Chem. Pharm. Bull. **39**(7) 1651—1654 (1991)

Amphiphile-Induced Erythrocyte Shape Change and Simultaneous Tetraethylammonium Ion Uptake

Takashi KATSU,* Kozo SANCHIKA, Hiroko OKAZAKI, Tomoyo KONDO, Takashi KAYAMOTO, and Yuzaburo FUJITA

Faculty of Pharmaceutical Sciences, Okayama University, Tsushima, Okayama 700, Japan. *Received January 10, 1991*

Amphiphile-induced tetraethylammonium ion (TEA^+) uptake into human erythrocytes was examined along with cell shape change. A TEA^+-sensitive electrode was used to determine the amount of uptake. TEA^+ was preferentially incorporated into erythrocytes when amphiphiles changed cell shape to an invaginated form. This was contrasted with the release of acetylcholinesterase outside cells which occurred markedly with the amphiphiles, causing the crenated form. It was suggested that the invagination of erythrocyte membrane stimulated the formation of vacuoles, in which TEA^+ existing in an external medium was entrapped.

Keywords amphiphile; erythrocyte shape; erythrocyte membrane; shape change; acetylcholinesterase release; tetraethylammonium ion uptake; membrane electrode; ion-selective electrode

The normal discoid shape of human erythrocytes is altered by the addition of amphiphilic compounds. Two types of changes have been mainly observed so far: the crenated and invaginated forms named echinocytes and stomatocytes, respectively.[1-6] Many have observed that the amphiphiles causing echinocytes stimulate the release of vesicles containing acetylcholinesterase (AChE) or phospholipids from the erythrocyte membrane.[7-10] Because such vesicles can be easily separated from the host erythrocytes by centrifugation, the degree of vesiculation depending on cell shape has been quantitatively analyzed.[9,10] In contrast, the vesicle release into inner cytoplasm, probably caused by stomatocyte-generating amphiphiles, is difficult to prove by chemical analysis because of the difficulty in separation of inner vesicles from host erythrocytes. Schrier and co-workers[11,12] applied ^{57}Co-vitamin B_{12} to this study. Creating the complex with plasma protein, this vitamin was absorbed on the cellular membrane, and the radioactivity of ^{57}Co trapped in cells was measured after residual membrane-bound vitamin B_{12} had been extensively removed by repeated washings and trypsin treatment. Concurrent electron microscopic measurements showed a correlation between inner vesiculation and the radioactivity trapped in cells.[11]

We were interested in a new methodology proving inner vesiculation without the use of a tracer. It was considered that when the vesicle release occurred inside cells, the intended marker dissolved in an outer medium would be entrapped in the vesicles drawn into erythrocyte cytoplasm. Electron microscopic observations[2,7-9,11,13] support the view that vesicles have sufficient space to incorporate the marker. Thus, the degree of inner vesiculation can be estimated from the amount of entrapped marker. The use of a water-soluble marker is preferable for easier removal of a residual marker from the cell surface. In the present study, tetraethylammonium ion (TEA^+) was chosen as the marker, and was detected with a TEA^+-sensitive electrode. The use of an ion-sensitive electrode has the inherent advantage of being simple, easy, and especially capable of detection without separation from assay mixtures. By using the TEA^+ marker, a correlation between inner vesiculation and shape change was investigated systematically. The amphiphiles tested were: chlorpromazine,[1-6,9,11] Triton X-100,[1,5,9] Tween 80,[14] and vitamin A[14,15] as the stomatocyte-forming agents; sodium dodecylsulfate (SDS),[5,9] *N*-dodecyl-*N*,*N*-dimethyl-3-ammonio-1-propanesulfonate (Zwittergent),[5,9] and egg lysophosphatidylcholine (egg lysoPC)[1,6] as the echinocyte-forming agents; and cetyltrimethylammonium bromide (CTAB)[1,5,9] as the agent forming both echinocytes and stomatocytes. It was found that TEA^+ was remarkably entrapped in erythrocytes when amphiphiles altered the cell shape to stomatocytes. Amphiphiles producing echinocytes did not induce the uptake to a significant extent.

Materials and Methods

Chemicals Chemical sources were as follows: Triton X-100, Tween 80, SDS, CTAB, and tetraethylammonium chloride (TEACl) from Tokyo Kasei Kogyo, Japan; chlorpromazine hydrochloride and egg lysoPC from Sigma, U.S.A.; vitamin A from Aldrich, U.S.A.; Zwittergent from Calbiochem, U.S.A.; sodium tetrakis[3,5-bis(trifluoromethyl)phenyl]-borate (NaTFPB) and 2-fluoro-2′-nitrodiphenyl ether (FNDPE) from Dojindo Laboratories, Japan; poly(vinyl chloride) (PVC) (degree of polymerization = 1020) from Nakarai Chemicals, Japan. Other chemicals used were all of analytical reagent grade.

Electrode System A TEA^+-sensitive electrode was constructed by the use of a PVC-based membrane. The PVC membrane had the following composition[16]: 0.5 mg of NaTFPB, 60 μl of FNDPE, and 30 mg of PVC. The materials dissolved in tetrahydrofuran were poured into a flat Petri dish of 30 mm diameter, and the solvent was evaporated at room temperature. The resulting PVC membrane was used as a sensor membrane. The electrochemical cell in this work is represented as follows: Ag, AgCl/10 mM TEACl (internal solution)/PVC sensor membrane/1 M NH_4NO_3 (salt bridge)/10 mM KCl/Ag, AgCl. The electromotive force between a pair of Ag/AgCl electrodes was measured with an appropriate field effect transistor-operational amplifier (input resistance: $>10^{12}\,\Omega$).

Erythrocytes Human erythrocytes were obtained on the day of an experiment from normal donors. Peripheral blood, drawn into ethylenediaminetetraacetic acid disodium salt (EDTA·2Na), was washed twice with 150 mM NaCl/5 mM 4-(2-hydroxyethyl)-1-piperazineethanesulfonic acid (Hepes)–NaOH (pH 7.4) and the intact cells were harvested by aspiration from under the "buffy" coat.

Assay Procedures Erythrocytes and amphiphiles were incubated at 37 °C for 30 min in 2.5 ml of a medium containing 100 mM TEACl/50 mM NaCl/5 mM glucose/5 mM Hepes–NaOH (pH 7.4). The final concentration of erythrocytes was 10% hematocrit (1×10^9 cells/ml). The addition of glucose improved the control shape of erythrocytes. After incubation, a cell suspension of a small amount (10 μl) was pipetted and added into 0.1 ml of 2% glutaraldehyde dissolved in 1/30 M NaH_2PO_4/Na_2HPO_4 (pH 7.4) for the fixation of cells. These cells were observed under an optical microscope connected to a video camera and a display television.[17] Shape changes were quantified by using the morphological indices defined by Fujii and co-workers.[4] After the remaining cell suspension was centrifuged out ($1300\times g$ for 5 min), K^+ efflux, hemolysis, and AChE activity in the supernatant were measured. The amount of K^+ efflux was measured with a K^+-selective electrode.[18] Hemolysis was estimated by measuring the absorbance at 540 nm.[17] AChE activity was determined by the method of Ellman *et al.*[19] The cell pellet was washed three times with 150 mM NaCl/5 mM Hepes–NaOH (pH 7.4), and was finally burst by

adding 500 μl of water to extrude TEA^+ trapped in the cells. The TEA^+ effused was determined using a TEA^+-sensitive electrode.

Results and Discussion

Response Characteristics of Electrode Figure 1 shows the calibration graph of the TEA^+ electrode in a buffer solution comprising 150 mM NaCl/5 mM Hepes–NaOH (pH 7.4). The electrode responded to TEA^+ down to 1 μM.

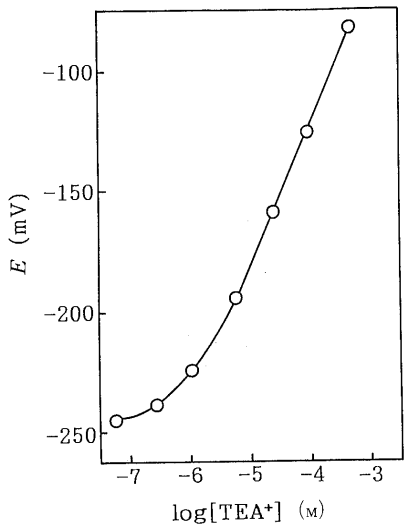

Fig. 1. Response of TEA^+-Sensitive Electrode in 0.15 M NaCl/5 mM Hepes–NaOH (pH 7.4) at 25 °C

The slope in the linear range was 58 mV/decade. The selectivity coefficients of the electrode against Na^+, K^+, Mg^{2+}, and Ca^{2+} were less than 10^{-4}, and substantially, these inorganic ions did not interfere. Because the TEA^+ electrode responded significantly to some amphiphiles, the following control experiments were performed; that is, erythrocytes and amphiphiles were incubated in a TEA^+-free solution comprising 150 mM NaCl/5 mM glucose/5 mM Hepes–NaOH (pH 7.4), and the cells were then washed and disrupted by the same procedures as in the TEA^+ uptake studies. With the amphiphiles used in the present study, serious interference was not observed. However, the electrode responded largely to some quaternary ammonium ions such as dodecyltrimethylammonium ion[5,9] and methochlorpromazine iodide,[3] and unfortunately, these amphiphiles could not been tested.

Erythrocyte Shape and TEA^+ Uptake Figure 2 shows the dose–response relations of TEA^+ uptake and shape change, together with AChE release, K^+ efflux, and hemolysis induced by chlorpromazine and Zwittergent. Chlorpromazine and Zwittergent were used as the representative agents causing stomatocytes and echinocytes, respectively. Both amphiphiles caused an efflux of K^+ before hemolysis, indicating that they initially formed a small membrane lesion and gradually a larger lesion, as has been observed with many amphiphilic compounds.[20-22] We were particularly interested in the fact that chlorpromazine induced the uptake of TEA^+ prior to the efflux of

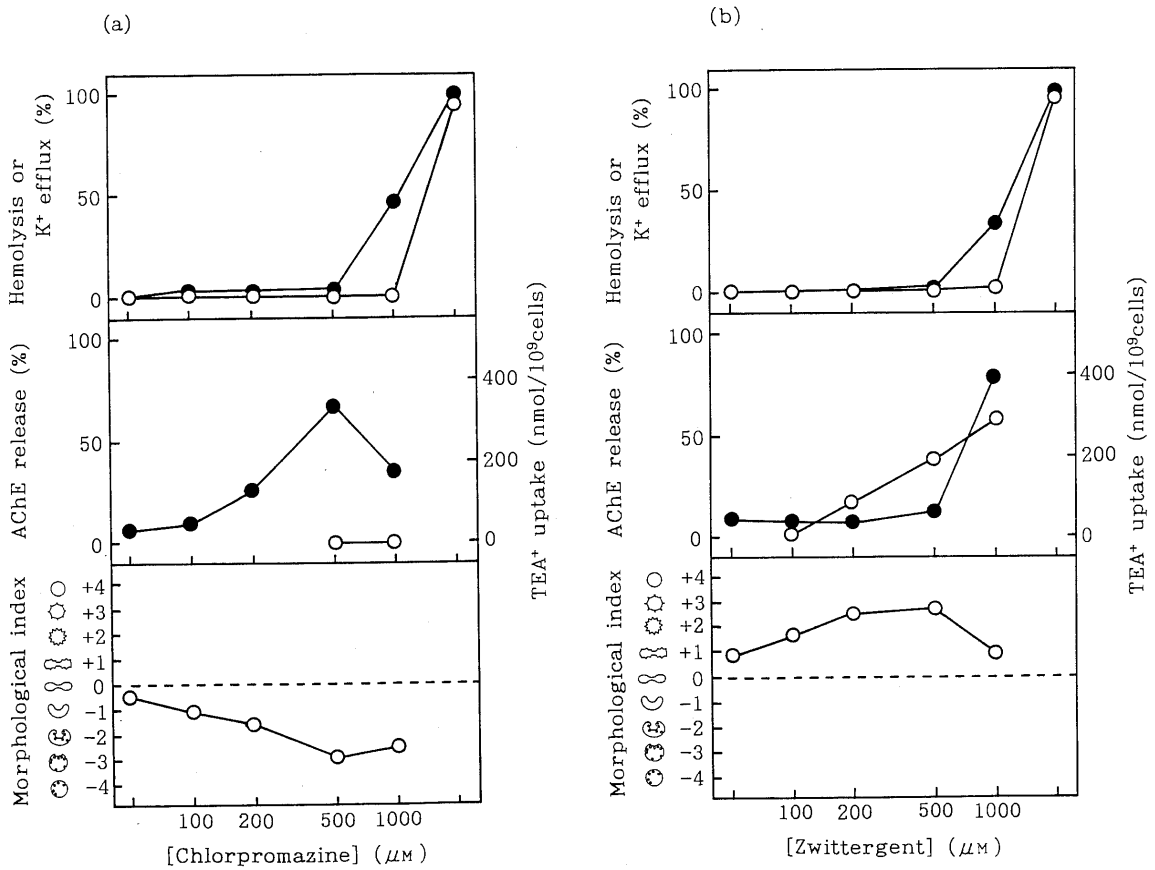

Fig. 2. The Dose–Response Curves of Hemolysis, K^+ Efflux, AChE Release, TEA^+ Uptake and Morphological Changes Induced by (a) Chlorpromazine and (b) Zwittergent

Upper drawing, hemolysis (○) and K^+ efflux (●); middle drawing, AChE release (○) and TEA^+ uptake (●); lower drawing, morphological index (○). Human erythrocytes (1×10^9 cells/ml) and amphiphiles were incubated at 37°C for 30 min in 100 mM TEACl/50 mM NaCl/5 mM glucose/5 mM Hepes–NaOH (pH 7.4).

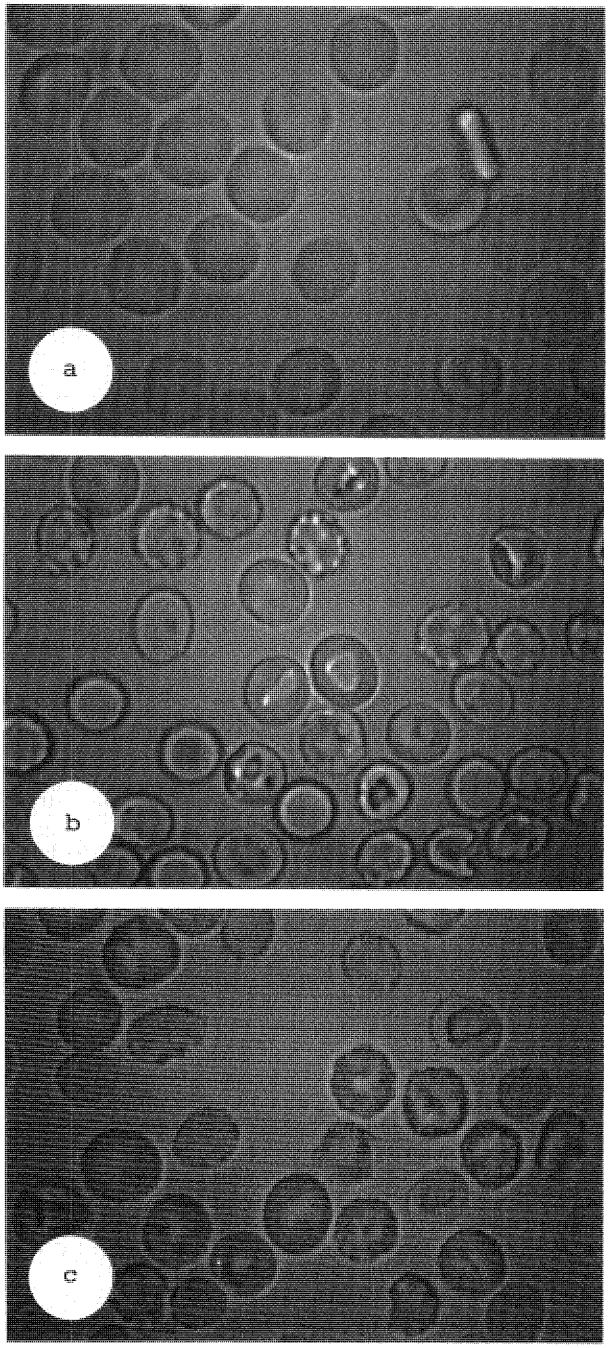

Fig. 3. Changes in the Morphology of Erythrocytes

(a) Control cells. Erythrocytes were incubated at 37 °C for 30 min with (b) 1 mM Zwittergent and (c) 200 μM SDS. They were observed under an optical microscope after being fixed with glutaraldehyde.

K^+. Because the size of TEA^+ is much larger than that of K^+,[23] TEA^+ seemed to have difficulty permeating the membrane more rapidly than K^+. The self-diffusion rate of TEA^+ through the liposomal membrane composed of egg phosphatidylcholine/cholesterol (molar ratio = 1 : 0.5 or 1 : 1) was also measured and found to be extremely slow (data not shown), indicating that the enhancement of TEA^+ uptake was not attributable to the lipophilic character of TEA^+. The dose–response of morphological changes revealed that TEA^+ uptake occurred at the stage of -2. It was reasonable to speculate that TEA^+ uptake originated from an inner vesiculation as mentioned in the introduction. Such TEA^+ uptake was also induced upon addition of Zwittergent at 1 mM, where stomatocytes were significantly observed as shown in Fig. 3b, although the average morphological index existed in the direction of echinocytes. However, in this instance, the uptake might partly be associated with an increase in membrane permeability, because a great deal of K^+ efflux was also observed at this concentration. As for AChE release, chlorpromazine did not cause it at all, while Zwittergent stimulated it largely at the stage of $+2$—$+3$. AChE release occurred through the stage of echinocytes.

The same experiments were performed using the various amphiphiles described in the introduction. After the dose–response relations were examined, the amounts of AChE release and TEA^+ uptake were plotted against a morphological index. The AChE release was clearly observed at the stage of echinocytes as shown in Fig. 4a. Although CTAB induced the release at the stage of stomatocytes (*ca.* -0.3), this was attributable to the time-dependent shape changes of CTAB[5,9]; that is, CTAB formed echinocytes releasing AChE at earlier period, and gradually the shape transformed to stomatocytes. Also, the release of AChE observed at the stage of *ca.* $+1$ (corresponding to the addition of SDS or Zwittergent at a high concentration) was attributable to such a time-dependent shape change. AChE was generally released through the stages above $+2$—$+3$. These results of AChE release were in good accordance with previous results.[9,24] Figure 4b shows a correlation between TEA^+ uptake and morphological index. The plots were limited to only a range where the amounts of K^+ efflux were relatively small (conventionally below 20%) to minimize the experimental error arising from spontaneous uptake due to an increase in membrane permeability. A marked uptake of TEA^+ was observed with the formation of stomatocytes, except for one instance of SDS. It should be pointed out, however, that SDS at this concentration (200 μM) produced stomatocytes significantly (Fig. 3c), similarly to the case of Zwittergent, but did not cause a remarkable efflux of K^+ (about 1%). Thus, also in this instance, the correlation between stomatocyte formation and TEA^+ uptake was actually recognized. There was a tendency for amphiphiles which form echinocytes initially (not only CTAB but also Zwittergent and SDS) to make stomatocytes, causing a TEA^+ uptake, especially in higher concentration ranges.

Concluding Remarks In this work, we showed that stomatocytes caused preferentiality for TEA^+ uptake, which contrasted with the release of AChE induced by echinocytes. Several advantages are mentioned in the use of TEA^+ marker. Firstly, the amount of marker uptake can easily be determined by using a TEA^+-sensitive electrode without any difficulty related to sample color or turbidity. Secondly, TEA^+ is certainly trapped into cells because of a low lipophilic character. Thirdly, erythrocyte shapes were not significantly affected in the presence of TEA^+. This enabled us to examine a correlation between shape changes and the amount of marker uptake. The present work, supported by chemical analyses, showed that amphiphiles forming echinocytes and stomatocytes led to further vesicle release outside and inside cells, respectively.

Acknowledgements We are grateful to Dr. M. Mio for valuable discussions. This work was supported in part by a Grant-in-Aid for Scien-

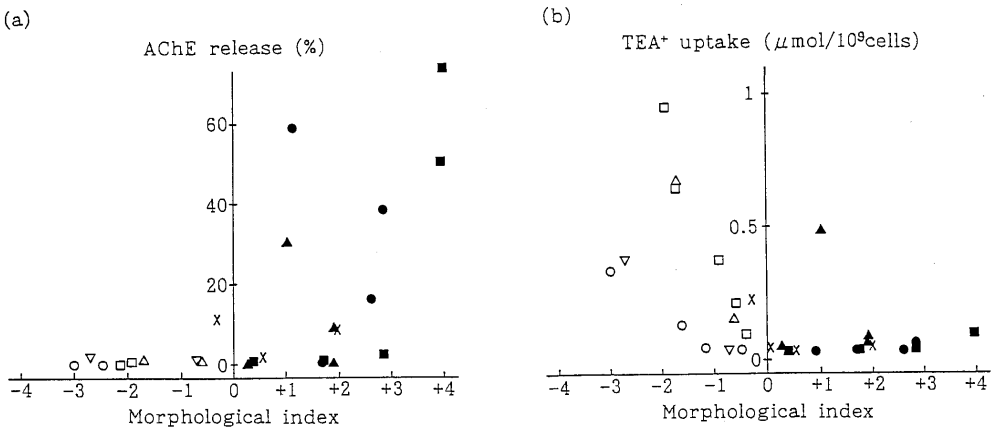

Fig. 4. Plots of (a) AChE Release and (b) TEA^+ Uptake as a Function of Morphological Index

Chlorpromazine (○), Triton X-100 (△), Tween 80 (□), vitamin A (▽), Zwittergent (●), SDS (▲), lysoPC (■), and CTAB (×).

tific Research from the Ministry of Education, Science and Culture of Japan.

References

1) B. Deuticke, *Biochim. Biophys. Acta*, **163**, 494 (1968).
2) B. Chailley, R. I. Weed, P. F. Leblond, and J. Maigné, *Neuv. Rev. Fr. Hématol.*, **13**, 71 (1973).
3) M. P. Sheetz and S. J. Singer, *Proc. Natl. Acad. Sci. U.S.A.*, **71**, 4457 (1974).
4) T. Fujii, T. Sato, A. Tamura, M. Wakatsuki, and Y. Kanaho, *Biochem. Pharmacol.*, **28**, 613 (1979).
5) B. Isomaa, H. Hägerstrand, and G. Paatero, *Biochim. Biophys. Acta*, **899**, 93 (1987).
6) J. E. Ferrell, Jr., K. T. Mitchell, and W. H. Huestis, *Biochim. Biophys. Acta*, **939**, 223 (1988).
7) D. Billington and R. Coleman, *Biochim. Biophys. Acta*, **509**, 33 (1978).
8) P. Ott, M. J. Hope, A. J. Verkleij, B. Roelofsen, U. Brodbeck, and L. L. M. Van Deenen, *Biochim. Biophys. Acta*, **641**, 79 (1981).
9) H. Hägerstrand and B. Isomaa, *Biochim. Biophys. Acta*, **982**, 179 (1989).
10) D. Allan, C. Hagelberg, K.-J. Kallen, and C. W. M. Haest, *Biochim. Biophys. Acta*, **986**, 115 (1989).
11) I. Ben-Bassat, K. G. Bensch, and S. L. Schrier, *J. Clin. Invest.*, **51**, 1833 (1972).
12) S. L. Schrier, I. Junga, and L. Ma, *Blood*, **68**, 1008 (1986).
13) K. Takahashi, T. Kobayashi, A. Yamada, Y. Tanaka, K. Inoue, and S. Nojima, *J. Biochem.* (Tokyo), **93**, 1691 (1983).
14) R. I. Weed and B. Chailley, "Red Cell Shape," ed. by M. Bessis, R. I. Weed, and P. F. Leblond, Springer–Verlag, New York, 1973, pp. 55—68.
15) M. J. Murphy, Jr., *Blood*, **41**, 893 (1973).
16) T. Katsu, T. Kayamoto, and Y. Fujita, *Anal. Chim. Acta*, **239**, 23 (1990).
17) T. Katsu, K. Sanchika, M. Takahashi, Y. Kishimoto, Y. Fujita, H. Yoshitomi, M. Waki, and Y. Shimohigashi, *Chem. Pharm. Bull.*, **38**, 2880 (1990).
18) T. Katsu, H. Kobayashi, and Y. Fujita, *Biochim. Biophys. Acta*, **860**, 608 (1986).
19) G. L. Ellman, K. D. Courtney, V. Andres, Jr., and R. M. Featherstone, *Biochem. Pharmacol.*, **7**, 88 (1961).
20) B. Isomaa, *Biochem. Pharmacol.*, **28**, 975 (1979).
21) T. Katsu, C. Ninomiya, M. Kuroko, H. Kobayashi, T. Hirota, and Y. Fujita, *Biochim. Biophys. Acta*, **939**, 57 (1988).
22) T. Katsu, M. Kuroko, K. Sanchika, T. Morikawa, Y. Kurosaki, T. Nakayama, T. Kimura, and Y. Fujita, *Int. J. Pharm.*, **53**, 61 (1989).
23) K. H. Stern and E. S. Amis, *Chem. Rev.*, **59**, 1 (1959).
24) T. J. Bierbaum, S. R. Bouma, and W. H. Huestis, *Biochim. Biophys. Acta*, **555**, 102 (1979).

Annelation Reactions of Enaminones with Ethyl Acetoacetate. Studies on the β-Carbonyl Compounds Connected with the β-Polyketides. XI[1)]

Naoki TAKEUCHI,* Satoko HANDA, Kumi KOYAMA, Kohji KAMATA, Kaori GOTO, and Seisho TOBINAGA*

Showa College of Pharmaceutical Sciences, Machida, Tokyo 194, Japan. *Received September 27, 1990*

Though condensation at either the carbonyl oxygen or the unsaturated carbon adjacent to nitrogen of enaminones can occur in the reaction with the active methylene of ethyl acetoacetate, the results obtained in the condensation reactions of the enaminones 1 and 2 with ethyl acetoacetate in the presence of Knoevenagel catalysts to give the α-pyranones 3 and 4 and with the dianion of ethyl acetoacetate to give the ethyl salicylates 6 and 19 show that these reactions proceed at the latter position.

Keywords condensation reaction; enaminone; ethyl acetoacetate; Knoevenagel catalyst; dianion; α-pyranone; ethyl salicylate

Enaminones are useful synthons in synthetic organic chemistry,[2)] and we have reported an aromatic annelation reaction by the reaction of an enaminone with dimethyl 3-oxoglutarate[3)] and an application of this reaction for the synthesis of *d,l*-phyllodulcin,[4,5)] a sweet dihydroisocoumarin.[6)] In the present paper, we describe the annelation reactions of enaminones with ethyl acetoacetate, investigated in connection with a previous report,[3)] to give several annelation products.

Two condensation patterns, namely, A and B, are possible in the condensation of the enaminones with the active methylene of ethyl acetoacetate, as shown in Chart 1.

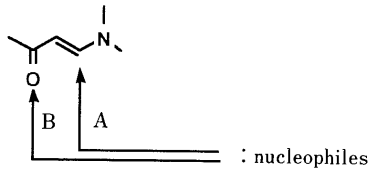

Chart 1

Two enaminones, 3-dimethylamino-1-phenyl-2-propenone (**1**)[3)] and 5-dimethylamino-1-phenyl-1,4-pentadien-3-one (**2**),[3)] were selected for the studies on the reactivity with ethyl acetoacetate. First, the condensation reactions in the presence of Knoevenagel catalysts were investigated by two methods. Reactions of the enaminone **1** with ethyl acetoacetate in the presence of AcONa, AcOH, and 18-crown-6 (method A) or in the presence of KF–AcOH (method B) afforded a condensation product **3** in a yield of 50.3 or 32.1%, respectively. Similar condensation reaction with the enaminone **2** by method A or B gave a condensation product **4** in 28.4 or 14.4% yield, respectively.

Four condensation products, namely, **3**, **5**, **6**, and **7**, are possible in the reaction of the enaminone **1** with ethyl acetoacetate (Chart 1). The following chemical transformations were performed to confirm the structure of 3-acetyl-6-phenyl-2-pyranone (**3**). Treatment of **3** with 10% KOH–MeOH (1 : 1) gave 3-phenylphenol (**8**)[7)] and reaction with NH_4OH in MeOH afforded 2-methyl-6-phenyl-3-nicotinic acid (**9**). The proton nuclear magnetic resonance spectrum (^{1}H-NMR) of **9** shows signals at δ 7.67 (1H, d, J=8.3 Hz) and δ 8.39 (1H, d, J=8.3 Hz).[8)] Therefore, the structures of **5**, **6**, **7**, and **10** are excluded as possible structures for the condensation product and the chemical

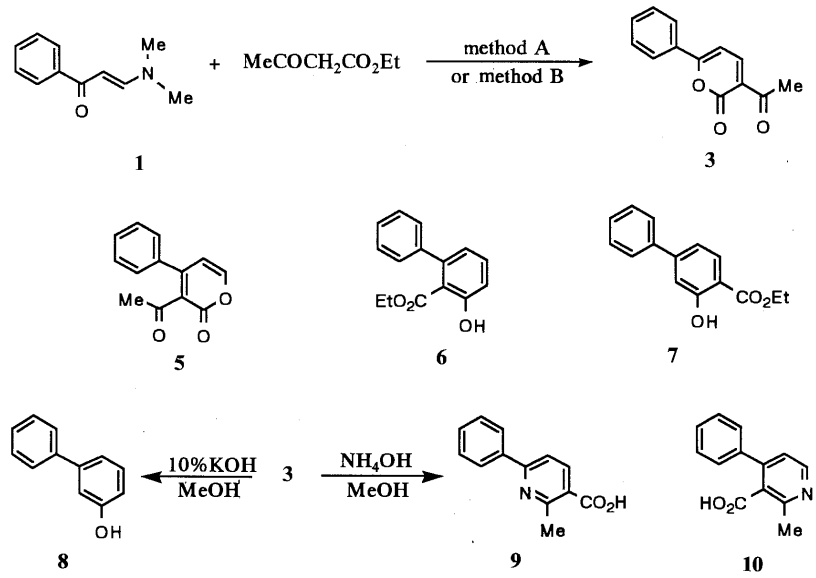

method A: AcONa, AcOH, 18-crown-6, toluene method B: KF, AcOH, dioxane

Chart 2

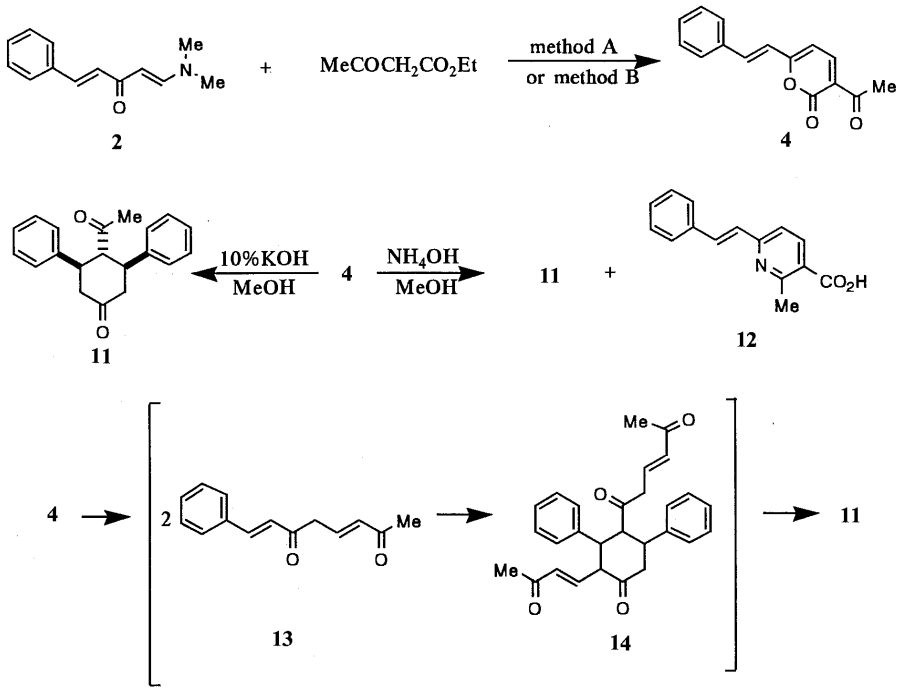

method A: AcONa, AcOH, 18-crown-6, toluene
method B: KF, AcOH, dioxane

Chart 3

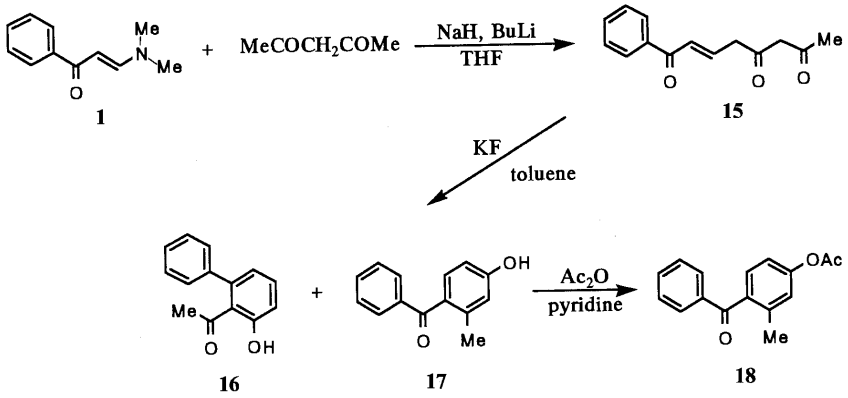

Chart 4

transformation product.

The structure of the condensation product **4** produced by the reaction of the enaminone **2** with ethyl acetoacetate was similarly established to be 3-acetyl-6-styryl-2-pyranone (**4**). Chemical transformations were performed as shown in Chart 3. Treatment of **4** with 10% KOH–MeOH (1 : 1) afforded 4-acetyl-3,5-diphenylcyclohexanone (**11**). An acetyl group and two phenyl groups of **11** may be equatorial in view of the ^{1}H-NMR signals at δ 3.43 (1H, t, J = 12.6 Hz) and δ 3.31 (2H, dt, J = 12.6 and 4.3 Hz). Compound **11** may be formed by the mechanism shown in Chart 3. That is, hydrolysis and decarboxylation of **4** may give **13**, which may dimerize to the intermediate **14**, and this in turn may be further hydrolyzed to yield **11**. Treatment of **4** with NH_4OH in MeOH afforded **11** and 2-methyl-6-styryl-3-nicotinic acid (**12**).

These results suggest that the reaction of enaminones with ethyl acetoacetate in the presence of Knoevenagel catalyst may proceed *via* pattern A shown in Chart 1.

Subsequently, the condensation reactions of the enaminones with ethyl acetoacetate through other procedures were investigated. The reaction of the enaminone **1** with the dianion prepared from the reaction of acetylacetone with NaH and butyl lithium in tetrahydrofuran (THF) (method C) was found in a preliminary experiment to give the condensation product **15**, which was transformed further to 2-acetyl-3-phenylphenol (**16**) and 4-hydroxy-2-methylbenzophenone (**17**) by treatment with KF in toluene. Acetylation of **17** with Ac_2O–pyridine afforded 4-acetoxy-2-methylbenzophenone (**18**).

Similarly, the reactions of the enaminones **1** and **2** with the dianion prepared from the reaction of ethyl acetoacetate with NaH and butyl lithium followed by treatment with KF afforded the condensation products **6** and **19** in yields of 14.8 and 24.0%, respectively (method C). The yields of condensation products **6** and **19** were raised to 33.1 and

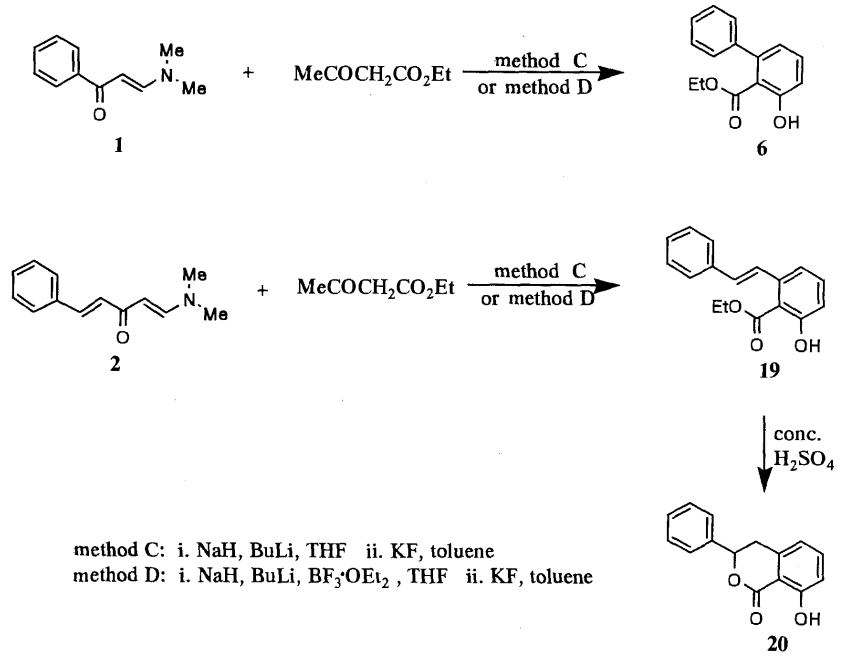

Chart 5

41.0%, respectively, by the addition of $BF_3 \cdot OEt_2$ to the above solution of the enaminones and the dianion of ethyl acetoacetate (method D).[9] The condensation product **19** was transformed subsequently to the dihydroisocoumarin **20** by treatment with concentrated H_2SO_4, in 69.9% yield.

The results obtained by the reactions of the enaminone **1** with the dianion of acetylacetone to give the products **16** and **17** and the enaminones **1** and **2** with the dianion of ethyl acetoacetate to give the products **6** and **19** show that these reactions proceed *via* pattern A shown in Chart 1, and may be applicable for the synthesis of natural dihydroisocoumarins, such as phyllodulcin,[4-6] hydrangenol,[4,10] *etc.*

Experimental

All melting points are uncorrected. Infrared (IR) spectra were recorded with a Hitachi 260-10 spectrometer, NMR spectra with a JEOL JNM-FX 100 spectrometer with tetramethylsilane as an internal standard, and mass spectra (MS) with a JEOL JMS-D 300 spectrometer. Elemental analyses were done by Ms. M. Takeda, Kissei Pharmaceutical Company, Ltd., Matsumoto, Japan. Mallinckrodt silica gel (100 mesh) and Merck Kieselgel G nach Stahl were used for column chromatography and thin layer chromatography (TLC), respectively.

3-Acetyl-6-phenyl-2-pyranone (3) Method A: Acetic acid (0.2 ml), dry sodium acetate (100 mg), and 18-crown-6 (200 mg) were added to a solution of the enaminone **1** (415 mg) and ethyl acetoacetate (470 mg) in dry toluene (20 ml), and the whole was refluxed for 6 h. The reaction mixture was concentrated under a vacuum, and the residue was acidified with 5% HCl and then extracted with ethyl acetate. The organic layer was washed with saturated $NaHCO_3$ and water, then dried and concentrated. The residue was subjected to silica gel chromatography. The chloroform eluate gave 255 mg (50.3%) of **3** as yellow needles (ether–hexane), mp 151—153 °C. IR (Nujol) cm^{-1}: 1720, 1675, 1550. ^{1}H-NMR ($CDCl_3$) δ: 2.66 (3H, s, –COMe), 6.69 (1H, d, J=6.1 Hz, olefinic H), 7.23—7.47 (3H, m, aromatic H), 7.63—7.83 (2H, m, aromatic H), 8.10 (1H, d, J=6.1 Hz, olefinic H). MS *m/z*: 214 (M^+), 199, 186, 171, 115, 109, 105. High-resolution MS *m/z*: Calcd for $C_{13}H_{10}O_3$ (M^+): 214.0630. Found: 214.0641. *Anal.* Calcd for $C_{13}H_{10}O_3$: C, 72.89; H, 4.70. Found: C, 72.71; H, 4.63.

Method B: Acetic acid (0.5 ml) and potassium fluoride (230 mg) were added to a solution of the enaminone **1** (175 mg) and ethyl acetoacetate (236 mg) in dry dioxane (5 ml), and the whole was refluxed overnight. The reaction mixture was worked up as described under method A to give 68.7 mg (32.1%) of **3**.

3-Phenylphenol (8) A mixture of **3** (100 mg), 10% KOH (5 ml), and methanol (5 ml) was refluxed overnight. The reaction mixture was poured into ice-water, acidified with 10% HCl, and then extracted with ether. The ether layer was washed with water, and then dried and concentrated. The residue was subjected to silica gel chromatography. The benzene eluate gave 17.9 mg (22.5%) of **8** as colorless prisms (ether–hexane), mp 76—78 °C (lit.[7] mp 76—78 °C).

2-Methyl-6-phenyl-3-nicotinic Acid (9) Ammonia water (5 ml) was added to a solution of **3** (50 mg) in methanol (3 ml) and the whole was refluxed overnight. The reaction mixture was poured into ice-water, acidified with 10% HCl, and then extracted with ether. The ether layer was washed with water, and then dried and concentrated. The residue was recrystallized from ether–hexane to yield 22 mg (44.2%) of **9** as orange-yellow prisms, mp 179—181 °C. IR (Nujol) cm^{-1}: 1685, 1580. ^{1}H-NMR ($CDCl_3$) δ: 2.98 (3H, s, –Me), 4.00 (1H, br, $-CO_2H$), 7.43—7.52 (3H, m, aromatic H), 7.67 (1H, d, J=8.3 Hz, olefinic H), 7.93—8.13 (2H, m, aromatic H), 8.39 (1H, d, J=8.3 Hz, olefinic H). High-resolution MS *m/z*: Calcd for $C_{13}H_{11}NO_2$: 213.0790. Found: 213.0785. *Anal.* Calcd for $C_{13}H_{11}NO_2$: C, 73.23; H, 5.20; N, 6.57. Found: C, 73.12; H, 5.19; N, 6.67.

3-Acetyl-6-styryl-2-pyranone (4) Compound **4** was obtained as yellow flaky crystals (ether), mp 145—147 °C, from the enaminone **2** by methods A and B described above in yields of 28.4 and 14.4%, respectively. IR (Nujol) cm^{-1}: 1710, 1680, 1630, 1535. ^{1}H-NMR ($CDCl_3$) δ: 2.68 (3H, s, –Me), 6.34 (1H, d, J=7.6 Hz, olefinic H), 6.69 (1H, d, J=15.9 Hz, olefinic H), 7.30—7.52 (5H, m, aromatic H), 7.67 (1H, d, J=15.9 Hz, olefinic H), 8.21 (1H, d, J=7.6 Hz, olefinic H). MS *m/z*: 240 (M^+), 225, 212, 197, 187, 169, 141, 131, 115, 109. High-resolution MS *m/z*: Calcd for $C_{15}H_{12}O_3$ (M^+): 240.0786. Found: 240.0807. *Anal.* Calcd for $C_{15}H_{12}O_3$: C, 74.99; H, 5.03. Found: C, 74.95; H, 5.00.

4-Acetyl-3,5-diphenylcyclohexanone (11) A mixture of **4** (50 mg), 10% KOH (3 ml), and methanol (3 ml) was refluxed for 3 h. The reaction mixture was poured into ice-water, acidified with 10% HCl, and then extracted with chloroform. The organic layer was washed with saturated $NaHCO_3$ and water, then dried and concentrated. The residue was subjected to silica gel chromatography. The chloroform eluate gave 25.5 mg (35.1%) of **11** as colorless prisms (ethyl acetate–chloroform), mp 207—209 °C. IR (Nujol) cm^{-1}: 1728, 1700, 1600, 1500. ^{1}H-NMR ($CDCl_3$) δ: 1.27 (3H, s, –Me), 2.67 (2H, dd, J=12.6, 4.3 Hz, methylene H), 2.80 (2H, t, J=12.6 Hz, methylene H), 3.31 (2H, dt, J=12.6, 4.3 Hz, methine H), 3.43 (1H, t, J=12.6 Hz, methine H), 7.20—7.36 (10H, m, aromatic H). High-resolution MS *m/z*: Calcd for $C_{20}H_{20}O_2$ (M^+): 292.1464. Found: 292.1470. *Anal.* Calcd for $C_{20}H_{20}O_2$: C, 82.15; H, 6.89. Found: C, 82.11; H, 6.94.

Reaction of 4 with Ammonia Water Ammonia water (5 ml) was added

to a solution of **4** (150 mg) in methanol (3 ml) and the whole was refluxed for 1.5 h. The reaction mixture was diluted with water and extracted with ethyl acetate. The organic layer was washed with water, then dried and concentrated. The residue was subjected to silica gel chromatography. The chloroform eluate gave 73.6 mg (33.8%) of **11** as colorless prisms (ethyl acetate–chloroform), mp 207—209 °C. The water layer was acidified with concentrated HCl and then extracted with ethyl acetate. The organic layer was washed with water, then dried and concentrated. The residue was recrystallized from methanol–ethyl acetate to yield 22.4 mg (12.6%) of 2-methyl-6-styryl-3-nicotinic acid (**12**) as colorless powdery crystals, mp 182—184 °C. IR (Nujol) cm^{-1}: 1700, 1595, 1490. ^{1}H-NMR ($CDCl_3$ + DMSO-d_6) δ: 3.16 (3H, s, –Me), 7.41—7.47 (2H, m, aromatic H), 7.69—7.79 (3H, m, aromatic H), 8.00 (2H, s, olefinic H), 8.18 (1H, d, J=8.8 Hz, aromatic H), 8.73 (1H, d, J=8.8 Hz, aromatic H). CI-MS m/z: 240 (M^++1). *Anal.* Calcd for $C_{15}H_{13}NO_2$: C, 75.30; H, 5.48; N, 5.85. Found: C, 75.28; H, 5.48; N, 5.89.

1-Phenyl-2-octene-1,5,7-trione (15) Sodium hydride (55%, 250 mg) was added to a solution of acetylacetone (330 mg) in dry THF (7.4 ml) with stirring at 0 °C for 10 min under a nitrogen atmosphere. A solution of 1.36 M butyl lithium in hexane (2.4 ml) was added and the mixture was stirred at 0 °C for 10 min under the same conditions. The enaminone **1** (500 mg) was then added, and the mixture was stirred at room temperature for 1 h under the same conditions. The reaction mixture was poured into ice-water, acidified with 10% HCl, and extracted with ether. The organic layer was washed with brine, then dried and concentrated. The residue was subjected to silica gel chromatography. The benzene eluate gave 373.2 mg (56.8%) of **15** as light yellow needles (ether–chloroform), mp 105—107 °C. IR (Nujol) cm^{-1}: 1678, 1645, 1592. High-resolution MS m/z: Calcd for $C_{14}H_{14}O_3$ (M^+): 230.0941. Found: 230.0940. *Anal.* Calcd for $C_{14}H_{14}O_3$: C, 73.03; H, 6.13. Found: C, 72.93; H, 6.11.

Reaction of 15 with Potassium Fluoride Potassium fluoride (75 mg) was added to a solution of **15** (100 mg) in dry toluene (5 ml), and the whole was refluxed overnight. The reaction mixture was concentrated under a vacuum, poured into ice-water, and then extracted with chloroform. The organic layer was washed with water, then dried and concentrated. The residue was subjected to silica gel chromatography. The first eluate with 30% hexane in chloroform gave 30.0 mg (32.5%) of 2-acetyl-3-phenylphenol (**16**) as a colorless oil. IR (neat) cm^{-1}: 1625, 1593, 1560, 1495. ^{1}H-NMR ($CDCl_3$) δ: 1.84 (3H, s, –COMe), 6.84 (1H, dd, J=7.3, 1.5 Hz, aromatic H), 6.99 (1H, dd, J=7.0, 1.5 Hz, aromatic H), 7.26—7.50 (6H, m, aromatic H), 11.6 (1H, s, –OH). High-resolution MS m/z: Calcd for $C_{14}H_{14}O_2$ (M^+): 212.0848. Found: 212.0859. The second eluate with 30% hexane in chloroform gave 39.9 mg (43.3%) of 4-hydroxy-2-methylbenzophenone (**17**) as a colorless oil. IR (neat) cm^{-1}: 3300, 1630, 1595, 1565, 1500. ^{1}H-NMR ($CDCl_3$) δ: 2.37 (3H, s, –Me), 6.12 (1H, br, –OH), 6.68 (1H, dd, J=8.4, 2.4 Hz, aromatic H), 6.75 (1H, d, J=2.4 Hz, aromatic H), 7.23—7.82 (6H, m, aromatic H). CI-MS m/z: 240 (M^++1).

4-Acetoxy-2-methylbenzophenone (18) Acetic anhydride (1.8 ml) was added to a solution of **17** (53 mg) in pyridine (0.6 ml) and the whole was allowed to stand overnight at room temperature. The reaction mixture was poured into ice-water and extracted with ether. The organic layer was washed with saturated $NaHCO_3$, 10% HCl, and water, then dried and concentrated. The residue was subjected to silica gel chromatography. The eluate with 50% hexane in ethyl acetate gave 54 mg (85%) of **18** as a colorless oil. IR (neat) cm^{-1}: 1770, 1668, 1602, 1585, 1500. ^{1}H-NMR ($CDCl_3$) δ: 2.25 (3H, s, –Me), 2.28 (3H, s, –Me), 6.92 (1H, dd, J=8.6, 2.2 Hz, aromatic H), 6.96 (1H, d, J=2.2 Hz, aromatic H), 7.19—7.54 (4H, m, aromatic H), 7.74 (2H, dd, J=7.8, 1.9 Hz, aromatic H). High-resolution MS m/z: Calcd for $C_{16}H_{14}O_3$ (M^+): 254.0943. Found: 254.0978.

Ethyl 6-Phenylsalicylate (6) Method C: Sodium hydride (55%, 52 mg) was added to a solution of ethyl acetoacetate (163 mg) in dry THF (3 ml) with stirring at 0 °C under a nitrogen atmosphere and the whole was stirred at 0 °C for 10 min. To the resulting mixture, a solution of 1.36 M butyl lithium in hexane (1.2 ml) was added, and the whole was stirred at 0 °C for 10 min under the same conditions. The enaminone **1** (200 mg) was then added, and the reaction mixture was stirred further at room temperature for 1 h under the same conditions, poured into ice-water, acidified with 10% HCl, and extracted with ether. The organic layer was washed with brine, dried and concentrated. The residue was dissolved in dry toluene (6.5 ml), potassium fluoride (104 mg) was added to the solution, and then the whole was refluxed overnight. The reaction mixture was concentrated under a vacuum, poured into ice-water, and extracted with chloroform. The organic layer was washed with water, then dried and concentrated. The residue was subjected to silica gel chromatography. The benzene eluate gave 41 mg (14.8%) of **6** as a colorless oil. IR (neat) cm^{-1}: 1658, 1598, 1566. ^{1}H-NMR ($CDCl_3$) δ: 0.75 (3H, t, J=7.3 Hz, –Me), 3.98 (2H, q, J=7.3 Hz, methylene H), 6.79 (1H, dd, J=7.3, 1.2 Hz, aromatic H), 6.99 (1H, dd, J=8.3, 1.2 Hz, aromatic H), 7.16—7.48 (6H, m, aromatic H), 10.79 (1H, s, –OH). High-resolution MS m/z: Calcd for $C_{15}H_{14}O_3$ (M^+): 242.0941. Found: 242.0928.

Method D: Sodium hydride (55%, 66 mg) was added to a solution of ethyl acetoacetate (325 mg) in dry THF (3 ml) with stirring at 0 °C under a nitrogen atmosphere and the whole was stirred similarly for an additional 10 min. A solution of 1.36 M butyl lithium in hexane (2.3 ml) was added to the mixture and the whole was stirred at 0 °C for 10 min under the same conditions. To the resultant solution, a solution of the enaminone **1** (52.5 mg) and $BF_3 \cdot OEt_2$ (0.4 ml) in dry THF (2 ml) was added, and the mixture was stirred at 0 °C for 1 h. The reaction mixture was worked up as described under method C to yield 24 mg (33.1%) of **6**.

Ethyl 6-Styrylsalicylate (19) Compound **19** was obtained as a colorless oil from the enaminone **2** by methods C and D described above in yields of 24.0 and 41.0%, respectively. IR (neat) cm^{-1}: 1678, 1622, 1598, 1520. ^{1}H-NMR ($CDCl_3$) δ: 1.41 (3H, t, J=7.1 Hz, –Me), 4.45 (2H, q, J=7.1 Hz, methylene H), 6.80 (1H, d, J=16.3 Hz, olefinic H), 6.90—7.50 (8H, m, aromatic H), 7.76 (1H, d, J=16.3 Hz, olefinic H), 11.30 (1H, s, –OH). High-resolution MS m/z: Calcd for $C_{17}H_{16}O_3$ (M^+): 268.1098. Found: 268.1083.

3,4-Dihydro-8-hydroxy-3-phenylisocoumarin (20) A solution of **19** (16 mg) in concentrated H_2SO_4 (0.4 ml) was stirred at 0 °C for 2 h. The reaction mixture was poured into ice-water and extracted with ethyl acetate. The organic layer was washed with saturated $NaHCO_3$, then dried and concentrated. The residue was recrystallized from ether–hexane to yield 10 mg (69.9%) of **20** as colorless prisms, mp 108—109.5 °C (lit.[11] mp 108—109.5 °C).

References and Notes

1) Part X: N. Takeuchi, Y. Sasaki, Y. Kosugi, and S. Tobinaga, *Chem. Pharm. Bull.*, **37**, 2012 (1989).
2) J. V. Greenhill, *Chem. Soc. Rev.*, **6**, 277 (1977).
3) N. Takeuchi, N. Okada, and S. Tobinaga, *Chem. Pharm. Bull.*, **31**, 4355 (1983).
4) Y. Asahina and J. Asano, *Chem. Ber.*, **62**, 171 (1929); *idem*, *ibid.*, **63**, 429 (1930); *idem*, *ibid.*, **64**, 1252 (1931); *idem*, *Yakugaku Zasshi*, **51**, 749 (1931); M. Watanabe, M. Sahara, S. Furukawa, J. Billedeu, and V. Snieckus, *Tetrahedron Lett.*, **23**, 1647 (1982); M. Watanabe, M. Sahara, M. Kubo, S. Furukawa, R. J. Billedeau, and V. Snieckus, *J. Org. Chem.*, **49**, 742 (1984); and references cited therein.
5) H. Arakawa, *Bull. Chem. Soc. Jpn.*, **33**, 200 (1960); Y. Naoi, S. Higuchi, H. Ito, T. Nakano, K. Sakai, T. Masui, S. Wagatsuma, A. Nishi, and S. Sano, *Org. Prep. Proc. Int.*, **7**, 129 (1975).
6) N. Takeuchi, K. Ochi, M. Murase, and S. Tobinaga, *J. Chem. Soc., Chem. Commun.*, **1980**, 593; *idem*, *Chem. Pharm. Bull.*, **31**, 4360 (1983).
7) This product was identified by comparison with an authentic sample obtained from a commercial supplier.
8) It was already known that the coupling constant between α and β protons in a pyridine ring is about 5—6 Hz and that between β and γ protons is about 7—9 Hz.
9) M. Yamaguchi, K. Shibato, and I. Hirao, *Chem. Lett.*, **1985**, 1145. 1145.
10) Y. Naoi, S. Higuchi, T. Nakano, K. Sakai, A. Nishi, and S. Sano, *Synth. Commun.*, **5**, 387 (1975); E. Napolitano, A. Ramacciotti, and R. Fiaschi, *Gazz. Chim. Ital.*, **118**, 101 (1988).
11) N. Takeuchi and S. Tobinaga, *Chem. Pharm. Bull.*, **28**, 3007 (1980).

[3,3]Sigmatropic Ring Expansion of Cyclic Thionocarbonates. IV.[1] Relationship between Ring Size of Cyclic Thionocarbonates and Geometry of Created Double Bond in Medium- and Large-Membered Thiolcarbonates

Shinya HARUSAWA, Hirotaka OSAKI, Toshiko KUROKAWA, Harumi FUJII, Ryuji YONEDA, and Takushi KURIHARA*

Osaka University of Pharmaceutical Sciences, 2–10–65, Kawai, Matsubara, Osaka 580, Japan. *Received November 19, 1990*

Medium- and large-membered cyclic thiolcarbonates containing an (*E*)- or (*Z*)-double bond were synthesized by two methods using [3,3]sigmatropic ring expansion of cyclic thionocarbonates. The [3,3]sigmatropic ring expansion proceeds exclusively *via* the transition state bearing the chain tethered in a *cis* relationship when the cyclic thionocarbonates are 8-membered or smaller. Importantly, the ring size of the cyclic thionocarbonate determines the double bond geometry of the thiolcarbonate.

Conversion of the cyclic thiolcarbonates into (*E*)- or (*Z*)-allylic sulfides is also described.

Keywords [3,3]sigmatropic rearrangement; cyclic thionocarbonate; cyclic thiolcarbonate; ring expansion; (*Z*)-selectivity; (*E*)-selectivity; (*Z*)-allylic sulfide; (*E*)-allylic sulfide; 1,1′-thiocarbonyldi-2,2′-pyridone; sodium bis(trimethylsilyl) amide

The exclusive (*E*)-selectivity of the double bond created by [3,3]sigmatropic rearrangement[2] has been extensively used for natural product synthesis.[3] However, few synthetic studies on the opposite (*Z*)-selective [3,3]sigmatropic rearrangement have been so far reported, probably owing to the lack of suitable methodology.[4] Garmaise and co-workers reported[5a] that the reaction of allyl alcohols with aryl chlorothionoformates yielded *S*-allyl aryl thiolcarbonates (Chart 1, Eq. 1). Faulkner and Peterson showed[5b] that treatment of 2-methyl-1-penten-3-ol with phenyl chlorothionoformate in pyridine at −20 °C afforded phenyl 2-methyl-2-pentenyl thiolcarbonate containing 96.5% (*E*)-olefin and 3.5% (*Z*)-olefin by rearrangement of the intermediate allylic thionocarbonate (Chart 1, Eq. 2).

Recently, we reported[6] that treatment of a diol monothionocarbonate (**5d**, $n=4$) with sodium hydride (NaH) or lithium diisopropylamide (LDA) resulted in the formation of an 8-membered thionocarbonate intermediate (**7d**) followed by spontaneous [3,3]-sigmatropic ring expansion to give a 10-membered heterocyclic thiolcarbonate (**8d**) containing a (*Z*)-double bond. This was easily converted into (*Z*)-allylic sulfides (**13** and **16**) of a type which has been widely used as intermediates for the formation of carbon–carbon bonds in organic synthesis.[7] We report herein the relationship between the ring size of cyclic thionocarbonates (**7**) and the geometry of the created double bond in medium- and large-membered thiolcarbonates (**8**), which could be prepared by two methods. We also present a full account of the work reported in a previous communication.[6] To our knowledge, there has been no previous report of a systematic study on [3,3]sigmatropic rearrangement applied in this fashion.[8]

Synthesis of Diol Monothionocarbonates (5a—g) The diol monothionocarbonates (**5c—g**) used in the present study were synthesized starting from commercially available ω-diols (**1**) *via* the three-step sequence outlined in Chart 2.

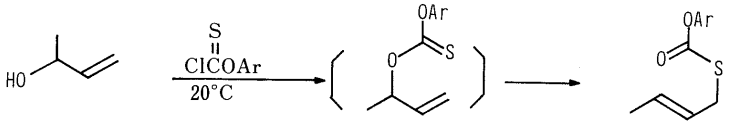

Eq. 1

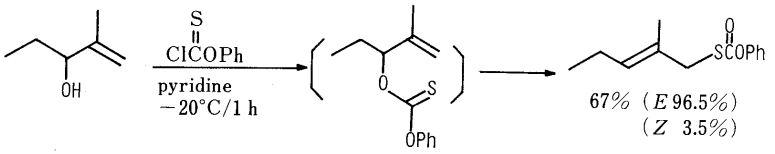

Eq. 2

Chart 1

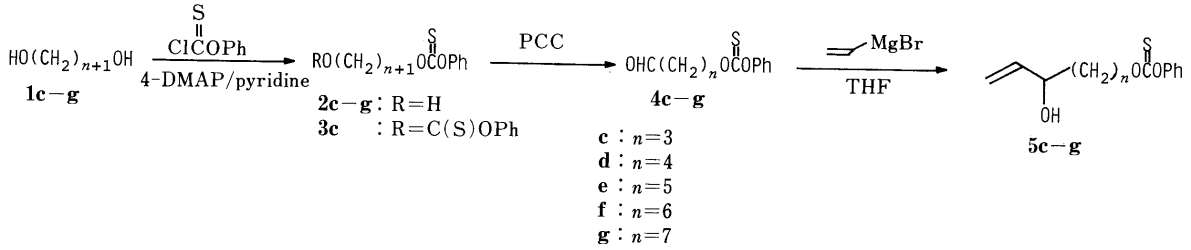

Chart 2

TABLE I. Yields and ^{1}H-NMR Spectral Data of Monothionocarbonates (**2**), Aldehydes (**4**), and Diol Monothionocarbonates (**5**)[a]

Compound No.	Yield (%)	^{1}H-NMR δ ($CDCl_3$, ppm)
2c	58	1.60—2.0 (4H, m, 2 × CH_2), 3.69 (2H, t, J=6.2 Hz, C$\underline{H}_2$OH), 4.54 (2H, t, J=6.4 Hz, CH_2O), 7.0—7.50 (5H, m, Ar-H)
2d	49	1.41—1.94 (6H, m, 3 × CH_2), 3.64 (2H, t, J=7.5 Hz, C$\underline{H}_2$OH), 4.51 (2H, t, J=7.5 Hz, CH_2O), 7.03—7.47 (5H, m, Ar-H)
2e	44	1.30—1.95 (8H, m, 4 × CH_2), 3.63 (2H, t, J=5.5 Hz, C$\underline{H}_2$OH), 4.50 (2H, t, J=5.5 Hz, CH_2O), 7.0—7.50 (5H, m, Ar-H)
2f	45	1.30—1.90 (10H, m, 5 × CH_2), 3.62 (2H, t, J=7.5 Hz, C$\underline{H}_2$OH), 4.49 (2H, t, J=8.0 Hz, CH_2O), 7.0—7.45 (5H, m, Ar-H)
2g	48	1.10—1.90 (12H, m, 6 × CH_2), 3.62 (2H, t, J=5.5 Hz, C$\underline{H}_2$OH), 4.49 (2H, t, J=5.5 Hz, CH_2O), 7.01—7.46 (5H, m, Ar-H)
4c	70	2.14 (2H, quint, J=5.5 Hz, CH_2), 2.64 (2H, t, J=6.0 Hz, C$\underline{H}_2$CHO), 4.54 (2H, t, J=5.5 Hz, CH_2O), 7.0—7.50 (5H, m, Ar-H), 9.81 (1H, s, CHO)
4d	68	1.68—1.96 (4H, m, 2 × CH_2), 2.51 (2H, t, J=5.0 Hz, C$\underline{H}_2$CHO), 4.52 (2H, t, J=5.0 Hz, CH_2O), 7.04—7.47 (5H, m, Ar-H), 9.78 (1H, s, CHO)
4e	63	1.35—1.95 (6H, m, 3 × CH_2), 2.44 (2H, t, J=6.0 Hz, C$\underline{H}_2$CHO), 4.51 (2H, t, J=5.5 Hz, CH_2O), 7.05—7.50 (5H, m, Ar-H), 9.77 (1H, s, CHO)
4f	58	1.18—1.92 (8H, m, 4 × CH_2), 2.45 (2H, t, J=9.0 Hz, C$\underline{H}_2$CHO), 4.51 (2H, t, J=8.0 Hz, CH_2O), 7.02—7.48 (5H, m, Ar-H), 9.77 (1H, s, CHO)
4g	63	1.13—1.92 (10H, m, 5 × CH_2), 2.41 (2H, t, J=6.0 Hz, C$\underline{H}_2$CHO), 4.48 (2H, t, J=6.0 Hz, CH_2O), 7.02—7.46 (5H, m, Ar-H), 9.76 (1H, s, CHO)
5a[b,c]	57	4.43 (1H, dd, J=11.4, 8.3 Hz, C$\underline{H}$OH), 4.59 (2H, dt, J=8.4, 3.2 Hz, CH_2O), 5.31 (1H, dt, J=10.6, 1.3 Hz, H$\underline{H}$C=CH), 5.46 (1H, J=17.2, 1.3 Hz, H$\underline{H}$C=CH), 5.92 (1H, ddd, J=17.2, 10.6, 5.3 Hz, =CH), 7.03—7.48 (5H, m, Ar-H)
5b[b]	76	1.90—2.15 (2H, m, CH_2), 4.32 (1H, br, C$\underline{H}$OH), 4.67 (2H, m, CH_2O), 5.17 (1H, d, J=11.0 Hz, H$\underline{H}$C=CH), 5.30 (1H, d, J=16.0 Hz, H$\underline{H}$C=CH), 5.92 (1H, ddd, J=16.0, 11.0, 7.0 Hz, =CH), 7.0—7.55 (5H, m, Ar-H)
5c	61	1.50—2.10 (4H, m, 2 × CH_2), 4.15 (1H, br, C$\underline{H}$OH), 4.55 (2H, t, J=5.5 Hz, CH_2O), 5.13 (1H, d, J=10.0 Hz, H$\underline{H}$C=CH),
	(47)[d]	5.23 (1H, d, J=16.0 Hz, H$\underline{H}$C=CH), 5.74 (1H, ddd, J=16.0, 10.0, 7.0, =CH), 7.0—7.50 (5H, m, Ar-H)
5d	70	1.40—1.60 (4H, m, 2 × CH_2), 1.85 (2H, quint, J=7.0 Hz, C$\underline{H}_2$CHOH), 4.12 (1H, br, C$\underline{H}$OH), 4.52 (2H, t, J=7.0 Hz,
	(75)[d]	CH_2O), 5.12 (1H, d, J=10.2 Hz, H$\underline{H}$C=CH), 5.21 (1H, d, J=18.0 Hz, H$\underline{H}$C=CH), 5.87 (1H, ddd, J=18.0, 10.0, 7.0 Hz, =CH), 7.05—7.50 (5H, m, Ar-H)
5e	55	1.30—1.95 (8H, m, 4 × CH_2), 4.10 (1H, br, C$\underline{H}$OH), 4.50 (2H, t, J=6.0 Hz, CH_2O), 5.10 (1H, d, J=10.5 Hz, H$\underline{H}$C=CH), 5.22 (1H, d, J=18.5 Hz, H$\underline{H}$C=CH), 5.83 (1H, ddd, J=18.5, 10.5, 6.0 Hz, =CH), 7.05—7.45 (5H, m, Ar-H)
5f	69	1.0—1.90 (10H, m, 5 × CH_2), 3.92—4.17 (1H, br, C$\underline{H}$OH), 4.49 (2H, t, J=8.0 Hz, CH_2O), 5.09 (1H, d, J=12.0 Hz, H$\underline{H}$C=CH), 5.20 (1H, d, J=18.0 Hz, H$\underline{H}$C=CH), 5.85 (1H, ddd, J=18.0, 12.0, 7.0 Hz, =CH), 6.9—7.48 (5H, m, Ar-H)
5g	61	1.15—1.98 (12H, m, 6 × CH_2), 4.08 (1H, br, C$\underline{H}$OH), 4.48 (2H, t, J=6.0 Hz, CH_2O), 5.08 (1H, d, J=12.0 Hz, H$\underline{H}$C=CH), 5.19 (1H, d, J=18.0 Hz, H$\underline{H}$C=CH), 5.85 (1H, ddd, J=18.0, 12.0, 7.0 Hz, =CH), 7.0—7.45 (5H, m, Ar-H)

a) Diol monothionocarbonates (**5**) showed an OH absorption band at 3380—3390 cm^{-1} in the IR spectra and did not give the expected MS peaks because of their thermal instability. b) Prepared from the diol (**6a** or **6b**). c) 4-Ethenyl-1,3-oxathiolan-2-one (**11**) (22%) was also obtained. d) Yield from the diol (**6c** or **6b**).

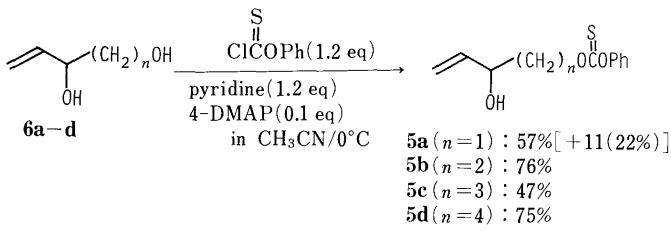

Chart 3

Thus, the diol (**1c**, n=3) was treated with phenyl chlorothionoformate (PCTF) (1 eq) in the presence of pyridine (1 eq) and 4-dimethylaminopyridine (4-DMAP) (0.1 eq) in acetonitrile at 0 °C to give a mixture of monothionocarbonate (**2c**) (58%) and bis-thionocarbonate (**3c**) (15%), which were separated by flash column chromatography (SiO_2). Formation of only **2c** could not be achieved in this reaction. The monothionocarbonate (**2c**) was then oxidized with pyridinium chlorochromate (PCC) in dichloromethane to give the aldehyde (**4c**) in 70% yield. Reaction of **4c** with vinylmagnesium bromide gave **5c** in 61% yield. Similarly, the diol monothionocarbonates (**5d—g**) were prepared. The yields and proton nuclear magnetic resonance (^{1}H-NMR) spectral data of the monothionocarbonates (**2**), aldehydes (**4**) and diol monothionocarbonates (**5**) are summarized in Table I. The monothionocarbonates (**5a—d**) were also prepared from unsaturated diols (**6**) by slow addition (7 h) of PCTF (1.2 eq) in the presence of pyridine (1.2 eq) and 4-DMAP (0.1 eq) in acetonitrile at 0 °C (Chart 3). The starting diols (**6a—d**) employed in this method were prepared according to the literature.[9]

Relationship between the Ring Size of Cyclic Thionocarbonates and the Geometry of the Created Double Bond in Medium- and Large-Membered Thiolcarbonates We have recently reported[6] that treatment of **5d** with LDA or NaH in tetrahydrofuran (THF) followed by refluxing for 1 h gives a 10-membered thiolcarbonate (**8d**) with a (*Z*)-double bond in 73% or 71% yield, respectively, *via* a spontaneous [3,3]sigmatropic rearrangement of the cyclic thionocarbonate (**7d**). We further found that the reaction proceeded at room temperature by the use of a sodium bis(trimethylsilyl)-amide [$(TMS)_2NNa$] (method A) as opposed to the elevated temperature often required for [3,3]sigmatropic rearrangement.[2] When a dry THF solution of $(TMS)_2NNa$ (1 eq) was rapidly added to a THF solution of **5d** (10 mM concentration) at room temperature, the reaction went to completion immediately and after usual work-up the

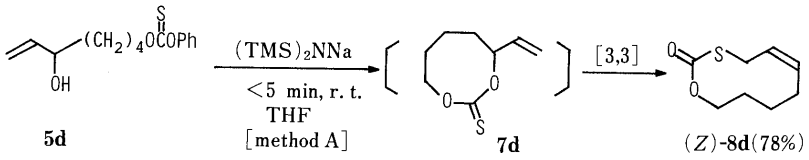

Chart 4

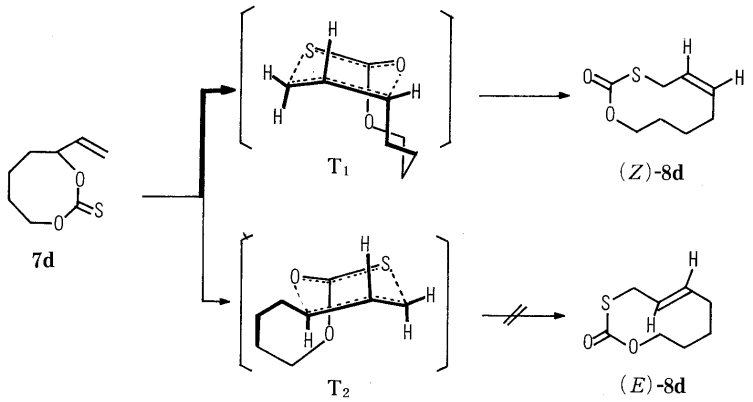

Chart 5

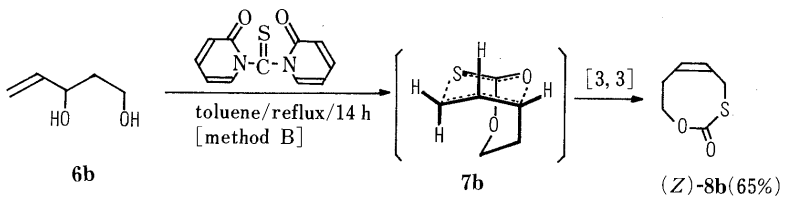

Chart 6

TABLE II. Synthesis of Cyclic Thiolcarbonates (**8**) Containing (*Z*)- or (*E*)-Double Bond

Compound		Yield (%)[a]	
8	*n*	Method A	Method B
a	1	—[b]	—[b]
b	2	—[c]	65 (*Z*)
c	3	(25)[b] (*E*)	—[c]
d	4	78 (*Z*)	46 (*Z*)
e	5	55[b] (*E*)	21 (*E*)
f	6	40 (*E*)	
g	7	—[b]	

a) Isolated yield. *b*) See text. *c*) Decomposed.

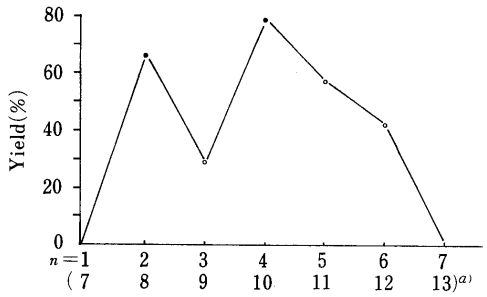

Fig. 1. Effect of the Ring Size on Selectivity of Double Bond Geometry of Cyclic Thiolcarbonates (**8**)

a) Number of atoms in cyclic thiolcarbonates (=*n*+6). ●, (*Z*)-double bond; ○, (*E*)-double bond.

product (**8d**) was isolated by flash column chromatography in 78% yield. Inspection of the ^{1}H-NMR [$CH_a=CH_bCH_2S$: δ 5.37 (H_a) (ddd, J=10.7, 8.4, 7.4 Hz), 5.57 (H_b) (dt, J=10.7, 8.2 Hz)] and carbon-13 (CH=CH: δ 126.1, 132.6 ppm) nuclear magnetic resonance (^{13}C-NMR) spectra of **8d** clearly showed the presence of a (*Z*)-double bond. Its stereochemical purity was also established by a vapor phase chromatography (VPC) analysis, using a 1.5% silicon OV-17 column. These results indicate that the reaction proceeds with high stereoselectivity. The cyclic thionocarbonates (**7d**) generated *in situ* were not isolated. The formation of a (*Z*)-double bond in **8d** can be rationalized as follows. In the [3,3]sigmatropic rearrangement, **7d** can adopt two possible conformations (T_1 and T_2) as the transition states, as shown Chart 5.[10] The T_1 with a 1,3-diaxial interaction would lead to the observed (*Z*)-olefin. On the other hand, the transition state (T_2) bearing the tethered chain in a *trans* relationship should be excluded because of the strain incurred in the four-carbon tether during proper alignment of the thiocarbonyl group and the double bond for the [3,3]sigmatropic ring expansion. Presumably, in the case of a larger membered thionocarbonate, the carbon bridge would be sufficiently long to allow the latter conformation.

In the case of **5b** (n=2), since the desired 8-membered thiolcarbonate (**8b**) was not obtained by method A, we employed an alternative approach using 1,1′-thiocarbon-

yldi-2,2′-pyridone (TCDP)[11] as the thiocarbonyl source. Refluxing 4-penten-1,3-diol (**6b**)[9a] with TCDP (1.1 eq) in toluene (method B) for 14 h cleanly gave an 8-membered thiolcarbonate (**8b**) containing a (*Z*)-double bond in 65% yield as shown in Chart 6. The (*Z*)-stereochemistry of **8b** was determined by ^{1}H-NMR [$CH_a=CH_bCH_2S$: δ 5.72 (H_a) (dt, $J=11.2$, 8.4 Hz), 5.98 (H_b) (dt, $J=11.2$, 9.1 Hz)]. The complete isomeric purity was confirmed by VPC analysis. The formation of the (*Z*)-olefin is reasonably accounted for by the all-chair transition state (**7b**). The remarkable ease of methods A and B is noteworthy and the results obtained are summarized in Table II and Fig. 1, making clear their characteristics in relation to the varying ring size of **8**. In these cases, the (*Z*)- and (*E*)-double bond in the cyclic thiolcarbonates (**8**) was distinguished clearly depending upon ring size. The [3,3]sigmatropic rearrangement of the 8-membered thionocarbonate (**7d**) was best carried out by method A and provided the 10-membered thiolcarbonate (**8d**) containing a (*Z*)-double bond in high yield.

Reaction of **5e** ($n=5$) with $(TMS)_2NNa$ by method A afforded an 11-membered thiolcarbonate (*E*-**8e**) in 55% yield. Inspection of the ^{1}H-NMR spectrum of the product (**8e**) showed an (*E*)-double bond [$CH_a=CH_bCH_2S$: δ 5.40 (H_a) (dt, $J=15.0$, 6.5 Hz), 5.51 (H_b) (dt, $J=15.0$, 6.5 Hz)]. Reaction of 7-octen-1,6-diol (**6e**) with TCDP by method B described above gave the product (**8e**) in 21% yield. The formation of the (*E*)-olefin shows that [3,3]sigmatropic ring expansion of **7e** proceeded through a relatively strain-free transition state (T_3) bearing the tethered chain in a *trans* relationship. Therefore, these observations have revealed that the [3,3]sigmatropic ring expansion proceeds exclusively *via* the transition state bearing the chain tethered in a *cis* relationship when the cyclic thionocarbonate (**7**) is 8-membered or smaller ($n\leqq 4$).

When **5f** ($n=6$) was similarly treated with $(TMS)_2NNa$, a mixture of a 12-membered thiolcarbonate (**8f**) and an unexpected product (**9f**) was obtained in 40% and 19% yields, respectively. The ^{1}H-NMR spectrum of **8f** showed an (*E*)-double bond [$CH_a=CH_bCH_2S$: 5.43 (H_a) (dt, $J=15.4$, 6.0 Hz), 5.58 (H_b) (dt, $J=15.4$, 6.0 Hz)]. Although the ^{1}H-NMR [δ 5.47 (2H, dt, $J=14.8$, 6.7 Hz), 5.64 (2H, dt, $J=14.8$ Hz, 6.7 Hz)] and infrared (IR) (960 cm^{-1}) spectra of **9f** closely resembled those of (*E*)-**8f**, the structure of **9f** was finally determined to be a dimer having two (*E*)-allylic thiolcarbonate moieties and a 24-membered cyclic system by examination of its mass spectrum (MS), which exhibited a parent peak at *m/z* 400. The similar reaction of **5g** ($n=7$) gave a dimer **9g** having a 26-membered cyclic system in 39% yield, together with decomposed materials. The structure of **9g** was supported by the MS (M^+, 428), ^{1}H-NMR ([δ 5.48 (2H, dt, $J=15.2$, 6.9 Hz), 5.66 (2H, dt, $J=15.2$, 6.9 Hz)] and IR (960 cm^{-1}) spectra. The presence of (*E*)-double bonds in the dimer **9g** was ultimately clarified by conversion of **9g** into an (*E*)-allylic thiolcarbamate (**10g**) (75%) by alkaline hydrolysis followed by treatment of the resulting allylic thiol with dimethylcarbamoyl chloride in

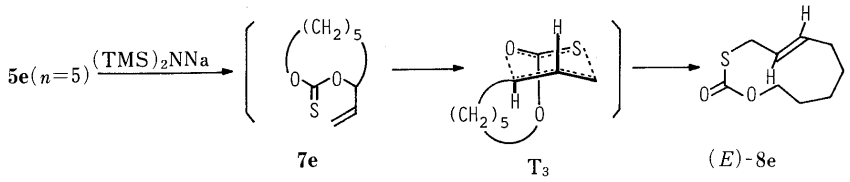

Chart 7

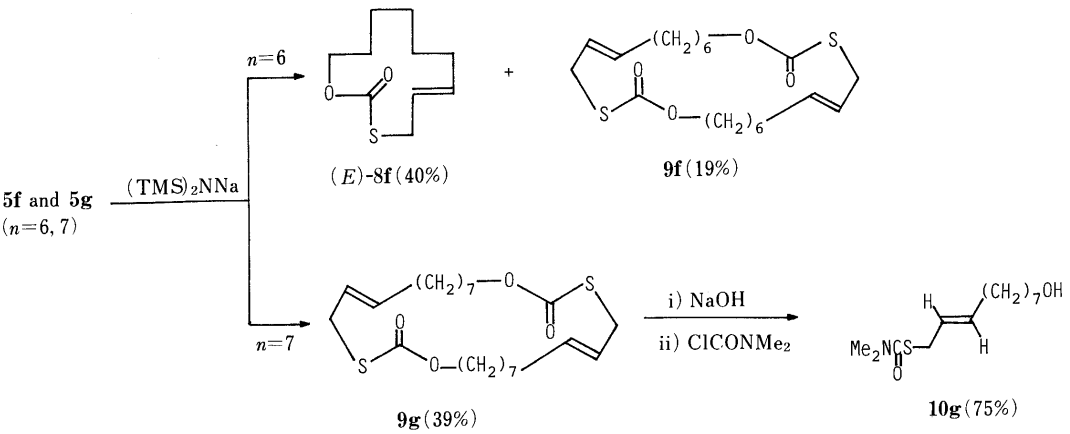

Chart 8

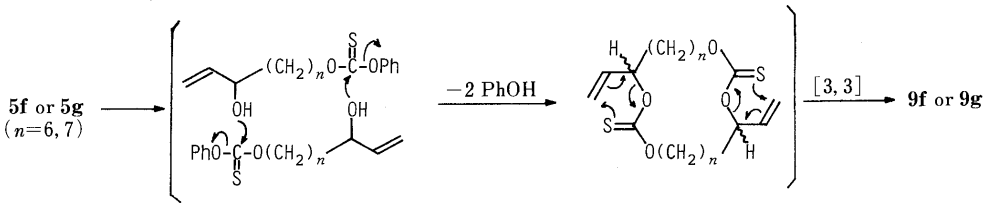

Chart 9

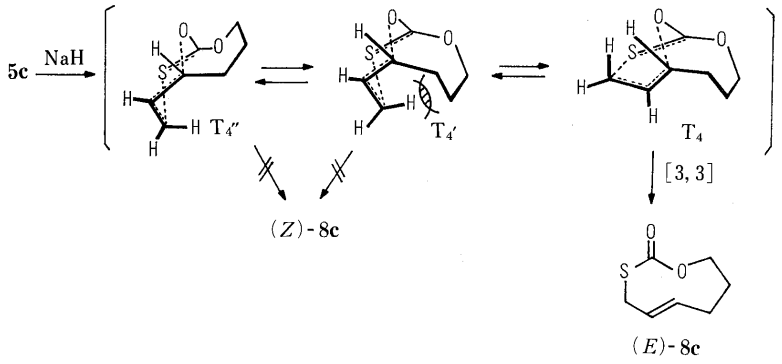

Chart 10

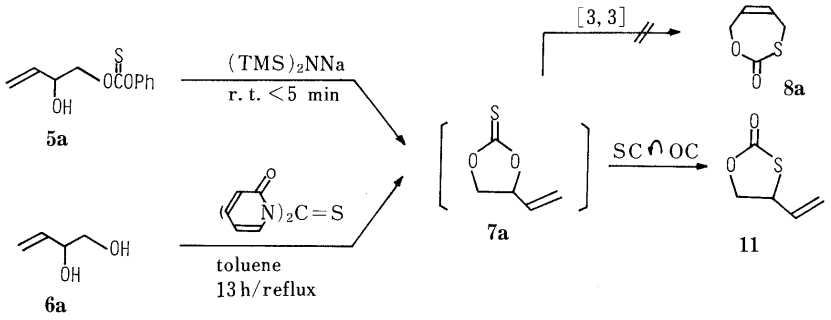

Chart 11

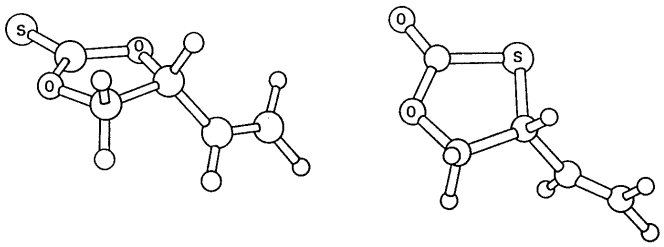

7a, $H_f = -47.13$ kcal/mol 11, $H_f = -64.14$ kcal/mol

Fig. 2. MNDO-Optimized Structures for **7a** and **11**

the presence of triethylamine and 4-DMAP. The formation of **9f** and **9g** may be easily explained by dimerization of the substrates (**5f** and **5g**) followed by a [3,3]sigmatropic ring expansion as depicted in Chart 9. Meanwhile, although **5c** ($n=3$) did not give a satisfactory result by method A or B, refluxing of **5c** with NaH[6] in THF for 20 min gave a 25% yield of (*E*)-**8c**. The formation of the (*E*)-isomer may be accounted for by the conformational preference of a boatlike transition state (T_4) over the more congested chairlike transition state ($T_{4'}$) or a boat 1,3-dioxepane ring ($T_{4''}$) leading to the (*Z*)-isomer.[10] The low yield of (*E*)-**8c** may be a consequence of the known difficulty in synthesis of medium rings and the inclusion of the (*E*)-double bond in the 9-membered ring.

In the case of **5a** ($n=1$), the methods A and B gave only 4-ethenyl-1,3-oxathiolan-2-one (**11**) (65% and 68% yields, respectively), which is an O,S-rearrangement product of the 5-membered thionocarbonate (**7a**), and the corresponding **8a** was not produced at all. The product **11** was also obtained as a by-product at the stage of preparation of the diol monothionocarbonate (**5a**) (Chart 3). In order to evaluate this isomerization, we carried out a molecular modeling study. Energy calculations[12] on **7a** and **11** were performed using the modified neglect of diatomic overlap (MNDO) program[13] in MOPAC.[14] The value of the calculated heat of formation energy (H_f) for each optimized conformer (**7a** and **11**) is shown with the molecular graphics in Fig. 2, wherein the ethenyl π-orbital in **7a** is restricted to a location perpendicular to the thiocarbonyl group. The energy of the conformer of **11** was lower by 17.01 kcal/mol than that of **7a**. The large difference of H_f value between **7a** and **11** is consistent with ease of isomerization.

Conversion of the Cyclic Thiolcarbonates [(*Z*)- or (*E*)-8] into (*E*)- or (*Z*)-Allylic Sulfides (10, 13 and 16) Allylic sulfides and their oxidation products, *i.e.*, sulfoxide or sulfones, play an important role in organic reactions, in particular carbon skeletal construction, because of the diversity of their chemical reactions.[6] (*E*)-Allylic sulfides are synthesized by a variety of methods involving [3,3]-sigmatropic rearragement.[15] On the other hand, the existing method[16] for the (*Z*)-allylic sulfides still relies on Lindlar hydrogenation of the corresponding acetylenes.[16a,b] Hayashi and co-workers[16a] derived (*Z*)-2-alkenyl *N*,*N*-dimethylthiolcarbamates from propargyl alcohol *via* several steps. However, hydrolysis of cyclic thiolcarbonates (**8**) containing a (*Z*)- or (*E*)-double bond with sodium hydroxide in aqueous methanol at room temperature easily gave the (*Z*)- or (*E*)-allylic thiols (**12b—e**) in quantitative yields, respectively. To avoid the undesirable formation of bisallylic sulfide in air, the products have been characterized by their conversion of allylic thiolcarbamates (**10b—e**) with dimethylcarbamoyl chloride in the presence of triethylamine and 4-DMAP. The reaction of the allylic thiol (**12d**) with electrophiles (methyl iodide, 2-bromocyclopentanone, 2-cyclopentenone, dimethylthiocarbamoyl chloride) led to the corresponding (*Z*)-allylic sulfides (**13a—d**), having a

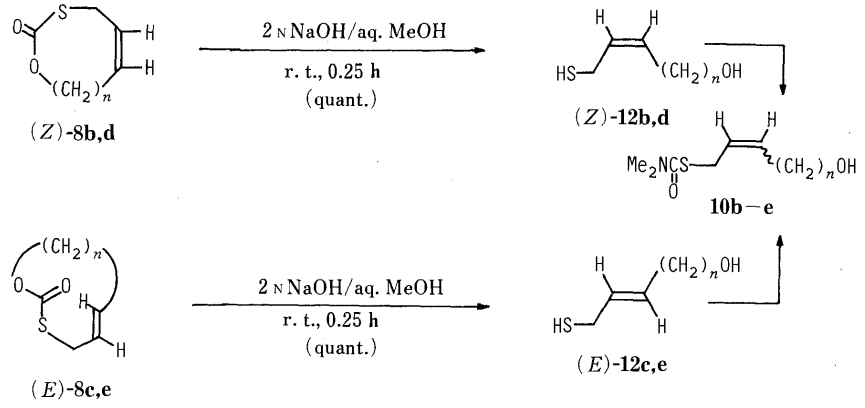

Chart 12

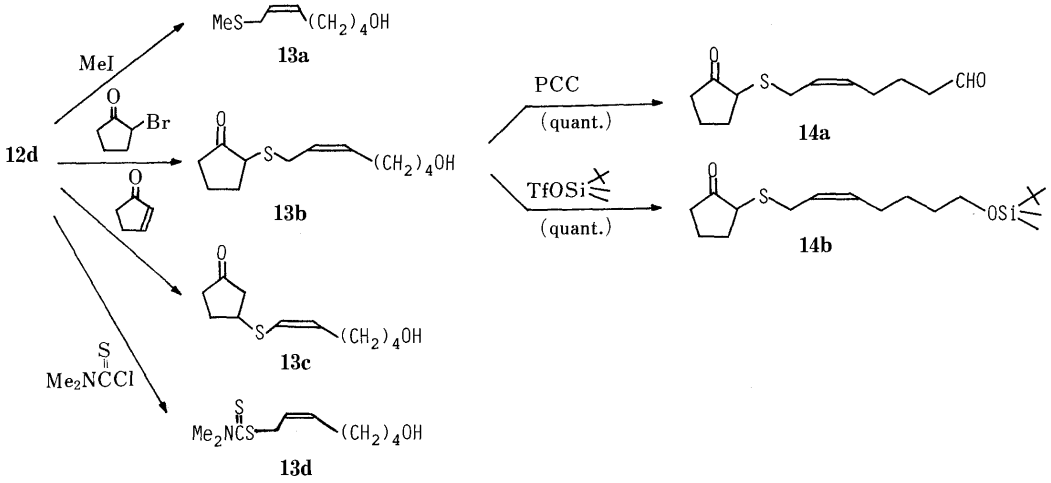

Chart 13

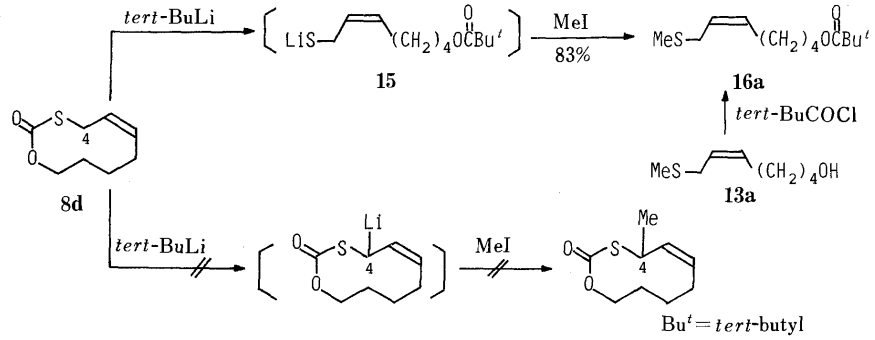

Chart 14

versatile alcohol function at the terminal position. The alcohol function of **13b** was easily converted into an aldehyde (**14a**) or silyl ether (**14b**) in quantitative yield, as shown in Chart 13.

We were further interested in a carbon–carbon bond formation reaction at the C-4 allylic position in the 10-membered thiolcarbonate (**8d**), as illustrated in Chart 14. However, treatment of **8d** with *tert*-butyllithium (*tert*-BuLi) at −78 °C in THF followed by addition of methyl iodide gave an unexpected (*Z*)-allylic sulfide (**16a**) with a pivaloate ester function in 83% yield. The structure of **16a** was established by an alternative synthesis from (*Z*)-allyl methylsulfide (**13a**) with pivaloyl chloride. This obviously means that *tert*-BuLi attacks the carbonyl group of **8d** to cleave the carbon–sulfur bond, followed by spontaneous coupling of the generated thiol anion (**15**) with methyl iodide. The thiol anion (**15**) was coupled with various alkyl halides as well as cyclolkenones to give the corresponding (*Z*)-allylic sulfides (**16**) containing a pivaloate moiety in good yield. The results are summarized in Table III. The method described here would provide new routes for (*Z*)-allylic sulfides.

Conclusion

Diol monothionocarbonates employed in this study could be prepared by two different routes. Methods A and B are useful for the preparation of medium- and large-membered thiolcarbonates (**8**) containing a (*Z*)- or (*E*)-double bond.

TABLE III. Yields of (*Z*)-Allylic Sulfides (**16**) Containing a Pivaloate Moiety

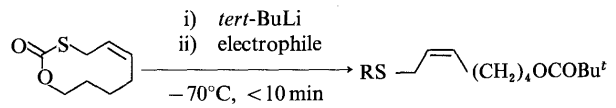

Electrophile	Product No.	Product	Yield (%)
MeI	**16a**	MeS–Y	83
Benzyl bromide	**16b**	$C_6H_5CH_2S$–Y	76
Geranyl bromide	**16c**	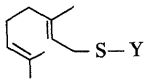	81
Propyl iodide	**16d**	$Me(CH_2)_2S$–Y	40
2-Cyclopentenone	**16e**	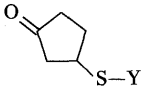	77
2-Cyclohexenone	**16f**	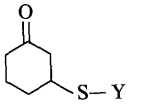	89
2-Bromocyclopentanone	**16g**	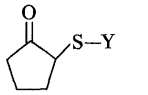	44[a]

Y =  $(CH_2)_4OCOBu^t$. *a*) **8d** (33%) was recovered.

This study has revealed that [3,3]sigmatropic ring expansion proceeds *via* the transition state bearing the chain tethered in a *cis* relationship when the cyclic thionocarbonate is 8-membered or smaller. This observation may provide an interesting insight into the factors influencing the transition state of the [3,3]sigmatropic rearrangement. Moreover, the ring size of cyclic thionocarbonates (**7**) is claimed to be an important factor for stereocontrolled olefin synthesis *via* [3,3]sigmatropic ring expansion. Further, conversion of cyclic thiolcarbonates (**8**) containing a (*Z*)- or (*E*)-double bond into **10**, **12**, **13** and **16** may provide a versatile and flexible approach for (*Z*)- or (*E*)-allylic sulfides. Further synthetic applications of cyclic thiolcarbonates (**8**) containing a (*Z*)- or (*E*)-double bond are being investigated in our laboratory.

Experimental

The IR spectra were recorded on a Shimadzu IR-435, and MS on a Hitachi M-80 spectrometer. ^{1}H- and ^{13}C-NMR spectra were taken with tetramethylsilane as an internal standard on a Varian Gemini-200 spectrometer in $CDCl_3$. Vapor-phase chromatographic analyses were performed with a Shimadzu GC-4BMPF gas chromatograph with a flame ionization detector using a 1.5% silicon OV-17 column (3 mm i.d. × 3 m, programed at 140—270 °C, 10 °C/min). For column chromatography, SiO_2 (Merck 9385) was used. All reactions were carried out under a nitrogen stream unless otherwise noted.

Synthesis of Diol Monothionocarbonate (5c) Method i (General Procedure): A solution of phenyl chlorothionoformate[17] (0.98 ml, 7 mM) in acetonitrile (10 ml) was added dropwise to a solution of 1,4-butanediol (**1c**) (630 mg, 7 mM) in acetonitrile (70 ml) in the presence of pyridine (0.56 ml, 7 mM) and 4-DMAP (85 mg, 0.7 mM) over 3 h at 0 °C under argon. After being stirred for 1 h, the mixture was evaporated under reduced pressure. The oily residue was dissolved in EtOAc–hexane (1 : 1). The organic layer was washed with H_2O and brine, dried over anhydrous Na_2SO_4, and then evaporated under reduced pressure. The residue was purified by column chromatography using hexane–EtOAc (1 : 1) as the eluent to give butane-1,4-bis (*O*-phenylthionocarbonate) (**3c**) (380 mg, 15%) [^{1}H-NMR spectrum: δ 1.55 (4H, m, 2 × CH_2), 4.52 (4H, t, J = 6.5 Hz, 2 × OCH_2), 7.10—7.55 (10H, m, Ar-H)] from the first fraction and *O*-4-hydroxybutyl *O*-phenyl thionocarbonate (**2c**) (920 mg, 58%) from the second fraction, each as an oil. Compound **2c** (920 mg, 4.3 mM) in dichloromethane (2 ml) was added to a suspension of PCC[17] (965 mg, 4.5 mM) in dichloromethane (3 ml) and the mixture was stirred at room temperature for 2 h. The mixture was filtered through a Celite pad and the filtrate was concentrated *in vacuo* to give a crude oil, which was purified by column chromatography (eluent: 20% EtOAc in hexane) to give *O*-3-formylpropyl *O*-phenyl thionocarbonate (**4c**) (638 mg, 70%) as an oil. A solution of vinylmagnesium bromide[17] (0.93 M in THF) (1.42 ml, 1.33 mM) was added dropwise to a solution of **4c** (298 mg, 1.33 mM) in THF (15 ml) over 10 min at 0 °C and the mixture was stirred for 20 min at the same temperature. The reaction was quenched by the addition of H_2O, and the mixture was extracted with EtOAc–hexane (1 : 1). The extract was washed with brine, dried over anhydrous Na_2SO_4, and then evaporated under reduced pressure. The residue was purified by column chromatography using 20% EtOAc in hexane for elution to give *O*-(4-hydroxy-5-hexenyl) *O*-phenyl thionocarbonate (**5c**) (206 mg, 61%) as an oil.

Similar treatments of **1d**—**g** afforded the monothionocarbonates (**2d**, **2e**, **2f** and **2g**) [no attempt was made to isolate the corresponding undesired bis-thionocarbonates (**3d**—**g**)], aldehydes (**4d**, **4e**, **4f** and **4g**) and diol monothionocarbonates (**5d**, **5e**, **5f** and **5g**), of which yields and ^{1}H-NMR spectral data are shown in Table I.

Synthesis of Diol Monothionocarbonate (5d) Method ii (General Procedure): A solution of phenyl chloroformate (2.46 g, 14.2 mM) in acetonitrile (8 ml) was added slowly over 7 h to a solution of 6-heptene-1,5-diol (**6d**)[9b] (1.54 g, 11.8 mM) in acetonitrile (70 ml) in the presence of pyridine (1.12 g, 14.2 mM) and 4-DMAP (0.144 g, 1.18 mM) at 0 °C under argon by a syringe pump technique. The solvent was evaporated off under reduced pressure to give an oil, which was subsequently diluted with EtOAc–hexane (1 : 1). The organic layer was washed with H_2O, and brine, dried over anhydrous Na_2SO_4, and then evaporated *in vacuo*. The residue was purified by column chromatography using 20% EtOAc–hexane for elution to give *O*-(5-hydroxy-6-heptenyl) *O*-phenyl thionocarbonate (**5d**) (2.33 g, 75%) as an oil.

Similar treatments of the diols (**6a**—**c**) gave the diol monothionocarbonates (**5a**, **5b** and **5c**), of which the yields and spectral data are shown in Table I.

General Procedure for the Preparation of Cyclic Thiolcarbonates (8) Method A (General Procedure): A 1 M solution of $(TMS)_2NNa$[17] in THF (0.5 ml) was added rapidly to a solution of a diol monothionocarbonate (**5**) (0.5 mM) in THF (50 ml) at room temperature, and the mixture was stirred for 5 min. The reaction was quenched by the addition of H_2O and the solvent was evaporated off under reduced pressure. The residue was extracted with EtOAc–hexane (1 : 1) and the extract was washed with brine, dried over anhydrous Na_2SO_4, and then evaporated under reduced pressure. The residual oil was purified by column chromatography using 5% or 10% EtOAc in hexane of elution to give the corresponding cyclic thiolcarbonate as an oil. Reaction of **5f** with $(TMS)_2NNa$ afforded **8f**, accompanied with a dimeric product (**9f**, 19%).

Method B (General Procedure): TCDP[17] (0.55 mM) was added to a solution of a diol (**6**)[9b] (0.5 mM) in toluene (50 ml), and the mixture was refluxed for 14 h. The solvent was evaporated off under reduced pressure. The residue was purified by column chromatography to give the corresponding cyclic thiolcarbonate as an oil.

(*Z*)-7,8,9,10-Tetrahydro-4*H*-1,3-oxathiecin-2-one (**8d**): IR (film) cm^{-1}: 1690 (C=O). ^{1}H-NMR δ: 1.5—1.8 (4H, m, 2 × CH_2), 2.37 (2H, br q, $CH=C\underline{H}_2$), 3.40 (2H, br, SCH_2), 4.39 (2H, br s, OCH_2), 5.37 (1H, ddd, J = 10.7, 8.4, 7.4 Hz, C_6-H), 5.57 (1H, dt, J = 10.7, 8.2 Hz, C_5-H). ^{13}C-NMR δ: 26.0, 27.2, 27.3, 29.8, 68.7, 126.1, 132.6, 169.8. MS *m/z*: 172 (M^+). HRMS Calcd for $C_8H_{12}O_2S$: 172.0558. Found: 172.0556. VPC analysis: t_R = 6.0 min.

(*Z*)-7,8-Dihydro-4*H*-1,3-oxathiocin-2-one (**8b**): IR (film) cm^{-1}: 1700 (C=O), 1100 (C–O–C), 1060, 965. ^{1}H-NMR δ: 2.47 (2H, m, $OCH_2C\underline{H}_2$), 3.55 (2H, d, J = 8.8 Hz, SCH_2), 4.26 (2H, t, J = 4.8 Hz, OCH_2), 5.72 (1H, dt, J = 11.2, 8.4 Hz, C_6-H), 5.98 (1H, dt, J = 11.2, 9.1 Hz, C_5-H). MS *m/z*: 144 (M^+). HRMS Calcd for $C_6H_8O_2S$: 144.0243. Found: 144.0239. VPC analysis: t_R = 3.7 min.

(*E*)-1-Oxa-3-thia-5-cycloundecen-2-one (**8e**): IR (film) cm^{-1}: 1690 (C=O), 1140, 965. ^{1}H-NMR δ: 1.30—1.85 (6H, br, 3 × CH_2), 2.10 (2H, quint, J = 5.0 Hz, $=CHC\underline{H}_2$), 3.40 (2H, d, J = 5.0 Hz, SCH_2), 4.23 (2H, t, J = 5.0 Hz, OCH_2), 5.40 (1H, dt, J = 15.0, 6.5 Hz, C_6-H), 5.51 (1H, dt, J = 15.0, 6.5 Hz, C_5-H). ^{13}C-NMR δ: 21.8, 25.9, 28.7, 33.1, 36.2, 67.9, 127.1, 135.0, 170.1. MS *m/z*: 186 (M^+). HRMS Calcd for $C_9H_{14}O_2S$: 186.0714. Found: 186.0717.

(*E*)-1-Oxa-3-thia-5-cyclododecen-2-one (**8f**): IR (film) cm^{-1}: 1685

(C=O), 960. ^{1}H-NMR δ: 1.20—1.90 (8H, m, 4×CH_2), 2.10 (2H, br s, =CHC$\underline{H}_2$), 3.38 (2H, d, J=8.0 Hz, SCH_2), 4.32 (2H, t, J=8.0 Hz, OCH_2), 5.43 (1H, dt, J=15.4, 6.0 Hz, C_6-H), 5.58 (1H, dt, J=15.4, 6.0 Hz, C_5-H). MS m/z: 200 (M^+). HRMS Calcd for $C_{10}H_{16}O_2S$: 200.0870. Found: 200.0871.

(*E,E*)-1,13-Dioxa-3,15-dithia-5,17-cyclotetracosandien-2,14-dione (**9f**): IR (film) cm^{-1}: 1695 (C=O), 960. ^{1}H-NMR δ: 1.10—1.50 (16H, m, 8×CH_2), 2.0 (4H, m, 2×=CHC$\underline{H}_2$), 3.41 (4H, d, J=8.0 Hz, 2×SCH_2), 4.21 (4H, t, J=7.0 Hz, 2×OCH_2), 5.47, 5.64 (each 2H, each dt, J=14.8, 6.7 Hz, 2×CH=CH). MS m/z: 400 (M^+). HRMS Calcd for $C_{20}H_{32}O_4S_2$: 400.1739. Found: 400.1740.

(*E*)-7,8-Dihydro-4*H*,9*H*-1,3-oxathionin-2-one (8c) A suspension of **5c** (172 mg, 0.68 mM) and 60% NaH (33 mg, 0.82 mM) in THF (70 ml) was refluxed for 20 min. The reaction mixture was cooled and quenched by the addition of H_2O and extracted with hexane–EtOAc (2 : 1). The extract was washed with H_2O, brine, and dried over anhydrous Na_2SO_4. After evaporation of the solvent under reduced pressure, the residue was purified by column chromatography using 5% EtOAc in hexane for elution to give **8c** (27 mg, 25%). IR (film) cm^{-1}: 1695 (C=O), 1150, 965. ^{1}H-NMR δ: 1.75 (2H, quint, J=5.5 Hz, CH_2), 2.13 (2H, q, J=5.5 Hz, =CHC$\underline{H}_2$), 3.30 (2H, d, J=5.5 Hz, SCH_2), 4.10 (2H, t, J=6.0 Hz, OCH_2), 5.42 (1H, dt, J=15.0, 6.9 Hz, C_5-H), 5.55 (1H, dt, J=15.0, 6.9 Hz, C_6-H). MS m/z: 158 (M^+). MRMS Calcd for $C_7H_{10}O_2S$: 158.0401. Found: 158.0408.

4-Ethenyl-1,3-oxathiolan-2-one (11) When treated according to the method A (or B), **5a** (or **6a**) gave **11** in 65% (or 68%) yield as an oil. IR (film) cm^{-1}: 1790 (C=O). ^{1}H-NMR δ: 4.32 and 4.75 (each 1H, each t, J=8.2 Hz, OCH_2), 5.32 (1H, q, J=8.0 Hz, SCH), 5.46 (1H, d, J=10.2 Hz, H⟩=⟨$\underline{H}$), 5.51 (1H, d, J=17.2 Hz, H⟩=⟨$\underline{H}$), 5.89 (1H, ddd, J=17.2, 10.2, 7.2 Hz, =CH). MS m/z: 130 (M^+). HRMS Calcd for $C_5H_6O_2S$: 130.0088. Found: 130.0093.

(*E,E*)-1,14-Dioxa-3,16-dithia-5,18-cyclohexacosandien-2,15-dione (9g) A 1 M solution of $(TMS)_2NNa$ (0.5 ml, 0.5 mM) in THF was added over 1.5 h to a solution of **5g** (154 mg, 0.5 mM) in THF (50 ml) at room temperature by a syringe pump technique. The ordinary work-up afforded **9g** (41 mg, 39%) as an oil. IR (film) cm^{-1}: 1695 (C=O), 1140, 960. ^{1}H-NMR δ: 1.10—1.80 (20H, m, 10×CH_2), 2.0 (4H, m, 2×CH=C$\underline{H}_2$), 3.42 (4H, d, J=8.0 Hz, 2×OCH_2), 4.19 (4H, t, J=8.0 Hz, 2×SCH_2), 5.48, 5.66 (each 2H, each dt, J=15.2, 6.9 Hz, 2×CH=CH). MS m/z: 428 (M^+). HRMS Calcd for $C_{22}H_{36}O_4S_2$: 428.2053. Found: 428.2052.

General Precedure for Hydrolysis of Cyclic Thiolcarbonates (8b—e) Aqueous 2 N sodium hydroxide solution (0.8 ml) was added to a thiolcarbonate (**8**) (1 mM) in MeOH (4 ml) at 0°C, and the mixture was stirred for 15 min at room temperature. The solvent was removed by evaporation and the residue was neutralized with 5% HCl. Extraction with CH_2Cl_2 by a salting-out technique gave almost pure allylic thiol as an oil in almost quantitative yield.

(*Z*)-5-Mercapto-3-penten-1-ol (**12b**): IR (film) cm^{-1}: 3400 (OH). ^{1}H-NMR δ: 2.30 (2H, q, J=7.5 Hz, =CHC$\underline{H}_2$), 3.16 (2H, t, J=7.5 Hz, SCH_2), 3.62 (2H, t, J=7.5 Hz, OCH_2), 5.41 (1H, dt, J=10.5, 10.0 Hz, C_4-H), 5.68 (1H, dt, J=10.5, 9.0 Hz, C_3-H). MS m/z: 118 (M^+).

(*E*)-6-Mercapto-4-hexen-1-ol (**12c**): IR (film) cm^{-1}: 3400 (OH). ^{1}H-NMR δ: 1.55—1.75 (2H, m, CH_2), 1.95—2.20 (2H, m, SCH_2), 3.09 (2H, t, J=5.5 Hz, SCH_2), 3.63 (2H, t, J=5.5 Hz, OCH_2), 5.5—5.6 (2H, br, CH=CH). MS m/z: 132 (M^+).

(*Z*)-7-Mercapto-5-hepten-1-ol (**12d**): IR (film) cm^{-1}: 3400 (OH). ^{1}H-NMR δ: 1.30—1.65 (4H, m, 2×CH_2), 2.10 (2H, q, J=7.0 Hz, =CHC$\underline{H}_2$), 3.16 (2H, t, J=8.0 Hz, SCH_2), 3.66 (2H, t, J=6.0 Hz, HOC$\underline{H}_2$), 5.31—5.65 (2H, m, CH=CH). MS m/z: 147 (M^+). HRMS Calcd for $C_7H_{15}OS$: 147.0843. Found: 147.0841.

(*E*)-8-Mercapto-6-octen-1-ol (**12e**): IR (film) cm^{-1}: 3400 (OH). ^{1}H-NMR δ: 1.10—1.70 (6H, m, 3×CH_2), 2.0 (2H, br, =CHC$\underline{H}_2$), 3.08 (2H, br, SCH_2), 3.59 (2H, t, J=6.5 Hz, OCH_2), 5.50 (2H, br, CH=CH). MS m/z: 160 (M^+).

General Procedure for Preparation of Thiolcarbamates (10b—e and 10g) A mixture of **12** (0.27 mM), dimethylcarbamoyl chloride (0.32 mM), triethylamine (0.32 mM) and 4-DMAP (0.054 mM) in THF (1 ml) was stirred overnight at room temperature under argon. The solvent was evaported off and the residue was diluted with EtOAc–hexane (1 : 1). The organic layer was washed with H_2O and brine, and dried over anhydrous Na_2SO_4. Evaporation of the solvent left a crude oil, which was purified by column chromatography using 30% EtOAc in hexane for elution to give **10** as an oil.

(*Z*)-*S*-(5-Hydroxy-2-pentenyl)*N,N*-Dimethylcarbamothioate (**10b**): Yield 59%, IR (film) cm^{-1}: 3400 (OH), 1630 (NC=O), 1095, 1040. ^{1}H-NMR δ: 2.41 (2H, q, J=5.5 Hz, =CHC$\underline{H}_2$), 2.93 (6H, s, 2×CH_3), 3.53 (2H, d, J=6.0 Hz, SCH_2), 3.64 (2H, t, J=6.5 Hz, OCH_2), 5.40—5.65 (2H, m, CH=CH). MS m/z: 189 (M^+). HRMS Calcd for $C_8H_{15}O_2NS$ Calcd: 189.0822. Found: 189.0830. VPC analysis: t_R=8.5 min.

(*E*)-*S*-(6-Hydroxy-2-hexenyl) *N,N*-Dimethylcarbamothioate (**10c**): Yield 41%, IR (film) cm^{-1}: 3400 (OH), 1630 (NC=O). ^{1}H-NMR δ: 1.61 (2H, quint, J=6.0 Hz, CH_2), 2.08 (2H, q, J=5.5 Hz, =CHC$\underline{H}_2$), 2.95 (6H, s, 2×CH_3), 3.49 (2H, d, J=6.0 Hz, SCH_2), 3.60 (2H, t, J=5.5 Hz, OCH_2), 5.48 (1H, ddd, J=15.3, 6.6, 6.3 Hz, C_3-H), 5.65 (1H, ddd, J=15.3, 6.3, 5.9 Hz, C_2-H). MS m/z: 203 (M^+). HRMS Calcd for $C_9H_{17}NO_2S$: 203.0979. Found: 203.0981. VPC analysis: t_R=10.6 min.

(*Z*)-*S*-(7-Hydroxy-2-heptenyl) *N,N*-Dimethylcarbamothioate (**10d**): Yield 92%, IR (film) cm^{-1}: 3400 (OH), 1630 (NC=O). ^{1}H-NMR δ: 1.30—1.60 (4H, m, 2×CH_2), 2.05—2.25 (2H, m, =CHC$\underline{H}_2$), 2.93 (6H, s, 2×CH_3), 3.55 (4H, m, SCH_2 and OCH_2), 5.45 (2H, m, CH=CH). VPC analysis: t_R=11.3 min.

(*E*)-*S*-(8-Hydroxy-2-octenyl) *N,N*-Dimethylcarbamothioate (**10e**): Yield 40%, IR (film) cm^{-1}: 3450 (OH), 1635 (NC=O), 1095, 965. ^{1}H-NMR δ: 1.10—1.70 (6H, m, 3×CH_2), 2.0 (2H, q, J=6.5 Hz, =CHC$\underline{H}_2$), 2.95 (6H, s, 2×CH_3), 3.48 (2H, d, J=6.5 Hz, SCH_2), 3.60 (2H, t, J=6.0 Hz, OCH_2), 5.45 (1H, dt, J=16.0, 7.5 Hz, C_3-H), 5.62 (1H, dt, J=16.0, 6.0 Hz, C_2-H). MS m/z: 231 (M^+).
HRMS Calcd for $C_{11}H_{21}O_2NS$: 231.1292. Found: 231.1291. VPC analysis: t_R=12.4 min.

(*E*)-*S*-(10-Hydroxy-2-decenyl) *N,N*-Dimethylcarbamothioate (10g) Aqueous 2 N NaOH (0.35 ml) was added to a solution of **9g** (30 mg, 0.07 mM) in MeOH (5 ml) and the mixture was stirred for 20 min at room temperature. Evaporation and extractive work-up gave a thiol (**12g**) (26 mg), which was subsequently treated with dimethylcarbamoyl chloride as described above (general procedure) to give **10g** (27 mg, 75%) as an oil. IR (film) cm^{-1}: 3450 (OH), 1630 (NC=O), 1360, 1100, 960. ^{1}H-NMR δ: 1.16—1.38 (8H, m 2×CH_2), 1.44—1.55 (2H, br, CH_2), 1.94 (2H, q, J=6.6 Hz, =CHC$\underline{H}_2$), 2.93 (6H, s, 2×CH_3), 3.46 (2H, d, J=7.2 Hz, SCH_2), 3.57 (2H, t, J=7.2 Hz, OCH_2), 5.41 (1H, dt, J=15.0, 7.2 Hz, C_3-H), 5.58 (1H, dt, J=15.0, 7.2 Hz, C_2-H). MS m/z: 259 (M^+). HRMS Calcd for $C_{13}H_{25}NO_2S$: 259.1604. Found: 259.1602.

(*Z*)-7-Methylthio-5-hepten-1-ol (**13a**) Methyl iodide (60 mg, 0.42 mM) was added to a solution of **12d** (21 mg, 0.14 mM) and MeONa (23 mg, 0.42 mM) in MeOH (8 ml), and the mixture was stirred for 20 min at room temperature. The solvent was evaporated and the residue was diluted with H_2O and CH_2Cl_2. The organic layer was washed with brine and dried over anhydrous Na_2SO_4. After evaporation of the solvent, the residue was purified by column chromatography using 40% EtOAc in hexane for elution to give **13a** (20 mg, 90%) as an oil. ^{1}H-NMR δ: 1.30—1.70 (4H, m, 2×CH_2), 2.02 (3H, s, CH_3), 1.95—2.18 (2H, m, =CHC$\underline{H}_2$), 3.12 (2H, d, J=7.0 Hz, SCH_2), 3.65 (2H, t, J=6.5 Hz, OCH_2), 5.38—5.63 (2H, m, CH=CH). MS m/z: 160 (M^+). HRMS Calcd for $C_8H_{16}OS$: 160.0921. Found: 160.0913.

(*Z*)-2-(7-Hydroxy-2-heptenyl)thiocyclopentanone (13b) 2-Bromocyclopentanone (137 mg, 0.84 mM) was added to a solution of **12d** (120 mg, 0.70 mM) and MeONa (45 mg, 0.84 mM) in MeOH (4 ml), and the mixture was treated as described for the preparation of **13a** to give **13b** (92 mg, 58%) as an oil. IR (film) cm^{-1}: 3700—3100 (OH), 1725 (C=O). ^{1}H-NMR δ: 1.30—2.55 (13H, m, 6×CH_2 and OH), 3.10 (2H, m, SCH_2), 3.45 (1H, dd, J=12.0, 9.0 Hz, SCH), 3.65 (2H, t, J=7.0 Hz, OCH_2), 5.50 (2H, m, CH=CH). MS m/z: 228 (M^+). HRMS Calcd for $C_{12}H_{20}O_2S$: 228.1183. Found: 228.1185.

(*Z*)-3-(6-Hydroxy-1-hexenyl)thiocyclopentanone (13c) 2-Cyclopentenone (4 mg, 0.05 mM) was added to a solution of **12d** (8 mg, 0.05 mM) and MeONa (3 mg, 0.06 mM) in MeOH (1 ml), and the mixture was treated as described above to give **13c** (9 mg, 86%) as an oil. IR (film) cm^{-1}: 3600—3000 (OH), 1725 (C=O). ^{1}H-NMR δ: 1.30—2.67 (13H, m, 6×CH_2 and OH), 3.21 (2H, d, J=7.0 Hz, SCH_2), 3.40 (1H, quint, J=7.0 Hz, SCH), 3.64 (2H, t, J=7.0 Hz, OCH_2), 5.50 (2H, m, CH=CH). MS m/z: 228 (M^+). HRMS Calcd for $C_{12}H_{20}O_2S$: 228.1183. Found: 228.1185.

(*Z*)-Dimethyl 7-Hydroxy-2-heptenylcarbamodithioate (13d) A mixture of **12d** (136 mg, 0.93 mM), dimethylthiocarbamoyl chloride (149 mg, 1.2 mM), triethylamine (121 mg, 1.2 mM) and 4-DMAP (24 mg, 0.2 mM) in THF (1 ml) was treated as described for the preparation of **10** to give **13d** (152 mg, 70%) as an oil. ^{1}H-NMR δ: 1.30—1.60 (4H, m, 2×CH_2), 1.70 (1H, br s, OH), 2.05—2.25 (2H, q, J=8.0 Hz, =CHC$\underline{H}_2$), 3.30, 3.35 (each 3H, each s, 2×CH_3), 3.59 (2H, q, J=6.0, SCH_2), 3.90 (2H, d, J=8.0 Hz, OCH_2), 5.40—5.65 (2H, m, CH=CH). MS m/z: 233 (M^+). HRMS Calcd for $C_{10}H_{19}NOS_2$: 233.0908. Found: 233.0904.

(*Z*)-7-(2-Oxocyclopentyl)thio-5-hexenal (14a) A suspension of **13b** (7 mg, 0.031 mM) and PCC (10 mg, 0.047 mM) in dichloromethane (1 ml)

was stirred for 13 h at room temperature. The reaction mixture was diluted with ether and filtered through a Celite pad. The filtrate was evaporated to give a brown oil, which was purified by column chromatography using EtOAc–hexane (1 : 1) for elution to give **14a** (7 mg, 100%) as an oil. IR (film) cm^{-1}: 1725 (C=O). ^{1}H-NMR δ: 1.60—2.60 (12H, m, $6\times CH_2$), 3.10 (2H, m, SCH_2), 3.45 (1H, m, SCH), 5.50 (2H, m, CH=CH), 9.75 (1H, s, CHO). MS *m/z*: 226 (M^+). HRMS Calcd for $C_{12}H_{18}O_2S$: 226.1027. Found: 226.1029.

(*Z*)-2-(7-*tert*-Butyldimethylsilyloxy-2-heptenyl)thiocyclopentanone (14b) *tert*-Butyldimethylsilyl trifluoromethanesulfonate[17] (1 drop) was added to a solution of **13b** (4 mg, 0.018 mM) in pyridine (1 ml) at −10 °C, and the mixture was stirred for 10 min. The reaction was quenched by the addition of H_2O at this temperature and the mixture was diluted with EtOAc–hexane (1 : 1). The organic layer was washed with H_2O and brine, and dried over anhydrous Na_2SO_4. Evaporation of the solvent left a crude oil, which was purified by column chromatography using 20% EtOAc in hexane for elution to give **14b** (6 mg, 100%) as an oil. IR (film) cm^{-1}: 1725 (C=O). ^{1}H-NMR δ: 0.03 (6H, s, $2\times CH_3$), 0.86 (9H, s, *tert*-Bu), 1.30—2.55 (12H, br, $6\times CH_2$), 3.10 (2H, m, SCH_2), 3.44 (1H, dd, J=13.0, 7.0 Hz, SCH), 3.60 (2H, t, J=7.0 Hz, OCH_2), 5.50 (2H, m, CH=CH). MS *m/z*: 342 (M^+). HRMS Calcd for $C_{18}H_{34}O_2SSi$: 342.2047. Found: 342.2045.

General Procedure for Reaction of 8d with Electrophiles in the Presence of *tert*-BuLi An electrophile (methyl iodide, benzyl bromide, geranyl bromide, propyl iodide, 2-cyclopentenone, 2-cyclohexenone or 2-bromocyclopentanone) was added to a solution of **8d** (0.1 mM) and 1.5 M *tert*-BuLi (0.11 mM) in THF (4 ml) at −78 °C under argon, and the mixture was stirred for 10 min at this temperature. The reaction was quenched by the addition of H_2O and the solvent was evaporated off under reduced pressure. The residue was extracted with CH_2Cl_2 and the extract was washed with H_2O and brine, and dried over anhydrous Na_2SO_4. Evaporation of the solvent gave a crude oil, which was purified by column chromatography using 5% EtOAc in hexane for elution to give **16** as an oil.

(*Z*)-7-Methylthio-5-heptenyl 2,2-Dimethylpropionate **(16a)**: IR (film) cm^{-1}: 1720 (C=O). ^{1}H-NMR δ: 1.18 (9H, s, *tert*-Bu), 1.43 and 1.64 (each 2H, each q, J=7.5 Hz, $2\times CH_2$), 2.0 (3H, s, CH_3), 2.07 (2H, q, J=7.5 Hz, $=CHC\underline{H}_2$), 3.11 (2H, d, J=7.5 Hz, SCH_2), 4.03 (2H, t, J=7.5 Hz, OCH_2), 5.43 (1H, dt, J=10.5, 6.2 Hz, C_6-H), 5.52 (1H, dt, J=10.5 Hz, 6.8 Hz, C_5-H). MS *m/z*: 244 (M^+). HRMS Calcd for $C_{13}H_{24}O_2S$: 244.1496. Found: 244.1494.

This compound (**16a**) was alternatively prepared as follows: A mixture of **13a** (18 mg, 0.12 mM) and pivaloyl chloride (17 mg, 0.14 mM) was allowed to stand overnight in the presence of triethylamine (15 mg, 0.14 mM) and 4-DMAP (1.5 mg, 0.012 mM) in THF (4 ml). Extractive work-up and purification by column chromatography gave **16a** (10 mg, 35%).

(*Z*)-7-Benzylthio-5-heptenyl 2,2-Dimethylpropionate **(16b)**: IR (film) cm^{-1}: 1720 (C=O). ^{1}H-NMR δ 1.16 (9H, s, *tert*-Bu), 1.40—1.65 (4H, m, $2\times CH_2$), 1.97 (2H, q, $=CHC\underline{H}_2$), 3.05 (2H, d, J=7.0 Hz, SCH_2), 3.66 (2H, s, $ArCH_2$), 4.0 (2H, t, J=7.0 Hz, OCH_2), 5.46 (2H, m, CH=CH), 7.2—7.4 (5H, m, Ar-H). MS *m/z*: 320 (M^+). HRMS Calcd for $C_{19}H_{28}O_2S$: 320.1809. Found: 320.1810.

(*Z,E*)-7-(3,7-Dimethyl-2,6-octadienyl)thio-5-heptenyl 2,2-Dimethylpropionate **(16c)**: IR (film) cm^{-1}: 1720 (C=O). ^{1}H-NMR δ: 1.18 (9H, s, *tert*-Bu), 1.55—1.67 (13H, $3\times CH_3$ and $2\times CH_2$), 1.98—2.12 (6H, br, $3\times =CHC\underline{H}_2$), 3.10 (4H, d, J=7.5 Hz, CH_2SCH_2), 4.02 (2H, t, J=7.3 Hz, OCH_2), 5.06, 5.24 (each 1H, each m, $2\times =CH$), 5.48 (2H, m, CH=CH). MS *m/z*: 366 (M^+). HRMS Calcd for $C_{22}H_{38}O_2S$: 366.2591. Found: 366.2597.

(*Z*)-7-Propylthio-5-heptenyl 2,2-Dimethylpropionate **(16d)**: IR (film) cm^{-1}: 1725 (C=O). ^{1}H-NMR δ: 0.95 (3H, t, J=8.0 Hz, $CH_2C\underline{H}_3$), 1.17 (9H, s, *tert*-Bu), 1.36—1.66 (6H, m, $3\times CH_2$), 2.02—2.12 (2H, q, J=7.5 Hz, $=CHC\underline{H}_2$), 2.43 (2H, t, J=7.5 Hz, SCH_2), 3.10—3.15 (2H, d, J=7.5 Hz, $SC\underline{H}_2CH=$), 4.03 (2H, t, J=7.2 Hz, OCH_2), 5.46 (2H, m, CH=CH). MS *m/z*: 272 (M^+). HRMS Calcd for $C_{15}H_{28}O_2S$: 272.1809. Found: 272.1814.

(*Z*)-7-(3-Oxocyclopentyl)thio-5-heptenyl 2,2-Dimethylpropionate **(16e)**: IR (film) cm^{-1}: 1720 (C=O). ^{1}H-NMR δ: 1.17 (9H, s, *tert*-Bu), 1.30—2.65 (12H, m, $5\times CH_2$ and $=CHC\underline{H}_2$), 3.21 (2H, d, J=7.0 Hz, SCH_2), 3.40 (1H, quint, J=7.0 Hz, SCH), 4.04 (2H, t, J=7.0 Hz, OCH_2), 5.50 (2H, m, CH=CH). MS *m/z*: 312 (M^+). HRMS Calcd for $C_{17}H_{28}O_3S$: 312.1758. Found: 312.1780.

(*Z*)-7-(3-Oxocyclohexyl)thio-5-heptenyl 2,2-Dimethylpropionate **(16f)**: IR (film) cm^{-1}: 1710 (C=O). ^{1}H-NMR: 1.16 (9H, s, *tert*-Bu), 1.37—2.15 (12H, m, $6\times CH_2$), 2.25—2.39 (2H, m, $=CHC\underline{H}_2$), 3.0 (1H, m, SCH), 3.20 (2H, d, J=7.5 Hz, SCH_2), 4.03 (2H, t, J=7.2 Hz, OCH_2), 5.45 (2H, m, CH=CH). MS *m/z*: 326 (M^+). HRMS Calcd for $C_{18}H_{30}O_3S$: 326.1914. Found: 326.1921.

(*Z*)-7-(2-Oxocyclopentyl)thio-5-heptenyl 2,2-Dimethylpropionate **(16g)**: IR (film) cm^{-1}: 1720 (C=O). ^{1}H-NMR δ: 1.17 (9H, s, *tert*-Bu), 1.35—2.60 (12H, m, $5\times CH_2$ and $-CHC\underline{H}_2$), 3.10 (2H, m, SCH_2), 3.43 (1H, dd, J=14.0, 8.1 Hz, SCH), 4.02 (2H, t, J=7.0 Hz, OCH_2), 5.50 (2H, m, CH=CH). MS *m/z*: 312 (M^+). HRMS Calcd for $C_{17}H_{28}O_3S$: 312.1758. Found: 312.1782.

Acknowledgements This work was supported in part by a Grant-in-Aid for the Encouragement of Young Scientists, Japan. The authors thank Dr. H. Ohishi at Osaka University of Pharmaceutical Sciences Computational Center for helpful suggestions and discussions, and Miss M. Danjo for measurements of mass spectra.

References and Notes

1) Part, III: S. Harusawa, H. Osaki, R. Yoneda, T. Kurihara, and H. Ohishi, *Tetrahedron Lett.*, **32**, 1203 (1991).
2) *a*) F. G. Ziegler, *Chem. Rev.*, **88**, 1423 (1988); *b*) S. Blechert, *Synthesis*, **1989**, 71.
3) G. Desimoni, G. Tacconi, A. Barco, and G. P. Pollini, "Natural Products Synthesis through Pericyclic Reactions," ACS Monograph 180, American Chemical Society, Washington D. C., 1983, p. 274.
4) *a*) K. Nonoshita, H. Banno, K. Maruoka, and H. Yamamoto, *J. Am. Chem. Soc.*, **112**, 316 (1990); *b*) S. Harusawa, H. Osaki, H. Fujii, R. Yoneda, and T. Kurihara, *Tetrahedron Lett.*, **31**, 5471 (1990).
5) *a*) D. L. Garmaise, A. Uchiyama, and A. F. McKay, *J. Org. Chem.*, **27**, 4509 (1962); *b*) D. J. Faulkner and M. R. Petersen, *J. Am. Chem. Soc.*, **95**, 553 (1973).
6) S. Harusawa, T. Kurokawa, H. Fujii, R. Yoneda, and T. Kurihara, *Chem. Pharm. Bull.*, **37**, 2567 (1989).
7) *a*) For a general review: E. Block, "Reactions of Organosulfur Compounds," Academic Press, New York, 1978; *b*) J. F. Biellman and J. B. Ducep, "Organic Reactions," Vol. 27, ed. by W. G. Dauben, John Wiley & Sons, Inc., New York, 1982, Chapter 1.
8) *a*) M. Petrzilka, *Helv. Chim. Acta*, **61**, 3075 (1978); *b*) R. W. Carling and A. B. Holmes, *J. Chem. Soc., Chem. Commun.*, **1986**, 325.
9) *a*) Y. Tamaru, S. Kawamura, and Z. Yoshida, *Tetrahedron Lett.*, **26**, 2885 (1985); *b*) N. Cohen, B. L. Banner, J. F. Blount, G. Weber, M. Tsai, and G. Saucy, *J. Org. Chem.*, **39**, 1824 (1974); *c*) A. Carpita and R. Rossi, *Synthesis*, **1982**, 469.
10) *a*) R. S. Glass, ed., "Conformational Analysis of Medium Sized Heterocycles," VCH Publishers, Inc., 1988; *b*) V. Burkert, and N. L. Allinger, "Molecular Mechanics," ACS Monograph 177, American Chemical Society, Washington D. C., 1982.
11) S. Kim and K. Y. Yi, *J. Org. Chem.*, **51**, 2613 (1986).
12) All calculations were performed by using the QCPE 455 MOPAC program within the TEO/CHEMICAL system on a Nippon Data General work station (AV300C).
13) *a*) M. J. S. Dewar and W. Thiel, *J. Am. Chem. Soc.*, **99**, 4899 (1977); *b*) *Idem, ibid.*, **99**, 4907 (1977).
14) MOPAC is a general-purpose semi-empirical molecular orbital package for the study of chemical reactions, and was developed by J. J. P. Stewart and F. J. Seiler (Research Laboratory, U. S. Air Force Academy, Colorado Springs, CO, 80840).
15) K. Takeda, K. Tsuboyama, K. Torii, M. Murata, and H. Ogura, *Tetrahedron Lett.*, **29**, 4105 (1988) and references cited therein.
16) *a*) T. Hayashi, N. Fujitaka, T. Ohishi, and T. Takeshima, *Tetrahedron Lett.*, **21**, 303 (1980); *b*) F. Kido, S. C. Sinha, T. Abiko, and A. Yoshikoshi, *ibid.*, **30**, 1575 (1989); *c*) C. German, A. Alexakis, and J. F. Normant, *Synthesis*, **1984**, 43.
17) These are available from Aldrich Chemical Company.

New Carbazole Alkaloids from *Murraya euchrestifolia*

Chihiro ITO,[a] Mayumi NAKAGAWA,[a] Tian-Shung WU,[b] and Hiroshi FURUKAWA*,[a]

Faculty of Pharmacy, Meijo University,[a] Tempaku-ku, Nagoya 468, Japan and Department of Chemistry, National Cheng Kung University,[b] Tainan, Taiwan, R.O.C. *Received November 26, 1990*

Seven new carbazole alkaloids, named pyrayafolines-B (1), -C (3), and -D (5), and euchrestines-A (7), -B (9), -C (10), and -D (11) were isolated from stem bark of *Murraya euchrestifolia* HAYATA (Rutaceae) collected in Taiwan and their structures were characterized by means of spectral methods. Pyrayafoline-B (1) was also synthesized.

Keywords carbazole alkaloid; *Murraya*; *Murraya euchrestifolia*; Rutaceae; pyrayafoline; euchrestine; NOE

We have isolated many kinds of new carbazole and carbazolequinone alkaloids from *Murraya euchrestifolia* HAYATA (Rutaceae).[1] This paper deals with the isolation and structural elucidation of another seven new monomeric carbazole alkaloids from the stem bark of the same *Murraya* plant collected in Taiwan in May.

The acetone extract of the stem bark of the plant was subjected successively to silica gel column and preparative thin layer chromatographies (TLC) to give seven new carbazoles named pyrayafolines-B (**1**), -C (**3**), and -D (**5**), each having an alkylated pyran ring in the molecule, and euchrestines-A (**7**), -B (**9**), -C (**10**), and -D (**11**) bearing a terpenoid side chain on the carbazole nucleus.

Results and Discussion

Structure of Pyrayafolines Pyrayafoline-B (**1**) was obtained as a brown powder and found to have the molecular formula $C_{18}H_{17}NO_2$ by high resolution mass (HR-MS) spectrometry. The proton nuclear magnetic resonance (^{1}H-NMR) spectrum showed a singlet (3H) at δ2.37 due to an aryl methyl, a singlet (6H) at δ1.46 assignable to geminal dimethyls attached to an oxygenated carbon, and AB-type doublets at δ6.48 and 5.58 (each J=9.6 Hz), indicating the presence of a dimethylpyran ring system in the molecule. In the aromatic proton region of the ^{1}H-NMR spectrum, four 1H singlets at δ6.74, 7.62, 7.49, and 6.71 appeared. Among them, the lower field two singlets at δ7.62 and 7.49 were assignable to H-4 and H-5, respectively, which were deshielded by the aromatic ring on the carbazole nucleus.[2] Treatment of this alkaloid with diazomethane in ether–methanol gave a monomethyl ether (**2**), suggesting the presence of a phenolic hydroxy group in the original molecule. In a differential nuclear Overhauser effect (NOE) experiment on the methyl ether (**2**), irradiation of the aryl methyl signal at δ2.34 gave an 8% enhancement of the deshielded H-4 signal at δ7.64. Irradiation of the methoxy signal at δ3.88 caused a 15% increase of the signal at δ6.79 (H-1). On the basis of these

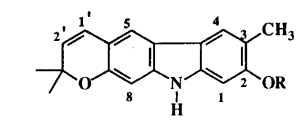

	R
1	H
2	CH_3

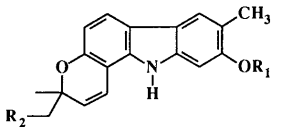

	R_1	R_2
3	H	H
4	CH_3	H
5	H	prenyl
6	CH_3	prenyl

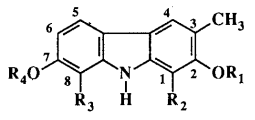

	R_1	R_2	R_3	R_4
7	H	H	prenyl	H
8	H	H	prenyl	CH_3
9	H	H	geranyl	CH_3
10	H	H	geranyl	H
11	H	geranyl	H	H
12	CH_3	geranyl	H	CH_3

prenyl = $-CH_2-CH=C(CH_3)_2$ geranyl = $-CH_2-\underset{\displaystyle CH_3}{\overset{\displaystyle H}{C}}=\underset{\displaystyle CH_3}{C}-CH_2CH_2-CH=C(CH_3)_2$

Chart 1

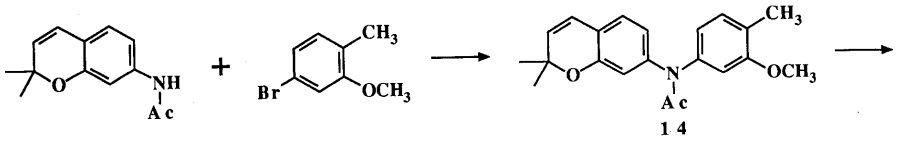

13 14

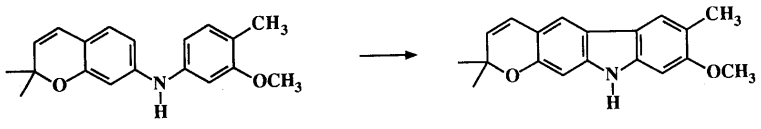

15

Chart 2

TABLE I. ^{1}H-NMR Data for Pyrayafolines

	1	2	3	5	6
H-1	6.74 (s)	6.79 (s)	6.82 (s)	6.83 (s)	6.86 (s)
3-CH_3	2.37 (3H, s)	2.34 (3H, s)	2.38 (3H, s)	2.38 (3H, s)	2.34 (3H, s)
H-4	7.62 (s)	7.64 (s)	7.64 (s)	7.64 (s)	7.64 (s)
H-5	7.49 (s)	7.50 (s)	7.63 (d, 8.4)	7.63 (d, 8.4)	7.64 (d, 8.4)
H-6	—	—	6.69 (d, 8.4)	6.68 (d, 8.4)	6.69 (d, 8.4)
H-8	6.71 (s)	6.78 (s)	—	—	—
OH	4.94 (br s)	—	—	4.74 (br s)	—
OCH_3	—	3.88 (3H, s)	—	—	3.90 (3H, s)
NH	7.70 (s)	7.76 (s)	7.78 (s)	7.75 (s)	7.79 (s)
H-1′	6.48 (d, 9.6)	6.49 (d, 9.6)	6.59 (d, 9.8)	6.62 (d, 10.1)	6.63 (d, 10.1)
H-2′	5.58 (d, 9.6)	5.57 (d, 9.6)	5.69 (d, 9.8)	5.66 (d, 10.1)	5.66 (d, 10.1)
H-5′	—	—	—	1.75 (2H, m)	1.75 (2H, m)
H-6′	—	—	—	2.15 (2H, m)	2.15 (2H, m)
H-7′	—	—	—	5.10 (t, 7.1)	5.10 (t, 7.1)
CH_3	1.46 (6H, s)	1.46 (6H, s)	1.47 (6H, s)	1.44 (3H, s)	1.44 (3H, s)
				1.57 (3H, s)	1.57 (3H, s)
				1.65 (3H, s)	1.65 (3H, s)

Values are in δ (ppm). Each signal corresponds to 1H, unless otherwise stated. Figures in parentheses are coupling constants (J) in Hz. s, singlet; d, doublet; t, triplet; m, multiplet; br, broad.

TABLE II. ^{1}H-NMR Data for Euchrestines

	7	8	9	10	11	12
H-1	6.83 (s)	6.82 (s)	6.80 (s)	6.81 (s)	—	—
3-CH_3	2.38 (3H, s)	2.38 (3H, s)	2.38 (3H, s)	2.38 (3H, s)	2.38 (3H, s)	2.44 (3H, s)
H-4	7.65 (s)	7.67 (s)	7.67 (s)	7.65 (s)	7.56 (s)	7.62 (s)
H-5	7.63 (d, 8.4)	7.70 (d, 8.0)	7.70 (d, 8.4)	7.63 (d, 8.4)	7.74 (d, 8.4)	7.82 (d, 8.4)
H-6	6.69 (d, 8.4)	6.82 (d, 8.0)	6.83 (d, 8.4)	6.70 (d, 8.4)	6.68 (dd, 8.4, 2.4)	6.80 (dd, 8.4, 2.4)
H-8	—	—	—	—	6.82 (d, 2.4)	6.87 (d, 2.2)
OH		4.74 (s)	4.75 (s)	—	5.12 (s)	—
OCH_3	—	3.90 (3H, s)	3.90 (3H, s)	—	—	3.88 (3H, s)
						3.78 (3H, s)
NH	7.72 (s)	7.70 (s)	7.73 (s)	7.73 (s)	7.73 (s)	7.82 (s)
H-1′	3.59 (2H, d, 6.7)	3.60 (2H, d, 7.0)	3.62 (2H, d, 6.7)	3.59 (2H, d, 7.1)	3.59 (2H, d, 6.7)	3.68 (2H, d, 7.0)
H-2′	5.36 (t, 6.7)	5.30 (t, 7.0)	5.32 (t, 6.7)	5.37 (t, 6.7)	5.36 (t, 6.7)	5.34 (t, 7.0)
H-5′, H-6′	—	—	2.06 (4H, m)	2.12 (4H, m)	2.11 (4H, m)	2.09 (4H, m)
H-7′	—	—	5.07 (m)	5.07 (m)	5.07 (m)	5.07 (m)
CH_3	1.89 (3H, s)	1.88 (3H, s)	1.87 (3H, s)	1.88 (3H, s)	1.89 (3H, s)	1.91 (3H, s)
	1.78 (3H, s)	1.74 (3H, s)	1.62 (3H, s)	1.65 (3H, s)	1.66 (3H, s)	1.62 (3H, s)
			1.57 (3H, s)	1.58 (3H, s)	1.59 (3H, s)	1.58 (3H, s)

Values are in δ (ppm). Each signal corresponds to 1H, unless otherwise stated. Figures in parentheses are coupling constants (J) in Hz. s, singlet; d, doublet; dd, double doublet; t, triplet; m, multiplet.

spectral data coupled with the ultraviolet (UV) spectrum (see Experimental), the structure of pyrayafoline-B was proposed to be represented by the formula **1**.

For confirmation of the structure of pyrayafoline-B (**1**), we tried to synthesize this alkaloid. According to our previous paper,[3] the reaction between 7-acetylaminochromene (**13**)[4] and 4-bromo-2-methoxytoluene was carried out in the presence of anhydrous potassium carbonate and copper in pyridine at reflux temperature for 43 h to give **14**. After hydrolysis of the *N*-acetyl group of **14** with KOH in ethanol, treatment of the amine (**15**) with $Pd(OAc)_2$ in dimethylformamide (DMF) for 2 h afforded a cyclization product having a carbazole nucleus. In the ^{1}H-NMR spectrum of this product, observation of two lower field 1H singlets at δ 7.64 and 7.50 assignable to deshielded H-4 and H-5 on the carbazole nucleus, respectively, indicated that cyclization had occurred in the linear direction, as shown by formula **2**. No other conceivable cyclization product could be detected. This synthetic compound **2** was found to be identical with the *O*-methyl ether derived from a natural specimen of pyrayafoline-B by spectrometric comparisons. From these results, the structure of pyrayafoline-B was confirmed to be as shown by formula **1**.

Pyrayafoline-C (**3**) was obtained as a pale yellow oil and found to have the same molecular formula $C_{18}H_{17}NO_2$ as that of pyrayafoline-B (**1**). The ^{1}H-NMR spectrum showed the presence of an aryl methyl, two geminal methyls attached to an oxygenated carbon, a disubstituted double bond, and four aromatic protons as *ortho*-located AB-type doublets and two 1H singlets (Table I). Treatment of this alkaloid with diazomethane gave a monomethyl ether, which was found to be identical with the synthetic specimen of **4** previously reported by us.[3] On the basis of these data, the structure of pyrayafoline-C was proposed to be as shown in formula **3** corresponding to the *O*-desmethyl analogue of pyrayafoline-A (**4**).[5]

Pyrayafoline-D (**5**) was isolated as a pale brown powder, $[\alpha]_D \pm 0°$ (MeOH). The molecular formula was determined as $C_{23}H_{25}NO_2$ by HR-MS. The ^{1}H-NMR spectrum differs from that of pyrayafoline-C (**3**) only in the presence of

signals [δ 1.75 (2H, m), 2.15 (2H, m), 5.10 (1H, t), 1.57 (3H, s), and 1.65 (3H, s)] assignable to the side chain [$-CH_2CH_2CH=C(CH_3)_2$] instead of the signal due to one of the methyls attached to the oxygenated carbon in the spectrum of **3**. The presence of this side chain in the molecule was also indicated by the observation of the characteristic mass fragment base peak at *m/z* 264 [M^+-83] in the MS. Treatment of this alkaloid with diazomethane afforded a monomethyl ether (**6**) as a colorless oil. The MS of the monomethyl ether (**6**) also showed the base fragment at *m/z* 278 corresponding to the loss of [$-CH_2CH_2CH=C(CH_3)_2$] from the molecular ion (*m/z* 361). In the NOE experiments on **6**, irradiation of the aryl methyl signal at δ 2.34 gave an 8% enhancement of the singlet signal at δ 7.64 (H-4). In irradiation of the methoxy signal at δ 3.90, a 15% increase of the singlet signal at δ 6.86 (H-1) was observed. On the basis of the results stated above, we assigned the structure **5** to pyrayafoline-D.

Structure of Euchrestines Euchrestines-A (**7**), -B (**9**), -C (**10**), and -D (**11**) were found to show the following common spectrometric features. 1) These alkaloids revealed analogous UV absorptions having high- and medium-intensity bands at λ_{max} 236—238 and 264—266 nm, respectively, along with twin low-intensity bands at λ_{max} 306—313 and 318—321 nm. These features are characteristic of the 2,7-dioxygenated carbazole chromophore.[6] 2) In the ^{1}H-NMR spectra, each euchrestine showed aromatic proton signals corresponding to four protons. Among them, as common features, lower-field proton signals appearing as a 1H singlet at δ 7.56—7.67 due to H-4, and an *ortho*-coupled 1H doublet at δ 7.63—7.74 (J=8.4 Hz) assignable to H-5, each proton deshielded by the aromatic ring, suggested the absence of substituents at C-4, C-5, and C-6 in the carbazole skeleton. 3) Appearance of a 3H singlet at δ 2.38 in each ^{1}H-NMR spectrum revealed the presence of an aryl methyl group, which was considered likely on biogenetic ground to be located at C-3 on the carbazole nucleus.[2] These results indicated the structure of euchrestines to be 2,7-oxygenated-3-methylcarbazole having a substituent at C-1 or C-8.

Euchrestine-A (**7**) was isolated as a colorless oil and its molecular formula was determined to be $C_{18}H_{19}NO_2$ by HR-MS. Observations of signals at δ 1.89 (3H, s), 1.78 (3H, s), 5.36 (1H, t, J=6.7 Hz), and 3.59 (2H, d, J=6.7 Hz), and a *para*-situated aromatic proton singlet at δ 6.83 besides the common ^{1}H-NMR signals described above indicated the presence of a prenyl group at C-8 of the carbazole nucleus. These spectral data together with the similarity of the ^{1}H-NMR spectrum (Table II) to that of isomurrayafoline-B (**8**) previously reported by us,[6] led us to assign structure **7** to euchrestine-A.

Euchrestine-B (**9**) was obtained as a pale yellow oil. The HR-MS analysis indicated the molecular formula to be $C_{24}H_{29}NO_2$. The presence of a geranyl moiety in the molecule was revealed by observations of proton signals at δ 3.62 (2H, d, J=6.7 Hz), 5.32 (1H, t, J=6.7 Hz), 2.06 (4H, m), 5.07 (1H, m), 1.87 (3H, s), 1.62 (3H, s), and 1.57 (3H, s), the NOE between the methyl group attached to the double bond (δ 1.87) and the benzylic methylene protons (δ 3.62), and a characteristic mass fragment at *m/z* 240 produced by cleavage at the benzylic position. Further, the ^{1}H-NMR spectrum showed a methoxy proton singlet at δ 3.90 and an additional aromatic proton signal at δ 6.80 as a singlet, indicating the location of the geranyl side chain at C-8. In the differential NOE experiment, irradiation of the methoxy signal at δ 3.90 gave a 9% increase of the doublet signal at δ 6.83 due to H-6 suggesting the location of the methoxy group at C-7. On the basis of these results, we proposed the structure **9** for euchrestine-B.

Euchrestine-C (**10**) was obtained as a colorless powder and the molecular formula was determined to be $C_{23}H_{27}NO_2$, different by CH_2 from that of euchrestine-B (**9**), by HR-MS. The presence of a geranyl moiety at C-8, the same as that of euchrestine-B (**9**), was indicated by the ^{1}H-NMR signals (Table II), a mass fragment at *m/z* 266 (M^+-83), and a singlet proton signal at δ 6.81 (H-1). No signal due to an *O*-methyl group was observed. On the basis of these results, euchrestine-C was assigned structure **10**.

Euchrestine-D (**11**) was isolated as a pale yellow oil. The molecular formula, $C_{23}H_{27}NO_2$, was found to be the same as that of euchrestine-C (**10**). The ^{1}H-NMR spectra and MS (Table II and Experimental) of euchrestine-D (**11**) and its *O*,*O*-dimethyl ether (**12**) also showed the presence of a geranyl moiety in the molecule. The appearance of ABC-type signals at δ 7.74 (1H, d, J=8.4 Hz), 6.68 (1H, dd, J=8.4, 2.4 Hz), and 6.82 (1H, d, J=2.4 Hz) assignable to H-5, H-6, and H-8, respectively, in the ^{1}H-NMR spectrum indicated the location of the geranyl moiety at C-1. Treatment of euchrestine-D (**11**) with diazomethane gave the *O*,*O*-dimethyl ether (**12**). In differential NOE experiments on the *O*,*O*-dimethyl ether (**12**), irradiation of the methoxy signal at δ 3.88 gave 2 and 7% increases of the signals at δ 6.80 (H-6) and 6.87 (H-8). On irradiation of another methoxy signal at δ 3.78, a 6% enhancement of the aryl methyl signal at δ 2.44 was seen. Irradiation of the aryl methyl signal at δ 2.44 caused 5 and 6% increases of the signals at δ 3.78 (O–CH_3) and 7.62 (H-4), respectively. Consequently, the structure of euchrestine-D was proposed to be as shown in formula **11**.

Experimental

^{1}H-NMR spectra were recorded on a GX-270 (JEOL) or GX-400 (JEOL) spectrometer in $CDCl_3$. Chemical shifts are shown in δ values (ppm) with tetramethylsilane (TMS) as an internal reference. EI- and HR-MS spectra were taken with an M-80 (Hitachi) spectrometer having a direct inlet system. Infrared (IR) spectra were recorded on a JASCO IR-810 IR spectrophotometer in $CHCl_3$, ultraviolet (UV) spectra on a JASCO UVIDEC-610C double beam spectrophotometer in MeOH, and optical rotation on a DIP-181 polarimeter (JASCO) in $CHCl_3$ at 20 °C. Preparative TLC was carried out with appropriate combinations of $CHCl_3$, hexane, isopropyl ether, benzene, and acetone.

Pyrayafoline-B (1) Brown powder. HR-MS Calcd for $C_{18}H_{17}NO_2$: 279.1258. Found: 279.1266. UV λ_{max} nm: 228, 252, 285, 296 (sh), 329, 353. IR ν_{max} cm^{-1}: 3600, 3470, 3380 (br). ^{1}H-NMR (Table I). EI-MS *m/z* (%): 279 (M^+, 34), 265 (20), 264 (100).

Pyrayafoline-C (3) Pale yellow oil. HR-MS Calcd for $C_{18}H_{17}NO_2$: 279.1258. Found: 279.1258. UV λ_{max} nm: 222, 238, 286 (sh), 296, 323, 351. IR ν_{max} cm^{-1}: 3600, 3470, 3380 (br). ^{1}H-NMR (Table I). EI-MS *m/z* (%): 279 (M^+, 36), 265 (21), 264 (100).

Pyrayafoline-D (5) Pale brown powder, $[\alpha]_D$ 0° (c=0.0013, MeOH). HR-MS Calcd for $C_{23}H_{25}NO_2$: 347.1883. Found: 347.1861. UV λ_{max} nm: 222, 238, 288 (sh), 296, 331, 342. IR ν_{max} cm^{-1}: 3600, 3480, 3380 (br). ^{1}H-NMR (Table I). EI-MS *m/z* (%): 347 (M^+, 22), 265 (19), 264 (100), 263 (12), 234 (6).

Euchrestine-A (7) Colorless oil. HR-MS Calcd for $C_{18}H_{19}NO_2$: 281.1414. Found: 281.1414. UV λ_{max} nm: 213, 236, 265, 295, 313, 318, 329. IR ν_{max} cm^{-1}: 3600, 3470, 3400 (br). ^{1}H-NMR (Table II). EI-MS *m/z* (%): 281 (M^+, 82), 266 (11), 264 (12), 227 (12), 226 (75), 225 (100), 224 (12).

Euchrestine-B (9) Pale yellow oil. HR-MS Calcd for $C_{24}H_{29}NO_2$: 363.2196. Found: 363.2173. UV λ_{max} nm: 212, 238, 264, 310, 318, 331. IR ν_{max} cm^{-1}: 3600, 3470, 3380 (br). ^{1}H-NMR (Table II). EI-MS *m/z* (%): 363 (M^+, 100), 294 (16), 280 (24), 264 (22), 263 (16), 240 (35), 227 (13), 210 (12). Differential NOE: irradiation of 7-OCH_3 (δ 3.90)-9% NOE at H-6 (δ 6.83, 1H, d); irradiation of H-1′ (δ 3.62, 2H, d)-8% NOE at CH_3 (δ 1.87).

Euchrestine-C (10) Colorless powder. HR-MS Calcd for $C_{23}H_{27}NO_2$: 349.2041. Found: 349.2058. UV λ_{max}nm: 212, 237, 266, 306, 320, 329. IR ν_{max} cm^{-1}: 3600, 3470, 3380 (br). ^{1}H-NMR (Table II). EI-MS *m/z* (%): 349 (M^+, 82), 280 (11), 266 (16), 264 (23), 227 (18), 226 (100), 225 (84), 213 (10).

Euchrestine-D (11) Pale yellow oil. HR-MS Calcd for $C_{23}H_{27}NO_2$: 349.2039. Found: 349.2011. UV λ_{max} nm: 212, 238, 265, 312, 321 (sh). IR ν_{max} cm^{-1}: 3600, 3470, 3380 (br). ^{1}H-NMR (Table II). EI-MS *m/z* (%): 349 (M^+, 61), 264 (25), 227 (17), 226 (80), 225 (100), 224 (10), 196 (17).

***O*-Methylation of 1, 3, 5, and 11 with Diazomethane** A large excess of ethereal diazomethane was added to a methanolic solution (20 ml) of **1**, **3**, **5**, or **11** (1—2 mg), and the mixture was left for 2 d at room temperature. The solvent was evaporated off, and the residue was purified by preparative TLC to give almost quantitatively **2**, **4**, **6**, or **12**, respectively. **2**: UV λ_{max} nm: 222, 247, 254, 284, 293, 328, 352. IR ν_{max} cm^{-1}: 3470, 3380 (br). ^{1}H-NMR (Table I). EI-MS *m/z* (%): 293 (M^+, 47), 279 (24), 278 (100), 263 (16). Differential NOE: irradiation of the aryl-CH_3 (δ 2.34)-8% NOE at H-4 (δ 7.64); irradiation of 2-OCH_3 (δ 3.88)-15% NOE at H-1 (δ 6.79). **4**: This product was found to be identical with synthetic pyrayafoline-A (**4**)[3,5] by ^{1}H-NMR and IR comparisons, and co-TLC. **6**: Colorless oil. UV λ_{max} nm: 221, 239, 286 (sh), 295, 333, 338. IR ν_{max} cm^{-1}: 3470, 3380 (br). ^{1}H-NMR (Table I). EI-MS *m/z* (%): 361 (M^+, 35), 279 (20), 278 (100). Differential NOE: irradiation of the aryl-CH_3 (δ 2.34)-8% NOE at H-4 (δ 7.64, 1H, s): irradiation of 2-OCH_3 (δ 3.90)-15% NOE at H-1 (δ 6.86, 1H, s). **12**: UV λ_{max} nm: 212, 238, 262, 305, 315 (sh). ^{1}H-NMR (Table II). EI-MS *m/z* (%): 377 (M^+, 24), 254 (8), 149 (10), 135 (49).

Preparation of *O*-Methylpyrayafoline-B (2) A mixture of 4-bromo-2-methoxytoluene (1.44 g), 7-acetylaminochromene (**13**)[4] (1.0 g), anhydrous K_2CO_3 (650 mg), and Cu (300 mg) in pyridine (2 ml) was refluxed for 43 h. The reaction mixture was diluted with $CHCl_3$, and washed with diluted HCl, and then with H_2O. The $CHCl_3$ solution was dried with anhydrous $MgSO_4$ and evaporated to dryness. The residue was subjected to silica gel chromatography with AcOEt–hexane (1 : 4) to afford **14** (610 mg) as an oil in 39% yield. **14**: HR-MS Calcd for $C_{21}H_{23}NO_3$: 337.1668. Found: 337.1678. IR ν_{max} cm^{-1}: 1660, 1610, 1500. ^{1}H-NMR δ: 7.09 (1H, br d, J=7.4 Hz), 6.94 (1H, d, J=7.4 Hz), 6.70—6.82 (3H, m), 6.65 (1H, s), 6.28 (1H, d, J=9.7 Hz), 5.58 (1H, d, J=9.7 Hz), 3.79 (3H, s), 2.19 (3H, s), 2.07 (3H, s), 1.41 (6H, s). EI-MS *m/z*: 337 (M^+), 323, 322, 280, 162, 161.

After treatment of **14** (380 mg) with 20% KOH–EtOH (20 ml) at reflux temperature for 1.5 h, the solvent was evaporated off and the residue was diluted with H_2O, then extracted with $CHCl_3$. The $CHCl_3$ extract was washed with H_2O and dried with anhydrous $MgSO_4$, and then the solvent was evaporated off to give **15** as an oil in 99% yield. **15**: HR-MS Calcd for $C_{19}H_{21}NO_2$: 295.1571. Found: 295.1561. IR ν_{max} cm^{-1}: 3430, 1610, 1570, 1510. ^{1}H-NMR δ: 7.02 (1H, br), 7.02 (1H, d, J=7.4 Hz), 6.83 (1H, d, J=7.4 Hz), 6.62 (1H, d, J=7.4 Hz), 6.60 (1H, s), 6.48 (1H, d, J=7.4 Hz), 6.46 (1H, s), 6.26 (1H, d, J=9.7 Hz), 5.44 (1H, d, J=9.7 Hz), 3.78 (3H, s), 2.16 (3H, s), 1.41 (6H, s). EI-MS *m/z*: 295, 281, 280 (100%), 265, 236, 144, 140. A solution of **15** (25 mg) in DMF (20 ml) was refluxed in the presence of $Pd(OAc)_2$ (20 mg) under argon gas for 2 h. The solvent was evaporated off and the residue was diluted with H_2O, and then extracted with AcOEt. The AcOEt extract was dried with anhydrous $MgSO_4$ and the solvent was evaporated off. The residue was subjected to preparative silica gel TLC to give **2** (2 mg, 9% yield) as a pale yellow oil, which was found to be identical with a natural specimen of *O*-methylpyrayafoline-B by NMR and IR comparisons, and co-TLC.

References and Notes

1) T.-S. Wu, T. Ohta, and H. Furukawa, *Heterocycles*, **20**, 1267 (1983); A. T. McPhail, T.-S. Wu, T. Ohta, and H. Furukawa, *Tetrahedron Lett.*, **24**, 5377 (1983); H. Furukawa, T.-S. Wu, and T. Ohta, *Chem. Pharm. Bull.*, **31**, 4202 (1983); H. Furukawa, M. Yogo, C. Ito, T.-S. Wu, and C.-S. Kuoh, *ibid.*, **33**, 1320 (1985); H. Furukawa, T.-S. Wu, and C.-S. Kuoh, *Heterocycles*, **23**, 1391 (1985); *idem*, *Chem. Pharm. Bull.*, **33**, 2611 (1985); H. Furukawa, T.-S. Wu, T. Ohta, and C.-S. Kuoh, *ibid.*, **33**, 4132 (1985); H. Furukawa, C. Ito, M. Yogo, and T.-S. Wu, *ibid.*, **34**, 2672 (1986); C. Ito, T.-S. Wu, and H. Furukawa, *ibid.*, **35**, 450 (1987); *idem*, *ibid.*, **36**, 2377 (1988); *idem*, *ibid.*, **38**, 1143 (1990); C. Ito and H. Furukawa, *ibid.*, **38**, 1548 (1990).

2) D. P. Chakraborty, *Fortschr. Chem. Org. Naturst.*, **34**, 299 (1977).

3) H. Furukawa, C. Ito, M. Yogo, and T.-S. Wu, *Chem. Pharm. Bull.*, **34**, 2672 (1986).

4) J. M. Evans, C. S. Fake, T. C. Hamilton, R. H. Poyser, and G. A. Showell, *J. Med. Chem.*, **27**, 1127 (1984).

5) Pyrayafoline (**4**) reported previously[3] will be renamed pyrayafoline-A (**4**).

6) C. Ito, T.-S. Wu, and H. Furukawa, *Chem. Pharm. Bull.*, **35**, 450 (1987) and our unpublished data.

The Pictet–Spengler Reaction of N_b-Hydroxytryptamines and Cysteinals. II. Temperature Effects, Stereochemistry and Mechanism

Jinjun LIU,[a] Masako NAKAGAWA,*[,b] Koreharu OGATA,[c] and Tohru HINO*[,b]

School of Pharmacy, Shanghai Medical University,[a] Yixue Yuan Road, 138, Shanghai, 200032, China and Faculty of Pharmaceutical Sciences,[b] and Chemical Analysis Center,[c] Chiba University, Yayoi-cho, Chiba-shi 260, Japan. *Received December 4, 1990*

The effect of temperature on the Pictet–Spengler reaction of N_b-hydroxytryptamines (1) and cysteinals (2) has been examined. The optically active nitrones (3), obtained from 1 and 2, gave the corresponding N_b-hydroxy-β-carbolines (4α and 4β) exclusively at −78 °C in the presence of an excess of trifluoroacetic acid. The mechanism is discussed in relation to the stereochemistry.

Keywords Pictet–Spengler reaction; N_b-hydroxytryptamine; cysteinal; N_b-hydroxy-β-carboline; nitrone; spiroindolenine; mechanism; temperature effect

Recently potent antiviral compounds, eudistomins, have been isolated from Caribbean and New Zealand colonial tunicates. They contain the previously unreported oxathiazepine ring system condensed with tetrahydro-β-carboline[1] (Chart 1).

In connection with our studies on the synthesis of eudistomins, we reported the Pictet–Spengler (P–S) reaction of hydroxytryptamine and aldehydes.[2] In the preceding paper,[2] we described the P–S reaction of N_b-hydroxytryptamines (**1**) and cysteinals (**2**) in the presence of trifluoroacetic acid (TFA) (1 mol eq) at room temperature, which provided a mixture of the corresponding N_b-hydroxytetrahydro-β-carbolines (**4**α and **4**β) together with unexpected tetracyclic compounds (**5**) (Table I, entries 8—14). Although both of the products (**5** and **4**) can be considered as precursors for the synthesis of the natural eudistomins, the tetracyclic compounds (**5**), which can easily be transformed into the corresponding β-carbolines (**4**) by treatment with excess TFA, seem to be more useful intermediates considering the ease of introduction of a substituent into the benzene ring by electrophilic substitution.[2b,3] In order to improve the selectivity for the tetracyclic compounds (**5**), we have investigated the effect of temperature on this P–S reaction.

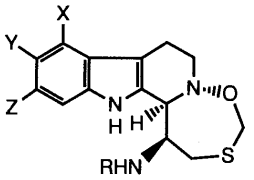

	X	Y	Z	R
eudistomin	H	H	H	H
eudistomin L	H	Br	H	H
eudistomin K	H	H	Br	H
eudistomin C	H	OH	Br	H
eudistomin E	Br	OH	H	H
eudistomin F	H	OH	Br	CO_2Me

Chart 1

Generally, the P–S reaction of tryptamine and an aldehyde has been carried out at room temperature[4] or at an elevated temperature[5] with an acid catalyst. On the other hand, unlike these Schiff's bases, the nitrones formed from N_b-hydroxytryptamine with an aldehyde were shown to have higher reactivity in the P–S reaction, and the reaction proceeded rapidly within 5 min,[6] so it was expected that the P–S reaction of nitrones could be achieved at lower temperature. Actually, the reaction occurred smoothly at −78 °C, although prolonged treatment (1—2 h) with an excess (2 or 5 eq) of TFA was necessary. When the optically active nitrone (**3a**) having no substituent at the indole nitrogen, obtained from N_b-hydroxytryptamine (**1a**) and *N*-methoxycarbonyl-*S*-methyl-L-cysteinal (**2a**), was treated with TFA (2 eq) at −78 °C, the reaction was completed within 1 h, and we unexpectedly obtained only two isomers of the N_b-hydroxytetrahydro-β-carboline (**4a**). None of the tetracyclic compound was detected (Table I, R_1=H, R_2=COOMe, R_3=Me). Furthermore, the ratio of **4a**α/**4a**β increased to 1/41, whereas the ratio of **4a**α/**4a**β obtained at room temperature was 1/7[2a] (Table I, entry 8).

The result at −78 °C was surprising, since the tetracyclic compound (**5a**) was most likely formed by an intramolecular cyclization of the spiroindolenine intermediate, and could be considered as a kinetically controlled product. This fact suggests that the formation of β-carboline (**4a**) at −78 °C may not have occurred *via* a spiroindolenine intermediate.

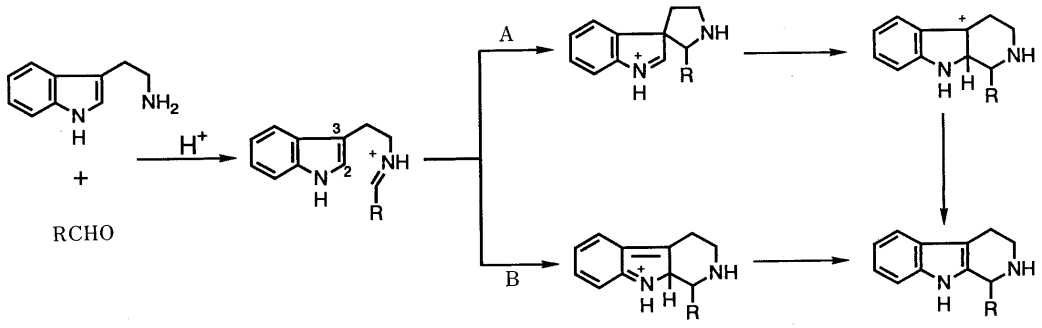

Chart 2

TABLE I. Cyclization of the Nitrones 3

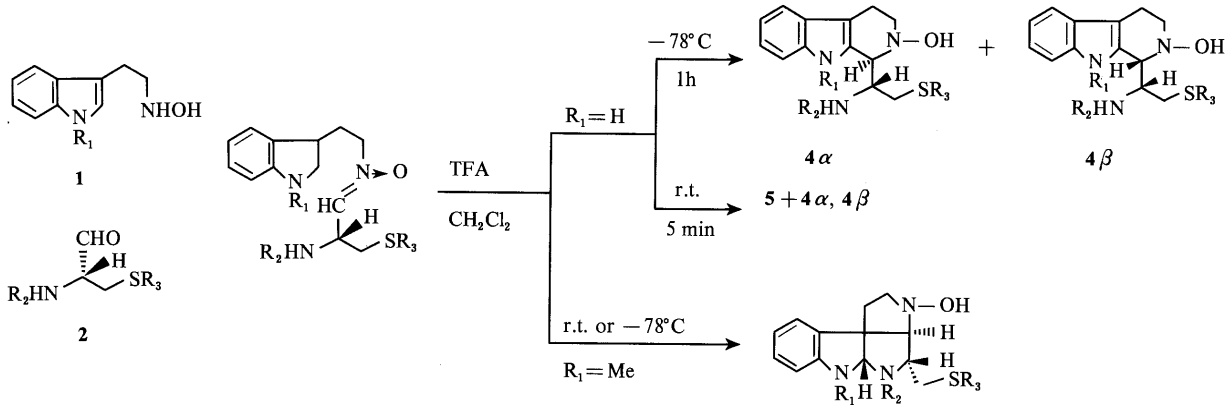

Entry	3	R_1	R_2	R_3	TFA (eq)	Conditions	5	Yield (%)	4	Yield (%)	(α:β)
1	**3a**	H	COOMe	Me	2	−78 °C/1 h			**4a**	97	(1:41)[a]
2	**3b**	H	Boc	Me	2	−78 °C/1 h			**4b**	96	(1:10)[b]
3	**3c**	H	COOMe	Troc	2	−78 °C/1 h			**4c**	100	(1:12)[b]
4	**3d**	H	Boc	Troc	5	−78 °C/2 h			**4d**	94	(1:10)[b]
5	**3e**	H	Cbz	Troc	2	−78 °C/1 h			**4e**	97	(1:12)[b]
6	**3f**	H	Troc	Me	5	−78 °C/2 h			**4f**	96	(1:21)[a]
7	**3g**	H	Troc	Cbz	5	−78 °C/1 h			**4g**	82	(1:8)[b]
8	**3a**	H	COOMe	Me	1	r.t./5 min	**5a**	75	**4a**	24	(1:7)[a]
9	**3b**	H	Boc	Me	1	r.t./5 min	**5b**	70	**4b**	21	(1:5)[b]
10	**3c**	H	COOMe	Troc	1	r.t./5 min	**5c**	35	**4c**	59	(1:6)[b]
11	**3d**	H	Boc	Troc	1	r.t./5 min	**5d**	49	**4d**	48	(1:5)[b]
12	**3e**	H	Cbz	Troc	2	r.t./1 hr	**5e**	28	**4e**	67	(1:4)[b]
13	**3f**	H	Troc	Me	1	r.t./5 min	**5f**	68	**4f**	25	(1:6)[a]
14	**3g**	H	Troc	Cbz	1[c]	r.t./1 h	**5g**	23	**4g**	58	(3:5)[b]
15	**3h**	Me	COOMe	Troc	1	r.t./5 min	**5h**	90			
16	**3i**	Me	COOMe	Me	1	r.t./5 min	**5i**	90			
17	**3h**	Me	COOMe	Troc	5	−78 °C/1 h	**5h**	93			
18	**3i**	Me	COOMe	Me	5	−78 °C/1 h	**5i**	90			

a) Ratio by isolation. *b*) Ratio by ^{1}H-NMR. *c*) TsOH was used instead of TFA. r.t. = room temperature.

Therefore, it was decided to make a detailed study of this observation.

A variety of nitrones (**3**) were employed in this cyclization at −78 °C; the results are shown in Table I together with the results obtained at room temperature.[2a] Excellent yields and high diastereoselectivity of tetrahydro-β-carbolines **4** (entries 1—7) were obtained with various nitrones **3** (R_1 = H) at −78 °C. On the other hand, *N*-methylated nitrones (**3h** and **3i**) gave the corresponding tetracyclic compounds (**5h** and **5i**) regardless of the reaction temperature (entries 15—18) as single isomers in high yields.

Two possible mechanistic pathways (Chart 2) for the P–S reaction of tryptamine and tryptophan derivatives have been proposed,[7] which involve either direct attack at the indole 2-position (path B) or attack at the 3-position of the indole ring to give a spiroindolenine intermediate followed by rearrangement (path A).

There is an increasing volume of data on the mechanisms and, in general, the cyclization is strongly suggested to proceed *via* the spiroindolenine intermediate (path A), whereas the direct attack at the indole 2-position could proceed through the geometrically more favoured 6-*endo*-Trig cyclization (path B).[8] Jackson and coworkers[9] have reported a substantial amount of evidence in support of the spiroindolenine mechanism stemming from an investigation of the electrophilic reactivity at the 3-position of the indole,

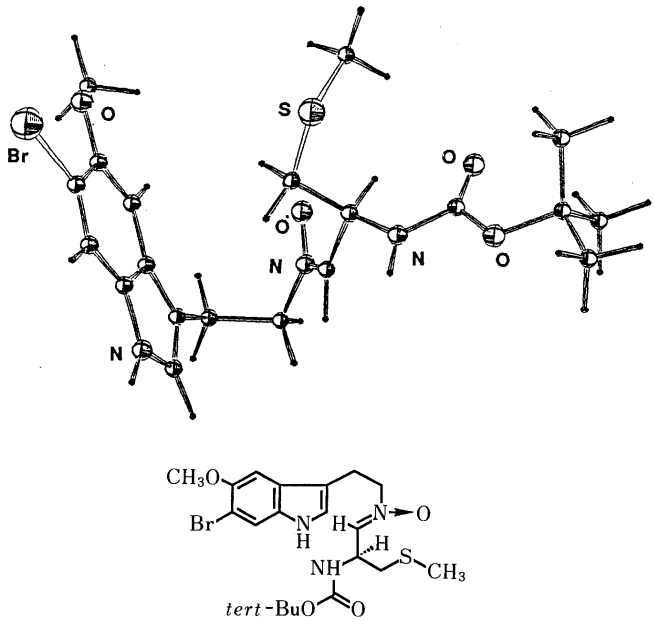

Fig. 1. ORTEP Drawing of (−)-**3k**

while Casnati and coworkers[10] have shown that direct attack at the 2-position (path B) competed with attack at the 3-position under some circumstances.

In our cases, the P–S reaction of N_b-hydroxytryptamine (**1**) and cysteinal (**2**) generates the corresponding nitrones (**3**) as the first intermediates which, unlike the imines from tryptamine derivatives, were isolable in a stable form as a single isomer. The configuration of the nitrones (**3**) has been confirmed as *Z*-form by X-ray analysis of the nitrone (**3k**) (Fig. 1, see also the experimental section).

Our result obtained at room temperature is qualitatively similar to the known mechanism which proceeds through the spiroindolenine intermediate. On the assumption that there is an allylic strain ($A^{1,3}$ strain)[11] in the stage of nitronium ions, the most stable conformation of the nitronium ions would be like **6**. The 3-position of the indole ring attacks on either the top or bottom face of the C=N bond to give the two corresponding spiroindolenine intermediates (**7**); the ratio of these spiroindolenines (**7**α and **7**β) may be governed by the chiral center adjacent to the C=N bond. The spiroindolenine (**7**α) would either rearrange to the minor isomer of β-carboline (**4**α) or be trapped by intramolecular cyclization to give the tetracyclic compound (**5**), competitively, whereas the spiroindolenine (**7**β) would preferentially rearrange to the major isomer of β-carboline (**4**β), or revert to **6** due to the instability of the corresponding tetracyclic compound (**5'**) (three five-membered rings are all *cis*-fused) (Chart 3).

Clearly, the isolation of the tetracyclic compound (**5**) provided strong evidence for the participation of the spiroindolenines in the P–S reaction. The results, however, can not exclude the other possibility that the spiroindolenines only take part in an equilibrium between spiroindolenines (**7**) and imininium ion (**6**) without leading to the corresponding β-carboline (**4**).[12] In fact, the presence of this equilibration was demonstrated by the formation of two β-carbolines, **4**β (major product) and **4**α (minor product) when the tetracyclic compound (**5**) was treated for a long time (24 h) with excess (10 mol eq) of TFA[2a] compared

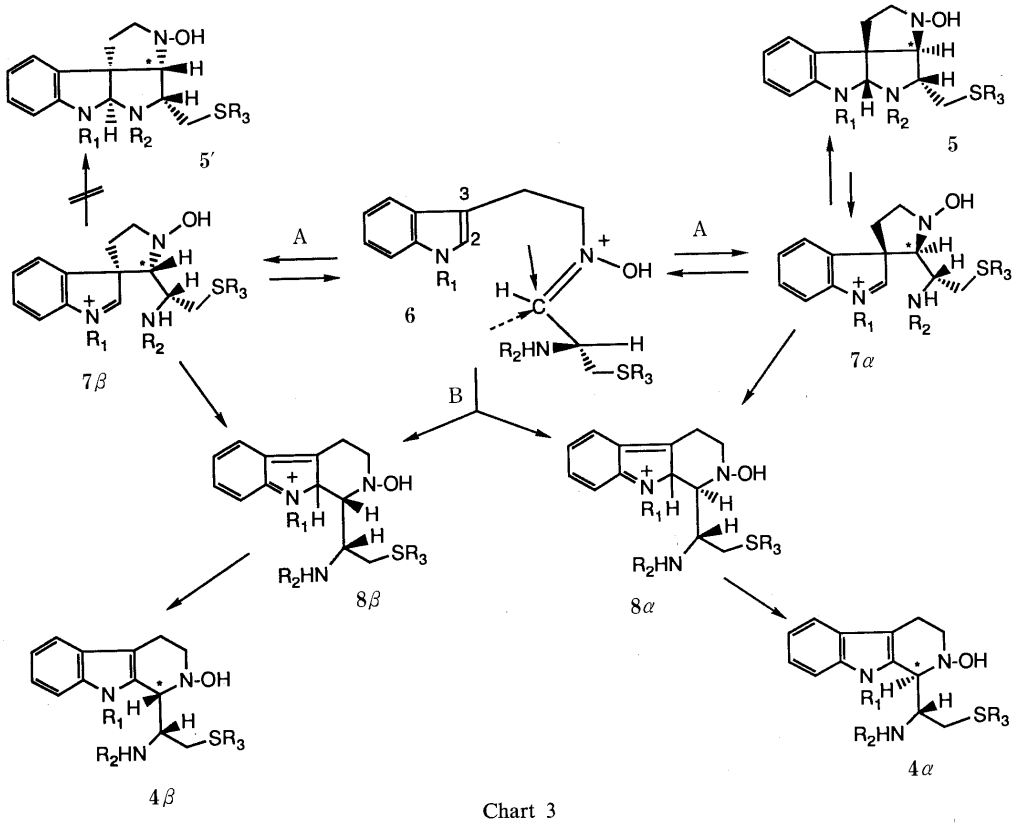

Chart 3

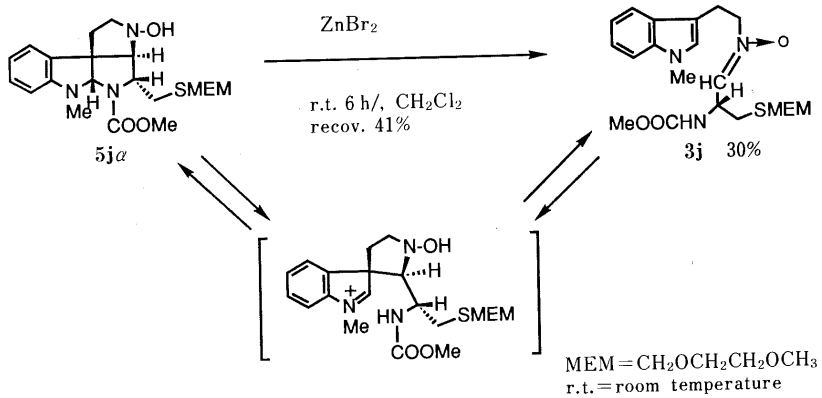

Chart 4

with that used in the direct reactions[1] (Table I, entries 8—14). Recent isotopic labelling experiments reported by Bailey[13] also suggested the presence of this equilibration in the P–S reaction.

Furthermore, more direct evidence for the presence of an equilibrium between **5** and **6** was obtained in our case. Thus, when the N_a-methyltetracyclic compound (**5j**)[2] was treated with $ZnBr_2$ in CH_2Cl_2 at room temperature for 6 h, the corresponding nitrone (**3j**) was obtained in 30% yield with recovery of the starting tetracyclic compound (**5j**) in 41% yield (Chart 4). The nitrone could only have been formed through the corresponding spiroindolenine; consequently, the result again supported the presence of an equilibrium between spiroindolenines (**7**) and nitrones (**3**).

Indeed, if the equilibration had to be considered, the isolation of the tetracyclic compounds (**5**) described herein and some other reported evidence[14,9d] are not necessarily significant support for a spiroindolenine intermediate for tetrahydro-β-carboline formation, and if the spiroindolenines only participate in the equilibration, β-carbolines must be formed *via* path B. Our results obtained from the low temperature experiments (Table I, entries 1—6) favor this possibility. Thus, the iminium ion (**6**) might cyclize to the intermediate (**8**) (Chart 3), *via* direct attack at the 2-position, and **8** in turn might deprotonate to give the corresponding β-carboline (**4**). On the other hand, when N_a-methyl nitrones (**3**) were used, the indolenium cation of the spiroindolenines (**7**) may be stabilized by the methyl group, so that the spiroindolenines (**7**) could be formed even at low temperature and then cyclized to give the tetracyclic compound (**5f**) while the corresponding β-carbolines (**4**) can not be formed, due to unfavorable $A^{1,2}$ strain,[11,15] by direct attack either at the 2-position or at the 3-position (*via* **7**).

The mechanisms outlined in Chart 3 provide a rational explanation for the results obtained at room temperature or at low temperature, as well as the stereochemical features of the P–S reaction of N_b-hydroxytryptamine (**1**) and cysteinals (**2**). The results described herein have been applied to the synthesis of the natural eudistomins.[16]

Experimental

Melting points were determined with Yamato MP-1 and Yanagimoto micro melting point apparatus, and are uncorrected. Ultraviolet (UV) spectra were recorded on a Hitachi 323 spectrophotometer. Infrared (IR) spectra were obtained with a Hitachi 260-10 spectrophotometer. Mass spectra (MS) were recorded on a Hitachi M-60 or a JMS-HX 100 mass spectrometer. Proton nuclear magnetic resonance (^{1}H-NMR) spectra were recorded on JEOL JNM-FX 270, JNM-GX 270, and JNM-GSX 500 apparatus. All chemical shifts are reported downfield from an internal Me_4Si standard and given as δ values (ppm). Optical rotations were recorded with a JASCO DIP-140 polarimeter. Microanalyses were performed on a Perkin-Elmer 240 C, H, and N analyzer. Unless otherwise noted, UV spectra (λ in nm) refer to a solution in 95% EtOH, IR spectra (ν in cm^{-1}) to KBr disks, and ^{1}H-NMR spectra to solutions in $CDCl_3$.

General Procedure for the Cyclization of the Nitrones (3) in Table I A solution of a nitrone (**3**) in dry CH_2Cl_2 was cooled to −78 °C and TFA (2—5 mol eq) was added by injection over 5 min in an argon atmosphere. After being stirred for 2 h at the same temperature, the reaction mixture was quenched carefully with saturated $NaHCO_3$ at −78 °C, diluted with CH_2Cl_2, washed with brine, dried over $MgSO_4$ and concentrated *in vacuo*. The residue was chromatographed over SiO_2 to give the product. For the structures of compounds **4a—d, f** and **5a—d, f**, see the preceding paper.[2a]

Compounds (**3e, g, 4e, g, 5e, g**) were prepared according to the procedure described in the preceding paper[2a] **4e**α and **4e**β (1 : 4 at room temperature, 1 : 12 at −78 °C): amorphous (diastereoisomeric mixture). UV λ_{max}^{EtOH} nm: 226, 275, 284, 291. ^{1}H-NMR (270 MHz, $CDCl_3$) δ: 8.46 (1H, br, NH, exchangeable), 7.08—7.50 (9H, m, ArH), 5.80 (1/5H, d, J=5 Hz, NH, exchangeable), 5.64 (4/5H, d, J=9Hz, NH), 5.12 (1H, d, J=12 Hz, OCHPh), 5.04 (1H, d, J=12 Hz, OCHPh), 5.04 (1H, br, OH, exchangeable), 4.87 (1H, d, J=12 Hz, $CHCCl_3$), 4.80 (1H, d, J=12 Hz, $CHCCl_3$), 4.65 (1H, br, C<u>H</u>NHCO$_2$), 4.47 (4/5H, br, C_1-βH), 4.25 (1/5H, br, C_1-αH), 3.65 (1H, m, CHN), 3.43 (1H, dd, J=5, 15 Hz, CHS), 3.30 (2H, m, CHS, C<u>H</u>NOH), 3.10 (1H, m, CH-Ind), 2.80 (1H, m, CH-Ind). **5e**: amorphous. UV λ_{max}^{EtOH} nm: 245, 303. ^{1}H-NMR (270 MHz, $CDCl_3$) δ: 7.39 (5H, s, PhH), 7.07—7.18 (2H, m, ArH), 6.80 (1H, m, ArH), 6.58 (1H, d, J=8 Hz, ArH), 5.60 (1H, br, OH, exchangeable), 5.39, 5.48 (1H, s, NCHN), 5.20 (2H, s, CH_2Ph), 5.00 (1H, br, NH, exchangeable), 4.60—4.80 (2H, m, CH_2CCl_3), 4.40 (1H, m, CHN), 3.50 (1H, s, C<u>H</u>NOH), 3.42 (1H, m, CH_2N), 3.17 (1H, m, CH_2N), 3.10 (1H, m, CHS), 2.40 (1H, m, CHS), 2.20 (2H, m, CH_2). MS *m/z*: 554, 552, 130, 91. **3g**: amorphous (64.5%), $[\alpha]_D^{17}$ +21.1° (c=0.65, MeOH). UV λ_{max}^{EtOH} nm: 220, 275, 284, 291. IR ν_{max}^{KBr} cm^{-1}: 3350, 1740, 1720, 1510, 1140. ^{1}H-NMR (270 MHz, $CDCl_3$) δ: 8.07 (1H, br s, NH, exchangeable), 7.57 (1H, m, ArH), 7.35 (5H, s, PhH), 7.10—7.33 (3H, m, ArH), 7.02 (1H, d, J=2 Hz, C_2-H), 6.67 (1H, br s, NH, exchangeable), 6.47 (1H, d, J=6 Hz, =CH), 5.21 (2H, s, CH_2Ph), 4.72 (1H, d, J=11 Hz, $CHCCl_3$), 4.68 (1H, d, J=11 Hz, $CHCCl_3$), 4.64 (1H, m, CH), 3.99 (2H, m, CH_2), 3.35 (2H, m, CH_2), 3.19 (2H, m, SCH_2). MS *m/z*: 368, 239, 186, 130. **4g**α and **4g**β (1 : 8): amorphous (diastereoisomeric mixture). IR ν_{max}^{KBr} cm^{-1}: 3340, 1710, 1510, 1140. ^{1}H-NMR (270 MHz, $CDCl_3$) δ: 8.58, 8.35 (1H, br s, NH, exchangeable), 7.06—7.48 (9H, m, ArH), 5.94 (1H, d, J=9 Hz, NH), 5.27 (2H, t-like q, J=7 Hz, OCH_2Ph), 5.18 (1H, br s, OH, exchangeable), 4.65 (2H, s, CH_2CCl_3), 4.60 (1H, m, NCH), 4.46 (8/9H, br, C_1-βH), 4.28 (1/9H, br, C_1-αH), 3.60 (1H, m, C_3-H), 3.42 (1H, m, SCH), 3.40 (1H, m, C_3-H), 3.30 (1H, m, SCH), 3.10 (1H, m, C_4-H), 2.80 (1H, m, C_4-H). MS *m/z*: 330, 239, 168, 91. **5g**: amorphous. UV λ_{max}^{EtOH} nm: 244, 300. IR ν_{max}^{KBr} cm^{-1}: 3400, 1710, 1140. ^{1}H-NMR (270 MHz, $CDCl_3$) δ: 7.28—7.40 (5H, s, PhH), 7.07—7.18 (2H, m, ArH), 6.80 (1H, m, ArH), 6.55—6.59 (1H, m, C_8-H), 5.40—5.50 (1H, br s, OH, exchangeable), 5.48 (1H, s, NCHN), 5.16—5.25 (2H, m, CH_2Ph), 4.86, 4.93 (1H, br s, NH, exchangeable), 4.69—4.95 (2H, m, CH_2CCl_3), 4.38—4.46 (1H, m, TrocNCH), 3.52, 3.59 (1H, s, C<u>H</u>NOH), 3.43 (1H, m, C_2-H), 3.18 (1H, m, C_2-H), 3.10 (1H, m, CHS), 2.37, 2.46 (1H, dd, J=10, 14 Hz, CHS), 2.17—2.26 (2H, m, CH_2). MS *m/z*: 555, 553, 480, 478, 130, 91.

Preparation of the Nitrone (3k) Freshly prepared Al(Hg) (from 4 g of Al) was added to a solution of 5-methoxy-6-bromo-3-nitroethylindole[6a] (1.00 g, 3.34 mmol) in tetrahydrofuran (THF)–H_2O (150 ml–15 ml) at 0 °C with vigorous stirring. After being stirred for 15 min, the reaction mixture was filtered through a Buchner funnel and then a Celite pad. The filtrates were evaporated and the residue was diluted with CH_2Cl_2 and washed successively with water and brine. Drying over $MgSO_4$ and removal of the solvent gave crude 5-methoxy-6-bromo-N_b-hydroxytryptamine (1.06 g), which was used in the next step without purification. A solution of the crude 5-methoxy-6-bromo-N_b-hydroxytryptamine in dry CH_2Cl_2 (50 ml) was treated with (−)-*N*-Boc-*S*-methylcysteinal (1.18 g, 5.39 mmol) at room temperature. After 2 h, the reaction mixture was evaporated *in vacuo* and the residue was chromatographed over SiO_2 to give **3k** (1.51 g, 92.9% from 5-methoxy-6-bromo-3-nitroethylindole) as a white solid, which was recrystallized from a mixture of MeOH–AcOEt to give colorless prisms, mp 163.5—165.5 °C, $[\alpha]_D^{22}$ −54.0° (c=0.20, MeOH). UV λ_{max}^{EtOH} nm: 226.5, 290s, 303, 315s. IR ν_{max}^{KBr} cm^{-1}: 3270, 1680, 1542. MS *m/z*: 423, 421 (M^+ − OH − SMe; 2, 2%). ^{1}H-NMR (500 MHz, $CDCl_3$) δ: 8.03 (1H, br s, NH, exchangeable), 7.56 (1H, s, C_7-H), 7.06 (1H, s, C_4-H), 7.03 (1H, d, J=2.5 Hz, C_2-H), 6.61 (1H, br s, N=CH), 5.90 (1H, br s, NHBoc, exchangeable), 4.56 (1H, m, C<u>H</u>NHBoc), 3.99 (2H, t, J=6.6 Hz, CH_2N), 3.94 (3H, s, OMe), 3.32 (2H, t-like, CH_2), 2.89 (1H, m, SCH), 2.70 (1H, m, SCH), 2.07 (3H, s, SMe), 1.43 (9H, s, *tert*-Bu). *Anal.* Calcd for $C_{20}H_{28}BrN_3O_4S$: C, 49.38; H, 5.80; N, 8.64. Found: C, 49.49; H, 5.77; N, 8.64.

Crystal Data for **3k**: $C_{20}H_{28}BrN_3O_4S$, monoclinic, space group $P2_1$, a=10.522 (7), b=11.547 (17), c=9.710 (8) Å, β=94.305°, U=1176.52 Å^3, Z=2, D_c=1.372 g cm^{-3}. Lattice constants and intensity data were measured using graphite-monochromated CuK_α (λ=1.542) radiation on a Rigaku AFC-5 diffractometer. A total of 1935 unique reflections with $F(\theta) > 3\sigma(F_o)$ were obtained using the $\omega < 30° < \omega - 2\theta$ scanning method with a 2θ scan speed of 4° min^{-1} to 2θ=120°. The structure was solved by the UNICS-III system MULTAN 80 (Library of Computer Center of Tokyo University, T. Sakurai and K. Kobayashi, *Rep. Inst. Phys. and Chem. Res.*, **55**, 69 (1979) based on direct methods and refined to a final

R value of 0.0546.

Transformation of the Tetracyclic Compound (5j) to the Nitrone (3j) Dry zinc bromide (200 mg, 0.89 mmol) was added to a solution of **5j** (100 mg, 0.24 mmol)[2a] in dry CH_2Cl_2 (20 ml) at room temperature in an atmosphere of Ar. After being stirred for 6 h, the reaction mixture was diluted with CH_2Cl_2 and filtered through a Celite pad. The filtrate was washed with brine, dried over $MgSO_4$ and concentrated *in vacuo*. The residue (110 mg) was chromatographed over SiO_2 to give the starting **5j** (41 mg, 41%) and **3j** (30 mg, 30%). **3j**: UV λ_{max}^{EtOH} nm: 226, 276, 288, 300. IR ν_{max}^{KBr} cm^{-1}: 3400—3200, 1705, 1545, 1270. MS *m/z*: 424 ($M^+ + 1$), 157, 144. ^{1}H-NMR (270 MHz, $CDCl_3$) δ: 7.58—7.10 (4H, m, ArH), 6.92 (1H, s, C_2-H), 6.63 (2H, d, J=6.0 Hz, N=CH and NH, exchangeable), 4.77 (1H, m, CHNBoc), 4.68 (1H, d, J=12 Hz, SCHO), 4.56 (1H, d, J=12 Hz, SCHO), 3.99 (2H, t, J=7.0 Hz, CH_2), 3.74 (3H, s, NMe), 3.64 (3H, s, COOMe), 3.46—3.60 (4H, m, OCH_2CH_2O), 3.35 (2H, m, CH_2), 3.29 (3H, s, OMe), 3.19 (1H, d, J=14, 5 Hz, SCH), 2.92 (1H, d, J=14, 5 Hz, SCH). Exact MS *m/z*: M^+ Calcd for $C_{20}H_{29}N_3O_5S$: 423.1825. Found: 423.1824 (HRMS).

Acknowledgment We are grateful for support of this research by Grant-in-Aid for Scientific Research (62470134 and 63105005) from the Ministry of Education, Science, and Culture, Japan and by a grant from Uehara Memorial Foundation. One (J.-J. L) of the authors thanks the National Natural Science Foundation of China for a grant. We also thank Mrs. Seki, Miss Hara, Mr. Kuramochi, and Mrs. Imamoto of the Analytical Center of our University for spectral measurement (NMR and MS) and microanalysis.

References and Notes

1) *a*) K. L. Rinehart, Jr., J. Kobayashi, G. C. Harbour, R. G. Hughes, Jr., S. A. Mizsak, and T. A. Scahill, *J. Am. Chem. Soc.*, **106**, 1524 (1984); *b*) K. L. Rinehart, Jr., J. Kobayashi, G. C. Harbour, J. Gilmore, M. Mascal, T. G. Holt, L. S. Shield, and F. Lafargue, *ibid.*, **109**, 3378 (1987); *c*) J. W. Blunt, R. J. Lake, M. H. G. Munro, and T. Toyokuni, *Tetrahedron Lett.*, **28**, 1825 (1987); *d*) R. J. Lake, M. M. Brennan, J. W. Blunt, and M. H. G. Munro, *ibid.*, **29**, 2255 (1988); *e*) R. J. Lake, J. D. McCombs, J. W. Blunt, M. H. G. Munro, and W. T. Robinson, *ibid.*, **29**, 4971 (1988); *f*) R. J. Lake, J. W. Blunt, and W. H. G. Munro, *Aust. J. Chem.*, **42**, 1201 (1989).

2) *a*) J. J. Liu, M. Nakagawa, and T. Hino, *Tetrahedron*, **45**, 7729 (1989); *b*) M. Nakagawa, J. J. Liu, K. Ogata, and T. Hino, *J. Chem. Soc., Chem. Commun.*, **1988**, 463.

3) T. Hino and M. Taniguchi, *J. Am. Chem. Soc.*, **100**, 5564 (1978); M. Taniguchi, I. Yamamoto, M. Nakagawa, and T. Hino, *Chem. Pharm. Bull.*, **33**, 4783 (1985) and references cited therein.

4) *a*) G. Massiot and T. Mulamba, *J. Chem. Soc., Chem. Commun.*, **1983**, 1147; *b*) D. M. Harrison and R. B. Sharma, *Tetrahedron Lett.*, **27**, 521 (1986); *c*) M. Nakagawa, H. Fukushima, T. Kawate, M. Hongu, S. Kodato, T. Une, M. Taniguchi, and T. Hino, *ibid.*, **27**, 3235 (1986); *d*) M. Nakagawa, S. Kodato, M. Hongu, T. Kawate, and T. Hino, *ibid.*, **27**, 6217 (1986); *e*) P. D. Bailey, S. P. Hollinshead, and Z. Dauter, *J. Chem. Soc., Chem. Commun.*, **1985**, 1507.

5) D. Soerens, J. Sandrin, F. Ungemach, P. Mokry, G. S. Wu, E. Yamanaka, L. Hutchins, M. DiPierro, and J. M. Cook, *J. Org. Chem.*, **44**, 535 (1979) and references therein.

6) *a*) T. Hino, A. Hasegawa, J. J. Liu, and M. Nakagawa, *Chem. Pharm. Bull.*, **38**, 59 (1990); *b*) For the P–S reactions using *N*-hydroxytryptamines, see: S. Y. Han, M. V. Lakshmikantham, and M. P. Cava, *Heterocycles*, **23**, 1671 (1985); R. Plate, P. H. H. Hermkens, J. M. M. Smits, and H. C. J. Ottenheijm, *J. Org. Chem.*, **51**, 309 (1986); R. Plate, R. H. M. van Hout, H. Behm, and H. C. J. Ottenheijm, *ibid.*, **52**, 555 (1987); P. H. H. Hermkens, J. H. van Maarseveen, P. L. H. M. Cobben, H. C. J. Ottenheijm, C. G. Kruse, and H. W. Scheeren, *Tetrahedron*, **46**, 833 (1990); J. Sandrin, S. P. Hollinshead, and J. M. Cook, *J. Org. Chem.*, **54**, 5636 (1989).

7) For the mechanism of the P–S reaction see: *a*) F. Ungemach and J. M. Cook, *Heterocycles*, **9**, 1089 (1978); *b*) F. Ungemach, M. DiPierro, R. Weber, and J. M. Cook, *J. Org. Chem.*, **46**, 164 (1981); *c*) A. H. Jackson, P. V. R. Shannon, and D. J. Wilkins, *Tetrahedron Lett.*, **28**, 4901 (1987); *d*) P. D. Bailey, S. P. Hollinshead, and N. R. McLay, *ibid.*, **28**, 5177 (1987); *e*) P. D. Bailey, *ibid.*, **28**, 5181 (1987).

8) J. E. Baldwin, *J. Chem. Soc., Chem. Commun.*, **1976**, 734.

9) *a*) A. H. Jackson and A. E. Smith, *Tetrahedron*, **21**, 989 (1965); *b*) *Idem*, *ibid.*, **24**, 403 (1968); *c*) A. H. Jackson and P. Smith, *ibid.*, **24**, 2227 (1968); *d*) A. H. Jackson, B. Naidoo, and P. Smith, *Tetrahedron*, **24**, 6119 (1968).

10) G. Casnati, A. Dossena, and A. Pochini, *Tetrahedron Lett.*, **1972**, 5277.

11) *a*) F. Johnson, *Chem. Rev.*, **68**, 375 (1968); *b*) D. A. Evans, "Asymmetric Synthesis," Vol. 3, ed. by J. D. Morrison, Academic Press, New York, 1984, p. 1.

12) R. Grigg, H. Q. N. Gunaratne, and E. McNaghten, *J. Chem. Soc., Perkin Trans., 1*, **1983**, 185.

13) P. D. Bailey, *J. Chem. Res.*, **1987**, 202.

14) J. R. Williams and L. R. Unger, *J. Chem. Soc., Chem. Commun.*, **1970**, 1605.

15) *a*) F. Ungemach, D. Soerens, R. Weber, M. DiPierro, O. Campos, P. Mokry, J. M. Cook, and J. V. Silverton, *J. Am. Chem. Soc.*, **102**, 6976 (1980); *b*) J. Sandrin, D. Soerens, and J. M. Cook, *Heterocycles*, **4**, 1249 (1976).

16) *a*) M. Nakagawa, J. J. Liu, and T. Hino, *J. Am. Chem. Soc.*, **111**, 2721 (1989); *b*) J. J. Liu, M. Nakagawa, N. Harada, A. Tsuruoka, A. Hasegawa, J. Ma, and T. Hino, *Heterocycles*, **31**, 229 (1990); *c*) For recent syntheses of eudistomins, see: I. W. J. Still and J. R. Strautmanis, *Tetrahedron Lett.*, **30**, 1041 (1989); P. H. H. Hermkens, J. H. V. Haarseveen, C. G. Kruse, and H. W. Scheeren, *ibid.*, **30**, 5009 (1989); P. H. H. Hermkens, J. H. V. Maarseveen, H. W. Berens, J. M. M. Smits, C. G. Kruse, and H. W. Scheeren, *J. Org. Chem.*, **55**, 2200 (1990); M. P. Kirkup, B. B. Shankar, S. McCombie, A. K. Ganguly, and A. T. McPhail, *Tetrahedron Lett.*, **30**, 6809 (1989).

Chem. Pharm. Bull. **39**(7) 1677—1681 (1991)

Synthetic Studies on the Picraline-Type Indole Alkaloids-I: Improved Synthesis of *C*-Mavacurine-Type Compounds and a New Skeletal Rearrangement in a Corynanthe-Type Derivative

Takeshi KOIKE, Hiromitsu TAKAYAMA, and Shin-ichiro SAKAI*

Faculty of Pharmaceutical Sciences, Chiba University, 1–33 Yayoi-cho, Chiba 260, Japan. *Received December 7, 1990*

An efficient synthesis of the C/D ring-cleaved compounds (13S and 13R) from hirsutine (7) and their transformation into three different type of products, 8 (*C*-mavacurine type), 18 (isopleiocarpamine type), and 22 are described.

Keywords indole alkaloid; hirsutine; corynanthe type; picraline type; *C*-mavacurine type; chemical transformation; skeletal rearrangement

Picraline (**1**), a representative of the picraline- (or akuammiline-) type indole alkaloids, was first isolated from *Picralima nitida* (*Apocynaceae*),[1] which is used among west African natives as an antimalarial and antipyretic. At the present time, over eighty picraline-related alkaloids have been reported from many *Apocynaceae* plants.[2] These alkaloids possess an unusual and compact pentacyclic skeleton, which has fascinated synthetic organic chemists for a long time. However, chemical synthesis of these alkaloids has not been achieved to date.[3] Based on the fact that treatment of strictamine (**5**) with strong base brought about skeletal rearrangement to furnish akuammicine (**6**),[4] picraline-type alkaloids were postulated to be biogenetic precursors of the strychnos-type indole alkaloids. Generally, picraline-type alkaloids are biogenetically considered to be derived from geissoschizine (**3**) by ring closure between the C_7 and C_{16} positions.[5] A common intermediate, geissoschizine (**3**) would also provide the *C*-mavacurine type alkaloids, such as pleiocarpamine (**2**). In connection with synthetic studies on these structurally unique alkaloids based on the above biogenetic speculation, we have already succeeded in the chemical transformation of hirsutine (**7**) and geissoschizine methyl ether (**4**) to dihydro-16-*epi*-pleiocarpamine (**8**)[6,7] and 16-*epi*-pleiocarpamine,[7,8] respectively, by bond formation between the C_{16} and N_a positions in the corynanthe alkaloids. However, synthesis of picraline type alkaloids along this line still remains to be achieved. In order to examine the biomimetic construction of the picraline alkaloids, we reinvestigated the ring closure using the chlorides (**13**). Here, we would like to report an improved synthetic procedure of **13** from hirsutine (**7**) as well as some new results obtained by the attempts at ring closure, which led to the formation of 19,20β-dihydro-16-*epi*-pleiocarpamine (**8**) and a dihydroisopleiocarpamine type compound (**18**), and a new skeletal rearrangement of **13S** to **22**.

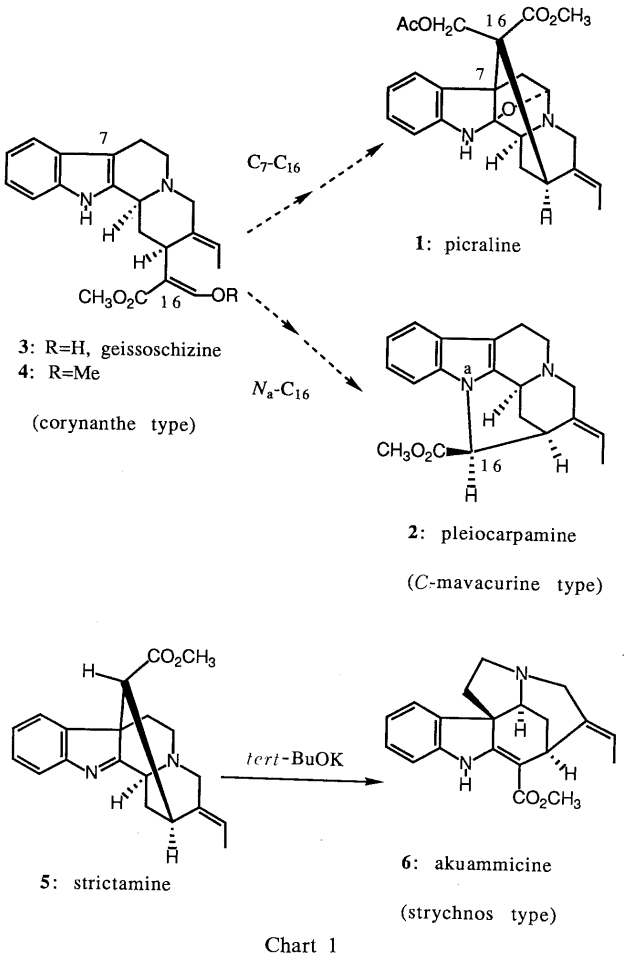

Chart 1

The initial step in this synthetic sequence was desmethylation of the enol ether in hirsutine (**7**). The use of concentrated HCl in acetic acid for the cleavage of the ether linkage overcame the problem of formation of a large amount of phorone (acetone polymer) in the known method (hydrogen chloride gas in acetone)[7] to afford the enol (**9**) in 80.4% yield after crystallization of the crude products. Next, after the C/D ring-cleavage of **9**, which would increase the flexibility of the resultant ten-membered ring, the new bond formation between C_7 and C_{16} could be expected. Direct treatment of **9** with cyanogen bromide (BrCN) gave by-products caused by the presence of a reactive β-hydroxyacrylate. After this functionality was protected as the *tert*-butyldimethylsilyl (TBS) ether, **10** was reacted with BrCN in MeOH–tetrahydrofuran (THF) (1 : 5) in the presence of magnesium oxide (MgO),[9] giving the C/D ring-opened compounds as a diastereomeric mixture at the C_3 position. Treatment of the crude products **11** with 1 N NaOH solution to remove the silyl protective group provided **12S** and **12R** in 65% and 6% yields from **7**, respectively. The configuration at the C_3 position in **12S** and **12R** was determined by comparison of the chemical shift of the C_3 protons in the proton nuclear magnetic resonance (^{1}H-NMR) spectra. It has been demonstrated that the signal of the C_3 proton in the C_3(*S*)-series appeared at lower field than that of the C_3(*R*)-series among C/D ring-opened derivatives of corynanthe- and yohimbine-type indole alkaloids.[10] Actually, H-3 in **12S** appeared at δ 4.68

(dd, $J=8.3$, 4.7 Hz), while it appeared at δ 4.36 (dd, $J=7.7$, 4.0 Hz) in **12R**. The aldehyde group at C_{16} in **12S** and **12R** was in turn replaced with a chlorine atom by treatment with *tert*-butyl hypochlorite (*tert*-BuOCl)[6-8] in CH_2Cl_2 at $-78\,^{\circ}C$, which presumably proceeded *via* a radical mechanism, to give the chlorides (**13S** and **13R**) in 81% and 74% yields, respectively.

Having obtained the key intermediates (**13S** and **13R**) in an efficient way, we next turned our attention to the ring closure reaction for connecting the C_{16} and C_7 positions. The results obtained are summarized in Table I. Generation of the indole anion with sodium hydride (NaH) (entries 1—4) resulted in cyclization between the C_{16} and N_a positions to afford **15S** and **15R** in 55% and 46% yields from **13S** and **13R**, respectively, when dimethyl sulfoxide (DMSO) was used as the solvent. The formation of the desired C_7–C_{16} cyclized product could not be observed at all. Previously, we had found that the cyclization of the C_3(*S*)-isomer (**14S**) having an ethoxy group in place of a methoxy group at the C_3 position gave **16S** in very low (2.6%) yield. In contrast to the reaction of **14S**, the methoxy derivative (**13S**) produced **15S** in 55% yield (entry 3). These phenomena can be interpreted as indicating that the steric hindrance of the ethoxy group in **14S** prevented the formation of the appropriate transition state in which the N_a anion could approach the C_{16} position. Regarding the conformation of the ring-closure products **15**, we previously proposed the structure (**15A**),[7] based on the fact that, in the ^{1}H-NMR spectra, one of the protons appeared at extraordinarily high field (around δ -0.9 ppm)[11] and it was assigned as 21-H. This unusual feature could be explained by the conformation (**15A**) in which 21-H lay just above the indole ring. However, this abnormal signal in **15S** and that in **15R** were unambiguously reassigned to 20-H based on examination of the ^{1}H–^{1}H and carbon-13 nuclear magnetic resonance (^{13}C-NMR)–^{1}H correlation spectroscopy (COSY) spectra. Therefore, another conformation (**15B**) might be the correct one for **15S** and **15R**, as depicted in Chart 3. The configuration at the C_{16} position was determined by the observation of nuclear Overhauser effects (NOEs) between H-16 and H-12/H-20. In order to obtain the pleiocarpamine-type compounds, we next attempted the reconstruction of the C/D ring by use of both stereoisomers at C_3. Treatment of **15R** with ammonium acetate ($AcONH_4$) in 5% aqueous acetic acid under reflux gave the amine (**8**) having the *C*-mavacurine skeleton in 45% yield as the major

Table I. Ring Closure Reactions of **13S** and **13R**

Entry	Substrates	Reagents and conditions	Products (Yield)
1	**13S**[b]	1) NaH–THF, room temp., 25 h 2) CH_2N_2, MeOH–Et_2O	**13S**
2	**13S**[a]	1) NaH–benzene, 18-crown-6-ether, reflux, 5.5 h 2) CH_2N_2, MeOH–Et_2O	**15S** (3.7%), **13S** (24%)
3	**13S**[a]	1) NaH–DMSO, 90 °C, 5 h 2) CH_2N_2, MeOH–Et_2O	**15S** (55%)
4	**13R**[a]	1) NaH–DMSO, 90 °C, 2.5 h 2) CH_2N_2, MeOH–Et_2O	**15R** (46%)
5	**13S**[b]	$AgBF_4$, CH_2Cl_2, room temp., 17.5 h	**19** (74%)
6	**13S**[c]	NaI, methyl ethyl ketone, reflux, 43 h	**22** (29%), **13S** (61%)

a) A diastereomeric mixture at the C_{16} position, *b*) less polar **13S**, and *c*) more polar **13S** were used.

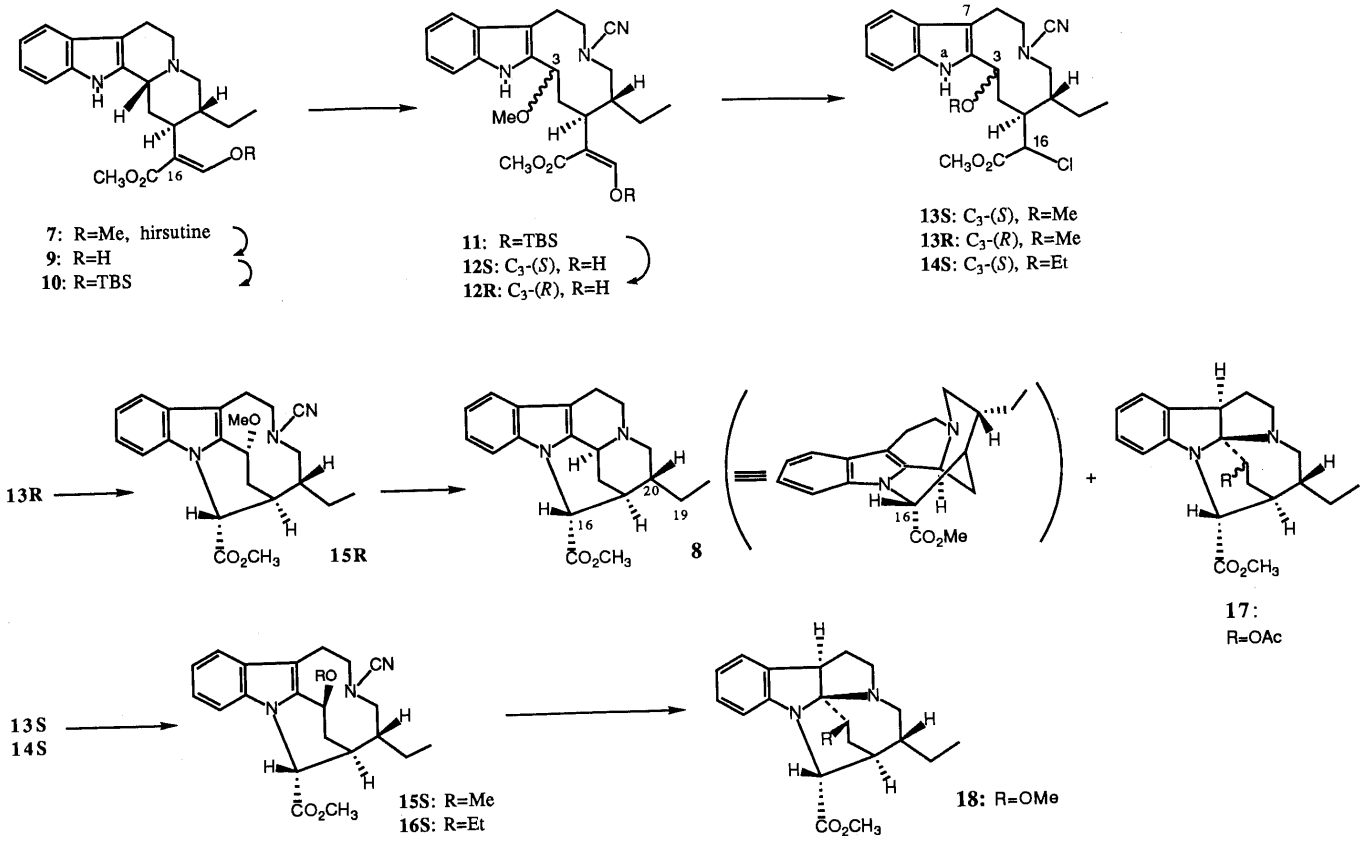

Chart 2

product. In contrast to the reaction of **15R**, **15S** was transformed selectively into the isopleiocarpamine-type compound **18** in 79% yield under the same reaction conditions. Compound **18** showed the characteristic ultraviolet (UV) absorptions at 252 and 305 nm due to the indoline chromophore. The structure of **18** including the stereochemistry at the C_{16} position was confirmed by means of two-dimensional (2D) NMR spectra (^1H–^1H and ^{13}C–^1H COSY and NOESY). Although this type of skelecton has not been isolated from nature, the preparation of isodihydropleiocarpamine from pleiocarpamine by reduction with zinc in HCl solution was reported by Schmid *et al.*[12] These two different reaction courses depending on the stereochemistry at the C_3 position can be rationalized as follows. In the case of the $C_3(R)$ isomer (**15R**), the nucleophilic center (N_b) is located at the back side position of the leaving group (OMe) so that *SN*2-like reaction proceeds smoothly to give the N_b–C_3 connected product (**8**). On the other hand, *SN*2-type reaction between the N_b and C_3 positions in the case of the $C_3(S)$ isomer (**15S**) would be sterically impossible. Then, the prdominant reaction between the N_b and the iminium function (N_a=C_2) generated by protonation at the C_7 position of the indole part would give the isopleiocarpamine skeleton (**18**). An attempt at C_7–C_{16} cyclization in **13S** by the use of silver tetrafluoroborate ($AgBF_4$) was unsuccessful (entry 5). The indolenine (**19**) produced by the reaction between C_7 and the cyano group was obtained in 74% yield as a sole product. Next, we expected that enhancement of the reactivity at C_{16} by replacement of the chlorine atom with iodine would enable ring closure between the C_7 and C_{16} positions to occur under non-basic conditions. Then, we treated **13S** with sodium iodide (NaI) in methyl ethyl ketone under reflux to obtain a novel product (**24**) in 29% yield, accompanied with 61% recovery of the starting material. The high-resolution mass spectrum of **24** showed M^+ at *m/z* 349.1794, corresponding to the formula $C_{21}H_{23}N_3O_2$. This is 32 mass units (MeOH) lower than the corresponding peak in **15S**. Since compound **24** showed the typical 1-vinylindole chromophore in the UV spectrum (224, 258, 302 nm), the $\Delta^{3,14}$ derivative generated by the elimination of methanol from **15S** could be excluded as a possible structure. The ^1H-NMR spectrum also suggested the presence of a ■–CH_a=CH_b–CH_c< system. The signal of H_a was observed at a markedly downfield position (δ 7.12 ppm) and showed NOE with the aromatic H-12. From the ^1H–^1H and ^{13}C–^1H COSY spectra, H_c was proven to be attached to the C_{15} position and a clear connectivity between H-15 and C_2 was observed in the long-range coupling (COLOC) spectrum.[13] Furthermore, strong NOE was observed between Hβ-6 and H-16. These data show that N_a is connected to C_3, while C_2 is bonded with C_{16}. A plausible mechanism of this unusual skeletal rearrangement is shown in Chart 4. Initially, the reactive C_2 of the indole part in **13S** might attack the C_{16} position which was replaced by iodine, and subsequent C_2–C_3 bond cleavage would give the indolic intermediate (**21**). Then, N_a would react with the C_3 position followed by methanol elimina-

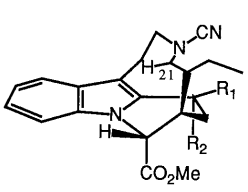

conformer **15A**

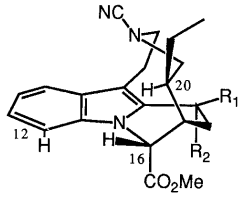

conformer **15B**

15S: R_1=OMe, R_2=H
15R: R_1=H, R_2=OMe

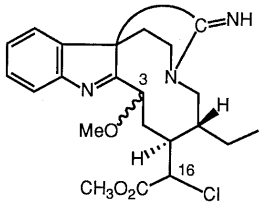

19: C_3-(*S*)

Chart 3

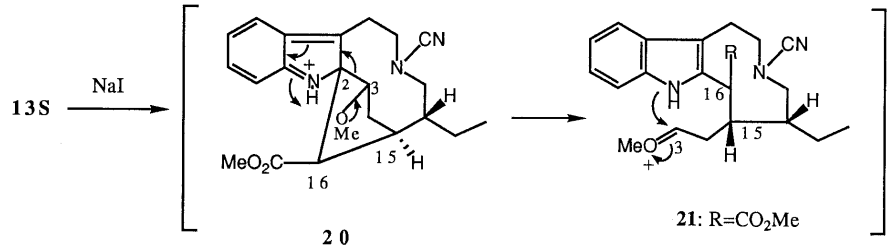

20

21: R=CO_2Me

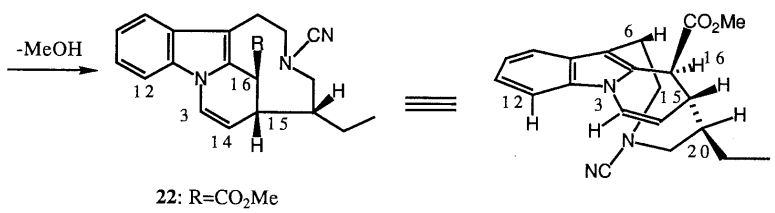

22: R=CO_2Me

Chart 4. A Plausible Mechanism of the Formation of **22** from **13S**

tion to produce **22**.

Although no picraline-type compound could be obtained during this investigation, we found some useful and significant chemical reactions and information. Further efforts on the biomimetic synthesis of the picraline-type alkaloids are in progress in this laboratory.

Experimental

All melting points were determined on a Yamato MP-21 apparatus and are uncorrected. The instruments used in this study were as follows; UV spectra, Hitachi U3400 spectrophotometer; infrared (IR) spectra, Hitachi 260 spectrophotometer; mass spectra (MS), Hitachi RMU-6E and RMU-7M spectrometers; ^{1}H- and ^{13}C-NMR spectra, JEOL JNM GX270, JEOL GSX400, and JEOL GSX500 instruments (compounds were dissolved in $CDCl_3$ with tetramethylsilane as an internal standard, and chemical shifts are recorded in δ values). Thin-layer chromatography was performed on Merck precoated Silica gel 60 F_{254} plates. Column chromatography was carried out on Merck Silica gel 60 (230—400 mesh for flash chromatography), pre-packed columns [silica gel, Kusano CPS-HS-221-05 (for medium-pressure column chromatograhy)], and Merck Al_2O_3 90 (activity II—III). Organic solutions were dried over anhydrous $MgSO_4$. Abbreviations used are: singlet (s), doublet (d), triplet (t), multiplet (m), shoulder (sh).

Desmethylhirsutine (9) A mixture of hirsutine (736 mg, 2.00 mmol) and concentrated HCl solution (1 ml) in acetic acid (4 ml) was stirred at room temperature for 24 h. After evaporation of the solvents under reduced pressure at below 30°C, the reaction mixture was diluted with chilled water and basified with saturated $NaHCO_3$ solution. The whole was extracted with $CHCl_3$. The organic phase was washed with water, dried and evaporated. The crude product was crystallized from acetone to give 569 mg (80.4%) of **9** as colorless needles, mp 121—122.5 °C (lit.[7] mp 116—119 °C), which was identical with an authentic sample.

Preparation of 12S and 12R from Hirsutine (7) A solution of hirsutine (**7**) (2.059 g, 5.60 mmol) in concentrated HCl solution (2.8 ml) and acetic acid (11.2 ml) was stirred at room temperature under argon for 24 h. Acetic acid was concentrated under reduced pressure at below 30 °C and then crushed ice was added to the residue. The mixture was basified with saturated $NaHCO_3$ solution and extracted with $CHCl_3$. The organic layer was washed with water, dried and evaporated to give a residue (1897 mg), which was subjected to the next reaction without purification. TBS chloride was added at intervals to a stirred solution of crude **9** and triethylamine (Et_3N) (2.24 ml, 16.07 mmol) in dry CH_2Cl_2 (58.8 ml) in the following manner: 0 min, 806 mg (5.35 mmol); 2 h, 806 mg; 3 h, 806 mg; 4.5 h, 806 mg. During this period, stirring was continued at room temperature under argon. After 5.5 h, the reaction mixture was diluted with water and extracted with $CHCl_3$. The organic phase was washed with water, dried and then evaporated. The silyl enol ether (**10**), which was labile during silica gel chromatography, was directly subjected to the next reaction. The crude residue containing the silyl ether (**10**) was dissolved in dry MeOH (10.7 ml) and dry THF (53.5 ml). MgO (1511 mg, 37.47 mmol) and BrCN (851 mg, 8.04 mmol) were added to the stirred solution at 0 °C and the mixture was stirred at room temperature for 2 h. The reaction mixture was filtered to remove MgO. The filtrate was evaporated *in vacuo* and the residue was taken up in water. The whole was extracted with $CHCl_3$. The organic layer was washed with water, dried and evaporated. The crude material was dissolved in MeOH and 1N NaOH solution (5 : 1, 128 ml), and the mixture was stirred at 0 °C under argon for 40 min. The solvent was evaporated off *in vacuo* and the residue was acidified with chilled 1N HCl solution. The whole was extracted with $CHCl_3$ and the organic phase was washed with water and dried. Evaporation of the solvents gave a residue, which was purified by flash column chromatography (benzene–EtOH–Et_3N, 100 : 5 : 10) to give 1492 mg (65%) of **12S** and 132 mg (5.7%) of **12R**.

(3*S*)-Methoxy-3,4-seco-cyanamide (**12S**): Colorless amorphous powder. UV λ_{max}^{EtOH} nm: 224, 271, 282, 291. UV $\lambda_{max}^{EtOH+1N\ NaOH}$ nm: 224, 277. IR $\nu_{max}^{CHCl_3}$ cm^{-1}: 3470, 3020, 2225 (CN), 1730, 1665, 1610. ^{1}H-NMR (500 MHz) δ: 8.33 (1H, br, NH), 7.04 (1H, s, 17-H), 4.68 (1H, dd, J=8.3, 4.7 Hz, 3-H), 3.70 (3H, s, CO_2CH_3), 3.28 (3H, s, OCH_3), 0.83 (3H, t, J=7.1 Hz, 18-CH_3). MS m/z (%): 411 (M^+, 4), 368 (24), 236 (26), 146 (100).

(3*R*)-Methoxy-3,4-seco-cyanamide (**12R**): Colorless amorphous powder. UV λ_{max}^{MeOH} nm: 224, 275, 283, 291. UV $\lambda_{max}^{MeOH+1N\ NaOH}$ nm: 225, 276. IR $\nu_{max}^{CHCl_3}$ cm^{-1}: 3460, 3000, 2210, 1720, 1660, 1600. ^{1}H-NMR (500 MHz) δ: 8.09 (1H, br, NH), 7.07 (1H, s, 17-H), 4.36 (1H, dd, J=7.7, 4.0 Hz, 3-H), 3.81 (3H, s, CO_2CH_3), 3.20 (3H, s, OCH_3), 0.48 (3H, t, J=7.1 Hz, 18-CH_3). MS m/z (%): 411 (M^+, 32), 368 (31), 236 (38), 156 (100).

Preparation of the Chloride (13S) A solution of 0.336 mmol of *tert*-BuOCl in CCl_4 (0.3 ml, 0.10 mmol) was added dropwise to a stirred solution of **12S** (41 mg, 0.10 mmol) and Et_3N (31 μl, 0.3 mmol) in dry CH_2Cl_2 (6 ml) at −78 °C under argon, and the reaction temperature was gradually raised to room temperature over 4 h. The reaction mixture was diluted with $CHCl_3$ and washed with water. The organic phase was dried and evaporated to leave a residue, which was subject to Al_2O_3 column chromatography (benzene–AcOEt, 100 : 17.5) to afford 34 mg (81%) of the chloride (**13S**) in a diastereomeric mixture at the C_{16} position. For the spectroscopic analysis a part of this mixture was separated by medium-pressure column chromatography (MPLC) (benzene–AcOEt, 5 : 1).

Less Polar (**13S**): Amorphous power. UV λ_{max}^{EtOH} nm: 224, 282, 291. IR $\nu_{max}^{CHCl_3}$ cm^{-1}: 3400, 3010, 2940, 2220, 1755. ^{1}H-NMR (500 MHz) δ: 8.28 (1H, br, NH), 4.62 (1H, dd, J=9.1, 5.5 Hz, 3-H), 4.29 (1H, d, J=2.8 Hz, 16-H), 3.48 (3H, s, CO_2CH_3), 3.28 (3H, s, OCH_3), 0.93 (3H, t, J=7.4 Hz, 18-CH_3). MS m/z(%): 419 (M^++2, 36), 417 (M^+, 98), 402 (100), 173 (50), 158 (66), 143 (73). Exact MS Calcd for $C_{22}H_{28}ClN_3O_3$: 417.1817. Found: 417.1815.

More Polar (**13S**): Amorphous powder. UV λ_{max}^{EtOH} nm: 223, 282, 291. IR $\nu_{max}^{CHCl_3}$ cm^{-1}: 3470, 3010, 2950, 2220, 1750. ^{1}H-NMR (500 MHz) δ: 8.20 (1H, br, NH), 4.62 (1H, dd, J=9.5, 5.1 Hz, 3-H), 4.26 (1H, d, J=9.1 Hz, 16-H), 3.69 (3H, s, CO_2CH_3), 3.25 (3H, s, OCH_3), 1.02 (3H, t, J=7.3 Hz, 18-CH_3). MS m/z(%): 419 (M^++2, 34), 417 (M^+, 100), 402 (94), 173 (45), 158 (60), 143 (68). Exact MS Calcd for $C_{22}H_{28}ClN_3O_3$: 417.1817. Found: 417.1826.

Preparation of the Chloride (13R) Treatment of 35 mg (0.086 mmol) of **12R** with *tert*-BuOCl and Et_3N in dry CH_2Cl_2 according to the same procedure described above afforded 26.5 mg (74%) of **13R** as a diastereomeric mixture at the C_{16} position. It was separated by MPLC (AcOEt–hexane, 1 : 1.5) for spectroscoic analysis.

Less Polar (**13R**): Amorphous powder. UV λ_{max}^{EtOH} nm: 224, 283, 291. IR $\nu_{max}^{CHCl_3}$ cm^{-1}: 3460, 2210, 1740. ^{1}H-NMR (270 MHz) δ: 8.17 (1H, br, NH), 4.37 (1H, dd, J=7.7, 4.5 Hz, 3-H), 4.41 (1H, d, J=3.0 Hz, 16-H), 3.86 (3H, s, CO_2CH_3), 3.23 (3H, s, OCH_3), 0.58 (3H, t, J=7.5 Hz, 18-CH_3). MS m/z (%): 419 (M^++2, 28), 417 (M^+, 78), 402 (89), 158 (73), 143 (100). Exact MS Calcd for $C_{22}H_{28}ClN_3O_3$: 417.1817. Found: 417.1808.

More Polar (**13R**): Amorphous powder. UV λ_{max}^{EtOH} nm: 224, 283, 292. IR $\nu_{max}^{CHCl_3}$ cm^{-1}: 3460, 2220, 1750. ^{1}H-NMR (270 MHz) δ: 8.17 (1H, br, NH), 4.42 (1H, dd, J=9.2, 3.5 Hz, 3-H), 4.26 (1H, d, J=8.9 Hz, 16-H), 3.82 (3H, s, CO_2CH_3), 3.21 (3H, s, OCH_3), 0.43 (3H, t, J=7.3 Hz, 18-CH_3). MS m/z(%): 419 (M^+ +2, 21), 417 (M^+, 60), 402 (67), 158 (60), 156 (51), 143 (100). Exact MS Calcd for $C_{22}H_{28}ClN_3O_3$: 417.1817. Found: 417.1814.

Ring Closure of 13S with NaH in DMSO A solution of NaH (50% in oil, 48 mg, 1.0 mmol) in dry DMSO was heated at 80 °C under argon for 40 min. To this solution was added **13S** (208.8 mg, 0.50 mmol) dissolved in dry DMSO (8 ml), and then the mixture was stirred at 90 °C under argon for 5 h. The reaction mixture was poured into cold water and then acidified with 1N HCl solution. It was extracted with AcOEt. The organic extract was washed with water, dried and evaporated. The residue was dissolved in MeOH and then treated with ethereal diazomethane (CH_2N_2). Evaporation of the solvent gave a residue, which was subjected twice to MPLC (acetone–hexane, 1 : 2 and benzene–AcOEt, 25 : 6) to afford 105 mg (55%) of **15S** as colorless columnar crystals, mp 140—141 °C (from ether–acetone). UV λ_{max}^{MeOH} nm: 229, 273, 283, 294. IR $\nu_{max}^{CHCl_3}$ cm^{-1}: 2200, 1750, 1460. ^{1}H-NMR (500 MHz) δ: 4.86 (1H, dd, J=10.2, 5.8 Hz, 3-H), 4.73 (1H, dd, J=2.2, 1.9 Hz, 16-H), 3.90 (3H, s, CO_2CH_3), 3.59 (3H, s, OCH_3), 2.87 (1H, m, 21-H), 2.17 (1H, br d, J=10.5 Hz, 21-H), 0.40 (3H, t, J=7.3 Hz, 18-CH_3), −0.90 (1H, m, 20-H). ^{13}C-NMR (100 MHz) δ: 145.5 (C2), 75.2 (C3), 54.0 (C5), 24.0 (C6), 112.4 (C7), 130.8 (C8), 118.6 (C9), 121.2 (C10), 123.1 (C11), 111.1 (C12), 142.5 (C13), 31.1 (C14), 43.7 (C15), 65.2 (C16), 11.7 (C18), 25.8 (C19), 38.9 (C20), 56.4 (C21), 171.3 (CO), 52.9 ($CO_2\underline{C}H_3$), 57.7 (OCH_3), 119.9 (CN). MS m/z (%): 381 (M^+, 46), 322 (100), 180 (27). Exact MS Calcd for $C_{22}H_{27}N_3O_3$: 381.2050. Found: 381.2050.

Ring Closure of 13R with NaH in DMSO **13R** (26.5 mg, 0.063 mmol) was treated with NaH (6.1 mg, 0.126 mmol) in DMSO and then with CH_2N_2 according to the procedure described above. After purification by MPLC (AcOEt–hexane, 1 : 1.5), 11 mg (46%) of **15R** was obtained as a colorless oil. UV λ_{max}^{EtOH} nm: 227, 273, 284. IR $\nu_{max}^{CHCl_3}$ cm^{-1}: 2200, 1730, 1455. ^{1}H-NMR (500 MHz) δ: 4.77 (1H, dd, J=8.8, 1.7 Hz, 3-H), 4.68 (1H, t, J=2.2 Hz, 16-H), 3.86 (3H, s, CO_2CH_3), 3.12 (3H, s, OCH_3), 0.46 (3H, t, J=7.4 Hz, 18-CH_3), −0.88 (1H, m, 20-H). ^{13}C-NMR (125 MHz) δ:

145.3 (C2), 69.8 (C3), 54.1 (C5), 24.2 (C6), 115.3 (C7), 128.9 (C8), 119.0 (C9), 121.1 (C10), 123.9 (C11), 111.3 (C12), 140.0 (C13), 30.2 (C14), 41.5 (C15), 63.5 (C16), 11.7 (C18), 25.7 (C19), 38.2 (C20), 56.2 (C21), 170.7 (CO), 52.6 ($CO_2\underline{C}H_3$), 55.3 (OCH_3), 119.0 (CN). MS *m/z* (%): 381 (M^+, 100), 322 (44), 180 (47). Exact MS Calcd for $C_{22}H_{27}N_3O_3$: 381.2050. Found: 381.2056.

Preparation of 8 from 15R A mixture of **8** (10 mg, 0.026 mmol) and $AcONH_4$ (10.1 mg, 0.13 mmol) in 5% aqueous acetic acid (2 ml) was heated at reflux under argon for 4 h. The reaction mixture was poured into chilled water and basified with concentrated ammonia water. The whole was extracted with $CHCl_3$ and the organic layer was washed with water and dried. Evaporation of the solvents gave a residue, which was separated by MPLC (acetone–hexane, 1 : 1) to provide 3.8 mg (45%) of **8** and 1.0 mg (10%) of **17**.

8: Colorless oil. UV λ_{max}^{MeOH} nm: 229, 286. IR $\nu_{max}^{CHCl_3}$ cm^{-1}: 1735. ^{1}H-NMR (400 MHz) δ: 4.66 (1H, s, 16-H), 3.74 (1H, m, 3-H), 3.86 (3H, s, CO_2CH_3), 3.30 (1H, ddd, J=13.0, 10.3, 2.6 Hz, 5-H), 3.15 (1H, ddd, J=16.1, 8.6, 2.6 Hz, 6-H), 2.65 (1H, ddd, J=16.1, 10.3, 6.0 Hz, 6-H), 2.55 (1H, m, 15-H), 2.28 (1H, dt, J=13.9, 2.7 Hz, 14-H), 2.20 (1H, d, J=13.9 Hz, 14-H), 2.13 (1H, ddd, J=13.0, 8.6, 6.0 Hz, 5-H), 1.92 (1H, d, J=12.3 Hz, 21-Hα), 1.77—1.66 (1H, m, 19-H), 1.60—1.51 (1H, m, 19-H), 1.25—1.09 (1H, m, 20-H), 0.87 (3H, t, J=7.4 Hz, 18-CH_3), 0.33 (1H, dd, J=12.3, 5.1 Hz, 21-Hβ). ^{13}C-NMR (100 MHz) δ: 137.5 (C2), 51.0 (C3), 50.0 (C5), 20.5 (C6), 108.9 (C7), 128.9 (C8), 118.2 (C9), 120.0 (C10), 121.3 (C11), 110.0 (C12), 139.4 (C13), 20.8 (C14), 34.5 (C15), 61.8 (C16), 12.4 (C18), 26.2 (C19), 40.3 (C20), 49.4 (C21), 171.5 (CO), 52.4 ($CO_2\underline{C}H_3$). MS *m/z* (%): 324 (M^+, 95), 265 (75), 182 (51), 180 (100). Exact MS Calcd for $C_{20}H_{24}N_2O_2$: 324.1836. Found: 324.1822.

17: Colorless oil. UV λ_{max}^{MeOH} nm: 205, 251, 304. UV $\lambda_{max}^{MeOH+1N\,HCl}$ nm: 204, 241, 293. IR $\nu_{max}^{CHCl_3}$ cm^{-1}: 1750 (sh), 1730, 1610. ^{1}H-NMR (500 MHz), δ: 5.12 (1H, br d, J=6.1 Hz, 3-H), 4.21 (1H, s, 16-H), 3.72 (3H, s, CO_2CH_3), 1.96 (3H, s, $COCH_3$), 1.01 (3H, t, J=7.4 Hz, 18-CH_3). MS *m/z* (%): 384 (M^+, 50), 325 (100), 265 (72), 194 (32). Exact MS Calcd for $C_{22}H_{28}N_2O_4$: 384.2047. Found: 384.2053.

Preparation of 18 from 15S A mixture of **15S** (36 mg, 0.095 mmol) and $AcONH_4$ (36.4 mg, 0.47 mmol) in 5% aqueous acetic acid (2 ml) was refluxed under argon for 4 h. The reaction mixture was poured into chilled water and basified with concentrated ammonia water. The whole was extracted with $CHCl_3$. The organic layer was washed with water, dried and evaporated to give a residue, which was purified by MPLC (acetone–hexane, 1 : 3) to provide 26.4 mg (79%) of **18** and 1.5 mg (4%) of the starting material.

18: Colorless oil. UV λ_{max}^{EtOH} nm: 205, 252, 305. UV $\lambda_{max}^{EtOH+1N\,HCl}$ nm: 204, 243, 293. IR $\nu_{max}^{CHCl_3}$ cm^{-1}: 1740, 1605. ^{1}H-NMR (500 MHz) δ: 4.17 (1H, s, 16-H), 3.84—3.81 (2H, m, 3-H, 7-H), 3.73 (3H, s, CO_2CH_3), 3.37 (3H, s, OCH_3), 3.12 (1H, ddd, J=8.5, 7.4, 4.8 Hz, 5-H), 2.73 (1H, dd, J=12.4, 5.9 Hz, 21-H), 2.63 (1H, dd, J=12.4, 5.0 Hz, 21-H), 2.07 (1H, ddd, J=14.9, 9.6, 6.0 Hz, 14-H), 1.72 (1H, dd, J=14.9, 4.3 Hz, 14-H), 0.94 (3H, t, J=7.4 Hz, 18-CH_3). MS *m/z*(%): 356 (M^+, 43), 341 (52), 297 (100), 239 (42). Exact MS Calcd for $C_{21}H_{28}N_2O_3$: 356.2098. Found: 356.2095.

Attempt at Ring Closure in 13S with $AgBF_4$ A mixture of less polar **13S** (20.8 mg, 0.05 mmol) and $AgBF_4$ (13 mg, 0.066 mmol) in dry CH_2Cl_2 was stirred at room temperature under argon for 17.5 h. The reaction mixture was diluted with $CHCl_3$ and washed with water. The organic layer was dried and evaporated to leave a residue, which was subjected to MPLC (4.5% MeOH–$CHCl_3$) to afford 15.4 mg (74%) of the indolenine **19** as a colorless amorphous solid. UV λ_{max}^{EtOH} nm: 219, 265. IR $\nu_{max}^{CHCl_3}$ cm^{-1}: 3310, 1760, 1640. ^{1}H-NMR (500 MHz) δ: 4.86 (1H, d, J=3.9 Hz, 16-H), 4.32 (1H, dd, J=5.0, 1.7 Hz, 3-H), 3.81 (3H, s, CO_2CH_3), 3.36 (3H, s, OCH_3), 1.01 (3H, t, J=7.4 Hz, 18-CH_3). ^{13}C-NMR (125 MHz) δ: 183.2 (C2), 75.8 (C3), 44.6 (C5), 26.9 (C6), 68.0 (C7), 135.0 (C8), 121.7 (C9), 129.9 (C10), 126.6 (C11), 123.3 (C12), 156.5 (C13), 35.7 (C14), 42.1 (C15), 61.9 (C16), 10.5 (C18), 24.2 (C19), 34.5 (C20), 47.5 (C21), 168.6 (CO)*, 53.3 ($CO_2\underline{C}H_3$), 57.7 (OCH_3), 167.7 (C=NH)* (assignments marked* may be interchanged). MS *m/z* (%): 419 (M^++2, 30), 417 (M^+, 90), 404 (35), 402 (100), 382 (76).

Skeletal Rearrangement of 13S to 22 A mixture of more polar **13S** (31.3 mg, 0.075 mmol) and NaI (16.9 mg, 0.11 mmol) in methyl ethyl ketone (2 ml) was refluxed under argon for 43 h. The reaction mixture was poured into water and extracted with AcOEt. The organic layer was washed successively with 10% $NaHSO_3$ solution, saturated $NaHCO_3$ solution and water, and then concentrated. The residue was subjected to MPLC (benzene–AcOEt, 12 : 1) to yield 19 mg (61%) of the starting material and 7.5 mg (29%) of **22** as a colorless oil. UV λ_{max}^{MeOH} nm: 224, 258, 302. IR $\nu_{max}^{CHCl_3}$ cm^{-1}: 2210, 1735, 1650. ^{1}H-NMR (500 MHz) δ: 7.48 (1H, d, J=7.7 Hz, 9-H), 7.41 (1H, d, J=8.0 Hz, 12-H), 7.27 (1H, t-like, J=8.0 Hz, 11-H), 7.18 (1H, t-like, J=7.7 Hz, 10-H), 7.12 (1H, d, J=7.7 Hz, 3-H), 5.12 (1H, ddd, J=7.7, 6.0, 1.2 Hz, 14-H), 4.61 (1H, s, 16-H), 3.67 (3H, s, CO_2CH_3), 3.58 (1H, m, 5-H), 3.40 (1H, t, J=6.2 Hz, 15-H), 3.21 (1H, ddd, J=15.1, 12.6, 3.3 Hz, 6-H), 3.01 (1H, m, 6-H), 2.86 (1H, d, J=12.9 Hz, 21-H), 2.67 (1H, ddd, J=14.0, 12.6, 1.7 Hz, 5-H), 2.13—2.07 (1H, m, 20-H), 1.79 (1H, dd, J=12.9, 10.2 Hz, 21-H), 0.99 (3H, t, J=6.6 Hz, 18-CH_3). The configuration at C_{16} was determined by the observation of NOEs between 16-H and 6-Hα/20-H. ^{13}C-NMR (67.8 MHz) δ: 131.2 (C2), 125.8 (C3), 52.3 (C5), 24.3 (C6), 113.2 (C7), 128.0 (C8), 118.5 (C9), 121.2 (C10), 123.3 (C11), 110.2 (C12), 136.8 (C13), 107.2 (C14), 35.4 (C15), 40.8 (C16), 11.9 (C18), 24.2 (C19), 43.1 (C20), 53.0 (C21), 171.6 (CO), 52.6 (OCH_3), 118.1 (CN). MS *m/z* (%): 349 (M^+, 63), 290 (55), 238 (89), 180 (100). Exact MS Calcd for $C_{21}H_{23}N_3O_2$: 349.1789. Found: 349.1794.

Acknowledgment Thanks are due to Mrs. H. Seki, Miss R. Hara, and Mr. T. Kuramochi in the Analytical Center of our University for measurements of spectral data (NMR and MS).

References

1) J. E. Saxton, "The Alkaloids," Vol. VIII, ed. by R. H. F. Manske, Academic Press, New York, 1965, Chapter 7.
2) J. W. Southon and J. Buckingham, "Dictionary of Alkaloids," Chapman and Hall Ltd., London, New York, 1989.
3) M. L. Bennasar, M. Alvarez, R. Lavilla, E. Zulaica, and J. Bosch, *J. Org. Chem.*, **55**, 1156 (1990).
4) Y. Ahmad, K. Fatima, A. Rahman, J. L. Occolowitz, B. A. Solheim, J. Clardy, R. L. Garnick, and P. W. Le Quesne, *J. Am. Chem. Soc.*, **99**, 1943 (1977).
5) E. Wenkert and B. Wickberk, *J. Am. Chem. Soc.*, **94**, 3205 (1972).
6) S. Sakai and N. Shinma, *Chem. Pharm. Bull.*, **22**, 3013 (1974).
7) S. Sakai and N. Shinma, *Yakugaku Zasshi*, **98**, 950 (1978).
8) S. Sakai and N. Shinma, *Heterocycles*, **4**, 985 (1976).
9) *a*) H. Takayama, K. Masubuchi, M. Kitajima, N. Aimi, and S. Sakai, *Tetrahedron*, **45**, 1327 (1989); *b*) H. Takayama, M. Horigome, N. Aimi, and S. Sakai, *Tetrahedron Lett.*, **31**, 1287 (1990).
10) S. Sakai, A. Kubo, K. Katano, N. Shinma, and K. Sasago, *Yakugaku Zasshi*, **93**, 1165 (1973).
11) D. D. O'Rell, F. G. H. Lee, and V. Boekelheid, *J. Am. Chem. Soc.*, **94**, 3205 (1972).
12) A. A. Gorman, N. J. Dastoor, M. Hesse, W. von Philipsborn, U. Renner, H. Schmid, *Helv. Chim. Acta*, **52**, 33 (1969).
13) H. Kessler, C. Griesinger, J. Zarbock, and H. R. Looshi, *J. Magn. Reson.*, **57**, 331 (1984).

Synthesis of Nucleosides and Related Compounds. XXII.[1] Carbocyclic Analogues of Thymidine and Related Compounds from 2-Azabicyclo[2.2.1]hept-5-en-3-ones

Nobuya KATAGIRI,* Masahiro NOMURA, Makoto MUTO, and Chikara KANEKO*

Pharmaceutical Institute, Tohoku University, Aobayama, Sendai 980, Japan. *Received December 13, 1990*

Reductive amido bond cleavage reaction, previously elaborated by our laboratory for the synthesis of carbocyclic ribothymidine from readily available 2-azabicyclo[2.2.1]hept-5-en-3-one, was successfully applied to the synthesis of carbocyclic analogues of thymidine and related compounds.

Keywords reductive amido bond cleavage; sodium borohydride; carbocyclic nucleoside; 2-azabicyclo[2.2.1]hept-5-en-3-one; epoxidation; cyclonucleoside; carbocyclic thymidine

In a recent paper in this series,[2] we reported a facile synthesis of carbocyclic ribothymidine (**5**) from readily available 2-azabicyclo[2.2.1]hept-5-en-3-one (**1**)[3] by the use of a reductive amido bond cleavage reaction as a key step. This method provides the shortest route to **5** among the methods so far reported and has the advantages that all reactions proceed with complete regio- and stereoselectivities and the 3-methoxy-2-methylacryloylcarbamoyl group on the nitrogen atom as the electron-withdrawing substituent which is essential for the above cleavage reaction acts as an equivalent of the thymine ring system. Furthermore, our methodology has not only permitted ready access to the cyclopentylurea (**7**), a versatile synthetic precursor of carbocyclic pyrimidine-type ribonucleosides, *via* the bicyclo amide (**6**), but also provided a new route to the cyclopentylamine (**8**),[4] which serves as a common precursor for the corresponding purine-type nucleosides.[5]

Compounds that interfere with the biosynthesis or utilization of thymidine and its nucleotides are of great interest because of the important role of thymidine nucleotides in deoxyribonucleic acid (DNA) synthesis.[6] Hence, a large number of analogues of the nucleoside constituents of deoxyribonucleic acids (as well as ribonucleic acids, which play an essential role in ribonucleic acid (RNA) synthesis) have been synthesized and their biological properties tested. Carbocyclic analogues of such nucleosides have, in this line of work, attracted much attention not only as potential tools for the study of nucleic acid metabolism, but also as potential anticancer and antiviral agents.[7] After elaboration of an effective synthetic method for carbocyclic ribothymidine,[2] we have continued to extend our methodology to the synthesis of carbocyclic analogues of thymidine and related compounds. In this paper, we report the synthesis of carbocyclic thymidine as well as several related thymines having a monohydroxycyclopentyl group at the 1-position.

Though a carbocyclic analogue of thymidine was claimed to have been synthesized from 1-(3-cyclopenten-1-yl)thymine (**9**) by means of the Prins reaction and to exhibit no biological activity by Murdock and Angier in 1962,[8] its structure was later revised by Shealy *et al.* to (±)-[3′α-hydroxy-4′α-(hydroxymethyl)cyclopent-1′β-yl]-5-methyl-2,4(1*H*,3*H*)-pyrimidinedione (**10′**).[9] Shealy *et al.* accomplished the synthesis of **10** from (±)-(1β,2α,4β)-4-amino-2-hydroxycyclopentanemethanol (**19**) and found that it had reproducible, though weak, activity against Leukemia L1210 in mice.[9-11] The synthesis of the amine (**19**)[10] from readily available *exo*-5-norbornen-2-ol acetate (**11**)[12] was, however, nonregioselective and involved many steps. Thus, oxidation of **11** with sodium permanganate gave the dicarboxylic acid (**12**), whose anhydride when treated with methanol gave a mixture of monomethyl esters (**13** and **14**). Two regioisomers were separated after their conversion to the corresponding carbamoylcyclopentanecarboxylates

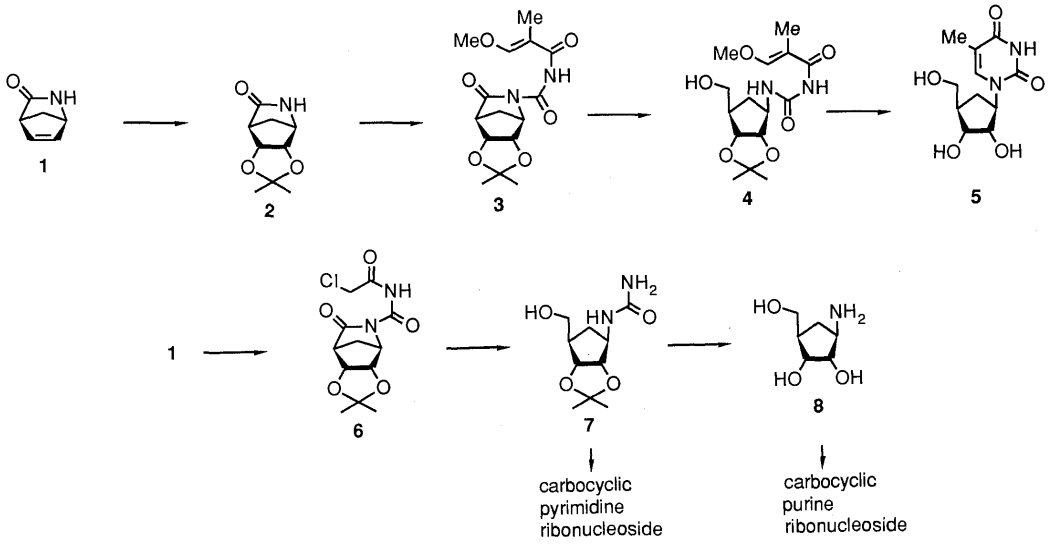

Chart 1

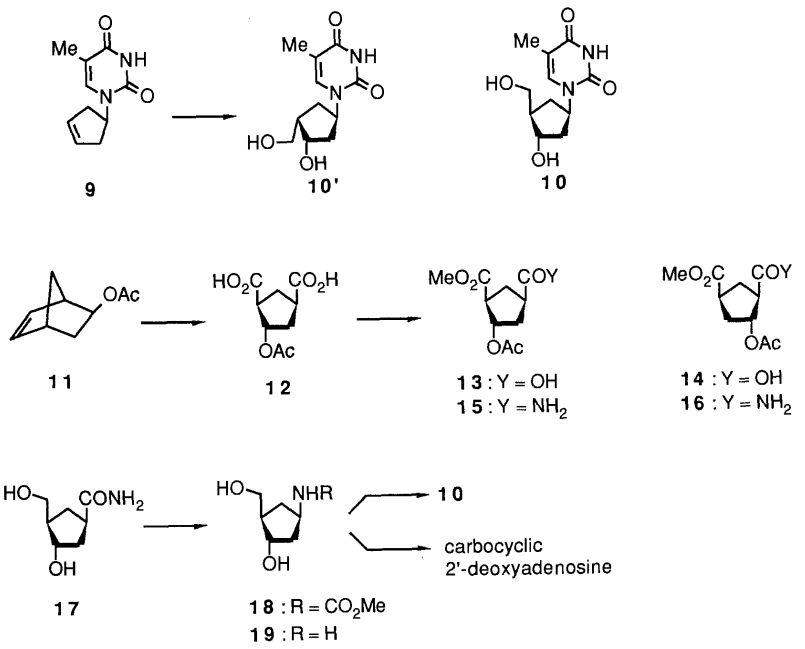

Chart 2

(**15** and **16**). Reduction of methyl (±)-2α-acetoxy-4β-carbamoylcyclopentane-1β-carboxylate (**15**) with $LiBH_4$ (formation of **17**), followed by Hofmann hypobromite reaction in methanol and acidic hydrolysis, afforded the amine (**19**).

In order to extend our methodology [use of the bicycloenamide (**1**) as the starting material with the aid of sodium borohydride mediated reductive amido bond cleavage as the key step] to the synthesis of **10** and related compounds, we have examined the following two routes: 1) epoxidation or hydration of the ene function of **1** in some stage of the reaction sequence and further manipulation of thus formed compounds and 2) removal of the 2′-hydroxyl group of carbocyclic ribothymidine (**5**), which is now readily available from **1** in essentially four steps.[2] To convenience, we report the results in separate sections.

Results and Discussion

Synthesis of Carbocyclic Analogue of Thymidine (10) by Epoxidation or Hydration of the Ene Function of the Bicycloenamide (1) Since carbocyclic ribothymidine (**5**) was synthesized from the bicycloenamide (**1**) *via* a small number of steps by the use of a reductive amide bond cleavage reaction as the key step (*cf.* **3**→**4** in Chart 1), we first planned to examine the route shown in Chart 3, involving epoxidation of **1** followed by appropriate reductive C–O bond cleavage. If the epoxidation from the less hindered side could be realized, the epoxide (**20**) would produce carbocyclic thymidine (**10**) or its isomer (**21**) on further reduction.

When the bicycloenamide (**1**) was treated with *m*-chloroperbenzoic acid (*m*-CPBA), the expected epoxide (**20**) was obtained as a sole product. It is obvious that this epoxidation has occurred stereospecifically from the less hindered *exo*-face.[2] The *exo*-epoxide structure of **20** was confirmed by later reactions.

The epoxide (**20**) was allowed to react with 3-ethoxyacryloyl or 3-methoxy-2-methylacryloyl isocyanate to give the corresponding *N*-acylcarbamoyl derivatives (**22** and **23**).[13]

As a model study, the epoxide (**22**) was subjected to reductive amido bond cleavage reaction. Though the expected product (**24**) was obtained, an attempted uracil ring formation reaction of the reductive amido bond cleavage product (**24**) by heating with ammonium hydroxide in methanol (sealed tube) afforded the cyclonucleoside (**28**).[14] On the contrary, when the epoxide (**25**) was used in the above ammonia-catalyzed cyclization reaction, the bicyclic oxazolidine derivative (**30**) was obtained as a by-product together with the cyclonucleoside (**29**). It should be noted that the same compound (**30**) was also formed even in the reaction of **23** with sodium borohydride in methanol, and the ratio of the products (**25** and **30**) was approximately 1 : 1. These facts indicate that the presence of a methyl group on the acryloyl side chain of **25** retards the thymine ring formation, but enhances the base-catalyzed oxazolidine ring formation leading to **30**. Thus, the route shown in Chart 3 was unsuccessful for the synthesis of the desired epoxide (**27**), though it provided a new route to carbocyclic cyclonucleosides (**28** and **29**). The yield of **29** was increased remarkably by employing a higher temperature in the reaction. This, as well as the fact that transformation of cyclonucleosides to arabinosyl nucleosides has well been documented already,[15] suggests strongly that the compounds (**28** and **29**) would serve as precursors of carbocyclic arabinosyl nucleosides. A detailed study along this line is in progress and the result will be reported in due course.

Since direct cyclization of the epoxides (**24** and **25**) had failed to give the desired products (**26** and **27**), an alternative route shown in Chart 4 was then examined. Thus, the carbamoylated product (**31**) derived from the bicycloenamide (**1**) was directly subjected to the reductive amide bond cleavage reaction to give the ring-opened product (**32**), which was cyclized to the corresponding thymine (**33**). Silylation of **33** with *tert*-butyldimethylsilyl chloride

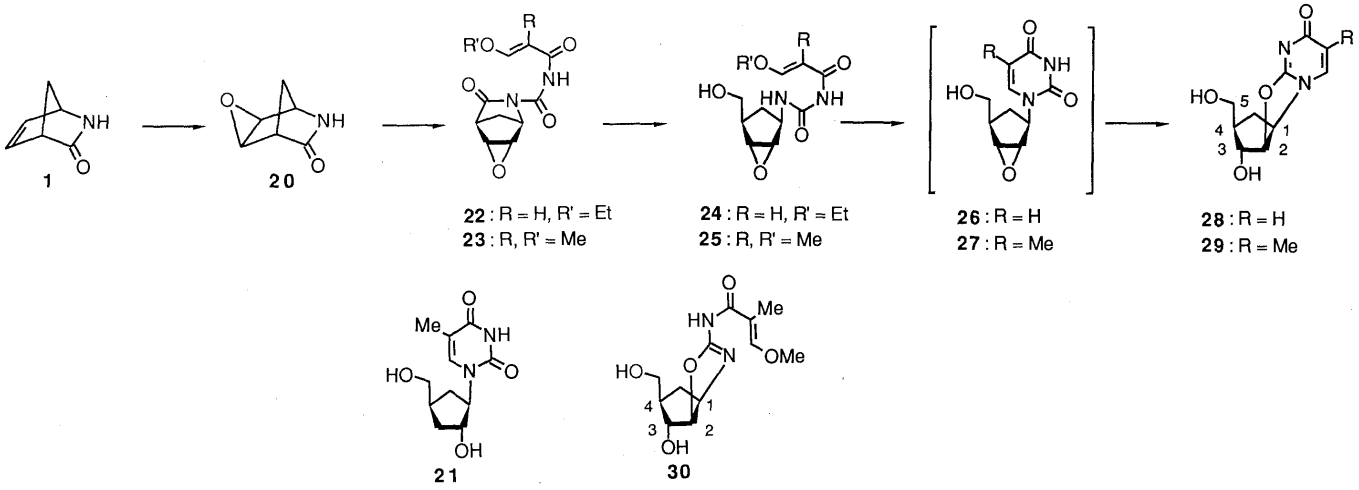

Chart 3

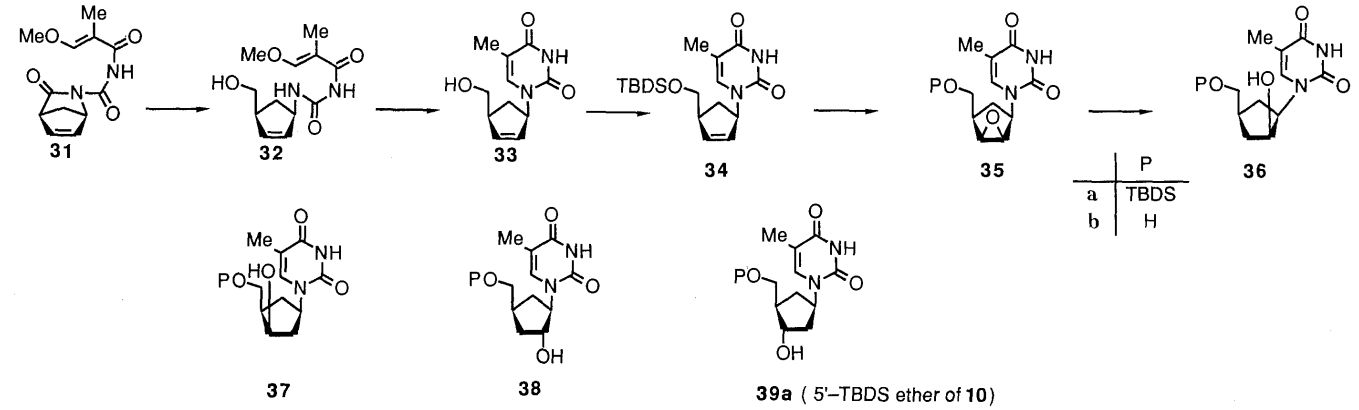

Chart 4

TABLE I. Reduction of **35a** to **36a** by Various Metal Hydrides

Entry	Reducing reagent	Solvent	Yield (%)
1	$LiEt_3BH$	THF	75
2	DIBAL	THF	48
3	Red-Al	THF	—
4	NaI, *n*-Bu_3SnH[17]	DMF	68

DIBAL = diisobutylaluminum hydride.

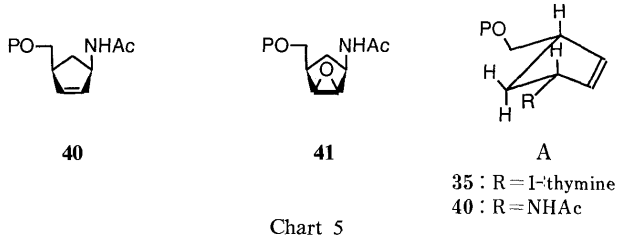

Chart 5

(TBDSCl) followed by epoxidation by *m*-CPBA gave the epoxide (**35a**) as a sole product. The epoxidation occurred from the more hindered face (the same face of both protected hydroxymethyl and 1-thymine groups) of **34** (*vide infra*).

Reduction of **35a** was then examined using a variety of reagents (Table I). In all cases, reductive C–O bond fission occurred at the 3'-position selectively to give the carbocyclic 3'-deoxyarabinothymine (**36a**) and none of its regioisomer (2'-deoxy derivative, **37a**) was obtained.[16] The same regioselectivity was also found when the unprotected cyclopentenol was used (**33**).

The structure of **36a** was determined after its hydrolysis to the corresponding alcohol (**36b**), whose melting point and spectral data were identical with those reported by Shealy *et al.*[9] Though the exact reason for the face selectivity in the epoxidation reaction is uncertain at present, Daluge and Vince reported that similar epoxidation of the corresponding amine derivative (**40**) also proceeded to give the all *cis*-epoxide (**41**).[18]

Though Daluge and Vince[18] rationalized this selectivity in terms of a favorable interaction between the peracid and the NH group in the allylamido function (allyl-NH-acyl),[19] it is more likely that the conformation depicted in formula A is a common factor (the upper face of A should be more hindered than the lower face due to the presence of two axial hydrogens irrespective of the amine moiety).

Alternatively, hydroboration–oxidation reaction of the protected cyclopentene (**34**) was examined (Chart 4). In this case, compound **38a** was obtained as the major product. However, regio- and stereoselectivities in this reaction were poor and two isomers (**36a** and **39a**), except for **37a**, were obtained concomitantly.

Synthesis of Carbocyclic Thymidine from the Corresponding Ribothymidine by Regioselective Removal of the 2'-Hydroxyl Group In this section, we describe how carbocyclic thymidine (**10**) was synthesized from the correspond-

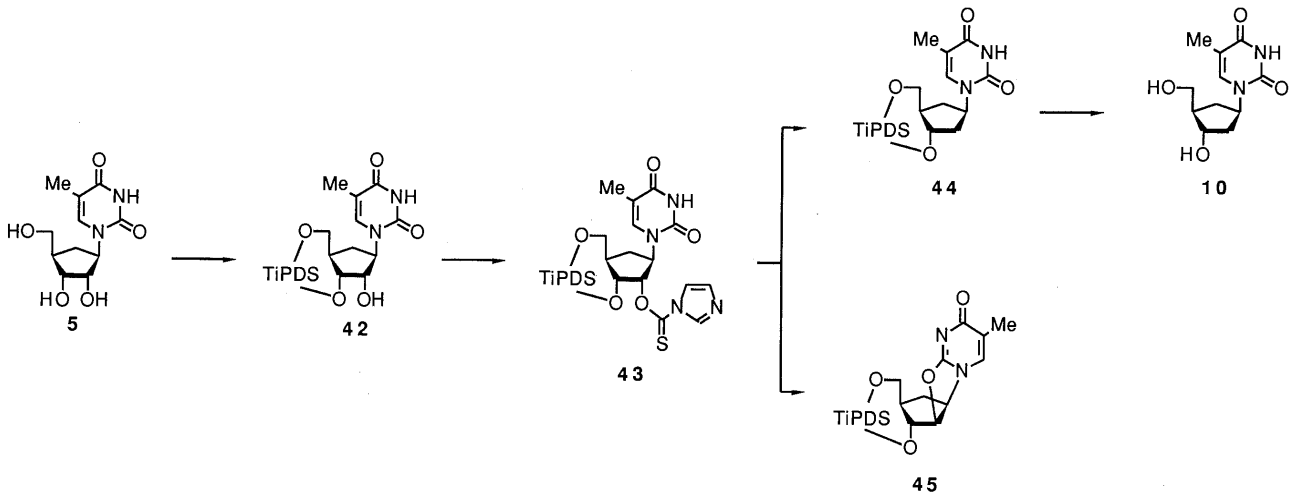

Chart 6

ing ribothymidine (**5**) by the route shown in Chart 6. This route, though long and used as a well-established procedure for nucleosides,[20] is advantageous for the present synthesis due to the ready availability of the starting ribothymidine (**5**) (*cf.* Chart 1).[2]

The 3′- and 5′-hydroxyl groups of **5** were protected with 1,3-dichloro-1,1,3,3-tetraisopropyldisiloxane ($TiPDSCl_2$) to give **42**. Then **42** was treated with bis(imidazol-1-yl)thione to give the 2′-*O*-(imidazol-1-yl)thiocarbonyl derivative (**43**). Reduction of **43** with tri-*n*-butyltin hydride then gave the 2′-deoxylated product (**44**), which, on treatment with tetrabutylammonium fluoride, led to the desired carbocyclic thymidine (**10**). It should be noted that mere heating of **43** in toluene afforded the cyclonucleoside (**45**). Obviously, in absence of an appropriate nucleophile, the intramolecular *SN*2 reaction proceeded due to the *trans* configuration of the 1′- and 2′-substituents.

Conclusion

The synthetic method for carbocyclic ribonucleosides previously developed in our laboratories[2] was employed for the synthesis of carbocyclic ribothymidine and related compounds by using the following three steps: 1) construction of the bicyclic enamide, 2) appropriate manipulation of the C=C bond, and 3) regioselective reductive amido bond cleavage under mild conditions with complete stereoselection. The present study has shown that the order of the second and third steps may be altered depending upon the structure of the target molecules. The main characteristics of the above methodology are: 1) the starting enamide (**1**) can be synthesized readily, 2) since the enamide has a rigid three dimensional shape, one can readily distinguish the two faces (*endo* and *exo*) of the C=C double bond and, thus, stereoselective manipulation at that function becomes possible, and 3) reductive amido bond cleavage, though it has some precedent,[21] has wide applicability and, if combined with the use of a suitable electron-withdrawing group which behaves as a masked heterocycle, provides the shortest route to the desired nucleosides.

Experimental

General All melting points were determined on a Yanagimoto micro-hot stage and are uncorrected. Infrared (IR) spectra were measured on a JASCO A-102 spectrometer. ^{1}H-Nuclear magnetic resonance (^{1}H-NMR) spectra were recorded with a JEOL JNM-PMX 60 or JEOL JNM-GX 500 spectrometer with tetramethylsilane (TMS) as an internal standard, and the abbreviations of signal patterns are as follows: s; singlet, d; doublet, t; triplet, q; quartet, m; multiplet, br; broad. High-resolution mass spectra (MS) were obtained on a JEOL JMS-DX-303 mass spectrometer. Wakogel (C-200) and Merck Kieselgel 60F 254 were employed for silica gel column and thin layer chromatography (TLC), respectively. The ratios of mixtures of solvents for chromatography are shown as volume/volume.

5,6-*exo*-Epoxy-2-azabicyclo[2.2.1]heptan-3-one (20) A solution of 2-azabicyclo[2.2.1]hept-5-en-3-one (**1**) (1.09 g, 10 mmol) and *m*-CPBA (3.45 g, 20 mmol) in CH_2Cl_2 (100 ml) was stirred at room temperature for 2 d. After removal of the precipitate by filtration, the filtrate was evaporated to dryness under reduced pressure. The residue was subjected to silica gel column chromatography. Elution with hexane–AcOEt (1 : 2) gave the product (**20**) (733 mg, 59%) as prisms (from CH_2Cl_2–hexane), mp 120 °C (sublimed). *Anal.* Calcd for $C_6H_7NO_2$: C, 57.58; H, 5.64; N, 11.20. Found: C, 57.79; H, 5.71; N, 11.04. IR ($CHCl_3$): 3360, 1720 cm^{-1}. ^{1}H-NMR ($CDCl_3$, 60 MHz) δ: 1.66 (1H, br d, J=10 Hz, CH–H), 1.92 (1H, br d, J=10 Hz, CH–H), 2.92 (1H, br s, C_4-H), 3.58 (1H, dd, J=4, 2 Hz, C_5-H or C_6-H), 3.72 (1H, dd, J=4, 2 Hz, C_5-H or C_6-H), 3.91 (1H, m, C_1-H), 6.90 (1H, br s, NH).

5,6-*exo*-Epoxy-2-[*N*-(3-ethoxyacryloyl)]carbamoyl-2-azabicyclo[2.2.1]-heptan-3-one (22)] A suspension of 3-ethoxyacryloyl chloride (804 mg, 6 mmol) and silver cyanate (900 mg, 6 mmol) in dry benzene (10 ml) was stirred at room temperature under an argon atmosphere for 3 h. The solution thus prepared contained 3-ethoxyacryloyl isocyanate. Compound **20** (250 mg, 2 mmol) was added to this suspension, and the mixture was stirred at room temperature for 3 h. After removal of the precipitate by filtration, the solvent was evaporated off under reduced pressure. The residue was subjected to silica gel column chromatography. Elution with AcOEt gave the product (**22**) (383 mg, 72%) as prisms (from CH_2Cl_2–hexane), mp 132—133 °C. *Anal.* Calcd for $C_{12}H_{14}N_2O_5$: C, 54.12; H, 5.30; N, 10.54. Found: C, 54.39; H, 5.30; N, 10.51. IR ($CHCl_3$): 3300, 1755, 1720, 1685 cm^{-1}. ^{1}H-NMR ($CDCl_3$, 60 MHz) δ: 1.36 (3H, t, J=7 Hz, Me), 1.80 (2H, m, CH_2), 3.20 (1H, m, C_4-H), 3.72 (1H, dd, J=4, 2 Hz, C_5-H or C_6-H), 3.92 (1H, dd, J=4, 2 Hz, C_5-H or C_6-H), 4.02 (2H, q, J=7 Hz, OCH_2Me), 4.92 (1H, m, C_1-H), 6.27 (1H, d, J=12 Hz, acryloyl C_2-H), 7.83 (1H, d, J=12 Hz, acryloyl C_3-H), 9.83 (1H, br s, NH).

(±)-2α,3α-Epoxy-1β-[*N*′-(3-ethoxyacryloyl)ureido]-4β-hydroxymethyl-cyclopentane (24) Sodium borohydride (190 mg, 5 mmol) was added to a stirred, ice-cooled solution of **22** (266 mg, 1 mmol) in MeOH (10 ml). The mixture was stirred at room temperature for 30 min, and neutralized with AcOH–MeOH (1 : 10). The solvent was evaporated off under reduced pressure, and water was added to the residue. The mixture was extracted with AcOEt. The extract was dried over anhydrous sodium sulfate, and concentrated under reduced pressure. The residue was subjected to silica gel column chromatography. Elution with AcOEt gave the product (**24**) (184 mg, 68%) as needles (from CH_2Cl_2–hexane), mp 140—141 °C. *Anal.* Calcd for $C_{12}H_{18}N_2O_5$: C, 53.31; H, 6.72; N, 10.37. Found: C, 53.32; H, 6.75; N, 10.32. IR ($CHCl_3$): 3650, 3450, 3300, 1700, 1675 cm^{-1}. ^{1}H-NMR

($CDCl_3$, 60 MHz) δ: 1.37 (3H, t, J=7 Hz, Me), 1.98—2.77 (4H, m, CH_2, C_4-H and OH), 3.50 (2H, t, J=3 Hz, C_2- and C_3-H), 3.80 (2H, d, J=4 Hz, $C\underline{H}_2OH$), 3.96 (2H, q, J=7 Hz, $OC\underline{H}_2Me$), 4.57 (1H, m, C_1-H), 5.37 (1H, d, J=12 Hz, acryloyl C_2-H), 7.63 (1H, d, J=12 Hz, acryloyl C_3-H), 9.12 (1H, br d, J=9 Hz, NH), 9.70 (1H, br s, NH).

5,6-*exo*-Epoxy-2-[*N*-(3-methoxy-2-methylacryloyl)carbamoyl]-2-azabicyclo[2.2.1]heptan-3-one (23) A suspension of 3-methoxy-2-methylacryloyl chloride (405 mg, 3 mmol) and silver cyanate (450 mg, 3 mmol) in dry benzene (5 ml) was refluxed under an argon atmosphere for 1 h. The solution thus prepared contained 3-methoxy-2-methylacryloyl isocyanate. Compound **20** (1.97 g, 10.8 mmol) was added to this solution. The mixture was then stirred at 50 °C for 3 h. After removal of the precipitate by filtration, the filtrate was evaporated to dryness under reduced pressure. The residue was subjected to silica gel column chromatography. Elution with hexane–AcOEt (1 : 1) gave the product (**23**) (437 mg, 82%) as an oil. High-resolution MS m/z Calcd for $C_{12}H_{14}N_2O_5$ (M^+): 266.0902. Found: 266.0879. IR ($CHCl_3$, 60 MHz): 3325, 1760, 1740, 1695 cm^{-1}. ^{1}H-NMR ($CDCl_3$, 60 MHz) δ: 1.66 (1H, br d, J=10 Hz, CH–H), 1.80 (3H, d, J=1 Hz, Me), 1.95 (1H, br d, J=10 Hz, CH–H), 3.20 (1H, m, C_4-H), 3.67 (1H, dd, J=4, 2 Hz, C_5-H or C_6-H), 3.90 (4H, br s, OMe and C_5-H or C_6-H), 4.97 (1H, m, C_1-H), 7.30 (1H, d, J=1 Hz, acryloyl C_3-H), 10.50 (1H, br s, NH).

(±)-2α,3α-Epoxy-4β-hydroxymethyl-1β-[*N'*-(3-methoxy-2-methylacryloyl)ureido]cyclopentane (25) Sodium borohydride (380 mg, 10 mmol) was added to a stirred, ice-cooled solution of **23** (532 mg, 2 mmol) in MeOH (20 ml). The mixture was stirred at room temperature for 30 min, and neutralized with AcOH–MeOH (1 : 10). The solvent was evaporated off under reduced pressure, and water was added to the residue. The mixture was extracted with AcOEt. The extract was dried over anhydrous sodium sulfate, and concentrated under reduced pressure. The residue was subjected to silica gel column chromatography. Elution with AcOEt gave the product (**25**) (237 mg, 44%) as a powder (from CH_2Cl_2–hexane), mp 152—154 °C. High-resolution MS m/z Calcd for $C_{12}H_{18}N_2O_5$ (M^+): 270.1215. Found: 270.1219. IR ($CHCl_3$): 3650, 3475, 3300, 1695, 1660 cm^{-1}. ^{1}H-NMR ($CDCl_3$, 60 MHz) δ: 1.00—2.66 (4H, m, CH_2, C_4-H and OH), 1.75 (3H, d, J=1 Hz, Me), 3.73 (5H, br and s, OMe and $C\underline{H}_2OH$), 4.53 (1H, td, J=8, 1 Hz, C_1-H), 7.33 (1H, d, J=1 Hz, acryloyl C_3-H), 8.23 (1H, br s, NH), 9.10 (1H, br d, J=8 Hz, NH). UV λ_{max}^{water} nm: 221. Further elution with AcOEt gave the product (**30**) (216 mg, 40%) as a powder (from AcOEt), mp 158—160 °C. High-resolution MS m/z Calcd for $C_{12}H_{18}N_2O_5$ (M^+): 270.1215. Found: 270.1208. IR (Nujol): 3320, 1715 cm^{-1}. ^{1}H-NMR (CD_3OD–$CDCl_3$, 60 MHz) δ: 1.20—2.50 (3H, m, CH_2 and C_4-H), 1.76 (3H, d, J=1 Hz, Me), 3.67 (2H, d, J=5 Hz, $C\underline{H}_2OH$), 3.90 (3H, s, OMe), 4.00—5.00 (3H, m, C_1-H, C_2-H and C_3-H), 7.30 (1H, d, J=1 Hz, acryloyl C_3-H). UV λ_{min}^{water} nm: 244.

Carbocyclic Analogue (28) of O^2,2'-Cyclouridine A solution of **24** (200 mg, 0.74 mmol) in a mixture of MeOH (10 ml) and concentrated NH_4OH (4 ml) was heated at 50 °C in a sealed tube for 12 h. The solvent was evaporated off under reduced pressure. The residue was subjected to silica gel column chromatography. Elution with 10% MeOH–AcOEt gave the product (**28**), mp 238—239 °C. High-resolution MS m/z Calcd for $C_{10}H_{12}N_2O_4$ (M^+): 224.0796. Found: 224.0841. IR (KBr): 3360, 3250, 1655 cm^{-1}. ^{1}H-NMR (DMSO-d_6–$CDCl_3$, 500 MHz) δ: 1.68 (1H, ddd, J=14, 7.5, 5 Hz, CH–H), 1.96 (1H, m, $C_{4'}$-H), 2.55 (1H, ddd, J=14, 7.5, 7.5 Hz, CH–H), 3.30 (1H, m, CHHOH), 3.40 (1H, ddd, J=10, 5, 5 Hz, CHHOH), 3.97 (1H, ddd, J=7.5, 7.5, 5 Hz, $C_{3'}$-H), 4.62 (1H, t, J=5 Hz, OH), 4.85 (1H, ddd, J=7.5, 7.5, 5 Hz, $C_{1'}$-H), 4.99 (1H, dd, J=7.5, 5 Hz, $C_{2'}$-H), 5.53 (1H, d, J=5 Hz, OH), 5.82 (1H, d, J=7.5 Hz, C_5-H), 7.75 (1H, d, J=7.5 Hz, C_6-H). UV λ_{max}^{water} nm: 256, 233; λ_{min}^{water}: 237.

Carbocyclic Analogue (29) of O^2,2'-Cycloribothymidine A solution of **25** (100 mg, 0.37 mmol) in a mixture of MeOH (5 ml) and concentrated NH_4OH (2 ml) was heated at 50 °C in a sealed tube for 12 h. The solvent was evaporated off under reduced pressure. The residue was subjected to silica gel column chromatography. Elution with AcOEt gave **30** (20 mg, 20%). Further elution with 10% MeOH–AcOEt gave **29** (47 mg, 53%) as a powder (from MeOH–AcOEt), mp 214—216 °C. High-resolution MS m/z Calcd for $C_{11}H_{14}N_2O_4$(M^+): 238.0953. Found: 238.0966. IR (Nujol): 3250, 1665 cm^{-1}. ^{1}H-NMR (CD_3OD–$CDCl_3$, 500 MHz) δ: 1.83 (1H, ddd, J=12, 7.5, 5 Hz, CH–H), 1.93 (3H, s, Me), 2.13 (1H, m, $C_{4'}$-H), 2.53 (1H, ddd, J=12, 7.5, 7.5 Hz, CH–H), 3.50 (1H, dd, J=11.3, 7.5 Hz, CHHOH), 3.61 (1H, dd, J=11.3, 5 Hz, CHHOH), 4.12 (1H, dd, J=7.5, 5 Hz, $C_{3'}$-H), 4.85 (1H, ddd, J=7.5, 7.5, 5 Hz, $C_{1'}$-H), 5.09 (1H, dd, J=7.5, 5 Hz, $C_{2'}$-H), 7.75 (1H, s, C_6-H). UV λ_{max}^{water} nm: 261, 226; λ_{min}^{water} nm: 238.

2-[*N*-(3-Methoxy-2-methylacryloyl)carbamoyl]-2-azabicyclo[2.2.1]hept-5-en-3-one (31) Silver cyanate (7.50 g, 50.0 mmol) was added to an anhydrous benzene solution (150 ml) of 3-methoxy-2-methylacryloyl chloride (5.04 g, 37.5 mmol) and the whole was stirred at 50 °C for 3 h, then filtered. To the filtrate was added the adduct (**1**) (2.72 g, 25.0 mmol) and the whole was again stirred at 50 °C for a further 5 h. The residue obtained by evaporation of the solvent was subjected to column chromatography over silica gel (270 g). Elution with hexane–AcOEt (1 : 1) gave 6.0 g (96%) of **31**, mp 126 °C (AcOEt). *Anal.* Calcd for $C_{12}H_{14}N_2O_4$: C, 57.59; H, 5.64; N, 11.20. Found: C, 57.68; H, 5.54; N, 11.13. IR ($CHCl_3$): 3280, 1750, 1725 cm^{-1}. ^{1}H-NMR ($CDCl_3$, 60 MHz) δ: 1.82 (3H, s, Me), 2.31 (2H, m, C_7-H), 3.53 (1H, m, C_4-H), 3.85 (3H, s, MeO), 5.33 (1H, m, C_1-H), 6.70 (1H, ddd, J=6, 4, 2 Hz, C_5- or C_6-H), 7.00 (1H, dd, J=6, 2 Hz, C_5- or C_6-H), 7.30 (1H, s, acryloyl C_3-H).

(±)-4β-Hydroxymethyl-1β-[*N'*-(3-methoxy-2-methylacryloyl)ureido]cyclopent-2-ene (32) Sodium borohydride (345 mg, 9.08 mmol) was added to a solution of **31** (1.14 g, 4.55 mmol) in absolute MeOH (45 ml) and the mixture was stirred at room temperature for 1 h. Excess sodium borohydride was decomposed by addition of AcOH–MeOH (1 : 1) and the solvent was evaporated off *in vacuo*. The residue thus obtained was chromatographed over silica gel (100 g). Elution with hexane–AcOEt (1 : 1) gave 1.06 g (91%) of **32**, mp 120—122 °C (AcOEt–hexane). *Anal.* Calcd for $C_{12}H_{18}N_2O_4$: C, 56.68; H, 7.14; N, 11.02. Found: C, 56.69; H, 7.07; N, 10.83. IR ($CHCl_3$): 3640, 3460, 3300, 1690, 1660 cm^{-1}. ^{1}H-NMR ($CDCl_3$, 60 MHz) δ: 1.78 (3H, s, Me), 1.3—3.0 (4H, m, OH, C_4- and C_5-H), 3.64 (2H, m, $C\underline{H}_2OH$), 3.84 (3H, s, MeO), 4.96 (1H, m, C_1-H), 5.85 (2H, s, C_2- and C_3-H), 7.34 (1H, s, acryloyl C_3-H), 8.36 (1H, br s, NH), 8.81 (1H, br d, J=10 Hz, NH).

(±)-1-(4'β-Hydroxymethylcyclopent-2'-en-1'β-yl)-5-methyl-2,4(1*H*,3*H*)-pyrimidinedione (33) Compound **32** (1.00 g, 3.94 mmol) in a mixture of MeOH (32 ml) and 25% ammonia (22 ml) was heated in a sealed cylinder at 85 °C for 24 h. The residue obtained after evaporation of the solvent was chromatographed over silica gel (100 g). Elution with $CHCl_3$–MeOH (30 : 1) gave 817 mg (93%) of **33**, mp 218 °C (MeOH). *Anal.* Calcd for $C_{11}H_{14}N_2O_3$: C, 59.45; H, 6.35; N, 12.61. Found: C, 59.61; H, 6.17; N, 12.55. IR (Nujol): 3450, 1710 cm^{-1}. ^{1}H-NMR (DMSO-d_6, 500 MHz) δ: 1.35 (1H, ddd, J=13, 7, 7 Hz, $C_{5'}$-H), 1.75 (3H, s, Me), 2.45—2.52 (1H, m, $C_{5'}$-H), 2.80 (1H, m, $C_{4'}$-H), 3.42 (1H, ddd, J=10, 5, 5 Hz, CHHOH), 3.49 (1H, ddd, J=10, 5, 5 Hz, CHHOH), 4.72 (1H, t, J=5 Hz, OH), 5.51 (1H, m, $C_{1'}$-H), 5.67 (1H, m, $C_{3'}$-H), 6.08 (1H, m, $C_{2'}$-H), 7.34 (1H, s, $C_{6'}$-H), 11.21 (1H, s, NH).

(±)-1-[4'β-(*tert*-Butyldimethylsilyloxy)methylcyclopent-2'-en-1'β-yl]-5-methyl-2,4(1*H*,3*H*)-pyrimidinedione (34) Under cooling by ice-water, *tert*-butyldimethylsilyl chloride (706 mg, 4.69 mmol) and imidazole (666 mg, 9.79 mmol) were added to a solution of **33** (871 mg, 3.92 mmol) in *N*,*N*-dimethylformamide (DMF) (8 ml) and the whole was stirred at room temperature for 15 h. After addition of ice-water to the reaction mixture, the product was extracted with ether. The extract was dried over Na_2SO_4, the solvent was evaporated off, and the residue was chromatographed over silica gel (40 g). Elution with hexane–AcOEt (2 : 1) afforded 1.29 g (98%) of **34**, mp 161 °C (Et_2O). *Anal.* Calcd for $C_{17}H_{28}N_2O_3Si$: C, 60.68; H, 8.39; N, 8.33. Found: C, 60.58; H, 8.45; N, 8.26. IR ($CHCl_3$): 1690 cm^{-1}. ^{1}H-NMR ($CDCl_3$, 60 MHz) δ: 0.06 (6H, s, Me_2Si), 0.86 (9H, s, *tert*-Bu), 1.1—1.5 (1H, m, $C_{5'}$-H), 1.92 (3H, d, J=1 Hz, Me), 2.5—3.1 (2H, m, $C_{4'}$- and $C_{5'}$-H), 3.65 (2H, m, $C\underline{H}_2OSi$), 5.61 (1H, m, $C_{1'}$-H), 5.76 (1H, m, $C_{3'}$-H), 6.06 (1H, m, $C_{2'}$-H), 7.06 (1H, q, J=1 Hz, C_6-H), 9.73 (1H, br s, NH).

(±)-1-[4'β-(*tert*-Butyldimethylsilyloxy)methyl-2'β,3'β-epoxycyclopent-1'β-yl]-5-methyl-2,4(1*H*,3*H*)-pyrimidinedione (35a) *m*-CPBA (211 mg, 1.22 mmol) was added to a solution of **34** (275 mg, 0.82 mmol) in anhydrous CH_2Cl_2 (5.5 ml) and the solution was kept standing at room temperature for 3 d. The residue obtained after evaporation of the solvent was chromatographed over silica gel (40 g). Elution with hexane–AcOEt (5 : 1) afforded 241 mg (84%) of **35a**. Further elution with the same solvent afforded 27 mg of the recovered material (**34**). **35a**: mp 151—153 °C (Et_2O). High-resolution MS m/z Calcd for $C_{13}H_{28}N_2O_4Si$ ($M^+ - tert$-Bu): 295.1114. Found: 295.1139. IR ($CHCl_3$): 1690 cm^{-1}. ^{1}H-NMR ($CDCl_3$, 500 MHz) δ: 0.09 and 0.10 (each 3H, s, Me_2Si). 0.92 (9H, s, *tert*-Bu), 1.95 (3H, d, J=1.0 Hz, Me), 2.30 (1H, ddd, J=13.0, 8.0, 8.0 Hz, $C_{5'}$-H), 2.33 (1H, m, $C_{4'}$-H), 3.61 and 3.62 (each 1H, dd, J=9.0, 1.0 Hz, $C\underline{H}_2OH$), 3.70 (1H, s, $C_{3'}$-H), 3.71 (1H, d, J=2.0 Hz, $C_{2'}$-H), 5.05 (1H, ddd, J=8.0, 8.0, 2.0 Hz, $C_{1'}$-H), 7.51 (1H, q, J=1.0 Hz, C_6-H).

(±)-1-[4'β-(*tert*-Butyldimethylsilyloxy)methyl-2'β-hydroxycyclopent-1'β-yl]-5-methyl-2,4(1*H*,3*H*)-pyrimidinedione (36a) Method A: Lithium triethylborohydride–tetrahydrofuran (THF) (1 M solution, 0.66 ml) was added under an argon atmosphere to an ice-cooled solution of **35a** (69 mg, 0.20 mmol) in THF (5 ml) and the mixture was stirred at room temperature

for 15 h. After decomposition of the reducing reagent by the addition of 5% aqueous AcOH (1.4 ml), THF (3 ml) and $MgSO_4$ were added to the solution and the whole was stirred vigorously. After 30 min, the solution was filtered and the solvent was evaporated off. The residue obtained was chromatographed over silica gel (8 g) with hexane–AcOEt (3 : 1) to give 52 mg (75%) of **36a**, mp 168—169 °C (Et_2O–hexane). High-resolution MS *m/z* Calcd for $C_{17}H_{30}N_2O_4Si$ (M^+): 354.1975. Found: 354.2021. IR ($CHCl_3$): 3420, 1690 cm^{-1}. ^{1}H-NMR ($CDCl_3$, 500 MHz) δ: *inter alia* 0.16 and 0.17 (each 3H, s, Me_2Si), 0.97 (9H, s, *tert*-Bu), 1.90 (3H, d, J=1.0 Hz, Me), 3.65 and 3.67 (each 1H, dd, J=12.0, 3.0 Hz, CH_2OSi), 4.09 (1H, ddd, J=9.0, 5.0, 5.0 Hz, $C_{2'}$-H), 4.75 (1H, ddd, J=14.0, 8.0, 3.0 Hz, $C_{1'}$-H), 7.79 (1H, q, J=1.0 Hz, C_6-H).

Method B: Under vigorous stirring in an argon atmosphere, diisobutylaluminum hydride–THF (1.5 M solution, 0.76 ml) was added to an anhydrous THF solution (5 ml) of **35a** (134 mg, 0.38 mmol) cooled at −78 °C. Stirring was continued at room temperature for 15 h, then excess reagent was decomposed by the addition of water (1.5 ml). After addition of THF (10 ml) and $MgSO_4$, the whole was kept stirring vigorously for several minutes, then filtered to remove insoluble inorganic materials. The filtrate was evaporated to dryness. The residue obtained was chromatographed over silica gel (7 g) with hexane–AcOEt (3 : 1) to give 65 mg (49%) of **36a**. Further elution with the same solvent gave 10 mg of the recovered material (**35a**).

Method C: Tetra-*n*-butyltin hydride (516 mg, 1.77 mmol) and azobisisobutyronitrile (AIBN, 76 mg, 0.46 mmol) were added to an anhydrous 1,2-dimethoxyethane (5.8 ml) solution of **35a** (204 mg, 0.58 mmol) under an argon atmosphere. After 3 h, the solvent was evaporated off and the residue was dissolved in a mixture of water and ether. The organic layer was separated and dried over $MgSO_4$. The residue obtained after evaporation of the solvent was chromatographed over silica gel (30 g) with hexane–AcOEt (3 : 1) to give 139 mg (68%) of **36a**.

(±)-1-(2′β-Hydroxy-4′β-hydroxymethylcyclopent-1′β-yl)-5-methyl-2,4(1*H*,3*H*)-pyrimidinedione (36b) A mixture of **36a** (24 mg, 0.067 mmol) and *n*-Bu_4NF–THF (1 M solution, 0.1 ml) in THF (2 ml) was kept standing at room temperature for 1 d. The residue obtained after evaporation of the solvent was chromatographed over silica gel (2 g) with $CHCl_3$–MeOH (30 : 1) to give 16 mg (97%) of **36b**, mp 220—222 °C (EtOH) [lit.[8] mp 219—221 °C (EtOH)].

(±)-1-(2′α-Hydroxy-4′β-hydroxymethylcyclopent-1′β-yl)-5-methyl-2,4(1*H*,3*H*)-pyrimidinedione (38b) BH_3–THF (1 M solution, 0.48 ml) was added to a solution of **34** (136 mg, 0.40 mmol) in THF (2 ml) under ice-cooling and the mixture was stirred at room temperature for 3 d. After evaporation of the solvent, the residue was dissolved in xylene (4 ml) and, after addition of trimethylamine *N*-oxide dihydrate (129 mg, 0.57 mmol), the whole was refluxed for 10 h. The residue obtained after evaporation of the solvent was chromatographed over silica gel (10 g) to give 65 mg of a mixture of **36a**, **38a**, and **39a**. Though attempts to separate these three products were unsuccessful, their structures and ratio were determined by analysis of the NMR spectrum. ^{1}H-NMR ($CDCl_3$, 500 MHz) δ: *inter alia* 4.61 (1H × 6/8, J=12.0, 7.0, 7.0 Hz, $C_{1'}$-H of **38a**), 4.72 (1H × 1/8, ddd, J=14.0, 8.0, 3.0 Hz, $C_{1'}$-H of **36a**), 5.14 [1H × 1/8, m, $C_{1'}$-H of **39a** (5′-TBDS ester of **10**)].

The mixture was dissolved in THF (3 ml) and, after addition of *n*-Bu_4NF–THF (1 M solution, 0.5 ml), the whole was stirred for 1 d. The residue obtained after evaporation of the solvent was chromatographed over silica gel (6 g) with $CHCl_3$–MeOH (30 : 1) to give 24 mg (25% from **34**) of **38b** (desilylated product of **38a**), mp 205—208 °C (EtOH) [lit.[10] mp 207—210 °C (EtOH)].

Carbocyclic (±)-3′,5′-*O*-(Tetraisopropyldisiloxanyl)ribothymidine (42) A mixture of **5** (338 mg, 1.32 mmol) and 1,3-dichloro-1,1,3,3-tetraisopropyldisiloxane (458 mg, 1.45 mmol) in DMF–pyridine (2 : 1, 20 ml) was stirred at 0 °C for 1 h. The reaction mixture was poured into ice-water, and extracted with ether. The extract was dried over anhydrous sodium sulfate, and the solvent was evaporated off under reduced pressure. The residue was subjected to silica gel column chromatography. Elution with hexane–AcOEt (2 : 1) gave the product (**42**) (446 mg, 68%) as a foam. High-resolution MS *m/z* Calcd for $C_{20}H_{35}N_2O_6Si_2$ [$M^+ - CH(CH_3)_2$]: 455.2031. Found: 455.2036. IR ($CHCl_3$): 3540, 3410, 1705, 1690 cm^{-1}. ^{1}H-NMR ($CDCl_3$, 60 MHz) δ: *inter alia* 1.92 (3H, s, Me), 2.18 (3H, m, $C_{4'}$-H and CH_2), 3.00 (1H, br s, OH), 3.90 (2H, m, CH_2OSi), 4.30 (3H, m, $C_{1'}$-H, $C_{2'}$-H and $C_{3'}$-H), 7.00 (1H, br s, C_6-H), 8.97 (1H, br s, NH).

Carbocyclic (±)-2′-*O*-(1*H*-Imidazol-1-yl)thiocarbonyl-3′,5′-*O*-(tetraisopropyldisiloxanyl)ribothymidine (43) A mixture of **42** (56 mg, 0.11 mmol) and bis(imidazol-1-yl)thione (49 mg, 0.27 mmol) in DMF (0.5 ml) was stirred for 12 h at room temperature. The reaction mixture was poured into ice-water, and extracted with ether. The extract was dried over anhydrous sodium sulfate and the solvent was evaporated off under reduced pressure. The residue was subjected to silica gel column chromatography. Elution with hexane–AcOEt (1 : 1) gave the product (**43**) (53 mg, 79%) as a foam. High-resolution MS *m/z* Calcd for $C_{23}H_{40}N_2O_5Si_2$ ($M^+ - C_4H_4N_2OS$): 480.2473. Found: 480.2441. IR ($CHCl_3$): 3410, 1705, 1690 cm^{-1}. ^{1}H-NMR ($CDCl_3$, 60 MHz) δ: *inter alia* 1.92 (3H, s, Me), 2.18 (3H, m, $C_{4'}$-H and CH_2), 3.95 (2H, m, CH_2OSi), 4.41 (1H, m, $C_{1'}$-H), 4.75 (1H, m, $C_{3'}$-H), 5.88 (1H, dd, J=6, 2 Hz, $C_{2'}$-H), 6.88 (1H, br s, imidazolyl C_4-H), 7.03 (1H, br s, imidazolyl C_5-H), 7.61 (1H, br s, C_6-H), 8.34 (1H, s, imidazolyl C_2-H), 9.12 (1H, br s, NH).

Carbocyclic (±)-3′,5′-*O*-(Tetraisopropyldisiloxanyl)thymidine (44) A mixture of 2,2′-azobis-2-methylpropionitrile (11 mg, 0.07 mmol) and tri-*n*-butyltin hydride (68 mg, 0.23 mmol) in dry toluene was added to a solution of **43** (60 mg, 0.10 mmol) in dry toluene, and the whole was heated at 75—80 °C under a nitrogen atmosphere. After 1 h, the solvent was evaporated off under reduced pressure, and the residue was subjected to silica gel column chromatography. Elution with hexane–AcOEt (3 : 1) gave the product (**44**) (32 mg, 67%) as colorless needles (from ether–hexane), mp 160—161 °C. High-resolution MS *m/z* Calcd for $C_{20}H_{35}N_2O_5Si_2$ [$M^+ - CH(Me)_2$]: 439.2082. Found: 439.2065. IR ($CHCl_3$): 3410, 1705, 1690 cm^{-1}. ^{1}H-NMR ($CDCl_3$, 60 MHz) δ: *inter alia* 1.92 (3H, s, Me), 3.70 (1H, dd, J=10, 3 Hz, $CHHOSi$), 4.02 (1H, dd, J=10, 2 Hz, $CHHOSi$), 4.42 (1H, m, $C_{3'}$-H), 5.12 (1H, m, $C_{1'}$-H), 6.95 (1H, br s, C_6-H), 9.22 (1H, br s, NH).

(±)-Carbocyclic Thymidine (10) A 1 N solution of tetrabutylammonium fluoride in THF (0.15 ml) was added to a solution of **44** (30 mg, 0.06 mmol) in THF (1 ml), and the mixture was stirred for 2 h at room temperature. The solvent was evaporated off *in vacuo*, and the residue was subjected to silica gel column chromatography. Elution with $CHCl_3$–MeOH (20 : 1) gave the product (**10**) (13 mg, 90%) as needles (from EtOH), mp 228—230 °C (lit.,[10] mp 218—220 °C).

Carbocyclic (±)-3′,5′-*O*-(Tetraisopropyldisiloxanyl)-*O*^{2},2′-cycloribothymidine (45) A solution of **43** (66 mg, 0.11 mmol) in absolute toluene (1 ml) was refluxed for 7 h. The residue obtained after evaporation of the solvent was chromatographed over silica gel (3 g). Elution with $CHCl_3$–MeOH (20 : 1) afforded 49 mg (94%) of **45**, mp 225—227 °C (Et_2O). High-resolution MS *m/z* Calcd for $C_{23}H_{40}N_2O_5Si_2$ (M^+): 480.2476. Found: 480.2482. UV λ_{max}^{MeOH}: 228, 259 nm. IR ($CHCl_3$): 1670, 1640 cm^{-1}. ^{1}H-NMR ($CDCl_3$, 60 MHz) δ: *inter alia* 1.96 (3H, d, J=1 Hz, Me), 3.86 (2H, m, CH_2OSi), 4.12 (1H, m, $C_{3'}$-H), 4.6—5.2 (2H, m, $C_{1'}$- and $C_{2'}$-H), 7.05 (1H, q, J=1 Hz, C_6-H). This compound (**45**) was deblocked by treatment with tetra-*n*-butylammonium fluoride to give the known carbocyclic cycloribothymidine.[2]

Acknowledgement This work was supported in part by a Grant-in-Aid for Cancer Research (No. 02152013) from the Ministry of Education, Science and Culture, Japan.

References and Notes

1) Part XXI: N. Katagiri, H. Sato, and C. Kaneko, *Chem. Pharm. Bull.*, **38**, 3184 (1990).
2) N. Katagiri, M. Muto, M. Nomura, T. Higashikawa, and C. Kaneko, *Chem. Pharm. Bull.*, **39**, 1112 (1991). See also, N. Katagiri, M. Muto, and C. Kaneko, *Tetrahedron Lett.*, **30**, 1645 (1989) and *idem*, *ibid.*, *Nucleic Acids Res., Symposium. Ser.*, **21**, 75 (1989).
3) This bicycloenamine (**1**) was synthesized from cyclopentadiene by means of the Diels–Alder reaction with either chlorosulfonyl isocyanate[3a] or tosyl cyanide[3b]: *a*) J. C. Jagt and A. M. van Leusen, *J. Org. Chem.*, **39**, 564 (1974); *b*) S. Daluge and R. Vince, *ibid.*, **43**, 2311 (1978).
4) Though conversion of the ureido function to the corresponding amine proceeds in **7** and related compounds (*e.g.* cyclobutyl- and cyclopentenylurea derivatives), the reaction sometimes gives the desired amines in poor yields. Recently, we have elaborated a more efficient method by using an alkoxycarbonyl group as the electron-withdrawing group before reductive amido bond cleavage, followed by basic hydrolysis of the resultant carbamates. Details of this method will be reported soon. N. Katagiri, M. Nomura, H. Sato, and C. Kaneko, *Nucleic Acids Res., Symposium Ser.*, **22**, 129 (1990).
5) Before our synthetic method[2] was elaborated, carbocyclic ribofuranosylamine had been synthesized from either norbornadiene,[5a] the corresponding dicarboxylate,[5b] or from the bicycloenamide (**1**)[5c]: *a*) Y. F. Shealy and J. D. Clayton, *J. Am. Chem. Soc.*, **88**, 3885 (1966);

idem, *ibid.*, **91**, 3075 (1969); *b*) M. Arita, K. Adachi, Y. Ito, H. Sawai, and M. Ohno, *ibid.*, **105**, 4049 (1983); *c*) R. C. Cermak and R. Vince, *Tetrahedron Lett.*, **22**, 2331 (1981).

6) Reviews for nucleosides: *a*) Y. Mizuno, "The Organic Chemistry of Nucleic Acids," Elsevier, Amsterdam, 1986; *b*) L. B. Townsend and R. S. Tipson (ed.), "Nucleic Acid Chemistry," Part 3, Wiley Interscience, New York, 1986.

7) *a*) Review of carbocyclic nucleosides: V. E. Marquez and M. I. Lim, *Med. Res. Rev.*, **6**, 1 (1986); *b*) Recent review of the synthesis of nucleoside derivatives aiming to obtain anti-HIV activity: F. G. De las Heras, M. J. Camarasa, and J. Fiandor, "Recent Progress in the Chemical Synthesis of Antibiotics," Springer-Verlag, Berlin, 1990, pp. 321—363.

8) K. C. Murdock and R. B. Angier, *J. Am. Chem. Soc.*, **84**, 3758 (1962).

9) Y. F. Shealy, C. A. O'Dell, M. C. Thorpe, and W. C. Coburn, Jr., *J. Heterocyclic Chem.*, **20**, 655 (1983) and references cited therein.

10) Y. F. Shealy and C. A. O'Dell, *J. Heterocyclic Chem.*, **13**, 1041 (1976).

11) Y. F. Shealy, C. A. O'Dell, and M. C. Thrope, *J. Heterocyclic Chem.*, **18**, 383 (1981).

12) G. Zweifel, K. Nagase, and H. C. Brown, *J. Am. Chem. Soc.*, **84**, 183 (1962).

13) It should be noted that the same epoxidation reaction if applied to the bicyclic enamide having an electron-withdrawing substituent at the 2-position proceeded at a much slower rate. Hence, in order to obtain **22** (or **23**), epoxidation prior to the acylcarbamoylation is superior to acylcarbamoylation prior to epoxidation.

14) References for cyclonucleosides (these compounds are also called anhydronucleosides): *a*) For a review: see reference 6*a*; *b*) For aza-analogues: S. Purkayastha and R. P. Panzica, *J. Heterocyclic Chem.*, **27**, 743 (1990); S. Purkayastha, C. J. Cheer, and R. P. Panzica, *ibid.*, **27**, 753 (1990).

15) D. M. Brown, D. B. Parihar, A. R. Todd, and S. Varadarajan, *J. Chem. Soc.*, **1958**, 3028.

16) Regioselective and reductive cleavage of epoxide by metal hydride has been successfully employed for the conversion of adenosine to 3′-deoxyadenosine (cordycepin): *a*) H. Bazin and J. Chattopadhyaya, *Synthesis*, **1985**, 1108; *b*) F. Hansske and M. J. Robins, *Tetrahedron Lett.*, **26**, 4295 (1985).

17) C. Banin, R. D. Fabio, G. Sotgiu, and S. Cavagnero, *Tetrahedron*, **45**, 2895 (1989).

18) S. Daluge and R. Vince, *J. Org. Chem.*, **43**, 2311 (1978).

19) G. Berti, *Top. Stereochem.*, **7**, 93 (1973) and references cited therein.

20) *a*) M. J. Robins and J. S. Wilson, *J. Am. Chem. Soc.*, **103**, 932 (1981); *b*) A. Matsuda, K. Pankiewicz, B. K. Marcus, K. A. Watanabe, and J. J. Fox, *Carbohydrate Res.*, **100**, 297 (1982).

21) The same methodology was applied successfully by Grieco *et al.* to base-catalyzed hydrolysis or methanolysis of lactams and amides. Thus, when *tert*-Boc was introduced at the nitrogen atom in the amide function, the corresponding ω-amino acids or esters were obtained under relatively mild conditions. D. L. Flynn, R. E. Zelle, and P. A. Grieco, *J. Org. Chem.*, **48**, 2424 (1983).

Tannins of *Stachyurus* Species. II.[1] Praecoxins A, B, C and D, Four New Hydrolyzable Tannins from *Stachyurus praecox* Leaves

Tsutomu HATANO, Kazufumi YAZAKI, Akira OKONOGI and Takuo OKUDA*

Faculty of Pharmaceutical Sciences, Okayama University, Tsushima, Okayama 700, Japan. *Received December 17, 1990*

Four new hydrolyzable tannins, praecoxins A (1), B (2), C (3) and D (4), were isolated from leaves of *Stachyurus praecox* SIEB. *et* ZUCC. (Stachyuraceae), and their structures were elucidated.

Keywords tannin; hydrolyzable tannin; *Stachyurus praecox*; Stachyuraceae; praecoxin A; praecoxin B; praecoxin C; praecoxin D; depsidone; valoneoyl group

Leaves and twigs of *Stachyurus praecox* SIEB. *et* ZUCC. (Stachyuraceae), known to be rich in tannins,[2] have been used as diuretics in Japan.[2] Isolation and structures of several hydrolyzable tannins, including *C*-glucosidic ellagitannins, from leaves of *Stachyurus praecox*,[1] and their biogenetic relationship[3] have been reported. Our further investigation of tannins of this plant has resulted in the isolation of additional hydrolyzable tannins, including four new tannins, from the leaves. We present here the full details of the isolation and structure elucidation of these new tannins, named praecoxins A (**1**), B (**2**), C (**3**) and D (**4**).[4]

Results and Discussion

Fresh leaves of *Stachyurus praecox* SIEB. *et* ZUCC. (Stachyuraceae) were homogenized in aqueous acetone, and the concentrated filtrate from the homogenate was extracted with Et_2O and EtOAc, successively. The EtOAc extract was separated by centrifugal partition chromatography (CPC),[5] and fractions containing tannins were further purified by column chromatography over Sephadex LH-20, to give **1**—**4**, along with 1,2,6-tri-*O*-galloyl-*β*-D-glucose,[6] tellimagrandin I,[1] casuarictin (**5**),[1] rugosin C (**6**)[7] and rugosin F.[8]

Praecoxin A (**1**) was obtained as a light-brown powder. The fast-atom bombardment mass spectrum (FAB-MS) of **1** showed the $[M+Na]^+$ ion peak at *m/z* 975, which corresponds to the molecular formula $C_{41}H_{28}O_{27}$. The proton nuclear magnetic resonance (^{1}H-NMR) spectrum of **1** showed signals of a hexahydroxydiphenoyl (HHDP) group [δ 6.54, 6.49 (1H in total, each s, H-3), 6.344, 6.340 (1H in total, each s, H-3′)], a valoneoyl group [δ 7.13 (1H, s, H-6″), 6.58, 6.57 (1H in total, each s, H-3), 6.25, 6.23 (1H, in total, each s, H-3′)] and a glucopyranose core (see Experimental), and the duplication of almost all of these signals indicated that **1** forms an anomer mixture. The coupling constants of the glucose protons are characteristic of those of a glucopyranose core taking the $^4C_1$ conformation. The large difference between the chemical shifts of the two H-6 protons on the $^4C_1$ glucose of each anomer of **1** (α-anomer, $\Delta\delta$ 1.50; β-anomer, $\Delta\delta$ 1.46) indicates that the HHDP moiety of the valoneoyl group (or the HHDP group) is at O-4/O-6 of the glucose core.[9] The remaining HHDP group (or the HHDP moiety of the valoneoyl group) is hence at O-2/O-3, since the chemical shifts of the glucose protons indicate that all the hydroxyl groups on the glucopyranose core, except for the anomeric hydroxyl group, are acylated.

Among the glucose proton signals in the ^{1}H-NMR spectrum of **1**, the H-4 and two H-6 protons showed some upfield shifts, relative to those of pedunculagin (**7**)[10] [$\Delta\delta$ 0.15 (H-4), 0.15 and 0.16 (H-6) (α-anomer); $\Delta\delta$ 0.14 (H-4), 0.14 and 0.15 (H-6) (β-anomer)], while the corresponding shifts of H-2 and H-3 are within 0.09 ppm. Analogous upfield shifts were also observed for the glucose H-4 and H-6 of **6** (which has a valoneoyl group at O-4/O-6),[7] relative to those of **5** [$\Delta\delta$ 0.11 (H-4), 0.15 and 0.12 (H-6)]. Therefore, the valoneoyl group in **1** is assumed to be at O-4/O-6 of the glucose core. A broad positive peak in the short-wavelength region[7,11] ($[\theta]_{223}+1.2\times10^5$, $[\theta]_{236}+1.1\times10^5$) of the circular dichroism (CD) spectrum of **1** indicated that the absolute configuration of the HHDP group and that of the valoneoyl group are both *S*. The orientation of the valoneoyl group in **1** is the same as that in **6**, since the chemical shifts of H-3 and H-3′ of the valoneoyl group in **1** are almost the same as those in **6** [δ 6.53 (H-3) and 6.23 (H-3′)].[7]

Structure **1** for praecoxin A was finally established by partial hydrolysis of **6** with tannase,[12] which afforded **1**. The carbon-13 nuclear magnetic resonance (^{13}C-NMR) spectrum of **1** is also consistent with this structure (see Experimental).

Praecoxin B (**2**) was obtained as a light-brown powder. The ^{1}H-NMR spectrum indicated that **2** consists of two galloyl groups [δ 7.142, 7.139 (2H in total, each s), 7.13, 7.10 (2H in total, each s)], an HHDP group [δ 6.60, 6.59 (1H in total, each s, H-3), 6.39 (1H, s, H-3′)] and a $^4C_1$ glucose core (see Experimental). A positive Cotton effect at 236 nm ($[\theta]_{236}+1.0\times10^5$) in the CD spectrum of **2** indicated the (*S*)-configuration of the HHDP group.[11] Therefore, praecoxin B is an isomer of tellimagrandin I (**8**)[1,9,10] concerning the locations of the acyl groups on the glucose core.

The upfield shifts of the glucose protons H-2 and H-3 of **2**, relative to the corresponding protons of **8** having galloyl groups at O-2 and O-3 on the glucose core,[10] are ascribable to the anisotropic effects of the HHDP group, which is therefore assigned to be at O-2/O-3.[7] The ^{13}C-NMR spectrum of **2** also shows the signals of two galloyl groups, an HHDP group and a glucose core (see Experimental). The difference between the chemical shifts of the glucose C-1 signals of the two anomers of **2** ($\Delta\delta$ 3.62), which is analogous to those of the tannins having an HHDP group at O-2/O-3,[13] is also consistent with the structure **2**.

The structure **2** was further substantiated by partial hydrolysis of praecoxin B with tannase, which afforded 2,3-*O*-(*S*)-hexahydroxydiphenoyl-D-glucose (**9**).[3,11,14]

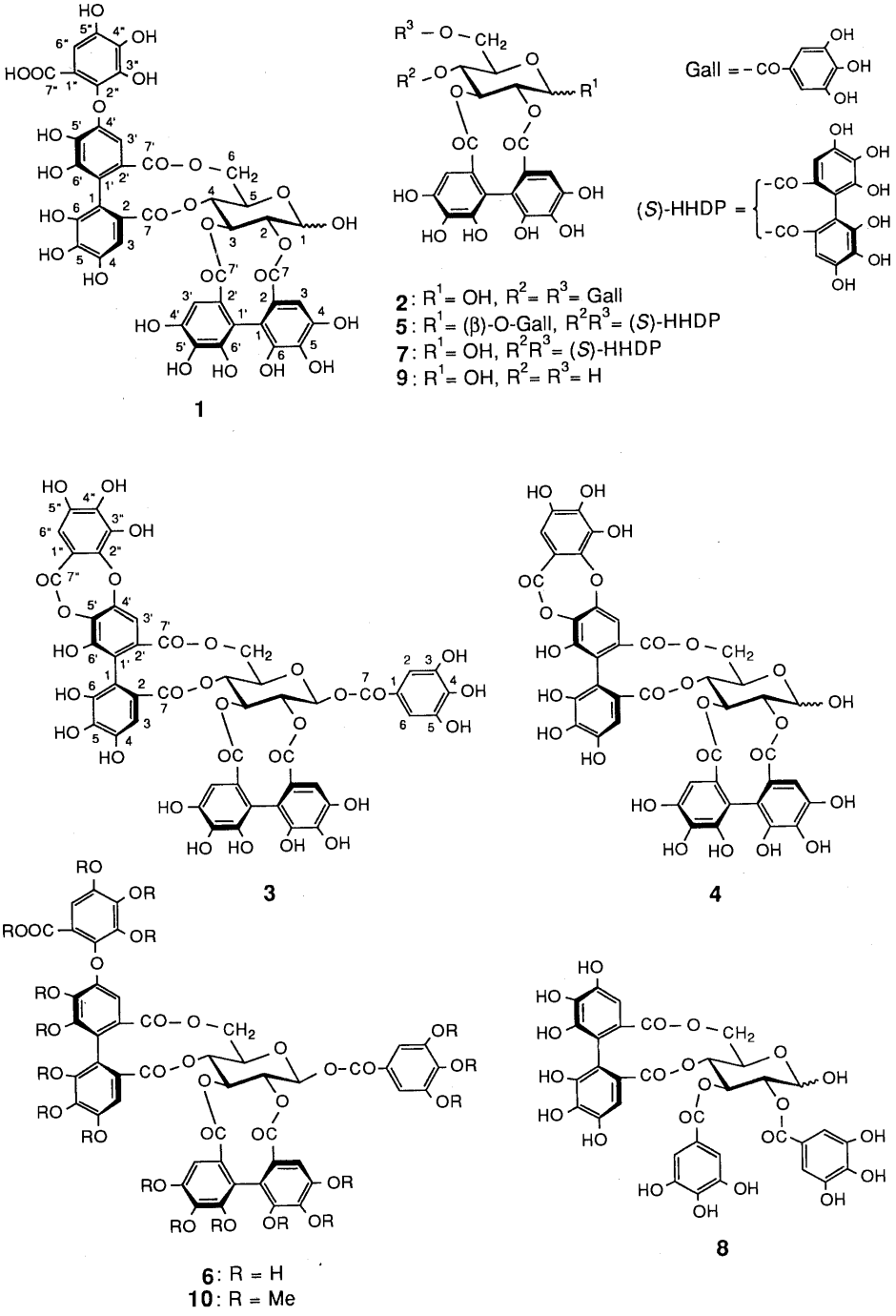

Chart 1

Praecoxin C (**3**) was obtained as a light-brown powder. The FAB-MS of **3** shows the $[M+Na]^+$ ion peak at *m/z* 1109, which corresponds to the molecular formula $C_{48}H_{30}O_{30}$. The ^{1}H-NMR spectrum shows the signals of a galloyl group [δ 7.17 (2H, s)], a valoneoyl group [δ 7.20, 6.95 and 6.58 (1H each, s)] and an HHDP group [δ 6.44 and 6.35 (1H each, s)], and also of a β-D-glucose core adopting $^4C_1$ conformation (see Experimental), suggesting that **3** has a structure closely related to **6**. The CD spectrum of **3** showed a broad positive peak at around 220—240 nm, which indicates that the absolute configuration of the HHDP group and that of the valoneoyl group are both *S*.[7,11]

Treatment of **3** with diazomethane afforded the octadecamethyl derivative (**10**) of rugosin C (**6**). Treatment of **3** in a way analogous to that employed for the selective cleavage of depside linkages in gallotannins[15] afforded **6**. From a solution containing these two compounds, **6** having a free carboxyl group was hardly extractable with EtOAc at pH 5.8, while **3** was easily extracted at this pH. These results and the molecular formula shown by the FAB-MS indicate that **3** has a depside linkage between the carboxyl group at C-1″ of the valoneoyl group and one of the phenolic hydroxyl groups in the molecule.

The ^{13}C-NMR spectrum of **3** showed the signals of a galloyl group, an HHDP group, a valoneoyl group and a glucose core as indicated by Table I. The assignments of the ^{13}C signals were based on the one-bond and long-range

TABLE I. One-Bond and Long-Range ^1H–^{13}C Correlation Data for Praecoxin C (**3**)

Carbon	δ_C	Correlated proton (δ_H)	
		Proton coupled *via* one bond	Proton coupled *via* two or three bonds[a]
Glucose (Glc)			
C-1	92.27	6.20	
C-2	75.84	5.21	
C-3	76.95	5.45	
C-4	69.37	5.15	
C-5	73.26	4.51	3.96 (Glc H-6)
C-6	63.97	5.26	
		3.96	
Galloyl (Gall)			
C-1	119.93		
C-2, C-6	110.25	7.17	
C-3, C-5	146.23		7.17 (Gall H-2, H-6)
C-4	139.88		7.17 (Gall H-2, H-6)
C-7	164.92		7.17 (Gall H-2, H-6)
Hexahydroxydiphenoyl (HHDP)			
C-1	114.92		6.44 (HHDP H-3)
C-2	126.03[b]		
C-3	107.21	6.44	
C-4	145.09		6.44 (HHDP H-3)
C-5	136.49		6.44 (HHDP H-3)
C-6	144.46[c]		
C-7	168.43		6.44 (HHDP H-3)
C-1′	114.14		6.35 (HHDP H-3′)
C-2′	126.37[b]		
C-3′	107.21	6.35	
C-4′	145.03		6.35 (HHDP H-3′)
C-5′	136.14		6.35 (HHDP H-3′)
C-6′	144.50[c]		
C-7′	169.13		6.35 (HHDP H-3′)
			5.45 (Glc H-3)
Valoneoyl (Val)			
C-1	114.58		6.58 (Val H-3)
C-2	124.98		
C-3	107.34	6.58	
C-4	145.77		6.58 (Val H-3)
C-5	136.67		6.58 (Val H-3)
C-6	145.29		
C-7	167.84		6.58 (Val H-3)
			5.15 (Glc H-4)
C-1′	122.07		7.20 (Val H-3′)
C-2′	132.82		
C-3′	111.25	7.20	
C-4′	151.67		7.20 (Val H-3′)
C-5′	135.54		7.20 (Val H-3′)
C-6′	148.49		
C-7′	167.01		
C-1″	111.38		
C-2″	141.43		6.95 (Val H-6″)
C-3″	137.10		
C-4″	143.39		6.95 (Val H-6″)
C-5″	143.80		
C-6″	109.96	6.95	
C-7″	163.21		6.95 (Val H-6″)

At 500 MHz for ^1H-NMR and 125.7 MHz for ^{13}C-NMR, in acetone-d_6. *a*) The long-range ^1H–^{13}C heteronuclear shift correlation spectrum was recorded under the average J_{CH} value of 7 Hz for two- or three-bond couplings. *b,c*) Assignments with the same superscript may be interchanged.

^1H–^{13}C shift correlation spectra.

Based on the following comparisons of the chemical shifts of the valoneoyl carbons of **3** with those of **6**,[7] the location of the depside linkage is assigned to be C-7″—O-5′ in the valoneoyl group of **3**: C-7″, δ 167.00 (**6**)→163.21 (**3**); C-4′, δ 146.97 (**6**)→151.67 (**3**); C-5′, δ 136.99 (**6**)→135.54 (**3**); C-6′, δ 144.63 (**6**)→148.49 (**3**).[16] The formula **3** in which the valoneoyl group forms a seven-membered lactone ring (a depsidone structure) was thus assigned for praecoxin C.

Transformation of rugosin C (**6**) to praecoxin C (**3**) was performed by using polyphosphoric acid as the dehydrating agent, to prove the structural correlation between **3** and **6**. The signals of the valoneoyl protons H-3′ [δ 6.23 (**6**)→7.20 (**3**)] and H-6″ [δ 7.09 (**6**)→6.95 (**3**)], which changed chemical shifts upon this transformation, were also compatible with the formation of the depside linkage. Recently, a depsidone-forming valoneoyl group has also been found in the molecule of prostratin C,[4c,17] a hydrolyzable tannin structurally related to rugosin A.[7]

Praecoxin D (**4**) was obtained as a light-brown powder. The $[M+Na]^+$ ion peak at *m/z* 957 in the FAB-MS and the microanalytical data indicated the molecular formula $C_{41}H_{28}O_{27}$ for **4**. The ^1H-NMR spectrum of **4** also shows the signals of a depsidone-forming valoneoyl group [δ 7.19, 7.17 (1H in total, each s, H-3′), 6.94 (1H, s, H-6″), 6.59, 6.568 (1H in total, each s, H-3)], along with those of an HHDP group [δ 6.571, 6.54 (1H in total, each s, HHDP H-3), 6.31 (1H, s, HHDP H-3′)] and of a glucose core (see Experimental). Duplication of these signals indicates that **4** exists as an anomeric mixture.

A broad positive peak in the short-wavelength region ($[\theta]_{220}$ $+1.0\times10^5$, $[\theta]_{235}+1.3\times10^5$) in the CD spectrum indicates that the valoneoyl group and the HHDP group in **4** have the (*S*)-configuration.[7,11]

Selective cleavage of the depside linkage in **4**, upon the incubation of its solution in a phosphate buffer (pH 5.8), afforded **1**. The structure **4** was thus assigned for praecoxin D. The ^{13}C-NMR spectrum of **4** was also consistent with this structure (see Experimental).

Experimental

Optical rotations were measured on a JASCO DIP-4 polarimeter. Ultraviolet (UV) and infrared (IR) spectra were recorded on a Hitachi 200-10 spectrophotometer and a JASCO A-102 spectrometer, respectively. CD spectra were recorded on a JASCO J-20 spectropolarimeter, or a J-500A spectropolarimeter equipped with a DP-501N data processor. Electron-impact mass spectra (EI-MS) were recorded on a Shimadzu LKB-9000 instrument, and FAB-MS spectra were recorded on a JEOL JMS-D300 or VG 70-SE mass spectrometer. ^1H- and ^{13}C-NMR spectra were recorded on a Varian VXR-500 instrument (500 MHz for ^1H-NMR and 125.7 MHz for ^{13}C-NMR) in acetone-d_6 or in acetone-d_6 containing D_2O (*ca.* 3%). Chemical shifts are given in δ values (ppm) from tetramethylsilane, based on the values of δ_H 2.04 and δ_C 29.8 of the signals of acetone-d_6. A Hitachi R22-FTS spectrometer was also used for measurements of the ^1H-NMR spectra (90 MHz). CPC was conducted on a Sanki L-90 centrifugal partition chromatograph equipped with twelve partition cell cartridges (240 ml in total). Normal-phase high-performance liquid chromatography (HPLC) was performed on a Superspher Si60 column (4×125 mm; Merck) or a Develosil 60-5 column (4×150 mm; Nomura), with *n*-hexane–MeOH–tetrahydrofuran–formic acid (55:33:11:1) containing oxalic acid (450 mg/l). Reversed-phase HPLC was performed on a LiChrospher RP-18 (5 μm) column (4×250 mm; Merck) with 0.01 M H_3PO_4–0.01 M KH_2PO_4–EtOH–EtOAc (83:83:24:10), or a LiChrosorb RP-18 (10 μm) column (4×300 mm; Merck) with 0.1 M H_3PO_4–0.1 M KH_2PO_4–EtOH–EtOAc (50:50:2:5),[3] at 40 °C. Light petroleum refers to the fraction boiling in the range of 75—120 °C. Identification of known compounds was based on comparisons of the ^1H-NMR spectral data with those of authentic samples and co-HPLC, unless otherwise mentioned.

Isolation of Tannins from Leaves of *Stachyurus praecox* Fresh leaves (3.6 kg) of *Stachyurus praecox*, collected from the trees grown at Takahashi River bank, Okayama Prefecture, in August 1982, were homogenized in a mixture of acetone and water (7:3, v/v) (15 l). The concentrated filtrate (940 ml) from the homogenate was extracted successively with Et_2O

(1 l × 10) and with EtOAc (1 l × 20), and then each solvent was evaporated off. A portion (26.6 g) of the ethyl acetate extract (48.0 g) was subjected to CPC with *n*-BuOH–*n*-PrOH–H_2O (2 : 1 : 3, v/v, normal-phase development), and the eluate was separated into fractions I—III (frs. I—III). Fraction I (3.5 g) was chromatographed over Sephadex LH-20, with EtOH→EtOH–MeOH (4 : 1), to give praecoxin C (**3**) (241 mg). Fraction II (5.1 g) was also chromatographed over Sephadex LH-20 with increasing concentrations of MeOH in EtOH, and each fraction containing tannins was further purified by column chromatography on Sephadex LH-20 or on Avicel (Funakoshi, with 5% acetic acid), to give 1,2,6-tri-*O*-galloyl-β-D-glucose (15 mg), praecoxin B (**2**) (198 mg), tellimagrandin I (515 mg), praecoxin A (**1**) (32 mg), praecoxin D (**4**) (188 mg), casuarictin (**5**) (248 mg), rugosin C (**6**) (337 mg) and rugosin F (43 mg). Strictinin, stachyurin, casuarinin and casuariin[1] were in fr. III from CPC.

Praecoxin A (1) A light-brown powder, $[\alpha]_D^{22}$ +45° (c=0.5, MeOH). *Anal.* Calcd for $C_{41}H_{28}O_{27}\cdot 3H_2O$: C, 48.91; H, 3.40. Found: C, 49.01; H, 3.54. FAB-MS m/z: 975 ($[M+Na]^+$). UV λ_{max}^{MeOH} nm (log ε): 217 (4.80), 260 (sh, 4.54). IR ν_{max}^{KBr} cm^{-1}: 1730, 1615. CD (MeOH): $[\theta]_{223}+1.2\times10^5$, $[\theta]_{236}+1.1\times10^5$, $[\theta]_{259}$ -5.4×10^4, $[\theta]_{282}$ $+3.4\times10^4$. ^{1}H-NMR (500 MHz, in acetone-d_6+D_2O) δ: 7.13 [α-anomer (α) and β-anomer (β); 1H, s, valoneoyl (Val) H-6″], 6.58 (α), 6.57 (β) (1H in total, each s, Val H-3), 6.54 (α), 6.49 (β) (1H in total, each s, HHDP H-3), 6.344 (α), 6.340 (β) (1H in total, each s, HHDP H-3′), 6.25 (β), 6.23 (α) (1H in total, each s, Val H-3′). Glucose protons δ: 5.36 (d, J=3.5 Hz, H-1), 5.00 (dd, J=3.5, 9.5 Hz, H-2), 5.42 (t, J=9.5 Hz, H-3), 4.95 (t, J=10 Hz, H-4), 4.52 (ddd, J=1, 6.5, 10 Hz, H-5), 5.14 (dd, J=6.5, 13 Hz, H-6), 3.64 (dd, J=1, 13 Hz, H-6) (α-anomer); 4.97 (d, J=8 Hz, H-1), 4.79 (dd, J=8, 9 Hz, H-2), 5.17 (t, J=9.5 Hz, H-3), 4.95 (t, J=9.5 Hz, H-4), 4.14 (br dd, J=6.5, 9.5 Hz, H-5), 5.17 (dd, J=6.5, 13 Hz, H-6), 3.71 (br d, J=13 Hz, H-6) (β-anomer). ^{13}C-NMR (125.7 MHz, in acetone-d_6+D_2O) δ: 63.49, 63.52 [glucose (Glc) C-6, α and β], 67.11 (Glc C-5, α), 69.56 (Glc C-4, β), 69.90 (Glc C-4, α), 72.17 (Glc C-5, β), 75.45 (Glc C-2, α), 75.65 (Glc C-3, α), 77.45 (Glc C-3, β), 78.13 (Glc C-2, β), 91.43 (Glc C-1, α), 95.12 (Glc C-1, β), 105.25, 105.34 (Val C-3′), 107.09, 107.23, 107.31, 107.57 (Val C-3, HHDP C-3 and C-3′), 109.73 (Val C-6″), 114.29, 114.38 (HHDP C-1′), 114.73, 114.80 (HHDP C-1), 115.29 (Val C-1″), 115.92 (Val C-1), 117.63, 117.66 (Val C-1′), 125.42, 125.47, 125.89, 125.93 (Val C-2 and C-2′), 126.33, 126.36, 126.53 (HHDP C-2 and C-2′), 136.01, 136.07 (HHDP C-5′), 136.27 (HHDP C-5), 136.50 (Val C-5), 136.91, 136.94 (Val C-5′), 137.04, 137.07 (Val C-2″), 139.89 (Val C-4″), 140.07 (Val C-3″), 143.18 (Val C-5″), 144.19, 144.29 (HHDP C-6 and C-6′), 144.66 (Val C-6′), 144.97, 145.06, 145.12 (Val C-6, HHDP C-4 and C-4′), 145.23 (Val C-4), 147.00, 147.03 (Val C-4′), 166.85, 166.88 (Val C-7″), 168.03, 168.08, 168.13 (Val C-7 and C-7′), 168.96, 169.07 (HHDP C-7), 169.41, 169.47 (HHDP C-7′).

Praecoxin B (2) A light-brown powder, $[\alpha]_D^{23}$ +49° (c=0.5, MeOH). *Anal.* Calcd for $C_{34}H_{26}O_{22}\cdot 3H_2O$: C, 48.57; H, 3.84. Found: C, 48.18; H, 3.82. UV λ_{max}^{MeOH} nm (log ε): 218 (4.78), 274 (4.40). IR ν_{max}^{KBr} cm^{-1}: 1710, 1615. CD (MeOH): $[\theta]_{236}$ $+1.0\times10^5$, $[\theta]_{270}-2.5\times10^4$. ^{1}H-NMR (500 MHz, in acetone-d_6+D_2O) δ: 7.142 (α), 7.139 (β) [2H in total, each s, galloyl (Gall) H-2 and H-6], 7.13 (α), 7.10 (β) (2H in total, each s, Gall H-2 and H-6), 6.60 (α), 6.59 (β) (1H in total, each s, HHDP H-3), 6.39 (α and β) (1H, s, HHDP H-3′). Glucose protons δ: 5.48 (d, J=3.5 Hz, H-1), 5.07 (dd, J=3.5, 9.5 Hz, H-2), 5.62 (t, J=9.5 Hz, H-3), 5.50 (t, J=10 Hz, H-4), 4.54 (ddd, J=2, 4, 10 Hz, H-5), 4.49 (dd, J=2, 12 Hz, H-6), 4.27 (dd, J=4, 12 Hz, H-6) (α-anomer); 5.17 (d, J=8 Hz, H-1), 4.88 (dd, J=8, 9.5 Hz, H-2), 5.35 (t, J=9.5 Hz, H-3), 5.46 (t, J=9.5 Hz, H-4), 4.22 (ddd, J=2, 5, 9.5 Hz, H-5), 4.49 (dd, J=2, 12 Hz, H-6), 4.26 (dd, J=5, 12 Hz, H-6) (β-anomer). ^{13}C-NMR (125.7 MHz, in acetone-d_6+D_2O) δ: 63.10 (Glc C-6, α), 63.16 (Glc C-6, β), 68.43 (Glc C-5, α), 68.46 (Glc C-4, β), 68.67 (Glc C-4, α), 73.08 (Glc C-5, β), 75.12 (Glc C-2, α), 75.39 (Glc C-3, α), 77.64 (Glc C-3, β), 77.73 (Glc C-2, β), 91.28 (Glc C-1, α), 94.90 (Glc C-1, β), 107.20, 107.28, 107.60 (HHDP C-3 and C-3′), 109.84, 109.99 (Gall C-2 and C-6), 114.33, 114.45 (HHDP C-1′), 114,55, 114.59 (HHDP C-1), 120.38, 120.43, 121.15, 121.21 (Gall C-1), 126.40, 126.49, 126.62 (HHDP C-2 and C-2′), 136.07, 136.16, 136.20, 136.24 (HHDP C-5 and C-5′), 138.89, 139.36 (Gall C-4), 144.23, 144.29 (HHDP C-6 and C-6′), 145.07, 145.14 (HHDP C-4 and C-4′), 145.95, 146.05 (Gall C-3 and C-5), 165.93, 166.64 (Gall C-7), 168.90, 169.06 (HHDP C-7), 169.18, 169.23 (HHDP C-7′).

Praecoxin C (3) A light-brown powder, $[\alpha]_D^{23}$ +41° (c=0.5, MeOH). *Anal.* Calcd for $C_{48}H_{30}O_{30}\cdot 5H_2O$: C, 48.98; H, 3.43. Found: C, 48.83; H, 3.78. FAB-MS m/z: 1109 ($[M+Na]^+$). UV λ_{max}^{MeOH} nm (log ε): 214 (4.92), 278 (4.49). IR ν_{max}^{KBr} cm^{-1}: 1720, 1605. CD (MeOH): $[\theta]_{223}$ $+1.1\times10^5$, $[\theta]_{233}+1.4\times10^5$, $[\theta]_{260}$ -3.2×10^4, $[\theta]_{282}+0.3\times10^4$. ^{1}H-NMR (500 MHz, in acetone-d_6) δ: 7.20 (1H, s, Val H-3′), 7.17 (2H, s, Gall H-2 and H-6), 6.95 (1H, s, Val H-6″), 6.58 (1H, s, Val H-3), 6.44 (1H, s, HHDP H-3), 6.35 (1H, s, HHDP H-3′). Glucose protons δ: 6.20 (d, J=8.5 Hz, H-1), 5.21 (t, J=9 Hz, H-2), 5.45 (dd, J=9, 10 Hz, H-3), 5.15 (t, J=10 Hz, H-4), 4.51 (br dd, J=6.5, 10 Hz, H-5), 5.26 (dd, J=6.5, 13 Hz, H-6), 3.96 (br d, J=13 Hz, H-6). ^{13}C-NMR: see Table I.

Praecoxin D (4) A light-brown powder, $[\alpha]_D^{23}$ +81° (c=0.5, MeOH). *Anal.* Calcd for $C_{41}H_{28}O_{27}\cdot 3H_2O$: C, 48.91; H, 3.40. Found: C, 49.01; H, 3.54. FAB-MS m/z: 957 ($[M+Na]^+$). UV λ_{max}^{MeOH} nm (log ε): 215 (4.87), 282 (sh, 4.44). IR ν_{max}^{KBr} cm^{-1}: 1730, 1610. CD (MeOH): $[\theta]_{220}+1.0\times10^5$, $[\theta]_{235}+1.3\times10^5$, $[\theta]_{260}-3.7\times10^4$, $[\theta]_{281}+1.8\times10^4$. ^{1}H-NMR (500 MHz, in acetone-d_6) δ: 7.19 (β), 7.17 (α) (1H in total, each s, Val H-3′), 6.94 (α and β) (1H, s, Val H-6″), 6.59 (α), 6.568 (β) (1H in total, each s, Val H-3), 6.571 (α), 6.54 (β) (1H in total, each s, HHDP H-3), 6.31 (α and β) (1H, s, HHDP H-3′). Glucose protons δ: 5.46 (d, J=3.5 Hz, H-1), 5.08 (dd, J=3.5, 9.5 Hz, H-2), 5.46 (t, J=9.5 Hz, H-3), 5.07 (t, J=10 Hz, H-4), 4.62 (ddd, J=1, 6.5, 10 Hz, H-5), 5.18 (dd, J=6.5, 13 Hz, H-6), 3.84 (dd, J=1, 13 Hz, H-6) (α-anomer); 5.06 (d, J=8 Hz, H-1), 4.84 (dd, J=8, 9 Hz, H-2), 5.24 (dd, J=9, 10 Hz, H-3), 5.06 (t, J=10 Hz, H-4), 4.24 (br dd, J=6.5, 10 Hz, H-5), 5.20 (dd, J=6.5, 13 Hz, H-6), 3.92 (br d, J=13 Hz, H-6) (β-anomer). ^{13}C-NMR (125.7 MHz, in acetone-d_6) δ: 64.41 (Glc C-6, α and β), 67.24 (Glc C-5, α), 69.78 (Glc C-4, β), 70.05 (Glc C-4, α), 72.21 (Glc C-5, β), 75.50 (Glc C-2, α), 75.56 (Glc C-3, α), 77.27 (Glc C-3, β), 78.34 (Glc C-2, β), 91.81 (Glc C-1, α), 95.51 (Glc C-1, β), 107.12, 107.21, 107.25, 107.35, 107.71 (Val C-3, HHDP C-3 and C-3′), 109.91 (Val C-6″), 111.08 (Val C-3′), 111.26 (Val C-1″), 114.02, 114.10 (HHDP C-1′), 114.57, 114.59 (Val C-1), 114.90, 114.99 (HHDP C-1), 122.12 (Val C-1′), 125.10, 125.15 (Val C-2), 126.52, 126.56, 126.58, 126.78 (HHDP C-2 and C-2′), 132.88, 132.92 (Val C-2′), 135.46, 135.49 (Val C-5′), 135.95, 136.03 (HHDP C-5′), 136.46 (HHDP C-5), 136.59 (Val C-5), 137.13 (Val C-3″), 141.50, 141.53 (Val C-2″), 143.30 (Val C-4″), 143.79, 143.81 (Val C-5″), 144.27, 144. 35, 144.39 (HHDP C-6 and C-6′), 144.95, 145.06, 145.12 (HHDP C-4 and C-4′), 145.27 (Val C-6), 145.71 (Val C-4), 148.54, 148.58 (Val C-6′), 151.60, 151.64 (Val C-4′), 163.42 (Val C-7″), 167.12, 167.22 (Val C-7′), 167.83, 167.87 (Val C-7), 168.67, 168.76 (HHDP C-7), 169.19, 169.27 (HHDP C-7′).

Partial Hydrolysis of Rugosin C with Tannase Rugosin C (**6**) (35 mg) dissolved in water (5 ml) was treated with tannase[12] at 37 °C for 24 h, and then the solvent was evaporated off. The EtOH-soluble portion of the residue was chromatographed over Sephadex LH-20 with EtOH and then with EtOH–MeOH (1 : 1), to give praecoxin A (**1**) (5 mg).

Partial Hydrolysis of Praecoxin B with Tannase Praecoxin B (**2**) (25 mg) dissolved in water (2 ml) was treated with tannase at 37 °C for 6 h. The solution was then concentrated, and was chromatographed over Sephadex LH-20 with EtOH, to afford 2,3-*O*-(*S*)-hexahydroxydiphenoyl-D-glucose (**9**) (5 mg).

Cleavage of Depside Linkage of Praecoxins C and D A solution of praecoxin C (**3**) (5 mg) in 0.03 M phosphate (KH_2PO_4–Na_2HPO_4) buffer (pH 5.8, 5 ml) was kept at 37 °C for 10 h, and then was extracted with EtOAc (to remove unchanged starting material). The aqueous layer was acidified with 10% HCl (1 ml), and was further extracted with EtOAc. Evaporation of the latter EtOAc layer gave rugosin C (**6**) (2 mg). A solution of praecoxin D (**4**) (30 mg) in phosphate buffer (15 ml) was also treated in an analogous way. After extraction of the acidified solution with EtOAc, the aqueous layer was passed through a BondElut C18 cartridge (Analytichem), and the adsorbed materials were eluted with water and then with 30% MeOH. The eluate with 30% MeOH afforded praecoxin A (**1**) (9 mg).

Treatment of Praecoxin C with Diazomethane Ethereal diazomethane was added to a solution of praecoxin C (**3**) (49 mg) in EtOH (7 ml), and the mixture was left to stand for 30 min. The solvent was evaporated off, and the residue was purified by preparative TLC on Kieselgel 60 PF_{254} with light petroleum–CH_2Cl_2–acetone (4 : 6 : 3), to give the octadecamethyl derivative (**10**) of rugosin C (**6**) (18 mg), which was identified from the ^{1}H-NMR spectrum,[18] the fragmentation pattern in the EI-MS, and $[\alpha]_D$. The identity with the derivative was further substantiated by methanolysis of this methylate to give methyl tri-*O*-methylgallate, dimethyl hexamethoxydiphenate and trimethyl octa-*O*-methylvaloneate (1 mg each),[7] which were identified by ^{1}H-NMR and EI-MS in comparison with authentic specimens.

Transformation of Rugosin C into Praecoxin C Polyphosphoric acid (250 mg) was added to a solution of rugosin C (**6**) (15 mg) in 1,4-dioxane (15 ml), and the mixture was refluxed for 1.5 h. After concentration, the reaction mixture was partitioned between water and EtOAc. The EtOAc layer was then extracted with 0.03 M phosphate buffer (pH 5.8). The organic layer was washed with 10% HCl, and the solvent was evaporated off, and

then the residue was chromatographed over Toyopearl HW-40SF with 70% EtOH, to give praecoxin C (**3**) (1 mg). The buffer solution was acidified with 10% HCl, and extracted with EtOAc, and evaporation of the EtOAc layer gave rugosin C (**6**) (3 mg).

Acknowledgements We thank Prof. T. Koga, Daiichi College of Pharmaceutical Sciences, and Dr. N. Toh, Kyushu Kyoritsu University, for the CD spectra. We also thank Assoc. Prof. Y. Takeda and Mrs. Y. Yoshioka, Faculty of Pharmaceutical Sciences, Tokushima University, for the FAB-MS. The 500 MHz ^{1}H-NMR and 125.7 MHz ^{13}C-NMR spectra were recorded on an instrument at the SC-NMR Laboratory of Okayama University. This study was supported in part by a Grant-in-Aid for Scientific Research from the Ministry of Education, Science and Culture.

References and Notes

1) Part I, T. Okuda, T. Yoshida, M. Ashida and K. Yazaki, *J. Chem Soc., Perkin Trans. 1*, **1983**, 1765.
2) H. Mitsuhashi (ed.), "Illustrated Medicinal Plants of the World in Colour," Hokuryukan, Tokyo, 1988, p. 320.
3) T. Okuda, T. Yoshida, T. Hatano, K. Yazaki and M. Ashida, *Phytochemistry*, **21**, 2871 (1982).
4) For preliminary reports, see *a*) T. Okuda, T. Hatano, K. Yazaki and N. Ogawa, *Chem. Pharm. Bull.*, **30**, 4230 (1982); *b*) T. Okuda, T. Hatano and K. Yazaki, *ibid.*, **31**, 333 (1983); *c*) T. Hatano, O. Namba, L. Chen, T. Yasuhara, K. Yazaki, T. Yoshida and T. Okuda, *Heterocycles*, **31**, 1221 (1990).
5) T. Okuda, T. Yoshida, T. Hatano, K. Yazaki, R. Kira and Y. Ikeda, *J. Chromatogr.*, **362**, 375 (1986).
6) *a*) E. A. Haddock, R. K. Gupta, S. M. K. Al-Shafi, E. Haslam and D. Magnolato, *J. Chem. Soc., Perkin Trans. 1*, **1982**, 2515; *b*) T. Hatano, N. Ogawa, R. Kira, T. Yasuhara and T. Okuda, *Chem. Pharm. Bull.*, **37**, 2083 (1989).
7) T. Hatano, N. Ogawa, T. Yasuhara and T. Okuda, *Chem. Pharm. Bull.*, **38**, 3308 (1990).
8) T. Okuda, T. Hatano and N. Ogawa, *Chem. Pharm. Bull.*, **30**, 4234 (1982); T. Hatano, N. Ogawa, T. Shingu and T. Okuda, *ibid.*, **38**, 3341 (1990).
9) C. K. Wilkins and B. A. Bohm, *Phytochemistry*, **15**, 211 (1976).
10) T. Hatano, T. Yoshida, T. Shingu and T. Okuda, *Chem. Pharm. Bull.*, **36**, 2925 (1988).
11) T. Okuda, T. Yoshida, T. Hatano, T. Koga, N. Toh and K. Kuriyama, *Tetrahedron Lett.*, **23**, 3937 (1982).
12) T. Yoshida, K. Tanaka, X.-M. Chen and T. Okuda, *Chem. Pharm. Bull.*, **37**, 920 (1989).
13) T. Yoshida, T. Hatano, T. Okuda, M. U. Memon, T. Shingu and K. Inoue, *Chem. Pharm. Bull.*, **32**, 1790 (1984).
14) *a*) O. T. Schmidt, L. Wurtele and A. Harreus, *Justus Liebigs Ann. Chem.*, **690**, 150 (1965); *b*) M. K. Seikel and W. E. Hillis, *Phytochemistry*, **9**, 1115 (1970).
15) R. Armitage, G. S. Bayliss, J. W. Gramshaw, E. Haslam, R. D. Haworth, K. Jones, H. J. Rogers and T. Searle, *J. Chem. Soc.*, **1961**, 1842.
16) The previous assignment[4b] of the location of the depside linkage in **3** was based on a comparison of the 22.6 MHz ^{13}C-NMR spectra of **3** and **6**. The discrimination of almost all the signals of the HHDP group from those of the HHDP moiety of the valoneoyl group, in the present study, has led to the structural revision. The previously reported structure for praecoxin D[4b] was also revised as described in this paper.
17) T. Yoshida, O. Namba, L. Chen, Y.-Z. Liu and T. Okuda, *Chem. Pharm. Bull.*, **38**, 3296 (1990).
18) The ^{1}H-NMR data of **10** in ref. 7, containing errors for the glucose and methoxyl protons, should be corrected as follows. δ: 6.25 (d, J=8 Hz, Glc H-1), 5.51 (t, J=9.5 Hz, Glc H-3), 5.20 (t, J=9 Hz, Glc H-2), 5.18 (dd, J=6, 10 Hz, Glc H-6), 5.06 (t, J=10 Hz, Glc H-4), 4.48 (m, Glc H-5), 4.05 (3H, s), 3.89 (6H, s), 3.87 (9H, s), 3.85, 3.85, 3.83, 3.82, 3.79, 3.76, 3.75, 3.75, 3.73, 3.69, 3.64, 3.60 (3H, each, s) (18 × OMe).

Quinazolin-2-ones Having a Spirohydantoin Ring. III.[1] A General and Efficient Synthesis of 3′-Substituted Spiro[imidazolidine-4,4′(1′*H*)-quinazoline]-2,2′,5(3′*H*)-triones[2]

Masafumi YAMAGISHI,*[a] Ken-ichi OZAKI,[a] Yoshihisa YAMADA,[a] Tadamasa DA-TE,[b] Kimio OKAMURA,[b] and Mamoru SUZUKI[a]

Research Laboratory of Applied Biochemistry, Tanabe Seiyaku Co., Ltd.,[a] 16-89, Kashima-3-chome, Yodogawa-ku, Osaka 532, Japan and Organic Chemistry Research Laboratory, Tanabe Seiyaku Co., Ltd.,[b] Kawagishi, Toda, Saitama 335, Japan. *Received December 19, 1990*

The reaction of 1-carbamoylisatins 2 with 2-ethyl-2-isothiourea hydrobromide in the presence of triethylamine followed by acid-catalyzed cyclization of the resulting 4-(2-ethyl-2-isothioureido)carbonyl-3,4-dihydro-4-hydroxy-2(1*H*)-quinazolinones 7 provides a general and high-yielding route to 3′-substituted spiro[imidazolidine-4,4′(1′*H*)-quinazoline]-2,2′,5(3′*H*)-triones 8.

Keywords aldose reductase inhibitor; spirohydantoin; 1-carbamoylisatin; thiourea; 2-ethyl-2-isothiourea hydrobromide; spiroquinazolin-2-one; spiro[imidazolidine-4,4′(1′*H*)-quinazoline]-2,2′,5(3′*H*)-trione

Aldose reductase inhibitors are of therapeutic interest for the chronic complications of diabetes such as retinopathy, neuropathy, nephropathy, and cataracts.[3] Recently, much attention has been paid to the aldose reductase inhibitory activity of several spirohydantoins and related cyclic amides.[4] In the course of our studies on quinazolines,[5] we have focussed on the syntheses and the biological activities of quinazolin-2-ones having such a spirohydantoin ring in the hope of finding potent and effective aldose reductase inhibitors.

A reported approach to such a ring system involves the reaction of either 3-iminoisatin or 1-carbamoylisatins with isocyanates followed by base treatment.[6,7] However, this method is not applicable for the synthesis of the desired quinazolin-2-one derivatives having an unsubstituted spirohydantoin ring. Recently we described a modification of this synthetic sequence using urea instead of isocyanates; it reacts with 1-methylcarbamoylisatin (**2a**) (method A)[8]or 1-ethoxycarbonylisatin (**9**) (method B),[1] yielding ultimately spiro[imidazolidine-4,4′(1′*H*)-quinazoline]-2,2′,5(3′*H*)-triones (**8**) (Chart 1). Unfortunately, method A suffers from low overall yield owing to the low solubility and poor nucleophilicity of urea, while method B cannot be applied to the synthesis of spiroquinazolin-2-ones having a bulky group such as benzyl at the 3-position for steric reasons. In this paper, we describe a new modification of the method using either thiourea or isothiourea.

Treatment of **2a** with thiourea in the presence of triethylamine in tetrahydrofuran (THF) at room temperature gave 3,4-dihydro-4-hydroxy-3-methyl-4-thioureidocarbonyl-2(1*H*)-quinazolinone (**3**) in 48% yield. When the resulting thioureido derivative **3** was refluxed in 1,2-dichlorobenzene, two spiro products **4** and **5** were obtained in 50% and 42% yields, respectively. The structure of **4** was determined by an X-ray analysis (Fig. 1). The spirothiohydantoin derivative **5** was assigned on the basis of spectroscopic and elemental analyses. The infrared (IR) spectrum of **5** showed absorption bands at 1780 and 1680 cm^{-1} due to two carbonyl groups.[9] The proton nuclear magnetic resonance (^{1}H-NMR) spectrum of **5** exhibited three singlet signals due to three NH protons at δ 10.00, 10.90 and 12.40, respectively. Interestingly, the spirothiazolinone **4** was converted into the spirothiohydantoin **5** upon heating with 10% HCl. This transformation would involve ring opening accompanied with the cleavage of the S–C bond of the spirothiazolinone ring, followed by recyclization by the attack of the amino group to the carbon at the 4-position of the quinazoline ring. In practice, **3** was heated with 10% HCl to give exclusively the spirothiohydantoin **5** in 83% yield. The spirothiohydantoin **5** was then converted into the desired spiroquinazolin-2-one **8a** by oxidation with 30% hydrogen peroxide (H_2O_2) in 10% sodium hydroxide (NaOH)[10] in a good yield.

Although the reaction of **2a** with thiourea, as we expected, proceeded smoothly, the yield of this step was still unsatisfactory. We then examined the reaction of **2a** with 2-

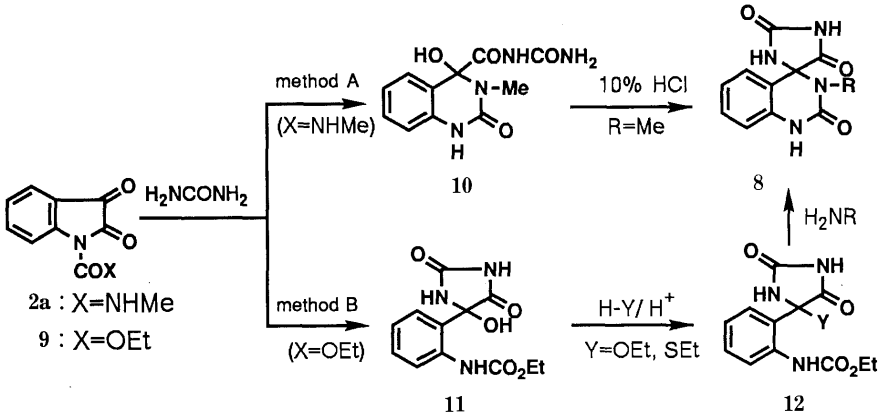

Chart 1

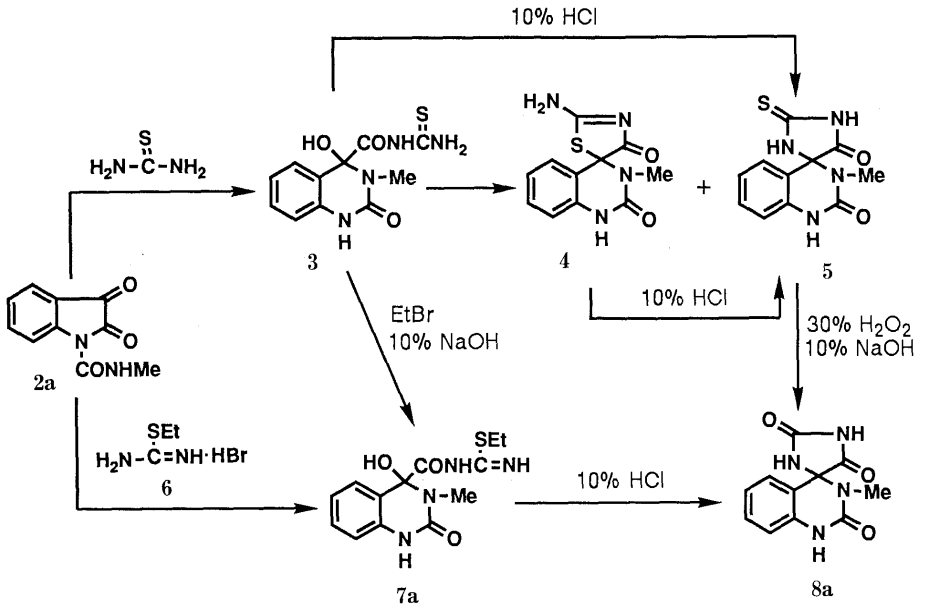

Chart 2

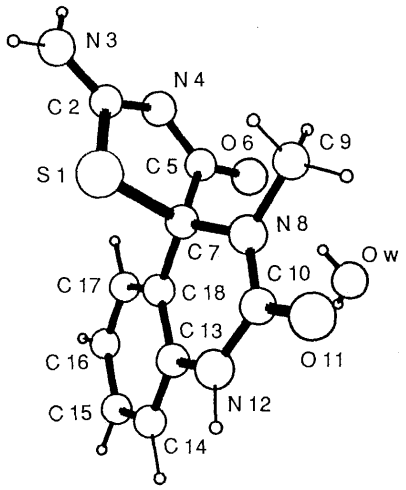

Fig. 1. Perspective View of Compound **4**

ethyl-2-isothiourea hydrobomide (**6**). When **2a** was allowed to react with **6** in the presence of triethylamine in THF at room temperature, the reaction proceeded more smoothly to afford **7a** in 65% yield. The product **7a** was identical with an authentic sample prepared by treatment of **3** with ethyl bromide in 10% NaOH. Compound **7a** was then treated with 10% HCl at 80 °C to give **8a** in 75% yield. It was found that these two step reactions can be done in one pot without isolation of relatively unstable **7a**. Thus, in the reaction of **2a** with **6**, the reaction mixture was concentrated under reduced pressure and treated with 10% HCl to give the desired spiroquinazolin-2-one **8a** in 85% overall yield. Apparently, this synthetic route for **8a** is superior to any previously reported method in terms of overall yield and ease of manipulation. We then applied this method to the synthesis of various 3-substituted spiroquinazolin-2-ones **8**.

A series of 1-carbamoylisatins **2** were firstly synthesized by the reaction of isatin (**1**) and isocyanates. The resulting products **2** were treated with **6** to afford the corresponding 3-substituted 4-hydroxyquinazolin-2-one derivatives **7**, which were directly converted into the target compounds

TABLE I. Synthesis of 3-Substituted Spiroquinazolin-2-ones (**8**)

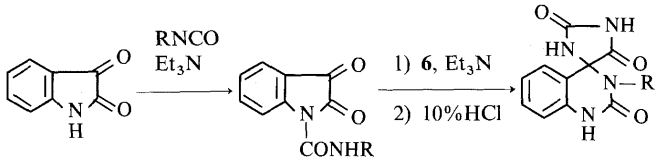

1 **2** **8**

Entry	R	**2** Yield (%)	**8** Yield (%)
a	Me	96	85
b	Et	—[a]	75[b]
c	iso-Pr	—[a]	69[b]
d	*n*-Bu	64	53
e	CH_2Ph	78	69
f	Ph	93	70

a) Not isolated. *b*) Yield from isatin (**1**).

8 by heating with 10% HCl. The results are summarized in Table I. We could synthesize in good yields the spiroquinazolin-2-ones **8** having bulky substituents such as isopropyl and phenyl groups at the 3-position, which could not be obtained by the previously reported methods.

A possible mechanism for the formation of **8** from **7** is depicted in Chart 3. The acid-catalyzed cyclization of **7** would give the imino oxazolidinium derivative **13** with the elimination of ethanethiol.[11] Subsequent ring opening of **13** would result in the formation of the acyl iminium cation intermediate **14**, which undergoes spontaneous recyclization by nucleophilic attack of the $-CONH_2$ group to give compound **8**.

In summary, we found a new, practical and versatile synthetic procedure for various 3-substituted spiroquinazolin-2-ones having a hydantoin ring which involves the reactions of 1-carbamoylisatins with 2-ethyl-2-isothiourea followed by acid treatment. The assay of the biological activities of the derivatives thus obtained is in progress.

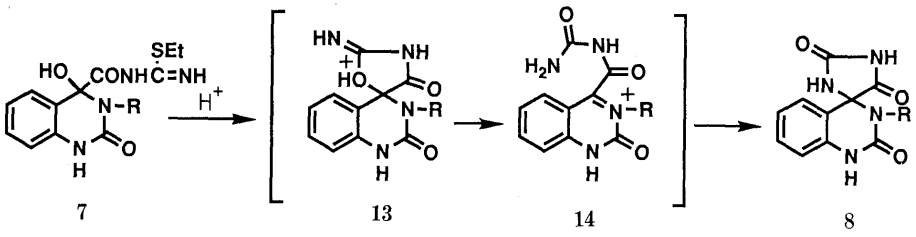

Chart 3

Experimental

All melting points were measured by the use of a Yamato MP-21 melting point apparatus and are uncorrected. IR spectra were recorded on a Shimadzu IR-420 spectrophotometer. Ultraviolet (UV) spectra were recorded on a Shimadzu UV-250 spectrophotometer. ^{1}H-NMR spectra were obtained using a Hitachi R-40 (90 MHz) spectrometer with tetramethylsilane (TMS) as an internal standard. Mass spectra (MS) were taken with a Hitachi M-60 mass spectrometer at an ionizing potential of 30 eV. All the data for X-ray structural analysis were collected with a Rigaku AFC/5 FOS four-circle diffractometer. Column chromatography was carried out with Kieselgel 60 (230—400 mesh, E. Merck) and analytical thin layer chromatography (TLC) was performed with precoated Kieselgel 60F_{254} plates (0.25 mm thickness, E. Merck).

Materials 1-Methylcarbamoylisatin (**2a**) and 1-phenylcarbamoylisatin (**2f**) were prepared from **1** according to the reported procedure.[12]

1-Butylcarbamoylisatin (2d) Butyl isocyanate (9.91 g, 0.1 mol) was added dropwise to a solution of **1** (14.71 g, 0.1 mol) and triethylamine (10.12 g, 0.1 mol) in *N*,*N*-dimethylformamide (DMF) (80 ml) at 0 °C and the mixture was stirred at the same temperature for 1 h. Then, the resulting crystals were collected, washed with diisopropyl ether (IPE), and recrystallized from ethyl acetate (AcOEt)–IPE to give **2d** (15.76 g, 64%), mp 97—99 °C. IR (Nujol): 3360, 1755, 1743, 1700 cm^{-1}. ^{1}H-NMR (DMSO-d_6) δ: 0.7—1.1 (3H, m, CH_3), 1.1—1.9 [4H, m, $(CH_2)_2$], 3.1—4.6 (2H, m, NHC$\underline{H}_2$), 7.1—7.4 (1H, m, NH), 7.5—7.8 (2H, m, ArH × 2), 8.0—8.4 (2H, m, ArH × 2). MS *m/z*: 246 (M^+). *Anal.* Calcd for $C_{13}H_{14}N_2O_3$: C, 63.40; H, 5.73: N, 11.38. Found: C, 63.08; H, 5.72; N, 11.41.

1-Benzylcarbamoylisatin (2e) This compound was synthesized from **1** (14.71 g, 0.1 mol) and benzyl isocyanate (13.32 g, 0.1 mol) in the same way as described for the preparation of **2d**. Yield 21.85 g (78%), mp 165—167 °C (from AcOEt). IR (Nujol): 3360, 1755, 1743, 1700 cm^{-1}. ^{1}H-NMR (DMSO-d_6) δ: 4.53 (2H, d, J=6 Hz, CH_2Ph), 7.16—7.83 (8H, m, ArH × 8), 8.28 (1H, d, J=8 Hz, ArH), 8.70 (1H, t, J=6 Hz, NH), MS *m/z*: 280 (M^+). *Anal.* Calcd for $C_{16}H_{12}N_2O_3$: C, 68.56; H, 4.32; N, 10.00. Found: C, 68.58; H, 4.38; N, 10.24.

3,4-Dihydro-4-hydroxy-3-methyl-4-thioureidocarbonyl-2(1*H*)-quinazolinone (3) Thiourea (1.7 g, 22 mmol) was added to a solution of **2a** (4.08 g, 20 mmol) and triethylamine (2.22 g, 22 mmol) in THF (50 ml) and the mixture was stirred at room temperature for 3 h. The resulting crystals were collected, washed with water, and recrystallized from DMSO–water to give **3** (2.7 g, 48%), mp >280 °C. IR (Nujol): 3350, 3300, 3150, 1705, 1650, 1605 cm^{-1}. ^{1}H-NMR (DMSO-d_6) δ: 2.80 (3H, s, CH_3), 6.70—7.50 (4H, m, ArH × 4), 8.25 (1H, s), 9.31 (1H, s), 9.72 (1H, s), 9.82 (2H, s), *Anal.* Calcd for $C_{11}H_{12}N_4O_3S$: C, 47.13; H, 4.32; N, 19.99; S, 11.44. Found: C, 47.05; H, 4.21; N, 19.89; S, 11.10.

2′-Amino-3-methylspiro[quinazoline-4(1*H*),5′-thiazoline]-2,4′-(3*H*)-dione (4) A suspension of **3** (2.24 g, 8 mmol) in 1,2-dichlorobenzene (20 ml) was refluxed of 2 h. After work-up, the crude product was charomatographed on silica gel using $CHCl_3$–ethanol (95 : 5) as an eluent. The first fraction gave **5** (0.91 g, 42%), mp >280 °C (from DMF–water). IR (Nujol): 3450, 3200, 1780, 1760 (sh), 1675, 1615 cm^{-1}. ^{1}H-NMR (DMSO-d_6) δ: 2.74 (3H, s, CH_3), 6.90—7.40 (4H, m, ArH × 4), 10.00 (1H, s, NH), 10.90 (1H, s, NH), 12.40 (1H, br, NH). UV λ_{max}^{MeOH} (log ε): 270 (4.30), 250 (4.23). MS *m/z*: 262 (M^+). *Anal.* Calcd for $C_{11}H_{10}N_4O_2S \cdot 1/2H_2O$: C, 48.70; H, 4.09; N, 20.65; S, 11.82. Found: C, 48.96; H, 3.91; N, 20.35; S, 12.07.

The second fraction gave **4** (1.09 g, 50%), mp >280 °C (from MeOH–water). IR (Nujol): 3400, 3200, 1680 (br), 1600 cm^{-1}. ^{1}H-NMR (DMSO-d_6) δ: 2.80 (3H, s, CH_3), 6.80—7.30 (4H, m, ArH × 4), 9.20 (1H, s, NH), 9.51 (1H, s, NH), 10.01 (1H, s, NH). UV λ_{max}^{MeOH} (log ε): 294 (sh) (4.29), 252 (sh) (3.93), 225 (3.33). MS *m/z*: 262 (M^+). *Anal.* Calcd for $C_{11}H_{10}N_4O_2S \cdot 3/5H_2O$: C, 48.38; H, 4.13; N, 20.52; S, 11.74. Found: C, 48.34; H, 4.28; N, 20.58; S, 11.58.

X-Ray Structure Analysis The diffraction experiment on **4**, $C_{11}H_{10}N_4O_2S \cdot H_2O$, was carried out using a colorless transparent prism with dimensions of 0.40 × 0.25 × 0.15 mm^3 obtained from MeOH solution with water by the vapor diffusion method. The four-circle diffractometer (AFC/5, RIGAKU) was used with graphite-monochromated Cu $K\alpha$ radiation (λ=1.5418 Å). The unit cell dimensions were determined from the angular setting of 25 reflections (2θ values in the range of 30—60°), and refined by the least-squares method. The crystal data are as follows: a=17.137(1), b=13.341(1), c=6.406(1) Å, α=90.00, β=116.43(1), γ=90.00°, U=1311.5 (2) Å^3, monoclinic, space group $P2_1/a$, Z=4, D_x=1.328 g/cm^3, F(000)=544, μ(Cu $K\alpha$)=21.564 cm^{-1}. Three dimensional intensity data were measured by the ω–2θ scan technique (2$\theta \leqq$120°); 1951 unique reflections were measured, of which 1729 with $|F_o| \geqq 2.67 \times \sigma(F)$ were considered as observed. No absorption corrections were applied. The structure was solved by the direct method using MULTAN80[13] and the difference Fourier method. The refinement of atomic parameters was carried out using the block-diagonal matrix least-squares method with anisotropic temperature factors for the non-hydrogen atoms. Of 12 hydrogen atoms, 4 atoms were located on the difference Fourier maps and refined with isotropic temperature factors. The positions of other hydrogen atoms were assumed geometrically and fixed. Throughout the refinement, the function $\Sigma w(|F_o|-|F_c|)^2$ was minimized. During the final refinement stage, the weighting scheme of $\sqrt{w} = 1/\sigma(F_o)$ was used. The final R value was 0.045 (R_w=0.058) and the maximum residual electron density was 0.3e/Å^3 on the final Fourier synthesis. The atomic scattering factors were taken from "International Tables for X-ray Crystallography".[14] The molecular structure is shown in Fig. 1. The fractional atomic coordinates, bond lengths and bond angles are listed in Tables II—IV, respectively.

Table II. Final Atomic Coordinates and Equivalent Isotropic or Isotropic Thermal Parameters with e.s.d. in Parentheses

Atom	x	y	z	B_{eq}
S1	0.24751 (4)	0.14756 (6)	0.61462 (11)	3.61 (3)
C2	0.1456 (2)	0.1501 (2)	0.3684 (4)	3.15 (10)
N3	0.0846 (1)	0.0903 (2)	0.3603 (4)	3.98 (10)
N4	0.1353 (1)	0.2129 (2)	0.1968 (3)	3.26 (8)
C5	0.2065 (2)	0.2688 (2)	0.2443 (4)	3.08 (10)
O6	0.2116 (1)	0.3366 (2)	0.1221 (3)	4.14 (8)
C7	0.2893 (2)	0.2425 (2)	0.4774 (4)	3.05 (10)
N8	0.3192 (1)	0.3314 (2)	0.6222 (3)	3.11 (8)
C9	0.2535 (2)	0.3917 (3)	0.6519 (5)	4.16 (12)
C10	0.4033 (2)	0.3381 (2)	0.7942 (4)	3.25 (10)
O11	0.4238 (1)	0.3984 (2)	0.9555 (3)	4.09 (8)
N12	0.4633 (1)	0.2774 (2)	0.7766 (4)	3.74 (9)
C13	0.4459 (2)	0.2162 (2)	0.5839 (4)	3.44 (10)
C14	0.5133 (2)	0.1737 (3)	0.5507 (6)	4.59 (13)
C15	0.4944 (2)	0.1135 (3)	0.3599 (6)	5.30 (15)
C16	0.4084 (2)	0.0948 (3)	0.2004 (5)	5.24 (15)
C17	0.3416 (2)	0.1372 (3)	0.2344 (5)	4.10 (12)
C18	0.3595 (2)	0.1986 (2)	0.4260 (4)	3.11 (10)
Ow	0.3521 (2)	0.4750 (2)	0.2364 (4)	5.86 (11)

$B_{eq}=4/3(B_{11}a^2+B_{22}b^2+B_{33}c^2+B_{13}ac)$.

5-Methyl-2-thioxospiro[imidazolidine-4,4′-(1′*H*)-quinazoline]-2′,5(3′*H*)-dione (5) (a) From **3**: A suspension of **3** (0.5 g, 1.8 mmol) in 10% HCl solution (10 ml) was stirred at 80 °C for 3 h. After cooling, the resulting crystals were collected, washed with water, and recrystallized from DMF–water to give **5** (0.40 g, 83%), mp >280 °C.

(b) From **4**: A suspension of **4** (2.1 g, 8 mmol) in 10% HCl solution (10 ml) was stirred at 80 °C for 3 h. After cooling, the resulting crystals were collected, washed with water, and recrystallized from DMF–water

TABLE III. Bond Lengths with e.s.d. in Parentheses

Atom 1–atom 2	Distance (Å)
S1–C2	1.757 (2)
S1–C7	1.857 (3)
C2–N3	1.297 (4)
C2–N4	1.330 (4)
N4–C5	1.345 (4)
C5–O6	1.224 (4)
C5–C7	1.575 (3)
C7–N8	1.451 (3)
C7–C18	1.501 (4)
N8–C9	1.463 (4)
N8–C10	1.372 (3)
C10–O11	1.231 (3)
C10–N12	1.353 (4)
N12–C13	1.397 (4)
C13–C14	1.386 (5)
C13–C18	1.391 (3)
C14–C15	1.375 (5)
C15–C16	1.392 (4)
C16–C17	1.379 (5)
C17–C18	1.391 (4)

TABLE IV. Bond Angles with e.s.d. in Parentheses

Atom 1–atom 2–atom 3	Angle (°)
C2–S1–C7	90.0 (1)
S1–C2–N3	119.0 (2)
S1–C2–N4	117.9 (2)
N3–C2–N4	123.1 (2)
C2–N4–C5	112.9 (2)
N4–C5–O6	125.5 (2)
N4–C5–C7	115.7 (2)
O6–C5–C7	118.7 (2)
S1–C7–C5	103.1 (2)
S1–C7–N8	110.8 (2)
S1–C7–C18	110.7 (2)
C5–C7–N8	109.7 (2)
C5–C7–C18	110.5 (2)
N8–C7–C18	111.7 (2)
C7–N8–C9	117.3 (2)
C7–N8–C10	120.8 (2)
C9–N8–C10	116.9 (2)
N8–C10–O11	121.5 (3)
N8–C10–N12	117.3 (2)
O11–C10–N12	121.2 (2)
C10–N12–C13	123.5 (2)
N12–C13–C14	120.6 (2)
N12–C13–C18	118.7 (3)
C14–C13–C18	120.6 (3)
C13–C14–C15	119.5 (3)
C14–C15–C16	120.7 (4)
C15–C16–C17	119.5 (3)
C16–C17–C18	120.6 (2)
C7–C18–C13	118.2 (2)
C7–C18–C17	122.7 (2)
C13–C18–C17	119.1 (3)

to give **5** (1.95 g, 93%), mp >280 °C.

4-(2-Ethyl-2-isothioureido)carbonyl-3,4-dihydro-4-hydroxy-3-methyl-2(1*H*)-quinazolinone (7a) (a) From **2a**: Triethylamine (4.5 g, 44 mmol) and **6**[15] (7.4 g, 40 mmol) were added to a solution of **2a** (8.16 g, 40 mmol) in THF (100 ml), and the mixture was stirred at room temperature for 3 h. The resulting crystals were collected, washed with water, and recrystallized from DMF–water to give **7a** (8.0 g, 65%), mp >280 °C. IR (Nujol): 3410, 3200, 3120, 1720, 1658, 1605 cm^{-1}. ^{1}H-NMR (DMSO-d_6) δ: 0.96 (3H, t, J=7 Hz, CH_2CH_3), 2.81 (3H, s, 3-CH_3), 3.05—3.72 (2H, m, SCH_2), 6.60—7.75 (6H, m), 9.72 (1H, br), 9.30—10.70 (1H, br). *Anal.* Calcd for $C_{13}H_{16}N_4O_3S$: C, 50.63; H, 5.23; N, 18.17; S, 10.40. Found: C, 50.56; H, 4.99; N, 18.12; S, 10.46.

(b) From **3**: A 10% NaOH solution (0.12 g, 3 mmol) was added to a solution of **3** (0.84 g, 3 mmol) in DMF (10 ml), and the mixture was stirred at room temperature for 30 min. Then, ethyl bromide (0.33 g, 3 mmol) was added dropwise to the mixture. After being stirred at room temperature for an additional 30 min, the resulting mixture was concentrated under reduced pressure and crystallized from water. The product was recrystallized from DMF–water to give **7a** (0.65 g, 70%), mp >280 °C.

3′-Methylspiro[imidazolidine-4,4′(1′*H*)-quinazoline]-2,2′,5(3′*H*)-trione (8a)[8] (a) From **2a**: Triethylamine (4.45 g, 44 mmol) and **6** (7.4 g, 40 mmol) were added to a solution of **2a** (8.16 g, 40 mmol) in THF (100 ml), and the mixture was stirred at room temperature for 3 h. Then, the reaction mixture was concentrated under reduced pressure. A 10% HCl solution (50 ml) was added to the residue, and the mixture was heated at 80 °C for 3 h. After cooling, the resulting crystals were collected, washed with water and recrystallized from DMSO to give **8a** (8.36 g, 85%), mp >280 °C.

(b) From **5**: A 30% hydrogen peroxide solution (2 ml) was added to a solution of **5** (1.0 g, 3.7 mmol) in 10% NaOH solution (10 ml), and the mixture was stirred at room temperature for 1 h. After being acidified with 10% HCl solution, the resulting crystals were collected, washed with water, and recrystallized from DMSO to give **8a** (0.85 g, 91%), mp >280 °C.

(c) From **7a**: A suspension of **7a** (2.0 g, 6.5 mmol) in 10% HCl solution (20 ml) was heated at 80 °C for 3 h. After cooling, the resulting crystals were collected, and recrystallized from DMSO to give **8a** (1.2 g, 75%), mp >280 °C.

3′-Ethylspiro[imidazolidine-4,4′(1′*H*)-quinazoline]-2,2′,5(3′*H*)-trione (8b)[1] Triethylamine (5.06 g, 50 mmol) and ethyl isocyanate (3.91 g, 55 mmol) were added to a solution of **1** (7.36 g, 50 mmol) in THF (75 ml) at 0°C, and the mixture was stirred at the same temperature for 1 h. Then, triethylamine (1.01 g, 10 mmol) and **6** (11.11 g, 60 mmol) were added to the reaction mixture, and the mixture was stirred at room temperature for 3 h. The resulting mixture was concentrated under reduced pressure. A 10% HCl solution (35 ml) was added to the residue and the mixture was heated at 80 °C for 3 h. After cooling, the resulting crystals were collected, washed with water, and recrystallized from DMF–water to give **8b** (9.76 g, 75%), mp >280 °C.

3′-Isopropylspiro[imidazolidine-4,4′(1′*H*)-quinazoline]-2,2′,5(3′*H*)-trione (8c) This compound was synthesized from **1** (7.36 g, 50 mmol) in the same way as described for the preparation of **8b**. Yield, 9.47 g, (69%), mp >280 °C (from DMF–water). IR (Nujol): 3330, 3210, 1790, 1740, 1672 cm^{-1}. ^{1}H-NMR (DMSO-d_6) δ: 1.40 [6H, d, J=6 Hz, $CH(CH_3)_2$], 3.0—3.4 (1H, sept., J=6 Hz, NCH), 6.6—7.4 (4H, m, ArH×4), 9.15 (1H, s, NH), 9.66 (1H, s, NH), 11.16 (1H, s, NH). MS *m/z*: 274 (M^+). *Anal.* Calcd for $C_{13}H_{14}N_4O_3$: C, 56.93; H, 5.15; N, 20.43. Found: C, 56.85; H, 5.22; N, 20.69.

3′-Butylspiro[imidazolidine-4,4′(1′*H*)-quinazoline]-2,2′,5(3′*H*)-trione (8d) This compound was synthesized from **2d** (2.46 g, 10 mmol) in the same way as described for the preparation of **8a**. Yield, 1.53 g, (53%), mp 263—266 °C (DMF–water). IR (Nujol): 3240, 1782, 1725, 1665 cm^{-1}. ^{1}H-NMR (DMSO-d_6) δ: 0.7—1.9 [7H, m, $(CH_2)_2CH_3$], 2.7—3.8 (2H, m, NCH_2), 6.7—7.4 (4H, m, ArH×4), 9.05 (1H, s, NH), 9.77 (1H, s, NH), 11.14 (1H, s, NH). MS *m/z*: 288 (M^+). *Anal.* Calcd for $C_{14}H_{16}N_4O_3$: C, 58.33; H, 5.59; N, 19.43. Found: C, 58.24; H, 5.64; N, 19.04.

3′-Benzylspiro[imidazolidine-4,4′(1′*H*)-quinazoline]-2,2′,5(3′*H*)-trione (8e) This compound was synthesized from **2e** (2.80 g, 10 mmol) in the same way as described for the preparation of **8a**. Yield, 2.22 g (69%), mp >280 °C (DMF–water). IR (Nujol): 3240, 3050, 1782, 1738, 1720 cm^{-1}. ^{1}H-NMR (DMSO-d_6) δ: 4.33, 4.66 (1H each, ABq, J=16 Hz, CH_2Ph), 6.87—7.50 (9H, m, ArH×9), 9.13 (1H, s, NH), 9.97 (1H, s, NH), 11.18 (1H, s, NH). MS *m/z*: 322 (M^+). *Anal.* Calcd for $C_{17}H_{14}N_4O_3$: C, 63.35; H, 4.38; N, 17.38. Found: C, 63.22; H, 4.29; N, 17.58.

3′-Phenylspiro[imidazolidine-4,4′(1′*H*)-quinazoline]-2,2′,5(3′*H*)-trione (8f) This compound was synthesized from **2f** (10.64 g, 40 mmol) in the same way as described for the preparation of **8a**. Yield, 8.87 g, (72%), mp >280 °C (DMF–water). IR (Nujol): 3400, 3050, 1785, 1738, 1660 cm^{-1}. ^{1}H-NMR (DMSO-d_6) δ: 6.64—7.50 (9H, m, ArH×9), 9.10 (1H, s, NH), 10.05 (1H, s, NH), 10.80 (1H, br, NH). MS *m/z*: 308 (M^+). *Anal.* Calcd for $C_{16}H_{12}N_4O_3 \cdot 1/2H_2O$: C, 60.56; H, 4.13; N, 17.66. Found: C, 60.63; H, 4.10; N, 17.54.

Acknowledgement We are grateful to Dr. I. Chibata, President and Dr. S. Saito, Research and Development Executive, for their encouragement and interest. Thanks are due to Drs. T. Tosa, M. Takeda, S. Oshiro, I. Inoue, T. Oine, K. Matsumoto for their valuable comments during this study.

References and Notes

1) Part II: M. Yamagishi, Y. Yamada, K. Ozaki, J. Tani, and M. Suzuki *Chem. Pharm. Bull.*, **39**, 626 (1991).
2) This study was presented at the 39th Annual Meeting of the Kinki Branch of the Pharmaceutical Society of Japan, Osaka, October 1989.
3) *a*) K. H. Gabbay, *Annu. Rev. Med.*, **26**, 521 (1975); *b*) J. H. Kinoshita, P. F. Kador, and M. Catiles, *J. Am. Med. Assoc.*, **246**, 257 (1981); *c*) P. F. Kador, W. G. Robinson, and J. H. Kinoshita, *Annu. Rev. Pharmacol. Toxicol.*, **25**, 691 (1985).
4) *a*) P. F. Kador, J. H. Kinoshita, and N. E. Sharpless, *J. Med. Chem.*, **28**, 841 (1985); *b*) N. Sakamoto and N. Hotta, *Farumashia*, **19**, 43 (1983); *c*) T. Tanimoto, *ibid.*, **24**, 459 (1988).
5) *a*) J. Tani, Y. Yamada, T. Ochiai, R. Ishida, I. Inoue, and T. Oine, *Chem. Pharm. Bull.*, **27**, 2675 (1979); *b*) J. Tani, Y. Yamada, T. Oine, T. Ochiai, R. Ishida, and I. Inoue, *J. Med. Chem.*, **22**, 95 (1979).
6) L. Capuano, M. Welter, and R. Zander, *Chem. Ber.*, **103**, 2394 (1970).
7) L. Capuano and K. Benz, *Chem. Ber.*, **110**, 3849 (1977).
8) M. Yamagishi, K. Ozaki, H. Ohmizu, Y. Yamada, and M. Suzuki, *Chem. Pherm. Bull.*, **38**, 2926 (1990).
9) D. T. Elmore, *J. Chem. Soc.*, **1958**, 3489.
10) *a*) J. D. Dutcher and A. Kjaer, *J. Am. Chem. Soc.*, **73**, 4139 (1951); *b*) C. Piantadosi, V. G. Skulason, J. L. Irvin, J. M. Powell, and L. Hall, *J. Med. Chem.*, **7**, 337 (1964).
11) E. Hoggarth, *J. Chem. Soc.*, **1949**, 1918.
12) S. Petersen, H. Heitzer, and L. Born, *Justus Liebigs Ann. Chem.*, **12**, 2003 (1974).
13) "MULTAN80: A computer program for automatic analysis of phase problem," produced by P. Main, G. German, and M. M. Woolfson, Univ. of York, England.
14) "International Tables for X-ray Crystallography," Vol. 4, Kynoch Press, Birmingham, 1974.
15) E. Brand and F. C. Brand, "Organic Syntheses," Coll. Vol. III, ed. by E. C. Horning, John Wiley and Sons, Inc., New York, 1955, p. 440.

Studies on the Constituents of *Aster scaber* THUNB. I. Structures of Scaberosides, Oleanolic Acid Glycosides Isolated from the Root

Tsuneatsu NAGAO, Ryuichiro TANAKA and HIKARU OKABE*

Faculty of Pharmaceutical Sciences, Fukuoka University, Nanakuma 8–19–1, Jonan-ku, Fukuoka 814–01, Japan. *Received December 19, 1990*

Six oleanolic acid glucuronide saponins, scaberosides B_1, B_2, B_3, B_4, B_5 and B_6 were isolated from the root of *Aster scaber* THUNB. (Compositae) as their methyl esters, and their structures were determined based on spectral and chemical evidence. Scaberosides have a common prosapogenin structure, oleanolic acid 3-*O*-glucopyranosiduronic acid, and differ in the structures of the 28-*O*-linked sugar moieties.

Scaberoside B_1 is a 28-[α-L-arabinopyranosyl] ester, scaberoside B_2, a 28-[β-D-xylopyranosyl] ester, scaberoside B_3, a 28-[*O*-α-L-rhamnopyranosyl-(1→2)-α-L-arabinopyranosyl] ester, scaberoside B_4, a 28-[*O*-α-L-rhamnopyranosyl-(1→2)-β-D-xylopyranosyl] ester, scaberoside B_5, a 28-[*O*-β-D-xylopyranosyl-(1→4)-*O*-α-L-rhamnopyranosyl-(1→2)-α-L-arabinopyranosyl] ester, and scaberoside B_6, a 28-[*O*-β-D-xylopyranosyl-(1→4)-*O*-α-L-rhamnopyranosyl-(1→2)-β-D-xylopyranosyl] ester of the prosapogenin.

Keywords *Aster scaber*; Compositae; scaberoside; triterpene glycoside; oleanolic acid; glucuronide saponin; 3,28-*O*-bisdesmoside

In a series of previous papers, we reported the isolation and structures of several oleanane-type triterpene saponins isolated from the root[1] and herb[2] of *Aster tataricus* L. f. (Compositae). As a continuation of the chemical investigation of the saponin constituents of *Aster* species, the root of *Aster scaber* THUNB. was investigated.

The glycoside fraction obtained from the fresh root was chromatographed on a polystyrene resin (Diaion HP-20) and divided into two saponin fractions (frs. A and B). The less polar fraction (fr. B) was treated with an ion-exchange resin, Amberlite IRC-84, and the acidic product was converted into the methyl ester with CH_2N_2. The methyl ester was repeatedly chromatographed on silica gel and reversed-phase material (ODS). Saponin methyl esters were finally purified by high-performance liquid chromatography (HPLC). They were named scaberosides B_1—B_6 methyl esters (I—VI) in order of increasing polarity. This paper deals with their structures. The polar saponin fraction (fr. A) contained several saponins of echinocystic acid. Isolation and structures of these saponins will be reported in the next paper.

Scaberoside B_1 methyl ester (I) was obtained as colorless needles, and it showed an $[M+Na]^+$ ion at *m/z* 779 in the fast atom bombardment mass spectrum (FAB-MS). The high-resolution FAB-MS gave the molecular formula $C_{42}H_{66}O_{13}$, and I gave L-arabinose and D-glucuronic acid on acid hydrolysis. The ^{1}H-nuclear magnetic resonance (^{1}H-NMR) spectrum showed signals of seven tertiary methyl groups (δ 0.84, 0.92, 0.96, 0.98, 1.02, 1.26 and 1.30), one trisubstituted olefinic proton (δ 5.43, dd, J=3, 3 Hz) and two anomeric protons (δ 4.96, d, J=8 Hz; 6.27, d, J=6 Hz). The ^{13}C-NMR spectrum (Tables I and II) showed signals of six C–C bonded quaternary carbons (δ 30.8, 36.9, 39.5, 39.9, 42.1 and 47.2), two ester carbonyl carbons (δ 170.7 ad 176.5), a pair of olefinic carbons (δ 122.9 and 144.2) and two anomeric carbons (δ 95.8 and 107.2). These NMR data indicated that I is an oleanolic acid 3,28-*O*-bisdesmoside containing L-arabinose and D-glucuronic acid methyl ester. The structure of I was determined to be as shown in the chart based on examination of the NMR spectra. The configuration and conformation of the ester-linked arabinopyranosyl group were determined from the coupling constants of C_1-H (6 Hz), C_2-H (6, 7 Hz), C_3-H (3, 7 Hz), although the coupling constant between C_1 and C_1-H ($J_{C_1H_1}$, 169 Hz) is inconsistent with the report[3] by Bock and Pedersen that the anomeric carbon which has an equatorial hydrogen shows the $J_{C_1H_1}$ value of *ca.* 170 Hz while the carbon having an axial hydrogen shows the $J_{C_1H_1}$ value of *ca.* 160 Hz.

Scaberoside B_2 methyl ester (II) was obtained as an amorphous powder and high-resolution FAB-MS gave the molecular formula $C_{42}H_{66}O_{13}$ (*m/z* 779). Compound II gave D-xylose and D-glucuronic acid on acid hydrolysis, and the NMR spectra indicated that II is also an oleanolic acid 3,28-*O*-bisdesmoside. The structure was determined to be as shown in the chart based on examination of the NMR spectra.

Scaberoside B_3 methyl ester (III), $C_{48}H_{76}O_{17}$, gave L-arabinose, L-rhamnose and D-glucuronic acid as component sugars on acid hydrolysis, and the NMR spectra indicated that III is an oleanolic acid 3,28-*O*-bisdesmoside having a β-D-glucuronic acid methyl ester linked to the C_3-OH group and a biose composed of L-arabinose and L-rhamnose which is linked to the carboxyl group of

TABLE I. ^{13}C-NMR Chemical Shifts of Aglycone Moieties of I[a] and VII

	I	VII		I	VII
1	38.7	38.6	16	23.2	23.4
2	26.5	26.5	17	47.2	47.0
3	89.2	89.1	18	41.7	41.8
4	39.5	39.5	19	46.2	46.1
5	55.8	55.8	20	30.8	30.8
6	18.5	18.4	21	34.1	34.0
7	33.1	33.0	22	32.7	32.8
8	39.9	39.6	23	28.2	28.1
9	48.0	47.9	24	16.9	16.9
10	36.9	36.9	25	15.5	15.4
11	23.8	23.7	26	17.4	17.1
12	122.9	122.8	27	26.0	26.1
13	144.2	144.1	28	176.5	177.9
14	42.1	41.9	29	33.1	33.1
15	28.2	28.0	30	23.6	23.6
			COOMe		51.5

a) Signals of the aglycone moieties of II, III, IV, V, VI have almost the same chemical shifts as those of I. The deviations are within 0.2 ppm.

TABLE II. ^{13}C-NMR Chemical Shifts of Sugar Moieties of I—IX

	I	II	III	IV	V	VI	VII	VIIIa	VIIIb	IXa	IXb
GlcUAMe											
1	107.2	107.2	107.2	107.2	107.2	107.1	107.2				
2	75.4	75.3	75.3	75.4	75.4	75.3	75.3				
3	77.9	77.9	77.9	77.9	77.9	77.9	77.9				
4	73.1	73.1	73.1	73.1	73.1	73.1	73.1				
5	77.2	77.1	77.1	77.2	77.1	77.1	77.1				
6	170.7	170.7	170.7	170.7	170.7	170.7	170.7				
COOMe	52.0	51.9	51.9	51.9	52.0	51.9	51.9				
	Ara	Xyl	Ara	Xyl	Ara	Xyl		Ara	Ara	Xyl	Xyl
1	95.8	96.2	93.5	95.3	93.4	95.2		103.6	101.1	104.3	100.5
2	71.3	73.6	75.0	75.5	75.2	76.1		76.8	78.7	78.7	81.4
3	73.8	78.1	70.4	78.0	70.1	77.7		74.2	69.1	79.0	74.1
4	67.9	70.8	66.3	70.9	66.2	70.9[a]		69.2	70.6	71.2	71.5
5	66.0	67.6	63.2	67.2	63.1	67.1		65.9	63.5	67.0	62.7
							OMe	55.9	55.1	56.2	54.9
Rha											
1			101.3	101.5	101.0	101.3		102.1	104.1	102.3	104.3
2			72.3	72.2	71.8	71.7		72.0	71.7	72.0	71.7
3			72.6	72.5	72.6	72.5		72.7	72.7	72.8	72.6
4			73.8	73.8	84.3	85.2		84.8	84.6	85.0	84.5
5			70.3	69.9	68.5	68.3		67.9	68.1	67.9	68.2
6			18.5	18.7	18.3	18.5		18.9	18.4	18.2	18.5
Xyl											
1					107.2	107.6		107.2	107.1	107.2	107.1
2					76.0	76.1		76.1	76.1	76.1	76.0
3					78.5	78.6		78.6	78.6	78.7	78.6
4					70.9	70.8[a]		70.9	70.9	70.9	70.9
5					67.4	67.5		67.5	67.5	67.5	67.4

Abbreviations: GlcUAMe, 6-*O*-methyl-β-D-glucuronopyranosyl; Ara, L-arabinopyranosyl; Xyl, D-xylopyranosyl; Rha, α-L-rhamnopyranosyl. *a*) Assignments may be reversed.

TABLE III. ^{1}H-NMR Chemical Shifts of Sugar Moieties of I—IX

	I	II	III	IV	V	VI	VII	VIIIa	VIIIb	IXa	IXb
GlcUAMe											
1	4.96 (d, 8)	4.97 (d, 8)	4.96 (d, 8)	4.96 (d, 8)	4.95 (d, 8)	4.94 (d, 8)	4.96 (d, 8)				
2	4.06 (dd, 8, 9)	4.07 (dd, 8, 9)	4.06 (dd, 8, 9)	4.06 (dd, 8, 9)	4.06 (dd, 8, 9)	4.05 (dd, 8, 9)	4.05 (dd, 8, 9)				
3	4.23 (dd, 9, 9)	4.25 (dd, 9, 9)	4.23 (dd, 9, 9)	4.24 (dd, 9, 9)	4.23 (dd, 9, 9)	4.22 (dd, 9, 9)	4.22 (dd, 9, 9)				
4	4.44 (dd, 9, 9)	4.45 (dd, 9, 9)	4.44 (dd, 9, 9)	4.45 (dd, 9, 9)	4.45 (dd, 9, 9)	4.44 (dd, 9, 9)	4.43 (dd, 9,				
5	4.56 (d, 9)	4.57 (d, 9)	4.56 (d, 9)	4.57 (d, 9)	4.56 (d, 9)	4.55 (d, 9)	10)				
COOMe	3.73	3.74	3.73	3.73	3.73	3.73	4.55 (d, 10) 3.73				
	Ara	Xyl	Ara	Xyl	Ara	Xyl		Ara	Ara	Xyl	Xyl
1	6.27 (d, 6)	6.22 (d, 7)	6.46 (d, 3)	6.16 (d, 7)	6.45 (d, 3)	6.14 (d, 7)		4.55 (d, 7)	5.29 (d, 4)	4.52 (d, 7)	5.20 (d,3)
2	4.57 (dd, 6, 7)	*ca.* 4.18	4.60 (dd, 3, 4)	4.40 (dd, 7, 8)	4.55 (dd, 3, 4)	*ca.* 4.31		4.45 (dd, 7, 8)	4.56 (dd, 9, 4)	*ca.* 4.07	*ca.* 3.95
3	4.35 (dd, 3, 7)	*ca.* 4.21	*ca.* 4.52	*ca.* 4.26	*ca.* 4.50	*ca.* 4.23		*ca.* 4.15	4.47 (br d)	*ca.* 4.07	*ca.* 4.45
4	*ca.* 4.45	*ca.* 4.21	*ca.* 4.40	*ca.* 4.16	*ca.* 4.40	4.14 (br m)		*ca.* 4.19	*ca.* 4.28	*ca.* 4.07	4.15 (br m)
5	3.91 (dd, 2, 11)	3.81 (dd, 9, 12)	3.91 (dd, 4, 11)	3.79 (dd, 9, 12)	3.94 (dd, 4, 11)	3.77 (dd, 9, 11)		3.67 (d-like, 10)	3.96 (2H, d-like, 2)	3.57 (dd, 9, 11)	*ca.* 3.95 (2H)
	4.40 (dd, 5, 11)	4.37 (dd, 4, 12)	*ca.* 4.47	4.33 (dd, 4, 12)	*ca.* 4.50	*ca.* 4.25		4.20 (dd, 4, 10)		4.25 (dd, 4, 11)	
							OMe	3.49	3.39	3.51	3.38
Rha											
1			5.83 (d, 2)	6.44 (br s)	5.77 (br s)	6.34 (d, 2)		5.95 (d, 1)	5.61 (br s)	6.17 (d, 2)	5.72 (br s)
2			*ca.* 4.57	4.75 (br s)	4.56 (br s)	4.77 (dd, 2, 3)		4.69 (br s)	4.62 (br s)	4.74 (br s)	4.64 (br s)
3			*ca.* 4.47	4.51 (dd, 3, 9)	*ca.* 4.55	4.64 (dd, 3, 9)		4.65 (br d)	*ca.* 4.63	*ca.* 4.66	4.62 (br dd)
4			4.25 (dd, 9, 9)	*ca.* 4.24	4.34 (dd, 9, 9)	4.34 (dd, 9, 9)		4.35 (dd, 9, 9)	4.32 (dd, 9, 9)	4.39 (dd, 9, 9)	4.35 (dd, 9, 9)
5			*ca.* 4.40	*ca.* 5.50	*ca.* 4.40	4.46 (dq, 9, 6)		4.53 (dq, 9, 6)	4.41 (dq, 9, 6)	*ca.* 4.66	*ca.* 4.45
6			1.71 (d, 6)	1.76 (d, 6)	1.77 (d, 6)	1.82 (d, 6)		1.70 (d, 6)	1.67 (d, 6)	1.77 (d, 6)	1.72 (d, 6)
Xyl											
1					5.09 (d, 7)	5.04 (d, 7)		5.13 (d, 7)	5.11 (d, 7)	5.15 (d, 7)	5.13 (d, 7)
2					4.01 (dd, 7, 8)	4.02 (dd, 7, 8)		4.04 (dd, 7, 8)	4.01 (dd, 7, 8)	*ca.* 4.05	4.01 (dd, 7, 8)
3					4.03 (dd, 8, 8)	*ca.* 4.06		4.08 (dd, 8, 8)	4.06 (dd, 8, 8)	*ca.* 4.07	4.06 (dd, 8, 8)
4					4.13 (br m)	4.14 (br m)		4.15 (br m)	4.14 (br m)	4.15 (br m)	4.15 (br m)
5					3.50 (dd, 10, 11)	3.53 (dd, 10, 11)		3.53 (dd, 10, 11)	3.52 (dd, 10, 11)	3.55 (dd, 10, 11)	3.54 (dd, 10, 11)
					4.21 (dd, 5, 11)	*ca.* 4.22		4.26 (dd, 5, 11)	4.25 (dd, 5, 11)	4.27 (dd, 5, 11)	4.26 (dd, 5, 11)

Abbreviations: GlcUAMe, 6-*O*-methyl-β-D-glucuronopyranosyl; Ara, L-arabinopyranosyl; Xyl, D-xylopyranosyl; Rha, α-L-rhamnopyranosyl. Numbers in parentheses are coupling constants in hertz (Hz).

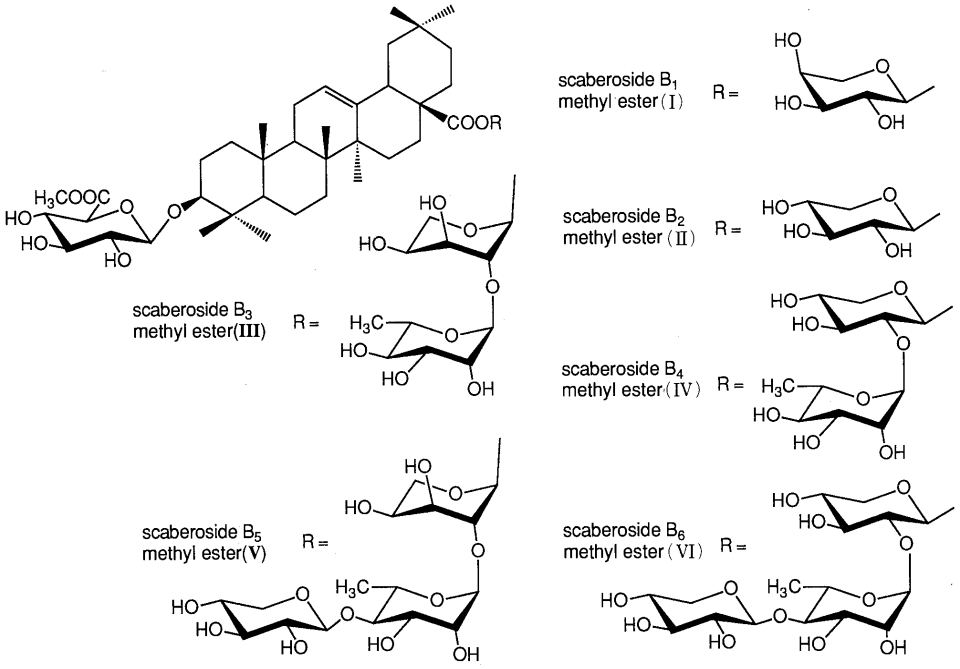

Chart 1

the aglycone. By investigation of the ^1H–^1H correlation spectroscopy (COSY) spectrum, ^1H–^{13}C COSY spectrum and nuclear Overhauser effect (NOE) difference spectrum of III, the ester-linked sugar was suggested to be *O*-α-L-rhamnopyranosyl-(1→2)-α-L-arabinopyranose. The NMR spectra of III were compared with those of I and 3-*O*-acetyl oleanolic acid 28-[*O*-α-L-rhamnopyranosyl-(1→2)-α-L-arabinopyranosyl] ester reported by Mizutani *et al.*[4] The ^{13}C-NMR chemical shifts of the prosapogenin moiety were superimposable on those of the former, and those of the ester-linked sugar moiety were the same as those of the latter. Therefore, the structure of III was elucidated to be as shown in the chart. The configuration and conformation of the arabinopyranosyl group were concluded to be α and $^1C_4$ judging from the values of $J_{H_1H_2}$ (3 Hz), $J_{H_2H_3}$ (4 Hz) and $J_{C_1H_1}$ (171 Hz).[3]

Scaberoside B_4 methyl ester (IV), $C_{48}H_{76}O_{17}$, has D-xylose, L-rhamnose and D-glucuronic acid as component sugars, and the NMR spectra suggested that IV is a similar glycoside having the same prosapogenin as that of III with the rhamnosyl–xylosyl group attached to the carboxyl group. The structure of the ester-linked sugar moiety was determined to be *O*-α-L-rhamnopyranosyl-(1→2)-β-D-xylopyranose by careful examination of NMR spectra, and the structure of IV was determined to be as shown in Chart 1. The configuration and conformation of the L-rhamnopyranosyl group were determined as α and $^1C_4$ on the basis of the coupling constants of C_1-H (br s), C_2-H (br s) and C_3-H (dd, $J=3$, 9 Hz) and from the $J_{C_1H_1}$ value (169 Hz).[3] The coupling constants of C_1-H (d, $J=7$ Hz) and C_2-H (dd, $J=7$, 8 Hz) of the ester-linked xylopyranosyl group undoubtedly indicate that the β-D-xylopyranosyl group is in the $^4C_1$ conformation although the $J_{C_1H_1}$ value (169 Hz) can not be reasonably explained.

Scaberoside B_5 methyl ester (V) gave an $[M+Na]^+$ ion at *m/z* 1079 in FAB-MS, and high-resolution FAB-MS indicated the molecular formula to be $C_{53}H_{84}O_{21}$. On acid hydrolysis, V gave L-arabinose, L-rhamnose, D-xylose and D-glucuronic acid as the component sugars. The NMR spectra suggested it also to be a 3,28-*O*-bisdesmosidic oleanolic acid glycoside having the same prosapogenin as that of IV and a triosyl group linked to the carboxyl group of the aglycone. On selective cleavage[5] of the ester-linked sugar moiety followed by treatment with CH_2N_2, V provided a prosapogenin methyl ester (VII) and an anomeric mixture (VIII) of a methyl trioside which is composed of L-arabinose, D-xylose and L-rhamnose. Compound VII was proved to be oleanolic acid 3-*O*-β-D-glucopyranosiduronic acid dimethyl ester by examination of the NMR spectra. Compound VIII showed in the negative ion FAB-MS an $[M-H]^-$ ion at *m/z* 441 and fragment ions at *m/z* 309 and 163, indicating that VIII is either a methyl arabinosyl-rhamnosyl-xyloside or a methyl xylosyl-rhamnosyl-arabinoside. The anomers were separated by HPLC and the NMR spectra of the α-anomer (VIIIa) and a β-anomer (VIIIb) were carefully examined. The signal assignments are summarized in Tables II and III. The results suggested that VIIIa is methyl *O*-β-D-xylopyranosyl-(1→4)-*O*-α-L-rhamnopyranosyl-(1→2)-α-L-arabinopyranoside and VIIIb, its β-anomer. The NMR spectra of VIIIa and VIIIb were superimposable on those of methyl triosides obtained by selective cleavage of foetidissimoside A {3-*O*-β-D-glucopyranosiduronyl echinocystic acid 28-[*O*-β-D-xylopyranosyl-(1→4)-*O*-α-L-rhamnopyranosyl-(1→2)-α-L-arabinosyl] ester} isolated from the herb of *Aster tataricus* L. f.[2] The ^{13}C-NMR chemical shifts of V were almost the same as those of foetidissimoside A methyl ester except for the signals of C_{15}, C_{16} and C_{17}. From the above-mentioned evidence, the structure of V was determined to be as shown in the chart. The configuration and conformation of the arabinosyl group were determined to be α and $^1C_4$ for the same reasons as in the case of III.

Scaberoside B_6 methyl ester (VI), $C_{53}H_{84}O_{21}$, gave D-xylose, L-rhamnose and D-glucuronic acid as component

sugars on acid hydrolysis. The NMR spectra suggested that VI is also a saponin similar to V. The ester-linked sugar moiety was selectively cleaved to give VII and an anomeric mixture (IX) of a methyl trioside. Compound IX showed the same negative ion FAB-MS as that of VIII, indicating that IX is a mixture of methyl α- and β-xylosyl-rhamnosyl-xylosides. Compound IX was subjected to HPLC and a β-anomer (IXa) and an α-anomer (IXb) were separated. By careful examination of the NMR spectra of IXa and IXb, they were suggested to be methyl *O*-β-D-xylopyranosyl-(1→4)-α-L-rhamnopyranosyl-(1→2)-β-D-xylopyranoside and its α-anomer, respectively. Compound IX was fully methylated according to Hakomori's method[6] and the permethylate was methanolysed. The methanolysate was acetylated and the product was analyzed by gas chromatography-chemical ionization mass spectrometry (GC-CI-MS). Methyl glycosides of 2,3,4-tri-*O*-methyl-D-xylopyranose, 2,3-di-*O*-methyl-4-*O*-acetyl-L-rhamnopyranose and 3,4-di-*O*-methyl-2-*O*-acetyl-D-xylopyranose were detected, thus supporting the structure suggested from the NMR spectra. Therefore, the structure of VI was determined to be as shown in the chart.

Scaberosides are contained in the root in a carboxylate form.

Experimental[7]

Extraction and Isolation of I—VI The plant material was collected in Fukuoka prefecture in August 1989. The fresh root (3 kg) of *Aster scaber* THUNB. was homogenized in MeOH, and percolated with MeOH (20 l) and then with 50% MeOH (20 l). After concentration under reduced pressure, the MeOH extract was suspended in H_2O and extracted with $CHCl_3$. The 50% MeOH extract was concentrated to half the initial volume. The H_2O layer from the MeOH extract and the H_2O solution from the 50% MeOH extract were combined and chromatographed on an MCI gel Diaion HP-20 column using H_2O–MeOH (40→100% MeOH, 10% step) as eluants and separated into two fractions, fr. A (eluted with 50 and 60% MeOH, 30.3 g) and fr. B (eluted with 70→90% MeOH, 19 g). Fraction B (10 g) was dissolved in 50% MeOH and passed through an Amberlite IRC-84 column. The acidic eluate was treated with CH_2N_2 and chromatographed on silica gel (eluant, EtOAc–MeOH–H_2O, 80:5:1→80:20:5) to obtain 12 fractions (fr. B-1—fr. B-12). Fraction B-3 (217 mg) was purified by silica gel column chromatography (EtOAc–1-propanol–H_2O, 100:5:1) and HPLC (column, Capcell pak C_{18}, 250 mm × 10 mm i.d., 80% MeOH) to yield I (75 mg) and II (15 mg). Fraction B-4 (1.02 g) and fr. B-5 (703 mg) were combined and repeatedly chromatographed on a silica gel column (EtOAc–1-propanol–H_2O, 100:5:1), and purified by HPLC (75% MeOH) to give III (244 mg) and IV (36 mg). Fraction B-6 (927 mg) and fr. B-7 (3.6 g) were also chromatographed on silica gel ($CHCl_3$–MeOH–H_2O, 150:40:5), YMC-gel ODS (70→75% MeOH), and finally purified by HPLC (75→80% MeOH) to give V (2.5 g) and VI (429 mg).

Scaberoside B_1 Methyl Ester (I): Colorless needles from H_2O–MeOH. mp 193—195 °C, $[\alpha]_D^{28}$ +8.4° (*c*=2.5, MeOH). Positive ion high resolution (HR)-FAB-MS *m/z*: 779.454 ($[M+H]^+$). $C_{42}H_{67}O_{13}$ requires 779.458. Negative ion FAB-MS *m/z*: 777 ($[M-H]^-$). ^{1}H-NMR δ: aglycone moiety: 3.36 (dd, *J*=4, 12 Hz, C_3-H), 5.43 (dd, *J*=3, 3 Hz, C_{12}-H), 3.25 (dd, *J*=4, 14 Hz, C_{18}-H), 1.30 (C_{23}-H), 0.98 (C_{24}-H), 0.84 (C_{25}-H), 1.02 (C_{26}-H), 1.26 (C_{27}-H), 0.92 (C_{29}-H), 0.96 (C_{30}-H). Sugar moiety: shown in Table III. ^{13}C-NMR: shown in Tables I and II. Coupling constant between anomeric C and H ($J_{C_1H_1}$): 169 Hz (Ara).

Scaberoside B_2 Methyl Ester (II): A white powder, $[\alpha]_D^{27}$ +3.1° (*c*=0.8, MeOH). Positive ion HR-FAB-MS *m/z*: 779.456 ($[M+H]^+$). $C_{42}H_{67}O_{13}$ requires 779.458. Negative ion FAB-MS *m/z*: 777 ($[M-H]^-$). ^{1}H-NMR δ: aglycone moiety: 3.37 (dd, *J*=4, 12 Hz, C_3-H), 5.44 (dd, *J*=3, 3 Hz, C_{12}-H), 3.24 (dd, *J*=4, 14 Hz, C_{18}-H), 1.30 (C_{23}-H), 0.98 (C_{24}-H), 0.84 (C_{25}-H), 1.06 (C_{26}-H), 1.26 (C_{27}-H), 0.92 (C_{29}-H), 0.94 (C_{30}-H). Sugar moiety: shown in Table III. ^{13}C-NMR: aglycone moiety: the chemical shifts are almost the same as those of I. Sugar moiety: shown in Table II. $J_{C_1H_1}$: 158 Hz (Xyl).

Scaberoside B_3 Methyl Ester (III): A white powder, $[\alpha]_D^{26}$ −37.9° (*c*=1.3, MeOH). Positive ion HR-FAB-MS *m/z*: 947.499 ($[M+Na]^+$). $C_{48}H_{76}NaO_{17}$ requires 947.498. Negative ion FAB-MS *m/z*: 923 ($[M-H]^-$). ^{1}H-NMR δ: aglycone moiety: 3.35 (dd, *J*=4, 12 Hz, C_3-H), 5.44 (dd, *J*=3, 3 Hz, C_{12}-H), 3.26 (dd, *J*=4, 14 Hz, C_{18}-H), 1.27 (C_{23}-H), 0.95 (C_{24}-H), 0.84 (C_{25}-H), 1.04 (C_{26}-H), 1.27 (C_{27}-H), 0.93 (C_{29}-H), 0.99 (C_{30}-H). Sugar moiety: shown in Table III. ^{13}C-NMR: aglycone moiety: the chemical shifts are almost the same as those of I. Sugar moiety: shown in Table II. $J_{C_1H_1}$: 171 Hz (Ara), 169 Hz (Rha).

Scaberoside B_4 Methyl Ester (IV): A white powder, $[\alpha]_D^{27}$ −24.2° (*c*=1.7, MeOH). Positive ion HR-FAB-MS *m/z*: 947.505 ($[M+Na]^+$). $C_{48}H_{76}NaO_{17}$ requires 947.498. Negative ion FAB-MS *m/z*: 923 ($[M-H]^-$). ^{1}H-NMR δ: aglycone moiety: 3.35 (dd, *J*=4, 12 Hz, C_3-H), 5.45 (dd, *J*=3, 3 Hz, C_{12}-H), 3.18 (dd, *J*=4, 14 Hz, C_{18}-H), 1.24 (C_{23}-H), 0.94 (C_{24}-H), 0.84 (C_{25}-H), 1.06 (C_{26}-H), 1.29 (C_{27}-H), 0.92 (C_{29}-H), 0.94 (C_{30}-H). Sugar moiety: shown in Table III. ^{13}C-NMR: aglycone moiety: the chemical shifts are almost the same as those of I. Sugar moiety: shown in Table II. $J_{C_1H_1}$: 169 Hz (Xyl), 169 Hz (Rha).

Scaberoside B_5 Methyl Ester (V): Colorless needles from H_2O–MeOH. mp 217—220 °C, $[\alpha]_D^{23}$ −33.3° (*c*=1.0, MeOH). Positive ion HR-FAB-MS *m/z*: 1079.543 ($[M+Na]^+$). $C_{53}H_{84}NaO_{21}$ requires 1079.540. Negative ion FAB-MS *m/z*: 1055 ($[M-H]^-$). ^{1}H-NMR δ: aglycone moiety: 3.36 (dd, *J*=4, 12 Hz, C_3-H), 5.43 (dd, *J*=3, 3 Hz, C_{12}-H), 3.26 (dd, *J*=4, 14 Hz, C_{18}-H), 1.29 (C_{23}-H), 0.96 (C_{24}-H), 0.83 (C_{25}-H), 1.05 (C_{26}-H), 1.28 (C_{27}-H), 0.93 (C_{29}-H), 1.00 (C_{30}-H). Sugar moiety: shown in Table III. ^{13}C-NMR: aglycone moiety: the chemical shifts are almost the same as those of I. Sugar moiety: shown in Table II. $J_{C_1H_1}$: 169 Hz (Ara), 169 Hz (Rha), 157 Hz (Xyl).

Scaberoside B_6 Methyl Ester (VI): Colorless needles from H_2O–MeOH. mp 214—216 °C. $[\alpha]_D^{24}$ −27.0° (*c*=1.0, MeOH). Positive ion HR-FAB-MS *m/z*: 1079.548 ($[M+Na]^+$). $C_{53}H_{84}NaO_{21}$ requires 1079.540. Negative ion FAB-MS *m/z*: 1055 ($[M-H]^-$). ^{1}H-NMR δ: aglycone moiety: 3.36 (dd, *J*=4, 12 Hz, C_3-H), 5.45 (dd, *J*=3, 3 Hz, C_{12}-H), 3.18 (dd, *J*=4, 14 Hz, C_{18}-H), 1.29 (C_{23}-H), 0.93 (C_{24}-H), 0.81 (C_{25}-H), 1.07 (C_{26}-H), 1.30 (C_{27}-H), 0.91 (C_{29}-H), 0.93 (C_{30}-H). Sugar moiety: shown in Table III. ^{13}C-NMR: aglycone moiety: the chemical shifts are almost the same as those of I. Sugar moiety: shown in Table II. $J_{C_1H_1}$: 167 Hz (inner Xyl), 175 Hz (Rha), 154 Hz (outer Xyl).

Determination of Sugar Species and Their Absolute Configurations A glycoside (*ca.* 3 mg) was dissolved in 1 N HCl–MeOH (1 ml) and heated at 95 °C for 2 h. The acidic solution was neutralized with Ag_2CO_3 and the precipitates were centrifuged off. The supernatant was concentrated and the residue was trimethylsilylated with trimethylsilylimidazole, and checked by gas liquid chromatography (GC). The GC conditions were as follows: column, Shimadzu HiCap-CBP-1 (50 m × 0.2 mm i.d.); column oven temperature, 190 °C (for pentose and methyl pentose) and 210 °C (for hexose and glucuronic acid derivatives); injection port temperature, 290 °C; carrier gas, He (linear velocity, 20 cm/s); split ratio, 1/110; make-up gas, He (50 ml/min). Determination of the absolute configuration was performed according to the method reported by Hara *et al.*[8] A glycoside (5—10 mg) was hydrolyzed in 1 N HCl (1 ml) at 95 °C for 2 h. The acidic solution was neutralized in the same manner as described above. The hydrolysate was suspended in H_2O and extracted with $CHCl_3$ to remove the aglycone. The aqueous layer was concentrated and the residue was dissolved in pyridine (0.2 ml). After addition of a pyridine solution (0.4 ml) of L-cysteine methyl ester hydrochloride (0.06 mol/l), the mixture was warmed at 60 °C for 1 h. The solvent was blown off under an N_2 stream, and the residue was trimethylsilylated and checked by GC. The absolute configuration of glucuronic acid was determined in the same way after $NaBH_4$ reduction of VII to methyl oleanolate 3-*O*-β-glucopyranoside. The GC conditions for the determination of the absolute configurations of the component monosaccharides were the same as those described above except for the column oven temperature (250 °C). The results are presented in the text.

Selective Cleavage of the Ester Glycoside Linkage Selective cleavage of the ester-linked sugar moiety was performed according to the method reported by Ohtani *et al.*[5] Compound V (1.1 g) and anhydrous LiI (1.5 g) were dissolved in a mixture of MeOH (4 ml) and 2,6-lutidine (9 ml). After heating at 180 °C for 3 h, the reaction solution was diluted with 50% MeOH and passed through the Amberlite MB-3 column. The eluate was concentrated to dryness, and the residue was dissolved in MeOH and treated with CH_2N_2. The reaction mixture was chromatographed on silica gel (EtOAc–MeOH–H_2O, 80:15:5) to give a prosapogenin methyl ester (VII, 700 mg) of V and an anomeric mixture (VIII, 250 mg) of a methyl glycoside.

Prosapogenin Methyl Ester (VII): Colorless needles from MeOH, mp

227—229 °C, $[\alpha]_D^{27}$ +11.6° (c=2.5, MeOH). Positive ion FAB-MS m/z: 683 ($[M+Na]^+$). ^{1}H-NMR δ: aglycone moiety: 3.37 (dd, J=4, 12 Hz, C_3-H), 5.37 (dd, J=3, 3 Hz, C_{12}-H), 3.08 (dd, J=4, 14 Hz, C_{18}-H), 1.30 (C_{23}-H), 0.98 (C_{24}-H), 0.86 (C_{25}-H), 0.82 (C_{26}-H), 1.24 (C_{27}-H), 0.92 (C_{29}-H), 0.94 (C_{30}-H), 3.60 (–COOMe). Sugar moiety: shown in Table III. ^{13}C-NMR: shown in Tables I and II.

VIII: A white powder. Positive ion FAB-MS m/z: 465 ($[M+Na]^+$). Negative ion FAB-MS m/z: 441 ($[M-H]^-$), 309 ($[M-Xyl-H]^-$), 163 ($[M-Xyl-Rha-H]^-$).

Compound VIII was chromatographed on HPLC (10% MeOH) to give an α-anomer (VIIIa, 63 mg) and a β-anomer (VIIIb, 151 mg) as amorphous powders.

VIIIa: $[\alpha]_D^{25}$ −59.9° (c=1.2, MeOH). ^{1}H-NMR: shown in Table III. ^{13}C-NMR: shown in Table II.

VIIIb: $[\alpha]_D^{26}$ +30.4° (c=1.1, MeOH). ^{1}H-NMR: shown in Table III. ^{13}C-NMR: shown in Table II.

Compound VI (220 mg) was treated in the same way as described for V to give a prosapogenin methyl ester (VII, 120 mg) and an anomeric mixture (IX, 50 mg) of a methyl glycoside. Compound IX was chromatographed on HPLC to give a β-anomer (IXa, 14 mg) and an α-anomer (IXb, 21 mg) as amorphous powders.

IX: A white powder. Positive ion FAB-MS m/z: 465 ($[M+Na]^+$). Negative ion FAB-MS m/z: 441 ($[M-H]^-$), 309 ($[M-Xyl-H]^-$), 163 ($[M-Xyl-Rha-H]^-$).

IXa: $[\alpha]_D^{26}$ −85.1° (c=0.7, MeOH). ^{1}H-NMR: shown in Table III. ^{13}C-NMR: shown in Table II.

IXb: $[\alpha]_D^{27}$ +7.4° (c=1.0, MeOH). ^{1}H-NMR: shown in Table III. ^{13}C-NMR: shown in Table II.

Permethylation of IX and GC-CI-MS Analysis of Component Methylated Sugars Compound IX (10 mg) was methylated according to Hakomori's method,[6] and the reaction product was purified by silica gel column chromatography (hexane–acetone, 9 : 1). The thin-layer-chromatographically homogeneous product (5 mg) was dissolved in 1 N HCl–MeOH and heated at 95 °C for 2 h. The reaction mixture was neutralized with Ag_2CO_3, acetylated with Ac_2O–pyridine and checked by GC-CI-MS. The permethylate of IX gave methyl glycosides of 2,3,4-tri-*O*-methyl-D-xylopyranose, 2,3-di-*O*-methyl-4-*O*-acetyl-L-rhamnopyranose and 3,4-di-*O*-methyl-2-*O*-acetyl-D-xylopyranose. GC-CI-MS conditions: GC part: column, 2% OV-17 on Uniport HP (80—100 mesh) packed in a glass column (1.0 m × 3 mm i.d.); column oven temperature, 130→190 °C (elevation rate, 3 °C/min); carrier gas, He (20 ml/min); injection port temperature, 250 °C. CI-MS part: reagent gas, isobutane (pressure, less than 1.5×10^{-5} Torr); ionization source temperature, 270 °C; ionization energy, 150 eV; scan range, m/z: 100—400; scan interval, 4 s.

Acknowledgement The authors are grateful to Ms. Y. Iwase, Miss J. Honda and Mr. H. Hanazono for measurements of NMR spectra and MS.

References and Notes

1) T. Nagao, S. Hachiyama, H. Okabe and T. Yamauchi, *Chem. Pharm. Bull.*, **37**, 1977 (1989); T. Nagao, H. Okabe and T. Yamauchi, *ibid.*, **38**, 783 (1990).
2) R. Tanaka, T. Nagao, H. Okabe and T. Yamauchi, *Chem. Pharm. Bull.*, **38**, 1153 (1990).
3) K. Bock and C. Pedersen, *J. Chem. Soc., Perkin Trans. 2*, **1974**, 293.
4) K. Mizutani, K. Ohtani, R. Kasai, O. Tanaka and H. Matsuura, *Chem. Pharm. Bull.*, **33**, 2266 (1985).
5) K. Ohtani, K. Mizutani, R. Kasai and O. Tanaka, *Tetrahedron Lett.*, **25**, 4537 (1984).
6) S. Hakomori, *J. Biochem.* (Tokyo), **55**, 205 (1964).
7) The instruments and materials used in this work were as follows: Yanaco micro melting point apparatus (melting points), JASCO DIP-360 digital polarimeter (specific rotation), JEOL JNM GX-400 spectrometer (^{1}H- and ^{13}C-NMR spectra), JEOL JMS DX-300 and HX-110 spectrometers (MS), Shimadzu GC-8APF gas chromatograph (GC), Shimadzu GC-MS-6020 gas chromatograph-mass spectrometer and GC-MS-PAK 500 FDG data analyzer (GC-CI-MS), Kiesel gel 60 (70—230 mesh, E. Merck), Diaion HP-20 (Mitsubishi Chemical Industries, Ltd.), Capcell pak C_{18}-AG120 Å (Shiseido Companyl Ltd.), YMC-Gel ODS (120 A, 70—230 mesh, Yamamura Chemical Laboratories Co., Ltd.). All melting points are uncorrected. NMR spectra were measured in pyridine-d_5 and chemical shifts are expressed in the δ scale using tetramethylsilane as an internal standard.
8) S. Hara, H. Okabe and K. Mihashi, *Chem. Pharm. Bull.*, **35**, 501 (1987).

Synthesis of Parvisoflavones A and B

Masao TSUKAYAMA,* Yasuhiko KAWAMURA, Hiroto TAMAKI, and Tokunaru HORIE

Department of Chemical Science and Technology, Faculty of Engineering, The University of Tokushima, Minamijosanjima-cho, Tokushima 770, Japan. *Received December 20, 1990*

Parvisoflavone B (2′,4′,5-trihydroxy-2″,2″-dimethylpyrano[5″,6″-*g*]isoflavone) (2) was synthesized by regioselective reduction of 7-[2,4-bis(benzyloxy)phenyl]-2,3-dihydro-5-methoxy-2,2-dimethyl-4*H*,6*H*-benzo[1,2-*b*:5,4-*b*′]dipyrano-4,6-dione (7) with sodium borohydride and dehydration of the resultant alcohol, followed by dealkylation with boron trichloride. Its angular isomer, parvisoflavone A (2′,4′,5-trihydroxy-2″,2″-dimethylpyrano[6″,5″-*h*]isoflavone) (1) was also synthesized from 3-[2,4-bis(benzyloxy)phenyl]-8,9-dihydro-5-methoxy-8,8-dimethyl-4*H*,10*H*-benzo[1,2-*b*:3,4-*b*′]-dipyran-4,10-dione (15) in a similar manner.

Keywords pyranoisoflavone; parvisoflavone A; parvisoflavone B; pyronochalcone; pyronoisoflavone; regioselective reduction; sodium borohydride; dealkylation; boron trichloride

A mixture of parvisoflavones A and B was separated from the trunk wood of *Poecilanthe parviflora* and their structures were shown to be 2′,4′,5-trihydroxy-2″,2″-dimethylpyrano-[6″,5″-*h*]isoflavone {systematic name 5-hydroxy-3-(2,4-dihydroxyphenyl)-8,8-dimethyl-4*H*,8*H*-benzo[1,2-*b*:3,4-*b*′]-dipyran-4-one} (**1**) and 2′,4′,5-trihydroxy-2″,2″-dimethylpyrano[5″,6″-*g*]isoflavone {5-hydroxy-7-(2,4-dihydroxyphenyl)-2,2-dimethyl-2*H*,6*H*-benzo[1,2-*b*:5,4-*b*′]dipyran-6-one} (**2**) by spectroscopy[1] and synthesis[2] of their trimethyl ethers. Recently, parvisoflavone B was also isolated from the root of *Lupinus albus* by Tahara *et al.* and they reported that it exhibited high antifungal activity.[3] During the course of our synthetic studies of pyranoisoflavones, we have already found a more convenient method for synthesizing linear and angular pyranoisoflavones from the corresponding pyronochalcones.[4] We report here on the synthesis of parvisoflavones A (**1**) and B (**2**) from the corresponding pyronochalcones by application of this method and confirm the identities of the two natural isomers.

Condensation of 6-acetyl-7-hydroxy-5-methoxy-2,2-dimethyl-4-chromanone[4] (**3**) with 2,4-bis(benzyloxy)-benzaldehyde (**4**) afforded the chalcone (**5**), which was converted into the acetate (**6**). The oxidative rearrangement of **6** with thallium(III) nitrate trihydrate (TTN), followed by cyclization of the resultant compound with diluted hydrochloric acid under reflux afforded the linear pyronoisoflavone (**7**). Debenzylation of **7** with palladium on charcoal was accompanied with hydrogenation of the 2,3-carbon–carbon double bond and afforded an about 1:1 mixture of the corresponding 2′,4′-dihydroxypyronoisoflavone and 2′,4′-dihydroxypyronoisoflavanone. Therefore, the debenzylation of **7** was examined and it was found that a solution of boron trichloride[5] in dichloromethane was the most appropriate reagent: it cleaved simultaneously the two benzyloxy groups and the methoxy group at the C_5-position under the conditions of −65——70 °C for 15 min to give quantitatively 2′,4′,5-trihydroxypyronoisoflavone. Furthermore, 2′,4′-bis(benzyloxy)-5-methoxypyranoisoflavone (**9**) was also easily dealkylated to linear 2′,4′,5-trihydroxypyranoisoflavone (**2**) without influencing the acid-labile dimethylchromene ring under similar dealkylating conditions. Thus, parvisoflavone B (**2**) was easily synthesized by using this dealkylation in the following manner. Compound **7** was regioselectively reduced with sodium borohydride in tetrahydrofuran (THF)–water[4,6] to give the desired monoalcohol (**8**) in good yield. The alcohol **8** was dehydrated with *p*-toluenesulfonic acid monohydrate in toluene to give the linear pyranoisoflavone (**9**), which was converted into **2** as described above. Acetylation and methylation of **2** afforded the triacetate (**10**) and the trimethyl ether[1] (**11**), respectively.

The isomeric angular pyranoisoflavone (**1**) was synthesized in a similar manner: the angular pyronoisoflavone (**15**) was derived from the acetate (**14**) of the corresponding chalcone (**13**), which was prepared from 6-acetyl-5-hydroxy-7-methoxy-2,2-dimethyl-4-chromanone[4] (**12**) and **4**. The angular 2′,4′,5-trihydroxypyranoisoflavone (parvisoflavone A) (**1**) was synthesized from **15** *via* the corresponding monoalcohol (**16**) and pyranoisoflavone (**17**). However, the cleavage of the C_5-methoxy group in **17** was more difficult than that in the linear pyranoisoflavone (**9**) because there is no substituent at the C_6-position adjacent to the 5-

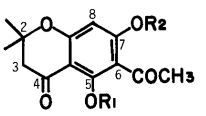

3 : R_1=Me, R_2=H
12 : R_1=H, R_2=Me

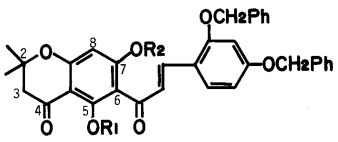

5 : R_1=Me, R_2=H
6 : R_1=Me, R_2=Ac
13 : R_1=H, R_2=Me
14 : R_1=Ac, R_2=Me

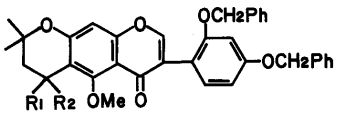

7 : R_1, R_2=O
8 : R_1=H, R_2=OH

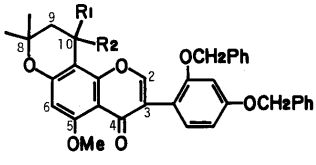

15 : R_1, R_2=O
16 : R_1=H, R_2=OH

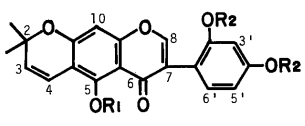

2 : R_1=R_2=H
9 : R_1=Me, R_2=$PhCH_2$
10 : R_1=R_2=Ac
11 : R_1=R_2=Me

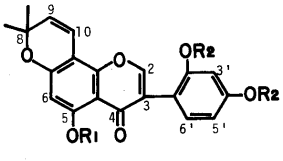

1 : R_1=R_2=H
17 : R_1=Me, R_2=$PhCH_2$
18 : R_1=R_2=Ac
19 : R_1=R_2=Me

TABLE I. ^{1}H-NMR ($CDCl_3$) Spectral Data for Parvisoflavones A (**1**), B (**2**), and Their Derivatives (**10**, **11**, **18**, and **19**)[a]

Compound	Me×2	$C_{3'}$-H	$C_{4'}$-H	C_6-H	C_8-H	$C_{3'}$-H	$C_{5'}$-H	$C_{6'}$-H	C_2-H	OH or Ac	OMe
2[b]	1.42 s	5.70 d	6.55 d		6.37 s	6.33 s	6.25 d′	6.93 d′	8.09 s	9.20 s, 9.29 s, 13.22 s	
Natural[c]	1.48 s	5.79 d	6.69 d		6.41 s	6.49 s	6.45 d′	7.13 d′	8.17 s	13.2 s	
10	1.46 s	5.66 d	6.40 d		6.62 s	6.98 s	6.95 d′	7.20 d′	7.61 s	2.12 s (3H), 2.25 s (3H) 2.37 s (3H)	
11	1.45 s	5.66 d	6.71 d		6.56 s	6.51 d″	6.51 d′,d″	7.20 d′	7.69 s		3.73 s (3H), 3.79 s (3H) 3.86 s (3H)
Natural[1]	1.52 s	5.72 d	6.78 d		6.62 s	6.57 s	6.57 d′	7.27 d′	7.74 s		3.80 s (3H), 3.90 s (3H) 3.94 s (3H)
1[b]	1.43 s	5.70 d	6.62 d	6.19 s		6.33 s	6.26 d′	6.96 d′	8.18 s	9.23 s, 9.32 s, 13.01 s	
18	1.47 s	5.62 d	6.68 d	6.43 s		7.00 s	6.97 d′	7.20 d′	7.68 s	2.13 s (3H), 2.26 s (3H) 2.33 s (3H)	
19	1.45 s	5.48 d	6.63 d	6.22 s		6.47 s	6.43 d′	7.13 d′	7.65 s		3.68 s (3H), 3.75 s (3H) 3.84 s (3H)
Natural[1]	1.50 s	5.60 d	6.75 d	6.23 s		6.55 s	6.55 d′	7.25 d′	7.75 s		3.77 s (3H), 3.88 s (3H) 3.95 s (3H)

a) s, singlet; d, doublet (J=10 Hz); d′, doublet (J=9 Hz); d″, doublet (J=2 Hz). *b*) Measured in DMSO-d_6. *c*) Lit. 3*a*: measured in acetone-d_6.

TABLE II. UV Spectral Data for Parvisoflavones A (**1**), B (**2**), and Their Derivatives (**10**, **11**, **18**, and **19**)[a]

Linear form				Angular form			
Compound	λ_{max} nm (log ε)			Compound	λ_{max} nm (log ε)		
2	284 (4.61)	347 sh (3.60)		**1**	270 (4.64)	307 i (3.88)	349 (3.53)
($AlCl_3$)	284 (4.61)	347 sh (3.61)		($AlCl_3$)	284 (4.64)	316 i (3.83)	408 (3.52)
10	265 (4.59)	294 i (3.93)	336 (3.88)	**18**	258 (4.61)	307 (3.76)	315 (3.73)
11	268 (4.59)	325 (3.84)		**19**	266 (4.62)	299 i (3.86)	332 (3.69)
Natural[1]	267 (4.65)			Natural[1]	263 (4.56)		

a) sh, shoulder; i, inflection point.

methoxy group,[7] and a small amount of 2′,4′-dihydroxy-5-methoxypyranoisoflavone was isolated as a by-product.

The proton nuclear magnetic resonance (^{1}H-NMR) and ultraviolet (UV) spectral data for the synthetic pyranoisoflavones **1** and **2** and their derivatives (**10**, **11**, **18**, and **19**) are summarized in Tables I and II. On the basis of these results, the structures of parvisoflavones A and B were confirmed to be 2′,4′,5-trihydroxy-2″,2″-dimethylpyrano-[6″,5″-*h*]isoflavone and 2′,4′,5-trihydroxy-2″,2″-dimethylpyrano[5″,6″-*g*]isoflavone, respectively.

Experimental

All the melting points are uncorrected. The UV spectra were taken in ethanol on a Hitachi 124 spectrophotometer. The ^{1}H-NMR spectra were measured with a Hitachi R-20 spectrometer (60 MHz), using tetramethylsilane as an internal standard (δ, ppm). Column chromatography and thin-layer chromatography were carried out on Kieselgel 60 (70—230 mesh) and with Kieselgel 60 F-254 (Merck).

7-Hydroxy-5-methoxy-2,2-dimethyl-6-[1-oxo-3-(2,4-bis(benzyloxy)-phenyl)-2-propenyl]-4-chromanone (5) A mixture of 6-acetyl-7-hydroxy-5-methoxy-2,2-dimethyl-4-chromanone[4] (**3**) (9.80 g) and 2,4-bis(benzyloxy)benzaldehyde (**4**) (14.17 g) was refluxed with stirring in the presence of KOH (6.2 g) in EtOH (400 ml) for 7 h. The reaction mixture was concentrated to *ca.* 200 ml under reduced pressure and then poured into ice-cold water and acidified with HCl. The separated precipitates were recrystallized from EtOAc–petroleum ether to give **5** (18.22 g, 81%) as yellow prisms: mp 162—164 °C. ^{1}H-NMR ($CDCl_3$) δ: 1.44 (6H, s, CH_3×2), 2.66 (2H, s, $COCH_2$), 3.77 (3H, s, OCH_3), 5.00 and 5.09 (each 2H, s, $C_6H_5C\underline{H}_2$), 6.20 (1H, s, C_8-H), 6.40—6.70 (2H, m, C_3-H and C_5-H), 7.68 (1H, d, J=9 Hz, C_6-H), 7.78 and 8.26 (each 1H, d, J=16 Hz, CH=), 13.74 (1H, s, OH). *Anal.* Calcd for $C_{35}H_{32}O_7$: C, 74.45; H, 5.71. Found: C, 74.59; H, 5.51.

The Acetate (6) Compound **5** (16.8 g) was converted into the acetate (**6**) as pale yellow needles by treatment with acetic anhydride–pyridine at 120 °C, mp 142—143 °C (MeOH–EtOAc). *Anal.* Calcd for $C_{37}H_{34}O_8$: C, 73.25; H, 5.66. Found: C, 73.42; H, 5.65.

7-[2,4-Bis(benzyloxy)phenyl]-2,3-dihydro-5-methoxy-2,2-dimethyl-4*H*,6*H*-benzo[1,2-*b*:5,4-*b*′]dipyran-4,6-dione (7) A mixture of **6** (7.0 g) and TTN (8 g) was stirred in MeOH (850 ml) and 1,2-dichloroethane (150 ml) at 35—38 °C for 6 h, then 10% HCl (80 ml) was added, and the mixture was refluxed for a further 3 h. After removal of the precipitates by filtration, the filtrate was concentrated to *ca.* 400 ml under reduced pressure and poured into a large amount of water to give precipitates. The separated precipitates were recrystallized from MeOH–EtOAc to give **7** (3.57 g, 55%) as pale yellow needles, mp 169—171 °C. ^{1}H-NMR ($CDCl_3$) δ: 1.46 (6H, s, CH_3×2), 2.71 (2H, s, $COCH_2$), 3.97 (3H, s, OCH_3), 5.01 and 5.03 (each 2H, s, $C_6H_5C\underline{H}_2$), 6.60 (1H, d, J=9 Hz, C_5-H), 7.22 (1H, d, J=9 Hz, $C_{6'}$-H), 6.64 (1H, s, $C_{3'}$-H), 6.67 (1H, s, C_{10}-H), 7.28 and 7.36 (each 5H, s, $C_6\underline{H}_5CH_2$), 7.69 (1H, s, C_8-H). *Anal.* Calcd for $C_{35}H_{30}O_7$: C, 74.72; H, 5.38. Found: C, 74.54; H, 5.23.

2′,4′-Bis(benzyloxy)-5-methoxy-2″,2″-dimethylpyrano[5″,6″-*g*]isoflavone (9) Compound **7** (4.0 g) in THF (240 ml) was stirred, with gradual addition of an aqueous solution (60 ml) of $NaBH_4$ (1.08 g), at 5—10 °C for 30 min, and then Me_2CO (5 ml) was added to the reaction mixture. The whole was diluted with water and the organic solvent was removed under reduced pressure. The residue was neutralized with HCl, and extracted with EtOAc. The extract was washed with water, dried (Na_2SO_4), and evaporated under reduced pressure to give the crude monoalcohol **8** (3.98 g) as a colorless paste: mp 140—142 °C (colorless needles from Me_2CO–Et_2O). ^{1}H-NMR ($CDCl_3$) δ: 1.38 and 1.43 (each 3H, s, CH_3), 2.07 (2H, d, J=6 Hz, $C\underline{H}_2CHOH$), 3.45 (1H, br, $CH_2CHO\underline{H}$), 3.88 (3H, s, OCH_3), 4.98 (4H, s, $C_6H_5C\underline{H}_2$×2), 5.02 (1H, t, J=6 Hz, $CH_2C\underline{H}OH$), 6.4—6.7 (3H, m, C_{10}-H, $C_{3'}$-H and $C_{5'}$-H), 7.0—7.4 (11H, m, $C_{6'}$-H and $C_6\underline{H}_5CH_2$×2), 7.67 (1H, s, C_8-H). *Anal.* Calcd for $C_{35}H_{32}O_7$: C, 74.45; H, 5.71. Found: C, 74.27; H, 5.68.

Crude **8** (3.98 g) was stirred in toluene (80 ml) in the presence of $TsOH \cdot H_2O$ (70 mg) at 110 °C for 20 min. The resulting compound was recrystallized from MeOH to give **9** (2.75 g, 71% based on **7**) as colorless needles, mp 124—126 °C. UV λ_{max}^{EtOH} nm (log ε): 268 (4.60), 325 (3.87). ^{1}H-NMR ($CDCl_3$) δ: 1.43 (6H, s, CH_3×2), 3.78 (3H, s, OCH_3), 4.98 (4H, s, $C_6H_5C\underline{H}_2$×2), 5.60 (1H, d, J=10 Hz, $C_{3'}$-H), 6.64 (1H, d, J=10 Hz, $C_{4'}$-H), 6.48 (1H, s, C_8-H), 6.53 (1H, d, J=9 Hz, $C_{5'}$-H), 7.16 (1H, d, J=9 Hz, $C_{6'}$-H), 6.60 (1H, s, $C_{3'}$-H), 7.20 and 7.28 (each 5H, s, $C_6\underline{H}_5CH_2$),

7.63 (1H, s, C_2-H). *Anal.* Calcd for $C_{35}H_{30}O_6$: C, 76.90; H, 5.53. Found: C, 76.86; H, 5.35.

2′,4′,5-Trihydroxy-2″,2″-dimethylpyrano[5″,6″-*g*]isoflavone (Parvisoflavone B) (2) A solution of BCl_3–CH_2Cl_2 (7 ml) [BCl_3 (25 g) had been dissolved in CH_2Cl_2 (48 ml)] was added to compound **9** (500 mg) in CH_2Cl_2 (12 ml) at −65——70°C. The reaction mixture was stirred at that temperature for 15 min, then water was added, and the solvent was removed at below 40 °C under reduced pressure to give a precipitate. The separated precipitate was extracted with EtOAc, washed with aqueous $NaHCO_3$ and water, and dried (Na_2SO_4). The resulting compound was chromatographed over a silica-gel column with $CHCl_3$–Me_2CO (5 : 1) to give **2** (250 mg, 78%) as yellow needles, mp 188.5—189.5 °C ($CHCl_3$). *Anal.* Calcd for $C_{20}H_{16}O_6$: C, 68.18; H, 4.58. Found: C, 68.01; H, 4.29.

The Triacetate (10) Compound **2** was converted into the acetate (**10**) as colorless needles by treatment with acetic anhydride–pyridine at 120 °C, mp 184—185 °C (MeOH). *Anal.* Calcd for $C_{26}H_{22}O_9$: C, 65.27; H, 4.64. Found: C, 65.16; H, 4.56.

The Trimethyl Ether (11) A mixture of **2**, dimethyl sulfate, and K_2CO_3 was refluxed with stirring in Me_2CO for 6 h. The resulting compound was recrystallized from MeOH–H_2O to give **11** as colorless needles, mp 150—151 °C. *Anal.* Calcd for $C_{23}H_{22}O_6$: C, 70.04; H, 5.62. Found: C, 69.80: H, 5.51.

5-Hydroxy-7-methoxy-2,2-dimethyl-6-[1-oxo-3-(2,4-bis(benzyloxy)-phenyl)-2-propenyl]-4-chromanone (13) A mixture of 6-acetyl-5-hydroxy-7-methoxy-2,2-dimethyl-4-chromanone[4] (**12**) (5.10 g) and **4** (7.26 g) was refluxed with stirring in the presence of piperidine (1.8 ml) in EtOH (200 ml) for 10 h. The resulting compound was recrystallized from MeOH–Me_2CO to give **13** (6.67 g, 61%) as yellow needles, mp 165—167 °C. ^{1}H-NMR ($CDCl_3$) δ: 1.45 (6H, s, $CH_3 \times 2$), 2.67 (2H, s, $COCH_2$), 3.67 (3H, s, OCH_3), 5.02 (4H, s, $C_6H_5C\underline{H}_2 \times 2$), 5.92 (1H, s, C_8-H), 6.40—6.70 (2H, m, C_3-H and C_5-H), 6.95 and 7.80 (each 1H, d, J=16 Hz, CH=), 7.26 and 7.30 (each 5H, s, $C_6\underline{H}_5CH_2$), 7.46 (1H, d, J=9 Hz, C_6-H), 12.30 (1H, s, OH). *Anal.* Calcd for $C_{35}H_{32}O_7$: C, 74.45; H, 5.71. Found: C, 74.51; H, 5.71.

The Acetate (14) mp 127—128 °C, pale yellow needles (MeOH). *Anal.* Calcd for $C_{37}H_{34}O_8$: C, 73.25; H, 5.66. Found: C, 73.11; H, 5.63.

3-[2,4-Bis(benzyloxy)phenyl]-8,9-dihydro-5-methoxy-8,8-dimethyl-4*H*,10*H*-benzo[1,2-*b*:3,4-*b*′]dipyran-4,10-dione (15) A mixture of **14** (4.70 g) and TTN (5.13 g) was stirred in MeOH (700 ml) and 1,2-dichloroethane (100 ml) at 35—38 °C for 10 h, and then cyclized with diluted HCl. The resulting compound was recrystallized from EtOAc–petroleum ether to give **15** (2.66 g, 61%) as colorless needles, mp 155—156 °C. ^{1}H-NMR ($CDCl_3$) δ: 1.47 (6H, s, $CH_3 \times 2$), 2.70 (2H, s, $COCH_2$), 3.90 (3H, s, OCH_3), 4.99 (4H, s, $C_6H_5C\underline{H}_2 \times 2$), 6.25 (1H, s, C_6-H), 6.40—6.75 (2H, m, C_3′-H and C_5′-H), 7.18 (1H, d, J=9 Hz, C_6′-H), 7.22 and 7.31 (each 5H, s, $C_6\underline{H}_5CH_2$), 7.87 (1H, s, C_2-H). *Anal.* Calcd for $C_{35}H_{30}O_7$: C, 74.72; H, 5.38. Found: C, 74.49; H, 5.27.

2′,4′-Bis(benzyloxy)-5-methoxy-2″,2″-dimethylpyrano[6″,5″-*h*]isoflavone (17) The selective reduction of **15** (350 mg) with $NaBH_4$ (100 mg) at 5—10 °C for 25 min gave the crude monoalcohol **16** (347 mg) as a colorless paste, mp 167—168.5 °C (colorless prisms from Me_2CO–Et_2O). ^{1}H-NMR ($CDCl_3$) δ: 1.36 and 1.44 (each 3H, s, CH_3), 1.85—2.15 (2H, m, $C\underline{H}_2CHOH$), 3.01 (1H, br, $CH_2CHO\underline{H}$), 3.79 (3H, s, OCH_3), 4.93 (4H, s, $C_6H_5C\underline{H}_2 \times 2$), 4.80—5.10 (1H, m, $CH_2C\underline{H}OH$), 6.19 (1H, s, C_6-H), 6.49 (1H, d, J=9 Hz, C_5′-H), 7.18 (1H, d, J=9 Hz, C_6′-H), 6.58 (1H, s, C_3′-H), 7.19 and 7.28 (each 5H, s, $C_6\underline{H}_5CH_2$), 7.63 (1H, s, C_2-H). *Anal.* Calcd for $C_{35}H_{32}O_7$: C, 74.45; H, 5.71. Found: C, 74.35; H, 5.78.

Dehydration of crude **16** (347 mg) with TsOH·H_2O (10 mg) gave **17** (260 mg, 76% based on **15**) as colorless needles, mp 151—152 °C. UV λ_{max}^{EtOH} nm (log ε): 265 (4.67), 299i (3.90), 332 (3.68). ^{1}H-NMR ($CDCl_3$) δ: 1.44 (6H, s, $CH_3 \times 2$), 3.84 (3H, s, OCH_3), 4.95 (4H, s, $C_6H_5C\underline{H}_2 \times 2$), 5.43 (1H, d, J=10 Hz, C_3″-H), 6.60 (1H, d, J=10 Hz, C_4″-H), 6.20 (1H, s, C_6-H), 6.52 (1H, d, J=9 Hz, C_5′-H), 7.10 (1H, d, J=9 Hz, C_6′-H), 6.56 (1H, s, C_3′-H), 7.18 and 7.25 (each 5H, s, $C_6\underline{H}_5CH_2$),7.63 (1H, s, C_2-H). *Anal.* Calcd for $C_{35}H_{30}O_6$: C, 76.90; H, 5.53. Found: C, 76.80; H, 5.58.

2′,4′,5-Trihydroxy-2″,2″-dimethylpyrano[6″,5″-*h*]isoflavone (Parvisoflavone A) (1) Compound **17** (220 mg) in CH_2Cl_2 (9 ml) was stirred with BCl_3–CH_2Cl_2 (5.5 ml) at −65——70 °C for 15 min. The resulting compound was chromatographed over a silica-gel column with $CHCl_3$–Me_2CO (5 : 1) to give **1** (105 mg, 73%) and 2′,4′-dihydroxy-5-methoxypyranoisoflavone (5 mg, 4%).

Parvisoflavone A (**1**): Pale yellow prisms, mp 236—238 °C ($CHCl_3$). *Anal.* Calcd for $C_{20}H_{16}O_6$: C, 68.18; H, 4.58. Found: C, 68.00; H, 4.60.

2′,4′-Dihydroxy-5-methoxypyranoisoflavone: Colorless prisms, mp 245—247 °C ($CHCl_3$). ^{1}H-NMR (DMSO) δ: 1.44 (6H, s, $CH_3 \times 2$), 3.78 (3H, s, OCH_3), 5.68 (1H, d, J=10 Hz, C_3″-H), 6.1—6.5 (3H, m, C_3′-, C_5′- and C_6-H), 6.63 (1H, d, J=10 Hz, C_4″-H), 6.88 (1H, d, J=9 Hz, C_6′-H), 7.92 (1H, s, C_2-H), 9.10 and 9.21 (each 1H, s, OH). *Anal.* Calcd for $C_{21}H_{18}O_6$: C, 68.84; H, 4.95. Found: C, 69.13; H, 4.70.

The Triacetate (18) Colorless needles, mp 152—154 °C (MeOH). *Anal.* Calcd for $C_{26}H_{22}O_9$: C, 65.27; H, 4.64. Found: C, 65.10; H, 4.51.

The Trimethyl Ether (19) Colorless needles, mp 165—167 °C (MeOH–H_2O). *Anal.* Calcd for $C_{23}H_{22}O_6$: C, 70.04; H, 5.62. Found: C, 69.79; H, 5.70.

References

1) R. M. V. Assumpcao and O. R. Gottlieb, *Phytochemistry*, **12**, 1188 (1973).
2) A. C. Jain, A. Kumar, and R. C. Gupta, *J. Chem. Soc., Perkin Trans. 1*, **1979**, 279.
3) *a*) S. Tahara, J. L. Ingham, S. Nakahara, J. Mizutani, and J. B. Harborne, *Phytochemistry*, **23**, 1889 (1984); *b*) S. Tahara, *Nippon Nogei Kagaku Kaishi*, **58**, 1247 (1984).
4) M. Tsukayama, Y. Kawamura, H. Tamaki, T. Kubo, and T. Horie, *Bull. Chem. Soc. Jpn.*, **62**, 826 (1989).
5) M. Fieser and L. F. Fieser, "Reagents for Organic Synthesis," Vol. 2, John Wiley & Sons, New York, 1979, p. 34.
6) M. Tsukayama, T. Sakamoto, T. Horie, M. Masumura, and M. Nakayama, *Heterocycles*, **16**, 955 (1981).
7) T. Horie, H. Kourai, and T. Fujita, *Bull. Chem. Soc. Jpn.*, **56**, 3773 (1983).

Studies on Trifluoromethyl Ketones. VII.[1] Ene Reaction of Trifluoroacetaldehyde and Its Application for Synthesis of Trifluoromethyl Compounds[2]

Keizo OGAWA, Takabumi NAGAI, Masahiko NONOMURA, Toshiyuki TAKAGI, Mayumi KOYAMA, Akira ANDO, Takuichi MIKI, and Itsumaro KUMADAKI*

Faculty of Pharmaceutical Sciences, Setsunan University, 45-1, Nagaotoge-cho, Hirakata, Osaka 573-01, Japan. *Received December 27, 1990*

As an extension of our studies on the ene reaction of trifluoromethyl ketones, the ene reaction of trifluoroacetaldehyde was examined. The aldehyde reacted with various ene compounds as a good enophile in the presence of Lewis acids, among which methylaluminum dichloride worked best, though polymerization of the aldehyde caused by the Lewis acid often lowered the isolation yields of the ene reaction. The ene reaction products were successfully oxidized to trifluoromethyl β,γ-unsaturated ketones with Dess–Martin reagent. Reduction of the ene reaction products followed by oxidation with Jones reagent gave saturated trifluoromethyl ketones. The β,γ-unsaturated ketone rearranged on thermolysis to an α,β-unsaturated ketone. These ketones obtained were converted to other types of trifluoromethyl compounds. Thus, the ene reaction of trifluoroacetaldehyde provides a versatile method for synthesis of many types of trifluoromethyl compounds. During this derivatization, a trifluoromethyl group was found to behave as a much larger substituent than a decyl group.

Keywords trifluoroacetaldehyde; ene reaction; trifluoromethyl; homoallyl alcohol; methylaluminum dichloride; Dess–Martin reagent; ketone; Grignard reaction; Wittig reaction; steric effect

We have already reported the ene reaction[3] of trifluoromethyl ketones with ene compounds and derivatization[4] of the products, trifluoromethylated homoallyl alcohols, to various types of trifluoromethyl compounds (see Chart 1). During that research, we noticed that the alkyl groups of trifluoromethyl ketones show a strong steric effect on their reactivities. Thus, we planned to examine the ene reaction of trifluoroacetaldehyde, which has the smallest substituent, a hydrogen. We expected that this small steric effect would help us to understand the steric effect on this reaction and that, if the reaction proceeded, the products would be α-trifluoromethylated secondary homoallyl alcohols that might be converted to trifluoromethyl ketones by oxidation. These ketones could be versatile intermediates for the synthesis of various types of trifluoromethyl compounds (see Chart 1).

Only one report on the reaction of trifluoroacetaldehyde with olefins was published, by Pautrat's group,[5] before the name "ene reaction" became familiar. They used ferric chloride as a catalyst for the reaction with cyclohexene and obtained 3-(2,2,2-trifluoro-1-hydroxyethyl)cyclohexene in the yield of 40%, though its purity was only 70%. They described its reaction with some olefins, but most of the products were mixtures and the yields were low. Thus, their method has little practical utility, and no attention has been paid to it for a long time. We examined this reaction more extensively, hoping to develop it into a useful synthetic method. The results are summarized in Table I.

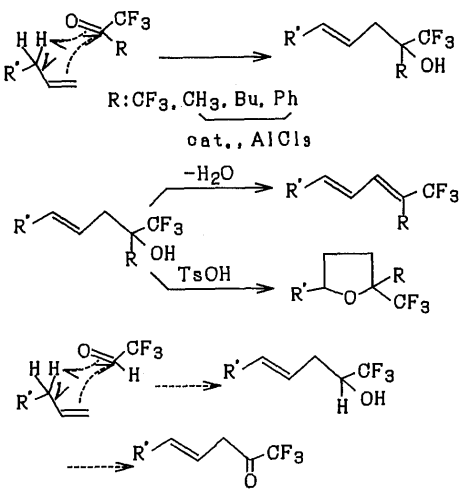

Chart 1

At first, 1-octene was heated with trifluoroacetaldehyde (**1**), which was generated from its hemiacetal, in the absence of a catalyst, but the olefin was recovered quantitatively. Hexafluoroacetone, which has two trifluoromethyl groups, reacts without a catalyst.[3a] The aldehyde (**1**) has only one trifluoromethyl group and is not reactive enough to react with an ene compound without a catalyst even though its steric hindrance may be small. The reaction in the presence of ferric chloride gave 1,1,1-trifluoro-4-decen-2-ol (**2**, 42%) with small amounts of 4-chloro-1,1,1-trifluoro-2-decanol (**3**, 1%) and 2-pentyl-5-(trifluoromethyl)tetrahydrofuran (**4**, 5%). The structure of **2** was determined by examination of the proton and fluorine nuclear magnetic resonance (^{1}H- and ^{19}F-NMR) spectra. Thus, a hydroxylic proton was observed at 2.20 ppm as a doublet, which disappeared on addition of D_2O. Usually, an alcoholic proton appears as a singlet. This splitting is characteristic of an α-trifluoromethyl alcohol. Two olefinic protons appeared at 5.33 and 5.69 ppm. The coupling constant between them was 15.4 Hz, which shows that the double bond is an *E*-form. Only one doublet was observed on ^{19}F-NMR. This suggests that the *Z*-isomer was not formed in an appreciable amount. Compound **3** showed a hydroxylic proton, two types of methylene protons and two methine protons, but no olefinic proton in its ^{1}H-NMR spectrum. Compound **4** is an isomer of **2**, but it does not have a hydroxyl group or olefinic protons. ^{19}F-NMR of **4** shows that it consists of two isomers, probably *cis* and *trans*. In this reaction, formation of polymers from **1** was significant and the yield of **2** was unsatisfactory. The ene reaction of trifluoromethyl ketones was catalyzed successfully with aluminum chloride at −78 °C.[3b,c] Thus, this condition was examined, but the yield of **2** was less than in the former case, and the yields

TABLE I. Ene Reaction of Trifluoroacetaldehyde

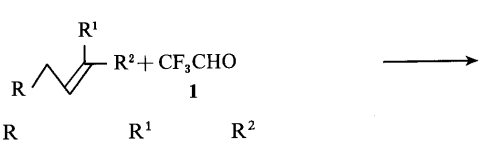

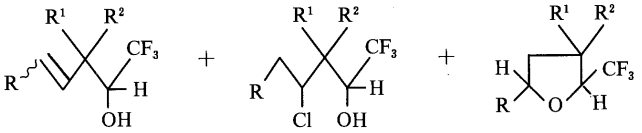

R	R^1	R^2							
Pen	H	H	$FeCl_3$, 80 °C	**2**	42%	**3**	1%	**4**	5%
			120 °C, 5 h		No reaction				
			$AlCl_3$, −78 °C		36%		6%		10%
			MADC, −78 °C		48%		1%		0.5%
$-(CH_2)_3-$		H	$AlCl_3$, −78 °C	**5**	9%	**6**[a]	12%		
			MADC, −78 °C		32%		2%		
			$(C_2H_5)_2AlCl_2$		No reaction				
Ph	H	H	$AlCl_3$, −78 °C	**7**	20%	**8**	17%	**9**	8%
			MADC, −78 °C		38%		14%		4%
Bu	Me	H	$FeCl_3$, 80 °C	**10**	22%				
			MADC, −78 °C		76%				
Hept	H	H	MADC, −78 °C	**11**	27%	**12**	1%		
			$AlCl_3$, −78 °C		77%		1%		

a) Concerning the structure, see text.

of the by-products were increased. Since polymerization of **1** seemed to be catalyzed by the Lewis acid, the reaction was carried out at −78 °C in the presence of methylaluminum dichloride (MADC), a weaker Lewis acid than $AlCl_3$. Now, the yield of **2** was improved to 48% and those of **3** and **4** were decreased remarkably. Formation of a chloro compound and a tetrahydrofuran compound was observed in the ene reaction of trifluoroacetone.[3b] Similar mechanisms are proposed. Compound **4** is formed by the cyclization of the ene reaction product (**2**), and **3** is formed from the transition state of the ene reaction. One to three equivalents of **1** were used in these experiments. Use of a large excess of **1** did not greatly improve the yield of **2**.

Next, the reaction of cyclohexene, a 1,2-disubstituted ene compound, was examined in the presence of aluminum chloride to give 3-(2,2,2-trifluoro-1-hydroxyethyl)cyclohexene (**5**, 9%) and 1-chloro-1-(2,2,2-trifluoro-1-hydroxyethyl)-cyclohexane (**6**, 12%), whereas in the presence of MADC, the yields of **5** and **6** were 32% and 2%, respectively. Here, polymerzation of **1** proceeded preferentially to the ene reaction. Thus, we tried diethylaluminum chloride as a catalyst, but no ene reaction product was formed, *i.e.*, diethylaluminum chloride is not effective for this reaction. The structure of **5** was determined from the following NMR data: six methylene protons, two olefinic protons at 5.66 and 6.03 ppm, one methine proton around 2.6 ppm, another methine proton at 3.76 ppm (qdd) and one OH proton at 2.31 ppm (d). One doublet was observed on ^{19}F-NMR. The ^{1}H-NMR spectrum of **6** showed only one methine proton (dq, changed to q with D_2O). Its ^{13}C-NMR spectrum showed five methylenes. These data support the structure of **6**. Formation of this product suggests a two-step mechanism through a carbocation, in contrast with the formation of **3**. Since no stereoisomer of **5** was detected, the ene reaction itself seems to be a concerted reaction.

The same reaction of allylbenzene with **1** in the presence of $AlCl_3$ gave 1,1,1-trifluoro-5-phenyl-4-penten-2-ol (**7**, 20%), 4-chloro-1,1,1-trifluoro-5-phenylpentanol (**8**, 17%) and 2-phenyl-5-(trifluoromethyl)tetrahydrofuran (**9**, 8%). The yields of **8** and **9** were quite large. Therefore, MADC was examined as a catalyst. The yield of **7** was slightly improved, but the by-products were still formed in fairly large amounts. This may be due to the high stability of a benzylic cation or a benzenonium ion.

The ene reaction of hexafluoroacetone with a 1,2-disubstituted olefin, 2-octene, hardly proceeded,[3a] while trifluoroacetone reacted with 2-octene in the presence of aluminum chloride.[3b] The difference of the reactivities seems to be attributable to the difference of steric effects of a methyl and a trifluoromethyl group. Thus, reaction of **1** with 2-octene was examined in the presence of $FeCl_3$ and MADC. While the former catalyst gave a poor yield of 3-methyl-1,1,1-trifluoro-4-nonen-2-ol (**10**, 22%), the latter gave a much better yield of **10** (76%). The ^{1}H-NMR spectrum of **10** shows two methyl protons, a doublet and a triplet, and two olefinic protons. This fact shows that a proton was abstracted not from the methyl group, but from the methylene part, though a methyl proton is abstracted in the usual ene reaction of 2-octene with non-fluorinated enophiles. No isomer of **10** was observed on ^{19}F-NMR. Thus, this reaction is highly regio- and steroselective. These selectivities will be discussed in the last part in this report. In the ene reaction of trifluoromethyl ketones, the reactivity of 2-octene is rather low. The high yield of **10** may be due to the lower steric hindrance of the hydrogen of trifluoroacetaldehyde than of other alkyl groups of trifluoromethyl ketones.

Finally, to investigate derivatization of trifluoromethyl compounds from the ene reaction product, a product of low volatility was required. For this purpose, the ene reaction of 1-decene was examined. MADC did not give a satisfactory result. As mentioned above, $AlCl_3$ seems to cause **1** to polymerize. Therefore, $AlCl_3$ was added gradually to a solution of 1-decene and **1** in CH_2Cl_2 at −78 °C, and 1,1,1-trifluoro-4-dodecen-2-ol(**11**, 77%) was obtained together with a very small amount of a chloro compound (**12**). The structure of **11** was determined by comparison of the spectral data with those of **2**.

Next, we planned to convert the ene reaction products, the secondary trifluoromethylated homoallyl alcohols, to other types of trifluoromethyl compounds. For this purpose, we chose **11** as a model compound, since the volatility of

the product was expected to be low enough to allow accurate estimation of the yield of reactions. Oxidation of **11** to a trifluoromethyl ketone was examined first. A trifluoromethyl carbinol is usually very stable, and in this case, we could not obtain the objective ketone by usual methods of oxidation, such as the use of Jones reagent, probably because the olefinic part reacted faster than the alcohol part. However, by means of Dess–Martin reagent,[6] **11** was oxidized smoothly to 1,1,1-trifluoro-4-dodecen-2-one (**13**, 74%). If **11** was hydrogenated first in the presence of Pd–C to 1,1,1-trifluoro-2-dodecanol (**14**, 99%), the latter was oxidized by Jones reagent to 1,1,1-trifluoro-2-dodecanone (**15**, 62%). Further, heating of **13** without a solvent at 180 °C afforded 1,1,1-trifluoro-3-dodecen-2-one (**16**) quantitatively. Thus, we could obtain three kinds of trifluoromethyl ketones from the ene reaction products of trifluoroacetaldehyde (see Chart 2). Oxidation of **2** gave 1,1,1-trifluoro-4-decen-2-one, but its isolation from methylene chloride was difficult due to the high volatility of the fluorine compound.

Next, some reactions of these carbonyl compounds for the introduction of carbon functions were examined.

Grignard reagents reacted with these ketones as normal carbonyl compounds. Thus, methyl magnesium iodide or phenyl magnesium bromide reacted with **13** to give 1,1,1-trifluoro-2-methyl-4-dodecen-2-ol (**17**, 60%) or 1,1,1-trifluoro-2-phenyl-4-dodecen-2-ol (**18**, 65%) without intervention of a fluorine as a halogen or the trifluoromethyl group as a pseudo halogen.[7] Similarly, **15** and **16** reacted to give trifluoromethylated tertiary alcohols (**19**, **20** and **21**). In the last case, no product of 1,4-addition reaction was detected, even in the presence of copper(I) iodide. The strong inductive effect of the trifluoromethyl group seems to make the alpha position highly electrophilic (see Chart 3).

As another reaction for carbon-chain elongation of the carbonyl group, the Wittig reaction was examined. When the ketone (**15**) was treated with benzyltriphenylphosphonium bromide in the presence of sodium ethoxide in ethanol, (1*E*)-1-phenyl-2-(trifluoromethyl)-1-dodecene (**22**) was obtained in only 9% yield. Ordinary ketones give good yields of olefins under this condition. The poor yield of the above reaction might be attributed to the fact that the high electronegativity of the trifluoromethyl group makes the carbonyl group highly electrophilic and that **15** forms a hemiacetal in ethanol. To avoid this acetal formation, the reaction was carried out in benzene in the presence of sodium hydride to give a 72% yield of **22**. The stereochemistry was determined from the coupling between the vinylic hydrogen and the trifluoromethyl fluorines in NMR. The reaction of **15** with triphenylphosphonium butylide gave 5-(trifluoromethyl)-4-pentadecene (**23**, 92%), which consisted of about 75% of (4*Z*) and about 25% of (4*E*) isomers. ^{19}F-NMR showed a singlet at −4.62 and a broad doublet at 2.60 (ratio 3 : 1). A small coupling of the latter with the olefinic hydrogen shows that this signal is attributable to the (4*E*) isomer.[4b] Namely, the (4*Z*) isomer was formed preferentially. In the Wittig reaction of ketones, a stable ylide such as benzyl ylide is reported to give a *trans* isomer preferentially for a larger substituent and an unstable ylide such as butyl ylide yields a *cis* isomer preferentially. If we apply this rule to our results, a trifluoromethyl group is larger than a decyl group. The ketone **13** gave a similar result to **15** (see Chart 3).

We have already reported derivatization of trifluoromethylated dienes from the ene reaction products of trifluoromethyl ketones by dehydration.[4b] Now, the ene reaction products were dehydrated similarly to the trifluoromethylated dienes with a hydrogen on the trifluoromethylated olefinic carbon. Thus, **11** was treated with phosphoryl chloride in pyridine to give (2*E*,4*E*)-1,1,1-

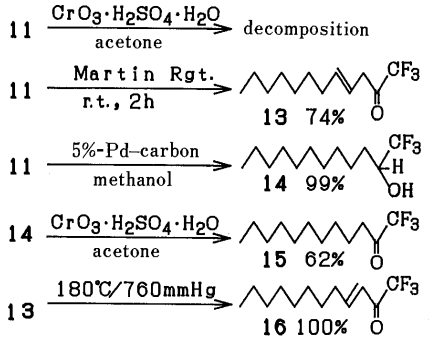

Chart 2

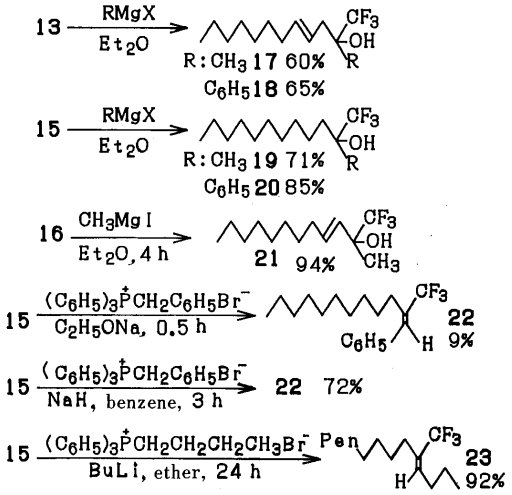

Chart 3

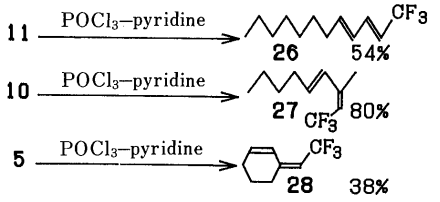

Chart 4

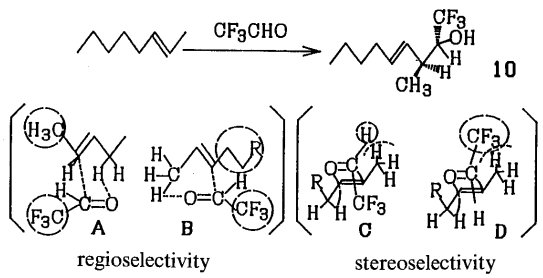

Chart 5

trifluoro-2,4-dodecadiene (**26**, 54%), which included very small amouts of its (2*Z*,4*E*)-isomer and the chlorination product of **11**. A similar reaction of **10** gave 1,1,1-trifluoro-3-methyl-2,4-nonadiene (**27**) selectively. Its stereochemistry was determined as (2*Z*,4*E*) based on the low chemical shift of the trifluoromethyl fluorine on ^{19}F-NMR and the small coupling constants between the methyl protons and the trifluoromethyl fluorines (see Chart 4). A similar dehydration of **5** gave predominantly (*Z*)-3-[(trifluoromethyl)methylene]cyclohexene (**28**), the structure of which was determined from the nuclear Overhauser effect (NOE) interaction between the *exo*-olefinic proton and the 4-methylene protons. A small amount of *E*-isomer was isolated and showed NOE interaction between the olefinic protons (see Chart 4).

As we have reported, this reaction proceeds predominantly through an anti-elimination.[4b] Therefore, these results shows that the stereochemistry of **10** and **5** is *l* (based on *l-u*: *like-unlike* notation.[8]) The regioselectivity is explained by a comparison of transition states A and B. Repulsion between the trifluoromethyl group and the pentyl group in B is larger than that between the trifluoromethyl group and the methyl group in A. The stereoselectivity can be explained similarly: repulsion between the olefinic hydrogen and the methyl group in trasition state C is smaller than that between the trifluoromethyl group and the methyl group in transition state D. Thus, **10** was formed through C (see Chart 5).

In conclusion, trifluoroacetaldehyde was found to react as a good enophile in the presence of a Lewis acid, though it also polymerizes in the presence of the Lewis acid. Therefore, the catalyst should be chosen carefully. The product was oxidized to a trifluoromethyl ketone, which was further converted to other types of trifluoromethyl compounds. In some of these transformations, it was found that a trifluoromethyl group behaves as a larger substituent than a decyl group.

Experimental

Gerneral Procedures Trifluoroacetaldehyde was obtained as follows. Trifluoroacetaldehyde ethyl hemiacetal was added dropwise to concentrated H_2SO_4 at 120 °C under stirring, and trifluoroacetaldehyde (**1**) was collected through a reflux condenser in a trap cooled at −78 °C. ^{1}H-NMR spectra were obtained on JNM-FX90Q and JNM-GX400 spectrometers. ^{19}F-NMR spectra were recorded on the JNM-FX90Q spectrometer, using benzotrifluoride as an internal standard (upper field taken as plus).

Reaction of 1 with 1-Octene 1) In the Presence of $FeCl_3$: $FeCl_3$ (0.1 g, 0.6 mmol), 1-octene (3.0 g, 27 mmol) and CH_2Cl_2 (10 ml) were put in a stainless steel tube, the tube was cooled to −78 °C, and **1** (3.3 ml) was introduced into the tube using a vacuum line. The tube was sealed and shaken at 80 °C for 5 h. After being cooled to room temperature, the tube was opened and the contents were treated with 10% NH_4OH (5 ml) and CH_2Cl_2 (10 ml). The mixture was filtered through a Celite layer. The filter cake was washed with CH_2Cl_2. The filtrate and washings were combined and extracted with CH_2Cl_2. The CH_2Cl_2 layer was dried over $MgSO_4$ and concentrated under vacuum. The residue was separated by a column chromatography (SiO_2, hexane–CH_2Cl_2, 4:1 to 1:1) to give 1,1,1-trifluoro-4-decen-2-ol (**2**, 2.43 g, 42%), 2-pentyl-5-(trifluoromethyl)tetrahydrofuran (**4**, 0.28 g, 5%) and 4-chloro-1,1,1-trifluoro-2-decanol (**3**, 0.07 g, 1%). **2**: A colorless oil. Mass spectrum (MS) *m/z*: 210 (M^+). High resolution MS (HRMS) Calcd for $C_{10}H_{17}F_3O$: 210.123. Found: 210.124. ^{1}H-NMR ($CDCl_3$) δ: 0.94 (3H, t, J=5.1 Hz), 1.07—1.57 (6H, m), 1.83—2.11 (2H, m), 2.20 (1H, d, J=5.9 Hz), 2.33—2.64 (2H, m), 3.68—4.17 (1H, m), 5.33 (1H, ddd, J=6.2, 6.7, 15.4 Hz), 5.69 (1H, td, J=5.7, 15.4 Hz). ^{19}F-NMR ($CDCl_3$) ppm: 15.06 (d, J=6.8 Hz). **3**: A colorless oil. MS *m/z*: 246 (M^+) HRMS Calcd for $C_{10}H_{18}ClF_3O$: 246.100. Found: 246.100. ^{1}H-NMR($CDCl_3$) δ: 0.97 (3H, m), 1.11—1.60 (11H, m), 1.62—1.84 (2H, m), 1.84—2.07 (2H, m), 2.45 (1H, d, J=6.2 Hz, disappeared on addition of D_2O), 3.92—4.61 (2H, m), ^{19}F-NMR ($CDCl_3$) ppm: 15.64 (d, J=6.8 Hz). **4**: A colorless oil. MS *m/z*: 210 (M^+). HRMS Calcd for $C_{10}H_{17}F_3O$: 210.123. Found: 210.124. ^{1}H-NMR ($CDCl_3$) δ: 0.81 (6H, t, J=5.1 Hz), 0.94—1.61 (12H, m), 1.72—2.24 (2H, m), 3.49—4.46 (2H, m). ^{19}F-NMR ($CDCl_3$) ppm: 14.40 (d, J=7.3 Hz), 14.55 (d, J=7.3 Hz) (ratio 1:1).

2) Thermal Reaction without a Catalyst: A solution of 1-octene (1.0 g, 9 mmol) in CH_2Cl_2 (10 ml) were sealed in a stainless steel tube and **1** (1.5 ml) was added as above. The tube was shaken at 120 °C for 5 h, and the mixture was treated as above. The analysis of the product by gas-liquid chromatography (GLC) showed only recovery of 1-octene. (The aldehyde **1** polymerized to an insoluble solid.)

3) In the Presence of $AlCl_3$: To a mixture of $AlCl_3$ (2.3 g, 17 mmol) and 1-octene (1.0 g, 9 mmol) in CH_2Cl_2 (10 ml), **1** (2.3 ml) was added through a cannula at −78 °C in an atmosphere of argon. The mixture was stirred at this temperature for 2 h, then poured into a mixture of 10% HCl and ice, and extracted with CH_2Cl_2. The CH_2Cl_2 layer was washed with H_2O and dried over $MgSO_4$. A similar separation to that descibed in section 1) gave **2** (1.57 g, 36%), **3** (0.31 g, 6%) and **4** (0.44 g, 10%).

4) In the Presence of MADC: In an atmosphere of Ar, **1** (6 ml) and CH_3AlCl_2 (MADC, 20 wt%/hexane, 16 ml) were added in that order at −78 °C to a solution of 1-octene (5.0 g, 45 mmol) in CH_2Cl_2 (28 ml), and the mixture was stirred at this temperature for 3 h. The mixture was treated as described in sec 1) to give **2** (4.5 g, 48%), **3** (0.11 g, 1%) and **4** (0.05 g, 0.5%).

Reaction of 1 with Cyclohexene 1) In the Presence of $AlCl_3$: In an atmosphere of Ar, cyclohexene (3.5 g, 42 mmol and **1** (11.5 g) were added to a suspension of $AlCl_3$ (12.0 g, 90 mmol) in CH_2Cl_2 (21 ml) at −78°C, and the mixture was stirred at this temperature for 1 h, then poured into a mixture of 10% HCl and ice, and extracted with CH_2Cl_2. The CH_2Cl_2 layer was washed with H_2O and dried over $MgSO_4$. After evaporation of the solvent, the residue was purified by a column chromatography (SiO_2, hexane–CH_2Cl_2, 4:1) to give 3-(2,2,2-trifluoro-1-hydroxyethyl)cyclohexene (**5**, 0.72 g, 9%) and 1-chloro-1-(2,2,2-trifluoro-1-hydroxyethyl)cyclohexane (**6**, 1.09 g, 12%). **5**: A colorless oil. bp 122 °C/100 mmHg. MS *m/z*: 180 (M^+). HRMS Calcd for $C_8H_{11}F_3O$: 180.076. Found 180.075. ^{1}H-NMR ($CDCl_3$) δ: 1.34—1.88 (4H, m), 1.88—2.17 (2H, m), 2.31 (1H, d, J=8.2 Hz), 2.44—2.84 (1H, m), 3.76 (1H, qdd, J=8.0, 8.2, 4.3 Hz), 5.66 (1H, bd, J=7.7 Hz), 6.03 (1H, dm, J=7.7 Hz). ^{19}F-NMR ($CDCl_3$) ppm: 12.31 (d, J=8.0 Hz). **6**: A colorless oil. MS *m/z*: 215 (M−1). HRMS Calcd for $C_8H_{12}ClF_3O$: 215.045. Found: 215.046. ^{1}H-NMR ($CDCl_3$) δ: 1.16—1.35 (1H, m), 1.61—1.86 (7H, m), 2.06—2.22 (2H, m), 2.98 (1H, d, J=9.2 Hz, disappeared on addition of D_2O), 3.76 (1H, qd, J=7.0, 9.2 Hz, q on addition of D_2O). ^{13}C-NMR ($CDCl_3$): 124.18 (CF_3), 76.43 (CF_3-C), 75.58 (C-Cl), 37.07, 34.64, 25.03, 21.66, 21.52 ($CH_2 \times 5$). ^{19}F-NMR ($CDCl_3$) ppm: 6.78 (d, J=7.0 Hz).

2) In the Presence of $(C_2H_5)_2$ AlCl: In a stream of Ar, **1** (2.3 ml) was added to a solution of cyclohexene (1.2 g, 15 mmol) in dry CH_2Cl_2 (7 ml). To this solution, 10% $(C_2H_5)_2AlCl$ (10 ml) was added at −78°C and the mixture was stirred at this temperature for 3 h, then worked up as above. Analysis by GLC showed that cyclohexene was recovered completely.

3) In the Presence of MADC: In an atmosphere of Ar, **1** (2.3 ml) and MADC (20 wt%/hexane, 17 ml) were added to a solution of cyclohexene (1.2 g, 15 mmol) in dry CH_2Cl_2 (7 ml) at −78 °C. The mixture was stirred at this temperature for 4 h, then poured into a mixture of 10% HCl and ice, and extracted with CH_2Cl_2. The organic layer was washed with H_2O and dried over $MgSO_4$. After evaporation of the solvent, the residue was separated by column chromatography (SiO_2, hexane–CH_2Cl_2, 4:1) to give **5** (0.84 g, 32%) and **6** (0.06 g, 2%).

Reaction of 1 with Allylbenzene 1) In the Presence of $AlCl_3$: In an atmosphere of Ar, **1** (2.2 ml) was added to a mixture of $AlCl_3$ (2.5 g, 19 mmol) and allylbenzene (1.5 g, 13 mmol) in dry CH_2Cl_2 (10 ml) at −78 °C, and the mixture was stirred at this temperature for 3 h, then poured into a mixture of 10% HCl and ice, and extracted with CH_2Cl_2. The CH_2Cl_2 layer was washed with H_2O and dried over $MgSO_4$. The solvent was evaporated off under vacuum, and the residue was separated by column chromatography (SiO_2, hexane–CH_2Cl_2, 4:1 to 1:1) to give 1,1,1-trifluoro-5-phenyl-4-penten-2-ol (**7**, 0.56 g, 20%), 4-chloro-1,1,1-trifluoro-5-phenylpentan-2-ol (**8**, 0.54 g, 17%) and 2-phenyl-5-(trifluoromethyl)tetrahydrofuran (**9**, 0.22 g, 8%). **7**: A colorless oil, bp 120 °C/20 mmHg, which solidified on standing. MS *m/z*: 216 (M^+). HRMS Calcd for $C_{11}H_{11}F_3O$: 216.076. Found: 216.076. ^{1}H-NMR ($CDCl_3$) δ: 2.29 (1H, d, J=6.7 Hz), 2.37—2.74 (2H, m), 3.80—4.29 (1H, m), 6.20 (1H,

ddd, J=15.9, 6.4, 6.4 Hz), 6.52 (1H, d, J=15.9 Hz), 6.74—7.57 (5H, m). ^{19}F-NMR ($CDCl_3$) ppm: 15.08 (d, J=6.8 Hz). **9**: A colorless oil. MS m/z: 216 (M^+). HRMS Calcd for $C_{11}H_{11}F_3O$: 216.076. Found: 216.076. ^{1}H-NMR ($CDCl_3$) δ: 1.67—2.73 (7H, m), 3.56 (1H, qdd, J=6.6, 7.2, 7.2 Hz), 3.89 (1H, m), 4.20—4.70 (2H, m), 4.86—5.19 (1H, m), 7.09—7.47 (10H, m). ^{19}F-NMR ($CDCl_3$) ppm: 14.02 (d, J=6.6 Hz), 14.34 (d, J=7.8 Hz). (ratio 2:1).

2) In the Presence of MADC: In an atmosphere of Ar, **1** (2.3 ml) and MADC (20 wt%/hexane, 5 ml) were added to a solution of allylbenzene (1.2 g, 10 mmol) in dry CH_2Cl_2 (7 ml) at −78 °C, and the mixture was stirred at this temperature for 2 h, then poured into a mixture of 10% HCl and ice, and extracted with CH_2Cl_2. The CH_2Cl_2 layer was washed with H_2O and dried over $MgSO_4$. After evaporation of the solvent, the residue was separated by column chromatography (SiO_2, hexane–CH_2Cl_2, 4:1 to 1:1) to give **7** (0.83 g, 38%), **8** (0.36 g, 14%) and **9** (0.09 g, 4%).

Reaction of 1 with 2-Octene 1) In the Presence of $FeCl_3$: Ferric chloride (0.1 g, 0.6 mmol), 2-octene (3.0 g, 27 mmol) and CH_2Cl_2 (10 ml) were placed in a stainless steel tube, and **1** (3.3 ml) was added at −78 °C under vacuum. The sealed tube was shaken at 80 °C for 4 h, then the mixture was worked up as in the case of the reaction of 1-octene and separated by column chromatography (SiO_2, hexane–CH_2Cl_2, 4:1 to 1:1) to give 3-methyl-1,1,1-trifluoro-4-nonen-2-ol (**10**, 1.25 g, 22%). **10**: A colorless oil. MS m/z: 210 (M^+). HRMS Calcd for $C_{10}H_{17}F_3O$: 210.123. Found: 210.124. ^{1}H-NMR ($CDCl_3$) δ: 0.89 (3H, t, J=6.2 Hz), 1.16 (3H, d, J=7.5 Hz), 1.21—1.45 (4H, m), 1.77—2.23 (2H, m), 2.48 (1H, s), 2.67 (1H, qdd, J=7.5, 7.2, 5.4 Hz), 3.76 (1H, qd, J=6.8, 5.4 Hz), 5.40 (1H, dd, J=15.4, 7.2 Hz), 5.53—5.87 (1H, m). ^{19}F-NMR ($CDCl_3$) ppm: 11.82 (d, J=6.8 Hz).

2) In the Presence of MADC: In an atmosphere of Ar, **1** (3.3 ml) and MADC (20wt%/hexane, 3 ml) were added to a solution of 2-octene (3.0 g, 27 mmol) in dry CH_2Cl_2 (10 ml) at −78 °C and the mixture was stirred at this temperature for 1.5 h. The reaction mixture was worked up as usual and the product was purified by column chromatography (SiO_2, hexane–CH_2Cl_2, 4:1 to 1:1) to give **10** (4.28 g, 76%).

Reaction of 1-Decene In an atomosphere of Ar, **1** (8.0 ml) was added through a cannula to a solution of 1-decene (5.0 g, 36 mmol) in dry CH_2Cl_2 (50 ml) at −78 °C. To this solution, $AlCl_3$ (5.0 g, 38 mmol) was added in small portions at −78 °C. The mixture was stirred at this temperature for 3 h, then poured into a mixture of 10% HCl and ice, and extracted with CH_2Cl_2. The CH_2Cl_2 layer was washed with H_2O and dried over $MgSO_4$. The solvent was evaporated off under vacuum, and the residue was purified by column chromatography (SiO_2, hexane–CH_2Cl_2, 4:1 to 1:1) to give 1,1,1-trifluoro-4-dodecen-2-ol (**11**, 6.61 g, 77%). **11**: A colorless oil. bp 130 °C/26 mmHg. MS m/z: 238 (M^+). HRMS Calcd for $C_{12}H_{21}F_3O$: 238.155. Found: 238.155. ^{1}H-NMR ($CDCl_3$) δ: 0.88 (3H, t, J=5.1 Hz), 1.06—1.61 (10H, m), 1.85—2.17 (3H, m), 2.23—2.53 (2H, m), 5.34 (1H, ddd, J=15.2, 7.2, 6.4 Hz), 5.63 (1H, td, J=5.1, 15.2 Hz). ^{19}F-NMR ($CDCl_3$ ppm: 15.14 (d, J=6.6 Hz). A chloro compound (**12**, 1%) was detected on GLC-MS.

1,1,1-Trifluoro-4-dodecen-2-one (13) Compound **11** (6.6 g, 28 mmol) was added to a solution of Dess–Martin reagent (29.2 g, 69 mmol) in dry CH_2Cl_2 (312 ml). The mixture was stirred at room temperature for 2 h, then treated with saturated $NaHCO_3$ (300 ml) containing $Na_2S_2O_3$ (68.2 g) and extracted with CH_2Cl_2. The CH_2Cl_2 layer was dried over $MgSO_4$. After evaporation of the solvent, the residue was purified by column chromatography (SiO_2, pentane) to give 1,1,1-trifluoro-4-dodecen-2-one (**13**, 4.8 g, 74%). **13**: bp 105 °C/20 mmHg. MS m/z: 236 (M^+) HRMS Calcd for $C_{12}H_{19}F_3O$: 236.139. Found 236.139. ^{1}H-NMR ($CDCl_3$) δ: 0.90 (3H, t, J=5.1 Hz), 1.08—1.46 (10H, m), 1.78—2.17 (2H, m), 3.44 (2H, d, J=5.7 Hz), 5.51 (1H, td, J=5.1, 15.1 Hz), 6.28 (1H, td, J=5.5, 15.1 Hz). ^{19}F-NMR ($CDCl_3$) ppm: 14.47 (s).

1,1,1-Trifluoro-2-dodecanol (14) A solution of **11** (4.0 g, 17 mmol) in MeOH (200 ml) was shaken with 5% Pd–C (0.2 g) in a stream of H_2. After removel of the catalyst by filtration, the reaction mixtue was concentrated under vacuum and purified by column chromatography (SiO_2, pentane to give 1,1,1-trifluoro-2-dodecanol **14**. 4.0 g, 99%). **14**: A colorless oil. MS m/z: 240 (M^+). HRMS Calcd for $C_{12}H_{23}F_3O$: 240.170. Found: 240.171. ^{1}H-NMR ($CDCl_3$) δ: 0.91 (3H, t, J=5.14 Hz), 1.15—1.43 (16H, br s), 1.49—1.78 (2H, m), 1.95 (1H, s), 3.70—4.10 (1H, m). ^{19}F-NMR ($CDCl_3$) ppm: 15.83 (d, J=6.84 Hz).

1,1,1-Trifluoro-2-dodecanone (15) Jones reagent (32 ml) was added to a solution of **14** (1.4 g, 5.8 mmol) in acetone (150 ml) added at 0 °C under stirring. Stirring was continued for a further 24 h. Isopropanol was then added dropwise till the red–brown color disappeared. Ice water was added to the mixture and the whole was extracted with CH_2Cl_2. The CH_2Cl_2 layer was washed with H_2O and dried over $MgSO_4$. After evaporation of the solvent, the residue was purified by column chromatography (SiO_2, pentane) to give 1,1,1-trifluoro-2-dodecanone (**15**, 0.83 g, 62%). **15**: A colorless oil. MS m/z: 238 (M^+). HRMS Calcd for $C_{12}H_{21}F_3O$: 238.155. Found: 238.155. ^{1}H-NMR ($CDCl_3$) δ: 0.89 (3H, t, J=5.14 Hz), 1.09—1.47 (14H, br s), 1.48—1.87 (2H, m), 2.73 (2H, t, J=7.46 Hz). ^{19}F-NMR ($CDCl_3$) ppm: 15.11 (s).

1,1,1-Trifluoro-3-dodecen-2-one (16) Heating of **13** without any solvent at 180 °C and purification by column chromatography (SiO_2, pentane) gave 1,1,1-trifluoro-3-dodecen-2-one (**16**) quantitatively. **16**: A colorless oil. bp 105 °C/20 mmHg. MS m/z: 236 (M^+). HRMS Calcd for $C_{12}H_{19}F_3O$: 236.139. Found: 236.139. ^{1}H-NMR ($CDCl_3$) δ: 0.91 (3H, t, J=5.1 Hz), 1.14—1.48 (12H, m), 2.06—2.49 (2H, m), 6.43 (1H, d, J=15.9 Hz), 7.16—7.58 (1H, m). ^{19}F-NMR ($CDCl_3$) ppm: 13.23 (s).

1,1,1-Trifluoro-2-methyl-4-dodecen-2-ol (17) A solution of **13** (0.3 g, 1.3 mmol) in dry Et_2O (5 ml) was added to a solution of MeMgI, which was prepared from Mg (113 mg, 4.7 mmol) and MeI (600 mg, 4.2 mmol) in dry Et_2O (15 ml), in an atmosphere of Ar. The mixture was stirred at room temperature for 4h, then poured into a mixture of 10% NH_4Cl and ice, and extracted with Et_2O. The Et_2O layer was washed with H_2O and dried over $MgSO_4$. After the evaporation of the solvent under vacuum, the residue was purified by column chromatography (SiO_2, hexane–CH_2Cl_2, 4:1) to give 1,1,1-trifluoro-2-methyl-4-dodecen-2-ol (**17**, 0.19 g, 60%). **17**: A colorless oil. MS m/z: 252 (M^+). HRMS Calcd for $C_{13}H_{23}F_3O$: 252.170. Found: 252.170. ^{1}H-NMR ($CDCl_3$) δ: 0.89 (3H, t, J=4.9 Hz), 1.05—1.49 (13H, m), 1.90—2.16 (2H, m), 2.12 (1H, s, disappeared on addition of D_2O), 2.26 (1H, dd, J=9.6, 7.4 Hz), 2.50 (1H, dd, J=9.6, 7.4 Hz), 5.36 (1H, ddd, J=7.4, 9.6, 15.1 Hz), 5.49 (1H, td, J=5.8, 15.1 Hz). ^{19}F-NMR ($CDCl_3$) ppm: 17.87 (s).

1,1,1-Trifluoro-2-phenyl-4-dodecen-2-ol (18) A solution of **13** (0.5 g, 2 mmol) in dry Et_2O (5 ml) was added to a solution of PhMgBr, which was prepared from Mg (160 mg, 6.6 mmol) and PhBr (1.0 g, 6.4 mmol) in dry Et_2O (30 ml) in an atmosphere of Ar. The mixture was stirred at room temperature for 3 h, then poured into 10% NH_4Cl and ice, and extracted with Et_2O. The Et_2O layer was washed with H_2O and dried over $MgSO_4$. After evaporation of the solvent under vacuum, the residue was purified by column chromatography (SiO_2, hexane–CH_2Cl_2, 4:1) to give 1,1,1-trifluoro-2-phenyl-4-dodecen-2-ol (**18**, 0.43 g, 65%). **18**: A colorless oil. MS m/z: 314 (M^+). HRMS Calcd for $C_{18}H_{25}F_3O$: 314.186. Found: 314.185. ^{1}H-NMR ($CDCl_3$) δ: 0.90 (3H, t, J=5.14 Hz), 1.06—1.48 (10H, m), 1.79—2.14 (2H, m), 2.63 (1H, s), 2.87 (2H, d, J=6.9 Hz), 5.14 (1H, td, J=6.7, 14.8 Hz), 5.66 (1H, td, J=6.4, 14.8 Hz), 7.23—7.71 (5H, m), ^{19}F-NMR ($CDCl_3$) ppm: 14.68 (s).

1,1,1-Trifluoro-2-methyl-2-dodecanol (19) A solution of **15** (0.3 g, 1.3 mmol) in dry Et_2O (5 ml) was added to a solution of MeMgI which was obtained by the reaction of Mg (113 mg, 4.7 mmol) and MeI (512 mg, 3.6 mmol) in dry Et_2O (15 ml) in atmosphere of Ar. The mixture was stirred at room temperature for 2 h, then poured into 10% NH_4Cl and ice, and extracted with Et_2O. The Et_2O layer was washed with H_2O and dried over $MgSO_4$. After evaporation of the solvent, the residue was purified by column chromatography (SiO_2, hexane–CH_2Cl_2, 4:1) to give 1,1,1-trifluoro-2-methyl-2-dodecanol (**19**, 229 mg, 71%). **19**: A colorless oil. MS m/z: 254 (M^+). HRMS Calcd for $C_{13}H_{25}F_3O$: 254.186. Found: 254.186. ^{1}H-NMR ($CDCl_3$) δ: 0.92 (3H, t, J=5.1 Hz), 1.09—1.45 (21H, m), 1.74 (1H, s). ^{19}F-NMR ($CDCl_3$) 18.83 (s).

1,1,1-Trifluoro-2-phenyl-2-dodecanol (20) A solution of **15** (0.5 g, 2 mmol) in dry Et_2O (5 ml) was added to a solution of PhMgBr, which was obtained by the reaction of Mg (160 mg, 6.6 mmol) and PhBr (1.0 g, 6.4 mmol) in dry Et_2O (20 ml), in an atmosphere of Ar. The mixture was stirred at room temperature for 2 h, then poured into a mixture of 10% NH_4Cl and ice, and extracted with Et_2O. The Et_2O layer was washed with H_2O and dried over $MgSO_4$. After evaporation of the solvent, the residue was purified by column chromatograhy (SiO_2, hexane–CH_2Cl_2, 4:1) to give 1,1,1-trifluoro-2-phenyl-2-dodecanol (**20**, 0.57 g, 85%). **20**: A colorless oil. MS m/z: 316 (M^+). HRMS Calcd for $C_{18}H_{27}F_3O$: 316.202. Found: 316.201. ^{1}H-NMR ($CDCl_3$) δ: 0.89 (3H, t, J=5.1 Hz), 1.07—1.37 (18H, m), 2.33 (1H, s), 7.23—7.64 (5H, m). ^{19}F-NMR ($CDCl_3$) ppm: 15.83 (s).

1,1,1-Trifluoro-2-methyl-3-dodecen-2-ol (21) A solution of **16** (0.3 g, 1.3 mmol) in dry Et_2O (5 ml) was added to a solution of MeMgI, which was obtained by the reaction of Mg (113 mg, 4.7 mmol) and MeI (600 mg, 4.2 mmol) in dry Et_2O (15 ml), in an atmosphere of Ar. The mixture was stirred at room temperature for 4 h, then poured into 10% NH_4Cl and ice, and extracted with Et_2O. The Et_2O layer was washed with H_2O and dried over $MgSO_4$. After evaporation of the solvent, the residue was purified by column chromatography (SiO_2, hexane–CH_2Cl_2, 4:1) to give

1,1,1-trifluoro-2-methyl-3-dodecen-2-ol (**21**, 0.31 g, 94%). **21**: A colorless oil. MS *m/z*: 252 (M^+). HRMS Calcd. for $C_{13}H_{23}F_3O$: 252.170. Found: 252.170. ^{1}H-NMR ($CDCl_3$) δ: 0.60—1.01 (3H, m), 1.10—1.42 (15H, m), 1.93—2.05 (3H, m), 5.59 (1H, d, J=15.9 Hz), 5.80—6.13 (1H, m). ^{19}F-NMR ($CDCl_3$) ppm: 18.41 (s).

(1*E*)-1-Phenyl-2-(trifluoromethyl)-1-dodecene (22) a) In EtOH: Sodium (110 mg, 4.8 mmol) was dissolved in EtOH (10 ml) and benzyltriphenylphosphonium bromide (1.65 g) was added to this solution in an atmosphere of Ar under vigous stirring. After 20 minutes' stirring, a solution of **15** (0.5 g, 2 mmol) in EtOH (5 ml) was added, and the whole was stirred at room temperature for a further 0.5 h then poured into ice-water and extracted with Et_2O. The Et_2O layer was washed with H_2O and dried over $MgSO_4$. After evaporation of the solvent, the residue was purified by column chromatography (SiO_2, hexane) to give (1*E*)-1-phenyl-2-(trifluoromethyl)-1-dodecene (**22**, 63 mg, 9%). **22**: A colorless oil. MS *m/z*: 312 (M^+). HRMS Calcd for $C_{19}H_{27}F_3$: 312.207. Found: 312.207. ^{1}H-NMR ($CDCl_3$) δ: 0.88 (3H, t, J=5.1 Hz), 1.09—1.40 (16H, m), 2.23—2.51 (2H, m), 6.99—7.09 (1H, m), 7.24—7.41 (5H, m). ^{19}F-NMR ($CDCl_3$) ppm: 2.24 (d, J=1.7 Hz). A very small singlet (less than 5%) observed at 5.20 ppm is attributed to the (1*Z*) isomer.

b) In Benzene: A suspension of benzyltriphenylphosphonium bromide (1.1 g) and NaH (about 60%, 0.13 g) in dry C_6H_6 (20 ml) was stirred at room temperature for 0.5 h in an atmosphere of Ar, and a solution of **15** (0.5 g, 2 mmol) in dry C_6H_6 (5 ml) was added to this suspension. Stirring was continued at room temperature for 3 h, then the reaction mixture was poured into ice-water and extracted with Et_2O. The Et_2O layer was washed with H_2O and dried over $MgSO_4$. After evaporation of the solvent, the residue was purified by column chromatography (SiO_2, hexane) to give **22** (0.52 g, 72%), which contained a trace of the (1*Z*) isomer.

(4*Z*)-5-(Trifluoromethyl)-4-pentadecene (23) BuLi (0.6 mmol/ml in hexane, 2.4 ml) was added to a suspension of butyltriphenylphosphonium bromide (1.4 g) in dry Et_2O (30 ml), and the mixture was stirred at room temperature for 2 h. A solution of **15** (0.5 g, 2 mmol) in dry Et_2O (5 ml) was added to the above mixture. The whole was stirred at room temperature for 24 h, then poured into ice-water and extracted with Et_2O. The Et_2O layer was washed with H_2O and dried over $MgSO_4$. After evaporation of the solvent, the residue was purified by column chromatography (SiO_2, hexane) to give (4*Z*)-5-(trifluoromethyl)-4-pentadecene (**23**, 0.54 g, 92%). **23**: A colorless oil. MS *m/z*: 278 (M^+). HRMS Calcd for $C_{16}H_{29}F_3$: 278.222. Found: 278.222. ^{1}H-NMR ($CDCl_3$) δ: 0.77—1.04 (6H, m), 1.08—1.54 (18H, m), 1.94—2.33 (4H, m), 5.66 (1H, t, J=7.7 Hz). Another small olefinic proton signal was observed at 6.05 (m). ^{19}F-NMR ($CDCl_3$) ppm: −4.62 (s), 2.60 (br d, J=1.4 Hz, ratio 3:1).

(1*E*,4*E*)-1-Phenyl-2-(trifluoromethyl)-1,4-dodecadiene (24) A solution of **13** (0.5 g, 2 mmol) in dry C_6H_6 (5 ml) was added to a solution of triphenylphosphonium benzylide, which was obtained by the reaction of benzyltriphenylphosphonium bromide (1.1 g) with NaH (about 60%, 0.13 g) in dry C_6H_6 (25 ml) at room temperature for 0.5 h in an atmosphere of Ar. The mixture was stirred at room temperature for 3 h, then poured into ice water and extracted with Et_2O. The Et_2O layer was washed with H_2O and dried over $MgSO_4$. After evaporation of the solvent, the residue was purified by column chromatography (SiO_2, hexane) to give (1*E*,4*E*)-1-phenyl-2-(trifluoromethyl)-1,4-dodecadiene (**24**, 82 mg, 12%). **24**: A colorless oil. MS *m/z*: 326 (M^+). HRMS Calcd for $C_{19}H_{25}F_3O$: 326.186. Found: 326.185. ^{1}H-NMR ($CDCl_3$) δ: 0.90 (3H, t, J=5.1 Hz), 1.05—1.46 (12H, br s), 1.88—2.28 (2H, m), 5.78—6.37 (2H, m), 7.03 (1H, d, J=2.2 Hz). 7.25—7.57 (5H, m). ^{19}F-NMR ($CDCl_3$) ppm: −0.10 (d, J=2.2 Hz).

(4*Z*,7*E*)-5-(Trifluoromethyl)-4,7-pentadecadiene (25) A solution of **13** (0.2 g, 0.8 mmol) in dry Et_2O (2 ml) was added to a solution which was obtained by the reaction of butyltriphenylphosphonium bromide (350 mg) and BuLi (0.6 ml) in dry Et_2O (7.6 ml) at room temperature for 2 h in an atmosphere of Ar. The mixture was stirred at room temperature for 24 h, then poured into ice water and extracted with Et_2O. The Et_2O layer was washed with H_2O and dried over $MgSO_4$. After evaporation of the solvent, the residue was purified by column chromatography (SiO_2, hexane) to give (4*Z*,7*E*)-5-(trifluoromethyl)-4,7-pentadecadiene (**25**, 29 mg, 12%). **25**: A colorless oil. MS *m/z*: 276 (M^+). HRMS Calcd for $C_{16}H_{27}F_3$: 276.206. Found: 276.205. ^{1}H-NMR ($CDCl_3$) δ: 0.81—0.98 (6H, m), 1.18—1.43 (12H, m), 1.95—2.29 (4H, m), 2.88 (2H, d, J=5.1 Hz), 5.28—5.52 (2H, m), 6.12 (1H, t, J=7.2 Hz). ^{19}F-NMR ($CDCl_3$) ppm: −4.29 (s).

1,1,1-Trifluoro-2,4-dodecadiene (26) A mixture of 1,1,1-trifluoro-4-dodecen-2-ol (**11**, 0.5 g, 2.1 mmol) in pyridine (1.12 ml) and $POCl_3$ (323 mg) was treated as above. After evaporation of the solvent, the residue was purified by a bulb-to-bulb distillation to give 1,1,1-trifluoro-2,4-dodecadiene (**26**, 0.25 g, 54%). **26**: A colorless oil. MS *m/z*: 220 (M^+). HRMS Calcd for $C_{12}H_{19}F_3$: 220.143. Found: 220.143. ^{1}H-NMR ($CDCl_3$) δ: 0.94 (3H, t, J=4.9 Hz), 1.07—1.50 (10H, m), 1.91—2.32 (2H, m), 5.61 (1H, qd, J=7.3, 15.4 Hz), 5.73—6.52 (2H, m), 6.55—6.97 (1H, m). ^{19}F-NMR ($CDCl_3$) ppm: −6.57 (d, J=8.5 Hz), −0.85 (d, J=7.3 Hz), 10.37 (d, J=6.1 Hz) ratio 1:14:1. The first peak is attributed to the (2*Z*,4*E*) isomer of **26**, the second to the (2*E*,4*E*) isomer, and the last to a chlorinated derivative of **11**.

1,1,1-Trifluoro-3-methyl-2,4-nonadiene (27) $POCl_3$ (250 mg) was added to a solution of 1,1,1-trifluoro-3-methyl-4-nonen-2-ol (**10**, 333 mg, 1.6 mmol) in pyridine (0.8 ml) at 0 °C, and the mixture was stirred at 110 °C for 48 h. After cooling, the mixture was treated with ice water and extracted with Et_2O. The Et_2O layer was washed with dilute HCl, H_2O and saturated $NaHCO_3$, and dried over $MgSO_4$. After evaporation of the solvent, the residue was purified by a bulb-to-bulb distillation to give (**27**, 0.24 g, 80%). **27**: A colorless oil. MS *m/z*: 192 (M^+). HRMS Calcd for $C_{10}H_{15}F_3$: 192.113. Found: 192.113. ^{1}H-NMR ($CDCl_3$) δ: 0.78—1.09 (3H, m), 1.12—1.54 (4H, m), 1,80—2.01 (3H, m), 2.03—2.36 (2H, m), 5.39 (1H, q, J=8.5 Hz), 5.98 (1H, td, J=5.7, 15.7 Hz), 6.54 (1H, d, J=15.7 Hz). ^{19}F-NMR ($CDCl_3$) ppm: −8.87 (dqd, J=8.5, 2.1, 2.1 Hz).

3-[(Trifluoromethyl)methylene]cyclohexene (28) A mixture of **5** (833 mg, 4.6 mmol), $POCl_3$ (1.45 g, 9.5 mmol) and pyridine (2 ml) was heated at 110 °C for 66 h. After usual work-up, the residue was distilled to give a colorless oil (371 mg, 50%), which was found to consist of three components (ratio 12:3:1) by gas liquid chromatography (GLC) (15% DEGS 4 mm × 2 m, 60 °C, carrier, N_2 at 30 ml/min), and ^{19}F-NMR analyses. The two main components were obtained by preparative GLC (15% DEGS 4 mm × 2 m, 25 °C, carrier, He at 30 ml/min). The major product: (*Z*)-3-[(Trifluoromethyl)methylene]cyclohexene (**28**): A colorless oil. MS *m/z*: 162 (M^+). ^{1}H-NMR ($CDCl_3$) δ: 1.73—1.82 (2H, m), 2.16—2.24 (2H, m), 2.33—2.40 (2H, m), 5.26 (1H, q, J=8.7 Hz), 6.17 (1H, dqd, J=10.3, 4.0, 1.5 Hz), 6.57 (1H, dqd, J=10.3, 2.0, 1.0 Hz). NOE interaction between the vinylic proton alpha to CF_3 at 5.26 ppm and the protons at 2.33 ppm was observed (1.3%). which shows that stereochemistry of the new double bond is *Z*. ^{19}F-NMR ($CDCl_3$) ppm: −7.38 (dd, J=8.7, 2.0 Hz). The minor product: (*E*)-3-[(Trifluoromethyl)methylene]cyclohexene: A colorless oil. MS *m/z*: 162 (M^+). ^{1}H-NMR ($CDCl_3$) δ: 1.74 (2H, tt, J=6.3, 6.3 Hz), 2.12—2.22 (2H, m), 2.53—2.60 (2H, m), 5.35 (1H, q, J=9.0 Hz), 6.06 (1H, d, J=12.1 Hz), 6.13 (1H, dt, J=12.1, 4.0 Hz). ^{19}F-NMR ($CDCl_3$) ppm: 6.65 (d, J=9.0 Hz). NOE interaction was observed between the two olefinic protons (16%).

Acknowledgment We thank the Central Glass Company for supplying trifluoroacetaldehyde ethyl hemiacetal.

References and Notes

1) Part VI: T. Nagai, K. Ogawa, M. Morita, M. Koyama, A. Ando, T. Miki, and I. Kumadaki, *Chem. Pharm. Bull.*, **37**, 1751 (1989).
2) Parts of this work were presented at the 109th and 110th Annual Meetings of the Pharmaceutical Society of Japan, Nagoya and Sapporo, 1989 and 1990.
3) *a*) Y. Kobayashi, T. Nagai, and I. Kumadaki, *Chem. Pharm. Bull.*, **32**, 5031 (1984); *b*) T. Nagai, I. Kumadaki, T. Miki, Y. Kobayashi, and G. Tomizawa, *ibid.*, **34**, 1546 (1986); *c*) T. Nagai, T. Miki, and I. Kumadaki, *ibid.*, **34**, 4782 (1986).
4) *a*) T. Nagai, T. Miki, and I. Kumadaki, *Chem. Pharm. Bull.*, **35**, 3620 (1987); *b*) T. Nagai, M. Hama, M. Yoshioka, M. Yuda, N. Yoshida, A. Ando, M. Koyama, T. Miki, and I. Kumadaki, *ibid.*, **37**, 177 (1989).
5) R. Pautrat, J. Marteau, and R. Cheritat, *Bull. Soc. Chim. Fr.*, **1968**, 1182.
6) D. B. Dess and J. C. Martin, *J. Org. Chem.*, **48**, 4156 (1983).
7) A trifluoromethyl group is easily replaced as it is a pseudo-halogen. See Y. Kobayashi, and I. Kumadaki, *Accounts Chem. Research*, **11**, 197 (1978).
8) D. Seebach and V. Prelog, *Angew. Chem. Int. Ed. Engl.*, **21**, 654 (1982).

Condensed Pyridazines. VIII.[1] Reaction of Diazolopyridazines with Ynamine. Formation of Benzodiazoles and Diazolodiazocines

Etsuo OISHI,[a] Naokata TAIDO,[b] Akira MIYASHITA,*[,a] Susumu SATO,[b] Syouji OHTA,[a] Hitoshi ISHIDA,[a] Ken-ichi TANJI,[a] and Takeo HIGASHINO[a]

School of Pharmaceutical Sciences, University of Shizuoka,[a] 395 Yada, Shizuoka 422, Japan and Central Research Laboratories, S S Pharmaceutical Co., Ltd.,[b] 1143 Nanpeidai, Narita 286, Japan. *Received January 7, 1991*

Reaction of the 7-(methylsulfonyl)-1*H*-imidazo[4,5-*d*]pyridazine (3) with 1-(*N*,*N*-diethylamino)-1-propyne (2) resulted in the formation of the benzimidazole (5) and the 3*H*-imidazo[4,5-*d*][1,2]diazocine (4) through the [4+2]- and [2+2]-cycloadducts. Similarly, reaction of the 7-(methylsulfonyl)- (9) and the 7-cyano-1*H*-pyrazolo[3,4-*d*]pyridazines (10) with 2 gave the corresponding indazoles (14, 16) and the 1*H*-pyrazolo[3,4-*d*][1,2]diazocines (15, 17). A similar reaction was also found to proceed between 7-(methylsulfonyl)-1*H*-1,2,3-triazolo[4,5-*d*]pyridazine (18) and 2, affording the corresponding benzotriazole (20) and the 3*H*-1,2,3-triazolo[4,5-*d*][1,2]diazocine (19).

Keywords condensed pyridazine; ynamine; cycloaddition; condensed diazocine

It has been reported by us that electron-poor condensed pyridazines react with electron-rich enamines and ynamines in an inverse-electron-demand Diels–Alder reaction mode, resulting in ring transformation into the corresponding benzoheteroarenes through the [4+2]-cycloadducts.[1,2] It has also been reported by us that similar inverse-electron-demand Diels–Alder reaction of electron-poor condensed pyrimidines with enamines gives condensed pyridines, while reaction with ynamines affords condensed diazocines through the [2+2]-cycloadducts. For example, reaction of the 3*H*-1,2,3-triazolo[4,5-*d*]pyrimidine (I) with 1-piperidinocyclopentene (**1a**) gave the 3*H*-1,2,3-triazolo[4,5-*b*]-pyridine (II), and reaction of I with 1-(*N*,*N*-diethylamino)-1-propyne (**2**) afforded the 3*H*-1,2,3-triazolo[4,5-*d*][1,3]-diazocine (III).[3]

In connection with the formation of the condensed diazocines, it was expected that the electron-poor condensed pyridazines might react with the ynamines in the same way as the condensed pyrimidines. Thus, we carried out reaction of the condensed pyridazines with **2**, and found that new condensed 1,2-diazocine ring systems are formed together with the benzodi(or tri)azoles. In the present paper, we describe the above reaction in detail.

The 1*H*-Imidazo[4,5-*d*]pyridazine Ring System We have shown that the electron-poor 7-(methylsulfonyl)-1*H*-imidazo[4,5-*d*]pyridazine (**3**) with its an electron-withdrawing methylsulfonyl group participates in an inverse-electron-demand Diels–Alder reaction with the enamine **1a**, to afford the indeno[5,6-*d*]imidazole (IV).[1]

On the other hand, two cycloadditions, [4+2]- and [2+2]-cycloadditions, proceeded when **3** was allowed to react with the ynamine **2**. The former resulted in the formation of the 1*H*-benzimidazole (**5**), and the latter gave the 3*H*-imidazo[4,5-*d*][1,2]diazocine (**4**).

It is reasonable that in the [4+2]-cycloaddition the nucleophilic carbon of the ynamine **2** would react at the more reactive C^4-ring atom[1] rather than the C^7 atom of the 1*H*-imidazo[4,5-*d*]pyridazine **3**, to form the cycloadduct (B). Loss of nitrogen from B affords the benzimidazole **5**. The above consideration and the spectral data of **5** suggest that the structure of **5** is 6-(*N*,*N*-diethylamino)-5-methyl-7-(methylsulfonyl)-1-phenyl-1*H*-benzimidazole.

The structure of **4** was determined by X-ray crystallography (Fig. 1 and Table I). The ORTEP view of **4** in Fig. 1 shows that the molecule consists of an unsaturated 1,2-diazocine ring condensed with an imidazole ring, and the conformation of the 1,2-diazocine ring can be drawn as a tub-shape.

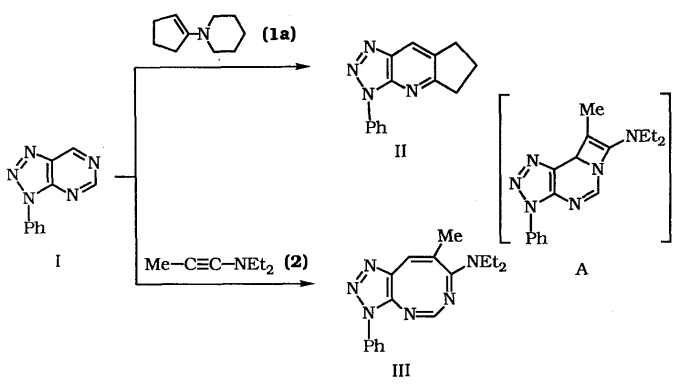

Chart 1

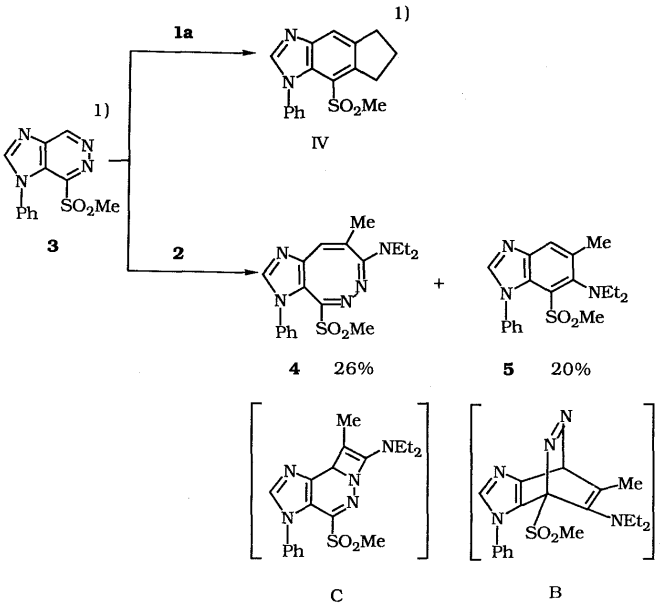

Chart 2

In the ^{1}H-nuclear magnetic resonance (^{1}H-NMR) spectrum of **4** (Table II), C^9-H (6.63 ppm) shows characteristic long-range coupling ($J=1.8$ Hz) with C^8-CH_3 (2.11 ppm). In the ^{13}C-NMR spectrum of **4** (Table III), the sp^2-hybridized C^4, C^7, and C^8 atoms of the diazocine ring resonate at 152.00, 152.83, and 119.19 ppm, respectively, as singlets, and the signal of the C^9 atom appears at 125.26 ppm as a doublet. The chemical shift of C^8-CH_3 (20.85 ppm) agrees well with that of C^8-$\underline{C}H_3$ in the reported 7-(diethylamino)-8-methyl-3-phenyl-3*H*-1,2,3-triazolo[4,5-*d*][1,3]diazocine (III).[3)]

The formation of **4** can be rationalized as follows. The reaction may occur by selective cycloaddition of the ynamine across the C^4–N^5 double bond of **3**, followed by isomerization of the initial [2+2]-adduct (**B**) to the fully unsaturated 3*H*-imidazo[3,4-*d*][1,2]diazocine **4**. An example of [2+2]-cycloaddition of an ynamine to the C–N double bond of the condensed heteroarenes has been reported by us in the reaction of the condensed pyrimidines with ynamines, affording the condensed 1,3-diazocines.[3)]

The 1*H*-Pyrazolo[3,4-*d*]pyridazine Ring System To our knowledge, no example of inverse-electron-demand Diels–Alder reaction on the 1*H*-pyrazolo[3,4-*d*]pyridazine ring has been reported so far. Thus, we examined the reaction of several 1*H*-pyrazolo[3,4-*d*]pyridazines (**6**, **9**, **10**) with the enamines **1a**—**c** and the ynamine **2**.

The 7-(methylsulfonyl)-1*H*-pyrazolo[3,4-*d*]pyridazine (**9**) was prepared by potassium permanganate oxidation of the methylthio derivative (**8**), which was obtained from the chloro derivative (**6**) by reaction with thiourea followed by methylation of the resultant **7**, in an overall yield of 60%.

TABLE I. Final Atomic Coordinates and Equivalent Isotropic Thermal Parameters for Non-hydrogen Atoms of **4**[a)]

No.	Atom	x	y	z	B_{eq}
1	N^1	1.1122 (1)	0.1429 (1)	0.5082 (1)	3.9
2	C^2	1.0819 (1)	0.2243 (1)	0.5584 (1)	3.8
3	N^3	0.9826 (1)	0.2589 (1)	0.5088 (1)	3.1
4	C^3a	0.9486 (1)	0.1938 (1)	0.4181 (1)	2.9
5	C^4	0.8422 (1)	0.1832 (1)	0.3478 (1)	2.9
6	N^5	0.8156 (1)	0.1810 (1)	0.2449 (1)	3.4
7	N^6	0.8880 (1)	0.2190 (1)	0.1922 (1)	3.7
8	C^7	0.9661 (1)	0.1589 (1)	0.1858 (1)	3.5
9	C^8	0.9910 (1)	0.0484 (1)	0.2347 (1)	3.7
10	C^9	1.0272 (1)	0.0359 (1)	0.3417 (1)	3.7
11	C^9a	1.0300 (1)	0.1234 (1)	0.4194 (1)	3.3
12	C^{10}	0.9323 (1)	0.3535 (1)	0.5347 (1)	3.2
13	C^{11}	0.8725 (1)	0.4172 (1)	0.4523 (1)	3.9
14	C^{12}	0.8250 (2)	0.5108 (2)	0.4773 (2)	5.1
15	C^{13}	0.8384 (2)	0.5408 (2)	0.5830 (2)	5.6
16	C^{14}	0.8990 (2)	0.4773 (2)	0.6648 (2)	5.6
17	C^{15}	0.9456 (2)	0.3825 (2)	0.6419 (2)	4.3
18	S^{16}	0.7345 (0)	0.1512 (0)	0.4048 (0)	3.4
19	C^{17}	0.6981 (2)	0.0189 (2)	0.3593 (2)	4.7
20	O^{18}	0.7753 (1)	0.1500 (1)	0.5203 (1)	4.9
21	O^{19}	0.6484 (1)	0.2221 (1)	0.3573 (1)	4.9
22	N^{20}	1.0296 (1)	0.1968 (1)	0.1246 (1)	4.4
23	C^{21}	1.1390 (2)	0.1606 (2)	0.1452 (2)	4.5
24	C^{22}	1.2123 (2)	0.2212 (3)	0.2372 (3)	6.4
25	C^{23}	1.0087 (2)	0.3072 (2)	0.0776 (2)	5.5
26	C^{24}	0.9220 (3)	0.3079 (3)	−0.0241 (3)	7.2
27	C^{25}	0.9775 (3)	−0.0461 (2)	0.1576 (2)	5.8

a) Estimated standard deviations are given in parentheses.

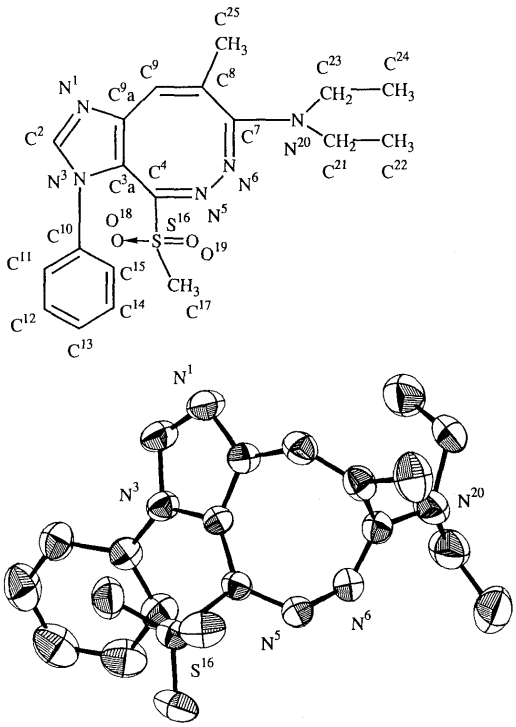

Fig. 1. Numbering and ORTEP Drawing for **4**

TABLE II. ^{1}H-NMR Spectral Data for Condensed Diazocines (**4**, **15**, **17**, **19**)

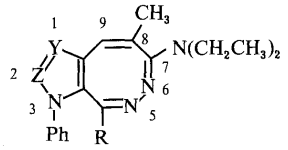

Compd.	R	Y	Z	^{1}H-NMR ($CDCl_3$) ppm						
				1-H (s)	2-H (s)	9-H (q)	N–C_6H_5 (m)	SO_2CH_3 (s)	$N(CH_2CH_3)_2$[b)]	8-CH_3 (d)
4	SO_2CH_3	N	CH	—	8.21	6.63[a)]	7.23—7.66	2.87	3.27 (q), 1.09 (t)	2.11[a)]
				7.62	—				3.25 (q), 1.08 (t)	
15	SO_2CH_3	CH	N	7.57	—	6.53[a)]	7.30—7.60	2.92	3.24 (q), 1.06 (t)	2.07[a)]
									3.22 (q), 1.05 (t)	
17	CN	CH	N	—	—	6.46[a)]	7.45—7.60	—	3.26 (q), 1.06 (t)	2.08[a)]
									3.24 (q), 1.05 (t)	
19	SO_2CH_3	N	N			6.70[c)]	7.53 (s)	2.96	3.24 (q), 1.05 (t)	2.12[c)]

a) $J=1.8$ Hz, b) $J=7.0$ Hz, c) $J=2.0$ Hz.

TABLE III. ^{13}C-NMR Spectral Data for Condensed Diazocines (**4**, **15**, **17**, **19**)

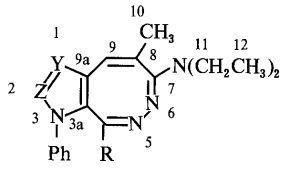

Compd.	R	Y	Z	^{13}C-NMR ($CDCl_3$) ppm											
				1(d)	2(d)	3a(s)	4(s)	7(s)	8(s)	9(d)	9a(s)	10(q)	11(t)	12(q)	SO_2CH_3(q)	N–C_6H_5
4	SO_2CH_3	N	CH	— 138.43	140.48 —	146.28	152.00 151.43	152.83 153.44	119.19 126.84	125.26 122.61	136.40 128.84	20.85 21.81	42.04 41.83	13.09 13.06	40.92	137.84(s), 129.99(d) 128.95(d), 123.40(d)
15	SO_2CH_3	CH	N	138.70	—	140.16	131.50	150.03	125.75	122.39	127.23	20.70	41.88	13.00	41.03	136.32(s), 129.44(d) 128.24(d), 123.25(d)
17	CN	CH	N	—	—	138.49	150.68	151.09	124.75	122.16	136.77	21.05	42.06	13.06	113.96(s) CN	137.13(s), 129.71(d) 128.57(d), 123.34(d)
19	SO_2CH_3	N	N			150.05									41.13	139.52(s), 129.95(d) 129.74(d), 123.03(d)

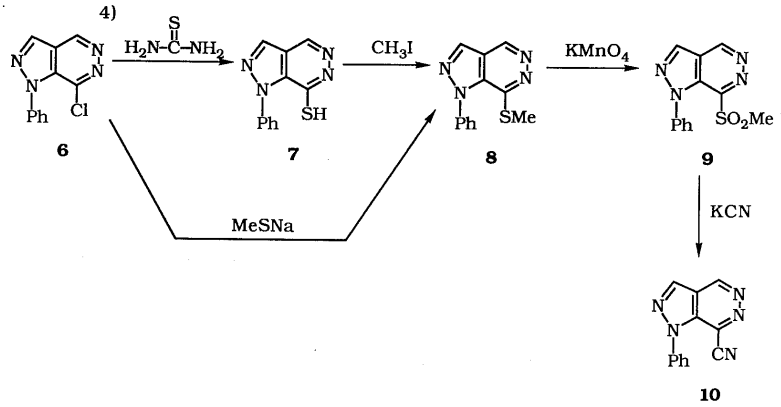

Chart 3

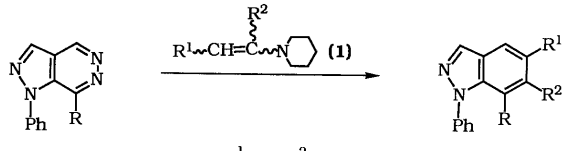

	R		R^1	R^2	yield (%)	
6	Cl	**1a**	$-(CH_2)_3-$		**11**	21
10	CN	**1a**	$-(CH_2)_3-$		**12a**	97
10	CN	**1b**	$-(CH_2)_4-$		**12b**	45
10	CN	**1c**	H	Ph	**13**	30

Chart 4

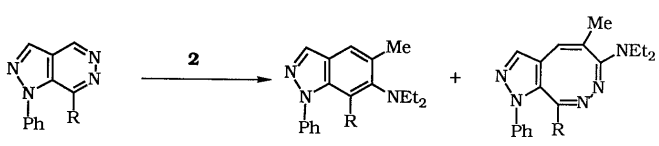

	R	yield (%)		yield (%)	
9	SO_2Me	**14**	39	**15**	11
10	CN	**16**	39	**17**	40
6	Cl		—		—

Chart 5

Compound **8** was also obtained by reaction of **6** with sodium methanethiolate. The 1*H*-pyrazolo[3,4-*d*]pyridazine-7-carbonitrile (**10**) was prepared by the nucleophilic substitution of **9** with potassium cyanide.

When a solution of **6** and the enamine **1a** in dioxane was heated at 120 °C for 8 h, inverse-electron-demand Diels–Alder reaction occurred, giving the 8-chlorocyclopenta-[*f*]indazole (**11**), while another enamine, 1-piperidino-1-phenylethene (**1c**) did not react with **6**, resulting in the recovery of **6**.

In the case of the more reactive **10**, **1a**, 1-piperidinocyclohexene (**1b**), and **1c** readily cycloadded across C^4 and C^7 of **10**, and the corresponding 1*H*-indazole-7-carbonitriles (**12a**, **b**, and **13**) were obtained. In particular, the formation of **13**, showing an *ortho* coupling constant (J=7.0 Hz) between C^4-H and C^5-H in the ^{1}H-NMR spectrum, demonstrates that the nucleophilic carbon of the enamines regioselectively attacks the C^4-ring atom of **10**.

The 7-chloro-1*H*-pyrazolo[3,4-*d*]pyridazine **6** did not react with the ynamine **2**, resulting in recovery of **6**. But both the 7-(methylsulfonyl)-1*H*-pyrazolo[3,4-*d*]pyridazine **9** and the 1*H*-pyrazolo[3,4-*d*]pyridazine-7-carbonitrile **10** underwent [4+2]- and [2+2]-cycloadditions with the ynamine **2**. The [4+2]-cycloaddition resulted in the formation of the corresponding 1*H*-indazoles (**14** and **16**), and the [2+2]-cycloaddition gave the corresponding 1*H*-pyrazolo-[3,4-*d*][1,2]diazocines (**15** and **17**).

Structural elucidation of the 1*H*-indazoles **14** and **16** was accomplished on the basis of the analytical and spectral data described in the experimental section. The structural elucidation of the 1*H*-pyrazolo[3,4-*d*][1,2]diazocines **15** and **17** was achieved as follows. The C^4-H proton resonating in the range of 6.53—6.46 ppm shows characteristic long-range coupling (J=1.8 Hz) with C^5-CH_3 in the range of 2.07—2.08 ppm in the ^{1}H-NMR spectra of **15** and **17**, as shown in Table II. In the ^{13}C-NMR spectrum of **15** and **17** (Table III), the chemical shifts of C^4, C^5, C^6, C^9, and C^5-CH_3 of the diazocine ring agree well with the chemical shifts of those in the 3*H*-imidazo[4,5-*d*][1,2]diazocine **4**, except for the chemical shift of C^9 in **17** (131.50 ppm), which is at higher field than that of **15** (151.43 ppm), because the former is shielded by the anisotropic effect of the cyano group at the 9-position.

The 1*H*-1,2,3-Triazolo[4,5-*d*]pyridazine Ring System In the previous paper we reported that the 1*H*-1,2,3-triazolo-[4,5-*d*]pyridazine **18** is able to undergo inverse-electron-demand Diels–Alder reaction with the enamines **1a, b**, resulting in the formation of the 1*H*-benzotriazoles (Va, b), while the ynamine **2** cycloadds across C^4 and C^7 of **18** to afford the cycloadduct (**21**) and the benzotriazole (**20**).[2b] We considered that the structure of the cycloadduct **21** is 8-(*N*,*N*-diethylamino)-4,7-dihydro-9-methyl-7-(methylsulfonyl)-1-phenyl-1*H*-4,7-etheno-1,2,3-triazolo[4,5-*d*]-pyridazine on the basis of its ^{1}H-NMR spectrum. The results on the formation of the condensed 1,2-diazocines (**4, 15, 17**) from the reaction of the 1*H*-imidazo[4,5-*d*]-pyridazine **3** and the 1*H*-pyrazolo[3,4-*d*]pyridazines **9, 10** with the ynamine **2** led us to reexamine the structure of **21**. We now report that the structure of **21** should be revised to 7-(*N*,*N*-diethylamino)-8-methyl-4-(methylsulfonyl)-3-phenyl-3*H*-1,2,3-triazolo[4,5-*d*][1,2]diazocine (**19**).

When **18** was allowed to react with two equivalents of the ynamine **2** in dry dioxane, the 1*H*-benzotriazole **20** and the 3*H*-1,2,3-triazolo[4,5-*d*][1,2]diazocine **19** were obtained in 46 and 22% yields, respectively.

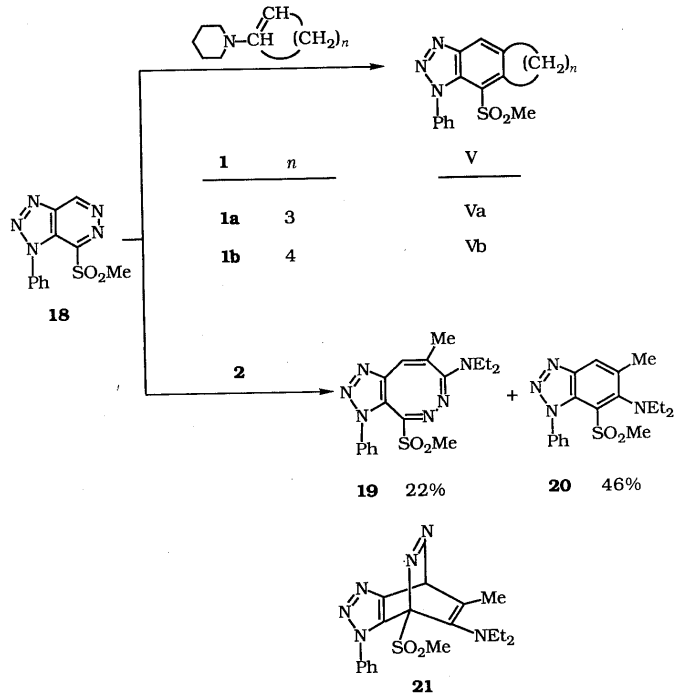

Chart 6

The ^{1}H- and ^{13}C-NMR spectral data for **19** are listed in Tables II and III. In the ^{1}H-NMR spectrum of **19**, C^9-H (6.70 ppm) shows characteristic long-range coupling (J= 2.0 Hz) with C^8-CH_3 (2.12 ppm). In the ^{13}C-NMR spectrum of the 1,2-diazocine part of **19**, the chemical shifts of the C^4, C^7, C^8, and C^9 atoms are 150.68, 151.09, 124.75, and 122.16, respectively. These NMR signals of the diazocine part of **19** agree well with those found for the new series of condensed 1,2-diazocines **4, 15, 17**, confirming that the molecule of **19** consists of a 1,2-diazocine ring fused to a 1,2,3-triazole ring.

The experimental results may be summarized as follows. Inverse-electron-demand [4+2]- and [2+2]-cycloadditions of the condensed pyridazines (**3, 9, 10**, and **18**) with the ynamine **2** proceeded competitively. The former resulted in the formation of the benzodi(or tri)azoles (**5, 14, 16**, and **20**) by way of the [4+2]-cycloadducts and the latter, which is reported here for the first time in a condensed pyridazine ring system, gave a new series of condensed 1,2-diazocines (**4, 15, 17**, and **19**) by way of the [2+2]-cycloadducts.

Experimental

All melting points are uncorrected. Infrared (IR) absorption spectra were recorded on a Jasco A-102 diffraction grating IR spectrometer. ^{1}H-NMR spectra were measured at 60 MHz on a Hitachi R-24B high-resolution NMR spectrometer, and ^{13}C-NMR spectra were obtained with a JEOL JNM-FX90Q FTNMR spectrometer. Chemical shifts are quoted in parts per million (ppm) with tetramethylsilane as an internal standard, and coupling constants (J) are given in hertz (Hz). The following abbreviations are used: s=singlet, d=doublet, t=triplet, q=quartet, quint=quintet, m=multiplet, and br=broad. Mass spectra (MS) were recorded on a JEOL JMS D-100 mass spectrometer. Samples were vaporized in a direct inlet system. Unit-cell parameters and intensity data for X-ray crystallography were measured on a Rigaku AFC-5R automatic four-circle diffractometer with graphite-monochromated MoK_α radiation at room temperature. The intensities of all the reflections were measured by the ω–2θ scanning technique. The structure was solved by direct methods using the program MULTAN 80.[4] The structure was refined by the full-matrix least-squares method with anisotropic thermal parameters for the nonhydrogen atoms and with isotropic thermal parameters for the hydrogen atoms. Column chromatography was carried out on SiO_2, Wakogel C-200 (200 mesh).

Reaction of 7-(Methylsulfonyl)-1-phenyl-1*H*-imidazo[4,5-*d*]pyridazine (3) with 1-(*N*,*N*-Diethylamino)-1-propyne (2) A solution of **3**[1] (200 mg, 0.73 mmol) and **2**[5] (163 mg, 1.46 mmol) in dioxane (2 ml) was refluxed for 30 h. After cooling, the reaction mixture was poured onto an excess of ice, neutralized with AcOH, and extracted with $CHCl_3$. The extract was washed with H_2O, and dried over Na_2SO_4. After removal of the solvent, the residue was chromatographed on a column of SiO_2 eluted with AcOEt–benzene (1:25) then AcOEt–benzene (1:7). The fraction eluted with AcOEt–benzene (1:25) gave 6-(*N*,*N*-diethylamino)-5-methyl-7-(methylsulfonyl)-1-phenyl-1*H*-benzimidazole (**5**), mp 143—144 °C, as yellow needles from benzene–petroleum benzin, in 20% yield (52 mg). *Anal.* Calcd for $C_{19}H_{23}N_3O_2S$: C, 63.84; H, 6.49; N, 11.75, S, 8.97. Found: C, 63.69; H, 6.49; N, 11.70; S, 8.84. MS m/z: 357 (M^+). ^{1}H-NMR ($CDCl_3$): 8.32 (1H, s, C^2-H), 7.97 (1H, s, C^4-H), 7.66—7.27 (5H, m, C_6H_5), 3.38 (2H, q, J=7.0, NCH_2Me), 3.36 (2H, q, J=7.0, NCH_2Me), 3.20 (3H, s, SO_2CH_3), 2.51 (3H, s, C^5-CH_3), 1.13 (6H, t, J=7.0, 2×$CH_2\underline{CH_3}$).

The first and second fractions eluted with AcOEt–benzene (1:7) gave the starting **3** and 7-(*N*,*N*-diethylamino)-8-methyl-4-(methylsulfonyl)-3-phenyl-3*H*-imidazo[4,5-*d*][1,2]diazocine (**4**) in 20 and 26% yields (40 and 73 mg), respectively. Compound **4**, mp 204—206 °C as yellow prisms from carbon tetrachloride. *Anal.* Calcd for $C_{19}H_{23}N_5O_2S$: C, 59.20; H, 6.01; N, 18.17; S, 8.32. Found: C, 59.44; H, 6.09; N, 18.28; S, 8.26. MS m/z: 385 (M^+). The ^{1}H- and ^{13}C-NMR spectral data of **4** are shown in Tables II and III.

Crystal Data of 4 for X-Ray Crystallographic Analysis A crystal of

4 for X-ray crystallographic analysis was obtained from a saturated solution of **4** in carbon tetrachloride. The crystal data are as follows: $C_{19}H_{23}N_5O_2S$, $M_r=385.49$, crystal dimensions $0.3\times0.3\times0.4$ mm, monoclinic, space group $P2_1/n$, $a=13.149(2)$ Å, $b=12.304(1)$ Å, $c=12.818(2)$ Å, $\beta=105.2(1)°$, $V=2001.6(6)$ Å^3, $D_{calcd}=1.28$ g cm^{-3} and $Z=4$. A total of 4041 independent reflections were measured, of which 3855 reflections with $|F_O|>3\sigma|F_O|$ were used for calculations.

The final residual values were $R=0.045$ and $R_W=0.058$.

7-Mercapto-1-phenyl-1*H*-pyrazolo[3,4-*d*]pyridazine (7) Thiourea (2.0 g, 26 mmol) was added to a solution of 7-chloro-1-phenyl-1*H*-pyrazolo-[3,4-*d*]pyridazine (**6**,[6] 5.0 g, 22 mmol) in MeOH (65 ml), and the mixture was refluxed for 30 min. After cooling, the separated crystals were collected by suction, and recrystallized from MeOH to give **7**, mp 240—241 °C, as yellow needles, in 71% yield (3.55 g). *Anal.* Calcd for $C_{11}H_8N_4S$: C, 57.88; H, 3.53; N, 24.55; S, 14.04. Found: C, 57.63; H, 3.50; N, 24.50; S, 13.95. IR ν_{max}^{KBr} cm^{-1}: 3200—3300 (SH). ^{1}H-NMR ($(CD_3)_2SO$): 14.50—14.22 (1H, br, SH), 8.75 (1H, s, C^4-H), 8.38 (1H, s, C^3-H), 7.40 (5H, s, C_6H_5).

7-Methylthio-1-phenyl-1*H*-pyrazolo[3,4-*d*]pyridazine (8) (i) Methyl iodide (4.43 g, 31 mmol) was added to a stirred solution of **7** (3.55 g, 16 mmol) in 2 N KOH (30 ml), and the mixture was stirred for 15 min. The reaction mixture was extracted with $CHCl_3$. The extract was washed with H_2O, dried over Na_2SO_4, and concentrated. The residue was recrystallized from benzene to give **8**, mp 179—180 °C, as colorless prisms, in 92% yield (3.46 g). *Anal.* Calcd for $C_{12}H_{10}N_4S$: C, 59.48; H, 4.16; N, 23.12; S, 13.23. Found: C, 59.39; H, 4.12; N, 23.03; S, 13.28. ^{1}H-NMR ($CDCl_3$): 9.33 (1H, s, C^4-H), 8.29 (1H, s, C^3-H), 7.54 (5H, s, C_6H_5), 2.68 (3H, s, SCH_3). ^{13}C-NMR ($CDCl_3$): 144.66 (s), 142.54 (d), 138.38 (s), 134.31 (d), 134.15 (s), 129.93 (d), 128.75 (d), 118.66 (s), 13.11 (q).

(ii) A solution of MeSH (1.7 g, 4.3 mmol) in 15% NaOH (15 ml) was added to a solution of **6** (1.0 g, 4.3 mmol) in dimethylformamide (20 ml), and the mixture was stirred for 1 h at 60 °C. After cooling, the reaction mixture was poured into an excess of H_2O, and extracted with benzene. The extract was washed with H_2O, dried over Na_2SO_4, and concentrated. The residue was chromatographed on a column of SiO_2. The fraction eluted with $CHCl_3$ gave **8** in 90% yield (947 mg).

7-(Methylsulfonyl)-1-phenyl-1*H*-pyrazolo[3,4-*d*]pyridazine (9) A solution of 3% potassium permanganate (160 ml) was dropped into a stirred solution of **8** (3.46 g, 15 mmol) in AcOH (100 ml) during 1 h, and the whole was stirred for a further 30 min. After decolorization of the potassium permanganate with $NaHSO_3$, the reaction mixture was diluted with H_2O (350 ml) and extracted with $CHCl_3$. The extract was washed with H_2O, dried over Na_2SO_4, and concentrated. The residue was chromatographed on a column of SiO_2 eluted with $CHCl_3$. The first fraction gave **9**, mp 169—170 °C, as colorless plates from benzene, in 92% yield (3.81 g). *Anal.* Calcd for $C_{12}H_{10}N_4O_2S$: C, 52.54; H, 3.67; N, 20.43; S, 11.69. Found: C, 52.70; H, 3.65; N, 20.37; S, 11.82. IR ν_{max}^{KBr} cm^{-1}: 1315, 1145 (SO_2). ^{1}H-NMR ($CDCl_3$): 9.69 (1H, s, C^4-H), 8.54 (1H, s, C^3-H), 7.56 (5H, s, C_6H_5), 3.45 (3H, s, SO_2CH_3). ^{13}C-NMR ($CDCl_3$): 143.50 (s), 147.91 (d), 139.26 (s), 135.04 (d), 129.85 (d), 128.50 (d), 127.10 (d), 123.15 (s), 40.03 (q).

1-Phenyl-1*H*-pyrazolo[3,4-*d*]pyridazine-7-carbonitrile (10) A mixture of **9** (100 mg, 0.36 mmol) and KCN (48 mg, 0.74 mmol) in dimethylsulfoxide (DMSO) (4 ml) was stirred for 1.5 h. The reaction mixture was diluted with H_2O, and extracted with benzene. The extract was washed with H_2O, dried over Na_2SO_4, and concentrated. The residue was chromatographed on a column of SiO_2. The fraction eluted with $CHCl_3$ gave **10**, mp 183—184 °C, as slightly brown needles from MeOH, in 47% yield (38 mg). *Anal.* Calcd for $C_{12}H_7N_5$: C, 65.15; H, 3.19; N, 31.66. Found: C, 65.29; H, 3.27; N, 31.40. IR ν_{max}^{KBr} cm^{-1}: 2250 (CN). ^{1}H-NMR ($(CD_3)_2SO$): 9.99 (1H, s, C^4-H), 8.90 (1H, s, C^3-H), 7.82—7.40 (5H, m, C_6H_5). ^{13}C-NMR ($(CD_3)_2SO$): 147.48 (d), 136.59 (s), 136.37 (d), 133.94 (s), 130.03 (d), 129.17 (d), 126.68 (d), 125.16 (s), 121.04 (s), 113.35 (s).

Reaction of 7-Chloro-1-phenyl-1*H*-pyrazolo[3,4-*d*]pyridazine (6) with 1-Piperidinocyclopentene (1a) A solution of **6** (200 mg, 0.87 mmol) and **1a** (263 mg, 1.74 mmol) in dioxane (0.21 ml) was heated at 120 °C for 8 h. After cooling, the reaction mixture was diluted with H_2O (5 ml), acidified with AcOH, and extracted with $CHCl_3$. The extract was washed with H_2O, dried over Na_2SO_4, and concentrated. The residue was chromatographed on a column of SiO_2. The first fraction eluted with $CHCl_3$ gave 8-chloro-1,5,6,7-tetrahydro-1-phenylcyclopenta[*f*]indazole (**11**), mp 118—119 °C, as colorless prisms from benzene–petroleum benzin, in 21% yield (49 mg). *Anal.* Calcd for $C_{16}H_{13}ClN_2$: C, 71.51; H, 4.88; N, 10.42. Found: C, 71.58; H, 4.84; N, 10.53. MS *m/z*: 268 (M$^+$). ^{1}H-NMR ($CDCl_3$): 8.05 (1H, s, C^3-H), 7.44 (5H, s, C_6H_5), 3.04 (2H, t, $J=7.0$, C^5H_2), 3.00 (2H, t, $J=7.0$, C^7H_2), 2.13 (2H, quint, $J=7.0$, C^6H_2).

From the second fraction, **6** was recovered in 54% yield (108 mg).

Reaction of 10 with the Enamines 1. General Procedure A mixture of **10** (100 mg, 0.45 mmol) and an enamine (**1**, 0.3 ml) was heated at 140 °C for 15 h. After cooling, the reaction mixture was diluted with H_2O, acidified with AcOH, and extracted with $CHCl_3$. The extract was washed with H_2O, dried over Na_2SO_4, and concentrated. The residue was chromatographed on a column of SiO_2. The first fraction eluted with $CHCl_3$ gave the indazoles, which were recrystallized from benzene–petroleum benzin.

Reaction of **10** with **1a** gave 1,5,6,7-tetrahydro-1-phenylcyclopenta[*f*]-indazole-8-carbonitrile (**12a**), mp 185—186 °C, as colorless needles, in 97% yield (114 mg). *Anal.* Calcd for $C_{17}H_{13}N_3$: C, 78.75; H, 5.05; N, 16.21. Found: C, 78.86; H, 5.17; N, 15.90. MS *m/z*: 259 (M$^+$). IR ν_{max}^{KBr} cm^{-1}: 2225 (CN). ^{1}H-NMR ($CDCl_3$): 8.12 (1H, s, C^3-H), 7.72 (1H, s, C^4-H), 7.53 (5H, s, C_6H_5), 3.15 (2H, t, $J=7.0$, C^5H_2), 3.02 (2H, t, $J=7.0$, C^7H_2), 2.18 (2H, quint, $J=7.0$, C^6H_2).

Reaction of **10** with 1-piperidinocyclohexene (**1b**) gave 5,6,7,8-tetrahydro-1-phenyl-1*H*-benz[*f*]indazole-9-carbonitrile (**12b**), mp 151—153 °C, as colorless needles, in 45% yield (55 mg). *Anal.* Calcd for $C_{18}H_{15}N_3$: C, 79.10; H, 5.53; N, 15.37. Found: C, 79.20: H, 5.51; N, 15.32. MS *m/z*: 273 (M$^+$). IR ν_{max}^{KBr} cm^{-1}: 2225 (CN). ^{1}H-NMR ($CDCl_3$): 8.11 (1H, s, C^3-H), 7.67 (1H, s, C^4-H), 7.52 (5H, s, C_6H_5), 3.16—2.67 (4H, m, C^5H_2 and C^8H_2), 2.00—1.60 (4H, m, C^6H_2 and C^7H_2).

Reaction of **10** with 1-phenyl-1-piperidinoethene (**1c**) gave 1,6-diphenyl-1*H*-indazole-7-carbonitrile (**13**), mp 179—180 °C, as slightly yellow needles, in 30% yield (40 mg). *Anal.* Calcd for $C_{20}H_{13}N_3$: C, 81.34; H, 4.44; N, 14.23. Found: C, 81.16; H, 4.46; N, 14.16. MS *m/z*: 295 (M$^+$). IR ν_{max}^{KBr} cm^{-1}: 2330 (CN). ^{1}H-NMR ($CDCl_3$): 8.28 (1H, s, C^3-H), 8.00 (1H, d, $J=7.0$, C^4-H or C^5-H), 7.70—7.20 (11H, m, aromatic H).

Reaction of 9 with the Ynamine 2 A solution of **9** (200 mg, 0.73 mmol) and **2** (163 mg, 1.46 mmol) in dioxane (2 ml) was refluxed for 5 h. After cooling, the reaction mixture was poured onto an excess of ice, and extracted with $CHCl_3$. The extract was washed with H_2O, dried over Na_2SO_4, and concentrated under reduced pressure. The residue was chromatographed on a column of SiO_2 eluted with benzene then benzene–ethyl acetate (20 : 1). The fraction eluted with benzene gave 6-(*N*,*N*-diethylamino)-5-methyl-7-(methylsulfonyl)-1-phenyl-1*H*-indazole (**14**), mp 128—129 °C, as slightly yellow prisms from benzene–petroleum benzin, in 39% yield (100 mg), *Anal.* Calcd for $C_{19}H_{23}N_3O_2S$: C, 63.84; H, 6.49; N, 11.76. Found: C, 63.79; H, 6.56; N, 11.79. MS *m/z*: 357 (M$^+$). IR ν_{max}^{KBr} cm^{-1}: 1300, 1130 (SO_2). ^{1}H-NMR ($CDCl_3$): 8.16 (1H, s, C^3-H), 7.72 (1H, s, C^4-H), 7.60—7.30 (5H, m, C_6H_5), 3.45 (4H, q, $J=7.0$, $2\times NCH_2Me$), 3.13 (3H, s, SO_2CH_3), 2.48 (3H, s, C^5-CH_3), 1.16 (6H, t, $J=7.0$, $2\times CH_2\underline{CH_3}$).

The fraction eluted with benzene–ethyl acetate (20 : 1) gave 6-(*N*,*N*-diethylamino)-5-methyl-9-(methylsulfonyl)-1-phenyl-1*H*-pyrazolo[3,4-*d*]-[1,2]diazocine (**15**), mp 142—143 °C, as yellow prisms from benzene–petroleum benzin, in 11% yield (30 mg). *Anal.* Calcd for $C_{19}H_{23}N_5O_2S$: C, 59.20; H, 6.01; N, 18.17. Found: C, 59.21; H, 6.01; N, 18.11. MS *m/z*: 385 (M$^+$). IR ν_{max}^{KBr} cm^{-1}: 1320, 1130 (SO_2). The ^{1}H- and ^{13}C-NMR spectral data are listed in Tables II and III.

Reaction of 10 with the Ynamine 2 A solution of **10** (150 mg, 0.68 mmol) and **2** (151 mg, 1.36 mmol) in dioxane (2 ml) was refluxed for 5 h. The same work-up of the reaction mixture as described for the reaction of **9** with **2** gave 6-(*N*,*N*-diethylamino)-5-methyl-1-phenyl-1*H*-indazole-7-carbonitrile (**16**), mp 104—105 °C, as slightly yellow prisms from benzene–petroleum benzin, and 6-(*N*,*N*-diethylamino)-5-methyl-1-phenyl-1*H*-pyrazolo[3,4-*d*][1,2]diazocine-9-carbonitrile (**17**), mp 121—122 °C, as yellow needles from benzene–petroleum benzin, in 39 and 40% yields (81 and 90 mg), respectively.

Compound **16**: *Anal.* Calcd for $C_{19}H_{20}N_4$: C, 74.97; H, 6.62; N, 18.41. Found: C, 75.22; H, 6.57, N, 18.67. MS *m/z*: 304 (M$^+$). IR ν_{max}^{KBr} cm^{-1}: 2240 (CN). ^{1}H-NMR ($CDCl_3$): 8.10 (1H, s, C^3-H), 7.77 (1H, s, C^4-H), 7.58—7.48 (5H, m, C_6H_5), 3.38 (4H, q, $J=7.0$, $2\times NCH_2Me$), 2.42 (3H, s, C^5-CH_3), 1.09 (6H, t, $J=7.0$, $2\times CH_2\underline{CH_3}$).

Compound **17**: *Anal.* Calcd for $C_{19}H_{20}N_6$: C, 68.66; H, 6.06; N, 25.28. Found: C, 68.56; H, 6.14; N, 25.18. MS *m/z*: 332 (M$^+$). IR ν_{max}^{KBr} cm^{-1}: 2240 (CN). The ^{1}H- and ^{13}C-NMR spectral data are listed in Tables II and III.

Reaction of 7-(Methylsulfonyl)-1-phenyl-1*H*-1,2,3-triazolo[4,5-*d*]pyridazine (18) with the Ynamine 2 Reaction of **10** (200 mg, 0.73 mmol) and **2** (162 mg, 1.46 mmol) in dioxane (2 ml) as described for the reaction of **10** with **2** reported in the literature[2b] gave 6-(*N*,*N*-diethylamino)-5-methyl-7-(methylsulfonyl)-1-phenyl-1*H*-benzotriazole (**20**), mp 149—150

°C, as white needles from MeOH, and 7-(*N*,*N*-diethylamino)-8-methyl-4-(methylsulfonyl)-3-phenyl-3*H*-1,2,3-triazolo[4,5-*d*][1,2]diazocine (**19**), mp 155—157 °C, as yellow needles from isopropyl alcohol, in 46 and 22% yields (122 and 62 mg), respectively.

Compound **19**: ν_{max}^{KBr} cm^{-1}: 1320, 1140 (SO_2). The ^1H- and ^{13}C-NMR spectral data for **19** are listed in Tables II and III.

Acknowledgement The authors are greatly indebted to the staff of the central analysis room of the University of Shizuoka for elemental analysis and mass spectral measurement.

References

1) Part VII: E. Oishi, A. Yamada, E. Hayashi, K. Tanji, A. Miyashita, and T. Higashino, *Chem. Pharm. Bull.*, **37**, 13 (1989).
2) *a*) E. Oishi, N. Taido, K. Iwamoto, A. Miyashita, and T. Higashino, *Chem. Pharm. Bull.*, **38**, 3268 (1990); *b*) E. Oishi, A. Yamada, E. Hayashi, and T. Higashino, *ibid.*, **35**, 2686 (1987).
3) A. Miyashita, N. Taido, S. Sato, K. Yamamoto, H. Ishida, and T. Higashino, *Chem. Pharm. Bull.*, **39**, 282 (1991).
4) P. Main, S. J. Fiske, S. E. Hull, L. Lessinger, G. Germain, J. Declercq, and M. M. Wollfson,"MULTAN 80, A System of Computer Programs for Automatic Solution of Crystal Structures from X-Ray Diffraction Data," Univ. of York, England, and Louvain, Belgium, 1980.
5) J. Ficini and C. Barbara, *Bull. Soc. Chim. Fr.*, **1965**, 2787.
6) E. Oishi, T. Endo, Y. Asahina, and E. Hayashi, *Yakugaku Zasshi*, **105**, 219 (1985).

Studies on the Constituents of *Aster scaber* THUNB. II.[1] Structures of Echinocystic Acid Glycosides Isolated from the Root

Tsuneatsu NAGAO, Ryuichiro TANAKA, Haruki SHIMOKAWA and Hikaru OKABE*

Faculty of Pharmaceutical Sciences, Fukuoka University, Nanakuma 8–19–1, Jonan-ku, Fukuoka 814–01, Japan. *Received January 11, 1991*

Four new echinocystic acid 3,28-*O*-bisdesmosides, scaberosides A_1, A_2, A_3 and A_4, were isolated together with aster saponin Ha, aster saponin Hb and foetidissimoside A from the polar glycoside fraction of the root of *Aster scaber* THUNB. (Compositae) as their methyl esters, and their structures were determined based on spectral and chemical evidence. Scaberosides have a common prosapogenin, echinocystic acid 3-*O*-β-D-glucopyranosiduronic acid, and differ in the structures of the ester-linked sugar moieties. Scaberoside A_1 is a 28-[*O*-β-D-apiofuranosyl-(1→3)-*O*-α-L-rhamnopyranosyl-(1→2)-α-L-arabinopyranosyl] ester, A_2, a 28-[*O*-β-D-xylopyranosyl-(1→4)-*O*-α-L-rhamnopyranosyl-(1→2)-β-D-xylopyranosyl] ester, A_3, a 28-{*O*-β-D-apiofuranosyl-(1→3)-[*O*-β-D-xylopyranosyl-(1→4)-]-*O*-α-L-rhamnopyranosyl-(1→2)-α-L-arabinopyranosyl} ester, and A_4, a 28-{*O*-β-D-xylopyranosyl-(1→3)-[*O*-β-D-xylopyranosyl-(1→3)-*O*-β-D-xylopyranosyl-(1→4)-]-*O*-α-L-rhamnopyranosyl-(1→2)-β-D-xylopyranosyl} ester of the prosapogenin.

Keywords *Aster scaber*; Compositae; scaberoside; triterpene glycoside; echinocystic acid; glucuronide saponin; 3,28-*O*-bisdesmoside; triterpene saponin

In the preceding paper[1] of this series, we reported the structures of six oleanolic acid glycosides, scaberosides B_1—B_6, isolated from the less polar saponin fraction (fr. B) of the foot of *Aster scaber* THUNB. (Compositae). This paper describes the structures of the echinocystic acid glycosides isolated from the polar glycoside fraction (fr. A).

The polar glycoside fraction was treated with an ion-exchange resin, IRC-84, and the acidic product was converted to a methyl ester with CH_2N_2. The methyl ester was repeatedly chromatographed on silica gel and reversed-phase materials, and seven methyl esters (I—VII, numbered in order of increasing polarity) were isolated as crystals or thin-layer-chromatographically homogeneous amorphous powders.

Compounds I, II and III were identified by direct comparison [thin-layer chromatograms (TLC), nuclear magnetic resonance (NMR) spectra and mass spectra (MS)] as aster saponin Ha methyl ester, aster saponin Hb methyl ester and foetidissimoside A methyl ester, respectively, which had previously been isolated from the herb of *Aster tataricus* L. f.[2]

Compound IV was obtained as an amorphous white powder, and the positive ion fast atom bombardment mass spectrum (FAB-MS) showed an $[M+Na]^+$ ion at m/z 1095, while the negative ion FAB-MS showed an $[M-H]^-$ ion at m/z 1071, indicating the molecular weight to be 1072. The high-resolution FAB-MS gave the molecular formula $C_{53}H_{84}O_{22}$. On acid hydrolysis, IV gave L-arabinose, L-rhamnose, D-apiose and D-glucuronic acid as component sugars. The ^{1}H-NMR spectrum showed signals of seven tertiary methyl groups (δ 0.89, 0.98, 1.02, 1.10, 1.15, 1.27, 1.81), one trisubstituted olefinic proton (δ 5.61, br s) and four sugar anomeric protons (δ 4.97, d, J=8 Hz; 5.72, s; 6.07, d, J=3 Hz; 6.49, d, J=2 Hz). The ^{13}C-NMR spectrum showed signals of six C–C bonded quaternary carbons (δ 30.9, 37.0, 39.5, 40.0, 42.0, 49.6), two ester carbonyl carbons (δ 170.7, 175.9), a pair of olefinic carbons (δ 122.8, 144.4) (Table I) and four anomeric carbons (δ 93.4, 101.5, 107.2, 111.9). The NMR data were compared with those of known compounds and IV was suggested to be a glycoside in which D-apiose is linked to the C_3-OH or C_4-OH group of the L-rhamnopyranosyl unit of aster saponin Hb methyl ester (II). Compound IV was fully methylated and methanolyzed. The methanolysate was acetylated and checked by gas chromatography-chemical ionization mass spectrometry (GC-CI-MS). The methyl glycosides of 2-*O*-acetyl-3,4-di-*O*-methyl-L-arabinopyranose, 3-*O*-acetyl-2,4-di-*O*-methyl-L-rhamnopyranose and 2,3,5-tri-*O*-methyl-D-apiofuranose were detected. Therefore, the structure of IV was determined to be as shown in the chart, and careful examination of the NMR spectra (Table II) of IV supported the above structure. The configuration of the D-apiofuranosyl group was determined to be β from the molecular rotation difference ($\Delta[M]_D$ −139.2°)[3] between IV ($[M]_D$ −649.6°) and II ($[M]_D$ −510.4°). Compound IV is a new glycoside of echinocystic acid and was named scaberoside A_1 methyl ester.

Compound V, $C_{53}H_{84}O_{22}$, gave L-rhamnose, D-xylose and D-glucuronic acid on acid hydrolysis, and the NMR data indicated that V has the same prosapogenin as IV and has an ester-linked triose composed of one mol of L-rhamnose and two mol of D-xylose. The ester-linked sugar

TABLE I. ^{13}C-NMR Chemical Shifts[a] of the Aglycone Moieties of III, IV and VIII

	III	IV	VIII		III	IV	VIII
1	38.8	38.8	38.7	16	74.0	74.0	74.3
2	26.2	26.6	26.6	17	49.5	49.6	49.0
3	89.1	89.2	89.1	18	41.3	41.3	42.2
4	39.5	39.5	39.5	19	47.1	47.1	46.9
5	55.9	55.9	55.8	20	30.8	30.9	30.8
6	18.5	18.5	18.5	21	36.0	36.1	35.9
7	33.4	33.5	33.3	22	32.0	32.0	32.4
8	40.0	40.0	39.8	23	28.1	28.2	28.1
9	47.1	47.1	47.0	24	15.6	15.6	15.6
10	37.0	37.0	37.0	25	16.9	16.9	16.9
11	23.8	23.8	23.7	26	17.5	17.6	17.2
12	122.7	122.8	122.6	27	27.1	27.2	27.1
13	144.4	144.4	144.4	28	175.8	175.9	177.7
14	42.0	42.0	41.9	29	33.2	33.2	33.1
15	36.0	36.0	35.9	30	24.7	24.8	24.6
				OMe	—	—	51.7

a) The data were obtained in pyridine-d_5. The chemical shifts of the aglycone moieties of V, VI and VII were almost the same as those of IV. The deviations are within 0.2 ppm.

TABLE II. NMR Chemical Shifts[a] of the Ester-Linked Sugar Moieties of IV, V, VI and VII

	IV		V		VI		VII	
	^1H	^{13}C	^1H	^{13}C	^1H	^{13}C	^1H	^{13}C
	Ara(1→ag)[b]		Xyl(1→ag)		Ara(1→ag)		Xyl(1→ag)	
1	6.49 (d, 2)	93.4	6.14 (d, 7)	95.2	6.51 (d, 2)	93.6	6.13 (d, 7)	95.4
2	*ca.* 4.55	75.6	*ca.* 4.37	75.7	*ca.* 4.48	75.5		
3	*ca.* 4.50	70.0	*ca.* 4.20	77.7	*ca.* 4.48	75.5		
4	*ca.* 4.45	65.9	4.12 (m)	70.7[e]	*ca.* 4.40	65.0		
5	3.90 (dd, 4, 11)	62.8	3.78 (dd, 10, 11)	67.2[f]	3.95 (dd, 4, 10)	63.2		
	ca. 4.50		*ca.* 4.35	[d]	*ca.* 4.57			
	Rha(1→2A)[c]		Rha(1→2X)		Rha(1→2A)		Rha(1→2X)	
1	5.72 (s)	101.5	6.32 (d, 1)	101.2	5.60 (s)	101.0	6.15 (d, 2)	101.2
2	4.73 (dd, 2, 2)	71.7	4.73 (s)	71.9	4.71 (dd, 2, 4)	71.6	4.94 (br s)	71.2
3	*ca.* 4.45	80.3	4.65 (dd, 3, 8)	72.5	4.44 (dd, 4, 8)	82.3	4.72 (dd, 3, 9)	82.5
4	*ca.* 4.24	73.6	*ca.* 4.40	83.6	*ca.* 4.50	77.9	*ca.* 4.54	78.1
5	*ca.* 4.30	71.7	*ca.* 4.44	68.4	*ca.* 4.17	71.2	*ca.* 4.52	68.8
6	1.68 (d, 4)	18.5	1.75 (d, 6)	18.6	1.72 (d, 6)	18.5	1.75 (d, 6)	18.7
	Api(1→3R)				Api(1→3R)		Xyl(1→3R)	
1	6.07 (d, 3)	111.9			5.98 (d, 4)	111.7	5.20 (d, 8)	105.5
2	4.71 (d, 3)	77.9			4.74 (d, 4)	77.5		
3	—	80.0			—	79.5	Xyl(1→4R)	
4	4.24 (d, 9)	75.0			4.17 (d, 9)	74.5	5.35 (d, 8)	105.0
	ca. 4.55				*ca.* 4.55			
5	4.10 (2H, s)	65.5			*ca.* 3.95	62.2	Xyl(1→3X)	
					ca. 4.55		5.07 (d, 7)	105.9
			Xyl(1→4R)		Xyl(1→4R)			
1			5.18 (d, 7)	106.8	5.34 (d, 8)	105.1		
2			*ca.* 4.07	76.0	*ca.* 4.00	75.5		
3			3.98 (dd, 8, 8)	78.6	*ca.* 4.05	78.2		
4			4.12 (m)	71.0[e]	*ca.* 4.24	73.1		
5			3.47 (dd, 11, 11)	67.4[f]	3.38 (dd, 10, 12)	67.2		
			ca. 4.20	[d]	*ca.* 4.17			

a) Data meaured in pyridine-d_5. *b*) Ara(1→ag) means the arabinopyranosyl group linked to the carboxyl group of the aglycone. *c*) Rha(1→2A) means the rhamnopyranosyl group linked to the C_2-OH group of the arabinopyranosyl group. *d, e, f*) Assignments are interchangeable.

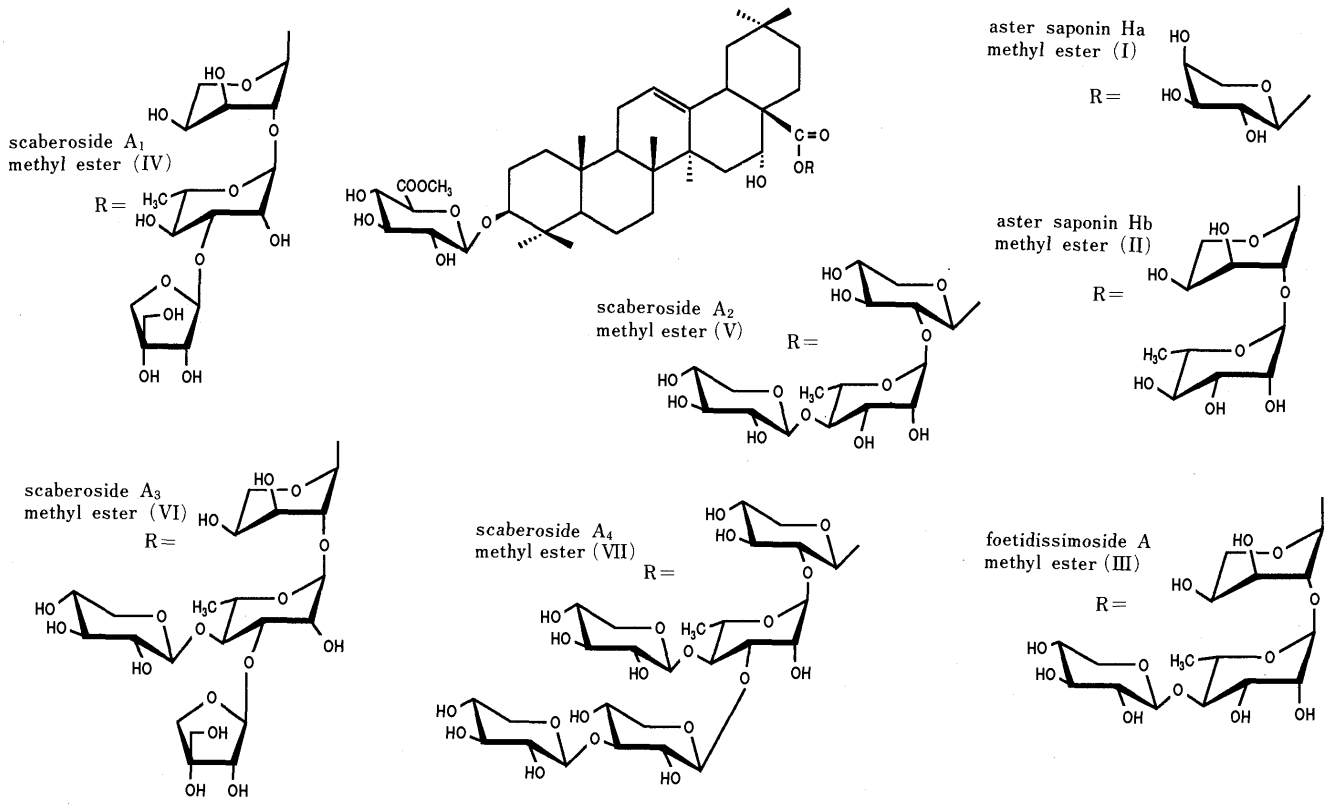

Chart 1

TABLE III. ^1H and ^{13}C-NMR Chemical Shifts of IX and X

		IX (β-anomer)		X (α-anomer)	
		^1H	^{13}C	^1H	^{13}C
Xyl(1→Me)	1	4.52 (d, 7)	104.4	5.20 (d, 4)	100.5
	2	*ca.* 4.07	79.0[d]	3.96 (dd, 4, 8)	81.5
	3	*ca.* 4.05	78.7[d]	4.48 (dd, 8, 8)	74.1
	4	*ca.* 4.05	71.2[b]	*ca.* 4.14	71.5
	5	3.55 (dd, 11, 11) 4.23 (dd, 4, 11)[a]	67.0[c]	3.92 (dd, 11, 11) 4.00 (dd, 4, 11)	62.7
	OMe	3.52 (s)	56.3	3.38 (s)	54.9
Rha(1→2X)	1	6.16 (d, 1)	102.3	5.72 (s)	104.3
	2	4.75 (br s)	72.0	4.65 (br s)	71.7
	3	4.66 (dd, 3, 10)	72.8	4.62 (br d)	72.7
	4	4.39 (dd, 10, 10)	85.0	4.35 (dd, 8, 8)	84.5
	5	4.67 (m)	67.9	4.42 (m)	68.2
	6	1.77 (d, 6)	18.3	1.72 (d, 6)	18.5
Xyl(1→4R)	1	5.15 (d, 8)	107.2	5.13 (d, 8)	107.1
	2	*ca.* 4.05	76.1	4.04 (dd, 8, 8)	76.0
	3	*ca.* 4.08	78.7[d]	4.06 (dd, 8, 8)	78.6
	4	*ca.* 4.15	71.0[b]	*ca.* 4.14	70.9
	5	3.55 (dd, 11, 11) 4.27 (dd, 5, 11)[a]	67.5[c]	3.53 (dd, 11, 11) 4.26 (dd, 5, 11)	67.5

Xyl(1→4R) means the xylopyranosyl group linked to the C_4-OH group of the rhamnosyl group. *a, b, c, d*) Signal assignments may be interchanged.

moiety was selectively cleaved by the method reported by Ohtani *et al.*[4] to give a prosapogenin and an anomeric mixture of a methyl triglycoside. The methyl ester (VIII) of the prosapogenin was identified as echinocystic acid 3-*O*-β-D-glucopyranosiduronic acid dimethyl ester by direct comparison with the prosapogenin methyl ester derived from III.[2] The methyl trioside was subjected to high-performance liquid chromatography (HPLC) on a reversed-phase material, and two anomers were separated. The faster-eluting anomer (IX) and the other (X) showed in the negative ion FAB-MS an $[M-H]^-$ ion at *m/z* 441 and fragment ions at *m/z* 309 and 163, indicating that they are methyl D-xylopyranosyl-L-rhamnopyranosyl-D-xylopyranosides. By careful examination of the NMR data of X (Table III), IX was suggested to be methyl β-D-xylopyranosyl-(1→4)-*O*-α-L-rhamnopyranosyl-(1→2)-β-D-xylopyranoside, and X, its α-anomer.

The permethylate of X gave methyl glycosides of 3,4-di-*O*-methyl-D-xylopyranose, 2,3-di-*O*-methyl-L-rhamnopyranose and 2,3,4-tri-*O*-methyl-D-xylopyranose on methanolysis, thus supporting the structure suggested by the NMR data. From the above-mentioned evidence, the structure of V was determined to be as shown in the chart, and the compound was named scaberoside A_2 methyl ester. The configuration and conformation of the ester-linked D-xylopyranosyl group were determined to be β and $^4C_1$ from the $J_{H_1H_2}$ value (7 Hz).

Compound VI, $C_{58}H_{92}O_{26}$, has L-arabinose, D-xylose, L-rhamnose, D-apiose and D-glucuronic acid as component sugars, and the NMR data indicated it to be a similar echinocystic acid pentaglycoside. When VI was methanolyzed in a methanolic CF_3COOH solution, it gave foetidissimoside A methyl ester (III). On selective cleavage of the ester-linked sugar moiety followed by methylation with CH_2N_2, VI gave VIII and an anomeric mixture of a methyl tetraglycoside, which was subjected to HPLC on a reversed-phase material, yielding the anomers (XI and XII). The NMR data for the anomers are summarized in Table IV. The permethylate of the faster-eluting anomer (XI) gave methyl glycosides of 3,4-di-*O*-methyl-L-arabinopyranose, 2-*O*-methyl-L-rhamnopyranose, 2,3,4-tri-*O*-methyl-D-xylopyranose and 2,3,5-tri-*O*-methyl-D-apiofuranose on methanolysis. Considering that VI gives foetidissimoside A methyl ester (III) on methanolysis, it is apparent from the above data that XI is methyl *O*-β-D-apiofuranosyl-(1→3)-[*O*-β-D-xylopyranosyl-(1→4)-]-*O*-α-L-rhamnopyranosyl-(1→2)-β-L-arabinopyranoside, and the other anomer (XII) is its α-anomer.

The structure of VI was, therefore, determined to be as shown in the chart, and VI was named scaberoside A_3 methyl ester. The configuration of the D-apiofuranosyl group was determined to be β from the $\Delta[M]_D$ value (−293.7°) between VI ($[M]_D$ −771.8°) and III ($[M]_D$ −478.1°).

Compound VII, $C_{63}H_{100}O_{30}$, has D-xylose, L-rhamnose and D-glucuronic acid as component sugars. The NMR spectra indicated that VII is a 3,28-*O*-bisdesmoside of echinocystic acid similar to VI, having the same prosapogenin and an ester-linked pentaose composed of 1 mol of L-rhamnose and 4 mol of D-xylose. Selective cleavage of the ester-linked sugar moiety and methylation with CH_2N_2 gave VIII and an anomeric mixture of a methyl pentaglycoside which was subjected to HPLC to yield the anomers (XIII and XIV). The faster-eluting anomer (XIII) showed in the negative ion FAB-MS an $[M-H]^-$ ion at *m/z* 705 and fragment ions at *m/z* 573, 441, 309 and 163, indicating that XIII is a linear MeO–Xyl–Rha–Xyl–Xyl–Xyl or a branched-chain sugar in which a xylosyl group and a xylobiosyl group are linked to the hydroxyl groups of the rhamnosyl group of MeO–Xyl–Rha, or a branched-chain sugar with three xylosyl groups attached to the rhamnosyl group of MeO–Xyl–Rha. The permethylate of XIII gave methyl glycosides of 2,3,4-tri-*O*-methyl-D-xylopyranose, 2,4-di-*O*-methyl-D-xylopyranose, 3,4-di-*O*-methyl-D-xylopyranose and 2-*O*-methyl-L-rhamnopyranose on methanolysis. Therefore, the sugar sequence and linkages in XIII were confined to one of the following four

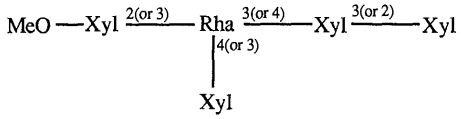

possibilities. In order to determine the positions of sugar linkages, the ^1H-NMR spectrum of the other anomer (XIV) measured in pyridine-d_5 was carefully examined. The anomeric proton signals were observed at δ 5.20 (d, *J*= 4 Hz, Xa-1H), 4.97 (d, *J*=8 Hz, Xb-1H), 5.11 (d, *J*=7 Hz, Xc-1H), 5.34 (d, *J*=8 Hz, Xd-1H) and 5.72 (br s, R-1H) (Fig. 1-A and Table IV), the last one being identified as the signal of the anomeric proton of the L-rhamnosyl group. The Xa-1H is the anomeric proton of the methyl glycosylated α-D-xylopyranosyl group. The signals at δ 4.82 (br s), 4.64 (dd, *J*=3, 9 Hz) and 4.50 (dd, *J*=9, 9 Hz) were assigned as R-2H, R-3H and R-4H, respectively, judged from the ^1H–^1H correlation spectroscopy (COSY) spectrum. The rotating frame nuclear Overhauser effect (ROE) difference spectrum (ROEDS) (Fig. 1-C) obtained by irradiation at the frequency of Xb-1H (δ 4.97) showed signals of R-2H, R-3H and R-4H and the intensities of the signals indicate that the xylose Xb is linked to the C_3-OH

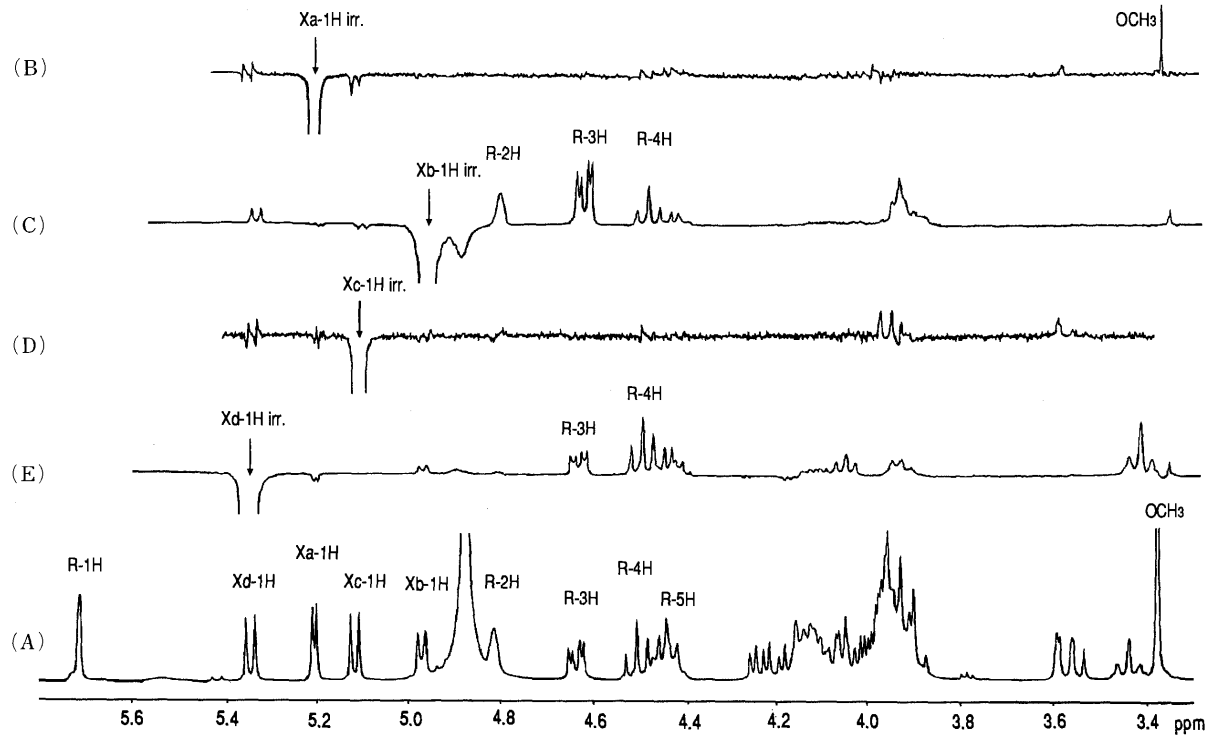

Fig. 1. ^{1}H-NMR Spectrum (A) and ROED Spectra (B, C, D, E) of XIV

TABLE IV. NMR Chemical Shifts of XI, XII, XIII and XIV

		XI (β-anomer)		XII (α-anomer)		XIII (β-anomer)		XIV (α-anomer)	
		^{1}H	^{13}C	^{1}H	^{13}C	^{1}H	^{13}C	^{1}H	^{13}C
Ara(1→Me)	1	5.30 (d, 3)	101.1	4.50 (d, 7)	103.4				
	2	4.53 (dd, 3, 9)	79.5	4.44 (dd, 7, 10)	77.1				
	3	*ca.* 4.43	68.6	*ca.* 4.10	74.1				
	4	*ca.* 4.14	71.2	*ca.* 4.15	71.3				
	5	3.96 (2H, d, 1)	63.4	3.68 (dd, 2, 12)	66.0				
				ca. 4.22					
	OMe	3.40 (s)	55.0	3.50 (s)	55.7				
Rha(1→2A)	1	5.56 (d, 1)	104.4	5.92 (d, 2)	102.3				
	2	4.83 (br d, 3)	71.4	4.88 (br s)	71.9				
	3	4.52 (dd, 3, 8)	82.5	4.55 (dd, 4, 8)	82.4				
	4	*ca.* 4.50	78.3	*ca.* 4.55	78.5				
	5	*ca.* 4.40	68.1	*ca.* 4.55	68.1				
	6	1.67 (d, 6)	18.6	1.67 (d, 6)	18.4				
Api(1→3R)	1	5.88 (d, 5)	111.5	6.11 (d, 4)	117.7				
	2	4.71 (d, 5)	77.4	4.77 (d, 4)	77.6				
	3	—	79.4	—	79.6				
	4	*ca.* 4.10	74.4	4.23 (dd, 3, 9)	74.6				
		ca. 4.53		*ca.* 4.55					
	5	3.96 (2H)	64.5	*ca.* 4.07 (2H)	64.7				
Xyl(1→4R)	1	5.34 (d, 8)	105.2	5.38 (d, 8)	105.2				
	2	*ca.* 3.96	75.5	3.98 (dd, 8, 8)	75.6				
	3	4.10 (dd, 8, 8)	78.3	*ca.* 4.10	78.5				
	4	4.18 (br s)	70.7	*ca.* 4.10	69.2				
	5	3.46 (dd, 10, 10)	67.2	3.48 (dd, 10, 12)	67.2				
		4.20 (dd, 4, 10)		*ca.* 4.22					
Xyl(1→Me)	1					4.52 (d, 7)	104.1	5.20 (d, 4)	100.5
	2					*ca.* 4.07	79.0	*ca.* 3.92	81.7
	OMe					3.51 (s)	56.1	3.38 (s)	54.8
Rha(1→2X)	1					6.15 (d, 1)	102.2	5.72 (s)	104.2
	2					4.92 (br s)	71.7	4.82 (br s)	71.2
	3					4.74 (dd, 3, 10)	82.3	4.64 (dd, 3, 9)	82.1
	4					4.57 (dd, 10, 10)	78.8	4.50 (dd, 9, 9)	78.5
	5					*ca.* 4.68	68.2	4.44 (m)	68.3
	6					1.75 (d, 6)	18.5	1.70 (d, 6)	18.7
Xyl(1→3R)	1					5.26 (d, 7)	105.8	4.97 (d, 8)	105.0
	3					*ca.* 4.15	86.4	3.95	86.3
Xyl(1→4R)	1					5.39 (d, 8)	105.1	5.34 (d, 8)	105.1
Xyl(1→3R)	1					5.11 (d, 8)	105.8	5.11 (d, 7)	105.8

group of the L-rhamnosyl group. In the same way, the signals of Xc-1H and Xd-1H were irradiated and ROEDS were measured. On irradiation on the signal of Xd-1H, ROE was observed at the signal of R-4H (Fig. 1-E). Irradiation on the signal of Xc-1H showed ROE on the signal at δ 3.95 (Fig. 1-D). This signal seemed to be due to C_2-H or C_3-H of a xylosyl group, but could not be definitively assigned because the C_2-H signals of all xylosyl groups and the C_3-H signals of some xylosyl groups overlapped in this region. In order to determine the position of the hydroxyl group of Xa to which rhamnose is linked, XIV was acetylated and ^{1}H-NMR spectrum of the acetate was measured in $CDCl_3$. The ^{1}H-NMR spectrum showed the signals of anomeric protons at δ 4.62 (d, J=6 Hz), 4.67 (d, J=6 Hz), 4.70 (d, J=2 Hz), 4.75 (d, J=3 Hz), 4.76 (d, J=7 Hz). The signal at δ 4.75 is due to the anomeric proton (Xa-1H) of the methyl glycosylated α-D-xylopyranosyl group, and the ^{1}H–^{1}H COSY spectrum showed the signal

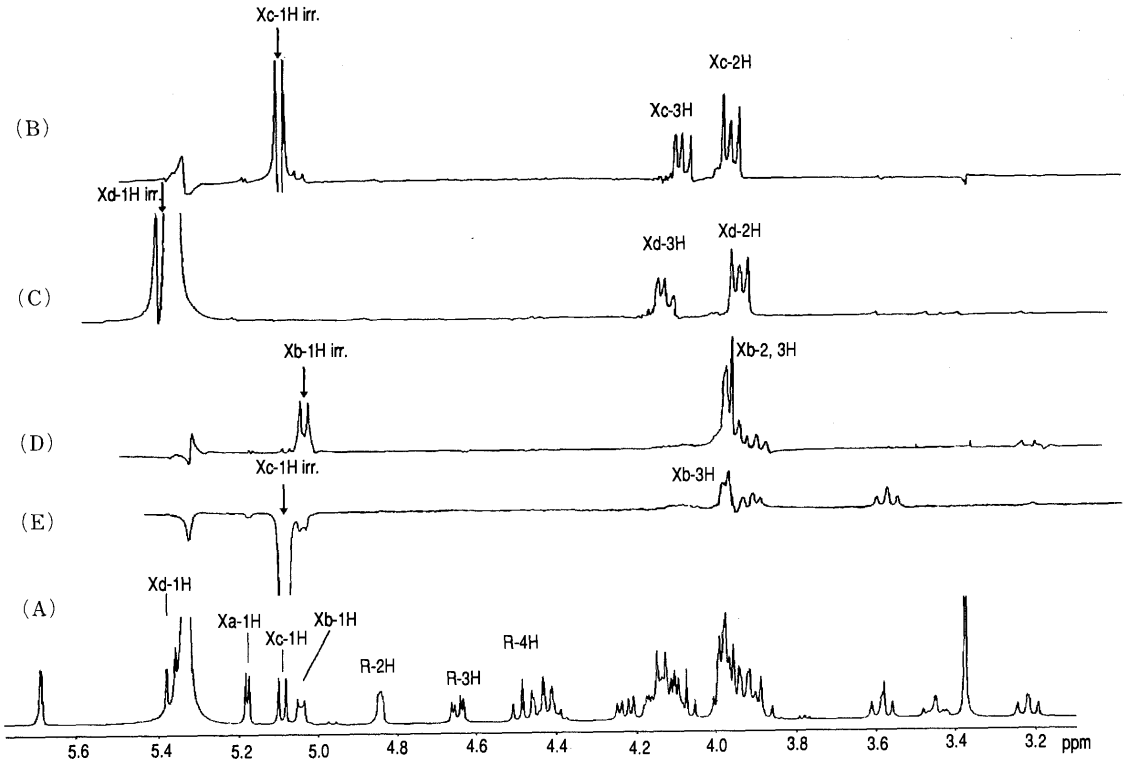

Fig. 2. ^{1}H-NMR Spectrum (A), ROED Spectrum (E) and 1D-HOHAHA Spectra (B, C, D) of XIV (in Pyridine-d_5 + D_2O)

of Xa-2H at δ 3.52 (dd, J=3, 10 Hz) overlapped by the signal of an axial C_5-H of a xylopyranosyl group. The signal at δ 5.36 (dd, J=10, 10 Hz) was assigned to Xa-3H from the ^{1}H–^{1}H COSY spectrum and the decoupling difference spectrum (DDS). The signals of Xa-2H and Xa-3H of this xylopyranosyl group in XIV appeared at δ 3.92 and 3.95, respectively, and the former signal is shifted up-field by 0.4 ppm and the latter is shifted down-field by 1.4 ppm by acetylation. These acetylation shifts clearly indicate that the L-rhamnopyranosyl group is linked to the C_2-OH group of Xa.

The last problem in the structure of XIV is the position of linkage of the terminal xylosyl group (Xc). In order to determine the position, C_3-OH of Xb or Xd, the ^{1}H-NMR spectrum of XIV was measured in the pyridine-d_5–D_2O solution, expecting shifts of the signals of C_2-H and C_3-H (Fig. 2). The ROEDS also indicated that Xa is the methyl glycosylated α-D-xylopyranosyl group, Xb, the xylosyl group linked to C_3-OH of the rhamnosyl group, and Xd, the xylosyl group linked to C_4-OH of the rhamnosyl group. The ROEDS (Fig. 2-E) obtained by irradiation at the frequency of Xc-1H showed the signal at δ *ca.* 3.95 and this signal was proved to be due to C_3-H of Xb from the 1D-homonuclear Hartmann–Hahn (HOHAHA) spectrum (Fig. 2-D). The Xd-3H appeared at lower magnetic field than the Xb-3H. From these NMR data, it was concluded that Xc is linked to the C_3-OH group of the xylosyl group (Xb) which is further linked to the C_3-OH group of the rhamnosyl group.

The structure of XIV was elucidated to be methyl *O*-β-D-xylopyranosyl-(1→3)-*O*-β-D-xylopyranosyl-(1→3)-[*O*-β-D-xylopyranosyl-(1→4)-]-*O*-α-L-rhamnopyranosyl-(1→2)-α-D-xylopyranoside, and therefore VII was determined to be as shown in the chart. Compound VII is also a new glycoside of echinocystic acid and was named scaberoside A_4 methyl ester. The configuration and conformation of the ester-linked xylopyranosyl group were determined to be β and $^4C_1$ from the $J_{H_1H_2}$ value (7 Hz).

Experimental

Extraction and Fractionation The polar glycoside fraction (fr. A) (15.3 g) obtained by factionation of the glycoside fraction of the root of *Aster scaber* THUNB.[1] was treated with Amberlite IRC-84 and the acidic product was methylated with CH_2N_2. The methyl ester was chromatographed on silica gel (EtOAc–MeOH–H_2O, 8:1:0.5) and fractionated into six fractions (fr. A-1—A-6). Fr. A-2 (1.39 g) was repeatedly chromatographed on silica gel ($CHCl_3$–MeOH–H_2O, 15:3:0.5, EtOAc–2-propanol–H_2O, 20:1:0.5) and then purified by chromatography on YMC gel (70% MeOH) to give aster saponin Ha methyl ester (I) (75 mg) and aster saponin Hb methyl ester (II) (165 mg). Fr. A-3 (4.58 g) was chromatographed on silica gel (EtOAc–2-propanol–H_2O, 9:1:0.5) and LiChroprep RP-8 (65% MeOH) to give foetidissimoside A methyl ester (III) (476 mg), IV (1.7 g) and V (122 mg). Fr. A-4 (3.61 g) was chromatographed on silica gel (EtOAc–MeOH–H_2O, 8:1:0.5) to give VI (3.23 g). Fr. A-5 was chromatographed on silica gel ($CHCl_3$–MeOH–H_2O, 15:6:1) and purified by HPLC (Capcell Pak C_{18}, 70% MeOH) to give VII (286 mg).

Aster Saponin Ha Methyl Ester (I): Colorless needles from MeOH–H_2O, mp 196—199 °C. $[\alpha]_D^{26}$ −15.3° (c=2.25, MeOH). Positive ion FAB-MS m/z: 795.450 ($[M+H]^+$). $C_{42}H_{67}O_{14}$ requires m/z 795.453.

Aster Saponin Hb Methyl ester (II): An amorphous powder. $[\alpha]_D^{29}$ −61.0° (c=2.0, MeOH). Positive ion FAB-MS m/z: 963.491 ($[M+Na]^+$). $C_{48}H_{76}NaO_{18}$ requires m/z 963.493.

Foetidissimoside A Methyl Ester (III): Colorless needles from MeOH–H_2O, mp 220—222 °C. $[\alpha]_D^{29}$ −42.7° (c=2.25, MeOH). Positive ion FAB-MS m/z: 1095.538 ($[M+Na]^+$). $C_{53}H_{84}NaO_{22}$ requires m/z 1095.535.

Scaberoside A_1 Methyl Ester (IV): An amorphous powder. $[\alpha]_D^{29}$ −60.6° (c=2.25, MeOH). Positive ion FAB-MS m/z: 1095.532 ($[M+Na]^+$). $C_{53}H_{84}NaO_{22}$ requires m/z 1095.535. Negative ion FAB-MS m/z: 1071 ($[M-H]^-$). ^{1}H-NMR δ: aglycone moiety; 3.38 (dd, 5, 5Hz, C_3-H), 5.24 (br s, C_{16}-H), 5.62 (br s, C_{12}-H), 1.27 (C_{23}-H), 1.10 (C_{24}-H), 0.98 (C_{25}-H), 0.89 (C_{26}-H), 1.81 (C_{27}-H), 1.02 (C_{29}-H), 1.15 (C_{30}-H). Sugar moiety; 3-*O*-β-D-glucuronic acid methyl ester; 4.97 (d, 8 Hz, C_1-H), 4.06 (dd, 8, 8 Hz, C_2-H), 4.25 (dd, 8, 8 Hz, C_3-H), 4.44 (dd, 8, 9 Hz, C_4-H), 4.56 (d,

9 Hz, C_5-H), 3.73 (OMe). ^{1}H-NMR data for the ester-linked sugar moiety are shown in Table II. ^{13}C-NMR δ: aglycone moiety; shown in Table I. 3-*O*-β-D-Glucuronic acid methyl ester; 107.2 (C_1), 75.4 (C_2), 77.9 (C_3), 73.1 (C_4), 77.1 (C_5), 170.7 (C_6), 52.0 (OCH_3). Ester-linked sugar moiety; shown in Table II.

Scaberoside A_2 Methyl Ester (V): An amorphous powder. $[\alpha]_D^{29}$ −42.9° (c=2.25, MeOH). Positive ion FAB-MS m/z: 1095.538 ($[M+Na]^+$). $C_{53}H_{84}NaO_{22}$ requires m/z 1095.535. Negative ion FAB-MS m/z: 1071 ($[M-H]^-$). ^{1}H-NMR, ^{13}C-NMR: prosapogenin moiety; almost the same as IV. Ester-linked sugar moiety; shown in Table II.

Scaberoside A_3 Methyl Ester (VI): An amorphous powder. $[\alpha]_D^{29}$ −64.1° (c=2.0, MeOH). Positive ion FAB-MS m/z: 1227.578 ($[M+Na]^+$). $C_{58}H_{92}NaO_{26}$ requires m/z 1227.577. Negative ion FAB-MS m/z: 1203 ($[M-H]^-$). ^{1}H-NMR, ^{13}C-NMR: prosapogenin moiety; almost the same as IV. Ester-linked sugar moiety; shown in Table II.

Scaberoside A_4 Methyl Ester (VII): An amorphous powder. $[\alpha]_D^{29}$ −46.2° (c=2.25, MeOH). Positive ion FAB-MS m/z: 1359.617 ($[M+Na]^+$). $C_{63}H_{100}NaO_{30}$ requires m/z 1359.619. Negative ion FAB-MS m/z: 1335 ($[M-H]^-$). ^{1}H-NMR, ^{13}C-NMR: prosapogenin moiety; almost the same as IV. Ester-linked sugar moiety; shown in Table II.

Determination of Sugar Species and Their Absolute Configurations A glycoside (*ca.* 3 mg) was dissolved in 1 N HCl–MeOH (1 ml) and heated at 95 °C for 2 h. The acid was neutralized with Ag_2CO_3 and the precipitates were centrifuged off. The supernatant was bubbled through with H_2S and concentrated. The residue was trimethylsilylated with trimethylsilylimidazole and checked by gas liquid chromatography (GC). The standard sugar samples and apiin were treated in the same way and retention times were compared with those of methanolysates of saponins. GC conditions were as follows: column, Shimadzu HiCap-CBP-1 (50 m × 0.2 mm i.d.); column oven temperature, 190 °C (for pentose and methylpentose) and 210 °C (for glucuronic acid); injection port temperature, 290 °C; carrier gas, He (linear velocity, 20 cm/s); split ratio, 1/110; make-up gas, He (50 ml/min). The sugar species identified for each saponin are given in the text. The retention times of the standard sugar derivatives were as follows: D-apiose, 9.5, 9.9; L-arabinose, 11.0, 11.3; D-xylose, 15.1, 16.1; L-rhamnose, 12.1, 12.7; D-glucuronic acid, 15.8, 17.6, 18.2.

Determination of the absolute configuration was performed according to the method reported by Hara *et al.*[6] Thus, a glycoside (5—10 mg) was hydrolyzed in 1 N HCl (1 ml) at 95 °C for 2 h. The acid was neutralized in the same manner as described above. The hydrolysate was suspended in H_2O and extracted with $CHCl_3$ to remove the aglycone. The aqueous layer was concentrated and the residue was dissolved in pyridine (0.2 ml). After addition of a pyridine solution (0.4 ml) of L-cysteine methyl ester hydrochloride (0.06 mol/l), the mixture was warmed at 60 °C for 1 h. The solvent was blown off under an N_2 stream, and the residue was trimethylsilylated and checked by GC. The absolute configuration of glucuronic acid was determined as glucose in the same way after $NaBH_4$ reduction of the prosapogenin methyl ester. The standard sugar samples and apiin hydrolysate were treated in the same way and the retention times were compared. The GC conditions were the same as those described above except for the column oven temperature (250 °C). The retention times of the standard sugar derivatives were as follows: L-arabinose, 11.9; D-arabinose, 12.5; L-rhamnose, 13.9; D-rhamnose, 14.2; D-xylose, 12.0; L-xylose, 12.4; D-apiose (from apiin), 11.7; D-glucose, 17.2; L-glucose, 17.7.

Methylation of IV, X, XI and XIII, Identification of Component Methylated Sugars by GC-CI-MS Methylation of a glycoside was performed according to the method reported by Hakomori.[7] Thus, IV (20 mg) was dissolved in dimethylsulfoxide (DMSO) (2 ml) and the solution was added to the dimethylsulfinyl carbanion solution prepared from NaH (oil-fused) (60 mg) and DMSO (1 ml) heated at 90 °C for 30 min. The mixture was stirred at room temperature for 10 min. CH_3I (2 ml) was added, and the whole was stirred for 24 h at room temperature. $CHCl_3$ (5 ml) was added to the solution, separated, and washed three times with H_2O. The $CHCl_3$ layer was dried over Na_2SO_4 and evaporated. The residue was chromatographed on silica gel (benzene–acetone, 3 : 2). The thin-layer-chromatographically homogeneous permethylate (23 mg) was methanolysed in 1 N HCl–MeOH. The methanolysate was treated with Ac_2O–pyridine (1 : 1) and the product was checked by GC-CI-MS. Compounds X, XI and XIII were methylated, methanolyzed, acetylated and checked by GC-CI-MS in the same way. GC-CI-MS conditions were as follows: GC part: column, 2% OV-17 on Uniport HP (80—100 mesh) packed in a glass column (1.0 m × 3 mm i.d.); column oven temperature, 130→190 °C (elevation rate, 3 °C/min); carrier gas, He (20 ml/min); injection port temperature, 250 °C. CI-MS part: reagent gas, isobutane (pressure, less than 1.5×10^{-5} Torr); ionization source temperature, 270 °C; ionization energy, 150 eV; scan range: 100→400 m/z; scan interval, 4 s.

The following methyl glycosides were identified as component methylated sugars of the permethylate of IV (the number in parentheses is the retention time in minutes): methyl 2,3,5-tri-*O*-methyl-α- or -β-D-apiofuranoside (1.60), methyl 2,3,5-tri-*O*-methyl-β- or -α-D-apiofuranoside (2.10), methyl 3-*O*-acetyl-2,4-di-*O*-methyl-α-L-rhamnopyranoside (5.43) and methyl 2-*O*-acetyl-3,4-di-*O*-methyl-α-L-arabinopyranoside (7.60). The peak at t_R 9.36 seemed to be a permethylate of glucuronic acid, but it was not identified because a standard sample was not available.

The permethylate of X gave methyl 2,3,4-tri-*O*-methyl-α-D-xylopyranoside (2.20), methyl 2,3,4-tri-*O*-methyl-β-D-xylopyranoside (1.70), methyl 2-*O*-acetyl-3,4-di-*O*-methyl-α-D-xylopyranoside (4.70), methyl 2-*O*-acetyl-3,4-di-*O*-methyl-β-D-xylopyranoside (6.10) and methyl 2,3-di-*O*-methyl-4-*O*-acetyl-α-L-rhamnopyranoside (6.40).

The permethylate of XI gave methyl 2,3,4-tri-*O*-methyl-α-D-xylopyranoside (2.20), methyl 2,3,4-tri-*O*-methyl-β-D-xylopyranoside (1.70), methyl 2,3,5-tri-*O*-methyl-α- or -β-D-apiofuranoside (2.10), methyl 2-*O*-acetyl-3,4-di-*O*-methyl-α-L-arabinopyranoside (7.60) and methyl 2-*O*-methyl-3,4-di-*O*-acetyl-α-L-rhamnopyranoside (9.60).

The permethylate of XIII gave methyl 2,3,4-tri-*O*-methyl-α-D-xylopyranoside (2.20) and its β-anomer (1.70), methyl 2,4-di-*O*-methyl-3-*O*-acetyl-α-D-xylopyranoside (7.50) and its β-anomer (6.10), methyl 2-*O*-acetyl-3,4-di-*O*-methyl-α-D-xylopyranoside (4.70) and its β-anomer (6.10) and methyl 2-*O*-methyl-3,4-di-*O*-acetyl-α-L-rhamnopyranoside (9.60).

Partial Methanolysis of VI with CF_3COOH Compound VI (148 mg) was dissolved in 2 N CF_3COOH–MeOH solution (3.5 ml) and the solution was heated at 60 °C for 6 h. After evaporation of the solvent, the residue was chromatographed on silica gel (EtOAc–MeOH–H_2O, 8 : 1 : 0.5) and the desapiosyl compound was purified by HPLC (Capcell Pak C_{18}, 72.5% MeOH) to give a thin-layer-chromatographically homogeneous product (40 mg) as an amorphous powder. $[\alpha]_D^{30}$ −44.6° (c=1.95, MeOH). The ^{1}H-NMR and ^{13}C-NMR spectra were identical with those of III.

Selective Cleavage of the Ester Glycoside Linkages of V, VI and VII Selective cleavage of the ester-linked sugar moiety was performed according to the method reported by Ohtani *et al.*[4] Compound V (294 mg) and LiI (300 mg) was added to a mixture of 2,6-lutidine (4 ml) and MeOH (2 ml). The mixture was heated in a sealed tube at 160—180 °C for 18 h. H_2O (6 ml) was added to the reaction mixture and passed through a column of Amberlite MB-3 (20 ml). The effluent was concentrated to dryness and the residue was dissolved in MeOH and treated with CH_2N_2. The reaction product (286 mg) was chromatographed on silica gel ($CHCl_3$–MeOH–H_2O, 15 : 4 : 0.2) to give a prosapogenin methyl ester fraction (144 mg) and a methyl glycoside fraction (89 mg). The former was further chromatographed on silica gel ($CHCl_3$–MeOH, 98 : 2) and then purified by HPLC (Capcell Pak C_{18}, 85% MeOH) to give VIII (80 mg). The methyl glycoside fraction was subjected to HPLC (Capcell Pak C_{18}, 10% MeOH) to give IX (25 mg) and X (33 mg). Compound VI (1.24 g) was treated in the same way to furnish VIII (121 mg), XI (106 mg) and XII (51 mg). Compound VII (188 mg) gave VIII (32 mg), XIII (21 mg) and XIV (35 mg).

VIII: An amorphous powder. $[\alpha]_D^{28}$ −11.1° (c=3.65, MeOH). Positive ion FAB-MS m/z: 699 ($[M+Na]^+$). The ^{1}H-NMR and ^{13}C-NMR spectra were identical with those of the prosapogenin methyl ester[2] derived from foetidissimoside A methyl ester (III).

IX: An amorphous powder. $[\alpha]_D^{30}$ −80.5° (c=1.25, MeOH). Positive ion FAB-MS m/z: 465 ($[M+Na]^+$). ^{1}H-NMR, ^{13}C-NMR: shown in Table III.

X: An amorphous powder. $[\alpha]_D^{30}$ +9.37° (c=1.65, MeOH). Positive ion FAB-MS m/z: 465 ($[M+Na]^+$). Negative ion FAB-MS m/z: 441 ($[M-H]^-$), 309, 163. ^{1}H-NMR, ^{13}C-NMR: shown in Table III.

XI: An amorphous powder. $[\alpha]_D^{28}$ −0.9° (c=2.00, MeOH). Positive ion FAB-MS m/z: 597 ($[M+Na]^+$). Negative ion FAB-MS m/z: 573 ($[M-H]^-$), 441, 309, 163. ^{1}H-NMR, ^{13}C-NMR: shown in Table IV.

XII: An amorphous powder. $[\alpha]_D^{29}$ −69.8° (c=2.15, MeOH). Positive ion FAB-MS m/z: 597 ($[M+Na]^+$). ^{1}H-NMR, ^{13}C-NMR: shown in Table IV.

XIII: An amorphous powder. $[\alpha]_D^{29}$ −58.0° (c=1.05, MeOH). Positive ion FAB-MS m/z: 729 ($[M+Na]^+$). Negative ion FAB-MS m/z: 705 ($[M-H]^-$), 573, 441, 309, 163. ^{1}H-NMR, ^{13}C-NMR: shown in Table IV.

XIV: An amorphous powder. $[\alpha]_D^{29}$ −12.2° (c=1.75, MeOH). Positive ion FAB-MS m/z: 729 ($[M+Na]^+$). ^{1}H-NMR, ^{13}C-NMR: shown in Table IV.

Acetylation of XIV Compound XIV (35 mg) was dissolved in Ac_2O–pyridine (1 : 1) (0.8 ml) and the mixture was stirred at room temperature

for 10 h. The solvent was blown off by an N_2 stream and the residue was checked by TLC (benzene–acetone, 3 : 1), which revealed a single spot of the product.

Acknowledgements The authors express their gratitude to Ms. Y. Iwase, Miss J. Honda and Mr. H. Hanazono for measurement of NMR spectra and MS.

References and Notes

1) Part I: T. Nagao, R. Tanaka and H. Okabe, *Chem. Pharm. Bull.*, **39**, 1699 (1991).
2) R. Tanaka, T. Nagao, H. Okabe and T. Yamauchi, *Chem. Pharm. Bull.*, **38**, 1153 (1990).
3) T. Nagao, H. Okabe and T. Yamauchi, *Chem. Pharm. Bull.*, **36**, 571 (1988); D. H. Ball, F. H. Bissett, I. L. Klundt and L. Long, Jr., *Carbohydr. Res.*, **17**, 165 (1971).
4) K. Ohtani, K. Mizutani, R. Kasai and O. Tanaka, *Tetrahedron Lett.*, **25**, 4537 (1984).
5) The instruments and materials used in this work were the same as those described in the preceding paper.[1] All melting points are uncorrected. The ^1H- and ^{13}C-NMR spectra were measured at 400 and 100 MHz, respectively in pyridine-d_5 solution unless otherwise stated, and the chemical shifts were expressed in the δ scale using tetramethylsilane as an internal standard.
6) S. Hara, H. Okabe and K. Mihashi, *Chem. Pharm. Bull.*, **35**, 501 (1987).
7) S. Hakomori, *J. Biochem.* (Tokyo), **55**, 255 (1964).

Studies on the Chemical Modification of Monensin. III. Synthesis and Sodium Ion Transport Activity of Macrocyclic Monensylamino Acid-1,29-lactones

Akito NAKAMURA,[a] Shin-ichi NAGAI,[a] Taisei UEDA,[a] Nobutoshi MURAKAMI,[a] Jinsaku SAKAKIBARA,*[,a] Hirotaka SHIBUYA,[b] and Isao KITAGAWA[b]

Faculty of Pharmaceutical Sciences, Nagoya City University,[a] Mizuho-ku, Nagoya 467, Japan and Faculty of Pharmaceutical Sciences, Osaka University,[b] 1-6, Yamada-oka, Suita, Osaka 565, Japan. *Received January 14, 1991*

Monensylglycine (2a) was lactonized to macrocyclic monensylglycine-1,29-lactone (3a) by Corey's method. Lactonization of monensylamino acids (2b—d) to monensylamino acid-1,29-lactones (3b—d) was carried out by utilizing the template effect of K^+ ion. Monobenzyl esters of dicarboxylic monensylamino acids (5e—f) also were lactonized followed by debenzylation to yield carboxylic monensylamino acid-1,29-lactones (3e—f). Sodium ion transport activity of monensin (1) and the lactones (3) was measured in a liquid membrane and in guinea pig erythrocyte membrane. Monensylaspartic acid-1,29-lactone (3e) exhibited 2.5 times higher activity than 1 in the liquid membrane. Monensylalanine-1,29-lactone (3b), monensylphenylalanine-1,29-lactone (3c), and monensyltyrosine-1,29-lactone (3d), having smaller Na^+ ion transport activity than 3e, showed weak antibacterial activity, while 3e was inactive in biological tests, probably due to the lower lipophilicity.

Keywords monensin; monensylamino acid-1,29-lactone; macrolactonization; Na^+ ion transport activity; lipophilicity; antibacterial activity

The antibiotic monensin (**1**, Fig. 1) is a typical representative of the polyether carboxylic ionophore family, and is known to preferentially transport Na^+ ion across biological membranes.[1] This ability results in a variety of biological activities,[2] anticoccidial activity[3] and a positive inotropic effect (PIE) on isolated guinea pig papillary muscle.[4]

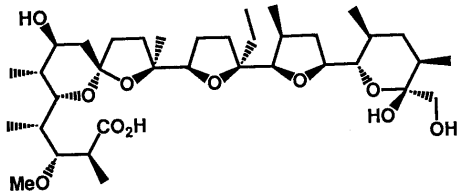

Fig. 1. Chemical Structure of Monensin (**1**)

We have recently synthesized a series of monensylamino acids (**2a—f**) by condensing the carboxylic group with optically active amino acids, and established, on the basis of X-ray analysis, that the NaBr complexes of **2a—f** (Fig. 2b) are quite different from the NaBr complex of **1** (Fig. 2a).[5] In addition, our technique to measure the Na^+ ion transport ability across the membrane of living guinea pig erythrocytes by using sodium-23 nuclear magnetic resonance (^{23}Na-NMR) spectroscopy revealed that **2a—f** showed much smaller initial increasing rates of Na^+ ion transport than **1**, probably due to their lower lipophilicity.[6] These observations suggested that chemical modifications of **2a—f** to produce more lipophilic compounds might lead to new monensin analogs with high initial increasing rate and potent biological activity.

Suzuki *et al.* found that monensin-1,26-lactone (Fig. 3) is a highly Li^+-selective ionophore[7] because the lactonization caused a reduction of the radius of the cavity at the position of Na^+ ion coordination. This interesting result prompted us to prepare monensylamino acid-1,29-lactones with increased lipophilicity which may have optimal cavity size for selective complexation with Na^+ ions. In the present paper, we describe the synthesis, Na^+ ion transport activity,

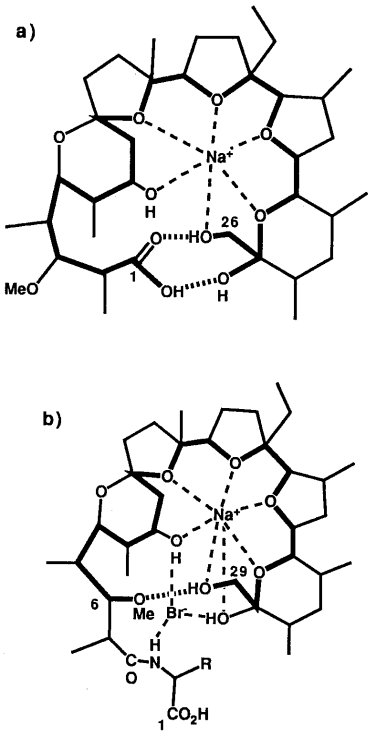

Fig. 2. Pseudocyclic Structure of a) NaBr Complex of Monensin (**1**) and b) NaBr Complexes of Monensylamino Acids (**2**)

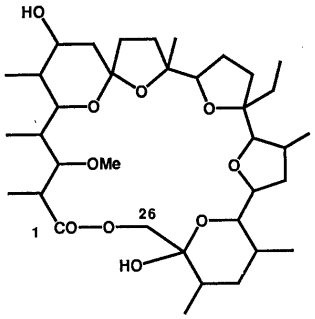

Fig. 3. Monensin 1,26-Lactone

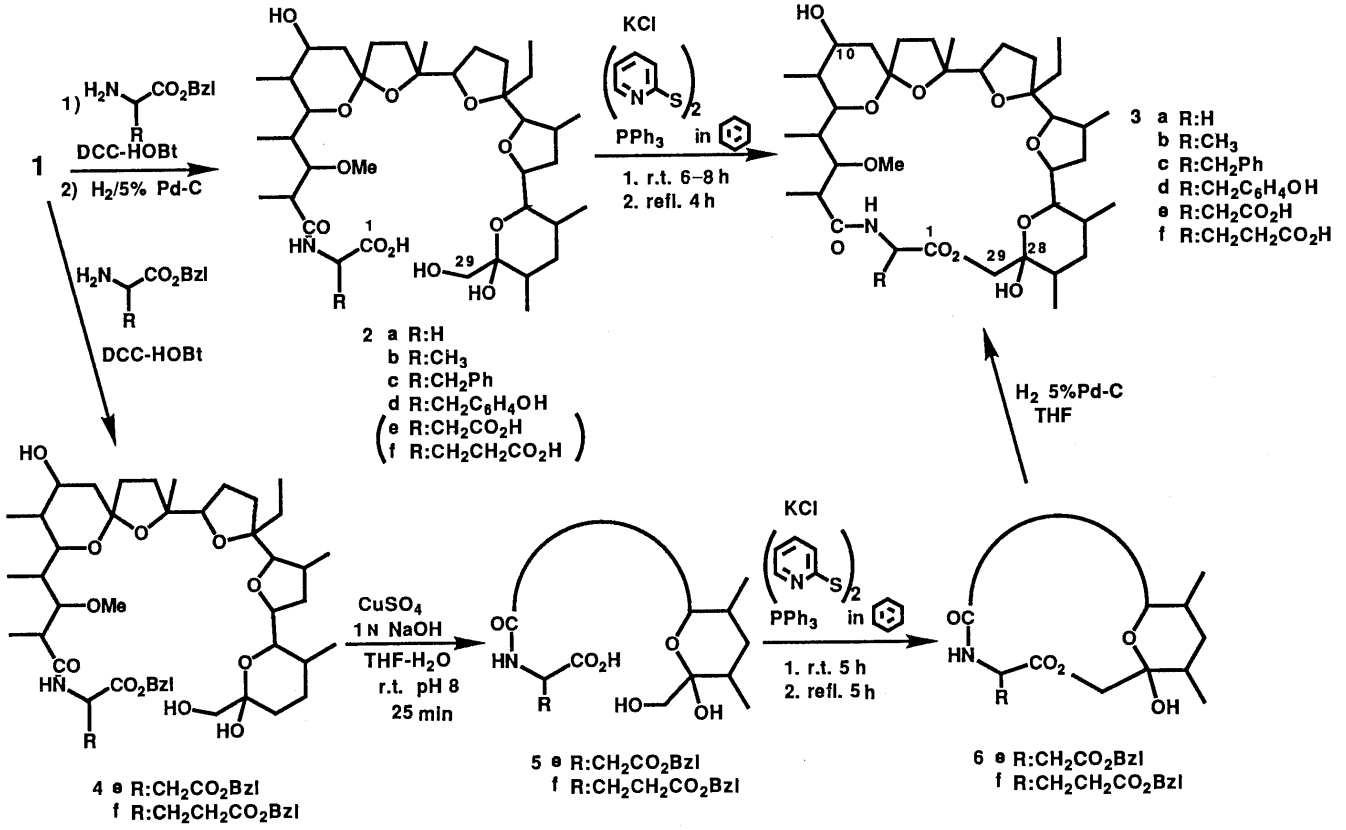

Chart 1

and biological activity of monensylamino acid-1,29-lactones (**3a**—**f**, Chart 1).

Results

Chemistry The preparation of macrocyclic monensylamino acid-1,29-lactones (**3a**—**d**) from monocarboxylic monensylamino acids (**2a**—**d**) was carried out according to Corey's method[8] as outlined in Chart 1, and compound **3a** was obtained from **2a** in 84% yield. The binding of the carboxyl group through oxygen to the C_{29} methylene is clear from the appearance in the ^{1}H-NMR spectrum of an AB doublet of doublets due to the C_{29} methylene of **3a** with doublet A at δ 3.71 ppm and doublet B at δ 4.92 ppm (J=11 Hz). The observed chemical shift values for H_A and H_B of the C_{29} methylene in **2a** itself are δ 3.56 and 3.65 (J=11 Hz), as summarized in Table I. The downfield shift of the C_{29} methylene protons of **3a** relative to **2a** and also the large chemical shift between H_A and H_B in **3a** offer reasonable evidence for structure **3a** and argue against the isomeric 1→10 or 1→28 lactones.

Lactonization of **2b** was similarly carried out, but the yield (57%) of **3b** was disappointingly low. This result stimulated us to utilize template cations[9] which hold two reacting groups in the correct orientation to allow easy lactonization. Thus, NaBr was initially added to the lactonization reaction as a source of readily available template cation. The yield of **3b**, however, was unsatisfactory (61%). This low yield appears to be attributable to the strong hydrogen bonding between the C_{29} hydroxy group and the C_6 methoxy oxygen[5] (Fig. 2b). We hence expected that the strong hydrogen bonding may be weakened, and consequently the C_{29} hydroxy and carboxylic groups may be more readily accessible to each other, if the cavity of complexed **2b** could be enlarged by using template cations with larger ion radius than that of Na^+ ion. We thus attempted the lactonization of **2b** in the presence of various template cations such as KCl, KBr, RbCl, RbBr, and $BaCl_2$. Among these cations, KCl was found to be the most effective compound to give **3b** in good yield (73%), while other compounds gave **3b** in 35—65% yields. Although the reasons for these differences in yield remain unclear, unambiguous evidence for weakened C_6–C_{29} hydrogen bonding in the **2b**–KCl complex was obtained from the ^{13}C-NMR spectrum. In the ^{13}C-NMR ($CDCl_3$) spectrum, the signal of the C_6 carbon of **2b**–NaBr complex appeared 4.13 ppm downfield compared to that of the free acid (**2b**), whereas the corresponding C_6 carbon signal of **2b**–KCl complex was shifted only 1.27 ppm downfield. These chemical shift differences arose from the appreciably weaker hydrogen

Table I. Reaction Times, Yields, and ^{1}H-NMR Data for Lactones

Compound	Reaction time (h)		Yield (%)	Chemical shifts of $C_{(29)}H_2$ (δ ppm) (each 1H, each d, J=11 Hz)	
	Stirring at r.t.	Reflux		Lactones **3** or **6**	ω-Hydroxy acids **2** or **5**
3a	8	4	84	3.71, 4.92	3.56, 3.65
3b	6	4	73	3.55, 4.96	3.54, 3.62
3c	6	4	75	3.49, 4.99	3.60, 3.70
3d	6	4	73	3.51, 5.00	3.60, 3.66
6e	5	5	72	3.53, 4.93	3.54, 3.57
6f	5	5	67	3.50, 4.94	3.52, 3.63

bonding between C_6 oxygen and C_{29} hydrogen. Guided by these results, other monensylamino acids (**2c—d**) were also reacted in the presence of KCl to give **3c—d** in the yields shown in Table I. The structures of **3c—d** were confirmed by the spectral data.

In order to prepare carboxylic lactones (**3e—f**), we examined a different approach as illustrated in Chart 1. Dibenzyl esters (**4e—f**) of monensylaspartic acid and monensylglutamic acid were selectively debenzylated in the presence of aqueous NaOH and $CuSO_4$[10] in tetrahydrofuran (THF) to give **5e—f**. In the ^{1}H-NMR spectra, the methine protons of amino acid moiety appeared downfield relative to the corresponding methines of **4e—f**. This finding demonstrates that selective debenzylation has indeed taken place. Lactonization of **5e—f** in the presence of KCl followed by debenzylation of **6e—f** over Pd–C provided the lactone compounds (**3e—f**).

We finally examined the lipophilicity of macrocyclic lactones (**3a—f**) by measuring *Rm* values.[11] All the lactones measured showed increased lipophilicity over the corresponding monensylamino acids (**2a—f**), and compounds **3a—d** were more lipophilic than monensin (**1**), as illustrated in Table II.

Ion Transport Activity Na^+ ion transport and binding activities of lactones in a $CHCl_3$ liquid membrane system were measured using the W-08 apparatus (Fig. 4).[12] The amount of Na^+ ion transported from the ion-containing water phase into the pure water phase and the amount of Na^+ ion in the $CHCl_3$ phase were determined by counting radioactivity with a γ-counter (Aloka NDW-35E). Interestingly, compound **3e** showed 1.5 times stronger binding activity and 2.5 times stronger transport activity than monensin (**1**), while the other lactones did not have any activity, as shown in Table III.

We also determined the Na^+ ion transport activity in a biological membrane. We employed the living erythrocytes of guinea pig and measured the concentration of intracellular Na^+ ion ($[Na^+_{in}]$) using ^{23}Na-NMR[6] spectros-

TABLE II. Rm_{50} Values of Monensin Derivatives

Compound	Rm_{50}	Compound	Rm_{50}[6]
1	1.83		
3a	1.86	**2a**	0.65
3b	1.99	**2b**	0.73
3c	2.54	**2c**	1.17
3d	1.94	**2d**	0.83
3e	0.82	**2e**	−0.04
3f	0.54	**2f**	−0.08

TABLE III. Na^+ Ion Transport and Binding Activities

Compound	Na^+ ion (nmol)	
	Transport	Binding
1	67.37	36.39
3a	0	0
3b	9.96	2.11
3c	2.51	0.08
3d	5.35	0.53
3e	170.03	56.93
3f	24.13	7.03

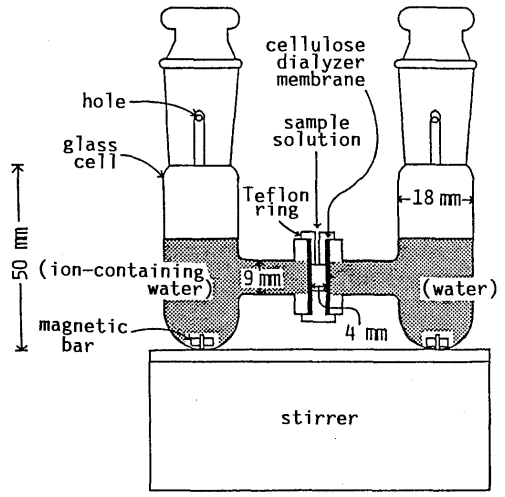

Fig. 4. Apparatus W-08 for Measurements of Ion-Transport and Ion-Binding Activity

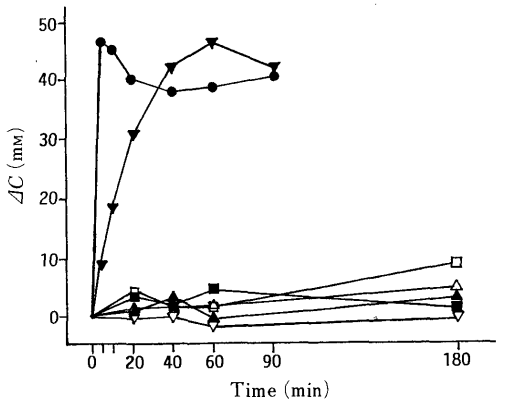

Fig. 5. Corrected Time–Dependent Change of $\Delta[Na_{in}]$ (ΔC)

●, **1**; ▲, **3a**; △, **3b**; ■, **3c**; □, **3d**; ▼, **3e**; ▽, **3f**. DMSO caused a slight decrease of $[Na_{in}]$, and therefore the corrected time dependent change of $\Delta[Na_{in}]$, ΔC ($=\Delta[Na_{in}]^i_t - \Delta[Na_{in}]^{DMSO}_t$) were indicated. $\Delta[Na_{in}]^i_t = [Na_{in}]^i_t - [Na_{in}]^i_0$.

TABLE IV. Minimum Inhibitory Concentrations of Monensin (**1**) and Lactones (**3**) against Anaerobic Bacteria

Organisms	MIC (ppm)						
	1	**3a**	**3b**	**3c**	**3d**	**3e**	**3f**
Peptococcus anaerobius B-40	0.20	>50	12.5	6.25	12.5	>50	>50
Peptostoreptococcus anaerobius B-30	1.56	>50	25	25	50	>50	>50
Propionibacterium acnes ATCC 11828	0.39	>50	25	12.5	6.25	>50	>50
Eubacterium entum BEERENS 515	1.56	>50	25	25	>50	>50	>50
Lactobacillus acidophilus ATCC 4356	0.78	>50	25	>50	1.56	>50	>50
Clostridium perfringens 7-heart	6.25	>50	50	50	25	>50	>50

copy. Among the lactones, compound **3e** showed the most remarkable increasing rate of $[Na^+_{in}]$ (Fig. 5). However, Fig. 5 indicates that the initial increasing rate of $[Na^+_{in}]$ within 0—5 min is markedly slower than that in the case of monensin (**1**).

Biological Activity The values of minimum inhibitory concentration against various bacteria were measured. Compounds **3b—d** showed weak antibacterial activity against anaerobic bacteria, as shown in Table IV, while compounds **3e—f** were inactive. Compounds **3a—f** showed no anticoccidial activity in *Eimeria tennella*-infected chicks. Compound **3e** showed a tendency to decrease the contraction of papillary muscle rather than to develop PIE.

Discussion

We found that the lactonization proceeded in satisfactory yield when KCl was added to Corey's reagents. The improved yields may be attributed to the template effect of K^+ ion.

Compounds **3e—f** showed effective Na^+ ion transport and binding activities in a $CHCl_3$ liquid membrane. In particular, the remarkable activity of **3e** suggested that the carboxylic acid group contributed to the stable complex formation with Na^+ ion by taking the most appropriate position to encapsulate the Na^+ ion in the cavity, as shown in Fig. 6. Compound **3f** may also complex with Na^+ ion in a similar fashion to **3e**, but the carboxylic side arm in this case seems unsuitable to shield the Na^+ ion completely.

Contrary to our expectation, compounds **3e—f** were less active in a variety of biological tests. These findings suggested that appearance of biological activity might depend not on the Na^+ ion transport activity but on the lipophilic character of the molecule. Low lipophilicity of **3e—f** obviously results from the hydrophilic carboxylic acid group appended to the periphery of the macrocyclic molecules. It is, therefore, difficult for **3e—f** to penetrate the bacterial cell membrane.

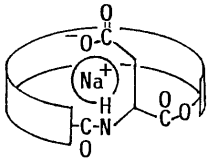

Fig. 6. Probable Structure of Complexed **3e**

The Na^+ ion is in a hydrophilic central cavity of the cyclic molecule and is covered by the ionic carboxylic arm.

In summary, we have synthesized macrocyclic monensylamino acid-1,29-lactones in sufficient yields, and investigated the Na^+ ion transport activity and the biological activity. Compound **3e** showed the largest Na^+ ion transport activity in the liquid membrane system, but **3e** did not show any biological activity, possibly due to its less lipophilic character resulting from the presence of the carboxylic acid group. Consequently, introduction of lipophilic substituents at the α-position to the carboxylic acid group will increase the lipophilicity of **3e** and improve membrane permeability. Our forthcoming paper will focus on further elaboration of **3e** analogues.

Experimental

The fast atom bombardment mass spectra (FAB-MS) were measured with a JEOL JMS DX-300 mass spectrometer, and the infrared (IR) spectra with a JASCO IRA-2 spectrometer. The ^{1}H-NMR spectra were recorded with a JEOL GSX-400 spectrometer in $CDCl_3$ using tetramethylsilane as an internal standard. The following abbreviations are used: d, doublet; dd, doublet of doublets; br, broad. Column chromatography was carried out on silica gel BW-200 (Fuji Davison Chemicals, Ltd.). High-performance liquid chromatography (HPLC) was carried out on C.I.G. ODS-C_{18}-10/20 (22 mm i.d. × 100 mm, Kusano Kagakukikai Co.).

Monensinamidoacetic Acid-1,29-lactone (3a) A solution of **2a** (100 mg), 2,2′-dithiodipyridine (10 eq) and triphenylphosphine (10 eq) in benzene (100 ml) was stirred for 8 h at room temperature followed by the addition of benzene (100 ml) and subsequent gentle boiling for 4 h. The solution was evaporated and the residue was chromatographed on silica gel (hexane–acetone) to afford **3a** as a syrup (82 mg, 84%). ^{1}H-NMR data for **3a** are summarized in Table I. The IR and FAB-MS data and physicochemical data for **3a** are shown in Table V.

General Procedure for Preparations of Lactones (3b—d) A solution of **2b—d** (100 mg) in $CHCl_3$ (5 ml) was treated with an equivalent amount of KCl in MeOH (5 ml). The mixture was evaporated to dryness to give syrups, which were subjected to lactonization using the same procedure as described for **3a** to give **3b—d** as syrups. The yield, the reaction time, and ^{1}H-NMR data for **3b—d** are summarized in Table I. The IR and FAB-MS data and physicochemical data for **3b—d** are shown in Table V.

3b: 2-Methylmonensinamidoacetic acid-1,29-lactone, **3c**: 2-phenylmethylmonensinamidoacetic acid-1,29-lactone, **3d**: 2-(4-hydroxyphenyl)-methylmonensinamidoacetic acid-1,29-lactone.

Monensylaspartic Acid β-Benzyl Ester (5e) and Monensylglutamic Acid γ-Benzyl Ester (5f) Compounds **4e, f** (200 mg) were each dissolved in THF

TABLE V. Physicochemical Data for Monensylamino Acid-1,29-lactones (3)

3	R	IR ν_{max}^{KBr} cm^{-1} (C=O)	$[\alpha]_D^{20}$ (c, $CHCl_3$)	FAB-MS m/z $(M+Na)^+$	Formula	Analysis (%) Found (Calcd)		
						C	H	N
a	H	1745, 1650	31.92 (0.30)	732	$C_{38}H_{63}NO_{11}\cdot 1/2H_2O$	63.50 (63.49)	9.20 8.97	1.71 1.94)
b	CH_3	1750, 1670	14.64 (0.38)	746	$C_{39}H_{65}NO_{11}$	64.49 (64.72)	9.31 9.05	1.72 1.93)
c	CH_2Ph	1735, 1665	−11.45 (0.50)	822	$C_{45}H_{69}NO_{11}$	67.61 (67.56)	8.78 8.69	1.41 1.75)
d	$CH_2C_6H_4OH$	1735, 1660	−10.30 (0.42)	838	$C_{45}H_{69}NO_{12}\cdot 1/2H_2O$	65.44 (65.51)	8.52 8.55	1.35 1.70)
e	CH_2CO_2H	1740, 1660	8.54 (0.41)	790, 812[a]	$C_{40}H_{64}NNaO_{13}$[b]	60.75 (60.82)	8.47 8.17	1.68 1.77)
f	$CH_2CH_2CO_2H$	1735, 1660	3.95 (0.30)	804	$C_{41}H_{67}NO_{13}$	62.78 (62.97)	8.79 8.63	1.79 1.79)

a) Pseudomolecular peak of $(M+2Na-H)^+$. *b*) Elemental analysis of **3e** was carried out as the sodium salt.

(10 ml) and aqueous $CuSO_4 \cdot 5H_2O$ (50 mg, 1 ml) was added. The pH was raised to pH 8 with 1 M NaOH and the solution was maintained at pH 8 for 30 min at room temperature, then extracted with AcOEt. The AcOEt layer was washed with 10% citric acid, 4% $NaHCO_3$, and water. The AcOEt layer was dried over $MgSO_4$, filtered, and evaporated to dryness. The residue was chromatographed on silica gel ($CHCl_3$–MeOH) to give the syrups **5e** and **5f**. **5e**: 2-Monensinamidobutanedioic acid β-benzyl ester, yield: 160 mg (88%). $[\alpha]_D^{23}$: 60.4° ($c=0.3$, $CHCl_3$). FAB-MS: 920 $(M+2Na-H)^+$. IR ν_{max}^{KBr} cm^{-1}: 1735, 1720, 1650. ^{1}H-NMR δ (ppm): 5.13 (1H, br, –NH–CH), 5.13, 5.15 (each 1H, each d, $J=12$ Hz, OCH_2Ph). **5f**: 2-Monensylamidopentanedioic acid γ-benzyl ester, yield: 151 mg (83%). $[\alpha]_D^{23}$: 42.0° ($c=0.3$, $CHCl_3$). FAB-MS: 912 $(M+Na)^+$, 934 $(M+2Na-H)^+$. IR ν_{max}^{KBr} cm^{-1}: 1735, 1720, 1650. ^{1}H-NMR δ (ppm): 4.73 (1H, dd, $J=14$, 8 Hz, NH–CH), 5.10, 5.11 (each 1H, each d, $J=12$ Hz, OCH_2Ph).

The elemental analysis of **5e, f** was carried out on their sodium salts. A solution of **5e, f** (20 mg) in $CHCl_3$ was washed with 4% $NaHCO_3$ in water. The $CHCl_3$ layer was separated, dried over Na_2SO_4, filtered, and evaporated to dryness. The residue was purified by HPLC to give an amorphous power.

Sodium Salt of **5e**: IR ν_{max}^{KBr} cm^{-1}: 1735, 1640, 1590. *Anal.* (%) Calcd for $C_{47}H_{72}NNaO_{14}$: C, 62.86; H, 8.08; N, 1.56. Found: C, 62.57; H, 8.22; N, 1.38.

Sodium Salt of **5f**: IR ν_{max}^{KBr} cm^{-1}: 1735, 1640, 1610. *Anal.* (%) Calcd for $C_{48}H_{74}NNaO_{14}$: C, 63.21; H, 8.18; N, 1.54. Found: C, 63.09; H, 8.40; N, 1.38.

2-Benzyloxycarbonylmethylmonensinamidoacetic Acid-1,29-lactone (6e) and 2-(2-Benzyloxycarbonylethyl)monensinamidoacetic Acid-1,29-lactone (6f) Compounds **5e, f** were cyclized to **6e, f** by the same procedure as described for **3b—d**. The reaction times, the yields, and ^{1}H-NMR data for **6e, f** are summarized in Table I. **6e**: syrup. $[\alpha]_D^{22}$: −7.7 ($c=0.3$, $CHCl_3$). IR ν_{max}^{KBr} cm^{-1}: 1745, 1735, 1670. FAB-MS: 880 (M+Na): **6f**; Syrup. $[\alpha]_D^{22}$: 5.0 ($c=0.3$, $CHCl_3$). IR ν_{max}^{KBr} cm^{-1}: 1740, 1735, 1675. FAB-MS: 894 $(M+Na)^+$.

2-Hydroxycarbonylmethylmonensinamidoacetic Acid-1,29-lactone (3e) and 2-(2-Hydroxycarbonylethyl)monensinamidoacetic Acid-1,29-lactone (3f) Compounds **6e** (96 mg) and **6f** (131 mg) were each hydrogenated in the presence of 5% palladium on charcoal (10 mg) in THF (4 ml) at atmospheric pressure of hydrogen for 30 min. The catalyst was filtered off and the filtrate was evaporated to dryness followed by silica gel chromatography ($CHCl_3$–MeOH) of the residue to give syrups (**3e, f**, respectively). The IR and FAB-MS data and physicochemical data for **3e, f** are summarized in Table V. **3e**: Yield: 85 mg (99%). ^{1}H-NMR δ (ppm): 3.63, 5.00 (each 1H, each d, $J=11$ Hz, CH_2–O–CO). **3f**: yield: 111 mg (95%). ^{1}H-NMR δ (ppm): 3.53, 5.08 (each 1H, each d, $J=11$ Hz, CH_2–O–CO).

The elemental analysis of **3e** (Table V) was performed as the sodium salt, which was prepared by the same procedure as described for the sodium salts of **5e, f**.

Sodium Salt of **3e**: IR ν_{max}^{KBr} cm^{-1}: 1740, 1640, 1595.

***Rm* Values** The *Rm* values were measured by the reported method.[6,11] The MeOH solution of a compound was spotted on precoated TLC plates of Silica gel 60 F_{254} silanized (layer thickness 0.25 mm, Merck no. 5747), and developed with 65, 70, 75, and 80% (w/v) aqueous MeOH solutions. The *Rm* values were calculated from *Rf* values by means of the following equation.

$$Rm = \log(1/Rf - 1)$$

Determination of Ion Transport Activity in a Liquid Membrane The ion transport activity of the lactones (**3**) and monensin (**1**) in a liquid membrane was determined using the W-08 apparatus by essentially the same method as described previously.[12] Two glass cells containing ion-containing water (6 ml, 1 mmol/l, Na^+ : $^{22}Na^+ = 12185:1$) and pure water (6 ml) sandwich the Teflon cell containing sample solution (0.03 mol/l in $CHCl_3$ saturated with water). The aqueous phases were gently stirred at 25 °C. After 10 h, each phase was sampled. The molar amounts of ions in the pure water phase and in the organic solution phase were calculated by using the equations in the previous paper.[12]

Determination of Ion Transport Activity in Erythrocyte Membrane Na^+ ion transport activity in guinea pig erythrocyte membrane was measured by essentially the same method as we have reported, using ^{23}Na-NMR.[6] ^{23}Na-NMR spectra were recorded using a JEOL EX-270 spectrometer at 71.32 MHz and 37 °C. The tube combination (1 mm o.d. tube inside a 5 mm o.d. NMR tube) contained 0.45 ml of guinea pig blood obtained by cardiocentesis, 0.05 ml of 100 mM dysprosium triethylenetetramine hexacetate ($DyTTHA^{3-}$) in water, and 5 μl of 10^{-2} M lactone in DMSO in the annular space. The inner tube contained an external reference (20 mM dysprosium sodium triphosphate, $Na_7Dy(PPPi) \cdot 3NaCl$). The intracellular Na^+ ion concentrations were calculated by using the reported equation.[6]

Acknowledgment We thank Mr. H. Ando, Dr. Y. Hotta, and Prof. K. Takeya of the Department of Pharmacology, Aichi Medical University, for measurement of PIE of **3e** and for providing of the guinea pig blood. This work was supported in part by a Grant-in-Aid for Scientific Research from the Ministry of Education, Science, and Culture of Japan.

References

1) R. W. Taylor, "Polyether Antibiotics: Naturally Occurring Acid Ionophores," Vol. 1, ed. by J. W. Westley, Marcel Dekker, New York, 1982, pp. 104—184.
2) P. W. Reed, "Polyether Antibiotics: Naturally Occurring Acid Ionophores," Vol. 1, ed. by J. W. Westley, Marcel Dekker, New York, 1982, pp. 186—302.
3) M. D. Ruff, "Polyether Antibiotics: Naturally Occurring Acid Ionophores," Vol. 1, ed. by J. W. Westley, Marcel Dekker, New York, 1982, p. 304—314.
4) J. G. Hugtenburg, M. J. Mathy, H. W. G. Boddeke, J. J. Beckeringh, and P. A. van Zweiten, *Naunyn-Schmiedeberg's Arch. Pharmcol.*, **340**, 558 (1989).
5) J. Sakakibara, A. Nakamura, S. Nagai, T. Ueda, and T. Ishida, *Chem. Pharm. Bull.*, **36**, 4776 (1988).
6) A. Nakamura, S. Nagai, T. Ueda, J. Sakakibara, Y. Hotta, and K. Takeya, *Chem. Pharm. Bull.*, **37**, 2330 (1989).
7) K. Suzuki, K. Tohda, H. Sasakura, H. Inoue, K. Tatsuta, and T. Shirai, *J. Chem. Soc., Chem. Commun.*, **1987**, 932.
8) E. J. Corey, K. C. Nicolaou, Lawrence S. Melvin, Jr., *J. Am. Chem. Soc.*, **97**, 653 (1975).
9) J. Fuhrhop and G. Penzlin, "Organic Synthesis: Concepts, Methods, Starting Materials," Verlag Chemie, Weinheim, 1983, pp. 223—238.
10) R. L. Prestidge, D. R. K. Harding, J. E. Battersby, and W. S. Hancock, *J. Org. Chem.*, **40**, 3287 (1975).
11) *a*) G. L. Biagi, M. C. Guerra, and A. M. Barbaro, *J. Med. Chem.*, **13**, 944 (1979); *b*) N. Shirai, J. Sakakibara, **T.** Kaiya, S. Kobayashi, Y. Hotta, and K. Takeya, *ibid.*, **26**, 851 (1983).
12) H. Shibuya, K. Kawashima, M. Sakagami, H. Kawashima, M. Shimomura, K. Ohashi, and I. Kitagawa, *Chem. Pharm. Bull.*, **38**, 2933 (1990).

3-*O*-Alkylascorbic Acids as Free Radical Quenchers. II. Inhibitory Effects on Some Lipid Peroxidation Models

Yasunori NIHRO,[a] Satoshi SOGAWA,[a] Tadamitsu SUDO,[b] Tokutaro MIKI,[b] Hitosi MATSUMOTO,[a] and Toshio SATOH*,[a]

Faculty of Pharmaceutical Sciences, Tokushima Bunri University,[a] Yamashiro-cho, Tokushima 770, Japan and Research and Development Division, Nippon Hypox Laboratories, Inc.,[b] 9420 Nanbu, Nanbu-cho, Minamikoma-gun, Yamanashi 409–22 Japan. *Received November 5, 1990*

We previously found that 3-*O*-dodecylcarbomethylascorbic acid (3-RASA, 3, HX-0112) exhibited a potent inhibitory effect on biochemical lipid peroxidation and that 3-RASA (3) alleviated myocardial lesions induced by ischemia-reperfusion treatment in rats. In this study we examined the mode of action of 3-RASA (3) on the inhibition of lipid peroxidation. There was no reducing activity by 3-RASA (3) (*i.e.*, no oxide was produced) against ferric ions and superoxide anion radicals. The low reducing activity of 3-RASA (3) against a radical as compared to that of α-tocopherol was obtained by using a stable radical. However, 3-RASA (3) had a potent inhibitory effect, almost equal to that of α-tocopherol, in the model of lipid peroxidation dependent on enzymatic superoxide generation. 3-RASA (3) very strongly inhibited the chain-reaction of the peroxidation induced by Fe^{2+}-linoleic acid hydroxyperoxide. On the basis of these findings, it appears that the anti-lipid-peroxidative effects of 3-RASA (3) are due to the inhibition of the radical chain-reaction, as a chain-breaking antioxidant.

Keywords 3-*O*-alkylascorbic acid; 3-*O*-dodecylcarbomethylascorbic acid; 3-*O*-decylascorbic acid; HX-0112; HX-0113; lipid peroxidation; antioxidant; linoleic acid hydroxyperoxide; site specific Fenton reaction; chain-breaking antioxidant

It has recently become clear that active oxygen species (AOS; such as superoxide anion radical, hydroxyl radical, ·OOH *etc.*) and free radicals derived from the biochemical utilization of O_2 and the prooxidant stimulation of O_2 metabolism participate in the development of exacerbation of various kinds of diseases: ischemia-reperfusion disturbances in the brain and heart, rheumatism, inflammation, gastric ulcers, and cancer.[1)]

Although the exact mechanism of lipid peroxidation and the roles of AOS in this biochemical phenomenon are not entirely clear, there have been numerous reports that disturbances of membranes which result in cell damage are derived from AOS-induced lipid peroxidation.[2)] The average level of lipid peroxidant in plasma is higher in some disease cases than in normal cases[3)]; the lipid peroxidation has been suggested to result from excess superoxide anion radical (superoxide) production.[4)]

In fact, unsaturated fatty acids, the constituents of cell membranes, are substantially susceptible to oxidation. Additionally, there is considerable evidence that inhibitors of biochemical lipid peroxidation, such as α-tocopherol (Toc.),[5)] idevenone,[6)] and cyanidanol[7)] have demonstrably valuable pharmacological effects. A thiazolidine derivative, CS-045,[8)] an ascorbic acid derivative, CV-3611,[9)] and ebselene, a selenium compound,[10)] which were developed as new antioxidants, have been studied for the treatment of angiopathy, postischemia-reperfusion disturbance and inflammation, respectively.

We synthesized a novel series of 3-*O*-alkylascorbic acids (3-RASA) in order to develop new antioxidants. We found that 3-*O*-decylascorbic acid (3-RASA (**2**), HX-0113) and 3-*O*-dodecylcarbomethylascorbic acid (3-RASA (**3**), HX-0112) were strong inhibitors of lipid peroxidation in rat liver microsomes.[11)] HX-0112 and HX-0113, which are stable lipophilic ascorbic acid derivatives, alleviated myocardial lesions induced by ischemia-reperfusion treatment in rats.[12)] This paper deals with 3-RASA's mode of antioxidative action, using chemical models of lipid peroxidation. We discuss, especially, whether 3-RASA (**3**) scavenges AOS to participate in biochemical lipid peroxidation or inhibits the radical chain-reaction in linoleic acid peroxidation.

Results

The chemical structures of the various 3-RASA (**1**—**4**) investigated are presented in Fig. 1.

Blois proposed a method for assessing antioxidant activity in which such activity was determined by using a stable radical, α,α-diphenyl-β-picryl hydrazyl (DPPH).[13)] The reducing activity of 3-RASA, ascrobic acid and Toc. was

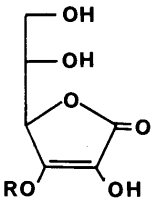

Fig. 1. Chemical Structure of 3-RASA

3-RASA; (**1**) R=CH_3CH_2–, (**2**) R=$CH_3(CH_2)_9$–, (**3**) R=$CH_3(CH_2)_{11}COCH_2$–, (**4**) R=$CH_3(CH_2)_{17}$–.

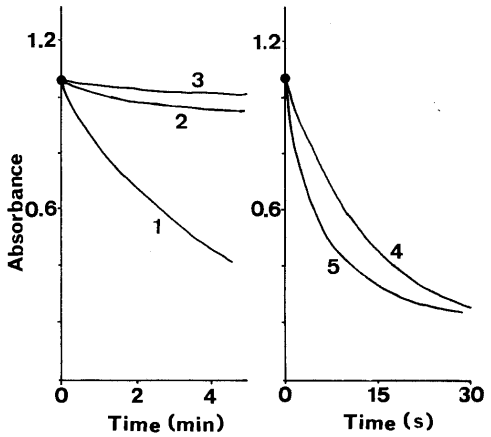

Fig. 2. Reducing Activity against DPPH hydrazyl with 3-RASA and Toc.

1, 3-RASA (**1**); 2, 3-RASA (**2**); 3, 3-RASA (**3**); 4, Toc.; 5, ascorbic acid. DPPH 0.1 mM and equimolar amount of compound exist in EtOH. The decrease of absorption of DPPH is continuously monitored by the absorption change at 517 nm.

determined by using DPPH, which is generally available in laboratories in which electron spin resonance experiments are conducted. The stable free radical was reduced by the test compounds, 3-RASA (**1**—**3**), ascorbic acid, and Toc. (Fig. 2). The reducing activities of 3-RASA (**1**—**3**) against this radical was much lower than that of ascorbic acid and Toc.

The redox potential is a valuable index for the electron donating potency required for a biologically beneficial radical scavenger. 3-RASA required much higher potentials than ascorbic acid in electrode oxidation, but the potentials of 3-RASA were estimated to be lower than those of superoxide/hydrogen peroxide[14] and those of Fe^{3+}/Fe^{2+} (Table I). Our electrochemical results suggest that 3-RASA (**3**) must be oxidized by superoxide and Fe^{3+}; however, a strong reducing agent has sometimes acted on the prooxidant and stimulated lipid peroxidation. For instance, a transition metal and ascorbic acid at a low concentration synergistically stimulate nonenzymic induced lipid peroxidation.[15] The reducing activity of ascorbic acid, Toc., and 3-RASA against Fe^{3+} was examined. Ascorbic acid and Toc. reduced against Fe^{3+} immediately, but 3-RASA could not reduce against Fe^{3+} (Table I). However, 3-RASA (**1**, **2**), but not 3-RASA (**4**) which bears an octadecyl group, demonstrated reducing activity against Fe^{3+} after the addition of *o*-phenanthroline (Table I).

TABLE I. Redox Potential of 3-RASA and Reducing Activity against Fe^{3+}: *o*-Phenanthroline

Compound	Redox potential[a] (mV)	Reducing Fe^{3+} (%)[b]	
		$FeCl_3$ alone	$FeCl_3$ + *o*-phenanthroline
3-RASA (**1**)	305	0	39
3-RASA (**2**)	300	0	32
3-RASA (**3**)	380	0	12
3-RASA (**4**)	—	0	3
Toc.	—	83	83
Ascorbic acid	210	87	87

a) The redox potentials are determined by differential pulse voltammetry; an Ag/AgCl reference electrode and a glassy carbon working electrode are used, voltammetric analysis is conducted in 0.01 M phosphate buffer at pH 7.4. *b*) The compound exsists at the molar ratio of 2.1 parts of Fe^{3+}.

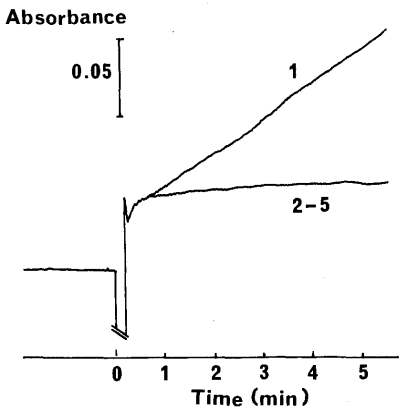

Fig. 3. Effect of 3-RASA and Toc. on XO-Dependent Peroxidation of Detergent-Dispended Linoleate

1, control; 2, (−)-EDTA-Fe^{3+}; 3, SOD (10 g/ml); 4, α-Toc (10 μM); 5, 3-RASA (**2**) (50 μM). The micelle solution of linoleate is made by sodium linoleate (5.7 mM) with XO (6.6 munits/ml), Lubrol (1%), CH_3CHO (35 mM), and EDTA–Fe^{3+} (0.11 mM EDTA, 0.1 mM $FeCl_3$) in 30 mM NaCl, pH 7.5. Diene conjugation during lipid peroxidation is continuously monitored at 234 nm.

The effects of 3-RASA (**1**—**4**) and Toc. on the lipid peroxidation of linoleic acid (LA), which is dependent on enzymatic superoxide generation, were also studied. The addition of ethylenediaminetetraacetic acid (EDTA)–Fe^{3+} to the xanthine oxidase (XO)-system resulted in the lipid peroxidation of LA, although no activity was observed in the absence of iron (Fig. 3). The effects of 3-RASA (**1**—**4**), Toc., superoxide dismutase (SOD), and catalase on the lipid peroxidation of the system are shown in Table II. Our results agreed with Tien's data[16] which showed that the addition of iron as an EDTA-chelate was necessary for XO-dependent peroxidation (XO-peroxidation); and further, indicated that SOD had an almost complete inhibiting effect and that catalase had a partially inhibiting effect. It appeared that 3-RASA (**1**—**4**) and Toc., at the molar ratio of 1 : 100 parts of LA, almost completely inhibited XO-peroxidation. Mannitol, at the molar ratio of about 2 : 1 parts of LA, resulted in partial inhibition of activity; 3-RASA (**2**) and Toc., which are more lipophilic compounds than 3-RASA (**1**), were capable of inhibiting activity at the molar ratio of $1/5 \times 10^3$ to LA. It is clear, as with the inhibitory effect of SOD, that XO-peroxidation is dependent on the generation of superoxide.

We assessed the effects of 3-RASA (**2**, **3**) on the XO superoxide generation system by continuous monitoring of the reduction against Fe^{3+}-cytochrome c. 3-RASA (**2**, **3**) did not affect the generating speed and level of superoxide; the ultraviolet (UV) spectra of 3-RASA (**2**, **3**) were not changed under these conditions (data not shown).

The effects of 3-RASA (**2**, **3**) and Toc. on the site-specific induction of lipid peroxidation by iron in charged micelles were studied according to the method of Fukuzawa.[17] At pH 3.5 both Fe^{2+} and H_2O_2 were necessary to induce lipid peroxidation in the positively charged tetradecyltrimethylammonium bromide (TTAB) micelles, in spite of the linoleic acid hydroperoxide (LOOH) which was present in LA. However, at pH 7, peroxidation of LA was induced by the addition of Fe^{2+} alone (Fig. 4). The Fe^{2+}-induced

TABLE II. Inhibitory Effect of Various Scavengers and Antioxidants on XO-Dependent Peroxidation of Dispersed Linoleate

Addition		ΔA_{234} (nm/min)	Inhibition (%)
None		0.029±0.002	—
3-RASA (**1**)	50 μM	<0.002	>93
	10 μM	0.022±0.003	24
3-RASA (**2**)	50 μM	<0.002	>93
	10 μM	0.011±0.002	62
	1 μM	0.023±0.026	20
3-RASA (**3**)	50 μM	<0.002	>93
	10 μM	0.013±0.002	55
3-RASA (**4**)	50 μM	<0.002	>93
	10 μM	0.017±0.003	41
Toc.	50 μM	<0.002	>93
	10 μM	<0.002	>93
	1 μM	0.011±0.003	62
SOD	10 μg/ml	<0.002	>93
Mannitol	10 mM	0.024±0.004	18
Catalase	10 μg/ml	0.017±0.005	41

The micelle solution of linoleate is made by sodium linoleate (5.7 mM) with XO (6.6 munits/ml). Lubrol (1%), CH_3CHO (35 mM), and EDTA–Fe^{3+} (0.11 mM EDTA, 0.1 mM $FeCl_3$) in 30 mM NaCl, pH 7.5. The rate of diene conjugation is lined up to approximately 4 min, after which a decrease in rate is observed. The rate is determined from the initial velocity of the reaction (mean±S.D., $n=5$).

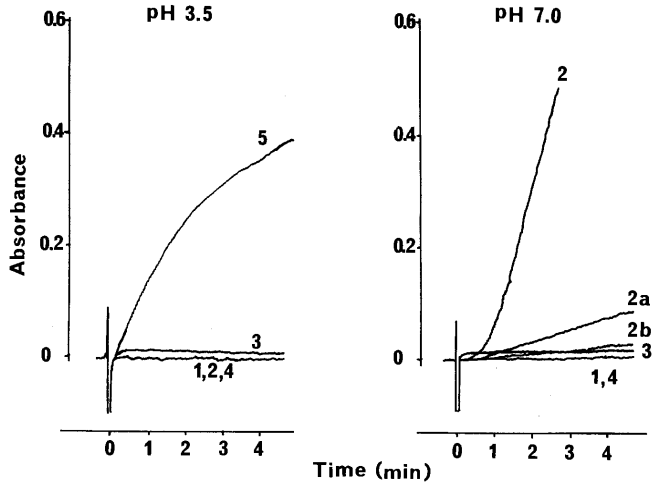

Fig. 4. Lipid Peroxidation of LA in TTAB Micelles

1, H_2O_2; 2, Fe^{2+}; 3, Fe^{3+}; 4, TPP+Fe^{2+}; 5, H_2O_2+Fe^{2+}, 2a, Fe^{2+}+3-RASA (**2**), 10 μM; 2b, Fe^{2+}+3-RASA (**2**), 50 μM. The reaction mixture contains LA (5 mM) with H_2O_2 (100 μM), $FeCl_3$ (20 μM), $FeSO_4$ (20 μM), and TPP (80 μM), in 50 mM TTAB micelle. Diene conjugation during lipid peroxidation is continuously monitored at 234 nm.

TABLE III. Inhibitory Effect of Ascorbic Acid Derivatives and Toc. on Lipid Peroxidation by Fe^{2+} in TTAB Micelles

Compound		Rate ΔA_{234} (nm/min)	Inhibition (%)
Control		0.263±0.020	—
3-RASA (**2**)	50 μM	0.025±0.005	90
	10 μM	0.040±0.015	84
3-RASA (**3**)	10 μM	0.027±0.005	90
Toc.	50 μM	0.013±0.001	95
	10 μM	0.025±0.005	90
EDTA	10 μM	0.039±0.024	84
TPP	80 μM	>0.002	100

The reaction mixture contains LA (5 mM) with $FeSO_4$ (20 μM) in 50 mM TTAB micelle at pH 7. The rate of diene conjugation is lined up to approximately 4 min, after which a decrease in rate is observed. The rate is determined from the initial velocity of the reaction (mean±S.D., $n=5$).

peroxidation at pH 7 was not observed using Fe^{3+} and triphenylphosphine (TPP) pretreatment to reduce against LOOH. The peroxidation was partially inhibited by EDTA at 1/2 molar ratio to Fe^{2+}, and it was completely inhibited by TPP at a molar ratio of almost 1:1 to LOOH (Table III). The peroxidation was strongly inhibited by 3-RASA (**2**, **3**) and Toc. at a molar ratio to LA of 1/500 and a molar ratio to LOOH of 1/7.

Discussion

We synthesized various novel antioxidants and selected 3-RASA (**2**, HX-0113) and 3-RASA (**3**, HX-0112) for further clinical testing. We determined their inhibitory effects of lipid peroxidation in rat liver microsomes and their stability against autooxidation in aqueous solution.[11] In this paper, we attempt to clarify 3-RASA's mode of action as an antioxidant. This attempt has been a significant addition to understanding the pharmacological effects of the inhibition of lipid peroxidation.

However, the reactive form(s) of AOS involved in superoxide-dependent lipid peroxidation has not been unequivocally established. Certainly there is much evidence of superoxide generation during many biological reaction.[18] Although superoxide itself is relatively unreactive, the hydroxyl radical is a very highly reactive AOS toward many compounds, including polyunsaturated fatty acids.[19] However, the hydroxyl radical is too short-lived in living organisms and thus it cannot reach the membrane from a distant place in extracelluluar fluid.[20]

Samuni *et al.* suggested a site-specific Fenton mechanism in which the binding of a transition metal ion to the biological target is a prerequisite for the production of hydroxyl radical-mediated cell damage.[21] The hydroxyl radical is probably derived from the superoxide as follows[22]:

$$O_2^- + Fe^{3+} \rightarrow O_2 + Fe^{2+} \quad (1)$$

$$2O_2^- + 2H^+ \rightarrow O_2 + H_2O_2 \quad (2)$$

$$Fe^{2+} + H_2O_2 \rightarrow Fe^{3+} + \cdot OH + OH^- \quad (3)$$

Recently, Fukuzawa *et al.* demonstrated lipid peroxidation induced by a site-specific Fenton mechanism in charged micelles.[23]

On this fairly reasonable hypothesis, we experimented with 3-RASA to find out the reactivity toward superoxide, the hydroxyl radical, and Fe^{3+}. No reactivity of 3-RASA was observed against superoxide and Fe^{3+}, in spite of 3-RASA's having a redox-potential suitable for oxidation with these entities. Only after the addition of *o*-phenanthroline was 3-RASA (**1**) capable of reducing activity against Fe^{3+}. The reducing ability of 3-RASA toward the Fe^{3+}: *o*-phenanthroline complex was inhibited by the steric hindrance of a long alkyl group. The shielding of the hydroxyl group of 3-RASA from Fe^{3+} is attributable to 3-RASA's long alkyl chain. The oxidation of 3-RASA with the hydroxyl radical was reported by Cabelli *et al.*[24] However, it is too difficult to make an exact comparison of the reactivity of an antioxidant with the hydroxyl radical because of the high reactivity of hydroxyl radical. We chose the stable radical (DPPH),[13] which Blois proposed as an assay for the antioxidant. 3-RASA obviously had less raducing activity against DPPH than did Toc., a typical inhibitor[25] of lipid peroxidation. The low reducing activity and the high redox potential of 3-RASA were in conflict with its potent inhibitory effect on lipid peroxidation. In other words, based on our data, 3-RASA will be characterized as a stable antioxidant.

While many organic compounds which have reducing activity, except for transition metal complexes,[26] are hardly oxidized or only slowly oxidized in aqueous solution by superoxide,[19a] 3-RASA was not oxidized in the enzymatic generation of superoxide, although it demonstrated complete inhibition toward lipid peroxidation dependent on superoxide generation. The XO-dependent peroxidation which became necessary with the addition of EDTA–Fe^{3+} might occur via the hydroxyl radical[16] (see. Eqs 1—3).

The 3-RASA, which bear a long alkyl chain, and Toc. showed potent inhibitory effects, but mannitol and 3-RASA (**1**), which bear an ethyl group, are lower in activity than the lipophilic hydroxyl-radical scavengers on XO-dependent perioxidation. SOD was also an effective protectant for the oxidation, but catalase did not lead to complete inhibition. The fact that SOD exists in the enzymatic superoxide generation area (outside the micelles) and that it is efficiently able to dismute superoxide,[27] and the fact that catalase is sensitive to superoxide,[28] account for this phenomenon [see the following section for further details]. On the basis of

our results, it is suggested that lipid peroxidation occurring from the site-specific Fenton reaction cannot be effectively inhibited by a hydrophilic antioxidant. In fact, the antioxidant efficiency of 3-RASA was influenced by its hydrophobic action on lipid peroxidation in rat liver microsomes.[11] 3-RASA, bearing a long alkyl chain, would be located in the lipid layer and might react as an antioxidant. Our hypothesis is also supported by the fact that the inhibitory effect of 3-RASA (**1**), which bears an ethyl group, was lower than that of 3-RASA (**2**), which bears a decyl group, on XO-dependent peroxidation.

It was reported that the antioxidant efficiency of Toc. in liposomes depends on its ability to react mainly with the chain-initiating and chain-propagating lipid radicals.[29] On the basis of these findings, since the mode of antilipid peroxidative action of the lipophilic 3-RASA (**2, 3**) is thought to be similar to that of Toc., the effects of 3-RASA on the lipid peroxidation model which involved site-specific chain-initiating lipid radicals, not initiated by AOS, were studied. The Fe^{2+}-LOOH-initiated peroxidation, which is a minor modification of the lipid peroxidation induced in TTAB micelles by site-specific Fenton reaction,[23] was suitable for our purpose. In this peroxidation, because of the results obtained from TPP treatment and the addition of Fe^{3+}, induction is clear, as shown in the following equations:

$$LOOH + Fe^{2+} \rightarrow LO\cdot + OH^- + Fe^{3+} \quad (4)$$

$$LO\cdot + LH \rightarrow LOH + L\cdot \quad (5)$$

The potent inhibitory effects of 3-RASA (**2, 3**) and Toc. on Fe^{2+}-LOOH-induced peroxidation are obviously due to reaction with the lipid radical (s) derived from LOOH. These lipid radicals, like the hydroxyl radical, show very high reactivity. These finding resolved the previous conflict, between the low reducing activity of 3-RASA (**2, 3**) and the potent inhibitory effects of these compounds on lipid peroxidation models. That is, the coflict probably involves the difference in chemical reactivity between DPPH as a radical and the lipid radicals. Since lipid peroxidation consists of high reactive chain-reactions, the difference in chemical reducing activity between Toc. and 3-RASA against low potential radicals, DPPH, will be compensated for by the high reactivity of lipid radicals, or may be compensated for by the negligible levels of each. Of course, this consideration is based on the localization of 3-RASA, like Toc.,[30] in the lipid layer as a site for the radical chain-reaction. Additionally, 3-RASA would be expressed in scavenging activity for same considerably reactive AOS (such as $^1O_2$,[31] oxygen and iron complex[32]), but this scavenging activity against remarkably reactive AOS, which is generated only at a distant place from the membrane, may not be very important as a protectant of the biomembranes. On the basis of these findings, it appears that the potent antioxidative effects of 3-RASA (**2, 3**) on biochemical lipid peroxidation are not due to scavenging activity for AOS which participates in the peroxidation, XO-dependent lipid peroxidation, but that 3-RASA (**2, 3**) inhibit the radical chain-reaction in linoleic acid peroxidation as a chain-breaking antioxidant.

Materials and Methods

Materials TTAB, bovine erythrocyte SOD (2900 units/mg protein), cytochrome c, beef liver catalase (30000 units/mg protein purified by redialysis before use) and XO (purified by redialysis before use) were purchased from the Sigma Chemical Co., St. Louis. LA, TPP, DPPH, Toc., and mannitol were obtained from Wako Pure Chemical Industries, Osaka. Lubrol was from Nakarai Tesque, Kyoto. 3-*O*-Ethylascorbic acid (3-RASA (**1**)), 3-RASA (**2**), 3-RASA (**3**), and 3-*O*-octadecylascorbic acid (3-RASA (**4**)) were synthesized by the method outlined in the provious paper.[11] All buffer and reagent solutions were passed through Chelex 100 (Bio-Rad Laboratories) ion-exchange resin to free them of contaminants.

Determination of the Reducting Activity of the Stable Radical DPPH[13] The test compound, in 40 μl dimethylformamide (DMF) (1×10^{-2} M), was added to a solution of a stable radical, DPPH, in 4 ml EtOH (1×10^{-4} M). The decrease of absorption during the reduction of DPPH was continuously monitored at 517 nm.

Determination of 3-RASA Redox Potentials Voltammetric analysis was conducted in 0.01 M phosphate buffer, at pH 7.4, which was degassed with argon before use. An Ag/AgCl reference electrode, a glassy carbon working electrode (3 mm i.d.), and a Pt counter electrode (0.05 mm i.d. × 2 cm) were used (BSA systems). The redox potentials were determined by using a BSA 100A electrochemical analyzer to obtain the peak potential in the voltammograms by using the differential pulse voltametry mode. The experimental conditions were: initial E (mV) = −100, final E (mV) = 500, V (mV/s) = 4, pulse amplitude (mV) = 50, pulse width (ms) = 60, pulse ratio (ms) = 1000. Test compound solutions were added to the buffer (final conc. 0.05 mM, final conc. of MeOH 5%). Electrochemical reversibility was assessed by analyzing the reversed differential pulse voltammograms (initial E (mV) = 500, final E (mV) = −100).

Measurement of Ferrous Ion Concentration[33] $FeCl_3$ 5 mM dissolved in 1 N-HCl was prepared for Fe^{3+} stock solution before use. The test sample was dissolved in MeOH. Reaction mixtures contained 0.5 mM $FeCl_3$ and 1 mM test compound in MeOH, which were mixed for 30 s and allowed to stand at room temperature for 3 min. The absorption of the solution was measured at 362 nm to assess the reduction of Fe^{3+}. In separate experiments, reaction mixtures contained 0.05 mM $FeCl_3$, 0.1 mM test compound, and 0.13 mM *o*-phenanthroline in MeOH : 2.5 M acetate buffer at pH 4.2 (9 : 1). The reaction was initiated by the addition of $FeCl_3$, and the production of Fe^{2+} for 25 min was monitored by measuring the absorbance at 510 nm.

XO-Dependent Peroxidation in Linoleate Dispersed Solution[15] Linoleate stock solution was made by suspending linoleic acid (100 mg) in N_2-purged Chelexed water and adding 5—10 drops of 6 N-NaOH to yield a clear solution. The pH of this solution was then slowly lowered to 7.5 by the addition of 6 N-HCl. The micelle solution of linoleate was made by incubating sodium linoleate (5.7 mM) with XO (6.6 munits/ml), Lubrol (1%), 35 mM CH_3CHO, and EDTA–Fe^{3+} (0.11 mM EDTA, 0.1 mM $FeCl_3$) in 30 mM NaCl, pH 7.5, at 20—22 °C, under air. Reactions were initiated by the addition of XO; the test sample solutions (1%; 3-RASA dissolved in DMF) were added before the addition of the enzyme. Diene conjugation during lipid peroxidation was continuously monitored at 234 nm.[33] The rate of diene conjugation was lined up to approximately 4 min, after which a decrease in rate was observed. All rates were determined from the initial velocity of the reaction.

Measurement of Enzymatic Superoxide Generation[27] Reaction mixtures contained 0.1 mM EDTA, 200 units/ml catalase, 80 μM cytochrome c, 35 mM CH_3CHO, and XO (6.6 munits/ml) in Chelexed 50 mM potassium phosphate buffer, pH 7.5, at 20—22 °C. The reduction of cytochrome c during the generation of superoxide was continuously monitored at 550 nm. The test sample was dissolved in DMF, and the DMF solution (1%, v/v) was added to the reaction mixture. Reactions were initiated by the addition of XO.

Iron-Induced Lipid Peroxidation in TTAB Micelles[23] LA micellar solutions were prepared as follows: The interior base of the apparatus was filmed with LA 25 μM (and test sample) by evaporation of the solvent. Five ml of TTAB 50 mM solution was added to the film, followed by vortexing and sonication in a Sanyo sonic bath. The pH was adjusted by adding 5% acetic acid and 5% $NaHCO_3$. Any LOOH present in LA was reduced by treatment with TPP in chloroform solution[34] before the preparation of micelles. Reactions were initiated by the addition of iron. The peroxidation was monitored as described in the XO-dependent peroxidation section. The LOOH content of LA was determined iodometrically.[35]

References

1) J. M. McCord, *Advance in Free Radical Biology and Medicine*, **2**, 325 (1986); B. Halliwell and J. M. C. Gutteridge, *Biochem. J.*, **222**, 1

(1984).
2) "Medical, Biochemical and Chemical Aspects of Free Radicals," Vol. 1, ed. by O. Hayaishi, E. Niki, M. Kondow, and T. Yoshikawa, Elsevier, Amsterdam, 1989.
3) K. Yagi, "Lipid Peroxidation in Biology and Medicine," Academic Press, New York and London, 1982.
4) J. Goodmann and P. Hochstein, *Biochem. Biophys. Res. Commun.*, **77**, 797 (1977).
5) D. D. Pyke and A. C. Chan, *Arch. Biochem. Biophys.*, **277**, 429 (1990).
6) M. Suno and A. Nakagawa, *Biochem. Biophys. Res. Commun.*, **125**, 1046 (1984).
7) L. A. Videla, C. G. Fraga, O. R. Koch, and A. Boveris, *Biochem. Pharmacol.*, **32**, 2822 (1983).
8) T. Yoshioka, T. Fujita, T. Kanai, Y. Aizawa, T. Kurumada, K. Hasegawa, and H. Horikoshi, *J. Med. Chem.*, **32**, 421 (1989).
9) K. Kato, S. Terao, N. Shimamoto, and M. Hirata, *J. Med. Chem.*, **31**, 793 (1988).
10) A. Muller, E. Cadenas, P. Graf, and H. Sies, *Biochem. Pharmacol.*, **33**, 3252 (1984).
11) Y. Nihro, H. Miyataka, T. Sudo, H. Matsumoto, and T. Satoh, Abstract of Papers, The 109th Annual Meeting of the Pharmaceutical Society of Japan, Nagoya, April 1989, p. 21. (*J. Med. Chem.*, in press, 1991).
12) A. Sasamori, A. Izumi, T. Sudo, T. Miki, Y. Nihro, H. Matsumoto, and T. Satoh, Abstract of Papers, Annual Meeting of the Pharmaceutical Society of Japan, Sapporo, 1990, p. 266. (to be submitted to *J. Med. Chem.*).
13) M. S. Blois, *Nature* (London), **181**, 1199 (1958).
14) K. Sugioka, H. Nakano, M. Nakano, S. Kubota, and Y. Ikegami, *Biocihm. Biophys. Acta*, **753**, 411 (1983).
15) D. M. Miller and S. D. Aust, *Arch. Biochem. Biophys.*, **271**, 113 (1989).
16) M. Tien, B. A. Svingen, and S. D. Aust, *Arch. Biochem. Biophys.*, **216**, 142 (1982).
17) K. Fukuzawa, T. Tadokoro, K. Kishikawa, K. Mukai, and J. M. Gebicki, *Arch. Biochem. Biophys.*, **260**, 146 (1988).
18) I. Fridovich, *Annu. Rev. Pharmacol. Toxicol.*, **23**, 239 (1983).
19) *a*) B. Halliwelll and J. M. C. Gutteridge, *Arch. Biochem. Biophys.*, **246**, 501 (1986); *b*) I. Fridovich, *ibid.*, **247**, 1 (1986).
20) K. Kobayashi, *Tampakushitsu Kakusan Koso*, **33**, 2678 (1988).
21) A. Samui, J. Aronovitch, D. Godinger, M. Chevion, and G. Czapski, *Eur. J. Biochem.*, **137**, 119 (1983).
22) B. Halliwell and J. M. C. Gutteride, *Arch. Biochem. Biophys.*, **260**, 146 (1988).
23) K. Fukuzawa, T. Tadokoro, K. Kishikawa, K. Mukai, and J. M. Gebicki, *Arch. Biochem. Biophys.*, **260**, 146 (1988).
24) D. E. Cabelli and B. H. J. Bielski, *Radiat. Phys. Chem.*, **23**, 419 (1984).
25) G. W. Burron and K. U. Ingold, *Ann. N. Y. Acad. Sci.*, **570**, 7 (1989).
26) S. Kubota and J. T. Yang, *Porc. Natl. Acad. Sci. U.S.A.*, **81**, 3283 (1984).
27) J. M. McCord and I. Fridovich, *J. Biol. Chem.*, **242**, 6049 (1969).
28) Y. Kono and I. Fridovich, *J. Biol. Chem.*, **257**, 5751 (1982).
29) E. Niki, A. Kawakami, M. Saito, J. Tuchiya and Y. Kamiya, *J. Biol. Chem.*, **260**, 2191 (1985); K. Fukuzawa, H. Chida, A. Tokumura, and H. Takatani, *Arch. Biochem. Biophys.*, **206**, 173 (1981).
30) S. L. Taylor, M. P. Lamden, and A. L. Tappel, *Lipids*, **11**, 530 (1976).
31) E. W. Kellogg and I. Fridovich, *J. Biol. Chem.*, **250**, 8812 (1975).
32) S. D. Aust, L. A. Morehouse, and L. A. Thomas, *J. Free Radical Biol. Med.*, **1**, 3 (1985).
33) "Standard Method of Analysis for Hygienic Chemists with Commentary," Pharmaceutical Society of Japan, Kanehara Press, Tokyo, 1980, p. 58.
34) R. Hiat and C. McColeman, *Can. J. Biochem.*, **49**, 1712 (1971).
35) J. A. Buege and S. D. Aust, "Methods in Enzymology," eds. by S. Fleischer and L. Parker, Vol. 52, Part C, Academic Press, New York, 1978, pp. 302—310.

Quantitative Structure–Activity Relationship of Catechol Derivatives Inhibiting 5-Lipoxygenase

Youichiro NAITO,[a,b] Masanori SUGIURA,[a] Yasunari YAMAURA,[a] Chikara FUKAYA,*[,a] Kazumasa YOKOYAMA,[a] Yoshiaki NAKAGAWA,[b] Tokuji IKEDA,[b] Mitsugi SENDA,[b] and Toshio FUJITA[b]

Central Research Laboratories, Green Cross Corporation,[a] Shodaiohtani, Hirakata, Osaka 573, Japan and Department of Agricultural Chemistry, Faculty of Agriculture, Kyoto University,[b] Sakyo-ku, Kyoto 606, Japan. *Received December 12, 1990*

Various catechol derivatives (β-substituted 3,4-dihydroxystyrenes, 1-substituted 3,4-dihydroxybenzenes, and 6-substituted 2,3-dihydroxynaphthalenes) were synthesized and their inhibition of 5-lipoxygenase was assayed. Their structure–activity relationships were examined quantitatively with substituent and structural parameters and regression analysis. The variations in the inhibitory activity were explained in bilinear hydrophobic parameter (log *P*) terms, and steric (molecular thickness) and electronic (proton nuclear magnetic resonance (^{1}H-NMR) chemical shift of the proton adjacent to the catechol group) parameter terms. The hydrophobicity of the inhibitor molecule was important, and the optimum value of log *P* was about 4.3—4.6, beyond which inhibition did not increase further. A lower electron density of the aromatic ring containing the catechol group and the greater thickness of the lipophilic side chains were unfavorable to the activity. The results added a physicochemical basis for the selection of candidate compounds for developmental studies.

Keywords quantitative structure–activity relationship; Kubinyi's Bilinear-model; Hansch–Fujita analysis; 5-lipoxygenase; 5-lipoxygenase inhibition; 1-(3,4-dihydroxyphenyl)-1-octen-3-one; caffeic acid octyl amide

Arachidonate 5-lipoxygenase is a key enzyme in the biosynthesis of leukotrienes, which seem to be related to many diseases such as allergic asthma,[1] psoriasis,[2] and myocardial infraction.[3] Therefore, potent inhibitors of this enzyme are candidate drugs for the treatment of these diseases.

Caffeic acid and its methyl ester are potent inhibitors of 5-lipoxygenase.[4] We have studied[5] the structure–activity relationships of 3,4-dihydroxystyrenes modified by various substituents at the β-position (series I; see Chart 1). Hoping to understand the physicochemical background of the structural effects of the side chains as well as the ring systems on the inhibition, we synthesized a number of 1-substituted 3,4-dihydroxybenzenes (series II) and 6-substituted 2,3-dihydroxynaphthalenes (series III) with various substituents and measured their inhibition of 5-lipoxygenase (Table I). Together with the results for the previously reported 3,4-dihydroxystyrenes, the structure–activity relationships were examined quantitatively with their substituent and structural parameters and by regression analysis.

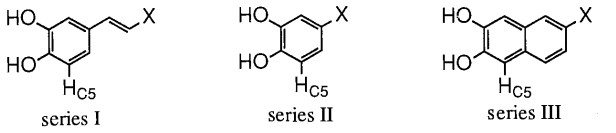

Chart 1

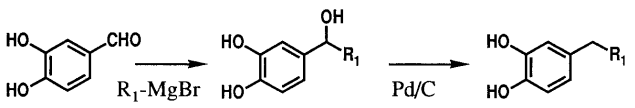

Chart 2

Synthesis

Some of the series I compounds (**3**, **5**, **6**, and **12**—**18**) were newly synthesized by a reported procedure.[5] Compounds **26**—**28** of series II were prepared similarly to compounds **7**—**11**.[5]

The 4-alkyl-1,2-dihydroxybenzene derivatives **32**—**34** were obtained by catalytic hydrogenation (palladium on carbon: Pd/C) of the corresponding benzylalcohols, **29**—**31**, which were prepared by the Grignard reaction of protocatechualdehyde (Chart 2). 4-Alkoxycatechols were prepared as shown in Chart 3. Baeyer–Villiger oxidation of the dibenzyl ether of protocatechualdehyde, **35**, with 3-chloroperoxybenzoic acid (*m*-CPBA) followed by hydrolysis with 3 N NaOH gave phenol **36**. The phenol was alkylated with alkyl bromide followed by debenzylation with Pd/C to yield 4-alkoxycatechols (**37**, **38**). The β-phenoxyacrylamides

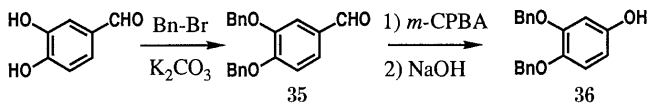

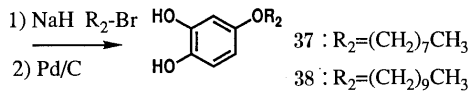

Chart 3

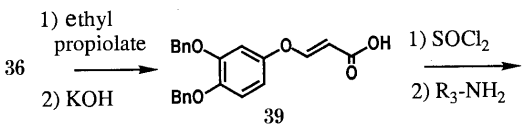

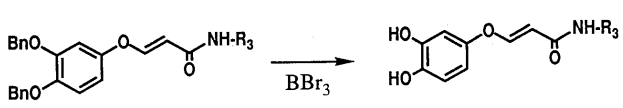

Chart 4

TABLE I. Physicochemical and Biological Data of the Compounds of Series I, II, and III

No.	Substituents X	mp (°C)[a]	Recrystn solvent[b]	Formula	Analysis (%) Calcd (Found) C	H	N	I_{50}[c] (M)
Series I								
1	$CO_2CH_2CH_3$	142—143	A	$C_{11}H_{12}O_4$	63.45 (63.36	5.81 5.77)		1.65×10^{-7}
2	$CO_2(CH_2)_3CH_3$	111—111.5	B	$C_{13}H_{16}O_4$	66.09 (65.94	6.83 6.84)		6.70×10^{-8}
3	$CO_2(CH_2)_4CH_3$	125—127	B	$C_{14}H_{18}O_4$		250.1204[d] (250.1219)		7.70×10^{-8}
4	$CO_2(CH_2)_8CH_3$	107—108	B	$C_{18}H_{26}O_4$	70.56 (70.41	8.55 8.76)		1.88×10^{-7}
5	$CONHCH_2CH_3$	Amorph.		$C_{11}H_{13}NO_3$		208.0972 (208.0968)		1.50×10^{-6}
6	$CONH(CH_2)_3CH_3$	Amorph.		$C_{13}H_{17}NO_3$		236.1286 (236.1306)		7.00×10^{-7}
7	$CONH(CH_2)_5CH_3$	141—143	A	$C_{15}H_{21}NO_3$	68.42 (68.34	8.04 8.07	5.32 5.22)	1.30×10^{-7}
8	$CONH(CH_2)_7CH_3$	126—128.5	A	$C_{17}H_{25}NO_3$	70.07 (70.10	8.65 8.92	4.81 5.08)	4.20×10^{-8}
9	$CONH(CH_2)_9CH_3$	Amorph.		$C_{19}H_{29}NO_3$		320.2224 (320.2222)		4.50×10^{-8}
10	$CONH(CH_2)_{11}CH_3$	124—125	A	$C_{21}H_{33}NO_3$		348.2536 (348.2534)		6.50×10^{-8}
11	$CONH(CH_2)_{13}CH_3$	119—120	A	$C_{23}H_{37}NO_3$		375.2712 (375.2792)		1.55×10^{-7}
12	$CONHCH_2Ph$	164—167	A	$C_{16}H_{15}NO_3$		270.1130 (270.1160)		1.15×10^{-7}
13	$CONH(CH_2)_2Ph$	157—159	A	$C_{17}H_{17}NO_3$	72.07 (72.30	6.05 6.19	4.94 4.78)	1.50×10^{-7}
14	CONHPh(4-butyl)	204—205.5	A	$C_{19}H_{21}NO_3$		312.1598 (312.1561)		8.10×10^{-8}
15	CONHPh(4-octyl)	173.5—175	A	$C_{23}H_{29}NO_3$		368.2224 (368.2180)		8.40×10^{-8}
16	CONHPh(3,4-OCH_3)	201—202	C	$C_{17}H_{17}NO_5$	64.75 (64.46	5.43 5.41	4.44 4.35)	1.20×10^{-7}
17	$CONHCH_2$Ph(3,4-OCH_3)	203—206	A	$C_{18}H_{19}NO_5$	65.64 (65.43	5.81 5.92	4.25 4.03)	1.70×10^{-7}
18	$CONH(CH_2)_2$Ph(3,4-OCH_3)	97—99	A	$C_{19}H_{20}NO_5$		344.1496 (344.1456)		2.60×10^{-7}
19	$CO(CH_2)_2CH_3$	131—132	D	$C_{12}H_{14}O_3$	69.89 (69.62	6.84 6.89)		2.75×10^{-7}
20	$CO(CH_2)_4CH_3$	130—131	D	$C_{14}H_{18}O_3$	71.77 (71.71	7.74 7.81)		3.50×10^{-8}
21	$CO(CH_2)_6CH_3$	115—116.5	D	$C_{16}H_{22}O_3$	73.25 (72.96	8.45 8.62)		5.80×10^{-8}
22	$CO(CH_2)_5OH$	Amorph.		$C_{14}H_{18}O_4$	67.18 (67.06	7.25 7.13)		5.95×10^{-7}
23	CH_2CH_3[e]	Liquid		$C_{10}H_{12}O_2$		165.0915 (165.0950)		9.50×10^{-8}
24	$(CH_2)_3CH_3$[e]	Liquid		$C_{12}H_{16}O_2$		193.1227 (193.1195)		1.20×10^{-8}
25	$(CH_2)_5CH_3$[e]	Liquid		$C_{14}H_{20}O_2$		221.1540 (221.1524)		1.50×10^{-8}
Series II								
26	$CONH(CH_2)_5CH_3$	139—140	E	$C_{13}H_{19}NO_3$	65.80 (65.52	8.07 8.21	5.90 5.89)	4.00×10^{-7}
27	$CONH(CH_2)_9CH_3$	129.5—130	A	$C_{17}H_{27}NO_3$	69.59 (69.61	9.28 9.25	4.77 4.69)	1.80×10^{-7}
28	$CONH(CH_2)_{11}CH_3$	119.5—120	E	$C_{19}H_{31}NO_3$	70.99 (70.80	9.72 9.74	4.36 4.35)	4.50×10^{-7}
29	$CH(OH)(CH_2)_2CH_3$	137—139	A	$C_{10}H_{14}O_3$	65.92 (65.88	7.74 7.75)		1.80×10^{-6}
30	$CH(OH)(CH_2)_4CH_3$	108—110	A	$C_{12}H_{18}O_3$	68.55 (68.44	8.63 8.68)		1.20×10^{-6}
31	$CH(OH)(CH_2)_6CH_3$	120—122.5	A	$C_{14}H_{22}O_3$	70.56 (70.46	9.30 9.56)		3.20×10^{-7}

TABLE I. (continued)

No.	Substituents X	mp (°C)[a]	Recrystn solvent[b]	Formula	Analysis (%) Calcd (Found) C	H	N	I_{50}[c] (M)
32	$(CH_2)_3CH_3$	Amorph.		$C_{10}H_{14}O_2$	72.26 (72.23	8.49 8.60)		6.30×10^{-7}
33	$(CH_2)_5CH_3$	Amorph.		$C_{12}H_{18}O_2$	74.19 (73.90	9.34 9.07)		2.50×10^{-7}
34	$(CH_2)_7CH_3$	60—61	F	$C_{14}H_{22}O_2$	75.63 (75.40	9.97 10.23)		1.90×10^{-7}
37	$O(CH_2)_7CH_3$	108—109	A	$C_{14}H_{22}O_3$	70.56 (70.33	9.30 9.31)		3.00×10^{-7}
38	$O(CH_2)_9CH_3$	112—113	A	$C_{16}H_{26}O_3$	72.14 (72.29	9.84 9.90)		1.60×10^{-7}
43	$OCH=CHCONH(CH_2)_5CH_3$	103—104	E	$C_{15}H_{21}NO_4$		280.1547 (280.1527)		2.50×10^{-7}
44	$OCH=CHCONH(CH_2)_7CH_3$	139—140	E	$C_{17}H_{25}NO_4$	66.43 (66.21	8.20 8.47	4.56 4.38)	1.70×10^{-7}
45	$OCH=CHCONH(CH_2)_9CH_3$	110—111	E	$C_{19}H_{29}NO_4$	68.03 (67.74	8.71 8.69	4.18 4.03)	7.20×10^{-8}
Series III								
50	$COCH_3$	169—170	E	$C_{12}H_{10}O_3$	71.28 (71.23	4.98 4.89)		3.00×10^{-6}
51	$CO(CH_2)_2CH_3$	180—181	E	$C_{14}H_{14}O_3$		231.1021 (231.1062)		4.60×10^{-7}
52	$CO(CH_2)_4CH_3$	173—174	E	$C_{16}H_{18}O_3$	74.40 (74.17	7.02 7.05)		2.00×10^{-7}
56	CH_2CH_3	148—149.5	E	$C_{12}H_{12}O_2$	76.57 (76.46	6.43 6.31)		3.00×10^{-6}
57	$(CH_2)_3CH_3$	137.5—139	E	$C_{14}H_{16}O_2$	77.75 (77.68	7.46 7.47)		8.00×10^{-7}
58	$(CH_2)_5CH_3$	138.5—139.5	E	$C_{16}H_{20}O_2$	78.65 (78.35	8.25 8.29)		9.00×10^{-7}
63	$CONH(CH_2)_3CH_3$	193.5—194	G	$C_{15}H_{17}NO_3$	69.48 (69.38	6.61 6.73	5.40 5.37)	5.00×10^{-6}
64	$CONH(CH_2)_5CH_3$	181—181.5	G	$C_{17}H_{21}NO_3$	71.06 (70.97	7.37 7.27	4.87 4.89)	1.40×10^{-6}
65	$CONH(CH_2)_7CH_3$	186—187.5	G	$C_{19}H_{25}NO_3$		316.1911 (316.1883)		2.00×10^{-7}
68	OCH_2CH_3	131—132	A	$C_{12}H_{12}O_3$	70.58 (70.38	5.92 5.88)		1.30×10^{-6}
69	$O(CH_2)_3CH_3$	141.5—143	A	$C_{14}H_{16}O_3$	72.39 (72.15	6.94 6.97)		4.00×10^{-7}
70	$O(CH_2)_5CH_3$	130.5—132	A	$C_{16}H_{20}O_3$	73.82 (73.98	7.74 7.84)		5.60×10^{-7}

a) Compounds that did not show a sharp mp are denoted "Amorph". *b*) Solvents: A, AcOEt–hexane; B, Et_2O–hexane; C, CH_3CN–Et_2O; D, EtOH–H_2O; E, $CHCl_3$–hexane; F, hexane; G, $CHCl_3$–MeOH. *c*) Concentration for 50% inhibition of 5-lipoxygenase from guinea pig leukocytes. Each value represents the mean of at least two experiments. *d*) High mass data. The upper value was calculated and the lower one was that found. The values are for $M+H^+$ (measured by the SIMS-positive mode) except for compounds **3** and **11**, where M^+ (measured by the EI-mode) was measured. *e*) The sample is a *cis–trans* mixture, although the *cis* isomer is generally predominant.

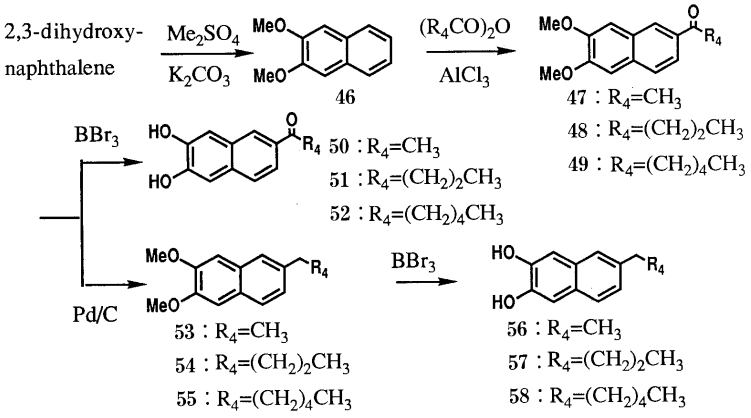

Chart 5

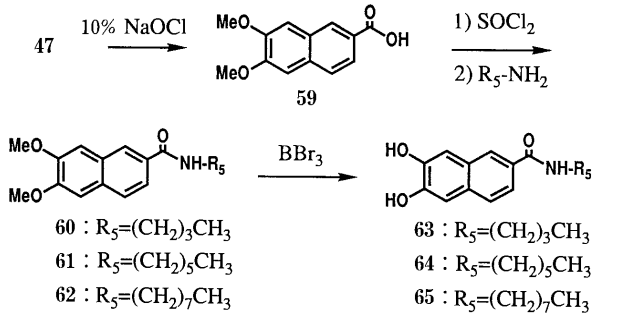

Chart 6

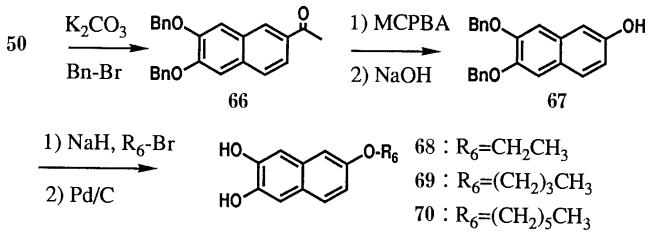

Chart 7

43—**45** were prepared[6] by the addition of phenol **36** to ethyl propiolate followed by amidation giving compounds **40**—**42**, which were debenzylated with boron tribromide as shown in Chart 4. The 6-acyl-2,3-dihydroxynaphthalenes **50**—**52** were prepared by the Friedel–Crafts reaction of 2,3-dimethoxynaphthalene, **46**, with acid anhydrides and aluminum chloride followed by demethylation by use of boron tribromide (Chart 5). The 6-alkyl-2,3-dihydroxynaphthalenes **56**—**58** were prepared by the reduction of the acyl derivatives **47**—**49** by catalytic hydrogenation followed by demethylation (Chart 5). The *N*-alkyl-6,7-dihydroxy-2-naphthamides **63**—**65** were prepared by procedures similar to those for compounds **43**—**45** from 6,7-dimethoxy-2-naphthoic acid, **59**, which was prepared by the Haloform reaction of **47** by use of a sodium hypochlorite solution (Chart 6). The 6-alkoxy-2,3-dihydroxynaphthalenes **68**—**70** were prepared similarly to the 4-alkoxy-2,3-dihydroxybenzene derivatives **37**, **38** (Chart 7).

All compounds used in this study are listed in Table I.

Biological Results and Discussion

The 50% inhibitory concentration of each compound (I_{50}) was measured against the production of leukotriene B_4 and 5-hydroxyeicosatetraenoic acid from arachidonic acid. The measurement was done by use of a reported procedure[5] in a $10000 \times g$ supernatant fraction from guinea-pig polymorphonuclear leukocytes. Inhibition of the enzyme by compounds of series I—III is listed in Table I.

In general, the series I compounds caused greater inhibition than series II or III compounds with the corresponding substituents X. The styrene double bond seemed favorable for inhibition. Within each series, the activity varied depending upon the substituents X. The physicochemical background for variations in the strength of inhibition was examined by quantitative structure–activity analysis with pI_{50} ($-\log I_{50}$) as the dependent variable.

First, analysis was made of the series I compounds (**1**—**25**) with the use of single parameters. The results indicated that the activity was parabolically related to the hydrophobic parameter ($\log P$), as shown in Eq. 1. P is the partition coefficient measured in the 1-octanol/water system.[7] The $\log P$ of some compounds with different chain lengths was estimated from the observed $\log P$ value of homologs by use of the $\pi(CH_3)$ value ($=0.54$).[8]

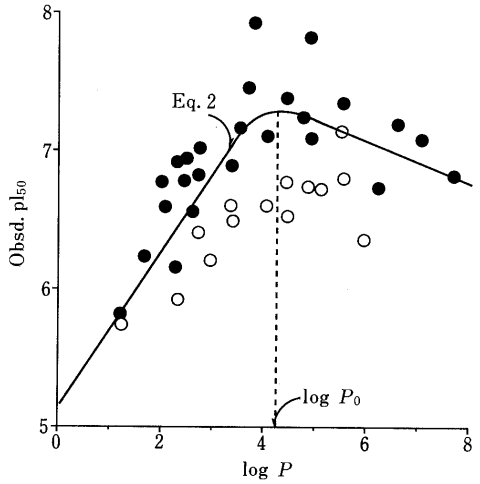

Fig. 1. Plots of pI_{50} *versus* $\log P$
●, series I; ○, series II.

$$pI_{50} = -0.10(\log P)^2 + 1.02 \log P + 4.87 \quad (1)$$
$$(0.04) \qquad (0.34) \qquad (0.66)$$

$n=25$, $r=0.82$, $s=0.28$, $F=23.24$, $\log P_0=5.1$

In this and the following equations, n is the number of compounds, r is the correlation coefficient, s is the standard deviation, F is the ratio between regression and residual variances, and $\log P_0$ is the optimum $\log P$ value.

The plots of pI_{50} versus $\log P$ are shown in Fig. 1. The shape of the relationship shown in Fig. 1 is a skewed "parabola." The "slope" of the ascending side of the parabola is steeper than that on the descending side. We examined the correlation using the bilinear model of Kubinyi.[9] Equation 2 (Table II) was derived as the counterpart of Eq. 1. The optimum value of $\log P$ was calculated to be 4.3, slightly lower than that calculated from Eq. 1. The quality of the correlation of Eq. 2 was better than that of Eq. 1, so further analyses were conducted using the bilinear model with respect to the $\log P$ value of compounds.

Next, we looked at incorporating the series II compounds (**26**—**34**, **37**, **38**, and **43**—**45**) into the series I compounds. The pI_{50} values of the series II compounds are also plotted in Fig. 1. They almost invariably deviated downward from the bilinear regression line for the series I compounds. By use of an indicator variable, D_{II}, which is unity for the series II compounds, Eq. 3, of good quality, was derived (Table II). The situation is summarized in Fig. 2.

Finally, analysis of series III compounds (**50**—**52**, **56**—**58**, **63**—**65**, and **68**—**70**) was attempted together with series I and II compounds. The inhibition caused by series III compounds was again lower than that of the series I compounds with the same $\log P$ values (Fig. 2). By consideration of a second indicator variable, D_{III}, which is unity for series III compounds, Eq. 4, which was of excellent

TABLE II. Correlation Equations for the 5-Lipoxygenase Inhibitory Activity of Compounds $pI_{50}=h(\log P)+i\log(\beta 10^{\log P}+1)+jD_{II}+kD_{III}+\text{const.}$

Eq. no.	Series	h	i	j	k	Const.	$\log P_0$[a]	$-\log\beta$[b]	n[c]	r[d]	s[e]	$F_{m,n-m-1}$[f]
2	I	0.64	−0.84			5.18	4.30	3.79	25	0.84	0.27	16.64
		(0.19)[g]	(0.29)			(0.52)						
3	I, II	0.52	−0.72	−0.61		5.47	4.50	4.11	39	0.87	0.25	26.57
		(0.12)	(0.22)	(0.17)		(0.36)						
4	I, II, III	0.49	−0.75	−0.62	−1.13	5.50	4.63	4.33	51	0.89	0.27	36.17
		(0.11)	(0.22)	(0.18)	(0.20)	(0.33)						

a) Optimum log *P* value. *b*) Estimated log *P* values where the slope changes from ascending to descending. *c*) Number of points used for calculation. *d*) Correlation coefficient. *e*) Standard deviation. *f*) *F* value of the correlation; *m* stands for the number of independent variables including β; theoretical *F* values are: $F_{3,21;\alpha=0.05}=3.07$ for Eq. 2, $F_{4,30;\alpha=0.05}=2.69$ for Eq. 3, and $F_{5,40;\alpha=0.05}=2.45$ for Eq. 4. *g*) Figures in parentheses are 95% confidence intervals.

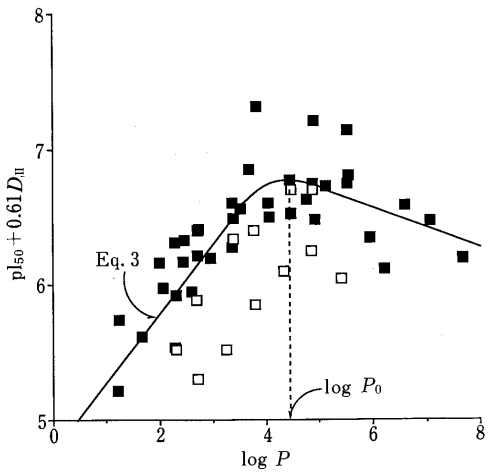

Fig. 2. Plots of $pI_{50}+0.61D_{II}$ *versus* log *P*

■, series I and II; □, series III.

TABLE III. Development of Eq. 4

Intercept	D_{III}	log *P*	D_{II}	$\log(\beta 10^{\log P}+1)$	s	r	$F_{X,Y}$[a]
6.79	−0.74				0.48	0.55	$F_{1,49}=21.72$
6.18	−0.73	0.16			0.42	0.69	$F_{1,48}=15.40$
6.33	−0.91	0.16	−0.49		0.37	0.78	$F_{1,47}=15.36$
5.50	−1.13	0.49	−0.62	−0.75	0.27	0.89	$F_{2,45}=22.14$

a) *F* statistic for the significance of the addition of each parameter; theoretical *F* values are: $F_{1,40,\alpha=0.05}=4.08$, $F_{1,60,\alpha=0.05}=4.00$, $F_{2,40,\alpha=0.05}=3.23$, and $F_{2,60,\alpha=0.05}=3.15$.

TABLE IV. Simple Correlation Matrix (r^2) for the Parameters of Eq. 4

	log *P*	$\log(\beta 10^{\log P}+1)$	D_{II}	D_{III}
log *P*	1.000			
$\log(\beta 10^{\log P}+1)$	0.769	1.000		
D_{II}	0.003	0.000	1.000	
D_{III}	0.000	0.021	0.116	1.000

quality, was formulated (Table II).

If differences in the skeletal structure were not considered, hydrophobicity was most important in governing the variations in activity. The effect of the skeletal structures was reflected in the terms D_{II} and D_{III} in Eq. 4. The styrene structure of series I compounds was most favorable to activity; in series II compounds, the deletion of the double bond lowered the activity. The naphthalene skeleton, which seems to involve a styrene-like substructure, further lowered the activity of series III compounds. The slope of the log *P* term in the ascending part in Eq. 4 is close to 0.5, suggesting that these compounds may interact with a hydrophobic protein surface, but are not engulfed in a hydrophobic pocket[10] until the log *P* value reaches about 4.3. Beyond this point, the inhibition did not increase, but decreased. The slope of the decrease, however, was not very steep. The compounds whose log *P* value was higher than the optimum generally had side chains longer than 8 or 10 bond units when the styrene double bond in series I compounds and the $\alpha\beta$ bond in series III compounds were included. The end of the side chain in these longer-chain compounds may not interact so tightly with the region where the shorter side-chain compounds are hydrophobically bound. Furthermore, the inhibitory mode of the binding of the shorter-chain region may be released by some conformational change in the enzyme structure caused by the additional hydrophobicity of the compounds. Another possibility is that the bilinear correlation equation may reflect pharmacokinetic processes being governed by the hydrophobicity of the compounds.[9] Enzyme preparation is considered to involve a number of "impurities." The compounds in which log *P* is beyond the optimum may be trapped with hydrophobic impurities to a higher extent than those with a lower log *P* value. The stepwise development of Eq. 4 for the 51 compounds studied here is shown in Table III. The intercorrelation between independent variables for the 51 derivatives in Eq. 4 was insignificant except for that between log *P* and $\log(\beta 10^{\log P}+1)$ (Table IV). The pI_{50} values and physicochemical independent variables of the compounds are listed in Table V.

Although Eq. 4 explains variations in the inhibitory activity fairly well, the physicochemical meaning of the indicator variables D_{II} and D_{III} should be clarified. When one or both of the hydroxy groups were replaced by a methoxy group in **20**, one of the most potent inhibitors, the activity was significantly decreased,[5] suggesting that a catechol structure with two vicinally located hydroxy groups is essential for strong inhibition; this is probably the pharmacophore of these compounds.

Recently, compounds containing catechol, such as nordihydroguaiaretic acid (see Chart 8), which is one of the most efficient inhibitors of lipoxygenase, have been shown to reduce the catalytically active ferric form of soybean lipoxygenase-1 to an inactive ferrous form.[12] The inhibition is increased by the introduction of electron-releasing substituents into catechol derivatives.[12] Thus, we analyzed variations in the activity of our compounds in terms of their electronic structure using the chemical shift of the proton at the C_5 position of the 3,4-dihydroxystyrene skeleton (see Chart 1) measured by proton nuclear magnetic

TABLE V. Inhibitory Activity and Physicochemical Parameters of the Compounds of Series I, II, and III

No.	Substituents X	log P[a]	D_{II}[b]	D_{III}[c]	ΔH_{C5}[d]	$E_{1/2}$[e]	ΔT_{max}[f]	pI_{50} Obsd.	pI_{50} Calcd[g]	pI_{50} (Δ)[h]
Series I										
1	$CO_2CH_2CH_3$	2.45[i]	0	0	1.5	1.40	0.60[m]	6.78	6.71	(0.07)
2	$CO_2(CH_2)_3CH_3$	3.53	0	0	1.5	1.40	0.60[m]	7.17	7.20	(−0.03)
3	$CO_2(CH_2)_4CH_3$	4.07[i]	0	0	1.5	1.40	0.60[m]	7.11	7.37	(−0.26)
4	$CO_2(CH_2)_8CH_3$	6.23[i]	0	0	1.5	1.40	0.60[m]	6.73	7.16	(−0.43)
5	$CONHCH_2CH_3$	1.21[i]	0	0	1.3	1.05	0.60[m]	5.82	6.10	(−0.28)
6	$CONH(CH_2)_3CH_3$	2.29[i]	0	0	1.3	1.05	0.60[m]	6.15	6.63	(−0.48)
7	$CONH(CH_2)_5CH_3$	3.37	0	0	1.3	1.05	0.60[m]	6.89	7.13	(−0.24)
8	$CONH(CH_2)_7CH_3$	4.45[i]	0	0	1.3	1.05	0.60[m]	7.38	7.43	(−0.05)
9	$CONH(CH_2)_9CH_3$	5.53[i]	0	0	1.3	1.05	0.60[m]	7.35	7.32	(0.03)
10	$CONH(CH_2)_{11}CH_3$	6.61[i]	0	0	1.3	1.05	0.60[m]	7.19	7.07	(0.12)
11	$CONH(CH_2)_{13}CH_3$	7.69[i]	0	0	1.3	1.05	0.60[m]	6.81	6.80	(0.01)
12	$CONHCH_2Ph$	2.48	0	0	1.3	1.05	0.60[m]	6.94	6.72	(0.22)
13	$CONH(CH_2)_2Ph$	2.72	0	0	1.3	1.05	0.60[m]	6.82	6.84	(−0.02)
14	CONHPh(4-butyl)	4.92[j]	0	0	1.3	1.05	0.60[m]	7.09	7.42	(−0.33)
15	CONHPh(4-octyl)	7.08[i]	0	0	1.3	1.05	0.60[m]	7.08	6.95	(0.13)
16	$CONHPh(3,4\text{-}OCH_3)$	2.30	0	0	1.3	1.05	0.60[m]	6.92	6.63	(0.29)
17	$CONHCH_2Ph(3,4\text{-}OCH_3)$	1.99	0	0	1.3	1.05	0.60[m]	6.77	6.48	(0.29)
18	$CONH(CH_2)_2Ph(3,4\text{-}OCH_3)$	2.07	0	0	1.3	1.05	0.60[m]	6.59	6.52	(0.07)
19	$CO(CH_2)_2CH_3$	2.61	0	0	1.6	1.25	0.60[m]	6.56	6.78	(−0.22)
20	$OC(CH_2)_4CH_3$	3.69[i]	0	0	1.6	1.25	0.60[m]	7.46	7.26	(0.20)
21	$CO(CH_2)_6CH_3$	4.77[i]	0	0	1.6	1.25	0.60[m]	7.24	7.43	(−0.19)
22	$CO(CH_2)_5OH$	1.67	0	0	1.6	1.25	0.60[m]	6.23	6.32	(−0.09)
23	CH_2CH_3	2.74[i]	0	0	0.9	0.525	0.60[m]	7.02	6.85	(0.17)
24	$(CH_2)_3CH_3$	3.82	0	0	0.9	0.525	0.60[m]	7.92	7.30	(0.62)
25	$(CH_2)_5CH_3$	4.90[i]	0	0	0.9	0.525	0.60[m]	7.82	7.42	(0.40)
Series II										
26	$CONH(CH_2)_5CH_3$	2.71	1	0	1.2	—[l]	2.07[n]	6.40	6.21	(0.19)
27	$CONH(CH_2)_9CH_3$	4.87[i]	1	0	1.2	—[l]	2.07[n]	6.74	6.80	(−0.06)
28	$CONH(CH_2)_{11}CH_3$	5.95[i]	1	0	1.2	—[l]	2.07[n]	6.35	6.60	(−0.25)
29	$CH(OH)(CH_2)_2CH_3$	1.24[i]	1	0	0.2	—[l]	2.17[o]	5.74	5.49	(0.25)
30	$CH(OH)(CH_2)_4CH_3$	2.32	1	0	0.2	—[l]	2.17[o]	5.92	6.02	(−0.10)
31	$CH(OH)(CH_2)_6CH_3$	3.40[i]	1	0	0.2	—[l]	2.17[o]	6.49	6.52	(−0.03)
32	$(CH_2)_3CH_3$	2.96	1	0	0	—[l]	2.17[p]	6.20	6.33	(−0.13)
33	$(CH_2)_5CH_3$	4.04[i]	1	0	0	—[l]	2.17[p]	6.60	6.74	(−0.14)
34	$(CH_2)_7CH_3$	5.12[i]	1	0	0	—[l]	2.17[p]	6.72	6.77	(−0.05)
37	$O(CH_2)_7CH_3$	4.47[k]	1	0	−0.2	—[l]	2.07[q]	6.52	6.81	(−0.29)
38	$O(CH_2)_9CH_3$	5.55[i]	1	0	−0.2	—[l]	2.07[q]	6.80	6.69	(0.11)
43	$OCH{=}CHCONH(CH_2)_5CH_3$	3.36	1	0	1	—[l]	2.07[q]	6.60	6.51	(0.09)
44	$OCH{=}CHCONH(CH_2)_7CH_3$	4.44[i]	1	0	1	—[l]	2.07[q]	6.77	6.81	(−0.04)
45	$OCH{=}CHCONH(CH_2)_9CH_3$	5.52[i]	1	0	1	—[l]	2.07[q]	7.14	6.70	(0.44)
Series III										
50	$COCH_3$	2.32	0	1	5.5	—[l]	0.71[r]	5.52	5.52	(0.00)
51	$CO(CH_2)_2CH_3$	3.40[i]	0	1	5.5	—[l]	0.71[r]	6.34	6.02	(0.32)
52	$CO(CH_2)_4CH_3$	4.48[i]	0	1	5.5	—[l]	0.71[r]	6.70	6.30	(0.40)
56	CH_2CH_3	3.25	0	1	4.3	—[l]	0.71[r]	5.52	5.95	(−0.43)
57	$(CH_2)_3CH_3$	4.33[i]	0	1	4.3	—[l]	0.71[r]	6.10	6.29	(−0.19)
58	$(CH_2)_5CH_3$	5.41[i]	0	1	4.3	—[l]	0.71[r]	6.05	6.22	(−0.17)
63	$CONH(CH_2)_3CH_3$	2.72	0	1	5.3	—[l]	0.71[r]	5.30	5.71	(−0.41)
64	$CONH(CH_2)_5CH_3$	3.80[i]	0	1	5.3	—[l]	0.71[r]	5.85	6.17	(−0.32)
65	$CONH(CH_2)_7CH_3$	4.88[i]	0	1	5.3	—[l]	0.71[r]	6.70	6.30	(0.40)
68	OCH_2CH_3	2.70	0	1	3.9	—[l]	0.71[r]	5.89	5.70	(0.19)
69	$O(CH_2)_3CH_3$	3.78[i]	0	1	3.9	—[l]	0.71[r]	6.40	6.16	(0.24)
70	$O(CH_2)_5CH_3$	4.86[i]	0	1	3.9	—[l]	0.71[r]	6.25	6.30	(−0.05)

a) Values were measured, unless otherwise noted. *b*) Indicator variable that is unity for the series II compounds. *c*) Indicator variable that is unity for the series III compounds. *d*) Calculated from the equation $\Delta H_{C5} = \{H_{C5}(R) - H_{C5}(\text{pyrocatechol})\} \times 10$. The value of $H_{C5}(R)$ indicated a ^{1}H-NMR chemical shift of the proton adjacent to the catechol (see Chart 1). The parameters of compounds **2**, **7**, **20**, **24**, **27**, **30**, **33**, **38**, **43**, **50**, **57**, **63**, and **70** were used for the derivatives **1**—**4**, **5**—**18**, **19**—**22**, **23**—**25**, **26**—**28**, **29**—**31**, **32**—**34**, **37**—**38**, **43**—**45**, **50**—**52**, **56**—**58**, **63**—**65**, and **68**—**70**, respectively. *e*) All values were scaled by 0.01 and the parameters of compounds **2**, **8**, **20**, **24**, **26**, **29**, **32**, **38**, and **44** were used for the derivatives **1**—**4**, **5**—**18**, **19**—**22**, **23**—**25**, **26**—**28**, **29**—**31**, **32**—**34**, **37**—**38**, and **43**—**45**, respectively. *f*) Values were estimated by use of a program or a brochure, both of which were provided by Dr. A. Verloop. All values were used as values relative to that of *H*. *g*) Estimated from Eq. 4. *h*) Δ, difference between observed and calculated values. *i*) Estimated from the observed log P values of each derivative by calculation of $\pi(CH_3)(=0.54)$.[8] *j*) Estimated from the measured log P value of caffeic acid phenyl amide (log P=2.78) by the addition of $\pi(n\text{-Bu})(=2.14)$.[11] *k*) Estimated from the measured log P value of 4-*n*-hexyloxycatechol (log P=3.39). *l*) Not listed because the values were unstable for series II compounds. Not obtained reversible anodic waves for series III compounds. *m*) B_1 parameter of vinyl was used. *n*) B_5 parameter of $CONH_2$ was used. *o*) B_5 parameter of $CH(OH)CH_3$ was used. *p*) B_5 parameter of CH_2CH_3 was used. *q*) B_5 parameter of OCH_3 was used. *r*) B_1 parameter of naphthyl was used.

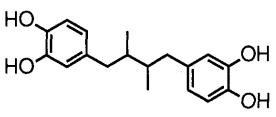

nordihydroguaiaretic acid

Chart 8

resonance (^{1}H-NMR) and the half-wave potential ($E_{1/2}$).[15] For series I compounds, almost equivalent Eqs. 5 and 6 were formulated.

$$pI_{50} = \underset{(0.16)}{0.62}\log P - \underset{(0.25)}{0.81}\log(\beta 10^{\log P}+1) - \underset{(0.49)}{0.71}\Delta H_{C5} + \underset{(0.82)}{6.19} \quad (5)$$

$$n=25,\ r=0.89,\ s=0.23,\ F=19.37,\ -\log\beta=3.81,\ F_{1,20}=8.39$$

$$pI_{50} = \underset{(0.16)}{0.63}\log P - \underset{(0.24)}{0.82}\log(\beta 10^{\log P}+1) - \underset{(0.38)}{0.63}E_{1/2} + \underset{(0.62)}{5.89} \quad (6)$$

$$n=25,\ r=0.90,\ s=0.22,\ F=21.31,\ -\log\beta=3.77,\ F_{1,20}=10.13$$

For simplicity, the chemical shift parameter was used in Eq. 5 as the value relative to that of pyrocatechol $\{\Delta H_{C5} = H_{C5}(R) - H_{C5}(\text{pyrocatechol})\}$. The ΔH_{C5} and $E_{1/2}$ used were the values of representative compounds for each of the homologous derivatives, because the length of alkane side chains did not significantly affect these parameters (see Table V); these values were multiplied by 10 and 0.01, respectively, to place them on a scale similar to that of $\log P$ in these equations. The ΔH_{C5} and $E_{1/2}$ parameters are highly correlated with each other ($r=0.95$).

The fact that the addition of the electronic term improved the quality of the correlation significantly over that of Eq. 2 is consistent with observations of nordihydroguaiaretic acid and its derivatives. The enzyme inhibition is governed not only by hydrophobicity but also by the electronic structure of the catechol skeleton. Equations 5 and 6 show that the lower the proton chemical shift or the $E_{1/2}$ value, the more potent is the activity, so high electron density at the catechol moiety is indeed necessary for potent inhibition. For the series I—III compounds, analysis was done by use of $\log P$ and ΔH_{C5}, and gave Eq. 7. The $E_{1/2}$ values for series II compounds were unstable and those for series III compounds were not measurable because irreversible anodic waves arose from these compounds.

$$pI_{50} = \underset{(0.13)}{0.47}\log P - \underset{(0.25)}{0.68}\log(\beta 10^{\log P}+1) - \underset{(0.23)}{0.82}D_{II} - \underset{(0.06)}{0.29}\Delta H_{C5} + \underset{(0.39)}{5.91} \quad (7)$$

$$n=51,\ r=0.86,\ s=0.31,\ F=24.92,\ \log\beta=-4.30,\ \log P_0=4.65$$

Equation 7 shows that the indicator variable D_{III} in Eq. 4 could be replaced by the parameter ΔH_{C5}, and that the D_{III} term reflects variations in the electron density of the catechol moiety.

Series III compounds contain a closed-ring styrene as a substructural feature in common with series I compounds. Thus, we expected the indicator variable D_{II} assigned to series II compounds to reflect the absence of the $\alpha\beta$ "double" bond. This factor could be steric. We examined various steric parameters to find if they could replace the D_{II} term and concluded that the STERIMOL width parameter[13] of the $\alpha\beta$ moiety works best when conformational factors are considered. That is, the vinyl group in series I compounds is likely to be coplanar with the benzene ring because of π electron resonance, as is the $\alpha\beta$-bond in series III (naphthalene) compounds. In series II compounds, the functional groups probably rotate around the bond which is connected directly with the benzene ring more easily than in series I compounds. Considering these conformational features, we used the maximum thickness, T_{max}, of the $\alpha\beta$-moiety from the ring plane as the steric parameter. For series I and III compounds, the half thickness, B_1, of the vinyl group and the naphthalene ring was used as the parameter. For the amides (**26**—**28**), benzylalcohols (**29**—**31**), alkanes (**32**—**34**), ethers (**37, 38**), and β-oxyacrylates (**43**—**45**), the maximum thickness, B_5, of the $CONH_2$, $CH(OH)CH_3$, CH_2CH_3, OCH_3, and OCH_3 groups, respectively, were used as the parameter, T_{max}. With the steric parameter estimated for these side chains, relative to that of H, ΔT_{max}, good correlation was obtained (Eq. 8).

$$pI_{50} = \underset{(0.13)}{0.47}\log P - \underset{(0.25)}{0.69}\log(\beta 10^{\log P}+1) - \underset{(0.15)}{0.55}\Delta T_{max} - \underset{(0.06)}{0.28}\Delta H_{C5} + \underset{(0.40)}{6.24} \quad (8)$$

$$n=51,\ r=0.86,\ s=0.30,\ F=26.49,\ -\log\beta=4.30,\ \log P_0=4.64$$

Equation 8 shows that indicator variable D_{II} could be replaced by the ΔT_{max} parameter. The D_{II} term in Eqs. 3 and 4 probably accounts for the largest thickness of the atomic group at the α and β positions of the catechol moiety.

In our previous paper,[5] compound **20** was shown to inhibit the enzyme non-competitively. Other catechol derivatives, such as circiliol, have also been indicated as non-competitive inhibitors.[14] Thus, compounds included in this study could also be non-competitive. In this work, they were suggested to interact with a hydrophobic milieu of the 5-lipoxygenase. Although the slope of the $\log P$ term (*ca.* 0.5) suggests that the interaction could occur on the hydrophobic proteinous surface but not in the hydrophobic pocket, the essential catechol part of the molecule, but not the side chain, may be engulfed in the pocket where the two hydroxy groups could chelate with prosthetic metal ions to inhibit the function of the oxygenase.

Based on the above results from analysis of the quantitative structure–activity relationships, the structural requirements for maximum potency can be summarized as follows.

(1) Hydrophobicity close to $\log P = 4.3$—4.7 is preferable.
(2) High electron density of the catechol moiety caused by electron-releasing side chains, not by the fused ring with delocalization of electrons, is preferable.
(3) Thickness of the lipophilic side chains close to the catechol benzene ring ($\alpha\beta$) is unfavorable to the activity.

The compounds that should cause the greatest inhibition, as predicted by Eqs. 4 and 8, are compounds **8** and **20**, both of series I with a $\log P$ value close to the optimum. The results were helpful in giving a physicochemical base for the selection of candidate compounds for developmental studies.

Experimental

5-Lipoxygenase Inhibitory Activity Inhibition by 5-lipoxygenase was assayed as described previously.[5]

Measurement of Substituent Parameters 1) log *P*: The partition ratio *P* (apparent partition coefficient), was measured by the flask-shaking method[7] at 25±3 °C with 1-octanol and water. After the partitioning equilibrium was reached, the concentration of each compound in the aqueous phase was measured by its ultraviolet (UV) absorbance.

2) H_{C5}: The ^{1}H-NMR chemical shift of the proton adjacent to the catechol group was measured on a Bruker AC-200 NMR in dimethyl sulfoxide-d_6 (DMSO-d_6) with tetramethylsilane (TMS) as an internal standard. The values for series III were assigned by use of nuclear Overhauser effect (NOE) analyses.

3) $E_{1/2}$: The half-wave potential (mV *vs.* a saturated calomel reference electrode) was measured as the midpoint of the cathodic and anodic peak potentials of cyclic voltammograms recorded as reported elsewhere,[15] except that a carbon-disk (i.d. = 3 mm) electrode (BAS Co.) was used as the working electrode. The carbon electrode surface was polished before each measurement with 0.05 μm alumina powder (Union Carbide, U.S.A.). Concentrations of about 1 mM of each sample in 50% EtOH that contained 0.1 M NaH_2PO_4–Na_2HPO_4 (pH 7.4) were used for voltammetric measurements.

Analyses Melting points were determined with a Yanaco melting point apparatus and are uncorrected. ^{1}H-NMR spectra were measured on a Bruker AC-200 NMR or a Hitachi R-24B NMR spectrometer with TMS as the internal standard; chemical shifts are given on the δ (ppm) scale. Infrared (IR) spectra were obtained on a Shimadzu IR-420 spectrometer.

The physicochemical data are summarized in Table I. The analytical data of previously prepared compounds are included here, because they were not given in our earlier report.[5]

Compounds and Syntheses: Caffeic Acid *n*-Pentyl Ester (3) Yield 20%. mp 125—127 °C. IR (KBr) cm^{-1}: 3480, 3310, 1675, 1635, 1600. ^{1}H-NMR (DMSO-d_6): 0.88 (3H, t, J=6.8 Hz), 1.2—1.7 (6H, m), 4.10 (2H, t, J=6.6 Hz), 6.26 (1H, d, J=15.9 Hz), 6.76 (1H, d, J=8.0 Hz), 7.01 (1H, dd, J=8.0, 1.8 Hz), 7.05 (1H, d, J=1.8 Hz), 7.47 (1H, d, J=15.9 Hz), 9.14 (1H, OH), 9.60 (1H, OH).

Caffeic Acid Ethyl Amide (5) Yield 29%. Amorphous solid. IR (KBr) cm^{-1}: 3480, 3370, 1645, 1578. ^{1}H-NMR (DMSO-d_6, $CDCl_3$): 1.16 (3H, t, J=7 Hz), 3.27 (2H, q, J=7 Hz), 6.31 (1H, d, J=16 Hz), 6.7—7.1 (3H, m), 7.41 (1H, d, J=16 Hz), 8.47 (1H, NH).

Caffeic Acid *n*-Butyl Amide (6) Yield 25%. Amorphous solid. IR (KBr) cm^{-1}: 3260, 1650. ^{1}H-NMR (DMSO-d_6, $CDCl_3$): 0.92 (3H, t, J=7 Hz), 1.15—1.7 (4H, m), 3.24 (2H, dt, J=4, 6 Hz), 6.38 (1H, d, J=16 Hz), 6.7—7.1 (3H, m), 7.32 (1H, d, J=16 Hz), 7.88 (1H, t, J=4 Hz, NH), 9.00 (2H, OH).

Caffeic Acid Benzyl Amide (12) Yield 37%. mp 164—167 °C. IR (KBr) cm^{-1}: 3250, 1670, 1640. ^{1}H-NMR (DMSO-d_6, $CDCl_3$): 4.42 (2H, d, J=6 Hz), 6.36 (1H, d, J=15 Hz), 6.65—7.5 (4H, m), 7.25 (5H, s), 8.27 (1H, t, J=6 Hz, NH), 8.80 (1H, OH), 9.00 (1H, OH).

Caffeic Acid Phenethyl Amide (13) Yield 24%. mp 157—159 °C. IR (KBr) cm^{-1}: 3450, 3300, 1640, 1600. ^{1}H-NMR (DMSO-d_6): 2.76 (2H, t, J=7.7 Hz), 3.40 (2H, m), 6.31 (1H, d, J=15.7 Hz), 6.73 (1H, d, J=8.1 Hz), 6.83 (1H, dd, J=8.1, 1.8 Hz), 6.93 (1H, d, J=1.8 Hz), 7.1—7.4 (6H, m), 8.07 (1H, t, J=5.8 Hz, NH), 9.12 (1H, OH), 9.36 (1H, OH).

Caffeic Acid 4-*n*-Butylphenyl Amide (14) Yield 31%. mp 204—205.5 °C. IR (KBr) cm^{-1}: 3490, 3390, 1660, 1620, 1600. ^{1}H-NMR (DMSO-d_6, $CDCl_3$): 0.90 (3H, t, J=6 Hz), 1.1—1.9 (4H, m), 2.52 (2H, t, J=6 Hz), 6.43 (1H, d, J=16 Hz), 6.7—7.8 (9H, m), 7.38 (1H, d, J=16 Hz), 9.58 (1H, NH).

Caffeic Acid 4-*n*-Octylphenyl Amide (15) Yield 37%. mp 173.5—175 °C. IR (KBr) cm^{-1}: 3260, 1655, 1620, 1600. ^{1}H-NMR (DMSO-d_6): 0.85 (3H, t, J=6.6 Hz), 1.1—1.7 (12H, m), 2.51 (2H, t, J=7.9 Hz), 6.53 (1H, d, J=15.7 Hz), 6.77 (1H, d, J=8.1 Hz), 6.8—7.0 (2H, m), 7.12 (2H, d, J=8.3 Hz), 7.38 (1H, d, J=15.7 Hz), 7.58 (2H, d, J=8.3 Hz), 9.19 (1H, OH), 9.44 (1H, OH), 9.98 (1H, NH).

Caffeic Acid 3,4-Dimethoxyphenyl Amide (16) Yield 27%. mp 201—202 °C. IR (KBr) cm^{-1}: 3250, 1650, 1600. ^{1}H-NMR (DMSO-d_6): 3.72 (3H, s), 3.74 (3H, s), 6.50 (1H, d, J=15.4 Hz), 6.7—7.4 (7H, m), 9.19 (1H, OH), 9.44 (1H, OH), 9.94 (1H, NH).

Caffeic Acid 3,4-Dimethoxybenzyl Amide (17) Yield 51%. mp 203—206 °C. IR (KBr) cm^{-1}: 3480, 1650, 1585. ^{1}H-NMR (DMSO-d_6, $CDCl_3$): 3.80 (6H, s), 4.38 (2H, d, J=6 Hz), 6.38 (1H, d, J=15 Hz), 6.6—7.2 (6H, m), 7.39 (1H, d, J=15 Hz), 7.85 (1H, NH), 8.0—8.3 (2H, OH).

Caffeic Acid 2-(3,4-Dimethoxyphenyl)ethyl Amide (18) Yield 10%. mp 97—99 °C. IR (KBr) cm^{-1}: 3300, 1650, 1600. ^{1}H-NMR (DMSO-d_6): 2.7 (2H, m), 3.4 (2H, m), 3.71 (3H, s), 3.73 (3H, s), 6.32 (1H, d, J=16 Hz), 6.7—7.0 (6H, m), 7.22 (1H, d, J=16 Hz), 8.02 (1H, NH), 9.12 (1H, OH), 9.35 (1H, OH).

***N*-*n*-Hexyl-3,4-dihydroxybenzamide (26)** Yield 20%. mp 139—140 °C. IR (KBr) cm^{-1}: 3480, 3350, 3150, 1615, 1580, 1540. ^{1}H-NMR (DMSO-d_6): 0.86 (3H, t, J=6.6 Hz), 1.2—1.8 (8H, m), 3.1—3.2 (2H, m), 6.73 (1H, d, J=8.2 Hz), 7.16 (1H, dd, J=8.2, 2.0 Hz), 7.26 (1H, d, J=2.0 Hz), 8.09 (1H, NH), 9.0—9.5 (2H, br, OH).

***N*-*n*-Decyl-3,4-dihydroxybenzamide (27)** Yield 16%. mp 129.5—130 °C. IR (KBr) cm^{-1}: 3480, 3350, 3180, 1610, 1580, 1540. ^{1}H-NMR (DMSO-d_6): 0.85 (3H, t, J=6.6 Hz), 1.2—1.8 (16H, m), 3.1—3.2 (2H, m), 6.73 (1H, d, J=8.4 Hz), 7.16 (1H, dd, J=8.4, 2.0 Hz), 7.26 (1H, d, J=2.0 Hz), 8.07 (1H, NH), 9.06 (1H, OH), 9.39 (1H, OH).

***N*-*n*-Dodecyl-3,4-dihydroxybenzamide (28)** Yield 13%. mp 119.5—120.0 °C. IR (KBr) cm^{-1}: 3480, 3350, 3150, 1615, 1580, 1540. ^{1}H-NMR (DMSO-d_6): 0.85 (3H, t, J=6.7 Hz), 1.2—1.8 (20H, m), 3.1—3.2 (2H, m), 6.73 (1H, d, J=8.2 Hz), 7.16 (1H, dd, J=8.2, 2.0 Hz), 7.26 (1H, d, J=2.0 Hz), 8.07 (1H, NH), 9.06 (1H, OH), 9.39 (1H, OH).

1-(3,4-Dihydroxyphenyl)-*n*-octanol (31) To a solution of *n*-heptylmagnesium bromide (prepared from 1.6 g of magnesium turnings and 9.4 ml of *n*-heptyl bromide in 100 ml of tetrahydrofuran (THF)) was added dropwise protocatechualdehyde (2.5 g) in THF (10 ml) at 0 °C for 10 min. The resultant solution was stirred at 0 °C for 30 min and then poured into ice water. The mixture was acidified to pH 2 with 1 N HCl and extracted with AcOEt. The extract was washed with water and brine in that order, and dried over $MgSO_4$. After evaporation of the solvent, **31** was collected by recrystallization from AcOEt–hexane (2.4 g, 57%). mp 120—122.5 °C. IR (KBr) cm^{-1} 3450, 3100, 1610, 1520. ^{1}H-NMR (DMSO-d_6, $CDCl_3$): 0.87 (3H, t, J=6 Hz), 1.1—2.0 (12H, m), 4.3—4.5 (2H, m), 6.5—7.0 (3H, m), 8.12 (2H, OH).

1-(3,4-Dihydroxyphenyl)-*n*-butanol (29) The procedure used for the preparation of **31** was repeated with protocatechualdehyde and *n*-propylmagnesium bromide to obtain **29** (2.3 g, 43%). mp 137—139 °C. IR (KBr) cm^{-1}: 3450, 3100, 1615, 1520. ^{1}H-NMR (DMSO-d_6, $CDCl_3$): 0.87 (3H, t, J=6 Hz), 1.1—2.0 (4H, m), 3.6 (1H, OH), 4.48 (1H, m), 6.5—7.0 (3H, m), 7.5—7.9 (2H, OH).

1-(3,4-Dihydroxyphenyl)-*n*-hexanol (30) The procedure used for the preparation of **31** was repeated with protocatechualdehyde and *n*-pentylmagnesium bromide to obtain **30** (2.8 g, 67%). mp 108—110 °C. IR (KBr) cm^{-1}: 3450, 3100, 1610, 1520. ^{1}H-NMR (DMSO-d_6): 0.83 (3H, t, J=6.5 Hz), 1.1—1.7 (8H, m), 4.29 (1H, m), 4.82 (1H, d, J=4.1 Hz, OH), 6.51 (1H, dd, J=8.0, 1.9 Hz), 6.63 (1H, d, J=8.0 Hz), 6.69 (1H, d, J=1.9 Hz), 8.62 (1H, OH), 8.72 (1H, OH).

4-*n*-Octylcatechol (34) Compound **31** (1.9 g) in EtOH (40 ml) containing five drops of 12 N HCl was hydrogenated over 10% Pd/C (380 mg) under atmospheric pressure at room temperature for 2 h. The catalyst was removed by filtration and the filtrate was concentrated under reduced pressure. The residue was extracted with AcOEt and the extract was washed with water and brine in that order, and dried over $MgSO_4$. After evaporation of the solvent, the residue was chromatographed on silica gel with AcOEt–hexane. Compound **34** was recrystallized from hexane (510 mg, 29%). mp 60—61 °C. IR (KBr) cm^{-1}: 3460, 3310, 1600, 1520. ^{1}H-NMR ($CDCl_3$): 0.86 (3H, t, J=6.0 Hz), 1.2—1.8 (12H, m), 2.42 (2H, t, J=7.0 Hz), 5.92 (2H, OH), 6.4—6.8 (3H, m).

4-*n*-Butylcatechol (32) The procedure used for the preparation of **34** was repeated with **29** to obtain **32** (1.1 g, 80%). Amorphous solid. IR (KBr) cm^{-1}: 3480, 3350, 1610, 1520. ^{1}H-NMR ($CDCl_3$): 0.86 (3H, t, J=6.0 Hz), 1.2—1.8 (4H, m), 2.42 (2H, t, J=7.0 Hz), 5.68 (2H, OH), 6.4—6.8 (3H, m).

4-*n*-Hexylcatechol (33) The procedure used for the preparation of **34** was repeated with **30** to obtain **33** (1.4 g, 91%). Amorphous solid. IR (KBr) cm^{-1}: 3480, 3350, 1610, 1520. ^{1}H-NMR (DMSO-d_6): 0.85 (3H, t, J=6.6 Hz), 1.2—1.7 (8H, m), 2.38 (2H, t, J=7.7 Hz), 6.40 (1H, dd, J=7.9, 2.0 Hz), 6.54 (1H, d, J=2.0 Hz), 6.61 (1H, d, J=7.9 Hz), 8.57 (1H, OH), 8.65 (1H, OH).

4-*n*-Octyloxycatechol (37) 1) Protocatechualdehyde Dibenzyl Ether (**35**): A solution of protocatechualdehyde (10 g), K_2CO_3 (20 g), and benzyl bromide (20 ml) in dimethylformamide (DMF) (200 ml) was stirred at 150 °C for 4 h. After the reaction mixture was cooled to 0 °C, it was poured into Et_2O. The organic layer was washed with water and brine in that order, and dried over $MgSO_4$. After evaporation of the solvent, **35** was collected by precipitation from AcOEt–hexane (18 g, 78%). IR (KBr) cm^{-1}: 1675, 1575, 1495. ^{1}H-NMR ($CDCl_3$): 5.20 (2H, s), 5.24 (2H, s),

7.00 (1H, d, J=8.2 Hz), 7.2—7.5 (12H, m), 9.80 (1H, s).

2) 3,4-Dibenzyloxyphenol (**36**): A solution of **35** (18 g) and *m*-CPBA (15 g) in AcOEt (200 ml) was stirred at room temperature for 6 h, and then AcOEt (300 ml) was added. The organic layer was washed with aqueous $NaHCO_3$, water and brine, in that order, and dried over $MgSO_4$. After evaporation of the solvent, the residue was dissolved in dioxane (50 ml). To this solution was added 3 N NaOH (50 ml), and the solution was stirred at room temperature for 30 min. The resultant solution was acidified with 3 N HCl to pH 2 at 0 °C and extracted with AcOEt. The extract was washed with brine and dried over $MgSO_4$. After evaporation of the solvent, **36** was collected by precipitation from $CHCl_3$–hexane (9.2 g, 53%). IR (KBr) cm^{-1}: 3300, 1600, 1500. ^{1}H-NMR ($CDCl_3$): 5.04 (2H, s), 5.05 (2H, s), 6.27 (1H, dd, J=8.5, 2.8 Hz), 6.47 (1H, d, J=2.8 Hz), 6.77 (1H, d, J=8.5 Hz), 7.2—7.5 (10H, m).

3) 4-*n*-Octyloxycatechol (**37**): To a cooled (0 °C) solution of **36** (0.7 g) in DMF (10 ml) was added NaH (140 mg) and 1-bromooctane (0.6 ml), in that order. The resultant solution was stirred at room temperature for 30 min, and cooled to 0 °C. Water was carefully added to the solution and the resultant mixture was extracted with AcOEt. The extract was washed with water and brine, and dried over $MgSO_4$. After evaporation of the solvent, the residue was chromatographed on silica gel (AcOEt–hexane). The obtained compound in AcOEt (10 ml) was hydrogenated over 10% Pd/C (500 mg) under atmospheric pressure at room temperature for 15 h. Then, the catalyst was removed by filtration. After evaporation of the solvent, the residue was chromatographed on silica gel with AcOEt–hexane. Compound **37** was recrystallized from AcOEt–hexane (230 mg, 42%). mp 108—109 °C. IR (KBr) cm^{-1}: 3400, 3300, 1615, 1525, 1510. ^{1}H-NMR (DMSO-d_6): 0.86 (3H, t, J=6.7 Hz), 1.2—1.8 (12H, m), 3.78 (2H, t, J=6.4 Hz), 6.16 (1H, dd, J=8.6, 2.9 Hz), 6.32 (1H, d, J=2.9 Hz), 6.60 (1H, d, J=8.6 Hz), 8.33 (1H, OH), 8.83 (1H, OH).

4-*n*-Decyloxycatechol (38) The procedure used for the preparation of **37** was repeated with **36** and 1-bromodecane to give **38** (270 mg, 44%). mp 112—113 °C. IR (KBr) cm^{-1}: 3400, 3300, 1615, 1525, 1510. ^{1}H-NMR (DMSO-d_6): 0.86 (3H, t, J=6.7 Hz), 1.2—1.8 (16H, m), 3.78 (2H, t, J=6.4 Hz), 6.16 (1H, dd, J=8.6, 2.9 Hz), 6.32 (1H, d, J=2.9 Hz), 6.59 (1H, d, J=8.6 Hz), 8.33 (1H, OH), 8.82 (1H, OH).

***trans*-*N*-*n*-Hexyl-β-(3,4-dihydroxyphenoxy)acrylamide (43)** 1) *trans*-β-(3,4-Dibenzyloxyphenoxy)acrylic Acid (**39**): By the procedure of Fujinami *et al.*,[6] **36** was converted to **39** (3.4 g, 42%). IR (KBr) cm^{-1}: 3020, 2550, 1655, 1590, 1510. ^{1}H-NMR ($CDCl_3$): 5.13 (2H, s), 5.15 (2H, s), 5.43 (1H, d, J=12.2 Hz), 6.57 (1H, dd, J=8.8, 2.8 Hz), 6.68 (1H, d, J=2.8 Hz), 6.89 (1H, d, J=8.8 Hz), 7.2—7.5 (10H, m), 7.78 (1H, d, J=12.2 Hz).

2) *trans*-*N*-*n*-Hexyl-β-(3,4-dibenzyloxyphenoxy)acrylamide (**40**): A solution of **39** (0.9 g), $SOCl_2$ (5 ml), and one drop of DMF was heated at reflux for 2 h. After the excess of $SOCl_2$ was removed by distillation, the residue obtained was dissolved in $CHCl_3$ (5 ml) and cooled to 0 °C. To the cooled solution was added triethylamine (0.4 ml) and *n*-hexylamine (0.4 ml), in that order, and the resultant solution was stirred at room temperature for 1 h. After the reaction, the solution was diluted with AcOEt. The organic layer was washed with water and brine, and dried over $MgSO_4$. After evaporation of the solvent, the residue was chromatographed on silica gel with AcOEt–hexane to give **40** (200 mg, 18%). IR (KBr) cm^{-1}: 3300, 1665, 1615, 1595. ^{1}H-NMR ($CDCl_3$): 0.89 (3H, t, J=6.5 Hz), 1.2—1.8 (8H, m), 3.2—3.4 (2H, m), 5.12 (2H, s), 5.13 (2H, s), 5.39 (1H, d, J=12.2 Hz), 6.56 (1H, dd, J=8.8, 2.8 Hz), 6.68 (1H, d, J=2.8 Hz), 6.88 (1H, d, J=8.8 Hz), 7.2—7.5 (10H, m), 7.67 (1H, d, J=12.2 Hz).

3) *trans*-*N*-*n*-Hexyl-β-(3,4-dihydroxyphenoxy)acrylamide (**43**): To a solution of **40** (200 mg) in dry CH_2Cl_2 (10 ml) was added dropwise 1 M BBr_3 in CH_2Cl_2 (2.6 ml) at −70 °C. After the addition, the reaction mixture was stirred at −70 °C for 10 min, and poured into ice water. The resultant mixture was extracted with AcOEt and the extract was washed with water and brine, and dried over $MgSO_4$. After evaporation of the solvent, the residue was chromatographed on silica gel with AcOEt–hexane, and recrystallized from $CHCl_3$–hexane to give **43** (30 mg, 25%). mp 103—104 °C. IR (KBr) cm^{-1}: 3460, 3100, 1670, 1595, 1520. ^{1}H-NMR (DMSO-d_6): 0.86 (3H, t, J=6.6 Hz), 1.2—1.8 (8H, m), 3.0—3.1 (2H, m), 5.50 (1H, d, J=12.1 Hz), 6.37 (1H, dd, J=8.5, 2.8 Hz), 6.49 (1H, d, J=2.8 Hz), 6.71 (1H, d, J=8.5 Hz), 7.41 (1H, d, J=12.1 Hz), 7.74 (1H, NH), 8.88 (1H, OH), 9.25 (1H, OH).

***trans*-*N*-*n*-Octyl-β-(3,4-dihydroxyphenoxy)acrylamide (44)** The procedure used for the preparation of **43** was repeated with **39** and *n*-octylamine to obtain **44** (60 mg, 8% yield from **39**). mp 139—140 °C. IR (KBr) cm^{-1}: 3400, 3230, 1660, 1620, 1575. ^{1}H-NMR (DMSO-d_6): 0.86 (3H, t, J=6.7 Hz), 1.2—1.8 (12H, m), 3.0—3.1 (2H, m), 5.50 (1H, d, J=12.1 Hz), 6.37 (1H, dd, J=8.5, 2.8 Hz), 6.49 (1H, d, J=2.8 Hz), 6.71 (1H, d, J=8.5 Hz), 7.41 (1H, d, J=12.1 Hz), 7.74 (1H, NH), 8.88 (1H, OH), 9.25 (1H, OH).

***trans*-*N*-*n*-Decyl-β-(3,4-dihydroxyphenoxy)acrylamide (45)** The procedure used for the preparation of **43** was repeated with **39** and *n*-decylamine to obtain **45** (70 mg, 8% yield from **39**). mp 110—111.0 °C. IR (KBr) cm^{-1}: 3450, 3300, 1660, 1620, 1580. ^{1}H-NMR (DMSO-d_6): 0.85 (3H, t, J=6.6 Hz), 1.2—1.8 (16H, m), 3.0—3.1 (2H, m), 5.50 (1H, d, J=12.1 Hz), 6.37 (1H, dd, J=8.5, 2.9 Hz), 6.49 (1H, d, J=2.9 Hz), 6.71 (1H, d, J=8.5 Hz), 7.41 (1H, d, J=12.1 Hz), 7.74 (1H, NH), 8.88 (1H, OH), 9.25 (1H, OH).

6-Acetyl-2,3-dihydroxynaphthalene (50) 1) 2,3-Dimethoxynaphthalene (**46**): The procedure used for preparation of **35** was repeated with 2,3-dihydroxynaphthalene (20 g), dimethyl sulfate (26 ml), and K_2CO_3 (50 g) in DMF (200 ml) to obtain **46** (10 g, 42%). IR (KBr) cm^{-1}: 1620, 1595. ^{1}H-NMR ($CDCl_3$): 4.00 (6H, s), 7.12 (2H, s), 7.35 (2H, dd, J=6.9, 3.6 Hz), 7.69 (2H, dd, 2H, J=6.9, 3.6 Hz).

2) 6-Acetyl-2,3-dimethoxynaphthalene (**47**): $AlCl_3$ (39 g) was added in portions to a solution of **46** (14.0 g), and acetic anhydride (11.5 ml) in nitrobenzene (80 ml) at 0 °C. The mixture was stirred at 0 °C for 1 h and poured into ice water. The mixture was extracted with Et_2O and the extract was washed with water, aqueous $NaHCO_3$, and brine, and dried over $MgSO_4$. After evaporation of the solvent, **47** was collected by precipitation from AcOEt–hexane (7.1 g, 41%). IR (KBr) cm^{-1}: 1675, 1620, 1600. ^{1}H-NMR ($CDCl_3$): 2.59 (3H, s), 3.91 (6H, s), 7.00 (1H, s), 7.06 (1H, s), 7.52 (1H, d, J=9.0 Hz), 7.78 (1H, dd, J=9.0, 2.0 Hz), 8.15 (1H, d, J=2.0 Hz).

3) 6-Acetyl-2,3-dihydroxynaphthalene (**50**): The procedure used for the preparation of **43** was repeated with **47** (7.1 g) in CH_2Cl_2 (150 ml) and 1 M BBr_3 (123 ml), except that the reaction temperature was −40 to 0 °C. After the reaction, **50** was recrystallized from $CHCl_3$–hexane (3.5 g, 56%). mp 169—170.0 °C. IR (KBr) cm^{-1}: 3300, 1640, 1525. ^{1}H-NMR (DMSO-d_6): 2.62 (3H, s), 7.16 (1H, s), 7.30 (1H, s), 7.63 (1H, d, J=9.0 Hz), 7.70 (1H, dd, J=9.0, 2.0 Hz), 8.32 (1H, d, J=2.0 Hz), 9.81 (1H, OH), 10.00 (1H, OH).

6-*n*-Butyloyl-2,3-dihydroxynaphthalene (51) The procedure used for the preparation of **50** was repeated with **46** and butyric anhydride to obtain **51** (230 mg, 3% yield from **46**). mp 180—181 °C. IR (KBr) cm^{-1}: 3500, 3300, 1660, 1625, 1600. ^{1}H-NMR (DMSO-d_6): 0.95 (3H, t, J=7.5 Hz), 1.67 (2H, qt, J=7.5, 7.1 Hz), 3.05 (2H, t, J=7.1 Hz), 7.16 (1H, s), 7.30 (1H, s), 7.63 (1H, d, J=8.6 Hz), 7.70 (1H, dd, J=8.6, 1.5 Hz), 8.32 (1H, d, J=1.5 Hz) 9.79 (1H, OH), 9.97 (1H, OH).

6-*n*-Hexanoyl-2,3-dihydroxynaphthalene (52) The procedure used for the preparation of **50** was repeated with **46** and hexanoic anhydride to obtain **52** (230 mg, 4% yield from **46**). mp 173—174 °C. IR (KBr) cm^{-1}: 3480, 3290, 1665, 1625, 1595. ^{1}H-NMR (DMSO-d_6): 0.88 (3H, t, J=6.8 Hz), 1.2—1.8 (6H, m), 3.06 (2H, t, J=7.2 Hz), 7.16 (1H, s), 7.30 (1H, s), 7.63 (1H, d, J=8.7 Hz), 7.70 (1H, dd, J=8.7, 1.5 Hz), 8.32 (1H, d, J=1.5 Hz), 9.80 (1H, OH), 9.95 (1H, OH).

6-Ethyl-2,3-dihydroxynaphthalene (56) 1) 6-Ethyl-2,3-dimethoxynaphthalene (**53**): The procedure used for the preparation of **34** was repeated with **47** (1.0 g), 10% Pd/C (1.0 g), and 12 N HCl (2 ml) in dioxane (15 ml) to obtain **53** (850 mg, 91%). IR (KBr) cm^{-1}: 1605, 1510. ^{1}H-NMR ($CDCl_3$): 1.31 (3H, t, J=7.6 Hz), 2.77 (2H, q, J=7.6 Hz), 3.99 (6H, s), 7.08 (1H, s), 7.09 (1H, s), 7.21 (1H, dd, J=8.3, 1.7 Hz), 7.49 (1H, d, J=1.7 Hz), 7.61 (1H, d, J=8.3 Hz).

2) 6-Ethyl-2,3-dihydroxynaphthalene (**56**): The procedure used for the preparation of **50** was repeated with **53** (600 mg) in CH_2Cl_2 (20 ml) and 1 M BBr_3 (5.5 ml) to obtain **56** (340 mg, 65%). mp 148—149.5 °C. IR (KBr) cm^{-1}: 3400, 1605, 1520. ^{1}H-NMR (DMSO-d_6): 1.21 (3H, t, J=7.6 Hz), 2.66 (2H, q, J=7.6 Hz), 7.03 (1H, s), 7.05 (1H, s), 7.05 (1H, m), 7.34 (1H, m), 7.48 (1H, d, J=8.4 Hz), 9.39 (2H, OH).

6-*n*-Butyl-2,3-dihydroxynaphthalene (57) The procedure used for the preparation of **56** was repeated with **48** to obtain **57** (140 mg, 48% yield from **48**). mp 137.5—139 °C. IR (KBr) cm^{-1}: 3400, 1605, 1520. ^{1}H-NMR (DMSO-d_6): 0.90 (3H, t, J=7.3 Hz), 1.2—1.7 (4H, m), 2.63 (2H, t, J=7.7 Hz), 7.02 (1H, s), 7.04 (1H, s), 7.03 (1H, m), 7.33 (1H, m), 7.47 (1H, d, J=8.4 Hz), 9.36 (1H, OH), 9.41 (1H, OH).

6-*n*-Hexyl-2,3-dihydroxynaphthalene (58) The procedure used for the preparation of **56** was repeated with **49** to obtain **58** (120 mg, 28% yield from **49**). mp 138.5—139.5 °C. IR (KBr) cm^{-1}: 3300, 1610, 1520. ^{1}H-NMR (DMSO-d_6): 0.85 (3H, t, J=6.6 Hz), 1.2—1.7 (8H, m), 2.62 (2H, t, J=7.7 Hz), 7.02 (1H, s), 7.04 (1H, s), 7.03 (1H, m), 7.32 (1H, m), 7.46 (1H, d, J=8.4 Hz), 9.39 (2H, OH).

***N*-*n*-Butyl-6,7-dihydroxy-2-naphthamide (63)** 1) 6,7-Dimethoxy-2-naphthoic Acid (**59**): A solution of **47** (10.8 g) and sodium hypochlorite

solution (available chlorine, min. 5%, 120 ml) was stirred at 100—115 °C for 1 h. After being cooled to room temperature, the solution was washed with Et_2O and cooled to 0 °C. The solution was acidified with 12 N HCl to pH 2 and extracted with AcOEt. The organic layer was washed with water and brine, and dried over $MgSO_4$. After evaporation of the solvent, **59** was precipitated from AcOEt–hexane (7.2 g, 66%). IR (KBr) cm^{-1}: 2600, 1680, 1620. ^{1}H-NMR (DMSO-d_6, $CDCl_3$): 3.9 (6H, s), 7.11 (1H, s), 7.21 (1H, s), 7.58 (1H, d, J=9 Hz), 7.76 (1H, dd, J=9, 2 Hz), 8.3 (1H, d, J=2 Hz).

2) *N*-*n*-Butyl-6,7-dimethoxy-2-naphthamide (**60**): The procedure used for the preparation of **40** was repeated with **59** (740 mg) and *n*-butylamine. After the reaction, the mixture was extracted with $CHCl_3$ and the extract was concentrated under reduced pressure to give **60** (650 mg, 71%). IR (KBr) cm^{-1}: 3300, 1620, 1540. ^{1}H-NMR ($CDCl_3$): 0.98 (3H, t, J=6.5 Hz), 1.2—1.8 (4H, m), 3.51 (2H, m), 3.99 (3H, s), 4.01 (3H, s), 6.30 (1H, NH), 7.13 (1H, s), 7.16 (1H, s), 7.66 (1H, dd, J=8.5, 1.5 Hz), 7.72 (1H, d, J=8.5 Hz), 8.15 (1H, d, J=1.5 Hz).

3) *N*-*n*-Butyl-6,7-dihydroxy-2-naphthamide (**63**): The procedure used for the preparation of **50** was repeated with **60** (600 mg) in CH_2Cl_2 (20 ml) and 1 M BBr_3 (6.7 ml). After the reaction, the solution was extracted with AcOEt and the residue obtained was chromatographed on silica gel ($CHCl_3$–MeOH) and recrystallized from $CHCl_3$–MeOH to give **63** (320 mg, 59%). mp 193.5—194 °C. IR (KBr) cm^{-1}: 3500, 3400, 3050, 1620, 1600, 1540. ^{1}H-NMR (DMSO-d_6): 0.91 (3H, t, J=7.2 Hz), 1.2—1.8 (4H, m), 3.28 (2H, m), 7.14 (1H, s), 7.18 (1H, s), 7.55—7.65 (2H, m), 8.10 (1H, m), 8.38 (1H, t, J=5.6 Hz, NH), 9.71 (1H, OH), 9.79 (1H, OH).

***N*-*n*-Hexyl-6,7-dihydroxy-2-naphthamide (64)** The procedure used for the preparation of **63** was repeated with **59** and *n*-hexylamine to obtain **64** (180 mg, 27%). mp 181—181.5 °C. IR (KBr) cm^{-1}: 3500, 3150, 1615, 1595, 1520. ^{1}H-NMR (DMSO-d_6): 0.87 (3H, t, J=7.2 Hz), 1.2—1.8 (8H, m), 3.27 (2H, m), 7.14 (1H, s), 7.18 (1H, s), 7.55—7.65 (2H, m), 8.10 (1H, m), 8.38 (1H, t, J=5.6 Hz, NH), 9.71 (1H, OH), 9.79 (1H, OH).

***N*-*n*-Octyl-6,7-dihydroxy-2-naphthamide (65)** The procedure used for the preparation of **63** was repeated with **59** and *n*-octylamine to obtain **65** (90 mg, 14%). mp 186—187.5 °C. IR (KBr) cm^{-1}: 3500, 3350, 3150, 1615, 1595, 1520. ^{1}H-NMR (DMSO-d_6): 0.86 (3H, t, J=6.5 Hz), 1.2—1.8 (12H, m), 3.26 (2H, m), 7.14 (1H, s), 7.18 (1H, s), 7.55—7.65 (2H, m), 8.09 (1H, m), 8.38 (1H, t, J=5.6 Hz, NH), 9.70 (1H, OH), 9.78 (1H, OH).

6-Ethoxy-2,3-dihydroxynaphthalene (68) 1) 6-Acetyl-2,3-dibenzyloxynaphthalene (**66**): The procedure used for the preparation of **35** was repeated with **50** (6.3 g), benzyl bromide (9.2 ml), and K_2CO_3 (12.8 g) in DMF (50 ml) to give **66** (5.2 g, 44%). IR (KBr) cm^{-1}: 1660, 1610. ^{1}H-NMR ($CDCl_3$): 2.62 (3H, s), 5.23 (4H, s), 7.1—7.7 (14H, m), 8.17 (1H, m).

2) 6,7-Dibenzyloxy-2-naphthol (**67**): The procedure used for the preparation of **36** was repeated with **66** (2.9 g), *p*-toluenesulfonic acid (1.0 g), and *m*-CPBA (2.6 g) in CH_2Cl_2 (30 ml). After the reaction, the residue obtained was chromatographed on silica gel (AcOEt–hexane) to give **67** (580 mg, 21%). IR (KBr) cm^{-1}: 3300, 1625, 1600. ^{1}H-NMR ($CDCl_3$): 5.24 (2H, s), 5.26 (2H, s), 6.91 (1H, dd, J=8.7, 2.4 Hz), 6.97 (1H, d, J=2.4 Hz), 7.05 (1H, s), 7.15 (1H, s), 7.2—7.5 (11H, m).

3) 6-Ethoxy-2,3-dihydroxynaphthalene (**68**): The procedure used for the preparation of **37** was repeated with **67** (0.25 g) and 1-bromoethane to obtain **68** (35 mg, 24%). mp 131—132 °C. IR (KBr) cm^{-1}: 3350, 1610, 1525. ^{1}H-NMR (DMSO-d_6): 1.35 (3H, t, J=7.0 Hz), 4.05 (2H, q, J=7.0 Hz), 6.82 (1H, dd, J=8.8, 2.5 Hz), 7.00 (1H, s), 7.02 (1H, s), 6.98 (1H, m), 7.45 (1H, d, J=8.8 Hz), 9.2—9.5 (2H, OH).

6-*n*-Butoxy-2,3-dihydroxynaphthalene (69) The procedure used for the preparation of **68** was repeated with **67** and 1-bromobutane to obtain **69** (25 mg, 13%). mp 141.5—143 °C. IR (KBr) cm^{-1}: 3350, 1610, 1525. ^{1}H-NMR (DMSO-d_6): 0.95 (3H, t, J=7.3 Hz), 1.4—1.8 (4H, m), 3.99 (2H, t, J=6.5 Hz), 6.82 (1H, dd, J=8.8, 2.5 Hz), 7.00 (1H, s), 7.01 (1H, s), 7.00 (1H, m), 7.45 (1H, d, J=8.8 Hz), 9.4 (2H, OH).

6-*n*-Hexyloxy-2,3-dihydroxynaphthalene (70) The procedure used for the preparation of **68** was repeated with **67** and 1-bromohexane to obtain **70** (50 mg, 27%). mp 130.5—132 °C. IR (KBr) cm^{-1}: 3350, 1610, 1525. ^{1}H-NMR (DMSO-d_6): 0.88 (3H, t, J=6.8 Hz), 1.3—1.8 (8H, m), 3.98 (2H, t, J=6.5 Hz), 6.82 (1H, dd, J=8.8, 2.5 Hz), 7.00 (1H, s), 7.02 (1H, s), 6.99 (1H, m), 7.45 (1H, d, J=8.8 Hz), 9.4 (2H, OH).

Acknowledgments We thank the staff of the Central Research Laboratories, Green Cross Corporation, for their cooperation in the biological and analytical examinations.

References and Notes

1) *a*) J. M. Drazen, K. F. Austen, R. A. Lewis, D. A. Clark, G. Goto, A. Marfat, and E. J. Corey, *Proc. Natl. Acad. Sci. U.S.A.*, **77**, 4354 (1980); *b*) A. Ueno, K. Tanaka, and M. Katori, *Prostaglandins*, **23**, 865 (1982); *c*) P. J. Piper, L. G. Letts, M. N. Samhoun, J. R. Tippins, and M. A. Palmer, "Advances in Prostaglandin, Thromboxane and Leukotriene Research," Vol. 9, Raven Press, New York, 1982, p. 169; *d*) A. F. Welton, H. J. Crowley, D. A. Miller, and B. Yaremko, *Prostaglandins*, **21**, 287 (1981).
2) *a*) S. D. Brain, R. D. R. Camp, P. M. Dowd, A. K. Black, P. M. Woollard, A. I. Mallet, and M. W. Greaves, *Lancet*, ii, 762 (1982); *b*) M. W. Greaves, *Br. J. Dermatol.*, **109**, 115 (1983).
3) *a*) S. Barst and K. Mullane, *Eur. J. Pharmacol.*, **114**, 383 (1985); *b*) M. Nishida, T. Kuzuya, S. Hoshida, Y. Kim, T. Kamada, and M. Tada, *Circulation*, **76**, Supp IV-482 (1987).
4) Y. Koshihara, T. Neichi, S. Murota, P. Lao, and T. Tatsuno, *Biochim. Biophys. Acta*, **792**, 92 (1984).
5) M. Sugiura, Y. Naito, Y. Yamaura, C. Fukaya, and K. Yokoyama, *Chem. Pharm. Bull.*, **37**, 1039 (1989).
6) *a*) A. Fujinami and A. Mine, *Agric. Biol. Chem.*, **34**, 1157 (1970); *b*) A. Fujinami, A. Mine, and T. Fujita, *ibid.*, **38**, 1399 (1974).
7) T. Fujita, J. Iwasa, and C. Hansch, *J. Am. Chem. Soc.*, **86**, 5157 (1964).
8) C. Hansch and A. J. Leo, "Substituent Constants for Correlation Analysis in Chemistry and Biology," John Wiley and Sons, New York, 1979, pp. 13—63.
9) H. Kubinyi, *Arzneim.-Forsch.*, **29**, 1067 (1979).
10) C. Hansch and T. E. Klein, *Acc. Chem. Res.*, **19**, 392 (1986).
11) Y. Nakagawa, K. Izumi, N. Oikawa, T. Sotomatsu, M. Shigemura, and T. Fujita, *Environ. Toxicl. Chem.*, in press.
12) *a*) C. Kemal, P. Louis-Flamberg, R. Krupinski-Olsen, and A. L. Shorter, *Biochemistry*, **26**, 7064 (1987); *b*) K. Yasumoto, A. Yamamoto, and H. Mitsuda, *Agric. Biol. Chem.*, **34**, 1162 (1970); *c*) M. L. Hammond, I. E. Kopka, R. A. Zambias, C. G. Caldwell, J. Boger, F. Baker, T. Bach, S. Luell, and D. E. MacIntyre, *J. Med. Chem.*, **32**, 1006 (1989).
13) A. Verloop, in "Pesticide Chemistry, Human Welfare and the Environment," ed. by J. Miyamoto and P. C. Kearney, Vol. 1, Pergamon, Oxford, 1983, p. 339.
14) T. Yoshimoto, M. Furukawa, S. Tamamoto, T. Horie, and S. Kohno, *Biochem. Biophys. Res. Commun.*, **116**, 612 (1983).
15) K. Kano, K. Mori, B. Uno, T. Kubota, T. Ikeda, and M. Senda, *Bioelectrochem. Bioenerg.*, **23**, 227 (1990).

Synthesis and Structure–Activity Relationships of *N*-Substituted 2-[(2-Imidazolylsulfinyl)methyl]anilines as a New Class of Gastric H^+/K^+-ATPase Inhibitors

Tomio YAMAKAWA,*[,a] Hitoshi MATSUKURA,[a] Yutaka NOMURA,[a] Mitsuko YOSHIOKA,[a] Mitsuo MASAKI,[a] Hideki IGATA[b] and Susumu OKABE[b]

Research Laboratories, Nippon Chemiphar Co., Ltd.,[a] 1–22, Hikokawato, Misato, Saitama 341, Japan and Department of Applied Pharmacology, Kyoto Pharmaceutical University,[b] Misasagi, Yamashina, Kyoto 607, Japan. *Received December 14, 1990*

A series of *N*-substituted 2-[(2-imidazolylsulfinyl)methyl]anilines (3) was synthesized and evaluated for its biological activity against gastric H^+/K^+-ATPase prepared from rabbit stomach and gastric acid secretions in Heidenhain pouch dogs. Monoalkyl substituents on the nitrogen atom of the aniline moiety markedly inhibited the enzyme activity to the same degree as omeprazole, a representative H^+/K^+-ATPase inhibitor. Most of these compounds, administered at 3 mg/kg i.v. inhibited histamine-stimulated gastric acid secretion. The inhibitory activity of these derivatives on the enzymes at pH 6.0 was more potent than that at pH 7.4, and was distinctly correlated to stability in aqueous solution at pH 5.0.

Keywords 2-[(2-imidazolylsulfinyl)methyl]aniline; H^+/K^+-ATPase inhibitor; proton pump inhibitor; antisecretory effect; stability; structure–activity relationship

In recent years there has been considerable interest in gastric H^+/K^+-ATPase as the proton pump in parietal cells. This enzyme is responsible for the secretion of acid into the gastric lumen, and has thus been widely regarded as an important target for peptic ulcer therapy. Since the discovery of the enzyme inhibitors 2-[(2-benzimidazolylsulfinyl)-

TABLE I. *N*-Substituted 2-[(2-Imidazolylthio)methyl]anilines (**2**)

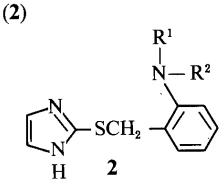

2

Compd. No.	R^1	R^2	Yield[a] (%)	Appearance	mp (°C)	HR-Mass Found	(Calcd)	^{1}H-NMR δ ($CDCl_3$), (J, Hz)
2a	H	H	81	Pale yellow powder	130—133	205.0677	(205.0674)	4.11 (2H, s), 6.4—7.1 (4H, m), 7.00 (2H, s)
2b	Me	H	66	White powder	173.5—175	219.0830	(219.0831)	2.84 (3H, s), 4.10 (2H, s), 6.3—7.2 (4H, m), 7.0 (2H, s)
2c	Me	Me	84	White powder	64—65	233.0986	(233.0987)	2.60 (6H, s), 4.22 (2H, s), 6.7—7.3 (6H, m)
2d	Et	H	100	Yellow powder	99.5—105	233.0989	(233.0987)	1.25 (3H, t, 7), 3.13 (2H, q, 7), 4.17 (2H, s), 6.3—7.3 (4H, m), 7.03 (2H, s)
2e	Me_2CH	H	59	Pale brown powder	125—126	247.1144	(247.1144)	1.19 (6H, d, 6), 3.4—3.8 (1H, m), 4.17 (2H, s), 6.3—7.2 (4H, m), 7.02 (2H, s)
2f	$Me(CH_2)_3$	H	71	White powder	95.5—97	261.1299	(261.1301)	0.7—1.8 (7H, m), 3.11 (2H, t, 7), 4.18 (2H, s), 6.3—7.2 (4H, m), 7.03 (2H, s)
2g	Me_2CHCH_2	H	94	White powder	106.5—107	261.1299	(261.1301)	0.88 (6H, d, 7), 1.84 (1H, m), 2.84 (2H, d, 7), 4.12 (2H, s), 6.2—7.1 (6H, m)
2h	$Me(CH_2)_4$	H	48	White powder	87	275.1457	(275.1457)	0.7—1.9 (9H, m), 3.11 (2H, t, 7), 4.19 (2H, s), 6.3—7.2 (4H, m), 7.03 (2H, s)
2i	$Me_2CHCH_2CH_2$	H	56	White powder	103—104	275.1455	(275.1457)	0.94 (6H, d, 6), 1.3—1.9 (3H, m), 3.13 (2H, t, 7), 4.19 (2H, s), 6.3—7.2 (4H, m), 7.03 (2H, s)
2j	Me_3CCH_2	H	43	White powder	127—128	275.1458	(275.1457)	1.00 (9H, s), 2.98 (2H, s), 4.20 (2H, s), 6.3—7.2 (4H, m), 7.02 (2H, s)
2k	$Me(CH_2)_5$	H	59	White powder	101	289.1617	(289.1614)	0.7—1.8 (11H, m), 3.10 (2H, t, 7), 4.18 (2H, s), 6.3—7.2 (4H, m), 7.03 (2H, s)
2l		H	61	White powder	93—97	259.1146	(259.1144)	0.1—0.4 (2H, m), 0.4—0.7 (2H, m), 0.8—1.3 (1H, m), 3.97 (2H, d, 7), 4.20 (2H, s), 6.4—7.3 (4H, m), 7.03 (2H, s)
2m		H	44	White powder	130—131.5	301.1616	(301.1614)	0.7—2.0 (11H, m), 2.97 (2H, d, 7), 4.20 (2H, s), 6.3—7.3 (4H, m), 7.03 (2H, s)
2n	$MeOCH_2CH_2$	H	88	Colorless prisms	73—74.5	263.1093	(263.1093)	3.44 (3H, s), 3.2—3.5 (2H, m), 3.6—3.8 (2H, m), 4.13 (2H, s), 6.4—7.2 (4H, m), 7.00 (2H, s)
2o	$EtOCH_2CH_2$	H	43	Pale yellow prisms	—[b]	—[b]	(277.1250)	1.22 (3H, t, 7), 3.37 (2H, t, 5), 3.61 (2H, q, 7), 3.78 (2H, t, 5), 4.13 (2H, s), 6.4—7.3 (4H, m), 6.99 (2H, s)
2p	$MeO(CH_2)_3$	H	66	Pale yellow oil		277.1252	(277.1250)	1.92 (2H, m), 3.23 (2H, t, 6), 3.32 (3H, s), 3.54 (2H, t, 6), 4.14 (2H, s), 6.3—7.2 (4H, m), 7.02 (2H, s)
2q	$Me_2CHOCH_2CH_2$	H	37	White powder	89.5—90.5	291.1406	(291.1406)	1.20 (6H, t, 6), 3.34 (2H, t, 5), 3.4—3.9 (3H, m), 4.12 (2H, s), 6.3—7.3 (4H, m), 6.98 (2H, s)
2r	$H_2C=CHCH_2$	H	79	White powder	103.5—105.5	245.0987	(245.0987)	3.76 (2H, dt, 2, 5), 4.19 (2H, s), 5.0—5.4 (2H, m), 5.6—6.1 (1H, m), 6.4—7.2 (4H, m), 7.04 (2H, s)
2s	$HC\equiv CCH_2$	H	71	Pale yellow powder	122—124	243.0831	(243.0831)	2.30 (1H, t, 2), 3.99 (2H, d, 2), 4.13 (2H, s), 6.5—7.3 (4H, m), 7.01 (2H, s)[c]
2t	$PhCH_2$	H	61	White powder	113—115	295.1141	(295.1144)	4.23 (2H, s), 4.36 (2H, s), 6.4—7.6 (11H, m)
2u	Thenyl	H	69	White powder	121—122	301.0707	(301.0708)	4.20 (2H, s), 4.55 (2H, s), 6.4—7.3 (7H, m), 6.95 (2H, s)
2v	Ph	H	68	Yellow prisms	126—128	281.0982	(281.0987)	4.23 (2H, s), 6.6—7.3 (9H, m), 7.03 (2H, s)

a) Yields from alcohol (**1**) to sulfide (**2**) have not been optimized. *b*) Melting point and HR-Mass for this compound was not determined. *c*) $CDCl_3 : CD_3OD = 3 : 1$.

TABLE II. *N*-Substituted 2-[(2-Imidazolylsulfinyl)methyl]anilines (**3**): Synthesis

Compd. No.	Method[a]	Yield[b] (%)	Appearance	Recrystn.[c] solv.	mp[d] (°C)	IR ν cm^{-1} (S→O)	Formula	Analysis (%) Found (Calcd) C	H	N	^{1}H-NMR δ (J, Hz)	Solvent[e]
3a	A	13	Pale brown powder	a	170—172	1035	$C_{10}H_{11}N_3OS$	54.45 (54.28)	4.84 5.01	18.88 18.99)	4.44 (2H, s), 5.16 (2H, br), 6.2—7.1 (4H, m), 7.26 (2H, s)	B
3b	A	66	Pale yellow prisms	a	168	1040	$C_{11}H_{13}N_3OS$	56.33 (56.15	5.47 5.57	17.71 17.86)	2.67 (3H, s), 4.37 (1H, d, 14), 4.52 (1H, d, 14), 5.60 (1H, br), 6.2—7.6 (6H, m)	C
3c	A	44	Colorless prisms	a	115—117	1005	$C_{12}H_{15}N_3OS$	57.78 (57.81	6.22 6.06	16.59 16.85)	2.66 (6H, s), 4.50 (1H, d, 12), 4.73 (1H, d, 12), 6.8—7.4 (4H, m), 7.22 (2H, s)	A
3d	B	82	Yellow prisms	b	145—146.5	995	$C_{12}H_{15}N_3OS$	57.65 (57.81	5.91 6.06	16.86 16.85)	1.27 (3H, t, 7), 3.11 (2H, q, 7), 4.32 (1H, d, 14), 4.52 (1H, d, 14), 6.4—7.3 (4H, m), 7.23 (2H, s)	B
3e	B	61	Pale brown powder	c	130—132	1040	$C_{13}H_{17}N_3OS$	59.22 (59.29	6.54 6.51	15.86 15.96)	1.21 (6H, d, 6), 3.60 (1H, m), 4.24 (1H, d, 14), 4.51 (1H, d, 14), 6.4—7.3 (4H, m), 7.21 (2H, s)	B
3f	A	46	Pale brown powder	a	136—139	1040	$C_{14}H_{19}N_3OS$	60.32 (60.62	6.98 6.90	14.97 15.15)	0.98 (3H, t, 6), 1.2—1.9 (4H, m), 3.07 (2H, t, 6), 4.29 (1H, d, 14), 4.52 (1H, d, 14), 6.4—7.3 (4H, m), 7.23 (2H, s)	B
3g	A	57	Colorless prisms	a	132—133	1020	$C_{14}H_{19}N_3OS$	60.47 (60.62	6.87 6.90	15.25 15.15)	1.02 (6H, d, 7), 1.94 (1H, m), 2.90 (2H, d, 7), 4.32 (1H, d, 13), 4.54 (1H, d, 13), 6.4—7.3 (4H, m), 7.24 (2H, s)	B
3h	B	63	White powder	a	137—138	1040	$C_{15}H_{21}N_3OS$	61.76 (61.82	7.22 7.26	14.52 14.42)	0.8—1.9 (9H, m), 3.06 (2H, t, 7), 4.31 (1H, d, 14), 4.52 (1H, d, 14), 6.4—7.3 (4H, m), 7.24 (2H, s)	B
3i	A	55	Pale brown powder	a	150—151	995	$C_{15}H_{21}N_3OS$	61.92 (61.82	7.25 7.26	14.17 14.42)	0.98 (6H, d, 6), 1.4—2.0 (3H, m), 3.08 (2H, t, 7), 4.31 (1H, d, 14), 4.53 (1H, d, 14), 6.4—7.3 (4H, m), 7.24 (2H, s)	B
3j	A	41	Pale yellow powder	d	133	1005	$C_{15}H_{21}N_3OS$	61.90 (61.82	7.35 7.26	14.28 14.42)	0.99 (9H,s), 2.79 (2H, d, 6), 4.25 (1H, d, 14), 4.62 (1H, d, 14), 6.4—7.3 (6H, m)	A
3k	B	69	White powder	c	151—154	1035	$C_{16}H_{23}N_3OS$	63.10 (62.92	7.52 7.59	13.55 13.76)	0.7—1.9 (11H, m), 3.06 (2H, t, 7), 4.30 (1H, d, 14), 4.53 (1H, d, 14), 6.4—7.3 (4H, m), 7.23 (2H, s)	B
3l	A	58	Pale yellow powder	c	138—138.5	1020	$C_{14}H_{17}N_3OS$	61.11 (61.06	6.27 6.22	15.13 15.26)	0.1—0.7 (4H, m), 0.9—1.2 (1H, m), 2.92 (2H, d, 7), 4.32 (1H, d, 14), 4.56 (1H, d, 14), 6.4—7.3 (4H, m), 7.22 (2H, s)	A
3m	B	46	White powder	c	145—146	1010	$C_{17}H_{23}N_3OS$	64.34 (64.32	7.47 7.30	13.06 13.24)	0.8—2.0 (11H, m), 2.91 (2H, d, 6), 4.25 (1H, d, 14), 4.53 (1H, d, 14), 6.4—7.3 (4H, m), 7.22 (2H, s)	B
3n	B	50	Colorless prisms	c	126—128	1000	$C_{13}H_{17}N_3O_2S$	55.93 (55.89	6.10 6.13	14.88 15.04)	3.0—3.4 (2H, m), 3.34 (3H, s), 3.44—3.70 (2H, m), 4.26 (1H, d, 14), 4.56 (1H, d, 14), 6.4—7.3 (6H, m)	B
3o	B	52	White powder	c	119—121	1040	$C_{14}H_{19}N_3O_2S$	57.19 (57.31	6.59 6.53	14.16 14.32)	1.24 (3H, t, 7), 3.28 (2H, t, 5), 3.59 (2H, q, 7), 3.69 (2H, t, 5), 4.31 (1H, d, 13), 4.53 (1H, d, 13), 6.4—7.3 (6H, m)	B
3p	A	31	Yellow prisms	d	100—107	1000	$C_{14}H_{19}N_3O_2S$	57.25 (57.31	6.44 6.53	14.54 14.32)	1.7—2.0 (2H, m), 2.9—3.2 (2H, m), 3.33 (3H, s), 3.49 (2H, t, 6), 4.24 (1H, d, 14), 4.54 (1H, d, 14), 6.4—7.3 (6H, m)	A
3q	B	76	White powder	c	140—142	1035	$C_{15}H_{21}N_3O_2S$	58.85 (58.61	6.94 6.89	13.33 13.67)	1.21 (6H, d, 6), 3.26 (2H, t, 5), 3.5—3.8 (3H, m), 4.31 (1H, d, 14), 4.54 (1H, d, 14), 6.4—7.3 (4H, m), 7.21 (2H, s)	B
3r	A	46	Colorless prisms	e	139	1000	$C_{13}H_{15}N_3OS$	59.90 (59.75	5.63 5.79	16.03 16.08)	3.72 (2H, d, 6), 4.31 (1H, d, 14), 4.53 (1H, d, 14), 4.9—5.4 (2H, m), 5.7—6.2 (1H, m), 6.4—7.4 (4H, m), 7.21 (2H, s)	B
3s	A	37	Pale yellow powder	c	158—159	1025	$C_{13}H_{13}N_3OS$	60.16 (60.21	4.91 5.05	15.99 16.20)	2.32 (1H, t, 3), 3.99 (2H, d, 3), 4.29 (1H, d, 13), 4.53 (2H, d, 13), 6.5—7.3 (4H, m), 7.22 (2H, s)	B
3t	A	43	Pale brown powder	a	135—138	1030	$C_{17}H_{17}N_3OS$	65.77 (65.57	5.48 5.50	13.63 13.49)	4.32 (2H, d, 6), 4.57 (2H, s), 6.2—7.5 (11H, m)	C
3u	A	72	White powder	f	137—139	1020	$C_{15}H_{15}N_3OS_2$	56.67 (56.76	4.47 4.76	13.00 13.24)	4.35 (1H, d, 14), 4.56 (1H, d, 14), 4.51 (2H, s), 6.4—7.3 (9H,m)	B
3v	A	42	Pale yellow powder	c	133—135	1025	$C_{16}H_{15}N_3OS$	63.87 (64.62	5.25 5.08	14.07 14.13)	4.33 (1H, d, 14), 4.62 (1H, d, 14), 6.6—7.4 (11H, m)	A

a) Method A: *m*-CPBA oxidation, method B: H_2O_2/NH_4VO_3 oxidation. *b*) Yields from sulfide have not been optimized. *c*) a, this compound was crystallized with addition of aqueous NH_4Cl solution to the NaOH solution of this compound; b, dichloromethane–ethanol; c, chloroform–ether; d, acetonitrile–ether; e, chloroform–acetonitrile; f, chloroform–hexane. *d*) Compounds decompose on melting; clearly defined melting points are not always obtainable. *e*) As the solvent of ^{1}H-NMR: A: $CDCl_3$, B: $CDCl_3/CD_3OD$, C: DMSO-d_6.

methyl]pyridines, represented by omeprazole,[1] there have been reports of many analogues with benzimidazole and pyridine moieties.[2]

In the replacement of the pyridine ring with other heterocycles, we previously reported the biochemical and pharmacological activities of *N*,*N*-dimethyl-2-[(2-benzimidazolylsulfinyl)methyl]anilines (NC-1300)[3] and *N*,*N*-dimethyl-2-[[2-(5-methoxy)benzimidazolylsulfinyl]-methyl]anilines (NC-1300-B)[4]; and Adelstein also reported those of *N*-unsubstituted 2-[[2-(5-methoxy)benzimidazolylsulfinyl]methyl]anilines.[5]

To obtain more potent compounds, we replaced the benzimidazole ring of NC-1300 with many other heterocycles. The fact that aniline (pK_a 4.60) is less basic than pyridine (pK_a 5.22) drew our attention to the imidazole ring (pK_a 6.95), which is a more basic heterocycle than benzimidazole (pK_a 5.48) coupled with the aniline ring.

In this paper, we report the synthesis and the pharmacological activities of *N*-substituted 2-[(2-imidazolylsulfinyl)methyl]anilines (**3**) as a new class of potent inhibitors of gastric H^+/K^+-ATPase. We also discuss the relationships between H^+/K^+-ATPase inhibitory activity (pH 6.0 and 7.4), antisecretory effects and stability in aqueous solutions (pH 3.0, 5.0, 7.0).

Synthesis *N*-Substituted 2-chloromethylaniline hydrochloride derivatives prepared by the chlorination of corresponding benzyl alcohols (**1**) with $SOCl_2$ in methylenechloride or gaseous HCl in ethanol were unstable and used without isolation. Condensation of 2-mercaptoimidazole with *N*-substituted 2-chloromethylanilines under neutral or acidic conditions gave the corresponding sulfides (**2**). The condensation reaction was carried out in ethanol and the sulfides (**2**) were isolated as the free bases by neutralization of the resultant hydrochlorides with aqueous Na_2CO_3 followed by extraction with chloroform or methylenechloride, as summarized in Table I.

Oxidation of the sulfides (**2**) with *m*-chloroperbenzoic acid (*m*-CPBA) in chloroform or methylenechloride at 0 °C gave sulfoxides (**3**) (method A). As an alternative method, sulfide was oxidized using H_2O_2 catalyzed by NH_4VO_3 in a mixed solvent (CH_2Cl_2–MeOH–AcOH) (method B). In the latter

TABLE III. *N*-Substituted 2-Aminobenzyl Alcohol (**1**)

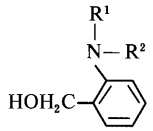

Compd. No.	R^1	R^2	Method	Yield	
				Step 1	Step 2
1b	Me	H	—	—[a]	100
1c	Me	Me	—	—[a]	100
1d	Et	H	D	100	80
1e	Me_2CH	H	D	66	100
1f	$Me(CH_2)_3$	H	C	95	100
1g	Me_2CHCH_2	H	D	77	100
1h	$Me(CH_2)_4$	H	C	82	59
1i	$Me_2CHCH_2CH_2$	H	C	100	66
1j	Me_3CCH_2	H	C	98	95
1k	$Me(CH_2)_5$	H	C	97	97
1l		H	C	62	41
1m		H	C	55	97
1n	$MeOCH_2CH_2$	H	C	81	41
1o	$EtOCH_2CH_2$	H	C	100	90
1p	$MeO(CH_2)_3$	H	C	37	94
1q	$Me_2CHOCH_2CH_2$	H	C	68	100
1t	$PhCH_2$	H	C	91	99
1u	Thenyl	H	C	56	29

a) Starting compound is commercially available.

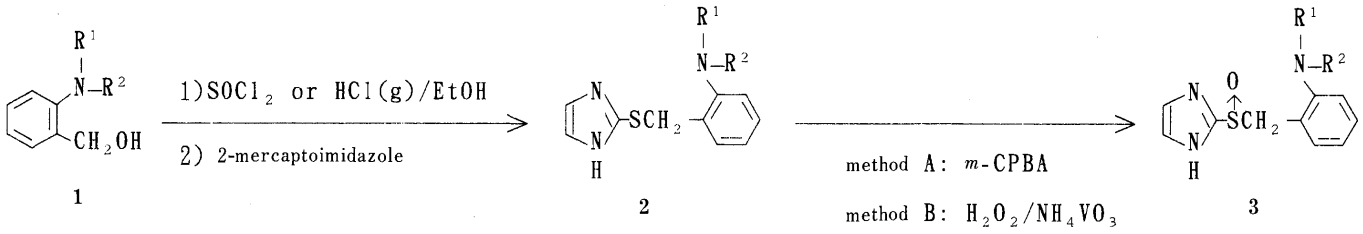

Chart 1

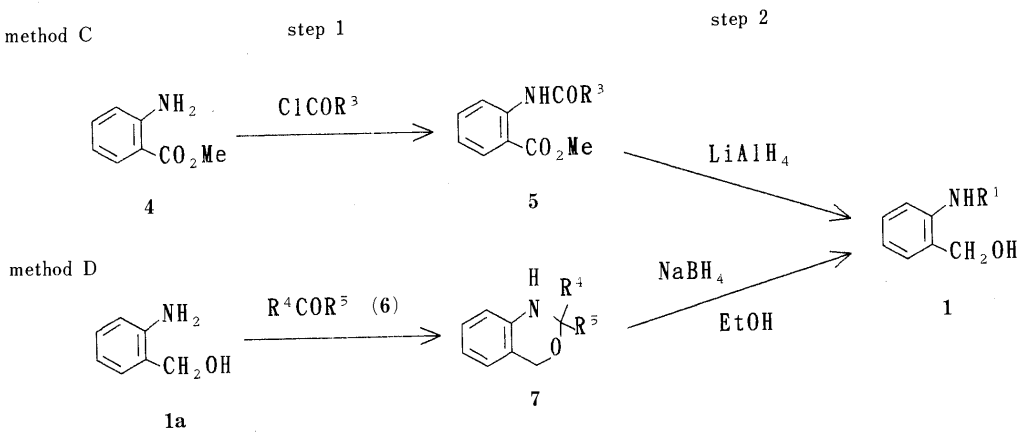

Chart 2

4 8 1r (19%) 1s (41%)

Chart 3

TABLE IV. *N*-Substituted 2-[(2-Imidazolylsulfinyl)methyl]anilines (**3**): Activity and Stability

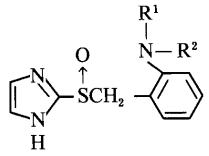

3

Group	Compd. No.	R^1	R^2	H^+/K^+ ATPase IC_{50} (μM)		Heidenhain pouch dog inhibn. at i.v.	$T_{1/2}$ (h)		
				pH 6.0	pH 7.4	% (3 mg/kg)	pH 3.0	pH 5.0	pH 7.0
I	**3a**	H	H	>100	>100	NE	—	—	—
	3b	Me	H	2.8	44	82	0.04	0.93	35.1
	3c	Me	Me	29	>100	NE	—	—	—
II	**3d**	Et	H	14	100	80	0.06	1.07	41.2
	3e	Me_2CH	H	10	>100	66	0.07	0.88	52.0
	3f	$Me(CH_2)_3$	H	5.2	23	92	0.04	0.76	29.0
	3g	Me_2CHCH_2	H	12	100	81	0.03	0.93	63.0
	3h	$Me(CH_2)_4$	H	19	96	86	0.04	0.93	60.3
	3i	$Me_2CHCH_2CH_2$	H	4.4	19	93	0.04	0.94	62.5
	3j	Me_3CCH_2	H	6.8	63	95	0.02	0.81	51.6
	3k	$Me(CH_2)_5$	H	8.4	>100	NE	0.04	0.99	55.3
	3l		H	6.2	18	52	0.07	1.34	61.8
	3m		H	8.6	98	77	0.02	0.83	45.0
III	**3n**	$MeOCH_2CH_2$	H	43	>100	89	0.15	4.60	175.0
	3o	$EtOCH_2CH_2$	H	22	53	98	0.16	4.00	65.4
	3p	$MeO(CH_2)_3$	H	13	60	92	0.07	1.77	50.9
	3q	$Me_2CHOCH_2CH_2$	H	46	>100	97	0.11	4.58	179.5
IV	**3r**	$H_2C=CHCH_2$	H	18	40	94	0.08	2.88	106.3
	3s	$HC\equiv CCH_2$	H	>100	140	70	1.03	79.1	155.9
	3t	$PhCH_2$	H	100	>100	57	0.14	8.16	180.6
	3u	Thenyl	H	>100	80	49	0.28	27.7	94.4
	3v	Ph	H	>100	>100	NE	7.53	54.1	46.6
	Omeprazole			3.8	54	95	0.05	0.34	27.1
	NC-1300			6.6	20	22	0.06	0.26	3.8

NE, not effective.

oxidation method, the formation of by-products was minor or not observed except for the corresponding sulfone. The sulfones were removed by washing the reaction mixture with a dilute aqueous alkaline solution. Sulfoxides were purified by extraction with 1 N NaOH followed by the addition of aqueous NH_4Cl solution. This purification method is critical as these sulfoxides are unstable under acidic solutions. The yield and chemical data of sulfoxides (**3**) are summarized in Table II.

2-Mercaptoimidazole was synthesized by a previously reported method.[6] *N*-Substituted 2-aminobenzyl alcohols (**1**) were also synthesized by accepted or modified methods. Alkyl groups were introduced into the aniline nitrogen atom by the acylation of methyl anthranilate (**4**), followed by the reduction of the resultant amide with $LiAlH_4$ (method C) or the cyclization of 2-aminobenzyl alcohol (**1a**) with aldehydes or ketones (**6**)[7] and subsequent reduction of the resultant benzoxazine derivatives (**7**) with $NaBH_4$ in ethanol (method D) as shown in Chart 2. The yield of the synthesis of **1** is summarized in Table III.

N-Allyl and *N*-propargyl derivatives (**1r** and **1s**) were synthesized by the pathway shown in Chart 3. Reduction with $LiAlH_4$ of *N*-propargyl derivative (**8**) prepared by the condensation of methyl anthranilate (**4**) and propargyl bromide gave the mixture of **1r** (19%) and **1s** (41%).

Results and Discussion

Three 2-[(2-imidazolylsulfinyl)methyl]anilines in which the nitrogen atoms of aniline moiety were unsubstituted (**3a**) and substituted with either a monomethyl (**3b**) or a dimethyl group (**3c**) were initially synthesized and evaluated for inhibitory activity against gastric H^+/K^+-ATPase prepared from rabbit stomach. A significant difference was found in the inhibitory activities between the three compounds shown as group I in Table IV. The *N*-methyl compound (**3b**) had potent inhibitory activity similar to

that of omeprazole or NC-1300, while the activity of the *N*,*N*-dimethyl derivative (**3c**) was one tenth that of **3b**, whereas the *N*-unsubstituted compound (**3a**) showed only a very weak inhibitory effect.

The inhibitory effects of these compounds against histamine-stimulated gastric acid secretion were also evaluated *in vivo* with Heidenhain pouch dogs by intravenous administration (3 mg/kg). The *N*-methyl compound (**3b**) showed a potent effect but the other two compounds were inactive.

On the basis of these results, a variety of *N*-monosubstituted derivatives were then synthesized and evaluated for H^+/K^+-ATPase inhibitory activity. Compounds investigated were classified into groups depending upon the type of substituent at the nitrogen atom of the aniline moiety: alkyl substituent group (II), alkoxyalkyl substituent group (III), and the π-electron-possessing substituent group (IV), as shown in Table IV.

Group II and III compounds all inhibited H^+/K^+-ATPase at pH 6.0, while group IV compounds had little or no inhibitory activity, with the exception of the *N*-allyl derivative (**3r**).

The pH dependent stability of omeprazole analogous in an aqueous solution serves as a model for the rate of activation essential for H^+/K^+-ATPase inhibition at low pH and for undesired reactions with other enzymes, such as Na^+/K^+-ATPase, under neutral conditions.[8] Accordingly, the stability of these new compounds in aqueous solution was measured at pH 7.0, 5.0 and 3.0. Half-lives of the compounds in the respective solutions are also listed in Table IV. All compounds synthesized were very stable in an aqueous solution at pH 7.0 but unstable at pH 3.0. The stability at pH 5.0 differed markedly depending on the compound.

The compounds with potent inhibitory activity against H^+/K^+-ATPase had half-lives of less than 5 h in an aqueous solution at pH 5.0. In contrast, compounds with little or no activity on the enzyme were stable in aqueous solution at pH 5.0 and the half-lives were more than 8 h. The *N*-allyl derivative (**3r**) had a half-life of 2.88 h, while other group IV compounds were very stable. The half-lives of group II or III compounds in aqueous solution at pH 5.0 were correlated with the potency of *in vitro* H^+/K^+-ATPase inhibitory activity at pH 6.0 as shown in Fig. 1 ($r=0.89$, $p<0.001$).

The compounds with shorter half-lives had highly potent H^+/K^+-ATPase inhibitory activity at pH 6.0. Most compounds with an IC_{50} against H^+/K^+-ATPase inhibitory activity of less than 10 μM, had half-lives of less than 1 h at pH 5.0, except **31**, whose IC_{50} was 6.2 μM despite a half-life of 1.34 h. The data for the group II compounds are consistent with that of omeprazole and NC-1300.

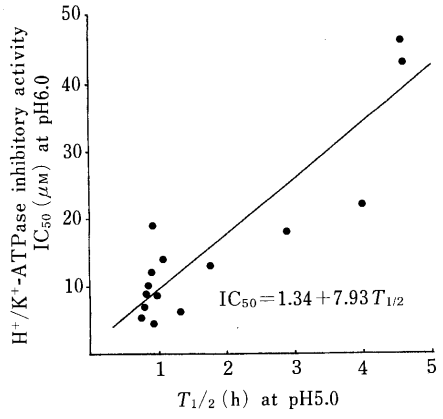

Fig. 1. Correlation of IC_{50} (pH 6.0) and $T_{1/2}$ (pH 5.0) for **3d**—**3r**
$r=0.89$, $p<0.001$.

Most group II and III compounds had good inhibitory effects against gastric acid secretion by intravenous administration (3 mg/kg), with the exception of the *n*-hexyl derivative (**3k**), although the potency differed somewhat depending on the compound. The difference in the potency of *in vivo* inhibitory activity against gastric acid secretion might be due to membrane permeability of the compounds or the ability of the compounds to reach the acidic compartments of the parietal cell.[9]

It is notable that compounds **3s**, **3t** and **3u** of group IV had moderate inhibitory effects against gastric acid secretion, whereas **3v** had no inhibitory effect. These compounds were very stable in aqueous solution at pH 5.0 and had little or no inhibitory effect in H^+/K^+-ATPase activity at pH 6.0.

Omeprazole is transformed under acidic conditions to give an active inhibitor, a cyclic sulfenamide.[10] An analogous mechanism of the inhibitory effect of H^+/K^+-ATPase activity for the new imidazole derivatives is suggested, based on the fact that the H^+/K^+-ATPase inhibitory activity of each compound at pH 6.0 was always more potent than that at pH 7.4 and that the lower stability in a solution at pH 5.0 was in proportion to higher inhibitory activity.

The *in vivo* inhibitory effect of **3s**, **3t** and **3u** against gastric acid secretion may be due to transformation into an active form under more acidic conditions in the parietal cell. In fact, **3s**, **3t** and **3u** were very unstable at pH 3.0 whereas **3v** was stable even at pH 3.0, as shown in Table IV.

These results show that *N*-alkyl or *N*-alkoxyalkyl 2-[(2-imidazolylsulfinyl)methyl]anilines in group II or III comprise a new class of H^+/K^+-ATPase inhibitors and that some of them might be candidates for antisecretory agents.

Experimental

Melting points determined with a Yamato MP-21 apparatus were uncorrected. Infrared (IR) spectra were recorded on a Hitachi 260-50 spectrometer. Nuclear magnetic resonance (NMR) spectra were recorded on a JEOL JNM-FX90Q NMR spectrometer with tetramethylsilane as the internal standard. High resolution mass spectra (MS) were obtained on a JEOL JMS-SX102 mass spectrometer. Elemental analyses (C, H, N) were performed on a Heraus C,H,N-Rapid instrument.

2-Aminobenzyl alcohol (**1a**) was commercially available. 2-Methylaminobenzyl alcohol (**1b**), 2-dimethylaminobenzyl alcohol (**1c**), and 2-phenylaminobenzyl alcohol (**1v**) were prepared by the reduction with $LiAlH_4$ of the corresponding benzoates which were commercially available.

Preparation of *N*-Substituted 2-Aminobenzyl Alcohol by Method C Step 1: Trimethylacetyl chloride (10.8 g, 89.6 mmol) and 12.3 g (89.6 mmol) of K_2CO_3 were added to a solution of 12.2 g (80.6 mmol) of methyl anthranilate (**4**) in 100 ml of benzene. The mixture was heated under reflux overnight, then cooled and poured into cold water (about 0 °C). The benzene layer was separated, washed with 6 N HCl and $NaHCO_3$ solution, dried over anhydrous Na_2SO_4, and evaporated *in vacuo* to yield 18.6 g (98%) of methyl *N*-trimethylacetylanthranilate (**5j**) as a pale brown oil. ^{1}H-NMR ($CDCl_3$) δ: 1.35 (9H, s), 3.92 (3H, s), 7.04 (1H, dt, $J=1$, 8 Hz), 7.52 (2H, dt, $J=2$, 8 Hz), 8.02 (1H, dd, $J=2$, 8 Hz), 8.77 (1H, dd, $J=1$, 8 Hz). Exact MS *m/z* Calcd for $C_{13}H_{17}NO_3$: 235.1209. Found: 235.1207.

Step 2: A solution of 10.0 g (42.6 mmol) of **5j** in 20 ml of dry tetrahydrofuran (THF) (Al_2O_3) was added dropwise to a suspension of

3.2 g (85.2 mmol) of $LiAlH_4$ in 100 ml of dry THF (Al_2O_3) at 0 °C during a period of over 30 min. The mixture was then stirred for 30 min and heated under reflux for 1 h. The reaction mixture was cooled and saturated aqueous Na_2SO_4 was added dropwise at 0 °C. After Et_2O (100 ml) was added to the mixture, the precipitate was filtered and the filtrate was evaporated *in vacuo* to yield 7.8 g (95%) of 2-neopentylaminobenzyl alcohol (**1j**) as a pale yellow oil. ^{1}H-NMR ($CDCl_3$) δ: 1.02 (9H, s), 2.90 (2H, s), 4.63 (2H, s), 6.5—7.3 (4H, m). Exact MS *m/z* Calcd for $C_{12}H_{19}NO$: 193.1468. Found: 193.1469.

Compounds **1f**, **h**, **i**, **k**—**q**, **t** and **u** were obtained by a similar procedure to that described for **1j**. The yields are listed in Table III.

Preparation of *N*-Substituted 2-Aminobenzyl Alcohol by Method D Step 1: Isobutylaldehyde (19.8 g, 275 mmol) and 12.3 g of $CaCl_2$ were added to 24.6 g (200 mmol) of 2-aminobenzyl alcohol (**1a**) in 123 ml of CH_2Cl_2. The mixture was stirred for 1 h and the precipitate was filtered through celite. The filtrate was evaporated *in vacuo* and the residue was crystallized by the addition of 75 ml of hexane to yield 27.0 g (77%) of 1,2-dihydro-2-isopropyl-4*H*-3,1-benzoxazine (**7g**) as a pale brown solid. ^{1}H-NMR ($CDCl_3$) δ: 1.05 (6H, d, J=7 Hz), 1.7—2.1 (1H, m), 3.84 (1H, br), 4.2—4.4 (1H, m), 4.76 (1H, d, J=14 Hz), 4.95 (1H, d, J=14 Hz), 6.5—7.2 (4H, m). IR (KBr): 3290, 1580, 1480, 1250, 1080, 1040, 1020, 980, 885, 745 cm^{-1}. *Anal.* Calcd for $C_{11}H_{15}NO$: C, 74.54; H, 8.53; N, 7.90%. Found: C, 74.36; H, 8.78; N, 8.05.

Step 2: Sodium borohydride (14.45 g, 380 mmol) was added in four portions over 4 h to a solution of 27.0 g (152 mmol) of 1,2-dihydro-2-isopropyl-4*H*-3,1-benzoxazine (**7g**) in 189 ml of EtOH and 81 ml of toluene. After the reaction was complete, the solvent was evaporated *in vacuo* and 20% aqueous NH_4Cl was added to the residue at 0 °C. A separated oil was extracted with ether and the ether layer was dried over anhydrous Na_2SO_4. Evaporation of the solvent yielded 27.2 g (100%) of 2-isobutylaminobenzyl alcohol (**1g**) as a pale brown oil. ^{1}H-NMR ($CDCl_3$) δ: 0.96 (6H, d, J=7 Hz), 1.6—2.1 (1H, m), 2.90 (2H, d, J=7 Hz), 4.52 (2H, s), 6.4—7.3 (4H, m). Exact MS *m/z* Calcd for $C_{11}H_{17}NO$: 179.1311. Found: 179.1311.

Compounds **1d** and **1e** were obtained by a procedure similar to that described for **1g**. The yields are listed in Table III.

Methyl *N*-Propargylanthranilate (8) A mixture of 45.6 g (303 mmol) of methyl anthranilate (**4**) and 18 g (151 mmol) of propargyl bromide in 50 ml of MeOH was heated under reflux for 40 h. The solvent was evaporated and 500 ml of Et_2O was added to the residue. Insoluble solid was filtered and the filtrate was washed with 30 ml of 1 N HCl and with 30 ml of 1 N NaOH. The extract was dried over Na_2SO_4, and concentrated *in vacuo*. The residue was crystallized by the addition of hexane (150 ml), collected by filtration and washed with cold hexane to yield 20.4 g (35%) of methyl *N*-propargylanthranilate (**8**) as a yellow solid. ^{1}H-NMR ($CDCl_3$) δ: 2.21 (1H, t, J=2 Hz), 3.85 (3H, s), 4.02 (2H, dd, J=2, 6 Hz), 6.5—8.0 (4H, m). *Anal.* Calcd for $C_{11}H_{11}NO_2$: C, 69.80; H, 5.86; N, 7.40%. Found; C, 69.73; H, 5.96; N, 7.70%.

2-Allylaminobenzyl Alcohol (1r) and 2-Propargylaminobenzyl Alcohol (1s) A solution of 5.0 g (26.4 mmol) of methyl *N*-propargylanthranilate (**8**) in 20 ml of dry THF (Al_2O_3) was added over 30 min under 0 °C to a suspension of 1.0 g of $LiAlH_4$ in 50 ml of dry THF (Al_2O_3) which was then cooled to −5 °C. After additional stirring for 30 min, a saturated aqueous Na_2SO_4 was added dropwise. The precipitate was filtered and the filtrate concentrated *in vacuo*. Column chromatography on silicagel (Et_2O : hexane = 5 : 2) of the residue yielded 0.8 g (19%) of 2-allylaminobenzyl alcohol (**1r**) as a colorless oil and 1.73 g (41%) of 2-propargylaminobenzyl alcohol (**1s**) as a white solid. ^{1}H-NMR ($CDCl_3$) for **1r**; δ: 1.7 (1H, br), 3.80 (2H, dt, J=2, 5 Hz), 4.64 (2H, s), 5.0—5.4 (2H, m), 5.7—6.2 (1H, m), 6.7—7.3 (4H, m). Exact MS *m/z* Calcd for $C_{10}H_{13}NO$: 163.0998. Found: 163.1002. ^{1}H-NMR ($CDCl_3$) for **1s**; δ: 1.84 (1H, br), 2.19 (1H, t, J=3 Hz), 3.93 (2H, d, J=3 Hz), 4.60 (2H, s), 5.0 (1H, br), 6.5—7.4 (4H, m). *Anal.* Calcd for $C_{10}H_{11}NO$: C, 74.51; H, 6.88; N, 8.69%. Found: C, 74.72; H, 6.85; N, 8.35%.

General Procedure for the Preparation of *N*-Substituted 2-[(2-imidazolylthio)methyl]anilines (2) A solution of 2.8 g (15.6 mmol) of 2-isobutylaminobenzyl alcohol (**1g**) in 23 ml of CH_2Cl_2 was cooled to −5 °C and 2.3 g of $SOCl_2$ was added dropwise. The mixture was stirred for 30 min, the solvent removed *in vacuo* under 40 °C and the residue was added to a suspension of 1.56 g (15.6 mmol) of 2-mercaptoimidazole in 15 ml of EtOH. The mixture was stirred for 1 h. The solvent was removed and $CHCl_3$ and water were added. The organic layer was separated, washed with 10% Na_2CO_3 solution, and dried over Na_2SO_4. The solvent was evaporated *in vacuo* and the addition of 6 ml of Et_2O–hexane (3 : 1) followed by filtration of the precipitate gave 4.1 g (94%) of *N*-isobutyl-2-[(2-imidazolylthio)methyl]aniline (**2g**) as a white powder. Most of the sulfides were obtained by a similar procedure to that described for **2g**. The yield, appearance, melting point, exact MS and ^{1}H-NMR data are given in Table I.

General Procedure for the Preparation of *N*-Substituted 2-[(2-Imidazolylsulfinyl)methyl]anilines (3) by Method A *m*-Chloroperbenzoic acid (purity 80%, 774 mg, 3.61 mmol) was added portionwise to a solution of 1.0 g (3.61 mmol) of *N*-isobutyl-2-[(2-imidazolylthio)methyl]aniline (**2g**) in 40 ml of $CHCl_3$ and 10 ml of MeOH, at a constant temperature of 0—5 °C. The mixture was stirred for 1 h, then the solution was washed with saturated aqueous Na_2CO_3. The $CHCl_3$ extract was shaken successively with 10 ml of 0.1 N NaOH and extracted three times with 2 ml of 1 N NaOH to transfer the reaction product into aqueous fractions. The combined extract was made ammonia-alkaline by the addition of a 20% NH_4Cl solution. A precipitate deposited from the ammonia-alkaline solution was collected by filtration, washed with ether, and dried to give 600 mg (57%) of *N*-isobutyl-2-[(2-imidazolylsulfinyl)methyl]aniline (**3g**) as a white colorless prism.

Compounds **3a**—**c**, **f**, **i**, **j**, **l**, **p** and **r**—**v** were obtained by a similar procedure to that described for **3g**.

General Procedure for the Preparation of *N*-Substituted 2-[(2-Imidazolylsulfinyl)methyl]anilines (3) by Method B A mixture of 1.45 g (5.5 mmol) of *N*-(2-methoxyethyl)-2-[(2-imidazolylthio)methyl]aniline (**2n**), 13 ml of CH_2Cl_2, 13 ml of MeOH, and 1.3 ml of AcOH was stirred for 30 min at room temperature to dissolve **2n** in the solvent. The solution was cooled with ice water to below 5 °C and 2.6 ml of 35% H_2O_2 and 37 mg of NH_4VO_3 were added successively. The mixture was stirred for approx. 2.5 h at temperatures between −3 and 3 °C. Chloroform and saturated aqueous $NaHCO_3$ were added and the $CHCl_3$ layer was separated. The $CHCl_3$ extract was shaken successively twice with 10 ml of 1 N NaOH to transfer the reaction product into the aqueous fractions. The combined aqueous extract was rendered ammonia-alkaline by the addition of 20% aqueous NH_4Cl. A separated oil was extracted with $CHCl_3$, washed with H_2O, dried over anhydrous Na_2SO_4, and evaporated *in vacuo*. Addition of Et_2O followed by filtration of the precipitate yielded 760 mg (50%) of *N*-(2-methoxyethyl)-2-[(2-imidazolylsulfinyl)methyl]aniline (**3n**) as a colorless prism.

Compounds **3d**, **e**, **h**, **k**, **m**, **o** and **q** were obtained by a similar procedure to that described for **3n**. The yield, appearance, mp, IR (S O), elemental analyses and ^{1}H-NMR of all sulfoxides (**3**) are given in Table II.

Preparation of H^+/K^+-ATPase Enriched Rabbit Gastric Membrane Gastric H^+/K^+-ATPase was purified from the parietal cell-rich fraction of rabbit stomach as described by Saccoman *et al.*[11] with slight modification. The fundic mucosa of male Japanese white rabbits was homogenized in about 10 volumes of a cold solution containing 250 mM sucrose, 1 mM EGTA, and 20 mM Tris–HCl buffer at pH 7.4. The resulting homogenate was centrifuged at 9000 *g* for 10 min. The pellet was re-homogenized, and the combined supernatants were centrifuged at 77000 *g* for 60 min to yield a crude microsomal pellet. The 77000 *g* pellet was resuspended in the same solution, homogenized and centrifuged at 77000 *g* for 180 min in a discontinuous density gradient. Vesicles enriched in the gastric H^+/K^+-ATPase were collected at the interface of 250 mM sucrose, 7% Ficoll (w/w) +250 mM sucrose layers. The vesicle preparation was stored in 250 mM sucrose (unbuffered) at 4 °C. Protein concentration was determined by the Lowry method using bovine serum albumin as the standard.[12]

Assay Procedure of H^+/K^+-ATPase Inhibitory Activity The enzyme (*ca.* 10 μg protein) was preincubated in medium consisting of 5 mM imidazole buffer (pH 6.0 or 7.4) and a test compound in a final volume of 0.5 ml. These agents were dissolved in dimethyl sulfoxide (DMSO). All incubations contained less than 1% DMSO, which had no influence on the assay. The incubation time was 25 min at room temperature followed by 5 min at 37 °C, after which the enzyme reaction was started by the addition of 0.5 ml of a mixture containing 4 mM $MgCl_2$, 4 mM ATP, and 80 mM imidazole buffer (pH 7.4), with or without 20 mM KCl. After incubation for 15 min at 37 °C, the reaction was terminated by adding 1 ml of 24% trichloroacetic acid. Inorganic phosphate from adenosine triphosphate (ATP) was measured by the method of Taussky and Shorr.[13]

Assay Procedure of Inhibitory Effect against Gastric Acid Secretion Beagles of both sexes (12—14 kg) with Heidenhain pouch were fasted for 18 h before the experiments. Histamine dihydrochloride was continuously administered i.v. at a dose of 160 μg/kg/h. Gastric juice was collected at 15 min intervals and the volume was determined. Acid concentration was measured by titration with 0.1 N NaOH to pH 7.0. Test compounds were administered i.v. 75 min after the initiation of histamine

administration. The percent inhibition of acid output was determined 30 min after the administration of each compound by comparison with the control value.

Assay of Stability Stability at 37 °C was determined in Britten–Robinson buffer which had been adjusted to the appropriate pH. Compounds were dissolved in this buffer by supersonic waves, and the filtered solution was monitored by high performance liquid chromatography (HPLC) (Tosoh TSK-gel ODS-120T 4.6—250 mm, CH_3CN/10 mM phosphate buffer (pH 7.0), 1 ml/min, room temperature (25 °C), detector ultraviolet (UV) 240—250 nm). Half-lives ($T_{1/2}$) were determined from linear regression of ln of the concentration *vs.* time (h).

References

1) A. Brändström, P. Lindberg, U. Junggren and B. Wallmark, *Scand. J. Gastroenterol.*, **21** (Suppl. 118), 54 (1986).
2) W. Beil, M. Eltze, K. Heintze, K. Klemm, R. Rieldel, C. Schudt, K.-Fr. Swing and A. Simon, *Br. J. Pharmac.*, **88**, 389 (1986); H. Satoh, N. Imatomi, H. Nagaya, I. Inada, A. Nohara, N. Nakamura and Y. Maki, *J. Pharmacol. Exp. Ther.*, **248**, 806 (1989); R. J. Ife, C. A. Dyke, D. J. Keeling, E. Meenan, M. L. Meeson, M. E. Parsons, C. A. Price, C. J. Theobald and A. H. Underwood, *J. Med. Chem.*, **32**, 1970 (1989); S. Souda, S. Miyazawa, N. Ueda, N. Shimomura, K. Tagami, H. Fuzisaki, K. Wakabayashi and I. Yamatsu, Abstracts of Papers IV, The 109th Annual Meeting of Pharmaceutical Society of Japan, Nagoya, April 1989, p. 8.
3) S. Okabe, E. Higaki, T. Higuchi, M. Sato and K. Hara, *Japan. J. Pharmacol.*, **40**, 239 (1986); S. Okabe, H. Miyake and Y. Awane, *ibid.*, **42**, 123 (1986); S. Okabe, Y. Akimoto, H. Miyake and J. Imada, *ibid.*, **44**, 7 (1987); S. Okabe, H. Miyake and S. Yamasaki, *Dig. Dis. Sci.*, **34**, 1035 (1989).
4) S. Okabe, Y. Akimoto, S. Yamasaki and H. Nagai, *Dig. Dis. Sci.*, **33**, 1425 (1988).
5) G. W. Adelstein, C. H. Yen, R. A. Haack, S. Yu, G. Gullikson, D. V. Price, C. Anglin, D. L. Decktor, H. Tsai and R. H. Keith, *J. Med. Chem.*, **31**, 1215 (1988).
6) I.B. Simon and I. I. Kovtunovskaya-Levshina, *Trudy Nauch. Konf.*, Kiev **1957**, 40.
7) F. W. Holly and A. C. Cope, *J. Am. Chem. Soc.*, **66**, 1875 (1944).
8) R. J. Ife, C. A. Dyke, D. J. Keeling, E. Meenan, M. L. Meeson, M. E. Parsons, C. A. Price, C. J. Theobald and A. H. Underwood, *J. Med. Chem.*, **32**, 1970 (1989).
9) T. H. Brown, R. J. Ife, D. J. Keeling, S. M. Laing, C. A. Leach, M. E. Parsons, C. A. Price, D. R. Reavill and K. J. Wiggall, *J. Med. Chem.*, **33**, 527 (1990).
10) V. Figala, K. Klemm, B. Kohl, U. Krüger, G. Rainer, H. Schaefer, J. Senn-Bilfinger and E. Sturm, *J. Chem. Soc., Chem. Commun.*, **1986**, 125; P. Lindberg, P. Nordberg, T. Alminger, A. Brändström and B. Wallmark, *J. Med. Chem.*, **29**, 1329 (1986); E. Sturm, U. Krüger, J. Senn-Bilfinger, V. Figala, K. Klemm, B. Kohl, G. Rainer, H. Schaefer, T. J. Blake, D. W. Darkin, R. J. Ife, C. A. Leach, R. C. Mitchell, E. S. Pepper, C. J. Salter, N. J. Viney, G. Huttner and L. Zsolnai, *J. Org. Chem.*, **52**, 4573 (1987); J. Senn-Bilfinger, U. Krüger, E. Sturm, V. Figala, K. Klemm, B. Kohl, G. Rainer, H. Schaefer, T. J. Blake, D. W. Darkin, R. J. Ife, C. A. Leach, R. C. Mitchell, E. S. Pepper, C. J. Salter, N. J. Viney, G. Huttner and L. Zsolnai, *ibid.*, **52**, 4582 (1987).
11) G. Saccomani, H. B. Stewart, D. Shaw, M. Lewin and G. Sachs, *Biochim. Biophys. Acta*, **465**, 311 (1977).
12) O. H. Lowry, N. J. Rosebrough, A. L. Farr and R. J. Randall, *J. Biol. Chem.*, **193**, 165 (1951).
13) H. H. Taussky and E. Shorr, *J. Biol. Chem.*, **202**, 675 (1953).

Studies on Hypotensive Agents. Synthesis of 1-Substituted 3-(2-Chlorophenyl)-6-ethoxycarbonyl-5,7-dimethyl-2,4(1*H*,3*H*)-quinazolinediones[1)]

Yukuo EGUCHI,*,[a] Fujinori SASAKI,[b] Akiko SUGIMOTO,[a] Hisashi EBISAWA,[c] and Masayuki ISHIKAWA[a]

Institute for Medical and Dental Engineering, Tokyo Medical and Dental University,[a] 2–3–10, Surugadai, Kanda, Chiyoda-ku, Tokyo, Japan, Research Laboratory, Banyu Pharmaceutical Co., Ltd.,[b] 2–9–3, Shimomeguro, Meguro-ku, Tokyo, Japan, and Life Science Research Laboratory, Showa Denko Co., Ltd.,[c] 2-24-25, Tamagawa, Ohta-ku, Tokyo, Japan. *Received December 20, 1990*

3-(2-Chlorophenyl)-6-ethoxycarbonyl-5,7-dimethyl-2,4(1*H*,3*H*)-quinazolinedione was newly prepared. 1-Hydrogen atoms of the compound were variously substituted in order to test for their hypotensive activities on relaxing effects of the blood vessels. The compounds with 2-(1-pyrrolidinyl) ethyl, 2-(1-piperidinyl)ethyl, 3-(dimethylamino)propyl, and 3-(*N*-benzyl-*N*-methylamino)propyl moieties showed significant activity. The 2-(1-piperidinyl)ethyl compound possessed activity approximately 23 times more potent than papaverine, however, it was less potent than cinnarizine.

Keywords synthesis; 1-substituted 3-(2-chlorophenyl)-6-ethoxycarbonyl-5,7-dimethyl-2,4-(1*H*, 3*H*)-quinazolinedione; hypotensive activity; relaxing effect, blood vessel

We reported[2)] earlier the synthesis and pharmacology of the quinazolinone derivative (I), which exerted considerably potent hypotensive activity in anesthetized rabbits. We also revealed results on a brief structure–activity relation[3)] of the compound that the 6-ethyl ester and 3-(2-chlorophenyl) moieties were important factors in improving the activity, particularly that the quinazolinone ring system was essential for the activity based on biological meaning given in the literature.[4–6)] 2,4(1*H*,3*H*)-Quinazolinediones as well as quinazolinones have been reported to demonstrate biological actions: vasodilater,[7)] sedative,[8)] and hypotensive[7–9)] activities. These activities were considered primarily attributable to the quinazolinone ring system. We prepared 2,4(1*H*,3*H*)-quinazolinediones (II) with functionalities of the 6-ethyl ester as well as 3-(2-chlorophenyl) in order to test for hypotensive activities (Fig. 1).

This report describes the synthesis and hypotensive activities on relaxing effects of the blood vessels of such 2,4(1*H*,3*H*)-quinazolinedione derivatives (II).

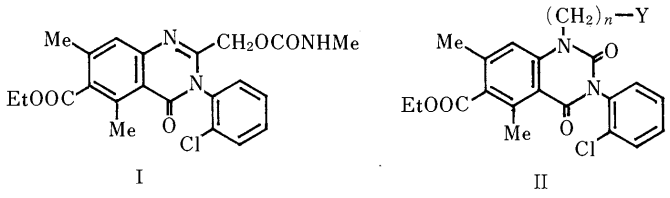

I II

Fig. 1

Synthesis

The starting 2,4(1*H*,3*H*)-quinazolinediones (**3a—d**) were prepared by a modified method[10)] from 2-amino-5-ethoxycarbonyl-4,6-dimethylbenzoic acid (**1a**)[11)] with aryl isocyanates to give the intermediate uramidobenzoic acids (**2a—d**) which, in turn, were cyclized by treatment with a solution of hydrochloric acid (HCl) in ethanol. The reactions gave mainly, the corresponding 2,4(1*H*,3*H*)-quinazolinediones **3a—d** with minor quantities of benzoxazolone derivatives (**4a—d**). Production of the latter compounds **4a—d** was avoidable when methyl ester (**1b**) was used as the starting material as described in the literature.[10)] (Chart 1).

Compounds chosen for the study are illustrated by the general formula II, where *n* is 1—4 and Y is as shown in the charts. The compounds (**5a—u**, **6a—c**) were prepared in the first stage by a displacement of the 1-hydrogen of **3b** with various alkyl halides in the presence of 50% sodium hydride (NaH) in 67—94% yield. The reactions were generally carried out in dimethylformamide at 70—140 °C, except **5d**. Compound **5d** could not be obtained under identical conditions using NaH and 3-bromopropionitrile and the starting material (**3b**) was recovered. Meanwhile, Michael type addition of acrylonitrile with **3b** in the presence of solid NaOH without solvents resulted in the corresponding product **5d** in a 92% yield (Chart 2).

The 1-free amines (**6d—f**) were prepared from the corresponding phthalimide derivatives (**6a—c**) in 74—91% yield by the reactions with hydrazine hydrate at room

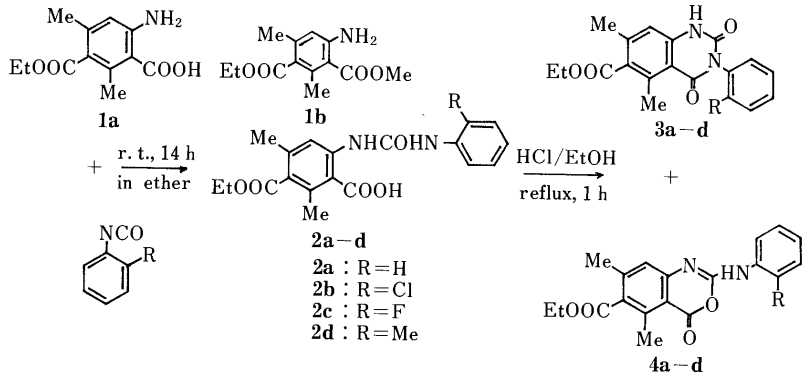

Chart 1

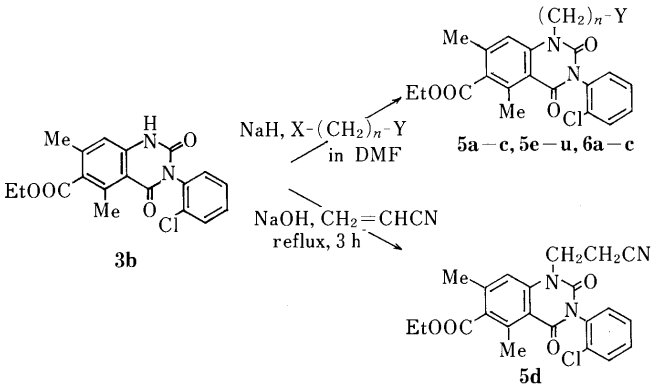

	n	Y	reaction conditions: alkyl halide (X)	temp. (°C)	time (h)	yield (%)
5a	1	H	I	80	4	63
5b	1	Ph	Cl	90	6	58
5c	1	α-pyridyl	Cl	80	4	70
5e	3	CN	Cl	80	4	73
5f	2	$N(Me)_2$	Cl	80	4	88
5g	2	N⊂	Cl	90	4	80
5h	2	N⊂	Cl	140	5	76
5i	2	N⊂O	Cl	90	4	72
5j	2	N⊂NCOOEt	Cl	80	3	62
5k	2	N⊂NCH_2COOEt	Cl	70	3	67
5l	2	N⊂$NCH_2COOC(Me)_3$	Cl	80	3	64
5m[a]	2	N⊂NCH_2COOH				
5n	2	N⊂$NCH_2CONHPh(2,6\text{-}Cl_2)$	Cl	80	4	78
5o	2	N⊂$NCH_2CH=CHPh$	Cl	80	2	65
5p	3	$N(Me)_2$	Cl	140	3	68
5q	3	$NMe(CH_2Ph)$	Cl	80	3	73
5r	1	COOEt	Cl	70	2	83
5s	1	$COOC(Me)_3$	Cl	80	1	96
5t	1	$COOCH_2Ph$	Cl	90	1	61
5u	3	COOEt	Br	140	4	59
6a	2		Br	80	4	53
6b	3		Cl	80	4	56
6c	4		Cl	80	4	47

a) prepared from **5l** by hydrolysis in conc. HCl

Chart 2

temperature. *N,N*-Disubstituted aminoalkylamido derivatives (**7a—d**) were obtained from **5r**, when high boiling amines were employed without solvents (Chart 3). Since hydrolysis of the *tert*-butyl ester of **5s** by an alkaline or the reported media[12,13] was accompanied by considerable decarboxylation, **5s** was simply stirred in concd. HCl at 40°C to afford a crystalline free acid (**8a**) in a moderate yield. The acid **8a** was then chlorinated with thionyl chloride, followed by treatment of appropriate amines or aminoalcohols in benzene to produce the 1-amido (**8c—h**) and ester derivatives (**8i—k**), respectively. Similarly, compounds **8l** and **8m** were prepared from the acid chloride of **8b**, which was prepared from the ethyl ester derivative **5u** under similar hydrolytic conditions in 38% yield (Chart 4).

The imidate (**9a**) and amidine (**9b**) salts were prepared from **5d** by the reported method.[14] On the other hand, compound **5e** afforded only ethyl ester derivative (**10**) under the identical reaction condition (Chart 5).

Results

The biological activities assessed in this study were relaxing effects of the blood vessels using basilar artery of albino rabbits. The relaxing effects of the test compounds were expressed as percentage of the maximum relaxation induced by papaverine (3×10^{-4} M), and was the mean value of three runs. Activities of test compounds were measured in a concentration of 3×10^{-6} M in the presence of KCl (40 mM). Several compounds were also measured in 3×10^{-7} M and the percentage values observed in the concentration are indicated in parenthesis in Table I.

In a preliminary test of the 1-unsubstituted compounds **3a—d**, **3b** with a chlorine moiety exhibited considerable effect. The 64% value was higher than that of the reference quinazolinone I, which showed a 57% relaxation in 3×10^{-6} M in the test.

Most compounds tested showed fairly potent activity compared to the reference quinazolinone I. Among them, an aminoalkyl moiety directly connected to **3b**, such as 2-(1-pyrrolidinyl)ethyl (**5g**), 2-(1-piperidinyl)ethyl (**5h**), 3-(dimethylamino) propyl (**5p**), and 3-(*N*-benzyl-*N*-methylamino) propyl (**5q**) compounds possessed significant activity for the relaxation of the artery. Similarly, an amido compound **7b** with an aminoalkyl moiety in its terminal chain also possessed fairly good activity. These results suggested that the aminoalkyl group considerably increased the relaxation effect of **3b** in this test. The activities of

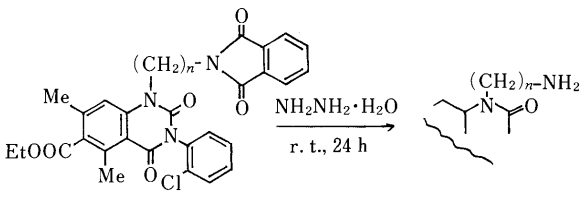

	n	yield (%)
6d	2	91
6e	3	86
6f	4	74

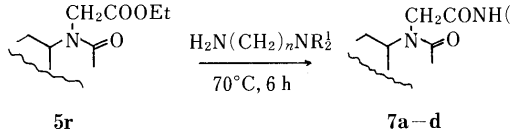

	n	NR_2^1	yield (%)
7a	2	diethylamino	78
7b	2	piperidino	54
7c	3	dimethylamino	82
7d	3	morpholino	67

Chart 3

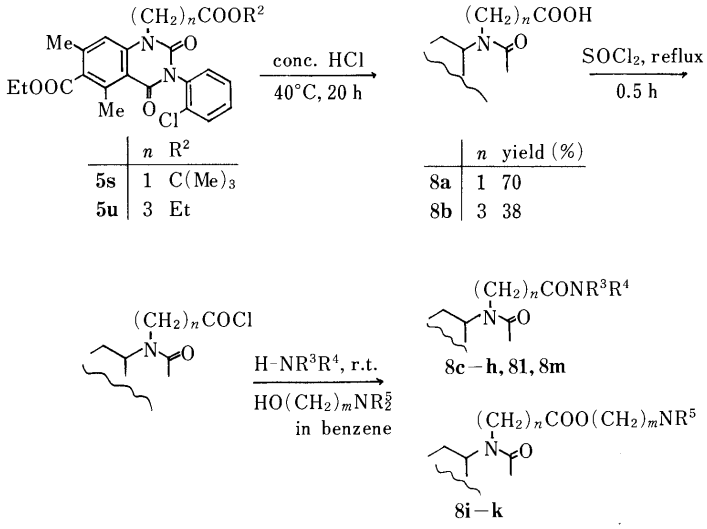

	n	R2
5s	1	C(Me)3
5u	3	Et

	n	yield (%)
8a	1	70
8b	3	38

	n	NR3R4	time (h)	yield (%)
8c	1	NH2	3	72
8d	1	NHMe	5	82
8e	1	N(Et)2	5	80
8f	1	N⊃	5	67
8g	1	N⊃NMe	3	69
8h	1	N(Me)CH2Ph	5	64
8l	3	NH2	5	42
8m	3	NHMe	5	62

	n	m	NR52	time (h)	yield (%)
8i	1	2	N(Me)2	40	47
8j	1	2	N⊃	40	45
8k	1	3	N(Me)2	40	38

Chart 4

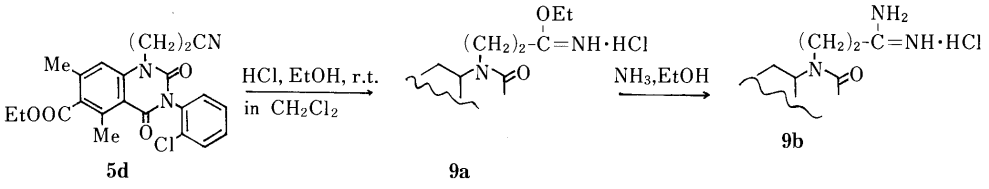

Chart 5

compounds **5g**, **5h**, **5p**, **5q**, **7b** were further measured in a cumulative concentration 3×10^{-7} M, and produced 70, 78, 62, 67, and 54% relaxation, respectively. Consequently, the 2-(1-piperidinyl)ethyl compound **5h** showed the highest relaxing activity among the test compounds.

The most active compound **5h** was again assessed in a comparative test for the relaxation of both basilar and mesenteric arteries. The effect was comparable to those of papaverine, quinazolinone I, and cinnarizine, respectively.

Thus, compound **5h** with the 2-(1-piperidinyl)ethyl moiety exhibited a potency 23 times greater than papaverine, but was less potent than cinnarizine (see Table II).

Discussion

Although the functionalities of the 6-ethyl ester and 3-(2-chlorophenyl) moieties were constructed to the 2,4-(1*H*,3*H*)-quinazolinedione, these effects were not evaluated in this test. Aminoalkyl moieties connected directly to the 2,4-(1*H*,3*H*)-quinazolinedione were found to have a greater tendency for hypotensive activity. Methylene chain and an adequate flexibility of these moieties might be needed.

Compound **5h** demonstrated significant activity, but was less potent than cinnarizine in the arterial relaxation test. In preliminary circulatory test in dogs on heart rate, blood flow, blood pressure, duration and selectivity to the arteries, **5h** showed a similar behavior to papaverine, and we consider the actions of the arterial relaxation induced by **5h** to be related to the blood flow rate. Under the consideration described in the literature[7] that a compound with cardiovascular action attributable to direct relaxation of vascular smooth muscle would elicit less side effect than an agent acting through impairment of adrenergic transmission, **5h** appeared to be worthy of further evaluation as a potential vasodilator hypotensive agent.

Experimental

All melting points were determined in a capillary tube and are uncorrected. Infrared (IR) spectra were determined with a Hitachi model 285 spectrometer, mass spectra (MS) were recorded by a Hitachi RMU-7L spectrometer, and proton nuclear magnetic resonance ^{1}H-(NMR) spectra with a JEOL-60HL machine. Merck Silica gel 60 was used for column chromatography. Physical and empirical analysis data of prepared compounds are shown in Table I and spectral data in Table III.

Preparation of 3a—d. 3-(2-Chlorophenyl)-6-ethoxycarbonyl-5,7-dimethyl-2,4-(1*H*,3*H*)-quinazolinedione (3b) A mixture of **1a** (2.37 g, 10 mmol) and *o*-chlorophenylisocyanate (1.84 g, 12 mmol) in ether (200 ml) was left at room temperature for 14 h. Precipitated materials were filtered. The materials were dissolved in a solution of concd. HCl (20 ml) and EtOH (80 ml), then the mixture was refluxed for 3 h. The reaction mixture was concentrated, neutralized with 10% K_2CO_3, and extracted with chloroform. The extract was purified by column chromatography with chloroform–EtOAc (10 : 1) to afford **3b** (2.65 g, 71.2%) in the later fractions. mp 224—225 °C (MeOH). *Anal.* Calcd for $C_{19}H_{17}ClN_2O_4$: C, 61.21; H, 4.60; N, 7.51. Found: C, 61.17; H, 4.60; N, 7.41. MS *m/z*: 373 (M^+), 337 (M^+-Et), 337 (M^+-Cl), 327 (M^+-OEt). IR ν_{max}^{KBr} cm^{-1}: 3400, 3300, 1740, 1690. ^{1}H-NMR (DMSO-d_6) δ: 1.39 (3H, t, J=7 Hz), 2.29 (3H, s), 2.69 (3H, s), 4.35 (2H, q, J=7 Hz), 6.68 (1H, s), 7.43 (4H, s), 10.31 (1H, s). Compound **4b** (R=Cl) was obtained in the early fractions in a yield

TABLE I. Physical and Biological Data for Compounds **3a—d**, **5a—9b**

No.	mp (°C) (solvent)[a]	Formula	Analysis (%) Calcd C	Calcd H	Calcd N	Found C	Found H	Found N	Relaxation effect on[b] blood vessel (%) concentration 3×10^{-6} M
3a	289—290 (EtOH)	$C_{19}H_{18}N_2O_4$	67.44	5.36	8.27	67.38	5.37	8.30	13
3b	233—234 (MeOH)	$C_{19}H_{17}ClN_2O_4$	61.21	4.60	7.51	61.17	4.60	7.41	64
3c	210—211 (ether–*n*-hexane)	$C_{19}H_{17}FN_2O_4$	64.04	4.89	7.86	64.12	4.73	7.91	44
3d	197—198 (ether–*n*-hexane)	$C_{20}H_{20}N_2O_4$	68.16	5.72	7.95	68.18	5.72	7.99	51
5a	216—217 (EtOH)	$C_{20}H_{19}ClN_2O_4$	62.09	4.95	7.24	62.03	4.94	7.30	69
5b	160—161 (ether–*n*-hexane)	$C_{26}H_{23}ClN_2O_4$	67.45	5.00	6.05	67.47	5.01	6.09	44
5c	161—162 (EtOH)	$C_{25}H_{22}ClN_3O_4$	64.72	4.78	9.05	64.77	4.81	9.00	NT[c]
5d	230—231 (MeOH)	$C_{22}H_{20}ClN_3O_4$	62.04	4.70	9.87	62.10	4.65	9.91	NT
5e	165—166 (MeOH)	$C_{23}H_{22}ClN_3O_4$	62.79	5.04	9.55	62.83	5.01	9.59	NT
5f	192—193 (ether–*n*-hexane)	$C_{23}H_{26}ClN_3O_4$	62.22	5.90	9.46	62.21	5.87	9.45	62
5g	144—145 (ether–*n*-hexane)	$C_{25}H_{28}ClN_3O_4$	63.89	6.00	8.94	63.93	6.01	9.01	83 (70)[d]
5h	138—139 (ether–*n*-hexane)	$C_{26}H_{30}ClN_3O_4$	64.52	6.20	8.68	64.49	6.21	8.72	87 (78)
5i	165—166 (EtOH–ether)	$C_{25}H_{28}ClN_3O_5\cdot HCl$	57.47	5.59	8.04	57.52	5.61	8.06	47
5j	155—157 (EtOH–ether)	$C_{28}H_{33}ClN_4O_6\cdot 2HCl$	53.38	5.60	8.89	53.41	5.58	8.94	NT
5k	189—191 (EtOH)	$C_{29}H_{35}ClN_4O_6\cdot 2HCl$	54.08	5.79	8.70	54.08	5.81	8.80	49
5l	101—102 (ether)	$C_{31}H_{39}ClN_4O_6$	62.14	6.56	9.35	62.20	6.60	9.31	NT
5m	179—180 (EtOH–*n*-hexane)	$C_{27}H_{31}ClN_4O_6\cdot 2HCl$	52.65	5.40	9.09	52.65	5.42	9.13	NT
5n	184—186 (EtOH–ether)	$C_{23}H_{35}Cl_3N_5O_5\cdot 2HCl$	43.10	5.82	10.92	13.14	5.86	11.03	NT
5o	240—241 (EtOH)	$C_{34}H_{37}ClN_4O_4\cdot 2HCl$	60.58	5.83	8.31	60.61	5.79	8.34	57
5p	155—156 (MeOH)	$C_{24}H_{28}ClN_3O_4$	62.94	6.16	9.17	63.02	6.17	9.25	88 (62)
5q	145—146 (ether)	$C_{30}H_{32}ClN_3O_4$	67.47	6.04	7.86	67.51	6.11	7.92	86 (67)
5r	158—159 (ether)	$C_{23}H_{23}ClN_2O_6$	60.19	5.05	6.10	60.14	5.08	6.18	65
5s	184—185 (ether)	$C_{25}H_{27}ClN_2O_6$	61.66	5.58	5.75	61.61	5.61	5.82	64
5t	128—129 (EtOAc–ether)	$C_{28}H_{25}ClN_2O_6$	64.55	4.83	5.37	64.59	4.90	5.41	74
5u	82— 83 (ether)	$C_{25}H_{27}ClN_2O_6$	61.66	5.89	5.75	61.55	5.60	5.81	50
6a	283—284 (MeOH)	$C_{29}H_{24}ClN_3O_6$	63.73	4.57	7.69	63.68	4.56	7.74	NT
6b	213—214 (MeOH)	$C_{30}H_{26}ClN_3O_6$	64.28	4.82	7.50	64.25	4.79	7.60	NT
6c	160—161 (MeOH)	$C_{31}H_{28}ClN_3O_6$	64.80	5.05	7.31	64.76	5.05	7.36	NT
6d	101—102 (EtOH–H_2O)	$C_{21}H_{22}ClN_3O_4$	60.64	5.29	10.10	60.57	5.32	10.16	48
6e	175—176 (EtOH–H_2O)	$C_{22}H_{24}ClN_3O_4$	61.46	5.62	9.77	61.43	5.65	9.82	NT
6f	160—161 (EtOH–ether)	$C_{23}H_{26}ClN_3O_4\cdot HCl$	57.50	5.66	8.74	57.55	5.66	8.77	NT
7a	193—194 (EtOAc–*n*-hexane)	$C_{27}H_{33}ClN_4O_5$	61.30	6.28	10.59	61.33	6.27	10.63	71
7b	179—180 (EtOAc–*n*-hexane)	$C_{28}H_{33}ClN_4O_5$	62.16	6.10	10.36	62.22	6.05	10.43	87 (54)
7c	173—175 (EtOAc–*n*-hexane)	$C_{26}H_{31}ClN_4O_5$	60.63	6.06	10.87	60.68	6.12	10.95	62
7d	197—198 (EtOAc–n-hexane)	$C_{28}H_{33}ClN_4O_6$	60.37	5.97	10.05	60.39	6.01	10.11	62
8a	181—183 (ether)	$C_{21}H_{19}ClN_2O_6$	58.53	4.41	6.50	58.61	4.43	6.49	61
8b	190—192 (ether)	$C_{23}H_{23}ClN_2O_6$	60.19	5.05	6.10	60.21	5.08	6.13	NT
8c	285—287 (MeOH)	$C_{21}H_{20}ClN_3O_5$	58.68	4.69	9.77	58.64	4.73	9.82	33
8d	249—250 (MeOH)	$C_{22}H_{22}ClN_3O_5$	59.52	4.99	9.46	59.58	5.04	9.52	52
8e	228—229 (MeOH)	$C_{25}H_{28}ClN_3O_5$	61.78	5.80	8.64	61.81	5.73	8.70	57
8f	173—175 (EtOAc)	$C_{26}H_{28}ClN_3O_5$	62.71	5.66	8.43	62.72	5.67	8.43	NT
8g	164—165 (EtOAc)	$C_{26}H_{29}ClN_4O_5$	60.87	5.65	10.92	60.77	5.63	11.11	NT
8h	172—173 (EtOAc)	$C_{29}H_{28}ClN_3O_5$	65.22	5.28	7.87	65.22	5.30	7.89	62
8i	112—113 (ether–*n*-hexane)	$C_{24}H_{26}ClN_3O_6$	59.07	5.37	8.61	59.11	5.40	8.65	55
8j	183—185 (EtOH–ether)	$C_{27}H_{30}ClN_3O_6\cdot HCl$	57.45	5.53	7.44	57.42	5.58	7.49	NT
8k	178—180 (EtOH–ether)	$C_{25}H_{28}ClN_3O_6\cdot HCl$	55.76	5.42	7.80	55.72	5.49	7.87	NT
8l	175—176 (EtOAc)	$C_{23}H_{24}ClN_3O_5$	60.32	5.28	9.17	60.33	5.31	9.21	NT
8m	200—201 (MeOH)	$C_{24}H_{26}ClN_3O_5$	61.08	5.55	8.90	61.09	5.61	9.01	NT
9a	128—129 (EtOH–ether)	$C_{24}H_{26}ClN_3O_5\cdot HCl$	56.69	5.31	8.26	56.74	5.40	8.30	NT
9b	219—220 (MeOH–ether)	$C_{20}H_{19}ClN_4O_4\cdot HCl$	53.21	4.43	12.41	53.19	4.42	12.48	78

a) Recrystallization solvent. *b*) Mean percentage observed in the basilar artery. *c*) Not tested. *d*) Percentage value observed in concentration 3×10^{-7} M.

TABLE II. Approximate ED_{50} and Relative Potencies for Relaxation of the Basilar and Mesenteric Arteries by Standardized Papaverine with Quinazolinone I, **5h**, and Cinnarizine

Compd.	Basilar artery ED_{50} (M)	Relative potency	Mesenteric artery ED_{50} (M)	Relative potency
Papaverine	6.6×10^{-6}	1.0	3.3×10^{-6}	1.0
Quinazolinone I	2.5×10^{-6}	2.5	3.3×10^{-6}	1.0
5h	2.9×10^{-7}	23	5.1×10^{-7}	7
Cinnarizine	5.4×10^{-8}	122	1.0×10^{-7}	33

of 0.32 g (8.6%). mp 215—216 °C (EtOAc–*n*-hexane). IR ν_{max}^{KBr} cm^{-1}: 3350, 1750, 1710, 1640. ^{1}H-NMR ($CDCl_3$) δ: 1.38 (3H, t, J=7 Hz), 2.30 (3H, s), 2.37 (3H, s), 4.32 (2H, q, J=7 Hz), 7.51 (4H, m), 8.12 (1H, s), 9.39 (1H, s).

Preparation of Alkyl Halides. 1-(2-Chloroethyl)-4-ethoxycarbonylpiperazine To a mixture of ethyl 1-piperazinecarboxylate (7.91 g, 0.05 mol) and ethylene bromohydrine (6.9 g, 0.055 mol) was added EtOH (50 ml) containing triethylamine (5.06 g, 0.05 mol). The mixture was refluxed for 3 h, then evaporated. The residue was diluted with chloroform. It was washed with 5% NaOH, water, and dried over anhyd. K_2CO_3. The solvent was evaporated to afford oil. Distillation of the oil afforded 7.6 g (75.2%) of 1-(2-hydroxyethyl)-4-ethoxycarbonylpiperazine. bp 140—142 °C MS m/z: 202 (M^+), 171 ($M^+ - CH_2OH$), 157 ($M^+ - OEt$), 143. A mixture of thus prepared compound (2.0 g) in chloroform (40 ml) containing thionyl

TABLE III. Spectral Data for **3a—d**

No.	MS (*m/z*)	IR (KBr, cm^{-1})	^{1}H-NMR ($CDCl_3$, J=Hz)
3a	338, 309, 293, 266	3400, 1730, 1720, 1660	1.38 (3H, t, 7), 2.21 (3H, s), 2.68 (3H, s), 4.42 (2H, q, 7), 6.72 (1H,s), 7.33 (5H, s), 10.21 (1H, s)
3b[a]	373, 343, 337, 327	3400, 3300, 1740, 1690	1.39 (3H, t, 7), 2.29 (3H, s), 2.69 (3H, s), 4.35 (2H, q, 7), 6.68 (1H, s), 7.43 (4H, s), 10.31 (1H, s)
3c	356, 327, 311	3000, 1730, 1680	1.39 (3H, t, 7), 2.22 (3H, s), 2.70 (3H, s), 4.35 (2H, q, 7), 6.68 (1H, s), 7.30 (4H, m), 10.23 (1H, s)
3d	352, 335, 323	3280, 1740, 1700, 1680	1.41 (3H, t, 7), 2.20 (3H, s), 2.34 (3H, s), 2.72 (3H, s), 4.41 (2H, q, 7), 6.64 (1H, s), 7.30 (4H, m), 10.20 (1H, s)

a) ^{1}H-NMR spectra was taken in DMSO-d_6.

TABLE IV. Spectral Data for **5a—u**

No.	MS (*m/z*)	IR (KBr, cm^{-1})	^{1}H-NMR ($CDCl_3$, J=Hz)
5a			1.40 (3H, t, 7), 2.42 (3H, s), 2.72 (3H, s), 3.60 (3H, s), 4.43 (2H, q, 7), 7.00 (1H, s), 7.40 (4H, m)
5b			1.36 (3H, t, 7), 2.28 (3H, s), 2.73 (3H, s), 4.38 (2H, q, 7), 5.39 (2H, q, 16), 6.91 (1H, s), 7.28 (5H, s), 7.40 (4H, m)
5c			1.38 (3H, t, 7), 2.31 (3H, s), 2.72 (3H, s), 4.40 (2H, q, 7), 5.51 (2H, q, 15), 7.15—7.80 (8H, m), 8.60 (1H, br)
5d	426, 391, 381, 363	3500, 3000, 2250, 1715, 1710, 1680	2.46 (3H, t, 7), 2.71 (3H, s), 2.73 (3H, s), 2.87 (2H, t, 6), 4.40 (2H, q, 7), 4.49 (2H, t, 6), 7.30 (1H, s), 7.43 (4H, m)
5e	440, 405, 395	3400, 3000, 2245, 1710, 1680	2.40 (3H, t, 7), 2.46 (3H, s), 2.73 (3H, s), 2.85 (2H, t, 6), 4.38 (2H, br), 4.40 (2H, q, 7), 4.49 (2H, t, 6), 7.00 (1H, s), 7.43 (4H, m)
5f			1.40 (3H, t, 7), 2.35 (6H, s), 2.45 (3H, s), 2.72 (3H, s), 4.12—4.60 (6H, m), 7.07 (1H, s), 7.70 (4H, m)
5g			1.40 (3H, t, 7), 1.70 (4H, br), 2.43 (3H, s), 2.68 (8H, br), 2.72 (3H, s), 4.40 (2H, q, 7), 7.10 (1H, s), 7.40 (4H, m)
5h			1.36 (3H, t, 7), 1.42 (6H, m), 2.26 (4H, m), 2.31 (3H, s), 2.55 (3H, s), 4.41 (2H, q, 7), 4.44 (2H, t, 6), 4.47 (2H, t, 6), 7.16 (1H, s), 7.42 (4H, m)
5i			1.40 (3H, t, 7), 2.41 (3H, s), 2.60 (6H, m), 2.70 (3H, s), 3.70 (4H, m), 4.30 (2H, br), 4.41 (2H, q, 7), 7.08 (1H, s), 7.40 (4H, m)
5j			1.28 (3H, t, 7), 1.42 (3H, t, 7), 2.46 (3H, s), 2.55 (4H, br), 2.75 (3H, t, 7), 3.50 (4H, br), 4.12 (2H, q, 7), 4.30 (4H, br), 4.42 (2H, q, 7), 7.08 (1H, s), 7.41 (4H, m)
5k			1.27 (3H, t, 7), 1.40 (3H, t, 7), 2.42 (3H, s), 2.50 (2H, br), 4.18 (2H, q, 7), 4.30 (4H, br), 4.40 (2H, q, 7), 7.08 (1H, s), 7.40 (4H, m)
5l			1.40 (3H, t, 7), 1.47 (9H, s), 1.92 (2H, br), 2.44 (3H, s), 2.62 (4H, br), 2.71 (3H, s), 3.09 (2H, s), 4.42 (2H, q, 7), 7.08 (1H, s), 7.41 (4H, m)
5m		3400, 3000, 2600, 1720, 1700, 1680, 1600, 1560	
5n	567		
5o	600, 555, 441		
5p			1.40 (3H, t, 7), 1.50—2.50 (4H, m), 2.26 (6H,s), 2.43 (3H, s), 2.72 (3H, s), 4.20 (2H, br), 4.42 (2H, q, 7), 7.42 (5H, m)
5q		3400, 3000, 2400, 1710, 1670, 1600	1.39 (3H, t, 7), 1.80—2.50 (6H, m), 2.21 (3H, s), 2.32 (3H, s), 2.70 (3H, s), 3.51 (2H, s), 4.40 (2H, q, 7), 7.12 (1H, s), 7.30 (5H, s), 7.36 (4H, m)
5r			1.28 (3H, t, 7), 1.39 (3H, t, 7), 2.40 (3H, s), 2.74 (3H, s), 4.28 (2H, q, 7), 4.42 (2H, q, 7), 4.92 (2H, s), 6.74 (1H, s), 7.41 (4H, m)
5s	486, 451, 395		1.45 (9H, s), 2.38 (3H, s), 2.72 (3H, s), 4.42 (2H, q, 7), 4.81 (2H, s), 6.72 (1H, s), 7.40 (4H, m)
5t	520, 485		
5u	486, 451		

chloride (8 ml) was refluxed for 3 h, then the solvent was removed. The reasidue was rinsed with benzene, and dried in air to afford crude 1-(2-chloroethyl)-4-ethoxycarbonylpiperazine.

1-Cinnamyl-4-(2-chloroethyl)-piperazine A mixture of 1-piperazine-ethanol (2.0 g, 16 mmol) and cinnamyl chloride (2.4 g, 16 mmol) in EtOH (50 ml) was refluxed for 8 h. The solvent was removed, and the residue was diluted with chloroform. It was washed with 10% NaOH, water, and evaporated to afford crude oil. The oil was purified by column chromatography with chloroform–MeOH (98 : 2) to afford 2.2 g (58%) of 1-cinnamyl-4-(2-hydroxyethyl)-piperazine, melted at 38—40 °C (ether–*n*-hexane). MS *m/z*: 246 (M^+), 215 ($M^+ - CH_2OH$), 117 ($M^+ - PhCH=CH-CH_2$). ^{1}H-NMR ($CDCl_3$) δ: 2.16 (1H, s), 2.58 (8H, s), 2.48—2.63 (2H, m), 3.18 (2H, d, J=6 Hz), 3.61 (2H, t, J=5 Hz), 6.23—6.45 (2H, m), 7.20—7.50 (5H, m). A mixture of thus prepared compound (0.5 g, 2 mmol) in dry benzene (10 ml) containing thionyl chloride (1 ml) was refluxed for 2 h. The mixture was washed with 10%-K_2CO_3, water, and evaporated to afford crude oil. It was purified by column chromatography with chloroform–MeOH (98 : 2) to afford 0.21 g (40%) of 1-cinnamyl-4-(2-chloroethyl)-piperazine in oil. MS *m/z*: 264 (M^+), 228 ($M^+ - HCl$), 147 ($M^+ - PhCH=CH-CH_2$). ^{1}H-NMR ($CDCl_3 + CD_3OD$) δ: 2.61 (8H, s), 2.73 (2H, t, J=6 Hz), 3.19 (2H, d, J=6 Hz), 3.60 (2H, t, J=6 Hz), 6.00—6.72 (2H, m), 7.30 (5H, m).

***N*-(2-Bromoethyl)phthalimide** A mixture of *N*-(2-hydroxyethyl)-phthalimide (2.0 g) in chloroform (20 ml) containing phosphorous tribromide (0.5 g) was refluxed for 3 h. To the reaction mixture was added water with stirring. The organic layer was washed with 5% NaOH, water, and then dried over anhyd. K_2CO_3. The solvent was evaporated to afford 1.4 g of crude *N*-(2-bromoethyl) phthalimide.

Preparation of 5a—u, 6a—c. 3-(2-Chlorophenyl)-6-ethoxycarbonyl-5,7-dimethyl-1-[2-(1-piperidinyl)ethyl]-2,4(1*H*,3*H*)-quinazolinedione (5h) A mixture of **3b** (932 mg, 2.5 mmol), 50% NaH (240 mg, 5 mmol) and 1-(2-chloroethyl)piperidine hydrochloride (465 mg, 2.5 mmol) in dimethylformamide (50 ml) was heated at 140—150 °C for 5 h with stirring. The mixture was concentrated *in vacuo*, and the residue was diluted with chloroform. The organic mixture was washed with 10% K_2CO_3, water, and dried. Purification by column chromatography with chloroform–MeOH (10 : 1) afforded 925 mg (76.4%) of **5h**, melted at 138—139 °C (ether–*n*-hexane). HCl salt: mp 243—244 °C (EtOH–ether). *Anal.* Calcd

for $C_{26}H_{30}ClN_3O_4$: C, 64.52; H, 6.20; N, 8.68. Found: C, 64.49; H, 6.21; N, 8.72. ^{1}H-NMR ($CDCl_3$) δ: 1.36 (3H, t, J=7 Hz), 1.42 (6H, m), 2.26 (4H, m), 2.31 (3H, s), 2.55 (3H, s), 4.41 (2H, q, J=7 Hz), 4.44 (2H, t, J=6 Hz), 4.47 (2H, t, J=6 Hz), 7.16 (1H, s), 7.42 (4H, m).

3-(2-Chlorophenyl)-1-(2-cyanoethyl)-6-ethoxycarbonyl-5,7-dimethyl-2,4(1*H*,3*H*)-quinazolinedione (5d) A mixture of **3b** (373 mg, 1 mmol) and solid NaOH (10 mg) in acrylonitrile (5 ml) was refluxed for 3 h with stirring. Excess acrylonitrile was evaporated to afford crude crystals. The crystals were purified by column chromatography with chloroform to afford 416 mg (92%) of **5d**, melted at 231—232 °C (MeOH). *Anal.* Calcd for $C_{22}H_{20}ClN_3O_4$: C, 62.04; H, 4.70; N, 9.87. Found: C, 62.10; H, 4.65; N, 9.91. MS *m/z*: 426, 391, 381, 363. IR ν_{max}^{KBr} cm^{-1}: 3000, 2250, 1715, 1690. ^{1}H-NMR ($CDCl_3$) δ: 2.36 (3H, t, J=7 Hz), 2.71 (3H, s), 2.73 (3H, s), 2.87 (2H, t, J=6 Hz), 4.40 (2H, q, J=7 Hz), 4.49 (2H, t, J=6 Hz), 7.30 (1H, s), 7.43 (4H, m).

3-(2-Chlorophenyl)-6-ethoxycarbonyl-5,7-dimethyl-1-(*N*-phthaloylamino)ethyl-2,4-(1*H*,3*H*)-quinazolinedione (6a) To a mixture of **3b** (746 mg, 2 mmol) and 50% NaH (96 mg, 2.5 mmol) in dimethylformamide (8 ml) was added *N*-(2-bromoethyl)phthalimide (580 mg, 2.3 mmol). The mixture was heated at 80 °C for 4 h, then it was concentrated. The residue was diluted with chloroform. The organic layer was washed with water and dried. Evaporation of the solvent afforded 580 mg (53%) of **6a**, melted at 283—284 °C (MeOH). *Anal.* Calcd for $C_{29}H_{24}ClN_3O_6$: C, 63.73; H, 4.57; N, 7.69. Found: C, 63.68; H, 4.56; N, 7.74. MS *m/z*: 545 ($M^+ - 1$), 510 ($M^+ - Cl$), 500 ($M^+ - OEt$), 363. ^{1}H-NMR ($CDCl_3$) δ: 1.38 (3H, t, J=7 Hz), 2.33 (3H, s), 2.67 (3H, s), 4.18 (2H, m), 4.44 (4H, m), 7.34 (5H, m), 7.72 (4H, s).

Compounds **6b**, **c** were prepared from **3b** in a similar manner.

Preparation of 6d—f. 1-(2-Aminoethyl)-3-(2-chlorophenyl)-6-ethoxycarbonyl-5,7-dimethyl-2,4(1*H*,3*H*)-quinazolinedione (6d) A mixture of 3-(2-chlorophenyl)-6-ethoxycarbonyl-5,7-dimethyl-1-(*N*-phthaloylamino)-ethyl-2,4(1*H*,3*H*)-quinazolinedione (**6a**) (mp 283—284 °C) (578 mg) in MeOH (50 ml) and hydrazine hydrate (1 ml) was stirred at room temperature for 24 h. The solvent was removed, then the residue was diluted with chloroform. The organic mixture was washed with water, dried, and evaporated. The resulting product was recrystallized from EtOH–water to afford 400 mg (91%) of **6a**, melted at 101—102 °C. *Anal.* Calcd for $C_{21}H_{22}ClN_3O_4$: C, 60.64; H, 5.29; N, 10.10. Found: C, 60.57; H, 5.32; N, 10.16. MS *m/z*: 415, 386, 372, 370, 351, 337. ^{1}H-NMR ($CDCl_3$) δ: 1.39 (3H, t, J=7 Hz), 1.89 (2H, br), 2.42 (3H, s), 2.72 (3H, s), 3.07 (2H, t, J=5 Hz), 4.42 (2H, q, J=7 Hz), 4.43 (2H, br), 7.06 (1H, s), 7.40 (4H, m).

Preparation of 7a—d. 3-(2-Chlorophenyl)-6-ethoxycarbonyl-5,7-dimethyl-1-[2-(1-piperidinyl)ethyl]acetyl-2,4(1*H*,3*H*)-quinazolinedione (7b) Compound **5r** (200 mg) and 1-(2-aminoethyl)piperidine (0.5 ml) was heated at 80 °C for 8 h. The reaction mixture was rinsed with ether, followed by recrystallization from EtOAc–ether to afford 120 mg (54%) of **7b**, melted at 179—180 °C. *Anal.* Calcd for $C_{28}H_{33}ClN_4O_5$: C, 62.16; H, 6.10; N, 10.36. Found: C, 62.22; H, 6.05; N, 10.43. MS *m/z*: 540, 495. ^{1}H-NMR ($CDCl_3$) δ: 1.35 (3H, t, J=7 Hz), 1.40 (6H, m), 2.30 (3H, s), 2.30 (2H, br), 2.42 (3H, s), 2.72 (3H, s), 3.30 (2H, q, J=6 Hz), 4.42 (2H, q, J=7 Hz), 4.80 (2H, d, J=5 Hz), 6.71 (1H, br), 7.08 (1H, s), 7.40 (4H, m).

Hydrolysis of 5s and 5u Hydrolysis of **5s** was carried out to stir in concd. HCl at 40 °C for 20 h to afford **8a** in 70% yield. **8a**: mp 181—183 °C (ether). *Anal.* Calcd for $C_{21}H_{10}ClN_2O_6$: C, 58.53; H, 4.41; N, 6.50. Found: C, 58.61; H, 4.43; N, 6.49. MS *m/z*: 430, 395. ^{1}H-NMR ($CDCl_3$) δ: 1.39 (3H, t, J=7 Hz), 2.43 (3H, s), 2.73 (3H, s), 4.43 (2H, q, J=7 Hz), 4.96 (2H, s), 6.75 (1H, s), 7.41 (4H, m).

Preparation of 8c—h. 3-(2-Chlorophenyl)-6-ethoxycarbonyl-5,7-dimethyl-1-(*N*-methylpiperazino)acetyl-2,4(1*H*,3*H*)-quinazolinedione (8g) A mixture of **8a** (300 mg) in thionyl chloride (6 ml) was heated to reflux gently for 30 min. Excess thionyl chloride was removed under reduced pressure to afford an oily residue. This was diluted with anhyd. benzene (50 ml), and *N*-methylpiperazine (0.5 ml) added. After stirring at room temperature for 3 h, the mixture was washed with 10% K_2CO_3, water, and dried. The solvent was evaporated to afford an oil. The oil was crystallized in a small amount of ether and stored in a refrigerator. Yield: 185 mg (69%). mp 164—165 °C (EtOAc–ether). *Anal.* Calcd for $C_{26}H_{29}ClN_4O_5$: C, 60.87; H, 5.65; N, 10.92. Found: C, 60.77; H, 5.63; N, 11.11. MS *m/z*: 512, 467, 413. ^{1}H-NMR ($CDCl_3$) δ: 1.39 (3H, t, J=7 Hz), 2.31 (3H, s), 2.39 (3H, s), 2.42 (4H, m), 2.71 (3H, s), 3.62 (4H, m), 4.40 (2H, q, J=7 Hz), 4.98 (2H, d, J=5 Hz), 6.75 (1H, s), 7.24 (4H, m).

Compounds **8i—k** were prepared in a similar manner using the cor-

TABLE V. Spectral Data for **6a—c**, **7a—d**, **8a—m**, and **9a—b**

No.	MS (*m/z*)	^{1}H-NMR ($CDCl_3$, J=Hz)
6a	415, 386, 372, 370, 351, 337	1.39 (3H, t, 7), 1.89 (2H, br), 2.42 (3H, s), 2.72 (3H, s), 3.07 (2H, t, 5), 4.42 (2H, q, 7), 4.43 (2H, br), 7.06 (1H, s), 7.40 (4H, m)
6b		1.40 (3H, t, 7), 1.55 (2H, s), 1.81 (4H, m), 2.42 (3H, s), 2.73 (3H, s), 2.82 (2H, br), 4.42 (2H, q, 7), 7.10 (1H, s), 7.40 (4H, m)
6c		1.40 (3H, t, 7), 1.64 (6H, m), 2.44 (3H, s), 2.72 (3H, s), 2.74 (2H, br), 4.20 (2H, m), 4.41 (2H, q, 7), 7.00 (1H, s), 7.38 (4H, m)
7a		0.85 (6H, t, 7), 1.40 (3H, t, 7), 2.40 (3H, s), 2.40 (4H, q, 7), 2.42 (2H, m), 3.28 (2H, q, 7), 4.40 (2H, q, 7), 4.78 (2H, d, 5), 6.70 (1H, br), 7.09 (1H, s), 7.40 (4H, m)
7b	540, 495	1.35 (3H, t, 7), 1.40 (6H, m), 2.30 (3H, s), 2.30 (2H, br), 2.42 (3H, s), 2.72 (3H, s), 3.30 (2H, q, 6), 4.42 (2H, q, 7), 4.80 (2H, d, 5), 6.71 (1H, br), 7.08 (1H, s), 7.40 (4H, m)
7c		1.39 (3H, t, 7), 1.63 (2H, m), 2.06 (6H, s), 2.25 (2H, m), 2.42 (3H, s), 2.73 (3H, s), 3.41 (2H, q, 7), 4.44 (2H, q, 7), 4.77 (2H, s), 7.10 (1H, s), 7.42 (4H, m)
7d	556, 525, 513	
8a	430, 395	1.39 (3H, t, 7), 2.43 (3H, s), 2.73 (3H, s), 4.43 (2H, q, 7), 4.96 (2H, s), 6.75 (1H, s), 7.41 (4H, m)
8b	458, 414	
8c[a]		1.32 (3H, t, 7), 2.34 (3H, s), 2.59 (3H, s), 4.36 (2H, q, 7), 4.77 (2H, s), 7.10 (1H, s), 7.51 (4H, m)
8d		1.39 (3H, t, 7), 2.44 (3H, s), 2.71 (3H, s), 2.80 (3H, d, 5), 4.42 (2H, q, 7), 4.73 (2H, d, 5), 6.21 (1H, br), 7.26 (5H, m)
8e		1.38 (9H, m), 2.39 (3H, s), 2.72 (3H, s), 3.45 (4H, q, 7), 4.40 (2H, q, 7), 4.95 (2H, d, 5), 6.75 (1H, s), 7.40 (4H, m)
8f		1.38 (3H, t, 7), 1.67 (6H, s), 2.38 (3H, s), 2.72 (3H, s), 3.54 (4H, br), 4.40 (2H, q, 7), 4.95 (2H, q, 9), 6.76 (1H, s), 7.40 (4H, m)
8g	512, 467, 413	1.39 (3H, t, 7), 2.31 (3H, s), 2.39 (3H, s), 2.42 (4H, m), 2.71 (3H, s), 3.62 (4H, m), 4.40 (2H, q, 7), 4.98 (2H, d, 5), 6.75 (1H, s), 7.24 (4H, m)
8h		1.39 (3H, t, 7), 2.36 (3H, s), 2.72 (3H, s), 3.07 (3H, s), 4.39 (2H, q, 7), 4.63 (2H, s), 5.10 (2H, br), 6.63 (1H, s), 7.28 (9H, m)
8i		1.40 (3H, t, 7), 2.26 (6H, s), 2.40 (3H, s), 2.58 (2H, t, 5), 2.73 (3H, s), 4.30 (2H, t, 5), 4.42 (2H, q, 7), 4.48 (2H, s), 6.75 (1H, s), 7.40 (4H, m)
8j		1.40 (3H, t, 7), 1.42 (6H, br), 2.40 (3H, s), 2.41 (4H, br), 2.58 (2H, t, 5), 2.72 (3H, s), 2.30 (2H, t, 5), 2.41 (2H, q, 7), 6.75 (1H, s), 7.40 (4H, m)
8k		1.38 (3H, t, 7), 1.82 (4H, q, 6), 2.13 (6H, s), 2.14 (2H, br), 2.38 (3H, s), 2.70 (3H, s), 4.38 (2H, q, 7), 4.92 (2H, s), 6.75 (1H, s), 7.40 (4H, m)
8l	457, 422	
8m	471, 436	
9a	472, 437, 408, 390, 337	
9b[a]	390, 372, 337	1.34 (3H, t, 7), 2.45 (3H, s), 2.61 (3H, s), 2.82 (2H, br), 4.40 (2H, q, 7), 5.05 (2H, br), 7.50 (1H, s), 7.51 (4H, s), 8.83 (2H, s), 9.42 (2H, s)

a) ^{1}H-NMR spectra were taken in DMSO-d_6.

responding aminoalcohols instead of amines.

Preparation of Imidate Salt (9a) An ice-cooled mixture of **5d** (350 mg) in anhyd. EtOH (3 ml) and anhyd. dichloromethane (6 ml) was saturated with hydrogen chloride. The mixture was allowed to stand at room temperature until **5d** was no longer observed on the thin layer chromatography developed by chloroform : MeOH (9 : 1). The mixture was evaporated, then the residue was crystallized from EtOH–ether to give 306 mg (73%) of **9a**, melted at 128—129 °C. *Anal.* Calcd for $C_{24}H_{27}Cl_2N_3O_5$: C, 56.69; H, 5.31; N, 8.26. Found: C, 56.74; H, 5.40; N, 8.30. MS *m/z*: 472, 437, 408, 390, 337. IR ν_{max}^{KBr} cm^{-1}: 3000, 2720, 1680, 1600, 1470, 1370.

Preparation of Amidine Salt (9b) To an ice-cooled mixture of **9a** (200 mg) in anhyd. EtOH (4 ml) was added ten drops of saturated ammonia–EtOH. The mixture was stirred under cooled condition until the salt dissolved; This took about 3 h. The solvent was evaporated, then the residue was crystallized from EtOH–ether to give 156 mg (88%) of **9b**. mp 219—220 °C. *Anal.* Calcd for $C_{20}H_{20}Cl_2N_4O_4$: C, 53.21; H, 4.43; N, 12.41. Found: C, 53.19; H, 4.42; N, 12.48. MS *m/z*: 390 ($M^+ - Cl$, NH_3), 372 ($M^+ - CH_2CH-\underset{\underset{NH}{\|}}{C}-NH_2$), 337. ^{1}H-NMR (DMSO-$d_6$) δ: 1.34 (3H, t, J=7 Hz), 2.45 (3H, s), 2.61 (3H, s), 2.82 (2H, br), 4.40 (2H, q, J=7 Hz), 5.05 (2H, br), 7.50 (1H, s), 7.51 (4H, s), 8.83 (2H, s), 9.42 (2H, s).

3-(2-Chlorophenyl)-6-ethoxycarbonyl-1-(3-ethoxycarbonylpropyl)-5,7-dimethyl-2,4(1*H*,3*H*)-quinazolinedione (10) An ice-cooled mixture of **5e** (370 mg, 1 mmol) in EtOH (5 ml) and anhyd. dichloromethane (10 ml) was saturated with hydrogen chloride, then allowed to stand at room temperature for 3 h. The mixture was diluted with chloroform (50 ml), washed with 5% NaOH, water, and dried over anhyd. Na_2SO_4. Evaporation of the solvent afforded crude crystals, which were recrystallized from ether to afford 230 mg (47%) of **10**. mp 82—83 °C. *Anal.* Calcd for $C_{25}H_{27}ClN_2O_6$: C, 61.66; H, 5.75; N, 5.75. Found: C, 61.70; H, 5.80; N, 5.69. MS *m/z*: 486, 451 ($M^+ - Cl$). ^{1}H-NMR ($CDCl_3$) δ: 1.26 (3H, t, J=7 Hz), 1.40 (3H, t, J=7 Hz), 2.10 (4H, br), 2.47 (3H, s), 2.72 (3H, s), 3.49 (2H, q, J=6 Hz), 4.20 (2H, q, J=7 Hz), 4.34 (2H, q, J=7 Hz), 7.25—7.50 (5H, m).

Biological Test The basilar arteries excised from albino rabbits were cut into strips, which were suspended in an organ bath filled with Krebs–Henseleit solution. After 2 h equilibration, each strip was constricted by the addition of 40 mM KCl. When this constriction reached maximum, a solution of test compound in DMSO was added to the bath in a concentration of 3×10^{-6} M, and the resulting relaxation was recorded. The concentration of the DMSO did not exceed 0.3%. At the end of each series of experiments, papaverine was added to the bath in a concentration of 3×10^{-4} M, and the relaxation induced by papaverine was taken as 100%. The relaxing effects of test compounds shown in Table I were expressed as percentage of the maximum relaxation induced by papaverine (3×10^{-4} M), and the relaxing effect is a mean value obtained from 3 runs.

Acknowledgement We thank Dr. S. Moriguchi, Life Science Research Laboratory, Showa Denko Co., Ltd., for his advice in the synthetic study.

References

1) *a*) Y. Eguchi, F. Sasaki, Y. Takashima, M. Nakajima, and M. Ishikawa, *Chem. Pharm. Bull.*, **39**, 795 (1991); *b*) Y. Eguchi and M. Ishikawa, *ibid.*, **39**, 1846 (1991).
2) M. Ishikawa, H. Azuma, Y. Eguchi, A. Sugimoto, S. Ito, Y. Takashima, H. Ebisawa, S. Moriguchi, I. Kotoku, and H. Suzuki, *Chem. Pharm. Bull.*, **30**, 744 (1982).
3) Unpublished observation.
4) W. L. F. Armarego, "Advances in Heterocyclic Chemistry," Vol. 1, Academic Press, New York and London, 1963, p. 243.
5) H.-J. Hess, T. H. Cronin, and A. Scriabine, *J. Med. Chem.*, **11**, 130 (1968).
6) K.-H. Boltze, H.-D. Dell, H. Lehwald, D. Lorenz, and M. R-Schweer, *Arzneim.-Forsch.*, **13**, 688 (1963).
7) H. H. Havera and H. Vidrio, *J. Med. Chem.*, **22**, 1548 (1979).
8) S. Hayao, H. J. Havera, W. G. Strycker, T. J. Leipzig, R. A. Kulp, and H. E. Hartzler, *J. Med. Chem.*, **8**, 807 (1965).
9) G. Pala and E. M.-Uberti, *Arzneim.-Forsch.*, **12**, 1204 (1962).
10) B. Taub and J. B. Hino, *J. Org. Chem.*, **26**, 5238 (1961).
11) M. Ishikawa and Y. Eguchi, *Heterocycles*, **16**, 31 (1981).
12) R. Schwyzer and H. Kappeler, *Helv. Chim. Acta*, **44**, 1991 (1961).
13) G. S. Fonken and W. S. Jhonson, *J. Am. Chem. Soc.*, **74**, 831 (1952).
14) F. C. Schaefer and G. A. Peters, *J. Org. Chem.*, **26**, 412 (1961).

Studies on Uricosuric Diuretics. II. Substituted 7,8-Dihydrofuro[2,3-*g*]-1,2-benzisoxazole-7-carboxylic Acids and 7,8-Dihydrofuro[2,3-*g*]benzoxazole-7-carboxylic Acids[1)]

Haruhiko SATO,* Takashi DAN, Etsuro ONUMA, Haruko TANAKA, Bunya AOKI, and Hiroshi KOGA*

Exploratory Research Laboratories, Chugai Pharmaceutical Co., Ltd., 135 Komakado 1-chome, Gotemba-shi, Shizuoka 412, Japan.
Received January 8, 1991

A series of substituted 7,8-dihydrofuro[2,3-*g*]-1,2-benzisoxazole-7-carboxylic acids 9 and 7,8-dihydrofuro[2,3-*g*]benzoxazole-7-carboxylic acids 12 were synthesized and evaluated for uricosuric and diuretic activities in rats. Many of the benzisoxazole derivatives 9 showed uricosuric and only weak diuretic activities, whereas the benzoxazoles 12 exhibited potent diuretic activities with little affecting urate excretion. Among these compounds, 5-chloro-7,8-dihydro-3-phenylfuro[2,3-*g*]-1,2-benzisoxazole-7-carboxylic acid (9b, AA-193) was found to be a potent uricosuric agent without diuretic activity and was selected for further development.

Keywords diuretic activity; uricosuric activity; 7,8-dihydrofuro[2,3-*g*]-1,2-benzisoxazole-7-carboxylic acid; 7,8-dihydrofuro[2,3-*g*]benzoxazole-7-carboxylic acid

Tienilic acid (**1**) (Chart 1), a member of aryloxyacetic acid diuretics, exhibits marked uricosuric activity as well as diuretic activity.[2)] This uricosuric effect is a rather unusual property for diuretics.[2)] In fact, most diuretics in clinical use today are uric acid retaining and frequently cause hyperuricemia as a side effect. Therefore, some uricosuric activity is a desirable attribute of a good diuretic agent. Unfortunately, however, this drug has been withdrawn from the market in most countries because of its liver toxicity.

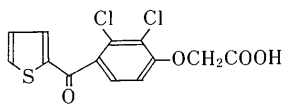

tienilic acid (1)

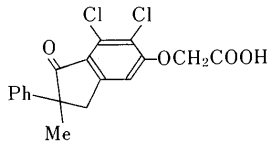

indacrinone (2)

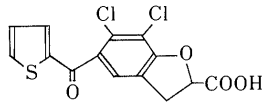

3

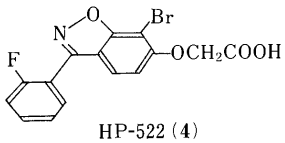

HP-522 (4)

Chart 1

The discovery of tienilic acid (**1**) has stimulated research on structurally related compounds, indacrinone (**2**),[2,3)] a tienilic acid analogue **3**,[2,4)] and HP-522 (**4**)[2,5)] (Chart 1). We noticed that these compounds had aryloxyacetic acid as a common structure and so aimed at discovering better uricosuric diuretics possessing the aryloxyacetic acid structure.

In a previous paper,[6)] we reported the syntheses, and diuretic and uricosuric activities of xanthonyloxyacetic acids **5** and **6** and dihydrofuroxanthone-2-carboxylic acids **7** and **8** (Chart 2). We also designed and prepared benzisoxazole derivatives **9**, **10**, and **11** and dihydrofurobenzoxazole-carboxylic acids **12** (Chart 2). After we completed the work, however, Plattner *et al.*[7)] reported the preparation of benzisoxazole derivatives **10** and **11**.

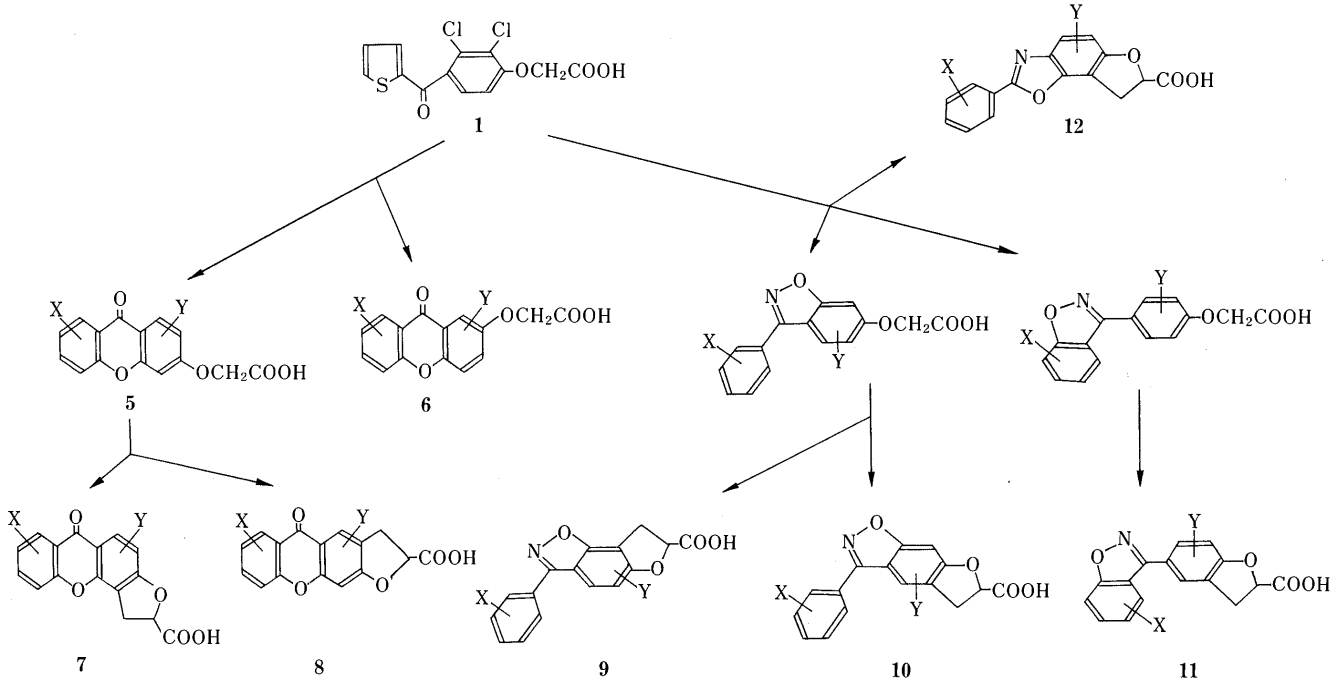

Chart 2

hypouricemic drugs

xanthine oxidase inhibitor

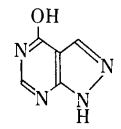

allopurinol (13)

uricosuric agents

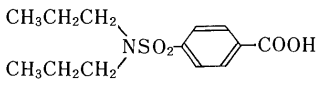

probenecid (14)

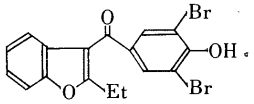

benzbromarone (15)

Chart 3

Herein we report the syntheses and biological activities of benzisoxazoles **9** and benzoxazoles **12**. We found that some of the benzisoxazoles **9** had weak diuretic and potent uricosuric activities and they seemed to be promising as a new class of uricosuric agents.

Allopurinol (**13**), probenecid (**14**), and benzbromarone (**15**) have been clinically used for the treatment of hyperuricemia and gout[8] (Chart 3). Allopurinol, a xanthine oxidase inhibitor, is generally well-tolerated with few significant adverse effects. However, a life-threatening toxicity syndrome has been described after its use, which includes an erythematous, skin rash, fever hepatitis, eosinophilia, and worsening renal function.[9] Although probenecid was the first generally acceptable uricosuric agent, it was originally developed as part of a planned pharmacologic attempt to develop an inhibitor of renal

TABLE I. 7,8-Dihydrofuro[2,3-*g*]-1,2-benzisoxazole-7-carboxylic Acids **9**

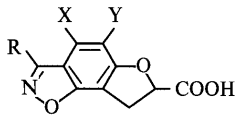

Compd. No.	R	X	Y	Method	Yield (%)	mp (°C)	Recrystn. solvent	Formula	Analysis (%) Calcd (Found)		
									C	H	N
9a	C_6H_5	H	H	B	74	219—220	CH_3CN	$C_{16}H_{11}NO_4$	68.32	3.94	4.98
									(67.96	3.91	5.14)
9aa	C_6H_5	H	Br	B	55	242—244	Acetone–H_2O	$C_{16}H_{10}BrNO_4$	53.36	2.80	3.89
									(53.66	2.89	3.73)
9b	C_6H_5	H	Cl	A	40	254—256	THF–Acetone	$C_{16}H_{10}ClNO_4$	60.87	3.19	4.44
				B	34				(61.08	3.22	4.39)
				C	99						
9c	C_6H_5	H	Me	B	61	214—216	Acetone–H_2O	$C_{17}H_{13}NO_4$	69.15	4.44	4.74
									(68.84	4.28	4.65)
9d	2-ClC_6H_4	H	Cl	B	55	220—222	Acetone–H_2O	$C_{16}H_9Cl_2NO_4$	54.88	2.59	4.00
									(54.86	2.66	4.01)
9e	2-FC_6H_4	H	Cl	B	89	199—200	Acetone–H_2O	$C_{16}H_9ClFNO_4$	57.59	2.72	4.20
									(57.50	2.77	4.40)
9f	2-$CH_3C_6H_4$	H	Cl	A	42	191—192	AcOEt–hexane	$C_{17}H_{12}ClNO_4$	61.92	3.67	4.25
									(61.88	3.63	4.31)
9g	3-ClC_6H_4	H	Cl	A	52	168—169	CH_3CN–H_2O	$C_{16}H_9Cl_2NO_4$	54.88	2.59	4.00
									(54.83	2.62	3.91)
9h	3-FC_6H_4	H	Cl	A	48	209—210	Acetone–H_2O	$C_{16}H_9ClFNO_4$	57.59	2.72	4.20
									(57.48	2.75	4.00)
9i	4-ClC_6H_4	H	Cl	A	64	240—243	Acetone–H_2O	$C_{16}H_9Cl_2NO_4$	54.88	2.59	4.00
									(55.05	2.69	3.82)
9j	4-FC_6H_4	H	Cl	A	38	215—218	Acetone–H_2O	$C_{16}H_9ClFNO_4$	57.59	2.72	4.20
									(57.53	2.79	4.04)
9k	4-OHC_6H_4	H	Cl	C	Quant.	263—265	AcOEt–hexane	$C_{16}H_{10}ClNO_5$	57.94	3.04	4.22
									(57.85	2.98	4.09)
9l	2,6-$F_2C_6H_3$	H	Cl	B	72	240—241	Acetone–H_2O	$C_{16}H_8ClF_2NO_4$	54.64	2.29	3.98
									(54.77	2.29	3.98)
9m	2,4-$F_2C_6H_3$	H	Cl	C	99	236—237	Acetone–H_2O	$C_{16}H_8ClF_2NO_4$	54.64	2.29	3.98
									(55.03	2.13	4.09)
9n	2-Thienyl	H	Cl	A	33	249—251	Acetone–H_2O	$C_{14}H_8ClNO_4S$	52.26	2.51	4.35
									(52.14	2.51	4.11)
9o	CH_3	H	Cl	C	Quant.	196—198	AcOEt–hexane	$C_{11}H_8ClNO_4$	52.09	3.18	5.52
									(52.13	3.11	5.48)
9p	$CH_2CH(CH_3)_2$	H	Cl	C	98	157—158	AcOEt–hexane	$C_{14}H_{14}ClNO_4$	56.86	4.77	4.74
									(56.81	4.72	4.79)
9q	Cyclo-C_5H_9	H	Cl	C	Quant.	165—167	AcOEt–hexane	$C_{15}H_{14}ClNO_4$	58.55	4.59	4.55
									(58.61	4.60	4.58)
9r	3-Pyridyl	H	Cl	C	74	>310	DMSO–$CHCl_3$	$C_{15}H_9ClN_2O_4$	56.89	2.86	8.85
									(56.49	2.49	8.45)
9s	2-FC_6H_4	Cl	H	B	60	191—193	Acetone–H_2O	$C_{16}H_9ClFNO_4$	57.59	2.72	4.20
									(57.75	2.65	4.15)

TABLE II. 7,8-Dihydrofuro[2,3-*g*]benzoxazole-7-carboxylic Acids **12**

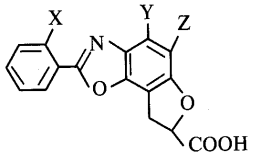

Compd. No.	X	Y	Z	Method	Yield (%)	mp (°C)	Recrystn. solvent	Formula	Analysis (%) Calcd C	Calcd H	Calcd N	Found C	Found H	Found N
12b	H	H	Cl	F	Quant.	242—243	Acetone–H_2O	$C_{16}H_{10}ClNO_4$	60.87	3.19	4.44	60.81	3.12	4.36
12s	F	Cl	H	D	65	234—235	CH_3CN	$C_{16}H_9FClNO_4$	57.59	2.72	4.20	57.77	2.60	4.31
12sa	F	Cl	Cl	D′	77	268—269	Acetone	$C_{16}H_8FCl_2NO_4$	52.20	2.19	3.80	52.28	2.25	3.86
12sb	F	H	H	D′	71	201—203	CH_3CN	$C_{16}H_{10}FNO_4$	64.22	3.37	4.68	64.11	3.26	4.94
12sc	F	H	Cl	D′	75	245—247	Acetone–H_2O	$C_{16}H_9FClNO_4$	57.59	2.72	4.20	57.43	2.82	4.08
12t	H	Cl	H	D	73	230—232	CH_3CN–H_2O	$C_{16}H_{10}ClNO_4$	60.87	3.19	4.44	61.05	3.33	4.56
12ta	H	Cl	Cl	D′	43	263—265	CH_3CN	$C_{16}H_9Cl_2NO_4$	54.88	2.59	4.00	54.91	2.73	4.40
12u	Me	H	H	E (D)	54	173—175	CH_3CN	$C_{17}H_{13}NO_4$	69.14	4.44	4.74	68.84	4.48	5.03

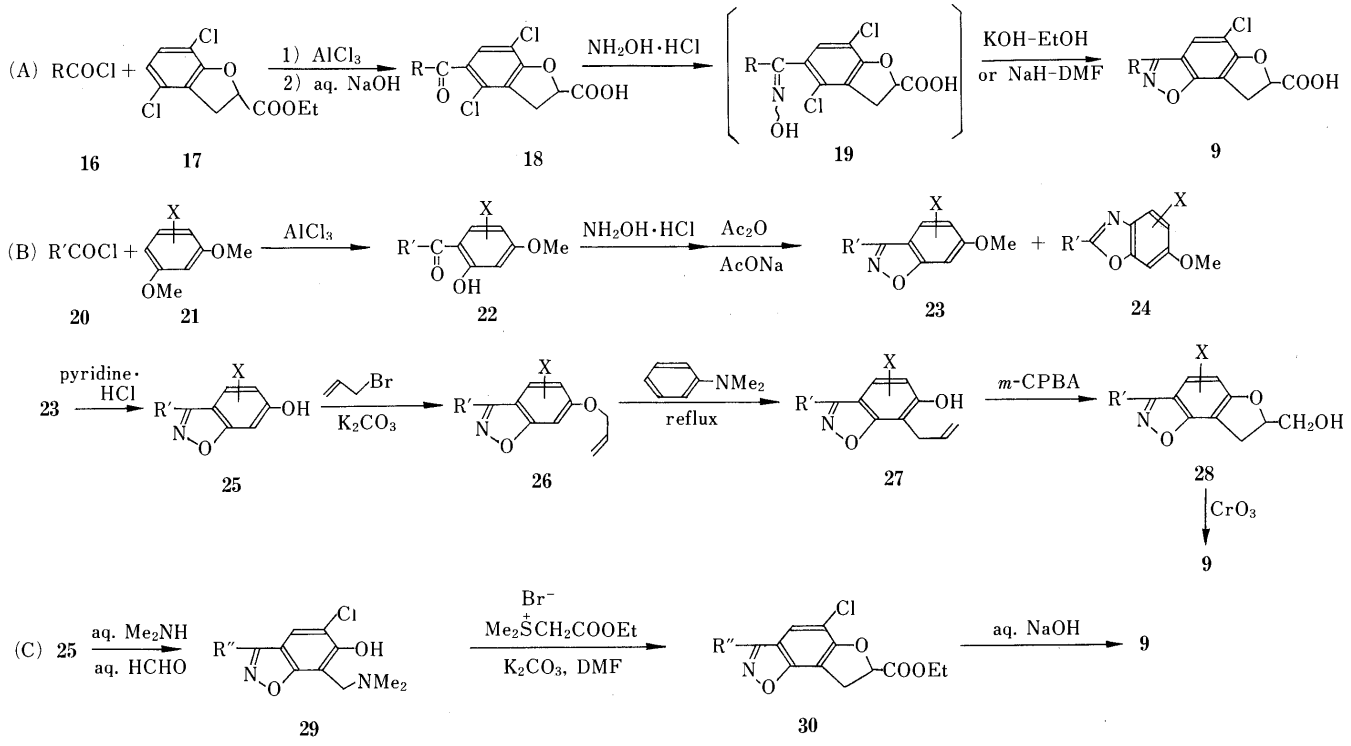

Chart 4

tubular secretion of penicillin and inhibits renal tubular secretion of many organic acids including *p*-aminohippuric acid (PAH) and penicillin. Benzbromarone is a potent uricosuric agent and appears to be a more selective inhibitor of the reabsorption of uric acid in the proximal tubules, but the preclinical studies showed that it has teratogenicity and carcinogenicity in rats.[10] Under these circumstances, there appears to exist a strong need for the development of safer uricosuric agents.

Chemistry The compounds prepared in this study are listed in Tables I and II, and their synthetic routes are outlined in Charts 4—6.

We have developed three general routes for the preparation of 7,8-dihydrofuro[2,3-*g*]-1,2-benzisoxazole-7-carboxylic acids **9** (Chart 4).

Method A was particularly useful for preparing compounds containing a chloro substituent at position 5 and an aryl ring (without an *ortho* halogen) at position 3 in **9**. Ethyl 4,7-dichloro-2,3-dihydrobenzo[*b*]furan-2-carboxylate (**17**)[4] was treated with an acyl chloride **16** (1 eq) and aluminum chloride (2 eq) in 1,2-dichloroethane, followed by hydrolysis with an alkaline solution, to afford the 5-acyl-4,7-dichloro-2,3-dihydrobenzo[*b*]furan-2-carboxylic acid **18** (Table IV). This compound **18** was heated with hydroxylamine hydrochloride in pyridine to give the corresponding oxime **19**, which was cyclized to the desired benzisoxazole **9** (Table I) upon treatment with ethanolic potassium hydroxide or sodium hydride in *N*,*N*-dimethylformamide (DMF).

Compounds containing an *o*-halo substituent on the

pendant phenyl ring in **9** were not readily accessible by method A due to competing cyclization of the oxime anion at both *ortho* positions. For these derivatives, as well as analogues containing variable substituents at positions 4 and 5, methods B and C shown in Chart 4 were used. In method B, a resorcinol dimethyl ether **21** was subjected to react with an acyl chloride **20** (1 eq) and aluminum chloride (1 eq) in 1,2-dichloroethane under the controlled conditions (see Experimental section) to afford the 2-acyl-5-methoxyphenol **22** (Table V). Treatment of **22** with hydroxylamine hydrochloride followed by the action of acetic anhydride and sodium acetate gave rise to the 6-methoxy-1,2-benzisoxazole **23** and the benzoxazole isomer **24**, which apparently arose from the Beckmann rearrangement of the oxime intermediate with the intramolecular capture by the phenol (Table VI). The methyl ether in **23** was smoothly cleaved with pyridine hydrochloride at 180—200 °C, giving the corresponding 6-hydroxy-1,2-benzisoxazole **25** (Table VII). The phenol **25** was alkylated with allyl bromide to give the 6-allyloxy-1,2-benzisoxazole **26** (Table VIII), which was transformed into the rearrangement product, 7-allyl-6-hydroxy-1,2-benzisoxazole **27** (Table IX) by heating in *N*,*N*-dimethylaniline. Oxidation of **27** with *m*-chloroperbenzoic acid (*m*-CPBA) gave the corresponding epoxide intermediate, which immediately cyclized to the dihydrobenzofuran **28** (Table X). Jones oxidation of **28** led to the desired carboxylic acid **9** (Table I).

Method C was originally developed for the large scale preparation of **9b** (AA-193),[11] an excellent candidate for a new uricosuric agent, and was also successfully employed for the synthesis of various derivatives of **9**. The 5-chloro-6-hydroxy-1,2-benzisoxazole **25** was treated with

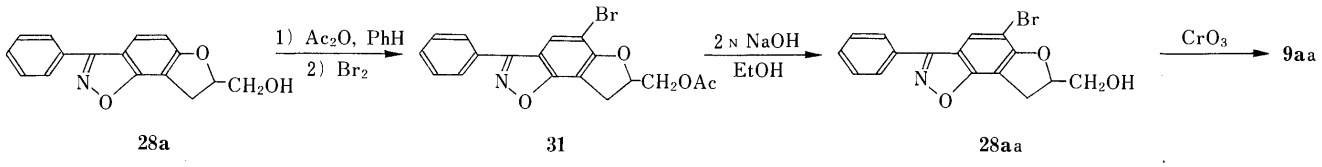

Chart 5

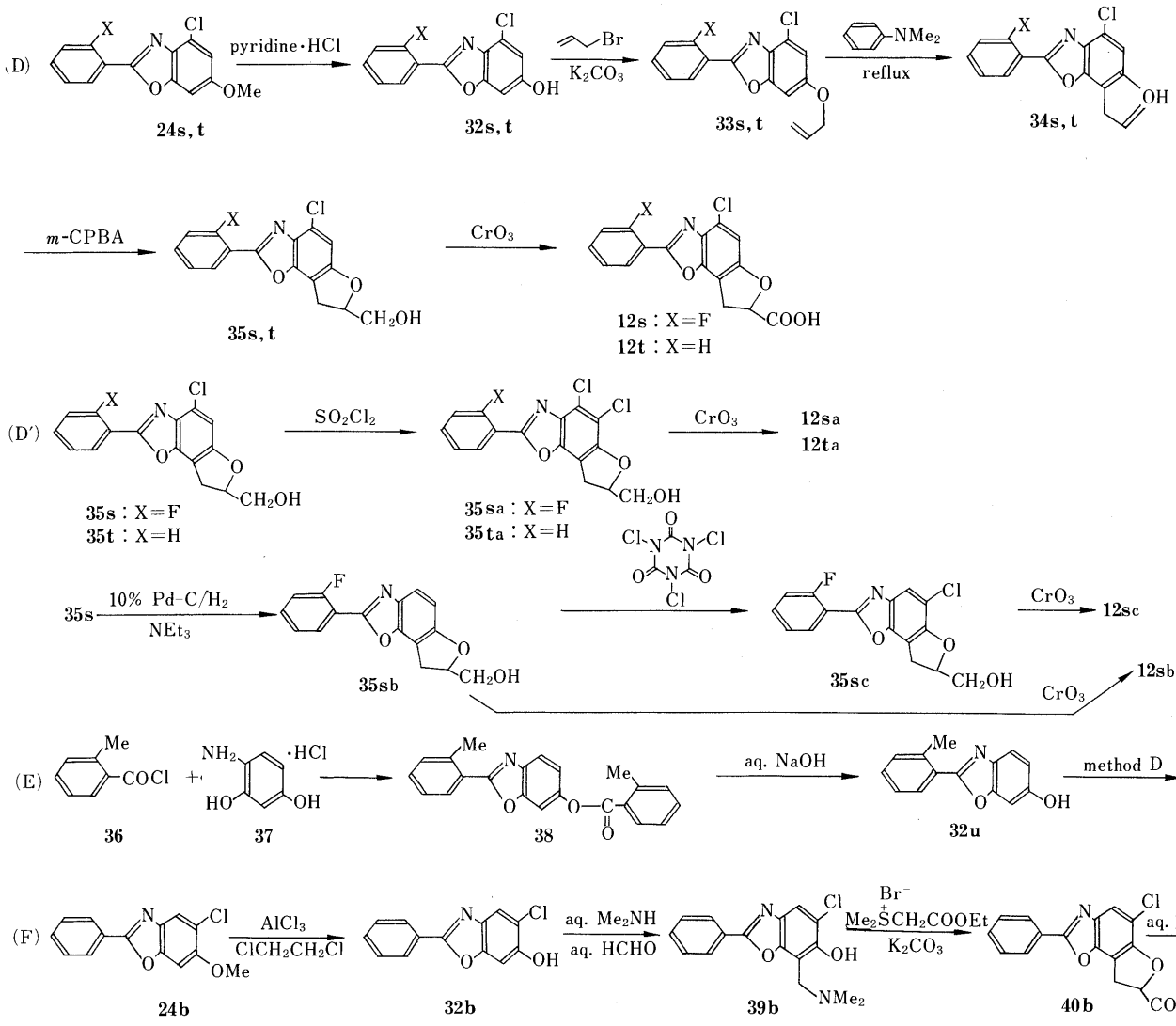

Chart 6

aqueous dimethylamine and formaline to give the Mannich base, the 6-hydroxy-7-dimethylaminomethylbenzisoxazole **29** (Table XI), which was converted into the dihydrobenzofuran **30** by reaction with dimethyl ethoxycarbonylmethylsulfonium bromide in the presence of anhydrous potassium carbonate (Table XII). Hydrolysis of **30** with aqueous sodium hydroxide gave the desired carboxylic acid **9** (Table I).

The 5-bromo derivative **9aa** was synthesized by the method shown in Chart 5.

Successive treatment of the dihydrobenzofuran **28a** with acetic anhydride and bromine gave the 7-acetoxymethyl-5-bromo derivative **31**. The compound **31** was hydrolyzed with aqueous sodium hydroxide to the methanol **28aa**. Jones oxidation of **28aa** afforded the desired **9aa** (Table I).

Synthesis of the 7,8-dihydrofuro[2,3-*g*]benzoxazole-7-carboxylic acids **12** were achieved by four methods shown in Chart 6.

Using the 4-chloro-6-methoxybenzoxazoles **24s** and **24t** formed in the method B procedure as the starting materials, the 4-chlorobenzoxazole derivatives, **12s** and **12t**, were prepared in the same way as the isomeric benzisoxazole **9** (method D) (Table II, XIII, XIV, XV, and XVI).

Compounds **12sa**, **12sb**, **12sc**, and **12ta** were prepared from the benzoxazoles, **35s** and **35t** (method D′). Treatment of **35s** and **35t** with sulfuryl chloride in dichloromethane gave the corresponding 4,5-dichloro derivatives **35sa** and **35ta**. Catalytic hydrogenolysis of **35s** led to the dechlorinated derivative **35sb**. Chlorination of **35sb** with trichloroisocyanuric acid in DMF afforded the 5-chloro derivative **35sc** (Table XVI). Jones oxidation of **35sa**, **35sb**, **35sc**, and **35ta** gave the corresponding carboxylic acids, **12sa**, **12sb**, **12sc**, and **12ta**, respectively (Table II).

The 6-hydroxy-2-(*o*-tolyl)-benzoxazole intermediate **32u** was also obtained by an alternative approach (method E). Treatment of 2-methylbenzoyl chloride (**36**) with 4-aminoresorcinol (**37**) gave the 6-acyloxybenzoxazole **38** which was hydrolyzed with aqueous sodium hydroxide to the 6-hydroxybenzoxazole **32u** (Table XIII). The compound **32u** was transformed into the corresponding carboxylic acid **12u** by method D.

The 5-chloro-2-phenyl derivative **12b** was synthesized by method F similar to method C starting from the 5-chloro-6-methoxybenzoxazole **24b** through the phenol **32b**, a Mannich base **39b** and the dihydrofurobenzoxazole **40b**.

Resolution of **9b** was accomplished by recrystallization of the (−)-cinchonidine salt to give (+)-**9b** and (+)-phenylethylamine salt to give (−)-**9b**.

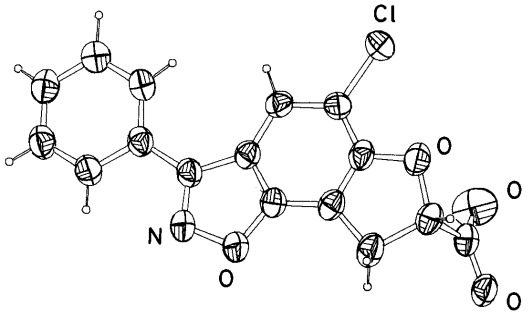

Fig. 1. ORTEP Drawing of (−)-**9b**

The absolute configuration of (−)-**9b** as determined from X-ray analysis of the corresponding (+)-phenylethylamine salt is 7*S* (see Fig. 1).[12]

Biological Activities Uricosuric and diuretic activities in rats of the compounds **9** and **12** are shown in Table III. Tienilic acid and indacrinone were used as the reference agents for the uricosuric and diuretic activities and probenecid and benzbromarone as those for the uricosuric activity. Tienilic acid showed moderate uricosuric and diuretic activities, whereas indacrinone showed potent uricosuric and diuretic activities. Probenecid exhibited only weak uricosuric activity, but benzbromarone did not increase urate excretion in this assay.

The uricosuric activity of most of the benzisoxazoles **9** was comparable to, or more potent than, that of tienilic acid, but the effect of **9** on diuresis was only marginal. On the other hand, the benzoxazoles **12**, the isomer of **9**, showed a high level of diuretic activity without significant uricosuric activity, except for **12sb**. It has been observed that a

Table III. Diuretic and Uricosuric Activities[a]

Compd. No.	Dose (mg/kg)	No. of animals	Uricosuric[b] (0—6 h)	Diuretic[b] (0—6 h)
9a	100	5	122	102
9aa	100	5	119[c]	153
9b	0.39	20	110[c]	109
	0.78	20	120[e]	96
	3.13	25	127[e]	94
	100	49	138[e]	107
S(−)-**9b**	1.56	15	139[e]	101
R(+)-**9b**	1.56	10	102	99
	25	5	104	105
9c	100	5	115	114
9d	100	5	109	96
9e	100	5	113	88
9f	100	5	142[c]	96
9g	100	5	102	144[c]
9h	100	5	132[d]	149[d]
9i	100	5	96	99
9j	100	5	114	114
9k	100	10	98	98
9l	100	5	115	125
9m	100	5	131[d]	123
9n	100	5	122[c]	125
9o	100	5	124[c]	98
9p	100	5	121[c]	165[d]
9q	100	5	129	128[c]
9r	100	5	148[c]	136
9s	100	5	104	151[c]
12b	100	5	101	248[e]
12s	100	5	123	335[e]
12sa	100	5	102	262[e]
12sb	100	5	135[e]	246[e]
12sc	100	5	102	242[e]
12t	100	5	75[c]	222[e]
12ta	100	5	97	419[e]
Tienilic acid	100	15	118[c]	143[e]
Indacrinone	100	19	156[e]	265[e]
Probenecid	400	5	118	88
	800	5	151[c]	59[d]
Benzbromarone	100	16	103	64[e]
	200	15	90	54[e]

a) Test compounds were orally administered to Wistar–Imamichi rats and the activities are shown as relative activity (%) to the control (100%). Details of the test protocol are described in the experimental section. *b*) Student's *t*-test: *c*) $p<0.05$, *d*) $p<0.01$, *e*) $p<0.001$ *vs.* control; values without marks are not statistically significant.

ring-annelation of phenoxyacetic acid diuretics results in a high ceiling uricosuric profile, as in compounds **2**, **3**, **4**, and **10**.[7] However, our results show that this is not the case for ring system **9**. No clear structure–activity relationships emerged for the substituents of compounds **9** and **12**.

With only the information in this study, it is impossible to rationalize why the benzoxazoles **12** have increasing diuretic activity compared to the benzisoxazoles **9**. Therefore, we examined the three-dimensional structure–activity relationships of the aryloxyacetic acid diuretics, including **1**, **2**, **3**, and their enantiomers, and created the receptor map. With this receptor model, we were able to semiquantitatively and elegantly rationalize the difference in the diuretic activity between **12** and **9**.[13]

Among these compounds, the benzoxazole derivative **12ta** showed the most potent diuretic activity, but it is devoid of uricosuric property. On the other hand, the benzisoxazoles **9b** and **9f** had potent uricosuric activity without diuretic activity. The dose–response study for uricosuric activity of **9b** demonstrated that it significantly increases urate excretion at a low dose of 0.39 mg/kg *p.o.*

The uricosuric activity of **9b** was evaluated in detail in rat, mice, and Cebus monkeys in comparison to tienilic acid (**1**), probenecid (**14**), and benzbromarone (**15**). Compound **9b** showed uricosuric activity in all the animals tested and was found to have a mode of action different from the reference drugs. It appeared to inhibit presecretory reabsorption in the proximal tubules.[14] Compound **9b** (AA-193) was selected for furthur development and is currently undergoing clinical evaluation as a new class of uricosurics.

Evaluation of the enantiomers of **9b** revealed that the *S*(−) isomer possesses all the uricosuric activity.

Experimental

Melting points were determined on a Yanagimoto micro melting point apparatus and are uncorrected. Infrared (IR) spectra were taken on a Hitachi 270-30 spectrophotometer. Nuclear magnetic resonance (NMR) spectra were recorded on a Hitachi R-24B spectrometer using tetramethylsilane as an internal standard. Chemical shifts are given in ppm and coupling constants are given in Hertz. The following abbreviations are used: s=singlet, d=doublet, t=triplet, q=quartet, dd=doublet of doublets, br=broad. For column chromatography, Wakogel C-200 (Wako, 0.074—0.149 mm) was used.

5-Benzoyl-4,7-dichloro-2,3-dihydrobenzo[*b*]furan-2-carboxylic Acid (18b) General Procedure: Ethyl 4,7-dichloro-2,3-dihydrobenzo[*b*]furan-2-carboxylate (**17**) (58.7 g, 0.23 mol) and benzoyl chloride (35 g, 0.25 mol) were dissolved in 1,2-dichloroethane (600 ml) and the solution was cooled to 0—5 °C. $AlCl_3$ (69 g, 0.52 mol) was added portionwise to the solution, and the resulting mixture was warmed to room temperature over an 8 h period and left to stand overnight. After addition of ice-water and conc. HCl to the solution, the mixture was extracted with Et_2O. The extract was washed with H_2O, dried over Na_2SO_4, and evaporated to give crude ethyl 5-benzoyl-4,7-dichloro-2,3-dihydrobenzo[*b*]furan-2-carboxylate. 1 N NaOH (1000 ml) was added to a solution of crude ester in EtOH (100 ml) and the mixture was refluxed for 2 h and then cooled. The mixture was acidified with conc. HCl and extracted with Et_2O. The extract was washed with H_2O, dried over Na_2SO_4, and evaporated. Recrystallization from benzene gave **18b** (35.8 g). MS *m/z*: 336 (M^+), 259. IR (KBr) cm^{-1}: 1736 (COOH), 1666 (C=O). NMR ($CDCl_3$–DMSO-d_6) δ: 3.53 (1H, d, J=7.8 Hz, Ph-C<u>H</u>$_2$), 3.61 (1H, d, J=9.8 Hz, Ph-C<u>H</u>$_2$), 5.41 (1H, dd, J=9.8, 7.8 Hz, Ph-CH$_2$-C<u>H</u>), 7.22 (1H, s, 6-H), 7.30—7.97 (5H, m, arom. H), 7.50 (1H, br s, COO<u>H</u>). Yields, melting points, recrystallization solvents, and microanalyses data for **18** are given in Table IV.

5-Chloro-7,8-dihydro-3-phenylfuro[2,3-*g*]-1,2-benzisoxazole-7-carboxylic Acid (9b) General Procedure, Method A: A solution of **18b** (47.2 g, 0.14 mol) and $NH_2OH \cdot HCl$ (100 g, 1.43 mol) in pyridine (700 ml) was refluxed for 24 h, and evaporated. The resulting mixture was acidified with HCl and extracted with Et_2O. The extract was washed with H_2O, dried over Na_2SO_4, and evaporated to give 50 g of 4,7-dichloro-2,3-dihydro-5-(α-hydroxyiminobenzyl)benzo[*b*]furan-2-carboxylic acid (**19b**). The crude **19b** (50 g) was dissolved in DMF (600 ml) and the solution was cooled to 0—5 °C. 60% NaH (17.0 g, 0.43 mol) was added portionwise to the solution, and the resulting mixture was warmed to room temperature over a 7 h period and left to stand overnight. After cooling, the mixture was acidified with HCl and extracted with Et_2O. The extract was washed with H_2O, dried over Na_2SO_4, and evaporated. Recrystallization gave **9b** (19.4 g) as crystals (acetone–H_2O), mp 224—227 °C, (tetrahydrofuran (THF)–acetone), mp 254—256 °C. MS *m/z*: 315 (M^+). IR (KBr) cm^{-1}: 1728 (COOH), 1712. NMR ($CDCl_3$–DMSO-d_6) δ: 3.74 (1H, d, J=7.8 Hz, Ph-C<u>H</u>$_2$), 3.79 (1H, d, J=9.8 Hz, Ph-C<u>H</u>$_2$), 5.44 (1H, dd, J=9.8, 7.8 Hz, Ph-CH$_2$-C<u>H</u>), 7.34—7.63 (3H, m, arom. H), 7.63—8.00 (2H, m, arom. H), 7.67 (1H, s, 4-H), 8.29 (1H, br s, COO<u>H</u>). Yields, melting points, recrystallization solvents, and microanalyses data for **9b**, **f**—**j**, **n** are given in Table I.

3-Chloro-6-hydroxy-4-methoxybenzophenone (22b) General Procedure: Dimethylresorcine (6.9 g, 0.050 mol) was dissolved in $CHCl_3$ (100 ml) and the solution was cooled to 0—5 °C. SO_2Cl_2 (7.6 g, 0.056 mol) was added portionwise to the solution and the resulting mixture was warmed to room temperature over 5 h and left to stand overnight, and evaporated to give crude 4-chlorodimethylresorcine. This crude resorcine and benzoyl chloride (7.4 g, 0.053 mol) were dissolved in 1,2-dichloroethane (100 ml) and the solution was cooled to 0—5 °C. $AlCl_3$ (7.0 g, 0.052 mol) was added portionwise to the solution, and the resulting mixture was warmed to room temperature over a 2 h period and then refluxed for 1 h. After cooling, ice-water and conc. HCl were added to the reaction mixture, and the whole mixture was stirred for 30 min. The slurry formed was extracted with Et_2O. The extract was washed with H_2O, dried over Na_2SO_4, and evaporated. Recrystallization from CH_2Cl_2–hexane gave **22b** (8.6 g). MS *m/z*: 262 (M^+), 261. IR (KBr) cm^{-1}: 1624 (C=O), 1604. NMR ($CDCl_3$) δ: 3.84 (3H, s, C<u>H</u>$_3$), 6.45 (1H, s, 5-H), 7.17—7.73 (6H, m, arom. H, 2-H), 12.60 (1H, s,

TABLE IV. 5-Acyl-4,7-dichloro-2,3-dihydrobenzo[*b*]furan-2-carboxylic Acids **18**

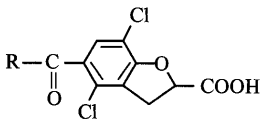

Compd. No.	R	Yield (%)	mp (°C)	Recrystn. solvent	Formula	Analysis (%) Calcd C	Calcd H	Found C	Found H
18b	C_6H_5	47	167—169	Benzene	$C_{16}H_{10}Cl_2O_4$	57.00	2.99	57.02	3.01
18f	2-$CH_3C_6H_4$	12	174—176	Benzene	$C_{17}H_{12}Cl_2O_4$	58.14	3.44	57.99	3.41
18g	3-ClC_6H_4	69	159—161	Benzene	$C_{16}H_9Cl_3O_4$	51.72	2.44	52.12	2.46
18h	3-FC_6H_4	84	183—184	Benzene	$C_{16}H_9Cl_2FO_4$	54.11	2.55	54.23	2.62
18i	4-ClC_6H_4	72	212—213	Benzene	$C_{16}H_9Cl_3O_4$	51.72	2.44	51.79	2.42
18j	4-FC_6H_4	72	188—190	Benzene	$C_{16}H_9Cl_2FO_4$	54.11	2.55	54.51	2.62
18n	2-Thienyl	22	167—168	Benzene	$C_{14}H_8Cl_2O_4S$	49.00	2.35	48.93	2.48

TABLE V. 2-Acyl-5-methoxyphenols **22**

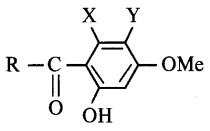

Compd. No.	R	X	Y	Yield (%)	mp (°C)	Recrystn. solvent	Formula	Analysis (%) Calcd (Found)		
								C	H	N
22a	C_6H_5	H	H	85	64—66 (Lit.[15] 66)	Hexane				
22b	C_6H_5	H	Cl	66	118—119	CH_2Cl_2–hexane	$C_{14}H_{11}ClO_3$	64.01 (63.96	4.22 4.15)	
22c	C_6H_5	H	Me	97	88—89 (Lit.[16] 188)	Hexane	$C_{15}H_{14}O_3$	74.36 (74.42	5.83 5.91)	
22d	2-ClC_6H_4	H	Cl	77	98—99	EtOH	$C_{14}H_{10}Cl_2O_3$	56.59 (56.73	3.39 3.26)	
22e	2-FC_6H_4	H	Cl	64	133—134	CH_2Cl_2–Et_2O	$C_{14}H_{10}ClFO_3$	59.91 (59.93	3.59 3.52)	
22k	4-$OCH_3C_6H_4$	H	Cl	85	130—132	CH_2Cl_2–Et_2O	$C_{15}H_{13}ClO_4$	61.55 (61.54	4.48 4.27)	
22l	2,6-$F_2C_6H_3$	H	Cl	92	132—133	CH_2Cl_2–Et_2O	$C_{14}H_9ClF_2O_3$	56.30 (56.30	3.04 3.04)	
22m	2,4-$F_2C_6H_3$	H	Cl	99	136—137	EtOH	$C_{14}H_9ClF_2O_3$	56.30 (56.43	3.04 3.01)	
22o	CH_3	H	Cl	79	154—155	EtOH	$C_9H_9ClO_3$	53.88 (53.58	4.52 4.37)	
22p	$CH_2CH(CH_3)_2$	H	Cl	92	81—82	EtOH	$C_{12}H_{15}ClO_3$	59.39 (59.28	6.23 6.19)	
22q	Cyclo-C_5H_9	H	Cl	87	88—89	EtOH	$C_{13}H_{15}ClO_3$	61.30 (61.41	5.94 6.18)	
22r	3-Pyridyl	H	Cl	29	157—159	EtOH	$C_{13}H_{10}ClNO_3$	59.22 (59.29	3.82 3.73	5.31 5.32)
22s	2-FC_6H_4	Cl	H	70	111—113 (Lit.[5] 108—110)	CH_2Cl_2–Et_2O	$C_{14}H_{10}ClFO_3$	59.91 (59.77	3.59 3.61)	
22t	C_6H_5	Cl	H	72	96—98	Et_2O–hexane	$C_{14}H_{11}ClO_3$	64.01 (64.20	4.22 4.17)	

OH). Yields, melting points, recrystallization solvents, and microanalyses data for **22** are given in Table V.

5-Chloro-6-methoxy-3-phenyl-1,2-benzisoxazole (23b), 5-Chloro-6-methoxy-2-phenylbenzoxazole (24b) General Procedure: A mixture of **22b** (76.5 g, 0.29 mol) and $NH_2OH \cdot HCl$ (122.0 g, 1.76 mol) in pyridine (500 ml) was refluxed for 4 h, and evaporated. The resulting mixture was acidified with HCl and extracted with Et_2O. The extract was washed with H_2O, dried over Na_2SO_4, and evaporated to give 4-chloro-2-(α-hydroxyiminobenzyl)-5-methoxyphenol. A mixture of this crude phenol, acetic anhydride (68.8 g, 0.67 mol) and sodium acetate (52.5 g, 0.64 mol) in DMF (600 ml) was refluxed for 3.5 h. The product crystallized upon the addition of H_2O was collected by filtration, washed with H_2O, dried, and chromatographed on silica gel with CH_2Cl_2 to give **23b** (38.9 g) and **24b** (29.1 g). Product **23b**: MS *m/z*: 259 (M^+). IR (KBr) cm^{-1}: 1618. NMR ($CDCl_3$) δ: 3.94 (3H, s, C<u>H</u>$_3$), 7.04 (1H, s, 7-H), 7.32—7.65 (3H, m, arom. H), 7.65—8.02 (2H, m, arom. H), 7.79 (1H, s, 4-H). Product **24b**: MS *m/z*: 259 (M^+), 244. IR (KBr) cm^{-1}: 1474. NMR ($CDCl_3$) δ: 3.84 (3H, s, C<u>H</u>$_3$), 6.99 (1H, s, 7-H), 7.25—7.54 (3H, m, arom. H), 7.64 (1H, s, 4-H), 7.83—8.22 (2H, m, arom. H). Yields, melting points, recrystallization solvents, and microanalyses data for **23** and **24** are given in Table VI.

5-Chloro-6-hydroxy-3-phenyl-1,2-benzisoxazole (25b) General Procedure: Compound **23b** (10.1 g, 0.039 mol) was heated with pyridine hydrochloride (129 g) at 180—190 °C for 7 h and then cooled to 70 °C. The product crystallized upon the addition of H_2O was collected by filtration and washed with H_2O to give **25b** (9.3 g). MS *m/z*: 245 (M^+). IR (KBr) cm^{-1}: 3072, 3042. NMR ($CDCl_3$–DMSO-d_6) δ: 7.19 (1H, s, 7-H), 7.34—7.67 (3H, m, arom. H), 7.67—8.09 (2H, m, arom. H), 7.80 (1H, s, 4-H), 10.57 (1H, br s, O<u>H</u>). Yields, melting points, recrystallization solvents, and microanalyses data for **25** are given in Table VII.

6-Allyloxy-5-chloro-3-phenyl-1,2-benzisoxazole (26b) General Procedure: A mixture of **25b** (9.3 g, 0.038 mol), allyl bromide (6.8 g, 0.056 mol) and anhydrous K_2CO_3 (7.9 g, 0.057 mol) in DMF (100 ml) was stirred at 50—60 °C for 2.5 h. The product crystallized upon the addition of H_2O was collected by filtration and washed with H_2O to give **26b** (10.8 g). MS *m/z*: 285 (M^+). IR (KBr) cm^{-1}: 1362, 1292. NMR ($CDCl_3$) δ: 4.63 (2H, dt, J=4.7, 1.4 Hz, O–C<u>H</u>$_2$), 5.14—5.70 (2H, m, –CH=C<u>H</u>$_2$), 5.70—6.47 (1H, m, –C<u>H</u>=CH$_2$), 7.03 (1H, s, 7-H), 7.30—7.65 (3H, m, arom. H), 7.65—8.04 (2H, m, arom. H), 7.80 (1H, s, 4-H). Yields, melting points, recrystallization solvents, and microanalyses data for **26** are given in Table VIII.

7-Allyl-5-chloro-6-hydroxy-3-phenyl-1,2-benzisoxazole (27b) General Procedure: A solution of **26b** (10.8 g, 0.038 mol) in *N*,*N*-dimethylaniline (100 ml) was refluxed for 1 h. After cooling, the mixture was acidified with conc. HCl and the deposited crystals were collected by filtration, washed with H_2O to give **27b** (7.5 g). MS *m/z*: 285 (M^+), 270. IR (KBr) cm^{-1}: 3256. NMR ($CDCl_3$–DMSO-d_6) δ: 3.72 (2H, dt, J=6.4, 1.4 Hz, Ph-C<u>H</u>$_2$), 4.82—5.50 (2H, m, –CH=C<u>H</u>$_2$), 5.70—6.57 (1H, m, –C<u>H</u>=CH$_2$), 7.40—7.70 (3H, m, arom. H), 7.70—8.20 (2H, m, arom. H), 7.73 (1H, s, 4-H), 9.00 (1H, br s, O<u>H</u>). Yields, melting points, recrystallization solvents, and microanalyses data for **27** are given in Table IX.

5-Chloro-7,8-dihydro-3-phenylfuro[2,3-*g*]-1,2-benzisoxazole-7-methanol (28b) General Procedure: To a stirred solution of **27b** (5.5 g, 0.019 mol) in $CHCl_3$ (100 ml), *m*-CPBA (5 g, 0.029 mol) was added in small portions at room temperature. The solution was refluxed for 2 h. After addition of *m*-CPBA (5 g, 0.029 mol), the solution was refluxed for 3 h further. After addition of an aqueous solution of NaOH to the solution, the mixture was extracted with $CHCl_3$. The $CHCl_3$ layer was dried over Na_2SO_4 and evaporated to give **28b** (5.0 g). MS *m/z*: 301 (M^+). IR (KBr) cm^{-1}: 3452 (OH), 1372. NMR ($CDCl_3$) δ: 2.65 (1H, br s, O<u>H</u>), 3.40 (1H, d, J=8.4 Hz, Ph-C<u>H</u>$_2$), 3.44 (1H, d, J=9 Hz, Ph-C<u>H</u>$_2$), 3.73—4.02 (2H, m, C<u>H</u>$_2$OH), 4.87—5.41 (1H, m, Ph-CH$_2$–C<u>H</u>), 7.30—7.67 (4H, m, arom. H, 4-H), 7.67—8.07 (2H, m, arom. H). Yields, melting points, recrystallization solvents, and microanalyses data for **28** are given in Table X.

5-Chloro-7,8-dihydro-3-phenylfuro[2,3-*g*]-1,2-benzisoxazole-7-carboxylic Acid (9b) General Procedure, Method B: To a stirred solution of **28b**

TABLE VI. 6-Methoxy-1,2-benzisoxazoles **23**, 6-Methoxybenzoxazoles **24**

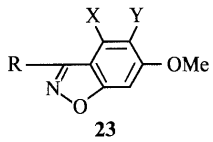

23

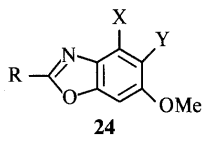

24

Starting Compd.	Product. No.	R	X	Y	Yield (%)	mp (°C)	Recrystn. solvent	Formula	Analysis (%) Calcd (Found) C	H	N
22a	**23a**	C_6H_5	H	H	56	81—82	Et_2O–hexane	$C_{14}H_{11}NO_2$	74.65	4.92	6.22
									(74.87	5.00	6.26)
	24a	C_6H_5	H	H	36	63—65	Et_2O–hexane	$C_{14}H_{11}NO_2$	74.65	4.92	6.22
									(74.64	4.97	6.20)
22b	**23b**	C_6H_5	H	Cl	51	156.5—158	EtOH	$C_{14}H_{10}ClNO_2$	64.75	3.88	5.39
									(64.85	3.82	5.36)
	24b	C_6H_5	H	Cl	39	140—141.5	EtOH	$C_{14}H_{10}ClNO_2$	64.75	3.88	5.39
									(64.86	3.84	5.36)
22c	**23c**	C_6H_5	H	Me	57	141—142	CH_2Cl_2–Et_2O	$C_{15}H_{13}NO_2$	75.30	5.48	5.85
									(75.57	5.48	5.88)
22d	**23d**	2-ClC_6H_4	H	Cl	50	144—145	CH_2Cl_2–Et_2O	$C_{14}H_9Cl_2NO_2$	57.17	3.08	4.76
									(57.19	3.07	4.81)
22e	**23e**	2-FC_6H_4	H	Cl	90	170—172 (Lit.[17] 165—166)	CH_2Cl_2	$C_{14}H_9ClFNO_2$	60.56	3.27	5.04
									(60.48	3.24	5.10)
22k	**23k**	4-$OCH_3C_6H_4$	H	Cl	48	200—201	EtOH	$C_{15}H_{12}ClNO_3$	62.19	4.18	4.84
									(62.46	3.96	4.87)
22l	**23l**	2,6-$F_2C_6H_3$	H	Cl	8	213—214	CH_2Cl_2–Et_2O–MeOH	$C_{14}H_8ClF_2NO_2$	56.87	2.73	4.74
									(56.92	2.77	4.72)
22m	**23m**	2,4-$F_2C_6H_3$	H	Cl	42	193—194	CH_2Cl_2–Et_2O	$C_{14}H_8ClF_2NO_2$	56.87	2.73	4.74
									(56.87	2.57	4.70)
22o	**23o**	CH_3	H	Cl	84	163—164	EtOH	$C_9H_8ClNO_2$	54.70	4.08	7.09
									(54.53	3.99	7.11)
22p	**23p**	$CH_2CH(CH_3)_2$	H	Cl	76	51—52	EtOH	$C_{12}H_{14}ClNO_2$	60.13	5.89	5.84
									(59.98	5.92	5.76)
	24p	$CH_2CH(CH_3)_2$	H	Cl	18	44—45	EtOH	$C_{12}H_{14}ClNO_2$	60.13	5.89	5.84
									(60.02	6.22	5.79)
22q	**23q**	Cyclo-C_5H_9	H	Cl	15	57—58	EtOH	$C_{13}H_{14}ClNO_2$	62.03	5.61	5.57
									(62.07	5.67	5.56)
	24q	Cyclo-C_5H_9	H	Cl	37	52—53	Hexane	$C_{13}H_{14}ClNO_2$	62.03	5.61	5.57
									(62.05	5.80	5.54)
22r	**23r**	3-Pyridyl	H	Cl	55	220—221	EtOH	$C_{13}H_9ClN_2O_2$	59.90	3.48	10.75
									(59.95	3.32	10.82)
22s	**23s**	2-FC_6H_4	Cl	H	17	106—107 (Lit.[5] 116—117)	EtOH	$C_{14}H_9ClFNO_2$	60.56	3.27	5.04
									(60.51	3.15	5.03)
	24s	2-FC_6H_4	Cl	H	36	118—119	EtOH	$C_{14}H_9ClFNO_2$	60.56	3.27	5.04
									(60.48	3.26	4.98)
22t	**23t**	C_6H_5	Cl	H	5	122—123	EtOH	$C_{14}H_{10}ClNO_2$	64.75	3.88	5.39
									(64.93	3.85	5.55)
	24t	C_6H_5	Cl	H	35	112—113	EtOH	$C_{14}H_{10}ClNO_2$	64.75	3.88	5.39
									(64.93	3.89	5.43)

(4.8 g, 0.016 mol) in acetone (100 ml), a mixture of CrO_3 (7.6 g, 0.076 mol), H_2O (17 ml) and conc. H_2SO_4 (10.9 g) was added at room temperature. The resulting mixture was stirred for 9 h and left to stand overnight. Iso-PrOH (20 ml) was added and the mixture was stirred for 1 h, and then filtered. The filtrate was evaporated to dryness *in vacuo*. After addition of an aq. solution of NaOH to the residue, the aqueous phase was washed with Et_2O. The aqueous solution was acidified with HCl and extracted with Et_2O. The extract was washed with H_2O, dried over Na_2SO_4, and evaporated. Recrystallization from THF–acetone gave **9b** (1.7 g). Yields, melting points, recrystallization solvents, and microanalyses data for **9a**, **9aa**, **9b—e**, **9l**, and **9s** are given in Table I.

5-Chloro-6-hydroxy-7-dimethylaminomethyl-3-phenyl-1,2-benzisoxazole (29b) General Procedure: To a mixture of **25b** (5.0 g, 0.020 mol), 50% Me_2NH (18.5 g, 0.21 mol) and H_2O (50 ml), a solution of 35% HCHO (17.5 g, 0.20 mol) in H_2O (25 ml) was added slowly at room temperature. The resulting mixture was stirred for 3 h and left to stand overnight. The deposited crystals were collected by filtration, washed with H_2O, and dried to give **29b** (6.0 g). MS *m/z*: 302 (M^+). IR (KBr) cm^{-1}: 2656, 2600, 2520, 2482. NMR ($CDCl_3$–DMSO-d_6) δ: 2.47 [6H, s, $N(C\underline{H}_3)_2$], 4.07 (2H, s, Ph-$C\underline{H}_2$), 7.32—7.68 (3H, m, arom. H), 7.68—8.04 (2H, m, arom. H), 7.74 (1H, s, 4-H), 9.01 (1H, s, O$\underline{H}$). Yields, melting points, recrystallization solvents, and microanalyses data for **29** are given in Table XI.

Ethyl 5-Chloro-7,8-dihydro-3-phenylfuro[2,3-*g*]-1,2-benzisoxazole-7-carboxylate (30b) General Procedure: A mixture of Me_2S (0.62 g, 0.010 mol) and $BrCH_2COOEt$ (1.67 g, 0.010 mol) was left to stand overnight. To a solution of this resulting solid in DMF (10 ml), K_2CO_3 (1.4 g, 0.010 mol) was added at room temperature. After stirring for 30 min, **29b** (1.0 g, 0.0033 mol) was added to the solution. The solution was stirred for 24 h. The product crystallized upon the addition of H_2O was collected by filtration and washed with H_2O to give **30b** (1.1 g). MS *m/z*: 343 (M^+), 315. IR (KBr) cm^{-1}: 1740 (COOEt). NMR ($CDCl_3$) δ: 1.30 (3H, t, J=7.2 Hz, $C\underline{H}_3$), 3.73 (1H, d, J=7.8 Hz, Ph-$C\underline{H}_2$), 3.78 (1H, d, J=9.8 Hz, Ph-$C\underline{H}_2$), 4.25 (2H, q, J=7.2 Hz, $C\underline{H}_2CH_3$), 5.41 (1H, dd, J=9.8 Hz, 7.8 Hz, Ph-CH_2-C$\underline{H}$), 7.30—7.62 (3H, m, arom. H), 7.62—8.00 (2H, m, arom. H), 7.66 (1H, s, 4-H). Yields, melting points, recrystallization solvents, and microanalyses data for **30** are given in Table XII.

5-Chloro-7,8-dihydro-3-phenylfuro[2,3-*g*]-1,2-benzisoxazole-7-carboxylic Acid (9b) General Procedure, Method C: A mixture of **30b** (1.1 g, 0.0032 mol), 2 N NaOH (10 ml) and EtOH (10 ml) was refluxed for 1 h. After cooling, H_2O was added to the mixture. The mixture was acidified

TABLE VII. 6-Hydroxy-1,2-benzisoxazoles **25**

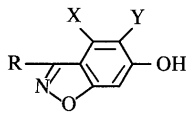

Compd. No.	R	X	Y	Yield (%)	mp (°C)	Recrystn. solvent	Formula	Analysis (%) Calcd (Found)		
								C	H	N
25a	C_6H_5	H	H	97	218—219	AcOEt–hexane	$C_{13}H_9NO_2$	73.92	4.30	6.63
								(73.94	4.19	6.63)
25b	C_6H_5	H	Cl	97	188.5—190.5	AcOEt–hexane	$C_{13}H_8ClNO_2$	63.56	3.28	5.70
								(63.55	3.38	5.55)
25c	C_6H_5	H	Me	Quant.	173—174	AcOEt–hexane	$C_{14}H_{11}NO_2$	74.65	4.92	6.22
								(74.77	5.29	6.02)
25d	2-ClC_6H_4	H	Cl	Quant.	205—206	CH_2Cl_2–hexane	$C_{13}H_7Cl_2NO_2$	55.74	2.52	5.00
								(55.50	2.64	4.89)
25e	2-FC_6H_4	H	Cl	Quant.	187—188 (Lit.[17] 180—182)	CH_2Cl_2–hexane	$C_{13}H_7ClFNO_2$	59.22	2.68	5.31
								(59.14	2.46	5.35)
25k	4-OHC_6H_4	H	Cl	Quant.	260—262	EtOH–H_2O	$C_{13}H_8ClNO_3$	59.67	3.08	5.35
								(59.83	2.99	5.38)
25l	2,6-$F_2C_6H_3$	H	Cl	Quant.	161—163	AcOEt–hexane	$C_{13}H_6ClF_2NO_2$	55.44	2.15	4.97
								(55.04	2.18	4.83)
25m	2,4-$F_2C_6H_3$	H	Cl	Quant.	167—169	AcOEt–hexane	$C_{13}H_6ClF_2NO_2$	55.44	2.15	4.97
								(55.06	2.38	4.74)
25o	CH_3	H	Cl	91	167—170	AcOEt–hexane	$C_8H_6ClNO_2$	52.34	3.29	7.63
								(51.94	3.48	7.27)
25p	$CH_2CH(CH_3)_2$	H	Cl	83	126—128	AcOEt–hexane	$C_{11}H_{12}ClNO_2$	58.55	5.36	6.21
								(58.55	5.38	6.34)
25q	Cyclo-C_5H_9	H	Cl	75	151—154	AcOEt–hexane	$C_{12}H_{12}ClNO_2$	60.64	5.09	5.89
								(60.56	5.12	5.88)
25r	3-Pyridyl	H	Cl	Quant.	277—279	EtOH	$C_{12}H_7ClN_2O_2$	58.44	2.86	11.36
								(58.51	2.81	11.25)
25s	2-FC_6H_4	Cl	H	96	248—249	CH_2Cl_2–MeOH–hexane	$C_{13}H_7ClFNO_2$	59.22	2.68	5.31
								(59.10	2.51	5.29)

TABLE VIII. 6-Allyloxy-1,2-benzisoxazoles **26**

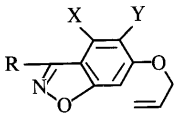

Compd. No.	R	X	Y	Yield (%)	mp (°C)	Recrystn. solvent	Formula	Analysis (%) Calcd			Found		
								C	H	N	C	H	N
26a	C_6H_5	H	H	98	55—56	EtOH	$C_{16}H_{13}NO_2$	76.47	5.22	5.57	76.61	5.26	5.59
26b	C_6H_5	H	Cl	Quant.	106—107	EtOH	$C_{16}H_{12}ClNO_2$	67.26	4.23	4.90	67.39	4.19	4.90
26c	C_6H_5	H	Me	93	81—82	EtOH	$C_{17}H_{15}NO_2$	76.96	5.70	5.28	77.24	5.59	5.31
26d	2-ClC_6H_4	H	Cl	94	144—145	EtOH	$C_{16}H_{11}Cl_2NO_2$	60.02	3.46	4.38	59.67	3.34	4.29
26e	2-FC_6H_4	H	Cl	96	132—133	EtOH	$C_{16}H_{11}ClFNO_2$	63.27	3.65	4.61	63.31	3.56	4.59
26l	2,6-$F_2C_6H_3$	H	Cl	92	145—146	EtOH	$C_{16}H_{10}ClF_2NO_2$	59.74	3.13	4.35	59.68	3.16	4.35
26s	2-FC_6H_4	Cl	H	Quant.	39—40	EtOH	$C_{16}H_{11}ClFNO_2$	63.27	3.65	4.61	63.24	3.69	4.63

with conc. HCl and deposited crystals were collected by filtration, washed with H_2O, and dried to give **9b** (1.0 g). Yields, melting points, recrystallization solvents, and microanalyses data for **9b**, **k**, **m**, **o**—**r** are given in Table I.

7-Acetoxymethyl-5-bromo-7,8-dihydro-3-phenylfuro[2,3-*g*]-1,2-benzisoxazole (31) A mixture of 7,8-dihydro-3-phenylfuro[2,3-*g*]-1,2-benzisoxazole-7-methanol (**28a**) (7.2 g, 0.027 mol), benzene (160 ml) and Ac_2O (35 ml) was refluxed for 5 h and evaporated. To a stirred solution of this residue in CH_2Cl_2 (200 ml), Br_2 (4.8 g, 0.030 mol) was added slowly at room temperature. The solution was stirred for 10 h and then evaporated. The resulting residue was chromatographed on silica gel with CH_2Cl_2 to give **31** (1.6 g, 15%) as crystals (AcOEt–hexane), mp 128—129 °C. *Anal.* Calcd for $C_{18}H_{14}BrNO_4$: C, 55.69; H, 3.64; N, 3.61. Found: C, 55.73; H, 3.50; N, 3.63. MS *m/z*: 387 (M^+), 327. IR (KBr) cm^{-1}: 1730 (C=O), 1370. NMR ($CDCl_3$) δ: 2.05 (3H, s, CH_3), 3.41 (1H, d, J=7.2 Hz, Ph-CH_2), 3.55 (1H, d, J=8.0 Hz, Ph-CH_2), 4.35 (2H, d, J=5.0 Hz, CH_2OAc), 5.00—5.53 (1H, m, Ph-CH_2–CH), 7.31—7.60 (3H, m, arom. H), 7.64—7.95 (2H, m, arom. H), 7.76 (1H, s, 4-H).

5-Bromo-7,8-dihydro-3-phenylfuro[2,3-*g*]-1,2-benzisoxazole-7-methanol (28aa) A mixture of **31** (1.5 g, 0.0038 mol), 2 N NaOH (10 ml) and EtOH (30 ml) was refluxed for 10 min. After cooling, H_2O was added to the mixture. The mixture was acidified with conc. HCl and deposited crystals were collected by filtration, washed with H_2O, dried, and chromatographed on silica gel with CH_2Cl_2 to give **28aa** (0.85 g, 64%) as crystals (EtOH), mp 165—166 °C. *Anal.* Calcd for $C_{16}H_{12}BrNO_3$: C, 55.51; H, 3.49; N, 4.05. Found: C, 55.49; H, 3.44; N, 4.04. MS *m/z*: 345 (M^+), 314. IR (KBr) cm^{-1}: 3440 (OH), 1370. NMR ($CDCl_3$–DMSO-d_6) δ: 3.50 (2H, br d, J=8.2 Hz, Ph-CH_2), 3.81 (2H, dd, J=6.0, 5.0 Hz, CH_2OH), 4.38 (1H, t,

TABLE IX. 7-Allyl-6-hydroxy-1,2-benzisoxazoles **27**

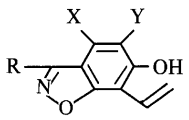

Compd. No.	R	X	Y	Yield (%)	mp (°C)	Recrystn. solvent	Formula	Analysis (%) Calcd C	Calcd H	Calcd N	Found C	Found H	Found N
27a	C_6H_5	H	H	44	171—172	AcOEt–hexane	$C_{16}H_{13}NO_2$	76.47	5.22	5.57	76.30	5.45	5.42
27b	C_6H_5	H	Cl	69	142—144	$CHCl_3$–hexane	$C_{16}H_{12}ClNO_2$	67.26	4.23	4.90	67.08	4.11	4.76
27c	C_6H_5	H	Me	71	133—134	EtOH	$C_{17}H_{15}NO_2$	76.96	5.70	5.28	77.05	5.66	5.26
27d	2-ClC_6H_4	H	Cl	60	111—112	CH_2Cl_2–hexane	$C_{16}H_{11}Cl_2NO_2$	60.02	3.46	4.38	60.10	3.43	4.34
27e	2-FC_6H_4	H	Cl	97	142—143	EtOH	$C_{16}H_{11}ClFNO_2$	63.27	3.65	4.61	63.05	3.78	4.70
27l	2,6-$F_2C_6H_3$	H	Cl	86	107—108	CH_2Cl_2–hexane	$C_{16}H_{10}ClF_2NO_2$	59.74	3.13	4.35	59.71	3.16	4.34
27s	2-FC_6H_4	Cl	H	72	211—212	CH_2Cl_2–MeOH–hexane	$C_{16}H_{11}ClFNO_2$	63.27	3.65	4.61	62.94	3.70	4.65

TABLE X. 7,8-Dihydrofuro[2,3-*g*]-1,2-benzisoxazole-7-methanols **28**

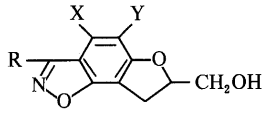

Compd. No.	R	X	Y	Yield (%)	mp (°C)	Recrystn. solvent	Formula	Analysis (%) Calcd C	Calcd H	Calcd N	Found C	Found H	Found N
28a	C_6H_5	H	H	99	109—112	EtOH	$C_{16}H_{13}NO_3$	71.90	4.90	5.24	71.83	4.96	5.32
28b	C_6H_5	H	Cl	86	135—138	EtOH	$C_{16}H_{12}ClNO_3$	63.69	4.01	4.64	63.54	4.05	4.57
28c	C_6H_5	H	Me	96	137—138	EtOH	$C_{17}H_{15}NO_3$	72.58	5.37	4.98	72.48	5.38	4.90
28d	2-ClC_6H_4	H	Cl	97	164—165	EtOH	$C_{16}H_{11}Cl_2NO_3$	57.17	3.30	4.17	57.28	3.15	4.17
28e	2-FC_6H_4	H	Cl	89	143—144	EtOH	$C_{16}H_{11}ClFNO_3$	60.11	3.47	4.38	60.14	3.42	4.35
28l	2,6-$F_2C_6H_3$	H	Cl	86	171—172	EtOH	$C_{16}H_{10}ClF_2NO_3$	56.91	2.99	4.15	56.88	3.01	4.12
28s	2-FC_6H_4	Cl	H	74	110—111	EtOH	$C_{16}H_{11}ClFNO_3$	60.11	3.47	4.38	59.96	3.37	4.31

TABLE XI. 5-Chloro-6-hydroxy-7-dimethylaminomethyl-1,2-benzisoxazoles **29**

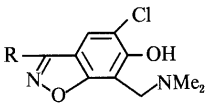

Compd. No.	R	Yield (%)	mp (°C)	Recrystn. solvent	Formula	Analysis (%) Calcd C	Calcd H	Calcd N	Found C	Found H	Found N
29b	C_6H_5	97	164—166	AcOEt–hexane	$C_{16}H_{15}ClN_2O_2$	63.48	4.99	9.25	63.47	5.09	9.09
29k	4-OHC_6H_4	89	>310	DMF–H_2O	$C_{16}H_{15}ClN_2O_3$	60.29	4.74	8.79	59.96	4.70	8.74
29m	2,4-$F_2C_6H_3$	52	87—88	AcOEt–hexane	$C_{16}H_{13}ClF_2N_2O_2$	56.73	3.87	8.27	56.37	3.89	8.16
29o	CH_3	95	100—103	AcOEt–hexane	$C_{11}H_{13}ClN_2O_2$	54.89	5.44	11.64	54.49	5.41	11.57
29p	$CH_2CH(CH_3)_2$	78	96—97	Hexane	$C_{14}H_{19}ClN_2O_2$	59.47	6.77	9.91	59.47	7.03	9.96
29q	Cyclo-C_5H_9	99	108—110	Hexane	$C_{15}H_{19}ClN_2O_2$	61.12	6.50	9.50	61.31	6.73	9.34
29r	3-Pyridyl	40	149—151	EtOH	$C_{15}H_{14}ClN_3O_2$	59.31	4.65	13.83	59.29	4.70	13.69

J=6.0 Hz, OH), 4.83—5.38 (1H, m, Ph-CH_2–CH), 7.28—7.60 (3H, m, arom. H), 7.60—7.95 (2H, m, arom. H), 7.72 (1H, s, 4-H).

5-Bromo-7,8-dihydro-3-phenylfuro[2,3-*g*]-1,2-benzisoxazole-7-carboxylic Acid (9aa) To a stirred solution of **28aa** (0.7 g, 0.002 mol) in acetone (50 ml), a mixture of CrO_3 (1.0 g, 0.010 mol), H_2O (3 ml) and conc. H_2SO_4 (1.4 g) was added at room temperature. The resulting mixture was stirred for 6 h and left to stand overnight. Iso-PrOH (20 ml) was added and the mixture was stirred for 1 h, and then filtered. The filtrate was evaporated to dryness *in vacuo*. After addition of an aqueous solution of NaOH to the residue, the aqueous phase was washed with Et_2O. The aqueous solution was acidified with HCl and extracted with Et_2O. The extract was washed with H_2O, dried over Na_2SO_4 and evaporated. Recrystallization from acetone–H_2O gave **9aa** (0.4 g). MS *m/z*: 359 (M^+), 314. IR (KBr) cm^{-1}: 1712 (COOH). NMR ($CDCl_3$–DMSO-d_6) δ: 3.79 (1H, d, J=7.8 Hz, Ph-CH_2), 3.84 (1H, d, J=9.8 Hz, Ph-CH_2), 5.43 (1H, dd, J=9.8, 7.8 Hz, Ph-CH_2-CH), 7.37—7.68 (3H, m, arom. H), 7.68—7.99 (2H, m, arom. H), 7.84 (1H, s, 4-H), 8.02 (1H, br s, COOH). Yield, melting point, recrystallization solvent, and microanalysis data for **9aa** are given in Table I.

4-Chloro-2-(2-fluorophenyl)-6-hydroxybenzoxazole (32s) General Procedure, Method D: 4-Chloro-2-(2-fluorophenyl)-6-methoxybenzoxazole (**24s**) (28.9 g, 0.10 mol) was heated with pyridine hydrochloride (250 g) at

TABLE XII. Ethyl 5-Chloro-7,8-dihydrofuro[2,3-*g*]-1,2-benzisoxazole-7-carboxylates **30**

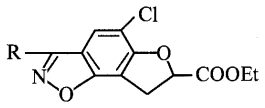

Compd. No.	R	Yield (%)	mp (°C)	Recrystn. solvent	Formula	Analysis (%) Calcd C	H	N	Found C	H	N
30b	C_6H_5	97	136—138	Et_2O–hexane	$C_{18}H_{14}ClNO_4$	62.89	4.11	4.07	62.97	4.07	4.05
30k	4-OHC_6H_4	80	135—136	CH_2Cl_2	$C_{18}H_{14}ClNO_5$	60.09	3.92	3.89	59.90	3.75	3.91
30m	2,4-$F_2C_6H_3$	72	139—140	EtOH	$C_{18}H_{12}ClF_2NO_4$	56.93	3.19	3.69	57.21	2.98	3.71
30o	CH_3	92	103—104	EtOH	$C_{13}H_{12}ClNO_4$	55.43	4.29	4.97	55.49	4.05	5.00
30p	$CH_2CH(CH_3)_2$	87	99—100	EtOH	$C_{16}H_{18}ClNO_4$	59.36	5.60	4.33	59.35	5.63	4.52
30q	Cyclo-C_5H_9	87	93—94	EtOH	$C_{17}H_{18}ClNO_4$	60.81	5.40	4.17	60.86	5.47	4.07
30r	3-Pyridyl	88	150—151	EtOH	$C_{17}H_{13}ClN_2O_4$	59.23	3.80	8.13	59.38	3.82	8.14

TABLE XIII. 6-Hydroxybenzoxazoles **32**

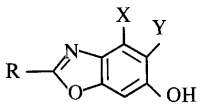

Compd. No.	R	X	Y	Method	Yield (%)	mp (°C)	Recrystn. solvent	Formula	Analysis (%) Calcd C	H	N	Found C	H	N
32b	C_6H_5	H	Cl	F	96	207—208	AcOEt–hexane	$C_{13}H_8ClNO_2$	63.56	3.28	5.70	63.52	3.20	5.68
32s	2-FC_6H_4	Cl	H	D	95	250—251	EtOH	$C_{13}H_7ClFNO_2$	59.22	2.68	5.31	59.44	2.51	5.33
32t	C_6H_5	Cl	H	D	91	259—260	AcOEt–hexane	$C_{13}H_8ClNO_2$	63.56	3.28	5.70	63.69	3.18	5.63
32u	2-$CH_3C_6H_4$	H	H	E	98	134—135	AcOEt–hexane	$C_{14}H_{11}NO_2$	74.65	4.92	6.22	74.73	4.92	6.19

TABLE XIV. 6-Allyloxybenzoxazoles **33**

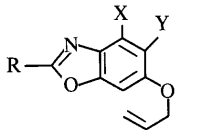

Compd. No.	R	X	Y	Yield (%)	mp (°C)	Recrystn. solvent	Formula	Analysis (%) Calcd C	H	N	Found C	H	N
33s	2-FC_6H_4	Cl	H	99	98—99	EtOH	$C_{16}H_{11}ClFNO_2$	63.27	3.65	4.61	63.54	3.62	4.60
33t	C_6H_5	Cl	H	60	73—74	EtOH	$C_{16}H_{12}ClNO_2$	67.26	4.23	4.90	67.60	4.07	5.04
33u	2-$CH_3C_6H_4$	H	H	98	33—34	EtOH	$C_{17}H_{15}NO_2$	76.96	5.70	5.28	76.89	5.64	5.27

170—180 °C for 7 h and then cooled to 70 °C. The product crystallized upon the addition of H_2O was collected by filtration and washed with H_2O to give **32s** (26.1 g). MS *m/z*: 263 (M^+). IR (KBr) cm^{-1}: 3180 (OH), 1620. NMR ($CDCl_3$–DMSO-d_6) δ: 6.96 (1H, d, J=2.4 Hz), 7.01 (1H, d, J=2.4 Hz), 7.11—7.77 (3H, m, arom. H), 7.92—8.41 (1H, m, arom. H), 9.20 (1H, br s, OH). Yields, melting points, recrystallization solvents, and microanalyses data for **32s** and **32t** are given in Table XIII.

6-Allyloxy-4-chloro-2-(2-fluorophenyl)benzoxazole (33s) General Procedure: A mixture of **32s** (26.0 g, 0.099 mol), allyl bromide (23.9 g, 0.20 mol) and anhydrous K_2CO_3 (29.3 g, 0.21 mol) in DMF (300 ml) was stirred at 50—60 °C for 2.5 h. The product crystallized upon the addition of H_2O was collected by filtration and washed with H_2O to give **33s** (29.7 g). MS *m/z*: 303 (M^+), 262. IR (KBr) cm^{-1}: 1626, 1600. NMR ($CDCl_3$) δ: 4.50 (2H, dt, J=4.6, 1.4 Hz, O-C<u>H</u>$_2$), 5.11—5.57 (2H, m, -CH=C<u>H</u>$_2$), 5.71—6.37 (1H, m, -C<u>H</u>=CH$_2$), 6.95 (1H, s, 1H, s, 5-H, 7-H), 7.05—7.66 (3H, m, arom. H), 8.00—8.35 (1H, m, arom. H). Yields, melting points, recrystallization solvents, and microanalyses data for **33** are given in Table XIV.

7-Allyl-4-chloro-2-(2-fluorophenyl)-6-hydroxybenzoxazole (34s) General Procedure: A solution of **33s** (29.7 g, 0.098 mol) in *N*,*N*-dimethylaniline (250 ml) was refluxed for 6 h. After cooling, the mixture was acidified with conc. HCl and the deposited crystals were collected by filtration, washed with H_2O, dried, and chromatographed on silica gel with CH_2Cl_2–hexane to give **34s** (20.2 g). MS *m/z*: 303 (M^+), 288. IR (KBr) cm^{-1}: 1620, 1396. NMR ($CDCl_3$) δ: 3.65 (2H, br d, J=6.0 Hz, Ph-C<u>H</u>$_2$), 4.90—5.39 (2H, m, -CH=C<u>H</u>$_2$), 5.71—6.44 (1H, m, -C<u>H</u>=CH$_2$), 6.97 (1H, s, 5-H), 7.05—7.70 (3H, m, arom. H), 7.92—8.35 (1H, m, arom. H). Yields, melting points, recrystallization solvents, and microanalyses data for **34** are given in Table XV.

4-Chloro-2-(2-fluorophenyl)-7,8-dihydrofuro[2,3-*g*]benzoxazole-7-methanol (35s) General Procedure, Method D (E): To a stirred solution of **34s** (20.0 g, 0.066 mol) in CH_2Cl_2 (250 ml), *m*-CPBA (13.9 g, 0.081 mol) was added in small portions at room temperature. The solution was stirred for 1 h. After addition of *m*-CPBA (2.4 g, 0.014 mol), the solution was refluxed for 1.5 h. After addition of an aqueous solution of NaOH to the solution, the mixture was extracted with CH_2Cl_2. The CH_2Cl_2 layer was dried over Na_2SO_4 and evaporated to give **35s** (14.5 g). MS *m/z*: 319 (M^+). IR (KBr) cm^{-1}: 3400 (OH), 1486. NMR ($CDCl_3$–DMSO-d_6) δ: 3.34 (1H, d, J=8.0 Hz, Ph-C<u>H</u>$_2$), 3.37 (1H, d, J=8.4 Hz, Ph-C<u>H</u>$_2$), 3.77 (2H, d, J=5.0 Hz, C<u>H</u>$_2$OH), 4.60 (1H, br s, O<u>H</u>), 4.77—5.30 (1H, m, Ph-CH$_2$-C<u>H</u>),

TABLE XV. 7-Allyl-6-hydroxybenzoxazoles **34**

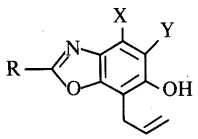

Compd. No.	R	X	Y	Yield (%)	mp (°C)	Recrystn. solvent	Formula	Analysis (%) Calcd C	H	N	Found C	H	N
34s	2-FC_6H_4	Cl	H	68	135—137	AcOEt–hexane	$C_{16}H_{11}ClFNO_2$	63.27	3.65	4.61	63.21	3.69	4.56
34t	C_6H_5	Cl	H	56	194—195	AcOEt–hexane	$C_{16}H_{12}ClNO_2$	67.26	4.23	4.90	67.54	4.14	4.91
34u	2-$CH_3C_6H_4$	H	H	67	120—122	AcOEt–hexane	$C_{17}H_{15}NO_2$	76.96	5.70	5.28	76.82	5.59	5.27

TABLE XVI. 7,8-Dihydrofuro[2,3-*g*]benzoxazole-7-methanols **35**

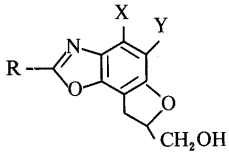

Compd. No.	R	X	Y	Method	Yield (%)	mp (°C)	Recrystn. solvent	Formula	Analysis (%) Calcd C	H	N	Found C	H	N
35s	2-FC_6H_4	Cl	H	D	69	160—161	CH_2Cl_2–hexane	$C_{16}H_{11}ClFNO_3$	60.11	3.47	4.38	60.08	3.48	4.22
35sa	2-FC_6H_4	Cl	Cl	D′	38	237—238	EtOH	$C_{16}H_{10}Cl_2FNO_3$	54.26	2.85	3.95	54.20	2.89	3.90
35sb	2-FC_6H_4	H	H	D′	98	148—149	EtOH	$C_{16}H_{12}FNO_3$	67.37	4.24	4.91	67.58	4.28	4.90
35sc	2-FC_6H_4	H	Cl	D′	87	181—183	EtOH	$C_{16}H_{11}ClFNO_3$	60.11	3.47	4.38	59.96	3.33	4.38
35t	C_6H_5	Cl	H	D	78	165—168	EtOH	$C_{16}H_{12}ClNO_3$	63.69	4.01	4.64	63.63	3.82	4.70
35ta	C_6H_5	Cl	Cl	D′	78	213—216	EtOH	$C_{16}H_{11}Cl_2NO_3$	57.17	3.30	4.17	57.22	3.28	4.13
35u	2-$CH_3C_6H_4$	H	H	E (D)	75	122—123	EtOH	$C_{17}H_{15}NO_3$	72.58	5.37	4.98	72.18	5.44	4.75

6.78 (1H, s, 5-H), 6.98—7.62 (3H, m, arom. H), 7.87—8.35 (1H, m, arom. H). Yields, melting points, recrystallization solvents, and microanalyses data for **35s**, **t**, **u** are given in Table XVI.

5-Chloro-2-(2-fluorophenyl)-7,8-dihydrofuro[2,3-*g*]benzoxazole-7-carboxylic Acid (12s) General Procedure, Methods D, D′, and E: To a stirred solution of **35s** (4.0 g, 0.013 mol) in acetone (150 ml), a mixture of CrO_3 (4.7 g, 0.047 mol), H_2O (8 ml) and conc. H_2SO_4 (6.7 g) was added at room temperature. The resulting mixture was stirred for 5.5 h and left to stand overnight. Iso-PrOH (20 ml) was added and the mixture was stirred for 1 h, and then filtered. The filtrate was evaporated to dryness *in vacuo*. After addition of an aqueous solution of NaOH to the residue, the aqueous phase was washed with Et_2O. The aqueous solution was acidified with HCl and extracted with Et_2O. The extract was washed with H_2O, dried over Na_2SO_4, and evaporated to give **12s** (2.7 g). MS *m/z*: 333 (M^+). IR (KBr) cm^{-1}: 1738 (COOH), 1622. NMR ($CDCl_3$–DMSO-d_6) δ: 3.65 (1H, d, J=7.8 Hz, Ph-C$\underline{H}_2$), 3.70 (1H, d, J=9.8 Hz, Ph-C$\underline{H}_2$), 5.36 (1H, dd, J=9.8, 7.8 Hz, Ph-CH_2-C$\underline{H}$), 6.95 (1H, s, 5-H), 7.02—7.76 (3H, m, arom. H), 8.00—8.40 (1H, m, arom. H), 9.03 (1H, br s, COO$\underline{H}$). Yields, melting points, recrystallization solvents, and microanalyses data for **12s**, **12sa**—**sc**, **12t**, **12ta**, and **12u** are given in Table II.

4,5-Dichloro-2-(2-fluorophenyl)-7,8-dihydrofuro[2,3-*g*]benzoxazole-7-methanol (35sa) General Procedure, Method D′: The compound **35s** (5.0 g, 0.016 mol) was dissolved in CH_2Cl_2 (150 ml) and the solution was cooled to 0—5 °C. SO_2Cl_2 (2.4 g, 0.018 mol) was added portionwise to the solution and the resulting mixture was warmed to room temperature over a 3 h. After addition of SO_2Cl_2 (0.6 g, 0.004 mol), the solution was stirred for 3 h further, evaporated, and chromatographed on silica gel with CH_2Cl_2 to give **35sa** (2.1 g). MS *m/z*: 353 (M^+). IR (KBr) cm^{-1}: 3480 (OH), 1452. NMR ($CDCl_3$–DMSO-d_6) δ: 3.51 (2H, d, J=8.0 Hz, Ph-C$\underline{H}_2$), 3.83 (2H, d, J=4.0 Hz, C$\underline{H}_2$OH), 4.90—5.47 (1H, m, Ph-CH_2-C$\underline{H}$), 4.95 (1H, br s, O$\underline{H}$), 7.03—7.84 (3H, m, arom. H), 7.95—8.40 (1H, m, arom. H). Yields, melting points, recrystallization solvents, and microanalyses data for **35sa** and **35ta** are given in Table XVI.

2-(2-Fluorophenyl)-7,8-dihydrofuro[2,3-*g*]benzoxazole-7-methanol (35sb) A solution of **35s** (8.1 g, 0.025 mol) and NEt_3 (4.4 g, 0.044 mol) in THF (300 ml) was stirred with 10% Pd–C (1.9 g) in an atmosphere of H_2 for 3 h and then filtered. The filtrate was evaporated and chromatographed on silica gel with 1% MeOH–CH_2Cl_2 to give **35sb** (7.1 g). MS *m/z*: 285 (M^+). IR (KBr) cm^{-1}: 3296 (OH), 1486. NMR ($CDCl_3$–DMSO-d_6) δ: 3.41 (2H, br d, J=8.4 Hz, Ph-C$\underline{H}_2$), 3.78 (2H, dd, J=5.8, 5.0 Hz, C$\underline{H}_2$OH), 4.59 (1H, t, J=5.8 Hz, O$\underline{H}$), 4.79—5.30 (1H, m, Ph-CH_2-C$\underline{H}$), 6.79 (1H, d, J=8.0 Hz, 5-H), 7.02—7.74 (3H, m, arom. H), 7.47 (1H, d, J=8.0 Hz, 4-H), 7.98—8.33 (1H, m, arom. H). Yield, melting point, recrystallization solvent, and microanalysis data for **35sb** are given in Table XVI.

5-Chloro-2-(2-fluorophenyl)-7,8-dihydrofuro[2,3-*g*]benzoxazole-7-methanol (35sc) The compound **35sb** (3.4 g, 0.012 mol) was dissolved in DMF (80 ml) and the solution was cooled to 0—5 °C. Trichloroisocyanuric acid (1.2 g, 0.0051 mol) was added portionwise to the solution and the resulting mixture was warmed to room temperature over a 2 h. After ice cooling, the product crystallized upon the addition of 0.1 N NaOH (500 ml) was collected by filtration, washed with H_2O, dried, and recrystallized from EtOH to give **35sc** (3.3 g). MS *m/z*: 319 (M^+). IR (KBr) cm^{-1}: 3380 (OH), 1430. NMR ($CDCl_3$–DMSO-d_6) δ: 3.49 (2H, d, J=8.4 Hz, Ph-C$\underline{H}_2$), 3.82 (2H, dd, J=5.8, 5.0 Hz, C$\underline{H}_2$OH), 4.72 (1H, t, J=5.8 Hz, O$\underline{H}$), 4.93—5.37 (1H, m, Ph-CH_2-C$\underline{H}$), 7.12—7.74 (3H, m, arom. H), 7.47 (1H, s, 4-H), 7.92—8.30 (1H, m, arom. H). Yield, melting point, recrystallization solvent, and microanalysis data for **35sc** are given in Table XVI.

6-(2-Methylbenzoyloxy)-2-(2-methylphenyl)benzoxazole(38) A mixture of 2-methylbenzoyl chloride (**36**) (14.0 g, 0.091 mol) and 4-aminoresorcinol hydrochloride (**37**) (3.0 g, 0.019 mol) was refluxed for 2 h and then cooled. After addition of aqueous K_2CO_3 to the solution, the mixture was extracted with CH_2Cl_2. The extract was washed with H_2O, dried, evaporated, and chromatographed on silica gel with CH_2Cl_2 to give **38** (5.0 g, 79%) as crystals (CH_2Cl_2–hexane), mp 98—100 °C. *Anal.* Calcd for $C_{22}H_{17}NO_3$: C, 76.95; H, 4.99; N, 4.08. Found: C, 76.78; H, 4.81; N, 3.99. MS *m/z*: 343 (M^+), 224, 119. IR (KBr) cm^{-1}: 1730 (COOAr). NMR ($CDCl_3$) δ: 2.65 (3H, s, C$\underline{H}_3$), 2.75 (3H, s, C$\underline{H}_3$), 7.00—7.50 (7H, m, 7-H, arom. H), 7.12 (1H, dd, J=8.0, 2.0 Hz, 5-H), 7.73 (1H, d, J=8.0 Hz, 4-H), 7.90—8.26

(2H, m, arom. H).

6-Hydroxy-2-(2-methylphenyl)benzoxazole (32u) Method E: A mixture of **38** (3.1 g, 0.0091 mol), 2 N NaOH (60 ml) and EtOH (60 ml) was refluxed for 1 h. After cooling, ice-water was added to the mixture. The mixture was weakly acidified with conc. HCl and then weakly basified with saturated $NaHCO_3$, and extracted with Et_2O. The extract was washed with H_2O, dried over Na_2SO_4, and evaporated to give **32u** (2.0 g). MS *m/z*: 225 (M^+), 224. IR (KBr) cm^{-1}: 3148 (OH), 1486. NMR ($CDCl_3$) δ: 2.72 (3H, s, C<u>H</u>$_3$), 6.82 (1H, dd, J=8.2, 2.2 Hz, 5-H), 7.03 (1H, d, J=2.2 Hz, 7-H), 7.12—7.42 (3H, m, arom. H), 7.51 (1H, d, J=8.2 Hz, 4-H), 7.73 (1H, br s, O<u>H</u>), 7.89—8.22 (1H, m, arom. H). Yield, melting point, recrystallization solvent, and microanalysis data for **32u** are given in Table XIII.

5-Chloro-6-hydroxy-2-phenylbenzoxazole (32b) Method F: To a stirred solution of 5-chloro-6-methoxy-2-phenylbenzoxazole (**24b**) (4.5 g, 0.017 mol) in 1,2-dichloroethane (90 ml), $AlCl_3$ (4.7 g, 0.035 mol) was added portionwise and the mixture was heated at 80 °C over a 3 h period. Ice-water and conc. HCl were added to the solution and the mixture was extracted with Et_2O. The extract was washed with H_2O, dried over Na_2SO_4, and evaporated to give **32b** (4.1 g). MS *m/z*: 245 (M^+). IR (KBr) cm^{-1}: 3472 (OH), 1442. NMR ($CDCl_3$–DMSO-d_6) δ: 7.22 (1H, s, 7-H), 7.30—7.71 (3H, m, arom. H), 7.60 (1H, s, 4-H), 7.90—8.33 (2H, m, arom. H), 9.82 (1H, br s, O<u>H</u>). Yield, melting point, recrystallization solvent, and microanalysis data for **32b** are given in Table XIII.

5-Chloro-6-hydroxy-7-dimethylaminomethyl-2-phenylbenzoxazole (39b) To a mixture of **32b** (4.1 g, 0.017 mol), 50% Me_2NH (15.1 g, 0.17 mol) and H_2O (40 ml), a solution of 35% HCHO (14.5 g, 0.17 mol) in H_2O (20 ml) was added slowly at room temperature. The resulting mixture was stirred for 24 h. The deposited crystals were collected by filtration, washed with H_2O, and dried to give **39b** (4.8 g, 95%) as crystals (AcOEt–hexane), mp 171—173 °C. *Anal.* Calcd for $C_{16}H_{15}ClN_2O_2$: C, 63.48; H, 4.99; N, 9.25. Found: C, 63.54; H, 5.01; N, 9.14. MS *m/z*: 302 (M^+), 257. IR (KBr) cm^{-1}: 2984, 2952, 2836, 2788. NMR ($CDCl_3$) δ: 2.40 [6H, s, N(C<u>H</u>$_3$)$_2$], 3.94 (2H, s, Ph-C<u>H</u>$_2$), 7.19—7.46 (3H, m, arom. H), 7.48 (1H, s, 4-H), 7.83—8.20 (2H, m, arom. H), 11.02 (1H, s, O<u>H</u>).

Ethyl 5-Chloro-7,8-dihydro-2-phenylfuro[2,3-*g*]benzoxazole-7-carboxylate (40b) To a mixture of **39b** (4.8 g, 0.016 mol), dimethyl ethoxycarbonylmethylsulfonium bromide (10.8 g, 0.047 mol) in DMF (100 ml), K_2CO_3 (6.5 g, 0.047 mol) was added at room temperature. The solution was stirred for 24 h. The product crystallized upon the addition of ice-water was collected by filtration, washed with H_2O, dried, and chromatographed on silica gel with CH_2Cl_2 to give **40b** (4.5 g, 83%) as crystals (EtOH), mp 135—137 °C. *Anal.* Calcd for $C_{18}H_{14}ClNO_4$: C, 62.89; H, 4.11; N, 4.07. Found: C, 62.94; H, 4.10; N, 4.03. MS *m/z*: 343 (M^+). IR (KBr) cm^{-1}: 1752 (COOEt). NMR ($CDCl_3$) δ: 1.29 (3H, t, J=7.2 Hz, C<u>H</u>$_3$), 3.64 (1H, d, J=7.8 Hz, Ph-C<u>H</u>$_2$), 3.66 (1H, d, J=9.8 Hz, Ph-C<u>H</u>$_2$), 4.21 (2H, q, J=7.2 Hz, C<u>H</u>$_2$CH$_3$), 5.29 (1H, dd, J=9.8, 7.8 Hz, Ph-CH$_2$-C<u>H</u>), 7.16—7.51 (3H, m, arom. H), 7.36 (1H, s, 4-H), 7.75—8.14 (2H, m, arom. H).

5-Chloro-7,8-dihydro-2-phenylfuro[2,3-*g*]benzoxazole-7-carboxylic Acid (12b) Method F: A mixture of **40b** (4.1 g, 0.012 mol), 2 N NaOH (60 ml) and EtOH (60 ml) was refluxed for 1 h. After cooling, ice-water was added to the mixture. The mixture was acidified with conc. HCl and deposited crystals were collected by filtration, washed with H_2O, and dried to give **12b** (3.8 g). MS *m/z*: 315 (M^+). IR (KBr) cm^{-1}: 1722 (COOH). NMR ($CDCl_3$–DMSO-d_6) δ: 3.73 (1H, d, J=7.8 Hz, Ph-C<u>H</u>$_2$), 3.79 (1H, d, J=9.8 Hz, Ph-C<u>H</u>$_2$), 5.37 (1H, dd, J=9.8, 7.8 Hz, Ph-CH$_2$-C<u>H</u>), 6.05 (1H, br s, COO<u>H</u>), 7.29—7.63 (3H, m, arom. H), 7.45 (1H, s, 4-H), 7.92—8.26 (2H, m, arom. H). Yield, melting point, recrystallization solvent, and microanalysis data for **12b** are given in Table II.

R(+)-**9b**: A solution of **9b** (50.0 g, 0.16 mol) in CH_3CN (3600 ml) was mixed with a solution of (−)-cinchonidine (47.0 g, 0.16 mol) in boiling EtOH (400 ml). The resultant solution was stored at 5 °C for 18 h. The insoluble salt (34.5 g) was collected by filtration and recrystallized (4 times) by dissolving the salt in CH_3CN (2000 ml) and then adding EtOH (80 ml) to yield the salt (16.5 g) of the pure (+) enantiomer. The salt was converted to carboxylic acid by treatment with the mixture of Et_2O and aqueous HCl. The Et_2O layer was separated, washed with H_2O, dried over Na_2SO_4, and evaporated to crude *R*(+)-**9b** (8.1 g, 16%). Recrystallization from AcOEt–hexane gave *R*(+)-**9b** (5.5 g) as crystals, mp 193—195 °C. $[\alpha]_D^{25}$ +6.4° (c=1.0, acetone).

S(−)-**9b**: *d*-(+)-1-Phenylethylamine (12.3 g, 0.10 mol) was added to partially resolved 5-chloro-7,8-dihydro-3-phenylfuro[2,3-*g*]-1,2-benzisoxazole-7-carboxylic acid (32.0 g, 0.10 mol) [obtained from the mother liquor of the resolution of the (+) enantiomer desribed above], dissolved in CH_3CN (2200 ml). The resulting salt (43.5 g) was recrystallized (5 times) from EtOH–CH_3CN (1 : 5, v/v) (1620 ml) to provide the salt (11.5 g) of the pure (−) enantiomer. The salt was converted to the carboxylic acid in the same manner as described above to give crude *S*(−)-**9b** (8.4 g, 26%). Recrystallization from AcOEt–hexane gave *S*(−)-**9b** (5.7 g) as crystals, mp 193—195 °C. $[\alpha]_D^{25}$ −6.1° (c=1.0, acetone).

Diuretic and Uricosuric Effects on Rats[14] Seven-week-old Wistar-Imamichi rats that had been fasted for 24 h were divided in groups of five heads so that the animals in each group would excrete almost the same amount of urine. After forced urination, the rats were orally administered the test compounds that were suspended in physiological saline containing 3% gum arabic in a dose volume of 25 ml per kg of body weight. The control rats were given only physiological saline containing 3% gum arabic. The animals were housed in separate metabolic cages and the urine excreted from each animal was collected over a period of 6 h following the administration of the test compounds or physiological saline after complete starvation. The urine volume was directly read on a measuring cylinder after forced urination thereinto, and the amount of urine per kg of body weight was calculated. The amount of uric acid excreted in the urine was determined by the uricase-catalase method.

Acknowledgement The authors are indebted to Drs. S. Hata, I. Matsunaga, and T. Mori for valuable suggestions throughout this work. We are also grateful to Dr. M. Hamana, Professor emeritus of Kyushu University, for helpful discussions. We also thank Dr. Y. Nawata for help in obtaining the X-ray analysis of **9b**.

References and Notes

1) Portions of this work were presented at the 108th Annual Meeting of the Pharmaceutical Society of Japan, Hiroshima, April 1988, Abstract of Papers, p. 681, and at the 9th Symposium on Medicinal Chemistry, Tokyo, November 1988, Abstract of Papers, p. 37.
2) E. J. Cragoe, Jr., "Diuretics-Chemistry, Pharmacology, and Medicine," ed. by E. J. Cragoe, Jr., John Wiley and Sons, Inc., New York, 1983, p. 201.
3) S. J. deSolms, O. W. Woltersdorf, Jr., E. J. Cragoe, Jr., L. S. Watson, and G. M. Fanelli, Jr., *J. Med. Chem.*, **21**, 437 (1978).
4) W. F. Hoffman, O. W. Woltersdorf, Jr., F. C. Novello, E. J. Cragoe, Jr., J. P. Springer, L. S. Watson, and G. M. Fanelli, Jr., *J. Med. Chem.*, **24**, 865 (1981).
5) G. M. Shutske, L. L. Setescak, R. C. Allen, L. Davis, R. C. Effland, K. Ranbom, J. M. Kitzen, J. C. Wilker, and W. J. Novick, Jr., *J. Med. Chem.*, **25**, 36 (1982).
6) H. Sato, T. Dan, E. Onuma, H. Tanaka, and H. Koga, *Chem. Pharm. Bull.*, **38**, 1266 (1990).
7) *a*) J. J. Plattner, A. K. L. Fung, J. A. Parks, R. J. Pariza, S. R. Crowly, A. G. Pernet, P. R. Bunnell, and P. W. Dodge, *J. Med. Chem.*, **27**, 1016 (1984); *b*) J. J. Plattner and A. K. Fung, U. S. Patent 4456612 (1984) [*Chem. Abstr.*, **101**, 702 (1984)].
8) "Uric Acid," ed. by W. N. Kelley and I. M. Weiner, Springer-Verlag, Berlin, 1978.
9) K. R. Hande, R. M. Noone, and W. J. Stone, *Am. J. Med.*, **76**, 47 (1984).
10) *a*) R. C. Heel, R. N. Brogden, T. M. Speight, and G. S. Avery, *Drugs*, **14**, 349 (1977); *b*) T. Aoyama, T. Hasegawa, M. Terabayashi, M. Shibuya, S. Komatsu, and W. Shimamura, *Shinryo To Shinyaku*, **16**, 1521 (1979); *c*) "Benzbromarone" Drug Information (1984), Torii Pharmaceutical Co., Ltd., Tokyo.
11) H. Sato, K. Kuromaru, T. Ishizawa, and H. Koga, *Chem. Pharm. Bull.*, in preparation.
12) Y. Nawata, H. Koga, and M. Sawada, *Acta Cryst.*, in preparation.
13) *a*) H. Sato, H. Koga, and T. Dan, 15th Symposium on Structure–Activity Relationships, Tokyo, November 1987, Abstract of Papers, p. 334; *b*) H. Koga, H. Sato, T. Dan, and B. Aoki, *J. Med. Chem.*, in press.
14) *a*) T. Dan, H. Koga, E. Onuma, H. Tanaka, H. Sato, and B. Aoki, *Adv. Exp. Med. Biol.*, **253A**, 301 (1989); *b*) T. Dan, H. Tanaka, and H. Koga, *J. Pharmacol. Exp. Ther.*, **253**, 437 (1990).
15) B. Konig and St. v. Kostanecki, *Ber.*, **39**, 4028 (1906).
16) A. H. Abdel Rahman and E. M. Ismail, *Arzneim.-Forsch.* (*Drug Res.*), **26**, 756 (1976).
17) G. M. Shutske, L. L. Setescak, and R. C. Allen, Eur. Patent 2666 (1979) [*Chem. Abstr.*, **92**, 592 (1980)].

Isolation of Neoanisatin Derivatives from the Pericarps of *Illicium majus* with Other Constituents

Isao KOUNO,*[,a] Miwa HASHIMOTO,[a] Sayuri ENJOJI,[a] Masakatsu TAKAHASHI,[a] Hiroshi KANETO,[a] and Chun-Shu YANG[b]

Faculty of Pharmaceutical Sciences, Nagasaki University,[a] Nagasaki 852, Japan and Beijing College of Traditional Medicine,[b] Beijing, People's Republic of China. *Received January 24, 1991*

Further studies on the constituents of *Illicium majus* have resulted in the isolation of five new neoanisatin derivatives and two known phytoquinoides together with two known neolignans. Two of the neoanisatin derivatives are 1-hydroxyl, which are the first examples isolated anisatin derivatives so far. Another one, 2-oxoneoanisatin, exhibited picrotoxin-like convulsions in mice, the same as anisatin. The other two 3,4-dehydroxy-2-oxoneoanisatin isomers could not be separated from each other, even with high performance liquid chromatography.

Keywords *Illicium majus*, Illiciaceae; pericarps; 1-hydroxylneoanisatin; 2-oxoneoanisatin; neolignan; phytoquinoid

In the course of our investigation of the toxic constituents of the pericarps of *Illicium majus* HOOK. f. *et* THOMS., which is one of the toxic *Illicium* plants in China, we reported the isolation and structure determination of sesquiterpene lactones.[1-3] In these reports, we described the isolation of anisatin and other anisatin-like sesquiterpenes, which we call "majucin-type" compounds. This paper deals with the isolation and structure determination of the neoanisatin derivatives and other constituents from the pericarps of *I. majus*.

As we described before,[2] the MeOH extract of *I. majus* was divided into *n*-hexane-, AcOEt-, *n*-BuOH- and H_2O-soluble parts. Then, the AcOEt-soluble part was partitioned between AcOEt and H_2O with a counter-current distribution apparatus to give five fractions (I—V). The isolation of fractions II, III and IV afforded pseudomajucin,[1] anisatin, neomajucin, 2,3-dehydroneomajucin,[2] and six 2-oxyneomajucins.[3] The investigation of fraction V afforded **1** (16.5 mg), **2** (132 mg), a mixture of **4** and **5** (10 mg in the total amount) and two known phytoquinoides (**6**) (61 mg) and (**7**) (11 mg), respectively. From the *n*-BuOH-soluble part (286 g), a large amount of shikimic acid was removed by repeated column chromatography on Amberlite IRA-400; and subsequent chromatography on silica gel gave pseudomajucin glucoside[1] and two known neolignans, **8** (83 mg) and **9** (180 mg), respectively, together with a neoanisatin derivative (**3**) (10 mg).

Compound **1** was obtained as a colorless oil, $[\alpha]_D$ −16.9° (c=0.41, dioxane), and has the molecular formula, $C_{15}H_{20}O_8$, the same as anisatin, as analyzed by electron impact mass spectrum (EI-MS), and carbon counts in the carbon-13 nuclear magnetic resonance (^{13}C-NMR) spectrum. Absorptions due to a hydroxyl group at 3320 cm^{-1}, β-lactone at 1820 cm^{-1}, and δ-lactone at 1720 cm^{-1} were shown in the infrared (IR) spectrum of **1**. The presence of the β-lactone moiety was also suggested by the signal at δ_C 168.1 in the ^{13}C-NMR spectrum, and the characteristic small coupling constant (J=6.2 Hz) of AB type doublet signals at δ_H 4.49 and 4.90 in the proton ^{1}H-nuclear magnetic resonance (^{1}H-NMR) spectrum of **1**. The ^{13}C-NMR spectral data of **1** (Table II), analyzed by the heteronuclear multiple bond correlation (HMBC) spectrum, were similar to those of anisatin, except for the signals due to C-1 and C-3. The C-1 signal, revealed by HMBC spectrum, was assigned as a singlet at δ_C 81.3, and the C-3 signal was triplet at δ_C 33.2. In connection with these results, one of two methyl signals, H-15 (δ_H 1.63), appeared as a singlet and shifted to a lower field in the ^{1}H-NMR spectrum of **1** compared to the doublet H-15 signal of anisatin. These findings indicated that **1** is substantiated at C-1 by a hydroxy group in the structure of neoanisatin.

The relative stereochemistries at C-1 and C-6 can be deduced from a consideration of the results of the differential nuclear Overhauser effect (NOE) experiments as 1β-methyl and 6β-methyl, respectively; *i.e.* irradiation of H-15 signal produced NOE enhancements at the signals of H-10, H-8β and H-2β. Whereas, irradiation of H-10 gave expected NOEs at H-15 and H-8β. On the other hand, irradiation of H-12 caused NOEs at H-14a signal along with an H-7 signal as shown in Fig. 2, indicating that the configuration of C-12 methyl is β. Consequently, the structure of **1** was established as 1-hydroxyneoanisatin. It is the first example of a 1-hydroxyl group in the anisatin-type structure.

Compound **3** was obtained as a colorless oil, $[\alpha]_D$ −7.6° (c=0.49, dioxane), and has the molecular formula, $C_{15}H_{20}O_7$, as analyzed by EI-MS, and thus has one oxygen less than the molecular formula of **1**. In the IR spectrum of **3**, absorptions due to a hydroxyl group at 3350 cm^{-1}, β-lactone at 1820 cm^{-1}, and δ-lactone at 1725 cm^{-1} were demonstrated. The presence of the β-lactone moiety was also indicated by the characteristic small coupling constant (J=6.2 Hz) of AB type signals at δ_H 4.54 and 4.92 in the ^{1}H-NMR spectrum, which also showed a singlet methyl signal at δ_H 1.63 and a doublet methyl signal at δ_H 1.30 (J=7.3 Hz). Although these spectral features were very similar to those of neoanisatin, two-dimensional proton–proton correlation spectroscopy (2D ^{1}H–^{1}H COSY) of **3**

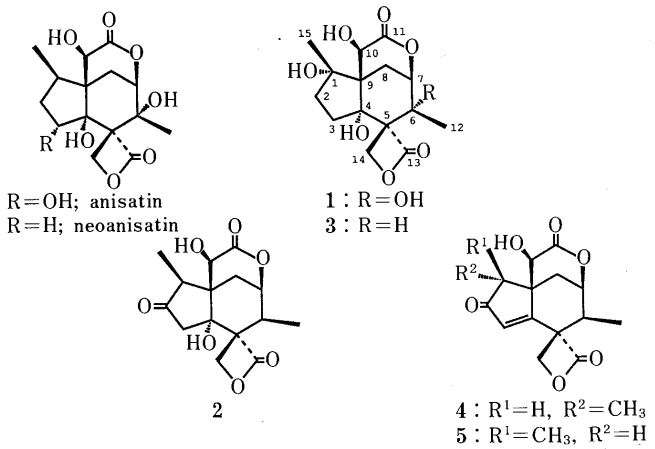

Fig. 1

TABLE I. ^{1}H-NMR Data for Anisatin and Compounds **1**—**5** (400 MHz, δ from TMS in Pyridine-d_5; J (Hz) in Parentheses)

Protons	Anisatin	1	2	3	4	5
1	2.73	—	3.20	—	3.01	2.38
	ddq (12.4, 11.0, 7.3)		q (7.3)		q (7.7)	q (7.3)
2α	2.18	2.39	—	2.46	—	—
	ddd (14.8, 11.0, 4.4)	ddd (13.9, 9.1, 6.9)		ddd (13.9, 9.2, 7.3)		
2β	2.37	2.52	—	2.56	—	—
	ddd (14.8, 12.4, 9.5)	ddd (13.9, 11.7, 2.5)		ddd (13.9, 12.1, 2.6)		
3α	—	2.24	2.85	2.27	6.50	6.59
		ddd (12.0, 9.1, 2.5)	d (17.6)	ddd (12.1, 9.2, 2.6)	s	s
3β	5.57	2.88	3.63	2.91	—	—
	dd (9.5, 4.4)	ddd (12.0, 11.7, 6.9)	d (17.6)	td (12.1, 7.3)		
6	—	—	3.33	3.27	2.47	2.56
			qd (7.3, 2.0)	qd (7.3, 2.2)	qd (7.0, 1.8)	qd (7.0, 1.5)
7	4.44	4.52	4.56	4.56	4.71	4.67
	dd (3.7, 2.0)	dd (3.6, 2.2)	ddd (4.0, 2.2, 2.0)	dt (3.3, 2.2)	dt (4.0, 1.8)	dt (4.4, 1.5)
8α	2.73	3.17	2.74	2.82	1.94	2.02
	dd (14.7, 2.0)	dd (15.0, 2.2)	dd (13.9, 2.2)	dd (14.3, 2.2)	dd (14.3, 1.8)	dd (13.9, 1.5)
8β	2.04	2.11	2.14	2.04	2.42	2.60
	dd (14.7, 3.7)	dd (15.0, 3.6)	dd (13.9, 4.0)	dd (14.3, 3.3)	dd (14.3, 4.0)	dd (13.9, 4.4)
10	4.49	4.61	4.53	4.53	4.60	4.55
	br d (4.4)	br s	s	br d (4.8)	s	s
10-OH	8.70	8.40	—	8.61	—	—
	br d (4.4)	br s		br d (4.8)		
H-12	1.79	1.80	1.32	1.30	1.30	1.30
	s	s	d (7.3)	d (7.3)	d (7.0)	d (7.0)
14a	4.50	4.49	4.59	4.54	4.77	4.75
	d (6.2)	d (6.2)	d (6.6)	d (6.2)	d (5.5)	d (5.5)
14b	5.06	4.90	4.90	4.92	4.80	4.56
	d (6.2)	d (6.2)	d (6.6)	d (6.2)	d (5.5)	d (5.5)
15	1.10	1.63	1.32	1.63	1.14	1.43
	d (7.3)	s	d (7.3)	s	d (7.7)	d (7.3)

Assignments were aided by ^{1}H–^{1}H 2D COSY spectra.

TABLE II. ^{13}C-NMR Data for Anisatin and Compounds **1**—**5** (100 MHz, δ from TMS in Pyridine-d_5)

Carbons	Anisatin	1	2	3	4	5
1	37.5 d	81.3 s	48.8 d	81.4 s	47.1 d	51.7 d
2	42.1 t	41.4 t	214.5 s	41.7 t	207.6 s	206.4 s
3	71.2 d	33.2 t	46.2 t	32.8 t	129.6 d	130.6 d
4	85.5 s	86.9 s	77.6 s	83.9 s	170.3 s	167.7 s
5	65.3 s	66.9 s	66.4 s	67.2 s	63.5 s	63.1 s
6	74.9 s	74.7 s	35.2 d	34.9 d	39.7 d	38.7 d
7	81.7 d	81.8 d	78.9 d	79.4 d	78.2 d	78.2 d
8	27.6 t	24.4 t	31.2 t	28.4 t	33.8 t	36.4 t
9	50.6 s	53.7 s	50.5 s	54.1 s	50.5 s	49.6 s
10	70.1 d	70.5 d	69.8 d	70.9 d	71.2 d	69.6 d
11	174.8 s	174.2 s	174.6 s	174.8 s	173.2 s	173.9 s
12	22.1 q	22.5 q	12.8 q	12.5 q	12.5 q	12.8 q
13	168.7 s	168.1 s	171.5 s	171.3 s	170.3 s	170.3 s
14	65.3 t	65.5 t	64.1 t	63.9 t	66.9 t	68.2 t
15	13.7 q	23.2 q	8.0 q	23.3 q	10.2 q	8.8 q

Assignments were made with the aid of HMQC and HMBC spectra.

showed the connectivity of H-12-H-6-H-7-H-8α,β and H-2α,β-H-3α,β. Thus, **3** should possess a 1-hydroxyl group the same as the structure of **1**, but has no 6-hydroxyl group; *i.e.* **3** was presumed to be a 6-dehydroxy-derivative of **1**, and the carbon connectivities of this structure was supported by HMBC spectrum of **3**.

The configurations of C-15 and C-12 methyl groups were deduced from NOE experiments. When irradiated at the frequency of H-14a, the signals of H-14b and H-12 were enhanced. On the other hand, the irradiation of the H-15 methyl signal caused the enhancement of the signals of

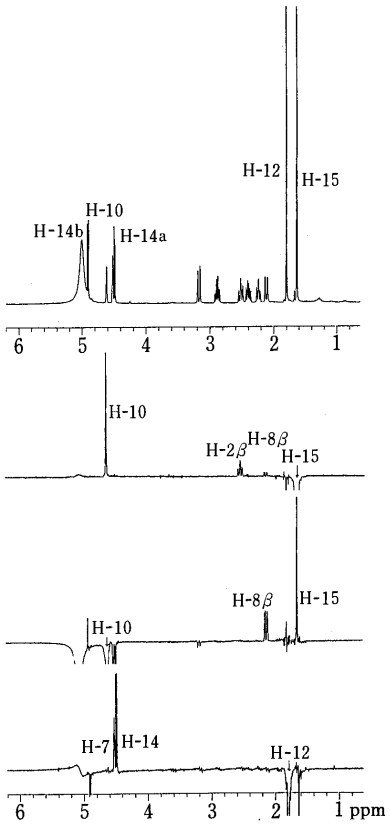

Fig. 2. ^{1}H-NMR Spectrum of **1** and NOE Spectra

TABLE III. ^1H and ^{13}C Correlations Shown in the HMBC Spectra of Compounds **1**—**5**[a]

Protons	1	2	3	4	5
H-1	—	—	C-8, 9, 10, 15	C-2, 15	C-2, 8, 9, 15
H-2β	b)	b)	—	—	—
H-2α	C-1	b)	—	—	—
H-3β	b)	b)	C-2	C-1, 2, 9	C-1, 2, 9
H-3α	b)	b)	C-4, 9	—	—
H-6	—	b)	C-5, 12, 13, 14	C-4, 5, 13, 14	C-5, 12, 13, 14
H-7	b)	b)	b)	b)	b)
H-8β	b)	C-6, 7	b)	b)	C-4
H-8α	C-9, 10	C-10	C-9, 10	C-9, 10	C-9, 10
H-10	C-4, 9, 11	C-4, 9, 11	C-1, 4, 9, 11	C-1, 4, 9, 11	C-4, 9, 11
H-14a	C-4, 6	C-4	C-4, 13	C-4, 13	C-4, 13
H-14b	C-4, 6, 13	b)	C-4, 13	C-4, 13	C-4, 13
H-15	C-1, 2, 9	C-1, 2, 9	C-1, 2, 9	C-1, 2, 9	C-1, 2

a) Measured in pyridine-d_5. b) No correlations were seen.

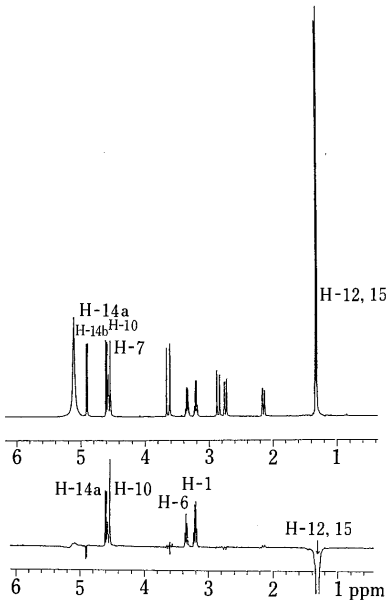

Fig. 3. ^1H-NMR Spectrum of **2** and NOE Spectrum

H-10 and H-2β, as summarized in Fig. 4. Consequently, the structure of compound **3** was determined to be a 6-dehydroxy compound of **1**.

Compound **2**, colorless prisms, mp 211—213 °C; $[\alpha]_D$ +67.4° (c=0.23) has the molecular formula, $C_{15}H_{18}O_7$, by elemental analysis and EI-MS. The IR spectrum of **2** showed absorptions due to hydroxyl groups at 3480 and 3460 cm^{-1}, and a δ-lactone carbonyl group at 1730 cm^{-1}, along with characteristic absorptions due to a β-lactone carbonyl group at 1825 cm^{-1} and a cyclopentanone carbonyl group at 1745 cm^{-1}. The presence of a β-lactone moiety was supported by the signals of an AB quartet at δ_H 4.59 and 4.90 (each doublet) with a small coupling constant (J=6.6 Hz) in the ^1H-NMR spectrum, which also suggested the presence of two secondary methyl groups in CD_3OD solution as two doublet signals at δ_H 1.05 (3H, d, J=7.0 Hz) and δ_H 1.22 (3H, d, J=7.3 Hz), and in C_5D_5N solution as one doublet signal at δ_H 1.32 (6H, d, J=7.3 Hz). In the ^1H–^1H 2D COSY of **2**, the connectivity was clarified between H-15-H-1, H-3α-H-3β, and H-6-H-7-H-8α,β, respectively. The assignment of signals in the ^{13}C-NMR spectrum and the connectivity of carbons and hydrogens

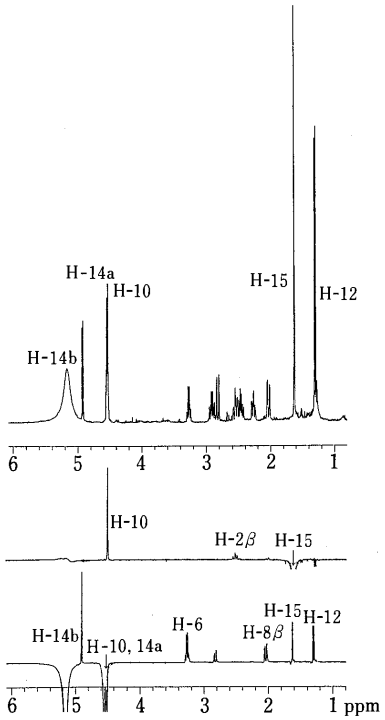

Fig. 4. ^1H-NMR Spectrum of **3** and NOE Spectra

TABLE IV. Dose-Dependent Mortality Induced by Compound **2**

Dose	Mortality
1.000	1/10
1.250	3/10
1.500	7/10
2.000	8/10
4.000	10/10

clarified with the aid of HMBC spectrum suggested that **2** is also an anisatin-type compound. These results propose that **2** is a 2-oxo-6-deoxyneoanisatin-derivative.[5]

The configurations at C-1 and C-6 were confirmed as 1β and 6β-methyl by an NOE experiment, which showed enhancement between the signals due to H-15 and H-10, whereas an NOE observed between the H-12 signal and one of the H-14 signals (δ_H 4.59) as shown in Fig. 3. These observations demonstrated that **2** has the same configura-

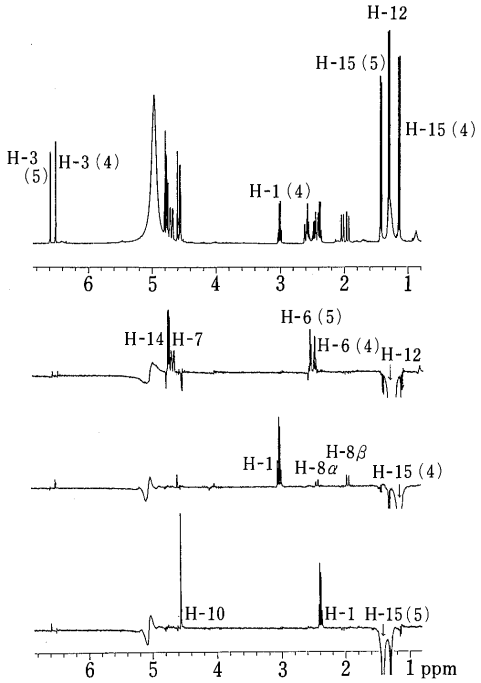

Fig. 5. ^{1}H-NMR Spectrum of a Mixture of **4** and **5**, and NOE Spectra

tion as that of neoanisatin; thus, the structure of **2** was determined to be 2-oxo-6-deoxyneoanisatin.

The toxicity of this compound was estimated as 1.46 mg/kg, which was examined using ddY-strain mice weighing 25—28 g, with 10 animals in each dose group. When the mice were treated with this compound, the animals exhibited picrotoxin-like convulsions, in a dose-dependent manner, which is shown in Table IV. As we reported before,[2,3] majucin-type compounds have no toxicity except for neomajucin, which is almost ten times less toxic than the toxicity of anisatin. We also confirmed that pseudoanisatin has no toxicity, as was reported by Lane *et al.*[4] Accordingly, the above result suggested that strong toxicity may be dependent upon the possession of β- and γ-lactone moieties in the anisatin-type structure, although other anisatin-type compounds reported herein were not examined because of their small quantities.

Compounds **4** and **5** were obtained as an epimeric mixture in spite of an attempt to purify each with high performance liquid chromatography (HPLC). However, it was possible to analyse their ^{1}H- and ^{13}C-NMR spectra by comparing the NMR spectra of the mixtures of **4**:**5**=2:1 and **4**:**5**=1:1. These mixtures were crystallized from AcOEt and showed a molecular ion peak at *m/z* 292 indicating a molecular formula of $C_{15}H_{16}O_6$. In the ^{1}H-NMR spectrum of this mixture, two sets of AB quartet signals with a small coupling constant (J=5.5 Hz) were seen, suggesting **4** and **5** have a β-lactone group. Two sets of two doublet methyl signals (H-12 and H-15 signals, and H-12 signals overlapping each other) were also seen in this spectrum, and the carbon signals in the ^{13}C-NMR spectrum of the mixture were very similar to those of compound **2** except for two sets of two olefinic carbon signals at δ_C 129.6 (d), 170.3 (s) and δ_C 130.6 (d), 167.7 (s). The olefinic singlet proton signals were seen at δ_H 6.50 and 6.59, respectively. These features indicated that **4** and **5** are a 3,4-dehydroxy compound of **3**, and therefore this mixture was the epimeric

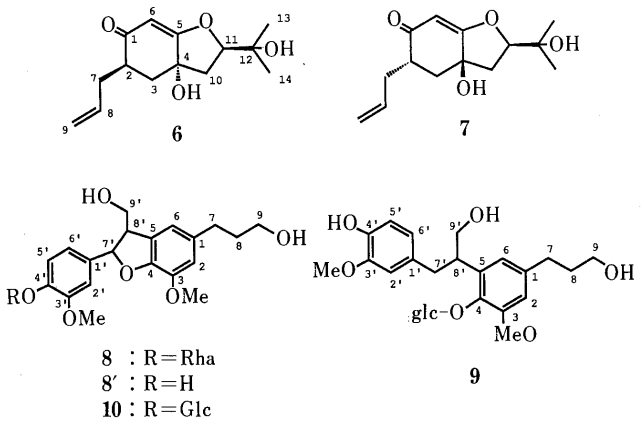

Fig. 6

mixture of C-1 α-methyl and C-1 β-methyl compounds.

To resolve the configuration at C-1, NOE experiments were performed in the ^{1}H-NMR spectrum of the 1:1 mixture. When the signal of H-15 (δ_H 1.14) in those proton signals ascribable to compound **4** was irradiated, the signals of H-1, H-8α and H-8β were enhanced. On the other hand, irradiation of H-15 (δ_H 1.43) belonging to compound **5** caused enhancements of the signals of H-1 and H-10, as shown in Fig. 5. These results indicated that **4** is the 3,4-dehydroxy 15α-methyl compound of **2**, and **5** is the 3,4-dehydroxy compound of **2**. In the majucin-type compounds, there were the same isomers as compounds **4** and **5**. But, it was possible to separate them from each other in the case of the majucin-type compounds.[3]

Compound **6** was isolated as a colorless oil. Its molecular formula was determined as $C_{14}H_{20}O_4$ by an analysis of MS (*m/z*: 252 [M^+]) and carbon counts in the ^{13}C-NMR spectrum. The IR spectrum of **6** showed the absorptions due to hydroxy groups (3580 and 3350 cm^{-1}) and an α,β-unsaturated carbonyl group (1640 cm^{-1}). The ^{1}H–^{1}H 2D COSY of **6** revealed the connectivity of CH_2=CH–CH_2–CH–CH_2– and –O–CH–CH_2–, and the ^{1}H-NMR spectrum showed the presence of a *tert*-dimethyl group and an α proton of α,β-unsaturated olefine. Compound **7**, which was obtained as colorless needles, mp 110—112 °C, has the same molecular formula as **6**, and the IR and ^{1}H- and ^{13}C-NMR spectra strongly resembled those of **6**. These results suggested that **6** and **7** should be analogous compounds each other. The structure, which satisfied these data and the partial structures derived from the ^{13}C–^{1}H long-range correlations in the HMBC spectra (in C_5D_5N solution) of **6** and **7**, was assigned for the structure of illifunone, which belongs to phytoquinoid and was obtained from *I. tashiroi* and *I. arborescens*,[6] both of which are the same species as *I. majus*. So far, four stereoisomers of illifunone, illifunone A, B, C and D, have been isolated from these plants in connection with the stereochemistry at the positions of C-2 and C-4. These compounds were easily distinguished from each other based on the consideration of the chemical shifts of axial H-3 and H-11 proton signals in the ^{1}H-NMR spectra of these compounds. Comparisons of the spectral and physical data of **6** and **7** with those of illifunones A, B, C and D, suggested that **6** is identical to illifunone C, and **7** to illifunone A. Phytoquinoid is constituted of a C_6–C_3 unit and isoprene, and is a rare compound found only in higher plants.

Compound **8** was isolated as a viscous oil, $[\alpha]_D$ −51.8° (c=0.26, MeOH). Its molecular formula was deduced $C_{26}H_{34}O_{10}$ by fast atom bombardment mass spectrum (FAB-MS) (m/z: 529 [M^+ + Na]) and by carbon counts in the ^{13}C-NMR spectrum. Acid hydrolysis of **8** with hesperidinase afforded an aglycone (**8'**) and a sugar. The sugar is rhamnose as corroborated by Avicel thin layer chromatography (TLC) developed with an authentic sample of rhamnose. In the ^{1}H-NMR spectrum of **8**, two methoxy signals were seen. In the ^{13}C-NMR spectrum of **8**, twelve aromatic and six aliphatic carbon signals were shown except for the carbon signals of rhamnose and methoxy groups. The ^{1}H–^{1}H 2D COSY spectrum of **8** suggested that the aromatic rings are 1,3,4-tri-substituted and 1,3,4,5-tetra-substituted benzene rings. Thus, **8** was proven a rhamnoside of dihydrodehydroconiferyl alcohol. The linkage position of rhamnose to dihydrodehydroconiferyl alcohol was clarified as 4' by HMBC spectrum of **8**. This compound was previously obtained from *Pinus massoniana* by O. Theander *et al.*[7] and from *Epimedium diphyllum* by A. Ueno *et al.*,[8] and the spectral data of **8**, including the optical rotation value, were approximately identical to those of the former compound.

The configurations at C-7' and C-8' were not specified in the compound obtained by O. Theander *et al.*, but A. Ueno *et al.* suggested C-7 and C-8 to be *R* and *S*, respectively, by circular dichroic (CD) spectroscopy. Although their proposal was derived from the results of 2-aryl-3-methyl-2,3-dihydrobenzofuran derivatives, it seems that these results cannot be applied to the derivatives of dihydrodehydroconiferyl alcohol. The plane structure of the aglycone of their compounds was identical to the aglycone of compound **10**, which was obtained by T. Yamauchi *et al.*[9] from *Trachelospermum asiaticum*, but they did not determine the configuration at C-7 and C-8, and suggested that this compound may have the same stereoisomeric structure as that obtained by Takemoto *et al.*[10] or by Satake *et al.*[11] comparing their optical rotation value. The negative optical rotation value of **8'** ($[\alpha]_D$ −3.9°) suggests that **8** has the same stereoisomeric structure as that of the aglycone ($[\alpha]_D$ −3.2°) of **10**, rather than that obtained by Theander *et al.* ($[\alpha]_D$ +4.7°). Since the sugar moiety was characterized as an α-linked rhamnose, **8** was deduced to be the 4'-*O*-α-D-rhamnoside of dihydrodehydroconiferyl alcohol.

Compound **9** was obtained as a colorless syrup, and its molecular formula was deduced as $C_{26}H_{36}O_{11}$ from FAB-MS (m/z: 525 [M^+ + 1]) and carbon counts in the ^{13}C-NMR spectrum. The presence of two benzene rings, two methoxy groups and a glucose moiety was clarified by its ^{1}H- and ^{13}C-NMR spectra, and six extra aliphatic carbons were also suggested by the ^{13}C-NMR spectrum. These findings indicated that **9** is also lignan. The ^{1}H-NMR spectrum of **9** indicated that one of two benzene rings is 1,3,4-tri-substituted and the other is 1,3,4,5-tetra-substituted ones, and the ^{1}H–^{1}H COSY spectrum suggested the connectivity of –CH_2–CH–CH_2O– and –CH_2–CH_2–CH_2O– moieties. The linkage position of glucose was elucidated by HMBC spectrum as 4. All this data and the HMBC correlations demonstrated the structure as shown in Fig. 6. This compound was isolated from *Epomedium grandiflorum* by A. Ueno *et al.*,[12] and named icariside E_3, whose ^{1}H- and ^{13}C-NMR spectral data and optical rotation value were identical with those of **9**.

Experimental

All melting points were determined on a Yanagimoto micro melting point apparatus and are uncorrected. ^{1}H- and ^{13}C-NMR spectra were taken with JEOL GX-400 and JEOL FX-90Q spectrometers. NOE and 2D COSY experiments were performed on the former apparatus. Chemical shifts are expressed in δ (ppm) values with tetramethylsilane as an internal standard. EI-MS and FAB-MS were recorded on a JEOL JMS-DX-303 spectrometer. IR spectra were recorded on a JASCO IR-180 or Shimadzu IR-408. CD spectrum was taken on a JASCO J-500A apparatus. Optical rotations were measured with a JASCO DIP-181 digital polarimeter. Medium-pressure liquid chromatography (MPLC) was carried out on a JASCO 880-PU pump using a Kusano Si-5 column and a Kusano ODS-20 column.

Isolation The MeOH extract of the pericarps (1.5 kg) of *I. majus* was extracted with AcOEt and *n*-BuOH successively, after extraction with *n*-hexane. The AcOEt-soluble part was subjected to counter-current distribution using the solvent system of H_2O and AcOEt to give five fractions (I—V) as described before. Of these fractions, fraction V was newly investigated to give compound **1** (16.5 mg), **2** (132 mg), and **4** and **5** as a 1 : 1 mixture (10 mg total) together with compounds **6** (61 mg) and **7** (11 mg), respectively. The separation of the *n*-BuOH soluble part (286 g) was performed, after the exclusion of a large amount of shikimic acid, to give three fractions (I—III). From fraction I, compound **3** (10 mg) was obtained and purified by a Kusano Si-5 column. Fraction III was subjected to a Sephadex LH-20 column and ODS-MPLC using a solvent system of H_2O–MeOH (4 : 6), successively, to give compounds **8** (83 mg) and **9** (180 mg).

Compound 1 Colorless oil. $[\alpha]_D^{23}$ −16.5° (c=0.41, dioxane). EI-MS m/z: 328 (M^+), $C_{15}H_{20}O_8$. IR ν_{max}^{Nujol} cm^{-1}: 3320 (OH), 1820 (β-lactone), 1720 (δ-lactone).

Compound 2 Colorless prisms from $CHCl_3$–AcOEt, mp 211—213 °C. $[\alpha]_D^{21}$ +67.4° (c=0.23, dioxane). EI-MS m/z: 310 (M^+). IR ν_{max}^{KBr} cm^{-1}: 3480, 3460 (OH), 1825 (β-lactone), 1745 (cyclopentenone), 1730 (δ-lactone). *Anal.* Calcd for $C_{15}H_{18}O_7 \cdot 1/2H_2O$: C, 56.42; H, 6.00. Found: C, 56.26; H, 5.95.

Compound 3 Colorless oil. $[\alpha]_D^{20}$ −7.6° (c=0.49, dioxane). EI-MS m/z: 312 (M^+), $C_{15}H_{20}O_7$. IR ν_{max}^{Nujol} cm^{-1}: 3350 (OH), 1820 (β-lactone), 1725 (δ-lactone).

Compounds 4 and 5 Colorless needles (as a 1:1 mixture). EI-MS m/z: 292 (M^+), $C_{15}H_{16}O_6$.

Compound 6 (Illifunone C) Colorless oil. $[\alpha]_D^{17}$ +61.9° (c=0.29, $CHCl_3$). EI-MS m/z: 252 (M^+), $C_{14}H_{20}O_4$. IR $\nu_{max}^{CHCl_3}$ cm^{-1}:3580, 3350 (OH), 1640 (α,β-unsaturated ketone), 1185. ^{1}H-NMR (400 MHz, C_5D_5N) δ: 3.19 (1H, m, H-2), 1.87 (1H, t, J=13.2 Hz, H-3β), 2.59 (1H, dd, J=13.2, 4.4 Hz, H-3α), 5.64 (1H, s, H-6), 2.36 (1H, m, H-7a), 2.92 (1H, m, H-7b), 5.86 (1H, m, H-8), 5.02 (1H, m, H-9a), 5.10 (1H, m, H-9b), 2.38 (1H, dd, J=12.8, 10.3 Hz, H-10α), 2.52 (1H, dd, J=12.8, 4.8 Hz, H-10β), 5.09 (1H, dd, J=10.3, 4.8 Hz, H-11), 1.33 (3H, s, H-13 or H-14), 1.52 (3H, s, H-14 or H-13). ^{1}H-NMR (90 MHz, $CDCl_3$) δ: 1.71 (1H, t, J=12 Hz, H-3), 5.27 (1H, s, H-6), 5.86 (1H, m, H-8), 5.06 (1H, m, H-9a), 4.92 (1H, m, H-9b), 1.95 (1H, dd, J=13, 10 Hz, H-10a), 2.36 (1H, dd, J=13, 5 Hz, H-10b), 4.68 (1H, dd, J=10, 5 Hz, H-11), 1.17 (3H, s, H-13 or H-14), 1.37 (3H, s, H-14 or H-13). ^{13}C-NMR (22.5 MHz, $CDCl_3$) δ: 200.6 (s, C-1), 39.9 (d, C-2), 38.5 (t, C-3), 75.7 (s, C-4), 179.4 (s, C-5), 100.1 (d, C-6), 34.0 (t, C-7), 135.5 (d, C-8), 116.6 (t, C-9), 38.8 (t, C-10), 91.0 (d, C-11), 70.2 (s, C-12), 24.4 (q, C-13 or C-14), 26.8 (q, C-14 or C-13).

Compound 7 (Illifunone A) Colorless needles from *n*-hexane–$CHCl_3$, mp 110—112 °C. $[\alpha]_D^{16}$ −83.4° (c=0.58, $CHCl_3$). EI-MS m/z: 252 (M^+), $C_{14}H_{20}O_4$. IR $\nu_{max}^{CHCl_3}$ cm^{-1}: 3600, 3340 (OH), 1640 (α,β-unsaturated ketone), 1180. ^{1}H-NMR (400 MHz, C_5D_5N) δ: 3.14 (1H, m, H-2), 1.72 (1H, t, J=12.8 Hz, H-3β), 2.56 (1H, dd, J=12.8, 4.4 Hz, H-3α), 5.66 (1H, s, H-6), 2.43 (1H, m, H-7a), 2.88 (1H, m, H-7b), 5.89 (1H, m, H-8), 5.04 (1H, m, H-9a), 5.12 (1H, m, H-9b), 2.25 (1H, dd, J=13.9, 9.5 Hz, H-10α), 2.56 (1H, dd, J=13.9, 1.1 Hz, H-10β), 4.61 (1H, dd, J=9.5, 1.1 Hz, H-11), 1.31 (3H, s, H-13 or H-14), 1.55 (3H, s, H-14 or H-13). ^{1}H-NMR (90 MHz, $CDCl_3$) δ: 1.63 (1H, t, J=12 Hz, H-3), 5.33 (1H, s, H-6), 5.71 (1H, m, H-8), 5.08 (1H, m, H-9a), 4.94 (1H, m, H-9b), 2.17 (1H, dd, J=14, 9 Hz, H-10a), 2.40 (1H, dd, J=14, 2 Hz, H-10b), 4.42 (1H, dd, J=9, 2 Hz, H-11), 1.28 (3H, s, H-13 or H-14), 1.50 (3H, s, H-14 or H-13). ^{13}C-NMR (22.5 MHz, $CDCl_3$) δ: 200.5 (s, C-1), 40.6 (d, C-2), 39.1 (t, C-3), 73.3 (s, C-4), 180.4 (s, C-5), 99.2 (d, C-6), 34.2 (t, C-7), 136.0 (d, C-8), 116.4 (t, C-9), 38.0 (t, C-10), 90.4 (d, C-11), 71.5 (s, C-12), 26.8(q,

C-13 or C-14), 26.9 (q, C-14 or C-13).

Compound 8 Amorphous powder. $[\alpha]_D^{20}$ −51.8° (c=0.26, MeOH). FAB-MS m/z: 529 $[M^+ + Na]$, $C_{26}H_{34}O_{10}$. IR ν_{max}^{KBr} cm^{-1}: 3400 (OH), 2930, 1605, 1510, 1460, 1420. ^{1}H-NMR (400 MHz, CD_3OD) δ: 6.72 (1H, s, H-2), 6.73 (1H, s, H-6), 2.62 (2H, t, J=7.5 Hz, H-7), 1.81 (2H, m, H-8), 3.57 (2H, t, J=6.4 Hz, H-9), 7.03 (1H, d, J=1.8 Hz, H-2′), 7.08 (1H, d, J=8.4 Hz, H-5′), 6.92 (1H, dd, J=8.4, 1.8 Hz, H-6′), 5.55 (1H, d, J=6.0 Hz, H-7′), 3.46 (1H, m, H-8′), 3.75 (1H, dd, J=11.0, 7.5 Hz, H-9′a), 3.85 (1H, dd, J=11.0, 5.0 Hz, H-9′b), 3.86 (3H, s, –OMe), 3.80 (3H, s, –OMe), 5.34 (1H, d, J=1.8 Hz, rha-1″), 4.06 (1H, dd, J=3.5, 1.8 Hz, rha-2″), 3.87 (1H, J=9.5, 3.5 Hz, rha-3″), 3.44 (1H, J=9.5 Hz, rha-4″), 3.78 (1H, dq, J=9.5, 6.2 Hz, rha-5″), 1.21 (3H, d, J=6.2 Hz, rha-6″). ^{13}C-NMR (100 MHz, CD_3OD) δ: 131.7 (s, C-1), 114.3 (d, C-2), 145.3 (s, C-3), 147.5 (s, C-4), 127.6 (s, C-5), 118.0 (d, C-6), 32.9 (t, C-7), 35.8 (t, C-8), 62.3 (t, C-9), 138.8 (s, C-1′), 111. 4 (d, C-2′), 152.1 (s, C-3′), 146.6 (s, C-4′), 119.6 (d, C-5′), 119.2 (d, C-6′), 88.5 (d, C-7′), 55.6 (d, C-8′), 65.2 (t, C-9′), 56.9 (q, –OMe), 56.6 (q, –OMe), 101.4 (d, rha-1″), 72.2 (d, rha-2″), 72.1 (d, rha-3″), 73.9 (d, rha-4″), 70.8 (d, rha-5″), 18.0 (q, rha-6″).

Hydrolysis of 8 Hesperidinase (Sigma Chemical Co.) (70 mg) was added to a solution of **8** (30 mg) in H_2O (5 ml), which was shaken at 37 °C for 2 d, then extracted with AcOEt. The AcOEt soluble portion was dried over Na_2SO_4, then evaporated under reduced pressure to give the residue. This was purified by SiO_2 column chromatography using the solvent of $CHCl_3$–MeOH (1 : 1) to give **8′** (16 mg). The water layer was concentrated under reduced pressure, and was examined by Avicel TLC (Funakoshi Yakuhin Co., Ltd.) developed with n-BuOH–pyridine–H_2O (6 : 4 : 3) together with an authentic sample of rhamnose.

Compound 8′ Colorless oil. $[\alpha]_D^{16}$ −3.9° (c=0.37, acetone). CD (c=0.0016 mol/l, MeOH) $[\theta]$ (nm): −3838 (294), −10800 (242). ^{1}H-NMR (400 MHz, C_5D_5N) δ: 7.06 (1H, br s, H-2), 6.92 (1H, br s, H-6), 2.87 (2H, t, J=7.7 Hz, H-7), 2.08 (2H, m, H-8), 3.92 (2H, t, J=6.2 Hz, H-9), 7.33 (1H, d, J=1.8 Hz, H-2′), 7.20 (1H, d, J=8.1 Hz, H-5′), 7.25 (1H, dd, J=8.1, 1.8 Hz, H-6′), 6.06 (1H, d, J=6.6 Hz, H-7′), 3.96 (1H, m, H-8′), 4.20 (1H, dd, J=11.0, 6.6 Hz, H-9′a), 4.27 (1H, dd, J=11.0, 5.5 Hz, H-9′b), 3.63, 3.83 (each 3H, s, –OMe). ^{13}C-NMR (100 MHz, C_5D_5N) δ: 130.2 (s, C-1), 113.8 (d, C-2), 144.7 (s, C-3), 147.4 (s, C-4), 136. 1(s, C-5), 117.6 (d, C-6), 32.7 (t, C-7), 36.0 (t, C-8), 61.5 (t, C-9), 133.9 (s, C-1′), 110.9 (d, C-2′), 148 (s, C-3′), 148.8 (s, C-4′), 116.5 (d, C-5′), 119.8 (d, C-6′), 88.4 (d, C-7′), 55.1 (d, C-8′), 64.4 (t, C-9′), 55.9, 56.3 (each q, –OMe × 2).

Compound 9 Amorphous powder. $[\alpha]_D^{18}$ −61.1° (c=0.26, MeOH). FAB-MS m/z: 525 $[M^+ + H]$, $C_{26}H_{36}O_{11}$. IR ν_{max}^{KBr} cm^{-1}: 3385, 2930, 1590, 1520, 1460, 1430. ^{1}H-NMR (400 MHz, C_5D_5N) δ: 7.05 (1H, d, J=1.8 Hz, H-2), 7.16 (1H, d, J=1.8 Hz, H-6), 2.85 (2H, br t, J=7.3 Hz, H-7), 2.05 (2H, m, H-8), 3.90 (2H, t, J=6.2 Hz, H-9), 6.78 (1H, d, J=1.8 Hz, H-2′), 6.99 (1H, d, J=7.7 Hz, H-5′), 6.88 (1H, dd, J=7.7, 1.8 Hz, H-6′), 3.11 (1H, dd, J=13.9, 9.1 Hz, H-7′a), 3.46 (1H, dd, J=13.9, 5.9 Hz, H-7′b), 4.79 (1H, m, H-8′), 3.64, 3.66 (each 3H, s, –OMe), 5.40 (1H, d, J=7.3 Hz, glc-1″). ^{13}C-NMR (100 MHz, C_5D_5N) δ: 139.6 (s, C-1), 113.3 (d, C-2), 152.5 (s, C-3), 143.2 (s, C-4), 139.1 (s, C-5), 122.3 (d, C-6), 32.9 (t, C-7), 35.7 (t, C-8), 61.5 (t, C-9), 132.4 (s, C-1′), 111.3 (d, C-2′), 148.2 (s, C-3′), 146.0 (s, C-4′), 116.0 (d, C-5′), 119.8 (d, C-6′), 39.2 (t, C-7′), 42.3 (d, C-8′), 66.9 (t, C-9′), 55.7, 55.9 (each q, –OMe), 105.7 (d, glc-1″), 76.2 (d, C-2″), 78.4 (d, C-3″), 71.1 (d, C-4″), 78.2 (d, C-5″), 62.4 (t, C-6″).

Acknowledgment We are grateful to Mr. Y. Ohama for valuable assistance in measuring the NMR spectra.

References

1) I. Kouno, N. Baba, M. Hashimoto, N. Kawano, C.-S. Yang, and S. Sato, *Chem. Pharm. Bull.*, **37**, 2427 (1989).
2) I. Kouno, N. Baba, M. Hashimoto, N. Kawano, M. Takahashi, H. Kaneto, C.-S. Yang, and S. Sato, *Chem. Pharm. Bull.*, **37**, 2448 (1989).
3) I. Kouno, N. Baba, M. Hashimoto, N. Kawano, M. Takahashi, H. Kaneto, and C.-S. Yang, *Chem. Pharm. Bull.*, **38**, 422 (1990).
4) J. F. Lane, W. T. Koch, N. S. Leeds, and G. Gorin, *J. Am. Chem. Soc.*, **74**, 3211 (1952).
5) C.-S. Yang, M. Hashimoto, N. Baba, M. Takahashi, H. Kaneto, N. Kawano, and I. Kouno, *Chem. Pharm. Bull.*, **38**, 291 (1990).
6) K. Yakushijin, T. Tohshima, E. Kitagawa, R. Suzuki, J. Sekikawa, T. Morishita, H. Murata, S.-T. Lu, and H. Furukawa, *Chem. Pharm. Bull.*, **32**, 11 (1984).
7) L. N. Lundgren, Z. Shen, and O. Theander, *Acta. Chem. Scan., Ser. B*, **39**, 241 (1985).
8) T. Miyase, A. Ueno, N. Takizawa, H. Kobayashi, and H. Oguchi, *Phytochemistry*, **28**, 3483 (1989).
9) F. Abe and T. Yamauchi, *Chem. Pharm. Bull.*, **34**, 4340 (1986).
10) T. Takemoto, T. Miyase, and G. Kusano, *Phytochemistry*, **14**, 1890 (1978).
11) T. Satake, T. Murakami, Y. Saiki, and C.-M. Chen, *Chem. Pharm. Bull.*, **26**, 1616 (1978).
12) T. Miyase, A. Ueno, N. Takagi, H. Kobayashi, and H. Oguchi, *Chem. Pharm. Bull.*, **36**, 2475 (1988).

Enzyme Immunoassay for the Drug of Anti-ulcer Using Avidin–Biotin System

Takao OKUMURA,[a] Takeshi ASANO,[a] Tetuo ADACHI[b] and Kazuyuki HIRANO[b]

Research Laboratories, Maruko Seiyaku Co., Ltd.,[a] 1212 Teramae, Gejo-cho, Kasugai 486, Japan and Gifu Pharmaceutical University,[b] 6–1 Mitahora-higashi, 5-chome, Gifu 502, Japan. *Received December 11, 1990*

We have developed a competitive enzyme immunoassay for a drug, which was a newly synthesized anti-ulcer agent, using an enzyme immunoassay. The polyclonal anti-drug antibody coupled to biotin, peroxidase labeled drug derivatives as a tracer, and a small column of Sepharose 4B covalently bound to avidin were used in the assay. This assay is simple and rapid, and the sensitivity and the measuring range can be controlled by the flow rate of the substrate solution. The correlation between serum drug concentrations (0.1—10 μg/ml) measured by gas chromatography and this assay was good ($r=0.991$). This principle for the assay is very practical and applicable to the enzyme immunoassay for small and large molecules.

Keywords enzyme immunoassay; anti-ulcer agent; avidin; biotin; peroxidase

The determination of drugs in body fluids must be specific and rapid in order to obtain the clinical data of the patients.[1] Therapeutic drug monitoring is necessary to depress the adverse reaction of the drug in the case of the narrow therapeutic range between its efficacy and toxicity. Effective treatment is furthermore complicated because the pharmacokinetics of therapeutic drugs are significantly changed in individual patients.[2] Measurement of therapeutic drugs is now provided as a service by the department of clinical chemistry or pharmacy.[3] Several techniques have been used for measuring therapeutic drugs, including ultraviolet spectroscopy,[4] gas chromatography,[5] high performance liquid chromatography[6] and enzyme immunoassay.[7]

Since newly synthesized (−)-*cis*-2,3-dihydro-3-(4-methylpiperazinylmethyl)-2-phenyl-1,5-benzothiazepin-4(5*H*)-one hydrochloride (BTM-1086) was a strong potential anti-ulcer agent, we have attempted to develop a determination system to evaluate the anti-ulcer activity. In a previous paper,[8] we had prepared the rabbit anti-BTM-1086 antibody and developed the competitive enzyme immunoassay which is not ideally suited as a drug monitoring method since it involves a lot of work and is time-consuming.

In this paper, we describe a simple and rapid assay system for BTM-1086 using the avidin-biotin binding reaction.

Materials and Methods

Materials BTM-1086 and its metabolites were synthesized by Maruko Seiyaku Co., Ltd., as shown in Fig. 1. Horseradish peroxidase (HRP type VI) was obtained from Sigma Chemical Co. (U.S.A.) and 1-ethyl-3-(3-dimethylaminopropyl)carbodiimide hydrochloride and glutaraldehyde were from Nakarai Chemicals, Ltd. (Kyoto). Bovine serum albumin (BSA fraction V) was from Wako Pure Chemical Industries, Ltd. (Osaka). All other solvents and chemicals were of special grade. Rabbit anti-BTM-1086 antibody and BTM-1086–HRP conjugate were prepared according to the method of the previous paper.[8]

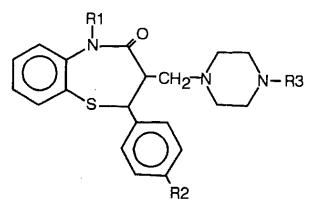

	R1	R2	R3
BTM-1086	H	H	CH_3
BTM-1066	H	H	H
BTM-1091	H	OH	H
BTM-1092	H	OH	CH_3

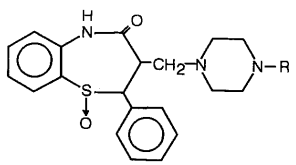

	R
BMS-053	CH_3
demethyl-BMS-053	H

Fig. 1. Chemical Structures of BTM-1086 and Its Metabolites

BTM-1066, BTM-1091, BTM-1092, BMS-053 and demethyl BMS-053 are metabolites of BTM-1086.

Buffer A 50 mM sodium phosphate buffer, pH 7.4, containing 0.02% Triton X-405 and 0.3 M NaCl.

Preparation of Biotinyl Antibody Six ml of anti-BTM antibody purified by protein A-Sepharose 4B was dissolved in 10 mM sodium phosphate buffer (pH 7.4) containing 0.15 M NaCl (2 mg protein/ml), then mixed with 200 μl of biotinyl *N*-succinimide dissolved in dimethylformamide (2 mg/ml). The mixture was allowed to stand for 2 h at room temperature according to the method of Jasiewicz, *et al.*[9] The resulting mixture was dialyzed against phosphate buffered saline at 4 °C overnight and diluted with buffer A before use.

Coupling of Avidin to Sepharose 4B Avidin was covalently linked to Sepharose 4B (10 mg avidin/30 ml gel) according to the method of March *et al.*[10]

Standard Procedure After 30 μl of normal rat serum as a carrier, 10 μl of serum sample and 40 μl of buffer A were mixed, 40 μl of BTM-1086–HRP conjugate (diluted 1:200 with buffer A) and 10 μl of biotinyl antibody solution (diluted 1:20 with buffer A) were added and the mixture was allowed to stand at room temperature for 20 min. 60 μl of the mixture was applied to column (4.4 × 13 mm) of 0.2 ml avidin coupled to Sepharose 4B, and the column was washed with 4 ml of buffer A at a flow rate of 7.5 ml/h. 0.5% of 3-(*p*-hydroxyphenyl)propionic acid solution, buffer A and 0.005% hydrogen peroxide solution were mixed at the ratio of 1:10:1 and used as a substrate solution. The substrate solution was applied on to the column at the same flow rate and after 5 min the fraction 0.5 ml was collected. 1.6 ml of 0.1 N NaOH were added into the 0.4 ml out of the 0.5 ml and the fluorescence of the resulting solution was measured at 320 nm for excitation and 405 nm for emission with a Hitachi model FPL-2 fluorometer. The calibration curve was prepared using the standard BTM dissolved in normal serum.

Correlation between Enzyme Immunoassay (EIA) and Gas Chromatography (GC) Wistar male rats were bled from the descending aorta at 0.5, 1, 2, 4, 6, 9 and 24 h after a single oral administration of BTM-1086 (30 mg/kg). The serum samples were assayed for BTM-1086 by EIA and GC. GC was performed on a Hitachi 163 gas chromatograph equipped with a hydrogen flame thermionic detector, and the conditions used were as follows; 1 m × 3 mm glass column packed with 2% OV-17 Chromosorb W (AW, DMCS); carrier gas, He, 50 ml/min; injection port temperature, 300 °C; column temperature, 280 °C.

Results and Discussion

Antigen–Antibody Reaction According to the standard assay system, we investigated the antigen–antibody reaction. The time course of the antigen–antibody reaction is shown in Fig. 2. The rate of the reaction was found to reach plateau

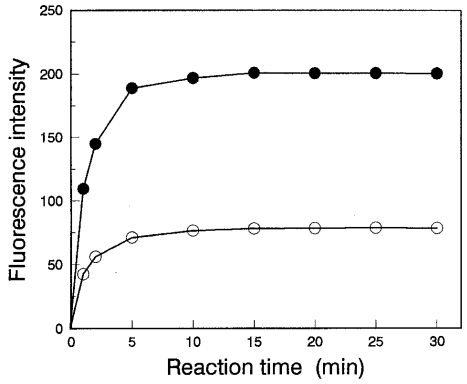

Fig. 2. Time Course of Antigen–Antibody Reaction

●, BTM-1086 (0 μg/ml); ○, BTM-1086 (2 μg/ml).

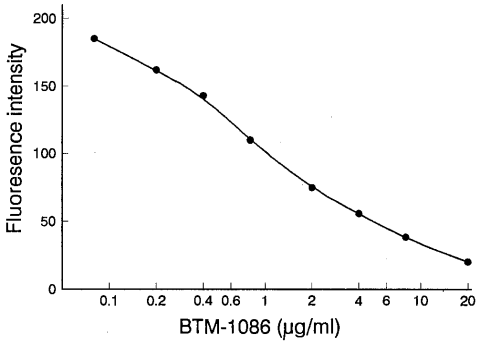

Fig. 3. Standard Curve for BTM-1086

TABLE I. The Influence of Flow Rate of Substrate Solution on the Sensitivity of the Assay System

Flow rate (ml/h)	Fluorescence intensity	
	BTM-1086 (0 μg/ml)	BTM-1086 (2 μg/ml)
3.8	313.6	125.9
7.5	200.6	78.3
15.0	112.9	42.2
30.0	42.3	15.0

TABLE II. Specificity of Antiserum against BTM-1086

Compound	Cross-reactivity (%)
BTM-1086	100.0
BTM-1066	11.5
BTM-1091	0.9
BTM-1092	18.9
BMS-053	0.4
Demethyl-BMS-053	0.1

within 15 min. The antigen–antibody reaction was known to be accelerated by the addition of polyethyleneglycol (0.1—0.05 M).[11] In this experiment, we examined the influence of polyethyleneglycol on the reaction, however, there is no difference between the rate of reactions in the presence and the absence of polyethyleneglycol.

Standard Curve for BTM-1086 The standard curve for BTM-1086 is obtained according to the standard assay as shown in Fig. 3. The measuring range was 0.05—20 μg/ml corresponding to the 0.5—200 ng/tube.

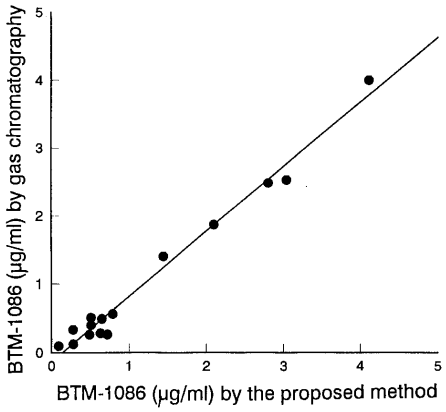

Fig. 4. Correlation between the Results of EIA and GC with Rat Serum Samples

Wister male rats were bled at 0, 0.5, 1, 2, 4, 6, 9 and 24 h after an oral administration of BTM-1086 (30 mg/kg). The serum levels of BTM-1086 were determined by EIA and GC. $Y=0.95X-0.13$, $r=0.991$, $n=15$.

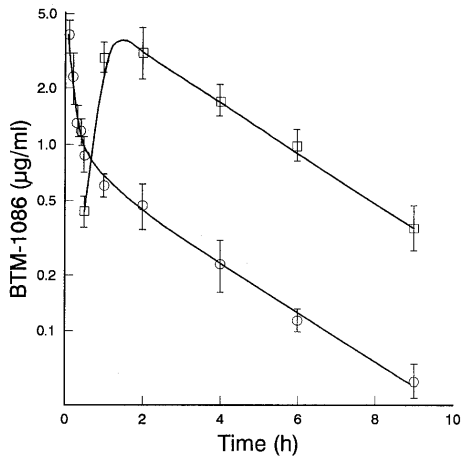

Fig. 5. Serum Levels of BTM-1086 after i.v. or *p.o.* Administration

○, i.v. dosing of 5 mg/kg of BTM-1086; □, *p.o.* dosing of 30 mg/kg of BTM-1086. The values are expressed as mean ± S.D. from three experiments.

The sensitivity of the assay depends on the flow rate of the substrate solution as shown in Table I. The slower flow rate offers more high sensitivity. In this assay system, 7.5 ml/h of flow rate is adopted.

Recovery of BTM-1086 from Sera We assayed the analytical recovery by using a human pool serum supplemented with different concentrations of the standards. Mean recoveries ranged from 98.5 to 101.4% for all the assays.

Specificity The results of the cross reaction study are summarized in Table II. The cross-reaction percentage was calculated at 50% displacement of the BTM-1086–HRP conjugate in the EIA system. Cross reactivity with BTM-1086 metabolites, BMS-053 and desmethyl BMS-053 is below 1% in this assay system. The cross reactivity with BTM-1086 antibody was almost identical with the results in the previous paper.[8]

Accuracy and Precision The inter and intra-assay coefficient of variation (C.V.) of serum samples were 3.95 and 4.07% at a level of 4 μg/ml, respectively.

Correlation between EIA and GC The serum levels of BTM-1086 were determined by the proposed method and gas chromatography. There was a good correlation ($r=0.991$) between two assays as shown in Fig. 4.

Serum Level of BTM-1086 after Oral or Intravenous Administration The serum levels of BTM-1086 in rat are shown in Fig. 5. In the case of a single intravenous injection (5 mg/kg), the pharmacokinetic parameters are almost the same as those in the previous paper.[8] It was found that β-phase in the excretion after *p.o.* administration of BTM-1086 is identical to that in the case of i.v. administration.

Although the sensitivity of the enzyme immunoassay used in this paper is lower than the previous immunoassay,[8] this assay system is more simple and rapid. Serum levels of BTM-1086 determined by EIA correlated well with those of GC. This suggests that the lower sensitivity is not a practical problem in the determination of the serum level of BTM-1086. These results indicated that this enzyme immunoassay of the drug is very convenient for monitoring the serum level of an active drug.

References

1) P. A. Routledge and D. G. Shand, *Clin. Pharmacokinet.*, **4**, 73 (1979).
2) K. Ohashi, A. Ebihara, K. Kondo and M. Usami, *Arzneim-Forsch.*, **34**, 507 (1984).
3) K. Onoyama, H. Hirata, K. Iseki, T. Omae, M. Kobayashi and Y. Kawahara, *Hypertension*, **3**, 456 (1981).
4) P. Jatlow, *Clin. Chem.*, **21**, 1518 (1975).
5) D. R. Jarvie and D. Simpson, *Ann. Clin. Biochem.*, **21**, 92 (1984).
6) J. D. Berg and B. M. Buckley, *Ann. Clin. Biochem.*, **23**, 559 (1986).
7) P. R. Wenham and H. M. Barbour, *Clin. Chem.*, **34**, 2080 (1988).
8) T. Asano, T. Okumura, K. Hirano, T. Adachi and M. Sugiura, *Chem. Pharm. Bull.*, **34**, 4238 (1986).
9) L. M. Jasiewicz, R. D. Schoenberg and C. G. Muelle, *Exp. Cell. Res.*, **100**, 213 (1976).
10) S. C. March, I. Parikh and P. Cuatrecasas, *Anal. Biochem.*, **60**, 149 (1974).
11) C. R. Brian and J. W. Charles, *Anal. Biochem.*, **121**, 257 (1982).

Partial Degradation and Biological Activities of an Antitumor Polysaccharide from Rice Bran

Yoshinori TANIGAMI,[a,1] Shoichi KUSUMOTO,[a] Shigeki NAGAO,[b] Susumu KOKEGUCHI,[c] Keijiro KATO,[c] Shozo KOTANI,[d] and Tetsuo SHIBA*,[a,2]

Department of Chemistry, Faculty of Science, Osaka University,[a] Toyonaka, Osaka 560, Japan, Department of Biochemistry, Shimane Medical University,[b] 89-1 Enya-cho, Izumo, Shimane 693, Japan, Department of Oral Microbiology, Okayama University Dental School,[c] 2-5-1 Shikata-cho, Okayama 700, Japan and Osaka College of Medical Technology,[d] Kita-ku, Osaka 530, Japan. *Received November 19, 1990*

A rice bran polysaccharide designated RON was subjected either to partial hydrolysis with formic acid or to partial degradation by ultrasonic irradiation. A significant change in the molecular size was also observed during simple chromatography of RON on a strongly acidic ion exchange resin, although the apparent molecular weight of RON had been assumed to be more than 1×10^6 daltons (Da). This fact indicates that RON exists as molecular aggregates, presumably mediated by metal cations. Degradation products with average molecular weights above *ca.* 1×10^4 Da which were obtained by any of the three methods still retained the following activities of RON: *in vivo* antitumor activity against Meth-A fibrosarcoma in mice by oral administration, and *in vitro* macrophage stimulatory effects to induce tumoricidal activity and interleukin 1 production. This molecular size was proven to be the minimum requisite for these activities because smaller fragments were scarcely active. The aggregation was characteristic of RON but not essential for its antitumor activity because definite, though slightly reduced, activity was exhibited even by the smaller fragments obtained after the ion exchange resin treatment.

Keywords rice bran; polysaccharide; RON; α(1—6)glucan; molecular size; partial degradation; antitumor activity; interleukin-1 induction; tumoricidal activity; cytotoxic activity

Introduction

A number of antitumor polysaccharides, such as lentinan from *Lentinus edodes*[3] and schizophyllan from *Schizophyllum commune*,[4] have been isolated from various natural sources. In spite of the difference in their origins, most of them have a same basic β-1,3-glucan structure. An antitumor polysaccharide recently isolated from rice bran and termed RON[5] has an α-1,6-glucan structure, which was not known as one of the described antitumor polysaccharides to date. It exhibits remarkable activity in inhibiting the growth of Meth-A fibrosarcoma, not only by intraperitoneal but also by oral administration.[5] We have elucidated by methylation analysis that RON is an α-1,6-glucan with 5% branching at the 3-positions of glucose residues of the backbone.[6-8] Unexpectedly, the primary chemical structure of RON was very similar to that of B512 dextran, which has neither antitumor nor any other particular immunostimulating activities.

We attempted to elucidate the structural characteristics of RON responsible for its antitumor activity. In this paper we describe the partial degradation of RON, chemical characterization of the degradation products, and their *in vivo* antitumor activity, *in vitro* activation of macrophages to induce cytotoxicity against EL4 leukemia cells, and interleukin-1 (IL-1) generation.

Results

Partial Hydrolysis of RON with Formic Acid RON was subjected to partial hydrolysis with 90% formic acid under the conditions given in Table I. The hydrolysates were fractionated by repeated column chromatography on Toyopearl HW-50F, as shown in Fig. 1. Fraction A-1 was obtained from the hydrolysate at 90 °C for 20 min, whereas two fractions with smaller molecular sizes, A-2 and -3, were isolated after elongated heating (30 min). The average molecular weights and the molecular weight distributions of the fractions were estimated by comparing their elution volume on gel permeation chromatography (GPC) with that of the standard polysaccharide Pullulan (Showa Denko P-82).[9,10] The results are given in Table I.

Methylation Analysis of Partial Hydrolysis Products The structures of the three fractions, A-1, -2, and -3, were examined by methylation analysis.[7,11] As shown in Table II, fractions A-1 and A-2 exhibit slightly increased but almost the same ratio of branching compared to the original RON. Fraction A-3, with the smallest molecular size, on the other hand, possesses distinctly fewer branches.

Degradation of RON and Dextran T2000 by Ultrasonic Irradiation Figure 2 shows the elution profiles on the GPC of degradation products of RON and dextran T2000 after ultrasonication at ambient temperature for 5 d, together with the profiles before ultrasonication.[12] The average

TABLE I. Conditions for Partial Hydrolysis and Molecular Weights of Hydrolysis Fractions of RON

Test materials	Conditions of hydrolysis		MW[a]	
	Temp (°C)	Time (min)	Average	Distribution
RON intact	—	—	$>10^6$	—
A-1	95	20	7.0×10^3	2.0×10^3—1.8×10^4
A-2	95	30	3.0×10^3	1.1×10^3—7.0×10^3
A-3	95	30	1.1×10^3	3.0×10^2—3.0×10^3
Dextran T2000	—	—	—	1.0×10^4—2.0×10^6

a) Molecular weights were determined on the basis of elution volumes on GPC (see text).

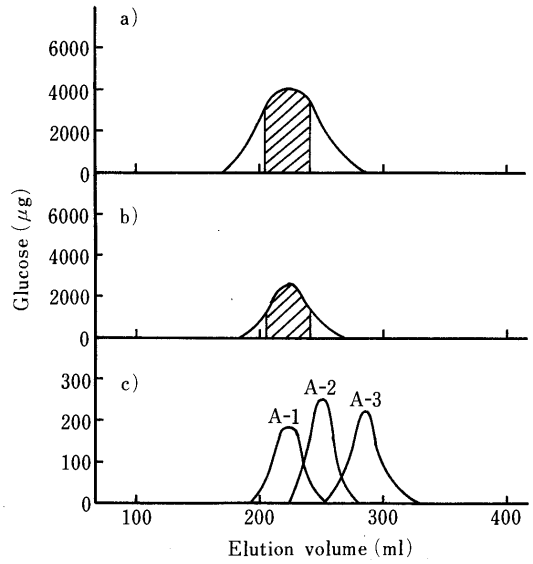

Fig. 1. Elution Profiles on Toyopearl HW-50F of Partial Hydrolysates of RON with 90% Formic Acid

a) Chromatography of the hydrolysate at 90 °C for 20 min. b) Rechromatography of the shaded part of a). c) Elution profiles of the fraction A-1 (shaded part of b), A-2 and A-3 obtained after hydrolysis for 30 min. Chromatographic conditions: column size 28 × 700 mm; eluent, H_2O; flow rate, 90 ml/h; sample size, 200 mg in a) and b) and 10 mg in c).

TABLE II. Methylation Analysis of RON and Its Fractions from Formic Acid Hydrolysis

Test materials	Relative amounts of methyl glucoside		
	2,3,4-Tri-*O*-Me-6-*O*-TMS	2,4-Di-*O*-Me-3,6-di-*O*-TMS	2,3,4,6-Tetra-*O*-Me
RON intact	17.8	1.0	1.1
A-1	15.5	1.0	0.92
A-2	14.4	1.0	0.93
A-3	36	1.0	10

TMS: trimethylsilyl.

molecular weights of the main ultrasonication products from both polysaccharides were estimated to be 1.7×10^4 daltons (Da) from the elution volumes. Fractions S-1 and S-2, corresponding to the two peaks in Fig. 2, were isolated for biological tests. No detectable changes in molecular size were observed by two additional days of ultrasonication of fraction S-2.

High performance liquid chromatographic (HPLC) analysis with an ERC-NH-1171 column proved that the ultrasonicated mixture of RON did not contain oligosaccharides with fewer than seven glucose residues. Furthermore, the endodextranase digest of the ultrasonicated mixture (S-1 + S-2) and that of intact RON gave superimposable HPLC chromatograms (data not shown).

Treatment of RON with Ion-Exchange Resins RON was subjected to dialysis and column chromatography on a cation-exchange resin (Dowex 50). Although the original RON supplied from Sapporo Breweries Ltd. gave a turbid suspension in water in a concentration of 10 mg/ml, the polysaccharide dissolved completely in the same concentration, giving a clear solution after Dowex 50 treatment. The dialyzed and Dowex 50-treated RON was then chromatographed on Toyopearl HW-65F. The polysaccharide was

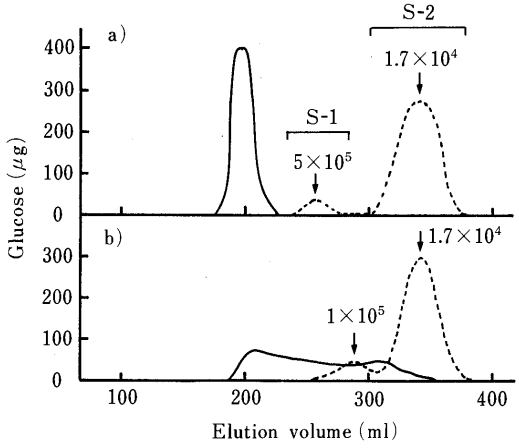

Fig. 2. Elution Profiles of RON (a) and Dextran T2000 (b) by GPC on Toyopearl HW-65F before and after Ultrasonication

Chromatographic conditions: eluent, H_2O; flow rate, 90 ml/h; sample, 10 mg. —, before ultrasonication; ---, after ultrasonication.

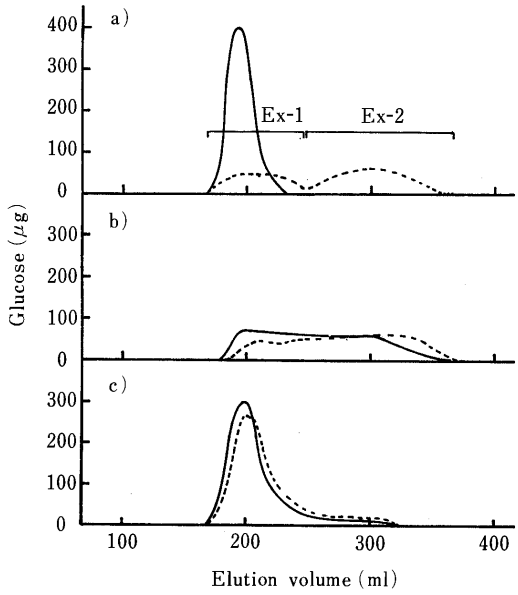

Fig. 3. Elution Profiles of GPC with Toyopearl HW-65F of RON (a), Dextran T2000 (b) and Native Dextran 5885 (c) before and after Dowex-50 Column Chromatography

Chromatographic conditions as in Fig. 2. —, not treated; ---, treated with a column of Dowex 50.

eluted in two peaks (Ex-1 and Ex-2, Fig. 3) with a total recovery of 97%. The molecular size of the latter peak (centered at 6×10^4) was remarkably lower than that of the original RON. When fraction Ex-2 was again treated after separation with the same ion-exchange resin, no change in molecular weight was observed. In contrast, about 50% of fraction Ex-1 was converted to a smaller fraction of the molecular size range of Ex-2 by the same treatment (data not shown). By repeated chromatography on the cation exchange resin, 90% of RON was converted into a smaller fragment corresponding to the fraction Ex-2, and 10% remained in the molecular size range of fraction Ex-1, which remained unchanged on the third treatment with the resin.

Dextran T2000 and native dextran ND-5885 which give a semitransparent solution and turbid suspension, respectively, in 1% concentration in water, were also treated

with a column of Dowex 50, but no significant changes in their molecular weights were observed (Fig. 3).

Determination of Inorganic Cations in RON and Its Degradation Products The amounts of inorganic cations were determined by the conventional atomic adsorption method for RON before and after dialysis and for fractions Ex-1 and Ex-2. Although some of the ions were removed by dialysis, column chromatography on a strongly acidic ion exchange resin was effective for a more complete removal of ions, as summarized in Table III. The amount of ions of other degradation products of RON determined by the same method is also given in Table III.

Antitumor Activity of Orally Administered Degradation Products Different in Molecular Sizes Suppressive activity against the growth of Meth-A fibrosarcoma by oral administration in BALB/C mice was tested for various partial degradation products described in the preceding sections. The results summarized in Table IV reveal the following. Among acid hydrolysis products, fraction A-1 appeared weaker than the original RON but had a definite, suppressive effect against Meth-A, whereas fractions A-2 and A-3, with smaller molecular sizes, lacked the antitumor activity. Fractions S-2 and Ex-2, obtained by ultrasonication and ion exchange chromatography, respectively, showed antitumor activity comparable to that of fraction A-1.

Induction of Tumoricidal Activity of Murine Peritoneal Macrophages RON and its partial degradation products were tested for the induction of cytotoxic activity of proteose peptone-irritated murine peritoneal macrophages on ^{51}Cr-labeled EL4 leukemia cells.[13] As presented in Fig. 4, intact RON exhibits definite activity in inducing a tumoricidal activity comparable to or stronger than that of a reference lipopolysaccharide (LPS) in terms of the extent of EL4 cell

TABLE III. Inorganic Ion Contents of Intact RON and Its Degradation Products

Test materials	Na	K	Mg	Ca	Zn	Fe	Cu (%)
RON intact dialyzed	0.094	0.230	0.015	0.028	0.018	ND	ND
	0.210	0.150	0.005	0.021	0.012	ND	ND
Ex-1	0.059	0.038	0.002	0.018	0.007	ND	ND
Ex-2	0.056	0.002	ND	ND	ND	ND	ND
S-1	0.039	0.004	0.003	0.013	—	—	—
S-2	0.140	0.214	0.061	0.010	—	—	—
A-1	—	—	—	0.008	—	—	—
Dextran T2000	0.043	0.003	ND	ND	ND	ND	ND
Limit of detection	—	—	0.001	0.007	0.002	0.008	0.007

ND: not detected. —: not done.

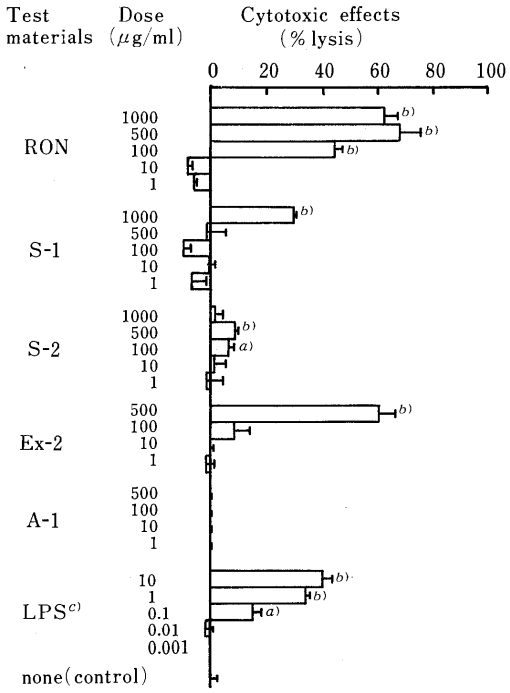

Fig. 4. Induction of Cytotoxic Activity of EL4 Leukemia Cells in Murine Peritoneal Macrophages by RON and RON Degradation Fractions

Statistical significance was evaluated by applying Student's t-test. Significance difference from control, *a*) $p<0.05$, *b*) $p<0.01$. *c*) LPS-W derived from *E. coli* 0111: B4.

TABLE IV. Antitumor Activity of RON and Its Degradation Products Against Meth-A Fibrosarcoma in Mice

Test materials[a]	MW		Tumor weight (g, mean±S.D.) Trial					Inhibition ratio (%)[b] Trial				
	Average	Distribution	1	2	3	4	5[e]	1	2	3	4	5
RON	$>10^6$	—	1.88±0.79	1.72±1.25	1.81±0.50	1.58±0.46	204±56	42.9[c]	60.0[d]	46.0[d]	55.4[d]	49.0[d]
A-1	7.0×10^3	2.0×10^3 -1.8×10^4	2.07±0.68	2.23±1.56		2.29±0.66		37.1	48.1[d]		35.3[d]	
A-2	3.0×10^3	1.1×10^3 -7.0×10^3	3.14±0.90					4.6				
A-3	1.0×10^3	0.3×10^3 -3.0×10^3	3.23±0.49					1.8				
S-1+S-2	—	—				2.01±0.73					43.2[d]	
S-2	1.7×10^4	1.0×10^3 -7.0×10^4					256±97					36.0[d]
Ex-1	9.0×10^5	$>6.0\times10^5$			2.04±0.65	1.69±0.57				39.1[d]	52.3[d]	
Ex-2	6.0×10^4	1.0×10^4 -6.0×10^5			2.61±1.15	2.13±0.70				22.1[c]	39.8[d]	
Dextran T2000	—	1.0×10^4 -2×10^6		4.39±1.99					−0.9			
None (control)			3.29±1.27	4.30±1.86	3.35±1.02	3.54±0.88	400±79	—	—	—	—	—

a) Dose: 30 mg/kg. *b*) (1 − tumor weight in test group/tumor weight in the reference control group) × 100 (%). Statistical significance was evaluated by applying Student's t-test. Significant difference from the respective control: *c*) $p<0.01$, *d*) $p<0.005$. *e*) Eight mice per group were used and tumor area (not tumor weight) was measured at day 22 in this trial.

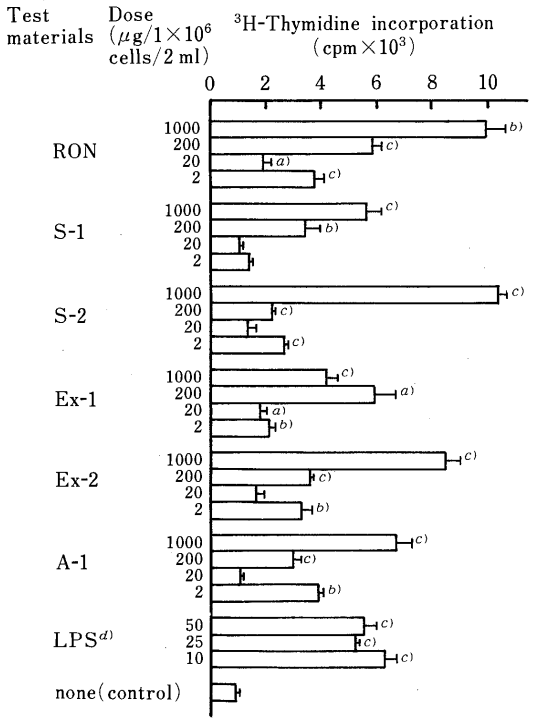

Fig. 5. IL-1 Inducing Activity of RON and RON Fractions

Statistical significance was evaluated by applying Student's *t*-test. Significant difference from control, *a*) $p<0.05$, *b*) $p<0.01$, *c*) $p<0.001$. *d*) *E. coli* 0111: B4 LPS.

TABLE V. *Limulus* Activity of RON and Its Degradation Products

Test materials	Equivalent of reference LPS (ng/mg)[a]
RON intact	145.5
A-1	0.02
S-1	6.7
S-2	2.3
Ex-2	66.5
Dextran T2000	0.001

a) Possible endotoxin contamination was assessed by Endospecy Test and expressed in terms of equivalency to a reference *E. coli* 0111: B4 LPS.

lysis, though the effective dose of RON was much higher than that of LPS. Fraction Ex-2 with an average molecular weight of 6×10^4 showed activity roughly comparable to RON itself, but fractions A-1 and S-2, with smaller molecular size than Ex-2, lacked this activity even at 500—1000 μg dose.

Induction of IL-1 of Murine Peritoneal Macrophages The stimulatory effects of RON and its degradation products on murine Tripticase peptone-irritated peritoneal macrophages were tested in terms of IL-1 induction by the method of Vacheron.[14] RON and all tested fractions showed activity roughly comparable to that of a reference LPS, although much higher doses than reference LPS were required (Fig. 5).

Check for Possible Endotoxin Contamination of RON and Its Degradation Products Contamination of the test preparations with extraneous endotoxin was assessed by use of a recently developed, colorimetric *Limulus* test, Endospecy test (ES-test).[15] Among the tested preparations, the original RON showed the highest *Limulus* activity (0.01% equivalent to a reference *Escherichia coli* endotoxin). About half of this activity was detected in fraction Ex-2. The *Limulus* activity of the other degradation product was hardly detectable (Table V).

Discussion

An antitumor active polysaccharide RON was partially degraded by three different methods, namely, partial hydrolysis with formic acid, ultrasonication, and treatment with a cation exchange resin. The degradation products were separated by GPC on columns of Toyopearl HW into fractions with limited ranges of molecular size, and were tested for biological activities.

In the case of partial hydrolysis with 90% formic acid, a mixture of polysaccharides with a wide range of molecular weights was obtained owing to the nonspecific nature of the reaction. By repeated column chromatography on HW-50F, three fractions, A-1, -2, and -3, were obtained, their average molecular weights being 7.0, 3.0 and 1.1×10^3, respectively (Table I). Methylation analysis showed that both fractions A-1 and A-2 have branch ratios similar to original RON (Table II). The component saccharides in the smallest fraction, A-3 contained practically no branch.

Degradation by ultrasonication afforded a main product with an average molecular weight of 1.7×10^4. The isolated main fraction did not show any further degradation on further ultrasonic irradiation, whereas another peak involving larger molecules demonstrated a decrease in size on repeated ultrasonication. Cleavage of a polysaccharide into a certain definite range of molecular size by ultrasonication has already been described.[16,17] As judged from the fact that no small oligosaccharides were formed by this degradation, the polysaccharide chains were cleaved not at random but at certain limited positions to give products with the observed molecular weight range. Furthermore, neither isomaltoheptaose (1.15×10^3 Da) nor fraction A-1 (7.0×10^3 Da) were degraded by ultrasonication. This fact indicates that a polysaccharide smaller than *ca.* 1×10^4 Da is not susceptible to ultrasound. HPLC analysis after endodextranase digestion indicated no detectable differences in the frequencies of α (1—3)-branches before and after ultrasonication.

Although the isolation procedure of RON included dialysis, ultrafiltration, and chromatography on diethylaminoetheyl (DEAE)-cellulose,[5] the RON preparation used in the present study still contained a considerable amount of inorganic ions (Table III). We therefore attempted to examine whether these ions have any effects on the antitumor activity of the RON polysaccharide. A simple dialysis procedure removed some of the ions in RON, but complete removal could not be effected. The dialyzed RON in water was then chromatographed successively on columns of strong anion- and cation-exchange resins. During the chromatography on a column of Dowex 50, a remarkable change was observed in the solubility of the polysaccharide. Analysis of the molecular weight distribution by a Toyopearl HW-65F column revealed that RON which had an apparent molecular weight of more than 10^6 Da was converted by Dowex 50 treatment into two broad peaks centered at the average molecular weights of 9×10^5 (fraction Ex-1) and 6.0×10^4 (Ex-2), respectively. The inorganic cation content in the smaller fraction, Ex-2, were very low, most ions being below the limits of detection (Table III).

Because no cleavage of glucosidic bonds could take place

during simple column chromatography on Dowex 50 at room temperature, we could assume that about 90% of RON composed of smaller polysaccharides with a molecular weight range of 1.0×10^4—6.0×10^5 Da and the remaining 10% of higher molecular sizes over 6.0×10^5 Da. In the native state, these polysaccharides of different sizes seem to form aggregates larger than 10^6 Da, possibly through interaction with cations like Ca^{2+} which were removed with Dowex 50. Several attempts to detect anionic counterparts such as uronic acids in RON were not successful, presumably because of the very low content, if any, of such acidic components. However, the addition of Ca^{2+} to a solution of Ex-2 had no effect on the solubility of the saccharide, and no regeneration of aggregates of higher molecular size was observed.

The antitumor activity against Meth-A fibrosarcoma by oral administration in mice, a characteristic activity of RON, was tested for various partial degradation products obtained in this study (Table IV). Whereas fraction A-2 and A-3 were inactive, all fractions larger than A-1 (with an average molecular weight of 7.0×10^3 Da) showed distinct Meth-A suppressive activity, though more or less weaker than RON itself. The minimum molecular size required for tumor suppression by RON was hence estimated to be around 10^4 Da. This value is similar to the reported minimum active molecular weight of a partial hydrolysate of lentinan,[18] in spite of the differences in primary chemical structure and administration routes of both polysaccharides.

Complete suppression of Meth-A tumor development was rarely accomplished by any of the test compounds, including the original RON, although in trial 2 (Table IV) two out of ten mice given RON were tomor-free on day 30 (data not shown).

RON and its partial degradation products stimulated murine macrophages to induce IL-1 production and tumoricidal activity, suggesting the participation of an immunological system for the *in vivo* antitumor activity of RON and degradation products of appropriate molecular size (Figs. 4 and 5). The intact RON and fractions Ex-2 and S-1 were active, provided that sufficiently high doses are used (Fig. 4). The minimum effective doses of RON and the fractions to make macrophages tumoricidal were again 100 times as high as that required for LPS. However, the present test method for the induction of macrophage-mediated cytotoxicity seems to be more sensitive to the reduction of the molecular size of the polysaccharides than the *in vivo* antitumor effects and *in vitro* enhancement of IL-1 production by macrophages. Fractions A-1 and S-2, which were positive in the latter two activity tests, exhibited no or negligible ability in inducing macrophage-mediated tumoricidal activity.

Another important point in the study on immunostimulating compounds is to check possible contamination with LPS which is a ubiquitous and extremely potent natural immunostimulant. For this purpose, RON and its degradation products were subjected to a colorimetric determination of LPS by use of Endospecy test.[15] This test was established specifically for LPS with a purified enzyme system of *Limulus* amoebocyte lysate, which is unaffected by β(1—3)glucans. In fact, *Limulus* activity corresponding to 146 ng of a reference *E. coli* LPS was detected in 1 mg of the intial RON preparation. However, this amount of LPS could never bring about the biological activities described above for RON. For example, 146 ng of LPS which possibly exists in 1 mg of RON would have only a slightly positive macrophage-mediated tumoricidal effect which is much weaker than that actually observed for that amount of RON (Fig. 4). The LPS content detected in all degradation products was less than in RON, possibly because the contaminated LPS was decomposed during the degradation procedures or removed through the subsequent fractionation steps. There is no correlation between the antitumor or related biological activities and the Endospecy activity among RON and its degradation products. In conclusion, the activities observed for RON or its degradation products should be attributed to the molecules themselves and not to contaminating LPS. It could be expected that even further reduction of the contaminating LPS in a preparation of RON is possible by careful improvement of the isolation procedure.

We demonstrated in this work that RON, which behaves as macromolecules over 10^6 Da on GPC, is composed of polysaccharides with different molecular weights. About 90% of the component polysaccharides have average molecular weights of 6×10^4. This type of aggregation is unique to RON, and was never observed in dextran which lacks antitumor activity. The apparent large molecular size due to the aggregation of intact RON seems to be favorable for its antitumor activity by oral administration. Nevertheless, degraded fractions proved to retain the activity if they were larger than 10^4 Da. Particularly, the definite antitumor and tumoricidal activities observed for fraction Ex-2, which was obtained by dissociation of the aggregate, indicate that the aggregation is not a prerequisite for the activities. We could speculate, however, that the structural characteristic which causes or enables such aggregation could be reflected in the unique biological function of RON. Further study on the structure of RON in comparison with dextran is being continued in order to elucidate the difference which is resposible for the different biological activities of these polysaccharides. The results will be presented elsewhere.[7]

Experimental

Materials, Apparatus, and General Considerations RON was isolated from rice bran by the method reported previously[5] and was generously supplied by Research and Development Laboratories, Sapporo Breweries Ltd. Dextran T2000, a partially hydrolyzed product of *L. mesenteroides* B512 dextran, was purchased from Pharmacia AB. *L. mesenteroides* N4 native dextran, ND-5885, was supplied by Meito Sangyo Co., Ltd. Isomaltoheptaose and endodextranase from *Chaetomium gracile* were purchased from Seikagaku Kogyo Co. Ltd.

HPLC was carried out on a Shimadzu LC-6A liquid chromatography apparatus equipped with an ERC-NH-1171 column (6×200 mm), Erma Optical Works, Japan. The peaks were monitored with a Showdex SE-11 refractometer, Showa Denko. Gas liquid chromatography (GLC) was carried out with a Shimadzu GC4CM-PF gas chromatography apparatus equipped with a PEG-HT capillary column (0.25 mm × 20 m).

Throughout the present study, meticulous precaution was taken to avoid contamination of all materials and utensils by extraneous endotoxins.

Partial Acid Hydrolysis of RON with Formic Acid RON (500 mg) was heated in 90% formic acid (100 ml) at 95 °C for period given in Table I. After evaporation of formic acid, the residue was heated in water (100 ml) at 100 °C for 6 h and evaporated *in vauco*. After lyophilization, complete removal of formyl residues in the product was assured by the lack of a band at 1710 cm^{-1} in its infrared (IR) spectrum.[18]

GPC of the Partial Hydrolysates of RON on Toyopearl Gels a) Preparative Scale Fractionation: Each formic acid hydrolysate (200 mg)

was dissolved in water (5 ml), applied to a column of Toyopearl HW-50F (28 × 700 mm) and eluted with water (90 ml/h). Each 10 ml eluate was pooled and its glucose content determined by the phenol–sulfuric acid method.[19] The appropriate fractions were combined and lyophilized.

b) Determination of Molecular Weight Distribution of Separated Fractions: An aliquot (10 mg) of each fraction obtained by preparative GPC was dissolved in water (1 ml) and chromatographed again on a column of HW-50F (28 × 700 mm) as described above in a). The molecular weight distribution was determined by comparison of the elution volume with those of a standard kit to pullulan.[9,10]

Degradation of RON by Ultrasonic Irradiation A suspension of RON (400 mg) in water (40 ml) in a 50 ml round-bottomed flask was dipped in an ultrasonic clearning bath (Bransonic 220 Branson) and ultrasonicated at an ambient temperature for 5 d, then lyophilized. The resultant colorless powder (400 mg) was fractionated with a column of Toyopeal HW-65F (28 mm × 700 mm), as described above for the formic acid hydrolysates, to give fraction S-1 (32 mg) and S-2 (364 mg), respectively.

Endodextranase Degradation of RON and Its Ultrasonication Product A sample (5 mg) was dissolved in 1.0 ml of 0.05 M acetate buffer, pH 5.1, and treated with 5 units[20] of *Chaetomium* endodextranase at 25 °C for 20 h. The progress of hydrolysis was followed by measuring the reducing sugar by the method of Somogyi–Nelson.[21] The enzyme digests were analyzed by HPLC on a column of ERC-NH-1171 eluted with water–acetonitrile (45 : 55) at a contstant flow rate of 1 ml/min.

Dialysis and Ion-Exchange Resin Treatment of RON A suspension of RON (500 mg) in water (50 ml) was dialyzed against water (2 l) for 72 h with two changes of water, then lyophilized (495 mg). Dialyzed RON (165 mg) was applied to a column of Dowex 50 × 8 (H^+ form, 20 ml) and eluted with water (100 ml). The eluate was lyophilized and chromatographed on a column of Toyopearl HW-65F (28 × 700 mm) to give fractions Ex-1 (48 mg) and Ex-2 (112 mg). The amount of cations in the fractions was determined by atomic absorption spectrometry.

Determination of Inorganic Cations About 30 mg of RON and it partial degradation products were weighed exactly and made into 25 ml solutions with 0.05 M hydrochloric acid. The solutions were subjected to atomic adsorption measurement on a model SAS 727 apparatus, Seiko Electronic Industry Co., Ltd. The content (wt %) of cations in each test sample was calculated conventionally.

***In Vivo* Antitumor Activity** Assays for the antitumor activity of orally administered test materials against Meth-A fibrosarcoma in BALB/c mice (7 weeks old, female, CRJ) was carried out at the Research and Development Laboratories, Sapporo Breweries Ltd., by the method described previously.[8]

***In Vitro* Induction of Macrophage-Mediated Cytotoxicity against EL4 Leukemia Cells** The activity was tested according to the procedure described elsewhere.[13] Briefly, exudated peritoneal macrophages (2×10^5 cells) of C3H/He Slc mice were incubated with or without a test specimen at 37 °C for 20 h. ^{51}Cr-labeled EL4 leukemia cells (1×10^4 cells) were added to the tested macrophages and the cell mixture was incubated for 20 h. After centrifugation for 10 min at 350 × *g*, aliquots of the cell-free supernatant fluid were counted for radioactivity. Cytotoxicity was expressed as the percentage of tumor cell lysis according to the following formula:

$$\% \text{ lysis} = \frac{\text{experimental release (cpm)} - \text{spontaneous release (cpm)}}{\text{maximal release (cpm)} - \text{spontaneous release (cpm)}} \times 100$$

Spontaneous release was considered to be the amount of radioactivity released from target EL4 cells cultured alone, and a maximal release was the amount obtained with target cells disrupted by freezing and thawing three times.

IL-1 Inducing Activity The activity was determined according to the method of Vacheron *et al.*[14] In brief, test materials were added to exudated peritoneal macrophages (1.0×10^6 cells/2 ml) of C3H/HeJ mice (8- to 10-week-old males). After incubation at 37 °C for 24 h, the culture supernatant was collected and filtered. Thymocytes from C3H/HeJ mice (1.5×10^6 cells in 0.1 ml RPMI-1640 supplemented with 10% fetal calf serum) were distributed in tissue culture plates. Equal volumes of the above macrophage supernatants and a submitogenic concentration (final 1 μg/ml) of phytohemagglutinin A were added to each cell culture. Cells in culture were pulsed with 0.5 μCi of ^{3}H-thymidine during the last 6 h of culture. Incorporation of ^{3}H-thymidine was measured by the conventional scintillation method.

Endospecy Test (ES-Test) The amount of LPS in RON and in its degradation products was determined by the colorimetric Limulus test, ES-test (Seikagaku Kogyo) as described in detail by Obayashi *et al.*[15] An LPS specimen from *E. coli* 0111: B4 (LPS-W; Difco) was used as a reference standard.

Acknowledgement The authors are gratefully indebted to Dr. N. Watanabe and Mr. S. Takeo of Research and Development Laboratories, Sapporo Breweries Ltd., for the generous gift of RON and for the *in vivo* antitumor tests. The authors also wish to express their gratitude to Dr. S. Tanaka, Tokyo Research Institute, Seikagaku Kogyo Co., Ltd., for carrying out the Endospecy test, and to Drs. H. Takada, M. Tsujimoto, T. Ogawa, and I. Takahashi, of the Osaka University Dental School, for generous help in the early stage of the present study. Thanks are further extended to Dr. H. Yagihara, Research Center, Daicel Chemical Industries, Ltd., for the kind measurement of atomic absorption spectroscopy. This work was supported in part by a Grant-in-Aid for scientific research (No. 62540406) from the Ministry of Education, Science and Culture of Japan.

References and Notes

1) Present address: *Yamamura Glass Co., Ltd., 2–1–18, Naruohama, Nishinomiya 663, Japan.*
2) Present address: *Peptide Institute, Protein Research Foundation, 4–1–2, Ina, Minoh, Osaka 562, Japan.*
3) G. Chihara, J. Hamuro, Y. Y. Maeda, Y. Arai, and F. Fukuoka, *Cancer Research*, **30**, 2776 (1970).
4) N. Komatsu, S. Okubo, S. Kikumoto, K. Kimura, G. Saito, and S. Sakai, *Gann*, **60**, 137 (1969).
5) E. Ito, S. Takeo, H. Kado, H. Yamamoto, N. Watanabe, M. Kamimura, E. Soma, K. Uchida, Y. Mori, and T. Morinaga, *Yakugaku Zasshi*, **105**, 188 (1985).
6) Parts of this work were presented at *a*) International Symposium on Immunological Adjuvants and Modulators of Nonspecific Resistance to Microbial Infections, Abstract of Papers, Columbia, Maryland, 1986, p. 14; *b*) The 9th Japanese Carbohydrate Symposium, Abstract of Papers, Tokyo, July 1986, p. 17.
7) T. Tanigami, S. Kusumoto, and T. Shiba, manuscript in preparation.
8) The result of our methylation analysis (ref. 6) was reconfirmed recently: S. Takeo, H. Kado, H. Yamamoto, M. Kamimura, N. Watanabe, K. Uchida, and Y. Mori, *Chem. Pharm Bull.*, **36**, 3609 (1988).
9) K. Kawahara, K. Ohta, H. Miyamoto, and S. Nakamura, *Carbohydr. Polym.*, **4**, 335 (1984).
10) T. Kato, T. Okamoto, T. Tokuya, and A. Takahashi, *Biopolymers*, **21**, 1623 (1982).
11) S. Hakomori, *J. Biochem.* (Tokyo), **55**, 205 (1964).
12) The time required to reach the ultimate stage of degradation depended on the amount of the polysaccharide used. For example, 10 mg of RON was completely degraded to fragments of 1.7×10^4 Da within 3 h. This might be due to the insufficient power of the ultrasound source employed.
13) S. K. Akagawa and T. Tokunage, *J. Exp. Med.*, **162**, 1444 (1985).
14) F. Vacheron, M. Guenounou, and C. Nauciel, *Infect. Immun.*, **42**, 1049 (1983).
15) T. Obayashi, H. Tamaru, S. Tanaka, M. Ohki, S. Takahashi, M. Arai, M. Masuda, and T. Kawai, *Clin. Chim. Acta*, **149**, 55 (1985).
16) T. Yanaki, W. Ito, K. Tabata, T. Kojima T. Norisuye, N. Takano, and H. Fujita, *Biophys. Chem.*, **17**, 337 (1983).
17) S. C. Szu, G. Zon, R. Schneerson, and J. B. Robbins, *Carbohydr. Res.*, **152**, 7 (1969).
18) T. Sasaki, N. Takasuka, G. Chihara, and Y. Y. Maeda, *Gann*, **67**, 191 (1976).
19) M. Dubois, K. A. Gilles, J. K. Hamilton, P. A, Rebers, and F. Smith, *Anal. Chem.*, **28**, 350 (1956).
20) One unit is defined as the amount of enzyme activity which produces reducing sugar equivalent to 1 μmol of glucose per minute.
21) M. Somogyi, *J. Biol. Chem.*, **195**, 19 (1952).

Production of Aliphatic Aldehydes on Peroxidation of Various Types of Lipids

Kyoji YOSHINO,*[,1)] Mitsuaki SANO, Masahiro FUJITA, and Isao TOMITA

Laboratory of Health Science, School of Pharmaceutical Sciences, University of Shizuoka, 395 Yada, Shizuoka 422, Japan. *Received December 3, 1990*

***In vitro* peroxidation by air, or xanthine–xanthine oxidase (xanthine–XOD) was performed to estimate the production of aliphatic aldehydes from free polyunsaturated fatty acids (PUFA), triglycerides, phospholipids and rat liver microsomes and mitochondria. The aldehyde contents in peroxidized lipids were determined by liquid chromatography and fluorescence detection. In both peroxidation, pentanal, (*E*)-4-hydroxy-2-nonenal (4-HN), and hexanal were produced from ω-6 PUFA rich lipids and propanal was mainly produced from ω-3 PUFA rich lipids. The aldehyde production was markedly enhanced by increasing the degree of fatty acid unsaturation. The ratios of 4-HN to hexanal production in xanthine–XOD peroxidation of the ω-6 PUFA rich lipids, and rat liver microsomes and mitochondria were much higher than those in air peroxidation. The ratios (4-HN/hexanal) obtained in microsomes and mitochondria by xanthine–XOD were similar to those in rat liver observed in vitamin E deficient studies. The determination of these aldehydes may be useful to estimate the kinds of fatty acids peroxidized and investigate *in vivo* lipid peroxidation mechanism.**

Keywords lipid peroxidation; aliphatic aldehyde; polyunsaturated fatty acid; rat liver microsome; mitochondria; 4-hydroxy nonenal; hexanal

Several investigators have reported that some aldehydes were produced *in vitro* or *in vivo* lipid peroxidation. Esterbauer[2)] demonstrated that hexanal and (*E*)-4-hydroxy-2-nonenal (4-HN) were mainly produced in the peroxidation of linoleic acid or arachidonic acid from the study of air oxidation in acetate buffer. The production of hexanal and 4-HN were also observed in rat liver microsomes by adenosine diphosphate (ADP)/Fe^{2}[,3)] or reduced nicotinamide adenine dinucleotide phosphate (NADPH)/Fe[4)] dependent *in vitro* lipid peroxidation and in mouse liver by the oral administration of bromobenzene.[5)] However, these reports did not include quantitative analysis of the aldehydes. We have shown recently that high levels of propanal, pentanal, hexanal, and 4-HN were observed in plasma and liver from vitamin E deficient rats compared with vitamin E supplemented rats by the high performance liquid chromatography (HPLC)-fluorometric method.[6)] The ratios of 4-HN to hexanal production in plasma and liver were 69% and 88%, respectively. While, in the report of Esterbauer,[3)] the ratios in air oxidation of free polyunsaturated fatty acids (PUFA) were lower than 20%. Most PUFA in biological tissues are in esterified forms,[7)] and the PUFA in triglyceride (TG) and phosphatidylcholine (PC) were peroxidized *in vivo* by the superoxide anion radical, lipoxygenase (EC 1.13.11.12), *etc.*[8-11)] The process of aldehyde production *in vivo* would be different from the *in vitro* production by air.

In this study, we compared the production of aliphatic aldehydes from various types of lipids and biological samples by atmospheric oxygen and xanthine–xanthine oxidase (EC 1.2.3.2) (xanthine–XOD) lipid peroxidation.

Experimental

Chemicals Linoleic acid and linolenic acid were purchased from Tokyo Kasei Kogyo Co., Ltd. Arachidonic acid was from Serdary Research Laboratories, Inc. and docosahexaenoic acid was from Nu-Chek-Prep, Inc. Safflower oil was obtained from Yuro Yakuhin Co. and linseed oil was from Wako Pure Chemical Industries, Ltd. L-α-Phosphatidylcholine (type VII-E, from frozen egg yolk) and XOD (grade IV, from milk) were purchased from Sigma Chemical Co. Other chemicals used were of reagent grade quality.

Preparation of Phosphatidylcholine Liposomes Vitelline PC liposomes were prepared by the method of Ursini *et al.*[12)]

Preparation of Rat Liver Microsomes and Mitochondria A male Wistar rat of 3 weeks old obtained from Clea Japan Inc. was sacrificed and the liver was removed after perfusion with ice-cold physiological saline. The liver was homogenized in 0.25 M sucrose solution including 5 mM Tris–HCl buffer (pH 7.2) and the microsomal and mitochondrial fraction were prepared by the method of Sato.[13)]

Peroxidation of Lipids and Rat Liver Fractions by Air Seven micro mol of each PUFA (linoleic acid, linolenic acid, arachidonic acid, and docosahexaenoic acid) or TG (safflower oil and linseed oil; *ca.* 98.5% of the oil was composed of TG) was put in the flasks and spread into the films by a rotary evaporator. These flasks were rotated at 37 °C for 24 h and for 48 h in the case of PUFA and TG peroxidation, respectively. After peroxidation, the lipids were diluted with ethanol–acetone (3 : 2) or distilled water. The suspensions of rat liver microsomes and mitochondria were added into 0.1 M phosphate buffer (pH 7.4) and incubated at 37 °C for 2 h. These samples were used for the determination of thiobarbituric acid reactive substances (TBARS) and aliphatic aldehydes.

Peroxidation of Lipids and Rat Liver Fractions by Xanthine–XOD PUFA and TG were diluted with ethanol–acetone (3 : 2). PC liposomes were suspended in 0.1 M Tris–HCl buffer (pH 7.5) and rat liver microsomes and mitochondria were in 0.01 M Tris–0.15 M KCl buffer (pH 7.4). These samples were used as the substrate for the peroxidation. Each substrate was added into 0.01 M Tris–0.15 M KCl buffer (pH 7.4) containing 10 μM ethylenediaminetetraacetic acid (EDTA), 0.15 M ADP, 0.01 M ferric chloride, 1 mM xanthine, and 0.032 units of XOD. Each substrate, 3.5 μM PUFA, 3.5 μM TG, 1 mg/ml PC liposomes, 4.8 mg protein/ml microsomes, or 6.4 mg protein/ml mitochondria, was added. The mixture was incubated at 25 °C for 60 min. TBARS and aliphatic aldehydes in the reaction mixture were assayed as follows.

Assay of TBARS and Aliphatic Aldehydes TBARS was determined by the method of Masugi *et al.*[14)] and was expressed as malondialdehyde equivalents. The determination of aliphatic aldehydes was performed by the method reported in a previous paper.[15)] The results shown in this study were obtained from the mean of the three experiments. The protein content was determined by the method of Lowry *et al.*[16)] with bovine serum albumin as the standard.

Results

Production of Aliphatic Aldehydes in Peroxidation of Free Polyunsaturated Fatty Acids Authentic free PUFA, *i.e.* linoleic acid, linolenic acid, arachidonic acid, and docosahexaenoic acid were peroxidized by two different peroxidations. Table I shows the production of aliphatic aldehydes from these lipids. The production of pentanal, 4-HN and hexanal were observed in the peroxidation of ω-6 PUFA such as linoleic acid and arachidonic acid by both lipid peroxidations. In air peroxidation, the ratios of

TABLE I. Formation of Aliphatic Aldehydes and TBARS in the Peroxidation of Free Polyunsaturated Fatty Acids

Aldehydes	Linoleic acid	Linolenic acid	Arachidonic acid	Docosahexaenoic acid
Non treatment (control)				
Propanal	Trace	0.20	Trace	1.80
Butanal	0.07	0.38	0.16	0.38
Pentanal	0.11	0.17	1.50	0.18
4-HN	0.10	Trace	0.17	0.10
Hexanal	0.27	0.15	1.18	Trace
Nonanal	Trace	Trace	Trace	Trace
Decanal	Trace	Trace	0.04	0.05
TBARS	0.04	0.11	0.07	1.85
Peroxidation by air				
Propanal	Trace	2.55	Trace	237.60
Butanal	1.84	3.70	12.94	9.35
Pentanal	3.13	1.06	124.60	9.68
4-HN	1.90	Trace	137.00	7.20
Hexanal	6.06	3.15	260.70	3.58
Nonanal	Trace	0.11	13.13	1.31
Decanal	Trace	Trace	4.55	0.43
TBARS	0.32	1.76	18.91	33.92
Peroxidation by xanthine–XOD				
Propanal	1.59	55.11	19.69	207.46
Butanal	2.71	9.66	30.09	20.63
Pentanal	86.72	10.34	150.60	16.85
4-HN	50.75	4.81	146.22	3.59
Hexanal	59.19	1.52	183.40	7.21
Nonanal	Trace	0.01	0.08	0.66
Decanal	0.01	Trace	0.01	0.67
TBARS	0.30	1.65	14.38	22.28

Aliphatic aldehydes, μmol/mmol free fatty acid. TBARS, μmol as malondialdehyde/mmol free fatty acid.

4-HN to hexanal production in the peroxidation of linoleic acid and arachidonic acid were 31% and 53%, respectively. While in xanthine–XOD peroxidation, the ratios were 86% and 80%, respectively. A large amount of propanal, and a small amount of butanal and pentanal were produced from ω-3 PUFA by xanthine–XOD, though the formation of propanal from linolenic acid by air was not significant. The amount of aldehydes and TBARS were associated with the number of double bonds in ω-6 and ω-3 PUFA.

Production of Aliphatic Aldehydes in Peroxidation of Esterified Fatty Acids Most fatty acids in biological tissues exist in TG or phospholipids as esterified form. Safflower oil and linseed oil, 98.5% of the oils were composed of TG, were peroxidized by air or xanthine–XOD. And PC liposomes were peroxidized by xanthine–XOD. Tables II and III show the production of aldehydes from the oils and PC liposomes, respectively. The species of aldehydes produced by air or xanthine–XOD peroxidation would be decided by the species of PUFA in the oil. Pentanal, 4-HN, and hexanal were produced by the peroxidation of safflower oil in which *ca.* 70% of the constituent PUFA is linoleic acid.[17] The ratios of 4-HN to hexanal production in air and xanthine–XOD peroxidation were 11% and 20%, respectively. While propanal was produced in the peroxidation of linseed oil in which *ca.* 60% of constituent PUFA is linolenic acid.[18] The 4-HN to hexanal ratios in xanthine–XOD peroxidation was higher than that in air peroxidation. In the peroxidation of PC liposomes in which

TABLE II. Formation of Aliphatic Aldehydes and TBARS in the Peroxidation of Safflower Oil and Linseed Oil

Aldehydes	Safflower oil	Linseed oil
Non treatment (control)		
Propanal	Trace	2.11
Butanal	Trace	Trace
Pentanal	1.18	0.01
4-HN	Trace	Trace
Hexanal	2.03	Trace
Nonanal	Trace	Trace
Decanal	Trace	Trace
TBARS	0.05	1.09
Peroxidation by air		
Propanal	Trace	7.95
Butanal	0.30	0.03
Pentanal	6.00	0.02
4-HN	1.60	Trace
Hexanal	14.91	0.20
Nonanal	0.10	Trace
Decanal	Trace	Trace
TBARS	0.43	10.87
Peroxidation by xanthine–XOD		
Propanal	0.51	66.80
Butanal	0.99	2.98
Pentanal	7.09	2.73
4-HN	13.35	0.71
Hexanal	68.11	4.32
Nonanal	0.01	0.02
Decanal	Trace	Trace
TBARS	3.89	19.16

Aliphatic aldehydes, μmol/g oil. TBARS, μmol as malondialdehyde/g oil.

TABLE III. Formation of Aliphatic Aldehydes and TBARS in the Peroxidation of Phosphatidylcholine Liposomes

Aldehydes	Non treatment (control)	Peroxidation by xanthine–XOD
Propanal	0.08	1.23
Butanal	0.02	1.69
Pentanal	0.61	5.62
4-HN	0.04	3.71
Hexanal	0.75	9.45
Nonanal	Trace	0.73
Decanal	Trace	0.01
TBARS	0.56	3.42

Aliphatic aldehydes, μmol/g phosphatidylcholine. TBARS, μmol as malondialdehyde/g phosphatidylcholine.

ca. 15% of constituent PUFA is linoleic acid and 5% of constituent PUFA is arachidonic acid, the productions of pentanal, 4-HN, and hexanal were observed, and the ratio of 4-HN to hexanal in the xanthine–XOD peroxidation was 39%.

Production of Aliphatic Aldehydes in Lipid Peroxidation of Rat Liver Microsomes and Mitochondria Rat liver microsomes and mitochondria containing a large amount of PUFA as phospholipid and TG forms[19] were frequently used for *in vitro* lipid peroxidation study. The productions of propanal, pentanal, 4-HN, and hexanal were observed in the peroxidation of these biological samples by xanthine–XOD as shown in Table IV. The ratios of 4-HN to hexanal production were 75% and 61% in microsomes

TABLE IV. Formation of Aliphatic Aldehydes and TBARS in the Peroxidation of Rat Liver Microsomes and Mitochondria

Aldehydes	Microsomes	Mitochondria
Non treatment (control)		
Propanal	0.86	1.10
Butanal	0.15	0.07
Pentanal	0.16	0.10
4-HN	0.16	0.06
Hexanal	0.20	0.12
Nonanal	0.04	0.05
Decanal	0.05	0.02
TBARS	0.86	0.85
Peroxidation by air		
Propanal	1.46	1.44
Butanal	0.26	0.13
Pentanal	0.20	0.17
4-HN	0.18	0.08
Hexanal	0.56	0.21
Nonanal	0.09	0.10
Decanal	0.06	0.03
TBARS	1.12	1.21
Peroxidation by xanthine–XOD		
Propanal	2.42	2.19
Butanal	1.09	0.05
Pentanal	2.95	1.83
4-HN	2.56	1.54
Hexanal	3.43	2.53
Nonanal	0.10	0.01
Decanal	0.01	Trace
TBARS	7.29	5.22

Aliphatic aldehydes, nmol/mg protein. TBARS, nmol as malondialdehyde/mg protein.

and mitochondria, respectively. The production of these aldehydes from microsomes and mitochondria by air were markedly low compared with production by xanthine–XOD. TBARS and aldehyde levels in the microsomes were slightly higher than those in the mitochondrial fraction.

Discussion

Some studies have been reported on the formation of aliphatic aldehydes from the breakdown of monohydroperoxides, hydroperoxy cyclicperoxides, or cyclic dioxides.[20,21]

Frankel *et al.*[20] have reported that propanal was formed by the thermal decomposition of hydroperoxy cyclicperoxide of methyl linolenate. We showed that a large amount of propanal was produced in the peroxidation of linolenic acid and docosahexaenoic acid, and linseed oil containing ω-3 fatty acids by air or xanthine–XOD.

Esterbauer[2] has shown that hexanal and 4-HN were produced from ω-6 free PUFA in the study of air oxidation of free PUFA. Our study in the peroxidation of various lipids by air and xanthine–XOD confirmed his findings. A marked difference of the ratio of 4-HN to hexanal production between air and xanthine–XOD peroxidation was observed. The ratios in the peroxidation of linoleic acid and arachidonic acid by air were 31% and 53%, respectively, while the ratios in the peroxidation by xanthine–XOD were 86% and 80%, respectively. The ratio observed in xanthine–XOD peroxidation was higher than that in air peroxidation. The high ratios of 4-HN to hexanal production were also observed in the peroxidation of rat liver microsomes and mitochondria by xanthine–XOD. Since 4-HN has several harmful effects on biological membranes compared with the other aliphatic aldehydes,[2,4] an increase of the ratio in the peroxidation by xanthine–XOD would be inconvenient in biological tissues. Our previous study with a rat fed vitamin E deficient diet showed increased levels of 4-HN and hexanal in plasma and liver and high ratios of 4-HN to hexanal production in their samples (69% and 88%, respectively).[6] The ratios in the peroxidation of these rat liver fractions by other peroxidation systems such as NADPH/Fe or lipoxygenase were lower (19—49%) than those by xanthine–XOD (data not shown). It is known that the superoxide anion radical is produced from the reaction of xanthine–XOD.[22] Lipid peroxidation observed in vitamin E deficient rats may be caused partly by the superoxide anion radical. Significant productions of 4-HN and hexanal were observed in the peroxidation of safflower oil and PC liposomes by xanthine–XOD, however, the ratios of 4-HN to hexanal were low (19.6%, 39.0%, respectively) compared with free PUFA or rat liver samples. Tappel[23] and Thayer[8] suggested that PUFA peroxidized in phospholipids were hydrolyzed first by phospholipase A_2 (EC 3.1.1.4) bound to the membrane and were treated with glutathione peroxidase (EC 1.11.1.9). We found the 4-HN to hexanal ratio in the peroxidation of free PUFA, mitochondria, and microsomes. Therefore, it was thought that lipid peroxides in microsomes and mitochondria were hydrolyzed to free PUFA peroxides by phospholipase A_2 before they were decomposed directly and then these aldehydes were produced. Rat liver microsomes and mitochondria contained a few ω-3 fatty acids, however, the ratios of propanal to hexanal production were very high. In our previous paper, the levels of propanal in plasma liver from vitamin E deficient rats were slightly higher than those of hexanal. These results might be explained by the evidence that ω-3 fatty acid could be peroxidized easily as compared with ω-6 fatty acids,[24] or that the specific activities of metabolic enzymes could be different between these aldehydes.[25,26]

References and Notes

1) Present address: *Department of Chemistry and Biochemistry, Numazu College of Technology, 3600 Ooka, Numazu-shi, Shizuoka 410, Japan.*
2) H. Esterbauer, "Aldehydic Products of Lipid Peroxidation, in Free Radicals, Lipid Peroxidation and Cancer," ed. by D. C. H. McBrien and T. F. Slater, Academic Press, New York, 1981, pp. 101—128.
3) H. Esterbauer, K. H. Cheeseman, M. U. Dianzani, G. Poli, and T. F. Slater, *Biochem. J.*, **208**, 129 (1982).
4) A. Benedetti, M. Comporti, and H. Esterbauer, *Biochim. Biophys. Acta*, **620**, 281 (1980).
5) A. Benedetti, A. Pompella, R. Fulceri, A. Romani, and M. Comporti, *Biochim. Biophys. Acta*, **876**, 658 (1986).
6) K. Yoshino, M. Sano, M. Fujita, and I. Tomita, *Chem. Pharm. Bull.*, **38**, 2212 (1990).
7) S. Cho and M. Sugano, *Nougeikagaku*, **49**, 27 (1975).
8) W. S. Thayer, *Biochem. Pharmacol.*, **33**, 2259 (1984).
9) H. Hughes, C. V. Smith, C. Horning, and J. R. Mitchell, *Anal. Biochem.*, **130**, 431 (1983).
10) J. Terao, I. Asano, and S. Matsushita, *Arch. Biochem. Biophys.*, **235**, 326 (1984).
11) J. F. G. Vliegenthart and G. A. Veldink, "Free Radicals in Biology," Vol. V, ed by W. A. Pryor, Academic Press, New York, 1982, pp. 29—64.
12) F. Ursini, M. Maiorino, M. Valente, L. Ferri, and C. Gregolin, *Biochim. Biophys. Acta*, **710**, 197 (1982).
13) R. Sato, "Saibou Bunkakuhou," Iwanami Shoten, Tokyo, 1967, pp.

219—229.
14) F. Masugi and T. Nakamura, *Vitamins*, **51**, 21 (1977).
15) K. Yoshino, T. Matsuura, M. Sano, S. Saito, and I. Tomita, *Chem. Pharm. Bull.*, **34**, 1694 (1986).
16) O. H. Lowry, N. Rosebrough, A. L. Farr, and R. J. Randall, *J. Biol. Chem.*, **191**, 265 (1951).
17) S. Watanabe and T. Nagai, *Yukagaku*, **28**, 433 (1979).
18) S. Watanabe and T. Nagai, *Yukagaku*, **27**, 557 (1978).
19) R. P. Cook, "Distribution of Sterols in Organisms and in Tissue, in Cholesterol," Academic Press, New York, 1958, p. 145.
20) E. N. Frankel, W. E. Neff, E. Selke, and D. Weisleder, *Lipids*, **17**, 11 (1982).
21) P. Winkler, W. Lindner, H. Esterbauer, E. Schauenstein, R. J. Schaur, and G. A. Khoschsorur, *Biochim. Biophys. Acta*, **796**, 232 (1984).
22) M. J. Thomas, K. S. Mehr, and W. A. Pryor, *Biochem. Biophys. Res. Commun.*, **83**, 927 (1978).
23) A. L. Tappel, "Free Radicals in Biology," Vol. IV, ed. by W. A. Pryor, Academic Press, New York, 1980, pp. 1—47.
24) E. E. Dumelin and A. L. Tappel, *Lipids*, **12**, 894 (1977).
25) H. Nakayasu, K. Mihara, and R. Sato, *Biochem. Biophys. Res. Commun.*, **83**, 697 (1978).
26) J. W. Kim and B. P. Yu, *Mech. Ageing Dev.*, **50**, 277 (1989).

Metabolic Fates of L-Tryptophan in *Saccharomyces uvarum* (*Saccharomyces carlsbergensis*)

Mariko SHIN, Tetsuro SHINGUU, Keiji SANO and Chisae UMEZAWA*

School of Pharmacy, Kobe-Gakuin University, Nishi-ku, Kobe 651–21, Japan. *Received December 14, 1990*

The metabolism of L-tryptophan by *Saccharomyces uvarum* (*carlsbergensis*) was investigated by simultaneous measuring of fluxes through kynureninase, through transaminases and into protein using L-[methylene-^{14}C]- and L-[side chain-2,3-^{3}H]tryptophan. In yeast cultivated in synthetic medium (S medium), the flux into protein was predominant, closely followed by the flux leading to 2-^{3}H liberation. The proportion of L-tryptophan metabolized *via* the latter flux increased over 10-fold (75% of total tryptophan metabolized) as the concentration of L-tryptophan was raised from 5×10^{-5} to 5×10^{-4} M. L-Tryptophan metabolized *via* the kynureninase flux was less than 5% of total tryptophan metabolized. In yeast extract-polypepton-glucose medium (YPG medium), more tryptophan was incorporated into protein than in the S medium. Contribution of the kynureninase flux remained very low. Tryptophan metabolism *via* each flux changed depending on the growth phase. 2-^{3}H liberation was shown to be primarily due to tryptophol synthesis by high performance liquid chromatography (HPLC) and nuclear magnetic resonance (NMR), indole-3-acetic acid and kynurenic acid also contributing to 2-^{3}H liberation but to a much lesser extent. 2-^{3}H liberation increased dose-dependently at tryptophan concentration higher than 10^{-5} M, while the kynureninase flux reached its plateau at 10^{-5} M. Formation of tryptophol and indole-3-acetic acid *via* indole-3-pyruvic acid and indole-3-acetaldehyde with indole aldehyde as a by-product was confirmed using exogenous tryptophan metabolites with indole rings.

Keywords *Saccharomyces uvarum* (*carlsbergensis*); L-tryptophan; metabolic flux; charcoal non-adsorbed metabolite; kynureninase; transaminase; tryptophol

Tryptophan is known to be metabolized by a variety of pathways and to supply physiologically important substances. In *Saccharomyces*, tryptophan was postulated to be catabolized *via* indole-3-pyruvic acid (IPA) to tryptophol (TOH),[1-4] which was later determined to be the main degradation product of tryptophan.[5,6] The degradation to anthranilic acid (AA)[7] and 3-hydroxy anthranilic acid[8,9] was postulated, and in aerobically grown *Saccharomyces cerevisiae* biosynthesis of nicotinic acid from tryptophan was also reported.[10] However, no studies have ever been done on the contribution rate of each metabolic pathway to total tryptophan metabolism in *Saccharomyces*.

Smith *et al.* examined tryptophan metabolism in rat hepatocytes by measuring charcoal-non-adsorptive radioisotope release from several radioisomers of tryptophan.[11] Kiyohara *et al.* reconfirmed the usefulness of this method in studying tryptophan metabolism in rat liver cells.[12] In the present study, we applied the method for estimating metabolic fluxes of tryptophan in yeast with several modifications and were able to elucidate the flux *via* each metabolic pathway simultaneously under several different conditions.

Experimental

Organism, Media, and Growth Conditions *Saccharomyces uvarum* (*Saccharomyces carlsbergensis*)ATCC 9080 was used throughout this work. In most studies, cultures were grown in S medium (glucose, 20 g; KH_2PO_4, 3 g; $(NH_4)_2SO_4$, 3 g; $MgSO_4\cdot7H_2O$, 0.25 g; $CaCl_2\cdot2H_2O$, 0.25 g; inositol, 10 mg, D-biotin, 2.2 μg; Ca-pantothenate, 1 mg; thiamine·HCl, 1 mg; pyridoxine·HCl, 1 mg per liter, pH 4.5).[13] YPG medium (yeast extract, 3.5 g; polypepton, 3.5 g; KH_2PO_4, 2.0 g; $(NH_4)_2SO_4$, 1.0 g; $MgSO_4$, 1.0 g; glucose, 10 g per liter, pH 6.2) was also used on some occasions. The yeast was cultivated aerobically in 1 l Meyer flasks containing 250 ml of medium at 30 °C at 110 oscillations min^{-1}. Cells in mid-logarithmic growth phase were washed and resuspended with fresh medium to a final density of 2.5 mg dry weight (wt.) cells/ml.

Chemicals Tryptophan, kynurenine (KN) sulphate, kynurenic acid (KA), xanthurenic acid (XA), *p*-phenylethylamine and charcoal Norit A were obtained from Nacalai Tesque Inc. Indole-3-acetaldehyde was purchased from Sigma, indole aldehyde (IAld) from Fluka AG Chem, indole-3-acetic acid (IAA) from Wako Pure Chemicals and TOH from Tokyo Kasei Co., Ltd. Scintillation cocktail ACS II and Soluene-350 were obtained from Amersham International and Packard Instruments, respectively. L-[Methylene-^{14}C]tryptophan (specific radioactivity 59 Ci/mol) and L-[side chain 2,3-^{3}H]tryptophan (specific radioactivity 62 Ci/mmol) were obtained from Amersham International and Commissariat à l'Énergie Atomique, respectively. Each radiolabelled tryptophan was further purified by high performance liquid chromatography (HPLC).

Measurement of Liberated $^{14}CO_2$ and Charcoal Non-adsorbed Metabolites from Radioisomers of Tryptophan The method of Smith *et al.*[11] was used with modifications as follows: Portions (0.25 ml) of cell suspension (2.5 mg dry wt. ml^{-1}) were bubbled with O_2 in a test tube (1.6 × 10.4 cm). The tubes were capped with rubber stoppers with suspended center wells. Incubations were started by the injection of 50 μl of radiolabelled tryptophan solution through the rubber stopper by a syringe, and carried out under an atmosphere of O_2 at 30 °C, at 110 oscillations min^{-1}. Incubations were terminated by the injection of 0.1 ml of 2.2 M-$HClO_4$. *p*-Phenylethylamine–methanol (1 : 1, 0.2 ml) was injected into the center well, which contained a piece of folded filter paper. Both additions were made through a septum in the stopper. All test tubes were then shaken at 75 oscillations min^{-1} at room temperature for a further 30 min, to ensure complete absorption of released CO_2. The filter paper, with 500 μl of methanol washing, was transferred to a vial containing 10 ml of ACS II for counting radioactivity.

Portions of the supernatant after centrifuging the $HClO_4$-treated reaction mixture were analyzed for charcoal non-adsorbed metabolites. Two hundred μl of cell-extract was treated with 60 μl of charcoal suspension (50 mg Norit A in 1 ml water). After thorough mixing and 30 min of standing, the charcoal was removed by centrifugation (13000 × *g*, 3 min) and charcoal non-adsorbed radioactivity in 180 μl of the supernatant was counted in ACS II. Residual tryptophan in the acidic supernatant was assayed by the method of Denckla and Dewey.[14]

Assay Method of Incorporation of Tryptophan into Protein A modification of the filter disc method of Mans and Novelli was employed.[15] Twenty or 40 μl of the $HClO_4$-treated samples incubated with either L-[side chain 2,3-^{3}H]- or L-[methylene-^{14}C]tryptophan was filtered through glass fiber filters (Advantec Toyo, GC50, i.d. 24 mm), and the residue was washed with 5 ml of 0.5 M $HClO_4$ followed by the same amount of ethanol. The washed filters were transferred to scintillation vials containing 0.5 ml of Soluene, 0.2 ml of 1 M-HCl and 10 ml of ACS II to count radioactivity.

Identification and Determination of Tryptophan Metabolites The yeast was cultivated aerobically in S medium with 5×10^{-4} M non-labelled tryptophan for 3 h. The major metabolite was extracted with acidic ethyl acetate from the broth. The concentrated extract was dissolved in methanol and subjected to HPLC [column, Finepak SIL C_{18-5}, 4.6 mm × 250 mm; mobile phase, 10^{-2} M phosphate buffer (pH 4.0)–methanol–acetonitrile

(9:1:1); absorbance, 280 nm]. The main metabolite corresponding to authentic TOH was analyzed by proton nuclear magnetic resonance (^{1}H-NMR) (400 MHz, Brucker) and also subjected to thin-layer chromatography (TLC) [Kiesel gel 60F_{254}, Merck, solvent: $CHCl_3$–CH_3COOH (95:5), benzene–ethanol (80:20)]. A portion of the culture broth was neutralized with 1 M-NaOH and subjected to HPLC to analyze other metabolites. IAA was analyzed as TOH. For the determination of KN, KA and XA, about 8 ml of the neutralized broth extract was applied to the columns of Dowex 50w × 8 (H^+, 200—400 mesh, 7 × 50 mm)[16] or Dowex 1 × 8 (formate, 200—400 mesh, 7 × 50 mm),[17] respectively, prior to HPLC [column, Finepak SIL C_{18-5}; mobile phase, 10^{-2} M phosphate buffer (pH 4.0)–10% methanol; absorbance, 340 nm]. KN was confirmed by the complete disappearance of the peak following pretreatment with kynureninase. Eluted peaks corresponding to each metabolite were pooled and analyzed by TLC with several solvent systems [solvent used for TOH identification; upper phase of *n*-butanol–CH_3COOH–water (4:1:5); water]. TOH and IAA developed a purple color with Ehrlich reagent, while KN and KA were visible under ultraviolet lamp (365 nm).

Results and Discussion

Chart 1 outlines the possible steps at which radiolabelled moieties may be released from L-[methylene-^{14}C]tryptophan or L-[side chain-2,3-^{3}H]tryptophan.

^{14}C from L-[methylene-^{14}C]tryptophan can be released only *via* the kynureninase pathway, and then L-[^{14}C]-alanine formed may be oxidized to $^{14}CO_2$. Therefore, a flux of tryptophan through kynureninase was estimated by the sum of the radioactivity of $^{14}CO_2$ and ^{14}C-labelled alanine. A preliminary experiment showed that L-[methylene-^{14}C]-tryptophan was completely (98.9 ± 0.26%) adsorbed by charcoal, while L-[1-^{14}C]alanine was not adsorbed (1.25 ± 0.15%). Tryptophan metabolized *via* the kynureninase flux was calculated from the equation:

$$[(^{14}CO_2 \text{ dpm}) + (^{14}\text{C non charcoal-adsorbed dpm})] \div (\text{specific radioactivity of } ^{14}\text{C-tryptophan})$$

On the other hand, radioisotope liberation from L-[side chain 2,3-^{3}H]tryptophan may occur at several stages of tryptophan metabolism by the following reactions: (1) L-[2,3-^{3}H]Alanine formation by the action of kynureninase or 3-hydroxy kynureninase; (2) 2-^{3}H liberation by the action of transaminases on tryptophan, KN or 3-hydroxy-kynurenine (OHKN). Therefore, total radioisotope release from L-[side chain-2,3-^{3}H]tryptophan may represent the sum of tryptophan metabolized *via* the kynureninase flux, and that metabolized *via* KN- or OHKN-transaminase (EC 2.6.1.7) and tryptophan transaminase (EC 2.6.1.27). As only one ^{3}H out of 3 is liberated, the transaminase flux (2-^{3}H liberation) was calculated from the equation:

$$[(^3\text{H non charcoal-adsorbed dpm}) - (\text{alanine formed nmol})$$

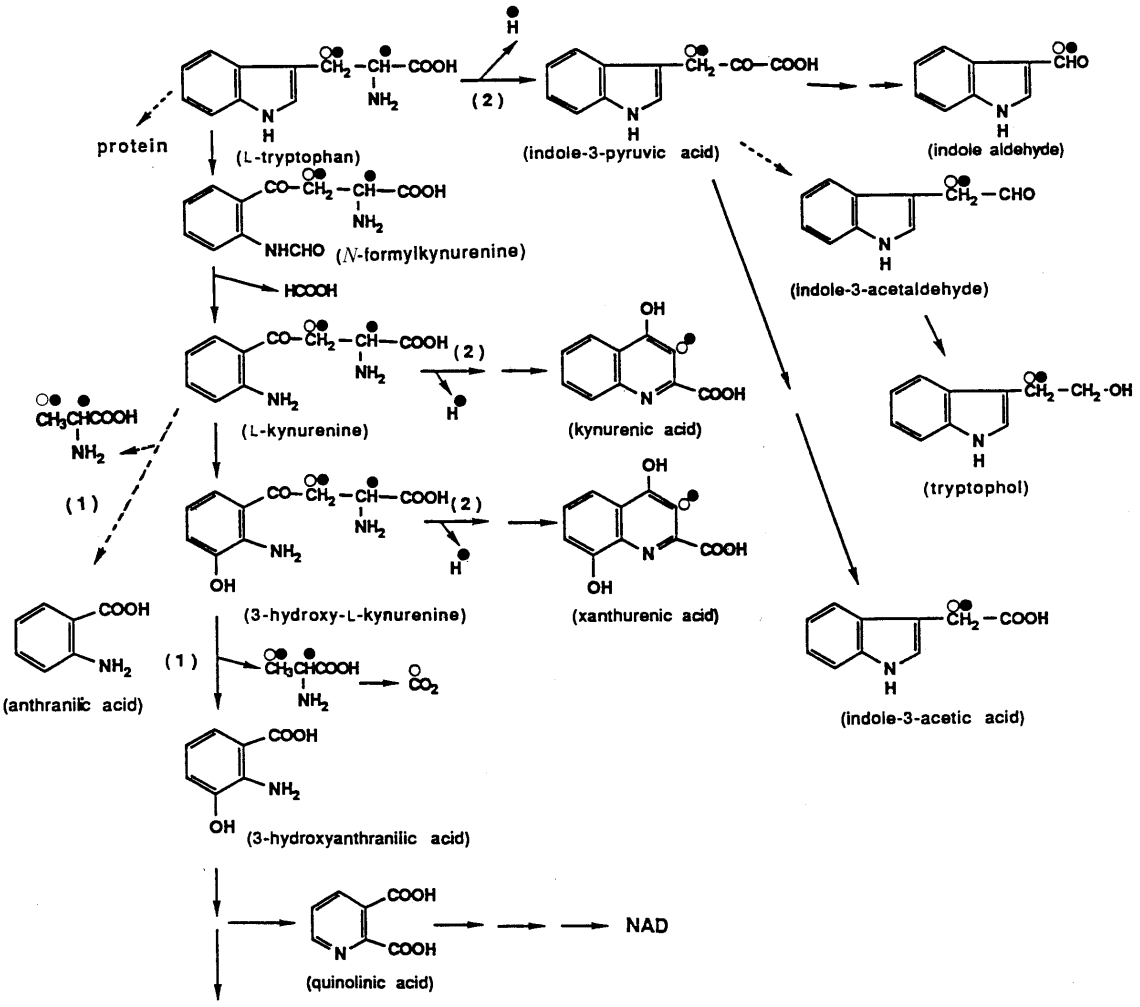

Chart 1. Metabolic Fate of Radioisotope from Specifically Radiolabelled L-Tryptophan

Outline of L-tryptophan expected in the yeast is shown. Radioisotope nomenclature: ○, L-[methylene-^{14}C]tryptophan; ●, L-[side chain-2,3-^{3}H]tryptophan. The metabolic fates: (1), alanine liberation (kynureninase flux); (2), 2-H liberation (transaminase flux).

× (specific radioactivity of L-[2,3-^{3}H]tryptophan)]

÷[(specific radioactivity of L-[2,3-^{3}H]tryptophan)/3]

A possibility that the metabolic flux of tryptophan to protein is overestimated by the simultaneous counting of the incorporation of ^{14}C-alanine formed from L-[methylene-^{14}C]tryptophan by kynureninase was checked. Pulse labelled protein was hydrolyzed with alkali and the hydrolysate was subjected to paper chromatography. The chromatograms (data not shown) showed that more than 90% of radioactivity found in the protein fraction was retained in tryptophan, which indicates that any L-[^{14}C]alanine secondarily formed from L-[methylene-^{14}C]-tryptophan was hardly incorporated into protein. This is probably due to the fact that the intracellular alanine pool is far bigger than that of tryptophan.[18]

Metabolism of 5×10^{-5} or 5×10^{-4} M tryptophan by yeast cultivated in S medium is shown in Fig. 1. In 5×10^{-5} M tryptophan (A), the flux into protein was predominant (40—50%) closely followed by the flux into 2-^{3}H liberation (40%). During 3 h-incubation, tryptophan incorporated into the acid-insoluble fraction and metabolized *via* the 2-^{3}H liberating reactions increased significantly. The kynureninase flux (alanine liberation) was very small (2—4%) throughout the entire incubation period. When the initial concentration of tryptophan was raised to 5×10^{-4} M (B), the flux leading to 2-^{3}H liberation increased 10 times (75%), the flux into the acid insoluble fraction and the flux through kynureninase also increased but to lesser extent.

In YPG medium, 30—40% of added tryptophan (5×10^{-4} M) was incorporated into the acid-insoluble fraction, the figure being much higher than that obtained in S medium. This is because in YPG medium, other amino acids exist in abundance and tryptophan may be a rate limiting factor for protein synthesis. The 2-H liberation flux increased with time, while the kynureninase flux remained small (2.5±0.9% of total tryptophan metabolized) during 3 h-incubation.

Metabolic fluxes of tryptophan in different growth phases were investigated by periodic collection of cultured broth in YPG medium. As shown in Fig. 2, the amount of tryptophan incorporated into protein was parallel to the cell growth, and at the stationary phase the incorporation ceased. On the other hand, the flux *via* alanine liberation was increased in the logarithmic phase, then reduced at the

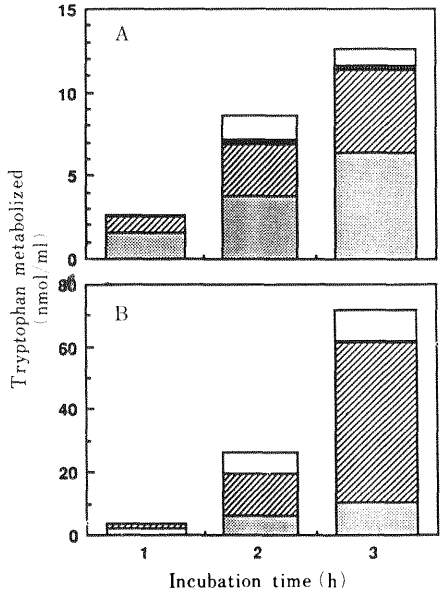

Fig. 1. Time Course of the Main Fluxes of L-Tryptophan Metabolism

Yeasts were cultivated in S medium with 5×10^{-5} M (A) or 5×10^{-4} M (B) tryptophan in a test tube containing 300 μl of broth. ⊠, acid insoluble fraction; ▨, 2-H liberation; ■, alanine liberation; □, unidentified.

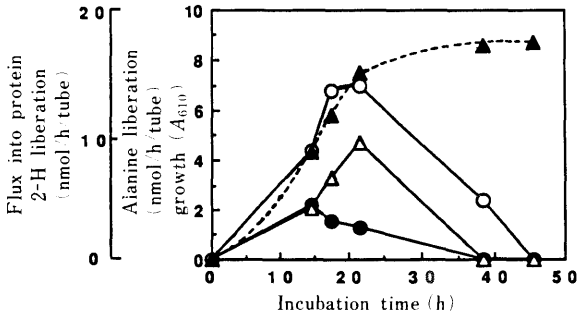

Fig. 2. Tryptophan Metabolism *via* Each Flux Throughout the Growth Phase

Yeasts cultivated in YPG medium were reincubated with radiolabelled tryptophan in a test tube containing 300 μl medium (150 nmol tryptophan added) for 1 h. ---▲---, growth; —●—, alanine liberation; —○—, 2-H liberation; —△—, flux into protein.

TABLE I. Comparison of the Amount of Tryptophan Metabolized *via* Side Chain 2-H Liberation with the Amounts of Metabolites Formed Following 2-H Liberation

Metabolites	Added tryptophan (nmol in test tube)			
	5×10^{-5} M (15 nmol)		5×10^{-4} M (150 nmol)	
	nmol	%	nmol	%
Metabolized tryptophan	12.7±0.76	100	75.2±7.76	100
Side chain 2-H liberation	6.09±0.90	47.9	52.5±4.82	69.9
KA	0.25±0.05	2.1	0.97±0.16	1.3
TOH	4.70±1.20	36.9	54.9±10.1	73.1
IAA	0.89±0.28	7.0	1.14±0.06	1.5

Yeast was cultivated in S medium at 30 °C for 3 h. 2-H liberation was determined by the flux assay using L-[methylene-^{14}C]- and L-[side chain-2,3-^{3}H]tryptophan. Metabolites were analyzed by HPLC directly or after ethyl acetate extraction. Data are means±S.D. for three experiments.

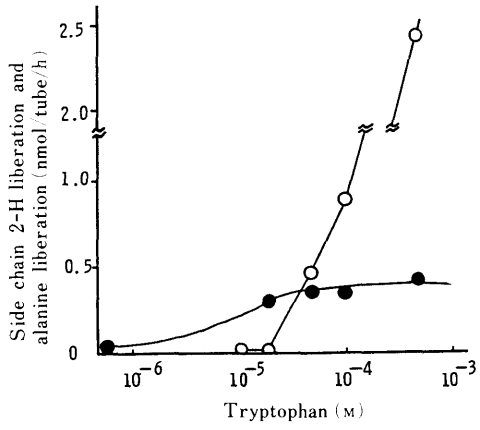

Fig. 3. Dose Response of Side Chain 2-H Liberation and Kynureninase Flux to Tryptophan Concentration in Reaction Medium

Yeasts were cultivated in S medium with various concentrations of tryptophan at 30 °C for 1 h in a test tube containing 300 μl of broth. —○—, 2-H liberation (transaminase flux), —●—; alanine liberation (kynureninase flux).

TABLE II. The Metabolism of IPA, IAAld, TOH and IAA

Substrate	Final conc. ($\times 10^{-6}$ M)	Presence of cells	Metabolites ($\times 10^{-6}$ M)		
			TOH	IAA	IAld
IPA	5	−	n.d.	n.d.	3.2
	100	−	n.d.	n.d.	14.6
	500	−	n.d.	n.d.	79.7
	5	+	n.d.	1.0	1.3
	100	+	n.d.	8.2	16.0
	500	+	n.d.	17.3	25.6
IAAld	500	−	n.d.	1.1	0.7
	10	+	1.9	n.d.	n.d.
	100	+	36.6	n.d.	n.d.
	500	+	218	n.d.	n.d.
TOH	100	−	102	n.d.	n.d.
	100	+	102	n.d.	n.d.
IAA	100	−	n.d.	108	n.d.
	100	+	n.d.	47	n.d.

Yeast was incubated with each substrate in 30 ml flasks containing 6 ml of S medium at 30 °C for 3 h. Metabolites were extracted with acidic ethyl acetate and analyzed by HPLC. n.d; not detected.

late logarithmic phase. Liberation of 2-^{3}H was maximally activated in the late logarithmic phase.

The main metabolite formed *via* the 2-H liberation reaction, which had an identical retention time as that of TOH, was further investigated by ^{1}H-NMR and identified as TOH. Chemical shifts (δ, $CDCl_3$) were as follows: 1.56 (1H?, br s, OH; overlapped to HDO signal), 3.90—3.93 (2H, t, $J=6.3$ Hz, $-CH_2-OH$), 3.03—3.06 (2H, t, $J=6.3$ Hz, $Ar-CH_2-$), 7.09—7.64 (5H, aromatic protons), 8.05 (1H, br s, NH).

The kynureninase flux is the pathway leading to the synthesis of nicotinamide adenine dinucleotide (NAD), an important cofactor for oxidoreductases, and the main metabolite of 2-H liberation reaction is TOH known as an autoregulatory substance in *Candida albicans*.[19] Differences in the activities of the two fluxes during cell growth may be due to the biological significance of the metabolite of each flux.

In the experiment with 5×10^{-5} M tryptophan, 47.9% of metabolized tryptophan went through the 2-^{3}H liberation reaction (Table I) and the sum of KA, TOH and IAA was close to this figure. With 5×10^{-4} M tryptophan, metabolism *via* the 2-^{3}H liberation reaction increased drastically and the percentage of TOH to total metabolites was also increased.

Dose response of the alanine liberation and the 2-^{3}H liberation is shown in Fig. 3. 2-^{3}H liberation from tryptophan occurred dose-dependently at 10^{-5} M and over. The kynureninase flux also increased but reached a plateau at about 10^{-5} M tryptophan. TOH was produced in detectable amounts at higher than 4×10^{-5} M tryptophan and increased dose-dependently (data not shown). On incubation with 5×10^{-3} M tryptophan for 3 h, 360 nmol/ml of TOH was synthesized, most of which distributed extracellularly. Under the same condition, 0.9 nmol/ml of KA was formed. The data indicate that tryptophan metabolism *via* the alanine liberation flux is strictly regulated, while that *via* 2-H liberation reaction was not saturated even with 10^{-3} M tryptophan.

A qualitative study was made to determine the capacity of the yeast to metabolize TOH, IAA, IAAld[20] and IPA (Table II). IPA was converted into IAld spontaneously or to IAA in the presence of cells. TOH, however, could not be detected even when IPA concentration was raised to 5×10^{-4} M. On the other hand, IAAld was readily converted into TOH without forming IAA. No metabolites were detected from either TOH or IAA. However, IAA was reduced to half in 3 h incubation with cells, which indicates that IAA may be metabolized further to another metabolite[21] not yet identified in the yeast. Consequently, tryptophan is mainly metabolized to TOH and a small amount of IAA was produced *via* IPA and IAAld with IAld as by-product. Evaluations of both metabolic fluxes of tryptophan and metabolite assay, showed that the kynureninase flux was much smaller than other fluxes under several conditions in this study. However, as the total amount of tryptophan metabolized *via* the fluxes (incorporation into protein, alanine liberation and 2-^{3}H liberation) was less than the amount of tryptophan consumed from the medium, metabolic intermediates before alanine liberation (KN or OHKN) were measured. KN formed was 2.3×10^{-7} or 1.03×10^{-6} M, respectively, with 5×10^{-5} or 5×10^{-4} M tryptophan for 3 h, 20—30% of which was distributed intracellularly. The quantity of OHKN formed was reported to be much less than that of KN.[22] Taking this into consideration, the tryptophan–NAD flux seems very small. The flux has a significant role in yeast,[10] so that it must be under the regulation of certain factors. This possibility is now under investigation.

References

1) F. Hagemann, *Arch. Mikrobiol.*, **49**, 150 (1964).
2) F. Hagemann, *Naturwissenschaften*, **22**, 626 (1965).
3) F. Lingens, W. Goebel and H. Uesseler, *Eur. J. Biochem.*, **1**, 363 (1967).
4) H. D. Heilmann and F. Lingens, *Hoppe-Seyler's Z. Physiol. Chem.*, **349**, 231 (1968).
5) P. Kradolfer and R. Hütter, *Experientia*, **36**, 1456 (1980).
6) P. Kradolfer, P. Niederberger and R. Hütter, *Arch. Microbiol.*, **133**, 242 (1982).
7) F. Schindler and H. Zähner, *Arch. Microbiol.*, **79**, 187 (1971).
8) A. S. Shetty and F. H. Gaertner, *J. Bacteriol.*, **113**, 1127 (1973).
9) F. H. Gaertner, *Acta Vitaminol. Enzymol.*, **29**, 332 (1975).
10) F. Ahmad and A. G. Moat, *J. Biol. Chem.*, **241**, 775 (1966).
11) S. A. Smith, F. P. Carr and C. I. Pogson, *Biochem. J.*, **192**, 673 (1980).
12) Y. Kiyohara, K. Shirasawa, M. Shin, K. Sano and C. Umezawa, *Int. J. Vitam. Nutr. Res.*, **59**, 88 (1989).
13) A. H. Rose and W. J. Nickerson, *J. Bacteriol.*, **72**, 324 (1956).
14) W. D. Denckla and H. K. Dewey, *J. Lab. Clin. Med.*, **69**, 160 (1967).
15) R. J. Mans and G. D. Novelli, *Arch. Biochem. Biophys.*, **94**, 48 (1962).
16) R. R. Brown, *J. Biol. Chem.*, **227**, 649 (1957).
17) J. M. Price and L. W. Dodge, *J. Biol. Chem.*, **223**, 699 (1956).
18) E. W. Jones and G. R. Fink, "The Molecular Biology of the Yeast Saccharomyces," ed. by J. N. Strathern, E. W. Jones and J. R. Broach, Cold Spring Harbor Laboratory, New York, 1982, p. 183.
19) B. T. Lingappa, M. Prasad and Y. Lingappa, *Science*, **163**, 192 (1969).
20) R. Rajagopal, *Physiol. Plant.*, **20**, 982 (1967).
21) G. Lacan, V. Magnus, S. Simaga, S. Iskric and P. J. Hall, *Plant Physiol.*, **78**, 447 (1985).
22) H. H. Schott and U. Krause, *Hoppe-Seyler's Z. Physiol. Chem.*, **360**, 481 (1979).

Effect of Cysteine on Bovine Serum Albumin (BSA) Denaturation Induced by Solar Ultraviolet (UVA, UVB) Irradiation

Yoshifumi WATANABE,*[,a,1)] Izumi HORII,[a] Yasuhisa NAKAYAMA[a] and Toshiaki OSAWA[b]

Department of Biological Sciences, Shiseido Basic Research Laboratories,[a] 1331 Nippa-cho, Kouhoku-ku, Yokohama 223, Japan and Division of Chemical Toxicology and Immunochemistry, Faculty of Pharmaceutical Sciences, University of Tokyo,[b] Tokyo 113, Japan. *Received December 26, 1990*

Long-term exposure to natural sun-light (UVA, UVB) induced fluorescence and caused disulfide bond formation in bovine serum albumin (BSA). The addition of cysteine enhanced the bond formation to such an extent that a solution of BSA was transformed into an insoluble gel. The disulfide bonds in the gels are derived from internal–SH groups of protein. This reaction occurred even if cysteine was added after exposure to ultraviolet (UV)-irradiation. Fluorescent substances seem to be involved in this reaction. On the other hand, low concentrations of cysteine (<5 mM) inhibited both fluorescence and disulfide bond formation. The addition of glutathione to BSA produced the same effect as that of cysteine. The addition of thiourea to BSA solution inhibited fluorescence, but did not inhibit disulfide bond formation. We assume that external–SH compounds such as cysteine and glutathione, which have high reactivity with hydroxyl radicals (.OH), act not only as free-radical scavengers, but also as radical mediators in the polymerization of protein through disulfide cross-links induced by UV-irradiation. Solar UVA as well as UVB irradiation are shown to have the same effect on the protein polymerization.

Keywords cysteine; protein denaturation; solar ultraviolet light (UVA, UVB); disulfide bond formation; fluorescence substance

Introduction

The effects of ultraviolet (UV)-light on living tissue are well documented.[2-5)] Of these effects, the denaturation of protein, including the formation of cross-linkages, has attracted much attention within the fields of dermatology and ophthalmology.[6-10)] In the present paper the authors also investigated the effects of solar UV-light on protein cross-linking and fluorescent substance generation, because cross-linking between protein molecules is thought to be a major cause of photo-aging in dermatology and of cataract formation in ophthalmology. In addition, there may be a relationship between the fluorescence induced by UV-irradiation and lipofuscin, a fluorescent pigment thought to be related to aging found in aged and sun-aged epidermal tissue. Interestingly, protein denaturation always follows fluorescence and cross-linking formation in aged skin tissues and cataract lens protein even though the trigger for denaturation may be different (*i.e.*, UV-light, heat in Maillard reaction or oxygen). In these reactions, radicals and reactive substances such as sulfhydryl (SH) compounds have an important role. SH compounds, such as cysteine and glutathione, which exist in living tissues are known to protein tissues by acting as radical scavengers.[11,12)] However, in the present study, cysteine and glutathione were shown to enhance disulfide bond formation between protein molecules exposed to UV-irradiation, while inhibiting the generation of fluorescent substances.

Materials and Methods

Reagents Bovine serum albumin (BSA), bovine casein and superoxide dismutase (SOD) were obtained from Sigma Chemical Co. (Tokyo, Japan); Mannitol, thiourea, 5,5'-dithiobis (2-nitrobenzoic acid) (DTNB), cysteine and glutathione were obtained from Wako Chemical Co., Ltd. (Osaka, Japan).

Preparation of UV-Irradiation Proteins Proteins (50 mg/ml) in 10 mM phosphate buffered saline (PBS) (pH 6.9) or an amino acid mixture in H_2O were irradiated with SE lamps (Toshiba Co., Ltd., Tokyo, Japan) for UVB, and BLB lamps (Toshiba Co., Ltd.) for UVA, and 25 °C in an incubator. Dosage levels in all experiments were 0.8 mW/cm^2 for UVB and 0.2 mW/cm^2 for UVA. Browning pigment was traced using absorbance at 350 nm.

Fluorescence Fluorescence spectra were measured on a JASCO FP-770 spectrofluorometer (Japan Spectroscopic Co., Ltd., Hachioji, Japan). Fluorescence excitation spectra were recorded at an emission wavelength of 440 nm; fluorescence intensity was expressed as relative intensity.

Sodium Dodecyl Sulfate–Polyacrylamide Gel Electrophoresis (SDS–PAGE) SDS–PAGE was performed using Laemmli's method.[13)] Samples were treated with a solubilizing buffer (0.1 M Tris, pH 6.8/2% SDS/2% glycerol/with or without 0.5% 2-mercaptoethanol (2-ME)) at 100 °C for 10 min before being subjected to SDS–PAGE. The gel formed when cysteine was added to UV-irradiation BSA was solubilized as follows: finally milled gel was suspended in 0.25 M oxalic acid (1 part gel to 8 parts acid, w/w) and heated in boiling water. As soon as the sample had been completely solubilized, it was applied to a Sephadex G-25 column (0.5 × 50 cm) equilibrated with 10 mM PBS to remove the oxalic acid. The solubilized samples were then treated as the other samples and subjected to SDS–PAGE. A stacking gel of 4% acrylamide and a resolving gel of 5—10% continuous-gradient acrylamide were employed. Gels were stained with Coomassie brilliant blue R. Arrows in figures show the position of aggregated protein.

Chromatography Gel filtration was performed using a Toyopearl HW-55 gel column (Toyo Soda Co., Ltd.) equilibrated with 10 mM PBS to separate polymerized BSA from unpolymerized BSA.

Quantitative Analysis of SH Groups The quantity of sulfhydryl groups in a protein was measured using the method described by Ellman.[14)]

Results

Changes in Protein Following UV Irradiation Protein subjected to UV-irradiation undergoes a number of important changes. Three major changes occurred in BSA after long-term UVB-irradiation under the conditions described above. As shown in Fig. 1A and 1B, both browning pigment and fluorescence intensity increased with increasing total dosage of UVB-irradiation. The fluorescence excitation spectra all exhibited the same pattern, with the minor peak at an excitation wavelength of 305 nm, which disappeared with continued irradiation. Based on the spectral analysis of various amino acids (data not shown), this minor peak is thought to be derived from the tryptophan of BSA. The third change is the formation of polymerized BSA. The irradiation sample was applied to a HW-55 column and gel filtration was performed. The chromatography pattern shown in Fig. 2A indicates that irradiated BSA consists of various polymerized molecules, and that there is no relationship between fluorescence and the degree

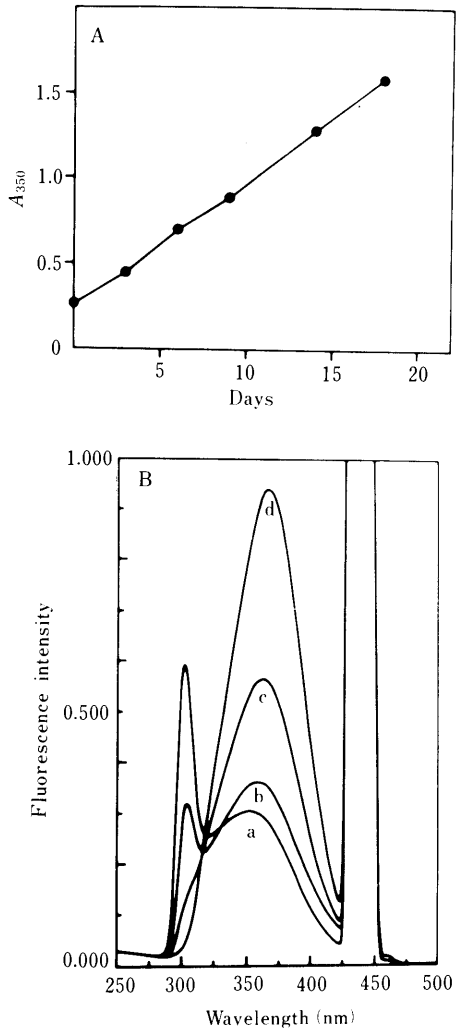

Fig. 1. Time Course of Increasing Absorbance at 350 nm (A) and Increasing Fluorescence at 370 nm (B, a = 0 d, b = 1 d, c = 3 d, d = 7 d) in UVB-Irradiated BSA

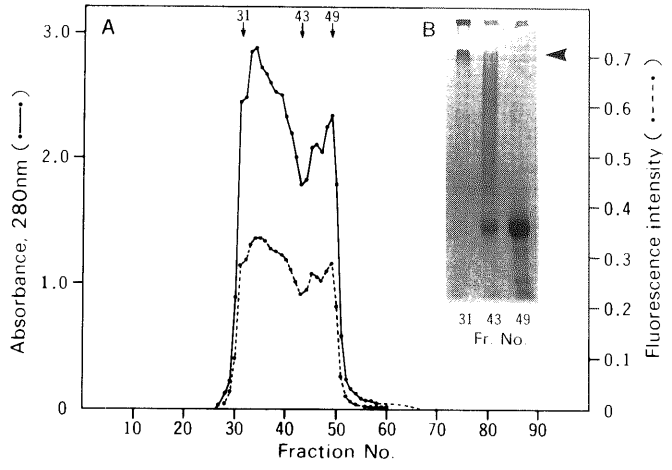

Fig. 2. Column Chromatography on Toyopearl HW-55

Five milliliter of UVB-irradiated BSA (50 mg/ml) were applied to a column of HW-55 (4 × 120 cm) and eluted with 10 mM PBS.

A) Chromatography pattern. (●—●) absorbance at 280 nm. (●- - -●) fluorescence intensity (Ex. 370 nm/Em. 440 nm). B) Results of SDS-PAGE (5—10% gradient gel).

of polymerization. This can be understood by the fact that fluorescence tracks absorbance rather than molecular weight. This suggests that the binding structure of polymerization is different from that of the fluorescent substances.

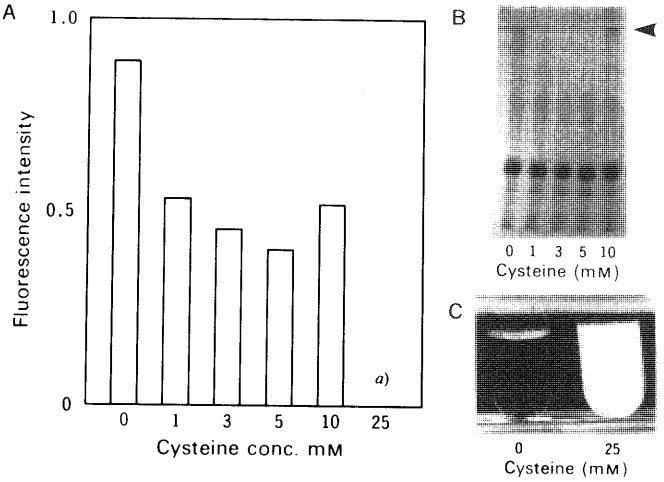

Fig. 3. Effects of Cysteine on the Changes of BSA Irradiated with UVB

BSA solution was irradiated with UVB as described in Materials and Methods for 5 d.

A) Effects of cysteine at various concentrations on the fluorescence generation (*a*) not measured because of gel formation.) B) Effects of cysteine at various concentrations on the polymerization. SDS-PAGE was performed with 5—10% gradient acrylamide gel. C) Photograph of the gel formed by UVB irradiation and cysteine (25 mM).

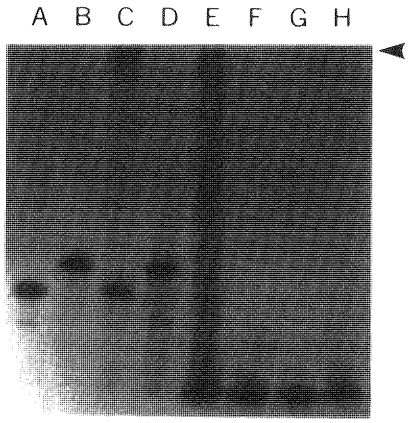

Fig. 4. Results of SDS-PAGE

SDS-PAGE was carried out with 5—10% gradient gel. Other experimental details are described in Materials and Methods

A, BSA; B, BSA treated with 2-Me; C, UVB-irradiated BSA (7-days); D, UVB-irradiated BSA treated with 2-ME; E, the gel treated with 0.25 M oxalic acid; F, the gel treated with 0.25 M oxalic acid and 2-ME; G, BSA treated with 0.25 M oxalic acid; H, BSA treated with 0.25 M oxalic acid and 2-ME.

Effects of Cysteine and Glutathione on UVB-Irradiated Protein Several specific changes occurred when BSA solution containing various concentrations of cysteine or glutathione was irradiated. At concentrations of less than 5 mM, both fluorescence intensity and polymerization were inhibited by increasing concentrations of these SH compounds as shown in Fig. 3A and 3B. However, at a concentration of 10 mM, some precipitation occurred, the fluorescence intensity recovered slightly (Fig. 3A), and polymerization was enhanced (Fig. 3B). In addition, an impermeable and insoluble gel formed at a concentration of 25 mM (Fig. 3C). The gel remained insoluble, even when immersed in a 2% SDS buffer at 90°C. Therefore, 0.25 M oxalic acid was used to solubilize the gel in preparation for analysis by SDS-PAGE, as described in Materials and

Methods. The results of SDS–PAGE are shown in Fig. 4. The BSA polymerized by UVB-irradiation was reduced with 2-ME to the normal BSA position on the SDS–PAGE gel (lanes C and D). The oxalic acid-treated gel consisted of highly polymerized BSA (lane E), which also was reduced with 2-ME to peptides similar to that of normal BSA treated with oxalic acid (lanes G and H). The amount of SH in control BSA and UVB-irradiated BSA was 1.3 mol SH/mol BSA and 0.94 mol SH/mol BSA, respectively. These results show that irradiation produced disulfide linkages between protein molecules, and that the gel formation by the addition of cysteine and UVB-irradiation is due to these excessive disulfide bonds between BSA molecules.

The same results were obtained when glutathione was used in place of cysteine (data not shown). Furthermore, UVA-irradiation under the conditions described in Materials and Methods yielded the same results as UVB-irradiation (Fig. 5). The former produced a greater degree of fluorescence than the latter on an equal-dosage basis. In other words, UVA is about 16 times more effective than UVB in producing fluorescence.

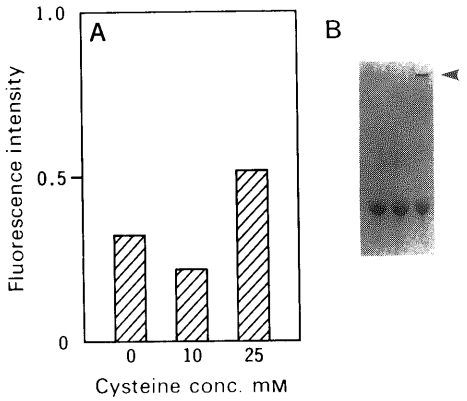

Fig. 5. Effects of Cysteine on the Change of BSA Induced by UVA-Irradiation

BSA solution (50 mg/ml) was irradiated with UVA (0.2 mW/cm^2) in the presence of cysteine for 2 d.

A) Effect on the fluorescence by UVA-irradiation. B) Results of SDS–PAGE (5—10% gradient gel). a, UVA-irradiated BSA; b, UVA-irradiated BSA with 10 mM cysteine. c, UVA-irradiated BSA with 25 mM cysteine.

The following experiment was carried out using bovine-casein, which is a protein lacking internal cysteine,[15] in an attempt to determine whether the disulfide bonds are derived from additive or internal cysteine. Bovine-casein was irradiated with UVB for 4 d both with and without 25 mM cysteine and subjected to SDS–PAGE. As shown in Fig. 6, UVB-irradiated bovine-casein exhibited intense fluorescence (Fig. 6A, B) which was inhibited by the addition of cysteine (Fig. 6A, C). However, as shown in Fig. 6B, polymerization did not occur and high performance liquid chromatography (HPLC) analysis revealed cystine precipitates in the solution of Fig. 6B (lane 3) following irradiation (data not shown).

The results indicate that the disulfide bonds of polymerization were derived from internal cysteine rather than cysteine addition, and that cysteine and glutathione additives acted to enhance the formation of disulfide bonds and inhibit the development of fluorescence in the presence of UV-irradiation.

Interaction between Fluorescence Substances and Disulfide Bond Formation We performed the following experiments to investigate the fluorescence substance in protein and the relationship between the fluorescence substances and disulfide bond formation. At first, we irradiated UVB to amino acid mixtures including cysteine and an aromatic amino acid in various combinations. The fluorescence intensity was measured, because cysteine seems to be deeply involved in both fluorescence and disulfide bond formation, as suggested by the results described above. In addition, there is a high probability that aromatic amino acids are also involved in these reactions because of their excitation capacity by UV-irradiation. As shown in Table I, although phenylalanine, tyrosine and tryptophan themselves do not have any fluorescence after UV-irradiation, the combination of cysteine and phenylalanine did have strong fluorescence after UVB irradiation. Their fluorescence pattern was similar to that of protein. The mixture of cysteine and tyrosine also gave some fluorescence, but the pattern was different from that of the protein. This suggests that the

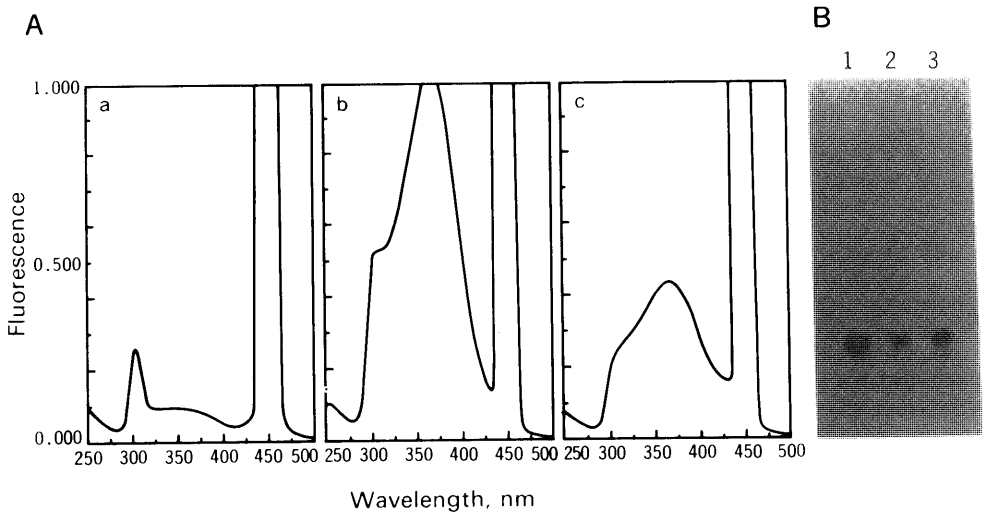

Fig. 6. Effects of UVB-Irradiation and Cysteine on Bovine-Casein

Bovine-casein (50 mg/ml) was irradiated with UVB for 3 d with or without cysteine.

A) Effect of cysteine on fluorescence. a, non-irradiated bovine-casein; b, UVB-irradiated bovine-casein; c, UVB-irradiated bovine-casein with 25 mM cysteine. B) SDS–PAGE with 5—10% gradient gel. 1, non-irradiated bovine-casein; 2, UVB-irradiated; 3, UVB-irradiated with 25 mM cysteine.

contribution of Cys–Tyr combination to the fluorescence of protein is small. According to the results in Table I, phenylalanine seems to have an important role in fluorescence formation; accordingly, we studied the combination of phenylalanine and other amino acids. Table II shows that there are some special amino acids that formed fluorescence substances with phenylalanine. The solution of cysteine, methionine or lysine in the presence of phenylalanine had strong fluorescence after UVB irradiation and the fluorescence pattern was similar to that of protein. On the other hand, the fluorescence of other amino acids (His, Asp, Leu *etc.*) with phenylalanine was relatively weak and the fluorescence patterns were completely different from that of protein (data not shown). We assume that the contribution of these amino acids to the fluorescence in protein is small. As these data shown, at least three fluorescent substances are involved in protein fluorescence induced by UV-irradiation, Cys–Phe, Met–Phe and Lys–Phe. They should be internal molecules because cysteine additives reduced the fluorescence intensity. Since bovine casein does not have any internal cysteines, its fluorescence may be derived from Phe–Lys. In addition, cysteine seems to be a reactive radical acceptor relative to other internal amino acids in bovine casein because cysteine additives inhibited fluorescent substances formation in Fig. 5C and formed cystine precipitation according to HPLC analysis (data not shown).

As described above, following UV-irradiation, the addition of cysteine to UV-irradiation BSA (50 mg/ml) which is fluorescent and slightly polymerized instantly resulted in gel formation. On the other hand, non-irradiated BSA was unaffected by the addition of cysteine. Therefore, since we assume that the fluorescent substances in UV-irradiated BSA molecules could work as radical donors that cause disulfide bond formation, the following experiments were carried out to confirm the interaction between fluorescent substances and disulfide bond formation. After UV-irradiation, the 3-day UVB-irradiated BSA was incubated with 25 mM cysteine at 4 °C for 3 weeks in the dark; gel formation did not occur at this concentration. Fluorescence was then measured and the mixture was subjected to SDS–PAGE (Fig. 7B). As shown in Fig. 7, the addition of cysteine after UV-irradiation reduced the

TABLE I. Fluorescence Intensity after UVB-Irradiation of Specific Amino Acids in the Presence of Cysteine

Amino acid	Fluorescence intensity		
	0 d	3rd day	5th day
Cys	0	0	0.08
+Phe	0	0.4	0.99
+His	0	0.05	0.1
+Tyr	0	0.07	0.35
+Pro	0	0	0
+Met	0	0	0
+Trp	0	0.15	0.15
Phe	0	—	0
Trp	0	—	0.05
Tyr	0	—	0.05

Amino acids were dissolved in distilled water at a final concentration of 50 mM each and continuously irradiated with UVB for 5 d. The fluorescence intensity was measured at 0, 3 and 5 d after the irradiation as described in Materials and Methods.

TABLE II. Fluorescence Intensity after UVB-Irradiation of Amino Acids with Phenylalanine

Amino acid	Fluorescence intensity		
	0 d	3rd day	5th day
Phe	0	0	0
+Val	0	0	0
+Ser	0	0	0
+Cys	0	0.52	0.95
+His	0	0.4	0.1
+Met	0	0.38	0.85
+Asp	0	0.52	0.4
+Leu	0	0.25	0.3
+Ala	0	0.3	0.2
+Arg	0	0.25	0.1
+Pro	0	0.45	0.2
+Tyr	0	—	0.15
+Trp	0	—	0
+Lys	0	0.85	0.95

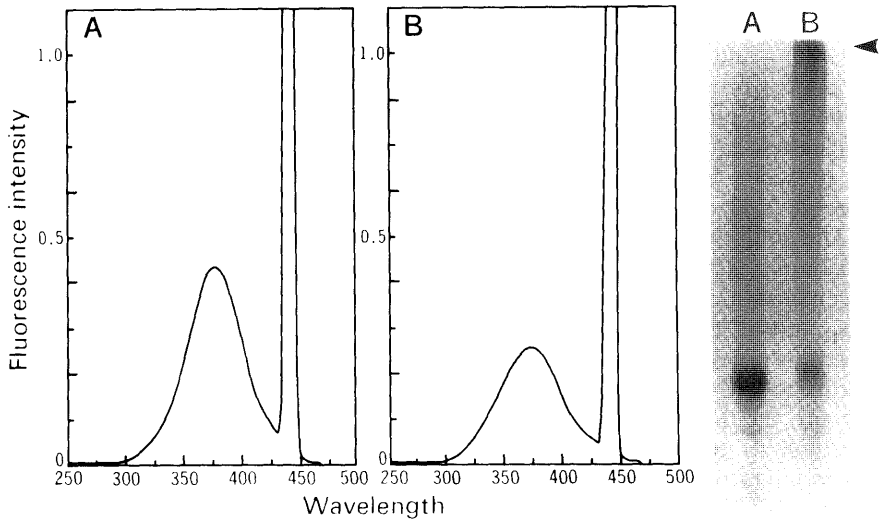

Fig. 7. Effects of Cysteine after Irradiation on UVB-Irradiated BSA

UVB-irradiated BSA (3 d) was incubated with or without 25 mM cysteine at 4 °C in the dark for 3 weeks after irradiation. The fluorescence spectra and SDS–PAGE are shown. A) UVB-irradiated BSA. B) UVB-irradiated BSA with 25 mM cysteine.

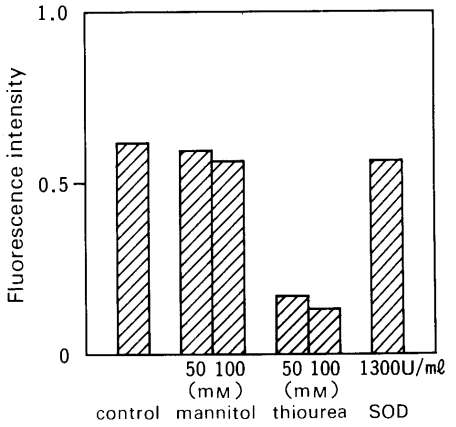

Fig. 8. Effects of Radical Scavengers on Fluorescence

BSA (50 mg/ml) was irradiated with UVB for 5 d in the presence of mannitol (50, 100 mM), thiourea (50, 100 mM) and SOD (1300 U/ml). The fluorescence intensity was measured.

fluorescence and increased the polymerization of BSA. These results show that there may be an association between fluorescent substances and disulfide bond formation which is mediated by external cysteine.

Effects of Radical Scavengers on Fluorescence and Polymerization Induced by UV-Irradiation Mannitol, thiourea and SOD were used as radial scavengers. BSA was irradiated for 4 d together with each radical scavenger using UVB. Fluorescence was then measured and samples were subjected to SDS–PAGE. Only thiourea inhibited fluorescence formation (Fig. 8). SDS–PAGE results indicated that radical scavengers did not inhibit polymerization of BSA or disulfide bond formation (data not shown). The same experiment was performed in the presence of 25 mM cysteine, but gel formation was not inhibited by radical scavengers.

Discussion

The results presented in this paper demonstrate that SH compounds such as cysteine and glutathione play an important role in the UV-induced denaturation of protein. Characteristic changes in protein exposed to UV-light are (1) an increase in brown pigmentation, (2) generation of fluorescent substances and (3) polymerization of protein molecules (Figs. 1 and 2). These changes also occur in the lens proteins of cataracts[6] and in non-enzymatically glycosylated protein.[16] As for brown pigmentation, most is reported to be the product of photolyzed tryptophan.[6]

High concentrations of cysteine and glutathione enhanced polymerization in the presence of UV-irradiation, but inhibited both fluorescence and polymerization at low concentration (Fig. 3). This inhibitory effect in the present experiment reached a maximum at a concentration of about 5 mM. The inhibitory mechanism might depend on the total dose of UV-irradiation, and/or the content of cysteine residue in a given protein. It is noteworthy that the addition of cysteine (50 mM or more) to UV-irradiated BSA solution (50 mg/ml) leads instantly to the formation of an insoluble gel. Gel formation was shown to result from the formation of disulfide bonds with internal rather than external cysteine (Figs. 4 and 6). The results also show that external cysteine acts as a mediator in the formation of disulfide linking between protein molecules. Goosey *et al.*[7] reported that singlet oxygen mediated the cross-linking process. Given that SH compounds such as cysteine (glutathione) react more easily with the hydroxyl radical (.OH) than with singlet oxygen, it is reasonable to assume that the hydroxyl radical rather than singlet oxygen plays a major role in protein polymerization mediated by external cysteine in these experiments. Since UVA irradiation (max.: 365 nm), which is not absorbed by any aromatic amino acids produced the same results as UVB irradiation (max.: 305 nm), it also seems reasonable to assume that the hydroxyl radical and aqueous electron (e_{aq}) are mostly derived from H_2O treated by UV-irradiation although partly derived from oxidization products of tryptophan.

Koster and Slee[17] suggested that hydroxyl radicals cause cross-linking by directly attacking a protein. In the present paper, the mechanism of disulfide formation enhanced by external cysteine is as follows. In the absence of free cysteine or glutathione, the hydroxyl radicals directly attack the cysteine contained in protein, causing polymerization. However, this reaction is sometimes slow due to protein conformation and the low rate of molecular association. On the other hand, in the presence of abundant SH compounds, hydroxyl radicals initially react with sulfydryl groups, resulting in the efficient formation of cysteinyl radicals (RS.); this reaction occurs quickly.

The effective radical mediation postulated above results in rapid protein cross-linking and gel formation. Hence, polymerization was not inhibited by radical scavengers regardless of the presence of cysteine because the rate of cysteine reaction is much higher than that of mannitol or thiourea. These facts suggest that SH compounds such as cysteine or glutathione play a dual role as both radical scavengers and radical mediators, especially in the formation of disulfide cross-links. The fact that UVA produced the same reactions as UVB (Fig. 5) suggests that the reaction described in this paper can occur not only in lens proteins but also in the dermis. The reason is that UVA has a longer wavelength than UVB and thus reaches the dermis through the epidermis.[18] In addition, hydroxyl radicals generated by the Fenton reaction might be involved in the protein cross-linking enhanced by SH compounds.

Only thiourea acted as a hydroxyl radical scavenger to inhibit the formation of fluorescent substances (Fig. 8). Interestingly, mannitol, which is also a hydroxyl radical scavenger, did not inhibit fluorescence formation. This is thought to depend on the reactivity of each drug. In addition, cysteine, which is a hydroxyl radical scavenger, inhibited fluorescence generation in bovine casein, where disulfide cross-linking did not occur. These acts suggest that fluorescent substances are generated through free radicals, possibly the hydroxyl radical.

The role of such fluorescent substances is not yet clear; however, according to our results, internal Cys–Phe, Met–Phe or Lys–Phe must have an important function in forming fluorescent substances in protein. Intriguingly, the sulfur-containing amino acids cysteine and methionine whose oxidation products are detected in proteins of advanced nuclear cataractous human lenses[19] are involved in this fluorescence formation. According to Pongor *et al.*,[16] lysine has also an important role in forming a fluorescent chromophore in Maillard products. In addition, the fact that fluorescence decreased and polymerization increased when cysteine was added to UV-irradiated BSA even after

UV-irradiation (Fig. 7) strongly suggests the existence of radical donors in UV-irradiated protein solution, and indicates that fluorescent substances might be a radical donor in the polymerization mediated by SH compounds. Our speculation is that cysteine is such a reactive radical acceptor that the fluorescent substances as radical donors give radicals to cysteines and that the cysteinyl radicals mediate the disulfide bond formation by passing radicals between internal cysteines. Given the present results, it is possible to speculate that the stable excited state species in human lens proteins[20] and the fluorescent substance bound to proteins in the human lens might be photosensitizers.[21] The specific fluorescence spectrum pattern of each protein depends on the composition ratio of the amino acids which constitute a given protein. Ongoing experiments will determine these fluorescent substances.

References and Notes

1) Present address: *Department of Bioengineering, Tokyo Institute of Technology, 4259 Nagatsuda-cho, Midori-ku, Yokohama 227, Japan.*
2) R. W. Gange and C. F. Rosen, *Photochem. Photobiol.*, **43**, 701 (1986).
3) S. Aktipis and A. J. Iammartino, *Biochem. Biophys. Res. Commun.*, **44**, 918 (1971).
4) L. I. Grossweiner, *Current Topics in Radiation Research Quarterly*, **11**, 141 (1976).
5) B. A. Gilchrest, *J. Gerontol.*, **35**, 537 (1980).
6) S. Zigman, *Photochem. Photobiol.*, **26**, 437 (1977).
7) J. D. Goosey, J. S. J. Zigler, and L. H. Kinoshita, *Science*, **208**, 1278 (1980).
8) M. P. Merville, J. Decuyper, J. Piette, C. M. Calberg-Bacq, and A. Van de Vorst, *Invest. Ophthalmol. Vis. Sci.*, **25**, 573 (1984).
9) K. J. Johnston, A. J. Olkarinen, N. J. Lowe, J. G. Clark, and J. Uitto, *J. Invest. Dermatol.*, **82**, 587 (1984).
10) G. J. H. Bessem, H. J. J. M. Rennen, and H. J. Hoender, *Exp. Eye Res.*, **44**, 691 (1987).
11) D. C. Srieve, J. Denekamp, and A. I. Minshinton, *Radiat. Res.*, **102**, 283 (1985).
12) R. M. Tyrrell and M. Pidoux, *Photochem. Photobiol.*, **44**, 561 (1986).
13) U. K. Laemmli, *Nature* (London), **227**, 680 (1970).
14) G. L. Ellman, *Arch. Biochem. Biophys.*, **32**, 70 (1959).
15) M. O. Dayhoff, "Atlas of Protein Sequence and Structure," National Biomedical Foundation, Washington D.C., 1972, p. 5.
16) S. Pongor, P. C. Ulrich, F. A. Bencsath, and A. Cerami, *Proc. Natl. Acad. Sci. U.S.A.*, **81**, 2684 (1984).
17) J. F. Koster and R. G. Slee, *Biochim. Biophys. Acta*, **752**, 233 (1983).
18) H. Ippen, "The Biologic Effects of Ultraviolet Radiation," (ed. by F. Urbach), Pergamon Press, New York, 1969, p. 681.
19) S. Zigman, G. Griess, T. Yulo, and J. Schultz, *Exp. Eye Res.*, **15**, 255 (1973).
20) M. H. Garner and A. Spector, *Proc. Natl. Acad. Sci. U.S.A.*, **77**, 1274 (1980).
21) A. Spector, D. Roy, and J. Stauffer, *Exp. Eye Res.*, **21**, 9 (1975).

Influence of Isosorbide Dinitrate Concentration on Its Skin Permeability from Adhesive Matrix Devices

Tomomi HATANAKA,[a] Manami OGUCHI,[a] Kenji SUGIBAYASHI[a,b] and Yasunori MORIMOTO*[,a,b]

Faculty of Pharmaceutical Sciences[a] and Life Science Research Center,[b] Josai University, 1–1 Keyakidai, Sakado, Saitama 350-02, Japan.
Received November 20, 1990

Adhesive matrix devices containing a model drug, isosorbide dinitrate (ISDN), were prepared with three different types of pressure sensitive adhesives (PSAs). ISDN permeation through excised hairless rat skin from the different devices was measured *in vitro*. For each PSA type, the steady state permeation rate of ISDN increased proportionally with an increase of ISDN concentration in the PSA and reached a maximum level at a certain concentration. Although the concentrations reaching the maximum skin permeation level varied among PSA types, the maximum rate for each PSA type was largely similar to that for ISDN aqueous suspension. The release rate of ISDN from devices was too fast to influence the skin permeation rate for all devices. In the PSA of devices showing maximum skin permeability, ISDN crystalline was observed by polarizing microscopy and differential scanning calorimetry. These results suggest that the skin permeation of ISDN from adhesive matrix devices was controlled by the thermodynamic activity of the drug in the PSAs.

Keywords adhesive matrix device; skin permeation; pressure sensitive adhesive; drug concentration; thermodynamic activity; isosorbide dinitrate

The objective of this study was to investigate the influence of physical and chemical properties of adhesive matrix devices on the skin permeability of drug. Adhesive matrix devices containing a model drug, isosorbide dinitrate (ISDN), were prepared using three different typical pressure sensitive adhesives (PSAs), namely acrylic, rubber and silicone adhesives. The effect of ISDN concentration and type of PSAs on ISDN permeability through the excised hairless rat skin from the devices was determined. Moreover, the adhesive properties and ISDN release for the devices were also evaluated.

Materials and Methods

Materials ISDN was a gift from Kyukyu Pharmaceutical Co. (Tokyo, Japan). An aqueous emulsion (50% solid content) of acrylic adhesive (methacrylic acid–butyl acrylate copolymer, mole ratio 50 : 1) was kindly supplied from Kyukyu Pharmaceutical Co. A rubber adhesive mixture made mainly from a styrene–isoprene-styrene block copolymer (weight ratio of styrene : isoprene 14 : 86) was supplied from Toko Pharmaceutical Industries Co. (Tokyo). Silicone adhesive (bio-PSA® Q7-2920) was purchased from Dow Corning Co. (Midland, MI, U.S.A.). Other chemicals were of a reagent grade and obtained commercially.

Preparation of Adhesive Matrix Devices The adhesive matrix devices were prepared by a casting method.[1] An appropriate volume of 20% ISDN ethyl acetate solution was added to the adhesive solution or emulsion and thoroughly stirred with a Teflon-spatula. The rubber-type adhesive solution (50% solid content) was formulated by adding chloroform to an additive-mixture containing styrene–isoprene–styrene block copolymer. The adhesive solution or emulsion containing ISDN was applied to a backing sheet, polyethylene terephthalate film. After allowing the solvent to evaporate off at 60 °C for 5 min, the adhesive samples were kept at room temperature for 24 h. The dried adhesive matrix devices were weighed and their thickness was measured with a dial thickness gauge (limit 0.1 μm). The devices with a thickness greater than 600 μm were obtained by laminating the PSA layers. The devices with various concentrations of ISDN (3—288 mg/g) were prepared by varying thicknesses of PSA layers with a constant ISDN content of 800 μg/cm^2. Table I shows the PSA type, ISDN concentration and thickness of the adhesive matrix devices prepared in this study.

Evaluation of Adhesive Properties The adhesive properties of adhesive matrix devices were evaluated after being kept at 23 °C, 60% relative humidity for 24 h. The ball tack test was done according the method of J. Dow.[2] The probe tack was measured with a Nichiban probe tack tester (Nichiban Co., Tokyo). Apparent viscosity and peel adhesion were measured by the shear strength test (PSTC no. 7)[3] and 180° peel test,[4] respectively.

Skin Permeation Procedure The abdominal skin of a male hairless rat (WBN/ILA-Ht, 6 weeks old, Life Science Research Center, Josai University, Saitama, Japan) was excised after being shaven carefully. An adhesive matrix device was applied on the stratum corneum side of the excised skin and the skin with the device was mounted between two half diffusion cells with a water jacket, having a volume of 2.5 ml and a 0.95 cm^2 effective diffusion area.[5] The receiver compartment (dermis side) of each cell was filled with 2.5 ml of distilled water and stirred throughout the experiment with a star-head bar in each half-cell, driven by a constant-speed synchronous motor (MC-301, Scinics, Tokyo) at 1200 rpm. The experiments were done at 37 °C by circulating warm water. At appropriate times, 500 μl samples were withdrawn from the receiver compartment and 500 μl of distilled water was added to keep the volume constant. Other experiments were done by filling the donor compartment (stratum corneum side) with 2.5 ml of ISDN aqueous suspension (3.0 mg/ml) instead of application of adhesive matrix devices.

Release Procedure The diffusion cell described above was employed for determining the release rate of ISDN from adhesive matrix devices. An adhesive matrix device was applied onto a half-cell, and the half-cell was filled with 2.5 ml of distilled water and stirred throughout the experiment. Samples (1 ml) were withdrawn from the half-cell for assay at appropriate times, and 1 ml of distilled water added to keep the volume constant.

ISDN Analysis ISDN was assayed by high performance liquid chromatography (HPLC). The HPLC system consisted of a pump (LC-6A, Shimadzu, Kyoto, Japan), an ultraviolet detector (SPD-6A, Shimadzu),

TABLE I. The PSA Type, ISDN Concentration and Thickness of Adhesive Matrix Devices Prepared in This Experiment

	PSA	ISDN concentration (mg/g)	Thickness (μm)
A-1	Acrylic	288	27.8
A-2		240	33.3
A-3		180	44.4
A-4		90	88.9
A-5		60	133.3
R-1	Rubber	203	39.4
R-2		102	78.4
R-3		68	117.6
R-4		10	800.0
R-5		5	1600.0
S-1	Silicone	165	48.5
S-2		83	96.4
S-3		55	145.5
S-4		5	1600.0
S-5		3	2666.7

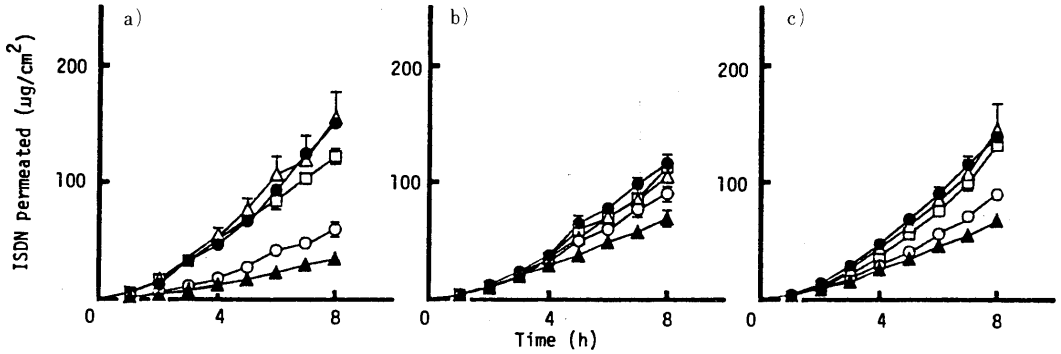

Fig. 1. Skin Permeation Profiles of ISDN from Several Adhesive Matrix Devices

a) Acrylic-type. ●, A-1; △, A-2; □, A-3: ○, A-4; ▲, A-5. *b*) Rubber-type. ●, R-1; △, R-2; □, R-3; ○, R-4; ▲, R-5. *c*) Silicone-type. ●, S-1; △, S-2; □, S-3; ○, S-4; ▲, S-5. Each value represents the mean±S.E. of 3 experiments.

a 4.6 mm × 250 mm stainless-steel column packed with Nucleosil® $5C_{18}$ (Macherey Nagel, Germany) and an integrator (C-R6A, Shimadzu). Analytical conditions were as follows: mobile phase, water–acetonitrile (45:55); flow rate, 1.2 ml/min; detector, UV 254 nm; internal standard, butyl *p*-hydroxybenzoate.

Polarizing Microscopy The PSA layer of adhesive matrix devices was observed by polarizing microscopy (Transmitted Light Nomarsky System Microscope, model BHS-N, Olympus, Tokyo) at 35×.

Differential Scanning Calorimetry (DSC) The PSA layer of adhesive matrix devices was studied by a differential scanning calorimeter (DSC-8240B, Rigaku Co., Tokyo). A weighed sample (about 9 mg) was packed in an aluminum pan. An empty pan was used as a reference. Each sample was heated at a rate of 10 °C/min from −100 to 100 °C.

Analysis of Release Profiles The solubility and diffusion coefficient of ISDN in PSAs were estimated by computer fitting the release profiles of ISDN in dissolved and suspended devices using W. I. Higuchi's (Eq. 1)[6] and T. Higuchi's (Eq. 2)[7] equations, respectively.

$$Q = hC_0\left\{1 - 8/\pi^2 \sum_{m=0}^{\infty} 1/(2m+1)^2 \exp(-D(2m+1)^2\pi^2 t/4h^2)\right\} \quad (1)$$

$$Q = \sqrt{D(2C_0 - C_S)C_S t} \quad (2)$$

where Q is the amount of drug released per unit area, h is the thickness of the PSA layer, D is the diffusion coefficient of the drug in the PSA, C_0 and C_S represent the total drug concentration and solubility in PSA, respectively, and t is time.

Results and Discussion

Evaluation of Adhesive Properties Table II shows the adhesive properties of adhesive matrix devices prepared without ISDN and commercial products, Frandol® tape and Frandol® tape S. Several adhesive properties, such as ball tack and peel, of devices prepared in this study were higher than those of commercial products, except for probe tack. Although the adhesive strength was lowered by adding ISDN, the value was high enough to maintain an intimate contact with the skin surface by comparison to the following standards: Ball tack, No. 16; $\log\eta$, 6; bakelite peel, 200 g/15 mm.[8]

Influence of ISDN Concentration in PSAs on Skin Permeation Figure 1 shows the time course of the cumulative amount of ISDN which permeated excised hairless rat skin from several devices. The cumulative amount of ISDN which permeated increased linearly with time after a short lag time (about 1 h), and the slope of linear portion, namely the steady state permeation rates, varied markedly dependent on the ISDN concentration of the devices (Fig. 2). For each type of PSA, the permeation rate increased proportionally with an increase of ISDN concentration in PSAs and reached a constant maximum level above a concentration. The concentrations reaching the maximum level were about 200, 10 and 5 mg/g for acrylic, rubber and silicone adhesives, respectively. But, the maximum level for each PSA type was largely similar to that for ISDN aqueous suspension (about 23 μg/cm² h), ass shown by the broken line in Fig. 2.

TABLE II. Evaluation of Adhesive Properties of Several Adhesive Matrix Devices

Device	Ball tack	Probe tack (g/5 mm i.d.)	$\log\eta$	Peel (g/15 mm)	
				Bakelite	Steel
Acrylic-type	No. 29	754±13[a)]	7.93	1202±127[a)]	696±17[a)]
Rubber-type	No. 32<	643±26[a)]	8.13	584± 11[a)]	584±14[a)]
Silicone-type	No. 26	115±13[a)]	7.96	920± 5[a)]	885± 8[a)]
Frandol® tape	No. 27	495	6.55	390	340
Frandol® tape S	No. 20	215	7.88	390	290

Each value represents the mean of 2 experiments. *a*) Each value represents the mean±S.E. of 3 experiments.

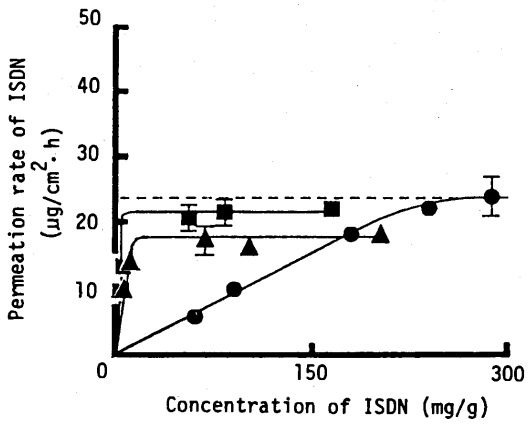

Fig. 2. Influence of ISDN Concentration in PSA on the Skin Permeation Rate of ISDN

●, acrylic-type; ▲, rubber-type; ■, silicone-type. Each value represents the mean ±S.E. of 3 experiments. The broken line represents the skin permeation rate from an ISDN aqueous suspension.

Release of ISDN from Adhesive Matrix Devices In order to evaluate the diffusivity of ISDN in PSA layers, the release of ISDN from several adhesive matrix devices was studied. Figure 3 illustrates the results of the release experiments. The release rate of ISDN for rubber adhesive was lower than that for acrylic and silicone adhesives. The release

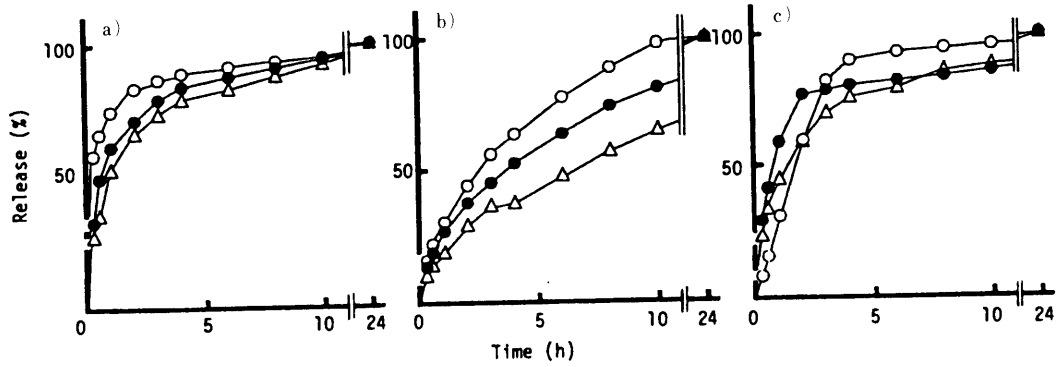

Fig. 3. Release Profiles of ISDN from Several Adhesive Matrix Devices

a) Acrylic-type. ○, A-3; ●, A-4; △, A-5. b) Rubber-type. ○, R-1; ●, R-2; △, R-3. c) Silicone-type. ○, S-1; ●, S-2; △, S-3. Each value represents the mean of 2 experiments.

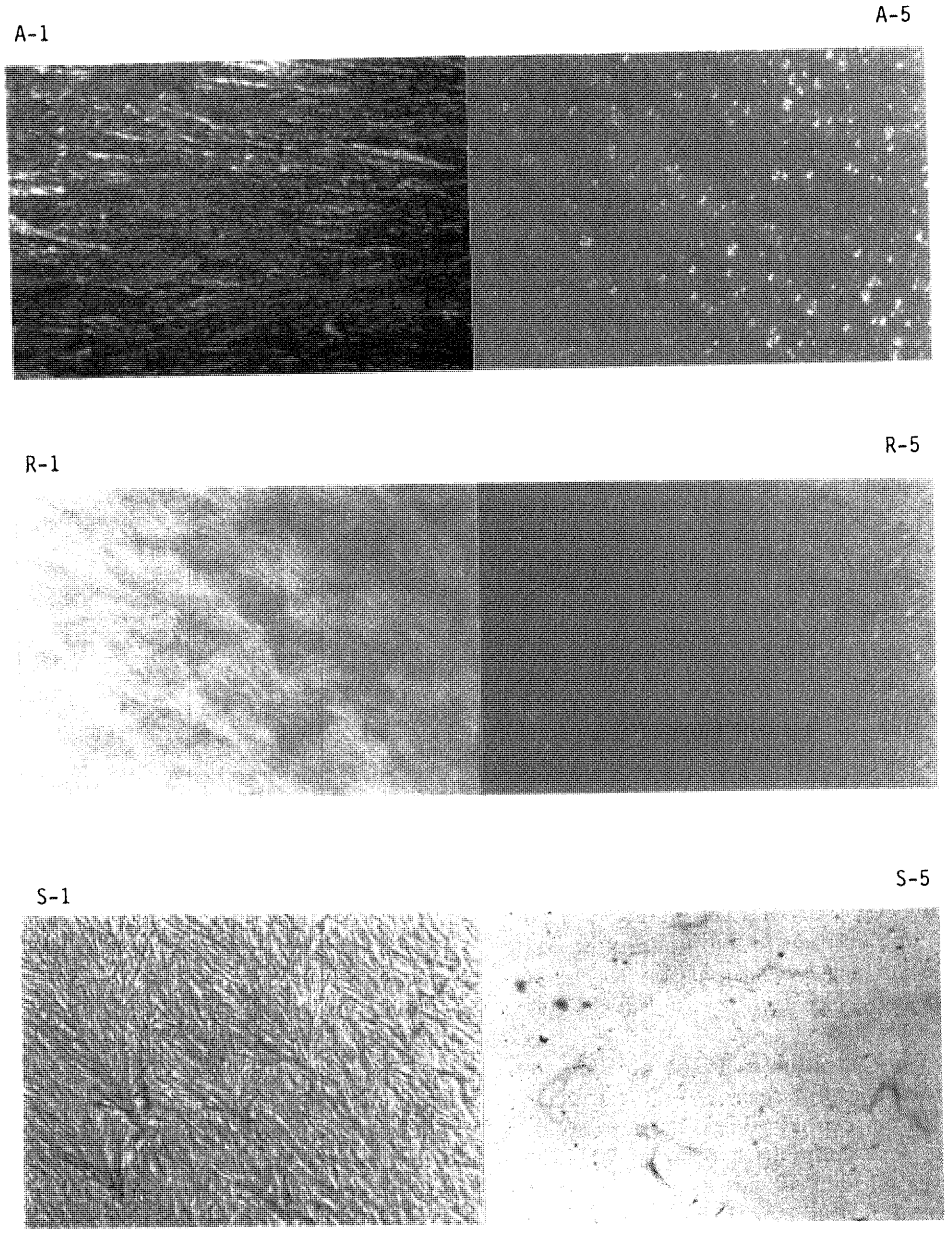

Fig. 4. Polarizing Micrographs of Several Adhesive Matrix Devices (Acrylic-Type A-1, A-5; Rubber-Type R-1, R-5; Silicone-Type S-1, S-5)

A-1, R-1 and S-1 were the typical devices which showed a maximum skin permeation rate, and A-5, R-5 and S-5 were the typical devices which didn't show a maximum permeation rate.

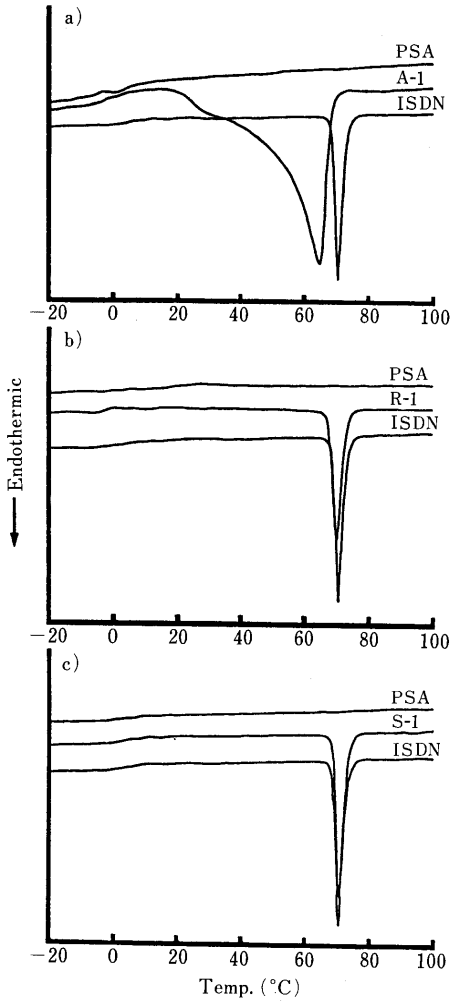

Fig. 5. DSC Thermograms of Several Adhesive Matrix Devices

a) Acrylic-type. b) Rubber-type. c) Silicone-type. A-1, R-1 and S-1 were the typical devices which showed a maximum skin permeation rate, and A-5, R-5 and S-5 were the typical devices which didn't show a maximum permeation rate.

rate of ISDN from each type of device had a tendency to increase with increasing ISDN concentration. The rate was too high to affect the skin permeability of ISDN. The swelling of the acrylic adhesive (2.34±0.21% after 24 h) was ignored in this study.

State of ISDN in PSAs Polarizing microscopy and DSC were employed to find out how the drug exists in PSAs. Comparison of the typical polarizing micrographs of three kinds of devices, with and without showing the maximum skin permeation rate, is shown in Fig. 4. ISDN crystalline was observed in devices with a maximum skin permeation rate, but no crystalline was found in the other devices for all types of PSA. It was suggested that the concentration of ISDN in a PSA was greater than the solubility for the devices having a maximum permeation rate, whereas only the dissolving ISDN existed in PSAs for the other devices.

The fact described above was further supported by the typical DSC thermograms of PSAs for devices having a maximum permeation rate (Fig. 5). A sharp endothermal peak was found at the melting point of ISDN (70 °C) in the rubber and silicone adhesives, suggesting the existence of ISDN crystalline in PSAs. A broad peak between 20 to 70 °C observed in the acrylic adhesive may be due to the influence of binding water and/or overlapping of the melting endotherm of ISDN neat crystalline and a solid solution.

TABLE III. Diffusion Coefficient and Solubility of ISDN in Several PSAs

Adhesive type	D ($cm^2/h \times 10^{-5}$)	C_s (mg/g)
Acrylic-type	3.583±0.576	156.1±18.21
Rubber-type	3.019±0.542	8.846±0.982
Silicone-type	24.44±0.333	1.931±0.294

Each value represents the mean±S.E. of 4 experiments.

Solubility and Diffusivity of ISDN in PSAs Analysis of the release profiles of ISDN was carried out to quantitatively evaluate the difference in solubility and diffusivity of ISDN among several PSAs. The estimated solubility and diffusion coefficient of ISDN in several PSAs is shown in Table III. The estimated solubilities were almost the same as the concentration reaching the maximum skin permeation rate for each type of PSA (Fig. 2). The diffusion coefficient in silicone adhesive was higher than in acrylic or rubber adhesives. The difference might reflect that the glass transition temperature of silicone adhesive (−116 °C) was remarkably lower than for acrylic or rubber adhesives (−41 and −48 °C).[9]

Conclusion

It was suggested from results in the present study that the skin permeation of ISDN from adhesive matrix devices was controlled by the thermodynamic activity of the drug in PSAs similar to the cases of solutions and ointment.[10] In the devices containing excess drug over solubility, the thermodynamic activity of the dissolving drug is generally the same as that of the solid (crystalline) drug. Whereas, in devices containing only the dissolving drug, the activity was proportional to the concentration. Therefore, the skin permeation rate reaches a maximum in the drug-suspended devices, and it is proportional to the concentration of the drug in the drug-dissolved devices. When the skin permeabilities of ISDN from several devices were compared under the same ISDN concentration, the higher permeation rate was obtained in the devices having a lower ISDN solubility. In order to develop novel adhesive matrix devices producing excellent skin permeability of drugs, PSAs with a low affinity against drugs (high thermodynamic activity of drugs) should be selected.

References and Notes

1) M. C. Musolf, "Transdermal Controlled Systemic Medications," eds. by Y. W. Chien, Marcel Dekker, Inc., New York, 1987, pp. 93—112.
2) JIS Z0237.
3) C. A. Dahlquist, "Handbook of Pressure Sensitive Adhesive Technology," eds. D. Satas, Van Nostrand Reinhold, New York, 1989, pp. 97—114.
4) JIS C2107.
5) M. Okumura, K. Sugibayashi, K. Ogawa and Y. Morimoto, *Chem. Pharm. Bull.*, **37**, 1404 (1989).
6) W. I. Higuchi, *J. Pharm. Sci.*, **51**, 802 (1962).
7) T. Higuchi, *J. Pharm. Sci.*, **50**, 874 (1961).
8) Private communication.
9) E. R. Cooper and G. Kasting, *J. Controlled Release*, **6**, 23 (1987).
10) T. Higuchi, *J. Soc. Cosmetic Chemists*, **11**, 85 (1960).

Microgranulation and Encapsulation of Pulverized Pharmaceutical Powders with Ethyl Cellulose by the Wurster Process

Yoshinobu FUKUMORI,*[,a] Hideki ICHIKAWA,[a] Yumiko YAMAOKA,[a] Eiichi AKAHO,[a] Yoshikazu TAKEUCHI,[a] Tomoaki FUKUDA,[a] Ryuichi KANAMORI[b] and Yoshifumi OSAKO[c]

Faculty of Pharmaceutical Sciences, Kobe-Gakuin University,[a] Arise, Ikawadani-cho, Nishi-ku, Kobe 651–21, Japan, Pharmacy, The City of Itami Hospital,[b] Konyoike 1–100, Itami, Hyogo 664, Japan and Fuji Paudal,[c] Chuo 2–2–30, Jyoto-ku, Osaka 536, Japan. *Received January 10, 1991*

A pulverized phenacetin powder with a mass median diameter of 11 μm was slightly granulated and subsequently coated to produce fine microcapsules by the Wurster process. As a membrane material, a 1:1:1 mixture of ethyl cellulose (EC), cholesterol (CH) and talc was used in the granulation, and a 1:1:0.06 mixture of EC, CH and stearyltrimethylammonium chloride in the coating. The produced microcapsules had a mass median diameter of 31 μm at 60% coating level and exhibited a practically useful sustained release at 40% or more coating.

In the granulation process, the membrane material solution was sprayed at a high rate of 14.2 ml/min upon 250 g of phenacetin powder. The mass median diameter was increased to 19 μm at a binder level of 3% (EC plus CH). The granules were then dried to reduce the particle size to 14 μm. This microgranulation and drying were effective for steady fluidization of the fine powder and to avoid excessive agglomeration. Coating was performed at a lower spray rate of 11.3 ml/min under a stronger agitation to avoid excessive agglomeration. During the coating process, however, an increase in the mass median diameter by 17 μm and the broadening of size distribution were unavoidable. The smallest size of particles which could be coated with no subsequent agglomeration was estimated to be 20 μm. The agglomeration of the particles smaller than 20 μm which occupied 78% of the raw powder accounted for the particle growth and the broadening of size distribution.

Keywords granulation; microcapsule; coating; ethyl cellulose; cholesterol; stearyltrimethylammonium chloride; Wurster process; powder; phenacetin; dissolution

The Wurster process is characterized by fine particle coating, and is a favorable technique for microencapsulation. However, there remain some problems to solve before it can be used practically.

In a previous paper,[1] calcium carbonate of 32—44 μm was layered with phenacetin and subsequently microencapsulated with a mixture of ethyl cellulose, cholesterol and stearyltrimethylammonium chloride (2:1:0.03). The produced microcapsules had a mass median diameter of 56 μm. In this study, the coating of finer pharmaceutical powders of the order of 10 μm was attempted. The previous calcium carbonate had a high density of 2.93 g/cm^3.[1] In the Wurster process, the particles blown up from partition have to fall down gravimetrically, therefore, heavier particles are more steadily fluidized. However, pharmaceutical powders very often have low particle densities, in addition, they are sometimes electrostatically charged, leading to retardation in particle recycling and to production of poorly coated microcapsules.[1] Although the Wurster method can process fine powder, it appeared that coating as fine a pharmaceutical powder as 10 μm as discrete particles would be difficult.

Ordinary top-sprayed granulation in a fluidized bed produces agglomerates with low apparent density and irregular, rough surface.[2] Since such agglomerates are not appropriate for subsequent coating, an additional consolidation and surface-smoothing by means of mechanical agitation are usually required.[2] As is well known, the particle motion in the Wurster process is very rapid, and particles collide with the inner surface of the partition, leading to the disintegration of large, weakly flocculated agglomerates.[3] Thus, this process can be expected to produce very fine, dense granules. Even if original particles were not coated as discrete particles and would unavoidably be agglomerated because of their fineness and low density, such dense agglomerates should be efficiently coated to produce fine microcapsules. Hence, the process in this study was designed for the fine powder to be first granulated and subsequently coated. Throughout both processes, materials known to be active as a permeation barrier were sprayed. The water soluble polymer used in usual fluidized granulation was not used.

Experimental

Materials As a model drug, phenacetin (Kawasaki Kagaku Kogyo Co., Ltd.) was used. The coarse phenacetin powder purchased was pulverized with a Sample-Mill (Fuji Paudal Co., Ltd.). Ethyl cellulose (EC, 30—50 cps), cholesterol (CH, SP reagent grade) and stearyltrimethylammonium chloride (STAC) were used as purchased from Nacalai Tesque Co., Ltd. Talc (JP XI grade, Maruishi) and anhydrous silica (Aerosil No. 200, Nippon Aerosil Co., Ltd.) were also used as purchased.

Coating A Glatt GPCG-1 Wurster was used. A spray nozzle of 0.6 mm diameter and a laminated filter with about 1 μm opening were set throughout all experiments.

Particle Size Distribution Sieve analysis was performed. All samples were premixed with anhydrous silica of 1%. An Alpine 200LS air jet sieve was operated at a charged weight of 10 g and a sieving time of 5 min in the range of 32 to 75 μm; in a range smaller than 32 μm, microsieves of 10, 20 and 30 μm were used at a charged weight of 1 g each, and the sieving was repeated until a constant weight was reached after 2 min of operation. In a range larger than 75 μm, a row-tap shaker (Iida Seisakusho Co., Ltd.) was used; the shaking time was 10 min and the charged weight was 20 g.

Droplet Size Distribution The sizes of sprayed droplets were determined at a distance of 30 mm from the nozzle by a light scattering spray analyzer (LDSA-1300A, Tonichi Computer Applications Co., Ltd.).

Dissolution Dissolution tests were performed as previously reported.[1]

Scanning Electron Microscopy (SEM) A Hitachi S430 was used.

Results and Discussion

Particle Design The attempt was made to finally produce as small microcapsules as possible. Since particles of 32 to 44 μm had been successfully processed and the microcapsules of 56 μm had been produced in a previous study,[1] it was attempted here to obtain products with a

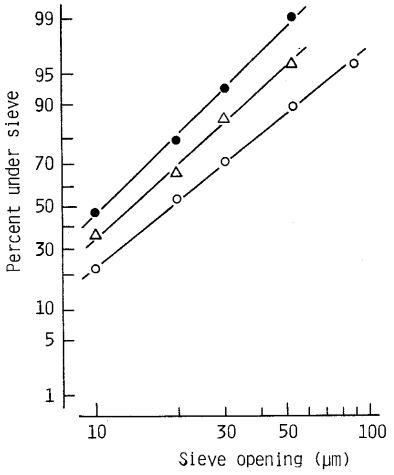

Fig. 1. Particle Size Distributions of Talc and Phenacetin Powders

○, phenacetin (P_a); ●, phenacetin (P_b); △, talc.

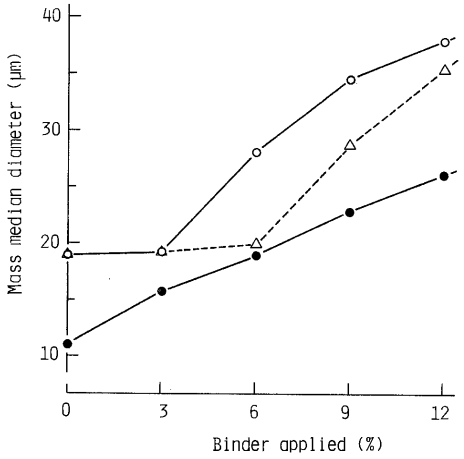

Fig. 2. Change of Mass Median Diameter in Granulation of the Powders of Different Size

Raw powder: ○, △, P_a; ●, P_b. Binder: EC–CH–talc (1 : 1 : 1). The binder applied is EC plus CH. Concentration of spray solution (EC plus CH, % (w/v)): ○, ●, 5; △, 3.

TABLE I. Operating Conditions in Granulation

Raw material: phenacetin P_a (19 μm) or P_b (11 μm)	250 g
Spray solution:	
EC	15 g
CH	15
Talc	15
Ethanol	
Total	600 ml
Operating conditions:	
Inlet air temperature (°C)	60
Outlet air temperature (°C)	24—28
Inlet air rate (m^3/min)	0.2
Spray rate (ml/min)	14.2
Spray pressure (atm)	2.5
Yield (%)	94

mass median diameter smaller than 30 μm.

The particle size distributions of pulverized phenacetin powders are shown in Fig. 1, where once or twice pulverized powder is respectively denoted by P_a or P_b. Mass median diameters were 19 and 11 μm, respectively, and particle sizes were well described by the log-normal distribution. Fine phenacetin particles with a low density of 1.24 g/cm^3 [4] did not seem to be discretely and steadily recycled in the Wurster chamber. Hence, the coating process was designed for fine particles to first be agglomerated at minimum until a steady fluidization was achieved and thereafter for the fine agglomerates to be coated under restrained agglomeration.

From the previous study,[1] the membrane thickness required for practically sustained release of phenacetin was estimated to be 1.5 μm, when EC–CH–STAC (2 : 1 : 0.03) was used as a membrane material. In that case, the coating level was 6.25% for cores of 32—44 μm. Hence, nearly 75 or 25% coating should respectively be required for 11 or 19 μm cores used in this study, if the particles were to be discretely coated without agglomeration. However, slightly agglomerated particles had exhibited a several times higher release rate.[1] A higher degree of agglomeration should not be avoided with the finer, lighter phenacetin particles, compared with calcium carbonate of 32—44 μm. In addition, the powders used in this study had a broader distribution of particle size (Fig. 1). These suggested that a stronger barrier against drug release might be required in this study.

The previous study also showed that, as the CH content became higher, phenacetin release and particle agglomeration were more suppressed.[1] Hence, the CH content was increased to EC : CH = 1 : 1. To reduce excessive agglomeration which might still occur even with EC–CH (1 : 1), talc was used as an anticoagulant in the granulation process. Although the talc powder had a large mass median diameter of 15 μm (Fig. 1), it should be brittle and easily flaked off, and was expected to lead to suppression of the size-enlargement of agglomerates.

Microgranulation Composition of the spray solution and the operating conditions for the microgranulation process with two phenacetin powders are shown in Table I. The concentration of EC–CH–talc (1 : 1 : 1) spray solution was 5% (w/v) (denoted as EC plus CH below). The operating conditions were specialized by a very high spray rate. This was because the phenacetin powder was adhered to the chamber wall in large quantity due to electrostatic charging, when sprayed at lower rates. At the beginning of the operation, the powder containing a great deal of solvent was remarkably flocculated and gradually began to flow freely. The phenacetin powder was granulated to the 3, 6, 9 or 12% level (denoted below as EC plus CH relative to phenacetin) and dried until the outlet air temperature had risen by 3 °C. Granules taken from the chamber were sieved for particle size analysis.

The change in mass median diameter (50% diameter) of granules is shown in Fig. 2 for the two phenacetin powders of different sizes. A significant difference in the time-course of agglomeration was observed between P_a and P_b. With P_a, the particle size distribution was little changed at the beginning of granulation and the mass median diameter was suddenly increased above the 3% binder level with 5% spray solution. A similar profile was observed with the 3% solution (Fig. 2), where the delay of size-enlargement was prolonged up to the 6% binder level. On the other hand, the mass median diameter was almost linearly increased for P_b.

A profile of delayed agglomeration was reported by

Shinoda *et al.* in the top-sprayed granulation of crystalline cellulose with water as a binder.[5] In their study, the granulation delay was not observed with corn starch, lactose or mannitol. The water-soluble lactose and mannitol were very quickly granulated and the insoluble corn starch more slowly. Since water was used as a binder, lactose and mannitol dissolved in spray droplets must have acted as interparticulate bridging material. The strong water-absorption of insoluble crystalline cellulose, in contrast, caused the delay, because the water absorbed by crystalline cellulose at the beginning of the granulation process could not effectively act as a binder, different from the case of corn starch.

The results of Shinoda *et al.*[5] suggested that the low coalescence probability[6] during the lag time accounted for the delay of granulation. In the Wurster process where particles are strongly agitated, the larger the particle size is, the lower is the coalescence probability. The delay observed only with the larger P_a in this study would partly result from easier disintegration of the flocculates composed of larger particles.

Sugimori *et al.*[7] analyzed their experimental results from fluidized bed granulation by computer simulation. When the granulation was assumed to proceed through the generation of nuclei, the experimental results agreed well with the simulation. When the nuclei were composed of 10 or less particles, there appeared a delay of granulation. It corresponded to the case where the ratio of droplet size to particle size was smaller than 1.2. The granulation proceeded more rapidly and was less delayed as the ratio became larger.

The droplet size measurement with the 5% spray solution in this study had complicated results. About 40% of the droplets were distributed in fractions smaller than 5 μm, and the residue was in the fraction of 8—30 μm. The mass median diameter of the latter was 15 μm. This suggested that the talc powder mixed into the spray solution (Fig. 1) might be causing the production of droplets of 15 μm. Since the ratios of the droplet size of 15 μm to the particle sizes of 11 and 19 μm were 1.4 and 0.8, respectively, the sizes of sprayed droplets might also explain why the delay of granulation was observed only with P_a.

In Fig. 3, the reduced mass median diameter, D_g/D_0, is plotted against the percentage of binder applied, where D_g and D_0 are the mass median diameters of granules and raw powders, respectively; with P_a the binder applied is made zero at the starting point of rapid size-enlargement. The data were well fitted to one line. This showed that granulation proceeded at the same rate for both powders and both concentrations in the case of P_a. However, in the granulation process, longer delay is usually followed by slower agglomeration, as well demonstrated by the simulation of Sugimori *et al.*[7] and the experimental results of Sagawa and Sakamoto[2] and Shinoda *et al.*[5] According to their results, the granulation in this study would have proceeded faster with P_b than with P_a and faster at 5% than at 3%.

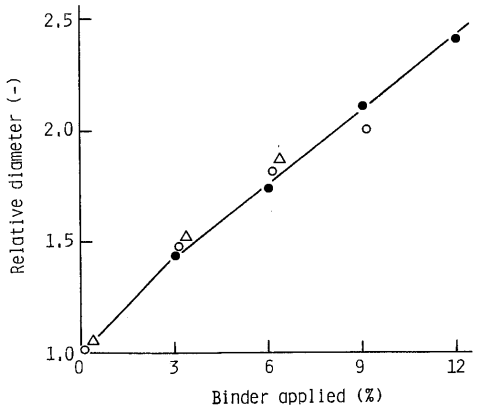

Fig. 3. Change of Relative Diameter, D_g/D_0, in Rapid Granulation Stage

Symbols and experimental conditions are the same as in Fig. 2.

In the present work, the difference of granulation between P_a and P_b in the Wurster process cannot be clearly explained. The strong agitation which acted on particles and agglomerates might have complicated the particle growth. Although P_a and P_b exhibited the same granulation rate after the delay in the experimental range used, the granulation of P_a even seemed to have a plateau after a longer granulation (Fig. 3). The complicated size distribution of the droplets containing solid particles also has to be further studied. Studies on elucidation of the mechanisms will be reported in the future.

As a model of fine powder, P_b was adopted below, because the particle size of P_a (Fig. 1) seemed too large and its agglomeration consequently led to the production of granules that were too coarse (Fig. 2).

Figure 4 shows the effect of drying in the chamber on the change of mass median diameter of P_b granules. The concentration of spray solution was fixed at 5% as EC plus CH. When the three kinds of formulations used were compared, talc was seen to be effective in restraining size-enlargement, though only a little. On the other hand, the difference of mass median diameter between undried and dried samples was very large: at 3 and 6% coating levels, becoming 6 and 9 μm (EC–CH–talc), respectively. These were very large compared with the desired size of the final product. These results suggested that the disintegration of weakly coagulated particles by drying prior to

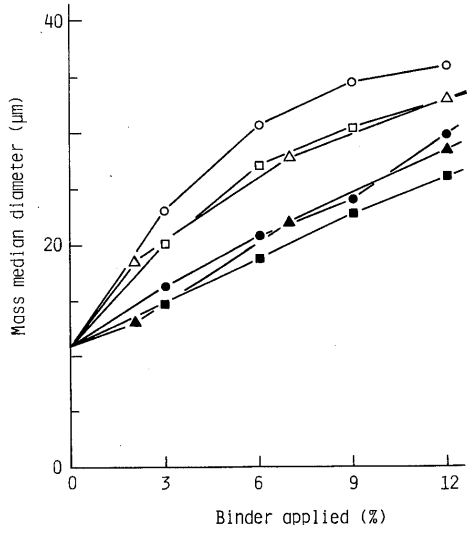

Fig. 4. Effect of Drying and Formulation of Binder on Change of Mass Median Diameter in Granulation of P_b

Closed symbols: after drying; open: before drying. Binder: ○, EC–CH (1 : 1); △, EC–CH–STAC (1 : 1 : 0.06); □, EC–CH–talc (1 : 1 : 1).

coating might be effective in reducing the particle size of microcapsules.

The granulation process has been studied in detail by Sekiguchi and Oota.[8] Granulation proceeds through the nuclei growth, transition and pellet growth (secondary agglomeration) regions. Apparently the granulation process demonstrated with the wet sample (undried) in Fig. 4 corresponded to the nuclei growth region. Sekiguchi and Oota[8] expressed the nuclei growth by Eq. 1, where the decrease in particle number was assumed to result from the coalescence and the destruction described by the second and first order kinetics, respectively.

$$dN/dt = -AN^2 + BN \quad (1)$$

where A and B are the rate constants and t the amount of binder applied (%). Equation 1 gave Eq. 2 by integration.

$$\ln \frac{D_{v,\infty}^3 - D_{v,t}^3}{D_{v,\infty}^3 - D_{v,0}^3} = -Bt \quad (2)$$

where $D_{v,0}$, $D_{v,t}$ and $D_{v,\infty}$ are the volume mean diameters at $t=0$, t and ∞, respectively. D_v can be replaced by the mass median diameter (D_{50}), when the particle size distributions during granulation are be described by the normal or log-normal probability law and their standard deviations are constant.

The size-enlargement of wet granules (Fig. 4) seemed to reach an equilibrium, as reported by Sekiguchi and Oota.[8] The particle size distributions of the wet granules were described on the log-normal probability paper by the lines broken at 32 μm; however, they seemed to be roughly approximated by the same standard deviation as that of P_b. By the least squares method based on Eq. 2 replaced D_v by D_{50}, D_{50} (μm) could be expressed by Eq. 3 for the wet granules prepared with EC–CH–talc.

$$D_{50}^3 = 51.1^3 - (51.1^3 - 10.8^3)\exp(-0.0257t) \quad (3)$$

The decrease in mass median diameter by drying clearly showed that weakly agglomerated particles still remained (Fig. 4). When the granule size would no longer be reduced by drying, the nucleation seemed to reach the equilibrium state, where the granules would become compact enough to accept an efficient coating. At the intersecting point of the linear regression line for dried granules (Fig. 4) and Eq. 3, the binder applied was 21.3% and the mass median diameter 38.5 μm. Granules of 38.5 μm were not available in this study which was aimed at producing small microcapsules, though they might be found useful for other applications.

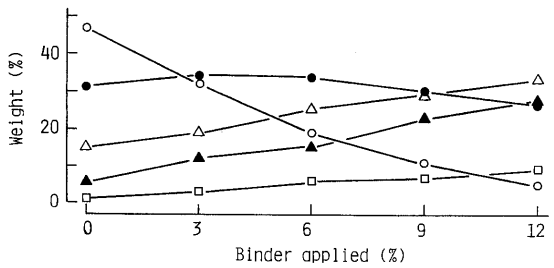

Fig. 5. Variation of the Weight of Dried Granules in Size Fractions during Granulation of P_b with EC–CH–Talc (1 : 1 : 1)

Size fraction: ○, −10 μm; ●, 10—20 μm; △, 20—32 μm; ▲, 32—53 μm; □, +53 μm.

The change of particle weight in each size fraction during granulation with EC–CH–talc is shown in Fig. 5 for dried granules. The weight of particles smaller than 10 μm was predominantly decreased, while that of particles larger than 20 μm was monotonously increased. The weight of 10—20 μm particles was at first increased due to the fast granulation of those smaller than 10 μm. It then decreased above the 6% binder level, which suggested that the 10—20 μm particles were also agglomerated. The production of particles larger than 53 μm was curtailed below 10%. The behavior of the 78% particles smaller than 20 μm which were contained in P_b played an important role in the granulation.

Microencapsulation with EC–CH–STAC (1 : 1 : 0.06) Details of the cores, the composition of spray solution and the operating conditions for both granulation and coating are listed in Table II. The spray solution of 5% and the phenacetin powder of P_b were used. At the beginning of the coating process, the operating conditions were changed to achieve a drier state and more rapid particle motion, and thus to suppress the agglomeration. For that purpose, the spray pressure and inlet air rate were increased to 3.5 atm and 0.5 m^3/min, respectively; the spray rate was decreased to about 11 ml/min. Talc was removed from the coating solution, since it had a large particle size of 15 μm, potentially resulting in formation of the particles with irregular, rough surface. Instead of talc, STAC was mixed to reduce particle adhesion due to electrostatic charge.[1]

In experiment-1 (exp.-1), the binder level in the granulation process was made 3%, where the powder seemed to achieve a free-flowing state. Wet granules (19 μm) were dried up to 3 °C higher outlet air temperature to reduce their size to 14 μm and thereafter coated at 11.3 ml/min.

TABLE II. Operating Conditions in Granulation and Coating

	Exp.-1		Exp.-2	
	Granulation	Coating	Granulation	Coating
Raw material: phenacetin, P_b (11 μm)				
Charged weight (g)	250		250	
Spray solution:				
EC	3.75 g	75 g	7.5 g	75 g
CH	3.75	75	7.5	75
Talc	3.75		7.5	
STAC		4.5		4.5
Ethanol				
Total	150 ml	3000 ml	300 ml	3000 ml
Operating conditions:				
Inlet air temperature (°C)	60	60	60	60
Outlet air temperature (°C)	28—29	26—29	28—31	27—30
Inlet air rate (m^3/min)	0.2	0.5	0.2	0.5
Spray rate (ml/min)	14.2	11.3	14.2	10.9
Spray pressure (atm)	2.5	3.5	2.5	3.5
Size of the product[a] (μm)	14	31	27	44
Yield (%)		90		90
Symbol of microcapsule		MC-1		MC-2

a) Mass median diameter.

The mass median diameter of the product was 31 μm at 60% coating level. The final yield was 90%.

As a reference, coating was performed under the same conditions without drying the wet granules, after the granulation was performed up to 6% binder level. Hence, at the beginning of the coating process, the mass median diameter of wet particles recycling in the chamber was 27 μm (Fig. 4). In this case, the mass median diameter of the product reached 44 μm at 60% coating level (Table II). In both exp.-1 and 2, there occurred a similar increase of 17 μm in the mass median diameter during coating.

In general, the agglomeration rate is strongly dependent on the sizes of sprayed droplets. Schaefer and Wørts[9] reported that the droplet size was dominated by air-to-liquid mass ratio at a constant concentration. Therefore, at a constant spray pressure, a lower spray rate should result in smaller droplet size and, consequently, in lower agglomeration due to weakening of the interparticulate bridge or decrease in the size of nuclei.[7] To reduce the agglomeration encountered in exp.-2, the spray rate was decreased to 6.2 ml/min. However, the mass median diameter of the product was contrarily increased to 99 μm. This can be explained by the view that the low spray rate led to the adhesion of small particles to the chamber wall due to the electrostatic charging, the coalescence of the oversprayed large particles and the layering of the small particles on large particles predominantly sprayed.[10]

The change of mass median diameter throughout the process is shown in Fig. 6. The wet sample was withdrawn at each coating level, mixed with 1% anhydrous silica and sieved without drying. In both exp.-1 and 2, the particle size was gradually increased until the 60% coating level. Comparison of exp.-1 and 2 revealed a difference only in the size of granules. The initial difference in granule size remained almost constant during coating. The granulation in exp.-1 reduced to the 3% level and the drying prior to coating were effective in decreasing the particle size of the product.

The particle size distributions of the products are shown in Fig. 7, compared with those of the related powder and granules. The product from exp.-1 (MC-1) was characterized by smaller mass median diameter and broader distribution. Although the product from exp.-2 (MC-2) had a large mass median diameter of 44 μm, its particle size distribution was sharper and the amount larger than 106 μm was not significantly different from that of MC-1.

The increase in particle size should continue until the smallest particles in the system became no longer agglomerated. The change of particle weight in each size fraction during coating is shown in Fig. 8. In both exp.-1 and 2, particles smaller than 20 μm were reduced in number and seemed to finally disappear; this is most clearly demonstrated by the results from exp.-2. The smallest size of the microcapsules coated as discrete particles without agglomeration was nearly 20 μm under the coating conditions set in this study (Table II). This lower particle size limit (20 μm) should be clearly dependent on the exerted agitation, the strength of interparticulate bridging materials and the droplet size. The coating conditions used in this study (Table II) were the strongest limit of agitation to be exerted on particles. The droplet size was also the lowest limit, since greater spray pressure caused the ejection of wet particles and droplets to the filter and a lower spray rate

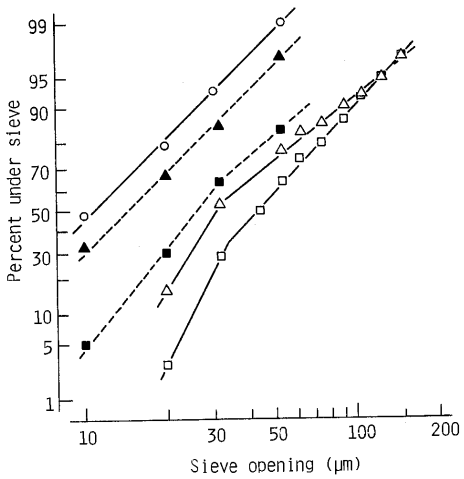

Fig. 7. Particle Size Distributions of MC-1, MC-2 and the Related Powder and Granules

○, P_b; △, ▲, MC-1; □, ■, MC-2. Closed symbols: before coating; open: after coating.

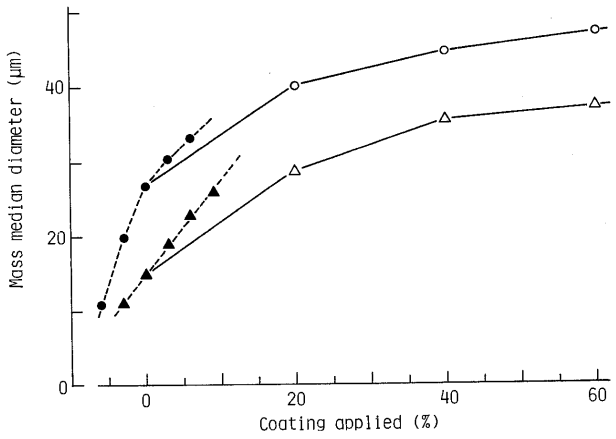

Fig. 6. Change of Mass Median Diameter in the Granulation and Coating Process

Microcapsule: △, ▲, MC-1; ○, ●, MC-2. Process: --, granulation; —, coating. Coating applied is EC plus CH.

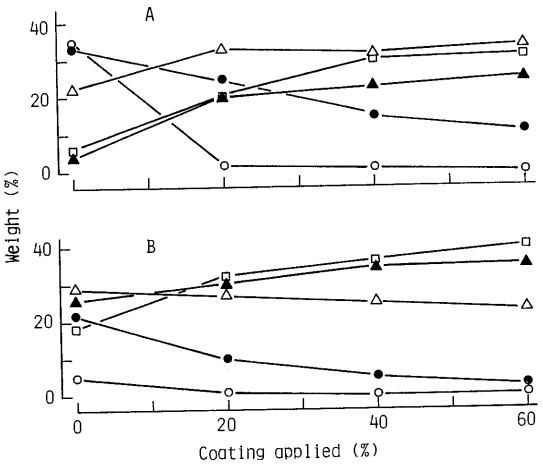

Fig. 8. Variation of Particle Weight in Size Fractions during Coating with EC–CH–STAC (1 : 1 : 0.06)

Size fraction: ○, −10 μm; ●, 10—20 μm; △, 20—32 μm; ▲, 32—53 μm; □, +53 μm. Operation: A, exp.-1; B, exp.-2.

caused particle adhesion to the wall due to electrostatic charging. Hence, if finer microcapsules from the Wurster process were desired, membrane materials of lower strength would have to be developed.

Sugimori *et al.*[7] reported the relation of the mean nucleus size *NN* (the number of particles in a nucleus) to the mean droplet size D_b in the granulation (Eq. 4).

$$NN = 6.44(D_b/D_p)^3 \quad (4)$$

where D_p is the mean particle size. The experiments of Sugimori *et al.*[7] were limited only to top-sprayed, fluidized bed granulation with a 5% hydroxypropyl cellulose aqueous solution. Although the analysis should be based on more comprehensive granulation processes, the difference in the agitation and the strength of membrane material or binder would roughly be reduced to that in the nucleus number *NN*. The size distribution of the droplets of EC–CH–STAC (1 : 1 : 0.06) solution sprayed in this study (Table II) was well explained by the log-normal probability law. The mass median diameter was 8.3 μm and the geometric standard deviation (σ_g) 1.79. Hence, it was estimated from Eq. 4 that the particles which could be granulated by the nucleation of two particles (the smallest nucleus size) might be 12 μm in diameter. Since this size of 12 μm was a mean diameter of core powder, the above estimation might explain the result that the lowest size of the particles to be coated without agglomeration was about 20 μm.

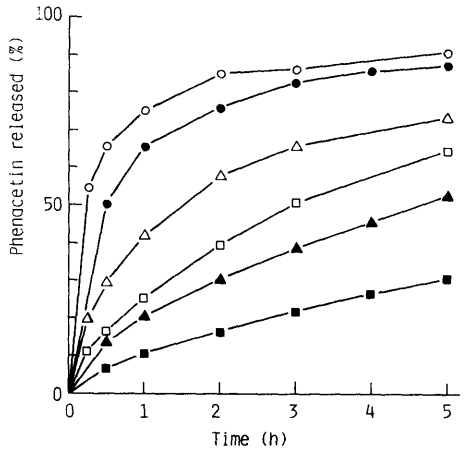

Fig. 9. Release of Phenacetin from EC Microcapsules Coated at Various Levels in JP XI Disintegration 2nd Fluid

Open symbols, MC-1; closed, MC-2. Coating level as EC plus CH (%): ○●, 20; △▲, 40; □■, 60.

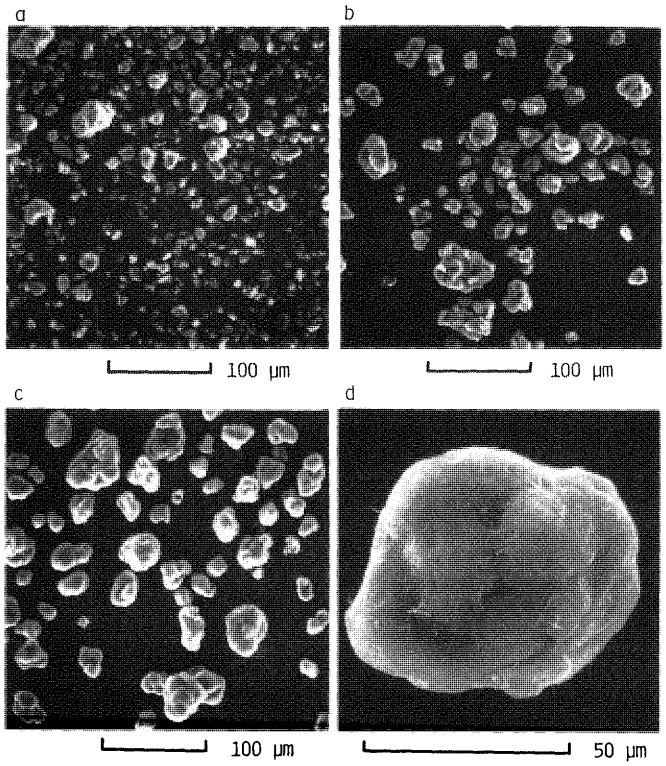

Fig. 10. Typical SEM Photographs of MC-1

Coating level (%): a, 0 (just before coating); b, 20; c and d, 60.

The dissolution profiles for MC-1 and 2 are shown in Fig. 9. The results showed 40% or more coated products to be practically useful for sustained release. The faster release from MC-1 than from MC-2 clearly resulted from its smaller particle size.

In Fig. 10 are shown SEM photographs of MC-1, which well demonstrate the process of size-enlargement. The granules (a) already contained coarse particles and fine particles adhered to the granular surfaces (Fig. 10a). After 20% coating (b), the fine particles seemed to disappear as expected from Fig. 8, but secondary agglomerates with irregular shape and porous structure were observed. Such insufficient encapsulation clearly led to the fast dissolution from 20% coated microcapsules (Fig. 9). At 60% coating level, the surfaces of particles became smooth and the pores became well covered with membrane (Figs. 10c and d). The fine particles around 20 μm were well coated at 60%, though the poor encapsulation of several percent of them might account for the bursting at the beginning of dissolution (Fig. 9).

Conclusion

A phenacetin powder with a mass median diameter of 11 μm was slightly granulated up to 19 μm using 3% binder, dried to reduce the size to 14 μm and subsequently coated by the Wurster process. The microcapsules produced had a mass median diameter of 31 μm at 60% coating level and exhibited a practically useful sustained release at 40% or above.

The agglomeration in the coating process seemed to continue until the smallest particles in the system were no longer agglomerated. The smallest size of the particles which could be processed with no successive agglomeration was estimated to be 20 μm. This would be the smallest microcapsules that the Wurster process has ever produced. To lower this limit further, the membrane material must be much weaker than EC–CH–STAC (1 : 1 : 0.06).

On the other hand, the agglomeration of particles smaller than the 20 μm current minimun led to the production of coarse particles, which accounted for a broad particle size distribution of product. The removal of particles smaller than the limit from raw powder would be effective for producting single-core microcapsules of the order of 20 μm.

Acknowledgements The authors would like to thank the staff of the Department of Research and Development, Okawara Seisakusho Co., Ltd., for their technical assistance in the measurement of droplet sizes.

References

1) Y. Fukumori, H. Ichikawa, Y. Yamaoka, Y. Takeuchi, T. Fukuda and Y. Osako, *Chem. Pharm. Bull.*, **39**, 164 (1991).
2) *a*) Y. Sagawa and T. Sakamoto, *Funtai Kogaku Kaishi*, **21**, 206 (1984); *b*) *Idem*, *ibid.*, **21**, 212 (1984); *c*) *Idem*, *ibid.*, **21**, 393 (1984).
3) Y. Fukumori, T. Fukuda, Y. Hanyu, Y. Takeuchi and Y. Osako, *Chem. Pharm. Bull.*, **35**, 2949 (1987).
4) J. Okada and Y. Fukumori, *Chem. Pharm. Bull.*, **23**, 326 (1975).
5) A. Shinoda, T. Nasu, M. Furukawa, S. Sakashita, K. Uesugi, Y. Miyake and S. Toyoshima, *Yakuzaigaku*, **36**, 83 (1976).
6) *a*) H. Sunada, A. Otsuka, Y. Kawashima and H. Takenaka, *Chem. Pharm. Bull.*, **27**, 3061 (1979); *b*) H. Sunada, A. Otsuka, Y. Tanaka, Y. Kawashima and H. Takenaka, *ibid.*, **29**, 273 (1981); *c*) Y. Kawashima, H. Takenaka, H. Sunada and A. Otsuka, *ibid.*, **30**, 280 (1982); *d*) Y. Kawashima, T. Keshikawa, H. Takenaka, H. Sunada and A. Otsuka, *ibid.*, **30**, 4457 (1982); *e*) Y. Kawashima, T. Handa, H. Takeuchi, K. Niwa, H. Sunada and A. Otsuka, *ibid.*, **34**, 833 (1986); *f*) H. Sunada, A. Otsuka, Y. Yamada, Y. Kawashima, H. Takenaka and J. T. Carstensen, *Powder Technol.*, **38**, 211 (1984).
7) K. Sugimori, S. Mori and Y. Kawashima, "Chemical Engineering Symposium Series 20," Society of Chemical Engineers, Tokyo, 1988, p. 20.
8) I. Sekiguchi and Y. Oota, Abstracts of Papers, 26th Summer Symposium of the Society of Power Technology, Kobe, 1990, p. 44.
9) T. Schaefer and O. Wørts, *Arch. Pharm. Chem. Sci. Ed.*, **5**, 178 (1977).
10) Y. Fukumori, Y. Yamaoka, H. Ichikawa, T. Fukuda, Y. Takeuchi and Y. Osako, *Chem. Pharm. Bull.*, **36**, 1491 (1988).

Kinetic Evaluation for Measurement of *in Vivo* Receptor Occupancy by Psychotropic Drug in Brain: Implication for Human Studies

Kiyomi ITO,*[,a] Yasufumi SAWADA,[a] Yuichi SUGIYAMA,[b] Manabu HANANO[b] and Tatsuji IGA[a]

Department of Pharmacy, University of Tokyo Hospital, Faculty of Medicine[a] and Department of Pharmaceutics, Faculty of Pharmaceutical Sciences,[b] University of Tokyo, Hongo, Bunkyo-ku, Tokyo 113, Japan. *Received January 10, 1991*

***In vivo* receptor occupancy of psychotropic drugs in brain can be estimated by measuring the tissue radioactivity of the tracer, which binds specifically to the receptor unoccupied by the drugs (back titration method). In this study, the validity of this method was evaluated by computer simulation, using various values for the plasma elimination rate, rate of transport across the blood–brain barrier, rate of receptor association and dissociation for both drug and tracer, and the sampling time. The differential equations based on a nonlinear three-compartment model including a plasma pool, precursor pool, and specific binding pool were solved numerically by the Runge–Kutta–Gill method. The receptor occupancy calculated by this method was close to the true value when the plasma concentration and specific binding fraction of the drug did not change greatly during circulation of the tracer. Although the error in calculated occupancy at 5 min after the tracer administration was smaller than that at 20 min, tracer may not greatly accumulate in brain tissue during the initial 5 min in some situations. Our analysis shows that it is necessary to adequately control the elimination rate of drug from plasma and to allow sufficient time for radioactivity to accumulate in the tissue. Therefore, this method requires previous knowledge of the pharmacokinetic behavior of both the drug and the tracer in plasma and tissue. The operation scheme that we suggest for the accurate measurement of the receptor occupancy *in vivo* can be used in human studies with positron emission tomography and may be useful for therapeutic drug monitoring.**

Keywords *in vivo* receptor occupancy; psychotropic drug; benzodiazepine; Ro 15-1788, kinetic simulation; brain

Introduction

In the therapy of neuro-psychiatric diseases, it is beneficial to monitor plasma concentration of a drug.[1] However, the receptor density and binding affinity of drugs to specific receptors can be altered by disease and/or chronic drug treatment. Even if similar plasma concentrations of a drug are achieved in all patients, there may be interindividual variations in the drug's therapeutic or side effects. According to the receptor occupancy theory, pharmacological effects of psychotropic drugs in the central nervous system should be proportional to their receptor occupancy.[2,3] Therefore, it is useful to relate pharmacologic effects directly to a measure of receptor occupancy *in vivo*.[4–7]

The techniques used for the measurement of receptor occupancy include *in vitro* measurement of radiolabeled ligand binding to membrane preparation from brain,[8] *in vitro* measurement of radiolabeled ligand binding after *in vivo* treatment of the drug (*ex vivo*),[6,7] and *in vitro* measurement of the remaining specific binding after *in vivo* treatment of both drug and radiolabeled ligand.[9,10] However, these three methods require tissue homogenization, centrifugation, and repeated washing to reduce nonspecific binding. These procedures may result in partial dissociation of the drug from the receptor.

In vivo receptor occupancy must be measured using a ligand which has a high specific/nonspecific binding ratio. Recently, it was suggested that the use of a specific antagonist [^{3}H]Ro 15-1788 made it possible to determine the time course of *in vivo* benzodiazepine receptor occupancy.[5,11,12] Farde *et al.* succeeded in measuring dopamine D_2 receptor occupancy of various antipsychotic agents in the living human brain using specific D_2 receptor antagonist ([^{11}C]raclopride) and positron emission tomography.[4,13] Thus, in order to carry out therapeutic drug monitoring in the treatment of schizophrenia, it may be useful to measure *in vivo* receptor occupancy of antipsychotic drugs. These methods are based on the *in vivo* measurement of specific and nonspecific binding of the radiolabeled tracer after the administration of therapeutic drug and tracer ligand.

In this study, the validity of the methodology for measuring *in vivo* receptor occupancy of psychotropic drugs was evaluated by pharmacokinetic modeling and computer simulation. We assumed the interaction of benzodiazepine/benzodiazepine receptor in the brain. The benzodiazepine receptor and receptor antagonist, [^{3}H]Ro 15-1788, were chosen as a model receptor–ligand system.

Theoretical

Radiolabeled tracer ligands, administered after psychotropic drug treatment, bind to the free receptors which are unoccupied by the drugs. When tracer ligands are administered in the absence of psychotropic drug (vehicle), however, all of the receptors are available for the tracer. The observed activities of tracer include not only its specific but also nonspecific binding which can be estimated in animal studies by the administration of excess drugs. Thus, the receptor occupancy is calculated as follows:

$$\text{percent occupancy} = \left(1 - \frac{A_{\text{drug}} - A_{\text{NS}}}{A_{\text{total}} - A_{\text{NS}}}\right) \times 100 \quad (1)$$

where A_{drug} and A_{total} are the radioactivities of tracer in the brain (dpm/mg tissue) in the presence and absence of the therapeutic dosing of the drug, respectively. A_{NS} is radioactivity in the presence of excess drug.

Based on this principle, Miller *et al.*[5] measured the benzodiazepine receptor occupancy of clonazepam and lorazepam using the antagonist [^{3}H]Ro 15-1788 as the tracer ligand. At 60 min after the administration of the drug or vehicle, radiolabeled tracer was administered intravenously. At 20 min after the tracer administration, the animal was decapitated and radioactivity in brain was measured (Fig. 1). In this study, the validity of this

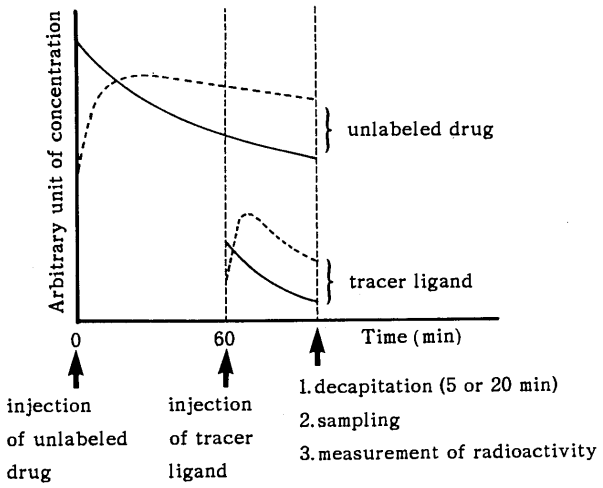

Fig. 1. Hypothetical Time Courses of Plasma (—) and Receptor-Bound (---) Concentrations of Unlabeled Drug and Radioactive Tracer Ligand

It is assumed that the radioactive tracer ligand was administered at 60 min after the treatment of psychotropic drug, and the radioactivity in brain was measured at 5 or 20 min later.

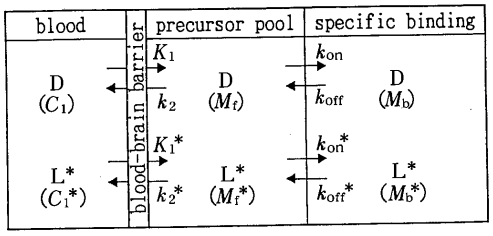

Fig. 2. Pharmacokinetic Model for Unlabeled Drug and Labeled Tracer Ligand

D and L* represent the drug and the tracer ligand, respectively. The following assumptions were made: $K_1=K_1^*$, $k_2=k_2^*$, $k_{on}=k_{on}^*$, and $k_{off}=k_{off}^*$. Density of the receptor unoccupied by the drug is represented as $B_{max}-M_b-M_b^*$. See text for the differential equations based on this model.

methodology was examined by computer simulation using various values for the plasma elimination rate, blood–brain barrier (BBB) transport rate constant, association/dissociation rate constants at the receptor site, and sampling time.

The three-compartmental model used in the simulation consisted of a plasma pool, precursor pool, and specific binding pool (Fig. 2). Nonspecific binding of the drug in the tissue was not incorporated in the model. Assuming that there is no difference in K_1 (influx clearance across BBB: ml/min/g), k_2 (efflux rate constant: min^{-1}), k_{on} (receptor association rate constant: min^{-1}/nM), and k_{off} (receptor dissociation rate constant: min^{-1}) between the drug and the tracer ligand, the following differential equations can be formed:

$$\frac{dM_f}{dt}=K_1C_1-k_{on}(B_{max}-M_b-M_b^*)M_f/V_d-k_2M_f+k_{off}M_b \quad (2)$$

$$\frac{dM_b}{dt}=k_{on}(B_{max}-M_b-M_b^*)M_f/V_d-k_{off}M_b \quad (3)$$

$$\frac{dM_f^*}{dt}=K_1C_1^*-k_{on}(B_{max}-M_b-M_b^*)M_f^*/V_d-k_2M_f^*+k_{off}M_b^* \quad (4)$$

$$\frac{dM_b^*}{dt}=k_{on}(B_{max}-M_b-M_b^*)M_f^*/V_d-k_{off}M_b^* \quad (5)$$

TABLE I. Parameters Used for the Simulation of *in Vivo* Receptor Occupancy

A (nM)	2000						
α (min^{-1})	0, 0.004, 0.04, 0.4						
A* (nM)	0.1						
α* (min^{-1})	0.07, 0.7, 7						
K_1 (ml/min/g)	0.01		0.1		1		
k_2 (min^{-1})	0.067		0.67		6.7		
K_1/k_2 (ml/g)	0.15		0.15		0.15		
k_{on} (min^{-1} nM^{-1})	0.00005	0.0001	0.0005	0.001	0.005	0.01	0.05
k_{off} (min^{-1})	0.001	0.005	0.01	0.05	0.1	0.5	1
$K_d(=k_{off}/k_{on})$[a] (nM)	20	20	20	20	20	20	20
B_{max}[b] (pmol/g)	20						

Parameters are based on binding of Ro15-1788 and clonazepam to the benzodiazepine receptor. Although K_1, k_2, k_{off} and k_{on} were changed within the range of three orders, the ratios K_1/k_2 and k_{off}/k_{on} ($=K_d$) were fixed at 0.15 ml/g and 20 nM, respectively. *a*) Taken from Inoue *et al.*[15] *b*) Taken from Pappata *et al.*[20]

where M_f and M_b represent the amount of drug (pmol/g) in the precursor pool and in the specific binding pool, respectively. M_f* and M_b* are the corresponding values of tracer ligand. B_{max} is the maximum concentration of specific binding sites (pmol/g). V_d is the physical volume of distribution of the ligand ($=0.8$ ml/g). C_1 and C_1* are plasma concentrations (nM) of the drug and the tracer, respectively. These input functions were assumed to decline monoexponentially:

$$C_1=A\exp(-\alpha t)$$

$$C_1^*=A^*\exp(-\alpha^* t)$$

Equations 2 to 5 were numerically solved by Runge–Kutta–Gill method.[14] As listed in Table I, we changed the values of parameters (K_1, k_2, k_{on}, k_{off}, α, and α*) in various ways. In order to simulate the situation of the animal experiments done by Miller *et al.*,[5] tracer ligand was administered 60 min after drug administration and circulated for 5 or 20 min in our modeling exercise (Fig. 1). First, we calculated the time course of tissue amount of unlabeled drug from 0 min to 80 min at intervals of 5 min based on Eqs. 2 and 3. Then, using the calculated amounts of drug at 60 min as the initial values, the time course of the tracer radioactivity in the presence of the therapeutic drug was estimated according to Eqs. 2 to 5. Finally, the amount of the tracer in the absence of drug administration was calculated by Eqs. 4 and 5. Using these estimated values, the percent receptor occupancy was calculated by the following Eq. 6 and compared with the "true occupancy" that was calculated by the computer program.

$$\text{percent occupancy}=\left(1-\frac{A_{drug}}{A_{total}}\right)\times 100 \quad (6)$$

Results

Effects of Plasma Elimination Rate, Brain Transport Rate and Receptor Binding Rate on the Recovery Ratio of the Estimated Receptor Occupancy The percent recovery of receptor occupancy is defined as the ratio of estimated occupancy to the true occupancy of a drug. Figure 3 shows the recovery ratio of receptor occupancy at 20 min after the tracer administration. The true occupancy was estimated from the drug amount in the specific binding pool at 0, 10, and 20 min after the tracer administration calculated

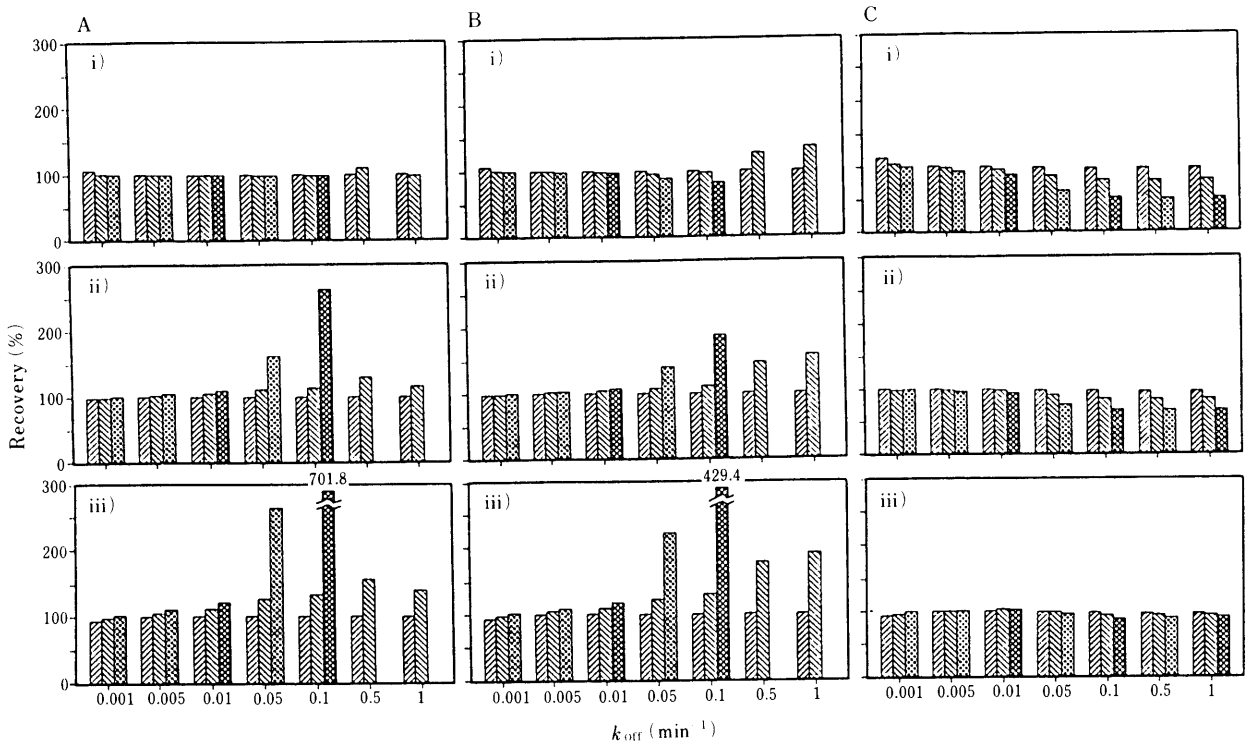

Fig. 3. Recovery Ratio of Receptor Occupancy at 20 min after the Tracer Administration

A: $K_1 = 1$ ml/min/g; B: $K_1 = 0.1$ ml/min/g; C: $K_1 = 0.01$ ml/min/g. Estimated occupancy was compared with true occupancy at τ min after the tracer administration [i) $\tau = 0$, ii) $\tau = 10$, iii) $\tau = 20$]. □: $\alpha = 0.004\,\text{min}^{-1}$, $\alpha^* = 0.07\,\text{min}^{-1}$; ▨: $\alpha = 0.04\,\text{min}^{-1}$, $\alpha^* = 0.7\,\text{min}^{-1}$; ■: $\alpha = 0.4\,\text{min}^{-1}$, $\alpha^* = 7\,\text{min}^{-1}$.

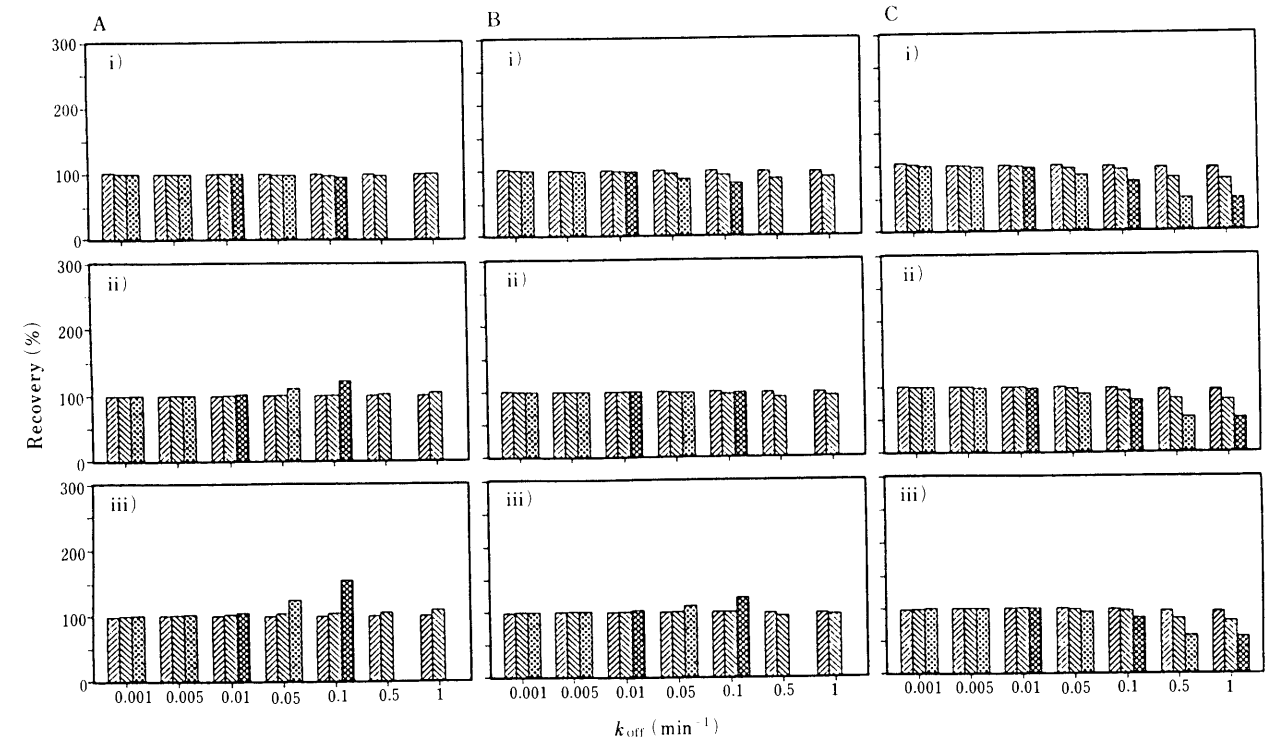

Fig. 4. Recovery Ratio of Receptor Occupancy at 5 min after the Tracer Administration

A: $K_1 = 1$ ml/min/g; B: $K_1 = 0.1$ ml/min/g; C: $K_1 = 0.01$ ml/min/g. Estimated occupancy was compared with true occupancy at τ min after the tracer administration [i) $\tau = 0$, ii) $\tau = 2.5$, iii) $\tau = 5$]. □: $\alpha = 0.004\,\text{min}^{-1}$, $\alpha^* = 0.07\,\text{min}^{-1}$; ▨: $\alpha = 0.04\,\text{min}^{-1}$, $\alpha^* = 0.7\,\text{min}^{-1}$; ■: $\alpha = 0.4\,\text{min}^{-1}$, $\alpha^* = 7\,\text{min}^{-1}$.

according to Eqs. 2 and 3. When the dissociation of the drug from the receptor was slow, a recovery of nearly 100% was observed for different plasma elimination rates. On the other hand, when the drug rapidly dissociated from the receptor and the plasma elimination was also rapid, the receptor occupancy was overestimated or underestimated at both rapid and slow BBB transport. Figure 4 shows the recovery ratio at 5 min after tracer administration using the

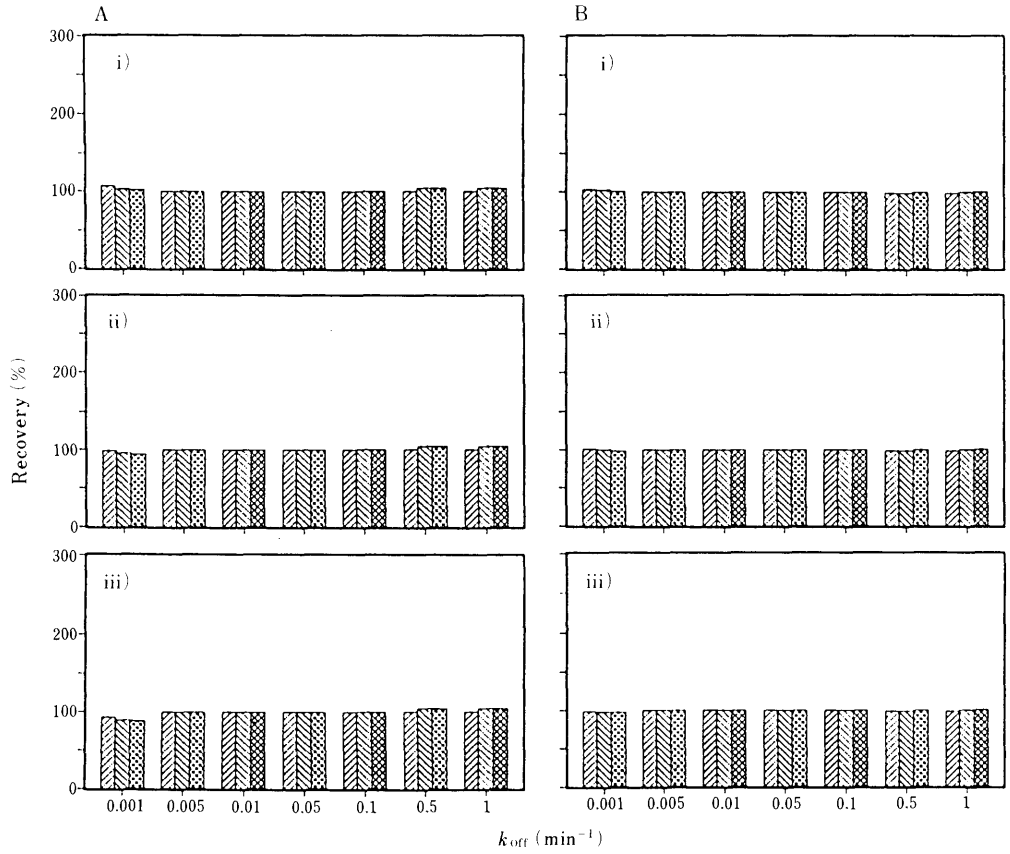

Fig. 5. Recovery Ratio of Receptor Occupancy at 20 (A) and 5 min (B) after the Tracer Administration when Plasma Concentration of the Drug Is in the Steady State

$K_1 = 0.1$ ml/min/g. Estimated occupancy was compared with true occupancy at τ min after the tracer administration [A) i) $\tau = 0$, ii) $\tau = 10$, iii) $\tau = 20$. B) i) $\tau = 0$, ii) $\tau = 2.5$, iii) $\tau = 5$]. ▨: $\alpha = 0\,\text{min}^{-1}$, $\alpha^* = 0.07\,\text{min}^{-1}$; □: $\alpha = 0\,\text{min}^{-1}$, $\alpha^* = 0.7\,\text{min}^{-1}$; ▩: $\alpha = 0\,\text{min}^{-1}$, $\alpha^* = 7\,\text{min}^{-1}$.

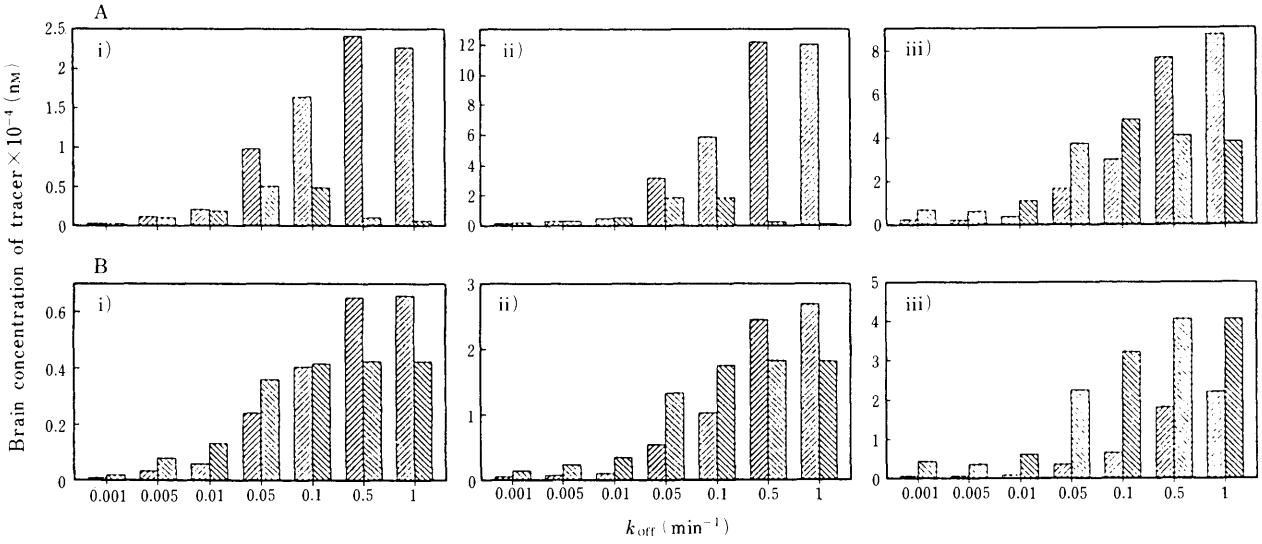

Fig. 6. Effects of Parameters on Tracer Radioactivity in Brain at 5 and 20 min after the Tracer Administration

A: $K_1 = 0.1$ ml/min/g; B: $K_1 = 0.01$ ml/min/g. ▨: At 5 min after tracer administration; □: At 20 min after tracer administration. i) $\alpha = 0.4\,\text{min}^{-1}$, $\alpha^* = 7\,\text{min}^{-1}$; ii) $\alpha = 0.04\,\text{min}^{-1}$, $\alpha^* = 0.7\,\text{min}^{-1}$; iii) $\alpha = 0.004\,\text{min}^{-1}$, $\alpha^* = 0.07\,\text{min}^{-1}$.

true values at 0, 2.5, and 5 min. The errors in Fig. 4 (at 5 min) are smaller than those in Fig. 3 (at 20 min). In both cases, when the plasma concentration of the drug is assumed to be in the steady state (*i.e.*, $\alpha = 0$), the recovery ratio of the occupancy was always around 100% (Fig. 5). This phenomenon was independent of the values of α^*, K_1, and k_{off}.

Effect of Sampling Time on the Radioactivity of the Tracer Ligand in Brain Figure 6 shows the bound concentration of the tracer ligand to the receptor at 5 and 20 min after the administration. The larger the values of K_1, k_{off}, and α are, the more rapid the elimination of the tracer from the

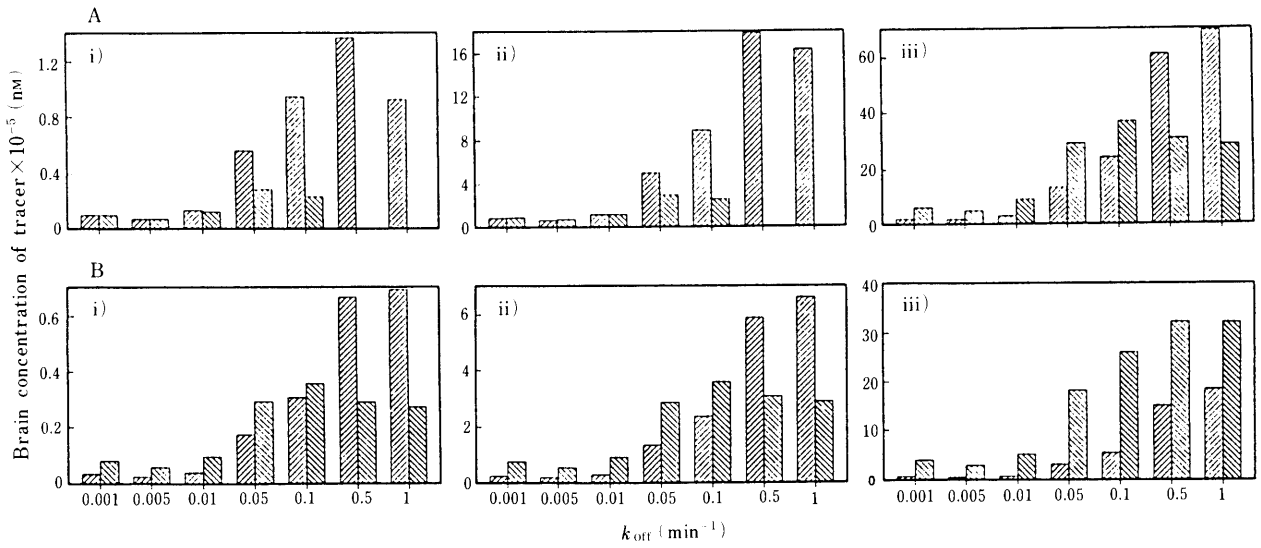

Fig. 7. Effects of Parameters on Tracer Radioactivity in Brain at 5 and 20 min after the Tracer Administration when Plasma Concentration of the Drug is in the Steady State

A: $K_1 = 0.1$ ml/min/g; B: $K_1 = 0.01$ ml/min/g. ▨: At 5 min after tracer administration; □: At 20 min after tracer administration. i) $\alpha = 0$ min^{-1}, $\alpha^* = 7$ min^{-1}; ii) $\alpha = 0$ min^{-1}, $\alpha^* = 0.7$ min^{-1}; iii) $\alpha = 0$ min^{-1}, $\alpha^* = 0.07$ min^{-1}.

tissue is. Furthermore, the radioactivity at 20 min was less than that at 5min. Figure 7 also indicates the effect of sampling time on the tissue radioactivity of the tracer. Simulation condition in Fig. 7 is the same as that in Fig. 6 except that plasma concentration of the drug was assumed to be in the steady state (*i.e.*, $\alpha = 0$). The ratio of the tracer radioactivity at 5 min and that at 20 min increased with the increases in K_1, k_{off}, and α^*, resulting from the rapid distribution and elimination of the tracer ligand.

Discussion

The simple method of measuring *in vivo* receptor occupancy in this study will be valid only when the following important points are assumed: 1) Transport of the tracer across BBB is based on a simple diffusion and is not affected by the therapeutic drug. 2) The tracer is not metabolized in the brain and the metabolites of the tracer in plasma do not cross the BBB and enter brain tissue. These assumptions seem to be reasonable for the benzodiazepine antagonist [^{3}H]Ro15-1788, because it is a highly lipophilic compound and none of its metabolites appear in the brain.[15] Furthermore, Miller *et al.*[5] reported that the brain concentrations of [^{3}H]Ro15-1788 in vehicle-treated control animals were similar to those in animals treated with a saturating dose of benzodiazepine (lorazepam). Thus, unlabeled benzodiazepines do not appear to alter the uptake of [^{3}H]Ro15-1788 into brain.

It is also necessary for the accurate measurement of *in vivo* receptor occupancy that a tracer ligand be selected which has a high specific/nonspecific binding ratio. Goeders and Kuhar[11] reported that the use of Ro15-1788 as tracer radioligand results in high specific/nonspecific binding ratios in tissues from intact animals without washing or homogenization. Therefore, in this regard, too, [^{3}H]Ro15-1788 seems to be a suitable tracer ligand for measuring benzodiazepine receptor occupancy *in vivo*.

In addition to the benzodiazepine receptor mentioned above, the receptors for which measurement of occupancy *in vivo* is now expected to be possible include dopamine D_2 receptor and opioid receptor, using raclopride and cyclofoxy as respective tracer ligands.[13,16] Based on rat studies, it has been suggested that the BBB transport of both ligands is rapid and their metabolites do not appear in the brain tissue.[15,17] These ligands, therefore, may possibly be used for measuring *in vivo* receptor occupancy of both receptors.

Optimal Condition for the Measurement of *in Vivo* Receptor Occupancy As shown in Figs. 3 and 4, the correct receptor occupancy of psychotropic drugs could be obtained by this simple method when the dissociation rate of the drug from the receptor sites was slow and the time-dependent change in receptor occupancy was small during the experimental period. On the other hand, error in the recovery of *in vivo* receptor occupancy would be large when the drug rapidly dissociates from the receptor sites, especially in the case of rapid plasma elimination. However, considering that plasma elimination constants of 0.4 min^{-1} for drug and 7 min^{-1} for radioactive tracer ligand are unlikely, this method seems valid for most cases.

In almost all cases, the recovery ratio at 5 min after tracer administration was nearly 100% as compared with that at 20 min. As shown in Figs. 6 and 7, however, the tracer may not yet have sufficiently accumulated in the brain at 5 min after administration.

From these findings, the optimal conditions for accurate measurement of *in vivo* receptor occupancy can be set up by scheduling a dosage regimen based on a slow plasma elimination rate and by obtaining sufficient brain radioactivity within a short period.

Clinical Application Positron emission tomography (PET) offers a new and exciting approach for the mapping of brain metabolism and neuro-receptors. The development of PET and single photon emission computed tomography (SPECT) makes it possible to evaluate the quantitative localization of the receptors in living human brain.[18] The receptor densities, affinities, and binding potential have been estimated using [^{11}C]methylspiperone[19] or [^{11}C]raclopride[13] for dopamine D_2 receptor, [^{11}C]Ro15-1788[20] for benzodiazepine receptor, and [^{18}F]cyclofoxy[16] for opioid

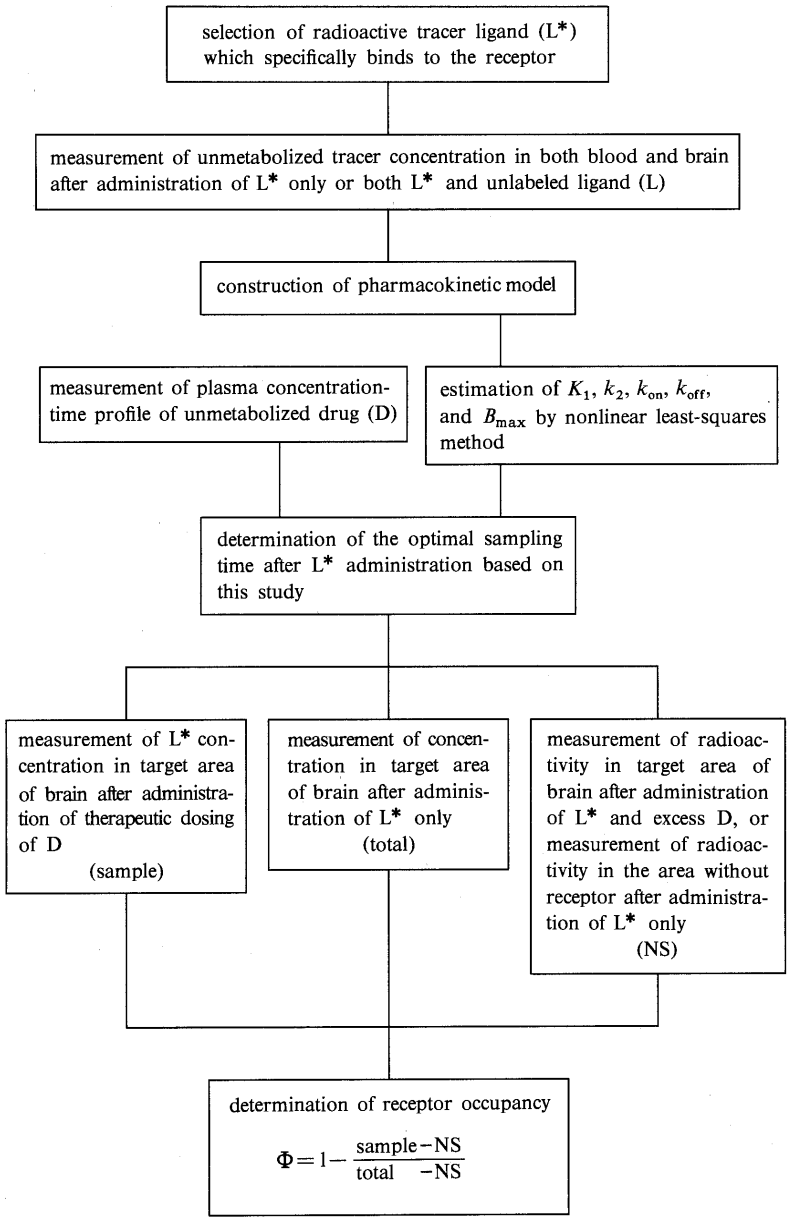

Fig. 8. Flow Chart for Determination of Receptor Occupancy *in Vivo*
See text for details.

receptor. Furthermore, Farde *et al.*[4] measured the *in vivo* receptor occupancy of various antipsychotics using [^{11}C]raclopride. Lee *et al.*[21] measured time dependency of *in vivo* receptor occupancy of naltrexone using [^{11}C]carfentanil. The methodologies which are used for the measurement of receptor occupancy in these human studies are almost the same as those presented by Goeders and Kuhar,[11] Miller *et al.*[5] and us. However, the validity of the method for determination of *in vivo* receptor occupancy has not been fully examined. In this study, we used a computer simulation to help in the evaluation of this technique. We also propose a scheme for accurately measuring receptor occupancy *in vivo* (Fig. 8).

First of all, in order to estimate the *in vivo* receptor occupancy of a psychotropic drug, various parameters (BBB transport rate constants and specific/nonspecific binding parameters) have to be determined based on pharmacokinetic behavior of the tracer in plasma and brain. If these parameters are obtained along with the plasma concentration–time profile of the drug, it should be possible to determine the optimal sampling time. Then, the tracer radioactivities in the brain are measured in the absence and presence of the therapeutic or excess dosing of the drug. Using these values, receptor occupancy can be calculated by Eq. 1. Nonspecific binding of tracer ligands can be estimated by the treatment of excess drug before administration of tracer. In human studies where the administration of excess drug is impossible, the radioactivity in a brain region without specific receptors may be used to estimate nonspecific binding. Since there is no dopamine D_2 receptor or opioid μ and/or κ receptor in cerebellum, the accumulation of raclopride or cyclofoxy in this organ are utilized as nonspecific binding potency of tracer ligands. In other cases, the nonspecific binding can be estimated

from the accumulation of the tracer enantiomer which has very low affinity for the receptor.[22-24] These methods make it possible to estimate the nonspecific binding of the tracer, and thus to measure the receptor occupancy *in vivo* in the living human brain.

In conclusion, the pharmacokinetical characteristics of a psychotropic drug and a tracer ligand (BBB permeability, association and dissociation rates at the receptor sites, metabolic process inside and outside the brain tissue, half-life of plasma elimination, *etc.*) have to be taken into consideration for the accurate measurement of *in vivo* receptor occupancy. In neuropsychiatric diseases, the simple method presented here may be useful for therapeutic drug monitoring under defined conditions and may result in achievement of a maximum therapeutic response with minimum side-effects.

Acknowledgements We thank Dr. Ronald G. Blasberg for his comments and suggestions.

References

1) S. G. Dahl, *Clin. Pharmacokin.*, **11**, 36 (1986).
2) A. J. Clark, *J. Physiol.* (London), **61**, 530 (1926a).
3) A. J. Clark, *J. Physiol.* (London), **61**, 547 (1926b).
4) L. Farde, F.-A. Wiesel, C. Halldin and G. Sedvall, *Arch. Gen. Psychiatry*, **45**, 71 (1988).
5) L. G. Miller, D. J. Greenblatt, S. M. Paul and R. I. Shader, *J. Pharmacol. Exp. Ther.*, **240**, 516 (1987).
6) S. M. Paul, P. J. Syapin, B. A. Paugh, V. Moncada and P. Skolnick, *Nature* (London), **281**, 688 (1979).
7) Y. Igari, Y. Sugiyama, Y. Sawada, T. Iga and M. Hanano, *Drug Metab. Disp.*, **13**, 102 (1985).
8) J. Dingemanse, M. Danhof and D. D. Breimer, *Pharmac. Ther.*, **38**, 1 (1988).
9) R. S. L. Chang and S. H. Snyder, *Eur. J. Pharmacol.*, **48**, 213 (1978).
10) M. J. Williamson, S. M. Paul and P. Skolnick, *Life Sci.*, **23**, 1935 (1978).
11) N. E. Goeders and M. J. Kuhar, *Life Sci.*, **37**, 345 (1985).
12) H. Ishizuka, Y. Sawada, K. Ito, Y. Sugiyama, H. Suzuki, T. Iga and M. Hanano, *J. Pharmacol. Exp. Ther.*, **251**, 362 (1989).
13) L. Farde, H. Hall, E. Ehrin and G. Sedvall, *Science*, **231**, 258 (1986).
14) K. Yamaoka and T. Tanigawara, "Maikon Ni Yoru Yakubutu Sokudoron Nyumon," Nanko-do, Tokyo, 1981.
15) O. Inoue, Y. Akimoto, K. Hashimoto and T. Yamasaki, *Int. J. Nucl. Med. Biol*, **12**, 369 (1985).
16) R. E. Carson, M. A. Channing, R. G. Blasberg, M. McManaway, R. M. Cohen, G. I. Jacobs, J. M. Benett, R. D. Finn, K. Rice, A. H. Neuman and S. M. Larson, *J. Cereb. Blood Flow Metab.*, **7**, s-343 (1987).
17) C. Kohler, H. Hall, S.-O. Ogren and L. Gawell, *Biochem. Pharmacol.*, **34**, 2251 (1985).
18) J. R. Barrio, S. C. Huang and M. E. Phelps, *Ann. Rev. Pharmacol. Toxicol.*, **28**, 213 (1988).
19) D. F. Wong, A. Gjedde, H. N. Jr. Wagner, R. F. Dannals, K. H. Douglass, J. M. Links and M. J. Kuhar., *J. Cereb. Blood Flow Metab.*, **6**, 147 (1986).
20) S. Pappata, Y. Samson, C. Chavoix, C. Prenant, M. Maziere and J. C. Baron, *J. Cereb. Blood Flow Metab.*, **8**, 304 (1988).
21) M. C. Lee, H. N. Jr. Wagner, S. Tanda, J. J. Frost, A. N. Bice and R. F. Dannals, *J. Nucl. Med.*, **29**, 1207 (1988).
22) Y. Sawada, S. Hiraga, B. Francis, C. Patlak, K. Pettigrew, K. Ito, E. Owens, R. Gibson, R. Reba, W. Eckelman, S. Larson and R. G. Blasberg, *J. Cereb. Blood Flow Metab.*, **10**, 781 (1990).
23) R. Kawai, Y. Sawada, M. Channing, A. H. Newman, K. C. Rice and R. G. Blasberg, *Am. J. Physiol.*, **259**, H1278 (1990).
24) R. Kawai, Y. Sawada, M. Channing, B. Dunn, A. H. Newman, K. C. Rice and R. G. Blasberg, *J. Pharmacol. Exp. Ther.*, **255**, 826 (1990).

Kinetic Evaluation of Pharmacological Effects Based on Allosteric Coupling of the Benzodiazepine/γ-Aminobutyric Acid$_A$ Receptor in the Brain

Yasufumi SAWADA,*[,a] Kiyomi ITO,[a] Yuichi SUGIYAMA,[b] Manabu HANANO[b] and Tatsuji IGA[a]

Department of Pharmacy, University of Tokyo Hospital, Faculty of Medicine,[a] Department of Pharmaceutics, Faculty of Pharmaceutical Sciences,[b] University of Tokyo, Hongo, Bunkyo-ku, Tokyo 113, Japan. *Received January 10, 1991*

A mathematical allosteric coupling model has been proposed to describe the process by which binding to the benzodiazepine/γ-aminobutyric acid (GABA) receptor complex initiates a biological response. The model states that the first receptors (benzodiazepine receptors) can diffuse independently in the plane of the membrane and reversibly associate with the second receptors (GABA receptors) to regulate their activity (induction of increased chloride ion flux due to the opening of the chloride ion channel). The ratio of agonist-bound to total GABA receptor density was defined to be directly proportional to the biological response in the model. The analysis makes the following assumptions: i) the binding affinity of agonists (muscimol or benzodiazepine) to the benzodiazepine receptor/GABA receptor complex is much greater than that to each receptor alone; ii) the double receptor–single agonist (benzodiazepine, muscimol or GABA) ternary complex binds to the other agonist with a high binding affinity as compared with that of each agonist to an agonist-free receptor complex; iii) benzodiazepine receptor–GABA receptor interaction is enhanced in the presence of each agonist; iv) the GABA receptor is desensitized after the binding of GABA agonist (GABA or muscimol) to the receptor. The modeling exercise shows that the benzodiazepine concentration required for half-maximal biological response is lower than that required for half-maximal receptor binding. In the case of the GABA agonist, a linear relationship between receptor occupancy and biological response was observed. The degree of discrepancy between the two profiles (receptor occupancy and biological response) concerning benzodiazepine concentration dependency and time dependency increased with a decrease in the dissociation constants based on the benzodiazepine receptor–GABA receptor interaction. This model offers a simple explanation for discrepancies between the receptor occupancy–concentration profile of benzodiazepine and the biological response–concentration curve that are often observed *in vivo* and/or *in vitro*.

Keywords benzodiazepine; benzodiazepine receptor; GABA; GABA receptor; muscimol; allosteric coupling; desensitization; chloride channel

Introduction

γ-Aminobutyric acid$_A$ (GABA$_A$) receptors are known to induce ionotrophic transmission by binding an agonist, GABA or muscimol. GABA receptors translocate chloride anions selectively by binding GABA or muscimol. The relationship between the biological response and agonist binding to the receptor results in inactivation (desensitization) of the receptor, as well as ion translocation.[1] Benzodiazepines produce their major pharmacological actions by augmenting the actions of the primary inhibitory neurotransmitter in the brain, GABA. Benzodiazepines bind to specific recognition sites associated with the postsynaptic GABA$_A$ receptor with affinities that are highly correlated with their behavioral potencies as anxiolytic, anticonvulsant, and sedative/hypnotic agents.[2-5] Furthermore, benzodiazepine agonists have been demonstrated to increase the affinity of GABA$_A$ recognition sites associated with the GABA receptor/chloride ion channel complex.[6-8] An oligomeric protein complex consists of several subunits with allosteric recognition sites for benzodiazepines and barbiturates that are structurally associated with a chloride ion channel.[4,9-11] It is very interesting to kinetically evaluate the cascade for intracellular transduction concerning the benzodiazepine receptor/GABA receptor/chloride channel complex.

Comparisons are often made between the concentration of agonist required for a half-maximal biological response (ED_{50}), and the concentration required for half-maximal receptor occupancy (K_d). In some cases these two concentration profiles are similar, but in many others, ED_{50} is much smaller or larger than K_d.[12-16] Various approaches have been used to account for these differences. Several models have been devised that predict a nonlinear relationship between agonist binding by functional receptors and biological response.[17,18-20] More recently, we have reported the nonlinear relationship between *in vivo* receptor occupancy of benzodiazepines, such as diazepam and clonazepam, and changes of pharmacological behavior and regional glucose utilization in rats and mice.[21,22]

Rigorous kinetic analyses concerning the quantitative relationship between benzodiazepine receptor–GABA receptor interaction and pharmacological effects have not been performed. Aoshima *et al.*[1] and Cash and Subbarao[23,24] estimated equilibrium and rate constants for GABA receptors from the results of five different measurements using a model and procedures similar to that described for the acetylcholine receptor.[25] Several mathematical approaches have been proposed to kinetically describe the biological responses based upon the receptor–effector interaction.[17,26,27] In this paper, we present a new mathematical model that addresses the dependence of the receptor occupancy of benzodiazepine and biological response upon agonist concentration in order to evaluate positive allosteric interactions between the GABA receptor and benzodiazepine receptors. This model illustrates the non-linear relationship between receptor occupancy and biological response.

Methods

System Components The model for kinetic analysis is shown in Fig. 1. The model consists of the benzodiazepine receptor (BR), the active form of the GABA receptor (GR), the inactive form of the GABA receptor (IR), and the following designations: benzodiazepine (B), GABA (G), muscimol (M), and cellular effect (E).

BR: Agonist, B interacts with BR, and BR can interact with the GABA

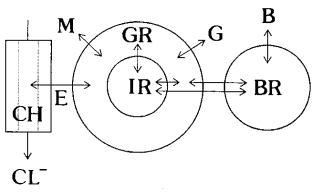

Fig. 1. A Schematic Representation of the Molecular Association of GABA Agonist, Benzodiazepine Agonist, GABA Receptor and Benzodiazepine Receptor

B, benzodiazepine; BR, benzodiazepine receptor; G, GABA; M, muscimol; GR, active form of GABA receptor; IR, inactive form of GABA receptor; CH, chloride channel; CL^-, chloride ion. Arrows show association/dissociation process of agonist–receptor and receptor–receptor interaction, activation/inactivation process of receptors and transport process of ions. See the text for detail.

receptor (GR or IR).

GR: Agonist, G or M interacts with GR, which has two binding sites; a domain for the binding of BR and a domain for interaction with the chloride channel.

IR: Desensitization (inactivation) of GR and recovery of IR to the GR state upon removal of the agonist are induced. IR does not interact with the chloride channel.

E: The response, E, is postulated to be a linear increasing function proportional to the concentration of the GABA receptor (GR)–agonists (G or M) complex.

Model Assumptions 1: Binding sites for GABA and benzodiazepines are located on the different polypeptide chains (or subunits).

2: Endogenous ligands for the benzodiazepine receptor are not considered.

3: B binds to a single site of BR, BR–GR, BR–GR–G or BR–IR–G.

4: G or M binds to a single site of GR, BR–GR or B–BR–GR.

5: Association and dissociation rates of agonists (B or G) to each receptor are rapid. Instantaneous equilibrium was assumed for the binding of G, M or B to the receptors. On the other hand, desensitization of the GABA receptor and the recovery processes are slow; rate constants for each process (on-rate and off-rate) can be established.[1)]

6: Rank order for binding affinity of B to BR, BR–GR and BR–GR–G (or BR–GR–M) are BR < BR–GR < BR–GR–G, BR–GR–M. This assumption is reasonable and is based on the report of Tallman.[28)]

7: The rank order for binding affinity of G (or M) to GR, BR–GR and B–BR–GR are GR < BR–GR < B–BR–GR. This assumption is also reasonable.[29)]

8: G (or M) and GR complexes (GR–G, GR–M, BR–GR–G, BR–GR–M, B–BR–GR–G and B–BR–GR–M) are desensitized to inactive forms of GR (IR–G, IR–M, BR–IR–G, BR–IR–M, B–BR–IR–G and B–BR–IR–M), respectively.

9: G (or M) and GR complexes (GR–G, GR–M, BR–GR–G, BR–GR–M, B–BR–GR–G and B–BR–GR–M) are only related to pharmacological effects (induction of chloride channel opening). There are no differences in intrinsic activity (ε) among these components. Therefore, the following equation for total activity (E_{all}) is obtained.

$$E_{all}=\varepsilon([GR–G]+[BR–GR–G]+[B–BR–GR–G]+[GR–M]+[BR–GR–M]+[B–BR–GR–M]) \quad (1)$$

10: Free agonist concentration is equal to total agonist concentration. The indicated concentration of agonists in this article means the free concentration around the receptors.

Model Development Conservation of the Benzodiazepine Receptor: The concentration of the total receptor, $[BR]_0$, is given by:

$$[BR]_0=[BR]+[B–BR]+[BR–GR]+[BR–GR–G]+[B–BR–GR]+[B–BR–GR–G]+[B–BR–IR–G]+[BR–IR–G]+[BR–GR–M]+[B–BR–GR–M]+[B–BR–IR–M]+[BR–IR–M] \quad (2)$$

where [BR] = free benzodiazepine receptor concentration, [B–BR] = concentration of the benzodiazepine receptor agonist complex, [BR–GR] = concentration of the benzodiazepine receptor GABA receptor complex, [BR–GR–G] = concentration of the ternary complex of BR, GR and G, [B–BR–GR] = concentration of the ternary complex of BR, GR and B, [B–BR–GR–G] = concentration of the quadruple complex of GR, BR, G, and B, [BR–IR–G] = concentration of the ternary complex of IR, BR and G and [B–BR–IR–G] = concentration of the quadruple complex of IR, G, BR and B, [BR–GR–M] = concentration of the ternary complex of BR, GR and M, [B–BR–GR–M] = concentration of the quadruple complex of GR, BR, M, and B, [BR–IR–M] = concentration of the ternary complex of IR, BR and M and [B–BR–IR–M] = concentration of the quadruple complex of IR, M, BR and B, respectively.

Conservation of the GABA Receptor: The concentration of the total receptor, $[GR]_0$, is given by:

$$[GR]_0=[GR]+[GR–G]+[BR–GR]+[BR–GR–G]+[B–BR–GR]+[B–BR–GR–G]+[B–BR–IR–G]+[BR–IR–G]+[IR–G]+[GR–M]+[BR–GR–M]+[B–BR–GR–M]+[B–BR–IR–M]+[BR–IR–M]+[IR–M] \quad (3)$$

where [GR] = GABA receptor concentration, [GR–G] = concentration of the GABA receptor and GABA complex, [IR–G] = concentration of the inactive GABA receptor and G complex, [GR–M] = concentration of the GABA receptor and M complex and [IR–M] = concentration of the inactive GABA receptor and M complex, respectively.

Equilibria between GABA (or Benzodiazepine) Receptor and Each Agonist: The law of mass action governs interactions involving receptor species:

$$K_{d,1}=[BR][B]/[B–Br] \quad (4)$$

$$K_{d,2}=[GR][G]/[GR–G] \quad (5)$$

$$K_{d,3}=[BR–GR][B]/[B–BR–GR] \quad (6)$$

$$K_{d,4}=[BR–GR][G]/[BR–GR–G] \quad (7)$$

$$K_{d,5}=[BR–GR–G][B]/[B–BR–GR–G] \quad (8)$$

$$K_{d,6}=[B–BR–GR][G]/[B–BR–GR–G] \quad (9)$$

$$K_{d,14}=[GR][M]/[GR–M] \quad (10)$$

$$K_{d,15}=[BR–GR][M]/[BR–GR–M] \quad (11)$$

$$K_{d,16}=[BR–GR–M][B]/[B–BR–GR–M] \quad (12)$$

$$K_{d,17}=[B–BR–GR][M]/[B–BR–GR–M] \quad (13)$$

$$K_{d,25}=[BR–IR–G][B]/[B–BR–IR–G] \quad (14)$$

$$K_{d,28}=[BR–IR–M][B]/[B–BR–IR–M] \quad (15)$$

where $K_{d,1-6}$, $K_{d,14-17}$, $K_{d,25}$ and $K_{d,28}$ are the dissociation constants (nM) for the receptor (GABA receptor or benzodiazepine receptor)–agonist (GABA, muscimol or benzodiazepine) complexes.

Equilibria between GABA Receptor and Benzodiazepine Receptor:

$$K_{d,7}=[BR][GR]/[BR–GR] \quad (16)$$

$$K_{d,8}=[BR][GR–G]/[BR–GR–G] \quad (17)$$

$$K_{d,9}=[B–BR][GR]/[B–BR–GR] \quad (18)$$

$$K_{d,10}=[B–BR][GR–G]/[B–BR–GR–G] \quad (19)$$

$$K_{d,18}=[BR][GR–M]/[BR–GR–M] \quad (20)$$

$$K_{d,19}=[B–BR][GR–M]/[B–BR–GR–M] \quad (21)$$

$$K_{d,23}=[BR][IR–G]/[BR–IR–G] \quad (22)$$

$$K_{d,24}=[B–BR][IR–G]/[B–BR–IR–G] \quad (23)$$

$$K_{d,26}=[BR][IR–M]/[BR–IR–M] \quad (24)$$

$$K_{d,27}=[B–BR][IR–M]/[B–BR–IR–M] \quad (25)$$

where $K_{d,7-10}$, $K_{d,18}$, $K_{d,19}$, $K_{d,23}$, $K_{d,24}$, $K_{d,26}$ and $K_{d,27}$ are the dissociation constants (nM) for the benzodiazepine receptor–GABA receptor complexes.

Equilibria between Active GABA Receptor and Inactive GABA Receptor:

$$K_{d,11}=[GR–G]/[IR–G] \quad (26)$$

$$K_{d,12}=[BR–GR–G]/[BR–IR–G] \quad (27)$$

$$K_{d,13}=[B–BR–GR–G]/[B–BR–IR–G] \quad (28)$$

$$K_{d,20}=[GR–M]/[IR–M] \quad (29)$$

$$K_{d,21}=[BR\text{–}GR\text{–}M]/[BR\text{–}IR\text{–}M] \quad (30)$$

$$K_{d,22}=[B\text{–}BR\text{–}GR\text{–}M]/[B\text{–}BR\text{–}IR\text{–}M] \quad (31)$$

where $K_{d,11-13}$ and $K_{d,20-22}$ are the equilibrium constants (no dimension) for the desensitization process of the GABA receptor. From these equations, the following relationships are tacitly obtained.

$$K_{d,3}=K_{d,1}\times K_{d,9}/K_{d,7} \quad (32)$$

$$K_{d,4}=K_{d,2}\times K_{d,8}/K_{d,7} \quad (33)$$

$$K_{d,5}=K_{d,1}\times K_{d,10}/K_{d,8} \quad (34)$$

$$K_{d,6}=K_{d,2}\times K_{d,10}/K_{d,9} \quad (35)$$

$$K_{d,15}=K_{d,14}\times K_{d,18}/K_{d,7} \quad (36)$$

$$K_{d,16}=K_{d,1}\times K_{d,19}/K_{d,18} \quad (37)$$

$$K_{d,17}=K_{d,14}\times K_{d,19}/K_{d,9} \quad (38)$$

$$K_{d,23}=K_{d,8}\times K_{d,12}/K_{d,11} \quad (39)$$

$$K_{d,24}=K_{d,10}\times K_{d,13}/K_{d,11} \quad (40)$$

$$K_{d,25}=K_{d,5}\times K_{d,13}/K_{d,12} \quad (41)$$

$$K_{d,26}=K_{d,18}\times K_{d,21}/K_{d,20} \quad (42)$$

$$K_{d,27}=K_{d,19}\times K_{d,22}/K_{d,20} \quad (43)$$

$$K_{d,28}=K_{d,16}\times K_{d,22}/K_{d,21} \quad (44)$$

Scatchard Plots and Hill Plots:

Let

$$[B_{bound}]=[B\text{–}BR]+[B\text{–}BR\text{–}GR]+[B\text{–}BR\text{–}GR\text{–}G]+[B\text{–}BR\text{–}IR\text{–}G]+[B\text{–}BR\text{–}GR\text{–}M]+[B\text{–}BR\text{–}IR\text{–}M] \quad (45)$$

$$[M_{bound}]=[GR\text{–}M]+[BR\text{–}GR\text{–}M]+[B\text{–}BR\text{–}GR\text{–}M]+[IR\text{–}M]+[BR\text{–}IR\text{–}M]+[B\text{–}BR\text{–}IR\text{–}M] \quad (46)$$

As x and y axes, $[B_{bound}]/[BR]_0$ and $[B_{bound}]/[B]/[BR]_0$ were taken for Scatchard plots of benzodiazepine, respectively. On the other hand, for Scatchard plots of muscimol, $[M_{bound}]/[GR]_0$ and $[M_{bound}]/[M]/[GR]_0$ are taken as x and y axes, respectively. For Hill plots, the relationships between ln ([B]) and ln $[B_{bound}]/([BR]_0-[B_{bound}])$, and between ln ([M]) and ln $[M_{bound}]/([GR]_0-[M_{bound}])$ are shown.

Pharmacological Effect and Receptor Occupancy: Fractional response (E_f) is expressed as follows.

$$E=([GR\text{–}G]+[BR\text{–}GR\text{–}G]+[B\text{–}BR\text{–}GR\text{–}G]+[GR\text{–}M]+[BR\text{–}GR\text{–}M]+[B\text{–}BR\text{–}GR\text{–}M])/([GR]_0)-E_0 \quad (47)$$

$$E_0=([GR\text{–}G]'_0+[BR\text{–}GR\text{–}G]'_0)/[GR]_0 \quad (48)$$

$$E_f=E/E_{max} \quad (49)$$

where E is the absolute effect of benzodiazepine (or muscimol). E_0 is the basal response in the absence of both benzodiazepine and muscimol. $[GR\text{–}G]'_0$ and $[BR\text{–}GR\text{–}G]'_0$ are GABA-occupied receptor concentrations in the basal condition. E_{max} is the maximum effect.

Fractional receptor occupancy of benzodiazepine or muscimol ($) is expressed as follows.

$$\$=[B_{bound}]/[BR]_0 \quad (50)$$

$$\$=[M_{bound}]/[GR]_0 \quad (51)$$

Computer Simulation: It is not easy to express each component by using several parameters under the equilibrium condition (see Eqs. 4—44). Therefore, we developed first-order ordinary differential equations suitable for each variable, and numerically solved the equations by using the intrinsic rate constants (on-rate constant: k^+ and off-rate constant: k^-). Simulation of the allosteric coupling model was carried out using the Runge Kutta Merson method, Hitachi Library Program.[30] A system of first-order ordinary differential equations was listed in the Appendix. In this analysis, the intrinsic parameters (k^+ and k^-) are necessary to solve the differential equations. As shown in "Model Assumptions," we assumed instantaneous equilibrium for the specific binding process and assigned large values to k^+ and k^- in each equation. However, fixed values were used for their ratios; $K_d=k^-/k^+$ (see Table I).

Parameter Values: The parameters which have been chosen to illustrate the properties of this allosteric coupling model are listed in Table I. For initial values of the variables at time 0 min, we used 20 pmol/g brain and 2.5 pmol/g brain for [BR] and [GR],[31,32] respectively. Further, 0 nM is assigned to [BR–GR], [BR–GR–G], [B–BR–GR], [B–BR], [GR–G], [B–BR–GR–G], [IR–G], [BR–IR–G], [B–BR–IR–G], [BR–GR–M], [GR–M], [B–BR–GR–M], [IR–M], [BR–IR–M] and [B–BR–IR–M], respectively. The GABA concentration (140 nM) in the extracellular space of brain is used as the input function for endogenous GABA (G).[33] Furthermore, benzodiazepine concentration [B] and muscimol concentration [M] were varied from 0.1 to 10000 nM and from 0.1 to 1000 nM, respectively, as fixed or constant values in one set of simulations. In another set of simulations, [B] was assumed to decreases by mono-exponential decay ($[B]=19300\times\exp(-0.66t)$).

TABLE I. Summary of Kinetic Parameters for Simulation Study

Parameters				
Dissociation constants of receptor/agonist interaction process (nM)				
$K_{d,1}$	43			
$K_{d,2}$	120000			
$K_{d,14}$	25			
$K_{d,3}$	21[a]			
$K_{d,4}$	60000[b]			
$K_{d,15}$	12.5[c]			
$K_{d,5}$, $K_{d,16}$, $K_{d,25}$, $K_{d,28}$	0.85			
$K_{d,6}$	2400			
$K_{d,17}$	0.5			
Dissociation constants of receptor/receptor interaction process (nM)	Case 1	Case 2	Case 3	Case 4
$K_{d,7}$	100	10	1	0.1
$K_{d,8}$, $K_{d,18}$, $K_{d,23}$, $K_{d,26}$	50	5	0.5	0.05
$K_{d,9}$	50	5	0.5	0.05
$K_{d,10}$, $K_{d,19}$, $K_{d,24}$, $K_{d,27}$	1	0.1	0.01	0.001
Rate constants of desensitization/reactivation process (min^{-1})[d]				
k^+_{11}, k^+_{20}	11.7			
k^-_{11}, k^-_{20}	0.25			
k^+_{12}, k^+_{21}	11.7			
k^-_{12}, k^-_{21}	0.25			
k^+_{13}, k^+_{22}	11.7			
k^-_{13}, k^-_{22}	0.25			

a) Taken from (Miller *et al.*,[58] Hollander-Jansen *et al.*).[47] *b*) Taken from (Aoshima *et al.*).[1] *c*) Taken from (Vaccarino *et al.*).[59] *d*) Taken from (Aoshima *et al.*).[1] The average values of two types of interconversion steps between active and inactive receptor sites were used. $K_{d,1}$, $K_{d,2}$, $K_{d,14}$, $K_{d,5}$, $K_{d,16}$, $K_{d,25}$, $K_{d,28}$, $K_{d,6}$ and $K_{d,17}$ were automatically determined (see Eqs. 32—44). $K_{d,7}$, $K_{d,8}$, $K_{d,9}$, $K_{d,10}$, $K_{d,18}$, $K_{d,19}$, $K_{d,23}$, $K_{d,24}$, $K_{d,26}$ and $K_{d,27}$ were arbitrarily set up based on the biochemical information.

Results

Concentration Dependency of Fractional Occupancy and Response As shown in Fig. 2, the pharmacological fractional response curve of benzodiazepine lies to the left of the curve for receptor occupancy. On the other hand, the response curve of muscimol was similar to the curve for fractional receptor occupancy (Fig. 3). The degree of discrepancy between the two curves in Fig. 2 increased with a decrease in the dissociation constants (K_d) for benzodiazepine receptor and GABA receptor interaction ($K_{d,7-10}$). However, in the case of muscimol (Fig. 3), the relationship between the two curves was not substantially affected by the K_d values for benzodiazepine receptor and GABA receptor interaction.

Time Dependency of Fractional Occupancy and Response In order to elucidate the relationship for time dependency between receptor occupancy and biological response, we set up a single exponential decay for the input functions of benzodiazepine. The receptor occupancy time profile of benzodiazepine showed a rapid decline, whereas the continuity of biological response was observed in the presence of benzodiazepine (Fig. 4). The degree of

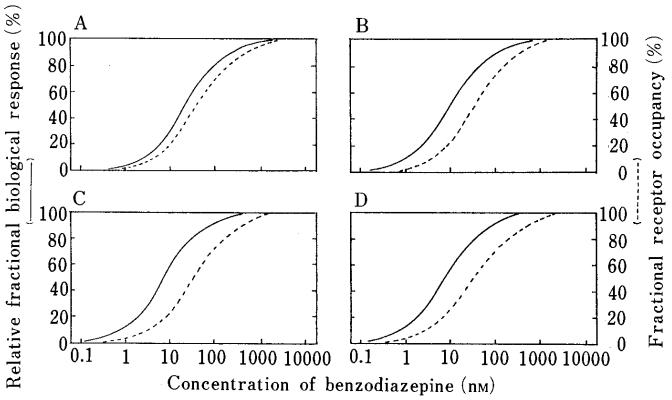

Fig. 2. Fractional Receptor Occupancy ($) and Fractional Biological Response (E_f) as Functions of the Logarithm of Benzodiazepine

The "E_f" was expressed as the ratio of biological response to the maximum response. A, case 1; B, case 2; C, case 3; D, case 4. See Table I and methods for simulation condition of cases 1 to 4.

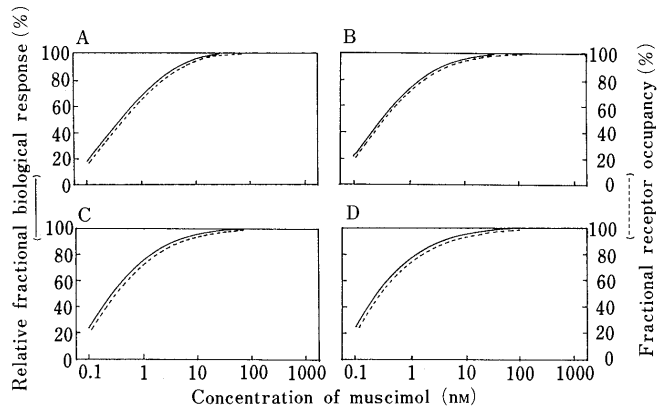

Fig. 3. Fractional Receptor Occupancy ($) and Fractional Biological Response (E_f) as Functions of the Logarithm of Muscimol

A, case 1; B, case 2; C, case 3; D, case 4. See Table I and methods for simulation condition of cases 1 to 4.

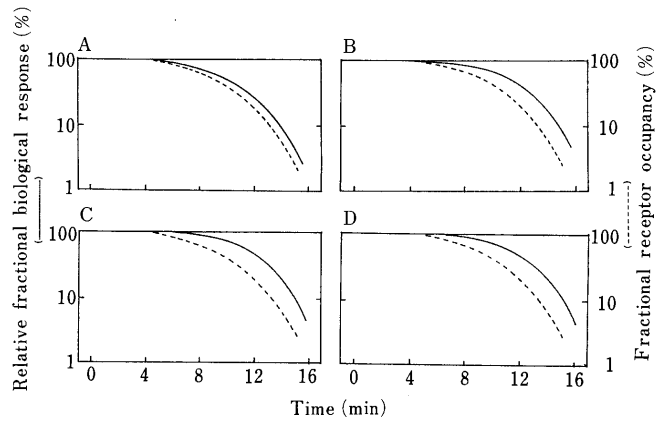

Fig. 4. Time Dependency of Fractional Receptor Occupancy ($) of Benzodiazepine and Fractional Biological Response (E_f)

It was assumed that the benzodiazepine concentration in the medium (precursor pool) monoexponentially decays. The "E_f" was expressed as the ratio of biological response to the maximum response. A, case 1; B, case 2; C, case 3; D, case 4. See Table I and methods for simulation condition of cases 1 to 4.

discrepancy of the two curves (pharmacological response and receptor occupancy for the benzodiazepine receptor) increased with the decrease in the dissociation constants (K_d) in benzodiazepine receptor and GABA receptor

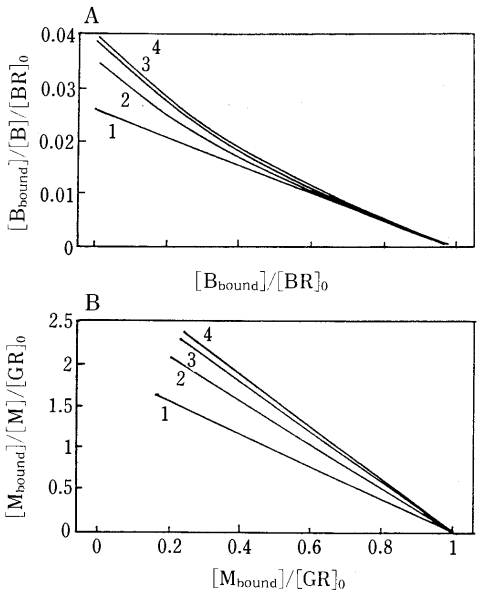

Fig. 5. Simulated Scatchard Plots of Benzodiazepine–Benzodiazepine Receptor Interaction and Muscimol–GABA Receptor Interaction

Calculations were made using Eqs. (45 or 46) in the text. See Table I and methods for simulation condition of cases 1 to 4. A, benzodiazepine; B, muscimol.

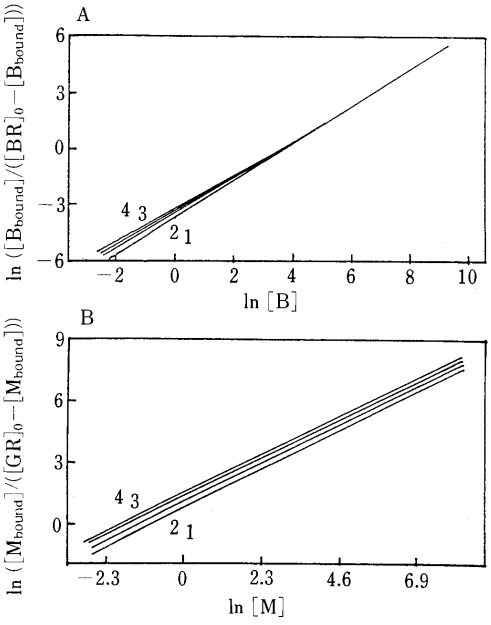

Fig. 6. Simulated Hill Plots of Benzodiazepine Binding to Benzodiazepine Receptor and Muscimol Binding to GABA Receptor

See Table I for simulation condition of cases 1 to 4. A, benzodiazepine; B, muscimol.

interaction ($K_{d,7-10}$).

Non-linear Scatchard Plots and Hill Plots In the case where $K_{d,7}=100$ nM, $K_{d,8}=50$ nM, $K_{d,9}=50$ nM and $K_{d,10}=1$ nM (case 1), benzodiazepine binding conforms to the classical hyperbolic binding isotherm and the Scatchard plot is almost linear (Fig. 5A). However, when $K_{d,7-10}$ decrease, the Scatchard plot is concave up, the degree of curvature depending upon the magnitude of these parameters (Fig. 5A). Hill plots determined by Eqs. 45 and 46 may be identical to those resulting from true negatively cooperative interactions (Fig. 6A). The magnitude of the Hill coefficient in the benzodiazepine–benzodiazepine

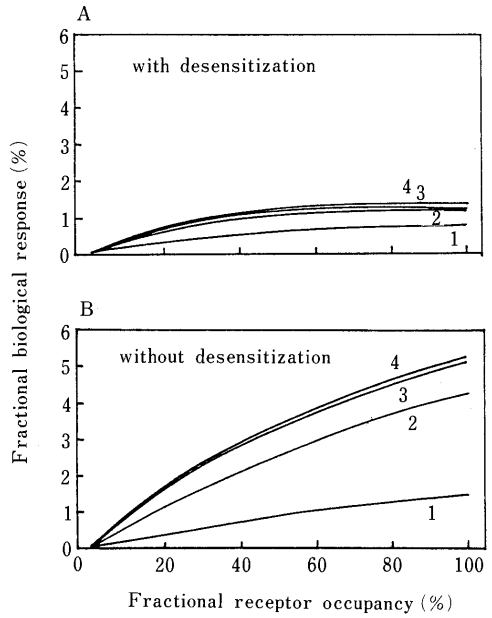

Fig. 7. Relationship between Benzodiazepine Receptor Binding Occupancy ($) and Biological Response (E)

See Table I and Methods for simulation condition of cases 1 to 4. A, with desensitization of GABA receptor; B, without desensitization of GABA receptor.

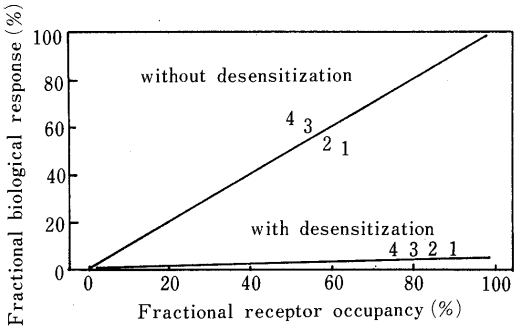

Fig. 8. Relationship between Muscimol Receptor Binding Occupancy ($) and Biological Response (E)

See Table I and Methods for simulation condition of cases 1 to 4.

receptor interaction decreased with the decrease in the dissociation constants (K_d) in benzodiazepine receptor–GABA receptor interaction ($K_{d,7-10}$) (Fig. 6A). On the other hand, the Scatchard plots of muscimol were almost linear for all 4 cases (Fig. 5B). When $K_{d,7}$, $K_{d,9}$, $K_{d,18}$ and $K_{d,19}$ decreased, the apparent binding affinity increased. The Hill coefficients in the muscimol–GABA receptor interaction were close to one in each case (Fig. 6B).

Non-linear Relationship between Fractional Occupancy and Fractional Response Classical receptor occupancy theory predicts that receptor occupancy will be linearly related to the biological response. If it is assumed that the benzodiazepine receptor interacts with the GABA receptor, a hyperbolic and non-linear relationship is obtained between benzodiazepine receptor occupancy and biological response (Fig. 7). The degree of curvilinearity between the two parameters increased with a decrease in the dissociation constants (K_d) for benzodiazepine receptor and GABA receptor interaction ($K_{d,7-10}$) (Fig. 7). On the other hand, a linear relationship between receptor occupancy of muscimol and biological response was observed (Fig. 8). The fractional response increased in the absence of GABA agonist-induced desensitization of the GABA receptor (Figs. 7B and 8).

Discussion

Elucidating the cellular mechanism underlying the coupling between neuromodulator and neurotransmitter receptors is important to understand central nervous system functions. The GABA receptor is a good model for studying these interactions because benzodiazepine and benzodiazepine receptor interaction modulates GABA receptor function. Biochemical studies have indicated that GABA enhances benzodiazepine binding[28] and that benzodiazepines enhance GABA binding,[29] indicating that the binding sites for benzodiazepines and GABA are allosterically coupled. In this study, we considered these biochemical observations and included them in our simulations by establishing $K_{d,3} > K_{d,5}$ and $K_{d,4} > K_{d,6}$. Although there is no actual measurement of binding affinity between the benzodiazepine receptor and the GABA receptor, we assumed that benzodiazepine (or GABA) enhance the binding affinity between these two receptors ($K_{d,9} < K_{d,7}$ and $K_{d,10} < K_{d,8}$) and that the association between the two receptors enhance the binding of each agonist to each receptor ($K_{d,3} < K_{d,1}$ and $K_{d,4} < K_{d,2}$) in order to account for the observed allosteric interactions noted above.

The positive allosteric interactions between benzodiazepine receptor and GABA receptor binding may contribute in part to the potentiation of the functional effects of GABA agonists on the chloride ion channel by benzodiazepine agonists. Indeed, diazepam has been reported to increase the affinity of ^{3}H-GABA binding to a low-affinity site[7] in good agreement with the decrease in the apparent ED_{50} for muscimol-stimulated $^{36}Cl^-$ uptake observed by Morrow and Paul.[34] We reproduced these phenomena in our simulation analysis (see Fig. 2). Although the actual subunit composition of the benzodiazepine receptor/GABA receptor complex has not been firmly established, it is believed that there are four subunits, α, β, γ, and δ.[10,11,35] Recent reports have investigated how the $GABA_A$ receptor and the benzodiazepine receptor are related to these subunits.[10,11,36-44] However, it is unclear whether the binding sites for GABA and benzodiazepines are located on the same or different polypeptide chains, nor is it known how the structure of the GABA receptor is related to the observed functional coupling between the GABA and benzodiazepine recognition sites.[35] In the present simulation study, receptor heterogeneity based on interactions among subunits is not considered. More precise calculation could be possible if more information was available concerning the details of the quantitative interaction among the receptor subunits.

Several groups have tried to evaluate the relationship between the receptor occupancy of benzodiazepine and pharmacological changes.[45-47] Mennini and Garattini[45] found that different benzodiazepines administered to rodents in equieffective anticonvulsant doses (ED_{50}) induce a similar degree of *in vivo* receptor occupancy (about 50%). By using a similar *in vivo* technique, Jochemsen *et al.*[48] indicated a receptor occupancy requirement of 20 to 40% for the near-maximal anti-pentylenetetrazole effect of metaclonazepam. Good linear correlations were established

between receptor occupancy and protection (with a low fractional occupancy of 30 to 40% receptor for maximum observed effect) against pentylenetetrazole-induced seizures after administration of diazepam in mice and rats.[21,49] Recently, Ishizuka *et al.* reported that the ID_{50} for the dose–response curve of receptor occupancy for clonazepam and the ED_{50} for a decrease in glucose utilization were 0.3 and 0.007 mg/kg in mouse brain *in vivo*, respectively.[22] A nonlinear and hyperbolic relationship was also observed between receptor occupancy and glucose metabolic rate, indicating that benzodiazepine exerts a maximum effect on glucose utilization at a low level of receptor occupancy (30—40%). Similar patterns of biological response *vs.* receptor occupancy were obtained with our simulation results (see Fig. 7). Therefore, the relationship between biological response and receptor occupancy may be accounted for by allosteric coupling between the benzodiazepine receptor and the GABA receptor. Similarly, the discrepancy in time dependency between receptor occupancy of benzodiazepine and biological response may be another explanation for allosteric coupling between the two receptors (Fig. 4). Other receptor binding-effect models have been presented to account for such a relationship,[50] *e.g.* 1) the spare receptor or receptor reserve hypothesis[51]; 2) the deglomeration-coupling model that assumes the existence of receptor oligomers and agonist activation by the monomer formation[52]; and 3) saturation of the physiological amplification cascade after the activation of only a fraction of the total receptor population.[26] However, the receptor binding-effector coupling hypothesis we propose in this study seems to account satisfactorily for the effect of benzodiazepine on the observed biological response.

A number of channel-opening neurotransmitter receptors are desensitized by their neurotransmitters. During exposure to the neurotransmitter, for times much longer than the channel-opening reaction, the receptor is transformed to a state that does not form open channels. Desensitization of the GABA receptor has been observed using electrophysiological techniques[53] in hippocampal neurons,[54] in ganglion cells,[55] in the rat brain receptor expressed in oocytes[56,57] and membrane vesicle preparations of rat brain.[23,24] As expected from the presence of desensitized forms in the model, Aoshima *et al.* reported that the dose dependence of electrophysiological responses before desensitization equilibrium was different from that of GABA binding, as calculated above from the kinetic model.[1] They assumed two types of interconversion steps between active and inactive receptor sites in the kinetic model. Furthermore, a large discrepancy was reported between the dose dependence of the electrophysiological response and that of radioligand binding measurements.[4,57] Based on *ex vivo* binding assay, Guidotti and Ferrero indicated no hyperbolic but a good relationship between the extent of ^{3}H-muscimol displacement by muscimol and its potency in delaying the onset of isoniazid-induced convulsion.[32] These findings are much different from the relationship between receptor binding of benzodiazepine and induced biological response.

An understanding of receptor occupancy by the agonist and benzodiazepine receptor–GABA receptor interaction is important to predict the effect of benzodiazepine and muscimol on the central nervous system. To our knowledge, this is the first investigation in which a simulation study was performed to evaluate the allosteric effect based on benzodiazepine receptor and GABA receptor interaction, and which related receptor occupancy in terms of both dose- and time-dependency of drug action in the central nervous system.

In the future, it is necessary to carry out *in vitro* studies using synaptoneurosomes and cultured cells that are based on the effect of benzodiazepine and GABA agonist on chloride ion transport and/or glucose metabolism in order to evaluate the relationship between receptor occupancy and the change in chloride ion flux.

Acknowledgements We thank Dr. R. G. Blasberg for his comments and suggestions.

Appendix The kinetic equations for agonist–receptor and receptor–receptor interaction are as follows.

$$BR + B \underset{k_1^-}{\overset{k_1^+}{\rightleftharpoons}} B\text{–}BR \tag{A1}$$

$$GR + G \underset{k_2^-}{\overset{k_2^+}{\rightleftharpoons}} GR\text{–}G \tag{A2}$$

$$BR\text{–}GR + B \underset{k_3^-}{\overset{k_3^+}{\rightleftharpoons}} B\text{–}BR\text{–}GR \tag{A3}$$

$$BR\text{–}GR + G \underset{k_4^-}{\overset{k_4^+}{\rightleftharpoons}} BR\text{–}GR\text{–}G \tag{A4}$$

$$BR\text{–}GR\text{–}G + B \underset{k_5^-}{\overset{k_5^+}{\rightleftharpoons}} B\text{–}BR\text{–}GR\text{–}G \tag{A5}$$

$$B\text{–}BR\text{–}GR + G \underset{k_6^-}{\overset{k_6^+}{\rightleftharpoons}} B\text{–}BR\text{–}GR\text{–}G \tag{A6}$$

$$BR + GR \underset{k_7^-}{\overset{k_7^+}{\rightleftharpoons}} BR\text{–}GR \tag{A7}$$

$$BR + GR\text{–}G \underset{k_8^-}{\overset{k_8^+}{\rightleftharpoons}} BR\text{–}GR\text{–}G \tag{A8}$$

$$B\text{–}BR + GR \underset{k_9^-}{\overset{k_9^+}{\rightleftharpoons}} B\text{–}BR\text{–}GR \tag{A9}$$

$$B\text{–}BR + GR\text{–}G \underset{k_{10}^-}{\overset{k_{10}^+}{\rightleftharpoons}} B\text{–}BR\text{–}GR\text{–}G \tag{A10}$$

$$GR\text{–}G \underset{k_{11}^-}{\overset{k_{11}^+}{\rightleftharpoons}} IR\text{–}G \tag{A11}$$

$$BR\text{–}GR\text{–}G \underset{k_{12}^-}{\overset{k_{12}^+}{\rightleftharpoons}} BR\text{–}IR\text{–}G \tag{A12}$$

$$B\text{–}BR\text{–}GR\text{–}G \underset{k_{13}^-}{\overset{k_{13}^+}{\rightleftharpoons}} B\text{–}BR\text{–}IR\text{–}G \tag{A13}$$

$$GR + M \underset{k_{14}^-}{\overset{k_{14}^+}{\rightleftharpoons}} GR\text{–}M \tag{A14}$$

$$BR\text{–}GR + M \underset{k_{15}^-}{\overset{k_{15}^+}{\rightleftharpoons}} BR\text{–}GR\text{–}M \tag{A15}$$

$$BR\text{–}GR\text{–}M + B \underset{k_{16}^-}{\overset{k_{16}^+}{\rightleftharpoons}} B\text{–}BR\text{–}GR\text{–}M \tag{A16}$$

$$B\text{–}BR\text{–}GR + M \underset{k_{17}^-}{\overset{k_{17}^+}{\rightleftharpoons}} B\text{–}BR\text{–}GR\text{–}M \tag{A17}$$

$$BR + GR\text{–}M \underset{k_{18}^-}{\overset{k_{18}^+}{\rightleftharpoons}} BR\text{–}GR\text{–}M \tag{A18}$$

$$\text{B–BR} + \text{GR–M} \underset{k_{19}^-}{\overset{k_{19}^+}{\rightleftarrows}} \text{B–BR–GR–M} \tag{A19}$$

$$\text{GR–M} \underset{k_{20}^-}{\overset{k_{20}^+}{\rightleftarrows}} \text{IR–M} \tag{A20}$$

$$\text{BR–GR–M} \underset{k_{21}^-}{\overset{k_{21}^+}{\rightleftarrows}} \text{BR–IR–M} \tag{A21}$$

$$\text{B–BR–GR–M} \underset{k_{22}^-}{\overset{k_{22}^+}{\rightleftarrows}} \text{B–BR–IR–M} \tag{A22}$$

$$\text{BR} + \text{IR–G} \underset{k_{23}}{\overset{k_{23}^+}{\rightleftarrows}} \text{BR–IR–G} \tag{A23}$$

$$\text{B–BR} + \text{IR–G} \underset{k_{24}^-}{\overset{k_{24}^+}{\rightleftarrows}} \text{B–BR–IR–G} \tag{A24}$$

$$\text{BR–IR–G} + \text{B} \underset{k_{25}^-}{\overset{k_{25}^+}{\rightleftarrows}} \text{B–BR–IR–G} \tag{A25}$$

$$\text{BR} + \text{IR–M} \underset{k_{26}^-}{\overset{k_{26}^+}{\rightleftarrows}} \text{BR–IR–M} \tag{A26}$$

$$\text{B–BR} + \text{IR–M} \underset{k_{27}^-}{\overset{k_{27}^+}{\rightleftarrows}} \text{B–BR–IR–M} \tag{A27}$$

$$\text{BR–IR–M} + \text{B} \underset{k_{28}^-}{\overset{k_{28}^+}{\rightleftarrows}} \text{B–BR–IR–M} \tag{A28}$$

where k^+ and k^- represent rate constants.

The first order ordinary differential equations are as follows.

$$\begin{aligned} d[\text{BR}]/dt = &-k_1^+[\text{BR}][\text{B}] + k_1^-[\text{B–BR}] - k_7^+[\text{BR}][\text{GR}] \\ &+ k_7^-[\text{BR–GR}] - k_8^+[\text{BR}][\text{GR–G}] + k_8^-[\text{BR–GR–G}] \\ &- k_{18}^+[\text{BR}][\text{GR–M}] + k_{18}^-[\text{BR–GR–M}] \\ &- k_{23}^+[\text{BR}][\text{IR–G}] + k_{23}^-[\text{BR–IR–G}] - k_{26}^+[\text{BR}][\text{IR–M}] \\ &+ k_{26}^-[\text{BR–IR–M}] \end{aligned} \tag{A29}$$

$$\begin{aligned} d[\text{GR}]/dt = &-k_2^+[\text{GR}][\text{G}] + k_2^-[\text{GR–G}] - k_7^+[\text{BR}][\text{GR}] \\ &+ k_7^-[\text{BR–GR}] - k_9^+[\text{B–BR}][\text{GR}] + k_9^-[\text{B–BR–GR}] \\ &- k_{14}^+[\text{GR}][\text{M}] - k_{14}^-[\text{GR–M}] \end{aligned} \tag{A30}$$

$$\begin{aligned} d[\text{BR–GR}]/dt = &-k_3^+[\text{BR–GR}][\text{B}] + k_3^-[\text{B–BR–GR}] \\ &- k_4^+[\text{BR–GR}][\text{G}] + k_4^-[\text{BR–GR–G}] \\ &+ k_7^+[\text{BR}][\text{GR}] - k_7^-[\text{BR–GR}] \\ &- k_{15}^+[\text{BR–GR}][\text{M}] + k_{15}^-[\text{BR–GR–M}] \end{aligned} \tag{A31}$$

$$\begin{aligned} d[\text{BR–GR–G}]/dt = &\, k_4^+[\text{BR–GR}][\text{G}] - k_4^-[\text{BR–GR–G}] \\ &- k_5^+[\text{BR–GR–G}][\text{B}] + k_5^-[\text{B–BR–GR–G}] \\ &+ k_8^+[\text{BR}][\text{GR–G}] - k_8^-[\text{BR–GR–G}] \\ &- k_{12}^+[\text{BR–GR–G}] + k_{12}^-[\text{BR–IR–G}] \end{aligned} \tag{A32}$$

$$\begin{aligned} d[\text{B–BR–GR}]/dt = &\, k_3^+[\text{BR–GR}][\text{B}] - k_3^-[\text{B–BR–GR}] \\ &- k_6^+[\text{B–BR–GR}][\text{G}] + k_6^-[\text{B–BR–GR–G}] \\ &+ k_9^+[\text{GR}][\text{B–BR}] - k_9^-[\text{B–BR–GR}] \\ &- k_{17}^+[\text{B–BR–GR}][\text{M}] + k_{17}^-[\text{B–BR–GR–M}] \end{aligned} \tag{A33}$$

$$\begin{aligned} d[\text{B–BR}]/dt = &\, k_1^+[\text{BR}][\text{B}] - k_1^-[\text{B–BR}] - k_9^+[\text{B–BR}][\text{GR}] \\ &+ k_9^-[\text{B–BR–GR}] - k_{10}^+[\text{B–BR}][\text{GR–G}] \\ &+ k_{10}^-[\text{B–BR–GR–G}] - k_{19}^+[\text{B–BR}][\text{GR–M}] \\ &+ k_{19}^-[\text{B–BR–GR–M}] - k_{24}^+[\text{B–BR}][\text{IR–G}] \\ &+ k_{24}^-[\text{B–BR–IR–G}] - k_{27}^+[\text{B–BR}][\text{IR–M}] \\ &+ k_{27}^-[\text{B–BR–IR–M}] \end{aligned} \tag{A34}$$

$$\begin{aligned} d[\text{GR–G}]/dt = &\, k_2^+[\text{GR}][\text{G}] - k_2^-[\text{GR–G}] - k_8^+[\text{BR}][\text{GR–G}] \\ &+ k_8^-[\text{BR–GR–G}] - k_{10}^+[\text{B–BR}][\text{GR–G}] \\ &+ k_{10}^-[\text{B–BR–GR–G}] - k_{11}^+[\text{GR–G}] + k_{11}^-[\text{IR–G}] \end{aligned} \tag{A35}$$

$$\begin{aligned} d[\text{B–BR–GR–G}]/dt = &\, k_5^+[\text{BR–GR–G}][\text{B}] - k_5^-[\text{B–BR–GR–G}] \\ &+ k_6^+[\text{B–BR–GR}][\text{G}] - k_6^-[\text{B–BR–GR–G}] \\ &+ k_{10}^+[\text{B–BR}][\text{GR–G}] - k_{10}^-[\text{B–BR–GR–G}] \\ &- k_{13}^+[\text{B–BR–GR–G}] + k_{13}^-[\text{B–BR–IR–G}] \end{aligned} \tag{A36}$$

$$\begin{aligned} d[\text{IR–G}]/dt = &\, k_{11}^+[\text{GR–G}] - k_{11}^-[\text{IR–G}] - k_{23}^+[\text{BR}][\text{IR–G}] \\ &+ k_{23}^-[\text{BR–IR–G}] - k_{24}^+[\text{B–BR}][\text{IR–G}] \\ &+ k_{24}^-[\text{B–BR–IR–G}] \end{aligned} \tag{A37}$$

$$\begin{aligned} d[\text{BR–IR–G}]/dt = &\, k_{12}^+[\text{BR–GR–G}] - k_{12}^-[\text{BR–IR–G}] \\ &- k_{25}^+[\text{BR–IR–G}][\text{B}] + k_{25}^-[\text{B–BR–IR–G}] \\ &+ k_{23}^+[\text{BR}][\text{IR–G}] - k_{23}^-[\text{BR–IR–G}] \end{aligned} \tag{A38}$$

$$\begin{aligned} d[\text{B–BR–IR–G}]/dt = &\, k_{13}^+[\text{B–BR–GR–G}] - k_{13}^-[\text{B–BR–IR–G}] \\ &+ k_{24}^+[\text{B–BR}][\text{IR–G}] - k_{24}^-[\text{B–BR–IR–G}] \\ &+ k_{25}^+[\text{BR–IR–G}][\text{B}] - k_{25}^-[\text{B–BR–IR–G}] \end{aligned} \tag{A39}$$

$$\begin{aligned} d[\text{BR–GR–M}]/dt = &-k_{16}^+[\text{BR–GR–M}][\text{B}] + k_{16}^-[\text{B–BR–GR–M}] \\ &+ k_{15}^+[\text{BR–GR}][\text{M}] - k_{15}^-[\text{BR–GR–M}] \\ &+ k_{18}^+[\text{BR}][\text{GR–M}] - k_{18}^-[\text{BR–GR–M}] \\ &- k_{21}^+[\text{BR–GR–M}] + k_{21}^-[\text{BR–IR–M}] \end{aligned} \tag{A40}$$

$$\begin{aligned} d[\text{GR–M}]/dt = &\, k_{14}^+[\text{GR}][\text{M}] - k_{14}^-[\text{GR–M}] - k_{18}^+[\text{BR}][\text{GR–M}] \\ &+ k_{18}^-[\text{BR–GR–M}] - k_{19}^+[\text{B–BR}][\text{GR–M}] \\ &+ k_{19}^-[\text{B–BR–GR–M}] - k_{20}^+[\text{GR–M}] + k_{20}^-[\text{IR–M}] \end{aligned} \tag{A41}$$

$$\begin{aligned} d[\text{B–BR–GR–M}]/dt = &\, k_{16}^+[\text{BR–GR–M}][\text{B}] - k_{16}^-[\text{B–BR–GR–M}] \\ &+ k_{17}^+[\text{B–BR–GR}][\text{M}] - k_{17}^-[\text{B–BR–GR–M}] \\ &+ k_{19}^+[\text{B–BR}][\text{GR–M}] - k_{19}^-[\text{B–BR–GR–M}] \\ &- k_{22}^+[\text{B–BR–GR–M}] + k_{22}^-[\text{B–BR–IR–M}] \end{aligned} \tag{A42}$$

$$\begin{aligned} d[\text{IR–M}]/dt = &\, k_{20}^+[\text{GR–M}] - k_{20}^-[\text{IR–M}] - k_{26}^+[\text{BR}][\text{IR–M}] \\ &+ k_{26}^-[\text{BR–IR–M}] - k_{27}^+[\text{B–BR}][\text{IR–M}] \\ &+ k_{27}^-[\text{B–BR–IR–M}] \end{aligned} \tag{A43}$$

$$\begin{aligned} d[\text{BR–IR–M}]/dt = &\, k_{21}^+[\text{BR–GR–M}] - k_{21}^-[\text{BR–IR–M}] \\ &- k_{28}^+[\text{BR–IR–M}][\text{B}] + k_{28}^-[\text{B–BR–IR–M}] \\ &+ k_{26}^+[\text{BR}][\text{IR–M}] - k_{26}^-[\text{BR–IR–M}] \end{aligned} \tag{A44}$$

$$\begin{aligned} d[\text{B–BR–IR–M}]/dt = &\, k_{22}^+[\text{B–BR–GR–M}] - k_{22}^-[\text{B–BR–IR–M}] \\ &+ k_{27}^+[\text{B–BR}][\text{IR–M}] - k_{27}^-[\text{B–BR–IR–M}] \\ &+ k_{28}^+[\text{BR–IR–M}][\text{B}] - k_{28}^-[\text{B–BR–IR–M}] \end{aligned} \tag{A45}$$

If the initial conditions and the values of the rate constants are known, these equations may be solved numerically (see text for details).

References

1) H. Aoshima, M. Anan, H. Ishii, H. Iio and S. Kobayashi, *Biochemistry*, **26**, 4811 (1987).
2) S. M. Paul, P. J. Marangos and P. Skolnick, *Biol. Psychiatry*, **16**, 213 (1981).
3) R. W. Olsen, *J. Neurochem.*, **37**, 1 (1981).
4) R. W. Olsen, *Annu. Rev. Pharmacol. Toxicol.*, **22**, 245 (1982).
5) P. Skolnick and S. M. Paul, *Int. Rev. Neurobiol.*, **23**, 103 (1982).
6) A. Guidotti, G. Tottano and E. Costa, *Nature* (London), **275**, 553 (1978).
7) J. H. Sakeritt, M. Willow and G. A. R. Johnston, *Neurosci. Lett.*, **29**, 63 (1982).
8) B. A. Meiners and A. I. Salama, *Eur. J. Pharmacol.*, **91**, 145 (1982).
9) P. Skolnick, V. Moncada, J. L. Barker and S. M. Paul, *Science*, **211**, 1448 (1981).
10) R. W. Olsen and A. J. Tobin, *FASEB J.*, **4**, 1469 (1990).
11) D. B. Pritchett, H. Sontheimer, B. D. Shivers, S. Ymer, H. Kettenmann, P. R. Schofield and P. H. Seeburg, *Nature* (London), **338**, 582 (1989).
12) T. Kono and F. W. Barham, *J. Biol. Chem.*, **246**, 6210 (1971).

13) S. Gammeltoft and J. Gliemann, *Biochim. Biophys. Acta*, **320**, 16 (1973).
14) K. J. Catt and M. L. Dufau, *Nature* (London), **244**, 219 (1973).
15) C. Mendelsn, M. Dufau and K. Catt, *J. Biol. Chem.*, **250**, 8818 (1975).
16) S. Jacobs and P. Cuatrecasas, *Biochim. Biophys. Acta*, **433**, 482 (1976).
17) H. Furukawa, J. P. Bilezikian and J. N. Loeb, *Biochim. Biophys. Acta*, **598**, 345 (1980).
18) Z. Kahn, *J. Cell Biol.*, **70**, 261 (1976).
19) J. M. Boeynaems and J. E. Dumont, *Mol. Cell Endocrinol*, **7**, 33 (1977).
20) R. N. Bergman and O. Hechter, *J. Biol. Chem.*, **253**, 3238 (1978).
21) Y. Igari, Y. Sugiyama, Y. Sawada, T. Iga and M. Hanano, *Drug Metab. Dispos.*, **13**, 102 (1985).
22) H. Ishizuka, Y. Sawada, K. Ito, Y. Sugiyama, H. Suzuki, T. Iga and M. Hanano, *J. Pharmacol. Exp. Ther.*, **251**, 362 (1989).
23) D. J. Cash and K. Subbarao, *Biochemistry*, **26**, 7556 (1987).
24) D. J. Cash and K. Subbarao, *Biochemistry*, **26**, 7570 (1987).
25) D. J. Cash, H. Aoshima, E. B. Pasquale and G. P. Hess, *Rev. Physiol. Biochem. Pharmacol.*, **102**, 73 (1985).
26) S. Strickland and J. N. Loeb, *Proc. Natl. Acad. Sci. U.S.A.*, **78**, 1366 (1981).
27) T. P. Kenakin and P. H. Morgan, *Mol. Pharmacol.*, **35**, 214 (1989).
28) J. F. Tallman, J. W. Thomas and D. W. Gallaner, *Nature* (London), **274**, 383 (1978).
29) B. A. Meiners and A. I. Salama, *Eur. J. Pharmacol.*, **119**, 61 (1985).
30) K. Ujiie, Hitachi Library Program (D2/TC/RKM), Runge Kutta Merson, 1966.
31) S. Pappata, Y. Samson, C. Chavoix, C. Prenant, M. Maziere and J. C. Baron, *J. Cerebral. Blood Flow Metab.*, **8**, 304 (1988).
32) A. Guidotti and P. Ferrero, *L.E.R.S. Monagr. Ser.*, **3**, 31 (1985).
33) U. Tossman, G. Jonsson and U. Ungerstedt, *Acta Physiol. Scand.*, **127**, 533 (1986).
34) A. L. Morrow and A. M. Paul, *J. Neurochem.*, **50**, 302 (1988).
35) C. Czajkowski, T. T. Gibbs and D. H. Farb, *Mol. Pharmacol.*, **35**, 75 (1989).
36) S. O. Cassalotti, F. A. Stephenson and E. A. Barnard, *J. Biol. Chem.*, **261**, 15013 (1986).
37) F. A. Stephenson and E. A. Barnard, "Benzodiazepine/GABA Receptors and Chloride Channels: Structural and Functional Properties," ed. by Olsen RW and Venter JC, Alan R. Liss, New York, 1987, p. 261.
38) E. A. Sigel, F. A. Stephenson, C. Mamalaki and E. A. Barnard, *J. Biol. Chem.*, **258**, 6965 (1982).
39) H. Mohler, M. K. Battersby and J. G. Richards, *Proc. Natl. Acad. Sci. U.S.A.*, **77**, 1666 (1980).
40) W. Sieghart and M. Karobath, *Proc. Natl. Acad. Sci. U.S.A.*, **77**, 1666 (1980).
41) A. S. Lippa, K. M. Garrett, B. Tabakoff, B. Beer, L. P. Wennogle and L. R. Meyerson, *Brain Res. Bull.*, **14**, 189 (1985).
42) J. W. Hebebrand, W. Friedl, B. Breidnbach and P. Propping, *J. Neurochem.*, **48**, 1103 (1987).
43) S. Fuchs, H. Mohler and W. Sieghart, *Neurosci. Lett.*, **90**, 314 (1988).
44) E. S. Levitan, P. R. Schofield, D. R. Burt, L. M. Rhee, W. Wisden, M. Kohler, N. Fujita, H. F. Rodriguez, A. Stephenson, M. G. Darlison, E. R. Barnard and P. H. Seeburg, *Nature* (London), **335**, 76 (1988).
45) T. Mennini and S. Garattini, "Benzodiazepine Recognition Site Ligands: Biochemistry and Pharmacology," Raven Press, New York, 1983, p. 189.
46) J. Dingemanse, J. Danhof and D. D. Breimer, *Pharmacol. Ther.*, **38**, 1 (1988).
47) M. Hollander-Jansen, J. Dingemanse, M. W. E. Langemeijer and M. Danhof, *Pharmaceu. Res.*, **6**, 585 (1989).
48) R. Jochemsen, G. Kato and M. Ruhland, *Drug Develop. Res.*, **9**, 115 (1986).
49) S. M. Paul and P. J. Syapin, *Nature* (London), **281**, 688 (1979).
50) D. C. Perry, J. S. Rosenbaum, M. Kurowski and W. Sadee, *Mol. Pharmacol.*, **21**, 272 (1982).
51) R. P. Stephenson, *Br. J. Pharmacol.*, **11**, 379 (1956).
52) M. Rodbell, *Nature* (London), **284**, 17 (1980).
53) K. Krnjevic, *Physiol. Rev.*, **54**, 418 (1974).
54) R. H. Thalman and N. Hershkowith, *Brain Res.*, **342**, 219 (1985).
55) N. Akaike, K. Hattori, N. Inomata and Y. Oomura, *J. Physiol.*, **360**, 367 (1985).
56) K. M. Houamed, G. Bilbe, T. G. Smart, A. Constanti, D. A. Brown, E. A. Barnard and B. M. Richards, *Nature* (London), **310**, 318 (1984).
57) I. Parker, C. B. Gundersen and R. Miledi, *J. Neurosci.*, **6**, 2290 (1986).
58) L. G. Miller, D. J. Greenblatt, S. M. Paul and R. S. Shader, *J. Pharmacol. Exp. Ther.*, **240**, 516 (1987).
59) F. M. Vaccarino, H. Alho, M. R. Santi and A. Guidotti, *J. Neurosci.*, **7**, 65 (1987).

Effects of 2-(*E*-2-Decenoylamino)ethyl 2-(Cyclohexylethyl) Sulfide on Various Ulcer Models in Rats

Isao KOHDA,*[,a] Hitoshi NAGAI,[a] Masakazu IWAI,[a] Masahiro WATANABE,[a] Kazumasa YOKOYAMA,[a] Kazutake TSUJIKAWA[b] and Tsutomu MIMURA[b]

Central Research Laboratories, The Green Cross Corporation,[a] Shodai Ohtani 2–1180–1, Hirakata, Osaka 573, Japan and Faculty of Pharmaceutical Sciences, Osaka University,[b] Yamadaoka 1–6, Suita, Osaka 565, Japan. *Received December 17, 1990*

The effects of 2-(*E*-2-decenoylamino)ethyl 2-(cyclohexylethyl) sulfide (compd. III-1a) on various experimental ulcers were investigated. The oral administration of compd. III-1a at doses ranging from 30 to 300 mg/kg inhibited the acute gastric ulcerations induced by ethanol, HCl·aspirin and indomethacin in rats. Compound III-1a significantly inhibited the water immersion stress-induced gastric ulcer at doses of 3 mg/kg, *p.o.* The anti-ulcer activity of plaunotol as a reference drug was equivalent on an ethanol-induced ulcer to that of compd. III-1a, but weaker on HCl·aspirin, indomethacin and stress-induced ulcers than that of compd. III-1a. On indomethacin-produced gastric antral ulcer, compd. III-1a showed the same significant inhibitory activity as spizofurone did at a dose of 100 mg/kg, *p.o.* Compound III-1a also inhibited hemorrhagic shock-, diethyldithiocarbamic acid (DDC)- and platelet activating factor (PAF)-induced ulcers dose-dependently. Plaunotol only showed significant inhibitory activity on PAF-induced ulcer in these three ucler models. The consecutive administration of compd. III-1a (100 mg/kg, *p.o.*) twice a day significantly accelerated the healing of an acetic acid-induced ulcer and that of plaunotol (200 mg/kg, *p.o.*) showed the same activity. Moreover, orally administered compd. III-1a at a dose of 100 mg/kg decreased the gastric acid secretion in pylorus-ligated rats. The results in the present study suggest that compd. III-1a has the dual action on ulcer formation.

Keywords 2-(*E*-2-decenoylamino)ethyl 2-(cyclohexylethyl) sulfide; ethanol-induced ucler; aspirin-induced ulcer; indomethacin-induced ulcer; water immersion stress-induced ulcer; indomethacin-produced gastric antral ulcer; hemorrhagic shock-induced ulcer; PAF-induced ulcer; acetic acid-induced ulcer; pylorus ligation gastric secretion

Previously, we reported that among the derivatives of 2-(*E*-2-alkenoylamino)ethyl alkyl sulfide, 2-(*E*-2-decenoylamino)ethyl 2-(cyclohexylethyl) sulfide (compd. III-1a) showed the strongest inhibitory activity on water immersion stress-induced ulcer and low toxicity.[1)]

In this work, the pharmacological profile of this compound as an anti-ucler agent was studied by using various ulcer models.

Experimental

Materials 2-(*E*-2-Decenoylamino)ethyl 2-(cyclohexylethyl) sulfide was synthesized as described previously.[1)] HCO-60 was obtained from Nikko Chemicals. Acetylsalicylic acid (aspirin) and diethyldithiocarbamic acid sodium salt, trihydrate (DDC) were obtained from Nakarai tesque. Indomethacin and platelet activating factor (PAF) were obtained from Sigma. Plaunotol (Kelnac®, Sankyo) and spizofurone (Maon®, Takeda) were used as a reference drugs.

Experimental Animal Male Wistar rats weighing 180 g (6 weeks)—250 g (7 weeks), fasted for 24 h, were purchased from Charles River Japan Inc.

Experimental Gastric Ulcer Models in Rats i) Ethanol-Induced Ulcer: This ulcer model was induced according to the method of Kuwata *et al.*[2)] The rats were given perorally 1 ml/rat of 70% ethanol. Each sample was suspended with 10% HCO-60 in saline and administered orally, 0.5 h before the ethanol administration. The animals were sacrificed 1 h later and their ulcer indices were evaluated.

ii) HCl·Aspirin-Induced Ulcer: According to the method of Guth *et al.*,[3)] the rats were given perorally 150 mg/kg of aspirin, suspended with 5% gum arabica in 150 mM HCl. Each sample was suspended with 10% HCO-60 in saline and administered orally, 0.5 h before the aspirin administration. The animals were sacrificed 1 h later and their ulcer indices were evaluated.

iii) Indomethacin-Induced Ulcer: By the method of Urusidani *et al.*,[4)] the rats were given subcutaneously 30 mg/kg of indomethacin. Each sample was suspended with 10% HCO-60 in saline and administered orally, immediately before the indomethacin administration. The animals were sacrificed 7 h later and their ulcer indices were evaluated.

iv) Water Immersion Stress-Induced Ulcer: The rats were subjected to stress following the method of Takagi and Okabe,[5)] in which animals were immobilized in a stress cage and immersed vertically in a water bath at 22 ± 1°C to the level of the xiphoid process. Each sample was suspended with 10% HCO-60 in saline and administered orally, immediately before the stress treatment. The animals were sacrificed 7 h after being subjected to the stress and their ulcer indices were evaluated.

v) Indomethacin-Produced Gastric Antral Ulcer: This ulcer model was induced according to the method of Satoh *et al.*[6)] Indomethacin (30 mg/kg) was given subcutaneously after the refeeding. Each sample was suspended with 10% HCO-60 in saline and administered orally, 0.5 h before the refeeding. One milliliter of a 1% Evans blue solution was injected into each rat *via* the tail vein immediately before the animals were sacrificed 8 h later and their ulcer indices were evaluated.

vi) Hemorrhagic Shock-Induced Ulcer: This ulcer model was induced according to the method of Ito *et al.*,[7)] with slight modification as followed. The rats were anesthetized with urethane. The blood which corresponded to 2% of the rat's body weight, was withdrawn from the carotid artery over a 5 min period into a syringe containing heparin. Half an hour after the hemorrhagic shock, the shed blood was returned into the carotid artery over 5 min. One milliliter of a 1% Evans blue solution was injected into each rat *via* the tail vein immediately before the animals were sacrificed 0.5 h after the reperfusion and their ulcer indices were evaluated. Each sample was suspended with 10% HCO-60 in saline and administered orally, 0.5 h before the hemorrhagic shock.

vii) DDC-Induced Ulcer: This ulcer model was induced according to the method of Ogino *et al.*[8)] The rats were given subcutaneously 1000 mg/kg of DDC. Each sample was suspended with 10% HCO-60 in saline and administered orally, 0.5 h before the DDC administration. The animals were sacrificed 7 h later and their ulcer indices were evaluated.

viii) PAF-Induced Ulcer: This ulcer model was induced according to the method of Satoh *et al.*[9)] The rats were given intravenously 8 μg/kg of PAF. Each sample was suspended with 10% HCO-60 in saline and administered orally, 0.5 h before the PAF administration. The animals were sacrificed 1 h later and their ulcer indices were evaluated.

ix) Acetic Acid-Induced Ulcer: The experiment was carried out according to the methods of Takagi *et al.*[10)] and Okabe *et al.*[11)] The rats were anesthetized with ether. The abdomen was incised and the stomach was exposed. 0.02 ml of 20% acetic acid was injected into the submucosal layer of the antral-oxyntic border on the anterior wall, then the abdomen was closed. Thereafter, the animals were fed normally and each sample was mixed with soybean oil and administered orally, twice a day for 14 d from the fifth day after the operation. The animals were sacrificed 16 h after the final administration of each sample and their ulcer indices were evaluated.

Evaluation of Gastric Ulcer Models Ulcered stomachs were removed, inflated with 10 ml of saline and immersed in 1% formalin solution for 5 min. The stomach was incised along the greater curvature and examined for gastric lesions. The total length (mm) of all lesions in the glandular portion of the stomach was used as an ulcer index on ethanol-, HCl·aspirin-, indomethacin-, water immersion stress-, hemorrhagic shock- and DDC-induced ulcer models. The total diameter (mm) of all

lesions in the antral portion of the stomach was used as an ulcer index on an indomethacin-produced gastric antral ulcer model. The ulcerous area (mm^2) was determined under a dissecting microscope ($\times 10$) with the aid of a square grid as an ulcer index on PAF- and acetic acid-induced ulcer models.

Gastric Acid Secretion in Pylorus-Ligated Rats The rats were anesthetized with ether and the pylorus was ligated. Each sample was mixed with soybean oil and administered perorally 2 or 4 h before pylorus ligation. Four hours after the pylorus ligation, the contents of the stomach were collected and centrifuged. Compound III-1a was an oily substance and it was separated from the gastric content by centrifugation. Furthermore, compd. III-1a did not have a buffer action in itself. Then, the content was analyzed for gastric volume and total acid output. The acidity was measured by titration with 0.05 N NaOH to pH 7.0 using autotitrator (Comtite-8; Hiranuma).

Statistics Results were expressed as the mean ± S.E. and analyzed by a one-way analysis of variance. When the analysis indicated that a significance existed, the treated groups were compared to the control by Dunnett's test.

Results

Anti-ulcer Effects of Compd. III-1a on Various Experimental Ulceration Models in Rats Compound III-1a administered at an oral dose of 300 mg/kg significantly inhibited the formation of gastric ulcer induced by ethanol. On the other hand, the anti-ulcer activity of plaunotol as a reference drug was equivalent to that of compd. III-1a on ethanol-induced ucler. Compound III-1a and plaunotol showed significant inhibitory activities in the rats having HCl·aspirin-induced gastric ulcer at 100 and 300 mg/kg, *p.o.* respectively. Both compd. III-1a and plaunotol showed a significant decrease in their indices for indomethacin-induced gastric ulcer at a dose of 100 mg/kg, *p.o.* Anti-stress ulcer activity of compd. III-1a was about 100-fold stronger than that of plaunotol (Table I).

1) Effect on Indomethacin-Produced Gastric Antral Ulcer As shown in Table II, compd. III-1a showed the same significant inhibitory activity as spizofurone did at a dose of 100 mg/kg, *p.o.* on indomethacin-produced gastric antral ucler.

2) Effect on Hemorrhagic Shock-, DDC- and PAF-Induced Ulcer As shown in Table III, compd. III-1a significantly inhibited the formation of gastric ulcers induced by hemorrhagic shock, DDC and PAF at doses of 100, 30 and 100 mg/kg, respectively. Plaunotol only showed significant

TABLE I. Effect of 2-(*E*-2-Decenoylamino)ethyl 2-(Cyclohexylethyl) Sulfide (Compd. III-1a) on Ethanol-, HCl·Aspirin-, Indomethacin- and Stress-Induced Ulceration in Rats

Ulceration	Treatment	Dose (mg/kg)	Ulcer index	Inhibition (%)
Ethanol-induced ulceration	Control[a,b]	—	47.5±5.0	—
	Compd. III-1a[b]	300	27.8±6.0[f]	41.5
		100	35.8±5.0	24.6
	Plaunotol[b]	300	28.1±5.3[f]	40.8
		100	38.0±5.4	20.0
		30	45.0±6.8	5.3
HCl·Aspirin-induced ulceration	Control[a,c]	—	44.5±5.4	—
	Compd. III-1a[c]	100	22.4±4.4[g]	49.7
		30	32.1±4.9	27.9
	Plaunotol[b]	300	28.9±4.2[f]	35.1
		100	29.2±5.9	34.4
		30	41.9±5.2	5.8
Indomethacin-induced ulceration	Control[a,d]	—	36.1±4.7	—
	Compd. III-1a[d]	100	16.6±2.6[g]	54.0
		30	32.9±4.5	8.9
	Plaunotol[b]	300	15.7±2.4[g]	56.5
		100	23.9±3.4	33.8
		30	28.5±3.7	21.1
Stress-induced ulceration	Control[a,e]	—	18.8±2.1	—
	Compd. III-1a[e]	3	8.9±0.9[g]	52.7
		1	10.9±1.3[g]	42.0
	Plaunotol[b]	100	11.3±1.7[f]	39.9
		30	12.1±2.0[f]	35.6
		10	18.8±2.2	0.0

All values represent the mean ± S.E. of 16 rats. *a*) HCO-60, 10% in saline. *b*) Each sample was administered perorally, 0.5 h before the peroral administration of 70% ethanol. *c*) Each sample was administered perorally, 0.5 h before the peroral administration of 100 mg/kg of aspirin, suspended in 1% gum arabic in 150 mM HCl. *d*) Each sample was administered perorally, immediately before the subcutaneous injection of 30 mg/kg of indomethacin. *e*) Each sample was administered perorally, immediately before the restraint and water immersion stress loading. Significantly different from the control group: *f*) $p<0.05$, *g*) $p<0.01$.

TABLE II. Effect of 2-(*E*-2-Decenoylamino)ethyl 2-(Cyclohexylethyl) Sulfide (Compd. III-1a) on Indomethacin-Produced Gastric Antral Ulceration in Refed Rats

Treatment	Dose (mg/kg)	Ulcer index	Inhibition (%)
Control[a]	—	3.4±0.7	—
Compd. III-1a	300	1.2±0.4[b]	64.7
	100	1.6±0.4[b]	52.9
	30	2.3±0.5	32.4
Spizofurone	100	1.5±0.3[b]	55.9

All values represent the mean ± S.E. of 16 rats. *a*) HCO-60, 10% in saline. Each sample was administered perorally 0.5 h before the refeeding. Significantly different from the control group: *b*) $p<0.05$.

TABLE III. Effect of 2-(*E*-2-Decenoylamino)ethyl 2-(Cyclohexylethyl) Sulfide (Compd. III-1a) on Hemorrhagic Shock-, DDC- and PAF-Induced Ulceration in Rats

Ulceration	Treatment	Dose (mg/kg)	Ulcer index	Inhibition (%)
Hemorrhagic shock-induced ulceration	Control[a,b]	—	19.2±2.3	—
	Compd. III-1a[b]	300	9.0±1.8[f]	53.1
		100	12.1±2.5[e]	37.0
	Plaunotol[b]	300	19.0±3.7	1.0
		100	21.9±3.8	(−14.1)
DDC-induced ulceration	Control[a,c]	—	8.1±1.7	—
	Compd. III-1a[c]	100	2.6±0.7[f]	67.9
		30	2.9±0.6[e]	64.2
	Plaunotol[c]	100	5.2±0.7	35.8
		30	7.5±2.0	7.4
PAF-induced ulceration	Control[a,d]	—	6.3±0.2	—
	Compd. III-1a[d]	300	4.7±0.3[f]	25.4
		100	5.0±0.1[f]	20.6
	Plaunotol[d]	300	4.8±0.4[e]	23.8
		100	5.0±0.2[f]	20.6

All values represent the mean ± S.E. of 8—12 rats. *a*) HCO-60, 10% in saline. *b*) Each sample was administered perorally, 0.5 h before the hemorrhagic shock. *c*) Each sample was administered perorally, 0.5 h before the subcutaneous injection of 1000 mg/kg of DDC. *d*) Each sample was administered perorally, 0.5 h before the intravenous injection of 8 μg/kg of PAF. Significantly different from the control group: *e*) $p<0.05$, *f*) $p<0.01$.

TABLE IV. Effect of 2-(*E*-2-Decenoylamino)ethyl 2-(Cyclohexylethyl) Sulfide (Compd. III-1a) on Acetic Acid-Induced Ulceration in Rats

Treatment	Dose (mg/kg/d)	Ulcer index	Healing rate (%)
Control[a]	—	10.6±1.2	—
Compd. III-1a	200×2	5.6±0.7[c]	47.2
	100×2	7.3±0.9[b]	31.1
	50×2	8.7±1.1	17.9
Plaunotol	200×2	7.4±0.8[b]	30.2

All values represent the mean ± S.E. of 15 rats. *a*) Soybean oil. Each sample was administered perorally, twice a day for 14 d from the 5th day after the operation. Significantly different from the control group: *b*) $p<0.05$, *c*) $p<0.01$.

TABLE V. Effect of 2-(*E*-2-Decenoylamino)ethyl 2-(Cyclohexylethyl) Sulfide (Compd. III-1a) on Gastric Secretion in Pylorus-Ligated Rats

Treatment	Dose (mg/kg)	Gastric volume (ml/100 g b.wt.)	Total acid output (μeq/100 g b.wt.)
Control[a,b]	—	2.65±0.32	202.9±33.1
Compd. III-1a[b]	200	1.79±0.23[d]	104.9±23.5[d]
	100	2.63±0.34	184.6±33.5
	50	2.65±0.32	194.0±37.2
Control[a,c]	—	2.34±0.42	195.0±44.5
Compd. III-1a[c]	100	1.39±0.23	88.0±22.3[d]
	50	1.78±0.23	124.5±22.7
	25	1.58±0.15	108.2±16.7

All values represent the mean±S.E. of 10 rats. *a*) Soybean oil. Each sample was administered perorally, 2 h[b] or 4 h[c] before pylorus ligation. Significantly different from the control group: *d*) $p<0.05$. b.wt., body weight.

inhibitory activity on PAF-induced ulcer in these three ulcer models at a dose of 100 mg/kg.

3) Effect on Acetic Acid-Induced Ulcer The consecutive administration of compd. III-1a (100 mg/kg, *p.o.*) twice a day significantly accelerated the healing of acetic acid-induced ulcer and that of plaunotol (200 mg/kg, *p.o.*) showed the same activity (Table IV).

4) Effect on Gastric Acid Secretion Gastric acid secretion was significantly reduced by compd. III-1a administration at doses of 200 and 100 mg/kg, *p.o.* at 2 and 4 h before pylorus ligation, respectively (Table V).

Discussion

We reported that among the derivatives of 2-(*E*-2-alkenoylamino)ethyl alkyl sulfide, 2-(*E*-2-decenoylamino)ethyl 2-(cyclohexylethyl) sulfide (compd. III-1a) showed the strongest inhibitory activity on water immersion stress-induced ulcer and low toxicity.[1] In the present study, the effects of compd. III-1a on various experimental ulcer models and gastric secretion were examined.

On ethanol-induced ulcer, ethanol directly harms gastric mucosa. Prostaglandins (PGs)[12] and leukotrienes (LTs)[13] play a significant role in the pathogenesis of this lesion. The potency of compd. III-1a on the ethanol-induced ulcer model was less than that on the other ulcer models. This result indicated that compd. III-1a did not have the cytoprotective activity by itself.

HCl·aspirin-induced ulcer is caused by the destruction of gastric mucosal barrier and the back-diffusion of H^+.[14] Furthermore, it was reported that the inhibition of cyclooxygenase activity by aspirin causes the decrease of PGs in gastric mucosa and the decrease is one of the important pathogenesis of the HCl·aspirin-induced ulcer model.[15] From the evidence that compd. III-1a significantly inhibited this model at a dose of 30 mg/kg, it was suggested that compd. III-1a retained the gastric mucosal barrier and maintained the PGs content.

Indomethacin is one of the nonsteroidal anti-inflammatory drugs (NSAIDs) and the general side effect of its gastrointestinal injury, which is caused by the reduction of PGs content in gastric mucosa.[16] From the results that compd. III-1a showed the anti-ulcerous activity on ethanol-, HCl·aspirin- and indomethacin-induced ulcer models, compd. III-1a seemed to maintain or increase PGs content in gastric mucosa. Furthermore, one of the anti-ulcerous activities of compd. III-1a might be dependency on cytoprotective activity of PGs. Further studies on PGs content and the enzyme related to PGs were scheduled.

The pathogenesis of the stress-induced ulcer model is complicated. But some of them seemed to be excitement of the autonamic nervous system,[17] acceleration of gastric motility,[18] increase of gastric secretion,[19] impairment of gastric mucosal blood flow,[20] decrease of PGs[21] and reduction of cell proliferation.[22] Compound III-1a showed the strongest activity on stress-induced ulcer among the gastric ulcer models we examined. This result suggested that compd. III-1a might have several effects on these pathogenesis. Further studies on them were scheduled.

Acute gastric ulcer models have the mucosal lesion in the fundic gland and the shape of the lesion is generally linear. On the other hand, the indomethacin-produced gastric antral ulcer model has the mucosal lesion in the pyloric antrum and its shape is round. From these points, the indomethacin-produced gastric antral ulcer model seems to resemble the human ulcer. It was reported that cimetidine and cetraxate did not show the effect on this model but PGE_2 did.[23,24] Spizofurone inhibited this ulcer model and potentiated the inhibitory effect of PGE_2 on this ulcer model.[24] Then we used spizofurone as a reference drug on this model. From the result that compd. III-1a showed the effect on this model, compd. III-1a seemed to become the unique anti-ulcer drug.

Recently it was reported that one of the pathogenesis of the stress-induced ulcer on which there was ischemia-reperfusion in a part of gastric mucosa, was generation of oxygen free radicals.[25] From the result that compd. III-1a showed strong inhibitory activity on the stress-induced ulcer, one of the anti-ulcerous actions of compd. III-1a seemed to be to depress the radical generation or accelerate the radical destruction. Then we examined the effects of compd. III-1a on hemorrhagic shock-, DDC- and PAF-induced ulcer models which seemed to be caused mainly by oxygen free radicals. Compound III-1a showed the significant inhibitory activities on these ulcer models and seemed to suppress the formation of the radicals or have a scavenger effect on them. But the compound which improved gastric mucosal blood flow (GMBF) was effective on these ulcer models. Then the effect of compd. III-1a on GMBF was scheduled.

There are many ulcer models but many of them are acute ulcer models. The acetic acid-induced ulcer model is thought to be the most useful chronic ulcer model for evaluating the curative effect of anti-ulcerous agents.[26] From the result that compd. III-1a accelerated the healing rate on it, compd. III-1a seemed to have both preventive and curative effects on the ulcer.

There are two types of anti-ulcerous drugs. One type is an anti-secretory agent to which histamine H_2 receptor antagonist, cimetidine and proton pump inhibitor, omeprazole belong. The other is the so-called defensive factor promoting agents. Recently, a dual type anti-ulcer drug was investigated.[27] Then we examined the inhibitory effect of compd. III-1a on the gastric secretion. Acid secretion in pylorus ligated rat which was thought to be basal secretion, could be inhibited significantly by the oral administration of compd. III-1a. Compound III-1a was thought to be absorbed in the duodenum or the small intestine followed by a time lag between the absorption and the action.

Furthermore, to show the inhibitory effect of compd. III-1a on the gastric secretion in pylorus ligation, compd. III-1a was thought to pass through the stomach. The administrative schedule in this time was employed from these points. The effective difference arising from the administrative schedule should be due to the absorptive rate of compd. III-1a.

The results in the present study suggest that compd. III-1a has dual action on ulcer formation.

References

1) I. Kohda, M. Iwai, M. Watanabe, Y. Arakawa, C. Fukaya, K. Yokoyama, Y. Kohama and T. Mimura, *Chem. Pharm. Bull.*, **39**, 1546 (1991).
2) H. Kuwata, K. Ishihara, M. Kakei, S. Ohara, H. Okabe and K. Hotta, *Jpn. J. Gastroenterol.*, **82**, 28 (1985).
3) P. H. Guth, D. Aures and G. Paulsen, *Gastroenterology*, **76**, 88 (1979).
4) T. Urushidani, S. Okabe, K. Takeuchi and K. Takagi, *Jpn. J. Pharmacol.*, **27**, 316 (1977).
5) K. Takagi and S. Okabe, *Jpn. J. Pharmacol.*, **18**, 9 (1968).
6) H. Satoh, I. Inada, T. Hirata and Y. Maki, *Gastroenterology*, **81**, 719 (1981).
7) M. Ito and P. H. Guth, *Gastroenterology*, **86**, 112 (1984).
8) K. Ogino, S. Oka, S. Matuura, I. Sakaida, S. Yoshimura, K. Matuda, Y. Sasaki, K. Yamamoto, T. Yoshikawa, Y. Okazaki and T. Takemoto, *J. Clin. Biochem. Nutr.*, **3**, 189 (1987).
9) H. Satoh, K. Iwasaki, N. Inatomi, A. Sino and Y. Maki, *Jpn. J. Pharmacol.*, **43** (Sup), 231 (1987).
10) K. Takagi, S. Okabe and R. Saziki, *Jpn. J. Pharmacol.*, **19**, 418 (1969).
11) S. Okabe, H. Jino and A. Nishida, *Jpn. J. Pharmacol.*, **40**, 329 (1986).
12) T. Mizui and M. Doteuchi, *Jpn. J. Pharmacol.*, **33**, 939 (1983).
13) B. M. Peskar, K. Lange, V. Floppe and B. A. Peskar, *Prostaglandins*, **31**, 283 (1986).
14) H. W. Davenport, *Gastroenterology*, **46**, 245 (1964).
15) J. R. Vane, *Nature New Biol.* (London), **231**, 232 (1971).
16) B. J. R. Whittle, *Gastroenterology*, **80**, 94 (1981).
17) Y. Osumi, S. Takaori and M. Fujiwara, *Jpn. J. Pharmacol.*, **23**, 904 (1973).
18) T. Garrick, F. W. Leung, S. Buack, K. Hirabayashi and P. H. Guth. *Gastroenterology*, **91**, 141 (1986).
19) H. Kitagawa, M. Fujiwara and Y. Osumi, *Gastroenterology*, **77**, 298 (1979).
20) M. Murakami, S. K. Lam, M. Inada and T. Miyake, *Gastroenterology*, **88**, 660 (1985).
21) T. Arakawa, K. Kobayashi, H. Nakamura, S. Chono, H. Yamada, T. Ono and S. Yamamoto, *Gastroenterol. Jpn.*, **16**, 236 (1981).
22) H. Kuwayama and G. L. Eastwood, *Gastroenterology*, **88**, 362 (1985).
23) N. Inatomi, H. Satoh, T. Hirata, I. Inada, K. Iwakasi and Y. Maki, *Yakuri To Chiryo*, **14**, 599 (1986).
24) N. Inatomi, H. Satoh, I. Inada, T. Hirata, H. Nagai and Y. Maki, *Eur. J. Pharmacol.*, **112**, 81 (1985).
25) T. Yoshikawa, H. Miyagawa, N. Yoshida, S. Sugino and M. Kondo, *J. Clin. Biochem. Nutr.*, **1**, 271 (1986).
26) M. Moriga, "Shyokaseikaiyou No Atarashii Tennkai," Kanishyobou, Tokyo, 1986, pp. 71—87.
27) T. Aizawa and Y. Matuo, *J. Clin. Sci.*, **26**, 50 (1990).

Further Studies on the Anti-ulcerogenic Effects of Compound, 2-(*E*-2-Decenoylamino)ethyl 2-(Cyclohexylethyl) Sulfide

Isao KOHDA,*[,a] Hitoshi NAGAI,[a] Masakazu IWAI,[a] Masahiro WATANABE,[a] Kazumasa YOKOYAMA,[a] Kazutaka TSUJIKAWA[b] and Tsutomu MIMURA[b]

Central Research Laboratories, The Green Cross Corporation,[a] Shodai Ohtani 2–1180–1, Hirakata, Osaka 573, Japan and Faculty of Pharmaceutical Sciences, Osaka University,[b] Yamadaoka 1–6, Suita, Osaka 565, Japan. *Received December 17, 1990*

Tha anti-ulcerogenic mechanism of 2-(*E*-2-decenoylamino)ethyl 2-(cyclohexylethyl) sulfide (compd. III-1a) was investigated in various gastric defensive factors. Compound III-1a maintained the high molecular glycoprotein (relative content of Fr. I hexose) and accelerated hexosamine synthesis which were reduced by water immersion stress. But plaunotol did not have these actions. The lipid peroxide level in the gastric mucosa from water immersion stressed rat was lowered by the administration of compd. III-1a. Compound III-1a maintained prostaglandin E_2 (PGE_2) and PGI_2 contents which were reduced in the early phase of the stress and accelerated PGs synthesis in the late phase of the stress. Furthermore, compd. III-1a maintained phospholipase A_2 (PLA_2) activity which was reduced by the stress. The plaunotol treated group showed the same tendency as the compd. III-1a treated group on the lipid peroxide level, PGE_2 and PGI_2 contents, and PLA_2 activity, but the potency of plaunotol was less than that of compd. III-1a. Compound III-1a accelerated gastric cell proliferation in pyloric glands of hydrocortisone treated rats. Tetragastrin accelerated significantly the cell proliferation in fundic glands. The sucralfate treated group showed the same tendency as the compd. III-1a treated group but the potency of sucralfate was less than that of compd. III-1a. The results in the present study suggest that compd. III-1a has a protective action on gastric mucosa.

Keywords 2-(*E*-2-decenoylamino)ethyl 2-(cyclohexylethyl) sulfide; anti-ulcerogenic activity; high molecular glycoprotein; Fr. I hexose; hexosamine; lipid peroxide; PGE_2; PGI_2; PLA_2; cell proliferation

Previously, we reported that among the derivatives of 2-(*E*-2-alkenoylamino)ethyl alkyl sulfide, 2-(*E*-2-decenoylamino)ethyl 2-(cyclohexylethyl) sulfide (compd. III-1a) showed the strongest inhibitory activity on stress-induced ulcer and low toxicity.[1] Compound III-1a showed inhibitory effects on various ulcer models and gastric secretion.[2] In the present paper, the effects of compd. III-1a on the gastric defensive factors were investigated by examining the amount of high molecular glycoprotein (relative content of Fr. I hexose), hexosamine, lipid peroxide, prostaglandin E_2 (PGE_2), PGI_2, and phospholipase A_2 (PLA_2) activity in gastric mucosa. Furthermore, the effect of compd. III-1a on cell proliferation of the generative zone was examined.

Experimental

Materials 2-(*E*-2-Decenoylamino)ethyl 2-(cyclohexylethyl) sulfide was synthesized as described previously.[1] HCO-60 was obtained from Nikko Chemicals. Plaunotol (Kelnac®, Sankyo), sucralfate (Ulcerlmin®, Chugai), and tetragastrin (UCB Bioproducts) were used as reference drugs.

Experimental Gastric Ulcer Model in Rats (Stress-Induced Ulcer) Male Wistar rats weighing 230—250 g (7 weeks, Charles River Japan), fasted for 24 h, were used as experimental animals. The rats were subjected to stress according to the method of Takagi and Okabe,[3] in which animals were immobilized in a stress cage and immersed vertically in a water bath at 22±1 °C to the level of the xiphoid process. Each sample was suspended with 10% HCO-60 in saline and administered perorally, immediately before (lipid peroxide, PGE_2, PGI_2 and PLA_2 activity) or twice a day for 3 d and immediately before the stress treatment (relative content of Fr. I hexose and hexosamine). The animals were sacrificed 7 h after the stress treatment, the stomach was removed and the gastric mucosa was examined as follows.

Determination of High Molecular Glycoprotein (Fr. I Hexose) Glycoprotein was extracted from the gastric glandular portion and Fr. I hexose was separated from the glycoprotein according to the method of Azuumi *et al.*[4] The gastric mucosa of three rats were pooled and lyophilized. The lyophilized tissue was weighed, grained and suspended in 0.05 M Tris–HCl buffer, pH 7.2, containing 2% Triton X-100 (2 ml/100 mg dry tissue). The suspension was boiled for 3 min and homogenized. The homogenate was incubated at 37 °C for 1 h and centrifuged at 10000 rpm for 30 min. The extraction of the precipitate was repeated twice. Two milliliters of the pooled supernatant were applied to Bio-Gel A-1.5 m column (1 × 45 cm), which had been preequilibrated with Tris–HCl buffer containing Triton X-100 as described above, and the column was eluted with this buffer. Hexose in each fraction was measured by the phenol–sulphuric acid method[5] using galactose as a standard. The eluted materials were divided into three fractions. The proportion of high molecular fraction (Fr. I hexose) in total hexose was called "relative content of Fr. I hexose."

Determination of Hexosamine According to the method of Hiroi *et al.*,[6] the scraped substance from each stomach was homogenized individually with 3 ml of papain solution (Sigma; 100 units of papain in 100 ml of 0.2 M acetate buffer, pH 5.6, containing 2 mM ethylenediaminetetraacetic acid (EDTA), 4 mM cystein, 0.88% NaCl) and digested for 20 h at 37 °C. Indigestive components were eliminated by centrifugation (3000 *g* × 10 min). A portion of the supernatant was hydrolyzed in 2 N HCl in a sealed ampoule at 110 °C for 14 h. Hexosamine was determined by the colorimetric method of Gunnar,[7] and calculated as glucosamine hydrochloride (Nakarai tesque).

Measurement of Lipid Peroxide Lipid peroxide in the gastric mucosa was measured according to the method of Ohkawa *et al.*[8] The tissue was homogenized (10% w/v) with 1.15% KCl. To 0.2 ml of the homogenate, 0.2 ml of 8.1% sodium dodecyl sulfate (SDS), 1.5 ml of 20% acetate buffer and 1.5 ml of 0.8 % thiobarbituric acid (TBA) were added, and the volume was brought up to 4 ml with distilled (dist.) water. The reaction mixture was heated in boiling water for 1 h, then allowed to cool. One milliliter of dist. water and 5 ml of *n*-butanol–pyridine (15 : 1) mixture were added to the reaction mixture and mixed. The chromophore formed by TBA was extracted into the *n*-butanol–pyridine layer after centrifugation (2000 g × 15 min). Lipid peroxide was determined by spectro-fluorometer (ex. :515 nm, em. :553 nm) and calculated as malondialdehyde (MDA).

Determinations of PGE_2 and PGI_2 (6-Keto-$PGF_1\alpha$) The mucosal tissue layer was separated according to the method of Arakawa *et al.*[9] The stomach was opened along the greater curvature and washed with cold saline (containing 10^{-5} M indomethacin). After removing the saline and mucus, the tissue from the fundus was mounted mucosal side down on a glass slide and covered with another glass slide. Each preparation was immersed in hexane in a dry ice-acetone bath, so that the frozen tissue adhered tightly to the slides. The mucosal tissue layer was obtained by pulling the two slides apart rapidly and weighed. PGE_2 and PGI_2 (6-keto-$PGF_1\alpha$) in mucosal tissue were extracted according to the method of Stein *et al.*[10] A phosphate-buffer, pH 7.4 (990 μl), and 1% sodium hydrogen carbonate (10 μl), containing 10% indomethacin, were added to the tissue. After shaking for 30 min, ethanol (750 μl) and dist. water (3250 μl) were added to the mixture. After centrifugation (3000 *g* × 20 min), the supernatant was adjusted at pH 3.0 with 1 N HCl. PGE_2 and PGI_2 (6-keto-$PGF_1\alpha$) were purified according to the method of Powell.[11] A

reversed-phase silica cartridge (Bond elut® C18: Analytichem International) was prepared by rinsing it with 10 ml of methanol followed by 10 ml of dist. water. The acidified sample was passed through the cartridge. The cartridge was washed with 15% ethanol (20 ml), dist. water (20 ml) and petroleum ether (20 ml), and eluted with methyl formate (10 ml). The contents of PGE_2 and PGI_2 (6-keto-$PGF_1\alpha$) were determined by radioimmunoassay (RIA) using Prostaglandin E_2 [^{125}I] RIA kit (Dupont) and 6-Keto-Prostaglandin $F_1\alpha$ [^{3}H] RIA kit (Dupont).

Measurement of PLA_2 Activity PLA_2 activity in gastric mucosa was measured according to the methods of Hirohara *et al.*, [12] and Teramoto *et al.*,[13] with slight modification. The gastric mucosa of the rats was removed and homogenized with 50 mM glycylglycine buffer, pH 7.4, containing 150 mM NaCl and 1 mM (*p*-amidino-phenyl)methanesulfonyl fluoride (5 ml/g mucosal wet tissue). The homogenate was sonicated for 2 min, diluted in 200 mM glycylglycine buffer, pH 8.0, containing 2 mM $CaCl_2$ to 2% solution and used as the enzyme source. The assay solution consisted of phosphatidylcholine, L- α-palmitoyl-2-linoleoyl, [*linoleoyl*-1-^{14}C]-(Dupont), 200 mM glycylglycine buffer, pH 8.0, 2 mM $CaCl_2$ and the enzyme solution were incubated at 37 °C for 15 min. The reaction was terminated by the addition of 100 mM EDTA. To the reaction mixture, 2 ml of isopropanol–heptane–1 N sulfuric acid (40 : 10 : 1, v/v/v) was added and the mixture was vortexed. Distilled water (0.75 ml) and heptane (1.2 ml) were then added, and the mixture was centrifuged (500 *g* × 10 min). One milliliter of the upper phase was mixed with 2 ml of heptane, and 100 mg of silicic acid powder was added to the mixture. After brief centrifugation, 1 ml of the heptane layer was transferred to a vial. The radioactivity was counted by the liquid scintillation counter.

Labeling Indices of Generative Zone Cells The kinetics of superficial epithelial cells of the mouse gastric mucosa was examined by the autoradiographic technique with ^{3}H-thymidine.[14] Each sample was administered perorally or intra-muscularly to ICR male mice twice a day for 7 d. Hydrocortisone (HC: 100 mg/kg, Sigma) was injected subcutaneously to half the number of mice of each treated group once a day for 7 d. After the last administration of the sample, ^{3}H-thymidine (Dupont: 1 μCi/g body wt.) was injected subcutaneously to the mice. The mice were sacrificed 90 min after the thymidine administration. The stomach was fixed with 10% buffered formalin, embedded in paraffin and sectioned longitudinally along the axis of the glandular tubles. Each section of 3 microns in thickness was mounted on a glass slide, dipped in Kodak NTB-2 nuclear emulsion and developed after 2 weeks exposure. They were stained with hematoxylin and eosin. The labeling index of the proliferation cell zone was counted and expressed as the percentage of labeled cell in total cells.

Statistics Results were expressed as the mean ± S.E. and analyzed by a one-way analysis of variance. When the analysis indicated that significance existed, the treated groups were compared to the control by Dunnett's test.

Results

Effect of Compd. III-1a on Relative Content of Fr. I Hexose in Gastric Mucosa of Normal Rats and Ulcerated Rats Induced by Water Immersed Restrained Stress As shown in Table I, the relative content of Fr. I hexose was reduced significantly during stress loading in the control group. Compound III-1a, given orally at a dose of 100 mg/kg, b.i.d. for 3 d and immediately before the stress maintained the relative content of Fr. I hexose in normal level. On the other hand, plaunotol as a reference drug did not show the effect.

Effect of Compd. III-1a on Hexosamine Content in Gastric Mucosa of Normal Rat and Ulcerated Rats Induced by Water Immersed Restrained Stress As shown in Table II, the hexosamine content was reduced significantly during stress loading in the control group. In the compd. III-1a treated group, the hexosamine content was reduced equally with the control group 4 h after the stress loading, but increased significantly 7 h after the stress loading. In the plaunotol treated group, the hexosamine content was reduced significantly during stress loading.

Effect of Compd. III-1a on Lipid Peroxide Content in Gastric Mucosa of Normal Rats and Ulcerated Rats Induced by Water Immersed Restrained Stress Lipid peroxide content was estimated from the TBA reacting substance. The stress loading increased lipid peroxide content significantly in the control group. At a dose of 100 mg/kg, the lipid peroxide content in the compd. III-1a treated group was kept at a normal level. The plaunotol treated group showed the same tendency as the compd. III-1a treated group but the potency of plaunotol was less than that of compd. III-1a (Table III).

Effect of Compd. III-1a on PGE_2 and PGI_2 Contents in

Table I. Effect of Compd. III-1a on Relative Content of Fr. I Hexose in Gastric Mucosa of Normal Rats and Ulcerated Rats Induced by Water Immersed Restrained Stress

Treatment	Sample	Dose (mg/kg)	Relative content of Fr. I hexose
Normal			40.2 ± 0.4
Stress (4 h)	Control[a]	—	30.5 ± 2.0 (−24.1)[b]
	Compd. III-1a	100	38.5 ± 3.2 (− 4.2)
	Plaunotol	100	32.8 ± 1.6 (−18.4)
Stress (7 h)	Control[a]	—	28.9 ± 0.2 (−28.1)[c]
	Compd. III-1a	100	37.7 ± 0.8 (− 6.2)[d]
	Plaunotol	100	32.1 ± 3.1 (−20.2)

a) HCO-60, 10% in saline. Each sample was administered perorally, twice a day for 3 d and immediately before the restraint and water (22 ± 1 °C) immersion. All values represent the mean ± S.E. of 5 experiments. Each value in parenthesis represents the rate of change to the normal. Significantly different from the normal group: *b*) $p<0.05$, *c*) $p<0.01$. Significantly different from the control group: *d*) $p<0.01$.

Table II. Effect of Compd. III-1a on Hexosamine Content in Gastric Mucosa of Normal Rats and Ulcerated Rats Induced by Water Immersed Restrained Stress

Treatment	Sample	Dose (mg/kg)	Hexosamine (μg/mg dry wt.)
Normal			43.1 ± 1.1
Stress (4 h)	Control[a]	—	35.5 ± 1.0 (−17.6)[b]
	Compd. III-1a	100	35.7 ± 1.2 (−17.2)[b]
	Plaunotol	100	33.3 ± 1.1 (−22.7)[b]
Stress (7 h)	Control[a]	—	36.2 ± 0.5 (−16.0)[b]
	Compd. III-1a	100	39.4 ± 0.9 (− 8.6)[c]
	Plaunotol	100	32.7 ± 1.2 (−24.1)[b]

a) HCO-60, 10% in saline. Each sample was administered perorally, twice a day for 3 d and immediately before the restraint and water (22 ± 1 °C) immersion. All values represent the mean ± S.E. of 6 rats. Each value in parenthesis represents the rate of change to the normal. Significantly different from the normal group: *b*) $p<0.05$. Significantly different from the control group: *c*) $p<0.05$.

Table III. Effect of Compd. III-1a on Lipid Peroxide Content in Gastric Mucosa of Normal Rats and Ulcerated Rats Induced by Water Immersed Restrained Stress

Treatment	Sample	Dose (mg/kg)	Lipid peroxide (nmol MDA/g wet wt.)
Normal			73.4 ± 5.7
Stress (4 h)	Control[a]	—	99.3 ± 5.2 (+35.3)[b]
	Compd. III-1a	100	83.6 ± 5.1 (+13.9)
	Plaunotol	100	85.3 ± 5.1 (+16.1)
Stress (7 h)	Control[a]	—	103.7 ± 5.3 (+41.3)[b]
	Compd. III-1a	100	85.8 ± 4.7 (+16.9)[c]
	Plaunotol	100	87.5 ± 5.0 (+19.2)

a) HCO-60, 10% in saline. Each sample was administered perorally, immediately before the restraint and water (22 ± 1 °C) immersion. All values represent the mean ± S.E. of 10 rats. Each value in parenthesis represents the rate of change to the normal. Significantly different from the normal group: *b*) $p<0.05$. Significantly different from the control group: *c*) $p<0.05$.

TABLE IV. Effect of Compd. III-1a on PGE_2 and PGI_2 Contents in Gastric Mucosa of the Normal Rats and the Ulcerated Rats Induced by Water Immersed Restrained Stress

Treatment	Sample	Dose (mg/kg)	PGE_2 (ng/100 mg wet wt.)	PGI_2 (ng/100 mg wet wt.)
Normal			8.5±1.3	10.5±1.7
Stress (0.5 h)	Control[a)]	—	3.7±0.4 (−56.5)[c)]	8.2±1.4 (−21.9)
	Compd. III-1a	25	7.3±1.0 (−14.1)[e)]	12.6±1.3 (+20.0)
	Plaunotol	25	6.4±1.3 (−24.7)	8.0±1.2 (−23.8)
Stress (1 h)	Control[a)]	—	3.7±0.9 (−56.5)[b)]	4.9±1.1 (−53.3)[b)]
	Compd. III-1a	25	4.4±1.3 (−48.2)[b)]	3.2±0.7 (−69.5)[c)]
	Plaunotol	25	2.2±0.4 (−74.1)[d)]	2.1±0.4 (−80.0)[d)]
Stress (4 h)	Control[a)]	—	2.8±0.5 (−67.1)[c)]	2.8±0.5 (−73.3)[c)]
	Compd. III-1a	25	3.5±0.6 (−58.8)[c)]	5.5±1.3 (−47.6)
	Plaunotol	25	3.8±1.0 (−55.3)[b)]	4.0±1.0 (−61.9)[b)]
Stress (7 h)	Control[a)]	—	10.9±2.2 (+28.2)	25.0±6.8 (+138.1)
	Compd. III-1a	25	16.9±3.1 (+98.8)[b)]	33.2±5.8 (+216.2)[b)]
	Plaunotol	25	13.5±2.3 (+58.8)	22.2±4.9 (+111.4)

a) HCO-60, 10% in saline. Each sample was administered perorally, immediately before the restraint and water (22±1 °C) immersion. All values represent the mean±S.E. of 10 rats. Each value in parenthesis represents the rate of change to the normal. Significantly different from the normal group: *b*) $p<0.05$, *c*) $p<0.01$, *d*) $p<0.001$. Significantly different from the control group: *e*) $p<0.05$.

TABLE V. Effect of Compd. III-1a on Phospholipase A_2 Activity in Gastric Mucosa of Normal Rats and Ulcerated Rats Induced by Water Immersed Restrained Stress

Treatment	Sample	Dose (mg/kg)	Phospholipase A_2 activity [^{14}C-Linoleic acid (pmol)]
Normal			5.92±0.36
Stress (4 h)	Control[a)]	—	1.64±0.24 (−72.3)[c)]
	Compd. III-1a	100	4.60±0.50 (−22.3)[d)]
	Plaunotol	100	2.39±0.52 (−59.6)[c)]
Stress (7 h)	Control[a)]	—	3.61±0.30 (−39.0)[b)]
	Compd. III-1a	100	4.73±0.46 (−20.1)
	Plaunotol	100	4.13±0.73 (−30.2)

a) HCO-60, 10% in saline. Each sample was administered perorally, immediately before the restraint and water (22±1 °C) immersion. All values represent the mean±S.E. of 7 rats. Each value in parenthesis represents the rate of change to the normal. Significantly different from the normal group: *b*) $p<0.05$, *c*) $p<0.01$. Significantly different from the control group: *d*) $p<0.01$.

Gastric Mucosa of Normal Rats and Ulcerated Rats Induced by Water Immersed Restrained Stress The content of PGI_2 was estimated from that of 6-keto $PGF_1\alpha$ which was a stable metabolite of PGI_2. As shown in Table IV, the PGE_2 content was reduced significantly 0.5—4 h after the stress loading and increased above normal level 7 h after the stress loading in the control group. At a dose of 25 mg/kg, compd. III-1a inhibited the reduction of PGE_2 in the early phase (0.5—4 h after the stress loading) of water immersion stress and accelerated the increase of PGE_2 in the late phase (7 h after the stress loading) of the stress. The plaunotol treated group showed the same tendency as the compd. III-1a treated group but the potency of plaunotol was less than that of compd. III-1a. On the other hand, compd. III-1a inhibited the reduction of PGI_2 in the early phase (0.5 h after the stress loading) of water immersion stress and accelerated the increase of PGI_2 in the late phase (7 h after the stress loading) of the stress. The variation of PGI_2 content in the plaunotol treated group, showed the same tendency as in the control group.

Effect of Compd. III-1a on PLA_2 Activity in Gastric Mucosa of Normal Rats and Ulcerated Rats Induced by Water Immersed Restrained Stress PLA_2 activity was estimated by releasing ^{14}C-linoleic acid from phosphatidylcholine, L-α-palmitoyl-2-linoleoyl, [*linoleoyl*-1-^{14}C]. As shown in Table V, PLA_2 activity was reduced significantly during stress loading in the control group. At a dose of 100 mg/kg, compd. III-1a maintained the PLA_2 activity at a normal level. The plaunotol treated group showed the same tendency as the compd. III-1a treated group but the potency of plaunotol was less than that of compd. III-1a.

TABLE VI. Effect of Compd. III-1a on Labeling Indices of Generative Zone Cell in Gastric Mucosa of Mice

Treatment	Route	Dose (mg/kg/d)	Labeling index (%)	
			Fundic glands	Pyloric glands
Control[a)]	*p.o.*	—	7.2±0.6	9.0±1.2
Compd. III-1a	*p.o.*	25×2	8.7±0.6 (+20.8)	8.4±0.8 (− 6.7)
Sucralfate	*p.o.*	200×2	7.5±0.3 (+ 4.2)	6.8±0.7 (−24.4)
Tetragastrin	i.m.	1×2	11.4±0.7 (+58.3)[b)]	9.1±0.3 (+ 1.1)
Hydrocortisone	s.c.	100		
+control[a)]	*p.o.*	—	5.1±0.6	3.8±0.4
Hydrocortisone	s.c.	100		
+compd. III-1a	*p.o.*	25×2	5.7±0.3 (+11.8)	6.2±0.6 (+63.2)[b)]
Hydrocortisone	s.c.	100		5.0±0.2 (+31.6)
+sucralfate	*p.o.*	200×2	6.1±0.5 (+19.6)	

a) Saline. All values represent the mean±S.E. of 5 mice. Each value in parenthesis represents the rate of change to the control. Significantly different from the control group: *b*) $p<0.05$.

Effect of Compd. III-1a on Labeling Indices of Generative Zone Cells in Gastric Mucosa of Mice The gastric cell proliferation was estimated by labeling indices of generative zone cells. Compound III-1a (25 mg/kg, b.i.d., *p.o*), sucralfate (200 mg/kg, b.i.d., *p.o.*), tetragastrin (1 mg/kg, b.i.d., i.m.) and hydrocortisone (HC; 100 mg/kg, sem. in d., s.c.) were administered for 7 d. Compound III-1a accelerated the cell proliferation in fundic glands but its effect was not significant. Furthermore, compd. III-1a significantly accelerated the cell proliferation which was reduced by HC in the pyloric glands. Tetragastrin significantly accelerated the cell proliferation in fundic glands. The sucralfate treated group showed the same tendency as the compd. III-1a treated group but the potency of sucralfate was less than that of compd. III-1a (Table VI).

Discussion

We have already reported that 2-(*E*-2-decenoylamino)ethyl 2-(cyclohexylethyl) sulfide (compd. III-1a) showed inhibitory effects on various ulcer models and gastric secretion.[2)] For example, the ulcer indices of the control and compd. III-1a (3 mg/kg, *p.o.*) on the stress-induced ulcer model were 23.4±3.2 and 10.1±1.1 ($p<0.001$), respectively.[2)] In the present paper, the anti-ulcerogenic effects of compd. III-1a on the gastric defensive factors were investigated. Plaunotol was used as a reference drug because its physical character (oily) was the same as compd. III-1a. Plaunotol exhibited its anti-ulcer effect mainly by potentiating the mucosal defensive factors. Compound III-1a showed the inhibitory activities on the acute gastric ulcer models (water immersion stress and indomethacin) which were caused by the degradation of gastric mucosa.[2)] Glycoprotein is a component of gastric mucosa and plays an important role in its defensive factor.[15)] But in order to play a defensive role, it must be high molecule. The ulcer index of 4 h after water immersed restrained stress was little

and that of 6 h after the stress rapidly increased.[16] It was reported that the high molecular glycoprotein is reduced significantly at 2 h after the stress loading[16] and this reduction seems to be the cause of ulceration which is caused by the activation of glucosidase.[17] We investigated the effect of compd. III-1a on the proportion of the high molecular fraction which was called "relative content of Fr. I hexose" in total hexose. Compound III-1a maintained the relative content of Fr. I hexose at a normal level. This indicated that the effect of compd. III-1a was based on an inhibition of the glycoprotein degradation system.

In general, the quantitation of hexosamine, which is the most important component in gastric mucosa, is the usual technique for evaluating the quantitation of glycoprotein.[18] Compound III-1a increased the hexosamine content to the normal level 7 h after the stress loading. This result suggested that compd. III-1a accelerated the hexosamine synthesis which was reduced by water immersion stress.

Recently it was reported that ischemic reperfusion injury is caused by oxygen free radicals,[19,20] the injury is accelerated by lipid peroxide which is induced by oxygen free radicals,[21] and the increase of lipid peroxide in gastric mucosa causes stress-induced gastric ulcer.[22] Compound III-1a showed anti-ulcerous activity on the stress-induced ulcer model. Furthermore, compd. III-1a showed anti-ulcerous activities on hemorrhagic schock-induced and diethyldithiocarbamic acid (DDC)-induced ulcer models.[2] These ulcers seemed to be caused by the radicals.[23,24] Superoxide dismutase, catalase and allopurinol, which eliminate the radicals, showed inhibitory activities on these ulcer models and depressed the increase of lipid peroxide.[25] From the result that the lipid peroxide content in compd. III-1a treated rats was kept at a normal level, compd. III-1a was considered to suppress the formation or scavenge the radicals.

Prostaglandins (PGs) are widely distributed throughout the gastrointestinal tract and prevent the damage of the mucosa by necrotizing agents (absolute ethanol, 0.6 N HCl, 0.2 N NaOH). This ability is designated as "cytoprotection."[26] The PGs content in the gastric mucosa of a patient with a gastric ulcer is lower than that of a healthy person.[27] PGE_2 and PGI_2 are the main components of the PGs in gastric mucosa and play an important role in gastric defensive mechanisms.[28] Compound III-1a showed anti-ulcerous activities on stress-, indomethacin- and HCl·aspirin-induced ulcer models[2] and these ulcer models seemed to be caused by a shortage of the PGs. In the preliminary study, the effect of compd. III-1a on the PGs content was examined at 25—100 mg/kg and the effect was shown at 25 mg/kg. Then we investigated the effects of compd. III-1a (25 mg/kg) on the PGE_2 and PGI_2 contents in gastric mucosa. Compound III-1a maintained PGE_2 and PGI_2 contents which were reduced in the early phase of the water immersed stress and accelerated their synthesis in the late phase of the stress. These results suggested that one of the mechanisms of the anti-ulcerous activity of compd. III-1a was due to maintenance of the PGs content in the gastric mucosa. But it was reported that the PGs contents increased at 30 min after stress loading and significantly decreased at 6 h after stress loading.[29] There is no appropriate explanation for the difference between our result and Arakawa's result[29] on the PGs content after stress loading. Further detailed study on the PGs content after stress loading was scheduled.

PGs are biosynthesized by the arachidonate cascade reaction, and phospholipase A_2 (PLA_2) is the starting enzyme of this cascade reaction. The decrease in the PGs content could be linked with the decrease in the activity of PLA_2.[30] Cimetidine, the antagonist of the histamine H_2 receptor, reduces the PGs content.[31] There is a report that the reduction is due to inhibition of the PLA_2 activity.[12] Compound III-1a maintained the PLA_2 activity which was reduced by the water immersed stress. The effect of compd. III-1a on the PGs seemed to be due to maintenance of the PLA_2 activity in the gastric mucosa. Furthermore, glucocoluticoids which increased after stress loading, induced lipomodulin and were a PLA_2 inhibitor.[32] Further studies on the relationship between glucocoluticoids, lipomodulin and PLA_2 activity were sheduled.

The cell proliferation kinetics in gastric mucosa played a significant role in the pathogenesis of gastric disease.[33] ^{3}H-Thymidine autoradiography was employed to evaluate the effect of compd. III-1a on the generative cell proliferation of gastric mucosa. Compound III-1a increased labeling indices of generative cells in the fundic gland but potency of compd. III-1a was less than that of tetragastrin. Gastrin (tetragastric) had strong trophic action on gastric mucosa.[34] On the other hand, HC showed inhibitory action on cell proliferation,[35] and delayed the healing of the ulcer.[36] Compound III-1a accelerated the cell proliferation which was reduced by HC and the antiulcerous activity of compd. III-1a may be due to acceleration of the cell proliferation under ulcer disease.

The results in the present study, therefore, suggest that compd. III-1a has a protective action on gastric mucosa.

References

1) I. Kohda, M. Iwai, M. Watanabe, Y. Arakawa, C. Fukaya, K. Yokoyama, Y. Kohama and T. Mimura, *Chem. Pharm. Bull.*, **39**, 1546 (1991).
2) I. Kohda, H. Nagai, M. Iwai, M. Watanabe, K. Yokoyama, K. Tsujikawa and T. Mimura, *Chem. Pharm. Bull.*, **39**, 1828 (1991).
3) K. Takagi and S. Okabe, *Jpn. J. Pharmacol.*, **18**, 9 (1968).
4) Y. Azuumi, S. Ohara, K. Ishihara, H. Okabe and K. Hotta, *Gut*, **21**, 533 (1980).
5) M. Dubois, K. A. Gilles, J. K. Hamilton, P. A. Robers and F. Smith, *Anal. Chem.*, **28**, 350 (1956).
6) J. Hiroi, T. Seki, M. Otsuka, S. Katsuki and F. Honda, *Jpn. J. Pharmacol.*, **31**, 144 (1981).
7) B. Gunner, *Acta Chem. Scand.*, **2**, 467 (1948).
8) H. Ohkawa, N. Ohnishi and K. Yagi, *Anal. Biochem.*, **95**, 351 (1979).
9) T. Arakawa, H. Nakamura, S. Chono, H. Yamada and K. Kobayashi, *Jpn. J. Gastroenterol.*, **77**, 1052 (1980).
10) T. A. Stein, L. Angus, E. Borrero, L. J. Auguste and L. Wise, *J. Chromatogr.*, **385**, 377 (1987).
11) W. S. Powell, *Prostaglandins*, **20**, 947 (1980).
12) J. Hirohara, J. Sugatani, T. Okumura, Y. Sameshima and K. Saito, *Biochim. Biophys. Acta.*, **919**, 231 (1987).
13) T. Teramoto, H. Tojo, T. Yamano and M. Okamoto, *J. Biochem.* (Tokyo), **93**, 1353 (1983).
14) Y. Kohno, K. Tanikawa, K. Ohta and T. Suwa, *Jpn. J. Pharmacol.*, **43**, 407 (1987).
15) Y. M. Takagaki and K. Hotta, *Biochim. Biophys. Acta*, **584**, 288 (1979).
16) T. Ohokubo, "Analysis of Gastric Mucus Secretions," ed. by M. Moriga and K. Hotta, Nihon-igakukan, Tokyo, 1989, pp. 17—22.
17) T. Okubo, Y. Watanabe and T. Kidokoro, *Jpn. J. Gastroenterol.*, **83**, 1111 (1986).
18) H. Uchida, S. Yorioka, T. Kodama, T. Takino, T. Oishi. S. Ohkuma, K. Kuriyama, and Y. Tsuchihashi, *Jpn. J. Gastroenterol.*, **85**, 1060

(1988).
19) D. N. Granger, G. Rutilli and J. M. McCord, *Gastroenterology*, **81**, 22 (1981).
20) F. Rossi, *Biochim. Biophys. Acta.*, **853**, 65 (1986).
21) K. Yagi, *Chem. Phys. Lipids*, **45**, 337 (1987).
22) T. Yoshikawa, H. Miyagawa, N. Yoshida, S. Sugio and M. Kondo, *J. Clin. Biochem. Nutr.*, **1**, 271 (1986).
23) M. Ito and P. H. Guth, *Gastroenterology*, **86**, 112 (1984).
24) K. Ogino, S. OKa, S. Matuura, I. Sakaida, S. Yoshimura, K. Matuda, Y. Sasaki, K. Yamamoto, T. Yoshikawa, Y. Okazaki and T. Takemoto, *J. Clin. Biochem. Nutr.*, **3**, 189 (1987).
25) M. A. Perry, S. Wadhwa, D. A. Parks, W. Pickard and D. N. Granger, *Gastroenterology*, **90**, 362 (1986).
26) A. Robert, J. E. Nezamis, C. Lancaster and A. J. Hanchar, *Gastroenterology*, **77**, 433 (1979).
27) J. P. Wright, G. O. Young, L. J. Klaff, L. A. Weers, S. K. Price and I. N. Marks, *Gastroenterology*, **82**, 263 (1982).
28) H. Nakamura, T. Arakawa and K. Kobayashi, *Gastroenterology*, **88**, 1514 (1985).
29) T. Arakawa, H. Nakamura and K. Kobayashi, *Jpn. J. Gastroenterol.*, **77**, 1711 (1980).
30) K. I. Takano, S. Sugiyama, S. Nakazawa and T. Ozawa, *Scand. J. Gastroenterol.*, **22**, 577 (1987).
31) K. Kobayashi, H. Nakamura and T. Arakawa, *Gastroenterology*, **88**, 1450 (1985).
32) G. J. Blackwell, R. Carnuccio, M. D. Rose, R. J. Flower, L. Parente and P. Persico, *Nature* (London), **287**, 147 (1980).
33) M. Lipkin, *Gut*, **12**, 599 (1971).
34) L. R. Johnson and P. D. Guthrie, *Gastroenterology*, **67**, 453 (1974).
35) Y. Tashiro, *Nichidai Igakuzasshi*, **44**, 749 (1985).

Application of Aqueous Suspensions and Latex Dispersions of Water-Insoluble Polymers for Tablet and Granule Coatings[1)]

Hiroaki NAKAGAMI,* Taketoshi KESHIKAWA, Manabu MATSUMURA, and Hisashi TSUKAMOTO[2)]

Pharmaceutical Formulation Research Center, Research Institute, Daiichi Pharmaceutical Co., Ltd., 16–13, Kita-kasai 1-chome, Edogawa-ku, Tokyo 134, Japan. *Received February 20, 1991*

An aqueous coating was studied using various water-insoluble polymers. In an aqueous suspension system of micronized polymers, the dissolving temperature (DT) of polymers dispersed in a plasticizer upon steady heating, and the cloud point (CP) of the resultant polymer solutions upon steady cooling was examined. The plasticizers with low DT and CP showed good compatibility with the polymers. The casting films obtained from various polymer suspensions showed intrinsic dissolution behavior in pH 1.2 to 7.5 aqueous media depending on the type of polymer used. Tablets coated with the aqueous suspension system showed the same dissolution profiles as those with an organic solution coating. A comparative study of the aqueous suspension and latex dispersion of ethylcellulose showed that the latex system needed less plasticizer for film formation than the aqueous suspension system. Tablet coating and granule coating were performed using the aqueous suspension system of a jet mill ground acid-alkaline soluble polymer with propylene glycol and the latex dispersion system of an enteric anionic methacrylate with polyethylene glycol 6000, respectively. The results indicate that propylene glycol can act as a temporary plasticizer which mostly evaporates during the coating process, and that water as well as the plasticizer plays an important role in the film formation of the latex particles.

Keywords aqueous coating; suspension; latex; micronization; plasticizer; tablet coating; granule coating

Introduction

Aqueous film coatings of pharmaceutical dosage forms have been extensively studied since the early 1970s, because they are free from the problems caused by organic solvents. At present, most film coatings can be made with water-based systems, and the available coating systems can be classified into three according to the state of the polymer dispersed in water: (a) an aqueous solution of a cellulose ether such as hydroxypropyl methylcellulose (HPMC)[3a)]; (b) colloidal polymer dispersions in latices such as acrylic latex[3b)] and ethylcellulose (EC) latex[3c)]; and (c) a suspension system of micronized water-insoluble polymer with a particle diameter less than 50 μm.[3a,4a,b,5)]

In this paper, the aqueous suspension system is described first according to our patented method.[4c)] Second, comparison between the suspension and latex systems of EC is made to clarify the characteristics of both aqueous systems. Third, the applications of each system for tablet and granule coatings are presented to show the factors affecting the film formation.

Experimental

Materials The polymers and plasticizers examined are listed in Tables I and II. These polymers were finely ground with a Supersonic jet mill (PJM-100, Nihon Pneumatic Co., Ltd.) under the following conditions: compressed air consumption, 2.1 Nm^3/min; air pressure, 7 kg/cm^2; sample feed, 2 kg/h. Poly (methacrylic acid ethylacrylate) latex (Eudragit L 30 D, Röhm Pharma), and EC latex (Aquacoat, FMC), micronized EC (N-10F, Shin Etsu Chemical Co., Ltd.) and HPMC (TC-5R, Shin Etsu Chemical Co., Ltd.) were also used.

Polyvinyl alcohol (Poval 205s, Kuraray Co., Ltd.) and hydroxypropyl cellulose (HPC-L, Nippon Soda Co., Ltd.) were used as binders in tablet formulations. The other excipients for the formulations of tablets, granules and coatings were of JP XI grade. The particle size distributions of latex and of the micronized particles of EC were measured in water with a Malvern zetasizer II and a Microtrac II (Leeds & Northrup, model SPA), respectively (Fig. 1). A small amount of nonionic dispersing agent (Hyonic PE-90, San Nopco Ltd.) was used to make homogeneous dispersion of micronized EC.

Plasticizer Effect The dissolving temperature (DT) of a polymer in plasticizer and the cloud point (CP) of the plasticizer solution of the polymer were measured with a JP melting point apparatus using a small test tube containing plasticizer with 1% (w/v) micronized polymer dispersed in it.

Film Formability The film formability of the aqueous suspension and latex of various polymers was evaluated using the following method: Aqueous coating dispersions containing 10—12% (w/v) polymer and various amounts of plasticizer were placed in a petri dish and dried in a thermostated chamber at constant temperature for 24—48 h.

Properties of Free Films Free films were made from various polymer suspensions according to the method described above. Dissolution time of a 20 mg free film was measured using a JP XI disintegration apparatus

TABLE I. Properties of Polymers

Key[a)]	Polymer	Dissolving pH	d (μm)[b)]
A	Polyvinylacetal diethylaminoacetate	$\leqq 5.8$	4.1
B	Dimethylaminoethyl methacrylate–methylmethacrylate copolymer	<6.0	12
C	2-Methyl-5-vinylpyridine–methyl-acrylate–methacrylic acid copolymer	$\leqq 4.0$ $\geqq 7.4$	4.9
D	Partial methyl ester of vinyl acetate–maleic anhydride copolymer	$\geqq 5.5$	6.9
E	HPMC phthalate	$\geqq 5.5$	2.9
F	Methylmethacrylate–methacrylic acid copolymer	$\geqq 6.0$	1.4
G	EC	—	5.6

a) A: AEA (Sankyo Co., Ltd.); B: Eudragit E (Röhm Pharma); C: MPM-47 (Tanabe Pharm. Co., Ltd., not on the market); D: VAE (Daiichi Pharmaceutical Co., Ltd., not on the market); E: HP-55 (Shin Etsu Chemical Co., Ltd.); F: Eudragit L (Röhm Pharma). *b*) d is a mean particle diameter which was measured by the air permeability method.

TABLE II. Properties of Plasticizers

Plasticizer	M.W.	Solubility in water
Propylene glycol	76.1	∞
PEG 400	400	∞
Triacetine	218.2	6.7%
Polysorbate 80	1100	Freely sol.
TEC	276.3	6.1%
DET	206.2	∞

M.W. = molecular weight.

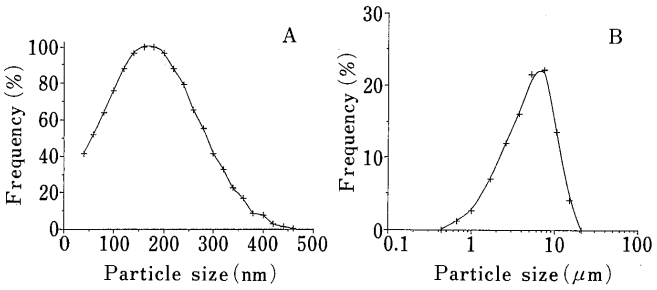

Fig. 1. Particle Size Distributions of Latex and Micronized Particles of EC

A, equivalent normal weight distribution of EC latex. B, volume distribution of micronized EC particles.

Table III. Formulations of Core Tablets

Ingredient	Amount (mg/tablet)	
	Formula I[a]	Formula II[b]
Nicotinamide	15	20
Lactose	247.5	170
Corn starch	30	14.37
Hydroxypropyl cellulose	6	—
Polyvinyl alcohol	—	4
Magnesium stearate	1.5	0.63
Total	300	209

The tablets were compressed with 9 mm[a] or 8 mm[b] concave punches.

Table IV. Formulations of Aqueous Suspensions and Organic Solution for Tablet Coating

Component	Suspension		Organic solution
	Formula I	Formula II	
Polymer C[a]	5.0 g	5.0 g	11.0 g
HPMC	—	1.0 g	—
Propylene glycol	10.0 g	10.0 g	—
Vinyl acetate	—	—	3.0 g
PEG 1500	—	—	2.0 g
Talc	2.5 g	2.5 g	32.5 g
Water	100 ml	100 ml	—
Ethanol	—	—	90 ml
1,1,1-Trichloroethane	—	—	40 ml
Film weight per tablet	10 mg	7 mg	10 mg

a) Polymer C: 2-methyl-5-vinylpyridine–methylacrylate–methacrylic acid copolymer.

without disks. JP XI 1st fluid (pH 1.2), purified water, JP XI 2nd fluid (pH 6.8) and 0.05 M phosphate buffer (pH 7.5) were used as the dissolution medium, and the measurement was done at 37 °C. Water uptake of the free films was determined by measuring their equilibrium weight gain after 3 d-immersion in water at room temperature.

The glass transition temperature of the Eudragit L 30 D film was determined using differential scanning calorimetry (DSC) (Du Pont 9900/910) according to the following conditions. The Eudragit latex dispersion (15% (w/v) as solid) with or without polyethylene glycol 6000 (PEG 6000) was casted in a petri dish and dried at 40 °C for 24 h. The free film thus obtained was placed in a desiccator over silica gel or a saturated solution of KNO_3 at 30 °C for 48 h, and then the water content of the film was determined by Karl Fischer method. A small amount of this film was placed in an aluminum sealed pan, heated at the rate of 20 °C/min to 110 °C and then held isothermally for 5 min. The sample was then rapidly cooled to near 0 °C and reheated at the rate of 20 °C/min to 180 °C.

Tablet Coating Mixtures of nicotinamide and excipients (Table III) were granulated by spraying a 5% (w/v) aqueous solution of hydroxypropyl cellulose or polyvinyl alcohol in a Glatt-type fluidized-bed granulator. The obtained granules were passed through a 20 mesh sieve, mixed with magnesium stearate, and compressed into tablets. The film coating of the tablets was made in a perforated pan (Freund hi-coater HCT-48 or HCF-100) using the formulations shown in Table IV. In formulae I and II, propylene glycol and HPMC were first dissolved in water, then polymer C and talc dispersed, and finally the suspension was passed through a 150 mesh sieve. In the organic solvent-based formula, polymer C, vinyl acetate and PEG 1500 were first dissolved in organic solvents, then talc was dispersed. The process parameters in a 5 kg batch size (HCT-48) were as follows: spray rates were 15 ml/min for aqueous coatings and 30 ml/min for organic coatings, and atomizing air pressure was 3 kg/cm^2; inlet air temperature was 75 °C for aqueous coatings and 50 °C for organic coatings; exhaust air temperature was 45 °C for aqueous coatings and 30 °C for organic coatings; pan speed was 15 rpm. In a 50 kg batch size (HCF-100), spray delivery was 100—120 ml/min using two air guns, and atomizing air pressure was 4 kg/cm^2; inlet and exhaust air temperatures were 75 °C and 45 °C, respectively; pan speed was 8—12 rpm.

The residual amount of propylene glycol in the films was determined using a gas chromatography assay. Twenty tablets were placed in a centrifuged tube, and 20 ml of 0.1 N HCl containing 0.1% isobutanol as an internal standard was added, then shaken for 30 min. This sample was centrifuged at 3000 rpm and the supernatant was filtered. The filtrate was used as a sample solution. Measurement conditions were as follows: a Shimadzu GC-4B gas chromatograph equipped with a flame ionization detector and a glass column (3 mm i.d. × 1 m) which was packed with Porapak Q, 80—100 mesh (GL Sciences Inc.) was used; the carrier gas was nitrogen (40 ml/min); the column, injection port and detector temperatures were 200 °C, 230 °C, 250 °C, respectively; sample size was 1 μl. The propylene glycol concentration was calculated from the calibration line constructed on the basis of peak area measurements.

Granule Coating The powder blend of lactose (34.1%), avicel (17.05%) and corn starch (47.05%) was granulated with a 5% (w/v) aqueous solution of HPMC (1.8%) using a high-shear mixer type granulator (high-speed mixer, FS-5, Fukae-kogyo Co., Ltd.). The wetted granules were dried in the fluidized-bed granulator and passed through a 32 mesh sieve. The granules thus obtained were coated in the fluidized-bed granulator with a top-spray gun (Glatt WSG-1) using a formulation containing Eudragit L 30 D (10% (w/v) as dry solid), PEG 6000 (0.5% (w/v)), and talc (4.31% (w/v)). Process parameters for the intermittent spray coatings under both wet and dry conditions in a 1 kg batch size were as follows: spraying-drying cycle was repeated three times; spray delivery was 30 ml/min and atomizing air pressure was 1.5 kg/cm^2; inlet air temperatures for wet conditions were room temperature during spraying in the first cycle, and 60—70 °C during both spraying in the following two cycles and drying; inlet air temperatures for dry conditions were 60—70 °C during both spraying and drying. The amount of coating applied was 113.6 mg per 1 g of granules.

The water content at which the granules were agglomerated during coating was examined with a 5 kg scale apparatus (FLO-5, Freund Co., Ltd./Okawara Co., Ltd.) using the continuous spray coating with the same formulation. Process parameters were as follows: spray rates ranging from 60 to 90 ml/min were used, and atomizing air pressure was 2.5 kg/cm^2; inlet air temperatures were 60—70 °C. The water content of granules was determined by loss when dried for 15 min at 80 °C.

Dissolution Test Dissolution test of tablets was performed by JP XI rotating basket method at 100 rpm in 900 ml of a test fluid at 37 °C. Nicotinamide was assayed spectrophotometrically (262 nm). Dissolution rate of lactose from the granules was determined using JP XI paddle method at 50 rpm in 500 ml of water at 37 °C. The amount of granules used was 980 mg, which was equivalent to 300 mg of lactose. Lactose was assayed using a high performance liquid chromatography (HPLC) system which consisted of a pump (880-PU, Japan Spectroscopic Co., Ltd.), a column (4.6 mm i.d. × 250 mm) packed with a porous silica gel chemically bonded with polyamino resins (YMC-pack PA-03, YMC Co., Ltd.), and a refraction index detector (ERC-7520, Erma Optical Works). Elutions were at 40 °C with a mobile phase of acetonitrile–water (60 : 40). The flow rate was 1 ml/min. Under these conditions, the retention time of lactose was 6.5 min. Lactose concentration was calculated from the calibration line constructed on the basis of peak area measurements.

Results and Discussion

Aqueous Suspension Coating of Water-Insoluble Polymers Table V shows the DT of polymers dispersed in

TABLE V. DT (°C) of Polymers and CP (°C) of Polymer Solutions

Polymer	Plasticizer											
	PG		PEG-400		TA		P-80		TEC		DET	
	DT	CP	DT	CP	DT	CP	DT	CP	DT	CP	DT	CP
A	124	114	109[a]	—	60[a]	—	62	43	<RT	<0	<RT	<0
B	71	65	147[a]	—	39[a]	—	55	39	RT	<0	<RT	<0
C	45	23	IS	—	IS	—	IS	—	IS	—	110	88
D	105	96	64	<0	83[a]	—	IS	—	IS	—	90	<0
E	96	85	42	<0	130[a]	—	IS	—	128[a]	—	79	<0
F	48	<0	45	<0	IS	—	IS	—	IS	—	IS	—
G	174[a]	—	RT	—	133[a]	—	139[a]	—	50[a]	—	RT	<0

PG, propylene glycol; TA, triacetine; P-80, polysorbate. RT, room temperature; IS, almost insoluble. *a*) Almost completely soluble.

TABLE VI. Compatibility[a] of Plasticizers with Polymers

Polymer	Plasticizer[b]					
	PG	PEG-400	TA	P-80	TEC	DET
A	**C**	**P**	**C**	**P**	**C**	**C**
B	**C**	**P**	**C**	**C**	**C**	**C**
C	**C**	**I**	**I**	**I**	**P**	**C**
D	**P**	**P**	**C**	**I**	**P**	**C**
E	**C**	**C**	**C**	**I**	**C**	**C**
F	**P**	**P**	**P**	**C**	**P**	**C**
G	**I**	**P**	**I**	**I**	**P**	**C**

PG, propylene glycol; TA, triacetine; P-80, polysorbate. *a*) **C**, compatible (transparent film formed); **P**, partially compatible (turbid film formed); **I**, incompatible (no film formed). *b*) The ratio of polymer to plasticizer was 1:0.5 (w/w).

plasticizer upon steady heating, and the CP of polymer solutions upon steady cooling. Toyoshima reported that DT is a measure of the solvent capacity of plasticizer required to break the bonds between polymer molecules, and that CP is a measure of the interaction force between polymer molecules and plasticizer molecules.[6] The solvent capacity may be expected to be stronger with plasticizers which dissolve the polymer at lower temperatures. CP is the temperature at which the interaction between polymer molecules becomes stronger than that between polymer and plasticizer molecules, causing the onset of precipitation. Thus, a plasticizer with a lower CP may be expected to give a stronger interaction force, and so the lower the DT and CP are, the better the compatibility of plasticizer. Plasticizers with the lowest DT and CP were triethyl citrate (TEC) and diethyl *d*-tartrate (DET) for polymers A and B; PG for polymer C; PEG-400 for polymers D, E and F; and DET for polymer G. These plasticizers also showed good compatibility with each polymer, as expected from the above discussion, except for polymers D and F (Table VI). Although polymer F was insoluble in pure P-80 and DET even at an elevated temperature, it became soluble at room temperature when these plasticizers contained a small amount of water. A similar effect of water was also reported for polymer E dispersed in TEC.[3a] These facts suggest that the water can act as a plasticizer for certain polymers. Water will interact with the polar groups of the polymer chains and weaken the intramolecular attraction between the polymer segments. Further interaction between polymer and plasticizer will provide the energy required to remove individual polymer chains from solid state, resulting in the polymer solution.

Table VII shows the dissolution time and water uptake of free films obtained from aqueous suspension systems. The intrinsic dissolution properties are shown for the films of acid-soluble polymer B, acid-alkaline soluble polymer C, enteric film-forming polymer D, and water-insoluble polymer G. The dissolution time and water uptake of enteric polymer D varied depending on the amount and type of the plasticizer used. The absorbed water caused polymer swelling and turbidity of the films. The water uptake into the film is partially through the pores formed by leaching of the plasticizer from the film and partially through the polymer phase. The uptake amount thus depends on the plasticizer's water solubility, the amount of plasticizer in the film, and the homogeneity of the film as a result of the polymer-plasticizer interaction. Therefore, the selection of the type and amount of plasticizers must be considered as affecting not only the film formability but also the film properties.

Tablets, containing nicotinamide as a model drug which has a bitter taste, were coated in a 5 kg batch size using an aqueous suspension system and an organic solvent system of polymer C. The formulations of the core tablets, aqueous coatings (formula I), and organic coatings are shown in Tables III and IV. No difference in dissolution profiles was observed between the tablets obtained by the two methods (Fig. 2). The masking time of the tablet was measured using three male subjects. Masking time is the time following the moment the subject puts the tablet into his mouth and tastes no bitterness until he tastes the bitterness. Both coating systems provided the tablets with a masking time of more than 60 s; thus, good taste masking was achieved. Scanning electron microscope analysis revealed that a continuous film was formed on the surface of the tablets obtained by both coating systems.

Film-Formation Mechanisms of Aqueous Suspension System and Latex System A comparative study of the aqueous suspension system and the latex system was carried out using EC as a model polymer. One of the greatest differences was in particle size distribution, as shown in Fig. 1. The mean diameter of the particles was 4.54 μm for the micronized EC used in the suspension system and 0.171 μm for the EC latex. The latex system needed less plasticizer for film formation than the suspension system (Table VIII). The latex system and aqueous suspension system showed

TABLE VII. Dissolution Time and Water Uptake of Free Films

Polymer (1)	Plasticizer (2)	Ratio (1)/(2)	Dissolution time (min)				Water uptake (%)
			pH 1.2	Water	pH 6.8	pH 7.5	
B	DET	1/0.3	3	> 60	>60	>60	—
C	DET	1/0.5	1.5	> 60	>60	14	—
D	DET	1/0.5	>120	>120	10	6.5	71.1
D	DET	1/0.25	>120	>120	10.5	6	28.2
D	Triacetine	1/0.3	>120	>120	4	5	60
D	TEC	1/0.3	>120	>120	6.3	5.5	4.7
G	DET	1/0.5	> 60	> 60	>60	>60	—

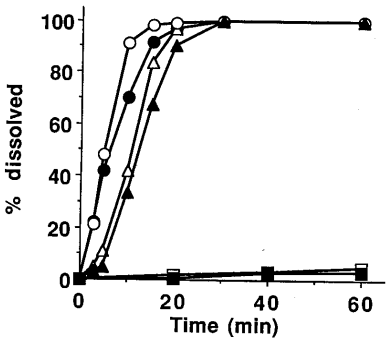

Fig. 2. Dissolution Profiles of Nicotinamide from Tablets Coated with Both Aqueous Suspension and Organic Solution of Polymer C

Aqueous-based coating: ○, pH 1.2; △, pH 7.5; □, water. Organic-based coating: ●, pH 1.2; ▲, pH 7.5; ■, water.

TABLE VIII. Influence of Plasticizer and Temperature on the Film Formation from Latex Dispersions and Aqueous Suspensions of EC

Temp. (°C)	Latex dispersion plasticizer level				Aqueous suspension plasticizer level			
	0%	10%	25%	40%	0%	10%	25%	40%
25	−	±	+	+	−	−	±	+
30	−	±	+	+	−	−	±	+
35	−	±	+	+	−	−	±	+
40	−	±	+	+	−	−	±	+
50	−	+	+	+	−	−	+	+
60	−	+	+	+	−	−	+	+

−: no film formation occurred. ±: cracked or partially transparent film was obtained. +: continuous transparent film was obtained.

no film formation at 25—60 °C unless the plasticizer was incorporated. The film formation was further examined at a temperature above T_g of the polymer. Steuernagel reported that T_g of EC latex and EC polymer are 89 °C and 129 °C, respectively.[3c] The latex system with no plasticizer gave a transparent film at 100 °C. In contrast, the micronized EC in the suspension system with no plasticizer showed no film formation even at 140 °C. These results indicate that the film-formation mechanism of the latex system is different from that of the aqueous suspension system.

The main driving force for film formation in a latex is the capillary force developed in the channels between the closely packed latex particles as water evaporates.[7] Since the capillary forces are inversely proportional to the radius of the particles, the force exerted on latex particles is estimated to be about 30 times greater than that on suspension particles. The capillary force causes coalescence of latex particles above the MFT (minimum film-forming temperature) of the latex polymer resulting in continuous-film formation. The MFT is directly related to T_g of the polymer and is usually less than T_g.[7] The film formation of EC latex with no plasticizer above the T_g is thus ascribed to particle coalescence by capillary force.

The role of the plasticizer incorporated in the latex system is to reduce the T_g of the polymer, thus decreasing MFT to the temperature of the usual film coating processes. The EC latex system (Aquacoat) contains sodium lauryl sulfate and cetyl alcohol at 4.6% and 10.3%, respectively, of the level of EC in the formulation.[3c] These stabilizers also have plasticizer efficiency, and hence decrease the T_g of EC polymer as described above (129 °C→89 °C).

On the other hand, the capillary force is too weak to bring about particle coalescence in a suspension system of micronized polymer with no plasticizer, resulting in no film formation above the T_g. Thus, the addition of a plasticizer is essential for film formation in a suspension system, because the plasticizer causes coalescence of particles through the gelation of the micronized polymer. The effects of particle size and the stabilizer explain why the EC latex system requires less plasticizer than the aqueous suspension system. However, further study is necessary in order to clarify the actual mechanism involved in the coalescence process of the micronized polymer particles of the suspension system.

Application of the Aqueous Suspension and Latex Systems The aqueous suspension coating of polymer C was applied to tablets in a 50 kg batch size using formula II shown in Tables III and IV. The dissolution of nicotinamide from tablets coated with polymer C–HPMC (5 : 1) mixture is shown in Fig. 3. The addition of water-soluble polymer HPMC to water-insoluble polymer C yielded an improved dissolution rate in water. The tablet thus coated had the masking time of 45—60 s, and retained the taste-masking effect of polymer C.

Free film was obtained from the aqueous suspension containing polymer C and propylene glycol in ratios ranging from 1 : 0.2 to 1 : 1. However, tablet coating required a range from 1 : 1 to 1 : 3. The amount of propylene glycol in the film on the tablet was found to be 20—35% of the theoretical value calculated based on the amount of propylene glycol in the coating formulation; and Skultety and Sims[8] reported that 81—96% of the propylene glycol was lost during the coating process using HPMC aqueous solution. This suggests that the propylene glycol can act as a temporary plasticizer which mostly evaporates during the coating process. Although free films of polymer C were obtained

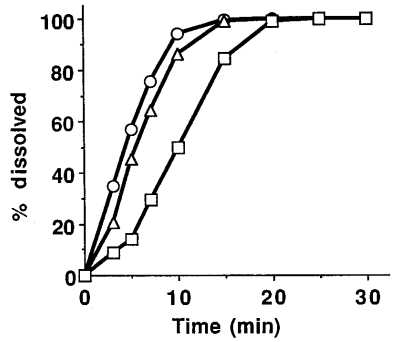

Fig. 3. Dissolution Profiles of Nicotinamide from Tablets Coated with Aqueous Suspension of Polymer C and HPMC

○, pH 1.2; △, pH 7.5; □, water.

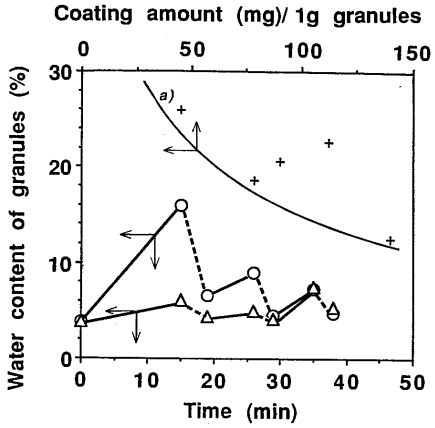

Fig. 4. Change of Water Content of Granules during Intermittent Spray Process for Granule Coating with Eudragit L 30 D Using a Fluidized-Bed Coater

○, wet condition; △, dry condition; +, water content at which agglomeration of the graules was observed. —, spraying process; ---, drying process. *a*) This line represents the estimated upper limit of water content of granules above which agglomeration of the granules will occur.

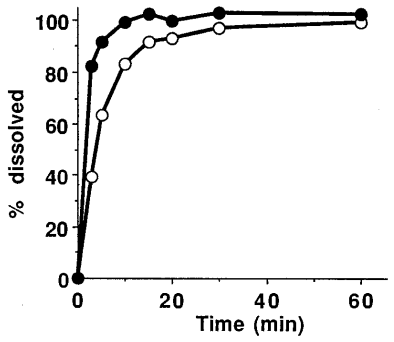

Fig. 5. Influence of Coating Conditions on Dissolution of Lactose from Granules Coated with Eudragit L 30 D

○, granules coated under wet conditions. ●, granules coated under dry conditions.

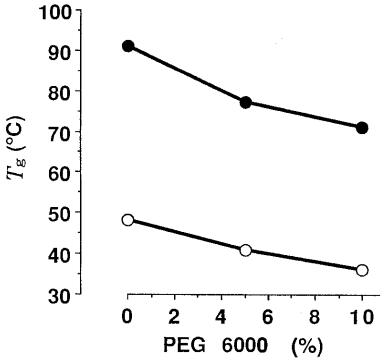

Fig. 6. Influence of Water and PEG 6000 Content on the T_g of Eudragit L 30 D Free Films

●, films stored in a desiccator containing silica gel at 30 °C (water content: 1.7—1.9%); ○, films stored at 30 °C, 92% R.H. (water content: 6.8—7.9%).

from the polymer particles under 150 μm, no film formation was observed above this particle size. This fact indicates that the particle size of polymer is an important formulation factor in the aqueous suspension coatings. Thus, we used a jet mill ground polymer C, which had an average diameter of *ca.* 5—5.5 μm and a maximum diameter of *ca.* 30—50 μm. Good film formation on the tablets was achieved with this micronized polymer.

The latex system of anionic methacrylate (Eudragit L 30 D) containing PEG 6000 as the plasticizer was used for granule coating using a fluidized-bed coater. Figure 4 shows changes of water content of granules during the coating process and the estimated upper limit of the water content above which the granule agglomeration will occur. This upper limit of water content that caused no agglomeration decreased as the amount of coating applied increased, as shown in Fig. 4.

Scanning electron microscopy of granules revealed that the granules coated under wet conditions had more smooth surfaces than those coated under dry conditions. The granules coated under wet conditions also showed slower dissolution of lactose than the latter (Fig. 5). These facts indicate that the water content of the granules affects film formability and the agglomeration of the granules.

The influence of absorbed moisture on the T_g of free films was examined using the Eudragit L 30 D films stored at 30 °C, 92% relative humidity. The amount of water in the film was measured by Karl Fischer method and thus included water initially present and moisture which was absorbed during storage. DSC study showed that the T_g of free films was decreased by the incorporation of not only the plasticizer but also of absorbed moisture (Fig. 6). This result indicates that the water can act as a plasticizer in the formation of anionic acrylic latex polymer films, as reported by Lehmann.[3b] The coalescence of latex particles is thus dependent upon the presence of enough water to soften them so that deformation can occur, resulting in smoother-surfaced and more homogeneous film when coating under wet conditions. However, an excess of water will cause undesirable sticking effects in the film-coating process owing to its softening effect on the polymer. Thus, regulation of the water content of granules is required to maintain optimal process conditions for granule coating with anionic methacrylate latex.

References and Notes

1) This paper was presented in preliminary form at the Pre-World Congress on Powder Technology in Gifu, Japan, September 1990.
2) Present address: *Quality Control Department, Head Office, Daiichi Pharmaceutical Co., Ltd., 10–7, Hachobori 1-chome, Chuo-ku, Tokyo 134, Japan.*
3) *a*) T. Nagai, F. Sekigawa, and N. Hoshi, "Aqueous Polymeric Coatings for Pharmaceutical Dosage Forms," ed. by J. W. McGinity, Marcel Dekker, Inc., New York and Basel, 1989, p. 81; *b*) K. Lehmann, *ibid.*, p. 153; *c*) C. R. Steuernagel, *ibid.*, p. 1.
4) *a*) H. Tsukamoto and H. Nakagami, Japan Kokai Tokkyo Koho,

Patent 54-84020 (1979) [*Chem. Abstr.*, **92**, 47217*r* (1980)]; *b*) *Idem*, Abstracts of Papers, the 101st Annual Meeting of the Pharmaceutical Society of Japan, Kumamoto, April 1981, p. 636; *c*) *Idem* (Daiichi Pharmaceutical Co., Ltd.), Japan. Patent 1478074 (1989).
5) H. Osterwald and K. H. Bauer, *Acta Pharm. Technol.*, **27**, 99 (1981).
6) K. Toyoshima, "Polyvinyl Alcohol," ed. by C. A. Finch, John Wiley & Sons, 1973, p. 339.
7) S. Muroi, "Chemistry of High Polymer Latices," Kobunshi Kanko-kai, 1976, p. 240.
8) P. F. Skultety and S. M. Sims, *Drug Dev. Ind. Pharm.*, **13**, 2209 (1987).

Introduction of Acetoxyl Group in Tropone and Azulene Nuclei Using Palladium(II) Acetate: Reactions of 2-Aminotropones and Azulenes with Palladium(II) Acetate

Katsuhiro SAITO,*,[a] Masatoshi KOZAKI,[a] Kazuya UENISHI,[a] Noritaka ABE,*,[b] and Kensuke TAKAHASHI[a]

Department of Applied Chemistry, Nagoya Institute of Technology,[a] Gokiso-cho, Showa-ku, Nagoya 466, Japan and Department of Chemistry, Faculty of Science, Yamaguchi University,[b] Yoshida 1677-1, Yamaguchi 753, Japan. *Received October 23, 1990*

Reactions of 2-(*N*,*N*-dimethylamino)- and 2-(*N*,*N*-diethylamino)tropones with palladium(II) acetate in benzene in the presence of sodium acetate afforded the corresponding 7-acetoxylated 2-aminotropones. A similar acetoxylation reaction proceeded with azulene to give 1-acetoxy- and 1,3-diacetoxyazulenes. On the other hand, phenylation at the 7-position occurred in the reaction using 2-(*N*-methyl)anilinotropone. The acetoxylations are considered to proceed through radical cation complexes formed through oxidation of amino groups by palladium.

Keywords acetoxylation; phenylation; 2-aminotropone; azulene; palladium acetate

Many studies on troponoid compounds have been reported,[1] but little work has been done on reactions with organometallic compounds except iron carbonyl compounds[2] and magnesium compounds such as Grignard reagents.[3] Recent researches on the reactions of palladium salts have established that they cause phenylation or vinylation of various kinds of olefinic, heterocyclic,[4] and aromatic[5] compounds, but little is known about the reactions with troponoid compounds. The vinylic substitution reactions on halotropones and halotropolones catalyzed by mercury and palladium complexes[6] and the phenylation reactions of tropones catalyzed by palladium(II) acetate[7] are the only reported examples. Concerning azulenes, we are unaware of any work on the reaction with palladium salts.

The reactivities of troponoid compounds toward palladium salts are interesting not only in comparison with those of benzenoid aromatic compounds but also from the viewpoint of elucidation of the electronic natures of nonbenzenoid aromatic compounds. Furthermore, considering that some kinds of tropones and azulenes have antiphlogistic or anticancer activity, researches on the reactions of these compounds with various types of organometallic compounds may have practical implications.

As a part of a series of studies on the reactions of palladium salts with cyclic olefins,[7,8] we studied reactions of palladium(II) acetate with 2-aminotropones and found that acetoxylation took place at the 7-position of the tropone nucleus. Similarly, azulene afforded acetoxylated azulenes. Here we report the results of these reactions.

Results and Discussion

2-(*N*,*N*-Dimethylamino)tropone (**1a**) was allowed to react with an equimolar amount of palladium(II) acetate in the presence of 5 molar eq of sodium acetate in benzene at 85 °C for 8 h. After treatment with water, the reaction mixture was subjected to thin-layer chromatography (TLC) to give 2-*N*,*N*-dimethylamino-7-acetoxytropone (**2a**). Under the same reaction conditions as above, 2-(*N*,*N*-diethylamino)tropone (**1b**) afforded 2-*N*,*N*-diethylamino-7-acetoxytropone (**2b**).

The structures of the products were deduced on the basis of their spectral, especially nuclear magnetic resonance (NMR) spectral, properties and comparisons of the spectra with those of analogous compounds.[9]

It is known that tropones without amino groups, such as tropone itself, 2-phenyltropone, and 2-methoxytropone take a completely different reaction path from the present one under the same reaction conditions as above. In the cases of these tropones, phenylation occurred at the 7-position,[7] while no acetoxylation was detected at all. There is no difference in the reaction conditions or in the structures of the starting materials between the reported case and the present case except for the amino group in the latter case. Thus, the amino group is the key to the acetoxylation.

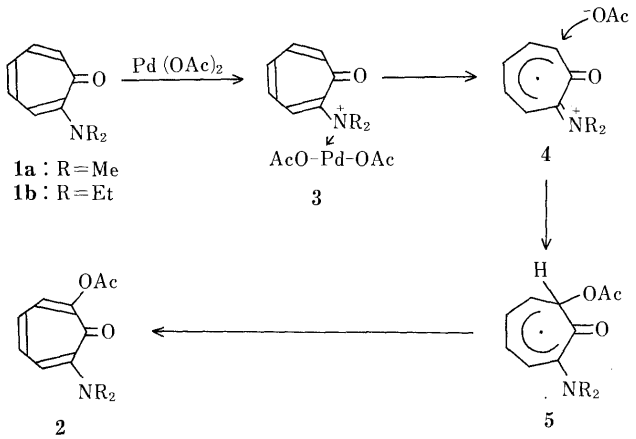

Fig. 1

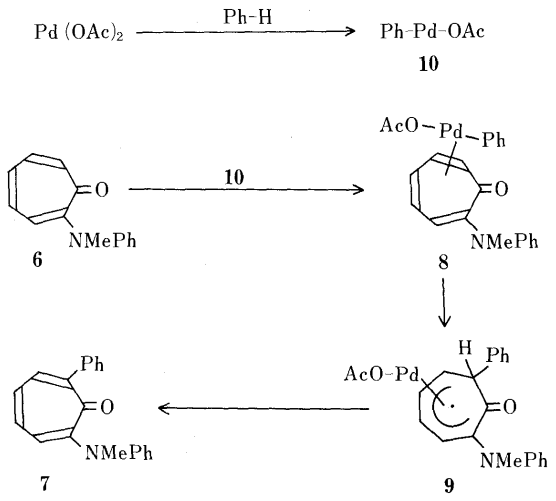

Fig. 2

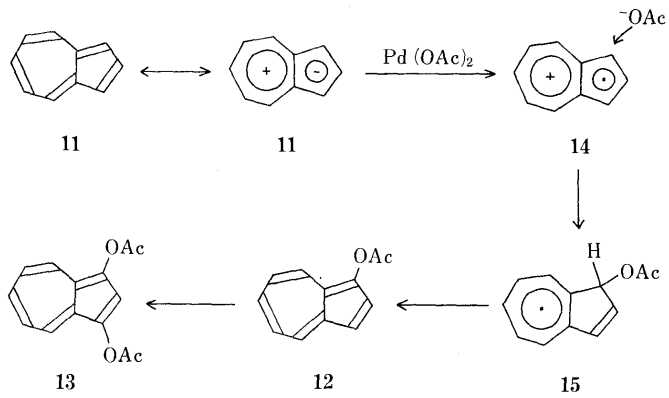

Fig. 3

It is not clear whether the reaction proceeds *via* a radical or an ionic process. However, the fact that amino groups are known to be oxidized by palladium(II) acetate[10] provides a clue. Thus, coordination of the palladium salt to the nitrogen atom of **1** may afford the complex (**3**). Oxidation of the lone pair electrons of the nitrogen atom of **3** by palladium acetate would generate a complex (**4**). Reaction of **4** with acetoxyl anion would then form an intermediate (**5**),[11] which affords the final product (**2**) *via* elimination of a hydrogen radical.

The analogous reaction using 2-(*N*-methylanilino)-tropone (**6**), however, afforded a phenylated product, 2-(*N*-methylanilino)-7-phenyltropone (**7**).[12] The difference between the reaction types of **1** and **6** is considered to be attributable to the different steric environments around the nitrogen atoms. The combination of phenyl and troponyl groups is sufficiently bulky to keep the palladium complex away from the nitrogen atom of **6**, preventing the oxidation. The reaction is considered to proceed through a complex (**8**) generated from **6** and phenyl–palladium complex (**10**).[7] Subsequent insertion of the tropone nucleus into the aryl–palladium bond yields the final product (**7**) *via* an intermediate (**9**).[11]

These results suggest that the acetoxylation reaction would be applicable to hydrocarbons which can form stable radical cation complexes, such as azulene. As was expected, the acetoxylation of azulene (**11**) proceeded to give 1-acetoxyazulene (**12**) and 1,3-diacetoxyazulene (**13**). The structure of **12** was deduced on the basis of agreements of its physical properties with literature values,[13] and the structure of **13** was deduced from the spectral properties and a comparison of the spectra with those of analogous compounds.[14]

By inference from the acetoxylation of 2-aminotropone derivatives, the reaction can be considered to proceed through an intermediate (**14**), formed *via* oxidation of the negatively charged five-membered ring part of **11** by palladium. Acetoxylation of **14** forms **12** *via* an intermediate (**15**), and a similar reaction of **12** can give **13**.

Experimental

Infrared (IR) and ultraviolet (UV) spectra were taken with JASCO A-102 and Hitachi 220A spectrophotometers, respectively. ^{1}H-NMR and ^{13}C-NMR spectra were measured with tetramethylsilane as an internal standard on a Varian XL-200 spectrometer. Mass spectra (MS) were measured with a JMX-DX300 spectrometer. Wako gel C-200 and Wako gel B-5F were used for column and TLCs, respectively. Palladium(II) acetate was commercially available from N. E. Chemcat Comp. Ltd. All the yields were calculated on the basis of the starting materials actually consumed.

Reaction of 1a with Palladium Acetate A mixture of **1a** (450 mg, 3 mmol), palladium acetate (680 mg, 3 mmol), and sodium acetate (1230 mg, 15 mmol) in benzene (30 ml) was refluxed for 10 h. After separation of a solid, the filtrate was poured into water, extracted with ethyl acetate, washed with water, and dried over anhydrous sodium sulfate. After filtration and evaporation of the filtrate on a rotary evaporator, the residual oil was subjected to TLC on silica gel using benzene–ether (7 : 3) as a developing solvent to give **2a** as a yellow oil (75 mg, 20%, Rf=0.65) and recovered **1a** (180 mg, 40%, Rf=0.40). **2a**: high-resolution MS Calcd for $C_{11}H_{13}NO_3$: 207.0895. Found: 207.0893. MS *m/z* (relative intensity): 207 (M^+, 6), 206 (28), 164 (100), 149 (57), 135 (59), 121 (36). IR (oil): 1746, 1562, 1552 cm^{-1}. UV EtOH nm (log ε): 202 (4.17), 256 (4.25), 355 (4.06), 424 (3.87). ^{1}H-NMR ($CDCl_3$) δ: 2.32 (s, 3H, Me), 3.05 (s, 6H, 2Me), 6.17—7.62 (m, 4H). ^{13}C-NMR ($CDCl_3$) δ: 20.6, 41.8, 115.1, 119.3, 127.5, 132.7, 150.4, 157.8, 168.5, 173.1.

Reaction of 1b with Palladium Acetate A mixture of **1b** (890 mg, 5 mmol), palladium acetate (1140 mg, 5 mmol), and sodium acetate (2050 mg, 25 mmol) in benzene (50 ml) was refluxed for 15 h. The same treatment of the reaction mixture as above using benzene–ether (6 : 4) as a developing solvent gave **2b** as a yellow oil (280 mg, 35%, Rf=0.70) and the recovered **1b** (280 mg, 31%, Rf=0.55). **2b**: high-resolution MS Calcd for $C_{13}H_{17}NO_3$: 235.1209. Found: 235.1202. MS *m/z* (relative intensity): 235 (M^+, 41), 192 (44), 164 (100), 113 (15). IR (oil): 1757, 1564 cm^{-1}. UV C_6H_{12} nm (log ε): 257 (4.11), 357 (3.94), 423 (3.80). ^{1}H-NMR ($CDCl_3$) δ: 1.22 (t, 6H, 2Me), 2.32 (s, 3H, Me), 3.50 (q, 4H, $2CH_2$), 6.43 (dd, 1H, J=9.8, 10.0 Hz), 6.62 (d, 1H, J=10.2 Hz), 6.98 (dd, 1H, J=10.0, 10.2 Hz), 7.09 (d, 1H, J=9.8 Hz). ^{13}C-NMR ($CDCl_3$) δ: 12.8, 20.8, 46.0, 114.5, 118.7, 127.6, 132.9, 150.1, 156.5, 168.8, 173.0.

Synthesis of 6 2-Chlorotropone (2.00 g, 14 mmol) was stirred in *N*-methylaniline (20 ml) for 12 h at 100 °C. After removal of the excess *N*-methylaniline under reduced pressure (62 °C, 1.0 Torr), the resulting residue was column-chromatographed on silica gel to give **6** (2.40 g, 81%) as a red oil from the eluate with hexane–ethyl acetate (7 : 3). **6**: high-resolution MS Calcd for $C_{14}H_{13}NO$: 211.0996. Found: 211.0996. MS *m/z* (relative intensity): 211 (M^+, 100), 194 (17), 182 (63), 167 (50). IR (oil): 1570, 1470, 1350 cm^{-1}. UV EtOH nm (log ε): 242 (4.09), 354 (3.79), 416 (3.79). ^{1}H-NMR ($CDCl_3$) δ: 3.39 (s, 3H, Me), 6.55—7.41 (m, 10H). ^{13}C-NMR ($CDCl_3$) δ: 41.5, 122.0, 122.4, 124.0, 127.0, 129.1, 133.2, 135.4, 136.2, 148.4, 158.0, 182.3.

Reaction of 6 with Palladium Acetate A mixture of **6** (630 mg, 3 mmol), palladium acetate (670 mg, 3 mmol), and sodium acetate (1230 mg, 15 mmol) in benzene (30 ml) was stirred for 3 h under reflux. After the usual treatment, the resulting mixture was subjected to TLC on silica gel using hexane–ethyl acetate (1 : 1) as a developing solvent to give **7** as a red oil (44 mg, 5%, Rf=0.44). **7**: high-resolution MS Calcd for $C_{20}H_{17}NO$: 287.1309. Found: 287.1293. MS *m/z* (relative intensity): 287 (M^+, 100), 270 (90), 258 (14), 181 (21). IR (oil): 1560, 1470, 1340 cm^{-1}. UV EtOH nm (log ε): 226 (4.55), 239 (sh, 4.48), 258 (4.42), 276 (sh, 4.26), 351 (4.14), 425 (3.97). ^{1}H-NMR ($CDCl_3$) δ: 3.37 (s, 3H, Me), 6.66—7.68 (m, 14H). ^{13}C-NMR ($CDCl_3$) δ: 41.6, 120.4, 122.2, 124.0, 125.5, 127.4, 128.0, 129.0, 129.3, 131.8, 135.2, 141.6, 145.3, 148.5, 157.1, 182.7.

Reaction of 11 with Palladium Acetate A mixture of **11** (130 mg, 1 mmol), palladium acetate (230 mg, 1 mmol), and sodium acetate (410 mg, 5 mmol) in acetic acid (11 ml) was stirred for 1 h at 60 °C. After the treatment of the reaction mixture as above, the resulting mixture was subjected to TLC on silica gel using hexane–ethyl acetate (9 : 1) as a developing solvent to give **12** (10 mg, 5%, Rf=0.44) and 13 (13 mg, 5%, Rf=0.28) as blue oils. **13**: high-resolution MS Calcd for $C_{14}H_{12}O_4$: 244.0733. Found: 244.0733. MS *m/z* (relative intensity): 244 (M^+, 38), 202 (40), 159 (100). IR (oil): 1759, 1200 cm^{-1}. UV 1,4-dioxane nm (log ε): 240 (4.05), 283 (4.46), 348 (3.53), 366 (3.48). ^{1}H-NMR ($CDCl_3$) δ: 2.40 (s, 6H, 2Me), 7.00 (dd, 2H, J=9.0, 10.0 Hz), 7.60 (t, 1H, J=10.0 Hz), 7.80 (s, 1H), 8.20 (d, 2H, J=9.0 Hz). ^{13}C-NMR ($CDCl_3$) δ: 20.9, 118.8, 121.4, 122.1, 133.1, 134.0, 139.8, 168.9.

Acknowledgement The authors are indebted to Professors H. Horino and M. Yasunami of Tohoku University for their fruitful suggestions.

References

1) T. Nozoe, K. Takase, H. Muramatsu, T. Asao, K. Kikuchi, S. Ito, and M. Kotake, "Daiyukikagaku," Vol. 13, "Nonbenzenoid Aromatic Compounds," Asakura Pub. Comp., Tokyo, 1959; G. R.

Yian, S. Sugiyama, A. Mori, and H. Takeshita, *Bull. Chem. Soc. Jpn.*, **61**, 2393 (1988); I. D. Reingold, K. S. Kwong, and M. M. Menard, *J. Org. Chem.*, **54**, 708 (1989); G. Mehta and S. R. Karra, *ibid.*, **54**, 2975 (1989); Y. Fukazawa, S. Usui, Y. Kurata, Y. Takeda, and N. Saito, *ibid.*, **54**, 2982 (1989); R. P. Gandi and M. P. S. Ishar, *Chem. Lett.*, **1989**, 101; K. Saito, T. Watanabe, and K. Takahashi, *ibid.*, **1989**, 2099; R. Hoferichter, G. Seitz, and H. Wassmuth, *Chem. Ber.*, **122**, 711 (1989).

2) D. F. Hunt, G. L. Farrant, and G. T. Rodeheaver, *J. Organometal. Chem.*, **38**, 349 (1972); A. Eisenstadt, *ibid.*, **97**, 443 (1975); N. Morita and T. Asano, *Chem. Lett.*, **1982**, 1574.

3) W. von E. Doering and C. F. Hiskey, *J. Am. Chem. Soc.*, **74**, 5688 (1952); R. D. Haworth and P. B. Tinker, *J. Chem. Soc.*, **1955**, 911; T. Mukai, *Bull. Chem. Soc. Jpn.*, **31**, 852 (1958).

4) H. Tanaka, Y. Fujiwara, I. Moritani, and S. Teranishi, *Bull. Chem. Soc. Jpn.*, **48**, 3372 (1975); O. Maruyama, M. Yoshidomi, Y. Fujiwara, and H. Taniguchi, *Chem. Lett.*, **1979**, 1229; T. Itahara, *J. Chem. Soc., Chem. Commun.*, **1981**, 254; Y. Fujiwara, O. Maruyama, M. Yoshidomi, and H. Taniguchi, *J. Org. Chem.*, **46**, 851 (1981); K. Saito, *Heterocycles*, **24**, 1831 (1986).

5) R. F. Heck, *J. Am. Chem. Soc.*, **90**, 5542 (1968); Y. Fujiwara, I. Moritani, S. Danno, R. Asano, and S. Teranishi, *ibid.*, **91**, 7166 (1969); R. F. Heck and J. P. Jolly, *J. Org. Chem.*, **47**, 2320 (1972); R. Asano, I. Moritani, Y. Fujiwara, and S. Teranishi, *Bull. Chem. Soc. Jpn.*, **46**, 663 (1973); H. A. Deck and R. F. Heck, *J. Am. Chem. Soc.*, **96**, 1133 (1974).

6) H. Horino, N. Inoue, and T. Asao, *Tetrahedron Lett.*, **22**, 741 (1981).

7) K. Saito, *J. Organometal. Chem.*, **338**, 265 (1988).

8) K. Saito, *J. Organometal. Chem.*, **363**, 231 (1989); K. Saito, M. Kozaki, and K. Takahashi, *Heterocycles*, **31**, 1491 (1990).

9) K. Imafuku and A. Shimazu, *Synthesis*, **12**, 1043 (1982); *idem, J. Heterocycl. Chem.*, **21**, 653 (1984).

10) J. Daridson and C. Triggs, *Chem. Ind.* (London), **1966**, 457; T. Sakakibara, J. Kotobuki, and Y. Dogomori, *Chem. Lett.*, **1977**, 25; T. Sakakibara, Y. Dogomori, and Y. Tsuzuki, *Bull. Chem. Soc. Jpn.*, **52**, 3592 (1979).

11) The regioselectivity of the attack of the acetoxyl or phenyl group can be explained by the formation of intermediates (**5** or **9**), which are stabilized by more extended conjugations.

12) Similar reactions using 2-aminotropones which have N–H protons, such as 2-aminotropone itself or 2-anilinotropone, afforded neither phenylated nor acetoxylated products but gave only intractable complex mixtures.

13) L. T. Scott and C. M. Adams, *J. Am. Chem. Soc.*, **106**, 4857 (1984).

14) A. J. Fry, B. W. Bowen, and P. A. Leermakers, *J. Org. Chem.*, **32**, 1970 (1967); L. J. Mathias and C. G. Overberger, *ibid.*, **45**, 1701 (1980).

Studies on Antiatherosclerotic Agents.[1] Synthesis of 5-Substituted Derivatives of 7-Ethoxycarbonyl-6,8-dimethyl-1(2*H*)-phthalazinone

Yukuo EGUCHI* and Masayuki ISHIKAWA

Institute for Medical and Dental Engineering, Tokyo Medical and Dental University, 2-3-10, Surugadai, Kanda, Chiyoda-ku, Tokyo 101, Japan.
Received November 1, 1990

Several 5-substituted derivatives of 7-ethoxycarbonyl-6,8-dimethyl-1(2*H*)-phthalazinone were prepared by means of nitration, reductive amination, and diazonium decomposition. The substituents introduced included NO_2, NH_2, F, Cl, CN. Among the derivatives, the fluorine compound was obtained only in poor yield because intramolecular cyclization occurred predominantly.

Keywords 7-ethoxycarbonyl-6,8-dimethyl-1(2*H*)-phthalazinone derivative; antiatherosclerotic agent; diazonium decomposition; 5-fluorine compound

Several new 5-substituted derivatives of 7-ethoxycarbonyl-6,8-dimethyl-1(2*H*)-phthalazinones were synthesized starting from the previously prepared compounds (**1a—c**).[1,2] As the synthetic procedures included nitration,[3,4] subsequent reduction and conventional diazonium salt decomposition[5,6] were convenient to introduce substituents, such as F, Cl, and CN, at the 5-position. Fluorine was an especially attractive substituent from the viewpoint of our medicinal studies.[7,8] The derivatives were required for examination of their potential as antiatherosclerotic agents.

The starting compounds **1a—c** were efficiently nitrated at the 5-position to afford **2a—c** in good yields using a mixture of potassium nitrate and concentrated sulfuric acid as a nitrating agent. In the reaction of **1a**, the dinitro derivative (**2d**) was produced as a by-product in 8% yield. The structures of these derivatives were confirmed by their proton nuclear magnetic resonance (^{1}H-NMR) spectra, which showed no aromatic protons, and infrared (IR) spectra, with typical $-NO_2$ absorption bands near 1540, 1370, and 1260 cm^{-1}, as well as mass spectra (MS).

The other nitro derivatives (**2e—j**) listed in Table I were also prepared by the following modified methods. Compound **2f** was obtained by hydrolysis of **2c** and subsequent decarboxylation of **2e** on heating at 220 °C in 90% yield. Compound **2g** was prepared from **2a** by heating with phosphoryl chloride. Treatment of **2g** with morpholine or sodium ethoxide afforded the corresponding products, **2h** and **2i**, respectively. The N^2-methyl derivative **2j** was obtained when **2f** was reacted with methyl iodide in alcoholic KOH.

Reduction of the nitro compounds **2a**, **b**, **f**, **h**, and **j** was carried out by hydrogenation over a catalyst of 5% palladium on carbon (Pd–C) under normal pressure, affording the corresponding 5-amino derivatives (**3a—e**) in good yields. On the other hand, reduction of **2c** afforded

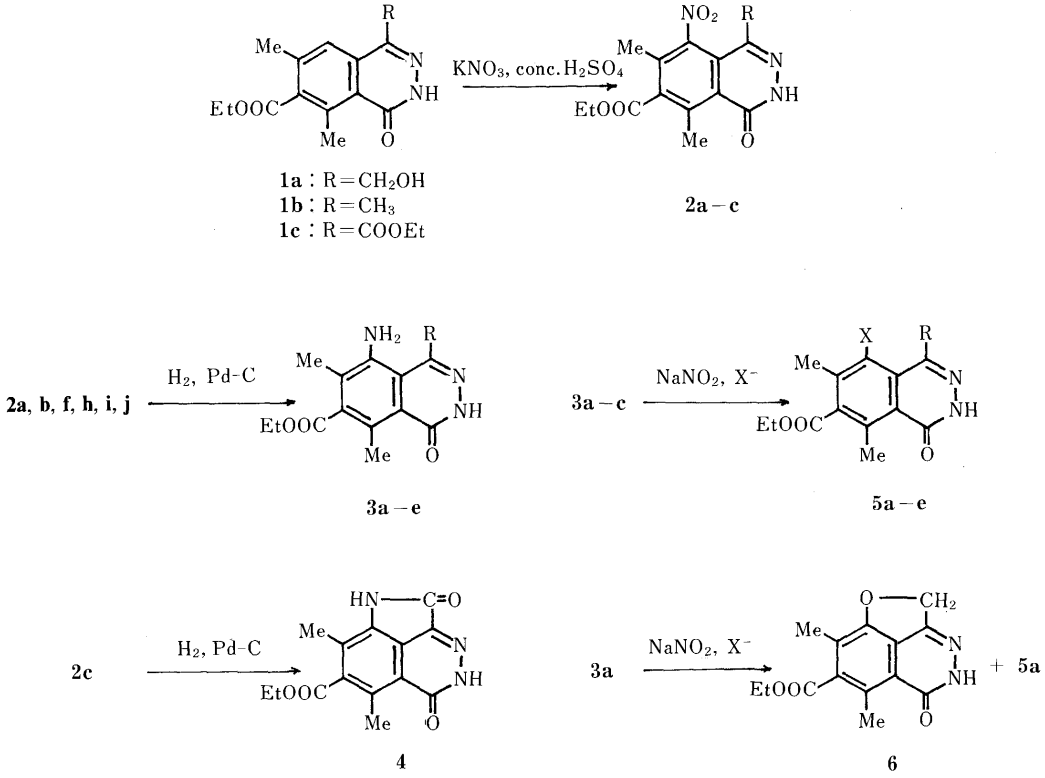

Chart 1

TABLE I

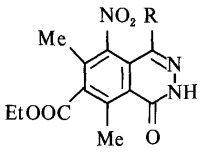

Compound	R	mp (°C) (Recryst. solvent)	Formula	Analysis (%) Calcd			Found		
				C	H	N	C	H	N
2a	CH_2OH	177—179 (MeOH)	$C_{14}H_{15}N_3O_6$	52.33	4.71	13.08	52.30	4.70	13.11
2b	CH_3	216—217 (MeOH)	$C_{14}H_{15}N_3O_5$	55.08	4.95	13.77	55.13	4.89	13.70
2c	$COOC_2H_5$	200—202 (MeOH)	$C_{16}H_{17}N_3O_7$	52.89	4.72	11.57	52.86	4.75	11.63
2d	CH_2ONO_2	183—185 (EtOAc–benzene)	$C_{14}H_{14}N_4O_8$	45.90	3.85	15.30	45.92	3.79	15.24
2e	COOH	212 (MeOH)	$C_{14}H_{13}N_3O_7$	50.15	3.91	12.53	50.18	3.95	12.48
2f	H	210 (MeOH)	$C_{13}H_{13}N_3O_5$	53.61	4.50	14.43	53.57	4.55	14.36
2g	CH_2Cl	207—209 (EtOH)	$C_{14}H_{14}ClN_3O_5$	49.45	4.12	12.36	49.42	4.11	12.44
2h	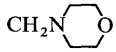	164—166 (MeOH)	$C_{18}H_{22}N_4O_6$	55.38	5.68	14.35	55.36	5.70	14.42
2i	$CH_2OC_2H_5$	150—152 (MeOH)	$C_{16}H_{19}N_3O_6$	55.01	5.48	12.03	55.05	5.50	12.08
2j	H, N^2–CH_3	137—138 (EtOAc–*n*-hexane)	$C_{14}H_{15}N_3O_5$	55.08	4.95	13.77	55.12	4.93	13.73

TABLE II

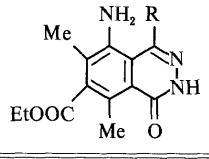

Compound	R	mp (°C) (Recryst. solvent)	Formula	Analysis (%) Calcd			Found		
				C	H	N	C	H	N
3a	CH_2OH	217—219 (MeOH)	$C_{14}H_{17}N_3O_4$	57.72	5.88	14.43	57.83	5.85	14.48
3b	CH_3	181—182 (MeOH)	$C_{14}H_{17}N_3O_3$	61.08	6.22	15.26	61.06	6.23	15.26
3c	H	205—206 (EtOAc–*n*-hexane)	$C_{13}H_{15}N_3O_3$	59.76	5.79	16.08	59.76	5.83	16.12
3d	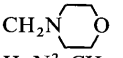	204—206 (MeOH)	$C_{18}H_{24}N_4O_4$	59.93	6.71	15.55	59.87	6.73	15.60
3e	H, N^2–CH_3	178—179 (EtOAc–ether)	$C_{14}H_{17}N_3O_3$	61.08	6.22	15.26	61.11	6.24	15.30
3f	CH_2OH, N^5–$COCH_3$	235—240 (MeOH)	$C_{16}H_{19}N_3O_5$	57.65	5.75	12.61	57.66	5.73	12.67

TABLE III

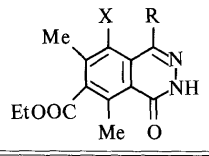

Compound	X	R	mp (°C) (Recryst. solvent)	Formula	Analysis (%) Calcd			Found		
					C	H	N	C	H	N
5a	F	CH_2OH	187—188 (EtOAc)	$C_{14}H_{15}FN_2O_4$	57.14	5.10	9.52	57.07	5.14	9.42
5b	Cl	CH_2OH	202—203 (MeOH)	$C_{14}H_{15}ClN_2O_4$	54.07	4.82	9.01	54.09	4.80	9.05
5c	CN	CH_2OH	203—205 (MeOH–EtOAc)	$C_{15}H_{15}N_3O_4$	59.79	5.02	13.95	59.77	5.01	13.97
5d	Cl	CH_3	188—189 (MeOH)	$C_{14}H_{15}ClN_2O_3$	57.04	5.09	9.50	57.07	5.06	9.57
5e	CN	H	190—192 (EtOH)	$C_{14}H_{13}N_3O_3$	61.98	4.83	15.49	61.96	4.81	15.52

the lactam derivative (**4**) as a sole product. The ultraviolet (UV) spectra of **3a**—**e** exhibited characteristic absorptions near 365 nm, which were not observed in the nitro compounds. Upon heating in acetic anhydride, **3a** provided the N^5-acetyl derivative (**3f**). The 5-amino derivatives obtained are listed in Table II.

It has been reported that [9] tetrabutylammonium fluoride is a powerful fluoride ion source able to displace aromatic nitro groups to yield fluoroaromatics. But, in the case of **2a**, no fluorinated products were obtained under similar

reaction conditions. However, the 5-fluorine compound (**5a**) was prepared in 7% yield by the thermal decomposition of the diazonium fluoroborate derived from **3a**, by the classical method.[5,10] Owing to radical decomposition,[11] the serious side reaction in which the *peri*-methylhydroxy group of **3a** acts as a donor to the radical center occurred to give an intramolecular cyclization product (**6**) exclusively in 30% yield. The other diazonium substitution products (**5b—e**) listed in Table III were prepared from the corresponding amino compounds in yields of 40—65% by the conventional procedures.[6]

Preliminary biological tests of the prepared compounds showed rather decreased inhibitory activities on platelet aggregation induced by both adenosine diphosphate and arachidonic acid as compared with **1a**.

Experimental

All melting points were determined in a capillary tube and are uncorrected. IR spectra were determined with a Hitachi model 285 spectrometer, MS were recorded on a Hitachi RMU-7L spectrometer, UV spectra with a Hitachi model 323 spectrometer, and NMR spectra with a JEOL C-60HL machine. Merck Silica gel 60 was used for column chromatography.

General Procedure for Preparation of the 5-Nitro Compounds Potassium nitrate (3.0 g) was added portionwise to a solution of **1a** (6.0 g) in concentrated sulfuric acid (40 ml), and the mixture was stirred for 7 h at room temperature, then poured into water (1.5 l). The whole was stirred for 20 h at room temperature. Precipitates were filtered off and washed with water on the filter. Recrystallization from MeOH gave 3.9 g of **2a**, melted at 177—179 °C (55.9%). *Anal.* Calcd for $C_{14}H_{15}N_3O_6$: C, 52.33; H, 4.71; N, 13.08. Found: C, 52.30; H, 4.70; N, 13.11. IR ν_{max}^{KBr} cm^{-1}: 1740, 1660, 1540, 1370, 1260. UV λ_{max}^{EtOH} nm: 215, 254, 263, 306. NMR ($CDCl_3$) δ: 1.43 (3H, t, J=7 Hz), 2.33 (3H, s), 2.92 (3H, s), 3.30 (1H, br), 4.50 (2H, q, J=7 Hz), 4.71 (2H, d, J=5 Hz), 10.92 (1H, s).

The mother liquor of **2a** was subjected to column chromatography with benzene–EtOAc (10 : 1) to give 640 mg of **2d** in 8.0% yield, mp 183—185 °C (EtOAc–benzene). *Anal.* Calcd for $C_{14}H_{14}N_4O_8$: C, 45.90; H, 3.85; N, 15.30. Found: C, 45.92; H, 3.79; N, 15.24. IR ν_{max}^{KBr} cm^{-1}: 1740, 1660, 1540, 1370, 1280, 1260. UV λ_{max}^{EtOH} nm: 213, 254, 264, 305, 313. NMR ($CDCl_3$) δ: 1.43 (3H, t, J=7Hz), 2.36 (3H, s), 2.92 (3H, s), 4.51 (2H, q, J=7 Hz), 5.47 (2H, s), 11.03 (1H, s).

Preparation of 2f Tableted **2e** (25 g) was placed in a 100 ml round-bottomed flask, which was filled with argon gas. When the flask was heated gradually to 210—225 °C, the tablets began to melt with evolution of gas. When evolution of the gas had ceased, the flask was allowed to stand at room temperature. A part of the solid was recrystallized from MeOH to give **2f**, mp 208 °C. Yield: 21 g (96%). *Anal.* Calcd for $C_{13}H_{13}N_3O_3$: C, 53.61; H, 4.50; N, 14.43. Found: C, 53.57; H, 4.55; N, 14.36. IR ν_{max}^{KBr} cm^{-1}: 1730, 1660, 1530, 1360, 1260. UV λ_{max}^{EtOH} nm: 214, 260, 302. NMR ($CDCl_3$) δ: 1.45 (3H, t, J=7 Hz), 2.41 (3H, s), 2.95 (3H, s), 4.82 (2H, q, J=7 Hz), 7.98 (1H, s), 10.72 (1H, s).

Compound **2g** was obtained from **2a** by reaction with $POCl_3$ under reflux for a short time (yield, 72%). Compounds **2h** and **2i** were obtained from **2g** in 65 and 57% yields by reaction with morpholine and EtONa, respectively. Compound **2j** was obtained from **2f** by reaction with CH_3I.

General Procedure for Preparation of the 5-Amino Compounds A solution of **2a** (1.3 g) in MeOH (40 ml) and EtOAc (20 ml) was shaken in H_2 on 5% Pd–C (0.3 g). After the theoretical amount of H_2 had been taken up, the catalyst was filtered off and the filtrate was concentrated to afford 1.0 g (85%) of **3a**. *Anal.* Calcd for $C_{14}H_{17}N_3O_4$: C, 57.72; H, 5.88; N, 14.43. Found: C, 57.83; H, 5.85; N, 14.48. IR ν_{max}^{KBr} cm^{-1}: 3420, 3350, 2980, 1740, 1700, 1640. UV λ_{max}^{EtOH} nm: 205, 224, 316, 367. NMR (DMSO-d_6) δ: 1.32 (3H, t, J=7 Hz), 2.12 (3H, s), 2.59 (3H, s), 4.38 (2H, d, J=7 Hz), 4.61 (2H, d, J=5 Hz), 5.65—6.30 (3H, m), 12.03 (1H, br).

Compound **4** was obtained from **2c** in 65% yield by a similar procedure. *Anal.* Calcd for $C_{14}H_{13}N_3O_4$: C, 58.53; H, 4.56; N, 14.63. Found: C, 58.62; H, 4.58; H, 14.70. MS m/z: 287, 259, 242. NMR (DMSO-d_6) δ: 1.35 (3H, t, J=7 Hz), 2.20 (3H, s), 2.56 (3H, s), 4.39 (2H, q, J=7 Hz), 11.15 (1H, s), 13.19 (1H, s).

7-Ethoxycarbonyl-5-fluoro-4-hydroxymethyl-6,8-dimethyl-1(2*H*)-phthalazinone (5a) A solution of **3a** (1.0 g) in 42% fluoroboric acid (4 ml) and water (4 ml) was chilled at 0 °C and a solution of sodium nitrate (400 mg) in water (2 ml) was added with vigorous stirring. Stirring was continued for 30 min, yielding precipitates. The salts were collected and washed with a small amount of cold water, then air-dried. The salts were placed in an argon gas-filled flask and heated gently with a flame. Evolution of gas occurred and the resulting mass was taken up in chloroform. Purification by column chromatography with benzene–EtOAc–MeOH (50 : 20 : 1) afforded 78 mg of **5a** from the later fractions in 7.2% yield. *Anal.* Calcd for $C_{14}H_{15}FN_2O_4$: C, 57.14; H, 5.10; N, 9.52. Found: C, 57.07; H, 5.14; N, 9.42. MS m/z: 294, 265, 249, 237. UV λ_{max}^{EtOH} nm: 215, 264, 293, 316, 329. The early fractions gave 290 mg (30.7%) of **6** as off-white crystals. *Anal.* Calcd for $C_{14}H_{14}N_2O_4$: C, 61.31; H, 5.15; N, 10.21. Found; C, 61.34; H, 5.18; N, 10.31. MS m/z: 274, 245, 229, 200. UV λ_{max}^{EtOH} nm: 216, 234, 275, 338, 354.

Compounds **5b—e** were obtained in 35—52% yields in the manner described in the literature.[6]

References

1) Y. Eguchi, F. Sasaki, M. Nakajima, Y. Takashima, and M. Ishikawa, *Chem. Pharm. Bull.*, **39**, 795 (1991).
2) M. Ishikawa, Y. Eguchi, and A. Sugimoto, *Chem. Pharm. Bull.*, **28**, 2770 (1980).
3) S. Kanahara, *Yakugaku Zasshi*, **84**, 483 (1964).
4) M. Ishikawa, Y. Eguchi, and A. Sugimoto, *Heterocycles*, **16**, 21 (1981).
5) A. Roe, *Organic Reactions*, **5**, 193 (1949).
6) H. Gilman, *Organic Syntheses*, **1**, 170, 514 (1956).
7) M. Schlosser, *Tetrahedron*, **34**, 3 (1978).
8) M. R. C. Gerstenberger and A. Haas, *Angew. Chem., Int. Ed. Engl.*, **20**, 647 (1981).
9) J. H. Clark and D. K. Smith, *Tetrahedron Lett.*, **26**, 2233 (1985).
10) H. Zollinger, "Diazo and Azo Chemistry," Interscience Publishers, Inc., New York, 1961.
11) A. H. Lewln and T. Cohen, *J. Org. Chem.*, **32**, 3844 (1967).

Alkaloidal Constituents of the Flowers of *Lycoris radiata* HERB. (Amaryllidaceae)

Masaru KIHARA,*[,a] Keiji KONISHI,[a] Lai XU,[a] and Shigeru KOBAYASHI[b]

Faculty of Pharmaceutical Sciences, The University of Tokushima,[a] Sho-machi, Tokushima 770, Japan and Faculty of Home Economics, Shikoku Women's University,[b] Ohjin-cho, Tokushima 771–11, Japan. *Received December 12, 1990*

A new alkaloid, hippeastrine *N*-oxide (7), was isolated from the flowers of *Lycoris radiata* HERB. (Amaryllidaceae) together with the known alkaloids galanthamine *N*-oxide (1), lycoramine *N*-oxide (3), galanthamine (4), lycoramine (6), hippeastrine (8), *O*-methyllycorenine *N*-oxide (9), *O*-methyllycorenine (10), homolycorine *N*-oxide (12), homolycorine (13), *O*-demethyllycoramine (14), vittatine (15), tazettine (16), lycorine (17), haemanthidine (18), and *O*-demethylhomolycorine (19), as well as dipalmitoylphosphatidylcholine (20) and 1-palmitoyl-2-linoleoylphosphatidylcholine (21).

Keywords *Lycoris radiata*; flower; Amaryllidaceae; alkaloid *N*-oxide; hippeastrine *N*-oxide; *O*-demethylhomolycorine; phosphatidylcholine

The flowers of Amaryllidaceae plants have not attracted much attention from phytochemists, although over 100 alkaloids have been isolated from the roots, bulbs, leaves, fruits, and seeds of these plants.[1] Recently, Ghosal *et al.* reported the isolation of new alkaloidal phospholipids from the flowers of *Zephyranthes flava*.[2] Previously, we reported the isolation of several new alkaloids, galanthamine *N*-oxide (**1**), sanguinine *N*-oxide (**2**), and lycoramine *N*-oxide (**3**), along with the corresponding free bases, galanthamine (**4**), sanguinine (**5**) and lycoramine (**6**), from *Lycoris sanguinea* MAXIM.[3] We now report the isolation of a new alkaloid, hippeastrine *N*-oxide (**7**) together with sixteen known alkaloids, hippeastrine (**8**), galanthamine *N*-oxide (**1**), galanthamine (**4**), lycoramine *N*-oxide (**3**), lycoramine (**6**), *O*-methyllycorenine *N*-oxide (**9**), *O*-methyllycorenine (**10**), homolycorine *N*-oxide (**12**), homolycorine (**13**), *O*-demethyllycoramine (**14**), vittatine (**15**), tazettine (**16**), lycorine (**17**), haemanthidine (**18**), and *O*-demethylhomolycorine (**19**) from the fresh flowers of *Lycoris radiata* HERB. Furthermore, dipalmitoylphosphatidylcholine (**20**) and 1-palmitoyl-2-linoleoylphosphatidylcholine (**21**) were obtained together with methyl palmitate (**22**) and methyl linoleate (**23**) from this plant.

Crude basic material extracted from the fresh flowers of *Lycoris radiata* by the modified method of Ghosal *et al.*[2] was subjected to column and preparative thin layer chromatography (PTLC), was described in Experimental, to give compounds **1**, **3**, **4**, **6**—**10**, **12**—**22** and **23**.

The new compound **7**, $C_{17}H_{17}NO_6$, was isolated as an amorphous powder. The infrared (IR) spectrum showed absorptions due to hydroxy group at 3401 cm^{-1} (broad) and a lactone ring at 1727 cm^{-1}. The proton nuclear magnetic resonance (^{1}H-NMR) spectrum showed the presence of two aromatic protons, an olefinic proton, and methylenedioxy protons in addition to deshielded *N*-methyl protons. The electron impact mass spectrum (EI-MS) was similar to that of hippeastrine (**8**),[4,5] except for the molecular ion peak. From these findings and the following facts, the new compound was concluded to be hippeastrine *N*-oxide (**7**): i) the molecular formula $C_{17}H_{17}NO_6$ has one more oxygen atom than that of hippeastrine (**8**), ii) the signals for the protons (H-11c, H-2 and NMe) attached to the nitrogen-bearing carbon atoms were shifted by *ca.* 0.5—1.2 ppm downfield from the corresponding signals in **8**.[5,6]

This assignment was confirmed by conversion of hippeastrine (**8**) to its *N*-oxide (**7**); oxidation of **8** in $CHCl_3$ with *m*-chloroperbenzoic acid (MCPBA) gave **7** as colorless cubes, $C_{17}H_{17}NO_6$, $[\alpha]_D$ +81.7° (MeOH).

The structures of compounds **9** and **12** were determined as *O*-methyllycorenine *N*-oxide and homolycorine *N*-oxide by comparisons of the ^{1}H-NMR spectra with those of 7β-*O*-methyllycorenine *N*-oxide (**11**) and homolycorine *N*-oxide (**12**) isolated from *Pancratium maritimum* (Amaryllidaceae) by Suau *et al.*[7] Although **11** had alpha configuration of H-7 (δ 5.50 in the ^{1}H-NMR spectrum), compound **9** is a mixture of epimers since the signals of H-7 of **9** were seen at δ 5.66 and 5.54 as two singlets. Thus, compound **9** might be an artifact derived from lycorenine *N*-oxide (**24**).[8] For the same reasons, *O*-methyllycorenine (**10**) isolated in this study seemed to be an artifact derived from lycorenine (**25**). The structure of homolycorine *N*-oxide (**12**) was confirmed by direct comparison with an authentic sample of **12**, $[\alpha]_D$ +17.4° (EtOH), mp 127—129 °C, prepared by oxidation of **13** with MCPBA.

Compound **19**, mp 127—130 °C, $[\alpha]_D$ +71.6° (EtOH), $C_{17}H_{19}NO_4$, was isolated as colorless pillars. The IR, ^{1}H-NMR and EI-MS spectra suggested the structure of compound **19** to be *O*-demethylhomolycorine. Recently, Jeffs *et al.*[6] reported that the structure of *O*-demethylhomolycorine with mp 138—140 °C was 9-*O*-demethylhomolycorine and speculated that *O*-demethylhomolycorine with mp 213—214 °C reported by Uyeo and Yanaihara[9] might be 10-*O*-demethylhomolycorine (**26**).[8] On the other hand, Tato *et al.*[10] isolated 9-*O*-demethylhomolycorine with mp 128—130 °C from *Pancratium* L. and suggested that the compound having mp 213—214 °C may be a polymorphic form. In order to clarify the situation, we measured the two-dimensional nuclear Overhauser effect correlation spectroscopy (2D-NOESY) spectra of **19** with mp 127—130 °C isolated in this study and of *O*-demethylhomolycorine with mp 207—208 °C isolated from the bulbs of *Lycoris radiata*.[5] The methoxy groups were correlated to H-11 but not to H-8 in both compounds. Therefore, *O*-demethylhomolycorine reported so far must be 9-*O*-demethylhomolycorine and the reported difference of the melting points was concluded to be due to polymorphism.[11]

Compounds **1**, **3**, **4**, **6**, **8**, **13**—**17** and **18** were identified as galanthamine *N*-oxide, lycoramine *N*-oxide, galanthamine, lycoramine, hippeastrine, homolycorine, *O*-de-

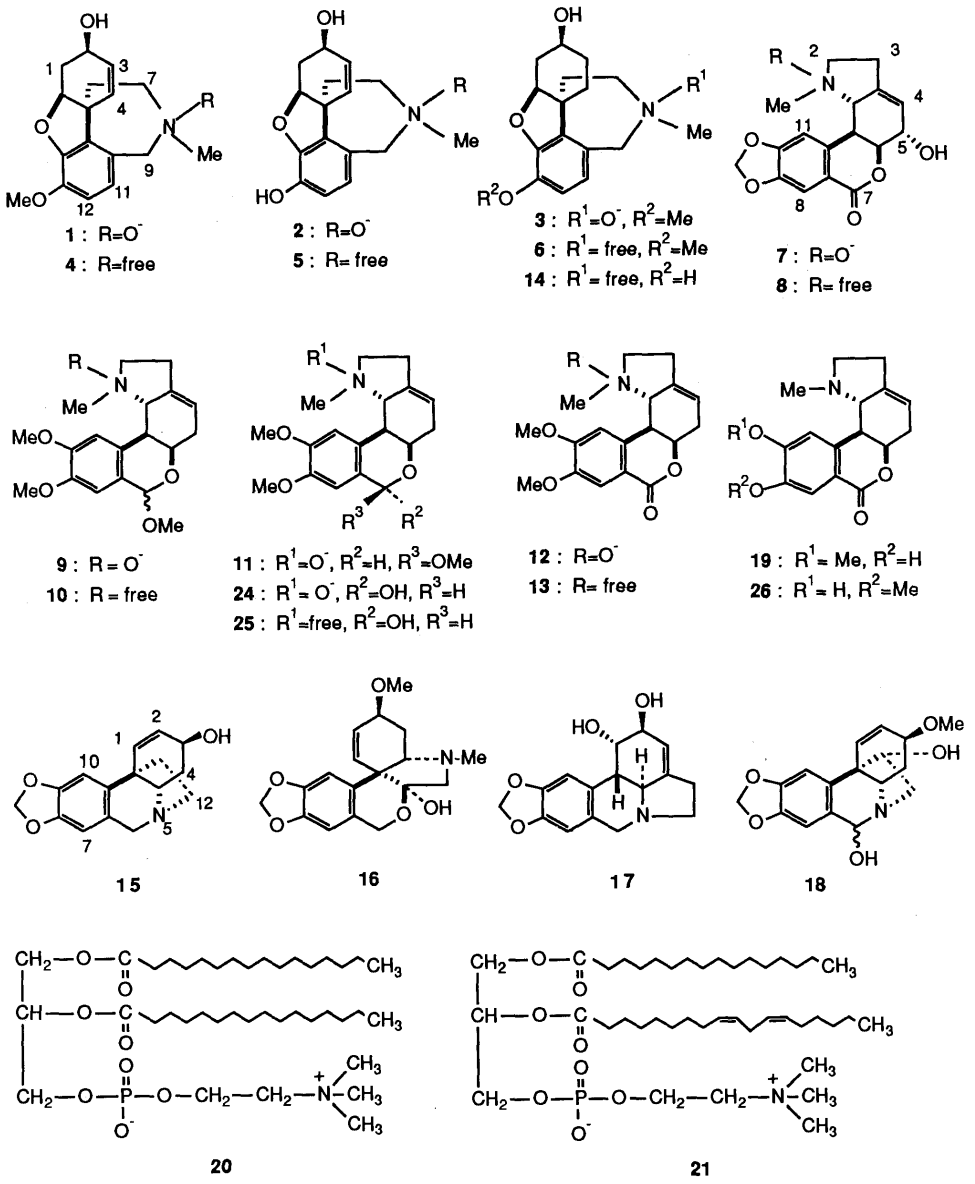

Chart 1

methyllycoramine, vittatine, tazettine, lycorine and haemanthidine by direct comparisons of their spectral data and thin layer chromatography (TLC) behavior with those of authentic samples.

A mixture of compounds **22** and **23** was isolated as an oil. The IR and ^{1}H-NMR spectra, and chemical ionization mass spectrum (CI-MS) of this oil indicated the structures of **22** and **23** to be methyl palmitate and methyl linoleate. The structures of **22** and **23** (a mixture of 1.4 : 1 from the ^{1}H-NMR spectrum) were confirmed by direct comparison of the ^{1}H-NMR and CI-MS spectra of this oil with those of a mixture (1 : 1) of authentic **22** and **23**.

Compound **21** gave a pale orange color with Dragendorff's reagent and a blue-violet color with molybdenum blue reagent.[12] The IR spectrum showed absorptions due to an ester at 1734 cm^{-1} and a phosphate group[13] at 1052 cm^{-1}. The ^{1}H-NMR spectrum indicated the presence of palmitate and linoleate groups in addition to a trimethylamino group (see Experimental). These findings suggested the structure of **21** to be a phosphatidylcholine derivative having a palmitate moiety and a linoleate moiety. The structure of compound **21** was determined as 1-palmitoyl-2-linoleoylphosphatidylcholine[14] by examination of the high resolution mass spectrum (high MS) and EI-MS[15-17] of **21** as follows. The intensity of the fragment at *m/z* 313 (90.6%) is higher than that of the fragment at *m/z* 337 (9.5%) as shown in Chart 2. This fact is consistent with the finding[16] that in the MS of phosphatidylcholines a fragment such as A generated by cleavage of an ester at C-2 is more stable than that such as B generated by cleavage of an ester at C-1.

In the same way, the structure of compound **20** was concluded to be 1,2-dipalmitoylphosphatidylcholine. The ^{1}H-NMR spectrum of **20** was similar to that of **21** except for the signals of a fatty acid moiety, which resemble those of methyl palmitate (**23**). The EI-MS of this compound was identical with that of **20** reported by Klein.[15]

This is the first time that the alkaloid *N*-oxides **7**, **1**, **3**, **9** and **12** have been isolated from *Lycoris radiata*. It is interesting that the flowers of this plant contain such a

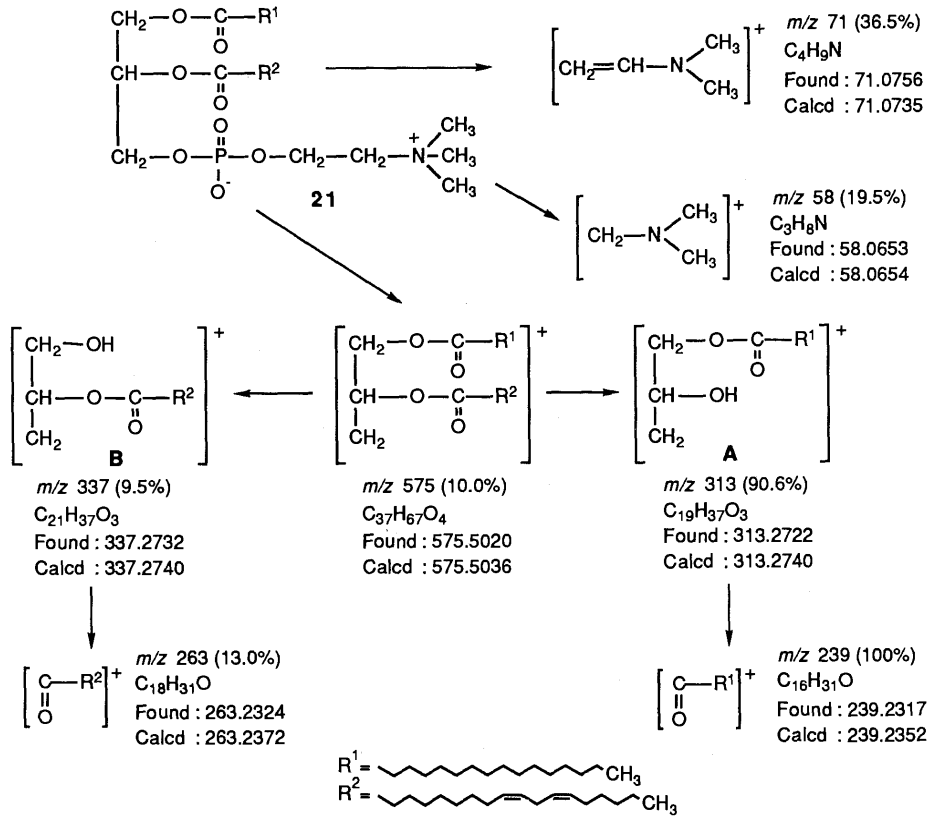

Chart 2

variety of alkaloids, even though in small amounts.

Experimental

All melting points are given as uncorrected values. The spectrophotometers used were a Perkin–Elmer 1720 infrared Fourier-transform spectrophotometer for IR spectra, a JEOL JMS-D 300 for MS, a Union PM-201 for optical rotation, a JASCO J-600 for optical rotatory dispersion (ORD), and JEOL JNM-FX 200 and JEOL JNM-GSX 400 spectrometers for ^{1}H-NMR spectra with tetramethylsilane as an internal standard. The plates used for PTLC were coated with silica gel (Kieselgel PF_{254} Merck) and aluminum oxide (PF_{254}, Merck). The following solvent systems were used: 1) $CHCl_3$–AcOEt (5:1); 2) $CHCl_3$–AcOEt–MeOH–H_2O (70:30:10:2), 3) $CHCl_3$–MeOH (20:1); 4) $CHCl_3$–MeOH–H_2O (60:35:10), 5) $CHCl_3$–MeOH–H_2O (65:25:4), 6) $CHCl_3$–MeOH (1:1), 7) $CHCl_3$–MeOH (7:1). UV light, I_2 vapor, Dragendorff's reagent and molybdenum blue reagent[12] were used for location of compounds.

Extraction Following the modified method of Ghosal *et al.*,[2] the fresh flowers (1.5 kg) of this plant collected in our Faculty plot were ground in 2 l of $CHCl_3$–MeOH (2:1) in a mixer. The extract was warmed at 60 °C for 1 h, then 0.1 M (EDTA) (20 ml) was added to retard the phospholipase activity and the mixture was kept at room temperature overnight. It was filtered to give two layers. The $CHCl_3$ and MeOH–H_2O layers were concentrated *in vacuo* to afford sticky extracts, 5.97 and 60 g, respectively.

Treatment of the $CHCl_3$ Extract The $CHCl_3$ extract was subjected to flash chromatography using HCl-washed Florisil (25 × 4 cm). Elution was carried out successively with benzene (1850 ml), $CHCl_3$ (2600 ml, fraction (fr.) I, 816 mg), $CHCl_3$–MeOH (95:5, 500 ml), $CHCl_3$–MeOH (9:1, 1000 ml), $CHCl_3$–MeOH (3:1, 500 ml, fr. II, 742 mg), $CHCl_3$–MeOH (1:1, 500 ml), and MeOH (1200 ml, fr. III, 342 mg).

Fraction I (816 mg) was subjected to column chromatography on SiO_2 using $CHCl_3$–MeOH–1% NH_4OH (70:16:2) to give four fractions (150 ml, fr. I-A: 142.5 mg; 75 ml, fr. I-B: 125.8 mg; 400 ml, fr. I-C: 50.6 mg; 700 ml, fr. I-D: 55.6 mg). Fraction I-A was subjected to PTLC (SiO_2, solvent 4) to give two fractions (fr. I-A-1, *Rf* 0.55—0.70 and fr. I-A-2, *Rf* 0.70—0.95). Purification of fr. I-A-1 and fr. I-A-2 by PTLC (Al_2O_3, solvent 2) afforded *O*-methyllycorenine *N*-oxide (**9**) (*Rf* 0.42—0.46, 4.9 mg) and *O*-methyllycorenine (**10**) (*Rf* 0.85—0.88, 2.1 mg). Fraction I-B was subjected to PTLC (SiO_2, $CHCl_3$–MeOH–AcOH (50:10:0.5)) to give hippeastrine *N*-oxide (**7**) (*Rf* 0.16—0.20, 1.9 mg) and galanthamine *N*-oxide (**1**) (*Rf* 0.20—0.40, 9 mg). Fraction I-C was purified by PTLC (SiO_2, solvent 5) to afford homolycorine *N*-oxide (**12**) (*Rf* 0.39—0.47, 3.5 mg). On PTLC (SiO_2, solvent 6), fr. I-D gave galanthamine *N*-oxide (**1**) (*Rf* 0.12—0.25, 5.4 mg, total yield 14.4 mg).

Fraction II (742 mg) was dissolved in MeOH and the solution, after filtration to remove undissolved material, was concentrated to afford an oily residue (385 mg), which was dissolved in ether. The ethereal solution was evaporated and the residue was subjected to PTLC (SiO_2, solvent 5) to give dipalmitoylphosphatidylcholine (**20**) (*Rf* 0.33—0.39, 200 mg). The insoluble material in ether was purified by PTLC (SiO_2, solvent 5) to afford 1-palmitoyl-2-linoleoylphosphatidylcholine (**21**) (*Rf* 0.33—0.43, 26.4 mg).

Fraction III (342 mg) was subjected to PTLC (SiO_2, solvent 2) to give lycoramine *N*-oxide (**3**) (*Rf* 0.11—0.25, 13.6 mg), lycoramine (**6**) (*Rf* 0.64—0.67, 53.9 mg), galanthamine (**4**) (*Rf* 0.64—0.79, 10 mg) and a mixture of methyl palmitate (**22**) and methyl linoleate (**23**) (*Rf* 0.79—1.0, 133 mg).

Treatment of the MeOH–H_2O Extract The MeOH–H_2O extract (60 g) was successively triturated with hot hexane, benzene, $CHCl_3$, $CHCl_3$–MeOH (1:1) (fr. IV, 4.04 g) and MeOH (fr. V, 37.5 g).

Fraction IV (4.04 g) was subjected to flash chromatography (SiO_2, $CHCl_3$–MeOH–NH_4OH–H_2O (70:25:2:2)) to give three fractions (250 ml, fr. IV-A, 59.8 mg; 500 ml, fr. IV-B, 80 mg; 650 ml, fr. IV-C, 35.4 mg). Fraction IV-A was purified by PTLC (SiO_2, solvent 4, Al_2O_3, solvent 2 and solvent 3 in succession) to afford homolycorine (**13**) (1.4 mg). Fraction IV-B was subjected to PTLC (Al_2O_3, solvent 2) to afford vittatine (**15**) (*Rf* 0.53—0.63, 28 mg) and a crude material (*Rf* 0.04—0.15), which was further purified by PTLC (Al_2O_3, solvent 7) to give *O*-demethyllycoramine (**14**) (*Rf* 0.43—0.53, 1.6 mg). On PTLC (SiO_2, solvent 4), fr. IV-C gave tazettine (**16**) (*Rf* 0.34—0.44, 2.6 mg).

Fraction V (37.5 g) was subjected to flash chromatography on SiO_2. Elution with $CHCl_3$–MeOH–NH_4OH–H_2O (70:25:2:2) gave a crude material (468 mg), which was subjected to PTLC (SiO_2, $CHCl_3$–MeOH–H_2O (60:30:5)) to give four fractions (fr. V-A, *Rf* 0.41—0.54, 67 mg; fr. V-B, *Rf* 0.64—0.72, 150 mg; fr. V-C, *Rf* 0.72—0.78, 25 mg; fr. V-D, *Rf* 0.78—0.86, 50.2 mg). Fraction V-A was purified by PTLC (Al_2O_3, solvent 1) to afford lycoramine (**6**) (*Rf* 0.22—0.45, 39 mg, total 92.9 mg). On trituration of fr. V-B with $CHCl_3$, lycorine (**17**) (56 mg) was obtained as precipitates and the $CHCl_3$ solution was subjected to PTLC (Al_2O_3, solvent 2) to afford haemanthidine (**18**) (*Rf* 0.28—0.36, 8.6 mg), lycorine (*Rf* 0.40–0.60, 37.6 mg, total 93.6 mg) and galanthamine (**4**) (*Rf* 0.75—0.82, 14 mg). Fraction V-C was subjected to PTLC (Al_2O_3, solvent 2) to give

O-demethylhomolycorine (**19**) (*Rf* 0.14—0.35, 12.5 mg) and galanthamine (**4**) (*Rf* 0.70—0.80, 7.9 mg, total 31.9 mg). Purification of fr. V-D by PTLC (Al_2O_3, solvent 3) gave hippeastrine (**8**) (*Rf* 0.71—0.78, 7.0 mg).

Hippeastrine *N*-Oxide (7) Amorphous powder. IR ν_{max}^{KBr} cm^{-1}: 3401 (OH), 1727 (C=O), 1611, 1484, 1385, 1295, 1252. High MS *m/z* [M^+]: Calcd for $C_{17}H_{17}NO_6$: 331.1053. Found: 331.1022. EI-MS *m/z* (%): 315 [M−O] (2), 313 (12), 307 (13), 293 (29), 253 (65), 190 (43), 162 (36), 125 (100). ^{1}H-NMR ($CDCl_3$, 200 MHz) δ: 7.50 (1H, s, H-8), 7.27 (1H, s, H-11), 6.09 (2H, s, OCH_2O), 5.98 (1H, br s, H-4), 4.73 (1H, br s, H-5a), 4.33 (1H, br s, H-5), 4.03 (1H, dd, J=2.1, 9.6 Hz, H-11b), 3.73 (1H, d, J=9.6 Hz, H-11c), 3.67 (1H, m, H-2), 3.50 (1H, m, H-2′), 3.10 (1H, m, H-3), 3.01 (3H, s, NMe), 2.68 (1H, m, H-3′).

Synthesis of 7 from 8 A solution of MCPBA (13.3 mg) in $CHCl_3$ (2 ml) was gradually added to a solution of **8** (16.4 mg) in $CHCl_3$ (2 ml) under ice-cooling. The mixture was stirred for 1 h and subjected to column chromatography on Al_2O_3. The fraction eluted with $CHCl_3$–MeOH (5:1) was concentrated and purified by PTLC (SiO_2, $CHCl_3$–MeOH (1:1)) to give **7** as colorless cubes (15 mg), mp 172—173 °C, $[\alpha]_D^{22}$ +81.7° (*c*=0.23, MeOH). High MS *m/z* [M^+]: Calcd for $C_{17}H_{17}NO_6$: 331.1053. Found: 331.1072. The MS, IR and ^{1}H-NMR spectra, and TLC behavior of this compound were identical with those of natural **7**.

Hippeastrine (8) Colorless cubes (from ethyl acetate), mp 206—210 °C (lit.[5] mp 210—212 °C). ^{1}H-NMR ($CDCl_3$, 200 MHz) δ: 7.49 (1H, s, H-8), 6.94 (1H, s, H-11), 6.09 and 6.07 (2H, each d, J=1.2 Hz, OCH_2O), 5.67 (1H, m, H-4), 4.61 (1H, br s, H-5a), 4.42 (1H, m, H-5), 3.16 (1H, m, H-2), 2.86 (1H, dd, J=9.3, 2.2 Hz, H-11b), 2.65 (1H, m, H-11c), 2.53 (2H, m, 2H-3), 2.25 (1H, m, H-2′), 2.06 (3H, s, NMe).

Galanthamine *N*-Oxide (1) Oil, $[\alpha]_D^{22}$ −118.2° (*c*=0.22, EtOH) (lit.[3] $[\alpha]_D^{26}$ −122.9° (*c*=0.38, EtOH)). High MS *m/z* [M^+]: Calcd for $C_{17}H_{21}NO_4$: 303.1469. Found: 303.1459. ^{1}H-NMR ($CDCl_3$, 200 MHz) δ: 6.76 (2H, s, H-11 and H-12), 6.08 (1H, dd, J=10, 4 Hz, H-3), 6.01 (1H, m, H-4), 4.65 (1H, br s, H-16), 4.84 and 4.39 (each 1H, d, J=15 Hz, 2H-9), 4.20 (1H, br s, H-2), 3.88 (3H, s, OMe), 3.70 (1H, m, H-7), 3.06 (3H, s, N^+Me), 2.74 (1H, d, J=16 Hz, H-1).

Galanthamine (4) Colorless pillars, $[\alpha]_D^{24}$ −87.4° (*c*=0.09, EtOH) (lit.[3] $[\alpha]_D^{23}$ −109.2° (*c*=0.85, EtOH)), mp 127–128 °C (lit.[3] 123—127 °C).

Lycoramine *N*-Oxide (3) Pale yellow oil, $[\alpha]_D^{26}$ −127.9° (*c*=0.08, EtOH) (lit.[3] $[\alpha]_D^{26}$ −111.6° (*c*=0.98, MeOH)). High MS *m/z* [M^+]: Calcd for $C_{17}H_{23}NO_4$: 305.1624. Found: 305.1606.

Lycoramine (6) Colorless pillars, $[\alpha]_D^{22}$ −78.6° (*c*=1.06, EtOH) (lit.[3] $[\alpha]_D^{26}$ −77.9° (*c*=0.35, MeOH)), mp 122—124 °C (lit.[5] mp 120—122 °C).

***O*-Methyllycorenine *N*-Oxide (9)** Colorless prisms, mp 109—111.5 °C (lit.[7] mp 136 °C). High MS *m/z* [M^+]: Calcd for $C_{19}H_{25}NO_5$: 347.1730. Found: 347.1707. ^{1}H-NMR ($CDCl_3$, 200 MHz) δ: 7.36 (1H, s, H-11), 6.80 (1H, s, H-8), 5.76 (1H, br s, H-4), 5.66 and 5.54 (1H, each s, H-7), 4.38 (1H, d, J=5.6 Hz, H-5a), 3.94 (2H, s, ArOMe), 3.89 (3H, s, ArOMe), 3.81 (1H, br s, H-11c), 3.64 (1H, ddd, J=11, 8.5, 1.8 Hz, H-2), 3.55 (3H, s, OMe-7), 3.44 (1H, dd, J=9.5, 1.7 Hz, H-11b), 3.08 (1H, m, H-3), 3.04 (3H, s, N^+Me).

***O*-Methyllycorenine (10)**[7] Pale yellow oil. High MS *m/z* [M^+]: Calcd for $C_{19}H_{25}NO_4$: 331.1782. Found: 331.1757. ^{1}H-NMR ($CDCl_3$, 200 MHz) δ: 6.91 (1H, s, H-11), 6.80 (1H, s, H-8), 5.66 and 5.54 (1H, each s, H-7), 5.50 (1H, br s, H-4), 4.30 (1H, br d, J=5 Hz, H-5a), 3.89 (3H, s, ArOMe), 3.87 (3H, s, ArOMe), 3.55 (3H, s, OMe-7), 2.11 (3H, s, NMe).

Homolycorine *N*-Oxide (12) Colorless needles, mp 125—128 °C (lit.[7] mp 134—136 °C). High MS *m/z* [M^+]: Calcd for $C_{18}H_{21}NO_5$: 331.1420. Found: 331.1433. ^{1}H-NMR ($CDCl_3$, 200 MHz) δ: 7.56 (1H, s, H-8), 7.34 (1H, s, H-11), 5.78 (1H, m, H-4), 4.88 (1H, m, H-5a), 4.03 (3H, s, OMe), 3.95 (3H, s, OMe), 3.83 (1H, br d, J=10 Hz, H-11c), 3.74 (1H, dd, J=9.8, 1.9 Hz, H-11b), 3.64 (1H, m, H-2), 3.49 (1H, m, H-2′), 3.08 (1H, m, H-3), 2.95 (3H, s, N^+Me), 2.67 (3H, m, H-3′ and 2H-5).

Synthesis of 12 from 13 A solution of MCPBA (18.2 mg) in $CHCl_3$ (3.5 ml) was added to a solution of **13** (15.1 mg) in $CHCl_3$ (1.5 ml) under ice-cooling and the mixture was stirred for 2 h. Work-up in the same way as described for **7** gave a crude product, which was purified by PTLC (SiO_2, $CHCl_3$–MeOH (2:1)) to give **12** as colorless needles (6 mg), mp 127—129 °C, $[\alpha]_D^{24}$ +17.4° (*c*=0.81, EtOH) (lit.[7] $[\alpha]_D^{25}$ +27.4° (*c*=0.1, MeOH). High MS *m/z* [M^+]: Calcd for $C_{18}H_{21}NO_5$: 331.1417. Found: 331.1382. The ^{1}H-NMR spectrum of this compound was identical with that of natural **12**.

Homolycorine (13) Amorphous powder (lit.[5] mp 167—169 °C). High MS *m/z* [M^+]: Calcd for $C_{18}H_{21}NO_4$: 315.1471. Found: 315.1501. ^{1}H-NMR ($CDCl_3$, 200 MHz) δ: 7.56 (1H, s, H-8), 7.04 (1H, s, H-11), 5.53 (1H, m, H-4), 4.81 (1H, m, H-5a), 3.96 (3H, s, OMe), 3.94 (3H, s, OMe), 3.19 (1H, m, H-11c), 2.03 (3H, s, NMe).

***O*-Demethylhomolycorine (19)** Colorless pillars, $[\alpha]_D^{25}$ +71.6° (*c*=0.20, EtOH) (lit.[18] $[\alpha]_D^{24}$ +89.6° (*c*=0.41, $CHCl_3$)), mp 127—130 °C (from AcOEt) (lit. mp 211—212 °C,[18] mp 207—208 °C,[5] mp 138—140 °C,[6] mp 213—214 °C,[9] mp 128—130 °C,[10]). IR ν_{max}^{KBr} cm^{-1}: 1790 (C=O). ^{1}H-NMR ($CDCl_3$, 200 MHz) δ: 7.61 (1H, s, H-8), 6.98 (1H, s, H-11), 5.51 (1H, br s, H-4), 4.79 (1H, br s, H-5a), 3.96 (3H, s, OMe), 3.15 (1H, m, H-11c), 2.80—2.40 (7H, m, 2H-3, 2H-5, H-11b and 2H-2), 2.00 (3H, s, NMe).

***O*-Demethyllycoramine (14)** Amorphous powder (lit.[5] mp 204—207 °C). High MS *m/z* [M^+]: Calcd for $C_{16}H_{21}NO_3$: 275.1518. Found: 275.1517. ^{1}H-NMR ($CDCl_3$, 200 MHz) δ: 6.65 and 6.53 (each 1H, d, J=8 Hz, H-11 and H-12), 4.36 (1H, m, H-16), 4.12 (1H, m, H-2), 3.99 and 3.58 (each 1H, d, J=15 Hz, 2H-9), 2.37 (3H, s, NMe).

Vittatine (15) Colorless needles, mp 206—209 °C (lit.[19] 206—208 °C). High MS *m/z* [M^+]: Calcd for $C_{16}H_{17}NO_3$: 271.1205. Found: 271.1204. ORD (*c*=0.016, MeOH) [*M*][23] (nm): +2491° (320), +4830° (311), +5745° (307) (peak), 0° (294), −4559° (270), −5745° (254) (trough), 0° (245), +5440° (240). ^{1}H-NMR ($CDCl_3$, 200 MHz) δ: 6.85 (1H, s, H-10), 6.59 (1H, d, J=10.8 Hz, H-1), 6.50 (1H, s, H-7), 5.96 (1H, ddd, J=10.8, 5.4, 1.2 Hz, H-2), 5.90 and 5.89 (each 1H, d, J=1.5 Hz, OCH_2O), 4.42 and 3.79 (each 1H, d, J=16.7 Hz, 2H-6), 4.33 (1H, m, H-3), 3.38 (2H, m, 2H-12), 2.93 (1H, m, H-4a).

Tazettine (16) Colorless pillars (from acetone), mp 211—215 °C (lit.[20] mp 209—210 °C). High MS *m/z* [M^+]: Calcd for $C_{18}H_{21}NO_5$: 331.1420. Found: 331.1441.

Lycorine (17) Colorless pillars (from MeOH), mp 257—258 °C (lit.[21] mp 256—262 °C).

Haemanthidine (18) Colorless pillars (from acetone), mp 162—166 °C (lit.[22] mp 189—190 °C). High MS *m/z* [M^+]: Calcd for $C_{17}H_{19}NO_5$: 317.1263. Found: 317.1268. This compound **18** was found to be a 1:1.4 mixture of the epimers[23] at C-7 by examination of the ^{1}H-NMR spectrum ($CDCl_3$, 200 MHz) δ: 6.97 and 6.78 (1H, each s, H-7), 6.82 and 6.81 (1H, each s, H-10), 6.40 (2H, s, H-1 and H-2), 5.93 and 5.91 (2H, each d, J=1.2 Hz, OCH_2O), 5.66 and 5.02 (1H, each s, H-6), 3.37 and 3.34 (3H, each s, OMe).

Mixture of Methyl Palmitate (22) and Methyl Linoleate (23) Pale yellow oil. CI-MS (isobutane) *m/z*: 271 (M+1 for **22**, 43%), 295 (M+1 for **23**, 100%). ^{1}H-NMR ($CDCl_3$, 200 MHz) δ: 5.34 (4H, m, olefinic H), 3.66 (6H, s, OMe×2), 2.77 (2H, m, =C–CH_2–C=), 2.30 (4H, t, J=7.6 Hz, $COCH_2$–×2), 2.05 (4H, m, =C–CH_2–×2), 1.62 (4H, m, $COCH_2C\underline{H}_2$–×2), 0.87 (6H, m, Me×2).

1,2-Dipalmitoylphophatidylcholine (20) Pale yellow oil. EI-MS *m/z* (%): 551 (4), 550 (10), 367 (2), 331 (9), 313 (45), 299 (12), 239 (67), 185 (5), 129 (32), 98 (45), 71 (65), 58 (80). FAB-MS (thioglycerol) *m/z* (%): 734 (M^+) (88), 735 (M+1) (44). IR ν_{max}^{KBr} cm^{-1}: 1733 (C=O), 1045 (phosphate). ^{1}H-NMR ($CDCl_3$, 200 MHz) δ: 5.22 (1H, m, –CH–), 3.72 (2H, br s, NCH_2–), 3.26 (9H, s, NMe_3), 2.31 (4H, m, $OC\underline{H}_2$–CH_2–×2), 1.57 (4H, br s, OCH_2–$C\underline{H}_2$–×2), 0.88 (6H, m, Me×2).

1-Palmitoyl-2-linoleoylphosphatidylcholine (21) Pale yellow oil. FAB-MS (M-NOBA) *m/z*: 758 (M+1). IR ν_{max}^{KBr} cm^{-1}: 1734 (C=O), 1052 (phosphate). ^{1}H-NMR ($CDCl_3$, 200 MHz) δ: 5.35 (4H, m, =CH×4), 5.21 (1H, br s, –CH–), 3.73 (2H, br s, CH_2N), 2.27 (9H, s, NMe_3), 2.75 (2H, t, J=6 Hz, =C–CH_2–C=), 2.29 (4H, m, $COC\underline{H}_2CH_2$–×2), 2.03 (4H, m, =CH–$C\underline{H}_2$–×2), 1.57 (4H, br s, $COCH_2C\underline{H}_2$–×2), 0.88 (6H, m, Me×2).

References and Notes

1) S. Ghosal, K. S. Saini, and S. Razdan, *Phytochemistry*, **24**, 2141 (1985).
2) S. Ghosal, S. K. Singh, and S. G. Unnikrishnan, *Phytochemistry*, **26**, 823 (1987).
3) S. Kobayashi, K. Satoh, A. Numata, T. Shingu, and M. Kihara, *Phytochemistry*, **30**, 675 (1991).
4) H. K. Schnoes, D. H. Smith, A. L. Burlingame, P. W. Jeffs, and W. Dopke, *Tetrahedron*, **24**, 2825 (1968).
5) S. Kobayashi, K. Yuasa, Y. Imakura, M. Kihara, and T. Shingu, *Chem. Pharm. Bull.*, **28**, 3433 (1980).
6) P. W. Jeffs, A. Abou-Donia, and D. Campau, *J. Org. Chem.*, **50**, 1732 (1985).
7) R. Suau, A. I. Gomez, R. Rico, M. P. V. Tato, L. Castedo and R. Riguera, *Phytochemistry*, **27**, 3285 (1988).
8) The isolation of these compounds has not been reported so far.
9) S. Uyeo and N. Yanaihara, *J. Chem. Soc.*, **1959**, 172.
10) M. P. V. Tato, L. Castedo, and R. Riguera, *Heterocycles*, **27**, 2833 (1988).
11) Y. Tsuda, N. Kashiwaba, and V. Kumar, *Chem. Pharm. Bull.*, **32**,

3023 (1984).
12) L. Gustavsson, *J. Chromatogr.*, **375**, 255 (1986).
13) M. B. Abramson, W. T. Norton, and R. Katzman, *J. Biol. Chem.*, **240**, 2389 (1965).
14) E. V. Dyatlovitskaya, V. I. Volkova, and L. D. Bergel'son, *Izv. Acad. Nauk SSSR, Ser. Khim.*, **1966**, 946 [*Chem. Abstr.*, **65**, 9318*h* (1966)].
15) R. A. Klein, *J. Lipid Res.*, **12**, 123 (1971).
16) R. A. Klein, *J. Lipid Res.*, **12**, 628 (1971).
17) R. A. Klein, *J. Lipid Res.*, **13**, 672 (1972).
18) S. Kobayashi, M. Kihara, K. Yuasa, Y. Imakura, T. Shingu, A. Katoh, and T. Hashimoto, *Chem. Pharm. Bull.*, **33**, 5258 (1985).
19) S. Uyeo, K. Kotera, T. Okada, S. Takagi, and Y. Tsuda, *Chem. Pharm. Bull.*, **14**, 793 (1966).
20) M. Kihara, T. Koike, Y. Imakura, K. Kida, T. Shingu, and S. Kobayashi, *Chem. Pharm. Bull.*, **35**, 1070 (1987).
21) S. Kobayashi, S. Takeda, H. Ishikawa, H. Matsumoto, M. Kihara, T. Shingu, A. Numata, and S. Uyeo, *Chem. Pharm. Bull.*, **24**, 1537 (1976).
22) H. G. Boit, *Chem. Ber.*, **87**, 1339 (1956).
23) R. W. King, C. W. Murphy, and W. C. Wildman, *J. Am. Chem. Soc.*, **87**, 4912 (1965).

Synthesis of Unsymmetrically Substituted Benzils *via* the Friedel–Crafts Reaction of Arenes with α-Chloro-α-(methylthio)acetophenones

Hiroyuki ISHIBASHI,* Kiyomi MATSUOKA, and Masazumi IKEDA

Kyoto Pharmaceutical University, Misasagi, Yamashina, Kyoto 607, Japan. *Received December 27, 1990*

Lewis acid-promoted reactions of arenes with α-chloro-α-(methylthio)acetophenones 6—8 gave the Friedel–Crafts reaction products 9, which were then treated with 3 molar eq of cupric chloride in aqueous acetone to afford the unsymmetrically substituted benzils 10.

Keywords Firedel–Crafts reaction; benzil; cupric chloride; α-chlorosulfide; Lewis acid; oxidation; β-ketosulfide; α-diketone; chlorination

In a series of papers,[1] we have shown that the α-chlorosulfides **1** having an electron-withdrawing group (EWG) such as an ethoxycarbonyl group react with arenes in the presence of Lewis acid to give the Friedel–Crafts (F–C) reaction products **2** in excellent yields. In an extension of these reactions, we have now examined the F–C reactions of arenes with a range of α-chloro-α-(methylthio)acetophenones **6**—**8**. The present paper describes a new convenient synthesis of the unsymmetrically substituted benzils **10** by oxidation of the F–C reaction products **9** with cupric chloride.

The requisite α-chlorosulfides **6**—**8** were prepared by treatment of the corresponding sulfides **3**—**5** with *N*-chlorosuccinimide (NCS). When a benzene solution of **6** was treated with a stoichiometric amount of stannic chloride ($SnCl_4$) at room temperature, the F–C reaction product **9a** ($R^1=R^2=H$) was obtained in 75% yield. Similarly the chloride **7** reacted with benzene to afford **9d** (R^1=4-MeO, $R^2=H$) in 69% yield. The reactions of **6**—**8** with an equimolar amount of electron-rich arenes such as veratrole or 1,3-benzodioxole were performed by using dichloromethane as a solvent to give the corresponding F–C reaction products. The results are summarized in Table I. In the cases of the reactions with 1,3-benzodioxole, the use of $SnCl_4$ as a Lewis acid sometimes led to the formation of by-products, so that a milder reagent, titanium tetrachloride ($TiCl_4$), was employed.

Recently, Caubere *et al.*[2] reported that the α-methylthio

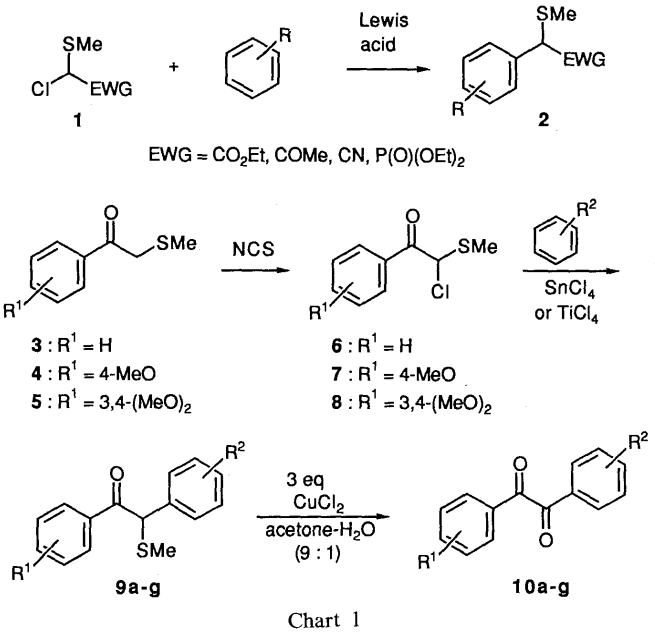

Chart 1

TABLE I. F–C Reaction of Arenes with **6**—**8** and Oxidation of **9** with $CuCl_2$

R¹	R²	F–C reaction of arenes with **6**—**8**				Oxidation of **9**	
		Lewis acid	Temp./time (min)	Products		Products	
				No.	Yield (%)	No.	Yield (%)
H	H	$SnCl_4$	r.t./40	**9a**	75	**10a**	99
H	3,4-(OMe)₂	$SnCl_4$	r.t./90	**9b**	57	**10b**	83
H	3,4-OCH₂O	$TiCl_4$	r.t./90	**9c**	76	**10c**	90
MeO	H	$SnCl_4$	r.t./60	**9d**	69	**10d**	70
MeO	3,4-(OMe)₂	$SnCl_4$	0 °C/60	**9e**	86	**10e**	73
MeO	3,4-OCH₂O	$TiCl_4$	0 °C/90	**9f**	93	**10f**	79
3,4-(MeO)₂	3,4-OCH₂O	$TiCl_4$	r.t./90	**9g**	62	**10g**	98

ketones **11**, on treatment with 2 molar eq of cupric chloride ($CuCl_2$) and 4 molar eq of cupric oxide (CuO) in 1% aqueous acetone, gave directly the α-diketones **13** in good yields. This reaction was suggested to proceed *via* the α-chloro-α-methylthio ketones **12** as intermediates, since $CuCl_2$ is known to chlorinate the α-position of simple ketones.[3] They also found that $CuCl_2$ alone, in a stoichiometric amount or in excess (a molar ratio was not given), led to a mixture of the starting sulfide **11** and the α-diketone **13**. Actually treatment of the β-ketosulfide **9a** ($R^1=R^2=H$) with combined $CuCl_2$ (2 eq) and CuO (4 eq) gave benzil (**10a**: $R^1=R^2=H$) quantitatively, whereas 1 or 2 molar eq of $CuCl_2$ alone resulted in the formation of a mixture of **9a** and **10a** in a ratio of 1:0.6 or 1:2.4, respectively. We found, however, that the oxidation of **9a** to **10a** was effected smoothly with 3 molar eq of $CuCl_2$ alone. Thus, heating of a homogeneous solution of **9a** and $CuCl_2$ (3 mol eq) in 10% aqueous acetone under reflux for 1 h gave **10a** quantitatively. Similar treatment of the F–C products **9b—g** gave the corresponding unsymmetrically substituted benzils **10b—g** in excellent yields.[4] The results are summarized in Table I.

Oxidation of **9** to **10** may proceed according to the stoichiometry shown in Chart 3. Thus, the β-ketosulfide **9** is chlorinated with 2 molar eq of $CuCl_2$ (probably *via* a radical process)[5] to give the α-chlorosulfide **14**, which is then hydrolyzed with the aid of an additional $CuCl_2$ giving the benzil **10**: the resultant methyl mercaptan might be oxidized with $CuCl_2$ to give dimethyl disulfide.

Finally, in order to test the applicability of this method to the synthesis of other α-dicarbonyl compounds, we

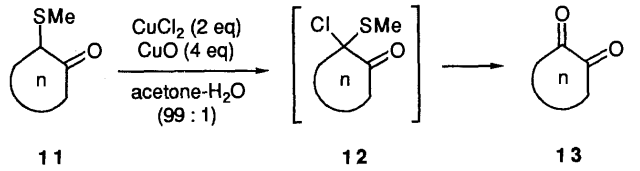

11 **12** **13**

Chart 2

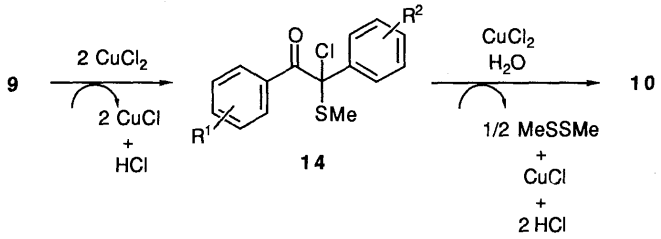

Chart 3

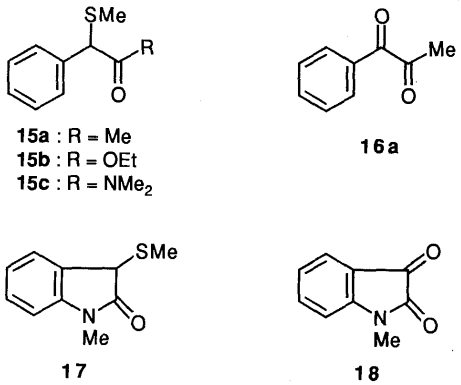

Chart 4

TABLE II. Physical Properties and Spectral Data for Compounds **9b—g** and **10b—g**

Compd. No.	mp (°C)[a] (lit. mp)	Analysis (%) Calcd (Found) C	H	Formula	IR cm^{-1}[b]	^{1}H-NMR ($CDCl_3$, δ)
9b	Oil	67.52 (67.27)	6.00 (6.15)	$C_{17}H_{18}O_3S$	1685	2.04 (3H, s), 3.83, 3.85 (3H × 2, s × 2), 5.46 (1H, s), 6.7—7.1 (3H, m), 7.2—7.6 (3H, m), 7.85—8.1 (2H, m)
9c	Oil	286.0662[c] (286.0643)		$C_{16}H_{14}O_3S$	1690	2.04 (3H, s), 5.40 (1H, s), 5.88 (2H, s), 6.6—7.1 (3H, m), 7.3—7.6 (3H, m), 7.85—8.1 (2H, m)
9d	Oil	70.56 (70.25	5.92 6.26)	$C_{16}H_{16}O_2S$	1680	2.03 (3H, s), 3.75 (3H, s), 5.46 (1H, s), 6.85 (2H, d, J=9 Hz), 7.1—7.65 (5H, m), 7.97 (2H, d, J=9 Hz)
9e	Oil	332.1081[c] (332.1063)		$C_{18}H_{20}O_4S$	1680	2.04 (3H, s), 3.77, 3.80, 3.83 (3H × 3, s × 3), 5.44 (1H, s), 6.65—7.1 (5H, m), 7.95 (2H, d, J=9 Hz)
9f	Oil	316.0769[c] (316.0781)		$C_{17}H_{16}O_4S$	1680	2.04 (3H, s), 3.83 (3H, s), 5.40 (1H, s), 5.93 (2H, s), 6.65—7.1 (5H, m), 7.98 (2H, d, J=9 Hz)
9g	Oil	346.0874[c] (346.0887)		$C_{18}H_{18}O_5S$	1680	2.03 (3H, s), 3.86 (6H, s), 5.39 (1H, s), 5.89 (2H, s), 6.6—7.05 (4H, m), 7.45—7.7 (2H, m)
10b	111—113 (111—113)[d]				1665	3.93 (6H, s), 6.87 (1H, d, J=9 Hz), 7.3—7.7 (5H, m), 7.8—8.1 (2H, m)
10c	104—106	70.86 (70.51	3.96 4.00)	$C_{15}H_{10}O_4$	1665	6.00 (2H, s), 6.80 (1H, d, J=9 Hz), 7.25—7.65 (5H, m), 7.8—8.1 (2H, m)
10d	59—60 (62—63)[d]				1665	3.83 (3H, s), 6.92 (2H, d, J=9 Hz), 7.2—7.7 (3H, m), 7.75—8.1 (4H, m)
10e	121—123 (123—124)[d]				1660	3.88 (3H, s), 3.93 (6H, s), 6.90 (1H, d, J=8 Hz), 6.97 (2H, d, J=9 Hz), 7.3—7.7 (2H, m), 7.95 (2H, d, J=9 Hz)
10f	109—111	67.60 (67.39	4.25 4.31)	$C_{16}H_{12}O_5$	1660	3.86 (3H, s), 6.04 (2H, s), 6.7—7.1 (3H, m), 7.35—7.6 (2H, m), 7.90 (2H, d, J=9 Hz)
10g	152—153	64.97 (64.79	4.49 4.53)	$C_{17}H_{14}O_6$	1660	3.95 (6H, s), 6.05 (2H, s), 6.7—7.0 (2H, m), 7.3—7.65 (4H, m)

a) Benzils **10** were recrystallized from ethanol except for **10b** (from methanol). *b*) Measured in CCl_4 for **9b—g** and in $CHCl_3$ for **10b—g**. *c*) High-resolution MS (M^+). *d*) Ref. 9 for **10b**, ref. 4*a* for **10d**, and ref. 10 for **10e**.

treated the α-methylthio carbonyl compounds **15a—c** with 3 molar eq of $CuCl_2$. The oxidation of **15a** occurred smoothly to give the α-diketone **16a** in 91% yield, whereas the reactions of **15b—c** with $CuCl_2$ were very sluggish, and prolonged heating of the mixture afforded a complex mixture of products. On the other hand, the 3-(methylthio)-oxindole **17** gave *N*-methylisatin (**18**) in 89% yield. These results suggest that the chlorination of α-methylthio carbonyl compounds with $CuCl_2$ proceeds *via* their enol forms.

Experimental

Melting points are uncorrected. Infrared (IR) spectra were recorded with a JASCO A-100 spectrophotometer. Proton nuclear magnetic resonance (^{1}H-NMR) spectra were determined with a JEOL JNM-PMX 60 (60 MHz) spectrometer using tetramethylsilane as an internal standard. High-resolution mass spectra (MS) were obtained with a Hitachi M-80 instrument at 20 eV. Column chromatography was performed on Silica gel 60 PF_{254} (Merck) under pressure.

General Procedure for the Preparation of α-Chlorosulfides 6—8 *N*-Chlorosuccinimide (0.68 g, 5 mmol) was added to a stirred solution of **3**,[6] **4**,[6] or **5**[6] (5 mmol) in CCl_4 (50 ml) at 0 °C and the stirring was continued at room temperature for 24 h. The precipitated succinimide was filtered off and the filtrate was concentrated *in vacuo* to give quantitatively the chlorosulfides **6**, **7**, and **8**, respectively, which, without further purification, were used immediately in the next step or stored in a refrigerator.

General Procedure for the Preparation of α-Methylthio Ketones 9a—g Method A: $SnCl_4$ (261 mg, 1 mmol) was added to a stirred solution of **6** or **7** (1 mmol) in benzene (3 ml) at 10 °C and the stirring was continued at room temperature for 40—60 min. Water (10 ml) was added to the reaction mixture and the organic layer was separated. The aqueous layer was further extracted with benzene and the combined organic layers were dried. The solvent was removed by evaporation and the residue was chromatographed on silica gel (hexane : ethyl acetate = 7 : 3) to give **9a**[7] (75%) and **9d** (69%), each as an oil. The physical data of **9d** are listed in Table II.

Method B: The Lewis acid (1 mmol) indicated in Table I was added to a stirred solution of **6—8** (1 mmol) and an arene such as veratrole or 1,3-benzodioxole (1 mmol) in CH_2Cl_2 (15 ml) at 0 °C and stirring was continued at the temperature indicated in Table I for 60—90 min. The reaction was quenched by the addition of water (10 ml) and the mixture was worked up to give the F–C reaction products **9b, c, e—g**, whose yields and physical data are listed in Tables I and II, respectively.

Benzil (10a): General Procedure for the Preparation of Unsymmetrically Substituted Benzils Cupric chloride dihydrate (303 mg, 1.78 mmol) was added to a solution of **9a** (153 mg, 0.59 mmol) in acetone (3.6 ml) and water (0.4 ml) and the mixture was heated under reflux for 1 h. After completion of the reaction (the green color of cupric ion faded), the reaction mixture was diluted with benzene (20 ml) and dried over $MgSO_4$ (3 g). The inorganic materials were removed by filtration, the filtrate was concentrated *in vacuo*, and the residue was chromatographed on silica gel (hexane : ethyl acetate = 9 : 1) to give **10a** (123 mg, 99%), mp 91—92 °C (from ethanol) (lit.[4a] mp 94—95 °C). IR $\nu_{max}^{CCl_4}$ cm^{-1}: 1675. ^{1}H-NMR ($CDCl_3$) δ: 7.2—7.7 (6H, m), 7.85—8.15 (4H, m). The yields and physical data of unsymmetrically substituted benzils **10b—g** are listed in Tables I and II, respectively.

1-Phenyl-1,2-propanedione (16a) Using a procedure similar to that described for the preparation of **10a**, 1-methylthio-1-phenyl-2-propanone (**15**)[1b] (204 mg, 1.13 mmol) was treated with $CuCl_2 \cdot 2H_2O$ (579 mg, 3.39 mmol) to give **16a** (153 mg, 91%) as an oil, whose spectral data were identical to those of an authentic sample purchased from Wako Pure Chemical Industries, Ltd. IR $\nu_{max}^{CCl_4}$ cm^{-1}: 1710, 1670. ^{1}H-NMR ($CDCl_3$) δ: 1.50 (3H, s), 7.3—7.9 (3H, m), 7.9—8.2 (2H, m).

1-Methyl-1*H*-indole-2,3-dione (18) Using a procedure similar to that described for the preparation of **10a**, 1-methyl-3-(methylthio)oxindole (**17**)[1d] (100 mg, 0.52 mmol) was treated with $CuCl_2 \cdot 2H_2O$ (265 mg, 1.55 mmol) to give **18** (75 mg, 89%), mp 128—129.5 °C (from ethanol), (lit.[8] mp 131—113 °C). IR $\nu_{max}^{CHCl_3}$ cm^{-1}: 1730. ^{1}H-NMR ($CDCl_3$) δ: 3.25 (3H, s), 6.8—7.3 (2H, m), 7.45—7.8 (2H, m).

Acknowledgment We thank Mr. T. Kobayashi for his technical assistance.

References and Notes

1) *a*) Y. Tamura, H. D. Choi, H. Shindo, and H. Ishibashi, *Chem. Pharm. Bull.*, **30**, 915 (1982); *b*) Y. Tamura, H. D. Choi, M. Mizutani, Y. Ueda, and H. Ishibashi, *ibid.*, **30**, 3574 (1982); *c*) H. Ishibashi, T. Sato, M. Irie, M. Ito, and M. Ikeda, *J. Chem. Soc., Perkin Trans. 1*, **1987**, 1095. See also *d*) Y. Tamura, J. Uenishi, H. Maeda, H. D. Choi, and H. Ishibashi, *Synthesis*, **1981**, 534; *e*) H. Ishibashi, H. Nakatani, Y. Umei, W. Yamamoto, and M. Ikeda, *J. Chem. Soc., Perkin Trans., 1*, **1987**, 589; *f*) H. Ishibashi, M. Okada, H. Nakatani, M. Ikeda, and Y. Tamura, *ibid.*, **1986**, 1763.
2) B. Gregoire, M.-C. Carre, and P. Caubere, *J. Org. Chem.*, **51**, 1419 (1986).
3) A. Lorenzini and C. Walling, *J. Org. Chem.*, **32**, 4008 (1967).
4) For other syntheses of unsymmetrically substituted benzils, see *a*) N. J. Leonard, R. T. Rapala, H. L. Herzog, and E. R. Blout, *J. Am. Chem. Soc.*, **71**, 2997 (1949); *b*) A. McKillop, O. H. Oldenziel, B. P. Swann, E. C. Taylor, and R. L. Robey, *ibid.*, **95**, 1296 (1973); *c*) A. McKillop, B. P. Swann, M. E. Ford, and E. C. Taylor, *ibid.*, **95**, 3641 (1973); *d*) R. Girard and H. B. Kagan, *Tetrahedron Lett.*, **1975**, 4513; *e*) D. Armesto, W. M. Horspool, M. J. Ortiz, and R. Perez-Ossorio, *Synthesis*, **1988**, 799.
5) Y. Ito, M. Nakatsuka, and T. Saegusa, *J. Org. Chem.*, **45**, 2022 (1980).
6) H. Ishibashi, I. Takamuro, Y. Mizukami, M. Irie, and M. Ikeda, *Synth. Commun.*, **19**, 443 (1989).
7) S. Kano, T. Yokomatsu, and S. Shibuya, *J. Org. Chem.*, **43**, 4366 (1978).
8) P. G. Gassmann, B. W. Cue, Jr., and T.-Y. Luh, *J. Org. Chem.*, **42**, 1344 (1977).
9) H. Hirano, K. Kurumaya, and M. Tada, *Bull. Chem. Soc. Jpn.*, **54**, 2708 (1981).
10) K. Oishi and K. Kurosawa, *Bull. Chem. Soc. Jpn.*, **53**, 179 (1980).

Studies on Sulfenamides. XIII.[1] Reaction of 2-Nitrobenzene-sulfenanilides with *N*-Bromosuccinimide

Takashi MICHIDA,* Michiko MIZUHARA, and Hiroteru SAYO

Faculty of Pharmaceutical Sciences, Kobe-Gakuin University, Ikawadani-cho, Nishi-ku, Kobe 651-21, Japan. *Received January 18, 1991*

The reaction of *N*-alkyl 2-nitrobenzenesulfenanilides (1a—3a) with *N*-bromosuccinimide (NBS) gave the corresponding monobrominated 2-nitrobenzenesulfenanilides (1b—3b) in good yields. The initial step of this reaction is the attack of NBS on the nitrogen atom of 1a—3a. The intermediate of this reaction is considered to be a cation radical of the sulfenanilides. A similar reaction of *N*-unsubstituted 2-nitrobenzenesulfenanilides (5a—10a) with NBS gave mono- or di-brominated 2-nitrobenzenesulfenanilides in low yields.

Keywords bromination; *N*-bromosuccinimide; sulfenamide; 2-nitrobenzenesulfenanilide

In this paper the bromination of the aromatic ring in the aniline moiety of sulfenanilides is reported. As shown in previous papers,[1,2] the oxidation of sulfenanilides involves various reactive intermediates, but neither their reactivity nor their fate in the oxidation process is known. 2-Nitrobenzenesulfenanilides [*N*-Me-4′-OMe (**1a**), *N*-Me (**2a**), *N*-Et (**3a**), 4′-Me (**5a**), 4′-COOEt (**6a**), unsubstituted (**7a**), 3′-OMe (**8a**), 3′-Me (**9a**), and 2′-COOEt (**10a**)] and *N*-(2-nitrophenylthio)-1,2,3,4-tetrahydroquinoline (**4a**) were subjected to reaction with *N*-bromosuccinimide (NBS) to elucidate the reactivity of the reactive intermediates derived from **1a**—**10a**. The feasibility of applying the method to the preparation of bromoanilines was also investigated, because a mild and facile synthesis of bromoanilines is still required.[3] The 2-nitrobenzenesulfenyl group, which is frequently used for protection of the amino group, can be easily removed by hydrogen chloride.[4]

Results and Discussion

The reaction of *N*-substituted 2-nitrobenzenesulfenanilides (**1a**—**4a**) with NBS in dry CH_2Cl_2 at room temperature gave the corresponding brominated compounds (**1b**—**4b**) in good yields as shown in Table I.

The *para* position to nitrogen in **2a**—**4a** was brominated selectively and almost quantitatively, but **1a**, which contains 4′-OMe, gave the 2′-brominated compound (**1b**). The oxidation mechanism of **1a**—**4a** has been reported in detail, base on the results of cyclic voltammetry and electron spin resonance (ESR) spectrometry.[2h] The conclusion in the previous paper suggests that the 4′-position of the cation radicals derived from sulfenanilides is the most reactive site. Chart 1 shows the bromination mechanism of **2a** as a typical example.

The electrophilic attack of NBS or Br^+ must take place at the position which has the highest electron density in the molecule of **2a**, that is, the lone pair of the nitrogen atom. Homolysis of the N–Br bond gives the cation radical B and a bromine atom, and the latter attacks the 4′-position of B to give C. A similar mechanism of generation of the cation radical was reported in the oxidation of triethylamine.[5] Subsequent deprotonation gives **2b** as the final product.

Compounds **5a** and **6a** did not give good results, as shown in Table I. Unreacted **5a** (29%) still remained in the reaction mixture, though the oxidation potential of **5a**[2d] was slightly lower than that of **2a**.[2h] When two equivalents of NBS was used, no unreacted **5a** was detected in the reaction mixture but the yield of **5b** was reduced to 3.4%. These facts suggest that the bromination of **5a** and **6a** proceeds *via* an alternative mechanism and the N–H bond must play an important role in it. In order to elucidate this phenomenon, **1a** and **5a**—**10a** were treated with NBS under basic conditions. The results are shown in Table II.

The following points are noteworthy. First, **1a** gave good results even under these conditions. Second, **5b**—**10b** also reacted with NBS. Although unreacted substrates were recovered from the reactions of **7a**, **8a**, and **9a**, only the dibrominated compounds were obtained without formation of the monobrominated compounds. This fact suggested

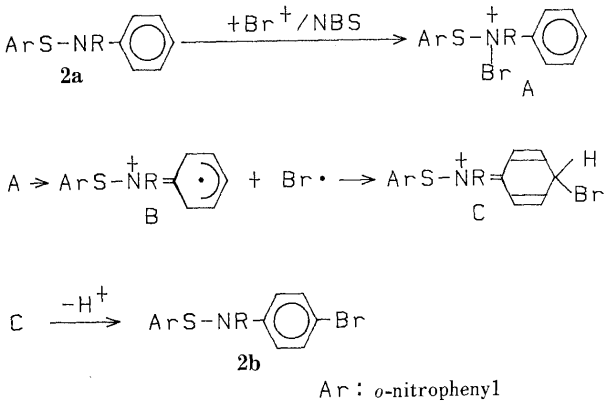

Chart 1

TABLE I. Results of Reaction of *N*-Substituted 2-Nitrobenzenesulfenanilides with NBS

Compd. no.	Sulfenanilide	Products identified (comp. no.)	Yields
1a	$ArSN(Me)C_6H_4$-4′-OMe	$ArSN(Me)C_6H_3$-2′-Br-4′-OMe (**1b**)	Quantitative
2a	$ArSN(Me)C_6H_5$	$ArSN(Me)C_6H_4$-4′-Br (**2b**)	98%
3a	$ArSN(Et)C_6H_5$	$ArSN(Et)C_6H_4$-4′-Br (**3b**)	Quantitative[a]
4a	*N*-ArS-1,2,3,4-tetrahydroquinoline	*N*-ArS-1,2,3,4-tetrahydro-6-Br-quinoline (**4b**)	99%
5a	$ArSNHC_6H_4$-4′-Me	$ArSNHC_6H_4$-2′-Br-4′-Me (**5b**)	40%
6a	$ArSNHC_6H_4$-4′-COOEt	$ArSNHC_6H_4$-2′-Br-4′-COOEt (**6b**)	44%

Ar: 2-nitrophenyl. *a*) One and half equivalents of NBS was used.

TABLE II. Results of Reaction of 2-Nitrobenzenesulfenanilides with NBS under Basic Conditions

Compd. no.	Sulfenanilides	Products identified (compd. no.)	Yield[a]	
			1 h	2 h[b]
1a	$ArSN(Me)C_6H_4$-4′-OMe	$ArSN(Me)C_6H_3$-2′-Br-4′-OMe (**1b**)	78% (44%)	96% (18%)
5a	$ArSNHC_6H_4$-4′-Me	$ArSNHC_6H_3$-2′-Br-4′-Me (**5b**)	26% (20%)	42% (10%)
6a	$ArSNHC_6H_4$-4′-COOEt	$ArSNHC_6H_3$-2′-Br-4′-COOEt (**6b**)	49% (53%)	35% (19%)
7a	$ArSNHC_6H_6$	$ArSNHC_6H_3$-2′,4′-Br_2 (**7b**)	11% (24%)	17% (8%)
8a	$ArSNHC_6H_4$-3′-OMe	$ArSNHC_6H_2$-2′,4′-Br_2-3′-OMe (**8b**)	74% (39%)	67% (24%)
9a	$ArSNHC_6H_4$-3′-Me	$ArSNHC_6H_2$-2′,4′-Br_2-3′-Me (**9b**)	20% (23%)	19% (2%)
10a	$ArSNHC_6H_4$-2′-COOEt	$ArSNHC_6H_3$-4′-Br-2′-COOEt (**10b**)	56% (55%)	33% (37%)

a) Yield based on the amount of consumed substrate. The amount of recovered substrate is shown in parentheses. Determined by HPLC. *b*) After 1 h, the same amounts of NBS and K_2CO_3 were added to the solution again.

that the monobrominated products were much more reactive than the starting materials.

It has already been reported that the Ep-value of the first anodic wave of **5a**—**10a** is decreased under basic conditions, because they gave conjugated bases by dissociation of the N–H bond in basic solution.[2f] Therefore, deprotonation of the N–H bond appears to play an important role in the reaction of **5a**—**10a** with NBS. The reaction of the conjugated bases generated from **5a**—**10a** gives monobrominated sulfenanilides (MBS). MBS will be oxidized faster than the parent **5a**—**10a**, because the bromosubstituent attracts electrons in the aromatic ring and increases the acidity of MBS. Oxidation of the conjugated base generated from MBS by NBS gives dibrominated sulfenanilides. However, it is impossible to rule out the existence of *N*-halogenated compounds as intermediates, just as in the chlorination of anilines with *N*-chlorosuccinimide.[6]

In conclusion, the oxidation of **1a**—**10a** with NBS brought about monobromination of the aniline moiety of the sulfenanilides, and **1b**—**4b**, with an alkyl group on the nitrogen atom, were not oxidized by NBS any further, whereas the monobrominated products derived from **7a**—**9a** were oxidized by NBS, because they gave conjugated bases with low oxidation potentials by dissociation of the N–H bond, to give dibrominated compounds **7b**—**9b**.

Monobromination can be often achieved in good yield but specific conditions are required in each case. NBS–dimethylformanide (DMF)[7] or anilinosilane–NBS[3a] has been reported to be a mild and selective monobromination reagent for reactive aromatic amines. Those reactions need a longer time than the reaction of **1a**—**10a** with NBS. Preparation of **1a**—**10a** is easier than that of anilinosilanes because 2-nitrobenzenesulfenyl chloride is commercially available. The oxidation of 2-nitrobenzenesulfenanilides with NBS is a mild and convenient method for their bromination but it is necessary to replace the *N*-hydrogen with an aliphatic substituent in order to increase the yield of monobrominated products.

Experimental

Materials The sulfenanilides were prepared from 2-nitrobenzenesulfenyl chloride and the corresponding amines in dry ether, and purified by recrystallization from ethanol.[2] Each compound gave analysis results consistent with the theoretical values. Dichloromethane was dried over molecular sieves. Methanol was dried with activated magnesium and distilled.

Apparatus Infrared (IR), nuclear magnetic resonance (NMR), and mass spectra (MS) were obtained as previously described.[2h] Melting points are not corrected. High-performance liquid chromatography (HPLC) was carried out as described previously.[2i]

2′-Bromo-4′-methoxy-*N*-methyl-2-nitrobenzenesulfenanilide (1b). Typical Examples of Isolation of Products from the Reaction Mixture a) NBS (0.36 g) was added to the solution of **1a** (576.8 mg) in dichloromethane (10 ml) and the mixture was stirred at room temperature for 1 h. CH_2Cl_2 (30 ml) was added to the reaction mixture, and the whole was washed with 30% aqueous Na_2CO_3 solution twice, and then once with water (30 ml). After being dried over $MgSO_4$, the organic layer was concentrated to dryness, and then the residue was purified on a Silica gel 60 (Merck) column using benzene–hexane (2 : 1) as an eluent to give **1b** (720.0 mg). mp 88—89 °C. (from EtOH). IR ν_{max}^{KBr} cm^{-1}: 1505 (NO_2), 1330 (NO_2). ^{1}H-NMR ($CDCl_3$) δ: 3.28 (3H, s, NCH_3), 3.77 (3H, s, OCH_3), 6.82 (1H, dd, J=2.91, 8.85 Hz, aromatic proton), 7.11 (1H, d, J=2.90 Hz, aromatic proton), 7.28 (1H, dt, J=1.34, 7.13 Hz, aromatic proton), 7.42 (1H, d, J=8.84 Hz, aromatic proton), 7.72 (1H, dt, J=1.40, 7.11 Hz, aromatic proton), 8.29 (1H, dd, J=1.33, 8.30 Hz, aromatic proton), 8.37 (1H, dd, J=1.28, 8.29 Hz, aromatic proton). MS *m/z*: 368, 370 (M^+), 214, 216 (H_3C–N^+–$C_6H_3BrOCH_3$), 154 (O_2N–$C_6H_4S^+$). *Anal.* Calcd for $C_{14}H_{13}BrN_2O_3S$: C, 45.54; H, 3.54; N, 7.85. Found: C, 45.42; H, 3.45; N, 7.54.

b) Potassium carbonate (0.4 g) and NBS (714.4 mg) were added to a solution of **1a** (578.8 mg) in dichloromethane (10 ml) and methanol (1 ml) and the mixture was stirred at room temperature for 1 h. CH_2Cl_2 (30 ml) was added to the reaction mixture, and the whole was washed with 30% aqueous Na_3CO_3 solution twice, and then once with water (30 ml). After being dried over $MgSO_4$, the organic layer was concentrated to dryness, and the residue was purified with LiChroprep Si 60 size C (Merck) using benzene as an eluent to give **1b** (720.0 mg).

The following compounds were obtained by essentially the same procedure and recrystallized from ethanol if necessary.

4′-Bromo-*N*-methyl-2-nitrobenzenesulfenanilide (**2b**): mp 118—119 °C. (from EtOH). IR ν_{max}^{KBr} cm^{-1}: 1490 (NO_2), 1310 (NO_2). ^{1}H-NMR ($CDCl_3$) δ: 3.47 (3H, s, NCH_3), 7.02 (2H, d, J=9.22 Hz, aromatic protons), 7.18 (1H, dd, J=1.42, 8.32 Hz, aromatic proton), 7.31 (1H, dt, J=1.36, 7.23 Hz, aromatic proton), 7.36 (2H, d, J=9.13 Hz, aromatic protons), 7.54 (1H, dt, J=1.33, 7.15 Hz, aromatic proton), 8.36 (1H, dd, J=1.32, 8.30 Hz, aromatic proton). MS *m/z*: 338, 340 (M^+), 184, 186 ($M^+ - O_2NC_6H_4S$), 154 ($O_2NC_6H_4S^+$). *Anal.* Calcd for $C_{13}H_{11}BrN_2O_2S$: C, 46.03; H, 3.26; N, 8.25. Found: C, 46.20; H, 3.23; N, 8.07.

4′-Bromo-*N*-ethyl-2-nitrobenzenesulfenanilide (**3b**): mp 105—107 °C. (from EtOH). IR ν_{max}^{KBr} cm^{-1}: 1510 (NO_2), 1350 (NO_2). ^{1}H-NMR ($CDCl_3$) δ: 1.38 (3H, t, J=7.08 Hz, CH_3), 3.53—3.63 (1H, m, CH_2), 3.90—3.99 (1H, m, CH_2), 7.01 (2H, d, J=9.23 Hz, aromatic protons), 7.27—7.36 (4H, m, aromatic protons), 7.54 (1H, dt, J=1.38, 7.64 Hz, aromatic proton), 8.35 (1H, md, J=8.05 Hz, aromatic proton). MS *m/z*: 352, 354 (M^+), 198, 200 ($M^+ - O_2NC_6H_4S$), 154 ($O_2NC_6H_4S^+$). *Anal.* Calcd for $C_{14}H_{13}BrN_2O_2S$: C, 47.60; H, 3.70; N, 7.93. Found: C, 47.90; H, 3.73; N, 7.89.

6-Bromo-1,2,3,4-tetrahydro-*N*-(2-nitrophenylthio)quinoline (**4b**): mp 146—148 °C. IR ν_{max}^{KBr} cm^{-1}: 1510 (NO_2), 1335 (NO_2). ^{1}H-NMR ($CDCl_3$) δ: 1.90—2.17 (2H, m, CH_2), 2.86 (2H, t, J=6.25 Hz, CH_2), 3.67—3.78 (2H, m, CH_2), 7.05 (1H, d, J=8.79 Hz, aromatic proton), 7.11 (1H, dd, J=2.44, 8.81 Hz, aromatic proton), 7.17 (1H, ds, J=2.22 Hz, aromatic proton), 7.28—7.34 (3H, m, aromatic protons), 8.35 (1H, d, J=8.10 Hz, aromatic proton). MS *m/z*: 364, 366 (M^+), 210, 212 ($M^+ - O_2NC_6H_4S$), 154 ($O_2NC_6H_4S^+$). *Anal.* Calcd for $C_{15}H_{13}BrN_2O_2S$: C, 49.32; H, 3.58; N, 7.66. Found: C, 49.32; H, 3.58; N, 7.59.

2′-Bromo-4′-methyl-2-nitrobenzenesulfenanilide (**5b**): mp 152—154 °C.

IR ν_{max}^{KBr} cm^{-1}: 3395 (NH), 1485 (NO_2), 1330 (NO_2). ^{1}H-NMR ($CDCl_3$) δ: 1.56 (3H, s, CH_3), 5.73 (1H, s, NH), 6.97 (1H, d, J=8.28 Hz, aromatic proton), 7.03 (1H, d, J=8.28 Hz, aromatic proton), 7.30 (1H, dt, J=1.45, 7.00 Hz, aromatic proton), 7.34 (1H, s, aromatic proton), 7.50 (1H, dd, J=1.43, 8.35 Hz, aromatic proton), 7.56 (1H, dt, J=1.42, 8.29 Hz, aromatic proton), 8.33 (1H, dd, J=1.48, 8.29 Hz, aromatic proton). MS m/z: 337, 339 (M^+), 183, 185 ($M^+ - O_2NC_6H_4S$), 154 ($O_2NC_6H_4S^+$). *Anal.* Calcd for $C_{13}H_{11}BrN_2O_2S$: C, 46.03; H, 3.26; N, 8.25. Found: C, 45.95; H, 3.05; N, 8.07.

2′-Bromo-4′-ethoxycarbonyl-2-nitrobenzenesulfenanilide (**6b**): mp 131—133 °C. IR ν_{max}^{KBr} cm^{-1}: 3475 (NH), 1710 (C=O), 1505 (NO_2), 1297 (NO_2). ^{1}H-NMR ($CDCl_3$) δ: 1.37 (3H, t, J=7.12 Hz, CH_3), 4.34 (2H, q, J=7.12 Hz, CH_2), 6.13 (1H, s, NH), 7.17 (1H, d, J=8.89 Hz, aromatic proton), 7.34 (1H, dt, J=1.26, 7.14 Hz, aromatic proton), 7.40 (1H, dd, J=1.15, 8.08 Hz, aromatic proton), 7.58 (1H, dt, J=1.34, 7.14 Hz, aromatic proton), 7.85 (1H, dd, J=1.88, 8.63 Hz, aromatic proton), 8.22 (1H, d, J=1.87 Hz, aromatic proton), 8.36 (1H, dd, J=1.39, 8.38 Hz, aromatic proton). MS m/z: 396, 398 (M^+), 242, 244 ($M^+ - O_2NC_6H_4S$), 154 ($O_2NC_6H_4S^+$). *Anal.* Calcd for $C_{15}H_{13}BrN_2O_4S$: C, 45.35; H, 3.29; N, 7.05. Found: C, 45.14; H, 3.26; N, 6.98.

2′,4′-Dibromo-2-nitrobenzenesulfenanilide (**7b**): mp 198—199 °C (recrystallized from CH_3COOEt). IR ν_{max}^{KBr} cm^{-1}: 3395 (NH), 1495 (NO_2), 1330 (NO_2). ^{1}H-NMR ($CDCl_3$) δ: 5.83 (1H, s, NH), 7.02 (1H, d, J=8.78 Hz, aromatic proton), 7.26—7.36 (2H, m, aromatic protons), 7.42 (1H, d, J=1.19, 8.30 Hz, aromatic proton), 7.58 (1H, dt, J=1.41, 7.14 Hz, aromatic proton), 7.65 (1H, d, J=2.19 Hz, aromatic proton), 8.34 (1H, dd, J=1.39, 8.30 Hz, aromatic proton). MS m/z 402, 404, 406 (M^+), 248, 250, 252 ($HN^+C_6H_3Br_2$), 154 ($O_2NC_6H_4S^+$). *Anal.* Calcd for $C_{12}H_8Br_2N_2O_2S$: C, 35.66; H, 1.99; N, 6.91. Found: C, 36.11; H, 2.06; N, 6.90.

2′,4′-Dibromo-3′-methoxy-2-nitrobenzenesulfenanilide (**8b**): mp 177—179 °C. IR ν_{max}^{KBr} cm^{-1}: 3400 (NH), 1510 (NO_2), 1340 (NO_2). ^{1}H-NMR ($CDCl_3$) δ: 3.73 (3H, s, OCH_3), 5.80 (1H, s, NH), 6.77 (1H, s, aromatic proton), 7.34 (1H, dt, J=1.34, 7.15 Hz, aromatic proton), 7.42 (1H, dd, J=1.16, 8.11 Hz, aromatic proton), 7.60 (1H, dt, J=1.42, 7.16 Hz, aromatic proton), 7.63 (1H, s, aromatic proton), 8.34 (1H, dd, J=1.16, 8.18 Hz, aromatic proton). MS m/z: 432, 434, 436 (M^+), 278, 280, 282 ($H_3CO-C_6H_3Br_2-N^+-H$), 154 ($O_2N-C_6H_4S^+$). *Anal.* Calcd for $C_{13}H_{10}Br_2N_2O_3S$: C, 35.96; H, 2.32; N, 6.45. Found: C, 36.18; H, 2.16; O, 6.44.

2′,4′-Dibromo-3′-methyl-2-nitrobenzenesulfenanilide (**9b**): mp 143—149 °C. IR ν_{max}^{KBr} cm^{-1}: 3400 (NH), 1510 (NO_2), 1335 (NO_2). ^{1}H-NMR ($CDCl_3$) δ: 1.55 (3H, s, CH_3), 5.74 (1H, s, NH), 7.03 (1H, s, aromatic proton), 7.33 (1H, dt, J=1.29, 8.24 Hz, aromatic proton), 7.44 (1H, dd, J=1.20, 8.22 Hz, aromatic proton), 7.59 (1H, dt, J=1.33, 8.34 Hz, aromatic proton), 7.65 (1H, s, aromatic proton), 8.35 (1H, dd, J=1.37, 8.35 Hz, aromatic proton). MS m/z: 415, 417, 419 (M^+), 261, 263, 265 ($M^+ - O_2NC_6H_4S$), 154 ($O_2NC_6H_4S^+$). *Anal.* Calcd for $C_{13}H_{10}Br_2N_2O_2S$: C, 37.34; H, 2.41; N, 6.70. Found: C, 37.79; H, 2.54; N, 6.76.

4′-Bromo-2′-ethoxycarbonyl-2-nitrobenzenesulfenanilide (**10b**): mp 122 °C. IR ν_{max}^{KBr} cm^{-1}: 3310 (NH), 1692 (C=O), 1510 (NO_2), 1310 (NO_2). ^{1}H-NMR ($CDCl_3$) δ: 1.45 (3H, t, J=7.12 Hz, CH_3), 4.41 (2H, q, J=7.13 Hz, CH_2), 7.17 (1H, d, J=8.96 Hz, aromatic proton), 7.30 (1H, t, J=2.19, 8.36 Hz, aromatic proton), 7.42—7.45 (2H, m, aromatic protons), 7.53 (1H, t, J=1.36, 7.05 Hz, aromatic proton), 8.11 (1H, d, J=2.41 Hz, aromatic proton), 8.33 (1H, dd, J=1.30, 8.33 Hz, aromatic proton), 9.04 (1H, s, NH). MS m/z: 396, 398 (M^+), 242, 244 ($HN^+C_6H_3BrCOOEt$), 154 ($O_2NC_6H_4S^+$).

Anal. Calcd for $C_{15}H_{13}BrN_2O_4S$: C, 45.35; H, 3.29; N, 7.05. Found: C, 45.26; H, 3.07; N, 7.02.

Determination of Products A typical example is described. An aliquot (0.2 ml) of the reaction mixture was filtered on a Columngard (Nihon Millipore Ltd.). One μl of filtrate was diluted to 20 μl with the mobile phase, MeOH–H_2O (3 : 1), and the rest of the filtrate was added to the reaction vessel. Five μl of the diluted solution was injected into a Nova-pak cartridge column. The detector was operated at 254 nm. After 1 h, NBS (365 mg, 2 mM) and K_2CO_3 (138 mg, 2 mM) were added to the solution again, and it was stirred at room temperature for 1 h. One-fifth ml of the resulting solution was treated as mentioned above.

Acknowledgment The authors wish to thank Miss H. Masunaga and Miss N. Sawashi for help with some of the experiments.

References

1) Part XII: H. Sayo, H. Hatsumura, and T. Michida, *Chem. Pharm. Bull.*, **34**, 4139 (1986).
2) *a*) H. Sayo, K. Mori, and A. Ueda, *Chem. Pharm. Bull.*, **25**, 525 (1977); *b*) H. Sayo, K. Mori, A. Ueda, and T. Michida, *ibid.*, **26**, 1682 (1978); *c*) H. Sayo, K. Mori, and T. Michida, *ibid.*, **27**, 351, (1979); *d*) *Idem*, *ibid.*, **27**, 2093 (1979); *e*) *Idem*, *ibid.*, **27**, 2316 (1979); *f*) *Idem*, *ibid.*, **29**, 2598 (1981); *g*) *Idem*, *ibid.*, **30**, 3782 (1982); *h*) H. Sayo, T. Michida, and H. Hatsumura, *ibid.*, **34**, 558 (1986); *i*) H. Sayo, H. Hatsumura, and T. Michida, *ibid.*, **34**, 4139 (1986).
3) See the following papers and references cited therein; *a*) W. Ando and T. Tsumaki, *Synthesis*, **1982**, 263; *b*) T. E. Nickson and C. A. Roche-Dolson, *ibid.*, **1985**, 669.
4) T. W. Greene, "Protective Groups in Organic Synthesis," John Wiley & Sons, Inc., New York, 1981, p. 283.
5) H. J. Dauben Jr. and L. L. McCoy, *J. Am. Chem. Soc.*, **81**, 4863 (1959).
6) *a*) R. S. Neale, R. G. Schepers, and M. R. Walsh, *J. Org. Chem.*, **29**, 3390 (1964); *b*) D. F. Paul, and P. Haberfield, *ibid.*, **41**, 3170 (1976).
7) R. H. Mitchell, Y. Lai, and R. V. Williams, *J. Org. Chem.*, **44**, 4733 (1979).

Synthesis of Diazipine and [^{3}H]Diazipine: Novel Dihydropyridines as Photoaffinity Probes of Calcium Channels

Motohiko TAKI, Akihiko KUNIYASU, Hitoshi NAKAYAMA,* and Yuichi KANAOKA

Faculty of Pharmaceutical Sciences, Hokkaido University, Sapporo 060, Japan. *Received January 21, 1991*

Diazipine and [^{3}H]diazipine were synthesized as new 1,4-dihydropyridine photoaffinity ligands containing a phenyldiazirine group. After simple high performance liquid chromatography separation, both compounds were purified in good overall yields. [^{3}H]Diazipine (21.2 Ci/mmol) was synthesized in two steps from commercially available [^{3}H]ethanolamine. Diazipine competitively inhibited [^{3}H]PN200-110 binding to the calcium channel of cardiac membranes with high affinity.

Keywords [^{3}H]diazipine; 1,4-dihydropyridine; calcium channel; photoaffinity ligand

Calcium channels are widely distributed in membrane, and are important for electrical excitability, excitation–contraction coupling, excitation–secretion coupling, and other cellular functions. A class of compounds known as 1,4-dihydropyridines (DHPs) functions either to block or activate voltage-regulated calcium channels in a variety of tissues and is, therefore, of considerable interest for both therapeutic and experimental purposes. A great number of DHPs have been developed and synthesized. DHPs are one of the most useful ligands to identify the L-type calcium channels, since they have high affinity even in broken cell preparations. DHPs bind to the alpha 1 subunit of the L-type channels.[1]

Photoaffinity labeling techniques using reagents with ligand structures have versatile roles to select and identify receptor molecules of the ligands in crude preparations, and even to locate or identify the binding sites of the ligands on the receptor molecules.[2] Azidopine is a currently employed photoreactive DHP with a nitrene precursor.[3] However, photoincorporated azidopine does not seem to be sufficiently chemically stable, and in fact, it was reported to be released to a considerable extent by reduction with dithiothreitol.[4] Such lability may hamper experiments to identify the labeled sites, for example. We have previously reported that phenyldiazirines are useful precursors to generate highly reactive carbenes which afford quite stable photoproducts.[5-7] As a extension of this line of work we report here the synthesis of novel photoactivatable dihydropyridines containing a phenyldiazirine.

A new dihydropyridine, 2-[4-(1-azi-2,2,2-trifluoroethyl)-benzoylamino]ethyl ethyl 2,6-dimethyl-4-(2-trifluoromethyl)phenyl-1,4-dihydropyridine-3,5-dicarboxylate, termed diazipine, has been synthesized as shown in Chart 1. The precursor dihydropyridine **1** is a common compound for azidopine synthesis. However, no synthetic details of **1** have been reported in the literature[8] and we prepared it by means of a conventional Hantzsch reaction[9] as described in the experimental section. Coupling of **1** with a phenyldiazirine **2** gave diazipine in good yield (80%) after high performance liquid chromatography (HPLC) purification.

In the binding experiments, diazipine competitively inhibited the [^{3}H](+)PN200-110 binding to calcium channels in cardiac membrane with an IC_{50} value of 3.81 nM (Fig. 1) or a K_i value of 1.48 nM. The binding affinity to the channel preparation was slightly lower than that of (−)azidopine (K_i = 1.05 nM), the active enantiomer of the currently used photoaffinity ligand, or of (±)PN200-110 (K_i = 0.96 nM), a typical DHP ligand, but the differences are only 1.5 times at most. Diazipine can be included in the

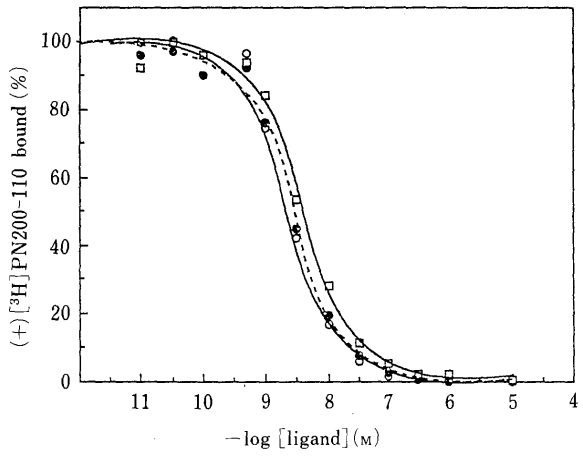

Fig. 1. Inhibition of [^{3}H](+)PN200-110 Binding by Dihydropyridines

□, diazipine; ●, (−)azidopine; ○, PN200-110. The experiment was performed by the incubation of various concentrations of each dihydropyridine with 200 μg/ml of porcine heart sarcolemma membranes and 0.17 nM [^{3}H](+)PN200-110 at 25 °C for 40 min.

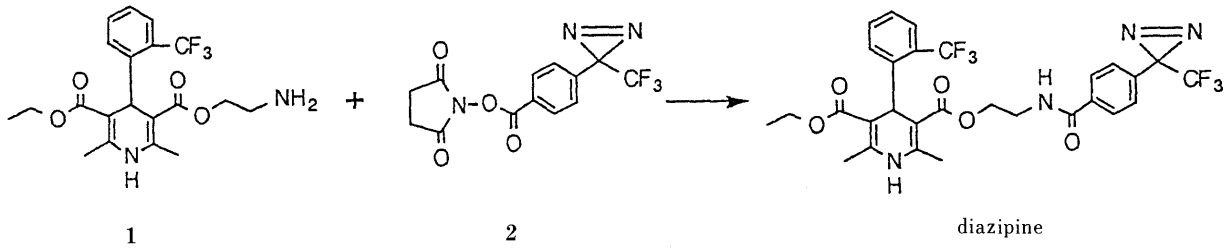

1 2 diazipine

Chart 1. Synthetic Scheme for Diazipine

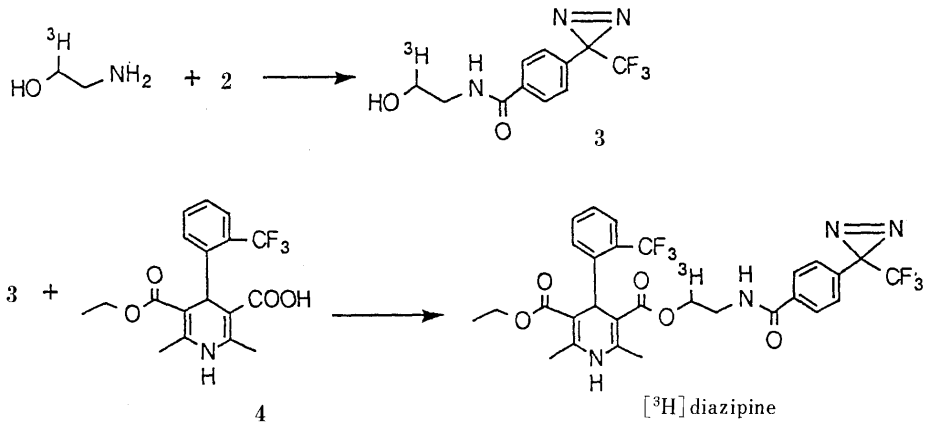

Chart 2. Synthetic Scheme for [^{3}H]Diazipine

series of DHP ligands for L-type calcium channels.

In the synthesis of [^{3}H]diazipine we used commercially available [1-^{3}H]ethan-1-ol-2-amine hydrochloride as a radioactive starting material and employed a different route than that used for the unlabeled diazipine, because as few steps as possible should be used in the synthesis of radioactive compounds. A two-step synthesis after introduction of [^{3}H]ethan-1-ol-2-amine was achieved, as shown in Chart 2. In order to optimize the radiosynthesis, all unlabeled reagents were used in 5- to 22-fold excess over the radioactive material. In the coupling of **3** with **4**, only the present method which is a modification of the described procedure[10] for this synthesis, gave a successful result. Other usual coupling methods which use acid chloride, dicyclohexylcarbodiimide, or carbonyldiimidazole, were unsuccessful. The overall yield of 40% after two reaction steps with subsequent HPLC purifications is satisfactory from a practical point of view. The specific radioactivity of 21.2 Ci/mmol is also good enough for studies on calcium channel preparations.

The above considerations, together with the result that diazipine has similarly high affinity to azidopine and PN200-110, suggest that diazipine, a novel dihydropyridine with phenyldiazirine group, will be useful for photoaffinity labeling of L-type calcium channels. An application study is under way.

Experimental

Instruments used in this study were as follows: MS, JEOL JMS-3000; proton nuclear magnetic resonance (^{1}H-NMR), JEOL JNX-FX 100, ultraviolet (UV), Hitachi UV-330, and liquid scintillation counter, Packard Tri-Carb 460C. HPLC was performed with a Waters HPLC system with two pumps (model 510) and an automated gradient controller. [^{3}H](+)PN200-110 was purchased from Amersham. (−)Azidopine was a kind gift from Prof. H. Glossmann and (±)PN200-110 was supplied by Sandoz.

Preparation of 1 2-(*N-tert*-Butyloxycarbonylamino)ethyl acetoacetate (2.45 g, 10 mmol), ethyl 3-aminocrotonate[11] (1.55 g, 12 mmol), and α,α,α-trifluoro-*o*-tolualdehyde (2.09 g, 12 mmol) were dissolved in ethanol (10 ml) and the solution was refluxed for 16 h. The solvent was evaporated off *in vacuo*, and the residue was purified by a silica-gel chromatography with benzene–ethyl acetate (2:1) as the solvent. A yellow oily material (2.59 g, 51% yield) was obtained. HRMS *m/z* Calcd for $C_{25}H_{31}F_3N_2O_6$: 512.21353. Found: 512.21062. The oil (2.56 g, 5 mmol) was dissolved in formic acid (19 ml) and the solution allowed to stand for 4 h at room temperature. After addition of water (25 ml), the aqueous solution was washed with chloroform three times. The aqueous layer was titrated to pH 11 with sodium hydroxide solution in an ice-bath followed by extraction with chloroform three times. The chloroform layer was dried over sodium sulfate, then the solvent was evaporated off *in vacuo*, and the residue was passed through an aluminum oxide column with chloroform–methanol (10:1) as the solvent to remove materials retained on top of the gel. The eluted fractions were evaporated to dryness *in vacuo* and the residue was recrystallized from benzene and *n*-hexane to give **1** as colorless prisms, 1.2 g (50% yield). mp 149.5—152.5°C, MS *m/z*: 412 (M^+). *Anal.* Calcd for $C_{20}H_{23}F_3N_2O_4$: C, 58.25; H, 5.62; N, 6.79. Found: C, 58.12; H, 5.62; N, 6.78. ^{1}H-NMR ($CDCl_3$) δ_{ppm}: 1.17 (t, 3H, J=7 Hz, C$\underline{H}_3$CH$_2$–), 1.47 (br, 2H, N$\underline{H}_2$CH$_2$–), 2.30, 2.32 (s, 6H, 2,6-dimethyl), 2.85 (t, 2H, J=5 Hz, –CH$_2$C$\underline{H}_2$NH$_2$), 3.9—4.3 (m, 4H, –COOC$\underline{H}_2$– × 2), 5.58 (s, 1H, 4-position of the dihydropyridine) 5.71 (s, 1H, –NH– at the 1-position of the dihydropyridine), 7.2—7.6 (m, 4H, $\underline{H}$-Ph × 4). UV λ_{max}^{EtOH} (ε): 355 (6100), 237 (18300).

Synthesis of Diazipine 4-(1-Azi-2,2,2-trifluoromethyl)benzoic acid *N*-hydroxysuccinimide ester (**2**)[12] (5 mg, 15 μmol) was dissolved in methylene dichloride (1 ml). Into this solution, 2-aminoethyl ethyl 2,6-dimethyl-4-(2-trifluoromethyl)phenyl-1,4-dihydropyridine-3,5-dicarboxylate **1**[8] (6.6 mg, 16 μmol) in methylene dichloride (0.2 ml) was added, and the mixture was stirred overnight at room temperature. The solvent was evaporated off *in vacuo*. The residue was dissolved in acetonitrile (0.2 ml) and 10 μl aliquots were separated by HPLC on a C18 column (Toso TSK 80TM, 4.6 × 250 mm) using CH_3OH–H_2O (4:1) as the solvent (flow rate: 0.5 ml/min). Eluates were monitored by using a UV detector at 240 nm and the peak at 15 min was collected as 2-[4-(1-azi-2,2,2-trifluoroethyl)benzoylamino]ethyl ethyl 2,6-dimethyl-4-(2-trifluoromethyl)-phenyl-1,4-dihydropyridine-3,5-dicarboxylate (termed diazipine). The overall yield of diazipine was 80%. *Anal.* Calcd for $C_{29}H_{26}F_6N_4O_5$: C, 55.77; H, 4.20; N, 8.97. Found: C, 55.58; H, 4.39; N, 8.75. MS *m/z*: 596 [$M^+ - N_2$]. UV λ_{max}^{EtOH} (ε): 356 (6330), 236 (32200).

Synthesis of [^{3}H]Diazipine Aqueous [1-^{3}H]ethan-1-ol-2-amine hydrochloride (223 nmol, 22.4 Ci/mmol from Amersham), was evaporated to dryness with a Speed-Vac (Savant) and the residue was dissolved in water (96 μl). To this, a 40 mM triethylamine solution in tetrahydrofuran (THF) (12 μl, 480 nmol), THF (190 μl), and finally a 50 mM solution of **2** in THF (22 μl, 1.1 μmol) were added and the whole was stirred for 12 h at room temperature. The reaction mixture was subjected to HPLC purification on a C18 column (Chemcosorb 7C18, 4.6 × 250 mm) with CH_3CN–H_2O (2:3) as the solvent (flow rate: 0.8 ml/min). The peak fractions eluted at 12 min was collected as the [^{3}H]ethanolamide derivative **3**. The fraction was evaporated to dryness and the residue was dried over P_2O_5 in a desiccator overnight *in vacuo*. The dry ethanolamide **3** (0.2 μmol) was dissolved in dry methylene dichloride (40 μl) and then 110 mM *N,N*-dimethylaminopyridine (40 μl, 4.4 μmol) was added to make 'solution A'. Separately, a 50 mM solution of 2,4-dinitrofluorobenzene (40 μl, 2 μmol) in dry methylene dichloride and a 50 mM solution of 2,6-dimethyl-4-(2-trifluoromethyl)phenyl-1,4-dihydropyridine-3,5-dicarboxylic acid monoethyl ester[13] (**4**) in dry methylene dichloride (40 μl, 2 μmol) was mixed to make 'solution B'. Solution B was added to solution A and the mixture was stirred for 12 h at room temperature. After evaporation of the solvent, the resultant residue was dissolved in acetonitrile (0.1 ml) and 5 μl aliquots were separated by HPLC in the same manner as described above for the unlabeled compound. A radiactive peak eluted at 15 min was collected. For further purification, pooled fractions were subjected to rechromatography under identical conditions. The overall yield of the purified [^{3}H]diazipine was 40% and its specific radioactivity was determined as

21.2 Ci/mmol, by measuring the radioactivity and absorption spectrum.

Binding Experiment Porcine heart sarcolemma membranes were prepared as described in the literature.[14] To the sarcolemma membranes (50 μg of protein) in 50 mM Tris–HCl (pH 7.4) containing 2 mM $CaCl_2$ 'binding buffer', either of diazipine, (−)azidopine, or PN200-110 (0.01 nM—10 μM) and then [^{3}H](+)PN200-110 (0.17 nM) were added, and the mixture (final volume: 250 μl) was incubated at 25 °C for 40 min. The incubation mixture was rapidly filtered through a Whatman GF/C filter on a filtration manifold (Brandel Cell Harvester M-24R) under reduced pressure, followed by rapid washing 5 times with cold binding buffer. Each of the filter disks was mixed with a scintillation cocktail and counted. Duplicate runs were performed for each data point.

Acknowledgements This work was supported by Grants-in-Aid for Scientific Research on Priority Areas (No. 01641501, No. 02250102, and No. 02257201) from the Ministry of Education, Science and Culture, and grants from the Mitsubishi Foundation and the Toray Foundation.

References and Notes

1) J. Striessnig, K. Mossburger, A. Goll, D. R. Ferry, and H. Glossmann, *Eur. J. Biochem.*, **161**, 603 (1986).
2) H. Bayley, "Photogenerated Reagents in Biochemistry and Molecular Biology," Elsevier, Amsterdam, New York, 1983
3) D. R. Ferry, M. Rombusch, A. Goll, and H. Glossmann, *FEBS Lett.*, **169**, 112 (1984).
4) P. L. Vaghy, J. Striessnig, K. Miwa, H.-G. Knaus, K. Itagaki, E. McKenna, H. Glossmann, and A. Schwartz, *J. Biol. Chem.*, **262**, 14337 (1987).
5) E. Yoshida, H. Nakayama, Y. Hatanaka, and Y. Kanaoka, *Chem. Pharm. Bull.*, **38**, 982 (1990).
6) Y. Hatanaka, E. Yoshida, H. Nakayama, and Y. Kanaoka, *Bioorg. Chem.*, **17**, 482 (1989).
7) Y. Hatanaka, E. Yoshida, H. Nakayama, and Y. Kanaoka, *FEBS Lett.*, **260**, 27 (1990).
8) The compound has been reported, but no synthetic details were given. D. R. Ferry and H. Glossmann, *Naunyn-Schmiedbergs Arch. Pharmacol.*, **325**, 186 (1984).
9) A. Hantzsch, *Justus Liebigs Ann. Chem.*, **215**, 1 (1882).
10) S. Kim and S. Yang, *Synthetic Commun.*, **11**, 121 (1981).
11) J. P. Celerier, E. Deloisy, P. Kapron, G. Lhommet, and P. Maitte, *Synthesis*, **1981**, 130.
12) M. Nassal, *Justus Liebigs Ann. Chem.*, **1983**, 1510.
13) R. B. Hargreaves, B. McLoughlin, J. Bernard, and S. D. Mills, PCT Int. Appl. WO 86 04581 [*Chem. Abstr.*, **106**, 32854*e* (1987)]; E. Wehinger and F. Bossert, Gen. Offen. 2847237 [*Chem. Abstr.*, **93**, 168138*v* (1980)].
14) L. R. Jones, H. R. Besch, Jr., J. W. Fleming, M. M. MaConnaughy, and A. M. Watanabe, *J. Biol. Chem.*, **254**, 530 (1979).

Constituents of the Roots of *Boerhaavia diffusa* L. IV.[1] Isolation and Structure Determination of Boeravinones D, E, and F

Nzunzu LAMI, Shigetoshi KADOTA, and Tohru KIKUCHI*

Research Institute for Wakan-Yaku (Oriental Medicines), Toyama Medical and Pharmaceutical University, 2630 Sugitani, Toyama 930-01, Japan. *Received January 31, 1991*

Three new rotenoids designated as boeravinones D, E, and F have been isolated from the methanol extract of the roots of *Boerhaavia diffusa* L. and their structures were determined based on spectral and chemical evidence.

Keywords *Boerhaavia diffusa*; Nyctaginaceae; 6a,12a-dehydrorotenoid; boeravinone D; boeravinone E; boeravinone F; NMR

In previous papers,[1,2] we reported the isolation and structure elucidation of three new rotenoids named boeravinones A (**4**), B (**5**), and C (**6**) and two known lignans, liriodendrin and syringaresinol mono-β-D-glucoside, from the ether extract and the methanol extract of the roots of *Boerhaavia diffusa* L., respectively. In a continuation of that work, we have recently isolated three new rotenoids, which were designated as boeravinones D (**1**), E (**2**), and F (**3**). This paper deals with the structure determination of these compounds.

Boeravinone D (**1**) is a very minor constituent obtained as an amorphous solid, and showed $[\alpha]_D$ 0° (acetone). In the electron impact mass spectrum (EI-MS) it showed the molecular ion peak at *m/z* 342 (M^+) along with fragment ion peaks at *m/z* 311 ($M^+ - OCH_3$) and 283 ($M^+ - OCH_3 - CO$) and its molecular formula was determined to be $C_{18}H_{14}O_7$ by high-resolution EI-MS measurement. The infrared (IR) spectrum of **1** revealed absorption bands at 3350 (OH), 1645 (conjugated CO), 1619 (olefin), 1597, 1510, and 1465 (phenyl) cm^{-1}, and the ultraviolet (UV) spectrum showed absorption bands at 217, 277, 301_{sh}, and 348_{sh} nm ($\log\varepsilon$: 4.49, 4.53, 4.28, and 3.71, respectively).

The proton nuclear magnetic resonance (^{1}H-NMR) spectrum of **1** showed characteristic signals assignable to 1,2,4-trisubstituted benzene protons at δ_H 7.07 (dd, J=8.5, 2.5 Hz), 7.14 (d, J=2.5 Hz), and 9.15 (d, J=8.5 Hz) and an

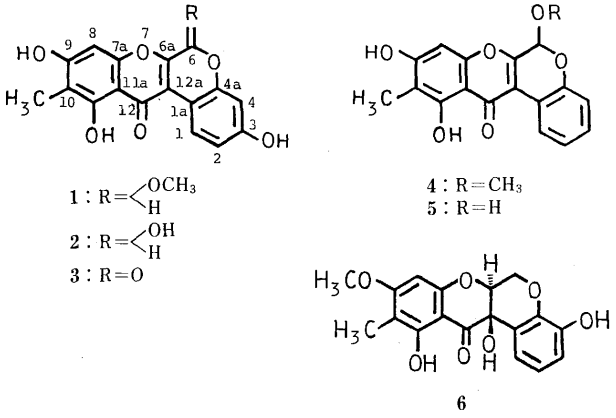

Chart 1

TABLE I. 400 MHz ^{1}H- and 100 MHz ^{13}C-NMR Data for Boeravinones D (**1**), E (**2**), F (**3**), and A (**4**) in Pyridine-d_5 (Coupling Constants in Parenthesis)

Position	1		2		3	4[a]	
	δ_H	δ_C	δ_H	δ_C	δ_H	δ_H	δ_C
1	9.15 d (8.5)	128.68 d	9.15 d (8.5)	128.60 d	9.44 d (9.0)	9.10 dd (8.0, 1.3)	127.48 d
1a	—	110.90 s	—	110.19 s	—	—	117.77 s
2	7.07 dd (8.5, 2.5)	111.11 d	7.06 dd (8.5, 2.5)	110.66 d	7.24 dd (9.0, 2.5)	7.16 ddd (8.0, 7.6, 1.3)	122.91 d
3	—	160.17 s	—	160.06 s	—	7.29 ddd (8.0, 7.6, 1.3)	129.06 d
4	7.14 d (2.5)	105.41 d	7.17 d (2.5)	105.63 d	7.12 d (2.5)	7.20 dd (8.0, 1.3)	117.48 d
4a	—	150.90 s	—	151.58 s	—	—	149.05 s
6	5.99 s	95.66 d	6.60 s	89.89 d	—	5.89 s	95.33 d
6a	—	153.11 s	—	155.27 s	—	—	154.82 s
7a	—	155.19 s	—	155.97 s	—	—	155.06 s
8	6.66 s	93.43 d	6.70 s	93.45 d	6.80 s	6.56 s	93.53 d
9	—	164.09 s	—	163.95 s	—	—	164.11 s
10	—	108.85 s	—	108.68 s	—	—	109.12 s
11	—	160.57 s	—	160.57 s	—	—	160.54 s
11a	—	105.41 s	—	105.35 s	—	—	105.32 s
12	—	180.66 s	—	180.85 s	—	—	180.40 s
12a	—	109.06 s	—	109.32 s	—	—	110.12 s
6-OMe	3.50 s	55.65 q	—	—	—	3.45 s	55.73 q
10-Me	2.47 s	8.06 q	2.47 s	8.08 q	2.44 s	2.39 s	7.92 q
11-OH	—	—	13.83 s	—	13.35 s	13.44 s	—

δ Values in ppm and coupling constants in Hz. Multiplicities of carbon signals were determined by means of the DEPT method and are indicated as s, d, t, and q. a) See reference 2*a*.

isolated benzene proton at δ_H 6.66 (s), together with signals due to a vinyl methyl group (δ_H 2.47, s) and a methoxy group (δ_H 3.50, s). The whole spectral pattern closely resembled that of boeravinone A (**4**), except for the disappearance of a signal due to the aromatic proton at the 3-position in **4** (see Table I). Also, the ^{13}C-NMR spectrum gave a pattern closely similar to that of **4**, except for the presence of six signals due to oxygenated sp^2 quaternary carbons instead of five in **4** (Table I).

In view of these spectral data and the molecular formula, the structure of boeravinone D was concluded to be 6-methoxy-3,9,11-trihydroxy-10-methyl-6a,12a-dehydrorotenoid, as represented by the formula **1**.[3]

Boeravinone E (**2**), a yellow amorphous solid, $[\alpha]_D$ 0° (acetone), showed UV and IR spectra similar to those of **1**. The positive ion fast atom bombardment mass spectrum (FAB-MS) and the negative ion FAB-MS of **2** exhibited the quasi-molecular ion peak at *m/z* 329 $[M+H]^+$ and at *m/z* 327 $[M-H]^-$, respectively, corresponding to the molecular formula $C_{17}H_{12}O_7$. The ^{1}H- and ^{13}C-NMR spectra of **2** were also very similar to those of **1**, respectively, except for the absence of signals due to the methoxy group (Table I), suggesting that **2** may be a demethyl compound of **1**.

Treatment of **2** with *p*-toluenesulfonic acid in dry methanol gave a methyl acetal, which was found to be identical with boeravinone D (**1**). Thus, the structure of boeravinone E was established to be 3,6,9,11-tetrahydroxy-10-methyl-6a,12a-dehydrorotenoid (**2**).[3]

Boeravinone F (**3**) is also a very minor component, obtained as a yellow amorphous solid. It exhibited the molecular ion peak at *m/z* 326 (M^+) in the EI-MS and its molecular formula was determined to be $C_{17}H_{10}O_7$ by high-resolution EI-MS measurement. The UV spectrum showed absorptions at 217, 265, 294, and 330 nm (log ε: 4.40, 4.05, 4.33, and 3.85, respectively), and the IR spectrum showed a carbonyl absorption band at 1721 cm^{-1},[4] besides the conjugated carbonyl band at 1646 cm^{-1}. The ^{1}H-NMR spectrum of **3** showed a pattern similar to that of boeravinone E (**2**), but it was characterized by the lack of signals assignable to acetal methine and methoxyl protons, suggesting that **3** may be the 6-oxo derivative of **2**.

Oxidation of boeravinone E (**2**) with manganese dioxide[5] afforded a lactone (**3**), which was shown to be identical with boeravinone F (**3**) by IR and ^{1}H-NMR comparisons. Thus, the structure of boeravinone F was assigned as the formula **3**.

We have isolated a total of six rotenoids from the roots of *B. diffusa*, five of which are dehydrorotenoids and one of which is a 12a-hydroxyrotenoid. These all have a methyl group at the C-10 position, in contrast to the fact that almost all known natural rotenoids contain an isoprenoid-derived substituent usually at the C-8 position and occasionally at the C-10 position.[6] Recently, Messana *et al.*[7] have reported the isolation and structure determination of two new 12a-hydroxyrotenoids, **7** and **8**, from the roots of a Brazilian plant *Boerhaavia coccinea*, which is used in traditional medicine for treatment of liver, loins, and urinary diseases. The structures of **7** and **8** closely resemble that of boeravinone C (**6**), but they have no methyl group at the C-10 position. Also, it is of interest from a chemotaxonomic viewpoint that boeravinones D (**1**), E (**2**), and F (**3**) are similar to stemonacetal (**9**), stemonal (**10**), and stemonone (**11**),[4] respectively, obtained from *Stemona collinsae* CRAIB., a plant of the family Stemonaceae which belongs to the order of Liliiflorae of Monocotyledoneae plants. The distribution of rotenoids in other Nyctaginaceae plants and their biological activities are worthy of further study.

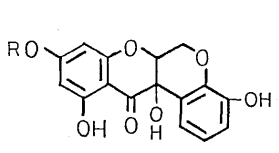

7 : R=CH_3
8 : R=H

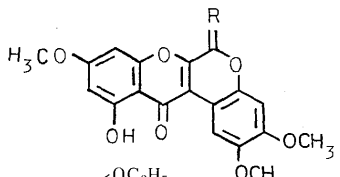

9 : R=
10 : R= 
11 : R=O

Chart 2

Experimental

UV spectra were taken with a Shimadzu 202 UV spectrometer in MeOH solutions and IR spectra with a JASCO IRA-2 or a Nicolet DX FT-IR spectrometer in KBr discs. ^{1}H- and ^{13}C-NMR spectra were taken on a JEOL JNM-GX 400 spectrometer with tetramethylsilane as an internal standard. Chemical shifts are recorded in δ values and coupling constants in hertz (Hz). Multiplicities of ^{13}C-NMR spectra were determined by means of the distortionless enhancement by polarization transfer (DEPT) method. ^{1}H–^{13}C shift correlation spectra (COSY) were obtained with the JEOL standard pulse sequence and data processing was performed with the JEOL standard software. EI-MS and high-resolution EI-MS were measured with a JEOL JMS-D 300 spectrometer (ionization voltage, 70 eV; accelerating voltage, 3 kV) using a direct inlet system, and FAB-MS was obtained with a JEOL SX-102 spectrometer (matrix: glycerol or *m*-nitrobenzyl alcohol). Preparative thin layer chromatography (TLC) was carried out on Merck Kieselgel GF_{254} plates and the plates were examined under UV light. Extraction of substances from silica gel was done with MeOH–$CHCl_3$ (3 : 7) and solutions were concentrated *in vacuo*. TLC analyses were done on Merck Kieselgel GF_{254} plates and spots were detected by the use of 1% $Ce(SO_4)_2$–aqueous H_2SO_4 (10%) reagent. For drying of organic solutions, anhydrous $MgSO_4$ was used.

Isolation of Boeravinones D (1), E (2), and F (3) As described in the preceding paper,[1] the BuOH-soluble fraction (8.5 g), obtained from the MeOH extract of the roots of *B. diffusa* L. (1.2 kg), was extracted with 1.5% HCl (100 ml)[8] at room temperature to give an insoluble material (1 g), which was separated by filtration and used in this experiment. This material was chromatographed on a column of Iatrobeads (33 g). A fraction (100 mg) eluted with MeOH–$CHCl_3$ (1 : 20) was further purified by preparative TLC with MeOH–$CHCl_3$ (1 : 20) to yield boeravinone F (**3**) (4.5 mg) from the less polar fraction and a mixture of sterol glucosides (40 mg)[9] from the more polar fraction. Another fraction (300 mg) eluted with MeOH–$CHCl_3$ (1 : 10) was also purified by preparative TLC with MeOH–$CHCl_3$ (1 : 10) to give two fractions. The less polar fraction yielded boeravinone D (**1**) (1.7 mg), while the more polar one gave boeravinone E (**2**) (12 mg).

Boeravinone D (1) Pale yellow amorphous solid, $[\alpha]_D^{27}$ 0° (*c*=0.1, acetone). IR ν_{max} cm^{-1}: 3350 (OH), 1654 (conj. CO), 1619 (C=C), 1597, 1510, 1465 (phenyl). UV λ_{max} nm (log ε): 217 (4.49), 277 (4.53), 301_{sh} (4.28), 348_{sh} (3.71). ^{1}H- and ^{13}C-NMR: Table I. EI-MS *m/z*: 342 (M^+), 311 (base peak, M^+-OCH_3), 283 (M^+-OCH_3-CO). High-resolution MS *m/z*: Found 342.0745, Calcd for $C_{18}H_{14}O_7$ (M^+) 342.0740.

Boeravinone E (2) Yellow amorphous solid, $[\alpha]_D^{27}$ 0° (*c*=0.1, acetone). IR ν_{max} cm^{-1}: 3350 (OH), 1654 (conj. CO), 1618 (C=C), 1596, 1512, 1456 (phenyl). UV λ_{max} nm (log ε): 217 (3.33), 278 (3.86), 300_{sh} (3.65), 349_{sh} (3.09). ^{1}H- and ^{13}C-NMR: Table I. Negative ion FAB-MS *m/z*: 327 $[M-H]^-$; positive ion FAB-MS *m/z*: 329 $[M+H]^+$.

Boeravinone F (3) Bright yellow amorphous solid, IR ν_{max} cm^{-1}: 3350 (OH), 1721 (lactone CO), 1646 (conj. CO), 1620 (C=C), 1589, 1510, 1465 (phenyl). UV λ_{max} nm (log ε): 217 (4.40), 265 (4.05), 294 (4.33), 330 (3.85). ^{1}H-NMR spectrum: Table I. EI-MS *m/z*: 326 (M^+) and 298 (M^+-CO). High-resolution MS *m/z*: Found 326.0400, Calcd for $C_{17}H_{10}O_7$ (M^+) 326.0426.

Boeravinone E Methyl Acetal (1) A mixture of **2** (2 mg), absolute MeOH (0.6 ml), and *p*-TsOH (0.5 mg) was refluxed for 1.5 h. After neutralization with saturated Na_2CO_3 and evaporation of MeOH, the mixture was extracted with ether. The combined ether solutions were dried and concentrated. The residue was subjected to preparative TLC with MeOH–$CHCl_3$ (1 : 10) to give a methyl acetal (**1**) (0.6 mg). This was identical with boeravinone D (**1**) by TLC, IR, and ^{1}H-NMR comparisons.

Manganese Dioxide Oxidation of Boeravinone E (2) Boeravinone E (**2**) (1.5 mg) was stirred vigorously with activated MnO_2 (12 mg) in acetone (1 ml) at room temperature for 24 h. After removal of the excess of MnO_2 by filtration, the acetone solution was evaporated *in vacuo* to leave an oil, which was purified by preparative TLC with MeOH–$CHCl_3$ (1 : 10) to give a lactone (**3**) (0.8 mg). The IR and ^{1}H-NMR of this product were superimposable upon those of boeravinone F (**3**).

Acknowledgements This work was supported in part by a Grant-in-Aid for Overseas Scientific Survey (No. 58041031) and a Grant-in-Aid for Scientific Research (No. 01571145) from the Ministry of Education, Science and Culture of Japan. We thank Mr. K. Tanaka of the National Research Institute of Police Science for the FAB-MS measurements. One of the authors (N. L.) is grateful to the Japanese Government for a scholarship.

References and Notes

1) Part III: N. Lami, S. Kadota, T. Kikuchi, and Y. Momose, *Chem. Pharm. Bull.*, **39**, 1551 (1991).
2) *a*) S. Kadota, N. Lami, Y. Tezuka, and T. Kikuchi, *Chem. Pharm. Bull.*, **37**, 3214 (1989); *b*) *Idem, ibid.*, **38**, 1558 (1990).
3) At present the possibility that **1** and/or **2** are artifacts formed during the extraction or separation procedure can not be excluded.
4) D. Shiengthong, T. Donavanik, V. Uaprasert, S. Roengsumran, and R. A. Nassy-Westropp, *Tetrahedron Lett.*, **1974**, 2015.
5) D. G. Carlson, D. Weisleder, and W. H. Tallent, *Tetrahedron*, **29**, 2731 (1973); M. E. Oberholzer, G. J. H. Rall, and D. G. Roux, *Phytochemistry*, **15**, 1283 (1976).
6) J. B. Harborne and T. J. Mabry (ed.), "The Flavonoids: Advances in Research," Chapman and Hall, London, 1982, pp. 564—576; J. B. Harborne (ed.), "The Flavonoids, Advances in Research Since 1980," Chapman and Hall, London, 1988, pp. 152—157.
7) I. Messana, F. Ferrari, and A. E. Goulart Sant'Ana, *Phytochemistry*, **25**, 2688 (1986).
8) Hydrochloric acid solution was used in order to separate effectively an alkaloidal component, which was reported to be contained in this plant by Indians workers. However, the content of the alkaloidal component was negligible. See: A. K. Nadkarni, "Dr. K. M. Nadkarni's Indian Materia Medica," Vol. I, A. K. Nadkarni Popular Prakashan Pvt. Ltd., Bombay 1976, pp. 203—205; I. G. Uasi and U. P. Kalintha, *J. Inst. Chem., Calcutta*, **51**, 214 (1979).
9) The ^{1}H-NMR spectrum of this substance was identical with that of the sample which was obtained from the ether extract and identified as a mixture of glucosides of sitosterol, stigmasterol, and campesterol. See reference 2*a*.

A Stereoselective Synthesis of (±)-Pestalotin

Toshio HONDA,* Akihiko OKUYAMA, Tomohisa HAYAKAWA, Hirotsune KONDOH, and Masayoshi TSUBUKI

Institute of Medicinal Chemistry, Hoshi University, Ebara 2–4–41, Shinagawa-ku, Tokyo 142, Japan. *Received February 1, 1991*

(±)-Pestalotin (1) was synthesized by employing a stereoselective reduction of a 5-alkyltetronate derivative (3) and a two-carbon elongation reaction of the aldehyde (13) with ethyl diazoacetate in the presence of stannous chloride as key steps.

Keywords (±)-pestalotin; tetronate; *syn*-glycol; stereoselective reduction; ethyl diazoacetate

Pestalotin (**1**) was isolated from culture filtrate of a phytopathogenic fungus, *Pestalotia cryptomeriaecola*, as an active principle showing gibberellin-synergistic activity.[1] Pestalotin has been the target of several syntheses owing to its interesting biological activity and *syn*-glycol structural feature.[2] We describe here a stereoselective synthesis of (±)-pestalotin using a catalytic reduction of a 5-alkyltetronate to construct the *syn*-glycol system as a key reaction.

Since the alkylation of tetronate has been established to afford the 5-alkylated product site-selectively,[3] methoxymethyl tetronate (**2**) was reacted with crotyl bromide in the presence of lithium cyclohexyl isopropylamide to give the desired compound (**3**) in 61% yield. In contrast, similar alkylation of **2** with *n*-butyl bromide yielded a trace amount of alkylated product. Catalytic reduction of the tetronate (**3**) over 5% rhodium on alumina under medium pressure (7 atm) of hydrogen provided the lactones (**4** and **5**) in 76 and 22% yields, respectively, where the reduction occurred predominantly from the opposite side to the substituent at the 5-position.[4]

Thus, the desired *syn*-glycol system was constructed stereoselectively, and we next attempted the conversion of **4** into (±)-pestalotin as follows.

Reduction of **4** with lithium aluminum hydride gave the diol (**6**) whose mono-silylation with *tert*-butyldimethylsilyl chloride and triethylamine afforded the silyl ether (**7**) in 78% yield from **4**. The secondary hydroxyl group of **7** was then benzylated in a usual manner with benzyl bromide and sodium hydride to give the benzyl ether, which (without

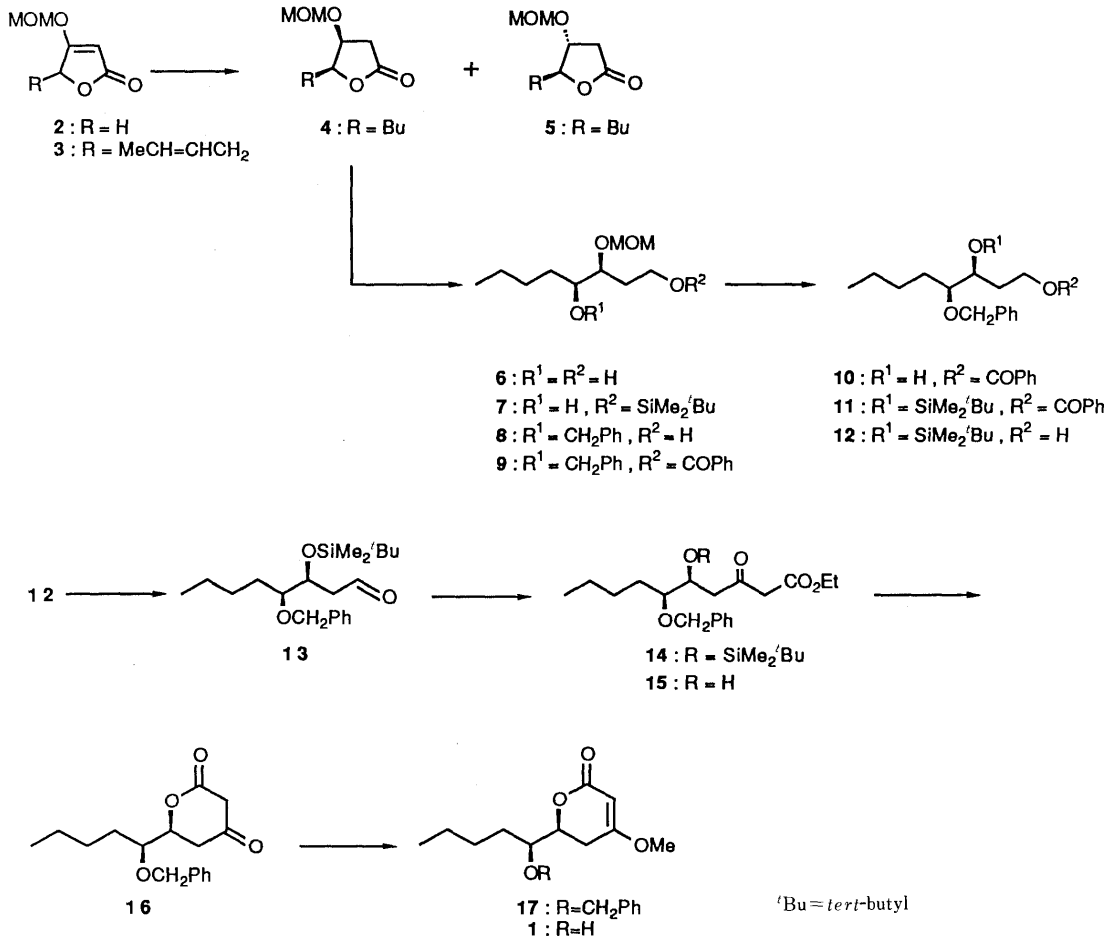

Chart 1

further purification) was subjected to desilylation with tetrabutylammonium fluoride to afford the alcohol (**8**) in 80% yield in two steps. Although we first employed **8** as a starting material, difficulties were encountered in removal of the methoxymethyl protecting group in the later stage of this synthesis. Compound **8** was, therefore, treated with benzoyl chloride in pyridine to give the benzoate (**9**), which, on treatment with aqueous hydrochloric acid, followed by silylation of the resulting alcohol (**10**) with *tert*-butyldimethylsilyl chloride and imidazole, gave the silyl ether (**11**) in 67% yield from **8**. Alkaline hydrolysis of **11** afforded the primary alcohol (**12**), which was subjected to oxidation with pyridinium chlorochromate (PCC) to provide the aldehyde (**13**). Two-carbon elongation reaction was achieved by treatment of **13** with ethyl diazoacetate in the presence of a catalytic amount of stannous chloride[5] to form the β-keto ester (**14**) in 94% yield. The silyl group of **14** was deprotected with aqueous hydrochloric acid, furnishing the alcohol (**15**), which on hydrolysis with 10% sodium hydroxide, followed by neutralization with 10% hydrochloric acid, brought about δ-lactone formation to give **16** in 72% yield from **14**. Finally, methylation of **16** with dimethyl sulfate and potassium carbonate in acetone gave benzyl pestalotin (**17**) whose spectroscopic data were identical with those reported.[2i] Since compound **17** has already been transformed into (±)-pestalotin,[2i] this synthesis constitutes a formal total synthesis of **1**.

The stereoselective reduction of a tetronate derivative yielding a *syn*-glycol system was thus applied successfully to the synthesis of (±)-pestalotin.

Experimental

Infrared (IR) spectra were measured in $CHCl_3$ solution and recorded with a Hitachi 260-10 spectrophotometer. Proton nuclear magnetic resonance (^{1}H-NMR) spectra were determined with a JEOL PMX GSX 270 spectrometer and δ values are quoted relative to tetramethylsilane. Mass spectra (MS) were measured with a JEOL JMS D300.

Methoxymethyl 5-Crotyltetronate (3) A solution of methoxymethyl tetronate (**2**) (5 g, 34.72 mmol) in dry tetrahydrofuran (THF) (10 ml) was added to a stirred solution of lithium cyclohexyl isopropylamide (1.2 eq) [prepared from cyclohexyl isopropylamine and *n*-butyllithium in dry THF (50 ml)] at −78 °C and the mixture was stirred for 2 h at −20 °C. After addition of crotyl bromide (4.46 ml, 45.09 mmol) at −78 °C, this solution was further stirred for 3 h at −20 °C. The reaction mixture was treated with aqueous NH_4Cl and extracted with $CHCl_3$. Evaporation of the solvent gave a residue, which was purified by column chromatography on silica gel using hexane–AcOEt (4 : 1) as the eluant to afford **3** (4.2 g, 61.1%) as a colorless oil. IR ($CHCl_3$) cm^{-1}: 1720, 1610. ^{1}H-NMR ($CDCl_3$) δ: 1.60 (3H, d, J=5.5 Hz, Me), 2.26—2.63 (2H, m, 6-H_2), 3.45 (3H, s, OMe), 4.74—4.81 (1H, m, 5-H), 5.09 (1H, d, J=6.1 Hz, OCH_2O), 5.11 (1H, d, J=6.1 Hz, OCH_2O), 5.30—5.38 (1H, m, 7-H), 5.50—5.61 (1H, m, 8-H). MS m/z: 198 (M^+).

(3*S,4*S**)-4-Butyl-3-methoxymethoxy-γ-butyrolactone (4) and (3*R**,4*S**)-4-Butyl-3-methoxymethoxy-γ-butyrolactone (5)** A solution of **3** (2.2 g, 11.1 mmol) in AcOEt (20 ml) containing 5% rhodium on alumina (0.45 g) was stirred under medium pressure (7 atm) of hydrogen for 4 h and an insoluble material was filtered off. The filtrate was concentrated to give a residue, which was subjected to column chromatography on silica gel. Elution with hexane–AcOEt (10 : 1) afforded **4** (1.7 g, 75.9%) as a colorless oil. IR ($CHCl_3$) cm^{-1}: 1760. ^{1}H-NMR ($CDCl_3$) δ: 0.90—1.85 (9H, m, *n*-Bu), 2.62 (1H, dd, J=1.8, 17.7 Hz, 3-H), 2.72 (1H, dd, J=4.9, 17.7 Hz, 3-H), 3.38 (3H, s, OMe), 4.33—4.47 (2H, m, 4-H, 5-H), 4.62, 4.67 (each 1H, each d, J=6.7 Hz, OCH_2O). MS m/z: 141 (M^+ − OMOM). Further elution with the same solvent gave **5** (0.51 g, 22.3%) as a colorless oil. IR ($CHCl_3$) cm^{-1}: 1765. ^{1}H-NMR ($CDCl_3$) δ: 0.90—1.69 (9H, m, *n*-Bu), 2.57 (1H, dd, J=4.3, 18.3 Hz, 3-H), 2.83 (1H, dd, J=6.7, 18.3 Hz, 3-H), 3.38 (3H, s, OMe), 4.10—4.46 (2H, m, 4-H, 5-H), 4.66 (2H, s, OCH_2O). MS m/z: 141 (M^+ − OMOM).

(3*S,4*S**)-1,4-Dihydroxy-3-methoxymethoxyoctane (6)** A solution of the lactone (**4**) (1.3 g, 6.44 mmol) in dry ether (20 ml) was added to a stirred suspension of lithium aluminum hydride in dry ether (30 ml) at 0 °C and the mixture was stirred at ambient temperature for 2 h. After quenching of the reaction by addition of 10% aqueous NaOH, the mixture was filtered through a Celite pad and the filtrate was concentrated to give a residue, which was purified by column chromatography on silica gel using hexane–AcOEt (1 : 1) as the eluant to afford **6** (1.3 g, 97.7%) as a colorless oil. IR ($CHCl_3$) cm^{-1}: 3300. ^{1}H-NMR ($CDCl_3$) δ: 0.88—1.92 (11H, m, *n*-Bu, 2-H_2), 3.41 (3H, s, OMe), 3.55—3.76 (4H, m, 1-H_2, 3-H, 4-H), 4.71 (2H, s, OCH_2O). MS m/z: 172 ($M^+ - 2\times$OH).

(3*S,4*S**)-1-*tert*-Butyldimethylsilyloxy-4-hydroxy-3-methoxymethoxyoctane (7)** A solution of **6** (2 g, 9.7 mmol), *tert*-butyldimethylsilyl chloride (1.54 g, 10.7 mmol) and triethylamine (1.49 ml, 10.7 mmol) in dry benzene (30 ml) was stirred at ambient temperature for 6 h and poured into brine. The mixture was extracted with AcOEt and the organic layer was washed with water and dried over Na_2SO_4. Evaporation of the solvent gave a residue, which was purified by column chromatography on silica gel using hexane–AcOEt (20 : 1) as the eluant to afford **7** (2.43 g, 78.3%) as a colorless oil. IR ($CHCl_3$) cm^{-1}: 3300. ^{1}H-NMR ($CDCl_3$) δ: 0.06, 0.07 (each 3H, each s, $SiMe_2$), 0.89 (9H, s, *tert*-Bu), 1.26—1.85 (11H, m, *n*-Bu, 2-H_2), 3.41 (3H, s, OMe), 3.54—3.77 (4H, m, 1-H_2, 3-H, 4-H). MS m/z: 259 (M^+ − OMOM).

(3*S,4*S**)-4-Benzyloxy-3-methoxymethoxyoctan-1-ol (8)** Sodium hydride (0.36 g, 60% oil dispersion, 9 mmol) and benzyl bromide (1.78 ml, 14.97 mmol) were added to a stirred solution of **7** (2.43 g, 7.59 mmol) in dry THF (20 ml) and the mixture was further stirred at ambient temperature for 6 h, then poured into aqueous NH_4Cl and extracted with AcOEt. The organic layer was washed with water and dried over Na_2SO_4. Evaporation of the solvent gave a residue, which was subjected to column chromatography on silica gel. Elution with hexane–AcOEt (40 : 1) gave the silyl ether (2.82 g, 90.6%) as a colorless oil, which (without further purification) was used in the next step. A mixture of the silyl ether (2.29 g, 5.59 mmol) and a 1 M solution of tetrabutylammonium fluoride (5.57 ml, 5.57 mmol) in THF was stirred at room temperature for 6 h. After evaporation of the solvent, the residue was extracted with AcOEt and the organic layer was washed with water and dried over Na_2SO_4. Evaporation of the solvent gave a residue, which was purified by column chromatography on silica gel using hexane–AcOEt (5 : 1) as the eluant to give **8** (1.80 g, 80.2%) as a colorless oil. IR ($CHCl_3$) cm^{-1}: 3300. ^{1}H-NMR ($CDCl_3$) δ: 0.86—1.92 (11H, m, *n*-Bu, 2-H_2), 2.60 (1H, br s, OH), 3.39 (3H, s, Me), 3.44—3.87 (4H, m, 1-H_2, 3-H, 4-H), 4.56, 4.61 (each 1H, each d, J=11.0 Hz, C$\underline{H}_2$Ph), 4.66, 4.72 (each 1H, each d, J=6.7 Hz, OCH_2O), 7.28—7.35 (5H, m, aromatic protons). MS m/z: 251 (M^+ − MOM).

(3*S,4*S**)-1-Benzoyloxy-4-benzyloxy-3-methoxymethoxyoctane (9)** A solution of **8** (550 mg, 1.86 mmol), benzoyl chloride (0.35 ml, 3.02 mmol) and pyridine (0.35 ml, 3.02 mmol) in THF (10 ml) was stirred at ambient temperature for 2 h and then poured into aqueous NH_4Cl. The aqueous layer was extracted with AcOEt and the organic layer was washed with aqueous $KHSO_4$ and dried over Na_2SO_4. Evaporation of the solvent gave a residue, which was subjected to column chromatography on silica gel. Elution with hexane–AcOEt (15 : 1) afforded **9** (707 mg, 95.1%) as a colorless oil. IR ($CHCl_3$) cm^{-1}: 1720. ^{1}H-NMR ($CDCl_3$) δ: 0.83—2.21 (11H, m, *n*-Bu, 2-H_2), 3.37 (3H, s, OMe), 3.49—3.91 (2H, m, 3-H, 4-H), 4.41—4.58 (2H, m, 1-H_2), 4.56, 4.61 (each 1H, each d, J=11.6 Hz, C$\underline{H}_2$Ph), 4.65, 4.71 (each 1H, each d, J=6.7 Hz, OCH_2O), 7.23—8.18 (10H, m, aromatic protons). MS m/z: 356 (M^+ − MOM).

(3*S,4*S**)-1-Benzoyloxy-4-benzyloxy-3-hydroxyoctane (10)** A solution of **9** (70 mg, 0.18 mmol) and 10% HCl in THF (5 ml) was heated at reflux for 2 h, and then diluted with AcOEt. The combined organic layer was washed with aqueous $NaHCO_3$ and dried over Na_2SO_4. Evaporation of the solvent gave a residue, which was purified by column chromatography on silica gel using hexane–AcOEt (8 : 1) as the eluant to afford **10** (51 mg, 81.9%) as a colorless oil. IR ($CHCl_3$) cm^{-1}: 1710. ^{1}H-NMR ($CDCl_3$) δ: 0.87—2.02 (11H, m, *n*-Bu and 2-H_2), 2.50 (1H, br s, OH), 3.33 (1H, dt, J=5.5, 10.5 Hz, 4-H), 3.79 (1H, m, 3-H), 4.47—4.69 (4H, m, 1-H_2, OC$\underline{H}_2$Ph), 7.25—8.04 (10H, m, aromatic protons). MS m/z: 339 (M^+ − OH).

(3*S,4*S**)-1-Benzoyloxy-4-benzyloxy-3-*tert*-butyldimethylsilyloxyoctane (11)** A solution of **10** (90 mg, 0.25 mmol), *tert*-butyldimethylsilyl chloride (114 mg, 0.76 mmol) and imidazole (52 mg, 0.76 mmol) in dry THF (5 ml) was stirred at room temperature for 6 h, then the mixture was poured into ice-cooled water and extracted with AcOEt. The extract was washed with water and dried over Na_2SO_4. Evaporation of the solvent gave a residue,

which was subjected to column chromatography on silica gel. Elution with hexane–AcOEt (30 : 1) afforded **11** (102 mg, 85.9%) as a colorless oil. IR ($CHCl_3$) cm^{-1}: 1710. ^{1}H-NMR ($CDCl_3$) δ: 0.01 (6H, s, $SiMe_2$), 0.89 (9H, s, *tert*-Bu), 0.93—2.14 (11H, m, *n*-Bu, 2-H_2), 3.37 (1H, ddd, J=2.4, 4.9, 9.2 Hz, 4-H), 4.01—4.08 (1H, m, 3-H), 4.28—4.53 (2H, m, 1-H_2), 4.55, 4.61 (each 1H, each d, J=11.6 Hz, CH_2Ph), 7.24—8.05 (10H, m, aromatic protons). MS *m/z*: 413 ($M^+ - tert$-Bu).

(3*S,4*S**)-4-Benzyloxy-3-*tert*-butyldimethylsilyloxyoctan-1-ol (12)** A solution of **11** (120 mg, 0.26 mmol) and 10% aqueous NaOH (0.5 ml) in MeOH (5 ml) was stirred at room temperature for 2 h, and then treated with water. The mixture was extracted with AcOEt and the extract was washed with water and dried over Na_2SO_4. Evaporation of the solvent gave a residue, which was purified by column chromatography on silica gel using hexane–AcOEt (9 : 1) as the eluant to afford **12** (81 mg, 86.7%) as a colorless oil. IR ($CHCl_3$) cm^{-1}: 3300. ^{1}H-NMR ($CDCl_3$) δ: 0.02, 0.05 (each 3H, each s, $SiMe_2$), 0.86—1.97 (11H, m, *n*-Bu, 2-H_2), 2.36 (1H, br s, OH), 3.33—3.39 (1H, m, 3-H), 3.71 (2H, br s, 1-H_2), 3.97 (1H, dt, J=4.3, 7.9 Hz, 4-H), 4.55, 4.61 (each 1H, each d, J=11.6 Hz, CH_2Ph), 7.28—7.35 (5H, m, aromatic protons). MS *m/z*: 309 ($M^+ - tert$-Bu).

(3*S,4*S**)-4-Benzyloxy-3-*tert*-butyldimethylsilyloxyoctanal (13)** A solution of **12** (105 mg, 0.29 mmol) in CH_2Cl_2 (10 ml) was added to a stirred suspension of PCC (180 mg, 0.84 mmol) and sodium acetate (20 mg, 0.24 mmol) in CH_2Cl_2 (70 ml) at room temperature and the mixture was further stirred for 1 h. After dilution with Et_2O, the mixture was filtered through a Celite pad to remove insoluble material and the filtrate was concentrated to give a residue, which was subjected to column chromatography on silica gel. Elution with hexane–AcOEt (20 : 1) gave **13** (95 mg, 91.0%) as a colorless oil. IR ($CHCl_3$) cm^{-1}: 1720. ^{1}H-NMR ($CDCl_3$) δ: 0.02, 0.04 (each 3H, each s, $SiMe_2$), 0.85 (9H, s, *tert*-Bu), 0.86—1.67 (9H, m, *n*-Bu), 2.49 (1H, ddd, J=2.2, 7.9, 15.8 Hz, 2-H), 2.68 (1H, ddd, J=1.8, 4.3, 15.8 Hz, 2-H), 3.32—3.38 (1H, m, 3-H), 4.39 (1H, ddd, J=3.7, 4.3, 7.9 Hz, 4-H), 4.52, 4.57 (each 1H, each d, J=11.6 Hz, CH_2Ph), 7.28—7.38 (5H, m, aromatic protons), 9.76 (1H, dd, J=1.8, 2.2 Hz, CHO). MS *m/z*: 307 ($M^+ - tert$-Bu).

Ethyl (5*S,6*S**)-6-Benzyloxy-5-*tert*-butyldimethylsilyloxy-3-oxodecanoate (14)** A solution of **13** (30 mg, 0.08 mmol) in CH_2Cl_2 (5 ml) was added dropwise to a stirred solution of ethyl diazoacetate (20 mg, 0.16 mmol) and a catalytic amount of $SnCl_2$ in CH_2Cl_2 (5 ml) at ambient temperature over a period of 10 min. The mixture was further stirred for 4 h, and then poured into aqueous NH_4Cl, and extracted with CH_2Cl_2. The extract was washed with water and dried over Na_2SO_4. Evaporation of the solvent gave a residue, which was subjected to column chromatography on silica gel. Elution with hexane–AcOEt (20 : 1) gave **14** (35 mg, 94%) as a colorless oil. IR ($CHCl_3$) cm^{-1}: 1720. ^{1}H-NMR ($CDCl_3$) δ: 0.04, 0.06 (each 3H, each s, $SiMe_2$), 0.89 (9H, s, *tert*-Bu), 0.91—1.71 (12H, m, *n*-Bu, Me), 2.66 (1H, dd, J=7.9, 15.9 Hz, 4-H), 2.81 (1H, dd, J=3.7, 15.9 Hz, 4-H), 3.33—3.38 (1H, m, 5-H), 3.47 (2H, s, 2-H_2), 4.22 (2H, q, J=7.3 Hz, OCH_2Me), 4.46—4.53 (1H, m, 6-H), 4.50, 4.62 (each 1H, each d, J=11.6 Hz, CH_2Ph), 7.30—7.41 (5H, m, aromatic protons). MS *m/z*: 393 ($M^+ - tert$-Bu).

Ethyl (5*S,6*S**)-6-Benzyloxy-5-hydroxy-3-oxodecanoate (15)** A solution of **14** (156 mg, 0.35 mmol) and 10% HCl (10 drops) in EtOH (10 ml) was stirred at room temperature for 2 h, and the mixture was extracted with an excess of CH_2Cl_2. The organic layer was washed with aqueous $NaHCO_3$ and dried over Na_2SO_4. Evaporation of the solvent gave a residue, which was purified by column chromatography on silica gel using hexane–AcOEt (5 : 1) to afford **15** (103.5 mg, 88.9%) as a colorless oil. IR ($CHCl_3$) cm^{-1}: 1720. ^{1}H-NMR ($CDCl_3$) δ: 0.91 (3H, t, J=7.3 Hz, Me), 1.24—1.71 (9H, m, Me, 3 × CH_2), 2.61—2.74 (3H, m, 4-H_2, OH), 3.32—3.45 (1H, m, 6-H), 3.51 (2H, s, 2-H_2), 4.12—4.17 (1H, m, 5-H), 4.18 (2H, q, J=7.3 Hz, OCH_2Me), 4.49, 4.63 (each 1H, each d, J=11.6 Hz, CH_2Ph), 7.26—7.39 (5H, m, aromatic protons). MS *m/z*: 318 ($M^+ - H_2O$).

(1*S,6*S**)-6-(1-Benzyloxypentyl)-3,4,5,6-tetrahydropyran-2,4-dione (16)** A 10% NaOH solution (2 ml) was added to a solution of **15** (10 mg, 0.03 mmol) in THF (5 ml) and the resulting mixture was stirred at room temperature for 2 h. After neutralization with 10% HCl, the mixture was extracted with AcOEt and the extract was washed with water and dried over Na_2SO_4. Evaporation of the solvent gave a residue, which was purified by column chromatography on silica gel using hexane–AcOEt (5 : 1) to afford **16** (7 mg, 81%) as a colorless oil. IR ($CHCl_3$) cm^{-1}: 1720. ^{1}H-NMR ($CDCl_3$) δ: 0.88—0.94 (3H, t, J=7.1 Hz, Me), 1.26—1.77 (6H, m, 3 × CH_2), 2.57 (1H, dd, J=4.3, 17.1 Hz, 5-H), 2.76 (1H, dd, J=5.5, 17.1 Hz, 5-H), 3.29, 3.34 (each 1H, each d, J=20.1 Hz, 3-H_2), 3.34—3.36 (1H, m, 7-H), 4.43, 4.58 (each 1H, each d, J=11.0 Hz, CH_2Ph), 4.62 (1H, ddd, J=4.3, 5.5, 7.9 Hz, 6-H), 7.24—7.39 (5H, m, aromatic protons). MS *m/z*: 290 (M^+). High-resolution MS Calcd for $C_{17}H_{22}O_4$ (M^+): 290.1516. Found: 290.1514.

(±)-Pestalotin Benzyl Ether (17) A solution of **16** (7 mg, 0.02 mmol), K_2CO_3, and Me_2SO_4 (3 drops) in acetone (5 ml) was stirred at room temperature for 2 h. After dilution with water, the mixture was extracted with AcOEt and the extract was washed with water and dried over Na_2SO_4. Evaporation of the solvent gave a residue, which was subjected to column chromatography on silica gel. Elution with hexane–AcOEt (2 : 1) gave **17** (6 mg, 81.9%) as a colorless oil, whose spectroscopic data were identical with those reported.[2i] IR ($CHCl_3$) cm^{-1}: 1690, 1620: ^{1}H-NMR ($CDCl_3$) δ: 0.89 (3H, t, J=7.3 Hz, Me), 1.26—1.74 (6H, m, 3 × CH_2), 2.26 (1H, dd, J=3.7, 17.1 Hz, 5-H), 2.69 (1H, ddd, J=1.8, 12.8, 17.1 Hz, 5-H), 3.59 (1H, dt, J=4.3, 8.5 Hz, 7-H), 3.74 (3H, s, OMe), 4.51 (1H, ddd, J=3.7, 4.3, 12.8 Hz, 6-H), 4.61, 4.66 (each 1H, each d, J=11.6 Hz, CH_2Ph), 5.13 (1H, d, J=1.8 Hz, 3-H), 7.26—7.35 (5H, m, aromatic protons). MS *m/z*: 304 (M^+). High-resolution MS Calcd for $C_{18}H_{24}O_4$ (M^+): 304.1673. Found: 304.1672.

References

1) Y. Kimura, K. Katagiri, and S. Tamura, *Tetrahedron Lett.*, **1971**, 3137; Y. Kimura and S. Tamura, *Agric. Biol. Chem.*, **36**, 1925 (1972); G. A. Ellestad, W. J. McGahren, and M. P. Kunstmann, *J. Org. Chem.*, **37**, 2045 (1972).
2) *a*) R. M. Carlson and A. R. Oyler, *Tetrahedron Lett.*, **1974**, 2615; *b*) D. Seebach and H. Meyer, *Angew. Chem., Int. Ed. Engl.*, **13**, 77 (1974); *c*) K. Mori, M. Oda, and M. Matsui, *Tetrahedron Lett.*, **1976**, 3137; *d*) A. Takeda, E. Amano, and S. Tsuboi, *Bull. Chem. Soc. Jpn.*, **50**, 2191 (1977); *e*) T. Izawa and T. Mukaiyama, *Chem. Lett.*, **1978**, 409; *f*) M. M. Midland and R. S. Graham, *J. Am. Chem. Soc.*, **106**, 4294 (1984); *g*) K. Mori, T. Otsuka, and M. Oda, *Tetrahedron*, **40**, 2929 (1984); *h*) Y. Masaki, K. Nagata, Y. Serizawa, and K. Kaji, *Tetrahedron Lett.*, **25**, 95 (1984); *i*) H. Hagiwara, K. Kimura, and H. Uda, *J. Chem. Soc., Chem. Commun.*, **1986**, 860.
3) A. Pelter, R. Al-Bayati, and W. Lewis, *Tetrahedron Lett.*, **23**, 353 (1982).
4) G. Stork and S. D. Rychnovsky, *J. Am. Chem. Soc.*, **109**, 1564 (1987); T. Kametani, T. Katoh, M. Tsubuki, and T. Honda, *ibid.*, **108**, 7055 (1986).
5) C. R. Holmquist and E. J. Roskamp, *J. Org. Chem.*, **54**, 3258 (1989).

Studies on the Agalwood (Jinkō). XI. Structure of Dioxan-Linked Bi-phenylethylchromone Derivative

Tenji KONISHI, Kiyoshi IWAGOE, Shiu KIYOSAWA,* and Yasuhiro FUJIWARA

Kyoto Pharmaceutical University, Nakauchi-cho, Misasagi, Yamashina-ku, Kyoto 607, Japan. *Received December 21, 1990*

New dioxan-linked bi-2-(2-phenylethyl)chromone, tentatively named AH_{21} was isolated from a pyridine extract of agalwood "Jinkō" and structurally characterized using proton and carbon-13 nuclear magnetic resonance spectra.

Keywords bi-2-(2-phenylethyl)chromone; agalwood; Aquilariaceae; dioxan-linkage; ^{1}H-NMR; ^{13}C-NMR; NOE

2-(2-Phenylethyl)chromone derivatives occur in agalwood "Jinkō" in various stages of polymerization. More recently six dimeric and four trimeric derivatives of 2-(2-phenylethyl)chromone have been found in the acetone and pyridine extracts of agalwood.[1] A new bi-2-(2-phenylethyl)chromone, AH_{21}, was isolated from the pyridine extracts of agalwood from Kalimantan.[1d]

This paper describes the characterization of the structure.

AH_{21} (**1**), white powder (mp 123—125 °C), $[\alpha]_D$ −75.2° (MeOH), in the infrared (IR) and ultraviolet (UV) spectra showed absorption maxima due to a γ-pyrone ring; 1660, 1630, 1600 cm^{-1} and 247 nm, ε=25971. It was suggested to be a bi-2-(2-phenylethyl)chromone derivative by its proton nuclear magnetic resonance (^{1}H-NMR) spectrum, which showed the presence of a pair of singlets at δ 6.07 and 6.13, and two sets of phenylethyl groups. One unit (unit A) of the dimer was considered to be agarotetrol[2] on the basis of the vicinal coupling system of four methine protons at δ 3.88, 4.30, 4.57 and 5.21 on the cyclohexene ring moiety of 5,6,7,8-tetrahydrochromone. Two hydroxy protons at δ 5.33 and 5.49 were confirmed by the saturation transfer method decreasing the signals of OH protons. The methine proton at δ 5.21 merely showed a doublet signal (J=7.9 Hz) coupled between the vicinal methine proton at δ 4.30, and it was ascribed to the C_5 position in comparison with the coupling constants of agarotetrol between 5- and 6-H. The downfield shift was considered to result from the bonding of ether at C_5 to another monomeric unit (unit B). The assignment of 5-H was also supported by the absence of the proton signal of 5-OH, which should appear in a field lower than the other hydroxylic protons at C_6, C_7 and C_8 because of the intramolecular bonding between 5-OH and 4-CO[3]; further, the carbon signal of 4-CO exhibited a chemical shift about 2 ppm upfield from that of agarotetrol in the carbon-13 nuclear magnetic resonance (^{13}C-NMR) spectrum.[1a] The double doublet methine proton at δ 4.30 was assigned to 6-H on the basis of the double-irradiation

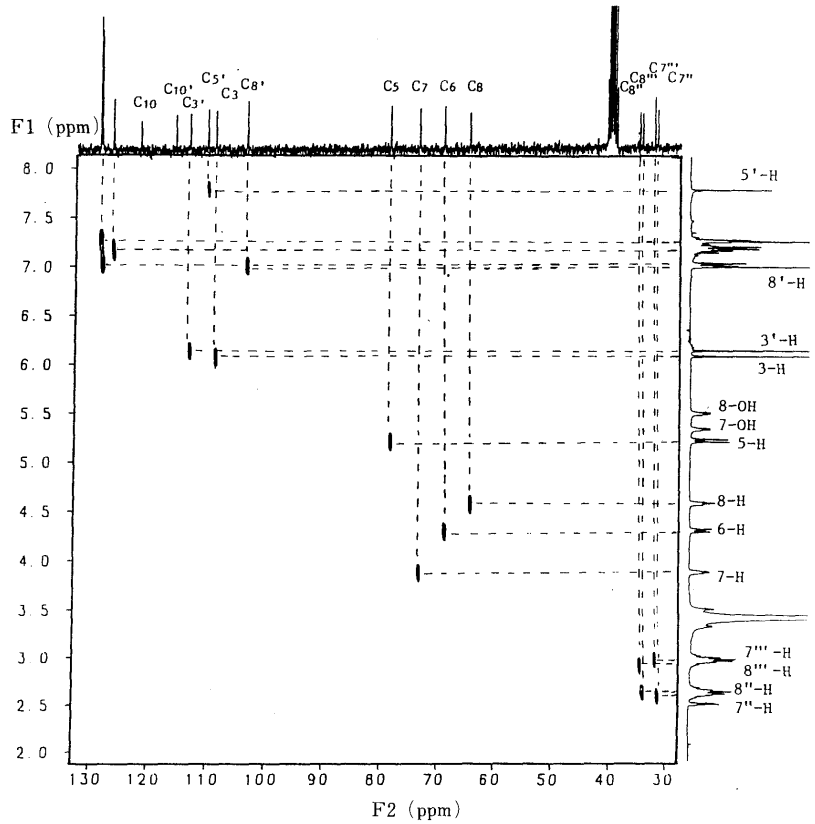

Fig. 1. ^{1}H–^{13}C Shift Correlated Spectrum AH_{21} (**1**) in DMSO-d_6

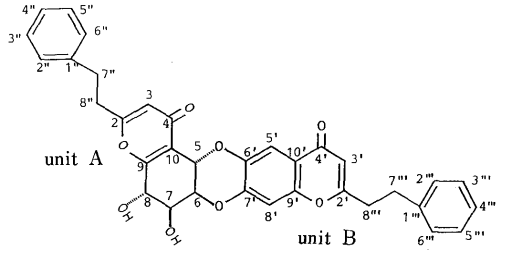

1

Chart 1

TABLE I. ^{1}H-NMR Spectral Data for AH_{21} (δ in DMSO-d_6)

	Unit A		Unit B	
5-H	5.21	(1H, d, J=7.9)	5′-H	7.78 (1H, s)
6-H	4.30	(1H, dd, J=7.9, 2.0)		
7-H	3.88	(1H, ddd, J=4.0, 3.5, 2.0)		
8-H	4.57	(1H, dd, J=4.9, 4.0)	8′-H	6.99 (1H, s)
7-OH	5.33	(1H, d, J=3.5)		
8-OH	5.49	(1H, d, J=4.9)		
3-H	6.07	(1H, s)	3′-H	6.13 (1H, s)
CH_2CH_2	2.63	(4H, m)	CH_2CH_2	2.97 (4H, m)
C_6H_5	7.00	(2H, dd, J=8.1, 1.7), 7.13, 7.78 (each 4H, m)		

TABLE II. ^{13}C-NMR Spectral Data for AH_{21} (δ in DMSO-d_6)

Carbon	Unit A	Carbon	Unit B	Carbon	Unit A	Unit B
2	167.72	2′	167.54	1″, 1‴	139.97	139.74
3	113.01	3′	108.01	2″, 6″	128.21	128.16
4	177.89	4′	175.85	2‴, 6‴		
5	78.27	5′	109.99	3″, 5″	127.97	127.97
6	68.70	6′	146.84	3‴, 6‴		
7	73.13	7′	153.70	7″, 7‴	31.52	32.01
8	64.14	8′	103.25	8″, 8‴	34.13	34.42
9	159.81	9′	152.39			
10	121.41	10′	115.40			

method between the 5-H signal, which showed the absence of the geminal coupling system with a hydroxy proton; thus the two hydroxy protons at δ 5.33 and 5.49 were ascribed to 7- and 8-OH, respectively. Subsequently, unit A was found to be agarotetrol dioxan-linked at C_5 and C_6, respectively to another monomeric unit B.

The structure of unit B was assumed to be the 6,7-dialkoxylate of 2-(2-phenylethyl)chromone because of the presence of two singlet signals of the aromatic protons at δ 7.78 and 6.99. The two protons were assigned to locations of $C_{5'}$ and $C_{8'}$ by ^{1}H and ^{13}C shift-correlated spectrum (2D-COSY) (Fig. 1, Tables I and II).[4] The two ether bonding positions between unit A and B were determined by measuring the difference in nuclear Overhauser effect (NOE) spectrum; irradiation of the 5-H at δ 5.21 caused an appreciable NOE increase of the 5′ proton signal at δ 7.78 and further showed an NOE increment of the 8′-H at δ 6.99 upon irradiation of the 6-H of unit A at 60 °C solution (Fig. 2). Therefore, it was determined that the C_5 and C_6 of unit A were linked *via* an ether bridge to $C_{6'}$ and $C_{7'}$ respectively, in unit B.

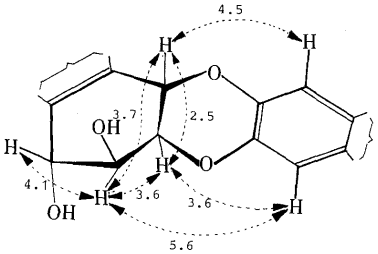

Fig. 2. NOEs of AH_{21} (1) (%)

Accordingly, AH_{21} was characterized as the dioxan-linked bi-2-(2-phenylethyl)chromone, **1**.

The polymers of 2-(2-phenylethyl)chromones isolated so far from "Jinkō" have proved to be dimers and trimers linked by ether bonds at the 5,6′-, 5,7′- or 8,6′-positions between agarotetrol or isoagarotetrol and another 2-(2-phenylethyl)chromone derivative. AH_{21} is specific as the first of a dioxan-linked biphenylethyl chromone derivative formed at the 5,6′- and 6,7′-positions between agarotetrol and 2-(2-phenylethyl)chromone.

Experimental

Isolation of AH_{21} A pyridine extract (300 g) from residue-2[4] was refluxed with MeOH to obtain a viscous extract (56.5 g) which, as a result of silica gel column chromatography ($CHCl_3$–MeOH–H_2O, 90 : 10 : 1 v/v), gave four fractions (monitored by thin layer chromatography (TLC) with detection under UV light). Fraction 1 (8.57 g) was chromatographed on silanized silica gel (MeOH–H_2O, 2 : 3 v/v) followed by silica gel ($CHCl_3$–MeOH–H_2O, 100 : 10 : 1 v/v) to give two fractions, A (543 mg) and B (1.18 g). Fraction A was subjected to column chromatography on Sephadex LH-20 (MeOH) and a silica gel (AcOEt–MeOH–H_2O, 10 : 1 : 0.1 v/v) to give three fractions, fr.$_1$ (236 mg), fr.$_2$ (190 mg) and fr.$_3$ (240 mg). Fr.$_2$ was followed with preparative high performance liquid chromatography on Lobar Rp-8 (acetonitril–H_2O, 4 : 6 v/v) an recycle preparative gel partition chromatography (column: Jaigel-310, elution: 4.0 ml/min, detection; UV) to afford AH_{21} as a white powder (14 mg) from AcOEt–MeOH.

AH_{21} (**1**): White powder (mp 123—125 °C). $[\alpha]_D$ −75.2° (c=1.09, MeOH). UV λ_{max}^{MeOH} nm (ε): 232 (28229), 247 (25971), IR (KBr) cm^{-1}: 3370 (OH), 1660, 1630, 1600 (γ-pyrone), 738, 690 (benzene ring). Field desorption mass spectrum (FD-MS) m/z: 565 $[M+H]^+$, 547 $[M+H-H_2O]^+$, 282 $[C_{17}H_{14}O_4]^+$, 192 $[C_{10}H_8O_4]^+$. ^{1}H-NMR and ^{13}C-NMR: Tables I and II.

Acknowledgement We thank Dr. K. Hashimoto, Kyoto Pharmaceutical University, for the FDMS data.

References

1) *a*) K. Iwagoe, T. Konishi, S. Kiyosawa, Y. Shimada, K. Miyahara, and T. Kawasaki, *Chem. Pharm. Bull.*, **34**, 4889 (1986); *b*) K. Iwagoe, S. Kodama, T. Konishi, S. Kiyosawa, Y. Fujiwara, and Y. Shimada, *ibid.*, **35**, 4680 (1987); *c*) K. Iwagoe, T. Kakae, T. Konishi, S. Kiyosawa, Y. Fujiwara, Y. Shimada, K. Miyahara, and T. Kawasaki, *ibid.*, **37**, 124 (1989); *d*) T. Konishi, K. Iwagoe, S. Kiyosawa, and Y. Fujiwara, *Phytochemistry*, **28**, 3548 (1989).
2) E. Yoshii, T. Koizumi, and T. Oribe, *Tetrahedron Lett.*, **41**, 3921 (1978).
3) Y. Shimada, T. Konishi, S. Kiyosawa, M. Nishi, K. Miyahara, and T. Kawasaki, *Chem. Pharm. Bull.*, **34**, 2766 (1986).
4) Y. Shimada, T. Tominaga, T. Konishi, and S. Kiyosawa, *Chem. Pharm. Bull.*, **30**, 3791 (1982).

An Additional Sweet Dihydroflavonol Glycoside from Leaves of *Engelhardtia chrysolepis*, a Chinese Folk Medicine, Huang-qi

Ryoji KASAI,*,[a] Satomi HIRONO,[a] Wen-Hua CHOU,[b] Osamu TANAKA[a] and Feng-Huai CHEN[b]

Institute of Pharmaceutical Sciences, Hiroshima University School of Medicine,[a] Kasumi, Minami-ku, Hiroshima 734, Japan and South China Institute of Botany, The Academy of Science of China,[b] Guangzhou, China. *Received January 14, 1991*

From leaves of *Engelhardtia crysolepis* HANCE (Juglandaceae), which have been used as a sweet tea in China, we have isolated a sweet dihydroflavonol glycoside, and the structure was elucidated on the basis of chemical and spectral evidence as 3-*O*-β-D-glucopyranosyl(1→3)-α-L-rhamnopyranosyl-(2*R*,3*R*)-taxifolin.

Keywords *Engelhardtia crysolepis;* Juglandaceae; Chinese folk medicine; dihydroflavonol glycoside; sweet glycoside; taxifolin glycoside; huangqioside E; neohuangqioside E; huang-qi

The leaves of *Engelhardtia crysolepis* HANCE (Juglandaceae) have been used as a sweet tea called huang-qi in China. In a preceding paper,[1] we reported on the isolation of neoastilbin (3-*O*-α-L-rhamnosyl-(2*S*,3*S*)-taxifolin, **1**) as a sweet principle of the leaves together with three non-sweet isomers of **1**, astilbin (**2**), neoisoastilbin (**3**) and isoastilbin (**4**). In further investigation of the sweet principle of the leaves, we isolated an additional new sweet dihydroflavonol glycoside (**5**) named huangqioside E. This paper deals with the structural elucidation and isomerization of **5**.

A methanolic extract of the leaves was defatted with ether and then repeatedly chromatographed to give a sweet compound (**5**) as colorless needls in a yield of 0.036%, $[\alpha]_D^{25}$ −20° (*c*=0.2, EtOH).

The ^{1}H- and ^{13}C-nuclear magnetic resonance (^{1}H- and ^{13}C-NMR) spectra revealed that **5** was a taxifolin glycoside having two monosaccharide units. Compound **5** afforded D-glucose and L-rhamnose after acid hydrolysis.[2] The circular dichroism (CD) spectrum of **5** showed almost the same curve to that of **2**, demonstrating that the aglycone of **5** is (2*R*,3*R*)-taxifolin (**6**). In a comparison of the ^{13}C-NMR spectrum of **5** with that of **6**, a glycosylation shift was observed at C-2, -3, -4 of the aglycone moiety of **5**,[3] indicating that **5** was a 3-*O*-glycosylated compound of **6**. The structure of the sugar moiety was determined as follows. The assignment of the proton signals due to the sugar moiety of **5** was performed by means of ^{1}H–^{1}H two dimensional correlation spectroscopy (2D COSY). In the two dimensional nuclear Overhauser effect (NOE) correlation spectroscopy (2D NOESY) spectrum of **5**, the cross peaks were observed between the H-3 of the aglycone moiety and the H-1 of the rhamnoside moiety as well as between the H-3 of the rhamnoside moiety and the H-1 of the glucoside moiety. The anomeric configuration of each sugar unit was elucidated by ^{1}H- and ^{13}C-NMR spectroscopy. Based on these results, **5** was formulated as 3-*O*-β-D-glucopyranosyl(1→3)-α-L-rhamnopyranosyl-(2*R*,3*R*)-taxifolin.

It is well known that dihydroflavonols are readily isomerized even under mild conditions to afford a mixture of stereoisomers arising from asymmetry at 2- and 3-positions. Tominaga has already reported on the formation of **1**, **3** and **4** from **2** by the isomerization reaction with mild alkaline conditions.[4] As shown in Table II, **5** afforded an equilibrium mixture of two isomers, **5** and **7**, but could not detect two other isomers, according to the method of Tominaga.[4] It was revealed that of these conditions, the heating of **5** in 10% pyridine–water was the most optimal condition for the formation of **7**. Compound **7** was isolated by high-performance liquid chromatography (HPLC) from the reaction mixture, and it was found that this isomerized compound, **7**, also tastes sweet. In the ^{1}H-NMR spectrum of **7**, the signals assignable to the H-2 and H-3 of the aglycone moiety appeared as doublets with J=11.2 Hz, showing that H-2 and H-3 are in the *trans* relationship, and the signals for H-2 of aglycone and H-6 of the rhamnosyl moiety are shifted upfield from those of **5**. On going from **5** to **7**, the ^{13}C-NMR signals due to C-3 and -4 were shifted, while other signals remained almost unshifted. Further, **7** exhibited a CD curve which is

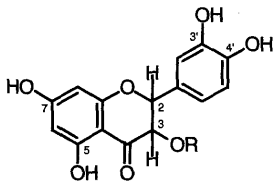

	R
1: (2*S*,3*S*)	-Rha
2: (2*R*,3*R*)	-Rha
3: (2*R*,3*S*)	-Rha
4: (2*S*,3*R*)	-Rha
5: (2*R*,3*R*)	-Rha^3–Glc
6: (2*R*,3*R*)	-H
7: (2*S*,3*S*)	-Rha^3–Glc

Rha: α-L-rhamnopyranosyl
Glc: β-D-glucopyranosyl

Chart 1

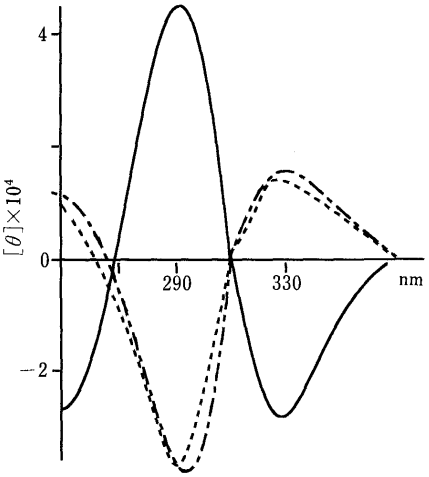

Fig. 1. CD Spectra of **2**, **5** and **7** in MeOH
——, **7**; – – –, **5**; – – –, **2**.

TABLE I. ^{13}C Chemical Shifts of **5**, **6** and **7** (in Acetone-d_6+D_2O)

Carbon No.	5	7	6
Aglycone moiety			
2	83.2	83.0	84.1
3	78.1	75.7	72.7
4	195.7	197.5	197.7
5	164.7	164.8	164.2
6	97.1	97.2	97.1
7	168.1	168.3	167.8
8	96.1	96.1	96.1
9	163.6	163.8	163.6
10	102.0	101.7	101.3
1′	128.6	129.4	129.1
2′	115.4	115.5	116.1
3′	145.8	146.1	145.4
4′	146.7	146.9	146.3
5′	116.3	116.1	115.8
6′	120.0	120.3	120.7
Rhamnosyl moiety			
1	101.5	101.9	
2	70.2[a]	70.6	
3	82.5	82.2	
4	70.4[a]	70.6	
5	69.8	69.5	
6	18.0	18.0	
Glucosyl moiety			
1	105.0	105.0	
2	74.6	74.9	
3	76.8[b]	77.0[a]	
4	71.6	71.5	
5	77.0[b]	77.3[a]	
6	61.7	62.0	

a, *b*) These assignments may be interchanged in each column.

TABLE II. Isomerization of **5**

Condition	5	7
10% pyridine–H_2O[a]	44.0%	56.0%
1% AcONa–EtOH[b]	97.8%	2.2%
H_2O[c]	95.0%	5.0%

a) See experimental. *b*) At room temperature. *c*) Heated at 90 °C.

antipodal to that of **5** as shown in Fig. 1. Based on these results, **7** can be formulated as 3-*O*-*β*-D-glucopyranosyl-(1→3)-α-L-rhamnopyranosyl-(2*S*,3*S*)-taxifolin. The name neohuangqioside E is proposed for **7**.

It has already been observed[1] that in the case of 3-*O*-α-rhamnosides of taxifolin, only the glycoside of the (2*S*,3*S*)-isomer (neoastilbin) is sweet and those of other stereoisomers are all tasteless. It is noteworthy that in the case of 3-*O*-(glucosyl-rhamnosides) of the present study, glycosides of both (2*S*,3*S*)- and (2*R*,3*R*)-isomers are found to taste sweet.

Experimental

The melting point was determined on a Yanaco micro hot stage and is uncorrected. NMR spectra were recorded on a JEOL JNM GX-400 instrument using tetramethylsilane (TMS) as an internal standard. Optical rotations were measured with a Union PM-101 automatic digital polarimeter. CD curves were taken on a JASCO J-40A spectropolarimeter. For gas liquid chromatography (GLC), a Shimadzu GC-8A apparatus was used. HPLC was carried out on a column of TSK-gel ODS-120T (7.8 mm × 30 cm) with a Tosoh HLC 803D pump and a Tosoh UV-8 model II spectrophotometer as a detector.

Extraction and Separation of 5 The leaves of *Engelhardtia chrysolepis* (1 kg) which were collected at Gaoyiao-Xian, Guangdon, China, and dried at room temperature, were extracted with hot MeOH. The MeOH extract (253 g) was defatted with Et_2O and chromatographed on a highly porous synthetic polymer (Diaion HP-20, Mitsubishi Chem. Ind. Co., Ltd) with H_2O, 50% MeOH, MeOH and Me_2CO, successively. The fraction eluted with 50% MeOH (93 g) was dissolved in H_2O, and insoluble substances were filtered off. The H_2O-soluble fraction (53.7 g) was chromatographed on a column of silica gel with $CHCl_3$–MeOH–H_2O (80:16:1, homogeneous), affording eight fractions (frs. 1—8), in increasing order of polarity. Fraction 6 was further chromatographed on a column of silica gel with $CHCl_3$–MeOH–H_2O (30:10:1, homogeneous) and then purified by HPLC [mobile phase, 20% CH_3CN–H_2O (containing 0.05% of trifluoroacetic acid, TFA); flow rate, 6 ml/min; detection, UV 254 nm], affording **5** in a yield of 0.036% from dried leaves.

Compound **5**: Colorless needles (from MeOH–H_2O), mp 229—231 °C, $[\alpha]_D^{25}$ −20° (*c*=0.2, EtOH). *Anal.* Calcd for $C_{27}H_{32}O_{16}\cdot 2H_2O$: C, 50.0; H, 5.60. Found: C, 50.26; H, 5.32. ^1H-NMR (acetone-d_6–D_2O) δ: 1.19 (3H, d, *J*=6.2 Hz, Rha H-6), 3.32 (1H, dd, *J*=7.7, 9.4 Hz, Glc H-2), 3.43 (1H, m, Glc H-5), 3.44 (1H, m, Glc H-4), 3.51 (1H, dd, *J*=9.4, 9.8 Hz, Glc H-3), 3.54 (1H, dd, *J*=9.5, 9.6 Hz, Rha H-4), 3.74 (1H, dd, *J*=4.2, 12.1 Hz, Glc H-6), 3.77 (1H, dd, *J*=3.3, 9.5 Hz, Rha H-3), 3.84 (1H, dd, *J*=1.7, 3.3 Hz, Rha H-2), 3.89 (1H, dd, *J*=2.0, 12.1 Hz, Glc H-6), 4.14 (1H, d, *J*=1.7 Hz, Rha H-1), 4.24 (1H, m, Rha H-5), 4.52 (1H, d, *J*=7.7 Hz, Glc H-1), 4.64 (1H, d, *J*=10.6 Hz, H-3), 5.16 (1H, d, *J*=10.6 Hz, H-2), 5.99 (1H, d, *J*=2.0 Hz, H-8), 6.01 (1H, d, *J*=2.0 Hz, H-6), 6.93 (1H, br s, H-5′), 6.93 (1H, br s, H-6′), 7.06 (1H, s, H-2′). ^{13}C-NMR data are given in Table I.

Acid hydrolysis of **5** followed by identification of the resulting monosaccharides were carried out as described in the previous paper.[2]

Isomerization of 5 and Isolation of 7 A solution of **5** (59 mg) in C_5H_5N–H_2O (1:9, 10 ml) was heated at 75 °C for 3.5 h, according to the method reported by Tominaga.[4] The equilibrium mixture was diluted with H_2O and then extracted with *n*-BuOH. The BuOH layer was concentrated to dryness. The residue was purified by HPLC (mobile phase, 20% CH_3CN–0.05% TFA; flow rate, 6 ml/min; detection, UV 254 nm) to give **7** (4.2 mg).

Compound **7**: A white powder, $[\alpha]_D^{18}$ −103° (*c*=0.21, EtOH). HR-FAB-MS *m/z* $(M+H)^+$: Calcd for $C_{27}H_{33}O_{16}$ 613.1769. Found: 613.1758. ^1H-NMR (acetone-d_6–D_2O) δ: 0.91 (3H, d, *J*=6.3 Hz, Rha H-6), 4.13 (1H, d, *J*=1.5 Hz, Rha-1), 4.54 (1H, d, *J*=7.9 Hz, Glc H-1), 4.70 (1H, d, *J*=11.2 Hz, H-3), 5.09 (1H, d, *J*=11.2 Hz, H-2), 5.97 (1H, d, *J*=2.0 Hz, H-8), 6.01 (1H, d, *J*=2.0 Hz, H-6), 6.91 (1H, br s, H-5′), 6.91 (1H, br s, H-6′), 7.07 (1H, s, H-2′). ^{13}C-NMR data are given in Table I.

Acknowledgments We are grateful to Dr. K. Harada, Faculty of Pharmaceutical Sciences, Meijyo University, for measurement of CD spectra. This study was financially supported by a Grant-in-Aid for Scientific Research (to R. Kasai, No. 02670955, 1990-1991) from the Ministry of Education, Science and Culture of Japan.

References

1) R. Kasai, S. Hirono, W.-H. Chou, O. Tanaka and F.-H. Chen, *Chem. Pharm. Bull.*, **36**, 4167 (1988).
2) K. Mizutani, K. Ohtani, J.-X. Wei, R. Kasai and O. Tanaka, *Planta Medica*, **1984**, 327.
3) R. Kasai, M. Suzuo, J. Asakawa and O. Tanaka, *Tetrahedron Lett.*, **1977**, 175.
4) T. Tominaga, *Yakugaku Zasshi*, **80**, 1202 (1960).

Studies on the Constituents of the Seeds of *Hernandia ovigera* L. IX.[1] Identification of Two Dibenzylbutyrolactone-Type Lignans and an Attempt of Conversion into Phenyltetralin-Type Lignan

Mariko TANOGUCHI, Etsuko HOSONO, Mayuko KITAOKA, Masao ARIMOTO and Hideo YAMAGUCHI*

Osaka University of Pharmaceutical Sciences, 2-10-65, Kawai, Matsubara, Osaka 580, Japan. *Received January 21, 1991*

Two kinds of lignans were isolated from the seeds of *Hernandia ovigera* L. in addition to the nine lignans previously reported. One was confirmed as (−)-dimethylmatairesinol (11) and the other was identified as 5′-methoxypodorhizol (14) by comparison with the authentic sample. An attempt at the cyclization of 14 afforded two compounds which were determined to be isohernandin (15) and an isomer of 15, 2-hydroxymethyl-5,6-methylenedioxy-7-methoxy-4-(3′,4′,5′-trimethoxyphenyl)-1,2,3,4-tetrahydronaphthoic acid lactone (16).

Keywords *Hernandia ovigera*; dimethylmatairesinol; 5′-methoxypodorhizol; lignan; isohernandin; phenyltetralin lignan

In the previous series of this study, the authors reported the isolation and structural determination of nine sorts of lignans from the seeds of *Hernandia ovigera* L. collected in Okinawa. Namely, desoxypodophyllotoxin (DPT) (**1**),[2] desoxypicropodophyllin (DPP) (**2**),[2] and hernandin (**3**)[3] as phenyltetralin-type lignans, bursehernin (**4**),[2] podorhizol (**5**),[2] (−)-yatein (**6**),[4] and hernolactone (**7**)[4] as dibenzylbutyrolactone-type lignans and 1,2,3,4-dehydro-DPT (**8**)[3] and 1,2,3,4-dehydropodophyllotoxin (**9**)[4] as phenylnaphthalene-type lignans were isolated, and their structures were clarified.

This time we reexamined the components of the original seeds and isolated two more known lignans. This paper describes the identification of these two lignans and the chemical transformation of a phenyltetralin-type lignan into one of them.

Compound A was isolated from the mother liquor, from which (−)-yatein (**6**) was afforded[4] by using preparative thin layer chromatography (PTLC). It was obtained as colorless needles, mp 123—125 °C, with an optical rotation of $[\alpha]_D$ −24.8° ($CHCl_3$). A molecular formula of $C_{22}H_{26}O_6$ and a molecular weight 386.1728 were deduced by means of high resolution mass spectrometry (HI-MS). In the mass spectrum (MS), fragment peaks were seen at 208, 177, 151, and 107. Fragment peak 208 corresponds to fragment ion (**10**) which is similar to that of **4**[2] (Fig. 2). In the ultraviolet (UV) spectrum, absorption maxima were observed at 281 and 230 nm. In the infrared (IR) spectrum, the existence of a carbonyl group was observed at 1770 cm^{-1}. Proton magnetic resonance (^{1}H-NMR) spectrum revealed the presence of six aromatic protons, two protons of lactone methylene, twelve protons of four methoxy groups, four protons of two benzyl methylenes and two protons of lactone junctions. This physical data coincides with that of (−)-dimethylmatairesinol (**11**) isolated from *Cinnamonium camphola* SIEB.[5] Direct comparison with the authentic sample was unavailable; however, additional confirmation was pursued by means of a circular dichroism (CD) spectrum. The CD spectrum showed negative Cotton effects at 233 an 276 nm as in the cases of **4**, **5**, **7**, and analogous compounds,[6] suggesting that the configurations of C-2 and C-3 are 2*R* and 3*R*. In conclusion, compound A was confirmed as (−)-dimethylmatairesinol (**11**).

Compound B was isolated from fraction 6-4 described in the previous paper.[4] Fraction 6-4 was purified by means of PTLC, followed by recrystallization from benzene–hexane. It was obtained as colorless needles, mp 127—129 °C, $[\alpha]_D$ −49.1° ($CHCl_3$). Its molecular formula of $C_{23}H_{26}O_9$ and molecular weight of 446.1583 were deduced by means of HI-MS. In the UV spectrum, absorption maxima were seen at 235 and 281 nm. In the IR spectrum, the existence of a hydroxy group, carbonyl group, and methylenedioxy group were seen at 3450, 1760, and 935 cm^{-1}, respectively. ^{1}H-NMR spectrum showed the presence of four aromatic protons, two methylenedioxy group protons, a proton of the hydroxy group junction, two lactone methylene protons,

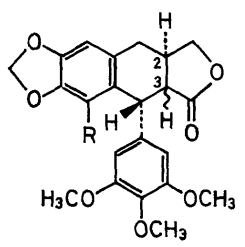

1: desoxypodophyllotoxin(DPT)
R=H, C_3-βH

2: desoxypicropodophyllin(DPP)
R=H, C_3-αH

3: hernandin
R=OCH_3, C_3-βH

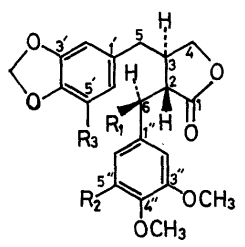

4: bursehernin
R_1=R_2=R_3=H,

5: podorhizol
R_1=OH, R_2=OCH_3, R_3=H

6: (-)-yatein
R_1=H, R_2=R_3=OCH_3

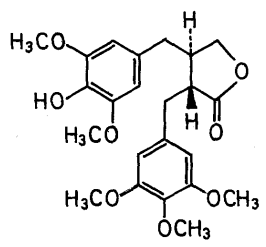

7: hernolactone

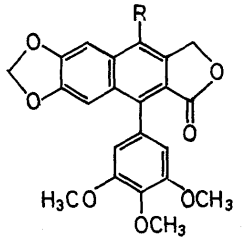

8: 1,2,3,4-dehydro-DPT
R=H

9: 1,2,3,4-dehydropodophyllotoxin
R=OH

Fig. 1

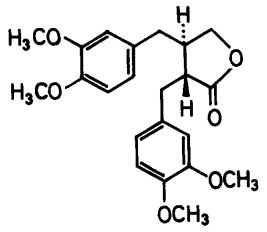

11: (-)-dimethylmatairesinol

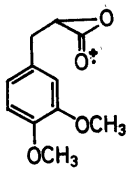

10: m/z 208

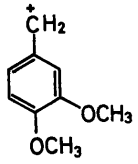

m/z 151

fragment ion of **11**

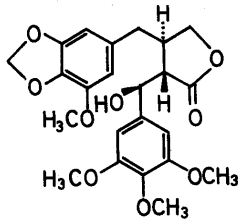

14: 5′-methoxypodorhizol

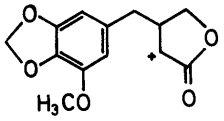

12: m/z 249

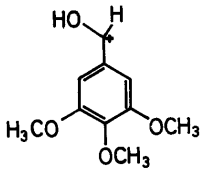

13: m/z 197

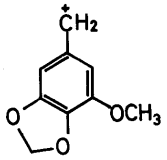

m/z 165

fragment ion of **14**

Fig. 2

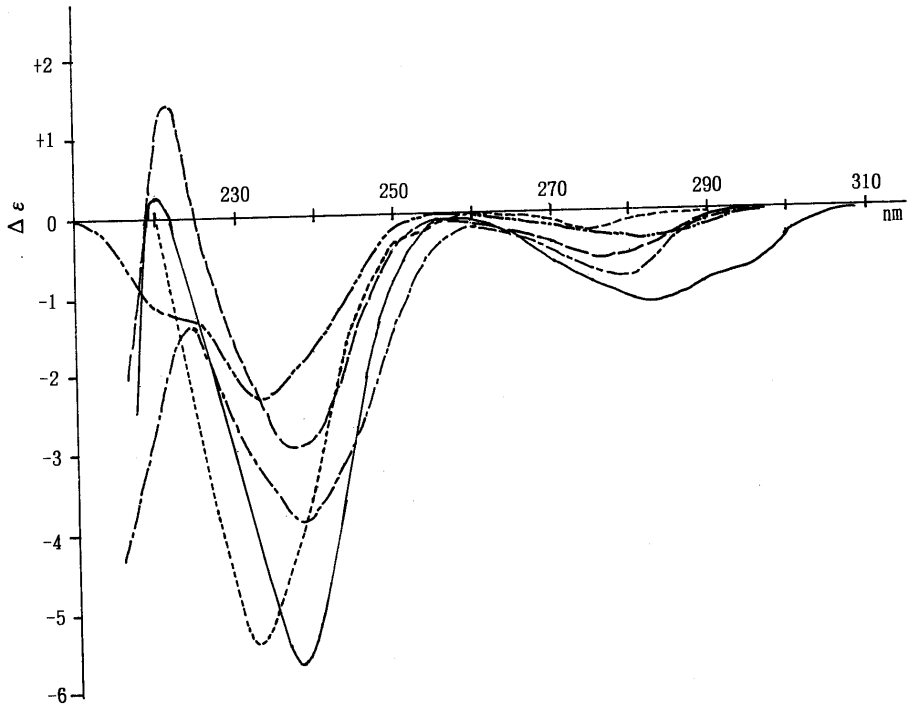

Chart 1. CD Curves of Dibenzylbutyrolactone in EtOH

------, compound A; — - —, compound B; ——, podorhizol (**5**); — - - —, bursehernin (**4**); — —, hernolactone (**7**).

twelve protons of four methoxy groups, two protons of benzyl methylene, and a hydroxy group which disappeared after the addition of D_2O. In the MS spectrum, ion peaks at 249 and 197 were assigned as fragment ions **12** and **13** (Fig. 2), respectively, revealing that one methoxy group existed in the same benzene nucleus together with the methylenedioxy group. The fact that two aromatic protons which have small J values appear at δ 6.03 (d, $J=1.5$ Hz) and δ 5.97 (d, $J=1.5$ Hz) in the NMR spectrum shows that a methoxy group is situated at the 5′ position. The CD spectrum shows negative Cotton effects at 238 and 280 nm, as in the cases of **4**, **5**, **7** and **11**, revealing that the configurations of C-2 and C-3 are 2*S* and 3*R*. Regarding the configuration of C-6, it was known that a proton of C-6 appeared at δ 5.28 ($J=2.0$ Hz) in **5** (C-6*S*) and δ 4.83 ($J=7.5$ Hz) in epipodorhizol (C-6*R*).[7] In this compound, a C-6 proton appears at δ 5.28 ($J=3.0$ Hz), revealing that the configuration of C-6 is *S*. From the above results, compound B was determined to be 5′-methoxypodorhizol (**14**) isolated from *Hernandia cordigera*.[8] However, a small

discrepancy was seen in the physical data of both compounds (lit.[8] mp 112—113 °C, $[\alpha]_D$ −20.5° ($CHCl_3$)). To clarify this ambiguity, direct comparison with the authentic sample, which was given through the generosity of Dr. P. Richomme, was examined by means of NMR spectra. Although the presented sample was low grade and a few ambiguous signals due to the impurity were observed in the spectrum, all essential absorptions to support the identity of both samples were confirmed.

It was expected that hernandin (**3**), a phenyltetralin-type lignan formerly isolated from the original seeds,[3] would be derived from **14** by cyclization. According to the Stevenson's method,[9] compound **14** was treated with excess trifluoroacetic acid in dichloromethane for 12 h at room temperature. As a result, two compounds, **15** and **16**, which had melting points of 180—182 °C and 204—206 °C respectively, were isolated by means of PTLC using the mixture of benzene, chloroform, and ethyl acetate (2 : 1 : 1). Both compounds showed the same molecular weight of 428 by means of MS spectra. The CD spectra showed a positive Cotton effect at 272 and 286 nm in **15** and 270 and 286 nm in **16**, contrary to that of **3**. In the NMR spectrum of **15**, a methylenedioxy group appeared at δ 5.90 and 5.91, similar to **3** (δ 5.92, 5.94). However, a methoxy group in the tetralin ring which was observed at δ 3.63 in **3** was revealed at a slightly higher magnetic field (δ 3.30), and a proton reduced to C-4 appeared at a higher magnetic field which had a larger J value (δ 4.33, J=9.4 Hz) than that of **3** (δ 4.81, J=4.8 Hz[10]). In the NMR spectrum of **16**, a proton of C-4 appeared at a higher magnetic field than that of **3**, similar to the case of **15** having a large J value (δ 4.24, J=10.3 Hz). However, the aspect of methylenedioxy and methoxy groups in the tetralin ring are different from those of **3** and **15**. Namely, the signal of the methylenedioxy group appeared at a higher magnetic field than those of **3** and **15** (δ 5.77, 5.66), and by contrast, the signal of methoxy group was revealed at a lower magnetic field than those of **3** and **15** (δ 3.91). The above results suggest that the configuration of C-4 of both **15** and **16** is 4β-aryl. In conclusion, compound **15** is isohernandin, 2-hydroxymethyl-5-methoxy-6,7-methylenedioxy-4-(3′,4′,5′-trimethoxyphenyl)-1,2,3,4-tetrahydronaphthoic acid lactone, and compound **16** is 2-hydroxymethyl-5,6-methylenedioxy-7-methoxy-4-(3′,4′,5′-trimethoxyphenyl)-1,2,3,4-tetrahydronaphthoic acid lactone, a positional isomer of **15** in relation to methylenedioxy and methoxy groups. The measurement of specific rotation was unattainable due to their small quantity.

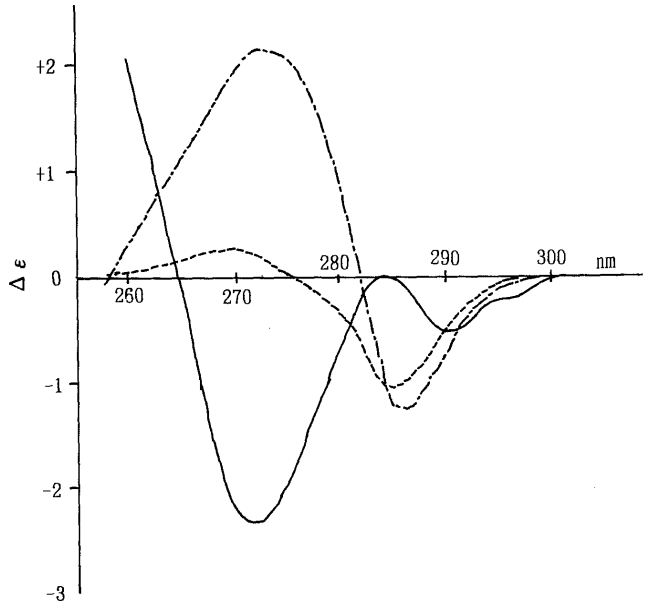

Chart 2. CD Curves of 4-Aryltetralin Lignan in EtOH
——, hernandin (**3**); — · —, compound **15**; ------, compound **16**.

Experimental

All melting points were determined on a Yanaco micro melting point apparatus and are uncorrected. IR spectra were taken with a Jasco infrared spectrometer, model IR-810. ^1H and ^{13}C-NMR spectra were measured with Varian XL-300 or with Varian Gemini-200 spectrometers. Chemical shift values are expressed in ppm relative to internal tetramethylsilane. Abbreviations are as follows: s, singlet; d, doublet; t, triplet; m, multiplet. MS spectra were taken with a Hitachi M-80 mass spectrometer. CD spectra were taken with a Jasco J-500 polarimeter. Optical rotations were measured on a Jasco DIP-181 polarimeter. Column chromatography was carried out on Merck silica gel (Kieselgel 60; 70—230 mesh). Precoated silica gel plates used in PTLC were Merck Kieselgel 60 F_{254} of 0.5 mm thickness.

Isolation Compound A was isolated from the mother liquor from which (−)-yatein (**6**) was separated as described in the previous report.[4] The residue of the mother liquor was subjected to PTLC (solvent; hexane : ethyl acetate = 5 : 1) and rechromatographed on PTLC (solvent; hexane : acetone = 3 : 1) to afford a crystalline material as colorless needles, mp 123—125 °C (from MeOH). Compound B was isolated from fraction 6-4 of the previous report.[4] Fraction 6-4 was purified by means of PTLC (solvent; hexane : ethyl acetate = 1 : 1) to afford a crystalline material as colorless needles, mp 127—129 °C (from benzene–hexane).

(−)-Dimethylmatairesinol (11) Colorless needles, mp 123—125 °C (from MeOH) (lit.[5] mp 126—127 °C). $[\alpha]_D$ −24.8° (c=1.41, $CHCl_3$). UV λ_{max}^{MeOH} nm (log ε): 230 (4.18), 281 (3.75). IR $\nu_{max}^{CHCl_3}$ cm^{-1}: 1770 (C=O), 1605, 1600, 1520. MS m/z: 386 (M^+, base peak), 208, 177, 151, 107. ^1H-NMR ($CDCl_3$) δ: 2.48—2.66 (4H, m), 2.93—2.97 (2H, m), 3.82, 3.84, 3.85, 3.86 (each 3H, s, OCH_3), 3.89 (1H, one of lactone-CH_2), 4.12 (1H, dd, J=9.2, 6.9 Hz, one of lactone-CH_2), 6.49—6.79 (6H, m, arom-H). ^{13}C-NMR ($CDCl_3$) δ: 34.5 (C-6), 38.2 (C-5), 41.1 (C-3), 46.6 (C-2), 55.9 (C-3′, 3″, 4′, 4″), 71.3 (C-4), 111.1 (C-2′), 111.4 (C-5′), 111.9 (C-2″), 112.4 (C-5″), 120.6 (C-6′), 121.4 (C-6″), 130.2 (C-1′), 130.5 (C-1″), 147.9 (C-4′), 148.0 (C-4″), 149.1 (C-3′, 3″), 178.7 (C-1). HI-MS Calcd for $C_{22}H_{26}O_6$ (M^+): 386.1729. Found: 386.1729.

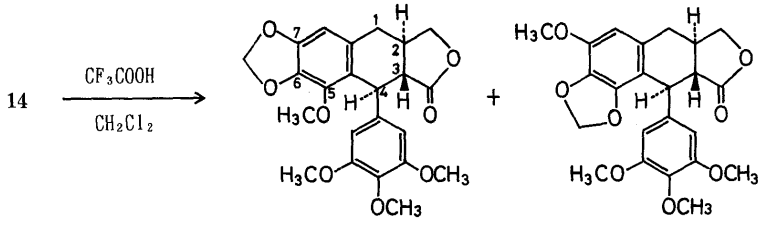

15 16

Fig. 3

(−)-5′-Methoxypodorhizol (14) mp 127—129 °C (from benzene–hexane) (lit.[9] 112—113 °C). $[\alpha]_D$ −49.1° (c=1.0, $CHCl_3$). UV λ_{max}^{EtOH} nm (log ε): 235 (4.06), 281 (3.19). IR $\nu_{max}^{CHCl_3}$ cm^{-1}: 3600, 3450 (OH), 1760 (C=O), 1635, 1595, 1510, 935 (OCH_2O). MS m/z: 446 (M^+), 249, 197 (base peak), 181, 165, 138, 125. ^{1}H-NMR ($CDCl_3$) δ: 2.26 (1H, dd, J=13.8, 7.8 Hz, C_5-H), 2.46 (1H, dd, J=13.8, 7.8 Hz, C_5-H), 2.56 (1H, br s, C_6-OH, disappeared on addition of D_2O), 2.66 (1H, dd, J=6.3, 3.0 Hz, C_2-H), 2.81 (1H, m, C_3-H), 3.84 (12H, s, $C_{5',3'',4'',5''}$-OCH_3), 3.98 (1H, dd, J=9.0, 5.7 Hz, C_4-H), 4.38 (1H, dd, J=9.0, 7.8 Hz, C_4-H), 5.29 (1H, br s, C_6-H), 5.92, 5.95 (each 1H, d, J=1.5 Hz, OCH_2O), 5.07 (1H, d, J=1.5 Hz, C_6-H), 6.03 (1H, d, J=1.5 Hz, $C_{2'}$-H), 6.50 (2H, s, $C_{2'',6''}$-H).

Cyclization of 14 A solution of compound **14** (54.4 mg, 0.122 mmol) in dichloromethane (4 ml) was added to a stirred solution of trifluoroacetic acid (1 ml) in dichloromethane (5 ml) at room temperature under a nitrogen atmosphere. After stirring for 12 h, the solvent was removed. A residual solid was purified by means of PTLC (solvent; hexane : $CHCl_3$: ethyl acetate = 2 : 1 : 1) affording two zones (Rf=0.25 and 0.16) from which **15** and **16** were respectively isolated.

Isohernandin (15) 35.1 mg, 67%. Colorless needles, mp 180—182 °C (from EtOH). IR $\nu_{max}^{CHCl_3}$ cm^{-1}: 1780 (C=O), 1620, 1595, 1500, 950. MS m/z: 428 (M^+, base peak), 413, 181, 165, 115. ^{1}H-NMR ($CDCl_3$) δ: 2.40 (2H, m, $C_{2,3}$-H), 2.86 (2H, m, C_1-H), 3.30 (3H, s, C_5-OCH_3), 3.81 (9H, s, $C_{3',4',5'}$-OCH_3), 3.92 (1H, dd, J=10.2, 8.5 Hz, one of lactone-CH_2), 4.30 (1H, d, J=9.4 Hz, C_4-H), 4.45 (1H, dd, J=8.5, 6.0 Hz, one of lactone-CH_2), 5.90, 5.91 (each 1H, d, J=1.4 Hz, OCH_2O), 6.40 (1H, s, C_8-H), 6.47 (2H, br s, $C_{2',6'}$-H). *Anal.* Calcd for $C_{23}H_{24}O_8$: C, 64.48; H, 5.65. Found: C, 64.47; H, 5.64.

2-Hydroxymethyl-5,6-methylenedioxy-7-methoxy-4-(3′,4′,5′-trimethoxyphenyl)-1,2,3,4-tetrahydronaphthoic Acid Lactone (16) 4.2 mg, 8%. Colorless needles, mp 204—206 °C (from EtOH). IR $\nu_{max}^{CHCl_3}$ cm^{-1}: 1780 (C=O), 1640, 1590, 1500, 940. MS m/z: 428 (M^+), 413, 181 (base peak), 165, 152, 115. ^{1}H-NMR ($CDCl_3$) δ: 2.35—2.65 (2H, m, $C_{2,3}$-H), 2.80—3.00 (2H, m, C_1-H), 3.80 (6H, s, $C_{3',5'}$-OCH_3), 3.83 (3H, s, $C_{4'}$-OCH_3), 3.91 (3H, s, C_7-OCH_3), 3.95 (1H, dd, J=11.0, 8.5 Hz, one of lactone-CH_2), 4.24 (1H, d, J=10.3 Hz, C_4-H), 4.49 (1H, dd, J=8.5, 6.4 Hz, one of lactone-CH_2), 5.66, 5.77 (each 1H, d, J=1.3 Hz, OCH_2O), 6.36 (1H, s, C_8-H), 6.51 (2H, s, $C_{2',6'}$-H).

Acknowledgement The authors express their deep gratitude to Dr. P. Richomme, Universite D'Angers, for his kind gift of the precious sample.

References and Notes

1) Part VIII: T. Kashima, M. Tanoguchi, M. Arimoto and H. Yamaguchi, *Chem. Pharm. Bull.*, **39**, 192 (1991). This work was presented at the 110th Annual Meeting of the Pharmaceutical Society of Japan, Sapporo, 1990.
2) H. Yamaguchi, M. Arimoto, K. Yamamoto and A. Numata, *Yakugaku Zasshi*, **99**, 674 (1979).
3) H. Yamaguchi, M. Arimoto, M. Tanoguchi, T. Ishida and M. Inoue, *Chem. Pharm. Bull.*, **30**, 3212 (1982).
4) M. Tanoguchi, M. Arimoto, H. Saika and H. Yamaguchi, *Chem. Pharm. Bull.*, **35**, 4162 (1987).
5) D. Takaoka, N. Takamatsu, Y. Saheki, K. Kono, C. Nakaoka and H. Hiroi, *Nippon Kagaku Kaishi*, **1975**, 2192.
6) S. Nishibe, S. Hisada and I. Inagaki, *Yakugaku Zasshi*, **94**, 522 (1974).
7) *a*) M. Kuhn and A. Von Wartburg, *Helv. Chim. Acta*, **50**, 1546 (1967); *b*) W. M. Kamil and P. M. Dewick, *Phytochemistry*, **25**, 2093 (1986).
8) P. Richomme, J. Bruneton and A. Cave, *Heterocycles*, **23**, 309 (1985).
9) P. A. Ganeshpure and R. Stevenson, *J. Chem. Soc., Perkin Trans. 1*, **1981**, 1681.
10) In our previous report[3] we described this signal as δ 4.84, J=10 Hz using a 90 Mc instrument. This time we reexamined it precisely by means of a 300 Mc instrument and confirmed the accurate datum.

Structures of Belamcandols A and B Isolated from the Seed of *Belamcanda chinensis*

Yoshiyasu FUKUYAMA,* Junko OKINO, and Mitsuaki KODAMA

Faculty of Pharmaceutical Sciences, Tokushima Bunri University, Yamashiro-cho, Tokushima 770, Japan. *Received February 1, 1991*

The structures of belamcandols A (1) and B (2) isolated from the seeds of *Belamcanda chinensis* have been assigned to 2,4-dimethoxy-6-((*Z*)-10′-pentadecenyl)phenol and 1-*O*-methyl-5-((*Z*)-10′-pentadecenyl)resorcinol, respectively, based on spectroscopic data and chemical degradation. Belamcandol A inhibits 5-lipoxygenase activity at IC_{50} 0.60 μM.

Keywords belamcandol A; belamcandol B; phenol; resorcinol; 1,4-benzoquinone; *Belamcanda chinensis*; Iridaceae; biosynthesis; 5-lipoxygenase inhibitor

A medicinal plant, *Belamcanda chinensis* L. (Iridaceae) has been used in Chinese herbs as antiinflammatory, antitussive, and expectorant agents.[1] Its rhizome, in particular, is prescribed as traditional crude drugs and elaborates a number of highly oxygenated isoflavones,[2,3] some of which are responsible for allergy inhibitors.[4] On the other hand, no chemical and pharmacological study on the seed of the title plant has been documented in spite of its folk medicinal value equivalent to the rhizome. As a part of our search for prostaglandin biosynthesis regulators in natural products,[5] we have investigated the chemical constituents of the seed of *B. chinensis*. A combination of silica gel and Sephadex LH-20 chromatographies of the methylene chloride extract has resulted in the isolation of two new phenols **1**, **2** named belamcandols A and B, respectively, along with the known 1, 4-benzoquinone (**3**).[6] In this paper, we deal with the structure elucidation and 5-lipoxygenase inhibitory activity of compounds **1** and **2**.

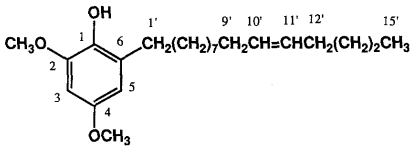

1

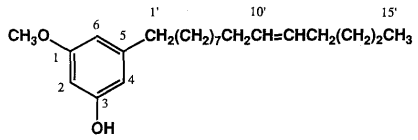

2

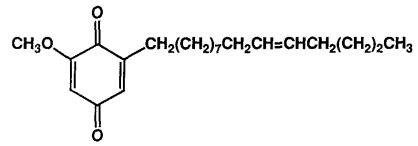

3

Fig. 1

Belamcandol A (**1**) had the molecular formula $C_{23}H_{38}O_3$ estimated from the molecular ion peak at *m/z* 362 in the positive fast atom bombardment mass spectrum (FABMS) together with the ^{13}C nuclear magnetic resonance (^{13}C-NMR) data. Its infrared (IR) spectrum showed characteristic bands at 3350, 1610 and 1490 cm^{-1}, attributable to a hydroxy group and an aromatic moiety, respectively. The 400 MHz ^1H nuclear magnetic resonance (^1H-NMR) spectrum of **1** revealed the presence of *meta* coupled aromatic protons at δ 6.29 (d, J=2.7 Hz) and 6.36 (d, J=2.7 Hz), and two methoxy groups at δ 3.76 and 3.85 as well as of signals due to a long alkenyl side chain at δ 5.37 (2H, t, J=4.5 Hz), 2.61 (2H, t, J=7.8 Hz), 2.02 (4H, m), 1.6 (2H, m), 1.3 (16H, m), and 0.90 (3H, t, J=7.1 Hz). The ^{13}C-NMR spectrum showed signals at δ 152.7 (s, C-4), 146.6 (s, C-2), 137.5 (s, C-1), 128.7 (s, C-6), 105.8 (d, C-5), and 96.6 (d, C-3) indicative of a tetrasubstituted benzene ring, at δ 129.8 (d, C-10′, 11′) for the double bond, at δ 55.7 and 55.9 (q, OCH_3) and signals ranging from 32.0—13.9 ppm (13 carbons) for the obtained side chain. These data suggested that belamcandol A is a phenol having two methoxy groups and a long side chain on the ring. It was also supported by the observation of a fragment ion peak at *m/z* 167 as follows. The position of the substituents on the benzene ring was determined by difference nuclear Overhauser effect (NOE) experiments as shown in Fig. 3. Upon irradiation of the benzylic proton signals at δ 2.61 (t), an NOE was observed for the one (δ 6.29) of the *meta* coupled aromatic signals, whereas irradiation of the methoxy signals at δ 3.76 and 3.85 gave NOEs on both the aromatic protons at δ 6.29 and 6.36, and only on the

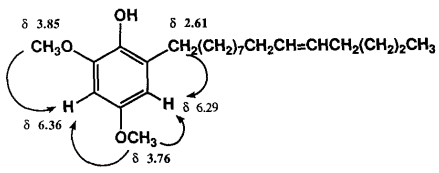

Fig. 3. The NOEs Observed for **1** are Denoted by Arrows

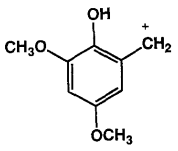

m/z 167

Fig. 2

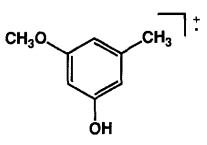

m/z 138

Fig. 4

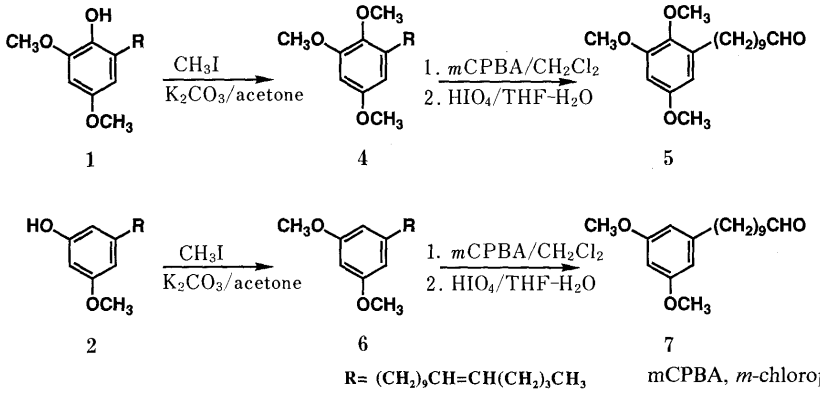

Fig. 5. Oxidative Cleavage of the Double Bond in **1** and **2**

aromatic one at δ 6.36, respectively, indicating the two methoxy groups to be located at C-2 and C-4, and the side chain to be at C-6. The double bond in the side chain was determined to be placed at C-10′ and 11′ on the basis of the molecular ion peak (*m/z* 322) for an aldehyde **5** which was obtained by oxidative degradation as shown in Fig. 5 (see Experimetal part). The stereochemistry on the double bond was assigned to *Z* from the diagnostic shifts of the two allylic methylene carbons at δ 26.8 and 27.1.[7] These results established that belamcandol A (**1**) is 2,4-dimethoxy-6-((*Z*)-10′-pentadecenyl)phenol.

Belamcandol B (**2**) was obtained as a viscous oil, and had the molecular formula $C_{22}H_{36}O_2$ in the high resolution electron impact mass spectrum (HREIMS). Its 400 MHz ^{1}H-NMR spectrum showed the presence of three aromatic protons *meta* coupled to each other at δ 6.23, 6.26, and 6.32 (each 1H, dd, J=2.3 and 2.3 Hz), a methoxy group at δ 3.76 and a C15 alkenyl side chain presumably identical to that which occurred in **1**. On the other hand, the ^{13}C-NMR spectrum indicated that the aromatic ring was substituted with a hydroxy group, a methoxy group, and a C15 side chain having one double bond (see Experimental part). It was also supported by the presence of a prominent fragment ion peak at *m/z* 138 as shown in Fig. 4. These spectral features disclosed **2** to be a resorcinol derivative.[8] In fact, **2** was converted to a symmetrical dimethoxy derivative **6** by methylation (CH_3I/K_2CO_3/acetone). The double bond of the side-chain in **6** was oxidized with *m*-chloroperbenzoic acid followed by HIO_4 to give a degraded product **7**, the molecular formula of which was confirmed as $C_{18}H_{28}O_3$ by HREIMS, and thereby the location of the double bond was verified to be at C-10′ and 11′. The stereochemistry of the double bond was assigned to *Z* from the chemical shifts (δ 26.9 and 27.2) of the allylic carbon signals. Thus, these data corroborated the structure of belamcandol B (**2**) to be 1-*O*-methyl-5-((*Z*)-10′-pentadecenyl)resorcinol.

Belamcandol A (**1**) and 1,4-benzoquinone (**3**) strongly inhibited 5-lipoxygenase activity at IC_{50} 0.60 and 1.57 μM, but belamcandol B (**2**) showed no inhibitory activity even at as high concentration as 10 μM by using the cytosol of quinea pig polymorphonuclear leukocytes.[9] From a biogenetic point of view, it is significant that three closely related compounds **1**, **2**, and **3** occurred in the same plant since **1** could be presumably oxidized *via* hydroquinone **2** to 1,4-benzoquinone (**3**). Finally, it is noted that no isoflavones, main ingredients in the rhizome of *B. chinensis*, have been detected in the seeds by the present chemical study.

Experimental

Ultraviolet (UV) spectra was recorded on a Shimazu UV-300 spectrophotometer. ^{1}H- and ^{13}C-NMR spectra were obtained at 400 or 90 MHz (^{1}H-NMR), and 100.16 MHz (^{13}C-NMR) using a JEOL GX-400 and a JX-90 spectrometers. Chemical shifts were expressed in δ (ppm) downfield from tetramethylsilane as an internal standard. Abbreviations are as follows: s, singlet; d, doublet; t, triplet; q, quartet; m, multiplet. The EI- and FABMS were taken on a JEOL JMS SX-102.

Extraction and Purification The dried seeds (150 g) of *Belamcanda chinensis* L. collected in Tokushima were immersed in CH_2Cl_2 at room temperature for a month. After filtration, the CH_2Cl_2 was evaporated *in vacuo* to leave an extract (13 g), which was chromatographed over silica gel (Merck Kieselgel 60, 70—230 mesh) using the solvent system of *n*-hexane–EtOAc (9 : 1, 7 : 3, and then 1 : 1) to divide into the thirteen fractions. The combined fractions 3 and 4 (4.28 g) were rechromatographed over silica gel (Wakogel C-300) eluting with *n*-hexane–EtOAc (9 : 1). The obtained 14th fraction (405 mg) was purified by silica gel chromatography (Merck Kieselgel 60, 230—400 mesh) with *n*-hexane–$CHCl_3$ (1 : 1) to give belamcandol A (**1**) (239 mg) as an oil and 1,4-benzoqinone (**3**) (97 mg) as a crystal. The 15th fraction was subjected to Sephadex LH-20 chromatography eluting with CH_2Cl_2–CH_3OH (3 : 7) to yield belamcandol B (**2**) (87.3 mg) as an oil.

Belamcandol A (1) HREIMS *m/z*: 362.2814 [M^+], Calcd 362.2812 for $C_{23}H_{38}O_3$. pos. FABMS *m/z*: 362 [M^+], 167 [M^+-195]. UV λ_{max}^{EtOH} nm (ε): 202.8 (42000), 285 (7020). IR $\nu_{max}^{CHCl_3}$ cm^{-1}: 3550 (OH), 1610, 1490 (aroma.). ^{1}H-NMR (400 MHz, $CDCl_3$) δ: 0.90 (3H, t, J=7.1 Hz, H-15′), 1.3 (16H, m), 2.02 (4H, m, H-9′, 12′), 2.61 (2H, t, J=7.8 Hz, H-1′), 3.76 (3H, s, C_4-OCH_3), 3.85 (3H, s, C_2-OCH_3), 5.26 (1H, s, OH), 5.37 (2H, t, J=4.5 Hz, H-10′, 11′), 6.29 (1H, d, J=2.7 Hz, H-5), 6.36 (1H, d, J=2.7 Hz, H-3). ^{13}C-NMR ($CDCl_3$) δ: 13.9 (q, C-15′), 26.8 (t, C-12′), 27.1 (t, C-9′), 29—30 (9 carbons), 31.9 (t, C-1′), 55.7 (s, OCH_3), 55.9 (s, OCH_3), 96.6 (d, C-3), 105.8 (d, C-5), 128.7 (s, C-6), 129.8 (d, C-10′, 11′), 137.5 (s, C-1), 146.6 (s, C-2), 152.7 (s, C-4).

Belamcandol B (2) HREIMS *m/z*: 332.2708 [M^+], Calcd 332.2716 for $C_{22}H_{36}O_2$. EIMS *m/z* (rel. int.): 332 [M^+] (13.4), 138 (45) [M^+-194]. UV λ_{max}^{EtOH} nm (ε): 202.5 (58400), 270 (3600). IR $\nu_{max}^{CHCl_3}$ cm^{-1}: 3600, 3300 (OH), 1600, 1460 (aroma.). ^{1}H-NMR (400 MHz, $CDCl_3$) δ: 0.89 (3H, t, J=7.1 Hz, H-15′), 1.3 (18 H, m), 2.02 (4H, m, H-9′, 12′), 2.51 (2H, t, J=7.7 Hz, H-1′), 3.76 (3H, s, C_1-OCH_3), 5.29 (1H, s, OH), 5.35 (2H, t, J=4.6 Hz, H-10′, 11′), 6.23 (1H, dd, J=2.3, 2.3 Hz, H-2), 6.26 (1H, dd, J=2.3, 2.3 Hz, H-6), 6.32 (1H, dd, J=2.3, 2.3 Hz, H-4). ^{13}C-NMR ($CDCl_3$) δ: 14.0 (q, C-15′), 26.9 (t, C-9′), 27.2 (t, C-12′), 29—30 (9 carbons), 36.1 (t, C-1′), 55.2 (s, OCH_3), 98.7 (d, C-2), 106.8 (d, C-6), 107.8 (d, C-4), 129.9 (d, C-10′, 11′), 145.8 (s, C-5), 156.5 (s, C-3), 160.8 (s, C-1).

Methylation of 1 A mixture of **1** (102.2 mg, 0.28 mmol), CH_3I (0.035 ml), K_2CO_3 (77.4 mg), and dry acetone (5 ml) was refluxed for 24 h. After filtration, the filtrate was evaporated *in vacuo* to leave the residue (250 mg), which was chromatographed on silica gel (Wakogel C-300, 10 g) with *n*-hexane–$CHCl_3$ (2 : 1) to give **4** (92 mg) as an oil. ^{1}H-NMR (90 MHz, $CDCl_3$) δ: 0.90 (3H, t, J=7.0 Hz, H-15′), 3.76 (3H, s, OCH_3), 3.77 (3H, s, OCH_3), 3.83 (3H, s, OCH_3), 5.35 (2-H, t, J=4.4 Hz, H-10′, 11′), 6.30 (1H, d, J=2.8 Hz, H-5), 6.34 (1H, d, J=2.8 Hz, H-3).

Oxidative Cleavage of the Double Bond in 4 A mixture of **4** (92 mg,

0.25 mmol), 85% *m*-chloroperbenzoic acid (37.5 mg) and CH_2Cl_2 (4 ml) was left standing at room temperature for 3 h. Ether (30 ml) was added to the reaction mixture and then the organic layer was washed with sat. $NaHCO_3$ sol., and sat. NaCl sol. After being dried over $MgSO_4$, the solvent was evaporated *in vacuo* to leave the residue (100 mg), which was purified by column chromatography on silica gel eluting with *n*-hexane–$CHCl_3$ (1 : 2) to afford an epoxide (39.4 mg) as an oil. ^{1}H-NMR (400 MHz, $CDCl_3$) δ: 0.92 (3H, t, J=6.9 Hz, H-15′), 2.59 (2H, dd, J=8.8, 6.9 Hz, H-10′, 11′), 2.90 (2H, t, J=4.4 Hz, H-1′), 3.74 (3H, s, OCH_3), 3.76 (3H, s, OCH_3), 3.82 (3H, s, OCH_3), 6.28 (1H, d, J=2.9 Hz, H-5), 6.35 (1H, d, J=2.9 Hz, H-3). To a solution of the obtained epoxide in tetrahydrofuran (THF)–H_2O (2 ml, 4 : 1) was added HIO_4 (27.6 mg) and the reaction mixture was stirred at room temperature for 2 h. To this reaction solution was added ether (20 ml), and then the organic layer was washed with sat. $NaHCO_3$ sol. and sat. NaCl sol. After being dried over $MgSO_4$, the solvent was evaporated *in vacuo* to leave the residue (50 mg), which was chromatographed on silica gel eluting with *n*-hexane–$CHCl_3$ (1 : 2) to afford an aldehyde **5** as an oil. IR $\nu_{max}^{CHCl_3}$ cm^{-1}: 2720, 1725 (CHO), 1600, 1490 (aroma.). EIMS *m/z* (rel. int.): 322 [M^+] (100), 167 (90). ^{1}H-NMR (90 MHz, $CDCl_3$) δ: 2.42 (2H, td, J=7.7, 1.8 Hz, H-9′), 2.59 (2H, t, J=8.4 Hz, H-1′), 3.74 (3H, s, OCH_3), 3.76 (3H, s, OCH_3), 3.82 (3H, s, OCH_3), 6.27 (1H, d, J=2.6 Hz, H-5), 6.34 (1H, d, J=2.6 Hz, H-3), 9.75 (1H, t, J=1.8 Hz, H-10′).

Methylation of 2 A mixture of **2** (22 mg, 0.066 mmol), CH_3I (0.09 ml), K_2CO_3 (18.2 mg), and dry acetone (1 ml) was refluxed for 24 h. The reaction solution was condensed *in vacuo* to leave the residue (50 mg), which was chromatographed on silica gel (Wakogel C-300, 5 g) with *n*-hexane–CH_2Cl_2 (1 : 2) to give **6** (13.0 mg) as an oil. HREIMS *m/z*: 346.2838 [M^+], Calcd 346.2871 for $C_{23}H_{38}O_2$; 152.0837, Calcd 152.0837 for $C_9H_{12}O_2$. ^{1}H-NMR (400 MHz, $CDCl_3$) δ: 0.89 (3H, t, J=5.8 Hz, H-15′), 2.02 (4H, m, H-9′, 12′), 2.54 (2H, t, J=7.7 Hz, H-1′), 3.78 (6H, s, OCH_3), 5.35 (2H, t, J=4.6 Hz, H-10′, 11′), 6.29 (1H, t, J=2.2 Hz, H-2), 6.34 (2H, d, J=2.2 Hz, H-4, 6).

Oxidative Cleavage of the Double Bond in 6 A mixture of **6** (13.0 mg, 0.038 mmol), 85% *m*-chloroperbenzoic acid (4.8 mg), and CH_2Cl_2 (2 ml) was left standing at room temperature for 4 h, Ether (10 ml) was added and then the organic solution was washed with sat. $NaHCO_3$ sol. and sat. NaCl sol. After being dried over $MgSO_4$, the solvent was removed *in vacuo* to leave the residue (35 mg), which was chromatographed on silica gel (Wakogel C-300, 5 g) eluting with *n*-hexane–CH_2Cl_2 (1 : 2) to yield an epoxide (4.8 mg) as an oil. This epoxide was dissolved in THF–H_2O (1 ml, 1 : 4) and then HIO_4 (3.64 mg) was added in one portion. The reaction mixture was stirred at room temperature for 24 h. Ether (10 ml) was added to the reaction solution and then the organic layer was washed with sat. $NaHCO_3$ sol. and sat. NaCl sol. After being dried over $MgSO_4$, the solvent was removed *in vacuo* to give an aldehyde **7** (1 mg) as an oil. HREIMS *m/z*: 292.2050 [M^+], Calcd 292.2038 for $C_{18}H_{28}O_3$; 152.0841, Calcd 152.0845 for $C_9H_{12}O_2$. ^{1}H-NMR (400 MHz, $CDCl_3$) δ: 2.42 (2H, td, J=6.8, 1.8 Hz, H-9′), 2.54 (2H, t, J=7.9 Hz, H-1′), 3.78 (6H, s, OCH_3), 6.30 (1H, t, J=2.2 Hz, H-2), 6.34 (2H, d, J=2.2 Hz, H-4, 6), 9.76 (1H, t, J=1.8 Hz, CHO).

Acknowledgment We are indebted to Dr. M. Sugawara and Mr. M. Nagasawa, Otsuka Pharmaceutical Co., Ltd. for the measurement of mass spectra.

References and Notes

1) Chang Su New Medical College (ed.), Dictionary of Chinese Crude Drugs, Shanghai Scientific Technologic Publisher, Shanghai, 1977, pp. 1883—1884.
2) N. Morita, M. Shimokoriyama, H. Shimizu, and M. Arisawa, *Chem. Parm. Bull.*, **20**, 730 (1972).
3) M. Yamaki, T. Kato, M. Kashihara, and S. Takagi, *Planta Med.*, **56**, 335 (1990).
4) H. Tsuchiya, Y. Iketani, H. Tsucha, and Y. Komatsu, Japan. Kokai Tokyo JP 86-171845 (1986) [*Chem. Abstr.*, **109**, 216001*t* (1988)].
5) Y. Fukuyama, K. Mizuta, K. Nakagawa, Q. Wenjuan, and W. Xiue, *Planta Med.*, **1986**, 433.
6) 1,4-Benzoquinone (**3**) was already isolated as a 5-lipoxygenase inhibitor from the Rhizome of *Ardisia japnonica* by us. Its detail will be reported in due course. H. Iwaki, Y. Fukuyama, and K. Matsui, *Eur. Pat. Appl.*, **151**, 995 (1986) [*Chem. Abstr.*, **104**, 23861 (1986)].
7) J. W. DE Haan and L. J. DE Ven, *Org. Magn. Resonance*, **5**, 147 (1973).
8) A number of naturally occurring resorcinol derivatives were isolated mainly from the Proteaceae. J. R. Cannon and B. W. Metcalf, *Aust. J. Chem.*, **24**, 1925 (1971) and references cited therein.
9) N. One, Y. Yamasaki, N, Yamamoto, A. Susami, and H. Miyake, *Jpn. J. Pharmacol.*, **42**, 431 (1986).

Detection of 8-Hydroxy-2′-deoxyguanosine in Deoxyribonucleic Acid by the ^{32}P-Postlabeling Method

Lee-Jane W. Lu,*[,a] Fumiyo Tasaka,[b] James A. Hokanson[c] and Kohfuku Kohda*[,b]

Division of Environmental Toxicology[a] and Division of Epidemiology and Biostatistics,[c] Department of Preventive Medicine and Community Health, The University of Texas Medical Branch, Galveston, TX 77550, U.S.A. and Faculty of Pharmaceutical Sciences, Nagoya City University,[b] Tanabe-Dori, Mizuho-ku, Nagoya 467, Japan. *Received February 1, 1991*

Using synthesized 8-hydroxy-2′-deoxyguanosine 3′-monophosphate as a marker, the ^{32}P-postlabeling method was adapted with minimum modifications for the analysis of 8-hydroxy-2′-deoxyguanosine (8-OH-dG) content in deoxyribonucleic acid (DNA). This method allows the analysis of one 8-OH-dG per 10^4 DNA nucleotides with only 10 pmoles of nucleotides required. The amounts of 8-OH-dG in DNA detected by the postlabeling method correlated well with the electrochemical detection method but were consistently lower.

Keywords ^{32}P-postlabeling; 8-hydroxydeoxyguanosine; DNA; oxidative damage

Introduction

8-Hydroxy-2′-deoxyguanosine (8-OH-dG) represents one specific type of deoxyribonucleic acid (DNA) damage product induced by oxygen radical producing agents.[1] Site specific mutagenesis analysis shows that 8-OH-dG is a mutagenic lesion.[2,3] Mechanistic studies concerning the formation of 8-OH-dG indicates the involvement of a singlet oxygen species.[4] An enzyme that specifically removes 8-OH-dG has been purified from *E. coli* implying the formation of this adduct *in vivo*.[5] This adduct was first detected in *in vivo* samples[1] through the combined use of high performance liquid chromatography (HPLC) and electrochemical detection developed by Floyd *et al.*[6] A fluorescence postlabeling method was also recently described for the analysis of this adduct.[7] Povey *et al.*, purified 8-hydroxy-2′-deoxyguanosine 3′-monophosphate (8-OH-dGp) from DNA by HPLC and quantitated this nucleotide using the postlabeling method.[8] The present report describes a simple modification of the ^{32}P-postlabeling method that allows the detection of one 8-OH-dG per 10^4 nucleotides in DNA without the prepurification of this nucleotide by HPLC. The HPLC purification step can enhance sensitivity but requires substantial amounts of DNA for analysis.

Experimental

Chemicals 2′-Deoxyguanosine 3′-monophosphate (dGp), calf thymus DNA, horseradish peroxidase, and hydrogen peroxide were purchased from Sigma Chem. Co. Sources of all reagents used for the ^{32}P-postlabeling method were described in detail.[9,10] [γ-^{32}P]adenosine triphosphate (ATP) was synthesized and activities determined in our laboratory as described.[10]

Synthesis of 8-OH-dGp 8-OH-dGp was synthesized as described[11] with the following modifications. dGp (10 mg) was dissolved in 10 ml of 0.1 M phosphate buffer, pH 6.8 containing 14 mM ascorbic acid, 6.5 mM ethylenediaminetetraacetic acid and 1.3 mM $FeSO_4$. The mixture was bubbled with oxygen at 37 °C for 3.5 h. The water was removed by lyophilization. The residue was solubilized with a minimum amount of water, applied to a Sephadex LH 20 column (2 × 38 cm), eluted with water, and detected by an electrochemical detector. Fractions containing 8-OH-dGp were pooled for further purification by HPLC. The pooled fractions were applied to a LiChrospher 100 RP-18(e) column (4.0 × 125 mm, Merck) and eluted isocratically with 10 mM NaH_2PO_4 containing 2% methanol. Salt was removed by HPLC using a TSKgel-ODS 80TM column (4.6 × 100 mm, Jasco). The solvent used for elution was water containing 10% methanol. Ultraviolet (UV) spectra (absorption maximum, nm) of 8-OH-dGp were 247 and 293 at pH 1 and pH 6, and 248 and 280 at pH 11. This spectra is identical to that of 8-OH-dG. Proton nuclear magnetic resonance (^{1}H-NMR) of 8-OH-dGp in D_2O revealed peaks (6.20 ppm, t, 1H, J=7.2 Hz, 1′-H) consistent with the presence of deoxyribose moiety. Treatment of 8-OH-dGp with alkaline phosphatase resulted in the formation of 8-OH-dG with spectral absorption identical to that of the authentic compound.[11]

Preparation of DNA Containing 8-OH-dG Calf thymus DNA was incubated with horseradish peroxidase and hydrogen peroxide as described.[4] The amounts of 8-OH-dG in each DNA preparation were determined using the electrochemical detection method[4,6] and by the postlabeling method described below.

Analysis of 8-OH-dG Using the ^{32}P-Postlabeling Method The ^{32}P-postlabeling conditions used were essentially as described.[9] Briefly, one μg of DNA was digested with 0.4 unit micrococcal nuclease (MN) and 4.0 μg spleen phosphodiesterase (SPD) at 37 °C for 3.5 h. Ten pmoles MN/SPD digest was then used for phosphate transfer reaction (omit P_1 digestion) using 200 μCi of ATP (carrier free, excess over 10 pmol) and 0.14 unit of T_4 polynucleotide kinase for each sample. After 30 min incubation at 37 °C, 20 mU of potato apyrase was added to each tube and incubation continued for an additional 10 min. One third of the labeled digest was then spotted on a 20 × 25 cm PEI (polyethyleneimine)-cellulose thin layer plate with a 10 cm Whatman No.1 wick attached to the top of the sheet. The digest was spotted at the lower left hand corner (2 × 2 cm from the bottom and left edges) of the chromatogram. The plate was then developed overnight in 1.25 M ammonium formate, pH 3.5 for *ca.* 15 h. The wick was then cut off with scissors. The sheets were then soaked in 500 ml of water with constant shaking for 7 min, dried with hot air and then developed in 0.3 M sodium phosphate, pH 6.0 at a right angle to the overnight direction to the top of the sheet (25 cm). After autoradiography, spots containing dG (2′-deoxyguanosine) and 8-OH-dG were excised and counted in a scintillation counter by Cerenkov counting. A blank area of the chromatogram neighboring, and with the size of the 8-OH-dG spot was excised and counted. This count was used as a surrogate background for the 8-OH-dG spot area and subtracted from cpm incorporated into the 8-OH-dG area for deriving true cpm due to the presence of 8-OH-dG in DNA. Results are expressed as %8-OH-dG/dG (=cpm incorporated into 8-OH-dGp/cpm in dGp). Markers of 8-OH-dGp and dGp were also ^{32}P-postlabeled as described for DNA digest. For co-chromatography, aliquot of [5′-^{32}P]8-OH-dpGp (3′,5′-bisphosphate of 8-OH-dG) was mixed with either ^{32}P-labeled digest of a DNA sample that contained 8-OH-dG or [5′-^{32}P]dpGp (3′,5′-bisphosphate of dG).

Results and Discussion

Figure 1 shows a suitable separation of 8-OH-dpGp from dpGp after two dimensional TLC (thin layer chromatography) on a PEI-cellulose plate. Figure 1A shows the pattern of control calf thymus DNA which has a background level of seven 8-OH-dG per 10^5 nucleotides as determined by the electrochemical detection method. Figure 1B shows the pattern of calf thymus DNA with 1493 8-OH-dG per 10^5 nucleotides. Figure 1C shows the pattern of a mixture consisting of a DNA sample (same as Fig. 1B) and an aliquot of [5′-^{32}P]8-OH-dpGp. Figure 1D represents authentic dpGp and 8-OH-dpGp. The result shown in Fig. 1C indicates that the 8-OH-dG moiety in DNA does co-chromatograph with an authentic marker.

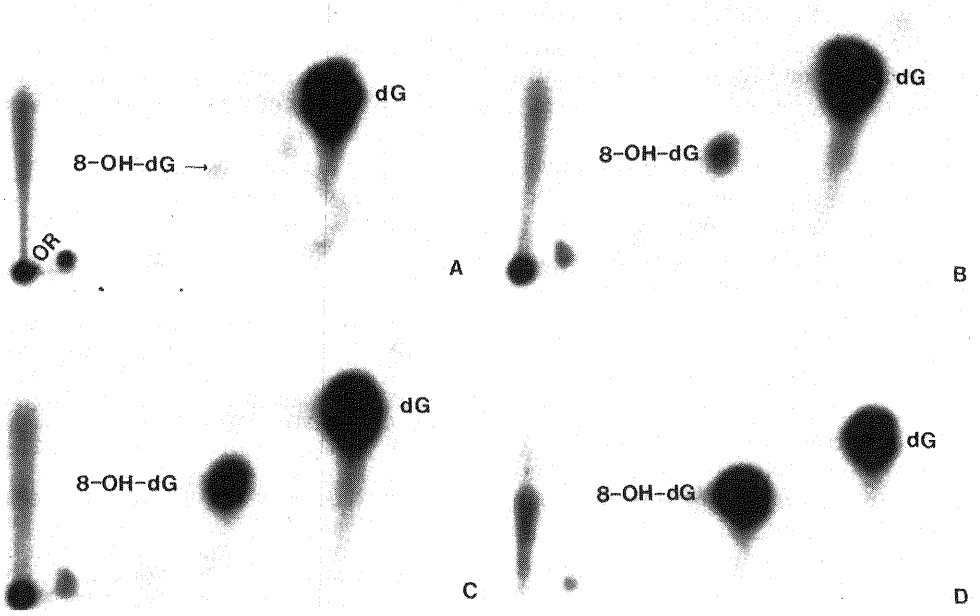

Fig. 1. Autoradiograms of Two Dimensional Thin Layer Chromatographic Separation of [5′-^{32}P]3′,5′-Bisphosphates of dG (2′-Deoxyguanosine) and 8-OH-dG (8-Hydroxy-dG)

Solvents used were 1.25 M ammonium formate, pH 3.5 for the first direction and 0.3 M sodium phosphate, pH 6.0 for the second direction. A, control calf thymus DNA not treated with horseradish peroxidase and H_2O_2; B, calf thymus DNA treated with horseradish peroxidase and H_2O_2[4]; C, a mixture of calf thymus DNA digest (same as sample in panel B) and marker of 8-OH-dG; D, a mixture of dG and 8-OH-dG markers; OR, origin of chromatography. Unmarked spots represent background labelings. Autoradiography was at room temp. for 15 min with DuPont Lightning Plus intensifying screen.

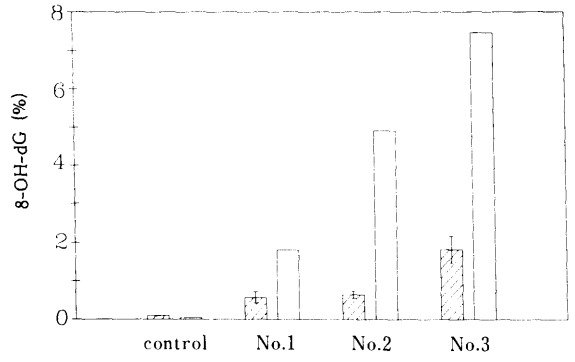

Fig. 2. 8-Hydroxy-2′-deoxyguanosine Contents in DNA Prepared by Reacting Calf Thymus DNA with Horseradish Peroxidase/H_2O_2[4]

The concentration of horseradish peroxidase (mg/ml)/ H_2O_2 (mg/ml) employed was: control, 0/0; No. 1, 0.1/0.7; No. 2, 0.2/1.5; No. 3, 0.3/2.25. ▨, postlabeling; □, electrochemical.

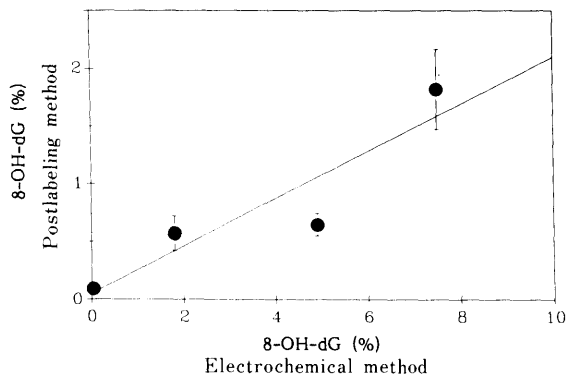

Fig. 3. A Comparison of the Levels of 8-OH-dG in DNA Analyzed by Postlabeling Method and Electrochemical Detection

Linear regression analysis was performed.

The 1.25 M ammonium formate, pH 3.5 and overnight development were chosen, since this condition retains only dpGp and 8-OH-dpGp on the TLC plate. The overnight development removed the remaining ^{32}P-labeled normal nucleotides and ^{32}Pi (from excess [γ-^{32}P]ATP after potato apyrase treatment), thus, reducing >90% of the radioactivity to which personnel would otherwise be exposed. Occasionally, 3′,5′-bisphosphate of 2′-deoxyadenosine was also retained at the upper right hand corner of the chromatogram. The overnight development can be performed for 15—17 h. 8-OH-dGp was found to be sensitive to the digestion of nuclease P_1. Therefore, nuclease P_1 cannot be used to enrich 8-OH-dGp. The amount of [γ-^{32}P]ATP used was greater than the amount of nucleotides used for this adaptation of the postlabeling method.[10]

Figure 2 compares the levels of 8-OH-dG contained in DNA samples analyzed by the postlabeling method and electrochemical detection. In general, 8-OH-dG contents were consistently lower by *ca.* 4-fold if analyzed by the postlabeling method compared to electrochemical detection. The reason for this difference is unknown. Whether this is due to suboptimal enzymatic digestion or reaction conditions is not known. We did not observe any significant differences in the 8-OH-dG content when the amount of ATP used was deficient (data not shown). More studies may be needed to explain the difference. However, in the postlabeling method, the same samples were simultaneously analyzed for both dG and 8-OH-dG. Since in this instance dG served as an internal standard, data obtained from the postlabeling method cannot be attributed to a variation in the amounts of nucleotides used for analysis. A 20% label-

ing effiiciency was reported for thymine glycol when the postlabeling method was used for the quantification of this type of oxidative DNA base damage.[12] The reduced labeling efficiency observed for both thymine glycol and 8-OH-dGp may result from the loss of their respective parent base ring structures.

In spite of the differences in the actual levels of 8-OH-dG determined using the postlabeling method and electrochemical detection, Fig. 3 shows that data obtained by the two methods do correlate well. The equation for linear regression analysis is $y=0.054+0.204x$, with the multiple correlation coefficient being 0.92 and the coefficient of determination being 0.85. From this equation, the actual background counts in the 8-OH-dG spot area is calculated to be 0.054% of dG (*e.g.*, $x=0$ based on electrochemical detection data) over the surrogate background area. From these parameters, assuming a sample size of 5, using a power of detection at 0.8, and a level of statistical significance equivalent to 0.05, a theoretical limit of the minimal value for detection above the background was calculated to be approximately 0.061% of dG (*ca.* 0.012% of total nucleotides).

One advantage of using the postlabeling method is that it requires substantially decreased amounts of DNA (1/300 μg DNA) compared to either electrochemical detection (100—500 μg DNA pending on the extent of modifications) or the fluorescence postlabeling method (100 μg DNA). The latter two procedures, however, do not expose personnel to radiation. Since the background levels of 8-OH-dG content in control DNA are *ca.* 1 modification per 10^4 nucleotides, this procedure is sufficient for the analysis of *in vitro* samples. DNA from cells or tissues contains 0.6—1.4 molecules of 8-OH-dG per 10^5 dG.[1] Improving the labeling efficiency will enable us to analyze the formation of 8-OH-dG in cells or tissues.

Acknowledgements We thank Prof. Y. Kawazoe of Nagoya City University for his encouragement. The technical help of Maria Yu Guo is appreciated. Supported in part by a USPHS grant CA44163.

References

1) H. Kasai, P. F. Crain, Y. Kuchino, S. Nishimura, A. Ootsuyama and H. Tanooka, *Carcinogenesis*, **7**, 1849 (1986).
2) Y. Kuchino, F. Mori, H. Kasai, H. Inoue, S. Iwai, K. Miura, E. Ohtsuka and S. Nishimura, *Nature* (London), **327**, 77 (1987).
3) M. L. Wood, M. Dizdaroglu, E. Gajewski and J. M. Essigmann, *Biochemistry*, **29**, 7024 (1990).
4) K. Kohda, T. Nakagawa and Y. Kawazoe, *Chem. Pharm. Bull.*, **38**, 3072 (1990).
5) H. Kasai, M.-H. Chung, S. Nishimura, H. Kamiya, and E. Ohtsuka, *J. Cancer Res. Clin. Oncol.*, **116** (Suppl, Part II), 1031 (1990).
6) R. A. Floyd, J. J. Watson, P. K. Wong, D. H. Altmiller and R. C. Richard, *Free Rad. Res. Commun.*, **1**, 163 (1986).
7) H. Sharma, H. C. Box and C. R. Paul, *Biochem. Biophys. Res. Commum.*, **167**, 419 (1990).
8) A. C. Povey, V. L. Wilson, B. G. Taffe, M. L. Wood, J. M. Essigmann and C. C. Harris, *Proc. Am. Assoc. Cancer Res.*, **30**, 201 (abstr. No. 796) (1989).
9) M. V. Reddy, R. C. Gupta and K. Randerath, *Anal. Biochem.*, **117**, 271 (1981).
10) M. V. Reddy and K. Randerath, *Carcinogenesis*, **7**, 1543 (1986).
11) H. Kasai and S. Nishimura, *Nucleic Acids Res.*, **12**, 2137 (1984).
12) M. E. Hegi, P. Sagelsdorff and W. K. Lutz, *Carcinogenesis*, **10**, 43 (1989).

An Enkephalin-Degrading Aminopeptidase from Rat Brain Catalyzes the Hydrolysis of a Neuropeptide, Kyotorphin (L-Tyr–L-Arg)

Kenji AKASAKI* and Hiroshi TSUJI

Faculty of Pharmacy & Pharmaceutical Sciences, Fukuyama University, Higashimura-cho, Fukuyama, Hiroshima 729–02, Japan.
Received February 4, 1991

We studied the hydrolysis of a neuropeptide kyotorphin (L-Tyr–L-Arg) by an enkephalin-degrading aminopeptidase purified from cytosol of rat brain *in vitro*. The purified enzyme was homogeneous as judged by sodium dodecyl sulfate (SDS)–polyacrylamide gel electrophoresis (PAGE), gel filtration and isoelectric focusing. The aminopeptidase with an apparent molecular weight (M_r) = 98000 catalyzed the hydrolysis of Leu- and Met–enkephalins with K_m values of 125 and 142 μM, respectively. The enzyme activity was inhibited by bestatin, amastatin and puromycin but not by pepstatin, leupeptin and phenylmethanesulfonyl fluoride (PMSF). Kyotorphin was degraded by the aminopeptidase at pH 7.0, and the V_{max} and K_m values were 9.2 μmol/min/mg protein and 95 μM, respectively. The K_m value for kyotorphin was compatible to those for Leu- and Met–enkephalins. Taken together, these results suggest a possible involvement of the enkephalin-degrading aminopeptidase in cytosolic degradation of kyotorphin in neuronal cells of rat brain.

Keywords aminopeptidase; kyotorphin (Tyr–Arg); enkephalin; bestatin; rat brain

Introduction

Kyotorphin is a neuropeptide isolated from bovine brain by Takagi *et al.*[1] This dipeptide is considered to produce analgesia *via* a release of enkephalin.[1,2] In cytosol of synaptosomes (synaptosol), kyotorphin is formed from free amino acids and/or precursor proteins by specific enzymes.[3,4] This peptide is rapidly degraded in the homogenate and synaptosol of rat brain.[3,5] The degradation is inhibited by bestatin, a inhibitor for cytosolic aminopeptidases.[6] Little is known, however, about the kyotorphin-degrading enzyme(s) in rat brain.

A major aminopeptidase was purified from the soluble fraction of rat brain as an enkephalin-hydrolyzing enzyme.[7,8] The enzyme has M_r = about 100000, and exhibits a broad specificity for arylamidase substrates such as Arg– and Ala–naphthylamides. It has further been shown that the aminopeptidase activity is effectively inhibited by bestatin and analogues of bestatin.[9] Such an aminopeptidase reportedly exists in monkey, bovine and human brains.[10–12] Taken together, these results raised the possibility that the kyotorphin degradation in the synaptosol can be ascribed to the enkephalin-degrading aminopeptidase. However, whether or not this aminopeptidase actually catalyzes the hydrolysis of kyotorphin has not been determined as yet.

In the present study, we purified the enkephalin-degrading aminopeptidase from rat brain to an apparent homogeneity and investigated its action on kyotorphin.

Materials and Methods

Materials Kyotorphin, Tyr–4-methyl-7-coumaryl-7-amide (Tyr–MCA), Ala–MCA, and Phe–MCA were obtained from Sigma (St. Louis, MO). Arg–MCA, Leu–MCA, Bz–Arg–Phe–MCA, Gly–Pro–MCA, Met– and Leu–enkephalins, bradykinin, substance P, bestatin, amastatin, leupeptin, pepstatin, actinonin and alphamenine B were purchased from Peptide Institute, Inc. (Osaka, Japan). Diethylaminoethyl (DEAE)-Sephacel, Sephadex G-150 and ampholine (pH 3.5—9.0) were from Pharmacia & LKB (Uppsala, Sweden). TSK gel G3000 SW, TSK gal DEAE-5PW and TSK gel ODS 80 TM were obtained from Tosoh Co. (Tokyo, Japan). Other chemicals of reagent grade were from various commercial sources.

Enzyme Purification The enkephalin-degrading aminopeptidase was purified from crude extracts of rat brain by a modified method of Wagner *et al.*[8]

Assay of Aminopeptidase Activity Enzyme (0.1 ml) was incubated for 10 min at 37 °C in a medium (total volume of 1 ml) containing 50 mM Tris–HCl buffer (pH 7.0), 2 mM 2-mercaptoethanol, and 0.1 mM Arg–MCA. Five mM 1,10-phenanthroline (2 ml) was added to terminate the reaction. The fluorescence of the liberated 7-amino-4-methylcoumarin was measured (λ_{ex} 380 nm; λ_{em} 450 nm) with reference to a fluorescence standard. The enzyme activity against other aminoacyl MCA derivatives was determined in the same way.

Analysis of Kyotorphin and Physiologically Active Peptides Degradation by Reversed-Phase High Performance Liquid Chromatography (HPLC) The purified enzyme was incubated with 100 μM kyotorphin at 37 °C for 10 min in a medium (total volume of 1.0 ml) containing 50 mM Tris–HCl (pH 7.0) and 2 mM 2-mercaptoethanol. Immediately after the reaction was terminated by cooling to 0 °C, the mixture was applied to reversed-phase HPLC using a TSK gel ODS 80 TM column (7.5 × 0.8 cm). In determination of the kyotorphin degradation, the incubation mixture was subjected to the column equilibrated with 0.1 M KH_2PO_4. The column was eluted with the equilibration buffer at a flow rate of 1.0 ml/min. Tyrosine and kyotorphin were monitored by an ultraviolet spectrophotometric detector (Tosoh model UV 8000) at 280 nm. For the other peptides, the column was equilibrated with 0.05% trifluoroacetic acid containing 20% acetonitrile. After application of the reaction mixture, elution was carried out with a linear gradient with acetonitrile concentrations from 20% to 80% at a flow rate of 1.0 ml/min.

Gel Electrophoresis Sodium dodecyl sulfate–polyacrylamide gel electrophoresis (SDS–PAGE) was carried out on 12% acrylamide gel according to the method of Laemmli.[13]

Protein Determination Protein concentrations were determined by the method of Lowry *et al.*[14] using bovine serum albumin as a standard.

Results and Discussion

Enzyme Homogeneity The aminopeptidase was purified 820-fold from the soluble fraction of rat brain. On SDS–PAGE (Fig. 1) the purified enzyme preparation gave only a single protein band with an apparent molecular weight (M_r) of 98000. When the purified enzyme was applied to size exclusion HPLC on a column of TSK gel G 3000 SW, the enzyme protein was eluted in a position corresponding to M_r = 109000 (data not shown). In isoelectric focusing, the enzyme showed a single peak of the enzyme activity at pH 5.0 (data not shown). By these criteria, the aminopeptidase was judged to be homogeneous. The M_r values of our enzyme preparation by SDS–PAGE and gel filtration are very similar to those of the aminopeptidase reported by Wagner *et al.*[8]

Effects of Inhibitors Effects of various protease inhibitors on the enzyme activity were tested, and the results obtained are summarized in Table I. Puromycin and

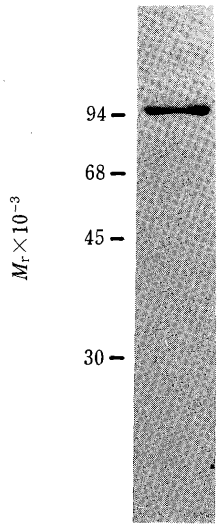

Fig. 1. SDS–PAGE of an Enkephalin-Degrading Aminopeptidase Purified from Rat Brain

Aminopeptidase purified from rat brain was analyzed by SDS–PAGE. Gel containing 2 μg of the purified enzyme was obtained after Coomassie blue staining. M_r values of marker proteins are shown to the left of the gel: phosphorylase b (M_r=94000); bovine serum albumin (68000); ovalbumin (45000); and carbonic anhydrase (30000).

TABLE I. Effect of Protease Inhibitors on the Aminopeptidase

Inhibitor	Concentration (μM)	Remaining activity (%)
No addition		100
Phenylmethanesulfonyl fluoride	1000	100
1,10-Phenanthroline	100	50
	500	0
Pepstatin	25	100
Leupeptin	15	100
Amastatin	0.48	50
Beststin	0.78	50
Puromycin	2.0	50
Actinonin	0.12	50
Arphamenine B	6.9	50

1,10-phenanthroline inhibited the enzyme activity but inhibitors for serine, thiol, and asparatic proteases had no effect on the aminopeptidase activity, indicating that this enzyme falls into the category of metalloproteases. As expected, bestatin was a potential inhibitor for this enzyme; aside from this antibiotic, actinonin, amastatin and arphamenine B strongly inhibited the enzyme activity.

Hydrolysis of Kyotorphin by the Enkephalin-Degrading Aminopeptidase The purified enzyme exhibited the greatest hydrolyzing activity for Arg–MCA at pH 7.0 in the presence of 2-mercaptoethanol. Substrate specificity of the aminopeptidase against various aminoacyl MCA derivatives and biologically active peptides is cited in Tables II and III. The enzyme hydrolyzed Leu–MCA with the highest rate among the amino acid MCA derivatives tested, while it did not catalyze the hydrolysis of Gly–Pro–MCA and Bz–Arg–Phe–MCA at all. The aminopeptidase liberated the N-terminal Tyr from Met– and Leu–enkephalin with respective K_m values of 142 and 125 μM (Table III); it also hydrolyzed delta sleep inducing peptide (DSIP). Substance P and bradykinin were resistant to hydrolysis by this aminopeptidase.

TABLE II. Activity of the Aminopeptidase on MCA Derivatives

Substrate	K_m (μM)	V_{max} (μmol/min/mg protein)	V_{max}/K_m
Arg–MCA	6.4	8.6	1.35
Leu–MCA	7.1	40.1	5.16
Phe–MCA	25.6	17.0	0.66
Ala–MCA	15.4	4.3	0.28
Tyr–MCA	7.7	5.2	0.67
Bz–Arg–Phe–MCA		Not reactive	
Gly–Pro–MCA		Not reactive	

TABLE III. Activity of the Aminopeptidase on Biologically Active Peptides

Peptide	Amino terminus	K_m (μM)	V_{max} (μmol/min/mg protein)
Met–enkephalin	Tyr–Gly	142	26.8
Leu–enkephalin	Tyr–Gly	125	10.8
Kyotorphin	Tyr–L-Arg	95	9.2
Kyotorphin analogue	Tyr–D-Arg	Not reactive	
DSIP	Trp–Ala	10	2.5
Substance P	Arg–Pro	Not reactive	
Bradykinin	Arg–Pro	Not reactive	

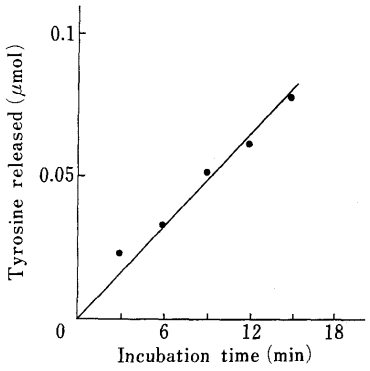

Fig. 2. Time Course of the Hydrolysis of Kyotorphin by the Enkephalin-Degrading Aminopeptidase

A reaction mixture (total volume of 1.0 ml) contained 50 mM Tris–HCl (pH 7.0), 2 mM 2-mercaptoethanol, 100 nmol kyotorphin and 500 ng of the purified enzyme. The mixture was incubated at 37 °C for the time indicated. After the reaction was terminated by cooling to 0 °C, amounts of tyrosine liberated were measured by reversed phase HPLC.

We next investigated whether or not the enkephalin aminopeptidase actually catalyzes degradation of kyotorphin *in vitro*. As shown in Fig. 2, kyotorphin was degraded by the purified enzyme in a linear reaction up to 15 min. At this time, about 85% of the initial substrates added were hydrolyzed by this enzyme. The degradation rate was dependent on the enzyme amounts and the concentration of kyotorphin. The apparent K_m and V_{max} values for kyotorphin were 95 μM and 9.2 μmol/min/mg protein (Table III). These values were compatible with those for Leu–enkephalin.

The enkephalin-degrading aminopeptidase showed a relatively broad specificity for arylamidase substrates. Arg–MCA is one of the favorable substrates for this enzyme; however, it does not exhibit the hydrolyzing activity for substance P and bradykinin in spite of the N-terminal Arg.

In addition, once D-Arg was substituted for L-Arg of kyotorphin (Table III), the enzyme did not demonstrate any hydrolyzing activity for the peptide. From these results, it is considered that the peptide conformation rather than the N-terminal amino acid residue is critical for the action of this enzyme. The enkephalin-degrading aminopeptidase has been shown to be widely distributed in rat tissues.[15] Such an enzyme has reportedly been purified from human skeletal muscles.[16,17] Together with the broad substrate specificity of this enzyme, these facts may reflect a central role of the aminopeptidase in degradation of di- or tripeptides presented at the final stage of general protein breakdown, as well as its possible function of controlling the kyotorphin level.

Acknowledgments We would like to thank Drs. A. Nakamura and H. Shiomi (Fukuyama University) for helpful comments.

References

1) H. Takagi, H. Shiomi, H. Ueda, and H. Amano, *Nature* (London), **282**, 410 (1979).
2) H. Takagi, *Nippon Yakurigaku Zasshi*, **96**, 85 (1990).
3) H. Ueda, Y. Yoshihara, N. Fukushima, H. Shiomi, A. Nakamura, and H. Takagi, *J. Biol. Chem.*, **262**, 8165 (1987).
4) Y. Yoshihara, H. Ueda, N, Fujii, A. Suda, H. Yajima, and M. Satoh, *J. Biol. Chem.*, **265**, 5809 (1990).
5) H. Ueda, G. Ming, T. Hazato, T. Katayama, and H. Takagi, *Life Sci.*, **36**, 1865 (1985).
6) H. Suda, T. Aoyagi, T. Takeuchi, and H. Umezawa, *Arch. Biochem. Biophys.*, **177**, 196 (1976).
7) H. P. Schnebli, M. A. Phillipps, and R. K. Barclay, *Biochim. Biophys. Acta*, **569**, 89 (1979).
8) G. W. Wagner, M. A. Tavianni, M. K. Herrmann, and J. E. Dixon, *Biochemistry*, **20**, 3884 (1981).
9) G. W. Wagner and J. E. Dixon, *J. Neurochem.*, **37**, 709 (1981).
10) M. Hayashi and K. Oshima, *J. Biochem.* (Tokyo), **94**, 631 (1977).
11) L. B. Hersh and J. F. McKelvy, *J. Neurochem.*, **36**, 171 (1981).
12) J. R. McDermott, D. Mantle, B. Lauffart, and A. M. Kidd, *J. Neurochem.*, **45**, 752 (1985).
13) U. K. Laemmli, *Nature* (London), **227**, 680 (1970).
14) O. H. Lowry, N. J. Rosebrough, A. L. Farr, and R. J. Randall, *J. Biol. Chem.*, **193**, 265 (1951).
15) S. McClellan, S. H. Dyer, G. Rodriguez, and L. B. Hersh, *J Neurochem.*, **51**, 1552 (1988).
16) D. Mantle, M. F. Hardy, B. Lauffart, J. R. McDermott, A. I. Smith, and R. J. T. Pennington, *Biochem. J.*, **221**, 567 (1983).
17) S. Ishiura, T. Yamamoto, M. Yamamoto, M. Nojima, T. Aoyagi, and H. Sugita, *J. Biochem.* (Tokyo), **102**, 1023 (1987).

Dissolution and Bioavailability of Phenobarbital in Solid Dispersion with Phosphatidylcholine[1)]

Makiko FUJII,* Katsuhiro HARADA, Keiko KAKINUMA and Mitsuo MATSUMOTO

Showa College of Pharmaceutical Sciences, 3-3165 Higashitamagawagakuen, Machida-shi, Tokyo 194, Japan. *Received November 2, 1990*

The dissolution of phenobarbital (PB) from solid dispersion with phosphatidylcholine (PC) was studied. PB was present in an amorphous state in solid dispersion (PB-PC) if the mole fraction of PB was under 0.75. Thus, supersaturation was observed when an excess amount of PB-PC was dispersed in pH 1.2 and 6.8 media. The degree of supersaturation was largest when the mole fraction of PB was 0.25, although it was only 1.3-fold of the PB solubility in this case. Dissolution from PB-PC was rapid and complete in both pH 1.2 and 6.8 media regardless of the mole fraction of PB, above 90% within 5 min. Bioavailability after the oral administration of PB-PC to rabbits with a dose of 15 mg/kg equivalent to PB was compared with that of PB crystals. The area under the plasma concentration curve was bigger, but not significant. The maximum concentration was significantly higher, and the time to maximum concentration was significantly faster. These results indicate that the absorption rate became high with PB-PC because the dissolution was rapid.

Keywords phenobarbital; phosphatidylcholine; solid dispersion; dissolution rate; amorphous; oral administration; rabbit; bioavailability

We previously reported the physicochemical properties of phenobarbital (PB) solid dispersion with phosphatidylcholine (PC).[1)] PB resembles indomethacin (IM) with a plane like molecular shape. PB is present in an amorphous state in solid dispersion with PC (PB-PC) when its mole fraction is less than 0.75, to the same extent as IM. The interaction between PC and PB is similar to that between PC and phenytoin (PHT) which also has an oxopyrimidine ring.

We examined the dissolution behavior of PB from solid dispersion and compared it with IM[2)] or PHT[3)] solid dispersion with PC (IM-PC, PHT-PC). Also, the plasma concentration of PB after its oral administration to rabbits was studied.

Experimental

Materials The same PB and PC as in the previous report were used.[1)] Other chemicals were of reagent grade.

Preparation of Solid Dispersion PB-PC and a physical mixture of PB and PC were prepared by the method previously reported.[1)] The figure in parentheses following PB-PC is the mole fraction of PB. In the case of PB-PC (0.50), the prepared PB-PC was held at 70 °C for 10 min or at 160 °C for 10 min to obtain the stable and metastable forms, respectively.

Solubility Studies An excess amount of sample (equivalent to 300 mg of PB) was put into 50 ml of the 1st fluid (pH 1.2) or the 2nd fluid (pH 6.8) of the JP XI disintegration test kept at 37±0.1 °C. Details have been previously reported.[3)] The concentration of PB was determined by ultraviolet absorption at 252 nm after diluting with 0.1 N NaOH solution. The determination was done within 2 h after diluting for PB degrades in alkaline solution. The results represent the mean of 3 experiments.

Dissolution Studies The dissolution patterns were tested by a method similar to PHT-PC.[3)] A sample equivalent to 250 mg of PB was dispersed in 4 ml of test solution and the suspension was dropped into 500 ml of test solution at 37±0.1 °C with stirring by a paddle at 100 rpm. The method for the determination of PB concentration is described in the solubility studies section. All studies were done in triplicate.

Animal Experiments Four white male rabbits (body weight 2.6—3.0 kg) were fasted for 24 h but allowed to take water freely. A sample equivalent to 15 mg/kg of PB suspended in 4 ml of water was orally administered to a rabbit followed by the administration of 26 ml of water. About 100 g of food was given after 24 h of blood sampling. Doses were administered by the cross-over arrangement after a two-week interval.

Determination of PB in Plasma The plasma concentration of PB was determined by high performance liquid chromatography (HPLC).[3,4)] The stationary phase, μBondapak C_{18} (3.9 × 150 mm), was kept at 50 °C. The mobile phase was a mixture of acetonitrile: pH 5.4 phosphate buffer solution (17:83, v/v). The flow rate was 1.0 ml/min. PB was detected

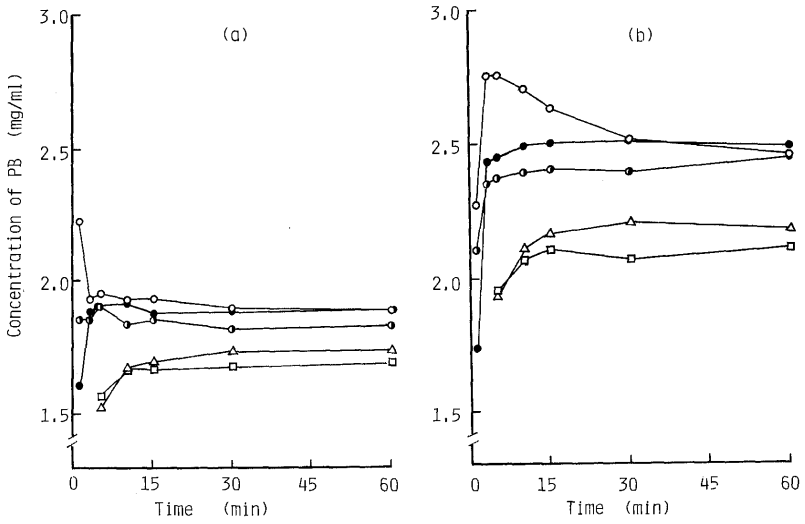

Fig. 1. Solubility Behavior of PB-PC in pH 1.2 (a) and 6.8 (b) Medium

△, PB crystals; □, physical mixture (0.75); ○, PB-PC (0.25); ◑, PB-PC (0.50); ●, PB-PC (0.75).

at 230 nm. PB concentrations were calibrated by an external standard method on the basis of peak height measurement.

Statistical Analysis Statistical analysis was performed using a one-way analysis of variance. Follow-up analysis was performed using Dunnett's test. A p value of <0.05 was accepted as demonstrating statistical significance.

Results and Discussion

Solubility and Dissolution Studies Figure 1 shows the time courses of the PB concentration in pH 1.2 and pH 6.8 media. The solubilities of PB in pH 1.2 and pH 6.8 media were 1.7 and 2.2 mg/ml, respectively. The PB concentrations with the physical mixture (0.75) were 1.7 mg/ml (pH 1.2) and 2.1 mg/ml (pH 6.8), and agreed with the PB solubilities. When PB-PC (0.25) was used, the PB concentrations rose temporarily to 2.2 mg/ml (pH 1.2) and to 2.8 mg/ml (pH 6.8) initially. When PB-PC (0.50) or (0.75) was used, the PB concentrations were slightly higher than the PB solubilities, 1.9 mg/ml (pH 1.2) and 2.5 mg/ml (pH 6.8). When PB-PC was used, PB concentrations after 24 h agreed with the solubility regardless of the PB mole fraction in PB-PC.

PB was present in an amorphous state in PB-PC when its mole fraction was under 0.75. When PB-PC was used, PB concentrations were temporarily higher than PB solubilities because of an amorphous state of PB, and the equilibrium concentrations agreed with solubilities. These time–concentration curves were similar to those of IM-PC and PHT-PC.[2,3]

In the case of IM-PC, the degree of supersaturation became higher when the mole fraction of the drug became higher as long as IM was present in an amorphous state.[2]

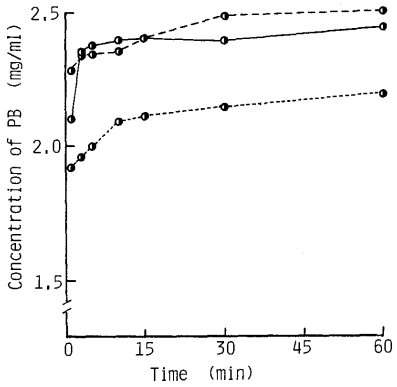

Fig. 2. Solubility Behavior of PB-PC (0.50) in Different Conditions
—, conventional PB-PC (0.50); ---, stable; – –, metastable.

It was considered that the diffusion of the drug in solid dispersion was the rate-limiting step because PC was insoluble in water. However, in the case of PB-PC, the degree of supersaturation was the largest when the mole fraction of PB was as low as 0.25. Thus, it was not explained merely by diffusion. When the mole fraction of PB was under 0.50, it was considered that the hydrogen bond exists between PB and a polar head group of PC.[1] Thus, PB exists first near the polar head group of PC and the remaining PB exists near the hydrophobic part of PC. It was considered that water has a higher affinity to the polar head group of PC than to the hydrophobic part, so that the PB existing near the polar head group dissolved faster than the PB existing near the hydrophobic part of PC; hence the dissolution might change.

PB-PC (0.50) showed two energy conditions, a metastable and a stable state.[1] They were induced by heating PB-PC at 70 °C (stable) or 160 °C (metastable). Figure 2 shows the effect of conditions on the solubility behavior in pH 6.8 medium. PB-PC (0.50) in the stable state showed no supersaturation. On the other hand, PB-PC in the metastable state showed similar solubility behavior to PB-PC. It became apparent that there is a difference in the solubility between the two conditions, and a metastable state was of greater advantage for the improvement of the solubility behavior of PB.

Figure 3 shows the dissolution patterns. In pH 1.2 medium, the dissolution percent of PB within 5 min was 35% from PB crystals, whereas it was above 90% from PB-PC. The dissolution was a little faster from PB-PC (0.25) than from PB-PC (0.75), but there was no marked difference. In pH 6.8 medium, the dissolution from PB crystals was faster than that in pH 1.2 because of the higher solubility. In contrast, dissolution from PB-PC (0.50) did not affect the pH; 90% of the PB dissolved within 5 min. PB dissolved almost completely from PB-PC though PHT dissolved only 75% from PHT-PC (0.25) in pH 6.8 medium,[3] although the same interaction pattern was indicated by infrared spectra and thermal analysis. It was considered to be because the solubility of PB is very much higher (about 100-fold) than PHT, and/or PB, but not PHT, is ionized in pH 6.8.

As mentioned above, the maximum concentration of PB with PB-PC was only 1.2 times the PB solubility, but the dissolution rate was improved, particularly in the pH 1.2 medium.

Bioavailability Studies PB is absorbed well by oral

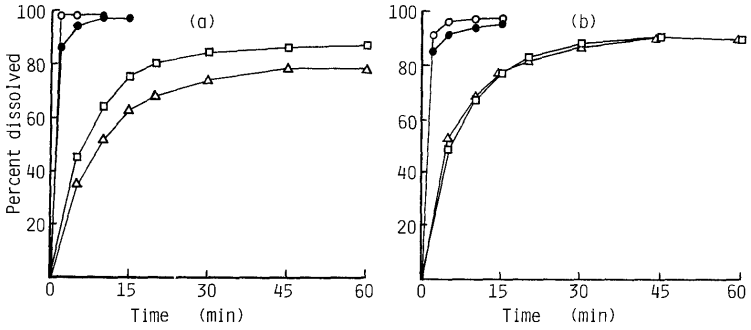

Fig. 3. Dissolution of PB from PB-PC in pH 1.2 (a) and 6.8 (b) Medium
△, PB crystals; □, physical mixture (0.75); ○, PB-PC (0.25); ●, PB-PC (0.75).

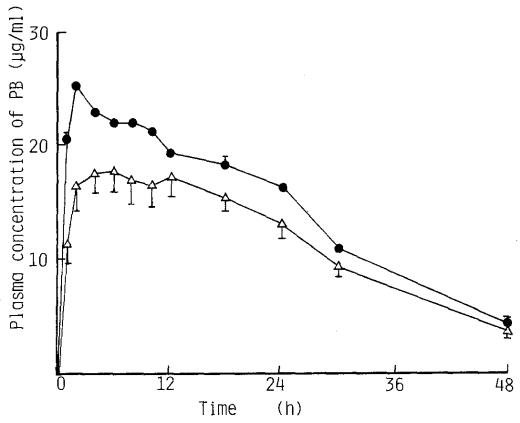

Fig. 4. Plasma Concentration of PB Following Administration of PB Crystals (△) and PB-PC (0.75) (●)

administration,[5] but sometimes the absorption is delayed because of slow dissolution.[6] There were not many problems in steady-state therapy of the convulsant, but some problems arose if PB was used as a hypnotic. The dissolution rate of PB is improved in both pH 1.2 and 6.8 by using PB-PC. Thus, the plasma concentration of PB following PB-PC administration was compared with that following PB crystals. PB-PC (0.75) was used because the dissolution rate showed no marked difference between the mole fraction of PB, the physicochemical property showed no change with time as did PB-PC (0.25) or (0.50),[1] and the amount of PC in PB-PC was minimum so that the influence of PC is thought to be small.

Figure 4 shows the plasma concentrations of PB following oral administration at a dose of 15 mg/kg PB equivalent. The bioavailability parameters (maximum concentration (C_{max}), time to maximum concentration (T_{max}) and area under the plasma concentration curve (AUC)) are shown in Table I. Following the administration of PB as PB-PC (0.75), the plasma concentration after 1 h was 20 μg/ml, and was 2-fold following an administration of PB crystals. C_{max} became significantly higher and T_{max} was faster than those with PB crystals. This suggests the improvement of the absorption rate. $AUC_{0-48\,h}$ after an administration of PB-PC (0.75) tended to be higher, but not significantly so. It was considered that the improvement of the dissolution rate affected the absorption rate.

TABLE I. Bioavailability Parameters after Oral Administration of PB at a Dose of 15 mg/kg

	C_{max} (μg/ml)	T_{max} (h)	$AUC_{0-48\,h}$ (μg·h/ml)
PB crystals	18.8±2.2	5.0±0.6	567±63
PB-PC (0.75)	25.3±0.6[a)]	2.0±0.0[a)]	692± 7

Each value represents mean ± S.E. of 4 rabbits. *a)* Significantly different ($p<0.05$) from PB crystals.

References and Notes

1) M. Fujii, K. Harada and M. Matsumoto, *Chem. Pharm. Bull.*, **38**, 2237 (1990).
2) M. Fujii, H. Terai, T. Mori, Y. Sawada and M. Matsumoto, *Chem. Pharm. Bull.*, **36**, 2186 (1988).
3) M. Fujii, K. Harada, K. Yamanobe and M. Matsumoto, *Chem. Pharm. Bull.*, **36**, 4908 (1988).
4) J. E. Slonek, G. W. Peng and W. L. Chiou, *J. Pharm. Sci.*, **67**, 1462 (1978).
5) S. E. Leucuta, L. Popa, M. Ariesan, L. Popa, R. D. Pop, M. Kory and S. Toader, *Pharm. Acta Helv.*, **52**, 261 (1977).
6) M. C. Meyer, A. B. Straughn, G. Raghow, W. L. Schary and K. S. Rotenberg, *J. Pharm. Sci.*, **73**, 485 (1984); F. Moolenaar, B. Koning and T. Huizinga, *Int. J. Pharmaceut.*, **4**, 99 (1979).

Effect of Inserted Bacteriohopane-32-ol on the Stability of Liposomal Membranes

Akira NAGUMO,* Kazuya TAKANASHI, and Yasuo SUZUKI

Pharmaceutical Institute, Tohoku University, Aobayama, Sendai 980, Japan. *Received November 5, 1990*

Bacteriohopane-32-ol (Monol), a hopanoid with one hydroxy group in the side chain, was prepared from hopanoids of *Rhodopseudomonas palustris* and incorporated into liposomal membrane composed of dipalmitoylphosphatidylcholine (DPPC). The effect of the inserted hopanoid on the stability of liposomes was compared with that of cholesterol (Cho) by measuring the release of 6-carboxyfluorescein (CF) entrapped in the liposomes. Monol has a stabilizing effect on liposomal membrane but its effect is different from that of Cho. Incorporation of Cho enhanced the stability of liposomes by increasing the contents. However, the incorporation of Monol at a low content of 20 mol% lowered, and that at higher contents increased, the stability. Furthermore, in the liposomes incorporated with Monol, there is no difference between the release of CF after incubation at 37 °C and 45 °C.

Keywords hopanoid; triterpenoid; liposome; cholesterol; membrane stability

Hopanoids are derivatives of a hopane family which has basic skeletons of pentacyclic triterpenes and are widely distributed in prokaryotes.[1] Hopanoids are considered to be structural and functional equivalents of sterols and to act as membrane reinforcers in prokaryotic systems as sterols do in the membranes of eukaryotes.[2] The function of cholesterol (Cho) is understood on the basis of its effect on artificial membranes.[3] By adding Cho to phospholipids composed of saturated fatty acyl chains, the calorimetic curve becomes progressively less sharp as the concentration increases, until it is abolished. Below the transition temperature (*Tm*), Cho tends to increase the disorder of phospholipid molecules, particularly in the hydrocarbon chains (fluidizing effect). Above *Tm*, Cho tightly assembles the molecules of phospholipid in bilayers (condensing effect) and the membrane is less permeable to small hydrophilic molecules and ions.[4] Hopanoids also have been shown to be effective in condensing phospholipid molecules in artificial membrane, and to provide a stable membrane.[5,6] Bacteriohopane-32-ol (Monol) is a semi-artificial molecule derived from many common hopanepolyols, and has a molecular resemblance to cholesterol particularly in polarity (Fig. 1). In this report, we describe the effect of Monol on the stabilization of liposomes composed of dipalmitoylphosphatidylcholine (DPPC) by measuring the release of 6-carboxyfluorescein (CF) entrapped in liposomes.[7,8]

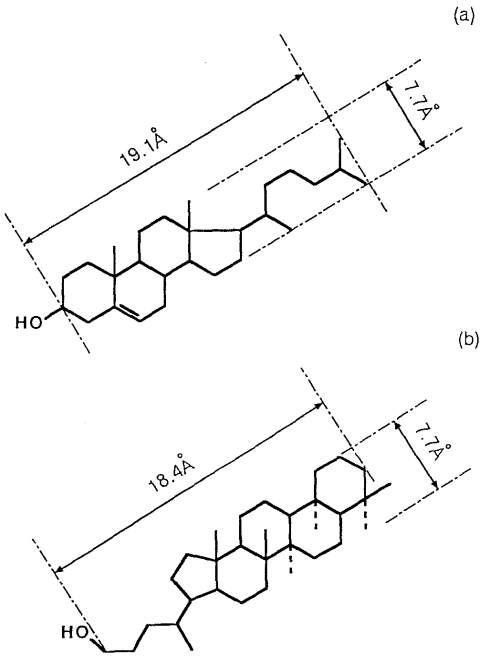

Fig. 1. Structure of Cho (a) and Monol (b)

Materials and Methods

Chemicals DPPC and dicetyl phosphate (DCP) were purchased from Nippon Oil & Fats Co., Ltd. and ICN K&K Laboratories, Inc., respectively. Cholesterol (Wako Pure Chemical Industries, Ltd.) was recrystallized from C_2H_5OH–H_2O. CF (Eastman-Kodak) was treated with activated charcoal, recrystallized from C_2H_5OH–H_2O (1 : 2) and purified by using a Sephadex LH-20 column with H_2O as the eluent.[9]

Purification of Monol Monol was prepared from *Rhodopseudomonas palustris* by the method of Rohmer *et al.*[10,11] with a slight modification as follows. The bacterial cells were harvested by centrifugation (10000 × *g*, 10 min), freeze-dried and extracted with $CHCl_3$–CH_3OH (2 : 1, v/v). The crude extract was submitted to H_5IO_6–$NaBH_4$ treatment and acetylated overnight at room temperature using acetic anhydride and pyridine (1 : 1, v/v). The acetylated Monol was separated by flash chromatography on silica gel using $CHCl_3$ as the eluent and deacetylated with 0.5% methanolic $NaOCH_3$ for 30 min at room temperature. The product was again separated by flash chromatography and further purified by thin layer chromatography (TLC) on silica gel using $CHCl_3$ as the eluent. Monol was identified by gas liquid chromatography (GLC) retention time and mass spectrum with the authentic standard which was a kind gift from Prof. M. Rohmer (Ecole Nationale Supérieure de Chimie de Mulhouse, France).

Preparation of Liposomes Reverse-phase evaporation vesicles (REV) were prepared by the method of Szoka *et al.*[12] with a slight modification. To the mixture of DPPC (10 μmol), DCP (2.5 μmol) and various amounts of Cho or Monol (2.5, 5, 7.5 μmol) dissolved in 2 ml of $CHCl_3$, 0.5 ml of phosphate buffered saline (PBS), pH 7.4, containing 50 mM CF was added. The resulting two-phase system was vigorously vortexed for 1 min and sonicated in a bath-type sonicator until the mixture became a homogeneous opalescent dispersion. $CHCl_3$ was removed under 360 mmHg for 10 min at 20 °C in a rotary evaporator and subsequently with maximum power of an aspirator for 40 min. Liposomes containing CF were separated from free CF by passing through a Sephadex G-50 column with PBS as the eluent.

Measurement of Liposomal Stability To 100 μl of liposomal suspension in a cuvette were added 3 ml of PBS containing 0.03% Triton X-100. Fluorescence (Dye_t) was measured at excitation and emission wavelengths of 490 and 515 nm, respectively. For the measurement of stability, liposomes were incubated in PBS at 37 °C or 45 °C. Aliquots of 100 μl were collected as the samples at time intervals, diluted to 3 ml with PBS and their fluorescences (Dye_f) measured. Liposomal stability was estimated as CF latency from 100 $(Dye_t - Dye_f)/Dye_t$ where t and f denote total and free dye, respectively.

Results and Discussion

Figure 2 shows the stabilizing effect of Cho and Monol on liposomal membranes at 37 °C. Both molecules have

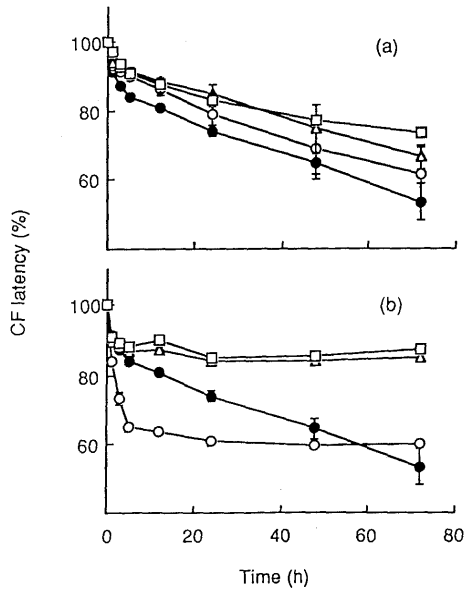

Fig. 2. Stability of Liposomes Containing Cho (a) and Monol (b)

Experiments were performed at 37 °C in PBS. Cho or Monol content: 0 mol% (—●—), 20.0 mol% (—○—), 33.3 mol% (—△—) and 42.9 mol% (—□—). Latency values were expressed as the mean ±S.D. ($n=4$).

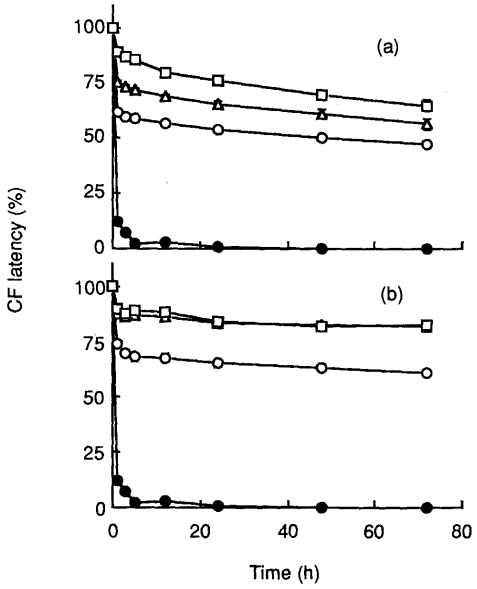

Fig. 3. Stability of Liposomes Containing Cho (a) and Monol (b)

Experiments were performed at 45 °C in PBS. The symbols are the same in Fig. 1.

differences with regard to the stabilization of liposomes. Incorporation of Cho enhanced the stability by increasing its content to 42.9 mol%. However, incorporation of Monol lowered, at a low content of 20 mol%, and that at higher contents drastically increased, the stability of the liposomes. The alicyclic ring structure of the hopanoid has perpendicularly oriented methyl groups on both sides of the pentacyclic ring plane. Its methyl groups will possibly disturb hydrophobic interaction of phospholipid acyl chains. At 45 °C, as shown in Fig. 3, incorporation of Cho into liposomes markedly enhanced the stability by increasing its content. These results agree with reports by other workers.[13-15] Monol stabilized liposomes more effectively than Cho at every contents.

The stability of liposomes at 37 °C was higher than that at 45 °C irrespective of the Cho contents. In contrast, there was little difference between the two temperatures in the stability of liposomes incorporated with Monol.

In addition to an almost planar steroid ring system, Cho possesses a 3β-hydroxyl group and hydrophobic tail giving the molecule an amphiphilic character. This makes Cho surface-active, causing its polar hydroxy group to orient with the hydrophilic headgroup of phospholipid bilayer in the aqueous phase, and its hydrophobic steroid ring to orient with the fatty acyl chains of the phospholipid. Cho may strongly influence the acyl chains of DPPC by its ability to restrict mainly the first ten carbon atoms of acyl chains.[4] On the other hand, as the pentacyclic ring of hopanoids is rigid, and as their molecular dimensions (length and cross sectional distance) fit well with those of the hydrophobic part of the phospholipid, cooperative van der Waals forces impart some additional rigidity to the hydrocarbon chains.[1] Monol seems to be oriented parallel to the fatty acyl chains of the phospholipids in an inverted orientation compared to Cho, as the hydroxy group is in the side chain and not in the ring structure. There was a well-established relationship between membrane fluidity and the permeability for small hydrophilic molecules and ions.[4] Liposomes containing Monol may increase the degree of order of phospholipid molecules in the liquid-crystalline state.

In all cases containing Cho, liposomes gradually released their content up to 72 h. However, liposomes containing Monol rapidly released their content to a certain extent and ceased from releasing at a constant level. This behavior may be a unique property of liposomes containing Monol. The distribution of hopanoids in the phospholipid bilayer is not known and it influences the properties of liposomes responsible for this behavior.

Although prokaryotic membranes generally do not contain Cho, there is a wide distribution of hopanoids in cytoplasmic membranes of Cyanobacteria, Rhodospirillaceae and Methylotrophes.[10,16] *Bacillus acidocaldarius* is a unique bacterium among Bacilli and grows optimally at pH 3 and 65 °C. The content of hopanoids in *B. acidocaldarius* increased from 4 to 16% of the total lipids when the temperature was raised from 50 to 65 °C.[17] The content of hopanoids in *Zymomonas mobilis*, which is an anaerobic ethanol-producing bacterium, also increased when the growth temperature was raised.[18] It therefore seems that hopanoids have a direct role in stabilizing bacterial membranes that are subjected to potential lysis-inducing stress.

Rohmer *et al.*[16] suggested that hopanoids are functional analogues and phylogenetic precursors of cholesterol. The functional analogy of hopanoids to Cho is further supported by our results showing the stabilizing effect of Monol on DPPC liposomes.

References

1) G. Ourisson, M. Rohmer, and K. Poralla, *Ann. Rev. Microbiol.*, **41**, 301 (1987).
2) R. F. Taylor, *Microbiol. Rev.*, **48**, 181 (1984).
3) L. Y. Philip, *Biochim. Biophys. Acta*, **822**, 267 (1985).
4) R. A. Demel and B. de Kruyff, *Biochim. Biophys. Acta*, **457**, 109 (1976).
5) K. Poralla, E. Kannenberg, and A. Blume, *FEBS Lett.*, **113**, 107

(1980).
6) E. Kannenberg and K. Poralla, *Naturwissenschaften*, **67**, 458 (1980).
7) J. N. Weinstein, S. Yoshikami, P. Henkart, R. Blumenthal, and W. A. Hagins, *Science*, **195**, 489 (1977).
8) D. H. Wreschner and G. Gregoriadis, *Biochem. Soc. Trans.*, **6**, 922 (1978).
9) J. N. Weinstein, R. Blumenthal, S. O. Sharrow, and P. A. Henkart, *Biochim. Biophys. Acta*, **509**, 272 (1978).
10) M. Rohmer, P. Bouvier-Nave, and G. Ourisson, *J. Gen. Microbiol.*, **130**, 1137 (1984).
11) S. Neunlist, P. Bisseret, and M. Rohmer, *Eur. J. Biochem.*, **171**, 245 (1988).
12) F. Szoka, Jr. and D. Papahadjopoulos, *Proc. Natl. Acad. Sci. U.S.A.*, **75**, 4194 (1978).
13) P. L. Yeagle, R. B. Martin, A. K. Lala, H-K. Lin, and K. Bloch, *Proc. Natl. Acad. Sci. U.S.A.*, **74**, 4924 (1977).
14) R. A. Demel, K. R. Bruckdorfer, and L. L. M. van Deenen, *Biochim. Biophys. Acta*, **255**, 321 (1972).
15) D. Papahadjopoulos, S. Nir, and S. Ohki, *Biochim. Biophys. Acta*, **266**, 561 (1971).
16) M. Rohmer, P. Bouvier, and G. Ourisson, *Proc. Natl. Acad. Sci. U.S.A.*, **76**, 847 (1979).
17) K. Poralla, T. Härtner, and E. Kannenberg, *FEMS Microbiol. Lett.*, **23**, 253 (1984).
18) A. Schmidt, S. Bringer-Meyer, K. Poralla, and H. Sahm, *Appl. Microbiol. Biotechnol.*, **25**, 32 (1986).

Insulin-Carrying Microspheres, *in Vitro* Studies

Sveinbjörn GIZURARSON*,[1] and Erik BECHGAARD

The Royal Danish School of Pharmacy, Department of Pharmaceutics, Universitetsparken 2, DK-2100 Copenhagen Ø, Denmark.
Received November 30, 1990

Loading and release characteristics of insulin-carrying albumin and starch microspheres have been studied *in vitro*. The sorption characteristics of ^{125}I-labelled insulin onto albumin microspheres were studied and were found to be completed within 5 h, and the loading capacity was found to be 0.14% w/w. Insulin did not show any sorption into the matrix of the starch microspheres. The release characteristics were analyzed by high performance liquid chromatography. About 80% was released within 5—10 min from albumin microspheres and starch microspheres, respectively.

Keywords adsorption; insulin; microsphere; release; sorption

Introduction

Growing attention has been paid to the preparation of delivery systems based on drug-loaded colloidal carriers such as microspheres. To attain the desired therapeutic effects in these systems, the release characteristics of a drug to the surrounding medium over a certain period of time is very important. More than 90 drugs have been incorporated into albumin microspheres and their release profiles have been reported, as reviewed.[2]

Bioadhesive microspheres, which form gel-like structures in contact with a mucous surface such as the nasal membrane, thereby prolonging the contact between the delivery system and the surface, have a potential for releasing the drug in a sustained and controlled manner, possibly increasing the absorption efficiency of the drug.[3] *In vitro* studies of insulin loaded microspheres have been investigated to achieve the prolonged release of insulin[4-6] and to increase absorption across the nasal membrane in rats.[7,8] The release of drugs from microspheres is generally biphasic, with an initial rapid release phase (called the "burst effect"), where the drug adsorbed on the surface is released, followed by a slower release phase where the drug incorporated into the matrix is released over a long period.

The purpose of the present paper is to study, *in vitro*, the sorption and release characteristics of insulin from produced albumin and commercially available starch microspheres.

Materials and Methods

Materials Zinc-free human insulin powder and mono-^{125}I-(Tyr A14)-human insulin (202 μCi/μg) was obtained as a gift from Novo Industry A/S and prepared in 0.1 M Tris buffer (pH = 7.4). 25% w/v 1.5-glutaraldehyde and rabbit serum albumin (RSA), (fraction V, RIA grade) were obtained from Sigma Chemical Company (St. Louis, MO. U.S.A.). Petroleum ether, highly refined olive oil and ethanol were obtained from Mecobenzon (Copenhagen, Denmark). Distilled water was used throughout and all other chemicals were of a reagent grade.

Microspheres Albumin microspheres were produced by an emulsification technique described by Burger *et al.*[9] with slight modifications. 500 ml of highly purified olive oil was mixed with 750 ml of petroleum ether and prestirred for 15 min in a 3000 ml flat-bottomed glass beaker (equipped with four 10 mm deep baffles positioned against the wall of the beaker) using a Heidolph mixer (Heidolph Electro Gmbh. Kelheim, Germany). In order to crosslink the microspheres, 20 ml of a 25% w/v aqueous solution of RSA in phosphate buffer (pH 7.4) was added in aliquots of 2.0 ml, and stirring was continued at 600 rpm for 15 min. The microspheres were isolated by centrifugation, washed with petroleum ether, filtered through a Millipore filter (Mitex: CJJ 621 A6) by washing with petroleum ether and ethanol and then freeze-dried overnight.

Freeze-dried starch microspheres (Spherex®) (swelling factor 8-10) were obtained as a gift from Pharmacia AB (Uppsala, Sweden), and used as obtained.

Particle Size Analysis The microspheres were sized in normal saline using a Coulter Counter model TA_{II}, Coulter Counter Electronics Ltd. (Herts, U.K.). The particle size was expressed as a mean volume diameter. The mean particle diameters of the swollen microsphere systems were found to be about 58 ± 13 and 40 ± 8 μm (swelled size) for the albumin and the starch microspheres, respectively.

Sorption Characteristics The sorption characteristics of insulin to the albumin and starch microspheres was evaluated by suspending the microspheres (70 mg) into 2.5 ml of an insulin solution containing ^{125}I-labelled insulin at about 20.8 mg/ml and about 180 nCi/ml. At selected time intervals (1, 3, 8, 16, 18, 22 and 46 h), about 10 mg samples of microspheres were taken from the suspension, filtered (no significant adsorption was found to occur to the filters) and washed with ethanol, and the activity detected by the γ-counter. The quantities measured at 24 h sorption time were taken as equilibrium values.

Release Characteristics The *in vitro* release of insulin was evaluated using about 10 mg of microspheres, carrying about 0.10—0.13 mg insulin/mg. The sorption of insulin to the microsphere systems was performed by suspending 100 mg of microspheres in 5 ml of an insulin solution containing about 20.8 mg/ml. After storage at ambient room temperature for 24 h, the albumin microspheres were separated from the solution by filtration, resuspended in water and then freeze-dried. In these experiments the starch microspheres were freeze-dried directly after storage without separation of the microspheres from the insulin solution. The microspheres were suspended in an 11 ml Tris-buffer at pH 7.4 (sink condition) and kept at 25 °C. At selected time intervals samples of 25 μl were taken from the top of the suspension and injected directly into the high performance liquid chromatography (HPLC) system. Prefiltration was not possible, since the HPLC-microfilters were found to adsorb about 14% (0.14 mg/cm^2) of the insulin. 25 μl of the buffer were added to the suspension after each sampling to maintain a constant volume.

Calculations The maximal sorption capacity was calculated by HPLC determination of the decrease in the insulin concentration after the addition of microspheres ($t = 24$ h).

Analytical Methods The amount of insulin sorbed to the microsphere systems was analyzed by means of a γ-counter. About 5—10 mg samples containing the labelled ^{125}I-insulin were detected by an LKB-Wallac 1272 CliniGamma (Pharmacia, Hillerød, Denmark) γ-counter, and the total amount of insulin sorbed to the microspheres was calculated using a standard curve, corrected for background.

The release of insulin from the microsphere system was analyzed by the HPLC method described by,[10] with slight modifications. The Hitachi HPLC-system was from Merck and consisted of a model 655A-11 pump, a model 655A variable wavelength ultraviolet-detector and a Rheodyne model 7125 injection valve. The column was a 4 × 250 mm LiChrosorb® RP-18, 5 μm, from Merck and the guard column was a 4 × 25 mm Perisorb® RP-8, 30—40 μm, from Merck. The mobile phase was a mixture of two solutions, A and B (4 : 3). Solution A consisted of 0.04 M phosphoric acid, 0.2 M sodiumsulphate, and 10% acetonitrile, and its pH was 2.5 with ethanolamine. Solution B was a 50% acetonitrile solution. Detection at 214 nm; flow rate 1 ml/min; column temperature 25 °C and injection volume 20 μl. The retention time (t_R) was about 10 min. The sample concentration was calculated on the basis of the peak height multiplied by t_R relative to an external insulin standard (0.8 mg/ml in 0.1 N hydrochloric acid).

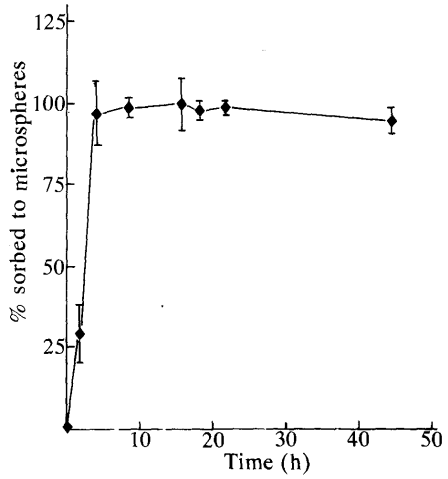

Fig. 1. The Sorption Profile of Insulin to Albumin Microspheres Expressed as a Percent of Maximal Loading Capacity; 0.14 mg/mg ($n=3$)

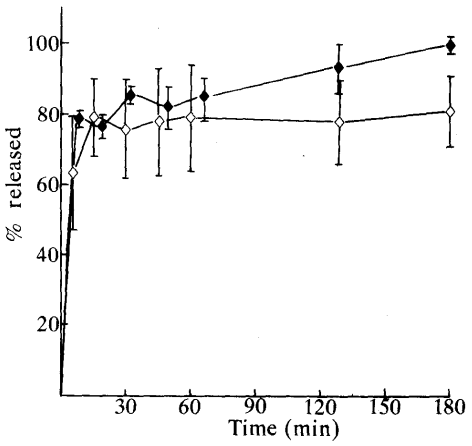

Fig. 2. The *in Vitro* Release of Insulin from Albumin ($n=6$) and Starch ($n=4$) Microspheres, Expressed Relative to the Amount Sorbed to the Microspheres

◆, albumin microspheres; ◇, starch microspheres.

Results and Discussion

Figure 1 gives the sorption profile of insulin to albumin microspheres. It shows that the sorption on and into the microspheres is completed within 3 h, as measured by labelled insulin, and the maximal sorption capacity was found to be 0.14 mg/mg microspheres, from an insulin solution containing 20.8 mg/ml. Since the loading of insulin to starch microspheres was performed by suspending the microspheres in insulin solution, followed by freeze-drying, the amount of insulin per weight microspheres could be adjusted as wanted. The sorption of insulin to albumin microspheres was found to be in accordance with Langmuir adsorption isotherm (data not shown).

In contrast to the albumin microspheres, the analysis of the insulin concentration, before and after addition of starch microspheres, showed that the concentration of insulin increased significantly from 16.7 to >20.8 mg/ml. This indicates that, during the swelling of the starch microspheres, water is removed from the insulin solution without allowing insulin molecules into the matrix. Hence, in all further experiments the "loading" of the starch microspheres with insulin was performed by freeze drying the microsphere–insulin suspension without prior separation.

Figure 2 shows the release profiles of insulin from albumin (about 0.14 mg/mg) and starch (about 0.11 mg/mg) microspheres as the percentage of insulin released with time. For both the albumin and starch microspheres, an initial fast release phase was observed. After the first 5—10 min about 80% of all insulin was released. In starch microspheres only, the initial phase tended to be followed by a second slower release phase, where about 20% of the insulin was released within 3 h. The rate and extent of release was not dependent on the amount sorbed to albumin or starch microspheres.

In conclusion, it has been demonstrated that in contrast to starch microspheres, albumin microspheres show the ability to sorb and carry native peptides such as insulin. The release profiles from albumin as well as from starch microspheres show a fast initial release phase which can be used clinically *e.g.* for the delivery of peptides to mucosal surfaces such as the nasal mucosa.[7,8] Microspheres are able to stick to the mucosal surface, thereby prolonging the duration of *e.g.* insulin at the absorption site. This could be preferable for increasing the amount absorbed intranasally,[11] but clinically relevant sustained release, from the studied microspheres, is not likely due to the fast *in vitro* release observed.

Acknowledgement This work was supported by Novo Nordisk A/S (Bagsværd, Denmark). The authors thank Mr. H. M. Højrup for skillful technical assistance.

References and Notes

1) Present address: *LYF H.F., The Icelandic Drug Delivery Group, Gardaflöt 16–18, IS-210 Gardabær, Iceland.*
2) E. Tomlinson, *Int. J. Pharm. Technol. Prod. Manuf.*, **4**, 49 (1983).
3) L. Illum, H. Jørgensen, H. Bisgaard, O. Krogsgaard and N. Rossing, *Int. J. Pharm.*, **39**, 189 (1987).
4) G. P. Royer, T. K. Lee and T. D. Sokoloski, *J. Parent. Sci. Techn.*, **37**, 34 (1983).
5) O. Saslawski, C. Weingarten, J. P. Benoit and P. Couvreur, *Life Sci.*, **42**, 1521 (1988).
6) S. Gizurarson and E. Bechgaard, in preparation.
7) E. Björk and P. Edman, *Int. J. Pharm.*, **47**, 233 (1988).
8) E. Björk and P. Edman, *Int. J. Pharm.*, **62**, 187 (1990).
9) J. J. Burger, E. Tomlinson, E. M. A. Mulder and J. G. McVie, *Int. J. Pharm.*, **23**, 333 (1985).
10) L. Snel, U. Damgaard and I. Mollerup, *Chromatographia*, **24**, 329 (1987).
11) S. Gizurarson, S. N. Rasmussen and F. Larsen, *J. Pharm. Sci.*, **80**, 505 (1991).

COOXIDATION OF ENONES DURING REACTION OF SUPEROXIDE WITH ACIDIC AROMATIC AMINES

Hiromasa TAKIZAWA, Tetsuo NAGANO and Masaaki HIROBE*

Faculty of Pharmaceutical Sciences, University of Tokyo, Hongo, Bunkyo-ku, Tokyo 113, Japan

Enones can be epoxidized by $O_2^{-\bullet}$ in the presence of various compounds having an acidic >NH group. Cyclic voltammetry and ESR study show that $O_2^{-\bullet}$ was disproportionated into H_2O_2 and O_2 by these compounds. Furthermore, H_2O_2 was deprotonated by unreacted $O_2^{-\bullet}$ and HOO^- was formed, which is widely known to be the effective oxidant in the epoxidation of enones. This confirms the strong basicity of $O_2^{-\bullet}$ in aprotic media, and we propose an alternative scheme for the Haber–Weiss reaction in the absence of metal ions.

KEYWORDS superoxide; Haber-Weiss reaction; hydroxyl radical; hydrogen peroxide; hydroperoxy anion; hydroperoxy radical; enone; oxidation

It has become clear that superoxide ($O_2^{-\bullet}$), a one-electron reduction product of dioxygen (O_2), plays important roles in various biological processes.[1] In spite of its involvement as a key intermediate, the chemical reactivity of $O_2^{-\bullet}$ itself is reported to be rather innocuous.[2] We have reported that $O_2^{-\bullet}$ can oxidize olefins and substrates having labile hydrogens in the presence of acyl halides,[3] polyhalides,[4] or CO_2.[5] In these reactions, $O_2^{-\bullet}$ reacts with halides to form peroxy intermediates which are more highly reactive than $O_2^{-\bullet}$ alone.[6] Furthermore, the phosphate moiety of nucleotides enhances the reactivity of $O_2^{-\bullet}$ in the nucleic base release reaction.[7]

A more intensive study of the $O_2^{-\bullet}$–adjunct agents system led us to the finding that $O_2^{-\bullet}$ can oxidize enones to the corresponding epoxides in the presence of nucleic bases and other compounds having an acidic >NH group (Table I).

These compounds were found to disproportionate $O_2^{-\bullet}$ into H_2O_2 and O_2 in DMSO. In this system, $O_2^{-\bullet}$ was shown to act as a base to form hydroperoxy anion (HOO^-) and hydroperoxy radical (HOO•) through deprotonation of H_2O_2 (Chart 1). The reaction of $O_2^{-\bullet}$ with H_2O_2 is well known to produce the hydroxyl radical (HO•) in the presence of Fe ions. This is called the Fe-catalyzed Haber-Weiss reaction (Chart 2).[8] In fact, adding Fe^{2+} to our system (KO_2-adjunct agent) produced no epoxide and the characteristic ESR signal of the PBN-CH_3 adduct was observed, ensuring HO• formation.[9] However, in the absence of a metal ion, the epoxidation of enones proceeded.

We used chalcone and its derivative (4'-methoxychalcone) as substrates. The reactivity of these

Table I. Epoxidation of Chalcone by KO_2–Adjunct Agent System

Adjunct agent	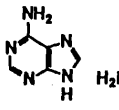 Adenine	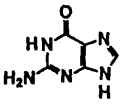 Guanine	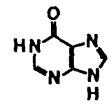 Hypoxanthine	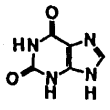 Xanthine	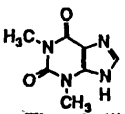 Theophylline
Yield% (Recovery%)	85 (2)	31 (59)	34 (44)	28 (59)	77 (0)
Adjunct agent	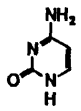 Cytosine	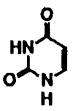 Uracil	 Imidazole	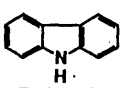 Carbazole	 Indole
Yield% (Recovery%)	53 (38)	80 (0)	61 (38)	54 (11)	21 (54)

Chart 1

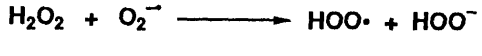

substrates was quite similar. Enones are decomposed by $O_2^{-\bullet}$ via base-catalyzed autoxidation, as reported by Frimer et al.[10] However, in the presence of the compounds shown in Table I, epoxidation of chalcone proceeded in fairly high yield (Chart 3).

Chart 2

$$H_2O_2 + O_2^{-\bullet} \xrightarrow[\text{Haber-Weiss reaction}]{Fe^{n+}} HO\bullet + HO^- + O_2$$

Chart 3

$$Ph\text{-}CH{=}CH\text{-}\overset{O}{\overset{\|}{C}}\text{-}Ph \xrightarrow[DMSO]{KO_2\text{-adjunct agent}} Ph\text{-}\underset{O}{CH}\text{-}\underset{O}{CH}\text{-}\overset{O}{\overset{\|}{C}}\text{-}Ph$$

Additive effects of adenine and adenosine on cyclic voltammogram of O_2 show that $O_2^{-\bullet}$ reacts with adenine, but not with adenosine (Fig. 1). $O_2^{-\bullet}$ was detected by ESR even after several hours without conversion into H_2O_2. But in the KO_2–adenine system, $O_2^{-\bullet}$ was not detected soon after the start of the reaction, and a large amount of H_2O_2 was formed (Fig. 2). This indicates that adenine can disproportionate $O_2^{-\bullet}$ into H_2O_2 and O_2 and that the acidic proton (of N-9 position) played an important role as a proton source.

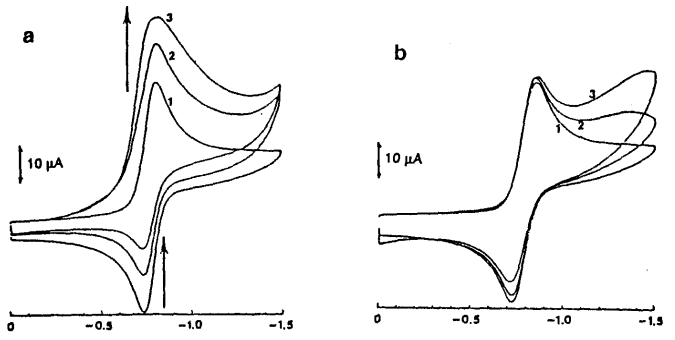

Fig. 1 Effect of Nucleic Bases on Cyclic Voltammogram of O_2.

Cyclic voltammograms of O_2 (curve 1), O_2 plus 0.5 mM adenine (a) or adenosine (b) (curve 2), and O_2 plus 1.0 mM adenine or adenosine (curve 3) in DMSO, containing 0.1 M tetraethylammonium perchlorate as a supporting electrolyte. Measurements were done using the platinum electrode at a scan rate of 0.05V/s.

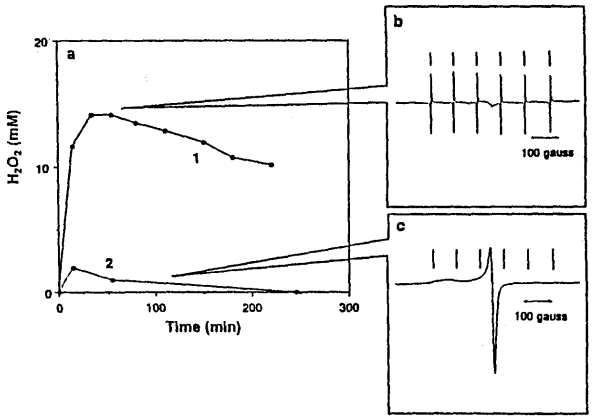

Fig. 2 Amounts of $O_2^{-\bullet}$ and H_2O_2 during the Reaction of KO_2 and Adenine or Adenosine

(a): line 1, amounts of H_2O_2 during the reaction of KO_2 and adenine; line 2, amounts of H_2O_2 during the reaction of KO_2 and adenosine. (b): ESR spectra of $O_2^{-\bullet}$ during the reaction of KO_2 and adenine. (c); ESR spectra of $O_2^{-\bullet}$ during the reaction of KO_2 and adenosine. H_2O_2 was measured by the method of Allen et al.[16] ESR spectra were recorded at 77K under the conditions as follows: microwave power 10 mW, modulation frequency 100 kHz with an amplitude of 6.3G, gain 4x100 (b), 4x1 (c), and response time 0.3s. The six arrows indicate the signal of Mn^{2+}.

We have also examined the correlation between the epoxidation yields and the pKa values in DMSO of these compounds.[11] In contrast to uracil, adenine, imidazole, carbazole and indole (pKa=14.1, 14.2, 18.6, 19.9, 20.95, respectively), pyrrole, 2-pyrrolidone and 2-piperidone (23.0, 24.2, 26.4, respectively) did not react with $O_2^{-\bullet}$, thus no H_2O_2 was formed, and no epoxidation of chalcone proceeded. Adenine, after deprotonation, was most probably converted into stable potassium salt, as Frimer et al. have reported,[12] since the consumption of adenine and the appearance of its oxidized products do not appear in HPLC. This shows that $O_2^{-\bullet}$ can abstract a proton from weakly acidic compounds whose pKa values are as high as *ca* 22.

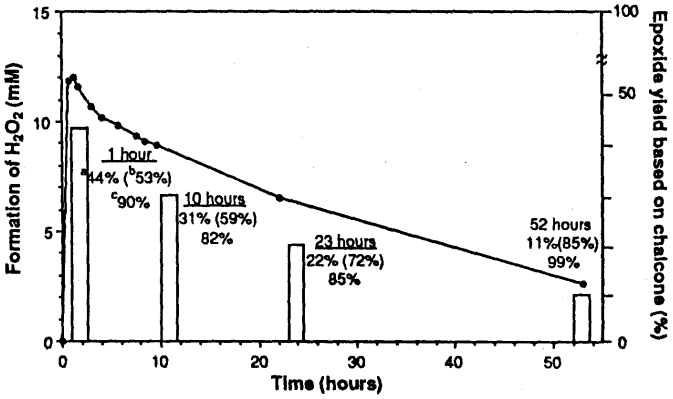

Fig. 3 Time Course of H_2O_2 Formation and H_2O_2 Concentration-Dependent Epoxidation of Chalcone.

Curve with solid circles shows H_2O_2 concentration in DMSO 90 ml containing adenine 4.2 mmol and KO_2 4.2 mmol (solution A). Open column shows the yield of chalcone epoxidation, when chalcone 0.35 mmol, 18-crown-6-ether 0.35 mmol and a small portion of KO_2 were dissolved in 15 ml of the solution A. [a]Yield of epoxide based on chalcone. [b]Chalcone recovery. [c]Yield of epoxide based on H_2O_2.

The H_2O_2 formed was then deprotonated by unreacted $O_2^{-\bullet}$ which acted as a strong base, and HOO^- was produced (Chart 1). HOO^- reacts with enones to form the corresponding epoxides.[13]

Figure 3 shows the time course of the formation of H_2O_2 in the KO_2-adenine system. The DMSO solution containing H_2O_2 produced from KO_2 and adenine with no $O_2^{-\bullet}$ remaining did not oxidize chalcone to the epoxide. However, the epoxidation did proceed upon addition of a small portion of KO_2 into the solution at 1 h, 10 h, 23 h, and 52 h after the first mixing of KO_2 and adenine. The yields based on H_2O_2 concentration were as high as 80~90% at each stage. The epoxide yield based on chalcone completely depended on the H_2O_2 concentration (Fig. 3). These data clearly show that H_2O_2 formed from the disproportionation of $O_2^{-\bullet}$ was deprotonated by $O_2^{-\bullet}$ to produce HOO^-, which was the ultimate reactant in the epoxidation of chalcone.

The Haber-Weiss reaction in the presence of Fe ion has been unanimously regarded as the most important one in the research concerning $O_2^{-\bullet}$. A number of reports have concluded that HO• produced through this reaction must be the ultimate toxin of reactive oxygen species.[14] The rate of the reaction is thought to be too slow in the absence of metal ions,[15] but no extensive investigation has been made in this respect. Our investigation carried out in the absence of metal ions in organic solvent shows the formation of HOO^- and HOO•, during which $O_2^{-\bullet}$ acted as a base. This is the alternative scheme for the Haber-Weiss reaction in the absence of metal ion, and proves meaningful in the field of $O_2^{-\bullet}$ study.

ACKNOWLEDGEMENT The authors are grateful for a research grant from the Ministry of Education , Science and Culture of Japan.

REFERENCES

1) J. M. McCord, *Science*, **185**, 529 (1974); B. N. Ames, *ibid*, **221**, 1256 (1983); L. Fucci, C. N. Oliver, M. J. Coon and E. R. Stadman, *Proc. Natl. Acad. Sci., U. S. A.*, **80**, 1521 (1983); I. Semsei, G. Rao and A. Richardson, *Biochem. Biophys. Res. Commun.*, **164**, 620 (1989); D. R. Ambruso, B. G. J. M. Bolscher, P. M. Stokman, A. J. Verhoeven and D. Roos, *J. Biol. Chem.*, **265**, 924 (1990); K. Kobayashi, K. Hayashi and M. Sono, *ibid.*, **264**, 15280 (1989).
2) D. T. Sawyer and S. Valentine, *Acc. Chem. Res.*, **14**, 393 (1981).
3) T. Nagano, K.Arakane and M. Hirobe, *Chem. Pharm. Bull.*, **28**, 3719 (1980); T. Nagano, K. Yokoohji and M. Hirobe, *Tetrahedron Lett.*, **24**, 3481 (1983); T. Nagano, K. Yokoohji and M. Hirobe, *ibid.*, **25**, 965 (1984).
4) H. Yamamoto, T. Nagano and H. Hirobe, *J. Biol. Chem.*, **263**, 12224 (1988); T. Nagano, H. Yamamoto and M. Hirobe, "The Biological Role of Reactive Oxygen Species in Skin," University of Tokyo Press, Tokyo, 1988, pp 241-251; H. Yamamoto, T. Mashino, T. Nagano and M. Hirobe, *J. Am. Chem. Soc.*, **108**, 539 (1986).
5) H. Yamamoto, T. Mashino, T. Nagano and M. Hirobe, *Tetrahedron Lett.*, **30**, 4133 (1989).
6) T. Nagano, H. Yamamoto and M. Hirobe, *J. Am. Chem. Soc.*, **112**, 3530 (1990).
7) H. Yamane, N. Yada, E. Katori, T. Mashino, T. Nagano and M. Hirobe, *Biochem. Biophys. Res. Commun.*, **142**, 1104 (1987).
8) F. Haber and J. Weiss, *Proc. R. Soc., London*, **A147**, 332 (1934); J. Weinstein and B. H. J. Bielski, *J. Am. Chem. Soc.*, **101**, 58 (1979).
9) W. Dixon, R. O. C. Norman and A. L. Buley, *J. Chem. Soc.*, **1964**, 3625; G. M. Rosen, Y. Chai and M. S. Cohen, *J. Biol. Chem.*, **261**, 4421 (1986); B. E. Britigan, T. J. Coffman and G. R. Buettner, *ibid.*, **265**, 2650 (1990).
10) A. A. Frimer and I. Rosenthal, *Photochem. Photobiol.*, **28**, 711 (1978); A. A. Frimer, P. G. Sharon, G. Aljadeff, H. E. Gottlieb, J. H. Buch, V. Marks, R. Philosof and Z. Rosental, *J. Org. Chem.*, **54**, 4853 (1989).
11) F. G. Bordwell, *Acc. Chem. Res.*, **21**, 456 (1988).
12) A. A. Frimer, G. Aljadeff and J. Ziv, *J. Org. Chem.*, **48**, 1700 (1983).
13) E. Weitz and A. Scheffer, *Ber.*, **54**, 2327 (1921); R. D. Temple, *J. Org. Chem.*, **35**, 1275 (1970).
14) O. I. Aruoma, B. Halliwell, E. Gajewski and M. Dizdaroglu, *J. Biol. Chem.*, **264**, 20509 (1989); J. A. Imlay and S. Linn, *Science*, **240**, 1302 (1988); K. Brawn and I. Fridovich, *Arch. Biochem. Biophys.*, **206**, 414 (1981).
15) W. H. Koppenol, J. Butler and J. W. Leeuwen, *Photochem. Photobiol.*, **28**, 655 (1978); C. Ferradini, J. Foos, C. Houee and J. Pucheault, *ibid.*, **28**, 697 (1978).
16) A. O. Allen, C. H. Hochanadel, J. A. Ghormley and T. W. Davis, *J. Phys. Chem.*, **56**, 575 (1952).

(Received May 13, 1991)

NOVEL DERIVATIZATION REAGENT WITH TETRATHIAFULVALENE AS AN ELECTROPHORE FOR PRE-COLUMN LABELING OF AMINES IN HIGH-PERFORMANCE LIQUID CHROMATOGRAPHY

Kazutake SHIMADA* and Tomoyuki OE
Faculty of Pharmaceutical Sciences, Kanazawa University, 13-1 Takara-machi, Kanazawa 920, Japan

A novel derivatization reagent with tetrathiafulvalene as an electrophore, N-succinimidyl tetrathiafulvalene-2-carboxylate, was prepared and evaluated for pre-column labeling of amine by using β-phenethylamine as a model compound in high-performance liquid chromatography with electrochemical detection. The reagent reacted readily with the primary amine at room temperature for 1 h, providing the amide which was highly responsive to an electrochemical detector (detection limit = 21 fmol, signal to noise ratio = 5) at a relatively low applied potential (+700 mV vs. Ag/AgCl). The characteristic two-stage oxidative pattern appeared on the hydrodynamic voltammogram of the derivative, which helped to identify the peak on the chromatogram.

KEYWORDS tetrathiafulvalene; electrophore; pre-column labeling; N-succinimidyl tetrathiafulvalene-2-carboxylate; amine; high-performance liquid chromatography; electrochemical detection

High-performance liquid chromatography (HPLC) with electrochemical detection (ED) is a useful way to determine trace components in biological fluids because it is selective and sensitive. Recently many pre- and post-column labeling methods have been developed to extend the applicability of HPLC-ED to electrochemically inactive compounds.[1] In our previous papers, we developed pre-column labeling reagents with guaiacol, aromatic amine or ferrocene as an electrophore to determine hydroxy, carboxy, thiol and amino compounds in HPLC-ED.[2] Recently much interest is focused on tetrathiafulvalene (TTF) and its derivatives whose charge transfer salts show metal-like properties such as high electroconductivity,[3] and many charge transfer salts of these compounds have been developed as organic superconductors.[4] We studied the intriguing electrochemical properties of TTF which is a two-stage redox system.[5, 6] The present paper deals with the preparation and properties of a novel derivatization reagent with TTF as an electrophore to determine amine in HPLC-ED.

A novel reagent, N-succinimidyl tetrathiafulvalene-2-carboxylate (**1**; **Chart 1**) was prepared from tetrathiafulvalene-2-carboxylic acid[6] by condensation with N-hydroxysuccinimide in the presence of dicyclohexylcarbodiimide. Properties of **1**: dark purple crystals from benzene. mp 172.5–173.5°C. ^{1}H-NMR ($CDCl_3$)δ : 2.87 [4H, s, $CO(CH_2)_2CO$], 6.35 and 6.36 (each 1H, each d, J=each 6.6 Hz, TTF-H), 7.69 (1H, s, TTF-H). High-resolution MS m/z: 344.9253 (M^+)(calculated for $C_{11}H_7NO_4S_4$, 344.9256). The reactivity and electrochemical properties of **1** were investigated using β-phenethylamine as a model compound. The apparatus used for HPLC was a TOSOH CCPD chromatograph equipped with an EICOM ECD-100 detector using glassy carbon as a working electrode. HPLC was carried out on a Chemcosorb 5-ODS-H (5 μm) column (15 cm x 0.46 cm i.d.) at a flow rate of 1 ml/min. β-Phenethylamine (10^{-5} M) with **1** (5 x 10^{-4} M) was quantitatively condensed at room temperature for 1 h in CH_3CN-pyridine-H_2O (5:1:4). This was confirmed by comparison with the peak area of the authentic derivative (**2**) [orange amorphous substance from benzene. mp 114.5–115.5°C. ^{1}H-NMR ($CDCl_3$)δ :2.86 (2H, t, J=6.9 Hz, $NCH_2\underline{CH_2}$-Ar), 3.58 (2H, q, convertible to t with 20% ND_3 in D_2O, J=6.9 Hz, $NC\underline{H_2}CH_2$-Ar), 5.58 (1H, br s, exchangeable with 20% ND_3 in D_2O, NH), 6.32 (2H, s, TTF-H), 7.01 (1H, s, TTF-H), 7.15–7.40 (5H, m, Ar-H). MS m/z: 351 (M^+)]. The derivatized amine showed a single peak of theoretical shape with a k' value of 5 [mobile phase; CH_3CN-H_2O (65:35) containing 0.05 M $NaClO_4$] and was highly responsive to the electrochemical detector with a detection limit of 21 fmol (signal to noise ratio = 5, +700 mV vs. Ag/AgCl), but the excess reagent came out at the solvent front.

The **Fig. 1** shows the hydrodynamic voltammograms of β-phenethylamine- together with the secondary amine-derivative [piperidine derivative (**3**): yellow amorphous substance from benzene. mp 149.5–151.0°C. ^{1}H-NMR

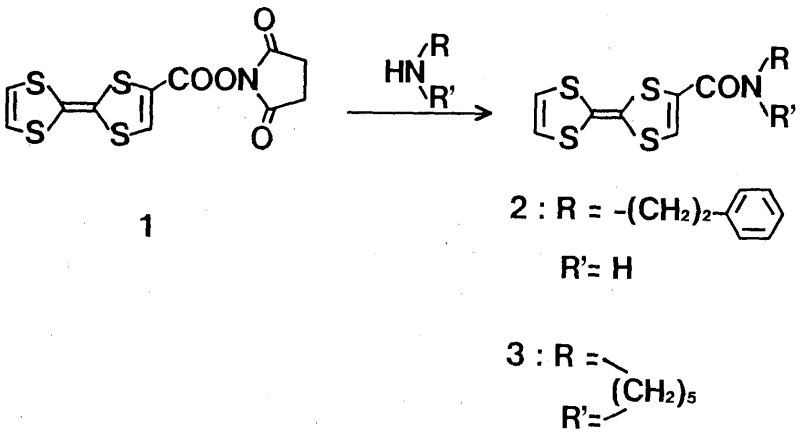

Chart 1

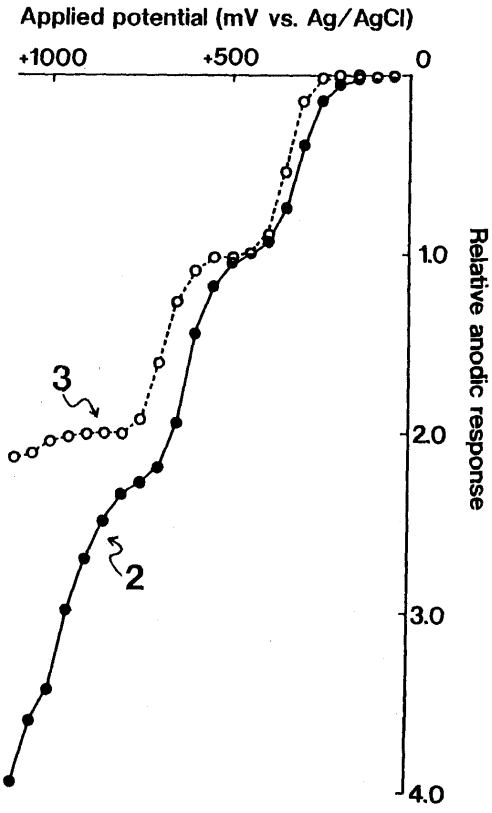

Fig. 1. Hydrodynamic Voltammograms of TTF Derivatives
Mobile phase: CH_3CN-H_2O (2, 70:30; 3, 65:35) containing 0.05 M $NaClO_4$. The response (peak height) of each compound at +450 mV was taken as 1.0.

($CDCl_3$) δ:1.50-1.75 (6H, m, piperidine-H), 3.56 (4H, br t, J= 5.4 Hz, piperidine-H), 6.32 (2H, s, TTF-H), 6.53 (1H, s, TTF-H). MS m/z: 315 (M^+)]. Both derivatives exhibited two-stage oxidative voltammograms due to the TTF moiety, which helped the selective detection of the TTF derivatives. In addition, derivative 2 showed a further increasing oxidative curve above +800 mV. This also occurred in the glycine ethyl ester derivative and may be due to the oxidation of amido and/or sulfur residues. These characteristic hydrodynamic voltammograms resulting from the amine moiety may be used to differentiate analytes having amine moieties. Although TTF has a redox system, these derivatives could not be detected by reductive ED after first oxidizing with a coulometric dual electrode detector (ESA 5100A). Such a phenomenon also occurs on polarographic reduction of TTF-radical cations in aqueous solution.[7] The details of this are now under investigation in our laboratories.

In conclusion, the newly developed derivatization reagent having tetrathiafulvalene as an electrophore has useful electrochemical properties for the sensitive analysis of biological substances. The development of this type of reagent having the reacting group toward the other functional group is now being conducted in our laboratories and the details will be reported elsewhere in near future.

ACKNOWLEDGEMENTS The authors are indebted to the staff of the central analytical laboratory of this Faculty for spectral measurements.

REFERENCES

1) K. Shimada and T. Oe, Yakugaku Zasshi, **111**, 225 (1991).
2) K. Shimada, Y. Kawai, T. Oe, and T. Nambara, J. Liquid Chromatogr., **12**, 359 (1989) and references cited therein.
3) J. Ferraris, D.O. Cowan, V. Walatka, Jr., and J.H. Perlstein, J. Am. Chem. Soc., **95**, 948 (1973).
4) H. Urayama, H. Yamochi, G. Saito, S. Sato, A. Kawamoto, J. Tanaka, T. Mori, Y. Maruyama, and H. Inokuchi, Chem. Lett., **1988**, 463 and references cited therein.
5) K. Nakasuji, M. Nakatsuka, and I. Murata, Yuki Gosei Kagaku Kyokaishi, **41**, 204 (1983).
6) D.C. Green, J. Org. Chem., **44**, 1476 (1979).
7) F. Wudl, G.M. Smith, and E.J. Hufnagel, J. Chem. Soc., Chem. Commun., **1970**, 1453.

(Received May 16, 1991)

ATOMIC FORCE MICROSCOPE IMAGES OF THE SURFACES OF ASPIRIN CRYSTALS AT SUBMOLECULAR RESOLUTION

Norio MASAKI,*, [a] Katsunosuke MACHIDA,[a] Hiroyuki KADO,[b] Kazuo YOKOYAMA [b] and Takao TOHDA[b]

Faculty of Pharmaceutical Sciences, Kyoto University,[a] Sakyo-ku, Kyoto 606, Japan and Central Research Laboratories, Matsushita Electric Industrial Co.Ltd.,[b] Moriguchi, Osaka 570, Japan

The atomic force microscope has been developed and used to image arrays of molecules at the (001) and (100) faces of aspirin crystals in water and in air. Lattice spacings composed of methyl groups and the part of the phenyl groups on the surface of the (001) in water, are consistent with X-ray diffraction data. The surface of (100) face which shows most perfect cleavage in bulk, is more difficult to image.

This initial success in imaging at drug crystal surfaces clarified the different structural behavior at the submolecular level for three crystal faces, and the close relationship to the differences in the dissolution velocity.

KEYWORDS atomic force microscopy; aspirin; submolecular resolution image; drug crystal surface; crystalline face

One of the most widely used drugs, aspirin, is commonly used by oral administration in solid dry form. The intestinal absorption rate of aspirin depends on its dissolution velocity and on the crystal habit.[1] Single crystals grown from ethanol solution were examined by X-ray diffraction [2] and the dissolution velocities for three crystal faces were measured.[3] Estimated lattice energy and surface energy were discussed in preceding papers.[2, 3] In this communication, we directly imaged the surfaces of those faces at the atomic level using the atomic force microscope.

The atomic force microscope (AFM) invented in 1986 by Binnig et al. [4] for insulators which do not generate tunnel current, is a variety of the scanning tunneling microscope. The atomic force microscope developed for this study is a modification of the improved original design. [5] The atomic forces between the tip of the stylus and the surface to be examined are detected by the deflection of a microfabricated cantilever with a tip made of silicon nitride Si_3N_4. The deflection was measured by the optical lever method monitoring laser light reflection from the cantilever at a two-segment photodiode. Scanning the specimen, including the vertical movement under the probing tip, is completed by a tripod type piezo complex with sub-angstrom scale sensitivity. Electronic equipment for feedback loop and imaging are used in the usual manner. A thin glass plate over the cantilever keeps a small amount of covering water on the specimen and the tip and prevents light scattering on the water drop surfaces.

Single crystals recrystallized from an ethanol solution of JP grade aspirin (99.5% acetylsalicylic acid C_6H_4 COOH $OCOCH_3$ in minimum) by slow evaporation,[3] were used throughout the experiments. They had developed (001) faces approximately 5-10 mm square and 1-3 mm thickness. Freshly cleaved surfaces of aspirin single crystals were prepared by hand with a razor blade at 20°C in

the room atmosphere. Silver paste or adhesive tape was used to mount the specimen on an aluminum plate which was screwed to the scanning device. Deionized water was applied before observation. Within a day after cleavage no significant change was observed under the AFM.

Molecular modeling of the surface of the aspirin crystals was done with the graphics software "MOLS system"[6] on a NEC9801 personal computer. The crystal data and atomic parameters including hydrogen atoms were taken from the previous paper[2] on X-ray diffraction analysis of aspirin.

An AFM image obtained from the surface of the (001) face of an aspirin crystal in water is shown in Fig. 1a. In the grey-scale image of raw data, the image size is 42 x 42 Å and 0.5 Å deep. This means that the brightest spots are 0.5 Å higher than the darkest background. A 0.7- Å thick surface model of the (001) faces calculated from 3-D crystal data of aspirin is shown in Fig. 1b with the same orientation as Fig. 1a, where hydrogen atoms are depicted with the van der Waals radius. Another 6- Å thick model including whole atoms of a molecule is shown in Fig. 1c in the same scale as Fig. 1b.

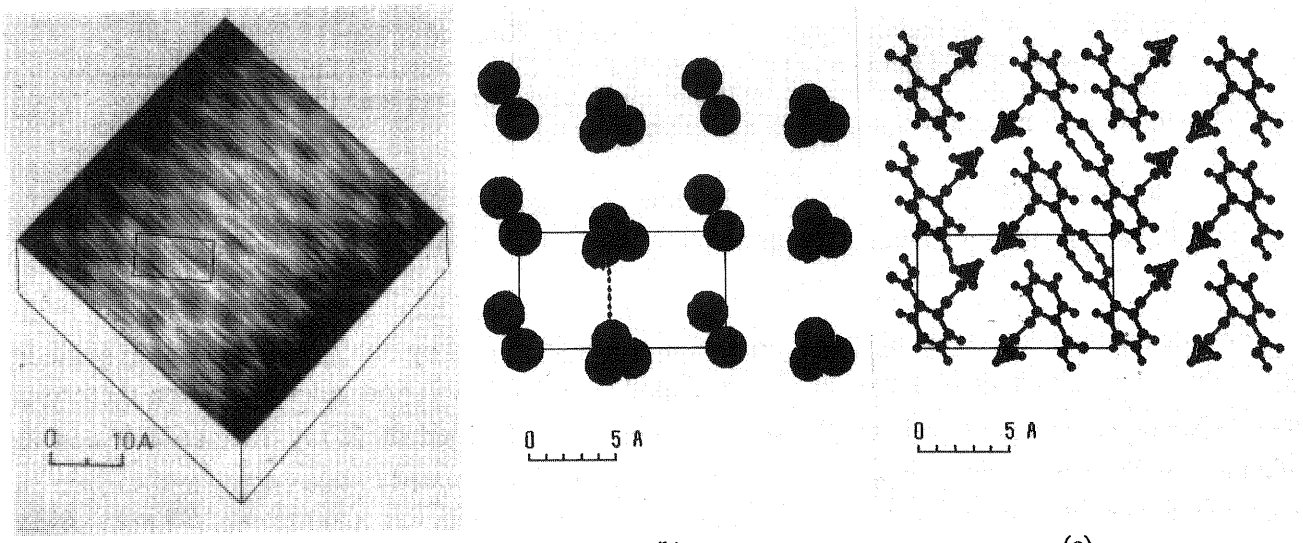

(a) (b) (c)

Fig. 1. Surfaces of the (001) Faces of Aspirin Crystals
(a) An AFM image of aspirin. The image area is 42 Å by 42Å. A 0.5-Å gradient from white, highest, to black, lowest, is shown as the gray scale image of the top view using the raw data. The unit cell, horizontal a-axis and vertical b-axis, of the lattice of the brightest spots is depicted. Arrays of the next highest spots are distinctly seen near half way but not exact half of the a-axis along the b-axis. (b) A 0.7-Å thick surface model. Hydrogen atoms within the space from the most jutted phenyl group hydrogen on the (001) surface are depicted using the van der Waals radius from x-ray diffraction data. The unit cell corresponding to Fig. 1a is shown as the most jutted hydrogen atom corners. (c) A 6Å thickness surface model. Whole atoms of a molecule are seen. Hydrogen bonds composing dimers and lines connecting the three hydrogen atoms of methyl groups are also depicted for convenience. The same scale and orientation of unit cell are applied as Fig.1b.

The AFM image of the surface of the (001) faces exhibits a clearly pronounced pattern of the lattice structure by the brightest spots, where a unit cell is depicted in the figure. The lattice constants a = 10.8 Å, b = 6.0 Å, $\gamma = 90°$ obtained from the AFM image are compared with the corresponding values in the crystal data a = 11.430 Å, b = 6.591 Å, c = 11.395 Å, $\beta = 95.68°$, ($\alpha = \gamma = 90°$), $P2_1 / a$, Z = 2.

The brightest spots with the diameters of approximately 2.4 Å are elongated to 4.5 Å in the hori-

zontal scanning direction. The most jutted atoms in the surface model for the (001) faces of the aspirin crystals are the hydrogen atoms HC5 [7] (four of these atoms are situated at the corner of the unit cell drawn in Fig. 1a and Fig. 1b.) of the phenyl groups. The second jutted atoms are hydrogen atoms HC9c (an array of these atoms are shown by the dotted line in Fig. 1b.) of the methyl groups situated 0.35 Å below the level of the top hydrogen HC5 of the phenyl groups. So the brightest spots in the AFM image are assumed to be the phenyl group hydrogen. And the next brighter but more diffused spots aligned along the b-axis between the array of the brightest spots are assumed to be the methyl group hydrogen. The distances between those two kinds of arrays, 6.0 Å and 4.7 Å, correspond respectively to the calculated values in the crystal, 6.46 Å and 4.97 Å. We therefore decided that those two kinds of spots were reduced to the part of the phenyl groups and to that of the methyl groups.

Even in air and on the uncleaved natural faces, we could image the surface of (001) faces by AFM, but for (100) and for (011) faces it became more difficult to image in this order. In bulk it is easier to have the perfect cleavage on (100) faces of aspirin crystals than on (001) faces though Niini[8] reported that the mineralogical cleavage for (001) was "vollkommen" and that for (100) was "deutrich". Umeyama et al.[9] calculated the interaction energies as −2.4 kcal/mol 100Å^2 for (001) faces of aspirin crystals and as −1.6 for (100) and concluded that (100) faces were the cleavage plane with the least interaction energy. It has been reported[10] that freshly cleaved surfaces are essential for AFM imaging because of contamination which exerts meniscus force and disturbs the atomic force measurement. In this study, the AFM imaging of the surface of the molecular crystals depended greatly on the crystal faces where anisotropic molecular arrangement was realized and cleavage in bulk did not always correspond to the easiness of the AFM imaging.

In conclusion, the initial success of AFM imaging of aspirin crystals at the submolecular level revealed that the molecular arrangement of aspirin on the surfaces of the (001) faces was as rigidly sustained as that inside the crystal examined by x-ray diffraction. On the other hand, the (100) and (011) faces become harder to image by AFM according to the order of dissolution velocity, including the (001)faces.

REFERENCES AND NOTES

1) H. Nogami and Y. Kato, Yakuzaigaku, 15, 154(1955);
A. Watanabe, Y. Yamaoka and K. Takada, Chem. Pharm. Bull., 30, 2958(1982)
2) Y. Kim, K. Machida, T. Taga and K. Osaki, Chem. Pharm. Bull., 33, 2641(1985).
3) Y. Kim, M. Matsumoto and K. Machida, Chem. Pharm. Bull., 33, 4125(1985)
4) G. Binnig, C. F. Quate and Ch. Gerber, Phys. Rev. Lett. , 56, 930(1986).
5) B. Drake,A.L. Prater, S. A. Weisenhorn, S.A.C. Gould, T.R. Albrecht, C.F. Quate, D.S.Cannell, H. G. Hansma and P.K. Hansma, Science, 243, 1586(1989) ; A.L. Weisenhorn, P.K. Hansma, T.R. Albrecht and C.F. Quate, Appl. Phys. Lett., 54, 2651(1989).
6) Y. Sasada, "Kobunshi No Kumitate (Polymer Construction in Japanese)", Kodansha Scientific Co.Ltd., Tokyo, 1990.
7) Nomenclature of the atoms in the aspirin molecule followed that of the preceding paper.
8) R. Niini, Z. Krist. , 79, 532(1931).
9) H. Umeyama, S. Nakagawa, and I. Moriguchi, J. Phys. Chem., 83, 2048(1979).
10) G. Meyer and N.M. Amer, Appl. Phys. Lett. 56, 2100(1990)

(Received May 21, 1991)

FACILE CONVERSION OF N^6-BENZOYLADENOSINES INTO 5'-CHLORO-5'-DEOXY-8-HYDROXYADENOSINES BY A REACTION WITH CUPRIC CHLORIDE: A PROMINENT SUBSTITUENT EFFECT OF THE N^6-BENZOYL GROUP

Yukio KITADE, Ryuji NAKANISHI, Magoichi SAKO, Kosaku HIROTA, and Yoshifumi MAKI*

Gifu Pharmaceutical University, 5-6-1, Mitahora-higashi, Gifu 502, Japan

Facile conversion of N^6-benzoyl-2',3'-*O*-isopropylideneadenosine (**1**) into N^6-benzoyl-5'-chloro-5'-deoxy-8-hydroxy-2',3'-*O*-isopropylideneadenosine (**3**) by a reaction with cupric chloride in acetonitrile provides a new method for the chemical modification of adenosines. This reflects the prominent substitutent effect of N^6-benzoyl group on the chemical reactivity of adenosines.

KEYWORDS adenosine derivative; 5'-*O*,8-cycloadenosine; oxidative cyclization; cupric chloride; imino-ether bond cleavage; 5'-chloro-8-hydoxyadenosine; N^6-substituent effect

In our research to develop methods for the chemical modification of adenosines,[1,2,3,4,5] the metal ion-catalyzed reactions of the adenosines have been examined as an intriguing target from the biochemical viewpoint.[6] This paper describes our discovery of the facile conversion of N^6-benzoyl-2',3'-*O*-isopropylideneadenosine (**1**) into N^6-bezoyl-5'-chloro-5'-deoxy-8-hydroxy-2',3'-*O*-isopropylidineadenosine (**3**) by a reaction with cupric chloride in acetonitrile. This provides a method for a new chemical modification of adenosines and clearly shows the prominent effect of the N^6-benzoyl group on the reactivity of adenosines.

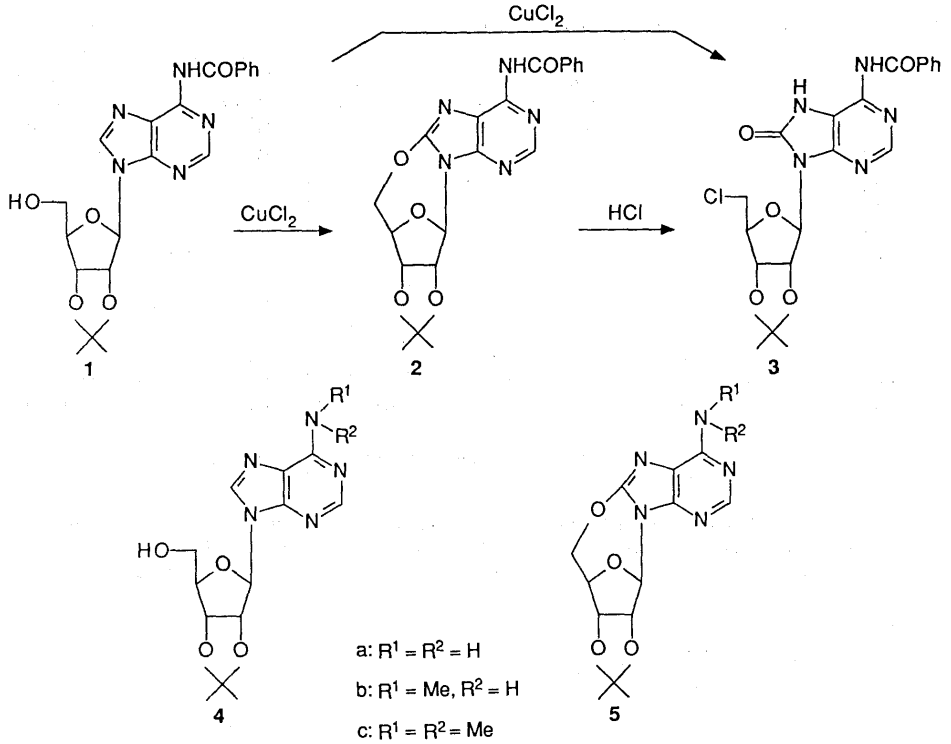

Chart 1

A mixture of **1** [5 mM] and cupric chloride [30 mM] in dry acetonitrile was refluxed under argon for 8 h. After removal of the solvent, the reaction mixture was chromatographed over Florisil (eluent: chloroform-methanol 20:1) to isolate **3** (mp 189-190°C from ethanol) in 90% yield.[7] The stoichiometric study showed that the use of excess cupric chloride is required for the smooth conversion of **1** into **3**. There was no catalytic action of cupric chloride under the aerobic condition. The structure of **3** was fully supported by mass, ^{1}H NMR, UV spectral data and microanalysis.

When the reaction was followed by thin-layer chromatography, a fairly stable intermediate was found. The intermediate was isolated in 35% yield by shortening the reaction time (3 h), together with **3** in 61% yield. The structure of the intermediate was found to be N^6-benzoyl-5'-*O*,8-cyclo-2',3'-*O*-isopropylideneadenosine (**2**) by spectral comparison with an authentic sample.[2] Analogous treatment of **2** with cupric chloride formed **3**. This was accelerated by adding a small amount of hydrochloric acid to the reaction medium. The above facts clearly show that the formation of **3** occurs *via* the initial oxidative cyclization of **1** to **2** by cupric ion followed by cleavage of the imino-ether bond of **2** by hydrochloric acid in the reaction medium as shown in Chart 1.

Recent works[3,4,5] from our laboratory have demonstrated the new type of the cyclization of 2',3'-*O*-isopropylideneadenosines by oxidation using lead tetraacetate[3] and *N*-bromosuccinimide[5] and photochemical oxidation in the presence of an electron acceptor.[4] The present oxidative cyclization of adenosines promoted by biologically important cupric ions[6] is of mechanistic interest. Cleavage of the imino-ether bond in 5'-*O*,8-cycloadenosines to give 5'-substituted 5'-deoxy-8-hydroxyadenosines by various agents under appropriate conditions has been well demonstrated.[8]

It should be noted that the present conversion easily occurs only when the N^6-benzoyladenosine (**1**) is the reactant, i.e. under analogous conditions, adenosine (**4a**), N^6-methyladenosine (**4b**) and N^6,N^6-dimethyladenosine (**4c**)[9] gave with comparative difficulty the corresponding 5'-*O*,8-cycloadenosines (**5a**), (**5b**),

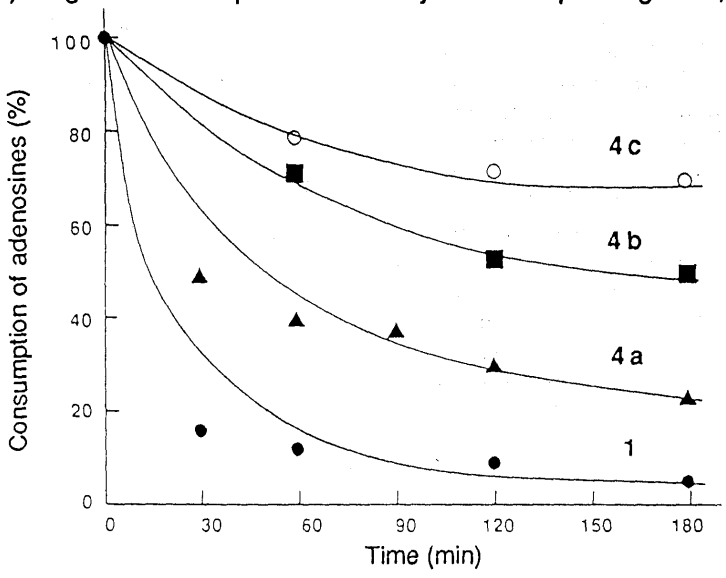

Fig. 1. Consumption of Adenosines, **1** and **4a-c**, in the Reaction with Cupric Chloride as a Function of Reaction Time
Reaction conditions: a mixture of adenosines, **1** and **4a-c**, [5 mM] and $CuCl_2$ [30 mM] in dry MeCN was refluxed under Ar for 3 h.

and (**5c**), without accompanying isolable amounts of 5'-chloro-5'-deoxy-8-hydroxyadenosines. Figure 1 shows the consumption of **1**, **4a**, **4b**, and **4c** in the reaction with cupric chloride as a function of reaction time. It indicates roughly that the ease of the oxidative cyclizations is in the order of **1** > **4a** > **4b** > **4c**. An independent experiment showed that the imino-ether bond of **5a** was almost inert against cupric chloride under the same reaction conditions. Thus, the prominent substituent effect of the N^6-benzoyl group on the present conversion is unequivocal.

It has been proved that the N^6-acyl group in the adenosines relatively increases the nucleophilicity of the imidazole ring nitrogen (N^7), e.g. contrary to the adenosines, protonation and alkylation of N^6-acyladenosines preferentially occurs at the N^7-position rather than the N^1-position.[1)]

In agreement with previous observations, the accelerative effect of N^6-benzoyl group on the present conversion may be explained in terms of preferable coordination of cupric ions at the N^7-position of **1** for the oxidative cyclization (intramolecular oxidative nucleophilic substitution) and by protonation at the N^7-position of **2** essential for the imino-ether bond cleavage.

ACKNOWLEDGMENTS This work was partly supported by Grant-in-Aid for Scientific Research from the Ministry of Education, Science, and Culture in Japan.

REFERENCES AND NOTES

1) Y. Maki, K. Kameyama, M. Suzuki, M. Sako, and K. Hirota, *J. Chem. Research (S)*, 1984, 388 and references cited therein.

2) M. Sako, T. Saito, K. Kameyama, K. Hirota, and Y. Maki, *J. Chem. Soc.,Chem. Commun.*, 1987, 1298.

3) K. Kameyama, M. Sako, K. Hirota, and Y. Maki, *J. Chem. Soc., Chem. Commun* ., 1984, 1658.

4) M. Sako, K. Shimada, K. Hirota, and Y. Maki, *J. Chem. Soc., Chem. Commun.*, 1986, 1704.

5) Y. Maki, M. Sako, T. Saito, and K. Hirota, *Heterocycles*, **27**, 347 (1988).

6) W. Saenger, in '*Principles of Nucleic Acid Structure*,' Springer-Verlag, New York, 1984, ch. 8, p 201.

7) Isopropylidene protection of adenosines and using acetonitrile as a solvent were pre-requisite for the smooth conversion of **1** to **3**. It is known that cupric ion is a weak oxidant in water but relatively strong in acetonitrile (E^0= 1.20 V). Among the cupric salts examined, cupric chloride gave the most satisfactory result for this type of conversion. Some other metal salts may be applicable in place of cupric salts.

8) M. Ikehara, *Acc. Chem. Res.*, **2**, 47 (1969); M. Ikehara and S. Uesugi, *Chem. Pharm. Bull.*, **17**, 348 (1969).

9) The formation of demethylated products (**4b**) and (**5b**) was also observed.

(Received May 21, 1991)

THE CHEMISTRY OF 1-HYDROXYINDOLES: SYNTHESES OF METHYL 1-HYDROXYINDOLE-3-ACETATE, Nb-ACETYL-1-HYDROXYTRYPTAMINE, (±)- AND (S)-1-HYDROXYTRYPTOPHAN DERIVATIVES[1)]

Masanori SOMEI,* Toshiya KAWASAKI, Kazuhisa SHIMIZU, Yoshikazu FUKUI, and Toshiharu OHTA
Faculty of Pharmaceutical Sciences, Kanazawa University, 13-1 Takara-machi, Kanazawa 920, Japan

Methyl 1-hydroxyindole-3-acetate, (±)-2-acetoamino-3-(1-hydroxyindol-3-yl)propanol, Nb-acetyl-1-hydroxytryptamine, (±)- and (S)-(+)-Nb-acetyl-1-hydroxytryptophan methyl ester, which are needed for inspecting our hypothesis regarding the metabolism of tryptophan, were prepared for the first time. The structural proof of (±)-Nb-acetyl-1-hydroxytryptophan methyl ester by X-ray crystallographic analysis is also reported.

KEYWORDS methyl 1-hydroxyindole-3-acetate; (±)-2-acetoamino-3-(1-hydroxyindol-3-yl)-propanol; Nb-acetyl-1-hydroxytryptamine; (±)-Nb-acetyl-1-hydroxytryptophan methyl ester; (S)-(+)-Nb-acetyl-1-hydroxytryptophan methyl ester; 1-hydroxyindole; 2,3-dihydroindole; oxidation; X-ray crystallographic analysis; tryptophan

1-Hydroxyindoles are generally believed to be unstable compounds except for cases where electron-withdrawing groups are placed at the proper positions.[2,3,4)] For a representative example, 1-hydroxyindole (2a) can exist only in an inert solvent under protection from light and attempts to isolate it have thus far been unsuccessful.[2,3)] Therefore, it is a quite interesting and challengeable theme to determine whether 1-hydroxytryptophan derivatives can exist or not. Furthermore, it is important to study 1-hydroxytryptophan derivatives as common intermediates for the formation of various indole metabolites *in vivo* in relation to the metabolism of tryptophan.[2)] Based on the hypothesis, we have long been engaged in the chemistry of 1-hydroxy- and 1-methoxyindoles,[2,4)] and developed simple synthesis methods for them.[4)] Here we report the first and simple synthesis of methyl 1-hydroxyindole-3-acetate (2b), (±)-2-acetoamino-3-(1-hydroxyindol-3-yl)propanol (2c), Nb-acetyl-1-hydroxytryptamine (2d), (±)- ((±)- 2e), and (S)-(+)-Nb-acetyl-1-hydroxytryptophan methyl ester ((S)-(+)-2f).

2,3-Dihydroindoles (1b-f) were prepared by reducing the corresponding indoles with sodium cyanoborohydride[5)] in acetic acid. Oxidation of methyl 2,3-dihydroindole-3-acetate (1b) with 30% aqueous hydrogen peroxide (H_2O_2, 10 mol eq.) in the presence of a catalytic amount of sodium tungstate dihydrate ($Na_2WO_4 \cdot 2H_2O$, 0.2 mol eq.) in methanol-water at room temperature for 30 min afforded methyl 1-hydroxyindole-3-acetate[6)] (2b) in 65% yield (Chart 1). The compound (2b) was stable enough for rapid silica gel column chromatography and isolable as a pure colorless oil. However, it gradually decomposed and after standing for one hour at room temperature, it formed unidentified products, though 2b was still the major component. The structure of 2b was determined by converting it to stable methyl 1-methoxyindole-3-acetate (3b)[2b)] by treating it with ethereal diazomethane in 91% yield.

Under similar oxidizing conditions, (±)-2-acetoamino-3-(2,3-dihydroindol-3-yl)propanol ((±)-1c), Nb-acetyl-2,3-dihydrotryptamine (1d), and (±)-Nb-acetyl-2,3-dihydrotryptophan methyl ester ((±)-1e) afforded

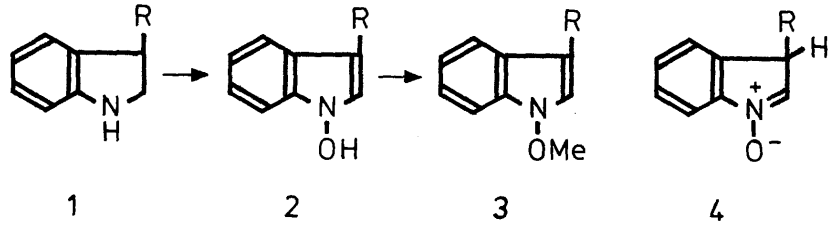

a R= H
b R= $-CH_2COOMe$
c R= (±)-$-CH_2CHCH_2OH$ (NHAc)
d R= $-CH_2CH_2NHAc$
e R= (±)-$-CH_2CHCOOMe$ (NHAc)
f R= (S)-$-CH_2CHCOOMe$ (NHAc)

Chart 1

the corresponding 1-hydroxyindole derivatives, ((±)-2c), (2d), and ((±)-2e), in 30, 55, and 73% yields, respectively. The compound ((±)-2c)[7] was an unstable oil, but more stable than 2b. To our surprise, the compounds (2d and (±)-2e)[8] were isolated as stable colorless prisms. The structures of (±)-2c, 2d, and (±)-2e were determined by converting them to the corresponding 1-methoxyindoles, ((±)-3c), (3d), and ((±)-3e), in 77, 83, and 83% yields, respectively, by treatment with ethereal diazomethane.

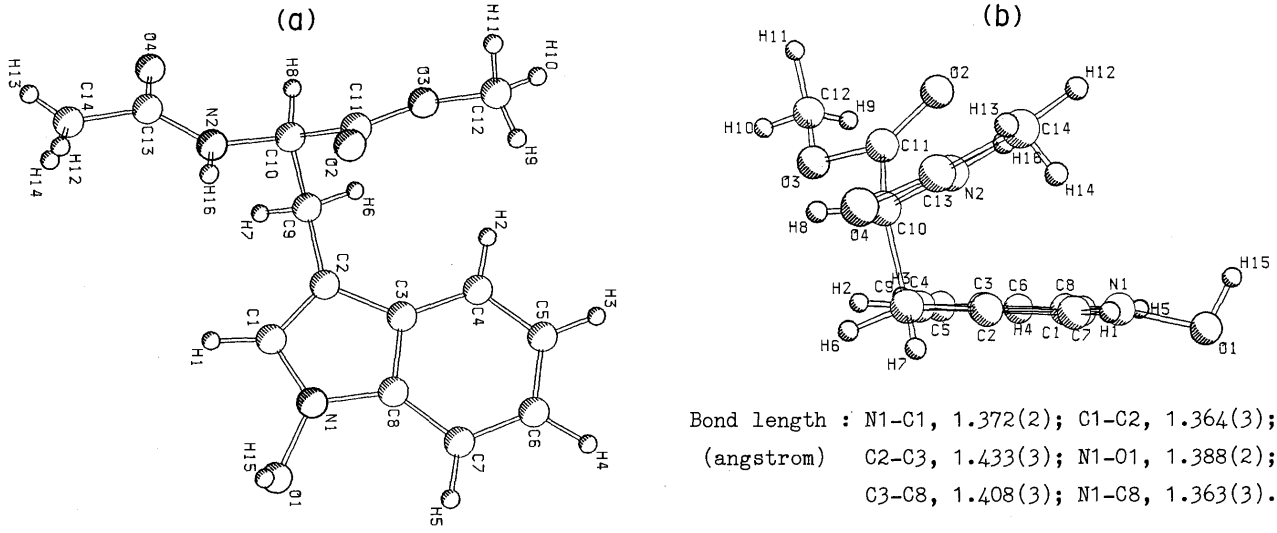

Fig. 1. Perspective View of (±)-Nb-Acetyl-1-hydroxytryptophan Methyl Ester ((±)-2e)

The structure of (±)-2e was unequivocally determined by X-ray single crystallographic analysis[9] as shown in Fig. 1. This is the first example of the X-ray analysis of 1-hydroxyindole itself. The ABX coupling pattern (^{1}H-NMR) of H6, H7, and H8 signals of (±)-2e and bond length between N1 and C1 proved that the contribution of the nitrone structure (4) was negligible in both the solution and solid states. It should be noted that the oxygen atom of the 1-hydroxy group deviates clearly from the plane of the indole nucleus,[3d] as Fig. 1b shows.

Finally, (S)-(+)-Nb-acetyl-1-hydroxytryptophan methyl ester[10] ((S)-(+)-2f) was obtained as stable colorless prisms (mp 116-117°C) in 53% yield from the corresponding 2,3-dihydroindole (1f) by the oxidation with 30% H_2O_2 and $Na_2WO_4 \cdot 2H_2O$. Treating (S)-(+)-2f with ethereal diazomethane afforded a 78% yield of (S)-(+)-Nb-acetyl-1-methoxytryptophan methyl ester[11] ((S)-(+)-3f).

These results show that the stability of 1-hydroxyindoles (2) is governed at least partly by the bulkiness of the 3-substituent. The most important point in the present work is that 1-hydroxytryptophan can exist in peptides and/or enzymes and plays a biologically significant role[2a] in vivo. Preparations of glycosides and phosphate esters and the biological activities of compounds (2 and 3) are currently under investigation.

ACKNOWLEDGMENT The authors express their gratitude to Prof. Y. Tsuda and Mr. S. Hosoi (Kanazawa University) for helpful discussions for X-ray crystallographic analysis. This work is partly supported by a Grant-in-Aid for Scientific Research from the Ministry of Education, Science and Culture of Japan, which is gratefully acknowledged.

REFERENCES AND NOTES

1) This report is part 57 of a series entitled "The Chemistry of Indoles". Part 56: K. Nakagawa and M. Somei, Heterocycles, 32, 873 (1991).

2) a) Leading reference (review): M. Somei, Yuki Gosei Kagaku Kyokai Shi, 49, 205 (1991); b) T. Kawasaki, A. Kodama, T. Nishida, K. Shimizu, and M. Somei, Heterocycles, 32, 221 (1991).

3) a) R.M. Acheson, D.M. Littlewood, and H.E. Rosenberg, J. Chem. Soc., Chem. Commun., 1974, 671 ; b) R.

M. Acheson, P.G. Hunt, D.M. Littlewood, B.A. Murrer, and H.E. Rosenberg, J. Chem. Soc., Perkin Trans. 1, 1978, 1117 ; c) R.M. Acheson, "New Trends in Heterocyclic Chemistry," Elsvier Scientific Pub. Co., New York, pp. 1-33 (1979); d) Acheson and co-workers found that 1-benzoyloxyindole has the pyramidal nitrogen atom (N1) by X-ray crystallographic analysis: R.M. Acheson, M.H. Benn, J. Jacyno, and J.D. Wallis, J. Chem. Soc., Perkin Trans. 2, 1983, 497; e) R.M. Acheson, "Advances in Heterocyclic Chemistry," Vol. 51, Academic Press, Inc., New York, pp. 105-175 (1990).

4) a) M. Somei and T. Shoda, Heterocycles, 16, 1523 (1981); b) M. Somei, H. Ohnishi, and Y. Shoken, Chem. Pharm. Bull., 34, 677 (1986); c) M. Somei and T. Kawasaki, Heterocycles, 29, 1251 (1989).

5) G.W. Gribble, P.D. Lord, J. Skotnicki, S.E. Dietz, J.T. Eaton, and J.L. Johnson, J. Am. Chem. Soc., 96, 7812 (1974).

6) Colorless unstable oil. IR (film) cm^{-1}: 3300, 2960, 1708, 1435, 1330, 1173, 1005, 738. ^{1}H-NMR (CD_3OD) δ : 3.66 (3H, s), 3.70 (2H, s), 6.96 (1H, dt, J=1.2 and 7 Hz), 7.06 (1H, dt, J=1.2 and 7.8 Hz), 7.18 (1H, s), 7.31 (1H, dm, J=7.8 Hz), 7.43 (1H, dm, J=7 Hz). High resolution MS m/z: Calcd for $C_{11}H_{11}NO_3$: 205.0738. Found: 205.0840. UV λ_{max}^{MeOH}nm: 222, 278, 291.

7) Colorless unstable oil. IR (film) cm^{-1}: 3265, 1629, 1547, 738. ^{1}H-NMR (CD_3OD) δ : 1.88 (3H, s), 2.80 (1H, dd, J=14.5 and 7.5 Hz), 3.00 (1H, dd, J=14.5 and 6.5 Hz), 3.53 (2H, d, J=5.1 Hz), 4.14 (1H, m), 6.96 (1H, dd, J=7.6 and 7.1 Hz), 7.10 (1H, s), 7.12 (1H, dd, J=7.6 and 6.8 Hz), 7.32 (1H, d, J=7.1 Hz), 7.57 (1H, d, J=6.8 Hz). High resolution MS m/z: Calcd for $C_{13}H_{16}N_2O_3$: 248.1159. Found: 248.1146. UV λ_{max}^{MeOH}nm: 224, 283, 293.

8) 2d: mp 138-139°C (recrystallized from AcOEt). IR (KBr) cm^{-1}: 3250, 3105, 1619, 1602, 1580, 743. ^{1}H-NMR (CD_3OD) δ : 1.89 (3H, s), 2.89 (2H, t, J=7.3 Hz), 3.43 (2H, t, J=7.3 Hz), 6.99 (1H, t, J=8.3 Hz), 7.10 (1H, s), 7.12 (1H, t, J=8.3 Hz), 7.34 (1H, d, J=8.3 Hz), 7.52 (1H, d, J=8.3 Hz). MS m/z: 218 (M^+), 202. Anal. Calcd for $C_{12}H_{14}N_2O_2$: C, 66.04; H, 6.47; N, 12.84. Found: C, 66.02; H, 6.53; N, 12.77. UV λ_{max}^{MeOH}nm (log ε): 225 (4.52), 281 (3.62), 295 (3.66).
(±)-2e: mp 153-154°C (dec., recrystallized from MeOH). IR (KBr) cm^{-1}: 3259, 3125, 1739, 1640, 1547, 727. ^{1}H-NMR (CD_3OD) δ: 1.92 (3H, s), 3.06 (1H, dd, J=13.9 and 7.6 Hz), 3.28 (1H, dd, J=13.9 and 5.9 Hz), 3.65 (3H, s), 4.66 (1H, dd, J=7.6 and 5.9 Hz), 6.97 (1H, ddd, J=7.1, 6.8, and 1.5 Hz), 7.09 (1H, s), 7.12 (1H, ddd, J=7.6, 6.8, and 1.5 Hz), 7.32 (1H, dm, J=7.1 Hz), 7.47 (1H, dm, J=7.6 Hz). MS m/z: 276 (M^+), 260. Anal. Calcd for $C_{14}H_{16}N_2O_4$: C, 60.86; H, 5.84; N, 10.14. Found: C, 60.78; H, 5.92; N, 10.09. UV λ_{max}^{MeOH}nm (log ε): 224 (4.55), 282 (3.65), 294 (3.68).

9) Crystal data for (±)-2e: $C_{14}H_{16}N_2O_4$, M=276.29, triclinic, space group $P\bar{1}$, with unit cell dimensions a=8.1707(8), b=12.105(1), c=8.019(1) Å, α=107.94(1)°, β=109.54(1)°, γ=73.156(8)°, V=695.6(1)Å^3, Z=2, and Dc=1.319 g/cm^3. The reflection data were collected on a Rigaku AFC-5 diffractometer for 3°< 2θ <55° using Mo Kα radiation (λ=0.71069A) and the ω-2θ scan method at a 2θ scan speed of 6°/min. The structure was solved by the direct method using the MITHRIL program and refined by full-matrix least squares. The final R value was 0.043 for 2210 independent reflections [I>3σ(I)].

10) (S)-(+)-2f: mp 116-117°C (recrystallized from MeOH-H_2O). $[\alpha]_D^{24}$ +11.8° (MeOH, c=0.102). IR (KBr) cm^{-1}: 3370, 3240, 1733, 1655, 1534, 745. ^{1}H-NMR (5% CD_3OD in $CDCl_3$) δ: 1.90 (3H, s), 3.19 (1H, dd, J= 15 and 5.8 Hz), 3.27 (1H, dd, J=15 and 5.2 Hz), 3.71 (3H, s), 4.86 (1H, dd, J=5.8 and 5.2 Hz), 7.01 (1H, s), 7.06 (1H, t, J=8.3 Hz), 7.19 (1H, t, J=8.3 Hz), 7.42 (1H, d, J=8.3 Hz), 7.45 (1H, d, J=8.3 Hz). MS m/z: 276 (M^+), 260. Anal. Calcd for $C_{14}H_{16}N_2O_4$: C, 60.86; H, 5.84; N, 10.14. Found: C, 60.85; H, 5.88; N, 10.14. UV λ_{max}^{MeOH}nm (log ε): 224 (4.53), 282 (3.64), 293 (3.66).

11) (S)-(+)-3f: Colorless oil. $[\alpha]_D^{20}$ +16.8° (MeOH, c=0.107). IR (film) cm^{-1}: 3270, 1741, 1658, 1540, 736. ^{1}H-NMR ($CDCl_3$) δ: 1.97 (3H, s), 3.25 (1H, dd, J=14.6 and 4.9 Hz), 3.31 (1H, dd, J=14.6 and 5.4 Hz), 3.70 (3H, s), 4.05 (3H, s), 4.93 (1H, ddd, J=7.8, 5.4, and 4.9 Hz), 6.03 (1H, d, J=7.8 Hz), 7.04 (1H, s), 7.11 (1H, dd, J=8.3 and 7.8 Hz), 7.24 (1H, t, J=8.3 Hz), 7.40 (1H, d, J=8.3 Hz), 7.49 (1H, d, J=7.8 Hz). High resolution MS m/z: Calcd for $C_{15}H_{18}N_2O_4$: 290.1266. Found: 290.1296. UV λ_{max}^{MeOH}nm (log ε): 223 (4.47), 276 (3.66), 289 (3.68).

(Received May 24, 1991)

FOUR NEW AND TWELVE KNOWN SAPOGENOLS FROM SOPHORAE SUBPROSTRATAE RADIX[1)]

Takashi TAKESHITA, Kei YOKOYAMA, Ding YI, Junei KINJO and Toshihiro NOHARA*

Faculty of Pharmaceutical Sciences, Kumamoto University, Oe-honmachi 5-1, Kumamoto 862, Japan

Four new oleanene sapogenols having 22-oxo group were obtained from the methanolysate of the crude glycosidic fraction in Sophorae Subprostratae Radix, the root of *Sophora subprostrata* CHUN et T. CHEN. Also, twelve known sapogenols were isolated from the same methanolysate.

KEYWORDS Sophorae Subprostratae Radix; *Sophora subprostrata*; Leguminosae; oleanene sapogenol; 22-oxoolean-12-ene; subprogenin A; subprogenin B; subprogenin C; subprogenin D

During our studies on the leguminous plants,[1)] we had obtained many oleanene sapogenols and described their structures.[2)] As a result of these studies, we found that the saponins which are effective for experimental liver cell injury have a methyl group at C-17 and several oxygen functions in an E-ring. These saponins, as represented by soyasaponin I, have various pharmacologoical effects.[3e)] In connection with these studies, we tried to clarify the constituents of Sophorae Subprostratae Radix, the root of *Sophora subprostrata* CHUN et CHEN. Now we have obtained four new sapogenols, named subprogenins A (**1**), B (**2**), C (**3**) and D (**4**), together with twelve known sapogenols(**5**~**16**) from the methanolysate of the crude saponin fraction of this drug. This paper deals with the structure of the subprogenins **1**~**4**.

The known sapogenols were identified as sohoradiol (**5**),[3a)] cantoniensistriol (**6**),[3b)] soyasapogenol B (**7**),[3b)] soyasapogenol A (**8**),[3a)] abrisapogenol C (**9**),[2c)] abrisapogenol D (**10**),[2b)] abrisapogenol E (**11**),[2b)] kudzusapogenol A (**12**),[2a)] abrisapogenol H (**13**),[2e)] wistariasapogenol A (**14**),[3c)] melilotigenin (**15**)[3d)] and abrisapogenol I (**16**),[2c)] by comparison of various data with those of the authentic samples.

Subprogenin A (**1**), colorless needles, mp 267-269°C, $[\alpha]_D$ +36.7°($CHCl_3$-MeOH=1:1, *c*=0.4), showed not only the same molecular ion peak (*m/z* 472) but also similar fragment peaks at *m/z* 224 (from the A/B ring) and 248 (from the D/E ring) by *retro* Diels-Alder fission[4)] in the EI-MS with those of wistariasapogenol A (**14**). In the ^{13}C-NMR spectra of **1** and **14**, the signals due to the A~D ring were consistent with each other, but the signals due to C-29 and 30 were completely different. Since the ^{1}H-NMR spectrum for the acetate (**1a**) of **1** showed an ABq (δ 3.93, 3.76, 2H, *J*=11.0Hz) signal which resembled the H-29(2H) signal of abrisapogenol C (**9**), the structure of **1** was determined to be 3β,24,29-trihydroxy-22-oxoolean-12-ene.

Subprogenin B (**2**), colorless needles, mp 235-237°C, $[\alpha]_D$ +53.1°($CHCl_3$-MeOH=1:1, *c*=0.1), showed a molecular ion peak at *m/z* 488 and a fragment peak at *m/z* 264 (from the D/E ring) which was larger by 16 mass units than that of **1** in the EI-MS. In the ^{13}C-NMR spectrum of **2**, the signals due to the A~D ring were in accordance with those of **1**. But a hydroxymethyl signal appeared instead of one methyl signal. Also, in comparison of the ^{13}C-NMR data of **2** with that of **1**, the respective shifts occurred at C-19(-3.8ppm), C-20(+4.4ppm) and C-21(-3.9ppm). This suggests the presence of a hydroxy group at C-29 and 30. So the structure of **2** was concluded to be 3β,24,29,30-tetrahydroxy-22-oxoolean-12-ene.

Subprogenin C (**3**) was obtained as the methyl ester (**3a**), colorless needles, mp 150-152°C, $[\alpha]_D$ +38.2°($CHCl_3$-MeOH=1:1, *c*=0.2), by methylation with CH_2N_2 during the isolation procedure. In the EI-MS of **3a**, a molecular ion peak at *m/z* 484 and fragment ion peaks at *m/z* 208 (from A/B ring) and *m/z* 276 (from D/E ring) indicated the presence of one hydroxy group in the A/B ring, and a carbonyl and a methoxycarbonyl group in the D/E ring. The ^{13}C-NMR spectrum of **3a** showed that the signals due to the A/B ring (C-1~10, 23~26) were the same as those of abrisapogenol H (**13**). But the signals due to C/D/E ring(C-12~22, 27~30) were in good agreement with those of abrisapogenol I methyl ester (**16a**). Consequently, the structure of **3** was deduced to be 3β-hydroxy-22-oxo-olean-12-ene-30-oic acid.

Subprogenin D (**4**) was also obtained as the methyl ester (**4a**), colorless needles, mp 221-223°C, $[\alpha]_D$ +9.4°($CHCl_3$-MeOH=1:1, *c*=0.5). Since the same molecular ion peak and fragment ion peaks similar to those of **3a** appeared in the EI-MS of **4a**, apparently **4a** was an isomer of **3a**. In the ^{13}C-NMR spectrum of **4a**, except the signals due to C-18~21, 29 and 30, the remaining signals were consistent with those of **3a**. In addition, on TLC, one of the reductive products of **4a** with $NaBH_4$ was the same as abrisapogenol A (**17**).[2c] Based on this evidence, the structure of **4** was 3β-hydroxy-22-oxo-olean-12-ene-29-oic acid.

These new sapogenols(**1**~**4**) have 22-oxo group in their molecules. They are members of

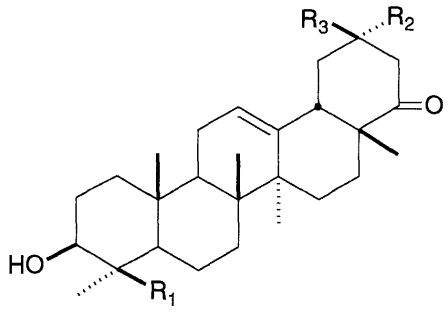

	R_1	R_2	R_3
subprogenin A (**1**)	CH_2OH	CH_2OH	Me
subprogenin B (**2**)	CH_2OH	CH_2OH	CH_2OH
subprogenin C (**3**)	Me	Me	COOH
methyl ester (**3a**)	Me	Me	COOMe
subprogenin D (**4**)	Me	COOH	Me
methyl ester (**4a**)	Me	COOMe	Me
abrisapogenol H (**13**)	Me	Me	CH_2OH
wistariasapogenol A (**14**)	CH_2OH	Me	CH_2OH
melilotigenin (**15**)	CH_2OH	COOH	Me
abrisapogenol I (**16**)	CH_2OH	Me	COOH

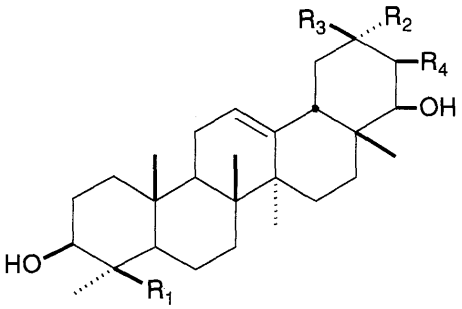

	R_1	R_2	R_3	R_4
sophoradiol (**5**)	Me	Me	Me	H
cantoniensistriol (**6**)	Me	Me	Me	OH
soyasapogenol B (**7**)	CH_2OH	Me	Me	H
soyasapogenol A (**8**)	CH_2OH	Me	Me	OH
abrisapogenol C (**9**)	Me	CH_2OH	Me	OH
abrisapogenol D (**10**)	Me	Me	CH_2OH	OH
abrisapogenol E (**11**)	CH_2OH	Me	CH_2OH	H
kudzusapogenol A (**12**)	CH_2OH	CH_2OH	Me	OH
abrisapogenol A (**17**)	Me	CH_2OH	Me	H

very rare class of oleanene. Since some compounds having such a functional group have been found as glycosides,[2c),3e)] they could not be an artifact caused by acid hydrolysis.

Seven saponins including three new saponins from this plant will be published.[5)]

Table I. ^{13}C-NMR Spectral Data for Sapogenols **1**, **2**, **3a**, **4a**, **13** and **14** (δ:ppm, in Pyridine-d_5)

	1	**2**	**3a**	**4a**	**13**	**14**
C-1	38.8	38.9	39.1	39.1	39.1	38.8
2	28.3	28.4	28.1	28.1	28.1	28.3
3	80.0	80.0	78.0	78.0	78.1	80.0
4	43.1	43.2	39.4	39.4	39.4	43.1
5	56.3	56.3	55.7	55.7	55.8	56.2
6	19.0	19.1	18.7	18.7	18.8	19.0
7	33.2	33.4	33.0	32.9	33.1	33.3
8	39.9	39.9	39.9	39.9	39.9	39.8
9	47.9	48.0	47.9	47.8	47.9	47.9
10	37.0	37.0	37.2	37.2	37.3	37.0
11	24.0	24.0	23.8	23.9	23.8	24.0
12	123.9	124.0	124.7	124.9	123.0	123.9
13	142.0	142.3	141.5	141.1	142.3	142.1
14	41.9	42.1	42.0	42.0	42.1	42.0
15	25.4	25.5	25.3	25.3	25.5	25.4
16	27.2	27.0	28.1	27.3	27.4	27.3
17	48.1	48.1	47.5	48.2	47.8	47.7
18	47.4	47.1	48.5	46.7	47.5	47.3
19	41.4	37.6	44.1	41.1	42.9	42.8
20	39.7	44.1	45.7	44.4	38.9	38.8
21	46.3	42.4	46.8	45.9	47.0	46.9
22	216.2	216.8	213.0	214.1	216.1	215.9
23	23.5	23.6	28.7	28.7	28.8	23.5
24	64.5	64.6	15.8	15.6	15.8	64.5
25	16.2	16.2	16.6	16.6	16.6	16.1
26	16.8	16.9	16.9	16.9	17.0	16.8
27	25.4	25.3	25.3	25.4	25.4	25.3
28	21.2	21.6	21.3	21.3	21.3	21.3
29	71.9	68.3	26.2	176.6	26.9	26.9
30	21.1	65.0	176.8	20.9	68.2	68.2
OMe			52.0	52.1		

REFERENCES AND NOTES

1) Part 27 in a series of studies on the leguminous plants.

2) *a)* J. Kinjo, I. Miyamoto, K. Murakami, K. Kida, T. Tomimatsu, M. Yamasaki and T. Nohara, *Chem. Pharm. Bull.*, **33**, 1293(1985); *b)* T. Takeshita, S. Hamada and T. Nohara, *Ibid.*, **37**, 846(1989); *c)* Y. Sakai, T. Takeshita, J. Kinjo, Y. Ito and T. Nohara, *Ibid.*, **38**, 824(1990); *d)* J. Kinjo, K. Matsumoto, M. Inoue, T. Takeshita and T. Nohara, *Ibid.*, **39**, 116(1991); *e)* T. Takeshita, S. Hamada, T. Nohara, N. Marubayashi and I. Ueda, Abstracts of Papers, 109th Annual Meetings of the Pharmaceutical Society of Japan, Nagoya, Apr. 1989, vol.3, P.146.

3) *a)* I. Kitagawa, H. K. Wang, M. Saito, U. Tosirisuk, T. Fujiwara and K. Tomita, *Chem. Pharm. Bull.*, **30**, 2294(1982); *b)* T. C. Chiang and H. M. Chang, *Planta Medica*, **46**, 52(1982); *c)* T. Konoshima, M. Kozuka, M. Haruna, K. Ito and T. Kimura, *Chem. Pharm. Bull.*, **37**, 1550(1989); *d)* S. S. Kang and W. S. Woo, *J. Natural Products*, **51**, 335(1988); *e)* I. Kitagawa, T. Taniyama, T. Murakami, M. Yoshihara and M. Yoshikawa, *Yakugaku Zasshi*, **108**, 547(1988); *e)* I. Kitagawa and M. Yoshikawa, *Kagaku to Seibutsu*, **21**, 224(1982).

4) H. Budzikiewicz, C, Djerassi and D. H. Williams, "Structure Elucidation of Natural Products by Mass Spectrometry," vol. 2, Holden-Day Inc., San Francisco, 1964, p. 121.

5) Y. Ding, T. Takeshita, K. Yokoyama, J. Kinjo and T. Nohara, *Chem. Pharm. Bull.*, submitted, B-7059.

(Received May 24, 1991)

ISOLATION, SEQUENCE AND BACTERIAL EXPRESSION OF A cDNA FOR CHALCONE SYNTHASE FROM THE CULTURED CELLS OF *PUERARIA LOBATA*

Osamu NAKAJIMA, Takumi AKIYAMA, Takashi HAKAMATSUKA, Masaaki SHIBUYA, Hiroshi NOGUCHI, Yutaka EBIZUKA and Ushio SANKAWA*

Faculty of Pharmaceutical Sciences, The University of Tokyo, 7-3-1, Hongo, Bynkyo-ku, Tokyo 113, Japan

cDNA clones for chalcone synthase (CHS) of *Pueraria lobata* cultured cells were isolated by screening the cDNA library using CHS cDNA of *Phaseolus vulgaris* as a probe. Analysis of nucleotide sequences of the cloned cDNA revealed a 1170-bp open reading frame that encoded a 390-amino acid polypeptide with an Mr of 43,000. The full-length cDNA was cloned into the expression vector pT7-7. CHS activity was found in the crude extracts of transformed *E. coli* after induction and two protein bands of ca. 43 and 34 kd were hybridized with anti-persley CHS antiserum.

KEYWORDS biosynthesis; secondary metabolism; chalcone synthase; elicitor; cDNA cloning; DNA sequence analysis; gene expression

The biosynthesis of flavonoids has been extensively studied at the enzyme level in many species of plants,[1] since flavonoids are ubiquitous in higher plants and have a wide variety of physiological functions in the plants. A typical example is the synthesis of phytoalexins in legumes against stress or microbial infection. In the last decade great attention has been paid to the study of the regulatory mechanism of flavonoid biosynthesis, since the recent progress of molecular biology made it possible to study flavonoid biosynthesis at the enzyme and gene levels. The first pathway-specific enzyme in flavonoid biosynthesis is chalcone synthase (CHS), which catalyzes the formation of chalcone from *p*-coumaroyl and malonyl CoAs. CHS cDNAs were cloned in several species of plants.[2] Studies of genomic CHS DNA were also reported.[3] We have been studying enzymology and the reaction mechanisms of isoflavonoid biosynthesis using cell suspension cultures of *Pueraria lobata*.[4] This paper reports the cloning, sequencing and bacterial expression of a cDNA for chalcone synthase (CHS) from the cultured cells of *P. lobata*.

In our previous studies on the enzymology of isoflavonoid biosynthesis we used an endogenous elicitor to induce CHS.[5] Later, yeast extract was found to be a better elicitor to induce the CHS activity in the cultured cells of *P. lobata* and was used as the elicitor to obtain mRNA. A northern blot analysis (Fig. 1) demonstrated that yeast extract induces CHS synthesis which is regulated at the transcriptional level, since the amount of mRNA in untreated cells was below the detectable level. The size of CHS mRNA, 1.5 kb which is sufficient to encode a protein of 43 kDa, was determined by the SDS-PAGE of purified CHS from the cultured cells of *P. lobata*. A cDNA library was constructed in λ gt10 and 2.0 x 10^5 recombinants were screened with ^{32}P labelled CHS cDNA of *Phaseolus vulgaris* as a probe.[6] Four hybridization-positive clones (designated as PlCHSI, PlCHSII, PlCHSIII and PlCHSIV) were obtained and sequenced by a DNA sequencer (Hitachi SQ-3000) after subcloning in pBluescript. The longest cDNA clone, pPlCHSI is a full-length clone comprising a single open reading frame (ORF) of 1170 bp that encoded a 390-amino acid polypeptide with an Mr of 43,000, 97 bp of 5' leader sequence and 188 bp of 3' untranslated sequence.[7] A part of the cDNA and deduced amino acid sequences are shown in Fig. 2. The other clones were not full-length cDNAs, but were 625 bp, 838 bp and 474 bp long, respectively. Their sequences of coding regions were the same as that of PlCHSI, but

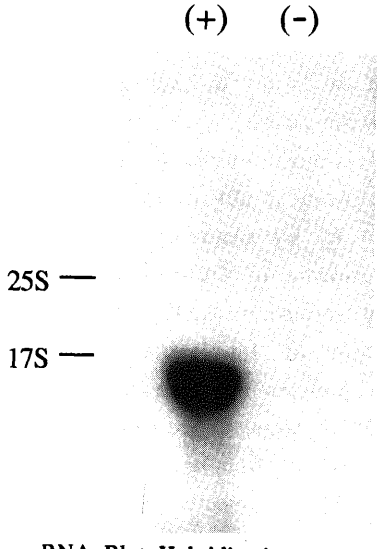

Fig. 1. RNA Blot Hybridization Analysis of *P. lobata* CHS mRNA
The total *P. lobata* RNA (2 μg) was separated on a 1.2% agarose gel, blotted and hybridized with radioactive probes (1.4-kbp *Eco*R I fragment of pCHS1[6]). The mobilities of the 25S (3.4 kb) and 17S (1.8 kb) rRNA are indicated by lines. The size of *P. lobata* CHS mRNA was estimated to be 1.5 kb. (+);elicitor-challenged with yeast ext, (-);no elicitor-challenged.

```
CTA GTA AAG TAC TGC TAG CTG TGA CTT GTT GAG TTC GAT CAA ATC GCA GTA CTT TGG TAT CAT CAT CAT CAT CAA TTA GAA GAA GGA AAA      0
 TER TER            TER     TER       TER                                                  TER       rbs
Met Val Ser Val Ala Glu Ile Arg Gln Ala Gln Arg Ala Glu Gly Pro Ala Thr Ile Leu Ala Ile Gly Thr Ala Asn Pro Pro Asn Cys
ATG GTG AGC GTA GCT GAG ATC CGC CAG GCA CAA AGG GCA GAA GGC CCA GCA ACC ATC CTT GCC ATT GGA ACT GCA AAC CCA CCA AAC TGT     90
 1
Val Asp Gln Ser Thr Tyr Pro Asp Tyr Tyr Phe Arg Ile Thr Asn Ser Glu His Met Thr Glu Leu Lys Glu Lys Phe Gln Arg Met Cys
GTT GAT CAG AGC ACC TAT CCT GAT TAC TAC TTC AGA ATC ACC AAC AGT GAG CAC ATG ACC GAG CTC AAA GAG AAA TTC CAG CGC ATG TGT    180

Asp Lys Ser Met Ile Lys Lys Arg Tyr Met Tyr Leu Thr Glu Glu Ile Leu Lys Glu Asn Pro Asn Met Cys Ala Tyr Met Ala Pro Ser
GAC AAG TCT ATG ATC AAG AAG AGA TAC ATG TAC TTA ACC GAA GAG ATC TTG AAA GAG AAT CCA AAC ATG TGT GCT TAC ATG GCA CCT TCT    270
                rbs             2                   rbs             3
Leu Asp Ala Arg Gln Asp Met Val Val Val Glu Val Pro Lys Leu Gly Lys Glu Ala Ala Thr Lys Ala Ile Lys Glu Trp Gly Gln Pro
TTG GAT GCT AGG CAA GAC ATG GTG GTG GTG GAG GTA CCA AAA CTA GGG AAA GAG GCT GCA ACA AAG GCC ATA AAG GAG TGG GGC CAG CCA    360
          rbs         4
Lys Ser Lys Ile Thr His Leu Ile Phe Cys Thr Thr Ser Gly Val Asp Met Pro Gly Ala Asp Tyr Gln Leu Thr Lys Gln Leu Gly Leu
AAG TCA AAG ATT ACC CAC TTG ATC TTT TGC ACC ACA AGT GGT GTG GAC ATG CCT GGT GCT GAT TAC CAA CTC ACC AAA CAA TTG GGC CTT    450

Arg Pro Tyr Val Lys Arg Tyr Met Met Tyr Gln Gln Gly Cys Phe Ala Gly Gly Thr Val Leu Arg Leu Ala Lys Asp Leu Ala Glu Asn
CGC CCC TAT GTG AAG AGG TAC ATG ATG TAC CAA CAA GGT TGC TTT GCA GGT GGC ACG GTG CTT CGT TTG GCC AAG GAT TTG GCT GAG AAC    540
               rbs         5
```

Fig. 2. A Part of Nucleotide and Deduced Amino Acid Sequences of the cDNA Insert in pPlCHSI
Nucleotides are numbered from the beginning of the initiation codon. Potential ribosome binding site in *E. coli* (rbs) and initiation codon were underlined.

the lack a part of the sequence in the 3' untranslated region, just before poly(A), by 18 bp, 15 bp and 8 bp, respectively. It is not clear that these deletions are due to different origins of the clones or to artifacts during the cloning procedure. Sequence comparison between the ORFs of *P. lobata* CHSI and *Phaseolus vulgaris* CHS cDNA[6] showed their high homology, 90.8% at nucleotide level and 95.9% at amino acid level as is expected from their close taxonomical relation.

The isolated cDNA of CHS has several stop codons in the 5' leader sequence and a sequence, AAGGA, which is identical to one of the ribosome binding sites (rbs) of *E. coli*, at 8-bp upstream from the initiation codon ATG. Since this AAGGA sequence was expected to function as rbs in transformed *E. coli*, we tried to express the isolated cDNA in *E. coli*. The *Bam*HI fragment of pPlCHSI was ligated to the *Bam*HI site of an expression vector pT7-7 (T7 RNA polymerase/T7 promoter expression system)[8a] without adjusting a frame to the translating frame of the expression vector. The construct was designated as pT7CHS. Induction was effected by raising the temperature, as described by S. Tabor.[8b] Though no distinct band of expressed CHS appeared at the expected molecular weight of CHS in silver stained SDS-PAGE, more than one distinct band were detected by immunoblotting analysis (western blotting) using anti-parsley CHS antiserum (Fig.3).[9a] The largest band blotted at 42-43 kd (lane 3) coincides with that of purified CHS from *P. lobata* cell cultures (lane 4).[9b] and the deduced Mr of a protein coded in the ORF of the cDNA. The other band corresponds to a protein of ca 34 kd. In addition to the initiation codon ATG which is accompanied by potential rbs, there are several ATG codons accompanied by potential rbs in the ORF of the cDNA. It is highly probable that translation started from the ATG codon at 208 and/or 247 to yield the protein(s) of ca. 34 k. An analogous case of translation initiated from the middle of ORF occurred in the expression of cDNA for ferredoxin NADP$^+$ reductase from spinach.[10] The protein of low molecular weight of the two expressed proteins of ferredoxin NADP$^+$ reductase is a product whose translation started from the GTG codon at 84-bp downstream from the initiation codon of ORF. This was caused by the potential rbs, AGGA, at 10 bp upstream from the GTG codon.[10]

To further determine the expression of the CHS cDNA, the CHS activity was measured using [^{14}C]-malonyl CoA as a substrate. As shown in Table 1, the CHS activity was found exclusively in the crude extract of *E. coli* transformed with pT7CHS. The radioactive naringenin, formed by chemical cyclization of naringenin chalcone, a product of the CHS reaction,

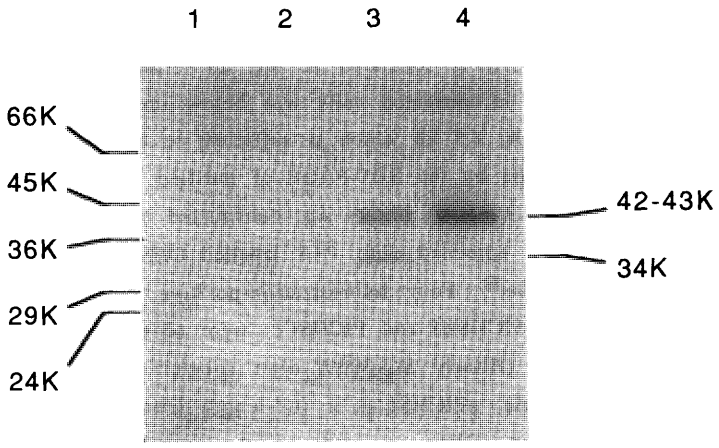

Fig. 3. Immunoblot Analysis of CHS Synthesis in *E. coli*. Proteins from a gel were transfered to a nitrocellulose membrane and probed with antiserum against parsley CHS. Lanes:1, *E.coli* DH5αF' containing pT7-7 alone; 2, *E. coli* DH5αF' containing pT7CHS before induction; 3, *E. coli* DH5αF' containing pT7CHS after induction; 4, purified CHS from *P. lobata*.

was determined by isotopic dilution analysis.[11] A radioactive fraction obtained by HPLC separation was diluted with non-labelled naringenin and recrystallized three times. Each sample showed constant specific activity (first; 257 dpm/mg, second; 246 dpm/mg, and third; 267 dpm/mg). The results rigorously demonstrated that the introduced cDNA was expressed in *E. coli* to yield CHS with catalytic activity. The CHS activity also appeared in an experiment using pBluescript as the expression vector (data not shown). The results so far obtained are unique, since full length cDNA is expressed by using the potential rbs site present in the cDNA.[12] Successful expression of CHS in *E. coli* will help in studying the association and cooperative action of the enzymes involved in 5-deoxychalcone synthesis,[13] and to investigate the stereochemistry of hydrogen loss in the process of aromatization subsequent to the condensation of *p*-coumaroyl CoA and the three molecules of malonyl CoA.[14]

Table I. CHS Activity in Crude Extract of Transformed *E. coli*.

Plasmid	Induction	Naringenin chalcone and naringenin (dpm)
pT7CHS	0 h	3084
	3 h	13831
pT7-7	0 h	684
	3 h	576

After lysis of the cells by lysozyme, the extract was incubated with ^{14}C-Malonyl CoA (1.11×10^5 dpm, 1.05 nmol) and *p*-coumaroyl CoA (2.5 nmol) at 30 °C for 20 min. The product was extracted with ethyl acetate, mixed with non-labeled standard sample and applied to reverse phase HPLC. The fraction of naringenin chalcone and naringenin were combined and radioactivity was measured.

ACKNOWLEDGEMENTS The authors thank Dr. C.J. Lamb of the Salk Institute for providing us cDNA for the CHS of *P. vulgaris*; Dr. S. Tabor of Harvard University Medical School for pT7-7 and pGP1-2; Dr. K. Hahlbrock of Max Planck Institut für Züchtungsforshung for the antiserum against parsley CHS; Dr. Y. Ozeki of College of Arts and Sciences, The University of Tokyo, for helpful suggestions; and Dr. T. Nishimura of Faculty of Medicine, The University of Tokyo, for many valuable suggestions.

REFERENCES AND NOTES

1) J. Ebel and K. Hahlbrock, " The Flavonoids: Advances in Research", ed. by J.B. Harborne and T.J. Mabry, Chapman and Hall, London 1982, p641.
2) a) (*Antirrhinum majus*) H. Sommer and H. Seadler, *Mol. Gen. Genet.*, **202**, 429 (1986);
b) (*Zea mays*) U. Wienand, U. Weydemann, U. Niesbach-Klosgen, P.A. Peterson and H. Seadler, *Mol. Gen. Genet*, **203**,202 (1986);
c) (*Petunia hybrida*) R.E. Spelt, H.J. Reif, P.J.M. van den Elzen, E. Veltkamp and J.N.M. Mol, Nucleic Acid Res., **14**, 5229 (1986);
d) (*Petroselinum hortense*) U. Reimold, M. Kroger, F. Kreuzaler and K. Hahlbrock, *EMBO* J., **2**, 1801 (1983);
e) (*Phaseolus vulgaris*) T.B. Ryder, C.L. Cramer, J.N. Bell, M.P. Robbins, R.A. Dixon and C.J. Lamb, *Proc. Natl. Acad. Sci. USA*, **81**, 5724 (1984);
f) (*Hordeum vulgare* and *Magnolia liliiflora*) U. Niesbach-Klosgen, E. Brazen, J. Bernhardt, W. Rohde, Z. Schwarz-Sornmer, H.J. Reif, U. Wienand and H. Seadler, *J. Mol. Evol.* **26**, 213 (1987);
g) (*Sinapis alba*) B. Ehmann and E. Schafer, *Plant Mol. Biol.* **11**, 869 (1988).
3) C.J. Lamb, M.A. Lawton, M. Dron and R.A. Dixon, *Cell*, **56**, 215 (1989).
4) a) M. Hashim, T. Hakamatsuka, Y. Ebizuka and U. Sankawa, *FEBS LETTERS*, **271**, 219 (1990);
b) M. Hashim, T. Hakamatsuka, Y. Ebizuka and U. Sankawa, *Tetrahedron* (1991), in press.
5) T. Hakamatsuka, H. Noguchi, Y. Ebizuka and U. Sankawa, *Chem. Pharm. Bull.* **37**, 249 (1989).
6) T. Ryder, S. Hedrick, J.N. Bell, X. Liang, S. Clous, C.J. Lamb, *Mol. Gen. Genet*, **210**, 219 (1987).
7) The nucleotide sequence of PlCHSI will appear in the DDBJ, EMBL and Genbank Nucleotide Sequence Databases under the accession number D01023.
8) a) S. Tabor, and C.C. Richardson, *Proc. Natl. Acad. Sci. USA*, **82**, 1074 (1985);
b) The *E. coli* carrying pT7CHS or pT7-7 was cultured at 30°C before induction. To induce T7 RNA polymerase gene under the λ P_L promoter, the temperature was raised to 42°C for 30 min., and then lowered to 37°C. The cultivation was continued for 3 h.
9) a) M. Lawton, R.A. Dixon, K. Hahlbrock and C.J. Lamb, *Eur. J. Biochem.*, **129**, 593 (1983);
b)Sequence comparison between *P. lobata* CHS and parsley CHS (Genbank, PETCHSR) revealed 70.7% homology at the nucleotide level. As expected from such homology, anti-parsley CHS antiserum reacted to the purified CHS from *P. lobata*.
10) A. Aliverti, T. Jansen, G. Zanetti, S. Ronchi, R.G. Herrmann and B. Curti, *Eur. J. Biochem*, **191**, 551 (1990).
11) Naringenin chalcone is reversibly converted to naringenin in a non-enzymatic manner. Its equilibrium lies very far to naringenin.
12) During the course of this study Schröder and his group also succeeded in the expression of CHS cDNA as a fusion protein having catalytic activity in *E. coli*. The authors thank Prof. Schröder for kindly supplying information.
13) T. Hakamatsuka, H. Noguchi, Y. Ebizuka and U. Sankawa, *Chem. Pharm. Bull.* **36**, 4225 (1988).
14) E. Woo, I. Fujii, Y. Ebizuka, U. Sankawa, A. Kawaguchi, S. Huang, J.M. Beale M. Shibuya, U. Mocek and H.G. Floss, *J. Am. Chem. Soc.*, **111**, 5498 (1989).

(Received May 24, 1991)

 Chem. Pharm. Bull. **39**(7) 1914—1916 (1991) Vol. 39, No. 7

REVERSIBLE ELECTROCHEMICAL REDUCTION OF 1,6,6a-TRITHIA-3,4-DIAZA-PENTALENES TO THEIR ANION RADICALS WITH THE PRODUCTION OF SUPEROXIDE

Tetsuo NAGANO, Maki TAKAHASHI and Masaaki HIROBE*

Faculty of Pharmaceutical Sciences, University of Tokyo, Hongo, Bunkyo-ku, Tokyo 113, Japan

1,6,6a-Trithia-3,4-diazapentalenes, which are hypervalent compounds, were reduced electrochemically and the resulting anion radicals reacted with dioxygen (O_2) to be re-oxidized to the starting materials, with the production of superoxide ($O_2^{-\bullet}$). We have already reported that 1,6-dioxa-6a-thia-2,5-diazapentalenes mediate $O_2^{-\bullet}$ production in living cells and do serious damage to the cells. These results suggest that hypervalent heteropentalenes generally generate $O_2^{-\bullet}$ in the presence of O_2 by chemical or biological reduction system.

KEYWORDS hypervalent; superoxide; reactive oxygen species; heteropentalene; lactoperoxidase; cyclic voltammogram

Paraquat (PQ^{2+}), a potent herbicide, can gain entry into living cells and is reduced one electron to the cation radical ($PQ^{+\bullet}$) at the expense of NAD(P)H in the biological system. $PQ^{+\bullet}$ reacts with dioxygen (O_2) to be re-oxidized to the starting material, with the production of superoxide ($O_2^{-\bullet}$) which does serious damage to the cells.[1] Thus PQ^{2+} can catalyze the production of $O_2^{-\bullet}$ in the presence of O_2 by the biological reduction system. Quinones,[2] benzofurazans[3] and nitrofurantoin[2] are also known as redox-active compounds like PQ^{2+}, and these compounds often have potent and various biological activities. As part of our reserach concerning reactive oxygen species,[4] we have reported that 1,6-dioxa-6a-thia-2,5-diazapentalenes (HEP, Chart 1) mediate $O_2^{-\bullet}$ production in *Escherichia coli*[5] and inactivate 2,3-dihydroxyisovalerate dehydratase to cause growth inhibition.[6] HEP compounds[7] have a hypervalent bond,[8] which is characteristic of the linear O-S-O arrangement. To determine whether hypervalent heteropentalenes can generally produce $O_2^{-\bullet}$, we examined the redox activity of 1,6,6a-trithia-3,4-diazapentalenes[9] (Chart 2).

Here, we report that 1,6,6a-trithia-3,4-diazapentalenes 1 ~ 3 (Chart 2) can be reduced electrochemically and be re-oxidized by O_2, with the production of $O_2^{-\bullet}$. These pentalenes containing hypervalent sulfur (IV) have electronic structures with formal expansion of the valence shell.

Cyclic voltammograms of compounds 1, 2 and 3 were measured in dimethylformamide (DMF) with tetraethyl

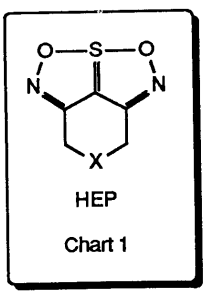

HEP

Chart 1

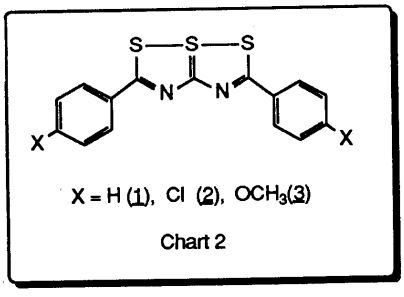

X = H (1), Cl (2), OCH_3(3)

Chart 2

Table I. Redox Potentials of Trithiadiazapentalenes

	Compound 1	Compound 2	Compound 3
$E_{1/2}$ (mV)	-818	-693	-913

$E_{1/2}$ potential *vs* SCE was determined by cyclic voltammetry in DMF.

ammonium perchlorate as the supporting electrolyte at Pt electrode. Figure 1 shows the cyclic voltammogram of compound 1 under anaerobic (solid line) and aerobic (dotted line) conditions. A quasi-reversible redox potential wave appeared at 0 ~ -1.5 V under anaerobic conditions. But the re-oxidation wave diminished under aerobic conditions which indicates that O_2 reacts with the reduced form of compound 1. As shown in Table I, the redox potential of compound 2, which has an electron-withdrawing functional group , was less negative. This indicates that compound 2 is more readily reduced than compounds 1 and 3.

We coulometrically reduced compounds 1, 2 and 3 in a two-compartment cell at E = -1.0 V, -0.9 V and -1.1 V *vs* S.C.E., respectively, for 40 min at room temperature in DMF at the Pt electrode under anaerobic conditions. The reduced forms of compounds 1 ~ 3 were all re-oxidized by exposure to O_2 to the starting materials. Figure 2 shows the spectral change when compound 2 is used. This demonstrates the increase at 320 nm and the decrease at 389 nm.

To determine whether $O_2^{-\bullet}$ is produced during the reaction of the reduced forms with O_2, a DMF solution of the reduced forms generated electrochemically was added to potassium phosphate buffer (pH 6.0), including lactoperoxidase. Generally, lactoperoxidase reacts with $O_2^{-\bullet}$ to form the complex known as Compound III,[10] which has a characteristic absorption maximum at 588 nm. The increase of absorbance at 588 nm was caused by the reduced 2 - O_2 - lactoperoxidase system (Fig. 3, line 2), and the increase was inhibited by superoxide dismutase (SOD)[11] which dismutates $O_2^{-\bullet}$ to H_2O_2 and O_2. The increase did not occur under anaerobic conditions. The excess amounts of H_2O_2 have also been reported to form Compound III, so to avoid the H_2O_2 effect, catalase was added to the reaction mixture

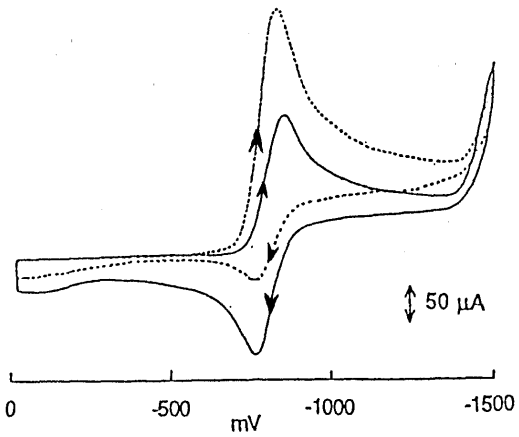

Fig. 1. Cyclic Voltammogram of Compound 1 under Anaerobic (——) and Aerobic (------) Conditions.

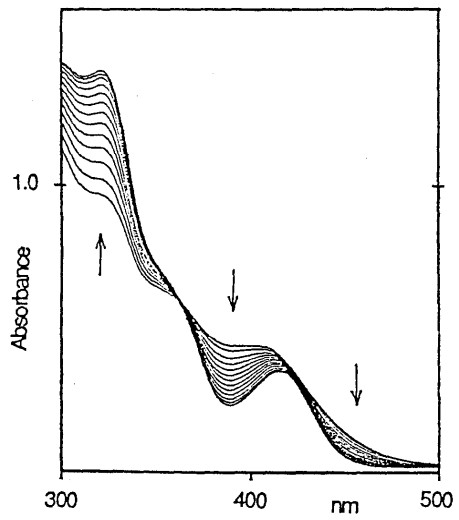

Fig. 2 . Spectral Change of Reduced 2 in the Presence of O_2

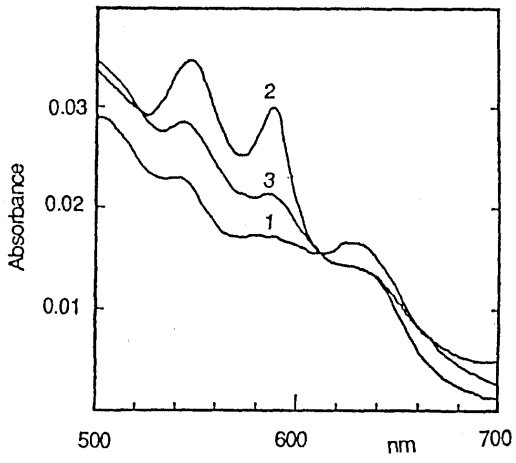

Fig. 3. Formation of Compound III in the Reaction of Reduced 2 with Lactoperoxidase in the Presence of O_2. line 1: Lactoperoxidase; line 2: Reduced 2 + Lactoperoxidase + O_2; line 3: Reduced 2 + Lactoperoxidase + Ar.

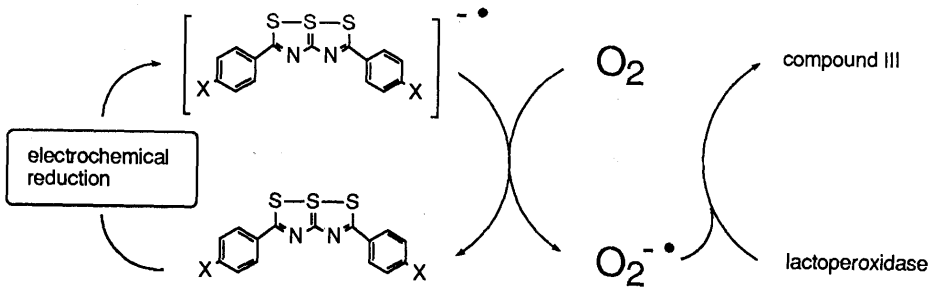

Chart 3

inducing no effect. This shows that reduced hypervalent heteropentalenes can react with O_2 and mediate electron transfer to O_2, producing $O_2^{-\bullet}$ (Chart 3).

From the results obtained by HEP and compounds 1 ~ 3, hypervalent heteropentalenes generally appear to generate $O_2^{-\bullet}$ in the presence of O_2 by chemical or biological reduction system.

ACKNOWLEDGEMENT The authors are grateful for the research grant from the Ministry of Education, Sciences and Culture of Japan.

REFERENCES

1) H. M. Hassan and I. Fridovich, *J. Biol. Chem.*, **253**, 8143 (1978); I. Fridovich and H. M. Hassan, *Trends Biochem.Sci.*, **4**, 113 (1979); H. M. Hassan and I. Fridovich, *J. Biol. Chem.*, **254**, 10846 (1979); D. J. Hassett, B. E. Britigan, T. Svendsen, G. M. Rosen and M. S. Cohn, *J. Biol. Chem.*, **262**, 13404 (1987).

2) H. M. Hassan and I. Fridovich, *Arch. Biochem. Biophys.*, **196**, 385 (1979); M. Boyd, H. Sesame, J. Mitchell and G. Catigmani, *Fed. Proc.*, **36**, 405 (1977).

3) T. Takabatake, M. Hasegawa, T. Nagano and M. Hirobe, *Chem. Pharm. Bull.*, **38**, 128 (1990); T. Takabatake, M. Hasegawa, T. Nagano and M. Hirobe, *ibid.*, in press.

4) T. Nagano, *Yakugaku Zasshi*, **111**, 103 (1991) and refs. cited therein.

5) M. Takabatake, T. Nagano and M. Hirobe, *Arch. Biochem. Biophys.*, **268**, 137 (1989).

6) Unpublished data.

7) P. Camilleri, J. R. Bowyer, M. T. Clark and O'Neill, *Biochim. Biophys. Acta*, **765**, 236 (1984); J. R. Bowyer, P. Camilleri and A. Stapleton, *FEBS Lett.*, **172**, 239 (1984); P. Camilleri, M. T. Clark, D. J. Cole-Hamilton and I. J. Gilmore, J. Chem. Soc. Perkin II, 833 (1985); P. Camilleri, J. R. Bowyer and R. C. Weaver, *Biochim. Biophys. Acta*, **810**, 385 (1985); P. Camilleri, J. R. Bowyer and P. H. McNeil, *Z. Naturforsch*, **42c**, 829 (1987).

8) K. Akiba, *Chemistry and Chemical Industry*, **40**, 112 (1987).

9) J-L. Derocque, M. Perrier and J. Vialle, *Bull. Soc. Chim. France*, 2062 (1968).

10) S. Nakamura and I. Yamazaki, *Biochim. Biophys. Acta*, **189**, 29 (1969); K. Sugioka, H. Nakano, T. Noguchi, J. Tsuchiya and M. Nakano, *Biochem. Biophys. Res. Commun.*, **100**, 1251 (1981).

11) J. M. McCord and I. Fridovich, *J. Biol. Chem.*, **244**, 6049 (1969).

(Received May 28, 1991)